International Indian Ocean Expedition

Collected reprints VIII

Published upon the recommendation
of the Scientific Committee on Oceanic Research (SCOR)
and the
Intergovernmental Oceanographic Commission (IOC)

Unesco, Paris 1972

International Indian Ocean Expedition. Collected reprints VIII

Collected edition published in 1972 by the United Nations
Educational, Scientific and Cultural Organization,
Place de Fontenoy, 75 Paris-7e
Printed by Les Presses Saint-Augustin, Bruges

SC.71/D.37.8/AFSR
Printed in Belgium

Preface

The eighth and last volume of collected reprints of the International Indian Ocean Expedition consists of papers received by Unesco between January 1970 and July 1971.

For convenience of presentation the papers have been grouped, in a very approximate classification, under the following main headings:

I. Marine biology;
II. Physical oceanography and marine meteorology;
III. Marine chemistry;
IV. Marine geology and geophysics;
V. General reports and comments;
VI. Papers presented by title or abstract only.

Author and subject indexes are now in preparation.

Collected reprints of the IIOE

List of reprints

Part I. Marine biology

Part II. Physical oceanography and marine meteorology

Part III. Marine chemistry

Part IV. Marine geology and geophysics

Part V. General reports and comments

Part VI. Papers presented by title or abstract only

Part I Marine biology

Reprinted from *Transactions, Royal Society of New Zealand (Botany)*, vol. 2, no. 15, 1963, p. 189-218

Studies on Australian and New Zealand Diatoms VI.—Tropical and Subtropical Species

By E. J. FERGUSON WOOD,
C.S.I.R.O. Division of Fisheries and Oceanography

[*Received by the Editor, June 7, 1963.*]

Abstract

THIS paper includes 133 diatom species, mainly from shallow waters and sediments of the Coral, Timor and Arafura Seas and Indonesian waters. A few species have been described but not figured in previous parts of this series Seven new species are described and named and eight species are described but not named, as they represent single occurrences.

INTRODUCTION

THIS paper, the last in this series, includes species which were collected during cruises of H.M.A.S. *Gascoyne* and H.M.A.S. *Diamantina* in tropical waters of the Indian and south-west Pacific Oceans, as well as a few species which had been omitted from the previous parts.

THE DIATOM SPECIES

Sub-Order DISCINEAE

Family COSCINODISCACEAE

Genus COSCINOSIRA Gran 1900

1. **Coscinosira oestrupii** Ostenfeld (Pl. 1, fig. 1; Pl. 5, fig. 1).

Ostenfeld, 1901, 52.

Cells in chains, cylindrical, with slightly rounded or occasionally concave valves; surface with irregular reticulations; marginal spinulae absent; cells united by numerous threads more or less parallel to the longitudinal axis. Diameter 35μ.

DISTRIBUTION. Off Timor.

Genus HYALODISCUS Ehr. 1845

2. **Hyalodiscus** sp. 1 (Pl. 1, fig. 2).

Cells in pairs or solitary, elliptical in girdle, circular in valve view; valves with central area about ⅓ valve diameter, clearly demarcated and with a vermiculate structure, marginal zone with fasciculate radial puncta. Diameter 40–60μ.

DISTRIBUTION. Bottom sediments off Port Moresby.

3. **Hyalodiscus** sp. 2 (Pl. 1, fig. 3)

Cells in pairs or solitary; elliptical in girdle, circular in valve view; surface with well-marked central area about ½ diameter of valve, irregularly punctate; marginal area with fasciculate puncta forming lines in three directions at an angle of about 30°. Puncta are coarser than those of *H. stelliger*. Diameter 50–60μ.

DISTRIBUTION. Indonesian waters.

Genus COSCINODISCUS Ehr. 1838

4. **Coscinodiscus africanus** Janisch (Pl. 1, fig. 4).

Janisch, 1875, 59, 24, 25.

Cells discoid; valves flat with small, hexagonal areolae radiating in narrow fascicles from an excentric area; areolae uniform in size; marginal spinulae numerous. Diameter 30–50μ.

DISTRIBUTION. Indonesian area, Arafura Sea, northern Coral Sea (Port Moresby area).

5. **Coscinodiscus apiculatus** Ehr. (Pl. 1, fig. 5).

Ehrenberg, 1844, 17.
A.S.A. 1886, 64, 5–8, 9, 10.

Valves circular; puncta in more or less radiate rows; central area hyaline. Close to *C. nitidus*. Diameter 40μ.

DISTRIBUTION. Moresby in shallow sediments.

6. **Coscinodiscus gazellae** Janisch (Pl. 1, fig. 6a, b).

Janisch in A.S.A. 1879, 688, 21, 8.
Wood, Crosby and Cassie 1959, 212, 15, 8.

A large form referred to *Ethmodiscus* by Hustedt. Depicted by Wood *et al.* by line drawing only. Plate shows fine striate markings.

DISTRIBUTION. Indonesian waters, Arafura Sea, Coral Sea.

7. **Coscinodiscus increscens** Karsten (Pl. 1, fig. 7).

Karsten 1907, 367, 35, 3, 3a.

Cells discoid; valves slightly convex, hexagonal areolae radiating from centre, no central area. Diameter 70–100μ.

DISTRIBUTION. Timor Sea.

8. **Coscinodiscus nodulifer** Janisch (Pl. 1, fig. 8).

Janisch in A.S.A. 1886, 59, 21, 23.
Karsten 1907, 36, 6.

Cells discoid; valves raised in the centre, areolate; areolae smaller towards the margin and with a raised nodule in the centre of the valve.

DISTRIBUTION. Indonesian waters.

9. **Coscinodiscus obscurus** A.S. (Pl. 1, fig. 9).

A.S.A. 1886, 61, 16.

Cells solitary; valves circular, with large, somewhat distant puncta which are roughly radial and slightly larger halfway to margin than at centre or margin; no central area or rosette. Diameter 50μ.

DISTRIBUTION. Off Mackay, Queensland.

10. **Coscinodiscus reniformis** Castracane (Pl. 1, fig. 10).

Castracane 1886, 160, 12, 12.
Stoschia admirabilis Janisch, Gazelle in A.S.A. 140, 17.
S. reniformis Heiden and Kolbe 1928, 476.

Valves irregularly reniform, one lobe usually larger than the other; areolae hexagonal, small, radiating. Length, 150–200μ.

DISTRIBUTION. Indonesia area, Arafura and Coral Seas.

11. **Coscinodiscus senarius** A.S. (Pl. 1, fig. 11).

A.S.A. 1875, 57, 24.
Karsten 1905, 87, 3, 10.

Valves convex, coarse areolae in a triangular arrangement one row of each series being radial, and dividing that series from the adjacent triangle of areolae. Diameter 40–60μ.

DISTRIBUTION. Indonesian waters.

12. **Coscinodiscus subtilissimus** Karsten (Pl. 1, fig. 12).

Karsten 1907, 363, 36, 2, 2a.

Valves convex near margins, otherwise flat; finely areolate in radial rows; no central area or rosette. Diameter 100 to 120μ.

DISTRIBUTION. Indonesian waters.

13. **Coscinodiscus** sp. (Pl. 1, fig. 13).

A.S.A. 1886, 64, 15.

Valves discoid, margin in this specimen apparently slightly crenate; surface flat, punctata, puncta random, no central area. Diameter 45μ.

DISTRIBUTION. Sediments off Port Moresby.

Genus PLANKTONIELLA (Wallich) Schütt 1893

14. **Planktoniella formosa** (Schimper ex Karsten) Karsten (Pl. 1, fig. 14).

Karsten 1928, 146, 218.
Hendey 1937, 258.
Valdiviella formosa Schimper ex Karsten 1907, 369, 39, 12.

Cells discoid, solitary; valves flat with hexagonal areolae similar to those of *Coscinodiscus excentricus* and a broad, circular wing with chambers separated by up to 75 rigid rays attached interiorly to a ring outside the valve margin and open exteriorly; upper and lower walls with radial striation; junction of rays and interior ring rounded. Diameter 100–200μ.

DISTRIBUTION. Indonesian waters and Arafura Sea.

Family ACTINODISCACEAE

Genus ACTINOCYCLUS Ehr. 1837 em. Ratt. 1890

15. **Actinocyclus alienus** Rattray (Pl. 1, fig. 15).

Rattray 1890, 144.

Valves flat, rounded at margins; central space irregular; surface areolate, areolae radial to sub-radial, obscurely fasciculate, secondarily oblique in decussating, outwardly convex rows; narrow sub-marginal zone inconspicuous; pseudo-ocellus circular. Diameter 100μ.

DISTRIBUTION. Timor Sea.

16. **Actinocyclus complanatus** Castracane (Pl. 1, fig. 16).

Castracane 1886, 145, 4, 9.
Rattray 1890, 165, 11, 10.

Frustules discoid; valves with rounded margin, circular; surface punctate, central space subcircular with irregularly arranged puncta; puncta radial, finer in marginal area, secondary rows straight or flexuous, becoming arcuate near margin; pseudonodule distinct, marginal. Diameter 100μ.

DISTRIBUTION. Sediments at 200m off Port Moresby.

17. **Actinocyclus disseminatus** Pantoczek (Pl. 1, fig. 17).

Pantoczek 1886–1893, 3, 35.
Rattray 1890, 141.

Frustules discoid; valves circular with small central space which is circular according to Rattray but almost triangular in the present specimen; surface irregularly punctate, puncta larger nearer the centre, decreasing to margin, irregularly arranged, secondary rows discernible, oblique. Diameter 60μ.

DISTRIBUTION. Sediments off Port Moresby.

18. **Actinocyclus dubiosus** Karsten (Pl. 1, fig. 18).

Karsten 1906, 157, 27, 1, 2.

Cells solitary, discoid; valves circular with very fine radial areolae and pear-shaped pseudo-ocellus. Diameter 100μ.

DISTRIBUTION. Off Mackay, Queensland.

19. **Actinocyclus mirabilis** Rattray (Pl. 1, fig. 19).

Rattray 1890, 159, 11, 16.

Cells discoid; valves with rounded margin; central space rounded with one or a few puncta, surface with radiating rows of puncta, closer near margin, with minute hyaline interspaces, especially near centre and at ends of shorter rows. Diameter 150μ.

DISTRIBUTION. Indonesian waters.

20. **Actinocyclus ovatus** sp. nov. (Pl. 1, fig. 20).

Cellae solae; valvae ovate cum areolis hexangulatis in ordine hexagonale.

Cells solitary, ovate in valve view, discoid in girdle view; surface with uniform hexagonal areolae arranged in three directions to give the appearance of an hexagonal system; pseudo-ocellus round, at apex of oval. Diameter 30–50μ.

DISTRIBUTION. Frequent in Indonesian region, Arafura and South Tasman Seas.

21. **Actinocyclus pyrotechnicus** Deby in Rattray (Pl. 1, fig. 21).

Rattray 1890, 144, 11, 15.

Valves discoid; surface areolate with large central granule or scattered small granules in central space, decreasing to margin in radial rows with hyaline spaces terminating the shorter rows of areolae, and irregular subhyaline rows separating fascicules of areolae; pseudonodule near margin (may be absent according to Rattray). Diameter 175μ.

DISTRIBUTION. Phytoplankton in Indonesian waters.

22. **Actinocyclus subocellatus** (Grunow) Rattray (Pl. 1, fig. 22).

Rattray 1890, 145.
Coscinodiscus curvatulus v. *subocellata* Grunow 1884, 83, 4d, 15.
A. curvatulus Janisch in A.S.A. 1875, 57, 31.
A. decipiens Castracane 1886.

Central area subcircular; areolae hexagonal, slightly smaller near centre and margins, in slightly curved, fasciculate and oblique arcuate secondary rows; pseudonodule circular. Diameter 120–150μ.

DISTRIBUTION. In sediment at 200m south of Port Moresby.

Genus ACTINOPTYCHUS Ehr. 1839

23. **Actinoptychus cathedralis** Brun (Pl. 2, fig. 23).

Brun in A.S.A. 1892, 154, 6.

Sectors 12 to 14; central space circular, slightly depressed; surface areolate giving a zig-zag pattern, inner stratum with round, more hyaline regions giving a dappled effect. Diameter 50μ.

DISTRIBUTION. Off Mackay, Queensland.

24. **Actinoptychus maculatus** Grove and Sturt (Pl. 2, fig. 24).

Grove and Sturt in A.S.A. 1892, 132, 18–20.

Valves circular, sectors 8 to 14, central area circular, surface areolate, inner stratum with large pores in irregular rows giving a dappled effect. Diameter 60–80μ.

DISTRIBUTION. Arafura Sea.

25. **Actinoptychus trilingulatus** (Br.) Ralfs (Pl. 2, fig. 25).

Ralfs in Pritchard 1861, 840.
Actinocyclus trilingulatus Br. 1860, 8, 93.
A.S. 1875, 1, 20.
Boyer 1927, 66.

Valves convex, slightly polygonal; surface finely and evenly areolate; sectors wedge-shaped; alternating sectors have a row of short spines near margin. Diameter 100μ.

DISTRIBUTION. Off Mackay, Queensland.

26. **Actinoptychus trifolium** Tempère and Brun (Pl. 2, fig. 26a-c).

Brun et Tempère 1889, 13, 7, 3.
A.S.A. 155, 12.

Cell in valve view polygonal with rounded corners; surface finely areolate, inner layer coarsely porulate; in valve view very twisted. Diameter 120–150μ

DISTRIBUTION. Indonesian waters.

Sub-Order AULISCINEAE
Family AULISCACEAE
Genus ASTEROLAMPRA Ehr. 1845

27. **Asterolampra dallasiana** Greville (Pl. 2, fig. 27).

Greville 1860, 115, 4, 10.
A.S.A. 1890, 137, 18.

Cells discoid; valves circular, with about 8 wedge-shaped sectors divided by hyaline rays, and finely punctate; central hyaline area about ⅓ diameter of valve; sectors joined to centre by straight lines. Diameter 60μ.

DISTRIBUTION. Coral Sea; Indian Ocean.

Genus ASTEROMPHALUS Ehr. 1844

28. **Asteromphalus cleveanus** Grunow (Pl. 2, fig. 28).

Grunow in A.S.A. 1875, 38, 13, 14.

Valves markedly oval; rays numerous, central hyaline area about half diameter of valve; sectors faintly marked. Diameter, 40–60μ.

DISTRIBUTION. Coral Sea; Lake Macquarie.

29. **Asteromphalus brookei** Bailey (Pl. 2, fig. 29).

Bailey 1856, 2, 1, 1.
A.S.A. 1875, 38, 21–23.
Boyer 1927, 73.

Valves circular, rays straight or angled, unbranched; segments numerous, with margins straight or curved, about half the radius, the two approximate segments with margins oblique towards centre; areolate, areolae diminishing from inner to outer portion of segments. Diameter 70–120μ.

DISTRIBUTION. Indian and Pacific Oceans in tropical waters.

30. **Asteromphalus heptactis** (Brebisson) Ralfs (Pl. 2, fig. 30).

Ralfs, in Pritchard, 1861, 838.
Boyer 1927, 73.
Spatangidium heptactis Brebisson 1857, 296.

Valves subcircular, hyaline area excentric, approximate rays longer than others, which are short and zig-zag; hyaline interspace between rays has a lunate line at its extremity, with a small marginal process; segments coarsely areolate. Diameter 50–70μ.

DISTRIBUTION. Indian Ocean, Indonesian waters.

31. **Asteromphalus-Coscinodiscus** (Pl. 2, fig. 31 a, b).

One valve has the characters of *Coscinodiscus excentricus*, the other of *Asteromphalus heptactis* except that the valve appears to be almost flat and not convoluted as in typical *Asteromphalus* or in the other cells of this type described by Wood, 1961, from the Antarctic. Several cells of this type were seen in three samples from the Timor Sea and Indonesian waters.

Genus STICTODISCUS Greville 1861

32. **Stictodiscus californicus** Greville (Pl. 2, fig. 32).

Greville 1861, 9, 79, 10, 1.

Cells discoid; valves circular or slightly deformed; with large radial puncta and broad, rather obscure hyaline rays becoming more evident near margin; marginal puncta smaller and more numerous, radiate. Diameter 40μ.

DISTRIBUTION. Lord Howe Island; Oamaru, fossil (Grove & Sturt 1887, 66).

33. **Stictodiscus hardmanianus** Greville (Pl. 2, fig. 33).

Greville 1865b, 98, 8, 4.
A.S.A. 1886, 74, 8; 131, 5.

Cells discoid, valves circular; hyaline central area; lines of radiating puncta separated by hyaline rays; margin with close radial puncta. Diameter, 50μ.

DISTRIBUTION. Maclean, New South Wales; Oamaru (Gr. & St. 1887, 66).

34. **Stictodiscus harrisonianus** (Norm. and Grev.) Castr. (Pl. 2, fig. 34).

Castracane 1886, 2, 112.
A.S.A. 1886, 75, 14–16.
Boyer 1927, 71.

Valves circular to triangular with straight or convex sides and sometimes slightly produced angles; rays strong, hyaline, radiate for over half radius, anastomosing, irregular towards centre, enclosing coarse puncta; marginal puncta radiate. Diameter 60–80μ.

DISTRIBUTION. Indonesian waters.

35. **Stictodiscus simplex**, A.S. (Pl. 2, fig. 35).

A.S.A. 1886, 74, 11.

Valves circular; puncta radial, separated by hyaline rays, large near centre, forming a single row between rays, replaced by two rows of smaller puncta nearer margin. Diameter, 60μ.

DISTRIBUTION. Sediments 20 miles south of Port Moresby.

Genus CYCLOTELLA (Kützing) Brebisson 1838

36. **Cyclotella comta** (Ehr.) Kützing (Pl. 2, fig. 36a).

Kützing 1849, 20.
Boyer 1916, 2, 7; 1927, 40.
Discoplea comta Ehr. 1844, 267.

Frustules not undulate, slightly inflated in girdle view; margin with radiate striae with an intramarginal zone apparently cellular, giving an appearance of spines; central portion of valve punctate or hyaline. Diameter, 30–40μ.

DISTRIBUTION. Sahul Bank sediments.

v. **unipunctata** Fricke (Pl. 2, fig. 36b).

Fricke in A.S.A. 1900, 224, 5–12.

Central area hyaline with a single punctum. Diameter 40μ.

DISTRIBUTION. Sediment off Port Moresby.

37. **Cyclotella kuetzingiana** Thwaites (Pl. 2, fig. 37).

Thwaites 1847, 8, 169.
Boyer 1927, 38.

Frustules in girdle view angular, undulate; valves circular, central part with scattered puncta, margin striate, striae may be oblique as in the plate. Diameter, 15–30μ.

DISTRIBUTION. Shallow water in the Timor Sea.

Genus AULACODISCUS Ehr. 1844

38. **Aulacodiscus formosus** Arnott (Pl. 2, fig. 38).

Arnott in Pritchard 1861, 843.
A.S.A. 1875, 35, 7, 8.

Valves circular with irregular, hyaline central area and radiating lines of puncta rather similar to *A. beeveriae* but puncta more numerous and smaller and to *A. margaritaceus*, but with raised cunieform processes which are not apparent in the illustration. Diameter, 80μ.

DISTRIBUTION. Sediments in Bate Bay, New South Wales. (34° S.).

Genus AULISCUS Ehr. 1888

39. **Auliscus compositus** A.S. (Pl. 2, fig. 39)

A.S.A. 1875, 30, 9.
Rattray 1888, 894.

Valves oblate, central area hyaline, stellate; elliptical area between the two processes with large, irregular areolae with a generally stellate arrangement and separated by irregularly reticulate meshwork; marginal area with radial subrectangular meshwork. Diameter, 120μ.

DISTRIBUTION. In sediments off Port Moresby.

Family BIDDULPHIACEAE

Genus CERATAULINA Peragallo 1892

40. **Cerataulina curvata** sp. nov. (Pl. 5, fig. 4; Pl. 2, fig. 40).

Cellae curvatae in serie; a duobus tuberis connectae; tuberis in extremis non oppositis.

Cells in chains connected by two spined processes; frustules curved, in appearance much resembling *Rhizosolenia stolterforthii*, but adjacent cells more closely depressed, processes of upper and lower valves not opposite; connective zone with numerous intercalary bands, Rhizosolenia-like. Length, 30 to 50μ.

DISTRIBUTION. Common in plankton of Timor and Arafura Seas.

41. **Cerataulina** sp. (Pl. 5, fig. 5; Pl. 2, fig. 41).

Cells cylindrical, in chains, attached by valve surface and two spined protuberances; aperture minute, thus differentiating this species from *C. compacta* and *C. pelagica*; intercalary bands scale-like. Diameter, 45–50μ.

DISTRIBUTION. North-east Indian Ocean, planktonic.

42. **Cerataulina compacta** Ostenfeld (Pl. 2, fig. 42).

Ostenfeld 1901, in Ostenfeld and Schmidt, 153 a-d.

Cells cylindrical, much longer than broad; valves slightly concave, processes short; cells in straight chains or solitary, weakly siliceous; puncta fine. Diameter 40–50μ.

DISTRIBUTION. North-west of Australia.

Genus BIDDULPHIA Gray 1821

43. **Biddulphia connecta** sp. nov. (Pl. 5, fig. 2).

Cellae binae; valvae circulares in medii in thalis sublatis cum duobus spinis longis et fasce filorum.

Cells in pairs, circular in valve view, subrotund in girdle view with narrow girdle zone and domed valves with raised central portion terminating in two long, angled spines; cells connected by a bundle of threads in a manner somewhat similar to Coscinosira. Diameter, 50μ.

This form is placed provisionally in the genus *Biddulphia* though it may merit generic rank.

DISTRIBUTION. Four cells observed in phytoplankton collected in the Java Sea.

44. **Biddulphia** sp. (Pl. 5, fig. 3).

Cells solitary, hyaline; girdle zone annulate; valves rounded in valve view circular, with four blunt processes. Length 150μ.

DISTRIBUTION. Arafura Sea.

Genus TRICERATIUM Ehr. 1839

45. **Triceratium antedeluvianum** (Ehr.) Grun. (Pl. 3, fig. 43).

Grunow 1868, 24.
Amphitetras antedeluvianum Ehr. 1839, 142.
Biddulphia antedeluviana Boyer 1901, 716.
Hendey 1937, 274.

Cells solitary; valves quadrangular with concave sides, centre depressed; surface coarsely areolate, radiate in central portion and also concentric, subradiate in outer part. Diameter, 65μ.

DISTRIBUTION. Bottom deposits off Port Moresby.

46. **Triceratium bicorne** Cleve (Pl. 3, fig. 44).

Cleve 1878, 17, 5, 30.
A.S.A. 1886 78, 24, 25.

This form is referred to *T. dubium* Brightwell by Mills 1916–32 but the identity seems doubtful. It is more closely related to *T. reticulum* but is much smaller. Valves quadrate with concave sides, one axis longer than the other; surface coarsely reticulate.

DISTRIBUTION. Rawson Collection; Indonesian waters.

47. **Triceratium biquadratum** Janisch (Pl. 3, fig. 45).

Janisch in A.S.A. 1886 98, 4–6.

Valves quadrilateral with slightly concave sides; angles rounded, with short, truncate processes, sculpture coarsely reticulate, central portion of valve raised with a circular or sub-rectangular depression between the centre and bases of the process; reticulations irregular, but with stronger radial lines in depressed portion of valve.

Hustedt synonymises this with *T. balearicum* as a variety, but Cleve (1881, 25) states distinctly that the sculpture of his species consists of "rounded puncta arranged in lines radiating from the centre to the angles."

DISTRIBUTION. Rawson Collection from Dunedin area, slide 92.

48. **Triceratium castelliferum** Grunow (Pl. 3, fig. 46).

Grunow in A.S.A. 128, 8, 17, 18; 152, 18.

Cells solitary; valves triangular with straight sides; surface punctate; in girdle view valves have long, capitate processes; girdle deep, punctate in rows parallel with the longitudinal axis. Diameter, 50μ.

DISTRIBUTION. Bottom sediment off Port Moresby.

49. **Triceratium constellatum** Tempère et Brun (Pl. 3, fig. 47).

Brün et Tempère 1889, 61, 6, 12.
A.S.A. 159, 10.

Valves triangular, margins slightly convex; surface irregularly punctate, puncta more numerous near margins; processes blunt, not extending beyond valve margin, with rows of fine puncta. Diameter, 80μ.

DISTRIBUTION. On reefs, Lord Howe Island; off Mackáy, Queensland.

50. **Triceratium picturatum** Greville (Pl. 3, fig. 48).

Greville, 1866, 9, 19.

Valves triangular, margins slightly convex, processes blunt, rounded, slightly capitate, hyaline; surface of valve punctate, puncta forming three small circles midway along sides and radiating more or less distinctly from these circles to margins and processes. Diameter, 60μ.

DISTRIBUTION. Dunedin, N.Z. (Rawson Coll. slide 52).

51. **Triceratium papillatum** Grove and Sturt (Pl. 3, fig. 49).

Grove and Sturt 1887, 76, 6, 14.
A.S.A. 128, 16.

Valves triangular with concave sides and rounded ends; with prominent nipple-shaped processes; centre raised wtih a few stout spines; valve surface with scattered puncta. Diameter, 40μ.

DISTRIBUTION. Timor Sea, sediments; Oamaru (Gr. and St.).

52. **Triceratium scitulum** Brightwell (Pl. 3, fig. 50).

Brightwell 1853, 246, 250, 4, 9.
A.S.A. 1886, 84, 5, 6.

Valves quadrate with concave sides; processes cylindrical, extending beyond ends of valve; valve surface convex, coarsely areolate, areolae larger in the centre. Diameter, 45μ.

DISTRIBUTION. Indonesian waters in shallows.

53. **Triceratium spinosum** Bailey (Pl. 3, fig. 51).

Bailey 1844, 46, 39.
A.S.A. 1886, 87, 2–5.
Biddulphia spinosum Boyer 1901, 703; 1927, 127.

Cell with girdle zone wider than valves, the latter domed, with digitate processes; in valve view triangular or quadrangular, with straight or slightly concave sides; surface reticulate; several spines occur near margin. Diameter, 85μ.

DISTRIBUTION. Indonesian waters.

Genus HEMIAULUS Ehr. 1844

54. **Hemiaulus polycistinorum** Ehr. (Pl. 5, fig. 6).

Ehrenberg 1854, 36.
A.S.A. 143, 23–29.
Boyer 1927, 142.

Valves lanceolate, concave with a narrow, longitudinal keel on surface, horns long, slightly sigmoid, with stout spines; surface coarsely reticulate, meshes prominent on the horns; chloroplasts 2. Length of valve 100μ. Boyer doubted whether this was an extant species; the presence of chloroplasts proves this

DISTRIBUTION. In plankton sample off Flores.

Family CHAETOCERACEAE

Genus CHAETOCEROS Ehr. 1844

55. **Chaetoceros dadayi** Pavillard (Pl. 5, fig. 7)

Pavillard 1913, 131, 2b.
Cupp 1943, 109, 64.

Cells usually in short chains; apertures small or absent; setae arising from valve corners, rudimentary on one side, on the other side one seta directed posteriorly, the other anteriorly, setae hirsute; chromatophores numerous, extending into setae. Diameter, 10μ.

DISTRIBUTION. Frequent but never abundant in Indonesian waters and the Arafura Sea.

56. **Chaetoceros seriacanthum** Gran (Pl. 5, fig. 8).

Gran 1897, 21, 3, 39–41.
Gran and Angst 1931, 478, 62.

Cells in straight chains, not touching at corners; apertures elliptical to rectangular; setae thin, issuing just inside slightly rounded corners, directed posteriorly; notch between valves and girdle; terminal setae diverging. Diameter, 25μ.

DISTRIBUTION. North-east Indian Ocean.

57. **Chaetoceros** sp. (Pl. 5, fig. 9).

Cells in short chains, cylindrical, with domed valves, slightly rostrate, connected by a central spine; setae arising within valve corners, then turning abruptly parallel to chain axis. Diameter, 20μ.

DISTRIBUTION. Off Onslow, W.A., in phytoplankton.

58. **Chaetoceros** sp. (Pl. 5, fig. 10).

Cells in chains attached by most of valve surface; apertures very reduced; setae fine, very short, emerging from rounded corners of valve; chromatophores numerous, plate-like: somewhat resembles *Ch. armatum* West but has not the fatty integument or the branched setae and the chains do not taper. Diameter, 40μ.

DISTRIBUTION. Indonesian waters.

59. **Chaetoceros tetrastichon** Cleve (Pl. 5, fig. 11).

Cleve 1897, 22, 1, 7.
Cupp 1943, 108, 63.

Cells in short chains; chains straight; valve surface flat, apertures almost absent, terminal valve domed; setae arising from valve margins at right angles to chain axis then turning parallel to this axis posteriorly, spined, not opposite; chromatophores numerous, extending into setae. Diameter, 20μ.

DISTRIBUTION. Indonesian waters; Arafura Sea.

Sub-Order SOLENIINEAE
Family BACTERIACEAE
Genus BACTERIASTRUM Shadbolt 1854

60. **Bacteriastrum elongatum** Cleve (Pl. 5, fig. 16).

Cleve 1897a, 19, 1, 19.
Hust. in A.S.A. 1920, 328, 10.

Cells cylindrical, in chains; valves circular in outline, hyaline; cells joined by about six setae, united at junction; setae straight, terminal setae curved posteriorly, spinulate. Diameter, 10μ.

DISTRIBUTION. Timor and Arafura Sea.

Family RHIZISOLENIACEAE
Genus RHIZOSOLENIA Ehr. (em. Brightw.) 1858

61. **Rhizosolenia arafurensis** sp. nov. (Pl. 5, fig. 12).

Cellae gracillimae; valvae conicae in processis cavis et obtusis extensis; vittis squamosis.

Cells slender, solitary; valves conical, slightly rounded at junction with girdle zone, tapering to hollow spines with rounded ends; intercalary bands scale-like. Length 150–220μ.

DISTRIBUTION. Arafura Sea, north of Darwin.

62. **Rhizosolenia curvatulus** sp. nov. (Pl. 5, fig. 13).

Cellae gracillimae et curvatae; valvae hemisphericae cum setis tenuis ad *R. cylindrus* similis; vittis squamosis.

A small, slender, curved species with rounded valves ending in a curved, thread-like spine resembling that of *R. cylindrus*; intercalary bands scale-like; cells often in pairs or threes; differs from *R. stolterforthii* in the shape of the valves and spines, and the slenderness of the cells. Length, 100μ.

DISTRIBUTION. Coral Sea; North-east Indian Ocean, Arafura Sea and Indonesian waters; not common.

63. **Rhizosolenia cochlea** Brun (Pl. 5, fig. 15).

Brun 1891, 43, 19, 9.
R. calcar avis v. *cochlea* Ostenfeld 1901, 228, 5.

Cells stout with rounded valves ending in a spur-like spine directed almost parallel to transverse axis of cell; connecting zone with numerous intercalary bands. Length, 100–200μ.

DISTRIBUTION. Indonesian waters.

64. **Rhizosolenia hyalina** Ostenfeld (Pl. 5, fig. 14).

Ostenfeld and Schmidt 1901 (Red Sea).

Cells solitary, broad, hyaline; valves tapering into a long, hollow spine, not rounded at junction with girdle; connecting zone hyaline, no intercalary banding observed. Length, 300μ.

DISTRIBUTION. Indonesian waters.

Genus GUINARDIA H. Peragallo 1892

65. **Guinardia blavyana** H. Peragallo (Pl. 5, fig. 17).

Peragallo 1892, 107, 13, 2.
Karsten 1906, 161, 29, 3, 3a.

Cells in chains, cylindrical; frustule more strongly silicified than that of *G. flaccida*; valves somewhat undulate, adjacent; intercalary bands overlapping, evident; chromatophores numerous. Length 50–70μ, diameter 20–40μ.

DISTRIBUTION. Indonesian waters; Arafura Sea.

66. **Guinardia victoriae** Karsten (Pl. 5, fig. 18).

Karsten 1906, 161, 29, 5.

Cells in chains, evenly bent on longitudinal axis, more markedly so than that depicted by Karsten, but variable; valves and intercalary bands as in *G. blavyana*. Diameter, 20–40μ.

DISTRIBUTION. Indonesian waters; Arafura Sea.

Sub-Order ARAPHIDINEAE
Family FRAGILARIACEAE
Genus DIATOMA De Candolle 1805

67. **Diatoma vulgare** Bory (Pl. 6, fig. 19).

Bory 1828, 20.
Boyer 1916, 10, 9, 10; 1927, 174.

Frustules quadrangular, sides straight or slightly constricted, valves lanceolate with rounded apices; costae unequal, transverse; pore present at one end of valve. Length 40μ.

DISTRIBUTION. Indonesian waters.

Genus CAMPYLOSIRA Grunow 1880-85

Cells in bands connected by delicate plates with numerous ribs; cells in girdle view curved, ventral valve being less convex than dorsal, or concave; no pseudoraphe or hyaline areas.

68. **Campylosira cymbelliformis** (A. Schmidt) Grunow (Pl. 6, fig. 20).

Cells in bands united by ribbed plates on valves, fusiform, with clavate ends, dorsal valve more convex than ventral; areolate in more or less longitudinal rows. Length, 40μ.

DISTRIBUTION. Off Darwin.

Genus THALASSIOTHRIX Cleve and Grunow 1880

69. **Thalassiothrix heteromorpha** Karsten (Pl. 6, fig. 21a, b).

Karsten 1906, 397, 12, 11.
T. delicatula Cupp 1943, 188, 137.

Cells solitary, very long and tenuous with tapering base and paddle-shaped apex in valve view; striae fine; base not swollen as in *T. mediterranea* and fan-shaped colonies not formed. Length 500–1,000μ. Cupp distinguished her species by greater twisting and length and fineness of striations, but such differences can be expected from Antarctic and tropical regions and there seems no reason to justify separation of the forms into separate species.

DISTRIBUTION. Indonesian waters and Arafura Sea.

70. **Thalassiothrix mediterranea** Pavillard (Pl. 6, fig. 22a-c).

Pavillard 1916, 39, 2, 3.

Cells slender, long, frequently united by their tapering basal portions into fan-shaped colonies; base tapered to a blunt point, slightly swollen above; apex rounded in valve, blunt in girdle view; surface faintly striate. Length, 500–1,000μ.

DISTRIBUTION. Indonesian waters.

Genus SYNEDRA Ehr. 1830

71. **Synedra tabulata** (Agardh) Kützing (Pl. 3, fig. 52).

Kützing 1844, 68, 15, X, 1-3.
Boyer 1927, 206.
S. affinis Kütz. 1844, 68, 15, 6, 9, 25 1-5.
Diatoma tabulata Agardh 1832, 40.

Valves fusiform-lanceolate with obtuse, rostrate to slightly capitate ends; striae marginal; pseudoraphe broadly lanceolate. Length 80–150μ.

DISTRIBUTION. Lord Howe Island. in shallows; northern Coral Sea: Indonesia; recorded as *S. affinis* from Kerguelen by Heiden and Kolbe, 1928.

72. **Synedra rostrata** (Hantzsch) A.S. (Pl. 3, fig. 53).

A.S.A. 1920, 305.
Toxarium rostratum Hantzsch in Rabenhorst 1863, 1, 19.
Valves elongate, tumid in the middle and at ends; puncta scattered or in arcuate rows; frustules arcuate. Length 500μ.

DISTRIBUTION. Planktonic, marine at Lord Howe Island.

Genus ENTOPYLA Ehr. 1848

73. **Entopyla ocellata** (Arnott) Grunow (Pl. 3, fig. 54).

E. ocellata v. *pulchella* has already been described in Part V.
The present typical form is more lanceolate and smaller than v. *pulchella.*

DISTRIBUTION. Port Hacking; sediments off Port Moresby and by Heiden and Kolbe 1928, from Kerguelen.

Genus PLAGIOGRAMMA Greville 1859

74. **Plagiogramma spinosum** Cleve (Pl. 3, fig. 55).

Cleve 1881, 4, 55.
Boyer 1927, 178.
Valves constricted in the middle and with rostrate, blunt ends; pseudoraphe scarcely evident; central space rounded as shown by Cleve (not oblong as in Boyer); terminal spaces elongate; valve surface punctate in transverse rows; marginal spines present. Length, 75μ.

DISTRIBUTION. Sediments 20 miles south of Port Moresby.

75. **Plagiogramma validum** Greville (Pl. 3, fig. 56).

Greville 1859, 7, 209.
Boyer 1927, 179.
Valves linear-lanceolate, slightly inflated in the middle; central space oblong, terminal spaces semicircular; pseudoraphe evident; valve surface with transverse rows of puncta. Length 80–90μ.

DISTRIBUTION. Sediments at 20m off Port Moresby.

Genus CYMATOSIRA Grunow 1862

76. **Cymatosira lorenziana** Grunow (Pl. 3, fig. 57).

Described with line drawing in Part IV. Plate illustration.

DISTRIBUTION. Timor Sea.

Genus PSEUDOEUNOTIA Grunow

Cells united into bands by valve surfaces, forming a semicircular band; valves linear with arcuate dorsal and straight or slightly curved ventral margins; pseudoraphe and nodules absent.

77. **Pseudoeunotia doliolus** (Wallich) Grunow (Pl. 3, fig. 58).

Grunow 1880-85 in van Heurck, 35, 22.
Cupp 1943, 190, 140.
Synedra doliolus Wallich 1860, 48, 2, 19.
Cells united into semicircular bands by valve surfaces; valves with arcuate dorsal and straight ventral margins and bluntly rounded ends; no nodules or pseudoraphe; surface with transverse striae separated by two rows of fine areolae. Length, 40–50μ.

DISTRIBUTION. Common in Indonesian waters, found in Coral Sea.

Genus CLIMACOSPHENIA Ehr. 1841

78. **Climacosphenia elongata** Bailey (Pl. 3, fig. 59).

Bailey 1853, 7, 8, 3, 10, 11.
A.S.A. 308, 5–10.

Frustules flabellate, on long branching stipes, narrowly cuneate; valves clavate, rounded at apex, slightly rounded at base; septa 2, with numerous oval foramina. Length 150–200μ.

DISTRIBUTION. Lord Howe Island; Madras by Subrahmanyan 1946.

Sub-Order MONORAPHIDINEAE
Family ACHNANTHACEAE
Genus CAMPYLONEIS Grunow 1862

79. **Campyloneis** sp. (Pl. 3, figs. 60a, b).

Cells elliptical in outline; upper valve with raphe and narrow axial area with transverse and longitudinal striae, the latter parallel to the margin, forming a square pattern, longitudinal striae absent towards inner part of valve forming an elliptic-lanceolate area; lower valve punctate, with depressed elliptic-lanceolate central portion and distinct, punctate margin; between valves a series of loculi with a·central rib. Length, 40–50μ.

DISTRIBUTION. Lord Howe Island (fresh water).

Genus COCCONEIS Ehr. 1838 em. Grun. 1868

80. **Cocconeis disculus** (Schum.) Cleve (Pl. 3, figs. 61a, b).

Cleve 1895, 172.
Hustedt 1933, 345, 799.
Navicula disculus Schumann 1864, 21, 2, 23.

Valves flat, elliptic lanceolate to elliptic; upper valve with evident pseudoraphe and coarse oblong striae, lower valve with straight raphe, narrow axial area, small central nodule and fine striae. Length 25–30μ.

DISTRIBUTION. Off Port Moresby on surface of sediments.

81. **Cocconeis nummularia** (Greville) Peragallo (Pl. 3, fig. 62).

Peragallo 1897, 3, 8, 9.
Hustedt 1933, 334, 548.
Navicula nummularia Greville 1859, 6, 249, 5, 6.

Valves flat, elliptical; upper valve with punctate radial striae and lanceolate pseudoraphe; lower valve with straight raphe narrow axial area; valve surface with transverse punctate striae interrupted by lyrate hyaline areas resembling those of *Navicula forcipata*. Length, 40μ.

DISTRIBUTION. Bottom sediments off Port Moresby.

82. **Cocconeis pseudomarginata** Gregory (Pl. 3, fig. 63).

Gregory 1857, 20, 1, 27.
Hustedt 1933, 359, 813.

Cells elliptical; valves, upper with radial transapical striae interrupted by several arcuate depressions on either side of lanceolate axial area; lower valve with straight raphe and radial lines of puncta terminating short of the margin in single larger puncta forming a sub-marginal ring. Length 35–50μ.

DISTRIBUTION. Port Hacking; recorded by Bunbury 1902 from Tasmania, Petit 1877 from Lyall Bay, Grove and Sturt 1887 from Oamaru (fossil) and Heiden and Kolbe 1928 from St. Paul.

Sub-Order BIRAPHIDINEAE
Family NAVICULACEAE
Genus NAVICULA Bory 1794

83. **Navicula acus** Cleve (Pl. 3, fig. 64).

Cleve 1894, 106, 3, 29, 30.

Cells in girdle view with rounded valves, in valve view naviculate with acute ends; raphe straight, striae transverse, faint; cell rectilinearly cuspidate. Length, 150–200μ.

DISTRIBUTION. Common in phytoplankton in Coral Sea, Arafura Sea and Indonesian waters.

84. **Navicula humerosa** Breb. v. **arabica** (Grunow) Peragallo (Pl. 3, fig. 65).

Peragallo 1897, 146, 27, 23.
N. arabica Grunow in A.S.A. 1875, 6, 14.

Form as in type but puncta more distant especially towards centre of valve, and resembling in their distribution those of *N. granulata*. This was referred by Cleve 1895, 49, to *N. brasiliensis* v. *bicuneata*.

DISTRIBUTION. Timor Sea.

85. **Navicula cancellata** Donkin (Pl. 3, fig. 66).

Donkin 1871, 55.
Boyer 1927, 398.

Valves linear-lanceolate, ends subacute, rounded; axial area indistinct, assymmetrical; central area circular; striae coarse, transverse.

v. **retusa** (Brebisson) Cleve.

Cleve 1894, 30.
Navicula retusa Brebisson 1867, 116, 6.

Valves linear, ends rounded. Length, 100μ.

DISTRIBUTION. Indonesian waters.

86. **Navicula clavata** Gregory (Pl. 3, fig. 67).

Gregory 1856, 46, 5, 17.
A.S.A. 1886, 70, 50.
Boyer 1927, 415.

Valves elliptic, ends rostrate; raphe straight, curved at ends; axial areas narrow, dilated at centre to form a very broadly lyrate hyaline area reaching the margin on each side of the axial area but separated from it by transverse punctata striae; marginal striae transverse to radial, punctate. Length, 75–90μ.

DISTRIBUTION. Sediments in Port Moresby region.

87. **Navicula cronullensis** sp. nov. (Pl. 3, fig. 68).

Navicula sp. n. A.S.A. 1875, 6, 35.

Cellae solitariae; valvae ovatae, terminibus obtusis, cum striis punctatis tenuis, punctis proximis distantioribus; vide Schmidt, 6, 35.

Cells solitary; valves elliptical with slightly acute but rounded ends; raphe straight; axial area narrow; central area small, circular; surface finely striate, punctate, striae marked near valve margin but puncta more distant nearer axial area. This species is depicted by Schmidt and is united with other forms which he suggested are a new species but did not name. Two of the illustrations are later referred to *N. glacialis* Grunow, but no name appears to have been given to A.S.A. 6, 35. The species could be a variety of the highly variable *N. granulata*. As Schmidt did not give a locality for his specimens the name *Cronullensis* refers to the locality of my specimens.

DISTRIBUTION. Port Hacking.

88. **Navicula directa** (W. Smith) Ralfs (Pl. 6, fig. 23).

Ralfs 1861, 906.
Karsten 1905, 18, 1.
A.S.A. 1875, 47, 1–5.
Boyer 1927, 395.
Pinnularia directa W. Smith 1853, 56, 18, 172.

Valves naviculate, ends acute; axial area indistinct; raphe straight; central area small; striae transverse, fine; chromatophores H-shaped. Length, 70–100μ.

DISTRIBUTION. Indonesian and Arafura Sea waters.

Genus MASTOGLOIA Thwaites 1856

89. **Mastogloia delicatula** Cleve (Pl. 3, fig. 69).

Cleve 1894, 16, 1, 20.
Hustedt 1933, 483, 904.

Valves elliptic-lanceolate with rostrate ends; raphe bent; axial and central areas narrow; valves slightly depressed each side of raphe to about half way to margin; surface punctate, puncta arranged in three intersecting systems; loculi of even size, numerous, reaching apices. Length, 35–45μ.

DISTRIBUTION. Lord Howe Island (common); off Port Moresby, in sediments.

90. **Mastogloia elegans** Lewis (Pl. 3, fig. 70).

Lewis 1865, 19, 1, 9.
Hustedt 1933, 498, 924.

Valves semielliptic with rostrate ends; loculi small, numerous, rectangular with widest sides parallel to margin; raphe sinuate; valve surface striate parallel to transverse axis with wavy longitudinal ribs. Length, 70μ.

DISTRIBUTION. Great Barrier Reef, near Mackay.

91. **Mastogloia jelineckii** (Grunow) Grunow (Pl. 3, fig. 71).

Grunow 1867, 99, 1, 11.
Hustedt 1937, 544, 977.
Navicula jelineckii Grunow 1863, 151, 5, 12.

Valves elliptic-lanceolate to rhombic-lanceolate with more or less rostrate ends; raphe straight or slightly curved; axial area narrow; loculi narrow, numerous, even; inner portion of valve surface raised above marginal portion, which is continuous with a narrow linear area adjacent to axial area; striae transverse, outer part crossed by longitudinal striae of two orders at about 60°. Length, 80–100μ.

DISTRIBUTION. Sediments off Port Moresby.

92. **Mastogloia ovulum** Hustedt 1933 (Pl. 6, fig. 24).

Hustedt 1933, 474, 648.

Valves elliptic or elongate-elliptic; raphe straight or slightly undulating; axial and central areas narrow; valves areolate-punctate in transapical rows and straight but irregular longitudinal rows; loculi narrow, ovate, few, reaching apex, varying in number and spacing. Length, 20–30μ.

DISTRIBUTION. Lord Howe Island (common); Borneo (Hustedt).

Genus DIPLONEIS Ehr. 1840

93. **Diploneis adonis** (Brun) Cleve (Pl. 3, fig. 72).

Cleve 1894, 85.
Hustedt 1937, 613, 1027.
Navicula adonis Brun 1889, 41, 5, 3.

Valves linear-elliptic more or less constricted in the middle, ends rounded; central nodule moderate, quadrate; horns diverging from the middle, converging towards ends; transapical ribs strong, radial, not reaching margin. Length 100–135μ.

DISTRIBUTION. Sediments off Port Moresby.

94. **Diploneis bombus** Ehr. (Pl. 3, fig. 73).

Ehr. 1844, 19, 31.

A description was given in Part IV, but only v. *bombiformis* recorded.

DISTRIBUTION. Sediments off Port Moresby.

95. **Diploneis gemmata** (Greville) Cleve (Pl. 3, fig. 74).

Cleve 1894, 98.

This species was described in Part IV, but only v. *pristiophora* recorded and figured. Length, 120μ.

DISTRIBUTION. Sediments at 20m off Port Moresby.

96. **Diploneis mediterranea** (Grunow) Cleve (Pl. 3, fig. 75).

Cleve 1894, 82.
Hustedt 1937, 596, 1014.
Navicula gemmata v. *mediterranea* Grunow in A.S.A. 1875, 8, 42.

Valves elliptic to linear-elliptic with convex or parallel sides; central nodule small, quadrate; horns parallel or slightly diverging from base; chambers not divided. Length, 60μ.

DISTRIBUTION. Sediments south of Port Moresby.

97. **Diploneis pseudobombiformis** Hustedt (Pl. 3, fig. 76).

Hustedt 1937, 708, 1087.

Resembles *D. bombus* in shape but is nearer *D. adonis*; longitudinal ribs are absent; inner openings to loculi present and a band crossing the transapical ribs is marked. Length, 80μ.

DISTRIBUTION. Sediments off Port Moresby.

Genus PINNULARIA Ehr. 1843

98. **Pinnularia stauroptera** v. **interrupta** Cleve (Pl. 4, fig. 77).

Cleve 1895, 83.
Boyer 1916, 30, 11.

Valve shape as for type (Pt. II), but central area much larger; stauros much wider and striae much shorter, particularly in the central region.

DISTRIBUTION. Botany swamps near Sydney, fresh water.

Genus TRACHYNEIS Cleve 1894

99. **Trachyneis antillarum** Cleve (Pl. 4, fig. 78).

Cleve 1878, 5, 8, 2, 11.
Boyer 1927, 429.

Valves lanceolate, ends obtuse, rounded; raphe curved; axial area unilaterally broad and lanceolate, on opposite side narrow, dilated into rounded central area; alveoli in transverse to radial rows; surface of valve rounded. Length, 130–200μ.

DISTRIBUTION. In sediments off Port Moresby.

Genus PLEUROSIGMA W. Smith 1853

100. **Pleurosigma acuminatum** (Kützing) Grunow (Pl. 6, fig. 25).

Grunow 1860, 561, 4, 6.
Frustulia acuminata Kützing 1833, 14, 39.
Navicula acuminata Kützing 1844, 102, 4, 26, 30, 15.

Valves sigmoid, sides parallel in the middle, then sharply bent, acute; ends acute or rounded; raphe central, sigmoid; striae transverse and longitudinal. Length, 120μ.

DISTRIBUTION. Shallow waters in Indonesian region.

101. **Pleurosigma arcticum** Cleve (Pl. 6, fig. 26).

Cleve 1894, 4, 119.

Both margins of valve continuously sigmoid, raphe evenly sigmoid, close to outer margin near apices. Length 50–70μ.

DISTRIBUTION. Planktonic off Solomon Islands.

102. **Pleurosigma distortum** W. Smith (Pl. 6, fig. 27).

Valves lanceolate with abruptly bent, subrostrate ends, sides evenly rounded; raphe central, sigmoid; striae longitudinal and transverse. Length, 60–100μ.

DISTRIBUTION. Indonesian waters and Arafura Sea in plankton.

103. **Pleurosigma elongatum** W. Smith (Pl. 6, fig. 28).

Valves lanceolate, rather slender, sigmoid, ends acute, tapering; raphe central sigmoid; striae oblique. Length, 150–200μ.

DISTRIBUTION. Indonesian waters; Arafura Sea.

104. **Pleurosigma galapagense** Cleve (Pl. 6, fig. 29).

Cleve 1894, 36, 4, 16.
Boyer 1927, 469.

Valves linear-lanceolate, slightly sigmoid at ends; raphe central, slightly bent at ends; striae oblique. Length 140–180μ.

DISTRIBUTION. Indonesian waters; Arafura Sea; northern Coral Sea and Torres Strait.

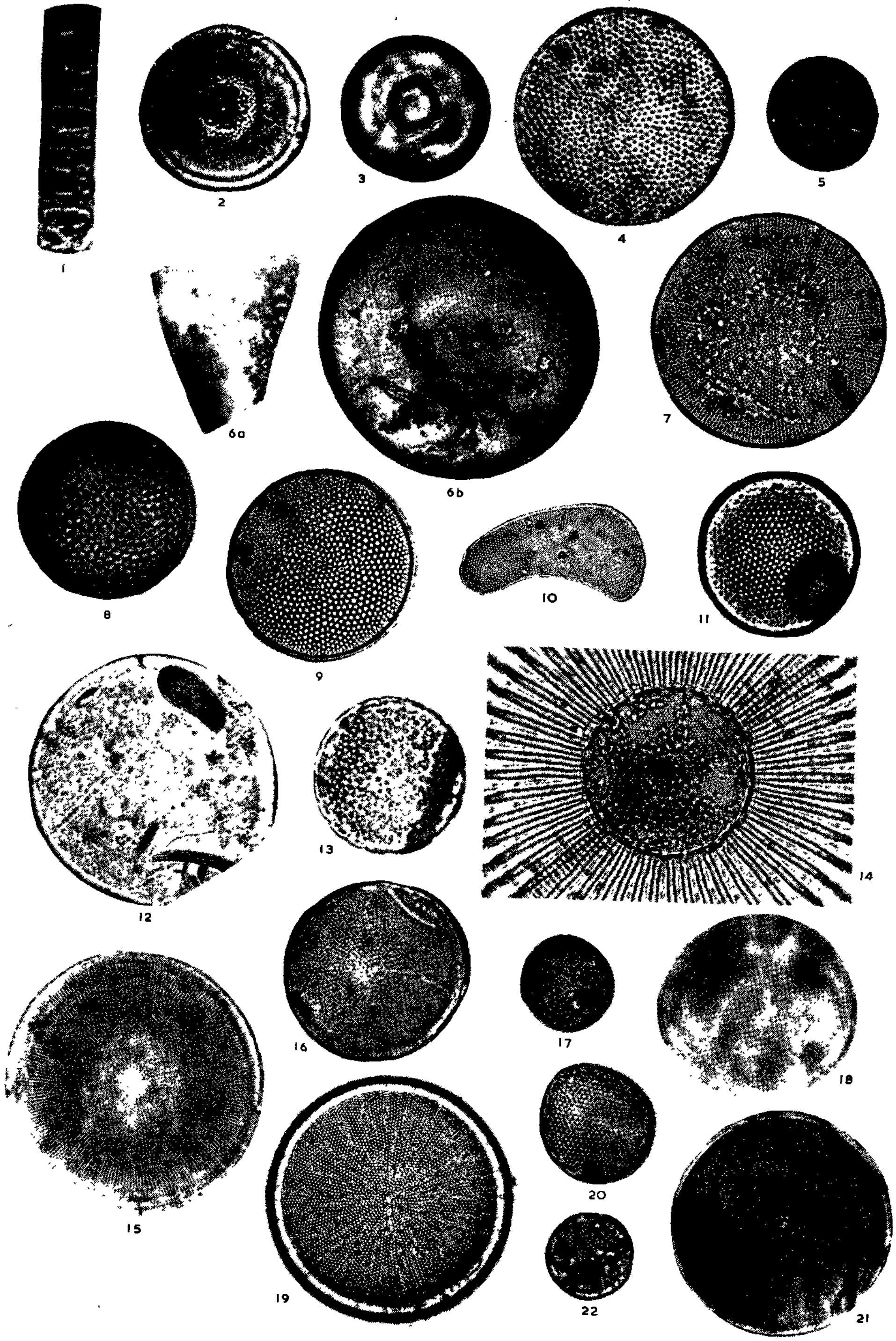

FIG. 1.—*Coscinosira oestrupii*. FIG. 2.—*Hyalodiscus* sp. 1. FIG. 3.—*Hyalodiscus* sp. 2. FIG. 4.—*Coscinodiscus africanus*. FIG. 5.—*C. apiculatus*. FIG. 6a, b.—*C. gazellae*. FIG. 7.—*C. increscens*. FIG. 8.—*C. nodulifer*. FIG. 9.—*C. obscurus*. FIG. 10.—*C. reniformis*. FIG. 11.—*C. senarius*. FIG. 12.—*C. subtilissimus*. FIG. 13.—*Coscinodiscus* sp. FIG. 14.—*Planktoniella formosa*. FIG. 15.—*Actinocyclus alienus*. FIG. 16.—*A. complanatus*. FIG. 17.—*A. disseminatus*. FIG. 18.—*A. dubiosus*. FIG. 19.—*A. mirabilis*. FIG. 20.—*A. ovatus*. FIG. 21.—*A. pyrotechnicus*. FIG. 22.—*A. subocellatus*.

PLATE II

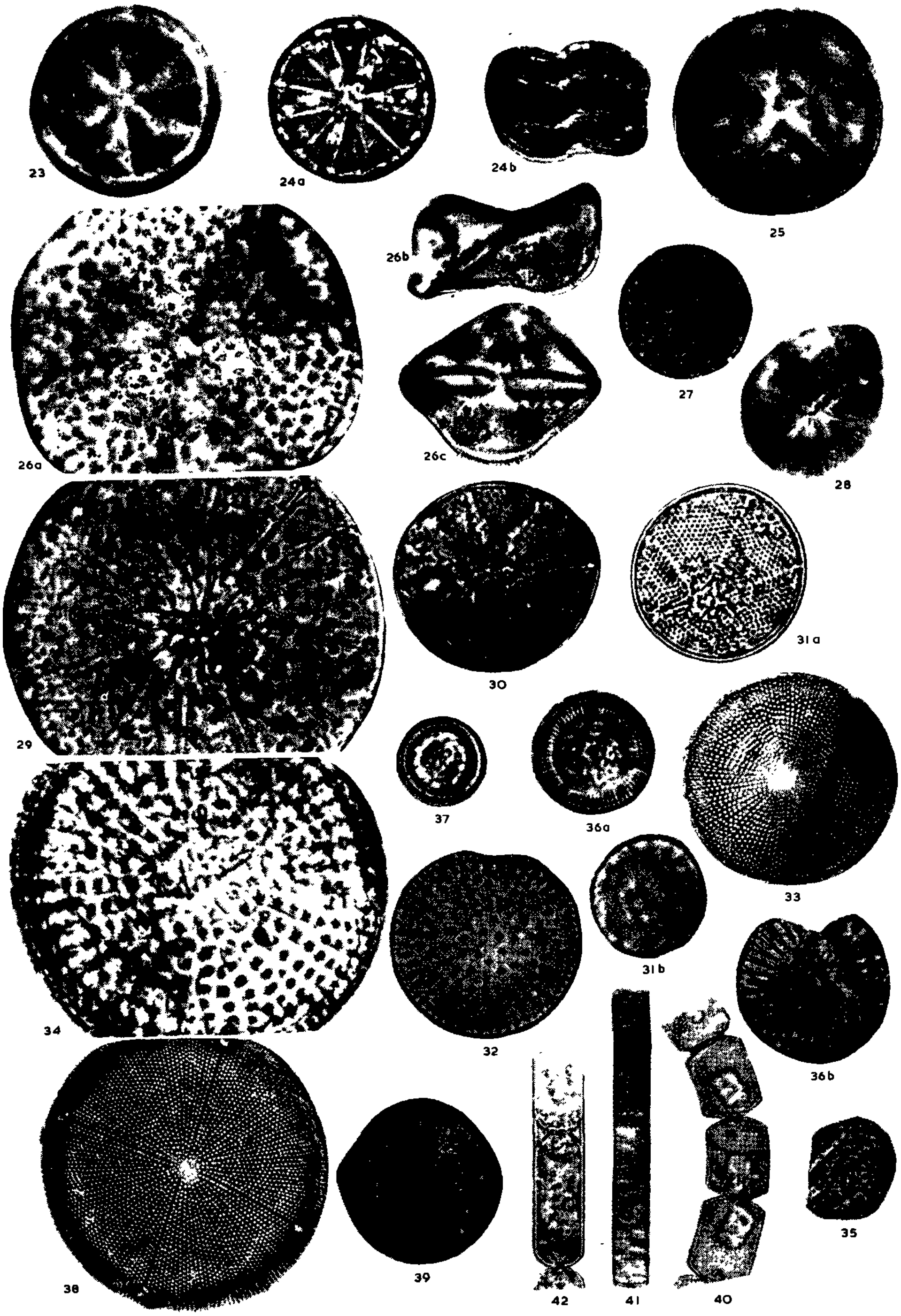

FIG. 23.—*Actinoptychus cathedralis.* FIG. 24.—*A. maculatus.* FIG. 25.—*A. trilingulatus.* FIG. 26a-c.—*A. trifolium.* FIG. 27.—*Asterolampra dallasiana.* FIG. 28.—*Asteromphalus cleveanus.* FIG. 29.—*A. brookei.* FIG. 30.—*A. heptactis.* FIG. 31.—*Asteromphalus-Coscinodiscus.* FIG. 32.—*Stictodiscus californicus.* FIG. 33.—*S. hardmanianus.* FIG. 34.—*S. harrisonianus.* FIG. 35.—*S. simplex.* FIG. 36a.—*Cyclotella comta,* b., var. *punctata.* FIG. 37.—*C. kuetzingiana.* FIG. 38.—*Aulacodiscus formosus.* FIG. 39.—*Auliscus compositus.* FIG. 40.—*Cerataulina curvata.* FIG. 41.—*C.* sp. FIG. 42.—*C. compacta.*

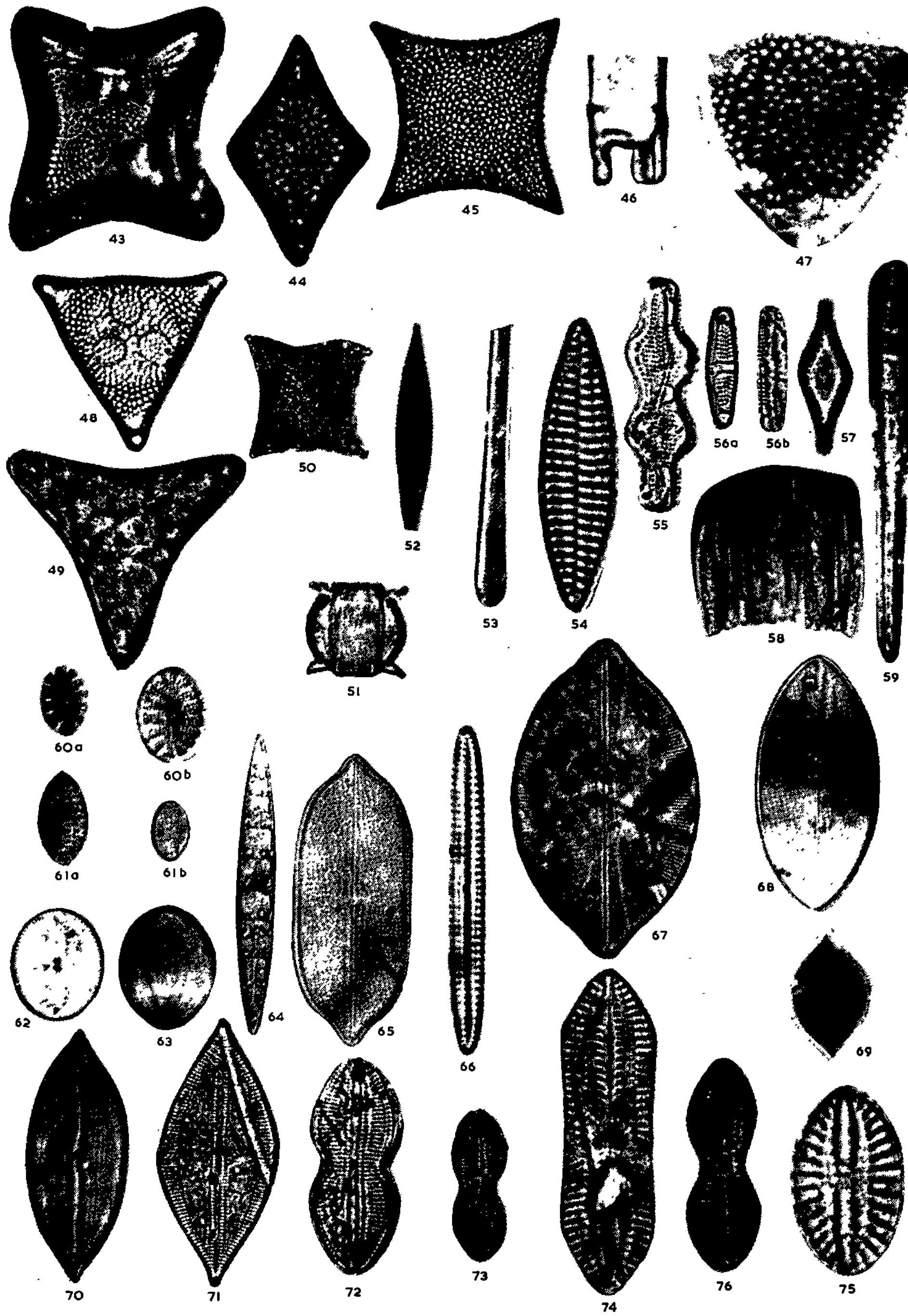

FIG. 43.—*Triceratium antedeluvianum.* FIG. 44.—*T. bicorne.* FIG. 45.—*T. biquadratum.* FIG. 46.—*T. castelliferum.* FIG. 47.—*T. constellatum.* FIG. 48.—*T. picturatum.* FIG. 49.—*T. papillatum.* FIG. 50.—*T. scitulum.* FIG. 51.—*T. spinosum.* FIG. 52.—*Synedra tabulata.* FIG. 53.—*S. rostrata.* FIG. 54.—*Entopyla ocellata.* FIG. 55.—*Plagiogramma spinosum.* FIG. 56.—*P. validum.* FIG. 57.—*Cymatosira lorenziana.* FIG. 58.—*Pseudoeunotia doliolus.* FIG. 59.—*Climacosphenia elongata.* FIG. 60a-b.—*Campyloneis* sp. FIG. 61a-b.—*Cocconeis disculus.* FIG. 62.—*C. nummularia.* FIG. 63.—*C. pseudomarginata.* FIG. 64.—*Navicula acus.* FIG. 65.—*N. humerosa* var. *arabica.* FIG. 66.—*N. cancellata.* FIG. 67.—*N. clavata.* FIG. 68.—*N. cronullensis.* FIG. 69.—*Mastogloia delicatula.* FIG. 70.—*M. elegans.* FIG. 71.—*M. jelineckii.* FIG. 72.—*Diploneis adonis.* FIG. 73.—*D. bombus.* FIG. 74.—*D. gemmata.* FIG. 75.—*D. mediterranea.* FIG. 76.—*D. pseudobombiformis.*

PLATE IV

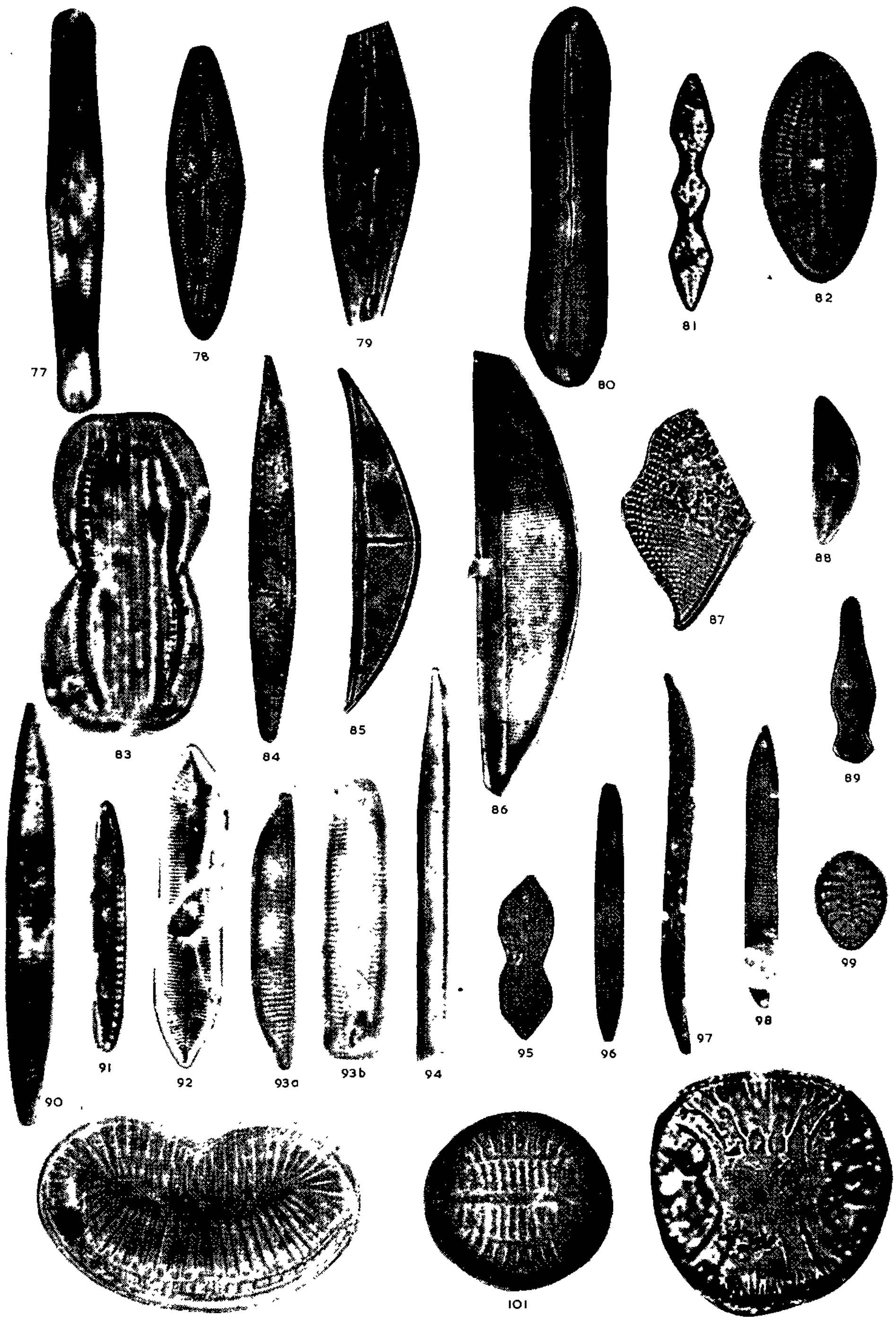

FIG. 77.—*Pinnularia stauroptera* var. *interrupta*. FIG. 78.—*Trachyneis antillarum*. FIG. 79.—*Pleurosigma heros*. FIG. 80.—*Caloneis bicuneata*. FIG. 81.—*C. ophiocephala*. FIG. 82.—*C. permagna*. FIG. 83.—*Amphiprora gigantea*. FIG. 84.—*Tropidoneis approximata*. FIG. 85.—*Amphora acuta* var. *labyrinthula*. FIG. 86.—*A. groenlandica*. FIG. 87.—*A. corpulenta*. FIG. 88.—*Gomphocymbella brunii*. FIG. 89.—*Gomphonema constrictum*. FIG. 90.—*Nitzschia distans*. FIG. 91.—*N. gruendleri*. FIG. 92.—*N. hungarica*. FIG. 93.—*N. kittlii*. FIG. 94.—*N. linearis*. FIG. 95.—*N. mediterranea*. FIG. 96.—*N. recta*. FIG. 97.—*N. vermicularis*. FIG. 98.—*Hantzschia marina*. FIG. 99.—*Surirella arachnoidea*. FIG. 100.—*S. neumeyeri*. FIG. 101.—*Campylodiscus brightwellii*. FIG. 102.—*C. pacificus*.

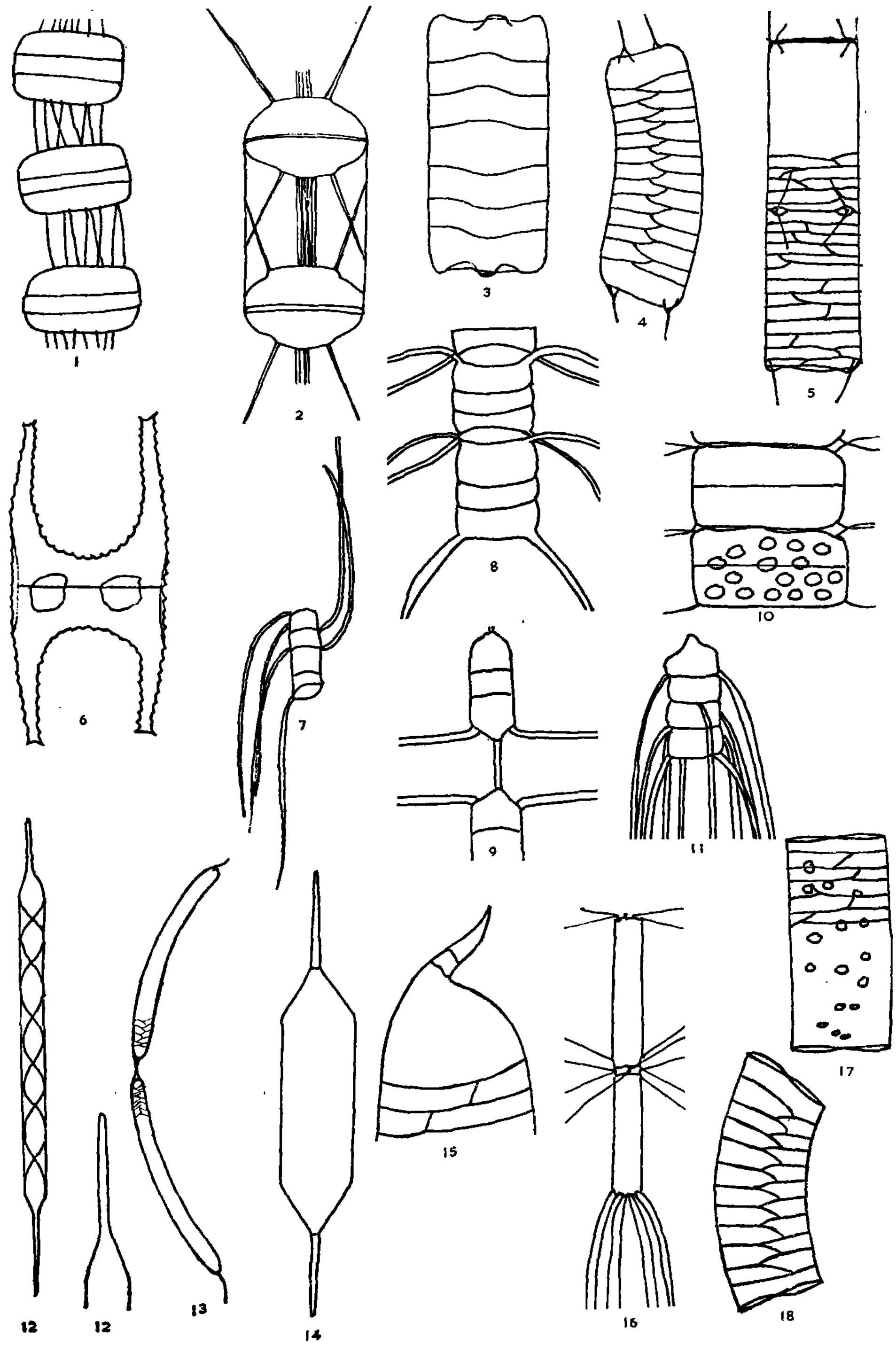

FIG. 1.—*Coscinosira oestrupii*. FIG. 2.—*Biddulphia connecta*. FIG. 3.—*Biddulphia* sp. FIG. 4.—*Cerataulina curvata*. FIG. 5.—*Cerataulina* sp. FIG. 6.—*Hemiaulus polycistinorum*. FIG. 7.—*Chaetoceros dadayi*. FIG. 8.—*C. seriacanthum*. FIG. 9.—*C.* sp. FIG. 10.—*C.* sp. FIG. 11.—*C. tetrastichon*. FIG. 12.—*Rhizosolenia arafurensis*. FIG. 13.—*R. curvatulus*. FIG. 14.—*R. hyalina*. FIG. 15.—*R. cochlea*. FIG. 16.—*Bacteriastrum elongatum*. FIG. 17.—*Guinardia blavyana*. FIG. 18.—*G. victoriae*.

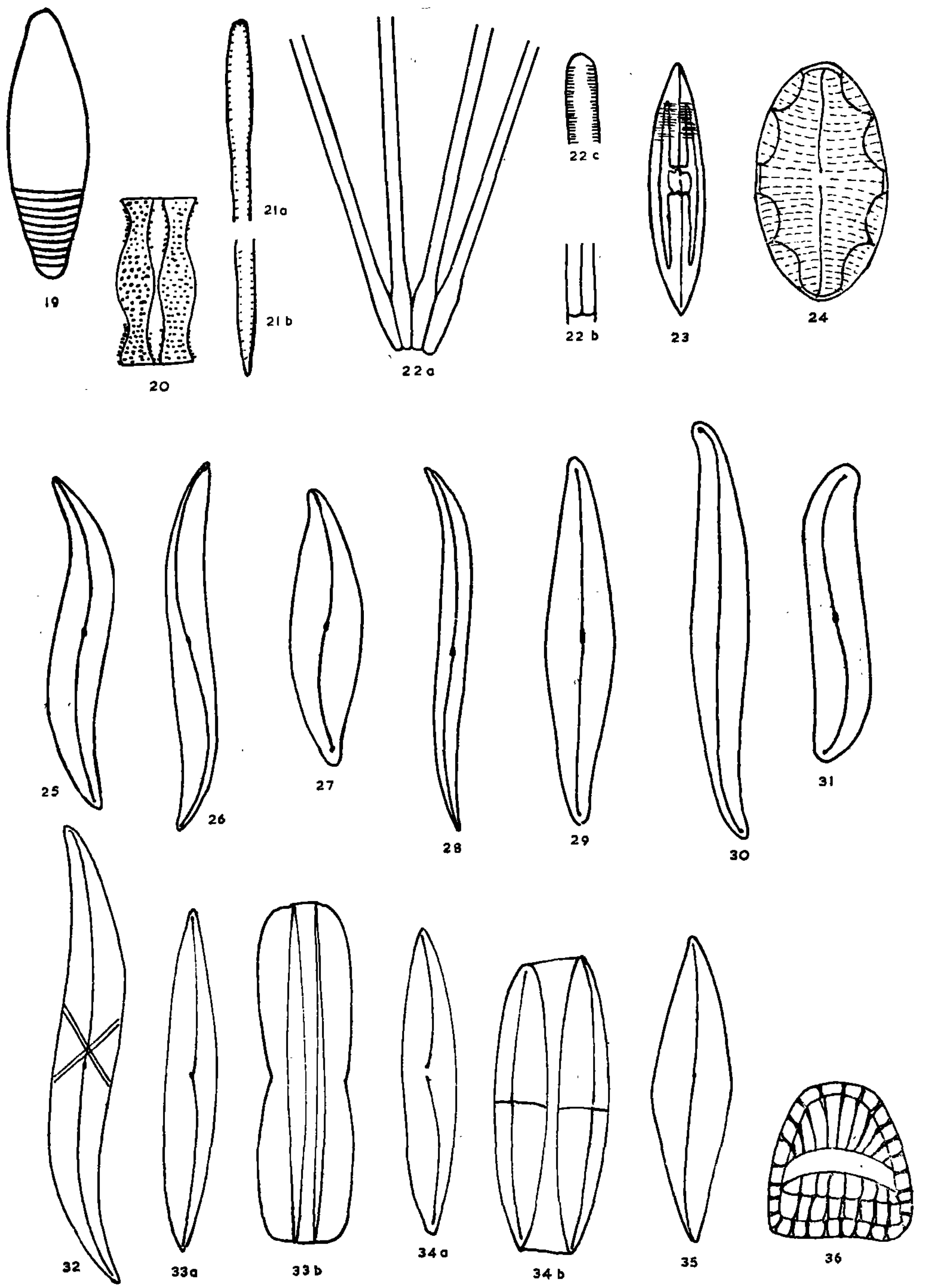

FIG. 19.—*Diatoma vulgare*. FIG. 20.—*Campylosira cymbelliformis*. FIG. 21a-b.—*Thalassiothrix heteromorpha*. FIG. 22a-c.—*T. mediterranea*. FIG. 23.—*Navicula directa*. FIG. 24.—*Mastogloia ovulum*. FIG. 25.—*Pleurosigma acuminatum*. FIG. 26.—*P. arcticum*. FIG. 27.—*P. distortum*. FIG. 28.—*P. elongatum*. FIG. 29.—*P. galapagense*. FIG. 30.—*P. majus*. FIG. 31.—*P. simile*. FIG. 32.—*P. strigosum*. FIG. 33a-b.—*Tropidoneis approximata*. FIG. 34a-b.—*T. maxima*. FIG. 35.—*Pleurosigma heros*. FIG. 36.—*Campylodiscus thuretii*.

105. **Pleurosigma heros** Cleve (Pl. 4, fig. 79; Pl. 6, fig. 35).

Cleve 1894, 44, 4, 20.

Valves lanceolate, somewhat angular in the middle, resembling *P. angulatum*; ends, however, are only slightly bent and acute; raphe sigmoid, central; valve surface with oblique striae. Length, 150μ.

DISTRIBUTION. North of Kangaroo Island, South Australia, in plankton. Type locality, Macassar Strait.

106. **Pleurosigma majus** (Grunow) Cleve (Pl. 6, fig. 30).

Cleve 1894, 44, 4, 15.

P. speciosum v. *major* Grunow in Cleve and Grun. 1880.

Valves lanceolate, slightly sigmoid, slightly wider at the middle, ends subacute, rounded; raphe central, displaced near ends; striae oblique. Length, 130μ.

DISTRIBUTION. Indonesian waters.

107. **Pleurosigma simile** Grunow (Pl. 6, fig. 31).

Grunow in Cleve and Grunow 1880, 56.

Gyrosigma simile Boyer 1916, 76, 23, 4; 1927.

Valves very slightly sigmoid, sides parallel, ends rounded, obtuse; raphe more sigmoid than valve margins, nearly central; striae transverse and longitudinal. Length, 120μ.

DISTRIBUTION. Indonesian waters.

108. **Pleurosigma strigosum** W. Smith (Pl. 6, fig. 32).

W. Smith 1853, 64, 21, 203.

Valves lanceolate, sigmoid; sides evenly rounded, ends subacute; raphe strongly sigmoid, excentric at ends; striae oblique. Length, 150–200μ.

DISTRIBUTION. Indonesian waters; Arafura Sea.

Genus CALONEIS Cleve 1894

109. **Caloneis bicuneata** (Grunow) Boyer (Pl. 4, fig. 80).

Boyer 1927, 311.

Navicula bicuneata Grunow 1860, 10, 546.

A.S.A. 1875, 50, 37.

Valves lanceolate, sigmoid; sides evenly rounded, ends subacute; raphe strongly sigmoid, raphe curved; central area small, circular; longitudinal lines irregular; surface striate, punctate. Length, 100–200μ.

DISTRIBUTION. Lake Macquarie; sediments south of Port Moresby.

110. **Caloneis ophiocephala** (Cleve and Grove) Cleve (Pl. 4, fig. 81).

Cleve 1894, 66.

Navicula ophiocephala Cleve and Grove 1887, 57, 9, 13.

Valves with lanceolate ends, round middle part and constricted between; raphe straight; axial area swollen in the middle and in each lobe; striae transverse, interrupted. Length, 75μ.

DISTRIBUTION. Sediments off Port Moresby.

111. **Caloneis permagna** (Bailey) Cleve (Pl. 4, fig. 82).

Cleve 1894, 59.

Navicula permagna Bailey 1850, 2, 40.

Valves ovate-lanceolate with ends more or less produced; raphe nearly straight; axial area narrow, linear, striae radiate, indistinctly punctate; longitudinal lines double. Length, 150μ.

DISTRIBUTION. Sediments 20 miles south of Port Moresby.

Genus AMPHIPRORA Ehr. 1843

112. **Amphiprora gigantea** Grunow (Pl. 4, fig. 83).

Grunow 1860, 568, 4, 12.

Cleve 1894, 1, 6.

Frustules sharply constricted; raphe sigmoid, junction line arcuate; striae curved, punctate; dorsal puncta appear in rows in three directions; more ventral puncta in transverse curved striae. Length, 150μ.

DISTRIBUTION. Indonesian waters.

Genus TROPIDONEIS Cleve 1891

113. **Tropidoneis approximata** Cleve (Pl. 4, fig. 84; Pl. 6, fig. 33a, b).

Cleve 1894, 26, 3, 20.
Boyer 1927, 480.

Valves narrow, lanceolate, ends acute, valve very convex; central area indistinct; wing unilateral, close to raphe. Length, 200–300μ.

DISTRIBUTION. Coral Sea; Indonesian waters; Arafura Sea. Type locality Java.

114. **Tropidoneis maxima** (Gregory) Cleve (Pl. 6, fig. 34a, b).

Cleve 1894, 26, 3, 24, 25.
Boyer 1927, 480.
Amphiprora maxima Gregory 1957, 507.

Frustules constricted; wing elevated above central nodule; valves lanceolate; wing unilateral; striae fine. Length, 150μ.

DISTRIBUTION. Indonesian waters.

Family CYMBELLACEAE
Genus AMPHORA Ehr. 1840

115. **Amphora acuta** v. **labyrinthula** (Grunow) Cleve (Pl. 4, fig. 85).

Cleve 1895, 4, 23.

As for type (Part IV) but surface with irregular rows of puncta.

DISTRIBUTION. Indonesian waters.

116. **Amphora groenlandica** Cleve (Pl. 4, fig. 86).

Cleve 1895, 128, 4, 1.

Valves with arcuate dorsal, straight ventral margins; raphe straight or slightly biarcuate, close to ventral margin; axial area linear; transverse rows of puncta on dorsal and ventral sides of raphe. Length 70–100μ.

DISTRIBUTION. Off Mackay, Queensland.

117. **Amphora corpulenta** Cleve and Grove (Pl. 4, fig. 87).

Cleve and Grove 1891, 68, 10, 14.

Valves papillionate; ventral margin slightly convex; raphe ventral, almost parallel to margin; dorsal margin almost semicircular but with central indentation; striae transverse, punctate, puncta more numerous towards dorsal margin. Length, 150μ.

DISTRIBUTION. Sediments off Port Moresby.

Genus GOMPHOCYMBELLA O. Müller 1905

118. **Gomphocymbella brunii** (Fricke) O. Müller (Pl. 4, fig. 88).

O. Müller 1905, 150, 1, 2–3.
Gomphonema brunii Fricke in A.S.A. 238, 4–6.

Valves asymmetric with respect to longitudinal and transverse axes, one side strongly convex, the other almost straight, ends slightly rostrate; raphe curved, axial area narrow, linear; striae coarse, transverse. Length, 40μ.

DISTRIBUTION. Sydney water supply.

Genus GOMPHONEMA Agardh 1824

119. **Gomphonema constrictum** Ehr. (Pl. 4, fig. 89).

Described in Part IV, but not illustrated.

DISTRIBUTION. Sydney and Wellington water supplies.

Family BACILLARIACEAE

Genus Nitzschia Hass. em. Grunow 1880

120. **Nitzschia distans** Gregory (Pl. 4, fig. 90).

Gregory 1857, 530, 14, 103, 103b.
Boyer 1927, 512.
Described in Part IV but not figured.

Distribution. In plankton off Mackay, Queensland.

121. **Nitzschia gruendleri** Grunow (Pl. 4, fig. 91).

Grunow 1878, 14, 4, 24.
Valves linear with subconical subacuate ends; keel excentric; keel costae wide, uneven. Length, 180μ.

Distribution. Lord Howe Island.

122. **Nitzschia hungarica** Grunow (Pl. 4, fig. 92).

Grunow 1862, 568.
Described in Part II. Present figure is much clearer.

Distribution. Lord Howe Island; present along east Australian coast.

123. **Nitzschia kittlii** Grunow (Pl. 4, fig. 93).

Grunow 1882, 155, 29, 24, 25.
A.S.A. 347, 15, 16.
Valves bean-shaped, coarsely striate, ends rostrate; no longitudinal fold; keel puncta even.

Distribution. Sahul Bank.

124. **Nitzschia linearis** (Agardh) W. Smith (Pl. 4, fig. 94).

W. Smith 1853, 39, 13, 110.
Boyer 1927, 518.
Frustulia linearis Agardh fide W. Smith..
Frustule linear, narrow, attenuate towards truncate ends; valves linear, attenuate, slightly curved but not sigmoid, ends truncate; keel puncta even but two median distant; striae transverse. Length, 150μ.

Distribution. Lord Howe Island, fresh water.

125. **Nitzschia mediterranea** Hustedt (Pl. 4, fig. 95).

Hustedt in A.S.A. 1912, 331, 22.
Valves deeply constricted in the middle into two sub-circular parts with rostrate ends; fold evident; keel puncta even; valve surface with large hexagonal areolae. Length, 70μ.

Distribution. Sediments off Port Moresby.

126. **Nitzschia recta** Hantzsch (Pl. 4, fig. 96).

Hantzsch in Rabenhorst 1864, 1283.
A.S.A. 334, 19–21.
Frustule linear, ends truncate; valves linear with attenuate ends; keel puncta distinct, more distant near centre of valve. Length, 120μ.

Distribution. Sydney water supply.

127. **Nitzschia vermicularis** (Kützing) Hantzsch (Pl. 4, fig. 97).

Hantzsch in Rabenhorst 1864, 1, 155.
Synedra vermicularis Kützing 1844, 67.
Valves linear, sigmoid, attenuated towards the obtusely rounded ends, almost rostrate. Length, 160μ.

Distribution. Off Mackay, Queensland; Lord Howe Island (fresh water).

Genus Hantzschia Grunow 1880

128. **Hantzschia marina** (Donkin) Grunow (Pl. 4, fig. 98).

Grunow in Cleve and Grunow 1880, 105.

Boyer 1916, 32, 22; 1927, 527.
Epithemia marina Donkin 1858, 29, 3, 14.
Valves with dorsal margin slightly concave, ventral almost straight, ends rostrate, curved; keel puncta prolonged into costae extending across valve, with striae formed by a double row of puncta between costae. Length 100μ.

DISTRIBUTION. Lord Howe Island.

Sub-Order SURIRELLINEAE
Family SURIRELLACEAE
Genus SURIRELLA Turpin 1828

129. **Surirella arachnoidea** sp. nov. (Pl. 4, fig. 99).

Valve ovate, cum area depressa et margine levata; costis 8–9, elevatis ad marginem areae, tum depressis.
Valves elliptic-ovate; central area depressed, with raised margin giving an arachnoid appearance to the valve; costae 8–9, coarse, abruptly raised at margin of central area, then abruptly depressed, meeting at central ridge. Length 40–50μ. Somewhat like *S. fluminensis* Grunow, differing in shape of valve surface.

DISTRIBUTION. Indonesian waters.

130. **Surirella neumeyeri** Janisch (Pl. 4, fig. 100).

Jan. Gaz. 31, 33.
A.S.A. 1886, 56, 1.
Valves reniform, with radiating septa and narrowly reniform axial area. Length, 120μ.

DISTRIBUTION. Cook Strait.

Genus CAMPYLODISCUS Ehr. 1841

131. **Campylodiscus brightwellii** Grunow (Pl. 4, fig. 101).

Grunow 1862, 445, 9, 5; in A.S.A. 1875, 15, 6, 7.
C. kinkeri, A.S.A. 207, 16.
Valves sub-spherical to ovate; marginal costae coarse, radiate: area elliptical to sub-rectangular, coarsely costate; median space narrow, lanceolate. Diameter 60–70μ.

DISTRIBUTION. Timor Sea.

132. **Campylodiscus pacificus** Grunow (Pl. 4, fig. 102).

Grunow in A.S.A. 1875, 16, 12.
Valves circular to sub-circular in outline, central area depressed, elliptical: costae anastomosing close to margin and near central area; central area elliptic, finely striate, median space difficult to distinguish. Length, 60–80μ.

DISTRIBUTION. Sediments south of Port Moresby.

133. **Campylodiscus thuretii** Brebisson (Pl. 6, fig. 36).

Brebisson 1854, 13.
A.S.A. 1886, 51, 15, 16.
Boyer 1927, 554.
Valves almost circular, costae wide; central area lanceolate, traversed by transverse lines. Diameter 50μ.

DISTRIBUTION. Arafura Sea.

CONCLUSION

Quantitative and qualitative studies have shown that, in tropical and sub-tropical waters of the Southern Hemisphere, diatoms are largely neritic. In Antarctic and sub-Antarctic waters, many species are Oceanic. It will be recognized that many species in this paper, though recorded from the plankton, belong to genera associated with the benthos, and are no doubt carried into the plankton by turbulence. Such species belong to the Pleurosigmas, Cyclotellas, Biddulphias, Triceratiums as well as many of the Coscinodiscaceae. They were most frequent in plankton from the shallow Timor and Arafura Seas, the waters inside the Great Barrier Reef and the island chains.

Study of the sediment flora of the coral shelf south of Port Moresby revealed a typical benthic flora, but included parts of the setae of *Chaetoceros messanense* and valves of *Rhizosolenia,* thus differing from the floras of sediments from deeper waters.

References

AGARDH, C., 1824–1832. *Conspectus Criticus Diatomacearum.* Parts 1–3. Lund.

ALEEM, A. A., 1950. The diatom community inhabiting the mud-flats at Whitstable, Kent. *New Phytol. 49*: 174–188.

ALLEN, W. E., and CUPP, EASTER E., 1935. Plankton Diatoms of the Java Sea. *Ann. Jard. Bot. Buitenz. 44*: 101–174.

APSTEIN, C., 1909. *Chaetoceros gracile* Schmidt and *Chaetoceros vistulae* n.sp. *Ber. wiss. Untersuch. Meeres.* Kiel N.F. *11*: 133–137.

ATKINS, W. R. G., 1945. Autotrophic flagellates as the major constituent of the oceanic phytoplankton. *Nature, 156*: 446–7.

BAAS BECKING, L. G. M., and WOOD, E. J. F., 1955. Biological processes in the estuarine environment, 1 and 2. Ecology of the sulphur cycle. *Proc. Kon. Ned. Akad.* Wet. *58B*: 160–181.

BAILEY, J. W., 1844. Account of some new infusorial forms discovered in the fossil infusoria from St. Petersburg, Va. and Piscataway. *Md. Amer. J. Sci. 46*: 137–141.

——— 1851. Microscopical observations made in South Carolina, Georgia and Florida. *Smithson. Contr. Knowl.* 2: 8.

——— 1853–54. Notes on new species and localities of microscopical organisms. *Smithson. Contr. Knowl. 7*: 1–16.

——— 1855. New species of the Diatomaceae. *Quart. J. Micr. Sci.* 3.

——— 1856. On microscopic forms in the Sea of Kamchatka. *Amer. J. Sci. Arts,* 2: 22.

BAILEY, L. W., 1862. Notes on new species of microscopical organisms chiefly from the Para River, South America. *Bost. J. Nat. Hist.* 7.

BERGON, P., 1903. Etudes sur la flore diatomique du Bassin d'Arcachon et des parages de l'Atlantique voisins de cette station. *Bull. Soc. d'Arcachon Stat. Biol.* 6.

BODEN, B. P., 1950. Some marine plankton diatoms from the west coast of South Africa. *Trans. Roy. Soc. S. Afr. 32*: 321–434.

BORY DE SAINT VINCENT, 1822–31. *Dict. Class. Hist. Nat. 1*: 79 (Paris).

BOYER, C. S., 1900. The biddulphoid forms of North American Diatomaceae. *Proc. Acad. Nat. Sci. Philad. 52*: 685–748, 1900.

——— 1916. *The Diatomaceae of Philadelphia and Vicinity.* (J. B. Lippincott: Philadelphia.

——— 1927a. Synopsis of North American Diatomaceae. Part 1. Coscinodiscatae, Rhizoselenatae, Biddulphiatae, Fragilariatae. *Proc. Akad. Nat. Sci. Philad. 78*: Suppl. 1–228, 1926.

——— 1927b. Synopsis of North American Diatomaceae. Part II. Naviculatae, Surirellatae. *Proc. Acad. Nat. Sci. Philad.* 79, Suppl.: 229–582.

BRAARUD, T., 1937. A quantitative method for the experimental study of plankton diatoms. *J. Cons. int. Explor. Mer. 12*: 321–32.

BREBISSON, A. DE, 1838. *Considérations sur les diatomées et essai d'une classification des genres et des éspèces appartenant à cette famille.* Falaise, 1838.

——— (1854) 1867. Notes sur quelques diatomées marines, nouvelles ou rares du littoral de Cherbourg. *Mem. Soc. Imp. Cherbourg,* 1854.

BRIGHTWELL, T., 1853. On the genus *Triceratium* with descriptions and figures of the species. *Quart. J. Micro. Sci. 1*: 245–252.

——— 1856. On the filamentous, long-horned Diatomacea. *Quart. J. Micr. Sci. 4.*

——— 1858a. Remarks on the genus *Rhizosolenia* of Ehrenberg. *Quart. J. Micr. Sci. 6.*

BRIGHTWELL, T., 1858b. Further observations on the genera *Triceratium* and *Chaetoceros*. *Quart. J. Micr. Sci. 6.*

——— 1859–60. On some of the rarer or undescribed species of Diatomacea. Parts 1 and 2. *Quart. J. Micr. Sci. 7,* 8.

BRUN, J., 1891. Diatomées éspèces nouvelles marine fossiles ou pelagique. *Mem. Soc. Phys. Hist. Nat. Geneve. 31*: 1–47.

——— and TEMPERE, J., 1889. Diatomées fossiles du Japon. *Mem. Soc. Phys. Hist. Nat. Geneve. 30*: 1–75.

CALLAME, B., and DEBUYSER, J., 1954. Observations sur les mouvèments des diatomées à la surface des sédiments marins de la zone intercotidiale. *Vie et Milieu 5*: 243–249.

CASTRACANE, A. F. DE, 1886. Report on the Diatomaceae collected by H.M.S. *Challenger* during the years 1873–76. *Rept. Challenger Exp. Botany,* 2.

CLARKE, G. L., and GELLIS, S. S., 1935. The nutrition of copepods in relation to the food cycle of the sea. *Biol. Bull. 68*: 231–246.

CLEVE, P. T., 1873a. Examination of diatoms found on the surface of the Sea of Java. *Bih. svensk. Vetenskakad. Handl. 1* (11): 1–13.

——— 1873b. On diatoms from the Arctic Sea. *Bih. svensk. Vetenskakad. Handl. 1* (13): 1–28.

——— 1878. Diatoms from the West Indian archipelago. *Bih. svensk. Vetenskakad. Handl. 5* (8): 1–22.

——— 1881. On some new and little known diatoms. *Bih. svensk. Vetenskakad. Handl. 18* (5): 1–28.

——— 1883. Diatoms collected during the expedition of the *Vega*. *Vega-Exped. Vetensk. Arbet. Iakttag. 3*: 457–517.

——— 1889. Pelagiske Diatomeer från Kattegat. Vidensk. Udbytte kanonbaaden. *"Hauchs" Togter Danske Have.* (1): 53–6.

——— 1891. Diatoms of Finland. *Acta. Soc. Fauna Flora Fenn.* 8:

——— 1894. Planktonunterskningar. Cilioflagellater og Diatomaceer. *Bih. svensk. Vetenskakad. Handl.* 20 (3), 2.

——— 1894–5. Synopsis of the naviculoid diatoms. Part 1 and 2. *Bih. svensk. Vetenskakad. Handl.* 26 (2): 1–194. 27 (3): 1–219.

——— 1896. Planktonuntersokningar. Vegetabiliskt Plankton. *Bih. svensk. Vetenskakad. Handl.* 22 (3) 5.

——— 1897a. *A treatise on the phytoplankton of the Atlantic and its tributaries.* Uppsala.

——— 1897b. Report on the phytoplankton collected on the expedition of H.M.S. *Research*, 1896. *15th Ann. Rep. Fish. Bd. Scot.* (3): 297–304.

——— 1900a. Notes on some Atlantic plankton organisms. *Bih. svensk. Vetenskakad. Handl.* 34 (1): 1–22.

——— 1900b. Plankton from the Southern Atlantic and the Southern Indian Oceans. *Ofver. svensk. Vetenskakad. Forh.* 8.

——— 1901. The seasonal distribution of Atlantic plankton organisms. *K. Vet. och Vett. Samh. Handl.* 17.

——— and GROVE, J., 1891. *Le Diatomiste. 1*: 68.

——— and GRUNOW, A., 1880. Beitrage zur Kenntnis der arctischen Diatomeen. *Bih. svensk. Vetenskakad.* Handl. *17* (2): 1–121.

——— and MOLLER, J. D., 1877–1882. *Diatoms*, Parts I–VI. Uppsala u. Wedel.

CLEVE-EULER, A., 1953a. Die Diatomeen von Schweden und Finnland. Teil II. Araphideae. Brachyraphideae. *K. svenska Vetenskakad Handl.* (4) 4 (1): 1–158.

——— 1953b. Die Diatomeen von Schweden und Finnland. Teil III. Monoraphideae, Biraphideae 1. *K. svenska Vetenskakad. Handl.* (4) 4 (5): 1–255.

CROSBY, L. H., and WOOD, E. J. F., 1958. Studies on Australian and New Zealand diatoms. I. *Trans. Roy. Soc. N.Z. 85*: 483–536.

——— 1959. Studies on Australian and New Zealand Diatoms, II. *Trans. Roy. Soc. N.Z. 86*: 1–58.

CUPP, E. E., 1943. Marine plankton diatoms of the west coast of North America. *Bull. Scripps Instn. Oceanogr. tech. 5* (1): 1–238.

DAKIN, W. J., and COLEFAX, A. N., 1940. The plankton of the Australian coastal waters off New South Wales. 1. *Publ. Univ. Dept. Zool. Monogr.* 1.

DE TONI, G. B., 1891–1894. "*Sylloge Algarum Omnium Hucusque Cognitarum. 2. Sylloge Bacillariarum, sect. III.*" (Typis Seminarii: Patavii.)

DILLWYN, L. W., 1809. *British Confervae,* London.

DONKIN, A. S., 1858. On the marine diatomaceae of Northumberland, with a description of 18 new species. *Trans. Micr. Soc. 6*: 12–34.

——— 1871. *The natural history of the British Diatomaceae.* 1.

EHRENBERG, C. G., 1828. *Die geographische Verbreitung der Infusionsthierchen in Nord-Afrika und West-Asien, beobachtet auf Hemprich und Ehrenbergs Reisen.*

——— 1830. Beitrage zur Kenntnis der Organisation der Infusorien und ihrer geographischen Verbreitung, besonders in Sibirien. *Abh. Kgl. Akad. dtsch. Wiss. Berl.* 1830: 1–88.

——— 1832. Zur Erkenntnis der Organisation in der Richtung des kleinsten Raumes. Zweiter Beitrag. *Abh. Kgl. Akad. dtsch. Wiss. Berl.*

——— 1836. Über das Massenverhaltnis der jetzt lebenden Kiesel-Infusorien und über neues Infusorien-Conglomerat als Polirschiefer von Jastraba in Ungarn. *Abh. Kgl. Akad. dtsch. Wiss. Berl.* 1836: 109–132.

——— 1838. *Die Infusionsthierchen als vollkommene Organismen. Ein Blick in das tiefere organische Leben der Natur.* Leipzig. Leopold Voss.

——— 1839. Die Bildung der europäischen, libyschen, und arabischen Kreidefelsen und des Kreidemergels aus mikroskopischen Organismen. (*Abh. Kgl. Akad. dtsch. Wiss. Berl.*) 56–147.

——— 1840. Über noch zahlreich jetzt lebende Tierarten der Kreidebildung und den Organismus der Polythalamien. *Abh. Kgl. Akad. dtsch. Wiss. Berl. 4*: 81–174.

——— 1843a. Neue Beobachtungen über den sichtlichen Einfluss der mikroskopischen Meeres-Organismen auf den Boden des Elbbettes bis oberhalb Hamburg. *Mon. Akad. Wiss. Berl.*

——— 1843b. Verbreitung und Einfluss des mikroskopischen Lebens in Sud- und Nord-Amerika. *Abh. Kgl. Akad. dtsch. Wiss. Berl.* 1841: 291–446.

——— 1844. Einige vorläufige Resultate seiner Undersuchungen der ihm von der Sudpolreise des Capitan Ross sowie von den Herre Schayer und Darwin zugekommen Materiel en. *Mon. Akad. Wiss. Berl.* 182–207.

——— 1845. Neue Untersuchungen über das kleinste Leben als geologisches Moment. *Mon. Akad. Wiss. Berl.* 53–88.

——— 1849. Passatstaub und Blutregen. Ein grosses organisches unsichtbares Wirken und Leben in der Atmosphäre. *Abh. Kgl. Akad. dtsch. Wiss. Berl.* 1847. 269–460.

——— 1854. *Mikrogeologie.* Leipzig.

——— 1869. Über mächtige Gebirgs-Schichten vorherrschend aus mikroskopischen Bacillarien unter und bei der Stadt Mexico. *Abh. Kgl. Akad. dtsch. Wiss.* Berlin.

——— 1873. Mikrogeologische Studien über das kleinste Leben der Meeres Tiefgrunde aller Zonen und dessen geologischen Einfluss. *Abh. Kgl. Akad. dtsch. Wiss. Berl.* 1872: 131–397.

ENGLER, A., 1883. Über die pelagischen Diatomeen der Ostsee. *Ber. deut. bot. Ges.* 1. Berlin.

GOUGH, LEWIS H., 1905. Report of the plankton in the English Channel, in 1903. *Mar. Biol. Ass. Internat. Inv. Rept.* 1. 325–77.

GRAN, H. H., 1897. Protophyta; Diatomacea, Silico-flagellata and Cilioflagellata. Norske *Nordhaus. Exped.* 1876–78. *24*: 1–36.

——— 1900. Bermerkungen über einige Planktondiatomeen. *Nyt. Mag. Naturvidensk. 38*: 103–6.

——— 1904. Die Diatomeen der Arktischen Meere I. Die Diatomeen des Planktons. *Fauna Antarctica 3*: 511–54.

——— 1905. Diatomeen. *Nord. Plankt. 3* (19): 1–146.

Gran, H. H. and Angst, E. C., 1931. Plankton diatoms of Puget Sound. *Publ. Puget Sd. Mar. (Biol.) Sta. 7*: 417–519.

——— and Thompson, T. G., 1930. The diatoms and the physical and chemical condition of the sea water of the San Juan archipelago. *Publ. Puget Sd. Mar. Biol. Sta. 7*: 169–204.

Gray, S. F., 1821. *A natural arrangement of British plants.*

Gregory, R. W., 1856. Notice on some new species of British freshwater diatoms. *Quart. J. Micr. Sci.* 4.

Gregory, W., 1857. On new forms of marine Diatomaceae found in the Firth of Clyde and in Loch Fyne. *Trans. Roy. Soc. Edinb. 21*: 473–542.

Greville, R. K., 1827. *Scottish cryptogram flora.*

——— 1855. Report on a collection of Diatomaceae made by Prof. Balfour and M. G. Lawson in the district of Braemar. *Ann. Mag. Nat. Hist. Ser.* 2, 15.

——— 1859. Descriptions of diatomaceae observed in California guano. *Quart. J. Micr. Sci. 7*: 155–66.

——— 1860. A monograph on the genus *Asterolampra* including *Asteromphalus* and *Spatangidium*. *Trans. Micr. Soc. 8*: 102–24.

——— 1861. Descriptions of new and rare diatoms. 1–4. *Trans. Micro. Soc.*, 9, 39–45, 67–87.

——— 1862. Descriptions of new and rare diatoms. 5–6. *Trans. Micro. Soc.* 10, 18–29, 89–96, 7, *Quart. J. Micr. Sci.* n.s. 2, 231–236.

——— 1863a. A monograph of the genus *Auliscus*. *Trans. Micro. Soc. 11*: 36–53.

——— 1863b. Descriptions of new and rare diatoms. 8–9. *Trans. Micro. Soc. 11*: 13–21, 63–76. 10, *Quart. J. Micr. Sci. 3*: 227–237.

——— 1863c. Descriptions of new genera and species from the South Pacific. *Edinburgh New Phil. J.* 18, 34–43; 181–187.

——— 1864. Descriptions of new and rare diatoms. 11–13. *Trans. Micr. Soc. 12*: 8–14, 81–86, 86–94.

——— 1865a. Descriptions of new and rare diatoms. 14–17. *Trans. Micr. Soc. 13*: 1–10; 24–34; 43–56; 97–105.

——— 1865b. Descriptions of genera and species from Hong Kong. *Ann. Mag. Nat. Hist.* 16.

——— 1866. Descriptions of new and rare diatoms. 18–20. *Trans. Micr. Soc. 14*: 1–9, 77–86, 121–130.

——— and Arnot, 1857. See Gregory, W., 1857.

Gross, F., and Zeuthen, F., 1948. The buoyancy of diatoms; a problem in cell physiology. *Proc. Roy. Soc. Edinb.* B135.

Grove, E., and Sturt, G., 1886–7. On a fossil marine diatomaceous deposit from Oamaru, Otago, New Zealand. *Quart. J. Micr. Sci. 17*: 321–330. *18*: 7–12, 63–78, 131–148.

Grunow, A., 1860. Über neue oder ungenügend gekannte Algen. *Verh. Zool.-bot. Ges. Wien.* 1860: 503–582.

——— 1862. Die österreichischen Diatomaceen nebst anschluss einiger neuen Arten von ändern Lokalitäten und einer kritischen Übersicht der bisher bekannten Gattungen und Arten, 1 and 2. *Verh. Zool.-bot. Ges. Wien. 12*: 315–472, 544–588.

——— 1863. Über einige neue ungenugend bekannte Arten und Gattungen von Diatomaceen. *Verh. Zool. bot. Ges. Wien.* 13, 137–162.

——— 1867. Nachträgliche Bermerkungen über die von Herrn Lindig gesammelten Diatomeen von Honduras. *Hedwigia* 6, 33–37.

——— 1868. Reise seiner Majestat Fregatte *Novara* um die Erde. Bot. Teil. *1*: 1–104.

——— 1877. Trans. of Grunow 1867 by F. Kitton. *Trans. Micr. Soc.* 18.

——— 1878. Algen und Diatomaceen aus dem Kaspischen Meere. In Dr Schneider, *Naturw. Beit. zur Kauk auf Grunde sein Sammel.* Dresden.

——— 1882. Beiträge zur Kenntnis der fossilen Diatomeen österreich-ungarns. *Mojs. u. Neum. Beitr. Palaont. Ost.-ung.* II: 136–159.

Grunow, A., 1884. Die Diatomeen von Franz Josefs-Land. *Denkschr. Akad. Wiss. Math. Naturw. Klasse. 48*: 53–112.

Hantzsch, C. A., 1862. Uber einige Diatomaceen aus dem Ostindischen Archipel. Rabenh. *Beitr.* 1.4.

Hart, T. M., 1937. *Rhizosolenia curvata* Zacharias, an indicator species of the Southern Ocean. *"Discovery" Rep. 16*: 413–446.

Harvey, H. W., 1937. Notes on selective feeding by *Calanus. J. Mar. Biol. Ass. U.K. 22*: 97–100.

——— 1945. *Recent advances in the chemistry and biology of seawater.* (Univ. Press, Cambridge.)

Hassall, A. H., 1855. *Diatomaceae in the water supplied to the inhabitants of London. Microscopic examination of the water.* London.

Heiberg, P. H. C., 1863. *Conspectus criticus Diatomacearum danicarum.*

Heiden, H., and Kolbe, R. W., 1928. Die marinen Diatomeen der deutsche Sudpolar-Expedition. *Deut. Sudp. Exped. 8* (5): 450–714.

Hendey, N. I., 1937. The plankton diatoms of the southern seas. *"Discovery" Rep. 16*: 151–364.

——— 1951. Littoral diatoms of Chichester Harbour with special reference to fouling. *J. R. Micr. Soc. 71*: 1–86.

——— 1953. Taxonomic studies on some Naviculae punctatae. *J. R. Micr. Soc. 73*: 156–161.

Hensen, V., 1887. Über die Bestimmung des Planktons. *Ber. Wiss. Untersuch dtsch. Meere, Kiel.* 1882. *6*: 1–108.

Hohn, M. H., 1951. A study of the distribution of diatoms in western New York State. *Mem. 308, Cornell agric. Exp. Sta.*: 1–37.

Hooker, —, 1833. In Smith, J. E., *English Flora* 5.

Hustedt, F., 1924. Die Bacillariaceen-Vegetation des Sarekgebirges. *Naturw. Untersuch Sarekgeb. Bot.* 3 (6): 525–626.

——— 1927–1937. Die Kieselalgen Deutschlands, Osterreichs und der Schweiz, mit berücksichtigung der übrigen Länder Europas sowie der angrenzenden Meeresgebeite, in Rabenhorst, *Kryptogamenflora.* Part 1, 1–272 (1927), 273–464 (1928), 465–608 (1929), 609–784 (1930), 785–920 (1930). Part 2. 1–176 (1931), 177–320 (1932), 321–432 (1933), 433–576 (1933), 577–736 (1937).

Janisch, C., 1862. Zur Characteristik des Guanos von Verschiedenen Fundorten. *Abh. Schles. Ges. Vatarl. Kult. Nat.-Med. Abt.*

Jorgensen, E., 1901. Protistenplankton aus dem Nordmeere in den Jahren 1897–1900. *Bergens Mus. Aarb.* 1900, 6.

——— 1905. Protistplankton and diatoms in bottom samples. Hydrographical and biological investigations in Norwegian fjords. *Bergens Mus. Skr. 7*: 49–148.

Karsten, G., 1905–7. Das phytoplankton des Antarktischen Meeres nach dem Material der Deutschen Tiefsee-Expedition, 1898–9. *Wiss. Ergebn. dtsch. Tiefsee-Exped. 2*: 1–136, 137–219, 223–544.

Kolbe, R. W., 1954. Diatoms from equatorial Pacific cores. Repts. Swedish Deep-Sea Exp., 1947–8. *Göteborgs Kungl. Vetensk. och vitterh.* samh. 6 (1), 1–49.

Kützing, F. T., 1834. Synopsis Diatomearum oder Versuch einer systematischen Zusammenstellung der Diatomeen. *Linnaea. 8*: 529–620.

——— 1844. *Die Kieselschaligen Bacillarien oder Diatomeen.* Kohne, 152 pp.

——— 1849. *Species algarum.* Lipsiae, F. A. Brochaus. 992 pp.

Lagerstet, N. G. W., 1873. Sölvattens-Diatomaceer fran Spetsbergen och Beeren Eiland. *Akad. Afh. Vidtb. Filosof. Fakult.* Uppsala Samt. 1–52.

Lauder, H. S., 1864. Remarks on the marine Diatomaceae found at Hong Kong, with descriptions of new species. *Trans. Micr. Soc. 12*: 75–9.

Lebour, Marie V., 1930. *The Planktonic Diatoms of Northern Seas.* (Ray Society: London.)

Leuduger-Fortmorel, G., 1898. *Diatomes marines de la cote occidentale d'Afrique.* Saint Brieuc.

LEWIN, JOYCE C., 1953. Heterotrophy in diatoms. *J. Gen. Microbiol. 9*: 305–13.

LEWIS, F. W., 1865. On extreme and exceptional variations of diatoms in some White Mountain localities. *Proc. Acad. Phila.* pp. 7–18.

LYNGBYE, H. C., 1819. "*Tentamen Hydrophytologiae Danicae.*" (Copenhagen.)

MANGIN, L., 1917. Sur le *Chaetoceros criophilus* Castr. éspèce charactéristique des mers antarctiques. *C. R. Acad. Sci. 164*: 704, 770.

MANGUIN, E., 1954. Diatomées marines provénant de L'île Heard. Australian Nat. Antarctic Research Expedition. *Rev. Algol. 1* (1): 14–24.

MANN, A., 1937. Diatoms. *Aust. Antarctic Exp. Sci. Repts.* C.1 (1): 1–82.

MANTEUFEL, B. P., 1941. Plankton and herring in the Barents Sea. *Trans. Knipovich Polar Sci. Inst. Sea Fish. Oceanogr.* 7: 125–210.

MARSHALL, S. M., and ORR, A. P., 1955. Experimental feeding of the copepod *Calanus finmarchicus* (Gunner) on phytoplankton cultures labelled with radioactive carbon (^{14}C). *Deep Sea Res.* 3 (Supp): 110–114.

MERESCHKOWSKY, C., 1902. Note sur quelques diatomées de la Mer Noir suivie d'une liste de formes obsérvées dans cette mer. *J. Bot. Paris 16*: 319–324, 358–360.

MEUNIER, A., 1910. Microplancton des Mers de Barents et de Kara. *Duc. d'Orleans, Campagne Arctique de 1907.* Brussels.

——— 1913. Microplancton de la Mer Flamande. 1 er partie. Le genre *Chaetoceros* Ehrg. *Mem. Mus. r. Hist. nat. Belg. 7*: 1–55.

MÜLLER, O., 1871 Über den feineren Bau der Zellwand der Bacillariaceen insbesondere des *Triceratium favus* Ehrbg. und der *Pleurosigma. Arch. Anat. Physiol. Wiss. Med. Lptz.* 5–6: 619–643.

——— 1895. *Rhopalodia* ein neues genus de Bacillariaceen. Engler's *Bot. Jahrb.* 22. Leipzig.

——— 1905–10. Bacillariaceen aus dem Nyassaland. Engler's *Bot. Jahrb.* Vols. 34, 36, 45.

MÜLLER, O. F., 1786. *Animalia, infusoria et marina quae detexit, etc.* Hauniae in-4.

NITZSCH, C. L., 1817. Beitrag zur Infusorienkunde oder Naturbeschreibung der Zerkarien und Bacillarien. *Neue Schr. Naturf. Ges. Halle,* 3 (1):1–128.

NORMAN, G., 1861. On some undescribed species of Diatomaceae. *Trans. Micro. Soc.* 9.

O'MEARA, E., 1875–7. Report on the Irish Diatomaceae. *Proc. R. Irish Acad.* (2). *2*: 235–425.

OSTENFELD, C. H., 1899. *Plankton in 1898. Iagttagelser over Overfladevandets Temperatur, Saltholdighed og Plankton paa islandske og gronlandske Skibsrouter i 1898 udgivne Martin Knudsen og C. Ostenfeld,* Copenhagen.

——— 1901. Iagttagelser over Plankton-Diatomeer. *Nyt. Mag. Naturvid.* 39.

——— 1902. Marine plankton diatoms in Johs. Schmidt, Flora of Koh Chang. Part 7 (Repr. *Bot. Tidskr.* 25) 219–45.

——— 1908. The immigration of *Biddulphia sinensis* Greville and its occurrence in the North Sea during 1903–7. *Medd. Kom. Hav S. Plankton.* 1 (6) Copenhagen.

——— 1915. A list of phytoplankton from Boeoton Strait, Celebes. *Dansk. Bot. Ark.* 2 (4). Note.

——— and SCHMIDT, JOHS., 1901. Plankton fra det Rode Hav og Adenbugten. *Vidensk. Med. Naturh. For. Koybenhaven*: 141–90.

ØSTRUP, E., 1910. *Danske Diatomeer.* 323 pp. Reitzels. Copenhagen.

PANTOCSEK, J., 1886–1893. *Fossilen Bacillarien Ungarns.* 1.

——— 1902. Kieselalgen oder Bacillarien des Balaton. *Result. Wiss. Erg. Balatonsees 2* (2): 1–112, Wien.

PAVILLARD, J., 1913. Obsérvations sur les Diatomées. 2. *Bull. Soc. bot. Fr. 60*: 126–133.

——— 1916. Réchérches sur les diatomées pelagiques du Golfe de Lion. *Trav. Inst. Bot. Univ. Montpellier, Mixt. Mem.* 5: 63.

——— 1925. Bacillariales. *Rept. Danish Exp.* (1908–10) *to Mediterranean and adjacent seas.* 2, Biol. J4: 1–72.

PERAGALLO, H., 1880. Diatomees de la baie de Villefranche (Alpes Maritimes). *Bull. Soc. Hist. Nat. Toulouse. 22*: 13–100.

——— 1892. Monographie du genre *Rhizosolenia* et de quelques genres voisins. *Le Diatomiste 1*: 79-82, 99–117. Paris.

PERAGALLO, M., 1921. Diatomees d'eau douce, et Diatomees d'eau salar 2 *Exped. Antarct. franc.* 1908–10.

PETERSEN, C. G. J., 1918. The sea bottom and its production of fishfood: a survey of the work done in connection with valuation of the Danish waters from 1883–1917. *Rep. Danish Biol. Sta.* 1918: 1–62.

PETIT, P., 1877. Catalogue des diatomees de l'ile Campbell et de la Nouvelle Zelande. *Fonds de la Mer. 3*: 164–198.

PFITZER, E., 1871. *Untersuchungen über Bau und Enticklung der Bacillariaceen (Diatomaceen)*. Adolph Marcus: Bonn.

PRITCHARD, A., 1861. *History of the Infusoria.* 4th Ed. (Diatoms by J. Ralfs) (London).

PROVASOLI, L., and PINTNER, I. F., 1953. Ecological implications of *in vitro* nutritional requirements of algal flagellates. *Ann. N.Y. Acad. Sci. 56*: 839–51.

QUECKETT, J., 1848. *A Practical Treatise on the Microscope.* (London.)

RABENHORST, L., 1864. *Flora europaea Algarum.* 1. Algae, Diatomaceae.

RALFS, J., 1843a. On the Diatomaceae. *Ann. Mag. Nat. Hist. 11*: 447–57; 12: 104–11, 270–6, 346–52.

——— 1843b. On the British species of *Meridion* and *Gomphonema. Ann. Mag. Nat. Hist. 12,* Suppl: 457–67.

——— 1844a. On the British species of *Grammonema* and *Eunotia. Ann. Mag. Nat. Hist. 13*: 457–61.

——— 1844b. On the British species *Achnanthes. Ann. Mag. Nat. Hist. 13*: Suppl.: 489–93.

——— 1845. On the British Diatomaceae. *Ann. Mag. Nat. Hist. 16*: 109–12.

——— 1861. Diatoms in Pritchard's *Infusoria.* q.v.

——— 1864. See Lauder, 1864, notes by Ralfs.

RATTRAY, J., 1888. A revision of the genus *Auliscus* and some allied genera. *J. Roy. Micr. Soc.* 8.

——— 1890. A revision of the genus *Coscinodiscus* and some allied genera. *Proc. Roy. Soc. Edinb. 16*: 449-692.

——— 1890. A revision of the genus *Actinocyclus*, Ehr. *J. Queck. Micro. Club.* 4 (Ser. II): 137.

ROPER, F. C. S., 1858. Notes on some new species and varieties of British Marine Diatomaceae. *Quart. J. Micr. Sci. 6*: 17–25.

——— 1859. On the genus *Biddulphia* and its affinities. *Trans. Micr. Soc. 7.*

——— 1863. On the genus *Licmophora* (Agardh). *Trans. Micr. Soc. 11*: 53–62.

SCHMIDT, A., 1875–1934. *Atlas der Diatomaceen-Kunde.* (Ernst Schlegel: Aschersleben).

VON SCHONFELD, H., 1907. *Diatomaceae Germania. Die deutschen Diatomeen des Süswassers und des Brackwassers.* (Theodor Oswald Weigel: Leipzig.)

SCHRODER, B., 1900. Das Phytoplankton des Golfes von Neapel. *Mitt Zool. Sta. Neapel,* 14.

——— 1906. Beiträge zur Kenntnis der Phytoplanktons warmer Meere. *Vischr. naturf. Ges. Zurich, 51*: 319–377.

SCHÜLTZE, M. S., 1858. Innere Bewegungserscheinungen bei Diatomeen der Nordsee aus den Gattungen *Coscinodiscus, Denticella, Rhizosolenia.* Mullers Arch. 1858. (summ. *Quart. J. micr. Sci.* 7: 13–21. 1859).

SCHUMANN, J., 1864–1869. Preussische Diatomeen. *Phys. Ok. Gesell. Konigsberg.*

SCHÜTT, F., 1889. Über die Auxosporebildung der Gattung *Chaetoceros. Ber. dtsch. bot. Ges.*

——— 1893. *Des Pflanzenleben der Hochsee.* Kiel u. Leipzig.

——— 1895. Arten von *Chaetoceros* und *Peragallia.* Ein Beitrag zur Hochseeflora. *Ber. dtsch. Bot. Ges. 13*: 35–48.

SCHÜTT, F., 1896. Bacillariales in Engler u. Prantl. *Die natürlichen Pflanzenfamilien,* 1 (1b): 31–150.

SHADBOLT, G., 1854. A note on the proposed new genus *Actinosphenia. Trans. Micr. Soc.* 2.

SHRUBSOLE, W. H., 1890. On a new diatom from the estuary of the Thames. *J. Queckett micr. Club* (Ser. 2) *4*: 259–262.

SMITH, J. E., 1807. English Botany. 23, 25, 27. Lond.

SMITH, W., 1853–1856. *A synopsis of the British Diatomaceae.* Smith and Beck, London.

DE SOUSA E. SILVA ESTELA (1953) 1956. Diatomacees do plankton marinho de Angola. *Trab. Miss. Biol. Marit.* 1–56.

STANBURY, F. H., 1944. Experiments in the growth of marine plants with special reference to the effects of copper and mercury salts. *Marine Corrosion Sub. Com. Rept. Iron & Steel Corr. Comm. M.S.*

SUBRAHMANYAN, R., 1946. A systematic account of the marine plankton diatoms of the Madras coast. *Proc. Ind. Acad. Sci.* B.24: 85–197.

SVERDRUP. H. U., JOHNSON, M. W., and FLEMING, R. H., 1942. *The Oceans.* (Prentice-Hall, N.Y.).

THWAITES, G. H. K., 1848. Further observations on the diatomaceae with descriptions of new genera and species. *Ann. Mag. Nat. Hist.* 20 (Ser. III): 161–172.

VAN HEURCK, H., 1880–1895. *Synopsis des Diatomees de Belgique.* (Anvers.)

VANHOFFEN, E., 1897. Die Fauna und Flora Groenlands. Groenland Exp. Ges. Erdkunde, 10: Bd. 2 Berlin.

VENKATARAMAN, G., 1939. A systematic account of some South Indian Diatoms. *Proc. Ind. Acad. Sci. B10*: 293–368.

WALLICH, G. C., 1858. On *Triceratium* and some new allied forms, with figures of same. *Quart. J. Micr. Sci. 6*: 242–253.

——— 1860. On the siliceous organisms found in the digestive cavities of the Salpae. *Trans. Micr. Soc.* n.s. *8*: 36–55.

WEST, TUFFEN, 1860. Remarks on some Diatomaceae new or imperfectly described, and a new desmid. *Trans. Micr. Soc.* n.s. *8*: 147–153.

WOOD, E. J. F., 1950. Investigations in underwater fouling. 1. The role of bacteria in the early stages of fouling. *Aust. J. Mar. Freshw. Res.* 1. 85.

——— 1953. Heterotrophic bacteria in marine environments of eastern Australia. *Aust. J. Mar. Freshw. Res. 4*: 160–200.

——— 1954. Dinoflagellates in the Australian region. *Aust. J. Mar. Freshw. Res. 5*: 171–351.

——— 1955. Effect of temperature and flow rate on some marine fouling organisms. *Aust. J. Sci. 18*: 33–4.

——— 1956. Diatoms in the ocean deeps. *Pac. Sci. 10*: 377–381.

——— 1961. Studies on Australian and New Zealand Diatoms, IV and V. *Trans. Roy. Soc. N.Z. 88*: 669–712.

WOOD, E. J. F., CROSBY, L. H., and CASSIE, VIVIENNE, 1959. Studies on Australian and New Zealand Diatoms, III. *Trans. Roy. Soc. N.Z. 87*: 211–219.

ZACHARIAS, O., 1905. *Rhizosolenia curvata* mihi, eine neue marine Plankton diatomee. *Arch. Hydrobiol. v. Planktonkunde 1*: 120–121.

ZOBELL, C. E., 1946. *Marine Microbiology.* Chronica Botanica Co., Waltham, Mass.

PROFESSOR E. J. FERGUSON WOOD,
Institute of Marine Science,
University of Miami,
1 Rickenbacker Causeway,
Virginia Key,
Miami 49, Flo., U.S.A.

Reprinted from *Ibis*, vol. 107, 1965, p. 385-386

A SUMMARY OF BIRDS SEEN OVER THE WESTERN INDIAN OCEAN August–November 1963*

The Woods Hole Oceanographic Institution vessel ' R.V. Atlantis II ' participated in the International Indian Ocean Expedition 1 August–11 November 1963. She passed through the Red Sea and Gulf of Aden and traversed that part of the western portion of the Indian Ocean from 20° N. to 25° S. bordered on the west by the east coast of Africa, and on the east by the west coast of India–Ceylon–The Chagos Archipelago–Mauritius–the southern tip of Madagascar. About one-third of the total area of the Indian Ocean falls within these bounds. Though there was no full-time ornithologist aboard, a regular bird-watch was maintained by Dr. R. Risebrough, Mr. M. Palmieri and myself. Our combined field-notes have been reported elsewhere (' Bird Log Data, Atlantis II Cruise 8 ', 1964 (WHO I Reference No. 64–31)), but are here summarised and related to certain properties of the surface waters, in particular temperature and the concentration of inorganic nutrients. Identifications and nomenclature follow the ' Preliminary Field Guide to the Birds of the Indian Ocean ', (Watson, G. E., Zusi, R. L., & Storer, R. W., 1963, Smithsonian Institution, Washington).

The water throughout the whole region, with the exception of the waters about Socotra, was warmer than 23°C. in the top metre. Thus the western portion of the Indian Ocean at this season falls within the tropical zone as defined by Murphy (' Oceanic Birds of South America ', 1936, Vol. 1 : 78–81). This contrasts with the South Atlantic Ocean where the 23°C. summer isotherm lies much further north, at approximately 15° S. There was, therefore, little in terms of temperature to distinguish the surface waters of the region and their bird populations.

We encountered the following species which are also found in the Atlantic and Pacific Oceans: Audubon's Shearwater *Puffinus l'herminieri;* Red-billed Tropic-bird *Phaethon aethereus* and White-tailed Tropic-bird *P. lepturus;* Blue-faced Booby *Sula dactylatra,* Red-footed Booby *S. sula* and Brown Booby *S. leucogaster;* Greater Frigate-bird *Fregata minor* and Lesser Frigate-bird *F. ariel;* Bridled Tern *Sterna anaethetus,* Sooty Tern *S. fuscata,* Roseate Tern *S. dougallii,* Little Tern *S. albifrons,* Common Noddy *Anous stolidus* and Fairy Tern *Gygis alba.*

Palaearctic breeding species seen at sea were: Ruddy Turnstone *Arenaria interpres,* a Curlew *Numenius* sp. (not *madagascarensis*), Curlew Sandpiper *Erolia testacea,* Lesser Black-backed Gull *Larus fuscus,* a Roller *Coracias* sp. (not *garrulus*), Swallow *Hirundo rustica,* Spotted Flycatcher *Muscicapa striata.*

Of those species peculiar to the Indo-Pacific Oceans we saw: Wedge-tailed Shearwater *Puffinus pacificus* and Crested Tern *Thalasseus bergii;* and of those found only in the Indian Ocean we saw: the Sooty Gull *Larus hemprichii* and of Indo-Atlantic species the Lesser Noddy *Anous tenuirostris.* Pan-antarctic breeding species were represented by the wide-ranging Wilson's Storm-petrel *Oceanites oceanicus* and the Great Skua *Catharacta skua.*

The colder water around Socotra did not have a distinctive non-tropical bird fauna. This agrees with oceanographic evidence which suggests that this cool surface water is seasonal, dependent upon the monsoons, and not sufficiently permanent to maintain singular populations such as, for example, those occurring in the waters of the Humbolt Current off Peru. In his analysis of the pelagic bird faunas of the Indo-Pacific Oceans, Serventy (' 8th Pac. Sci. Congr.' 1953 : 461–488) states that "No evidence of a trans-

* Contribution No. 1610 from the Woods Hole Oceanographic Institution. This work was done under Contract NSF GP–821 with the Office of Naval Research.

gression [of cool-water species during Glacial Periods] exists in the Indian Ocean; if it occurred no southern elements could have survived in the absence of cool-water refuges in the geographically limited northern Indian Ocean ". Unfortunately, conditions for observation in the area were poor, and the Socotra Cormorant *Phalacocorax nigrogularis*, and a recently-described gad-fly petrel, Jouanin's Petrel *Bulweria fallax*, neither of which were seen, may prove to be exclusively associated with this seasonal sub-tropical water-body.

There was no particular correlation between the total number of birds seen per day and the concentration of inorganic nutrients in the surface-water. High surface nitrate and phosphate concentrations and a high nitrate/phosphate ratio are conducive to greater densities of phytoplankton growth and, consequently, to more zooplankton, fish, and ultimately birds, as in the Antarctic zone (Murphy, ' Proc. Roy. Soc.' 152B : 642–654). Low levels of nutrients should have the opposite effect, though waters clear by reason of sparse plankton populations may benefit those birds such as the Sulidae which dive for prey detected from above. Our log revealed no particularly great number of birds in the areas of high surface nutrients—around Socotra and off the South Arabian Coast—which were also the regions of highest chlorophyll density, though large numbers have been recorded at this season closer to shore (R. Bailey, R.R.S. ' Discovery ', Cruise 1. South East Arabian Upwelling Region, Cruise Report, 1963. The Royal Society). By far the largest congregations of sea-birds were seen around the Seychelles, where nutrient concentrations were low, but large-scale breeding was in progress at the time on the outer islands of the group (R. Bailey, pers. comm.).

In general our log indicated that the presence of islands or at least of submerged banks (e.g. Saha de Mahya Bank) was necessary for large congregations of assorted species to be seen; the concentration of species and individuals about the islands contrasted with the empty mid-ocean sections. This finding applies not only to the land-based Sulidae, Fregatidae, and Laridae but, more surprisingly, also to the Procellaridae, as noted by Murphy (' Oceanic Birds of South America', 1936, Vol. 1 : 78–79)..." The pan-tropical oceanic birds tend to be more local and sedentary... Many must be regarded as more or less land-bound, rather than pelagic, and this applies even to the Procellariiformes."

Tropic-birds were occasionally seen singly far from shore; a specimen of *Phaethon aethereus* was, for example, sighted at 20° N., 66° E., 210 nautical miles from India and twice as far from Arabia, which was down-wind. Small groups of frigate-birds were often seen far from land, e.g. *Fregata minor* at 4° 53′ N., 57° 20′ E., 480 miles from the Somali Coast and 540 miles north of the Seychelles. The most numerous and most widely-ranging species of the Laridae was the Sooty Tern *Sterna fuscata*, observed on one occasion at 5° N., 63° E., 570 miles from the Maldives and 660 miles from the Seychelles.

One notable feature of our records was the apparent absence of overlap in the ranges of related species among the Phaethontidae and Sulidae; individuals of different species of the same genus were not seen together or even in the same surface-water region: *Sula leucogaster*—Red Sea, Somali Coast; *S. dactylatra*—Arabian Basin, Mascarene Basin; *S. sula*—Saha de Mahya Bank; *Phaethon lepturus*—Gulf of Aden, Arabian Basin, Seychelles; *P. aethereus*—Arabian Sea, Socotra. These species may therefore be allopatric in their pelagic distribution, even if sympatric at some breeding stations.

The number of our observations, taken on their own, is insufficient to establish a definite pattern, but combined with other data from the region, they should be useful in establishing the ranges of species at sea and relating this to the differing surface water-bodies.

Woods Hole Oceanographic Institution, R. POCKLINGTON.
Woods Hole, Massachusetts, U.S.A.
19 November 1964.

Reprinted from *Ibis*, vol. 107, 1965, p. 387

BIRDS SEEN ON COCO ISLAND, CARGADOS CARAJOS SHOALS, INDIAN OCEAN*

On 1 November 1963 a party of three scientists and one officer from the Woods Hole Oceanographic Institution vessel ' R. V. Atlantis II ' spent three hours ashore on a small treeless island at the southen tip of the Cargados Carajos Shoals (16° 49′ S., 59° 30′ E.) about 215 miles N.N.E. of Mauritius. The island visited was most probably the one designated as " Coco Island " on the chart reproduced in the ' Preliminary Field Guide to the Birds of the Indian Ocean ' (Watson, G. E., Zusi, R. L., & Storer, R. W., 1963, Smithsonian Institution, Washington). According to the Guide the Cargados Carajos Shoals have been visited by scientific parties only twice; " the Percy Sladen Trust Expedition " worked in the group mainly making observations incidental to dredgings from 26 August to 1 September 1905, and R. Newton worked in the islands 9–15 January 1955 and 7–21 January 1956. However, ornithologists from Mauritius are fairly regularly visiting these islands at present. The following identifications (and nomenclature) are taken from the Guide.

LESSER FRIGATE-BIRD *Fregata ariel.* About 200 pairs were nesting in low bushes, 1–2 ft. from the ground. None of the males was in full courtship plumage, though several of the males which were incubating eggs still showed some green iridescence of the nape feathers and a small shrunken throat-pouch. However, all other stages of the nesting cycle were observed, from which it can be inferred that breeding is continuous throughout the year. Plumage of the adult nesting females was surprisingly variable. Some had a complete white collar, on others the back of the neck was brownish-black; the eye-ring was either red or blackish, and the amount of rufous on the chest showed appreciable individual variation. This species, unlike the Greater Frigate-bird *F. minor* was not observed at sea, and it is therefore possible that *F. ariel* feeds only close to shore. If so, this would contribute to the ecological separation of the two species.

RUDDY TURNSTONE *Arenaria interpres.* Two groups of six individuals in non-breeding plumage were seen: one on a coral-sand spit south of, and separate from, Coco Island, the other on Coco itself.

SAND PLOVER *Charadrius* sp. One party of a dozen small plovers in dull plumage was seen on Coco Island. They were either Greater Sand Plover *C. leschenaultii* or Lesser Sand Plover *C. mongolus* which are difficult to separate in the field unless seen together. The Guide lists only *C. leschenaultii* as having been recorded from the Islands.

ROSEATE TERN *Sterna dougallii.* Confined to the spit of coral sand south of Coco Island. Young birds in all stages of development were seen, but no eggs were found. Tracks in the sand indicated that the terns share this breeding site with turtles.

SOOTY TERN *Sterna fuscata.* Many were seen flying over the water as we approached the islands, but were not seen ashore, though this species was nesting during October on the outer islands of the Seychelles.

GREATER NODDY *Anous stolidus.* Widespread as a solitary nester on the ground. It actively defended its nest-site when approached.

LESSER NODDY *Anous tenuirostris.* Confined to nesting sites above ground, occurring in groups of 5–10 pairs in those portions of the low bush not occupied by *Fregata ariel*, and dispersing without protest when approached.

FAIRY TERN *Gygis alba.* Though normally a tree-nester, on Coco Island it was largely excluded from the shrubbery by the other nesting species, and was sitting on its solitary egg upon elevated pieces of coral, and even on the ground.

Woods Hole Oceanographic Institution, R. POCKLINGTON.
Woods Hole, Massachusetts, U.S.A.
19 November 1964.

* Contribution No. 1611 from the Woods Hole Oceanographic Institution. This work was done under Contract NSF GP–821 with the Office of Naval Research.

Reprinted from *Arch. Oceanogr. Limnol.*, vol. 15. 1967, p. 63-67

ON THE OCCURRENCE OF ACANTHARIA IN THE ARABIAN SEA

E. MASSERA BOTTAZZI, K. VIJAYAKRISHNAN NAIR and M. C. BALANI

Department of Zoology and Comparative Anatomy, Parma University, Italy
Health Physics Division, Atomic Energy Establishment Trombay, India
Received April 29, 1967

ABSTRACT

A taxonomical study on the Acantharia of the Indian Ocean has been carried out by means of the examination of four plankton samples collected with a plankton net in the Arabian Sea during the cruise of INS « Kistna » (August 1963). Percentage abundance of total Acantharia and relative frequency of different species are taken into consideration.

The Acantharia are a group of Protozoa characterized by their specific and unique capacity to concentrate strontium in their skeletal structures in place of calcium. Following the early work of Buetschli on the chemical nature of these protozoans, Schreiber confirmed the presence of strontium in their skeletal structures. In recent years with the increasing interest of « fallout », the radioecology of Acantharia and their role in distributing strontium in the marine environment have become subjects of renewed interest and investigation. In a programme of work sponsored by IAEA, Italian workers have taken an active part in studies on Acantharia in the Mediterranean. Records of Acantharia from Indian Ocean, however, are practically nonexistent. It was of interest, therefore, to find these protozoans in significant concentrations in plankton hauls at four stations in the XIII IIOE Cruise of INS « Kistna » (August 1963). The plankton collections were accomplished with a standard bolting silk plankton net of 50 cm diameter and No. 20 mesh, by making a vertical haul from 200-0 m. The percentage abundance of total Acantharia in the four samples is given in Table 1 and the relative frequency of different species at a station is given in Table 2.

TABLE 1. Percentage composition of Acantharia in four plankton samples

IIOE I.N.S. « Kistna » Station No.	*Position*		*Percentage*	*Displacement volume (cm³)*
296	03°00'N	71°30'E	0.02	1.00
298	00°50'N	71°15.5'E	1.12	1.50
299	00°05'N	71°29.3'E	12.34	10.50
304	02°00'N	75°00'E	2.39	2.75

TABLE 2. Relative frequency of different Acantharia species

Order	*Family*	*Species*	*Relative * frequency*
HOLACANTHA	ACANTHOCHIASMIDAE	*Acanthochiasma fusiforme*	+
	ACANTHOPLEGMIDAE	*Acanthoplegma krohni*	+
		Acanthocolla cruciata	++++
SYMPHYACANTHA	AMPHILITHIDAE	*Amphilithium clavarium*	++
		Amphibelone hydrotomica	++++
		Amphibelone anomala	++++
		Quadristaurus crux	+
CHAUNACANTHA	GIGARTACONIDAE	*Gigartacon muelleri*	++++
		Gigartacon sp.	+
		Heteracon biformis	++
ARTHRACANTHA sub order:			
SPHAENACANTHA	ACANTHOMETRIDAE	*Acanthometra pellucida*	+
		Acanthometra tetracopa	++
		Amphilonche elongata	++++
	LITHOPTERIDAE	*Lithoptera fenestrata*	+
	DORATASPIDAE	*Pleuraspis costata*	++++
		Lychnaspis giltschi	+++
		Lychnaspis polyancistra	+++
		Lychnaspis undulata	++++
		Lychnaspis maxima	++
		Lychnaspis serrata	+++

Table 2 (Contd.)

Order	*Family*	*Species*	*Relative * frequency*
		Icosaspis elegans	+
		Dorataspis loricata	++++
		Dorataspis gladiata	+++
		Dorataspis micropora	++
		Hystrichaspis dorsata	++++
		Dictyaspis solidissima	++
	HEXALASPIDAE	*Hexalaspis* sp.	++
		Hexaconus sp.	++
	DIPLOCONIDAE	*Diploconus fasces*	++++
	PHRACTOPELTIDAE	*Phractopelta dorataspis*	++
		Phractopelta sp.	++++
Sub order:			
PHYLLACANTHA	PHYLLOSTAURIDAE	*Phyllostaurus siculus*	++++
		Phyllostaurus siculus var. *catervatus*	++
		Phyllostaurus siculus var. *quadrifolius*	+
		Phyllostaurus cuspidatus	++++
		Amphistaurus complanatus	++++
		Amphistaurus tetrapterus	++
		Amphistaurus atlanticus	++
		Acanthostaurus purpurascens	++++
		Acanthostaurus conacanthus	++
		Lonchostaurus rombicus	++++
		Zygostaurus amphitectus	++
	STAURACANTHIDAE	*Xiphacantha quadridentata*	+
		Xiphacantha alata	+
		Stauracantha orthostaura	+

* The signs indicated correspond to the following codex:
++++ = 16 or more findings.
+++ = 8 to 15 findings.
++ = 3 to 7 findings.
+ = 1 to 2 findings.

ACKNOWLEDGEMENTS

We are grateful to the International Atomic Energy Agency, Vienna for partly financing this work under IAEA-AEET Research Contract No. 155/RB (Project Marina). Our thanks are due to Professor Schreiber, Parma University, Italy and Dr. A. K. Ganguly, Principal, Scientific Investigator, Project Marina for their keen interest in the work.

RIASSUNTO

GLI ACANTARI DEL MARE ARABICO

È stato fatto uno studio sistematico sugli Acantari dell'Oceano Indiano, esaminando quattro campioni di plancton raccolti nel Mar Arabico durante la Crociera dell'INS « Kistna » (agosto 1963). Si danno le percentuali degli Acantari totali, l'elenco delle specie e la loro relativa frequenza.

REFERENCES

Bottazzi Massera, E. 1964. Gli Acantari dell'Oceano Atlantico. Osservazioni sistematiche ed ecologiche. *Boll. Zool.* *31*(2), 1115-1123.

Buetschli, O. 1906. Ueber die chemische Natur der Skelettsubstanz der Acantharia. *Zool. Anz.* *30*, 784-789.

Haeckel, E. 1862. Die Radiolarien (Rhizopoda radiaria). Eine Monographie, mit 1 Atlas, Berlin.

Haeckel, E. 1887. Report on the Radiolaria collected by H.M.S. Challenger during the years 1873-1876. Pag. 716-888 London.

Haeckel, E. 1888. Die Radiolarien. Eine Monographie, 3° Teil. Die Acantharien oder Actypileen. Radiolarien, Berlin.

Massera Bottazzi, E. Vannucci, A. 1964. Acantharia in the Atlantic Ocean. A systematic and ecological analysis of planktonic collections made during Cruises Chain 17 and Chain 21 of the Woods Hole Oceanographic Institution. 1st Contribution. *Arch. Oceanogr. Limnol.* *13*, 315-385.

Massera Bottazzi, E. Vannucci, A. 1965. Acantharia in the Atlantic Ocean. A systematic and ecological analysis of plankton collections made during Cruise 25 of R. V. Chain, of the Woods Hole Oceanographic Institution. 2nd Contribution. *Arch. Oceanogr. Limnol.* *14*, 1-68.

Popofsky, A. 1904. Die Acantharia der Plankton Expedition. T. 1. Acanthometra, *Ergebn. Plankt. Exped. Humboldt*, *3*, L. f. α, 1-158.

Popofsky, A. 1905. Weiteres ueber die Acanthometriden der Plankton Expedition. *Arch. Protistenk.* *5*, 340-357; Taf. 14-15.

Popofsky, A. 1905. Die nordischen Acantharien. Th. 1. Acanthometriden. *Nord. Plankt.* *3*, 43-69.

POPOFSKY, A. 1906. Die Acantharia der Plankton Expedition. T. 2, Acanthophracta. *Ergebn. Plankt. Exped. Humboldt*, *3*, L. f. β, 1-160.

POPOFSKY, A. 1906. Ueber Acanthometriden des Indischen und Atlantischen Oceans. *Arch. Protistenk.* *7*, 345-394.

SCHEWIAKOFF, W. 1926. Die Acantharia des Golfes von Neaples. *Fauna u. Flora Neapel*, *37*.

SCHREIBER, B. CAVALCA, L. BOTTAZZI MASSERA, E. 1959. Ecologia degli Acantari e la circolazione dello Sr nel mare. *Boll. Zool.* *26*, 213-219.

SCHREIBER, B. 1960. Ecology of Acantharia and Strontium circulation in the sea. Disposal of Radioactive Wastes, I.A.E.A. 26-27.

SCHREIBER, B. BOTTAZZI MASSERA, E. FANO SCHREIBER, A. GUERRA, F. PELATI, L. 1962. Ricerche sulla presenza dello Sr nel plancton marino in rapporto alla ecologia degli Acantari. *Pubbl. Staz. zool. Napoli* *32* (suppl.), 400-426.

Reprinted from *The Emu*, vol. 76, Parts 1 and 2, 1967, p. 133-138

BIRDS SEEN AT SEA OFF N.W. AUSTRALIA JULY 23-30, 1965*

By ROGER POCKLINGTON

During Cruise 15 (International Indian Ocean Expedition and Cooperative Kuroshio Investigations) of the Woods Hole Oceanographic Institution vessel R/V Atlantis II, a regular bird-watch was maintained by Mr M. Palmieri, 2nd Mate, Mr P. R. Willis, Medical Officer, and myself. Our combined field-notes will eventually be presented as a Woods Hole Oceanographic Institution Data Report: what follows is a report on the small portion relevant to Australia.

Our cruise course paralleled the coast from Fremantle to NW. Cape then struck NE. towards Timor. A list of noon positions with distance and bearing to nearest land is given in Table 1.

TABLE 1

Day	Latitude	Longitude	Place	Distance n. miles	Bearing
23	29°21'S	113°31'E	Geraldton	70	065°
24	25°34'S	112°02'E	Dorre I.	50	090°
25	22°05'S	113°07'E	N.W. Cape	40	090°
26	19°03'S	115°41'E	Monte Bello Is.	80	190°
27	16°06'S	118°03'E	Lacepede I.	240	100°
28	13°28'S	120°12'E	Seringapatam Reef	90	100°
29	13°26'S	120°19'E	Adele I. (as above)	150	130°
30	11°02'S	122°00'E	Sawu I.	30	010°

Four hydrographic stations were occupied; the one complete one showed low nutrients—nitrate, phosphate and silicate—in the top 150 metres. Weather conditions were good; winds light and mainly from the SE. (100°-165°).

The birds seen are listed by species in Table 2.

No Albatross, Cape Pigeons, Prions, Great-winged or Soft-plumaged Petrels were seen north of 21°S., i.e. over waters warmer than 24·5°C., which indicates that the northern limit of range of these species, in the absence of strong winds or other accidents, can be correlated with sea surface temperatures of 23-25°C., as we found to be the case in the western portion of the Indian Ocean one month before. Such typically tropical species as *Puffinus pacificus*, the *Phaethontidae* and the *Fregatidae* were first encountered over waters warmer than 24·5°C.

* Contribution No. 1957 from the Woods Hole Oceanographic Institution. This work was done under N.S.F. grant 821.

Table 2

Day	Hour	Sea Surface Temperature	Latitude	Longitude	Species—Numbers—Remarks
			ALBATROSS		*Diomedea sp.*
23	0950	22·2			1 small, black and white
24	1640	22·8			3 black-backed, on water
25	1000	23·9	22°20′S	112°50′E	1, reported by watch
			YELLOW-NOSED ALBATROSS		*D. chlororhynchos*
23	1045	22·1			1, immature, black bill
24	0925	20·9			1, immature
	1520	22·5			1, immature
			CAPE PIGEON		*Daption capensis*
23	0830	22·2			1, flying with gad-fly petrels in wake
	1745	21·4			2, crossed bows
24	0800	19·3			2, reported by officer of the watch
25	1800	24·5	21°00′S	113°50′E	1, the last one seen
			PRION		*Pachyptila sp.*
23	0845	22·2			1
			WEDGE-TAILED SHEARWATER		*Puffinus pacificus*
26	0700	24·6	19°40′S	115°00′E	2, all dark
	1400		18°30′S	116°00′E	Two flocks of *ca.* 20 birds, half with light breast and bill light horn colour
27	0630				2, dark-breasted
	1230	25·2	16°50′S	117°30′E	1

TABLE 2 continued

Day	Hour	Sea Surface Temperature	Latitude	Longitude	Species—Numbers—Remarks
			GREAT-WINGED PETREL		*Pterodroma macroptera*
23	0720	22·2			2, close to ship, little white about the face
	0845				1, pursuing a *P. mollis*, forced it to disgorge a fish which the larger petrel ate on the water, wings extended
			SOFT-PLUMAGED PETREL		*Pterodroma mollis*
23	0700	22·2			6, close about ship
	0830				many about; light line on dark underwing
24	0700	20·4	26°30′S	112°05′E	12+, around all morning
	1310	22·8			1
	1520				2
25	0700	23·2			1
	1500	24·0	21°30′S	113°20′E	1
			WILSON'S STORM-PETREL		*Oceanites oceanicus*
28	1400	25·4	13°40′S	120°20′E	1, in flock of 5 *Oceanodroma sp.*
29	1210				3
30	1250	25·3			1, stayed until 1515 hours in the wake
			MATSUDEIRA'S STORM-PETREL		*Oceanodroma matsudeirae*
26	1330	24·6	18°50′S	115°50′E	A storm-petrel, all dark brown with lighter upper wing coverts, long wing and tail, direct flight with constant flapping, not trailing legs, was seen to land on the water for thrown food
	1500				2, as above

TABLE 2 continued

Day	Hour	Sea Surface Temperature	Latitude	Longitude	Species—Numbers—Remarks
			MATSUDEIRA'S STORM-PETREL		*Oceanodroma matsudeirae* (Cont)
27	1630	25·6	15°48′S	118°18′E	One specimen was collected from a flock of 30 feeding astern
28	1300	25·6	13°28′S	120°12′E	15+
	1400				5, with 1 *Oceanites oceanicus*
29	0635	25·2			12, criss-crossing wake
	1210				12, with 3 *O. oceanicus*
	1320		13°38′S	120°15′E	One collected from flock of 20
30	1250	25·3			2-6, around all afternoon
			TROPIC-BIRDS		*Phaethon sp.*
26	1500		18°30′S	116°00′E	1, adult, no long streamers, pink plumage
27	1630	25·6	15°48′S	118°18′E	*Phaethon lepturus*, 5, one collected and identified as *P. l, fulvus?*, apricot plumage
28	1315	25·7	13°28′S	120°12′E	*P. lepturus*, 2, pure white plumage
	1430				*P. lepturus*, 1, white plumes and tail
29	0635				*P. lepturus*, 1, white
	0845				*P. lepturus*, 1, close astern, apricot colour
			BOOBYS		*Sula sp.*
29	1340	25·2			1, at a distance, NOT *Sula leucogaster*
27	1800	26·0	15°30′S	118°50′E	1
			FRIGATE-BIRDS		*Fregatidae*
28	1420	25·7	13°28′S	120°12′E	3, hanging over a flock of terns. NOT male *F. minor*, probably *F. ariel*

TABLE 2 continued

Day	Hour	Sea Surface Temperature	Latitude	Longitude	Species—Numbers—Remarks
			FRIGATE-BIRDS		*Fregatidae* (Cont)
29	0630	25·2			1, at a distance
	0845		13°28′S	120°12′E	Three flew over ship; 2 were all-black male *F. minor*, other was male *F. ariel*, smaller with white thigh patches
	1505				3, females
			GREAT SKUA		*Catharacta skua*
23	0950	22·2			Last one seen going north
			TERNS		*Sternidae*
26	1210	25·0			1, large, grey above, white below, prob. *Thalasseus bergii* or *T. bengalensis*
28	1420	25·7	13°28′S	120°12′E	Flock of 12, either *Sterna fuscata* or *S. anaethetus*
29	1505	25·9			Sooty-type terns (*S. fuscata* and/or *anaethetus*, 1 distant flock of 10
30	0717	25·0			2, as above
	0740				*S. fuscata*, 14, diving over tuna but not getting into water
	0800				*S. fuscata*, 2
	1115				*S. fuscata*, flock of 10+

Wilson's Storm-Petrels were not encountered south of 14°S., but from there on they were seen in small numbers well into the Banda Sea.

The specimens of Matsudeira's Storm-Petrel, *Oceanodroma matsudeirae*, are, to our knowledge, the first for this species in the Indian Ocean. There are sight records of large, all-dark, fork-tailed Storm-Petrels from around the equator at all times of the year in the western Indian Ocean (Bailey, R., *R.R.S. Discovery III*, and Gill, F. B., *R. V. Anton Bruun*, pers. comm.) which are distinct from the dark-rumped race of Leach's Storm-Petrel, known as Swinhoe's Storm-Petrel, *Oceanodroma leucorhoa monorhis*, which has been collected off the Arabian coast (R. Bailey).

The finding of White-tailed, rather than Red-tailed, Tropic-birds in this region was rather a surprise to us. According to the reference books aboard (Alexander 1955, Fisher and Lockley 1954, Palmer 1962, Watson, Zusi and Storer 1963) the nearest known breeding colony of this species is on Christmas Island, 800 naut. miles West, and the apricot colour of the plumage of our specimen appears to indicate this race (*Phaethon lepturus fulvus*). It is interesting to note that in flight the tail-streamers, though broad, appeared pinkish and, if the small size of body and the extensive black patches on the upper-wing are not noticed, the bird might be recorded as *Phaethon rubricauda*, the Tropic-bird to be expected in the area (Serventy and Whittell, 1962).

The specimens of *Oceanodroma matsudeirae* and *Phaethon lepturus* (*fulvus?*) were delivered to the Division of Birds, U.S. National Museum, Washington, D.C., at the end of the cruise.

REFERENCES

Alexander, W. B. 1955. *Birds of the Ocean*, 2nd ed., Putnam, London.
Fisher, J. and Lockley, R. M. 1954. *Sea Birds*, Collins, London.
Palmer, R. S. Ed. 1962. *Handbook of North American Birds*, vol. 1, Yale University Press, New Haven and London.
Serventy, D. L., and Whittell, H. M. 1962. *Birds of Western Australia*, 3rd. ed., Paterson Brokensha, Perth, W.A.
Watson, G. E., Zusi, R. L., and Storer, R. W. 1963. *Preliminary Field Guide to the Birds of the Indian Ocean*, Smithsonian Institution, Washington, D.C.

Institute of Oceanography, Dalhousie University, Halifax, N.S., Canada.
Manuscript received: April 5, 1966.

Reprinted from *Applied Microbiology*, vol. 16, no. 5, 1968, p. 708-713

Correlation of Taxonomic Criteria for a Collection of Marine Bacteria

ROY M. JOHNSON, MARY E. KATARSKI,[1] AND WILLIAM P. WEISROCK[2]

Botany Department, Arizona State University, Tempe, Arizona 85281

Received for publication 8 February 1968

Numerical taxonomy was done on 208 strains of marine bacteria. The collection was segregated into eight groups, seven of which contained *Vibrio* spp. Nucleic acid base ratio studies on a typical *Vibrio* sp. from each group and other genera were done. The phenotypically different *Vibrio* sp. had a narrow range of base ratios. The other genera had base ratios more similar to the base ratios reported for their genus than to each other as marine bacteria. The taxonomic groups are compared with generic classification and the strains' sources of isolations.

During the eighth cruise of the *Anton Bruun* in the Indian Ocean, a collection of over 200 bacteria was made. The results of attempts to classify the gram-negative isolates even to genera on the basis of current (15) information proved conflicting. Accordingly, the isolates were characterized generically by minimal tests using currently accepted major criteria (Table 2). Subsequently, a numerical taxonomy study was done on the entire collection to examine the validity of the above-used generic criteria and to afford another approach to classification of the collection. Much of the early work with numerical taxonomy was done with established cultures either to validate the method or to investigate relationships of specific groups. Pfister and Burkholder (13) used numerical taxonomy on 151 isolates from seawater with a view to establishing a pattern of characteristics for future marine isolations. Splittstoesser et al. (20) similarly used numerical taxonomy to group bacteria isolated from frozen vegetables. Unfortunately, both apparently deleted 50 and 25% of their cultures, respectively, that did not fit the groups produced by the remaining strains. It was essentially this inability to group some gram-negative bacteria into discrete units that we wished to examine. Leifson (8) criticized numerical taxonomy as adding nothing new in principle to taxonomy; however, it can provide an excellent tool, when properly used to investigate possible correlations between taxonomic criteria of established taxonomic groups. The relationship of the deoxyribonucleic acid (DNA) base composition and numerical analysis examined by Colwell and Mandel (3) is an example of this use.

[1] Present address: Department of Microbiology, University of California at Los Angeles, Calif.

[2] Trainee on Public Health Service grant TT-A-1259. Present address: Department of Microbiology, Washington State University, Pullman, Wash.

Materials and Methods

Organisms. A total of 208 bacteria isolated from seawater, mud, fish, shark, and an island in the Indian Ocean was studied. The strains were coded as to source of isolation with 100 being seawater, 200 mud, 300 fish, 400 shark, and 500 an island. The details of their isolation have been reported elsewhere (7).

Determination of properties. The 50 properties for each strain were examined (Table 1). All media were made with artificial seawater, except Chapman Stone (Difco) which was made with distilled water. Flagella stains were done by the method of Rhodes (14). The base medium for all tests contained 0.5% peptone and 0.05% yeast extract in artificial seawater (Aquarium Systems Inc., Wickliffe, Ohio). Antibiotic sensitivity was determined with standard BBL sensitivity discs impregnated with low levels of concentration for each antibiotic. Pteridine 0/129 was applied as a saturated solution to sterile filter-paper discs. Routine tests were done according to the *Manual of Microbiological Methods* (18) or Skerman (16). Lysine decarboxylase was examined with "pathotec" strips (Warner-Chilcot Laboratories, Richmond, Calif.).

Numerical analysis. The per cent similarity was computed according to the method of Sneath (17):

$$\%S = Nsp/(Nsp + Nd) \times 100$$

where $\%S$ = similarity coefficient; Nsp = number of similar positive matches; and Nd = number of dissimilar matches. The card. Fortran program was written by Paul Fisher at the Arizona State Computer Center and programmed on a General Electric 225 computer. Grouping of the values was done with the method of single-linkage clustering (19) by the investigator after inspection of the individual strain values. The 60% similarity level was used for grouping because inspection of the data showed only a few strains

TABLE 1. *Properties used in the characterization of marine bacteria*

General	*Carbohydrates*	*Antibiotics*
Gram stain	Acid from glucose	Chloramphenicol sensitive
Oxidase-positive	Acid from lactose	Tetracycline sensitive
Catalase-positive	Acid from xylose	Penicillin sensitive
Growth on McConkeys	Acid from arabinose	Erythromycin sensitive
Growth on SS agar	Gas from carbohydrates	Pteridine 0/129 sensitive
Growth on Chapman Stone	Oxidative glucose metabolism	
Growth on blood-agar	Fermentative glucose metabolism	*Miscellaneous*
Hemolysis on blood	Starch hydrolyzed	Pigment
Morphology	Cellulose utilized	Red
Rod or coccus	Chitin utilized	Yellow
Normal or pleomorphic	Inhibition by 5 carbon sugar	Violet
Flagella	*Nitrogen metabolism*	Other
Length	H_2S produced	Growth temperature
Polar	Gelatin hydrolyzed	Over 0 C
Lateral	Casein hydrolyzed	Over 20 C
Peritrichous	Indole produced	Over 40 C
Motile, not motile	Urease-positive	Luminescence
Spores present	Nitrate reduced	Require 0.1% agar for growth
Colony size	Lysine decarboxylase-positive	
Colony opaque		

TABLE 2. *Differential generic characteristics used for bacteria with bacillus-like morphology*

Genus	Gram stain	Spores	Pigment	Flagella	Hugh-Leifson glucose	Pteridine 0/129 sensitivity	Luminescence
Bacillus	+	+	+(−)	Peritrichous	No growth	(−)	(−)
Brevibacterium	+	(−)	+(−)	Peritrichous	No growth	+(−)	(−)
Corynebacterium	+	(−)	(−)	Variable	No growth	(−)	(−)
Pseudomonas	(−)	(−)	(−)	Polar	Oxidative	(−)	(−)
Xanthomonas	(−)	(−)	+	Polar	Oxidative	(−)	(−)
Achromobacter	(−)	(−)	(−)	Variable	Fermentative	(−)	(−)
Flavobacterium	(−)	(−)	+	Variable	Fermentative	(−)	(−)
Alcaligenes	(−)	(−)	(−)	Variable	Negative	(−)	(−)
Vibrio	(−)	(−)	(−)	Polar	Fermentative	+	+(−)
Spirillum	(−)	(−)	(−)	Bipolar	No growth	(−)	(−)
Photobacterium	(−)	(−)	(−)	Variable	Fermentative	(−)	+
Hyphomicrobium	(−)[a]	(−)	(−)	Polar	Fermentative	(−)	(−)

[a] Characterized by pleomorphic cells and budding.

above the 80% similarity level and virtually a continuum at the 50% similarity level.

Base ratio studies. DNA was isolated according to the method of Marmur (10) with Sipex (Alcolac Chemical Corp., Baltimore, Md.) for lysis of the cells. The base composition of the DNA was determined by the thermal denaturation method of Marmur and Doty (11), with the use of a Coleman Autoset spectrophotometer equipped with a special cuvette holder for temperature control.

RESULTS

Figure 1 shows the sorted and reordered matrix in which eight major groups can be observed. Table 2 gives the major criteria used to determine genera of the collection as reported in Table 3. Table 3 summarizes the characteristics of each group. At the 60% *S* value, strains of each group are interrelated with at least one other group (Fig. 1). Groups 4, 5, 6, and 7 may indeed be considered one group, and this is emphasized by group 6 which contains strains showing relationship at the 70% level to both groups 5 and 7.

The large number of organisms between group 3 and 4 include most of the genera in other groups plus some cocci. They relate in general below the 60% level to the rest of the collection and to each other. They appear to provide a logical continuum from the first three predominantly gram-positive groups to the last groups which are all gram-negative.

The following points from Table 3 appear significant: (i) The genus *Vibrio* was found in every

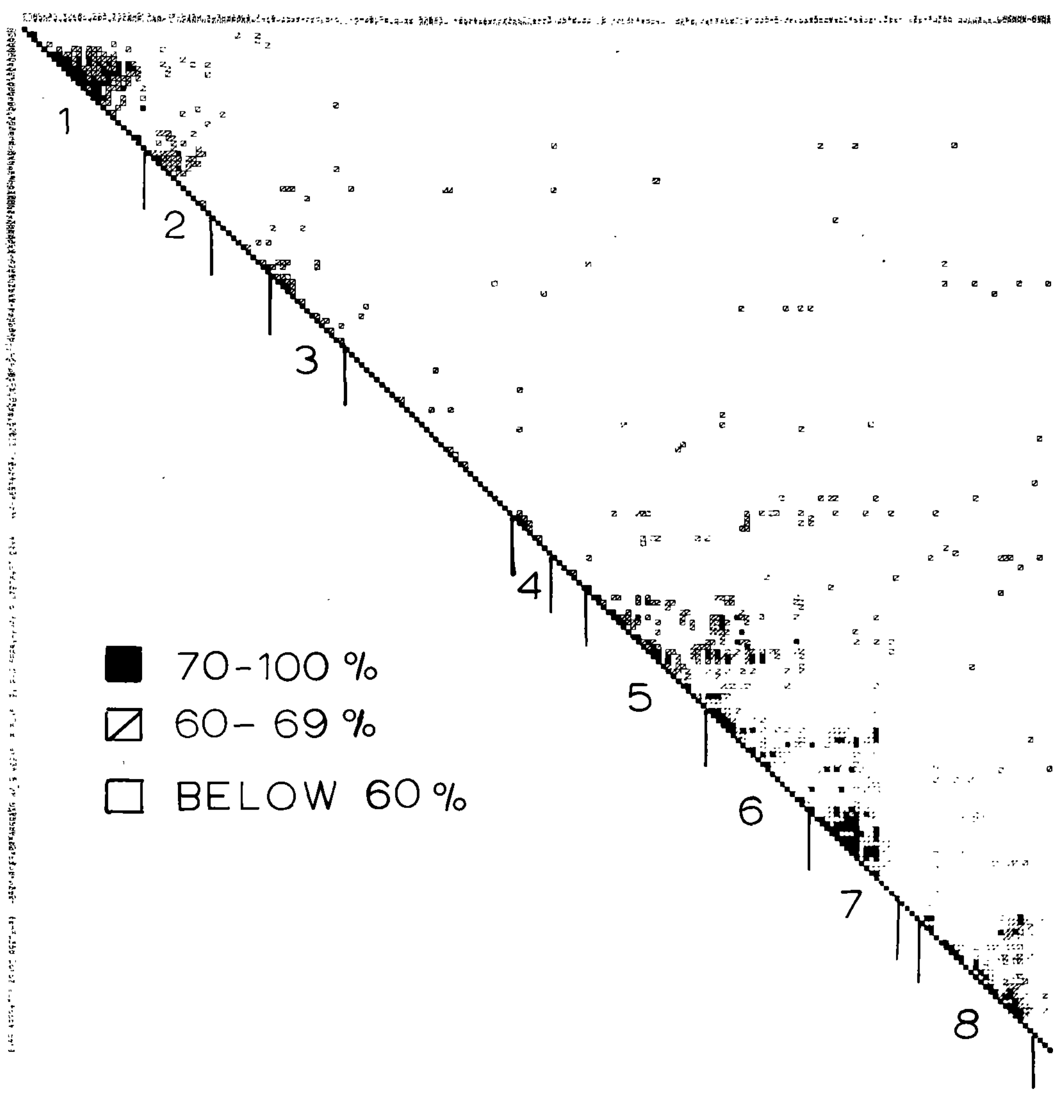

FIG. 1. *Matrix sorted and reordered by single linkage technique. Eight major groups are indicated. Values less than 60% were not plotted.*

group, except the one small *Pseudomonas* group (4). (ii) Strains from both shark and land are associated only with the first three groups which are predominantly gram-positive. (iii) All luminescent bacteria (genus *Vibrio* or *Photobacter*) are in one group (group 8). (iv) Group 6, showing the greatest crossing of similarity between groups, contains strains isolated primarily from marine mud. (v) Group 2, *Brevibacterium* shows a high correlation with a mud habitat. (vi) Pigment appears to be of little significance in grouping bacteria, as pigmented forms are found in most groups. (vii) Groups 7 and 8 isolated predominantly from fish intestine have no pigment, attack glucose, and are essentially either *Vibrio* or *Achromobacter* genera.

The wide distribution of the *Vibrio* genus, as well as the suggestion by Belser that marine bacteria may have a common narrow range of base ratio (1), prompted an examination of the base ratio of strains from each group. The majority of *Vibrio* strains are in the 35 to 40% guanine plus cytosine (GC) range (Table 4); the *Pseudomonas* strains are characteristically above this, whereas the remaining genera cover a range

TABLE 3. *Analysis and characteristics of numerical groups*

Group	No. of isolates	Genus	No.	Source	No.	Unique group characteristics[a]
1	25	*Bacillus*	18	Water	8	Catalase-positive
		Corynebacterium	4	Mud	4	
		Vibrio	2	Fish	2	
		Brevibacterium	1	Shark	10	
				Land	1	
2	12	*Brevibacterium*	11	Water	1	Sensitive, 5 antibiotics
		Vibrio	1	Mud	10	
				Land	1	
3	18	*Alcaligenes*	5	Water	7	Starch (−)
		Pseudomonas	4	Mud	3	
		Vibrio	3	Fish	3	
		Brevibacterium	2	Shark	1	
		Corynebacterium	2	Land	4	
		Bacillus	1			
		Achromobacter	1			
4	8	*Pseudomonas*	8	Water	4	Resistant to tetracycline, penicillin, erythromycin, pteridine 0/129; catalase-positive, chitin-positive, xylose-negative, arabinose-negative
				Mud	4	
5	25	*Alcaligenes*	10	Water	9	Resistant to tetracycline and penicillin; nitrate-negative
		Pseudomonas	5	Mud	8	
		Vibrio	4	Fish	8	
		Flavobacterium	3			
		Achromobacter	3			
6	20	*Achromobacter*	8	Water	2	Resistant to tetracycline, oxidase-positive
		Alcaligenes	6	Mud	16	
		Pseudomonas	2	Fish	2	
		Vibrio	2			
		Hyphomicrobium	1			
		Flavobacterium	1			
7	19	*Achromobacter*	11	Water	5	Glucose-positive, no pigment, gelatin-positive, and nitrate-positive
		Vibrio	6	Mud	2	
		Spirillum	2	Fish	12	
8	28	*Vibrio*	15	Water	10	Glucose-positive, no pigment, fermentative, and luminescent
		Photobacterium	6	Mud	1	
		Achromobacter	6	Fish	17	
		Flavobacterium	1			

[a] Characteristics possessed by all but one or two strains of the group.

more characteristic of their genus than of their marine origin.

DISCUSSION

It is not our purpose to review the present status of the art of classification of nonmedical gram-negative bacillus. The separation of gram-positive genera from each other and the gram-negative bacteria at the 60% level is taken as a control for the numerical analysis. Liston (9) further suggested the 60% similarity level for generic groups. The 32 isolates between groups 3 and 4 include all genera of the collection, except *Bacillus* and *Pseudomonas*. Two *Sarcina* spp. and one *Micrococcus* sp. are also in this group. As individual strains, these isolates have little in common; as a group, they appear to represent a transition from gram-positive to gram-negative bacteria and, perhaps, as Wood (21) has suggested based on other data, a transition from land and mud bacteria to seawater and fish bacteria. The appearance of *Vibrio* spp. in every group except one is considered significant in

TABLE 4. *Base ratio of typical generic strains within each group*

Group	Strain	Genus	Per cent GC		
			Vibrio	*Pseudomonas*	Other
1	360	*Vibrio*	39.3 (85.4)[a]		
2	237	*Brevibacterium*			37.0 (84.5)
3	110	*Vibrio*	40.7 (86.0)		
	339	*Pseudomonas*		64.3 (95.7)	
	505	*Bacillus*			43.6 (87.2)
4	156	*Pseudomonas*		43.0 (87.0)	
5	330	*Vibrio*	37.0 (84.5)		
	234	*Pseudomonas*		59.0 (93.5)	
6	319	*Alcaligenes*			58.3 (93.2)
	213	*Vibrio*	35.8 (84.0)		
	111	*Achromobacter*			44.3 (87.5)
	243	*Pseudomonas*		52.2 (90.7)	
	208	*Hyphomicrobium*			40.0[b]
	209	*Pseudomonas*		34.6 (83.5)	
7	353	*Vibrio*	39.4 (85.5)		
8	305[c]	*Vibrio*	39.5 (85.5)		
	306	*Vibrio*	39.0 (85.3)		
	307	*Vibrio*	43.1 (87.0)		
	329[c]	*Vibrio*	39.5 (85.5)		
	313[c]	*Photobacterium*	37.5 (84.8)		
Intergroup	510	*Micrococcus*			45.6 (88.0)
	368	*Vibrio*	39.5 (85.5)		
	231	*Flavobacterium*			60.5 (94.1)
	509	*Flavobacterium*			37.5 (84.7)
	182	*Achromobacter*			35.8 (84.0)

[a] Value in parentheses is T_m obtained in standard saline citrate.
[b] Value obtained by M. Mandel with buoyant density procedure.
[c] Luminescent.

view of other findings regarding the genus *Vibrio*. Colwell and Liston (2) found the same spread of *Vibrio* spp. in their work and attributed this to "oxidative and pigmented Vibrio." All of our *Vibrio* spp., however, are nonoxidative and nonpigmented. Both DeLey's review article (5) and the study of *Vibrio* spp. by Davis and Park (4) indicate that *Vibrio* spp. are phenotypically variable with a wide range of nucleic acid base ratios. Marmur et al. (11) reported base ratios for *Vibrio* spp. from 42 to 66% GC, suggesting the same interspersed spread of this genus. In spite of their phenotypic difference, our *Vibrio* spp. showed a narrower per cent GC, from 36 to 43. The characteristic pleomorphism of *Vibrio* sp. reported by Hallock (6) may provide a morphological corollary for this variability.

Flavobacter sp. have also been shown by Marmur et al. (12) to vary in base composition from 32 to 70% GC. Our data showed no grouping of pigmented bacteria, and Pfister and Burkholder (13) grouped only 6 of 76 as *Flavobacter* sp. This would suggest that pigment should not be used as a significant taxonomic criterion. The potential significance of habitat on taxonomy can be seen in groups 7 and 8. These strains obtained essentially from fish intestine could essentially be classified as *Vibrio* sp. with two variations: (i) luminescent (all *Photobacter* sp. and some *Vibrio* sp.); and (ii) pteridine 0/129 resistant (all *Achromobacter* sp.). The relationship of *Brevibacterium* sp. to mud is obvious in group 2 where the one water isolate is the one *Vibrio* sp. In conclusion, the relationship between all groups at the 60% level (Fig. 1) suggests a continuum of marine bacteria with all possible intergeneric strains. That such should be the case when isolating members of the largest group of bacteria (gram-negative rods) from the acknowledged site of the origin of all life should not be surprising. When generic criteria, established on evolved land and pathogenic bacteria, are applied to such marine isolates, it can be anticipated that some confusion will result. It is also apparent that the genus *Vibrio* is likely to be the major problem in the classification of marine gram-negative bacteria.

ACKNOWLEDGMENTS

This research was supported by a grant from the Arizona State University research committee.

The National Science Foundation supported the collection of bacteria used.

Pteridine 0/129 was graciously supplied by Alan Hanbury Ltd.

LITERATURE CITED

1. Belser, W. L. 1963. DNA base composition as an index to evolutionary affinities in marine bacteria. Evolution **18**:177-182.
2. Colwell, R. R., and J. Liston. 1961. Taxonomic relationships among the pseudomonads. J. Bacteriol. **82**:1-14.
3. Colwell, R. R., and M. Mandel. 1964. Adansonian analysis and deoxyribonucleic acid base composition of some gram-negative bacteria. J. Bacteriol. **87**:1412-1422.
4. Davis, G. H. G., and R. W. A. Park. 1962. A taxonomic study of certain bacteria currently classified as Vibrio species. J. Gen. Microbiol. **27**:101-119.
5. DeLey, J. 1964. Pseudomonas and related genera. Ann. Rev. Microbiol. **18**:17-36.
6. Hallock, F. A. 1959. The coccoid stage of vibrios. Trans. Am. Microscop. Soc. **78**:231-236.
7. Johnson, R. M., R. M. Schwent, and W. Press. 1968. The characteristics and ecological distribution of marine bacteria isolated from the Indian Ocean. Limnol. Oceanog., *in press*.
8. Leifson, E. 1966. Bacterial taxonomy: a critique. Bacteriol. Rev. **30**:257-266.
9. Liston, J. 1960. Some results of a computer analysis of strains of Pseudomonas and Achromobacter and other organisms. J. Appl. Bacteriol. **23**:391-394.
10. Marmur, J. 1961. A procedure for the isolation of deoxyribonucleic acid from microorganisms. J. Mol. Biol. **3**:208-218.
11. Marmur, J., and P. Doty. 1962. Determination of the base composition of deoxyribonucleic acid from its thermal denaturation temperature. J. Mol. Biol. **5**:109-118.
12. Marmur, J., S. Falkow, and M. Mandel. 1963. New approaches to bacterial taxonomy. Ann. Rev. Microbiol. **17**:329-372.
13. Pfister, R. M., and P. R. Burkholder. 1965. Numerical taxonomy of some bacteria isolated from Antarctic and tropical seawaters. J. Bacteriol. **90**:863-872.
14. Rhodes, M. E. 1958. The cytology of Pseudomonas spp. as revealed by a silver-plating staining method. J. Gen. Microbiol. **18**:639-648.
15. Shewan, J. M. 1963. The differentiation of certain genera of gram-negative bacteria frequently encountered in marine environments, 499-521. *In* Carl H. Oppenheimer [ed.], Marine Microbiology. Chas. C Thomas, Publisher, Springfield, Ill.
16. Skerman, V. B. D. 1959. A guide to the identification of the genera of bacteria. The Williams & Wilkins Co., Baltimore, Md.
17. Sneath, P. H. A. 1957. The application of computers to taxonomy. J. Gen. Microbiol. **17**:201-226.
18. Society of American Bacteriologists. 1957. Manual of microbiological methods. McGraw-Hill Book Co., Inc., New York.
19. Sokal, R. R., and P. H. A. Sneath. 1963. Principles of numerical taxonomy. W. H. Freeman & Co., San Francisco.
20. Splittstoesser, D. F., M. Wexler, J. White, and R. R. Colwell. 1967. Numerical taxonomy of gram-positive and catalase-positive rods isolated from frozen vegetables. Appl. Microbiol. **15**:158-162.
21. Wood, E. J. F. 1953. Heterotrophic bacteria in marine environments of Eastern Australia. Australian J. Marine Freshwater Res. **4**: 160-200.

Reprinted from *Bull. natn. Inst. Sci. India*, no. 38, 1968, p. 319-323

OBSERVATIONS ON THE SCATTERING LAYERS OVER THE CONTINENTAL SHELF OFF KONKAN COAST (INDIA)

by V.S. RAMA RAJU

Physical Oceanography Division, National Institute of Oceanography, Ernakulam

The echograms obtained by R.V. "VARUNA" using asdic during the September, 1963 cruise are analysed. Scattering layers observed over the shelf area, off Ratnagiri, are examined and studied in relation to the thermocline layer present. Comparison of the reflections from the layers in the thermocline region with similar observation in the North Sea has indicated that the layers are not directly due to the physical discontinuity.

INTRODUCTION

Extensive sound scattering layers are observed in many parts of the world oceans in deeper waters (day time layer depths 200—800 m) and few in shallow waters. Hersey and Moore (1948) summarized the results of observations of the scattering layers in the Atlantic Ocean and attributed their origin to biological agency plankton, especially euphausids from the evidence of net hauls. Weston (1958) reported in his paper a strong and extensive scattering layer at the thermocline depth in shallow water (depth about 37 fathoms) in the North Sea and proved by calculation that these layers are not directly related to physical discontinuity and therefore plankton or fish feeding on plankton is the probable source. Some of the earlier observers noticed the continuity of the layers over wide areas and their location sometimes coinciding with sharp temperature or density discontinuity; and thought the origin is possibly due to physical parameter such as temperature or density. But the more recent investigations have positively contributed to the idea that these layers are due to biological source, although there exist different layer types in different locations and they vary with time. Also the layers are not always caused by the same organisms and the sound reflective physical properties of the organisms under the observation conditions are not certain. It is known that, at least in some cases, the trawling operations conducted at locations where the scattering layers were observed by means of echo sounder or asdic have resulted in increased catches (Barnes 1959).

The present studies have been made from the echo sounder and asdic records of R.V. "VARUNA" obtained during the trawling operations. The scattering layers obtained in these records are quite interesting from the point of view of their occurrence at shallow depths, their vertical movements, their wavy pattern and also because of their double layered characteristics.

DESCRIPTION AND EXAMINATION OF THE LAYERS

The layers are recorded by asdic (Simrad type) on 20th and 21st September, 1963 and they extend at least over a distance of fifty miles to the north and north-east of 16°26′ N, 72°49′ E over the continental shelf where the bottom depth varied between 20 and 80 m. The asdic was in use for fish detection at trawling stations and in between the oceanographic stations. It has a scale range of 0-1500 m, frequency 30 KC. per second and chart speed 2 cm per minute. In operation the transducer of the asdic is lowered by about 1/2 m below the keel and the beam can be swept through 140°. The face of the transducer is slightly inclined from the vertical plane and the ultrasonic sound beam makes an angle of 3° downward with the horizontal. The beam width is 17°. The signal or ping length expressed as travel distance in water is about 10 m. The draught of the ship is 3.4 m and so only the scatterers below this depth are recorded.

The vertical temperature variation of the waters observed at the same time with reversing thermometers shows a small increase of temperature (0.5 to 1°C) with depth in the surface layer up to 10 m, and the thermocline layer thickness is 10 to 30 m with its upper surface at about 10 m depth. The thermocline layer shoaled towards the shore. The steepest temperature gradient in the thermocline is 0.33°C per metre. The thickness of the thermocline layer at different locations is shown in figures 1, 2, 3 and 4 along with the spatial and temporal variations of the scattering layer depths.

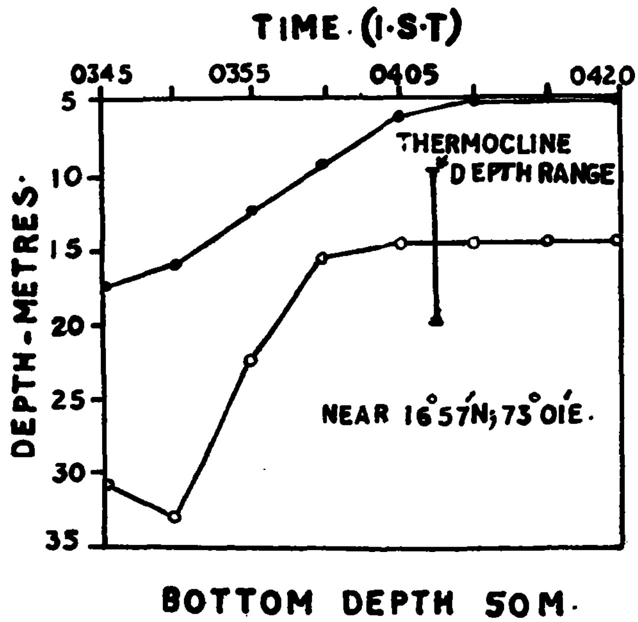

FIG. 1. Spatial and temporal variations of the depths of the scattering layers showing upward migration on 20th Sept, 1963. Ship underway at 8 Knots.

An examination of the records taken on 20th September by the asdic run in between the oceanographic stations from 0345 to 0735 hrs. (IST) reveals clearly the two reflective layers in the mid water and the sea bottom sounded by the echo sounder is definitely at a greater depth. These two layers are at a mean depth of 11 and 18 m. As the ship sailed west-ward, the upper layer present at 17 m at 0345 hrs. moved to the surface by 0400 hrs. and merged with the signal record of the outgoing pulse; and the lower layer also moved upwards from 30 m to 14 m depth. Similar vertical migration of the layers that do not seem to have any clear relation with the illumination of the water can be observed in all the figures. An interesting point noted from the records is that the sound scatterers observed in shallow water at a single level bifurcated to two levels, one moving upward and the other downward and later on maintained separate levels more or less parallel to one another, at least for some time. The bifurcation is clearly illustrated in figures 2 and 3.

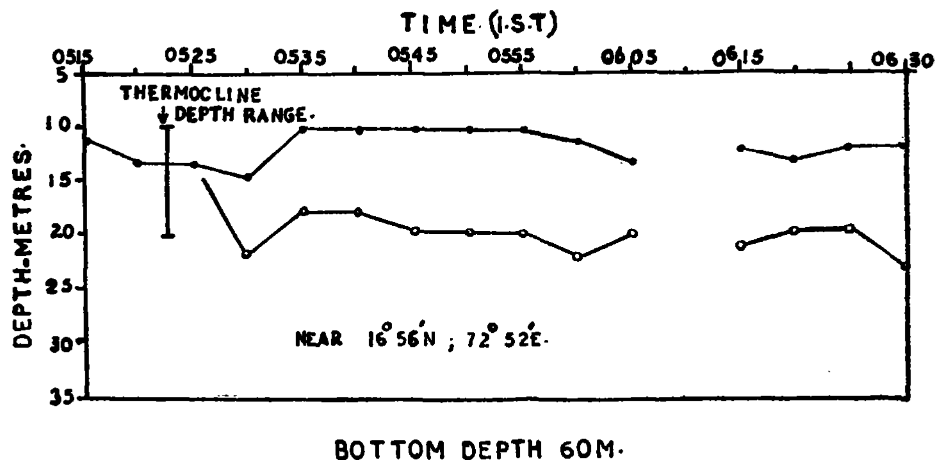

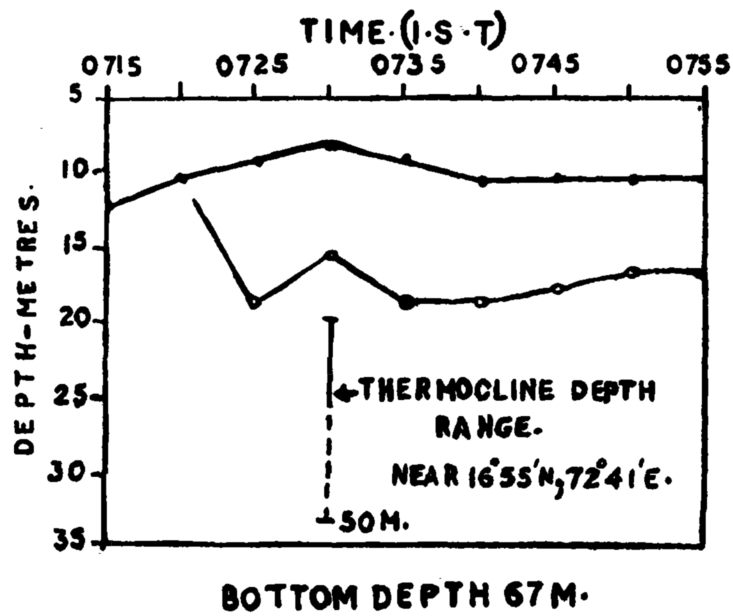

FIGS. 2, 3. Spatial and temporal variations of the depths of the scattering layers showing bifurcation of a single layer recorded on 20th Sept, 1963. Ship underway at 8 Knots.

The scattering layers are not always found in the region of the thermocline. Also it is difficult to ascertain exactly from the available data, from which part of the thermocline the reflections are arising. However, the records taken from 0515 to 0550 hrs. (IST) on 20th September, show that the scatterers are mostly confined to the thermocline and the bifurcated levels of the layers are situated near the top and bottom of the thermocline. And the temporal variation of the layer observed on 21st September shows that its level is mostly confined to the upper half of the thermocline. This particular record also shows superimposition of wave form on the layer suggesting that the scatterers are plausibly riding on an internal wave. The analysis reveals that the wave has periods varying between 2.5 and 7.5 minutes and heights between 2.0 and 8.0 metres. The mean period calculated is 3.5 minutes and wave height 4.5 metres. Well-defined wave forms superimposed on scattering layers caused by small organisms were recorded by echo sounder of frequency 30 KC per second in the shelf area off the Angola Coast (Vasco Valdez 1960).

The layers observed are, in general, diffuse in character and the few records obtained in the early hours of the day missed observations at sun rise. But the migration of the Deep Scattering Layers in the vertical with changes in illumination in the Sea water is well known.

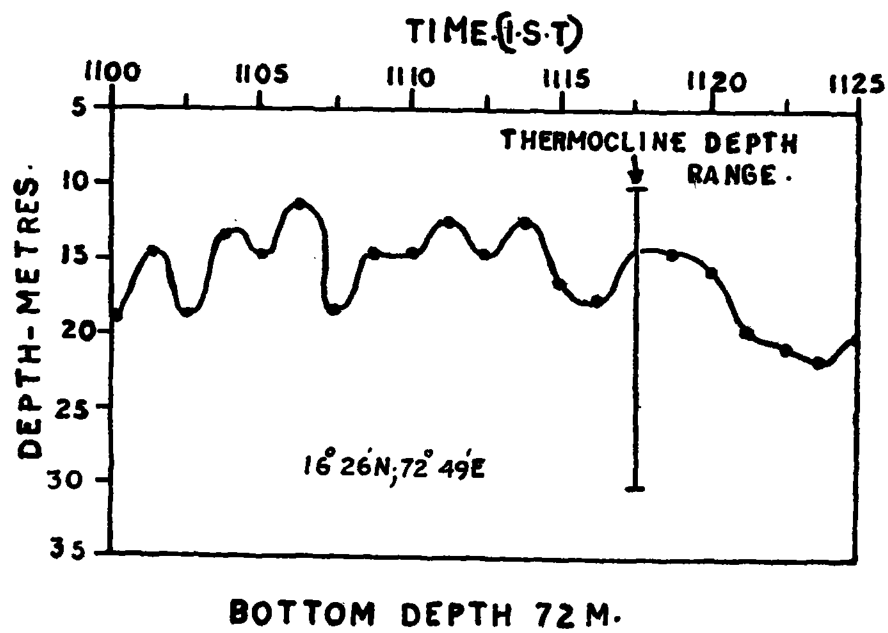

FIG. 4. Wave pattern of the shallow scattering layer recorded on 21st Sept. 1963. Ship trawling at about 0.5 Knot.

DISCUSSION

Ever since the scattering layers were recognized in 1942, various attempts are made to find out by direct and indirect means the exact source responsible for causing these so-called phantom bottoms on the echograms. These layers exist in most parts of the deep oceans (Dietz 1962). There are two main possibilities for a sound pulse sent down from a transducer getting reflected from the water layers. These are (1) a thermocline layer in which the temperature decreases rapidly with depth and consequently increases the density of the water column acting as a semi-reflector of sound waves and, (2) the presence of organisms containing air bladders which act as effective reflectors or organisms present in sufficient concentration and having chitinised carapace. Weston (1958) in his study of the scattering layer in the North Sea observed with a transducer of frequency 10 KC. per second at a thermocline of exceptionally steep gradient (2°C per metre) has proved that the density discontinuity is ineffective reflector. Comparing the present observed physical conditions clearly reveals that the reflections cannot be due to the physical discontinuity. Therefore, the shallow scattering layers observed must be due to some small organisms (such as euphausids, myctophids, etc.).

ACKNOWLEDGEMENTS

The author is grateful to the Indo-Norwegian Project, Ernakulam, for facilities given for this study and to Dr. N. K. Panikkar, Director, Indian Programme of the International Indian Ocean Expedition, for encouragement.

REFERENCES

Barnes, H. (1959). Oceanography and Marine Biology, George Allen Unwin Ltd.

Dietz, R.S. (1962). The Sea's Deep Scattering Layers—Scientific American, August, 1962.

Hersey, J.B., and Moore, H.B. (1948). Progress Report on scattering layer observations in the Atlantic Ocean. *Trans. A.G.U.*, **29**, 341-354.

Vasco Valdez (1960). Internal Waves on an echo sounder record. *Deep Sea Res.*, **7**, 148.

Weston, D.F. (1958). Observations on a scattering layer at the thermocline. *Deep Sea Res.*, **5**, 44-50.

Reprinted from *Bull. natn. Inst. Sci. India*, no. 38, 1968, p. 575-584

PRELIMINARY REPORT ON THE GEOGRAPHICAL DISTRIBUTION OF THE SPECIES OF CARINARIIDAE AND PTEROTRACHEIDAE (HETEROPODA, MOLLUSCA) FROM THE INTERNATIONAL INDIAN OCEAN EXPEDITION

by P. N. ARAVINDAKSHAN
Indian Ocean Biological Centre, National Institute of Oceanography, Cochin-16, S. India

This is a description of the distribution in the Indian Ocean of species belonging to two families of the Heteropoda, the Carinariidae and Pterotracheidae. The observations are based on plankton collected by *Anton Brunn, Argo, Pioneer* and *Vityaz* during the IIOE. The samples obtained by these vessels provide broad coverage of the Indian Ocean, including the Arabian Sea and Bay of Bengal and southward to 40° S. Beyond 40° S there were only three collections and these contained no specimens. Pterotracheids outnumber the Carinariids in abundance. The four species of the genus *Carinaria, Cardiapoda richardi, Pterotrachea scutata* and *Pt. minuta* deserve special mention because of their low density in the Indian Ocean. Most abundant and widely distributed are *Firoloida desmaresti* and *Pterotrachea hippocampus. Pterosoma planum* and *Cardiapoda placenta* appear to be more restricted to the tropical zone. The identification of the specimens is mainly based upon Tesch (1949).

INTRODUCTION

This paper is the first result of a continuing study of heteropod molluscs sorted out from the plankton collections deposited at the Indian Ocean Biological Centre by the nations that participated in the International Indian Ocean Expedition, 1960-1965. The heteropod molluscs are of particular interest because of their modifications for a pelagic mode of life. The three families, Atlantidae, Carinariidae and Pterotracheidae, are seen to be in a clear phylogenetic line when we take into consideration their shell-structure. In the case of Atlantidae the animal lives encased in the shell, in Carinariids the shell is much reduced, and in Pterotracheids it is absent. The Heteropoda is a small group, but it presents difficulties inasmuch as some forms lack clear diagnostic characters. Though the earliest publications are of limited use now, much knowledge of the group is obtained from the works of Smith (1888); Bonnevie (1920) and Tesch (1906, 1910, 1949). It was Tesch who arranged all the species in a systematic manner and largely solved the problems of identification. Dales (1952) has published a paper on the distribution of Carinariidae and Pterotracheidae off the Pacific coast of North America. Tokioka (1955) and Okutani (1957, 1961) have published a few papers on the heteropods of the Japanese waters.

Material Studied

The present discussion is limited to a consideration of Carinariidae and Pterotracheidae collected by the research vessels *Anton Brunn*, *Argo*, *Pioneer* and *Vityaz*. The area surveyed included the Arabian Sea, the Bay of Bengal and most of the rest of the Indian Ocean (Fig. 1), the southernmost collections being from a little beyond 40° S. Since only about one-fourth of the total samples on hand at the Indian Ocean Biological Centre have been examined for heteropods thus far the present paper is a preliminary one. The patterns of distribution as they appear at this stage of study will be indicated. From the 535 samples analysed till now, all the twelve species enumerated by Tesch (1949) have been obtained. The list of the species, the total number of stations at which each was represented and the total number of specimens present in all these stations together, are given below :

Species	Total number of stations	Total number of specimens in all stations together
Carinaria lamarcki challengeri	1	2
C. cristata	2	2
C. galea	1	1
C. cithara	6	6
Pterosoma planum	32	45
Cardiapoda placenta	43	143
C. richardi	1	1
Pterotrachea coronata	16	27
Pt. hippocampus	64	155
Pt. scutata	1	1
Pt. minuta	2	2
Firoloida desmaresti	206	1252

Review of Distribution of Species

Family Carinariidae

This family comprises three genera: *Carinaria, Ptrerosoma* and *Cardiapoda.* Not a single specimen was collected with the shell intact. Though the shell of *Carinaria* is more relied upon for identification characters, the soft parts also give certain clues. Of the three genera in this family, *Pterosoma* and *Cardiapoda* are more frequently represented than *Carinaria.*

Genus Carinaria *Lamarck* 1801

This includes four species: *Carinaria lamarcki* (with one variety, *Carinaria lamarcki challengeri*), *C. cristata, C. galea* and *C. cithara.* Of these *C. cithara* is more common in the Indian Ocean. Figure 2 shows the localities of capture of Carinaria.

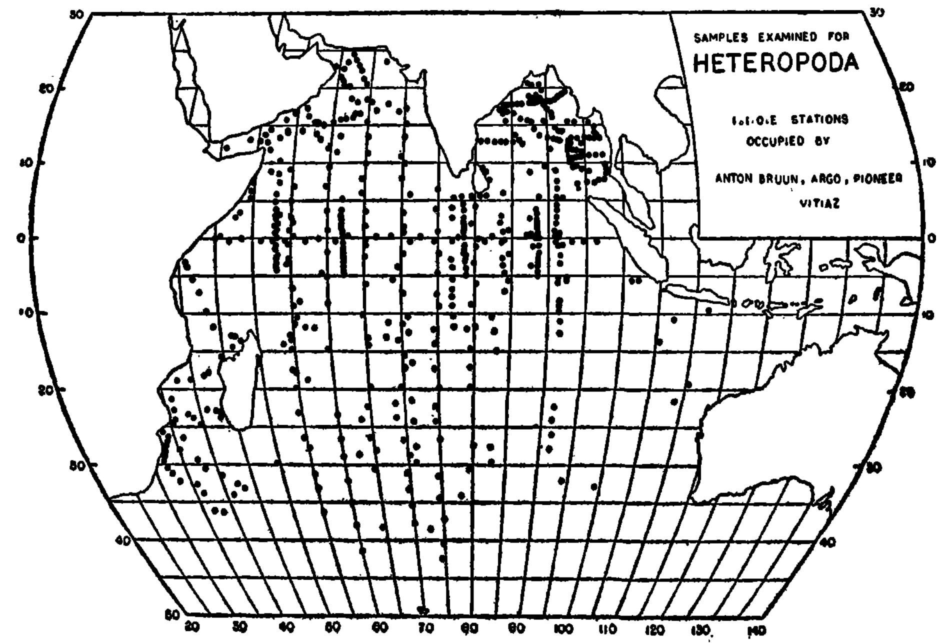

FIG. 1. I.I.O.E. stations occupied by *Anton Bruun, Argo Pioneer* and *Vityaz.*

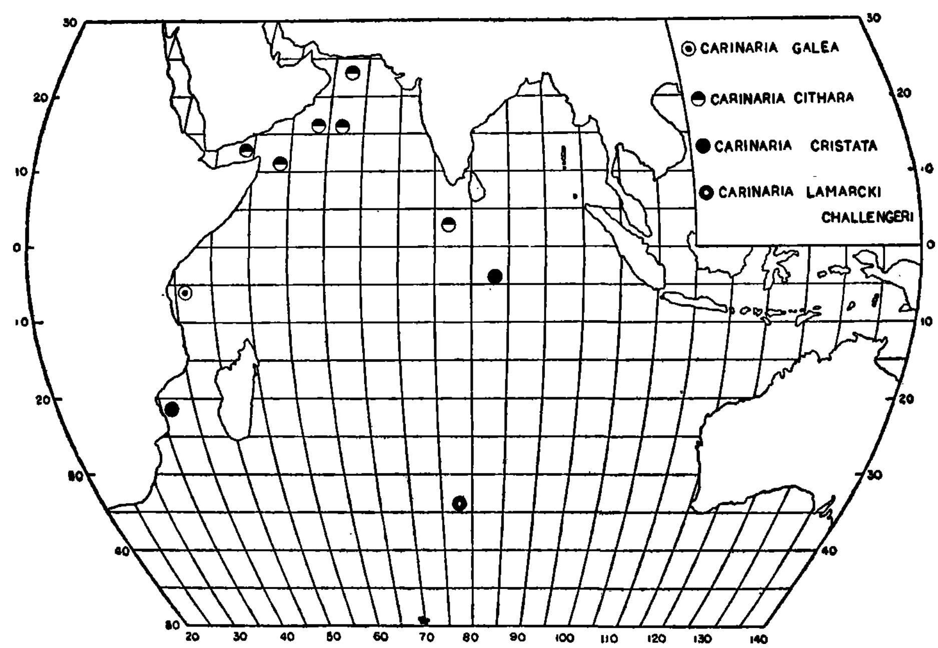

FIG. 2. Distribution of the species of *Carinaria.*

Carinaria lamarcki challengeri *Bonnevie*, 1920

The typical *Carinaria lamarcki* was not obtained. Two specimens of *Carinaria lamarcki challengeri* were collected at *Vityaz* station 5327 (34°18'S 77°56'E). The distribution of this species is interesting because, as Tesch points out, this is the only heteropod which penetrates into temperate waters. All other ranges are tropical-subtropical. These specimens are considered different from the typical *C. lamarcki* because they possess the "clasper" (Bonnevie 1920) consisting of a pair of folds on the posteroventral side of the body. Okutani (1961) has also not found the "clasper" in the typical specimens of *C. lamarcki.* One of the present specimens is a male (12 mm in length) and the other a female (21 mm). Both cephalic tentacles were present. The right tentacle was smaller than the left. This is contrary to the observations made by Okutani. In his 15 mm specimen the right tentacle was completely absent.

Carinaria galea *Benson,* 1835

Only a 13 mm female specimen was recorded. The locality was off Mombasa. In the Indian Ocean it is distributed from Sumatra to Mombasa, according to Tesch. On the East African coast its distribution extends to Durban. It has not been recorded from the Atlantic and may be considered an Indo-Pacific species.

Carinaria cristata (*Linne'* 1766)

The species is noted for its remarkably large size. In the present material there were only two specimens. The maximum length attained was 28 mm for a female. It was collected between Madagascar and Mozambique. In this species the right tentacle is longer than the left, an anomaly noted by Tesch is his 86 mm specimen. The other specimen was a male, collected north of equator in the eastern Indian Ocean. The distribution of *Carinaria cristata* is known to extend from the south-east coast of Africa northward to Mombasa and also includes the eastern part of the Indian Ocean.

Carinaria cithara *Benson,* 1835

Six specimens were obtained, five of them from the north-west part of the Indian Ocean. The other was from near the equator, south of the tip of India. An important aspect of its distribution is that not a single specimen was present in samples from the Bay of Bengal. Its southernmost record is towards Durban (Tesch). In the present material the maximum length was 52 mm for a female specimen from *Vityaz* station 5251 (3° 00' N 77° 01' E). The largest *Dana* specimen measured 50 mm. Tesch reported that *Carinaria cithara* was present at each station in the tropical region from Durban to Indo-Malayan waters. Now the distribution is known to extend into the Arabian Sea. There are more records from the Indian Ocean than from the other oceans. The distribution pattern indicates that it is a typical tropical species.

Genus Pterosoma *Lesson,* 1827

Pterosoma planum is the only species in the genus *Pterosoma.* It is Indo-Pacific and wholly confined to tropical waters. In the eastern Indian Ocean its northern most record is at 18° N in the Bay of Bengal (Fig. 3). There were numerous records

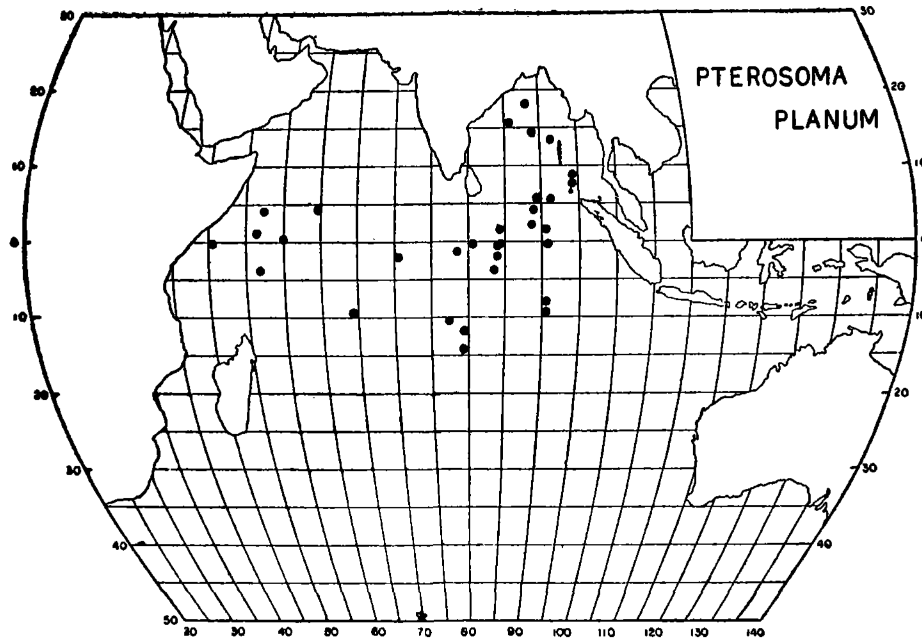

Fig. 3. Distribution of *Pterosoma planum.*

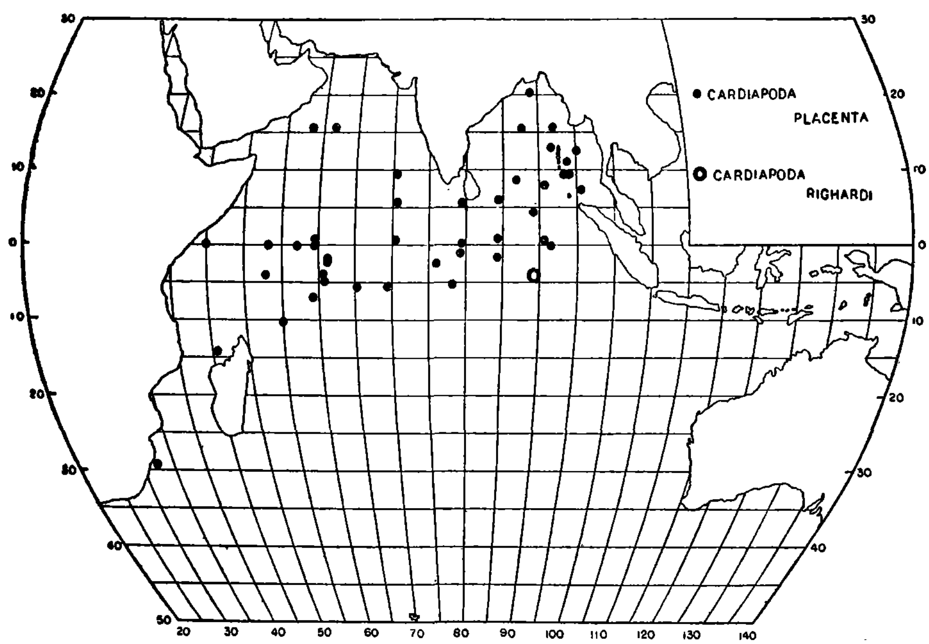

Fig. 4. Distribution of *Cardiapoda placenta* and *Cardiapoda richardi.*

from the eastern Indian Ocean. To the west, it was found off the Somali coast with the northernmost records near 5° N. Thus, it was not found in the Arabian Sea. According to the *Dana* investigations, the southernmost record is 35° 49′ S. The present records extend only to 15° S. In the present collection the largest specimen measured 35 mm in length (excluding the tail). Both cephalic tentacles were present, the right one being very small. However, in small specimens the right tentacle is absent. Lesson (1830) described a specimen of 80 mm length, while the largest specimens reported by Hedley (*cited from* Tesch) and Tesch measured only 30 mm.

Genus Cardiapoda *d' Orbigny*, 1836

The two species, *Cardiapoda placenta* and *C. richardi* are strikingly different morphologically, as well as in their distributional ranges. *Cardiapoda placenta* is common in the Indo-Pacific whereas *C. richardi* is more abundant in the Atlantic, particularly the Sargasso Sea. There are numerous records of *C. placenta* from the Caribbean Sea, but none for *C. richardi.* In turn, *C. placenta* is rare in the Sargasso Sea. The present records are shown in figure 4.

Cardiapoda placenta (*Lesson* 1830)

Most records for this species are from equatorial waters. There were also several records from the Bay of Bengal, but few from the Arabian Sea. They were present in large numbers in the eastern Indian Ocean. In the present investigation there were only three records south of 10°S. Previous records showed that *C. placenta* is abundant in Indo-Malayan waters. On the east African coast it was found near Madagascar and Mombasa. Its most southern *Dana* record was at 35° 49′S, 23° 09′E off the eastern edge of the Agulhas Bank. In the present study it was found to be only about 30°S.

Cardiapoda richardi *Vayssiere*, 1904

Cardiapoda richardi was present at only one locality, "Lusiad" Stn 85 (04° 01′S, 80° 00′ E). It was a small and damaged female specimen. Formerly the species was recorded between Ceylon and Seychelles and between Madagascar and east Africa. Now the distribution is known to extend to the eastern Indian Ocean. It is, clearly, rare and scattered in occurrence.

Family Pterotracheidae

All the known species of *Pterotrachea* were present. *Pterotrachea coronata* and *Pt. hippocampus* show wide distribution. *Pterotrachea scutata* and *Pt. minuta* are of special interest because of their rare occurrence. *Firoloida desmaresti* is the most abundant among all the species mentioned here. Figures 5 and 6 show the distribution of *Pterotrachea* species and figure 7 shows the distribution of *Firoloida desmaresti.*

Pterotrachea coronata : *Forskal,* 1775

This is one of the largest heteropods. It is widely distributed in the Indian Ocean, though the numbers caught are not as large as the catches reported from other oceans. In the present collection the largest specimen obtained measured 100 mm length (75 mm excluding the tail). It was a female and there was no sucker on the fin. Tesch could not find a single female with a sucker, but cited Fewkes (1883, 1888) and Paneth (1885) who concluded that this is not always the case, and that the sucker may occur in *Pt. coronata* females as well as in males. But the present author has not found any female specimen with sucker.

Pterotrachea hippocampus *Philippi,* 1836

According to Tesch *Pt. coronata* is more abundant than *Pt. hippocampus.* But the present observations show that *Pt. hippocampus* was obtained from 64 tations (Fig. 6) as against 16 stations for *Pt. coronata* (Fig. 5). In the Indian Ocean *Pt. hippocampus* was found to be most abundant between 5°S and 5°N. However, the southernmost record is at 28°00′S, on the African coast. In the Bay of Bengal it was not found north of the Andamans, as was the case with *Pt. coronata* (Fig. 5). No specimens were caught in the Arabian Sea.

Pterotrachea scutata *Gegenbaur,* 1855

Only one specimen was obtained, from *Vityaz* Stn 5199 (26° 02′ S, 91° 38′ E). The total length of the specimen was 39 mm. It was in a damaged condition. Evidently, this is not a common species in the Indian Ocean but in the Atlantic and Pacific it is known to have been caught in large numbers.

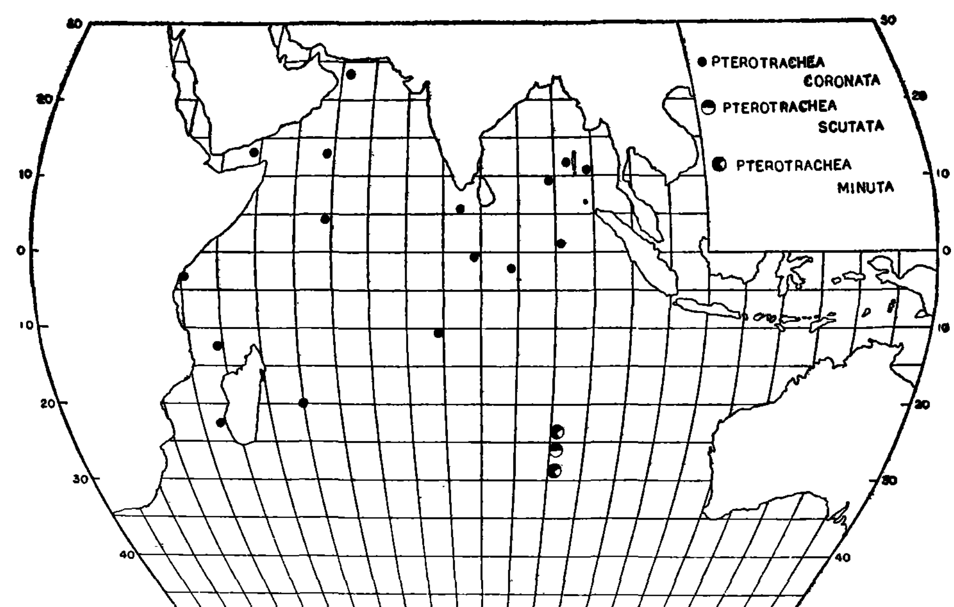

FIG. 5. Distribution of *Pterotrachea coronata, Pt. scutata* and *Pt. minuta.*

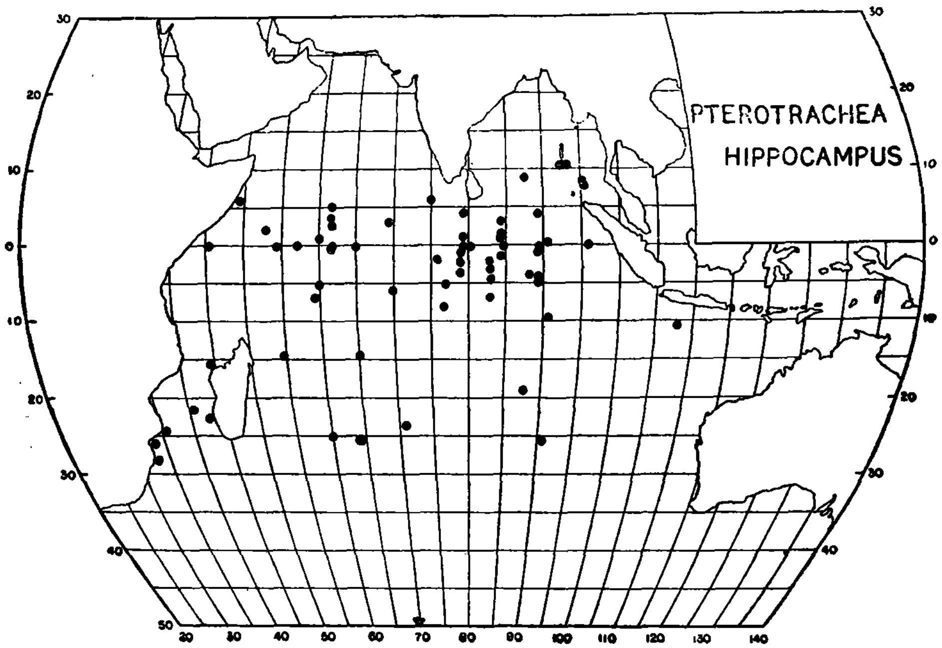

FIG. 6. Distribution of *Pterotrachea hippocampus.*

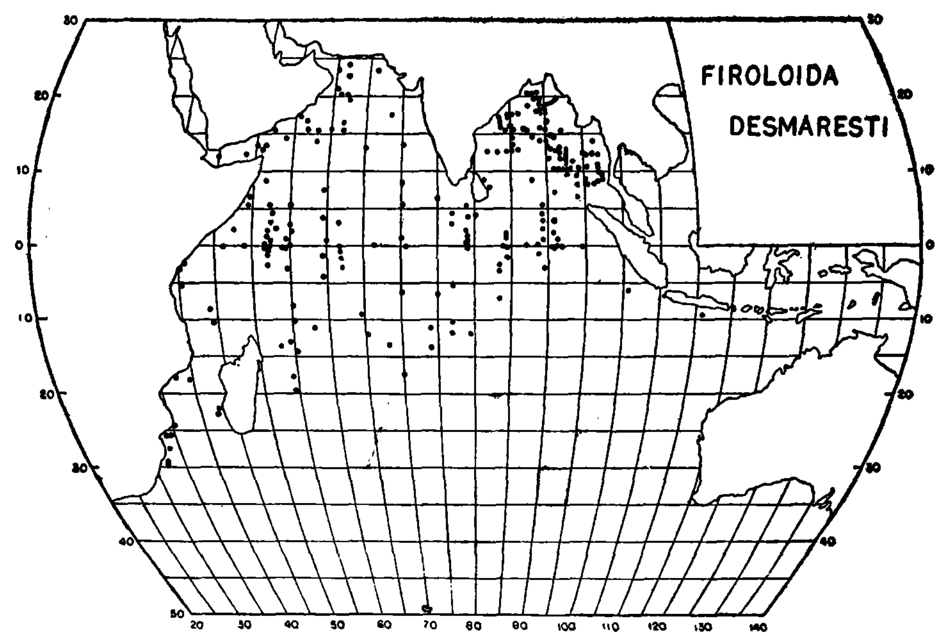

FIG. 7. Distribution of *Firoloida desmaresti.*

Pterotrachea minuta *Bonnevie*, 1920

Two specimens were obtained near the locality at which *Pt. scutata* was obtained. One specimen measured 13 mm and the other 29 mm in length. Bonnevie's specimen measured 13 mm and Tesch's was 25 mm. This species is rare in all oceans. Tesch reported it from near Mombasa and the present observation extends its distribution to the eastern Indian Ocean.

Firoloida desmaresti *Lesueur*, 1817

As has already been stated this is the most abundant species among the Carinariidae and Pterotracheidae. It is typically a tropical species, and Okutani did not find it in Japanese waters. In the Indian Ocean its southerly range extends to 30° S, along the African coast. East of the Agulhas Stream it is not found south of 20° S. The records are numerous from the Bay of Bengal, the Arabian Sea and the equatorial zone.

To summarise the above review of distribution, it may be said that all the species enumerated by Tesch were present in the material examined. *Carinaria cithara* was obtained from the Arabian Sea but not a single specimen was found in the Bay of Bengal. *Carinaria cristata, C. galea* and *C. lamarcki challengeri* were collected; but it is to be noted that not a single specimen was observed from the Arabian Sea or the Bay of Bengal. *Pterosoma planum* appears to be absent from the Arabian Sea. There were numerous records of *Cardiapoda placenta* from the Bay of Bengal but only scattered distribution in the Arabian Sea. Among the Pterotracheidae *Firoloida desmaresti* had the widest distribution. It seems to be rare beyond 20° S except on the African coast. Of the *Pterotrachea* species, *Pt. hippocampus* and *Pt. coronata* were relatively common. But the former was not obtained from the Arabian Sea. *Pt. Scutata* and *Pt. minuta* were noted to be rare. Only one specimen of *Pt. scutata* and two of *Pt. minuta* were collected.

Acknowledgement

The author is greatly indebted to Dr. N. K. Panikkar, the Director of the National Institute of Oceanography, for giving him permission to present this paper for the "Symposium on the Indian Ocean" and Dr. Edward Brinton, the Curator of the Indian Ocean Biological Centre, for his help and guidance. He is grateful to Mr. L. R. Kasturirangan, the Associate Curator, for his helpful criticisms of the manuscript.

References

Bonnevie, K. (1920). Heteropoda. *Rep. Sci. Res. "Michael Sars" N. Atl. Deep Sea Exped.*, 1910, **3**, 1-17.

Coan, E. (1965). Generic units in the Heteropoda. *Veliger*, **8**, 36-41.

Dales, R. P. (1952). The distribution of some heteropod molluscs off the Pacific coast of North America. *Proc. zool. Soc. Lond.*, **122**, 1007-1015.

Okutani, T. (1957). On Pterotrachean Fauna in Japanese waters. *Bull. Tokai reg. Fish. Res. Lab.*, **16**, 15-21.

————(1961). Notes on the genus *Carinaria* (Heteropoda) from Japanese and adjacent waters. *Publ. Seto mar. biol. Lab.*, **9**, 333-352.

Sebastian, M. J. (1963). On the occurrence of the pelagic mollusc, *Cardiapoda placenta* (Lesson) in the Arabian sea. *J. mar. biol. Ass. India*, **5**, 140-142.

Smith, E.A. (1888). Report on the Heteropoda collected by the H. M. S. Challenger during the years 1873-1876. *Sci. Rep. Voy. Challenger, Zool.*, **23**, 1-47.
Tesch, J. J. (1906). Die Heteropoden der Siboga—Expedite. *Siboga Exped.*, **51**, 1-112.
———(1910). Pterop. a. Heterop. Percy Sladen Trust exep. to the Indian Ocean in 1905. *Trans. Linn. Soc. Lond.*, **14**, 170-189.
———(1949). Heteropoda. *Dana Rep.*, **34**, 1-53.

Reprinted from *Bull. natn. Inst. Sci. India*, no. 38, 1968, p. 594-611

PRELIMINARY OBSERVATIONS ON THE DISTRIBUTION OF EUPHAUSIACEA FROM THE INTERNATIONAL INDIAN OCEAN EXPEDITION

by K. GOPALAKRISHNAN[1] *and* E. BRINTON

Indian Ocean Biological Centre, National Institute of Oceanography, Cochin 16

During the International Indian Ocean Expedition (IIOE), 1962-65, highest numerical densities of euphausiids were found on the western side of the Indian Ocean. A reduction in numbers occurred toward the east, but there was a secondary peak at 80°-90°E, the longitude of the western half of the Bay of Bengal. Numbers of euphausiids considered on a north-south basis show a picture of progressive decrease toward the southern limit of the Indian Ocean proper (40°-45° S) the zone of the Subtropical Convergence. The patterns hold for both seasons considered : April-October and October-April. Observed night-time numbers are twice as great as day-time numbers. Throughout the year, maximum numbers of euphausiids were found in the western most tropical part of the ocean, particularly off Arabia and Somaliland, agreeing with findings for most other taxa reported in the present series of papers. Numerical densities in the Bay of Bengal and in waters south of Java were somewhat higher during the Southwest Monsoon period than during the opposite season. A discussion of distribution of the separate euphausiid species is based on *Argo* samples from an equatorial zone 5°N-5° S extending the full breadth of the ocean. Typical Indo-Pacific tropical species are dominant, but surprising numbers of individuals representing faunas from mid-latitudes are mixed in, particularly toward the west and in the zone 0°-5° S.

INTRODUCTION

During IIOE, zooplankton samples were collected by research vessels from nine nations. The composite pattern of stations provides coverage of most of the ocean. Samples were received at the Indian Ocean Biological Centre (IOBC) for sorting and further analysis. Of the 2146 samples received, 1909 were collected according to the standard method prescribed for vessels participating in the IIOE (Currie 1963). Two hundred and thirty five samples are considered non-standard. The standard samples were collected by means of the Indian Ocean Standard Net, specially devised for the IIOE. The haul was as nearly vertical as possible, from approximately 200 m of depth to the surface. In waters over the continental shelf where the sonic depth was less than 200 m, the net was usually hauled up from within a few meters of the bottom. Such samples are also considered standard because the full water column was traversed.

The number of organisms in each of the gross taxa (e.g., Copepoda, fish larvae, foraminifera) is routinely determined for each sample. These counts provide data for study of the geographical distribution of abundances. In spite of the fact that Total Euphausiids, which we are now considering, is made up of many genera and species, and, furthermore, each species includes several developmental stages, there nevertheless appears to be justification for looking into the distribution of Euphausiacea as a whole.

[1]Present address : Scripps Institution of Oceanography, La Jolla, California, U.S.A.

First of all, the bulk of the present material consists of larvae and immature specimens. Inasmuch as all species pass through similar developmental stages, and the younger stages of most species are restricted to the near-surface strata (e.g. Brinton 1967), it is to be expected that the euphausiid community as a whole is representatively sampled.

Secondly, the morphological characters which distinguish genera are mainly concerned with limbs that function in feeding. Whether food is gathered selectively or by filtering, those species whose feeding habits have been studied are generally recognized as omnivores and, hence, play similar roles in the food chains. This may be particularly true in the epipelagic part of the tropical zone — with which we are mainly concerned here — because the species attain similar sizes at adulthood. We have therefore reasoned that euphausiids constitute an ecological entity, in a broad sense.

The importance of euphausiids in the economy of the sea stems only partly from the fact that these crustaceans are omniverous feeders, consuming diatoms, zooplankton, and detritus. In addition, they bulk second to the Copepoda as a stock of basic animal protein, if we exclude the larger protozoans from consideration. Euphausiids serve as fodder plankton, forming a part of the diets of many commercially important fishes, including both filtering and predaceous species. They are known as "krill"—the principal food of the baleen whales, particularly in northern and southern seas where euphausiid populations frequently form into great swarms at the surface. In tropical or subtropical oceanic waters such swarming has not been noted. The characteristics of the IIOE samples suggest that swarming in the Indian Ocean is infrequent, or that aggregations — if they occur at all — are small in relation to the volumes of water strained by the nets.

The distribution of Total Euphausiids has been compiled for the Pacific (Ponomareva 1966). Numerical densities were shown to be somewhat higher in tropical than in subtropical waters, but low as compared particularly with the far eastern seas which extend from the East China Sea to Alaska. These latter also yield the greater part of the North Pacific fish catch, which itself constitutes 40 per cent of the world catch. Maximum densities of euphausiids reported for the Pacific area are, it will be seen, no greater than those found in northern parts of the Indian Ocean, particularly the western part of the Arabian Sea.

Material and Methods

For the estimation of abundances of euphausiids in the Indian Ocean, 1275 samples were used. These include all of the standard samples sorted and counted at IOBC up to January, 1967.

Data for two six-month periods are contrasted. The period April 16—October 15 agrees with that of the wind regime of the Southwest Monsoon (Wooster, Schaefer and Robinson 1966), and the southern hemisphere's winter. October 16—April 15 includes the Northeast Monsoon and southern summer. Eight hundred and three samples are available for the first period and 472 for the second.

In the laboratory, a three or four ml portion of each sample is first sorted into its major taxonomic components. The specimens in each taxon are then counted and the counts are corrected so as to provide an estimate of numbers in the whole sample. The sorted fractions range from 5 per cent to 90 per cent of the whole sample, depending upon the sample's initial displacement volume.

In order to prepare generalized charts of the distribution of euphausiid abundance, values in each 5°-square of ocean were averaged. The 5°-squares are quadrants of 10° Marsden squares.[2] Each average then represents the number of euphausiids under 1 m^2 of sea surface to a depth of 200 m, for an area of approximately 160,000 km^2 of ocean. In those charts where the abundance values were contoured, each of the averages representing a Marsden quadrant was plotted at the midpoint of that quadrant, irrespective of the actual positions of the stations. These point values were then contoured using geometric intervals of abundance.

The adults of many euphausiid species carry out extensive diurnal vertical migrations, swimming down to depths of 300 m or more in the day-time and returning to the surface layer at night. Other species do not migrate but,to differing extents, avoid capture by nets in the near-surface part of the sea during the day-time (Brinton 1967). Day and night IIOE samples differ in euphausiid content by an average factor of about 2. As will be discussed in later paragraphs, this factor evidently is not constant for all parts of the ocean. Therefore, it seemed likely that inaccuracies might be introduced by applying a uniform correction factor. We shall therefore consider the night-time data as the basis for the present discussion. Night was considered to be sunset to sunrise.

In order to make fullest use of the available data (short of applying a correction factor to the day-time data), a few day-time samples which contained *more* euphausiids than the night-time average for the pertinent 5°-squares were used in the final calculation of that average.

The numbers of standard samples per 5°-square, including both day and night samples, that were available for the preparation of distributional charts are shown in Figure 1 for the period April 16—October 15, and in Figure 2 for the period October 16—April 15.

RESULTS

The distribution of euphausiid abundance for the April-October period, which includes the southwest monsoon, indicates that population maxima of >2000 per standard sample ($\cong 10/m^3$) lie off the coasts of Arabia, Somaliland and the Nicobar Islands of the Bay of Bengal. Somewhat less high densities, in the range of 750-2000 euphausiids per sample ($\cong$ 4 to $10/m^3$), were found along the coast of tropical Africa, and as far north as the Gulf of Oman at the head of the Arabian Sea. Waters off the southwest coast of India, and extending eastward around the tip of India to Ceylon and the Andaman Islands harboured similar numbers during this season. A rich area south of Java was separated from the equally rich southern part of the Bay of Bengal by an area west of Sumatra that was found to be poor in euphausiids. This relatively poor area lies at the eastern end of the easterly

[2]The standard method of coding the Marsden squares and their component quadrants is described in the National Oceanographic Data Center Publication G-1, 1963. The method proved useful and was followed in the processing.

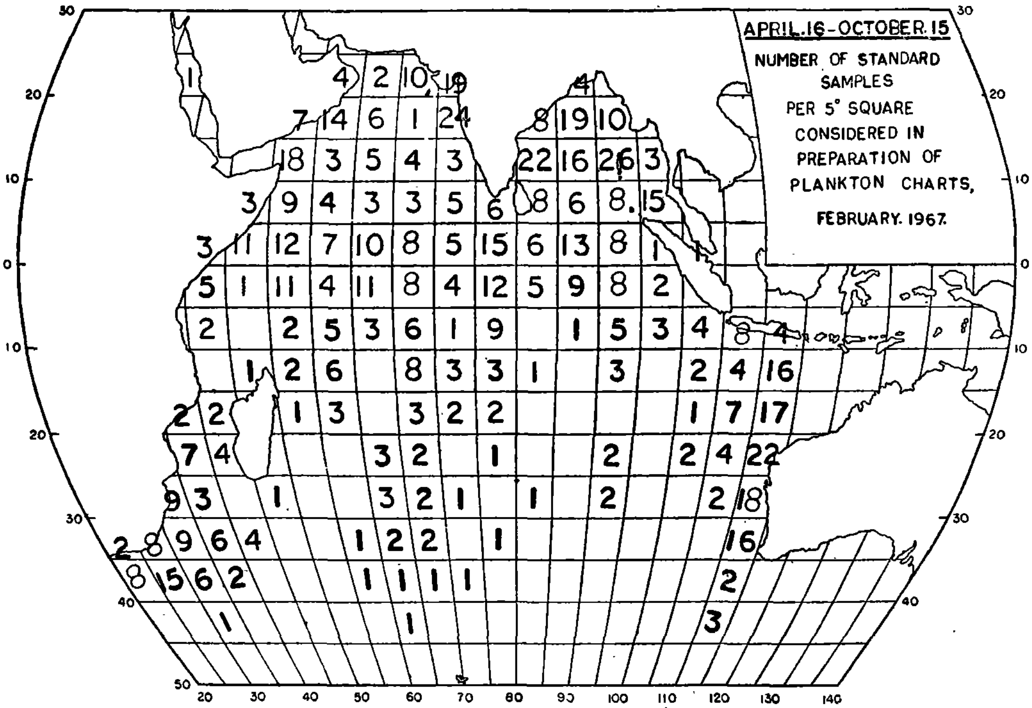

FIG. 1. Number of standard samples per 5°-square considered in preparation of plankton charts, April 16—October 15.

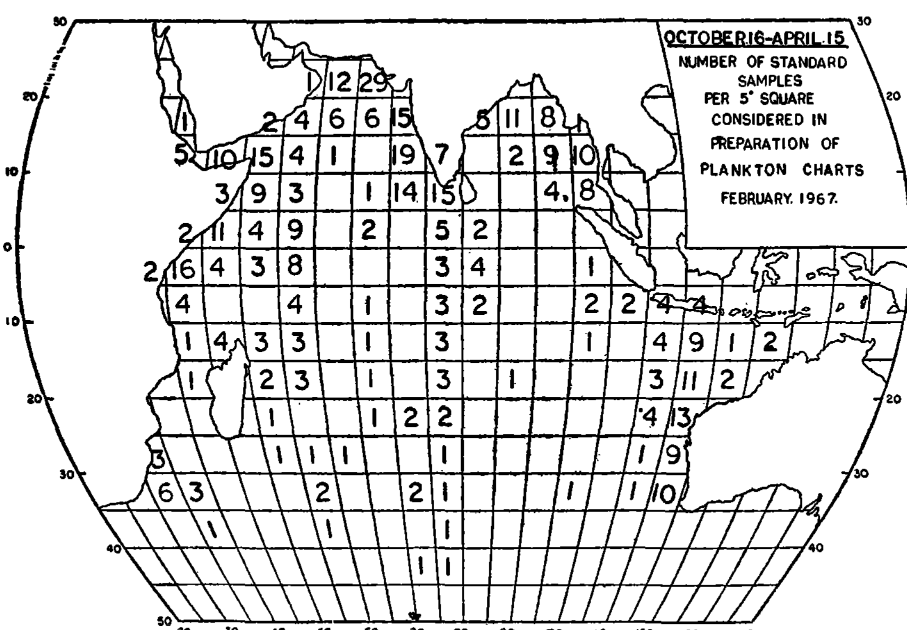

FIG. 2. Number of standard samples per 5°-square considered in preparation of plankton charts, October 16-April 15.

equatorial current system. Other areas of low euphausiid density were the region of the gyral of the central water mass, 15°-25° S, and oceanic waters southeast of South Africa. An attempt has been made in Figure 4 to clarify general features of the distribution by contouring the data shown in Figure 3.

During October-April, when the cold northeasterly Somali Current is no longer developed, the largest populations of euphausiids were nevertheless centered at the equator, on the Somali coast (Fig. 5). Off Arabia the population density also remained nearly as high as during April-October, but off the west coast of India it decreased appreciably. Contours drawn on the basis of individually plotted stations (Fig. 6) illustrate that the highest densities off Somalia, Arabia, and the tip of India were at near-shore stations, while those off west India lay somewhat farther offshore.

South of Java the numbers of euphausiids remained nearly constant year round. During October-April, the southern summer, South African and Australian coastal populations differed little in size from those measured during April-October. However, mid-ocean densities, based on the few data available, were then (October-April) somewhat higher in these mid-latitudes.

There is insufficient night-time data from mid-ocean south of the tropics. Day-time data have not been drawn upon to supplement this picture because in 5°-squares south of 25°S daytime values for abundance were in many cases disproportionately lower than night-time values, as compared with other parts of the ocean where night values consistently exceeded day values by a mean factor of 2 (Figs. 7, 8).

Day and night catches are compared (Figs. 7, 8) with respect to the number of euphausiids caught. All catches for each 12-hour period have been averaged for each 10° zone to provide north-south pictures of relative abundance. The extent of day-night variation is seen to be nearly constant from 20°N to 40°S and differs little between the two seasons. As has been noted above, the comparatively low day-time densities may be owing to the fact that during the day-time many animals either migrate into deeper water or are able to dodge the net. Because of the substantial extent of the day-night difference in catch, only night-time values were used in plotting the foregoing charts of distribution. Only for the Arabian Sea (Fig. 6) did we attempt to correct day-time values and incorporate them into a composite map. In this case a correction factor of 1.5 was applied to day-time values, using the lower limit of the ratio of night-to-day abundance (1.5 to 2) evident in Figures 7 and 8.

Another approach has been made to the study of seasonal and geographical variation by plotting mean abundances along east-west axes for each of the two seasons (Fig. 9). In each 10°-Zone a curve is plotted for each of the two 6-month periods. Values used in constructing the curves are mean night-catch sizes for each rectangular area circumscribed by 5° of longitude and 10° of latitude. The mean for each such area was determined by combining the means separately calculated for each of the two constituent 5°-squares. In this way, samples are to some extent weighted according to the size of the geographical area they represent.

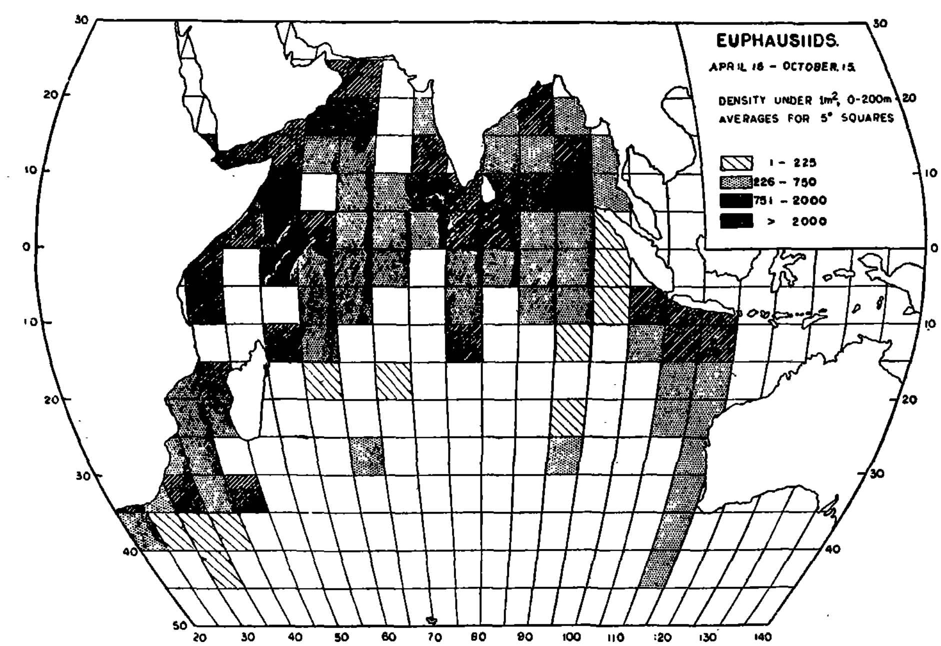

FIG. 3. April 16-October 15 period. Euphausiid population density under unit area, 0-200 m depth. Densities are averages of all night-time values for each 5°-square. Day-time values that exceed the night-time mean for the pertinent square are also included.

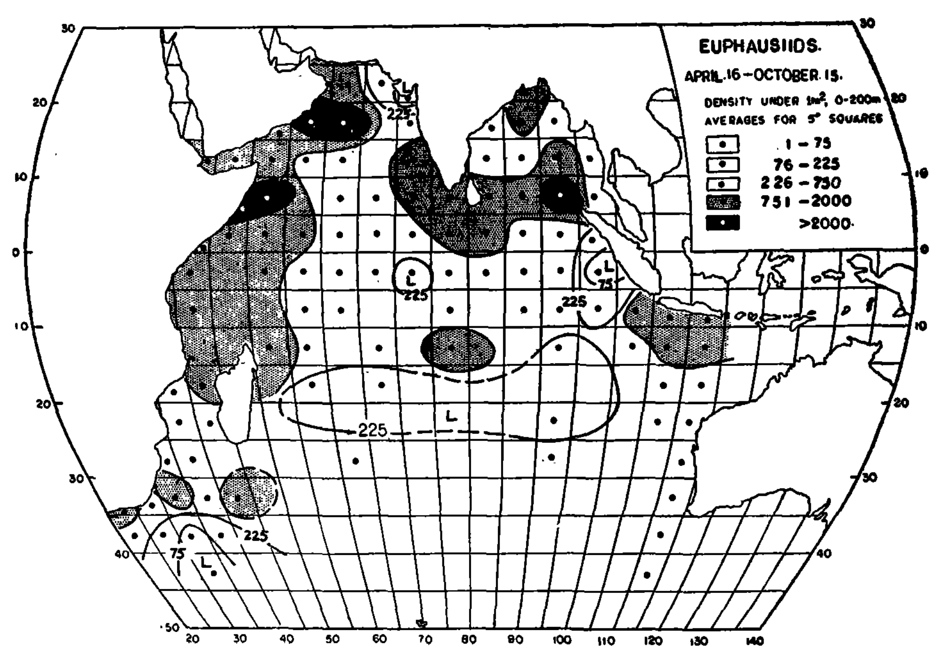

FIG. 4. April 16-October 15 period. Population densities shown in Figure 3 are contoured. Dots show the squares from which data are available.

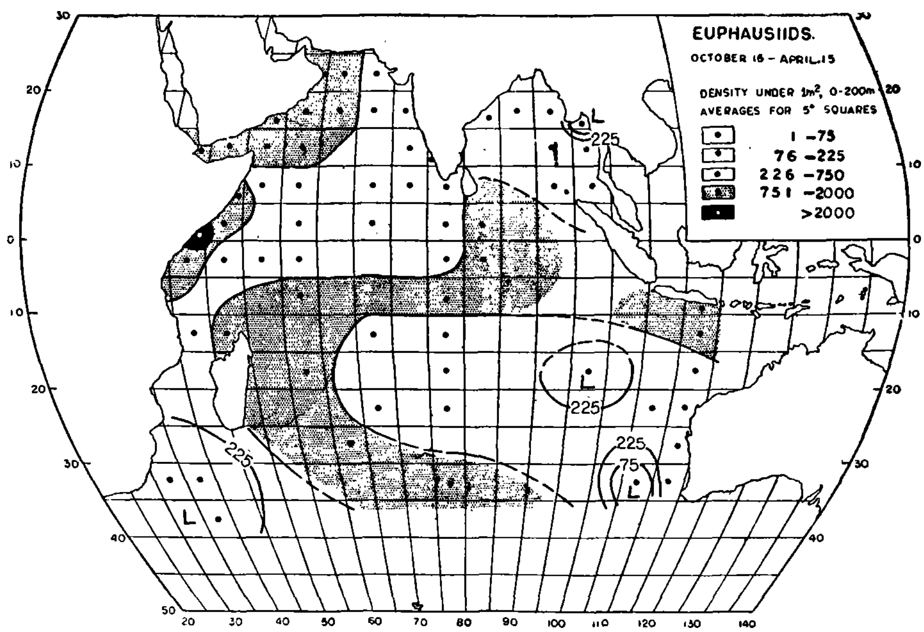

FIG. 5. October 16-April 15. Euphausiid population density under unit area, 0-200 m depth, contoured as in Figure 4.

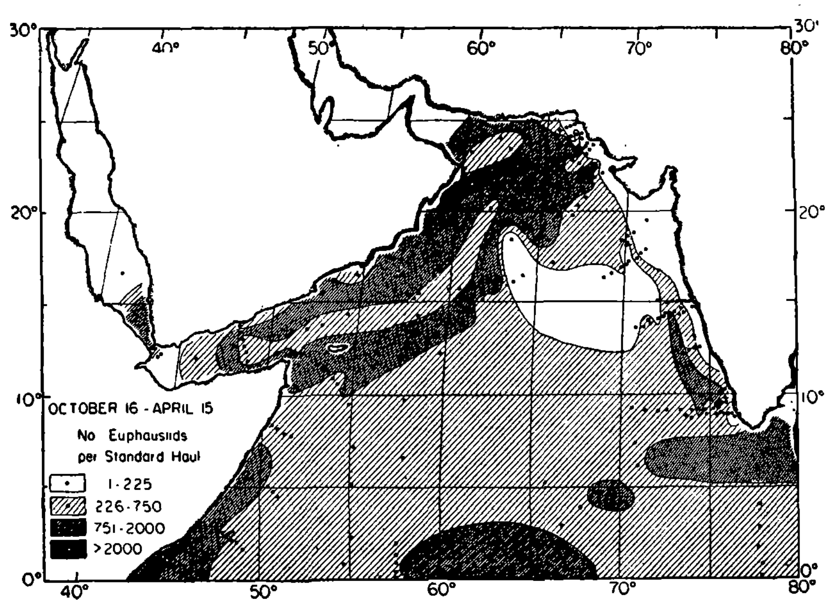

FIG. 6. October 16-April 15. Arabian Sea euphausiid population density, based on individual station positions. Day-time vaules have been multiplied by a factor of 1.5.

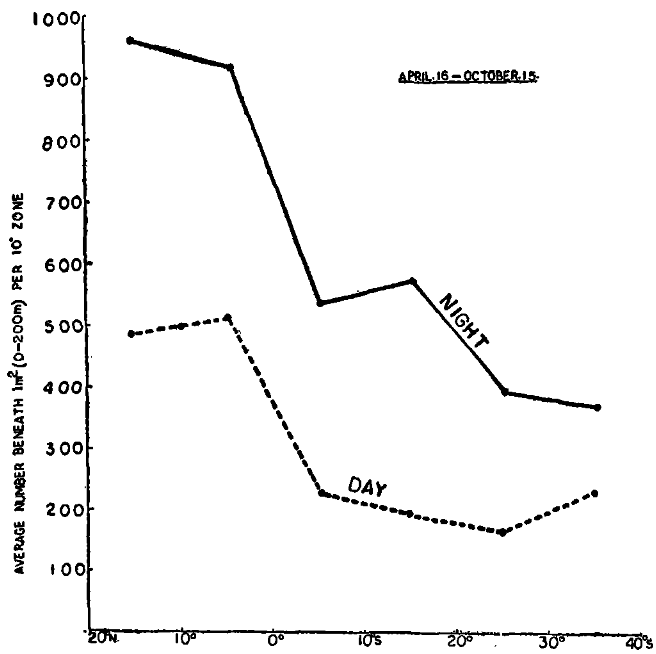

FIG. 7. April 16-October 15. Day-night variation in euphausiid population density. Curves are based on averages of the number of specimens, per standard sample, for each 10° zone.

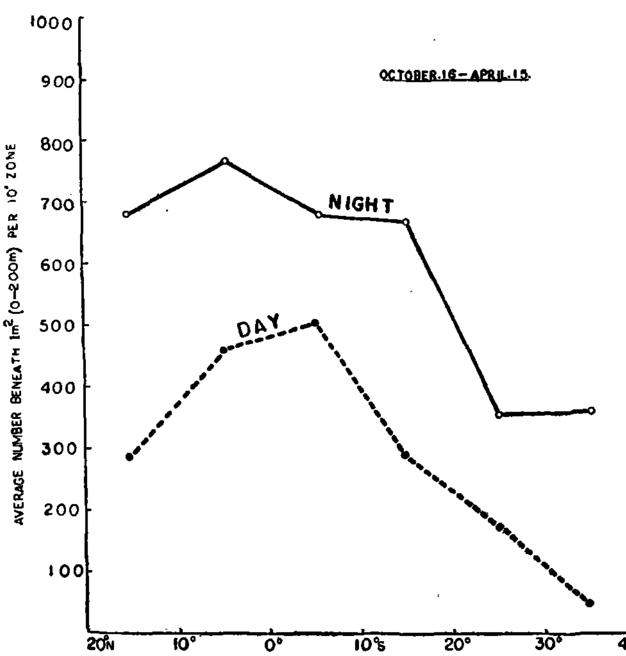

FIG. 8. October 16-April 15. Day-night variation per 10° zone, as in Figure 7, for the opposite season.

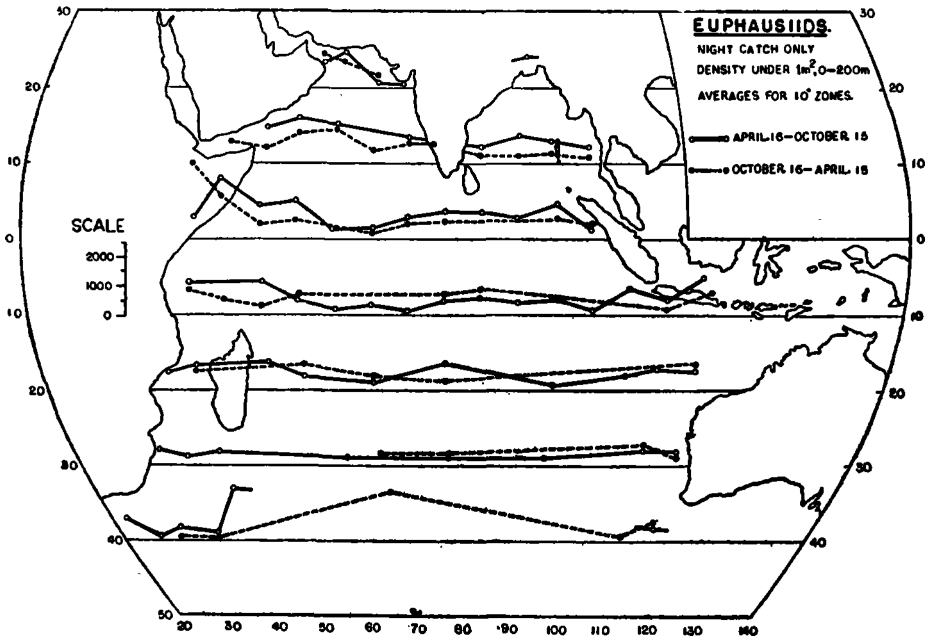

FIG. 9. Chart comparing east-west variation in Total Euphausiids for two seasons. Values are mean night-time densities, under unit area, for rectangular areas bounded by 5° of longitude and 10° of latitude.

The curves in Figure 9 indicate that seasonal change is small and generally consistent for each of the 10° zones north of the equator. Arabian Sea and Bay of Bengal peaks are somewhat more conspicuous than east-west variations in abundance noted in the southern hemisphere.

It is interesting to compare the foregoing pictures of euphausiid abundance in the Indian Ocean with that given by Ponomareva (1966) for the Pacific. The standard IOSN net-haul strains only 200 m³ of water (approx.), so that a correction factor of 5 must be applied to the present data before it can be compared with the Pacific data, which was standardized on the basis of 1000 m³. It seems unlikely that differences in depth-of-haul are of importance in this comparison; many of the data used by Ponomareva are from 0-140-0 m or 0-210-0 m tows, while the IOSN haul was from 200 m depth.

The Pacific estimates evidently are based on a combination of day and night data. For a comparable estimate of zonal abundances of euphausiids in the Indian Ocean we shall therefore consider a curve drawn equidistantly between the day and night curves given in each of Figures 7 and 8, and multiply the extrapolated values by a factor of five.

Mean euphausiid abundances for the 10° zones north of the equator in the Indian Ocean may then be seen to fall into a range of 2500-4000/1000 m³. The Pacific maxima, given as >1000/1000 m³, are shown to be restricted to the temperate and subarctic far eastern seas and parts of the California Current. An examination of Figures 4 and 5 (which illustrate abundances on the basis of approximately 200 m³ of water strained) shows that almost the entire Indian Ocean — excluding only the areas circumscribed by the two lowest intervals of abundance — contains more than 1000 euphausiids per 1000 m^3. Furthermore, the shaded areas circumscribed by the > 750/200 m^3 interval accommodate abundances greater than 3750/1000 m^3, while the blackened areas represent > 10,000/ 1000 m^3.

A comparison of the Pacific chart with the charts showing distribution and abundance of separate Pacific species given in Brinton (1962), on which Ponomareva's chart was partly based, indicates that the densities of Total Euphausiids in the Pacific were, indeed, minimal estimates. (This was probably unavoidable because the maximum abundance interval for most of the Pacific species was shown in the 1962 paper only as > 500/1000 m^3.) However, we may still reasonably conclude that the areas of high population density in the tropical Indian Ocean are proportionately large compared with those in the temperate and subarctic Pacific and that maximum Indian Ocean densities are at least as high and probably higher than those reported in the Pacific.

Distribution of Euphausiid Species During Lusiad Expedition

As part of the IIOE called "Lusiad" Expedition, the research vessel *Argo* studied the equatorial belt 5°N-5°S during July-September 1962. The samples afford an opportunity to examine geographical variation, particularly along an east-west axis, in the occurrence and abundance of tropical species.

Earlier knowledge of the distribution of Indian Ocean euphausiid species is based mainly on scattered records from four sources. These are the Deutsche Tiefsee Expedition (Illig 1930), the Percy Sladen Trust expedition to the islands of the southwestern part of the tropical zone (Tattersall 1912), the John Murray Expedition in the northwestern quadrant of the ocean (Tattersall 1939), and 1960-1961 work by *Vityaz* in the Arabian Sea and Bay of Bengal (Ponomareva 1964). Boden (1951) gives generalized distributions in South African waters. Baker (1965) compiles all Indian Ocean records of species in genus *Euphausia*, and describes the distribution of these species along the 90°E meridian, from the equator to Antarctica, using material collected by *Discovery* prior to IIOE. The most useful taxonomic study of the tropical species is contained in Hansen's (1910) *Siboga* report on collections from the Indo-Australian Archipelago.

The first part of the track of "Lusiad" Expedition consisted of an east-west line of stations spanning the ocean along the equator. The return track consisted of four north-south transects (5°N—5°S) of the equatorial current system, at 52° E, 62°E, 79° E and 89° E respectively.

Ninety-four "Lusiad" samples were analyzed at IOBC and the euphausiids were studied in detail. This is the first part of a taxonomic and zoogeographical study of Indian Ocean euphausiids based on the IOBC samples. All specimens were identified to species and classified as calyptopis, furcilia, juvenile, or adult. Counts were made of the specimens in the sorted fraction and, as was the case with Total Euphausiids discussed in the foregoing section, numbers were standardized on the basis of the total sample.

Of the 94 samples, 44 were collected during the night and 50 during the day. In the present preliminary study no attempt is made to correct for day-night differences in abundance. Also, the plotted densities represent aggregates of all developmental stages.

Of 31 species recorded, 10 were present at all or nearly all stations, while five others occurred at a majority of the stations.

The most characteristic species of this region, both from the standpoint of consistency of occurrence and numerical abundance were the following :

Stylocheiron carinatum G.O. Sars, 1883
Thysanopoda tricuspidata Milne-Edwards, 1830
Euphausia tenera Hansen, 1905
E. diomediae Ortmann, 1894
Nematoscelis gracilis Hansen, 1910

The first three are widely ranging species occupying tropical-subtropical zones of the three oceans. The last two species are confined to Indo-Pacific tropical waters (Brinton 1962).

It may be seen in Figure 10 that in each of the six genera a single species is numerically dominant in this area, with the exception of *Euphausia* in which two species, *E. diomediae* and *E. tenera* are of almost equal importance. In this connection it is probably significant that more than one author, following John's (1936) observations on Antarctic species, consider the genus *Euphausia* to consist of two natural groups. *Eusphausia diomediae* clearly belongs to John's "Group 1", while *E. tenera* belongs to "Group 2." *Euphausia tenera* proved to be the most abundant species in the equatorial belt of the Indian Ocean. Most maxima were at or to the north of the equator, as was also the case with *T. tricuspata* and *N. gracilis.* The maximum number of individuals at a station were of *Stylocheiron carinatum* (1160 specimens, at 0°, 51° E).

Seven species were regularly present throughout the "Lusiad" area, but in distinctly smaller numbers than the dominant species listed above. These were the following :

Thysanopoda aequalis Hansen, 1905
Nematoscelis tenella G.O. Sars, 1883
Stylocheiron affine Hansen 1910
S. abbreviatum G.O. Sars, 1883
S. longicorne G.O. Sars, 1883
S. microphthalma Hansen, 1910
Euphausia paragibba Hansen, 1910

All of these are pan-oceanic tropical-subtropical species, except *E. paragiaba* and *S. microphthalma* which, like *E. diomediae* and *N. gracilis*, are equatorial Indo-Pacific species.

The charts of *Euphausia tenera* and *Stylocheiron microphthalma* (Fig. 11), each of which is representative of one of the two groups of "Lusiad" species given above, contrast with respect to abundance but not occurrence. Both are present at most

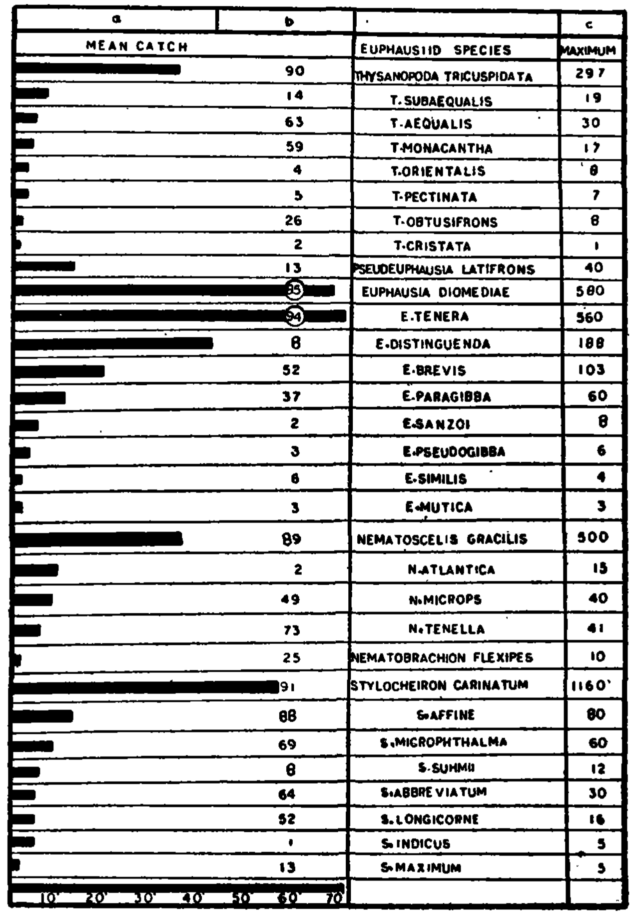

FIG. 10. Euphausiid species caught during "Lusiad" Expedition, July September, 1962. (*a*) mean catch per sample, considering only those samples in which the species was present, (*b*) the number of samples in which the species was present, (*c*) the maximum number of specimens caught in a sample.

stations. The mean density of *E. tenera* was 70 specimens per station, and *S. microphthalma*, 7.

In the Pacific the overall ranges of these two species almost coincide. Also, their actual and relative abundances (Brinton 1962, Figs. 43, 85) are the same as in the part of the Indian Ocean presently being considered. Population maxima for *E. tenera* in the Pacific were approximately 2000/1000 m^3.

The four stations near Africa at which maxima of *S. microphthalma* were recorded (Fig. 11) yielded 125-300/1000 m^3 ($\cong$25-60 per sample). Only five of the many Pacific records for this species were based on as many specimens, all five being in the range of 125-153/1000 m^3.

Nematoscelis gracilis is one of the species listed above as being abundant and consistently present in the "Lusiad" transects. Its maximum densities were found

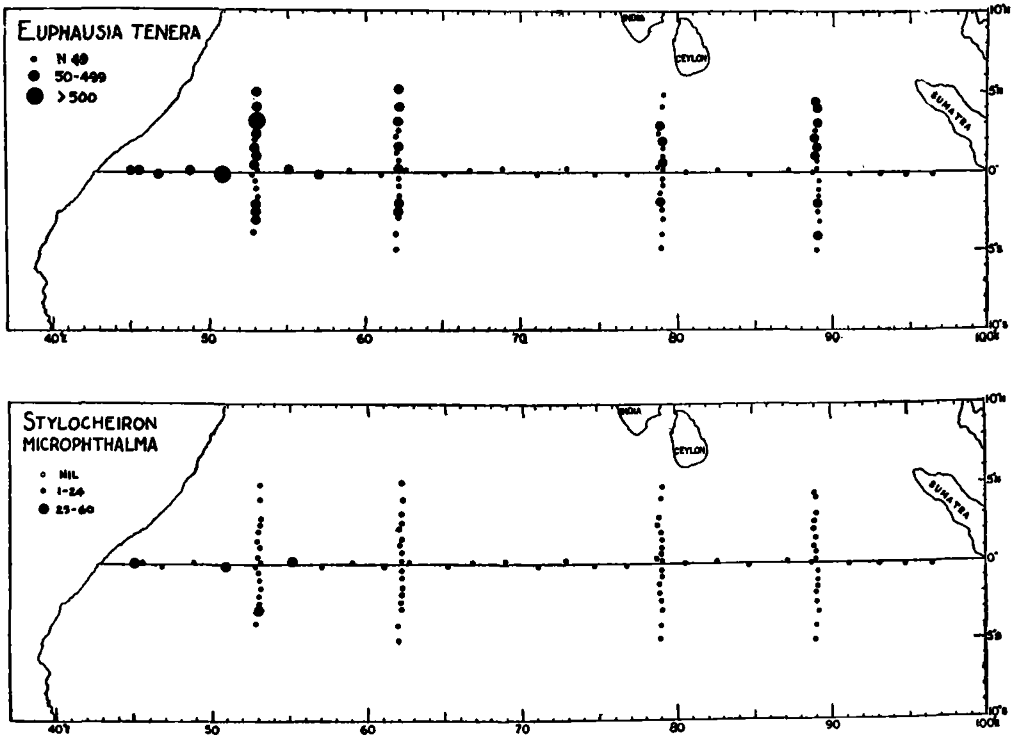

FIG. 11. "Lusiad" Expedition. Distributions of *Euphausia tenera* and *Stylocheiron microphthalma*. Population densities are No. per standard sample, 200-0 m (=200 m³ of water).

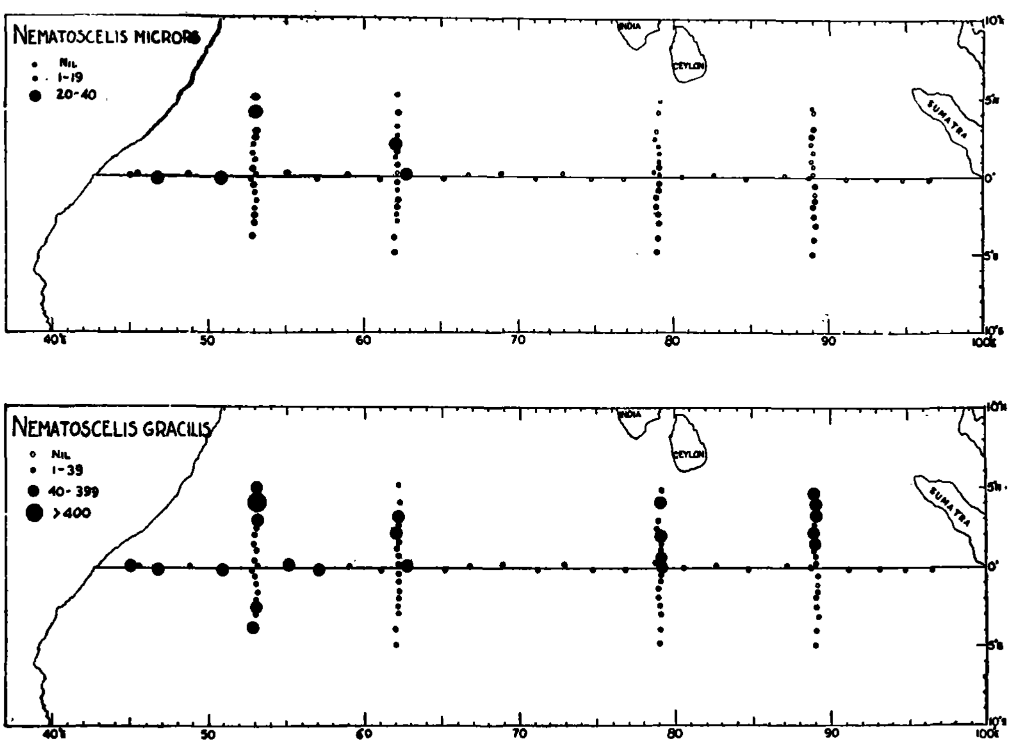

FIG. 12. "Lusiad" Expedition. Distributions of *Nematoscelis microps* and *Nematoscelis gracilis*.

north of the equator and, particularly, off east Africa where 500 specimens were caught at one station (Fig. 12). *Nematoscelis microps* is a closely related species which, in the Pacific, has a range that is almost mutually exclusive of that of *N. gracilis*.

In the eastern half of the "Lusiad" area the places of maximum abundance of these two species were separate, *N. microps* occurring mainly south of the equator, and *N. gracilis* to the north of it (Fig. 12). *N. gracilis*, the equatorial Indo-Pacific species, was the more abundant. Both species achieved maximum numbers in the western part of the ocean.

A third *Nematoscelis* species, *N. tenella*, was, like *S. microphthalma*, present at nearly all stations in small numbers, with maxima of 20 at three stations near Africa. Immature specimens believed to be *Nematoscelis atlantica* were caught at two stations on the western side of the ocean,—one at the northernmost (5° N) station of the 62° E transect, and the other near 3° N, 52° E. Both stations are somewhat to the east of the strong northeasterly Somali Current, which feeds water into the Arabian Sea from south of the equator. *N. atlantica* is recognized as a central water mass species in the Pacific and may prove to have affinities with the analogous zone, 10°-35° S, in the Indian Ocean.

Other species showing restricted distributions in the area of the "Lusiad" survey include *Euphausia mutica* (Fig. 13), the center of distribution of which appears to be to the south, and *E. distinguenda* which is abundant to the north, being perhaps the dominant species in the Arabian Sea (Tattersall 1939). Both were encountered in the easterly Southwest Monsoon Current, not far from Africa.

Pseudeuphausia latifrons (Fig. 13) is the characteristic euphausiid of tropical neritic waters,—from India to Samoa. Its occurrences in the eastern part of the ocean during "Lusiad" appear to reflect transport from coastal waters of India, Ceylon and Sumatra.

Of the species pair *Thysanopoda aequalis*—*T. subaequalis* (Boden and Brinton 1957), *T. aequalis* dominates throughout this equatorial zone, though *T. subaequalis* was recorded at 14 stations. The distribution of *T. subaequalis* was similar to that of *Nematoscelis microps*, in that all 11 records were south of the equator or on the western side of the ocean. Young of *Thysanopoda obtusifrons* were found at 25 stations, all but two of which were on or south of the equator.

The distribution of another species, *Euphausia brevis*, is similar to those of *Thysanopoda subaequalis* and *Nematoscelis microps*, just discussed. *E. brevis* was caught at 43 stations, all except five of which were at or south of the equator. The five exceptions were north of the equator on the two westernmost 5° N -5° S transects.

Euphausia similis, the curious polytypic species which has centers of distribution in the East China Sea and the Antarctic Ocean, but which has also been recorded sporadically in tropical waters of the Indian Ocean and the East Indian Archipelago, was caught at seven scattered stations. All were at or south of the equator, and only furcilia and juveniles were caught.

Specimens referable to *Euphausia pseudogibba* were caught at three stations, all north of the equator. *E. sanzoi*, known only from east African waters

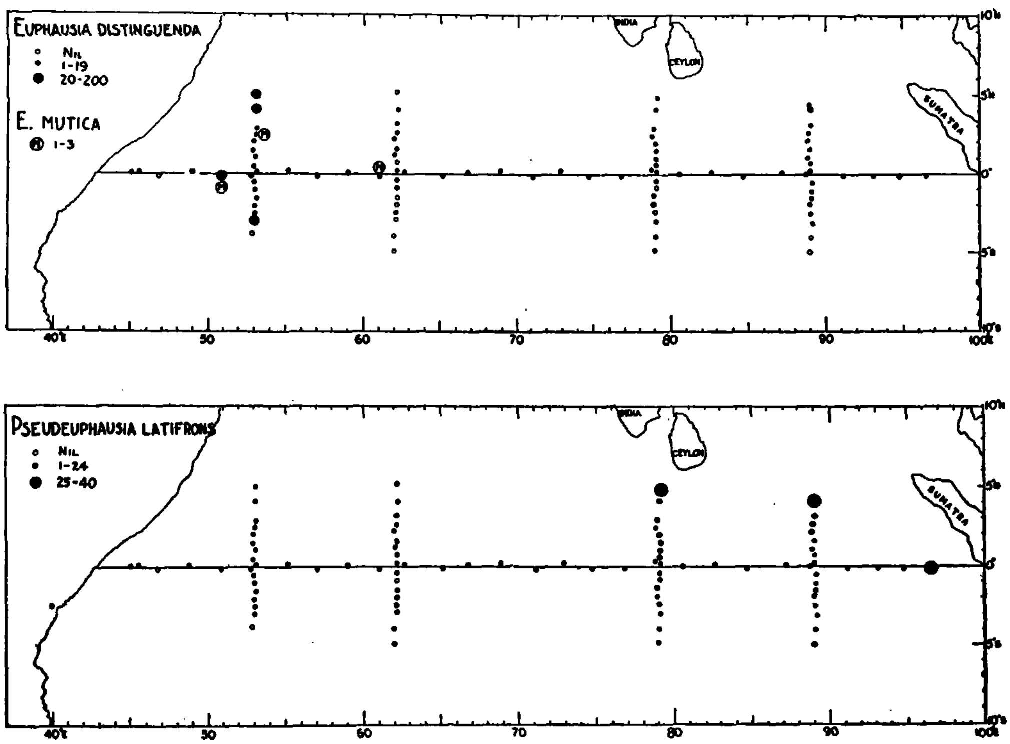

FIG. 13. "Lusiad" Expedition. Distributions of *Euphausia distinguenda*, *Euphausia mutica*, and *Pseudeuphausia latifrons*.

and the Red Sea, was caught twice, and only in the westernmost part of the "Lusiad" zone.

Stylocheiron suhmi, known in the Pacific as a Central water mass species (Brinton 1962), was caught at nine stations, all but one of which were west of 65° E. *Stylocheiron indicus*, recently described by Silas and Matthews (1967) from the south west coast of India, is represented in the "Lusiad" material by a single immature specimen from 62° E, north of the equator. Furcilia larvae of the deep-living cosmopolitan species *Stylocheiron maximum* were found at scattered localities throughout the area.

Other species represented only by larvae in the "Lusiad" collections or by sparse and scattered records include :

Nematobrachion flexipes (Ortmann) Calman, 1893
Thysanopoda monacantha Ortmann, 1893
T. orientalis Hansen, 1910
T. pectinata Ortmann, 1893
T. cristata G.O. Sars, 1883

Discussion

The ranges of most euphausiid species sampled by "Lusiad" Expedition (July-September, 1962) extended the breadth of the equatorial belt of the Indian Ocean. Off Africa, the aggregate of the large populations of individual species (Figs. 11, 12) contributed to the maximum of Total Euphausiids observed there during the Southwest Monsoon period (Fig. 4). This rich region was situated in and to the east of the Somali Current system, the northeasterly component of which is typically strongest during June-September (Wooster, Schaefer and Robinson 1967).

Upwelling enriches the Somali Current in this season. At the same time, the Southwest Monsoon Current evidently carries part of the dense Somali populations eastward.

During "Lusiad," the characteristics of the Southwest Monsoon Current differed between the western and eastern sides of the ocean. On the 53° E transect, flow was easterly only to the north of 2° N (Taft 1965); south of the equator the currents were poorly defined, but generally westerly. These observations, together with those made along the 62° E transect, suggested to Taft that in this western part of the ocean the circulation was in the form of a clockwise gyral, probably centered near 3° N. The northern part of the gyral formed the origin of the easterly Southwest Monsoon Current. Such a gyral of circulation in the rich area could help to explain the meridional type of distribution of species and abundances on the western side of the ocean, as compared with the more clearly zonal distributions found to the east, discussed below.

Physical and chemical profiles along the equator (Fisher, 1964; Taft 1965) show the presence of relatively cool (<26° C) water in the 0-100 m layer west of 55° E (Fig. 14). Salinity, oxygen and inorganic phosphate content are high in the upper layers of this westernmost area, suggesting that the water arose from depths below the thermocline.

On the eastern side of the ocean the species distributions tended to be zonal, as were the currents, which, for the most part, flowed from west to east. For example, *Nematoscelis microps* (Fig. 12) and *Euphausia brevis* were present at most stations south of the equator, but not north of it. *Stylocheiron microphthalma* was, on the average, four times as abundant south of the equator as north of it, while *Nematoscelis gracilis* was more abundant to the north of the equator, also by a factor of four.

These differences suggest that the easterly current north of the equator has a different origin from that in the 5° zone south of the equator. Some species were abundant in the 0° -5° S zone but were rare in the 0°-5° N zone, except to the west where transport from the south by means of the Somali Current system is evidently taking place. These species include *Nematoscelis microps*, *Thysanopoda subaequalis*, *T. obtusifrons*, *Stylocheiron suhmi*, and *Euphausia brevis*. All are recognized as having principal affinities with central water masses (Brinton 1962, discussing distributions in the Pacific), and have not been confirmed to be present in the Arabian Sea or Bay of Bengal.

Of the numerically important species found on the east-west transect along the equator proper, only *E. brevis* peaked in abundance on the eastern side of the ocean (Fig. 14). Baker (1965) also found *E. brevis* to be present as far north as the equator during *Discovery's* 90° E transect, but maximum numbers were found in the zone 15°-20° S.

Species which were present in greater numbers *north* of the equator than south of it (we continue to refer to the two easternmost N—S transects) were *Euphausia tenera, Thysanopoda tricuspidata*, and *Nematoscelis gracilis.* All three are abundant tropical species. They differ from the "central" species (discussed in the two previous paragraphs) in that they are among the dominant species in the *northern* parts of the Indian Ocean (Tattersall 1939; Ponomareva 1964). Baker found *E. tenera* to be scarce south of 2° S along the 90° E *Discovery transect.*

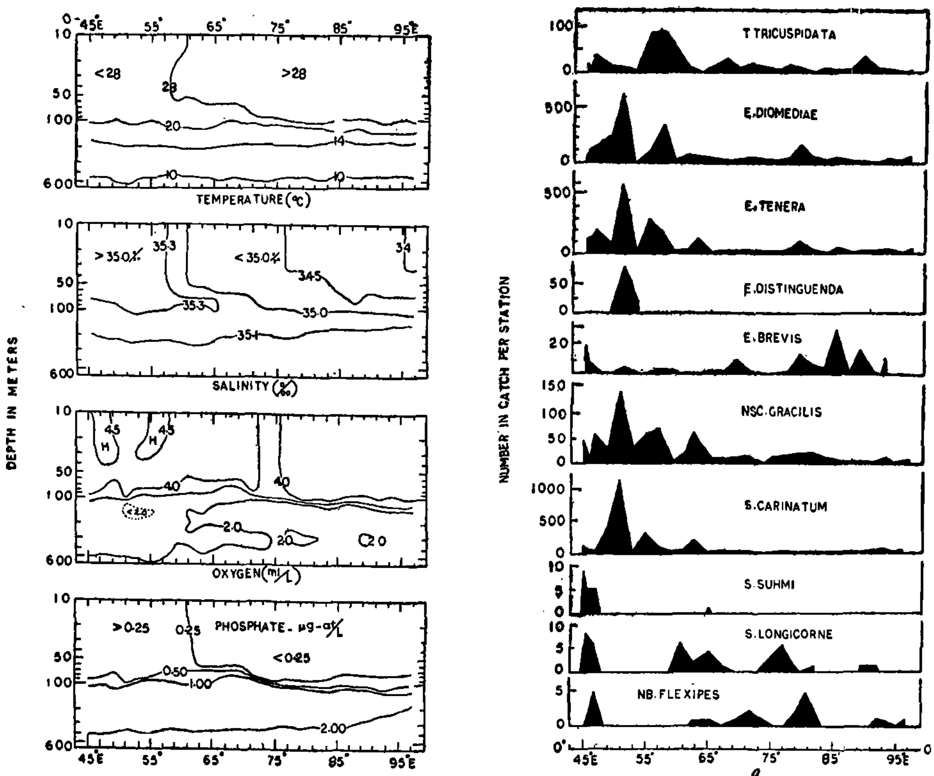

FIG. 14. "Lusiad" Expedition. Equatorial east-west transect, July 1-22, 1962 : (*a*) distribution of temperature, salinity, oxygen, and phosphate (from Fisher 1964) is compared with (*b*) distribution of ten euphausiid species. 27 stations between 45° E and 95° E are considered.

References

Baker, A. de C. (1965). The latitudinal distribution of *Euphausia* species in the surface waters of the Indian Ocean. *'Discovery' Rep.*, 33, 309-344.

Boden, B. P. (1951). The euphausiid crustaceans of southern African waters. *Trans. R. Soc. S. Afr.*, 36, 181-243.

Boden, B. P., and Brinton, E. (1957). The euphausiid crustaceans *Thysanopoda aequalis* Hansen and *Thysanopoda subaequalis* Boden, their taxonomy and distribution in the Pacific. *Limnol. Oceanogr.*, **2**, 337-341.

Brinton, E. (1962). The distribution of Pacific euphausiids. *Bull. Scripps Inst. Oceanogr.*, **8**, 51-270.

——————(1967). Vertical distribution and avoidance capability of euphausiids in the California Current. *Limnol. Oceanogr.*, **12**, 431-464.

Currie, R. I. (1963). The Indian Ocean Standard Net. *Deep Sea Res.*, **10**, 27-32.

Fisher, R. L. (*ed.*) (1964). Preliminary results of Scripps Institution of Oceanography Investigations in the Indian Ocean during Expeditions Monsoon and Lusiad. SIO Ref. 64-19, Univ. California, San Diego.

Hansen, H. J. (1910). The schizopoda of the Siboga Expedition. *Siboga Exped.*, **37**, 1-123.

Illig, G. (1930). Die Schizopoden der Deutschen Tiefsee-Expedition. *Wis. Ergensbn. dt. Tiefsee-Exped. 'Valdivia'*, **22**, 400-465.

John, D. D. (1936). The southern species of the genus *Euphausia*. *'Discovery' Rep.*, **14**, 193-324.

Ponomareva, L. A. (1964). On the Euphausiacea of the Arabian Sea and the Bay of Bengal. (*In Russian*) *Trudy Inst. Okeanol.*, **58**, 163-166.

——————(1966). Quantitative distribution of Pacific euphausiids. (*In Russian*). *Acad. Sci. USSR, Oceanology*, **6**, 690-693.

Silas, E. G., and Mathew, K. J. (1967). *Stylocheiron indicus*, a new euphausiid (Crustacea; Euphausiacea) from Indian Seas. *Curr. Sci.*, **36**, 169-172.

Taft, B. A. (1965). Current velocity structure at the equator in the Indian Ocean. Doctoral Dissertation, Univ. California, San Diego, pp. 1-182.

Tattersall, W. M. (1912). Reports of the Percy Sladen Trust Expedition to the Indian Ocean in 1905 IV, No. 9. On the Mysidacea and Euphausiacea collected in the Indian Ocean during 1905. *Trans. Linn. Soc. Lond.* (*Zool.*), Ser. 2, **15**, 119-136.

——————(1939). The Euphausiacea and Mysidacea of the John Murray Expedition to the Indian Ocean. *John Murray Exped.* (1933-34), *Sci. Rep.*, **5**, 203-246.

Wooster, W. S., Schaefer, M.B., and Robinson, M. K. (1967). Atlas of the Arabian Sea for Fisheries Oceanography. IMR Ref. 67-12, Univ. California, Inst. Mar. Resources, San Diego.

Reprinted from *Bull. natn. Inst. Sci. India*, no. 38, 1968, p. 641-648

A PRELIMINARY REPORT ON THE DISTRIBUTION AND ABUNDANCE OF PLANKTONIC OSTRACODS IN THE INDIAN OCEAN

by JACOB GEORGE

Indian Ocean Biological Centre, National Institute of Oceanography, Cochin-16, S. India

This paper deals with the distribution and abundance of planktonic ostracods as a whole, in the Indian Ocean based on the data from the I.I.O.E. Collections. The average number of ostracods per haul in each 5° Square has been plotted and the variation of population in south-west and north-east monsoon periods has been studied. The population of ostracods is found to be remarkably high in the northern part of the Arabian Sea. A few samples collected from different locations of the Arabian Sea have been analysed and out of the 24 species observed, *Cypridina dentata* is found to be the most dominant species.

INTRODUCTION

One of the main objects of the biological work of the International Indian Ocean Expedition is the study of the qualitative and quantitative distribution of planktonic organisms in the Indian Ocean. Since ostracods constitute a large portion of the planktonic collection in numerical abundance, their study has become particularly important. The main purpose of this paper is to discuss distribution of ostracods in the Indian Ocean, and to consider their comparative abundance. Having come to understand that the population of ostracods in the Arabian Sea is remarkably high, an attempt has been made to identify the main species accounting for the abundance. Samples from selected stations representing both coastal and offshore waters have been analysed. The majority of species that are found in the open sea belong to one family, Halocypridae. Except for two species belonging to the Cypridinidae, all species found in these samples come under Halocypridae. Previous marine expeditions have provided material which make it possible to identify the majority of the species in the present material. However, the juvenile stages of Halocypridae have not yet been adequately described. Therefore, the identification of most species listed here in this report has depended mainly on the availability of adult specimens.

MATERIALS EXAMINED

The observations on distribution and comparative abundance are based on 1223 standard samples from different parts of the Indian Ocean. These plankton samples were collected by means of the Indian Ocean Standard Net, in a vertical haul from 200 m to the surface. The average number of ostracods in a haul for each 5° square have been calculated and used in making the distributional charts (Figs. 1-3). Samples collected in two different seasons, i.e. April 16 to October 15

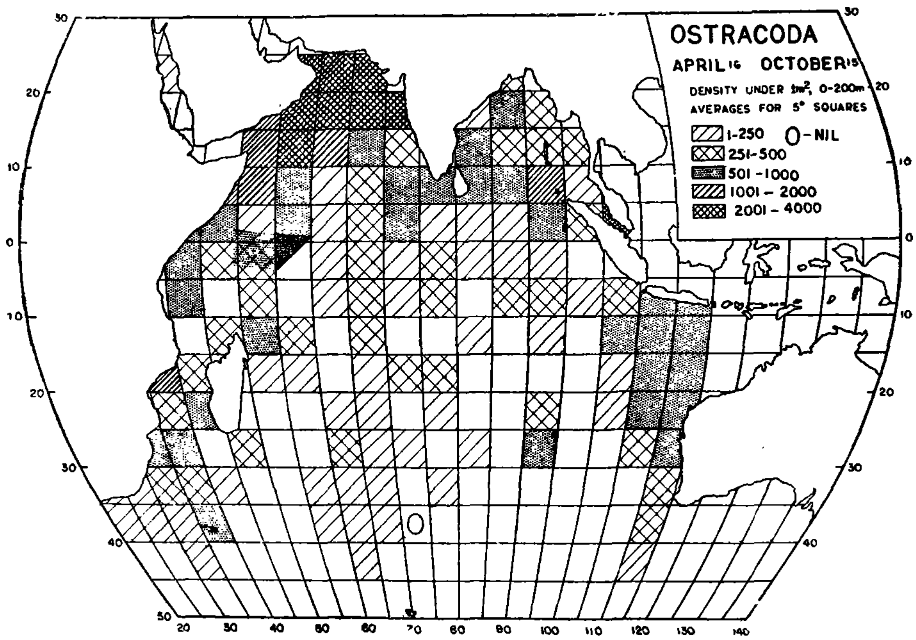

FIG. 1. Distribution of planktonic ostracods in the Indian Ocean, from April 16 to October 15.

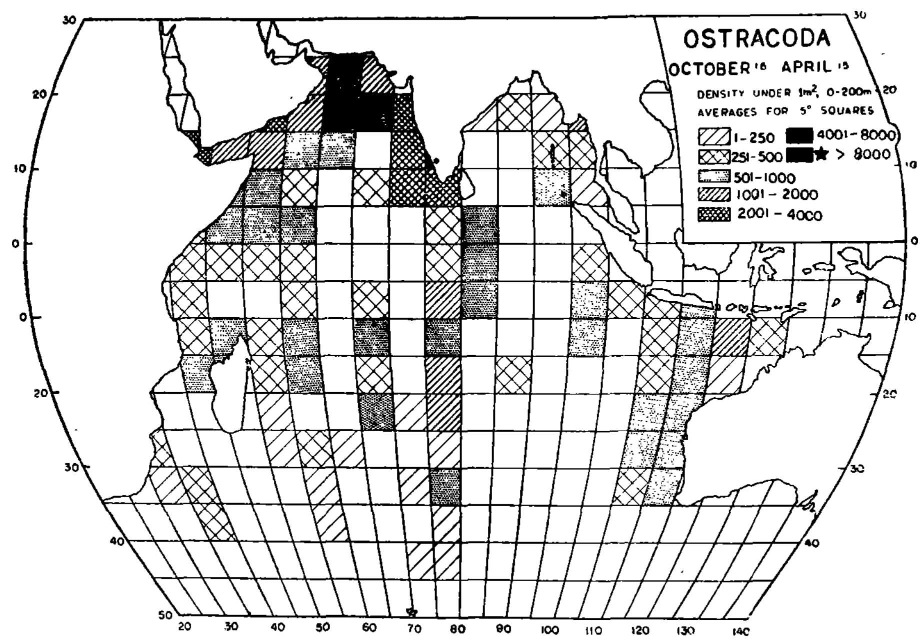

FIG. 2. Distribution of planktonic ostracods in the Indian Ocean from October 16 to April 15.

(Fig. 1) and October 16 to April 15 (Fig. 2), which correspond with the south-west and north-east monsoons respectively, are plotted separately. The study of the species occurrence in samples from the Arabian Sea is based on collections from 23 stations (Fig. 4). These include six collections of *Conch*, six of *Varuna*, seven of *Anton Bruun*, three of *Discovery* and one of *Meteor*.

Distribution and Abundance of Ostracods in the Indian Ocean

During the course of the present study it has become evident as an outstanding fact that ostracods occur far more abundantly in coastal waters than in open ocean. Samples collected near the Somali coast, off the south coasts of Arabia and Persia, the west coast of India and the west and north-west coasts of Australia indicate that the ostracod populations in these areas are of a higher order of density.

Northern parts of the Arabian Sea are found to be favourable regions for the massive development of ostracod populations. The population evidently is largest during the north-east monsoon period. The average number of ostracods per haul falls between 2001-4000 during the south-west monsoon period, and between 4001-8000 during the north-east monsoon, throughout the larger portion of the Arabian Sea. The particular 5° square falling in between 75°E-80° E and 10° N-15° N contained an average of more than 10,000 ostracods per haul, the highest population density observed in the Indian Ocean.

The Bay of Bengal is found to be somewhat less favourable for the development of ostracod populations, when compared to the Arabian Sea. The western part appears to harbour a moderately large population during April-October, but the data are not adequate for estimation of populations during the opposite season. Around the Andamans and in a part of the Straits of the Malacca a somewhat rich population is observed. A uniformly moderate population of ostracods is observed near the west and north-west coasts of Australia throughout the year. There is also a high abundance in the waters between Java and north-west coast of Australia. Near the Somali coast and particularly the south-west coast of Arabia, a moderate population is seen during south-west monsoon period (Fig. 1) and a higher one during the north-east monsoon period (Fig. 2). Around Madagascar the population is moderate in size throughout the year. An interesting point to be noted is the abundance of ostracods in the central part of Indian Ocean, between 75° E-80° E longitude and 5° S-25° S latitude in the October-April period. Except for this area, it is mainly in the coastal waters that maximum production of pelagic ostracods takes place.

Species of Ostracods Observed in the Arabian Sea

Cypridina dentata (Müller)

Stations :—C45, C49, C52, C55, C58, C62, V1797, V1802, V1808, V2040, V2041, AB183, AB198, AB200, D5265, M217.

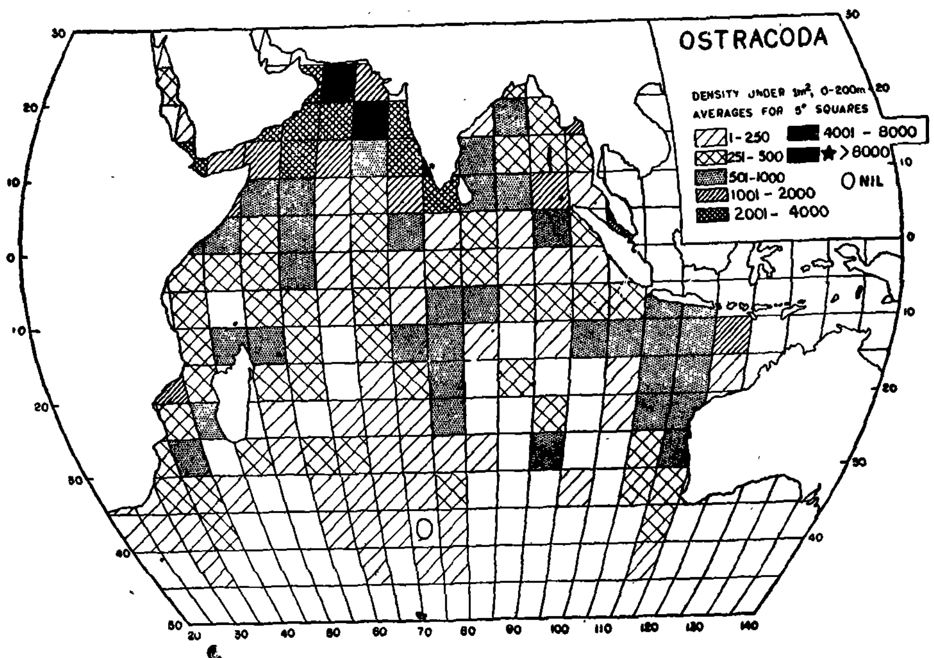

FIG. 3. Distribution of planktonic ostracods in the Indian Ocean, based on all collections taken during the period 1962-65.

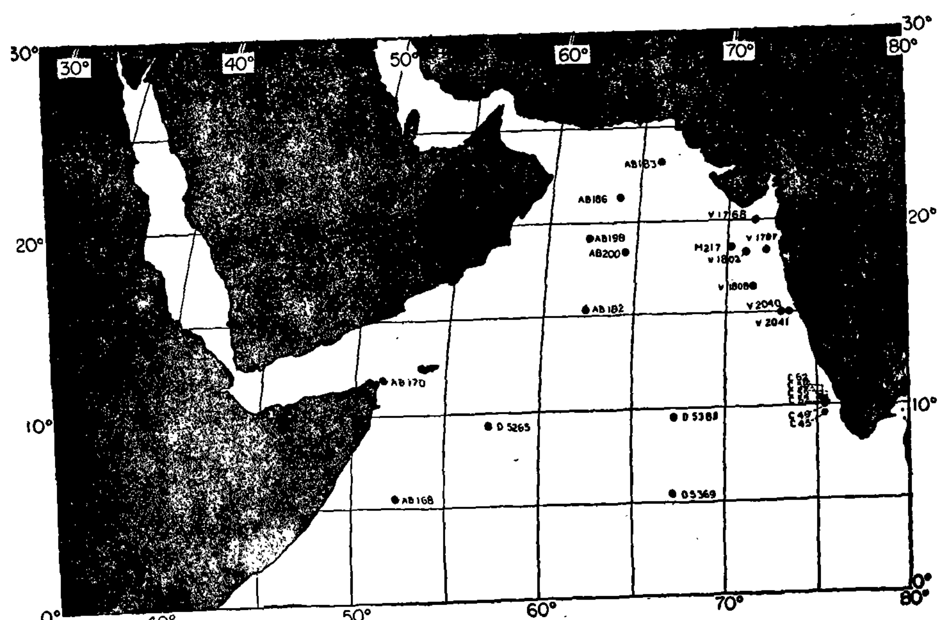

FIG. 4. Locations of stations selected for the study of species occurrence in the Arabian Sea. C—Conch, V—Varuna, AB—Anton Bruun, D—Discovery, M—Meteor,

Cypridina dentata is found to be the most abundant species in the Arabian Sea. In the majority of samples it constitutes more than 75 per cent of the total number of ostracods. It is interesting to note that, out of the 21436 ostracods collected by R.V. *Conch* at Stn. 58, in a single haul, more than 99 per cent are *C. dentata.* Even though *C. dentata* is found usually to be more or less restricted to coastal waters, offshore collections from the northern part of the Arabian Sea show high population densities. It may therefore be assumed that the remarkably high abundance of ostracods in the Arabian Sea is caused largely by this species.

Cypridina acuminata (Müller)

Station :—V1768

This species was found in a single station where there was a complete absence of *Cypridina dentata.* Out of the 23 ostracods found in the sample, 21 were *Cypridina acuminata*, the rest being *Euconchoecia aculeata.*

Halocypris inflata (Dana)

Stations :—C45, C49, C52, AB168, D5265, D5369.

This species was collected in few numbers, and only at stations south of 10° N latitude, but representing both coastal and offshore waters. At Stn. AB168, approximately 60 specimens were observed.

Archiconchoecia striata Müller

Stations :—C52, D5265.

One specimen from each station was obtained.

Euconchoecia aculeata (Thomas Scott.)

Stations :—C45, C49, C52, C58, C62, V1768, V1797, V1802, V1808, V2040, V2041, AB182, AB183, AB186, AB198, AB200, D5369, D5383, M217.

Observed in large numbers in a majority of the samples. An estimated number of 550 specimens were present at Stn. M217.

Euconchoecia chierchiae Müller

Station :—D5265.

A single specimen was obtained from the above station, at which there was a complete absence of *Euconchoecia aculeata.*

Grubea lacunosa (Müller)

Stations :—C49, V2041,

One female specimen 2.2 mm long from Stn. C49 and one male 3.15 mm long from Stn. V2041 were collected, which agree with Müller's (1908) description of *E. lacunosa* from a female larval specimen measuring 1.6 mm collected from Antarctic waters.

Conchoecia atlantica (Lubbock)

Stations :—C45, C49, C55, C58, C62, V2040, V2041, AB170, AB182, AB186, AB198, AB200, D5265, D5369, D5383.

Moderate numbers were obtained from these stations.

Conchoecia rotundata Müller

Stations :—C45, C49, C52, C55, C58, C62, V1808, V2040, V2041, AB168, AB170, AB182, AB183, AB186, AB198, AB200, D5265, D5369, D5383.

This species was collected in large numbers from coastal as well as offshore waters.

Iles (1953) confirms the hypothesis put forward by Skogsberg (1920) that *C. rotundata* is probably a mixture of closely allied species. He creates two new species, *C. skogsbergi* and *C. teretivalvata*, after examining the material from the Benguela Current and restricts the specific name *C. rotundata* to the Pacific material described by Müller. The specimens present in these samples do not agree with either of these two new species and hence the specific name, *C. rotundata* Müller is retained for the present even though the original description is quite inadequate, until a detailed study of the Indian Ocean material is completed.

Conchoecia kyrtophora Müller

Stations :—C58, D5369.

A few specimens were collected from the above stations.

Conchoecia procera Müller

Stations :—C45, C49, C52, C55, C58, V1808, V2040, V2041, AB168, AB182, AB183, AB186, D5383, M217, AB198, AB200, D5265, D5369.

As in the case of *Conchoecia rotundata*, this species was collected in large numbers. It is one of the most common species of the Arabian Sea.

Conchoecia acuminata (Claus)

Stations :—C45,C49,C52, C55, C58, C62, V2040, V2041, AB170, AB182, AB186, AB198, D5369, D5383.

Moderate numbers were collected from the above stations.

Conchoecia elegens Sars

Stations :—C45, C49,C52, C58, AB186.

This species was collected in moderate numbers.

Conchoecia discophora Müller

Stations :—D5383.

A few specimens were obtained from this station.

Conchoecia subarcuata Claus

Stations :—AB168, AB170, D5265.

Small numbers were collected from these stations.

Conchoecia magna Claus, var. *typica* Müller

Stations :—C45, C55, C62, AB168, AB170, AB182, AB183, AB198, D5265, D5369.

It was present in coastal as well as offshore waters, but found to be more abundant in offshore waters.

Conchoecia spinirostris Claus

Stations:—C55, V2040, AB168, AB170, AB182, AB186, D5369.

The distribution was found to be somewhat similar to that of *C. magna* var. *typica*.

Conchoecia curta Lubbock.

Stations:—C45, C49, C52, C55, C62, AB170, D5265, D5369.

This species is more abundant in coastal waters than offshore.

Conchoecia decipiens Müller

Stations:—C45, C49, C52, C55, C58, C62, V2040, AB170, AB182, AB186, AB198, D5265.

Moderate numbers were present.

Conchoecia echinata Müller

Stations:—C62, AB170.

This was found at only two stations, and the number of specimens is small.

Conchoecia alata alata Müller

Stations:—C55, V1808, V2041, AB168, AB170, AB182, AB198, AB200.
Most abundant in offshore waters.

Conchoecia parthenoda Müller

Stations:—C49, C62, AB168, AB170, D5369.

A few specimens were collected from the above stations.

Conchoecia bispinosa Claus

Stations:—AB170, D5369.

A few specimens were collected from these stations.

Conchoecia striola Müller

Stations:—C58, D5265, D5369.

This was present at three stations, and only in small numbers.

Conchoecia parvidentata Müller

One specimen was obtained at Station D5383.

ACKNOWLEDGEMENT

I wish to acknowledge my sincere thanks to Dr. N.K. Panikkar, Director, National Institute of Oceanography, for permitting me to present this paper and to Dr. Edward Brinton, and Mr. L. R. Kasturirangan, for going through the manuscript and giving me suggestions and encouragement for the work. I am particularly grateful to Dr. K. G. McKenzie who introduced me to the field of Ostracod studies, and for the continued interest he has shown in the progress of my work.

REFERENCES

Iles, E. J. (1953). A preliminary report on the Ostracoda of the Benguela current. '*Discovery*' *Rep.*, **26**, 261-279.

Müller, G. W. (1906). Ostracoda. *Wiss. Ergebn. dt. Tiefsee-Exped. Valdivia*, **8**, 29-154.

———(1908). Die Ostracoden der Deutschen Südpolar Expedition 1901-03. *Dt. Südpol. Exped.*, 1901-03, **10**, 52-181.

Skogsberg, T. (1920). Studies on Marine Ostracoda. Pt. 1. *Zool. Bid.*, *Uppsala*. (Suppl.) Bd. 1 1-784.

Reprinted from *Bull. natn. Inst. Sci. India*, no. 38, 1968, p. 700-717

A PRELIMINARY REPORT ON THE DISTRIBUTION AND RELATIVE ABUNDANCE OF EUTHECOSOMATA WITH A NOTE ON THE SEASONAL VARIATION OF *LIMACINA* SPECIES IN THE INDIAN OCEAN

by M. Sakthivel

Indian Ocean Biological Centre, National Institute of Oceanography, Cochin-16

Euthecosomata (holoplanktonic opisthobranch molluscs) sorted out from the collections of the International Indian Ocean Expedition are now being studied and the present communication is a first report based on an examination of material from 395 stations. Species were identified with the help of Tesch's studies (1946, 48) on the Dana Collections. *Limacina helicina* (Phipps) is newly recorded from the Indian Ocean. Including it, twenty-five species of euthecosomes are known to occur in this Ocean. This paper reports on twenty species, their distribution and numerical abundance over the Indian Ocean and compares present results with earlier records of the group in the Indian Ocean. The occurrence of a greater number of species as well as of larger numbers of individuals of particular species, is noted from the following areas: the sea east of Somalia, the Mozambique channel, the equatorial belt of the Indian Ocean, specified areas of the Arabian sea and Bay of Bengal. The most noteworthy of these areas is to the east of Somalia from where consistently high numbers of individuals were obtained for a good many species. This area is well-known for the upwelling of nutrient rich water during the south-west monsoon period and for its high biological productivity. A comparison of different months of the year with respect to the numerical abundance of three species of *Limacina*, indicated that all three species were at maximum abundance during August, which is the peak period of the south-west monsoon. Some species, e.g., *Styliola subula*, *Cuvierina columnella*, *Cavolinia globulosa* and *C. inflexa*, that are common in the equatorial belt and in Somali waters, are rare in the Bay of Bengal and the Arabian Sea, but the reasons for this are yet to be unravelled.

Introduction

Our present knowledge of the Thecosomata (formerly known as Pteropods) is based on the reports of the several expeditions carried out during the last hundred years. However, owing to the lack of intensive and systematic sampling, information on the pattern of distribution and relative abundance of these holoplanktonic forms in the Indian Ocean is incomplete. The available records are from the expeditions listed in Table I.

Table I

Name of the Expedition	Author of report	No. of species of euthecosomes recorded in the Indian Ocean
Voyage of H.M.S. Challenger (1873-76)	Pelseneer, P. (1888)	20
Deut. Tiefsee Expedition 'Valdivia' (1898-1899)	Meisenheimer, J. (1905)	21
John Murray Expedition (1933-34)	Stubbings, H.G. (1937)	16
Percy Sladen Trust Expedition (1905)	Tesch, J. J. (1910)	18
'Dana' (Indo-Pacific 1928-1930)	Tesch, J. J. (1948)	21
'Umitaka Maru' Expedition (Indo-Pacific 1956)	Taki, I. & Okutani, T. (1962)	16

The present report is based on an examination of Euthecosomata sorted out from 395 zooplankton samples collected by R.V. *Argo* and R.V. *Anton Bruun* during the International Indian Ocean Expedition. The areas explored by these two ships are the Arabian Sea, the Bay of Bengal, the equatorial zone and the south-western part of the Indian Ocean, to 80° E and 45° S. The positions of the stations of Cruises I to VIII of *Anton Bruun* and of the "Lusiad" and "Dodo" cruises of *Argo* are shown in figure 1 together with the distribution of *Limacina inflata*. No collections have been examined from the west coast of India, west coast of Sumatra and the south-eastern part of the Indian Ocean. The report is preliminary in that it includes data based on about a fifth of the samples in the international collections at the Indian Ocean Biological Centre. The Order Thecosomata includes two suborders, Euthecosomata and Pseudothecosomata. The present report deals only with the Euthecosomata, as the identification of the Pseudothecosomata has not yet been completed. McGowan (1960) states that there are 35 species of Euthecosomata recognized. Of these, 24 have so far been recorded from the Indian Ocean by previous expeditions. With a new record of *L. helicina*, the number of recorded species now increases to 25. Of the 25, not less than 20 have been found in the present collections. The attempt to relate distribution with hydrographical factors is done tentatively owing to the limited information available.

Review of Distribution of Species

Systematic List of Species

Family Limacinidae Gray 1847.
Genus *Limacina* (Cuvier) Lamarck 1819.

1. *L. inflata* (d' Orbigny 1836)
2. *L. bulimoides* (d' Orbigny 1836)
3. *L. trochiformis* (d' Orbigny 1836)
4. *L. lesueuri* (d' Orbigny 1836)
5. *L. helicina* (Phipps 1774)

Family Cavoliniidae (d' Orbigny 1841)
Genus *Clio* Linne' 1767

6. *C. pyramidata* Linne' 1767
7. *C. cuspidata* (Bosc 1802)
8. *C. balantium* (Rang 1834)

Genus *Creseis* Rang 1828

9. *C. virgula* Rang 1828
10. *C. acicula* Rang 1828

Genus *Styliola* Lesueur 1810

11. *S. subula* Quoy and Gaimard 1827

Genus *Hyalocylix* Fol 1875

12. *H. striata* (Rang 1828)

Genus *Cuvierina* Boas 1886

13. *C. columnella* (Rang 1827)

Genus *Diacria* Gray 1850

14. *D. quadridentata* (Lesueur 1821)
15. *D. trispinosa* (Lesueur 1821)

Genus *Cavolinia* Abilgaard 1791

16. *C. longirostris* (Lesueur 1821)
17. *C. globulosa* (Rang 1850)
18. *C. inflexa* (Lesueur 1813)
19. *C. uncinata* (Rang 1836)
20. *C. gibbosa* (Rang 1836)

Limacina inflata (d'Orbigny)

The distribution of this species (Fig. 1) is not uniform over the area of occurrence, but it does extend over a wide area with localized regions of greater abundance. Such areas are, except for one station, between 20° N and 20° S. They lie mainly off the coasts of equatorial Africa and Arabia, between 5° S and 10° N, 45° E and 55° E. According to McGowan (1960) in the Pacific "this species is responding to an 'enrichment' of its environment due to the upward mixing of nutrient rich deepwater in the equatorial current system....." This explanation seems also to be true in the present instance, since the areas of maximum abundance noticed here are regions associated with well-known centres of upwelling off the Somali and Arabian coasts during the period of the south-west monsoon. In the southern part of the Indian Ocean between 20° S and 40° S, 55° E and 80° E, where the hydrographic conditions are comparatively stable, the population density is low, a feature in which the present observation agrees well with what McGowan has noticed in the part of the eastern tropical Pacific in zone 10° - 20° N.

Limacina bulimoides (d'Orbigny)

The general pattern of distribution of this species resembles that of *L. inflata*, but occurrences are scarcer south of 30° S (Fig. 2). Maximum concentrations are between 10° S and 12° N, but mainly east of Somalia. This area is more restricted than the area of *L. inflata* maximum, suggesting an even closer tie with the upwelling-enriched conditions off Somalia where the temperature is low during June-September.

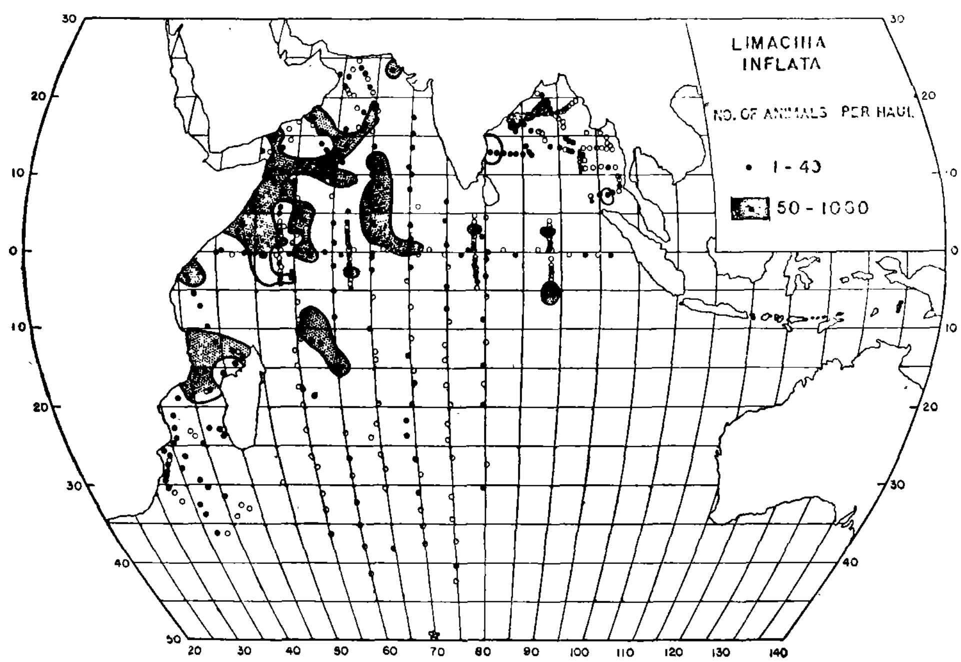

FIG. 1. The distribution of *Limacina inflata*.

Limacina trochiformis (d'Orbigny)

Unlike the reported distribution in the Pacific and Atlantic, *L. trochiformis* is a common and widespread species in the Indian Ocean (Fig. 3). But the area of maximum concentration is smaller than that of the two *Limacina* species discussed above. The high abundance of this species is similar to the other two species seen off the Somali coast between 0° and 10° N, 45° E and 55° E.

SEASONAL VARIATION IN *Limacina inflata, L. bulimoides* AND *L. trochiformis*

The above three species of *Limacina* showed seasonal changes in abundance (Fig. 4). Monthly values of population-density were calculated for each species for the period 1962-1964. These values represent the average number of specimens per standard sample, based on all samples containing positive records (Figs. 1-3). The period of December (no samples) and January (three samples) was poorly represented in the material examined, whereas April-May and July-October were well represented (22-47 samples per month). It can be seen that the three species have somewhat independent patterns of fluctuation during January-May, when populations are small. In June a decline is discernible, followed by an abrupt tenfold increase in July and August. After the August peak, there is a decline until November. The area of maximum population-density for all three *Limacina* species has been noted to be off the Somali coast. The strong correlation between season and abundance of the species is probably related to enrichment of that region by means of intensive upwelling during the south-west monsoon, June-September.

Limacina lesueuri (d' Orbigny)

Out of 395 samples examined, only 17 contained this species. On this basis it is considered rare in the Indian Ocean. From the nature of the distribution (Fig. 5) it is evident that all records except one are from south of the equator. There is no previous or present record of this species from the Arabian Sea, an area characterized by low oxygen concentration at intermediate depths one ml/l at 150 m, and high salinities 34-36.5‰ (Nejman 1961). It is interesting to note its most frequent presence in the Mozambique Channel and to the east of South Africa.

Limacina helicina (Phipps)

This is a cold water species not hitherto recorded from the Indian Ocean. There are only three records (Fig. 5), two of which are off Durban and one at 35° S, 60° E. These occurrences are clearly related to the temperate environment in the zone of 25-35° S.

Clio pyramidata Linne'*

According to Tesch (1948) this cosmopolitan species is eurythermic to a certain degree. In the North Atlantic it is known to penetrate regularly beyond 40° N.

*The variants of *Clio pyramidata* have not been identified yet consequent on the absence of the shell in most of the specimens.

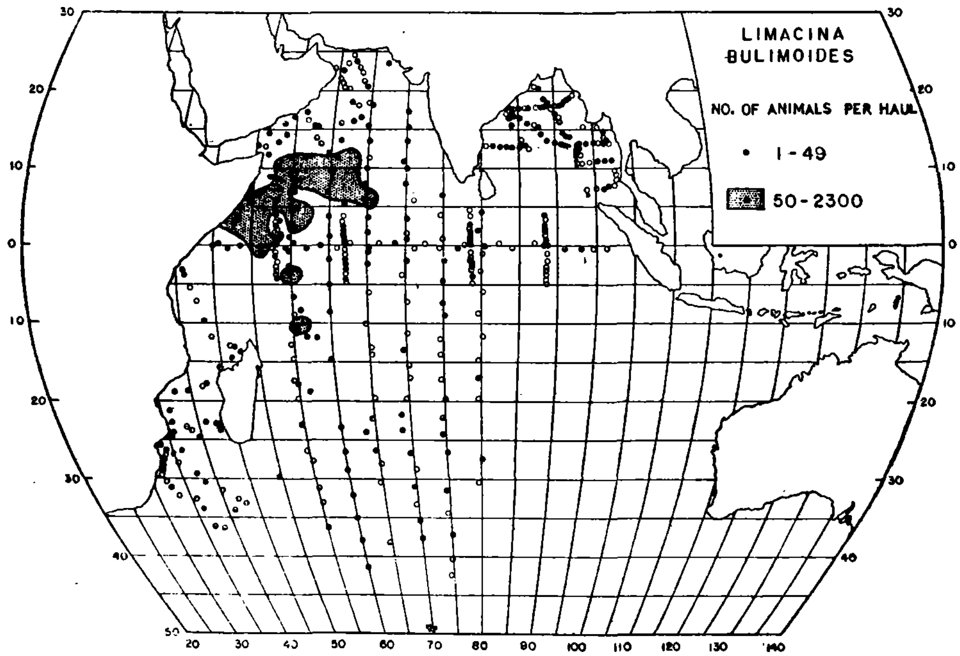

FIG. 2. The distribution of *Limacina bulimoides*.

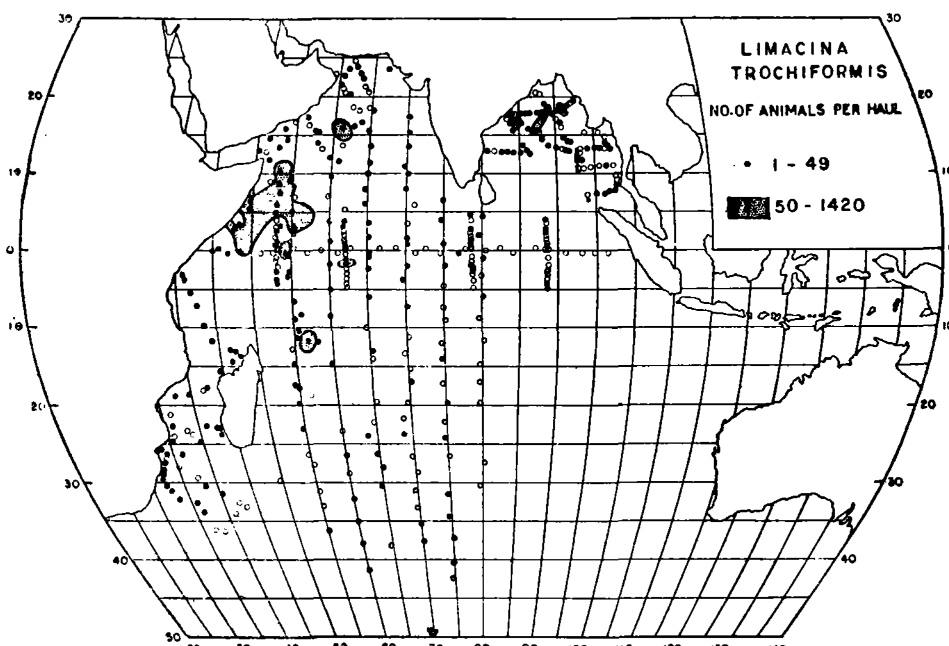

FIG. 3. The distribution of *Limacina trochiformis*.

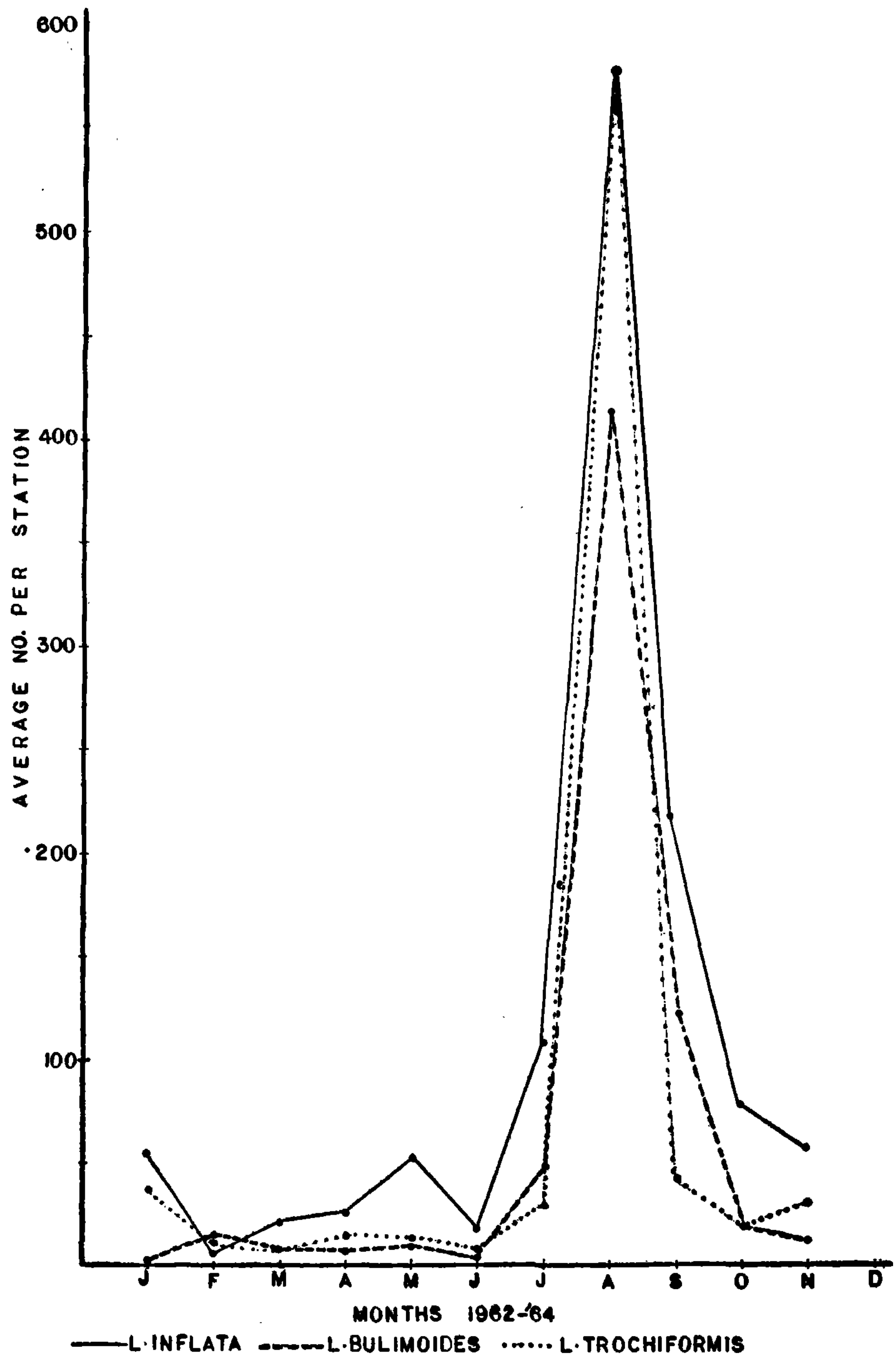

FIG. 4. Seasonal variation in *L. inflata*, *L. bulimoides*, *L. trochiformis*.

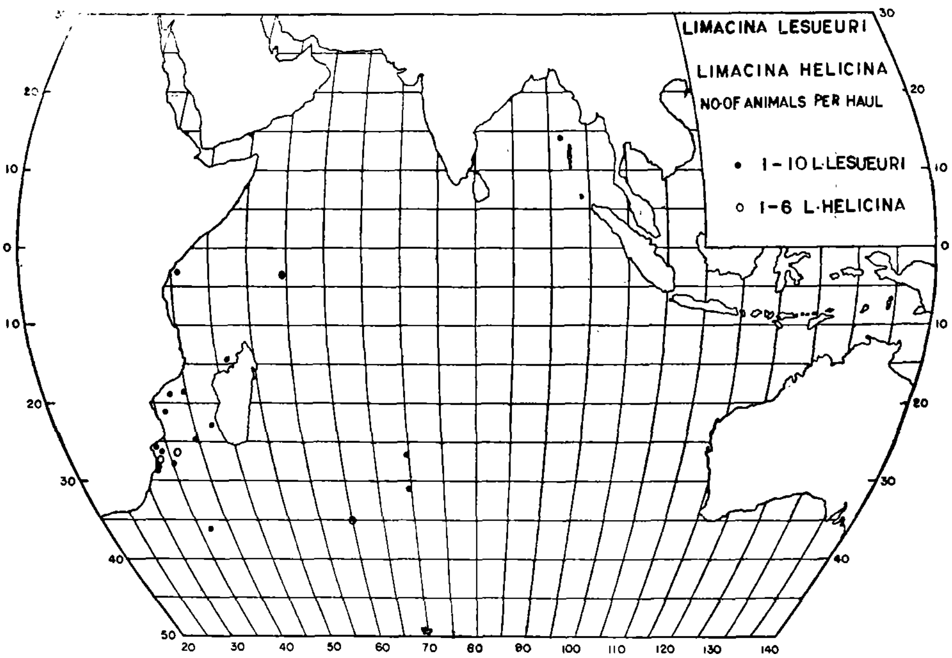

FIG. 5. The distribution of *Limacina lesueuri* and *L. helicina*.

"At the east coast of Africa it reaches, in isolated individuals, less than 50 specimens per hour's fishing, down to the latitude of Durban".

In the Indian Ocean this widespread species is apparently most common off the Somali coast, in the western equatorial Indian Ocean, the Bay of Bengal and northern Arabian Sea (Fig. 6).

Clio cuspidata (Bosc)

The rarity of the species in the present material is clear from the fact that there are only two records of adult specimens : 02° 00'S, 62° 20'E and 03° 34'S, 40° 53' E. Tesch (1948) however, found this to be a common species in the Indian Ocean. The rarity of *C. cuspidata* in the present samples may be due to the fact that juveniles have not yet been identified. McGowan (1960) attributed the rare occurrence of this species to an extreme form of patchiness in its distribution.

Clio balantium (Rang)

There are only five previous records in the Indian Ocean (Meisenheimer 1905; Tesch 1948) of which three are south-east and south of Madagascar, one south of Ceylon and the other off the west coast of Sumatra. All three of the present records are from the Bay of Bengal 18° 33'N, 91° 16'E, 12° 56'N, 92° 10'E; 14° 15'N 91° 50'E. Because of imperfect preservation and consequent distortion and damage, the identification is tentative. However, the broadly developed fins and the conspicuous posterior foot lobe indicate a close resemblance to *C. balantium*.

Creseis virgula Rang*

The scattered but widespread occurrences of this species are more consistent along the equatorial zone, off the Somali coast, the Bay of Bengal, and the Gulf of Oman (Fig. 7). All of the samples containing more than 50 specimens are from north of 10° S suggesting that this is mainly a tropical species. Occurrences south of 20° S are few. Tesch (1948) has also remarked on the wide occurrence of this species in the tropical Indo-Pacific.

Creseis acicula Rang

This species is of very general occurrence in the Arabian Sea, the Bay of Bengal, the western equatorial Indian Ocean and the Mozambique Channel (Fig. 8). High concentrations at a few stations off south-east Africa may be related to the influence of the land mass, as this species is recognized as being often abundant close to the shore in shallow bays and inlets. The southernmost occurrence was noted at 32° S.

Styliola subula Quoy and Gaimard

Meisenheimer (1905) was of the opinion that *S. subula* avoids strictly tropical waters and is most common beyond the 10° or 15° parallels, away from the equator. This sort of antitropical** distribution was not observed by Tesch (1948) since he noticed continuous distribution in the Pacific from the north central through the equatorial to the south central waters. Massay (1920) however, found that in the Atlantic *S. subula* avoided the very warm water near the equator. In the Pacific, McGowan (1960) points out that the distribution of the species is bisubtropical with "limited communication between the two segments of the population of the south and north subtropical Pacific". The distribution in the Indian Ocean further suggests that this is not a strictly antitropical species, since six stations of relatively high concentration were found in the western equatorial Indian Ocean (Fig. 9). However, Massay's explanation that "this species avoids the very warm water..." may still be applicable, inasmuch as the tropical maximum is in the area influenced by the cool Somali current.

The rare occurrence of the species in (1) the northern Indian Ocean (north of 7° N), (2) the southern part between 5° S and 15° S, and (3) the mid-part of the equatorial zone, may possibly be attributed to the excluding effect of high-temperature suggested by Massay, but both of the principal areas of high occurrence are mixing areas,—the terminus of the North Equatorial Current east of Africa, and the region of mixing of equatorial and subtropical water south of Madagascar (Orren 1963). Tesch (1948) noted that "there are some very rich stations at the west coast of Sumatra

*The identification of variants of *C. virgula* is not yet attempted as most of the specimens have lost their shells.

**Antitropical is defined by McGowan as follows. "Where the same or two closely related species inhabit areas both to the north and to the south of the tropical latitudes. These may be bipolar, biboreal, bitemperate or bisubtropical."

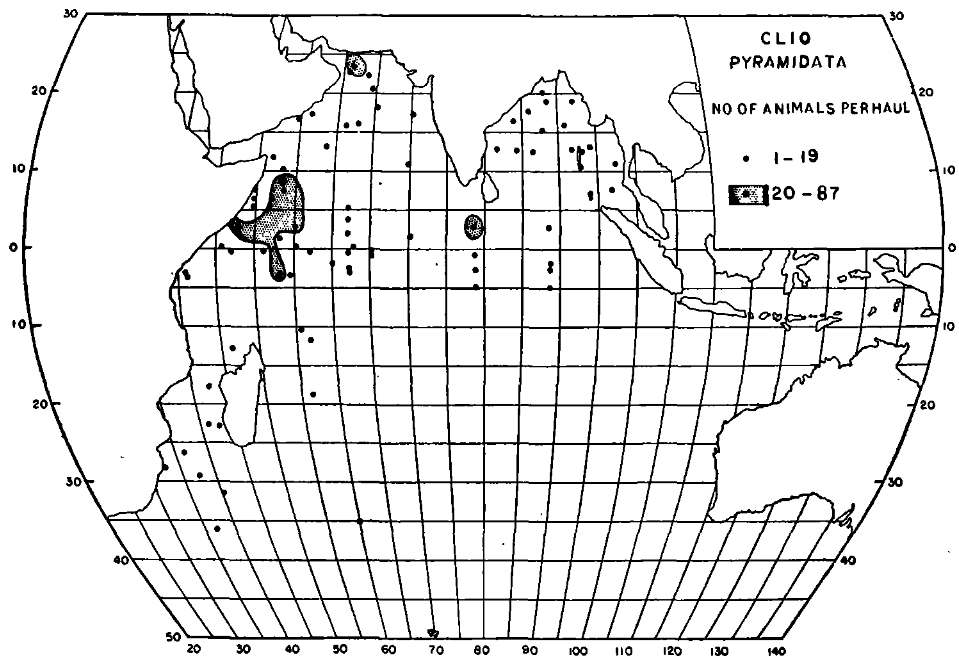

FIG. 6. The Distribution of *Clio pyramidata*.

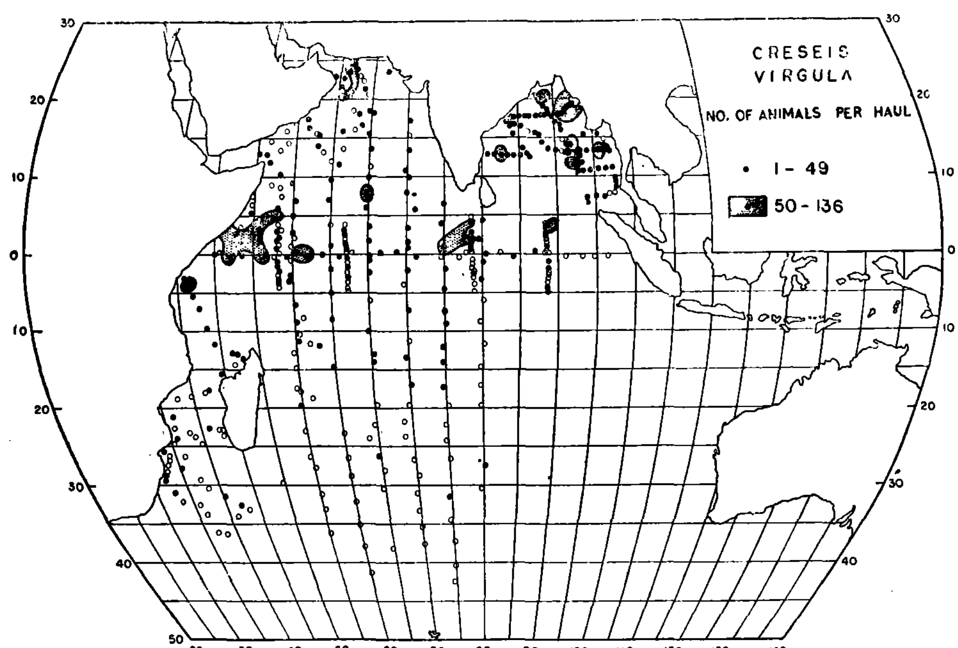

FIG. 7. The distribution of *Creseis virgula*.

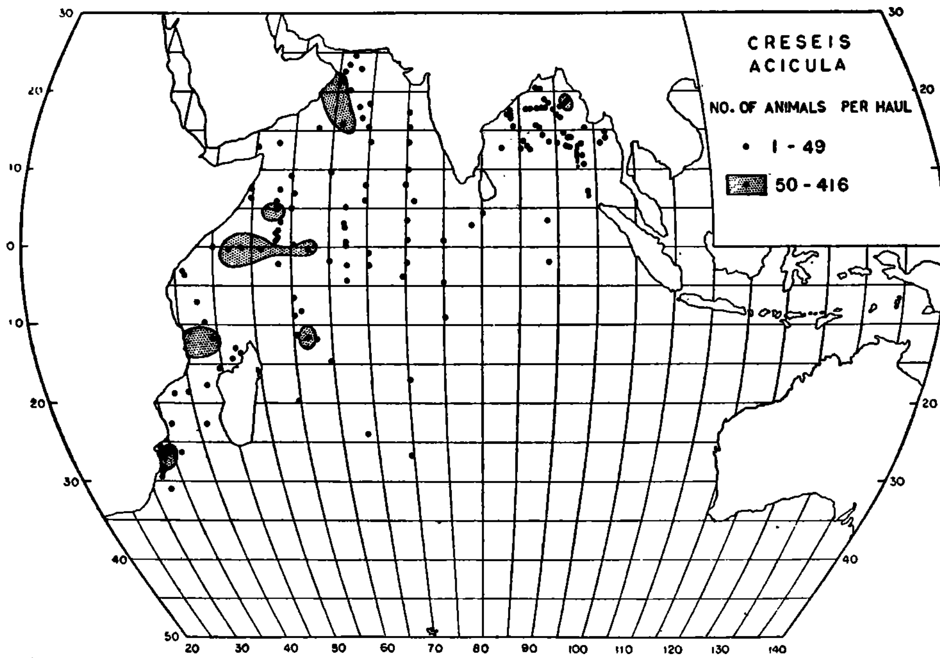

FIG. 8. The distribution of *Creseis acicula*.

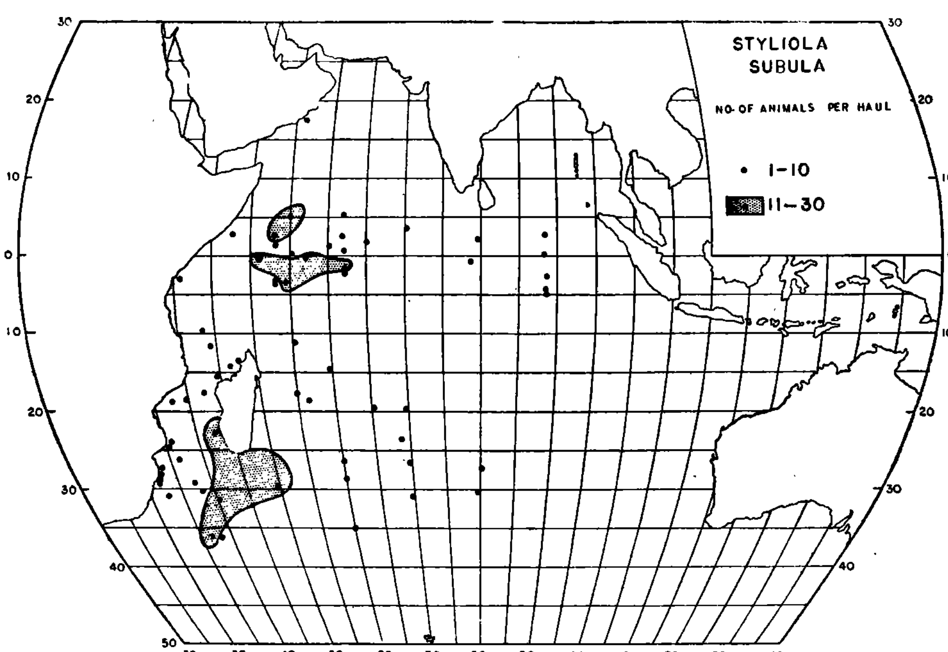

FIG. 9. The distribution of *Styliola subula*.

but on the track Nicobar-Ceylon-Seychelles it seemed rather scarce and only north of Madagascar, down to Duran was it again numerous". It is Stubbings's (1937) view that, in the Indian Ocean, this species is "more abundant between 25° S and 34° S except round the Cape of Good Hope; the scarcity in the northern part of Indian Ocean and Arabian Sea is in accordance with Meisenheimer's statements regarding its distribution. The distribution of the species on the east coast of Africa can possibly be attributed to the presence there of cooler Antarctic water flowing up the African coast".

Hyalocylix striata (Rang)

This is a typical tropical species, apparently very rare south of 20° S. The occurrence to 30° S in the Mozambique Channel may be, Tesch (1948) infers, owing to transport by the Agulhas Stream. The places of high abundance are along the equator, in the northern Arabian Sea, and in the northern and eastern parts of the Bay of Bengal (Fig. 10). According to McGowan (1960) "This species, like *L. inflata* and *D. trispinosa*, is adapted to warmer water conditions, but is able to achieve abundance only in those areas where either lateral or vertical movement of water mixes in cooler and presumably richer waters". The observed localities of high abundance are in such areas. At the western coast of Sumatra, Tesch (1948) has recorded it in every haul, sometimes in quantities of 2000 or even 3000. Stubbings (1937) too noted high concentration in the northern Arabian Sea and the Gulf of Aden.

Cuvierina columnella (Rang)

This species is most common along the equatorial zone (5° S - 5° N) and the Somali coast (Fig. 11). Previous records from Meisenheimer (1905), Stubbings (1937) and Tesch (1948) show more or less the same type of tropical distribution. Tesch (1948) noted that "from Nicobar to Durban this species was not encountered till after passing Ceylon, but from here on it was recorded at a series of stations, maximum being found at 8° 27'S, 50° 54'E. It could be followed up to Durban and it disappeared again on the route to Cape Town. Two largest catches were made close together at the west Sumatran coast by Dana". The scarcity of the species north of 10° N remains a point of interest.

Diacria quadridentata (Lesueur)

This species is found particularly in equatorial Indian Ocean (Fig. 12). High abundance is again noted along the Somali coast. Occurrences beyond 30° S are rare. Tesch (1948) found *D. quadridentata* throughout the tropical region.

Diacria trispinosa (Lesueur)

The distribution of this species in the Indian Ocean is similar to that observed by Tesch (1946) in the Atlantic. It ranges widely in tropical temperate waters, from 40° N to 35° S. High concentrations are noted along the east coast of Africa between 5° N and 15° S, 40° E and 60° E (Fig. 13). It should be pointed out, however, that forms clearly recognizable as adults of *D. trispinosa* occurred in five stations only out of

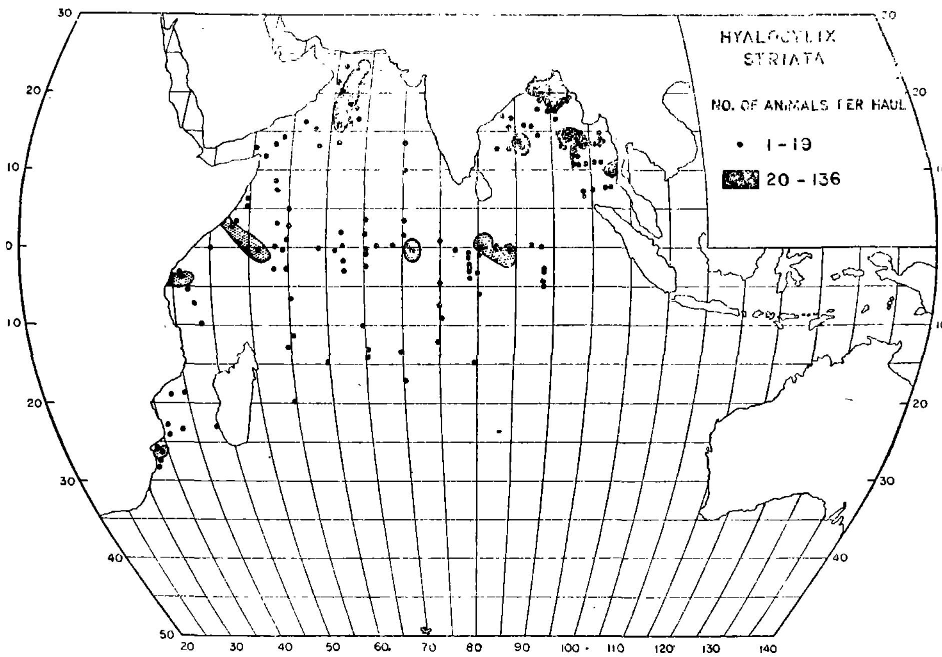

FIG. 10. The distribution of *Hyalocylix striata.*

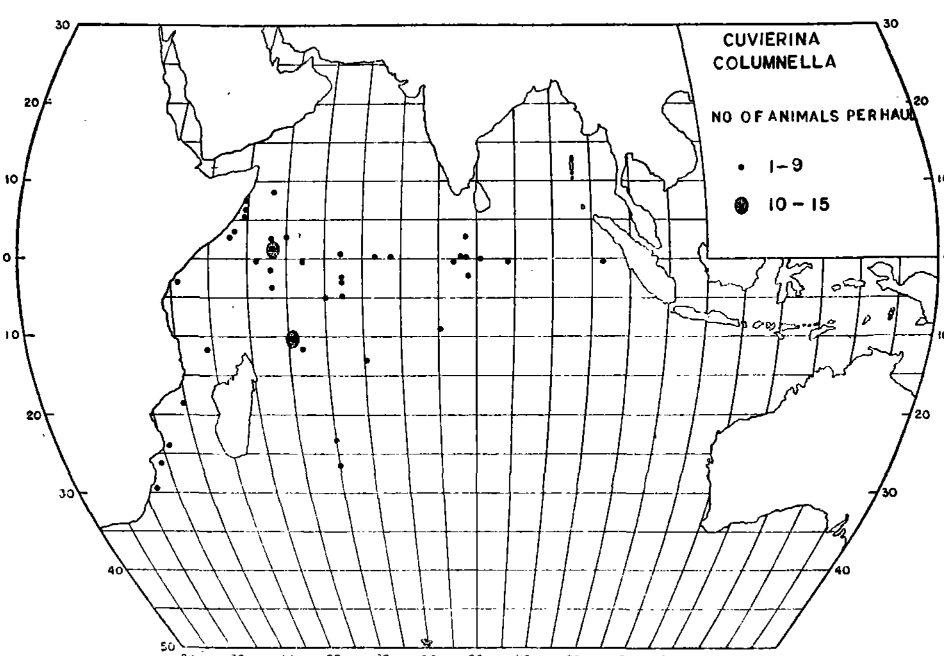

FIG. 11. The distribution of *Cuvierina columnella,*

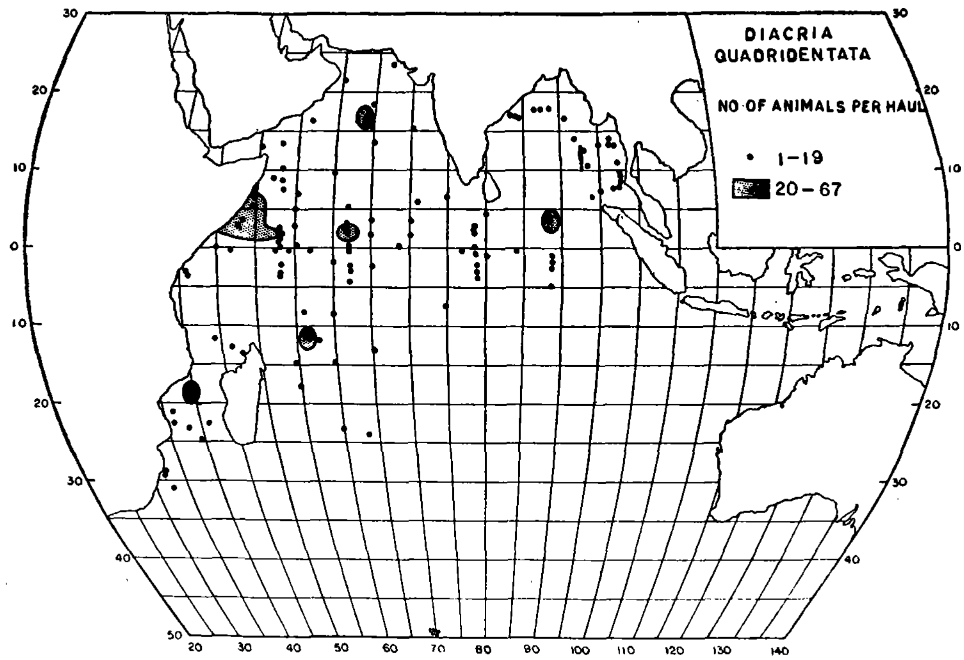

FIG. 12. The distribution of *Diacria quadridentata*.

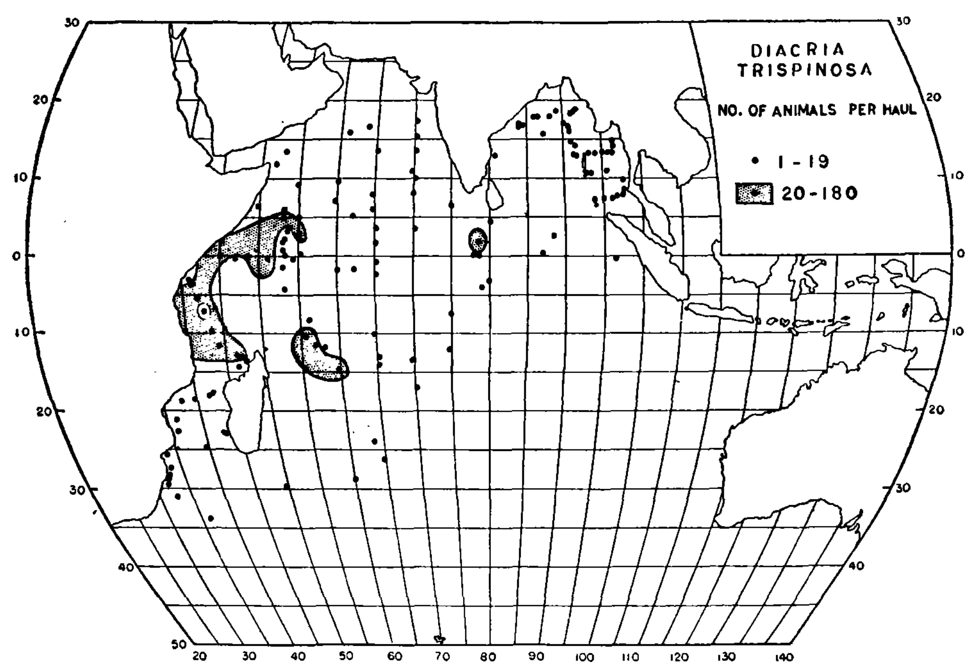

FIG. 13. The distribution of *Diacria trispinosa*.

395 (Fig. 13) and the forms observed in the remaining stations were more or less immatures or juveniles corresponding to *Cleodora compressa* (Souleyet); these juveniles belong mostly to *D. trispinosa* but some of these should perhaps be referred to *D. quadridentata* and the difficulty of separating juveniles of the cosomes according to species is too well known to need emphasis here. The distribution observed in figure 13 is in good agreement with the published records of Stubbings (1937) and Meisenheimer (1905). The paucity of this species in the northern Arabian sea (*see* Fig. 13) had been remarked upon by Stubbings (1937).

Cavolinia longirostris (Lesueur)

This species is not common south of 20° S (Fig. 14). Places of relatively high concentration are patchily distributed throughout the tropical zone. Tesch (1948) has recorded high abundance at the west coast of Sumatra. The records of Stubbings (1937) show that this species is very common in the Arabian Sea.

Cavolinia globulosa (Rang)

The distribution of this somewhat rare tropical species is centred at the equator, 10° N and 10° S. It is not common in the Bay of Bengal, the Arabian Sea and the central part of the southern Indian Ocean (Fig. 15). Tesch (1948) observed that this species is practically confined to the tropical belt of the Indo-Pacific and more common in Indo-Malayan waters and in the Indian Ocean; this is "foreign to the Atlantic". It is perhaps due to its rigid stenothermic habit that the species is unable to round the Cape of Good Hope. In the Pacific the occurrence is also rare (McGowan 1960). Stubbings (1937) was of the opinion that "this is common in the Bay of Bengal and eastern part of the Indian Ocean, and probably occurs almost as frequently in at least the central and southern parts of the Arabian sea; at present it is unknown from the northern part of the Gulf of Oman".

Cavolinia inflexa (Lesueur)

Stubbings (1937) was under the impression that except for a single record in the Bay of Bengal and his single shell-less specimen from the central Arabian Sea, all the previous records for the species in the Indian Ocean are south of the equator. Tesch (1948) recorded "many in Indo-Malayan waters and in the Indian Ocean up to S. of Durban". Meisenheimer (1905) found it to be most common between 20° S and 40° S. The present records are mostly from off the Somali coast and the western equatorial Indian Ocean, 15° N to 10° S and west of 65° E (Fig. 16). This is the cooler part of the tropical zone, enriched by the Somali upwelling. The scarcity of the species in the northern Indian Ocean remains a matter for further investigation.

Cavolinia uncinata (Rang)

Tesch (1948) concluded that "in accordance with Atlantic records this species seems to keep in the Indo-Pacific within tropical boundaries, 30° lat. being rarely

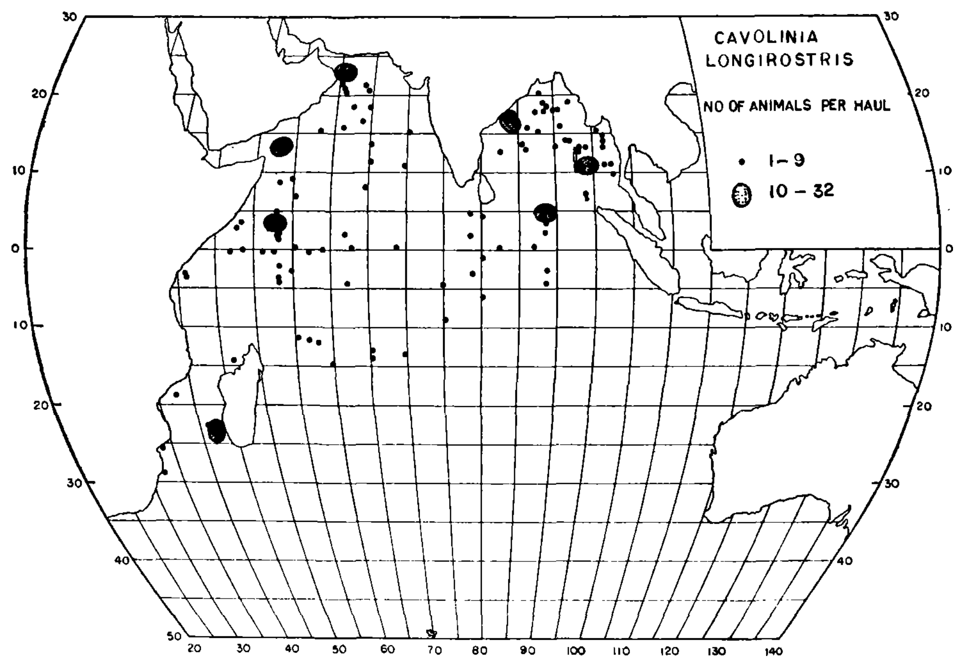

FIG. 14. The distribution of *Cavelinia longirostris.*

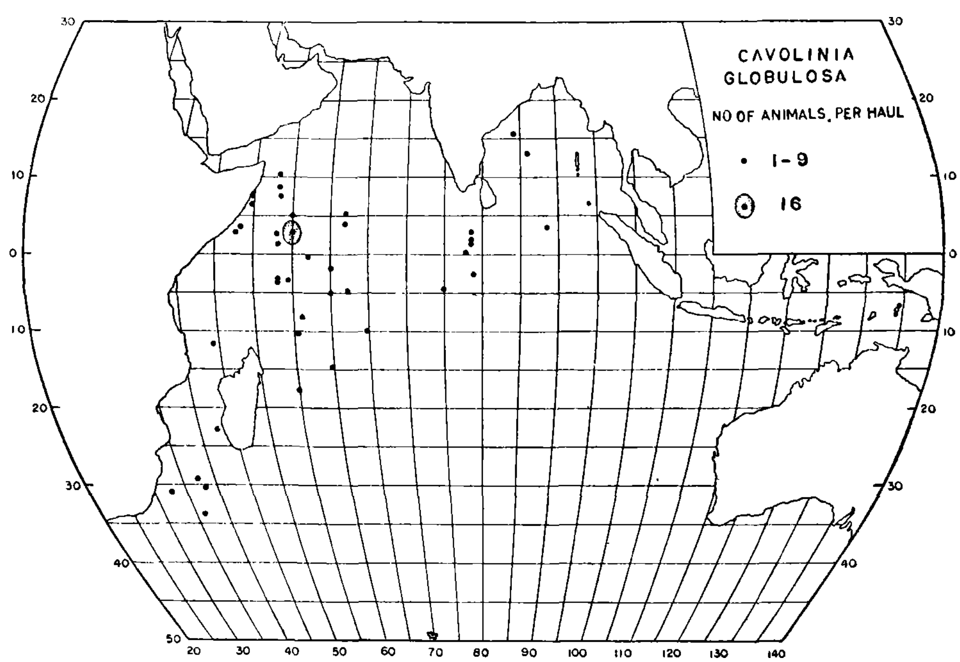

FIG. 15. The distribution of *Cavolinia globusa.*

reached. Within the tropic circles it is widely spread, but such large swarms as were sometimes encountered by the 'Dana' in the Atlantic (Tesch 1946) never occurred in the Indo-Pacific, the largest number being only 69 per haul at the West Sumatran coast. . . . ." On the basis of present observations and earlier records on the distribution of this species, it may be said that it occurs in the Bay of Bengal but is very rare in the Arabian sea and to the south of the equator (Fig. 17).

Cavolinia gibbosa (Rang)

The rarity of this species in all the world oceans is borne out by the single record in the present collections, at 10° S - 65° E (Fig. 17). In spite of intensive search along the west Sumatran coast Tesch could not find a single individual. All the previous records indicate that this species is more common in higher latitudes in the south-western part of the Indian Ocean. It is unknown in the northern Indian Ocean.

Discussion

The results derived from the present introductory study of the IIOE Collections do not permit definitive conclusions regarding the distribution of euthecosomes. This report is intended to provide a comparison of the first results with records from the early work in the Indian Ocean. The high concentration of most of the species in the region off the Somali coast suggests that this is a suitable habitat in several respects. The characteristic features of not only upwelling and enrichment of surface water but also a wide range of temperature probably provides a suitable environment or the breeding, spawning and feeding of several species of euthecosomes. Tesch (1948) has remarked on the great abundance of euthecosomes from west of Sumatra. As only two collections from off the coast of Sumatra have been examined in the present study, detailed comparisons with the results of Tesch will be attempted later. The Central zone of the southern Indian Ocean, 20°-45° S and 50°-85° E, appears to be sparsely populated by euthecosomes as is evidenced by the low numbers of all species. Because of the southerly transport between Mozambique and Africa, almost all species which occurred off the Somali coast were found to occur in the Mozambique Channel also. Scarcity or absence in the Arabian Sea and Bay of Bengal of certain otherwise common species, such as *Cuvierina columnella*, *Styliola subula*, *Cavolinia globulosa*, and *C. inflexa* is noteworthy. Possible reasons for this paucity in distribution can be considered later from the examination of further collections available at IOBC and in relation to environmental factors. As only a few specimens in the collections still retained their shells, identification of different varieties of the several species has not yet been attempted. Juveniles of uncertain identity and distorted specimens have also been excluded from this report. In due course, attempts will be made to identify the variants and juveniles.

Acknowledgement

I express my gratitude to Dr. N. K. Panikkar, for encouraging me to prepare this paper. I am grateful to Dr. John A. McGowan and Dr. Edward Brinton, for

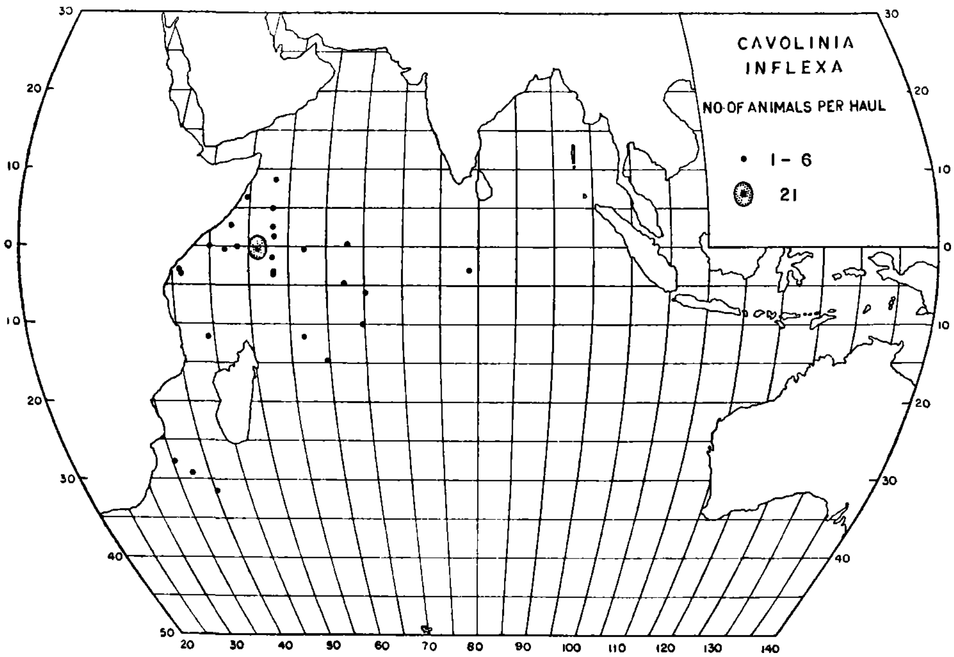

FIG. 16. The distribution of *Cavolinia inflexa*.

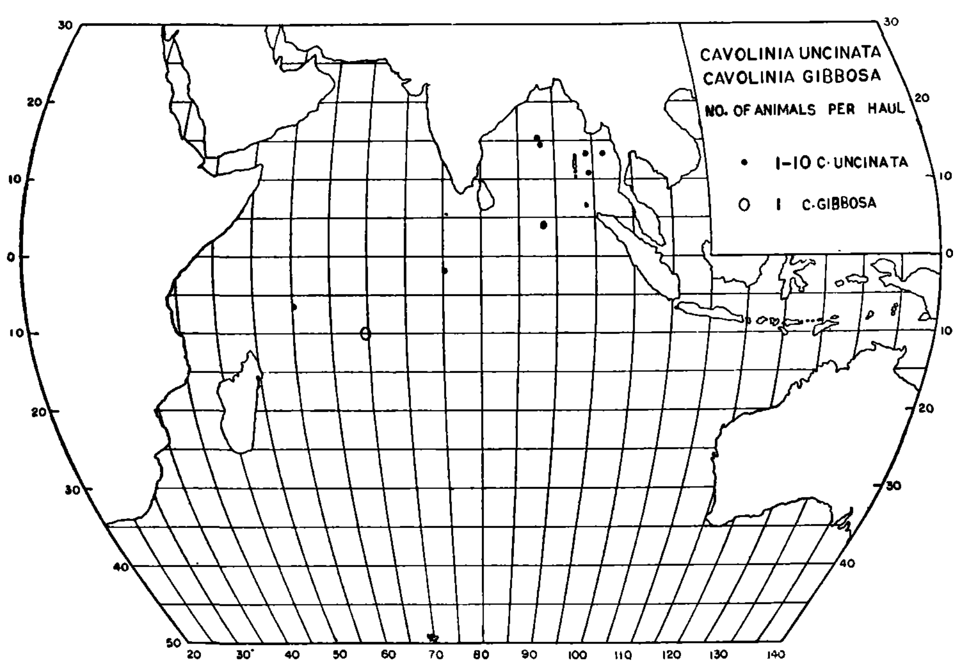

FIG. 17. The distribution of *Cavolinia uncinata* and *C. gibbosa*.

guidance and advice. I am also thankful to Mr. L. R. Kasturirangan, for going through this paper and offering me suggestions.

REFERENCES

Massay, A. L. (1920). Eupteropoda (Pteropoda Thecosomata) and Pterota (Pteropoda Gymnosomata). *Br. Antarct. Terra Nova Exped., Zool.*, **2**, 203-232.

———(1932). Mollusca, Gastropoda, Thecosomata and Gymnosomata. *'Discovery', Rep.*, **3**, 269-296.

McGowan, J. A. (1960). The systematics, distribution and abundance of Euthecosomata of the North Pacific. Ph. D. dissertation, Univ. of California at San Diego (*unpublished*).

Meisenheimer, J. (1905). Pteropoda. *Wiss. Ergebn. dt. Tiefsee-Exped. 'Valdivia'*, **9**, 1-34.

Morton, J. E. (1954). The Pelagic mollusca of the Benguela current. *'Discovery' Rep.*, **27**, 163-200.

Nejman, V. G. (1961). Formation of oxygen minimum in the sub-surface waters of the Arabian Sea. *Okearol. Issled*, **4**, 62-65.

Okutani, T. (1964). Thecosomatous pteropods collected during the second cruise of the Japanese expedition of deep sea. *Jap. J. Malac.*, **22**, 336-341.

Orren, M. J. (1963). Hydrological observations in the south-west Indian Ocean. *"Commerce & Industry", Cape Town, South Africa, Investigational Report*, **45**, 1-61.

Pelseneer, P. (1888). Report on Pteropoda collected by H.M.S. Challenger during the years 1873-76, ii. Thecosomata. *Rept. Voy., 'Challenger' Zool.*, **23** (Part 65), 1-132.

Stubbings, H. G. (1937). Pteropoda. *Scient. Rep. John Murray Exped.*, 1933-43, **5**, 15-53.

Taki, I., and Okutani, T. (1962). Planktonic gastropoda collected by the training vessel "Umitaka Maru"from the Pacific and Indian Oceans in the course of her Antarctic expedition, 1956. *J. Fac. Fish. Anim. Husb. Hiroshima Univ.*, **4**, 81-97.

———(1963). Thecosomatous Pteropods collected by the training vessel "Umitaka Maru" from the Antarctic Waters in 1957. *J. Fac. Fish. Anim. Husb. Hiroshima Univ.*, **5**, 95-105.

Tesch, J. J. (1910). Pteropoda and Heteropoda. Report Percy Sladon Trust expedition iii. *Trans. Linn. Soc. Lond., Zool.*, **14**, 165-189.

———(1946). The Thecosomatous Pteropods. I. Atlantic. *Dana Rep.*, **28**, 1-82.

———(1948). The Thecosomatous Pteropods. I. Indo-Pacific. *Dana Rep.*, **30**, 1-44.

Reprinted from *Bull. natn. Inst. Sci. India*, no. 38, 1968, p. 718-726

A PRELIMINARY REPORT ON THE GENERAL DISTRIBUTION AND VARIATION IN ABUNDANCE OF THE PLANKTONIC POLYCHAETES IN THE INDIAN OCEAN

by GEORGE PETER
Indian Ocean Biological Centre,
National Institute of Oceanography,
Cochin-16, S. India

Pelagic polychaetes in the International Indian Ocean Expedition collections are being studied taxonomically and zoogeographically and the present paper is a report on the general pattern of distribution exhibited by the polychaetes. Larval forms of bottom living polychaetes also occurred in the plankton and were included in enumeration. The year is divided into two periods; April 16th to October 15th and October 16th to April 15th, corresponding to the south-west and north-east monsoon seasons respectively. When these two periods are compared with each other with respect to the abundance of polychaetes the south-west monsoon season always shows a greater measure of abundance. When the computed values for population density of the day collection are compared with those of the night collections, the latter values are invariably higher. The Indian Ocean is divided into six regions and these are compared with one another both regionally and seasonally with respect to the abundance of polychaetes. As a general statement it may be remarked that northern parts of the ocean show greater number of polychaetes. In general the areas of high population density of polychaetes are seen to be in the regions characterized by regular upwelling.

INTRODUCTION

Planktonic polychaetes make up only, 0.15% of the organisms, numerically, in the so far analysed plankton samples of the International Indian Ocean Expedition and they rank ninth in numerical importance among the major taxa and are present in virtually all samples. It is the purpose of this report to present a general picture of the geographical distribution of planktonic polychaetes as a composite group. Our knowledge of these organisms in the Indian Ocean is very limited. The previously reported collections from this ocean have been confined to material from restricted areas (Dales 1963 ; east coast of Africa, 0-10° S and 1957 Pacific Ocean) or from a few scattered records (Fauvel 1953). The distribution of polychaete species have been extensively mapped for the South Atlantic and for the North Pacific by Tebble (1962) and for North Atlantic by Stop-Bowitz (1948). The present study of the Indian Ocean material has yet to be extended to the species level. For the present, only the ploychaetes as a whole and one family will be dealt with.

MATERIALS AND METHODS

The essential requirement for an oceanwide study of distribution is a large number of samples collected from all regions, during different seasons. This requirement was practically fulfilled by the IIOE. The data considered here are derived from the initial gross sorting of the IIOE samples, carried out at the Indian Ocean Biological Centre (IOBC). More than 2000 standard samples have been deposited in IOBC, of which 1250 have been processed and the organisms in the several major taxa counted. These samples were collected by nineteen ships taking part in the IIOE. The Indian Ocean Standard Net (IOSN), specially designed for this expedition, was used. Vertical hauls were made through a standard stratum of 200 to 0 meters, or to lesser depths in shoal water. These ships have covered all the parts of Indian Ocean, and seasonal data are available from most areas. It is convenient for the present, to divide the year into only two periods : April 16-October 15 and October 16-April 15. These periods generally coincide with the south-west and north-east monsoon respectively, in the northern hemisphere, and the winter and summer in the southern hemisphere. The planktonic polychaeta include five families, of which Tomopteridae, Typhloscolecidae and Alciopidae are holoplanktonic. Subfamily Lopadorhynchinae of the family Phyllodocidae and a few genera under Aphroditidae are also treated as pelagic. The text figures show distribution of Tomopteridae separately inasmuch as they have already been separated during sorting. All other groups of pelagic polychaetes are numerically lumped together, including both holoplanktonic species and the larvae and post larvae of many bottom dwelling polychaetes. Data from the several samples in each 5° square (following the Marsden Square system) have been averaged. These averages representing mean densities of polychaetes present under one square meter of sea surface, from surface to a depth of 200 meters have been used in making the figures.

RESULTS

It is clear from an examination of figures one to four that both the Tomopterids and the other polychaetes are more abundant in coastal regions than in oceanic waters. They are least abundant in the south-eastern part of the Indian Ocean. The Persian Gulf region is particularly rich in pelagic polychaetes, as is also the east coast of Arabia, the Somalia Coast, the west coast of India and the vicinity of the Andaman Islands. A generalized picture is given of the change in the distribution of pelagic polychaetes in different seasons. The two main seasons prevailing in the Indian Ocean, north of about 10°S, are the south-west and north-east monsoons. The former is believed to extend roughly from mid-April to mid-October and the latter from mid-October to mid-April. Transitional or intermonsoon periods are centered at April and October. For the sake of convenience the intermonsoon periods have been merged with the monsoon periods. The present study on the seasonal variation shows that Tomopteridae are more abundant during the south-west monsoon period than during the opposite season. This is also found to be true with the other pelagic polychaetes. The maximum abundance of this group (Tomopterids), is found in the Persian Gulf region during the south-west monsoon (Fig. 1); but during the north-east monsoon period (Fig. 2); it is seen to be on the west coast of India. In the case of other pelagic polychaetes, the corresponding shift is from the Persian Gulf region to the east coast of Arabia (Figs. 3, 4). It should be pointed out that the number of collections during the north-east monsoon

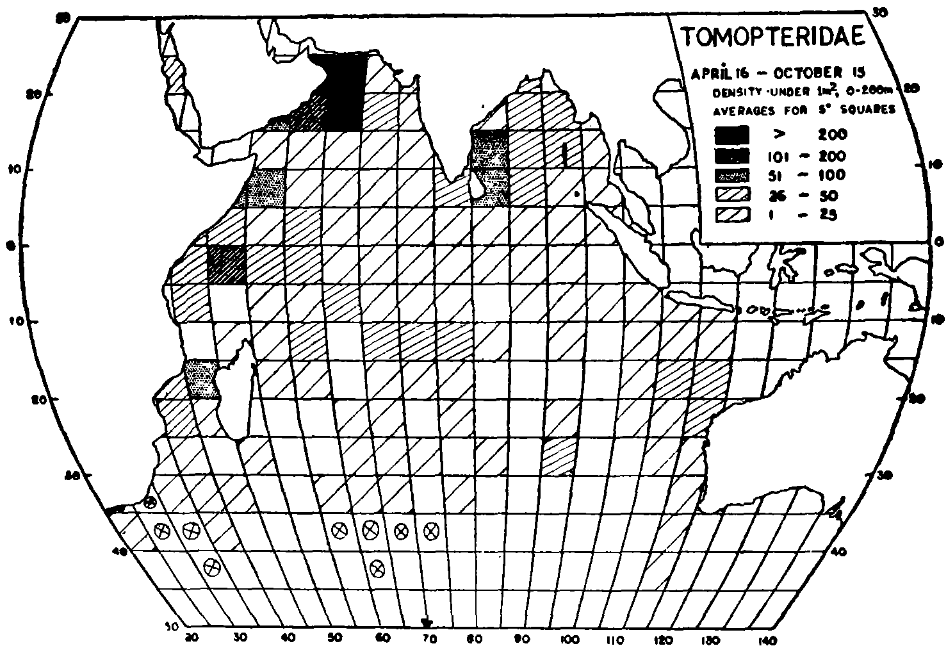

FIG. 1. Distribution of Tomopteridae during the south-west monsoon period (April 16-October 15) in the Indian Ocean.

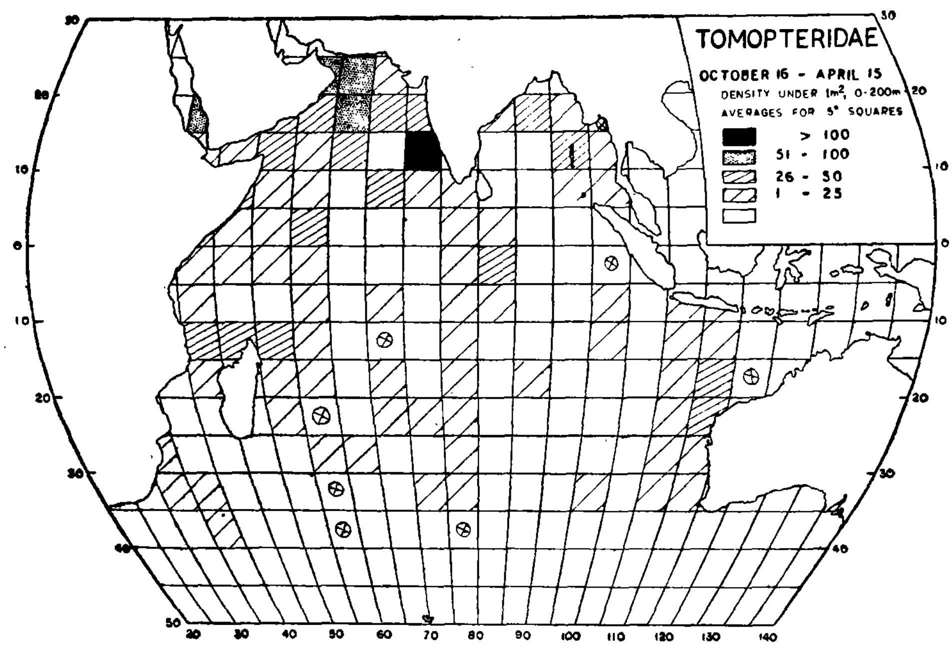

FIG. 2. Distribution of Tomopteridae during the north-east monsoon period (October 16-April 16) in the Indian Ocean.

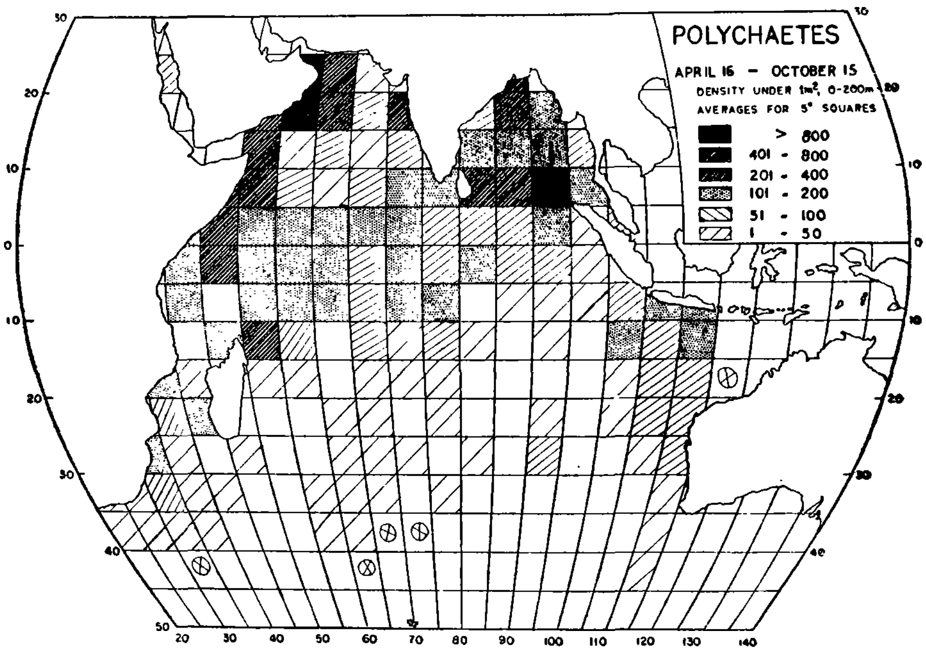

FIG. 3. Distribution of planktonic polychaetes (excluding Tomopteridae) during the south-west monsoon period (April 16-October 15) in the Indian Ocean.

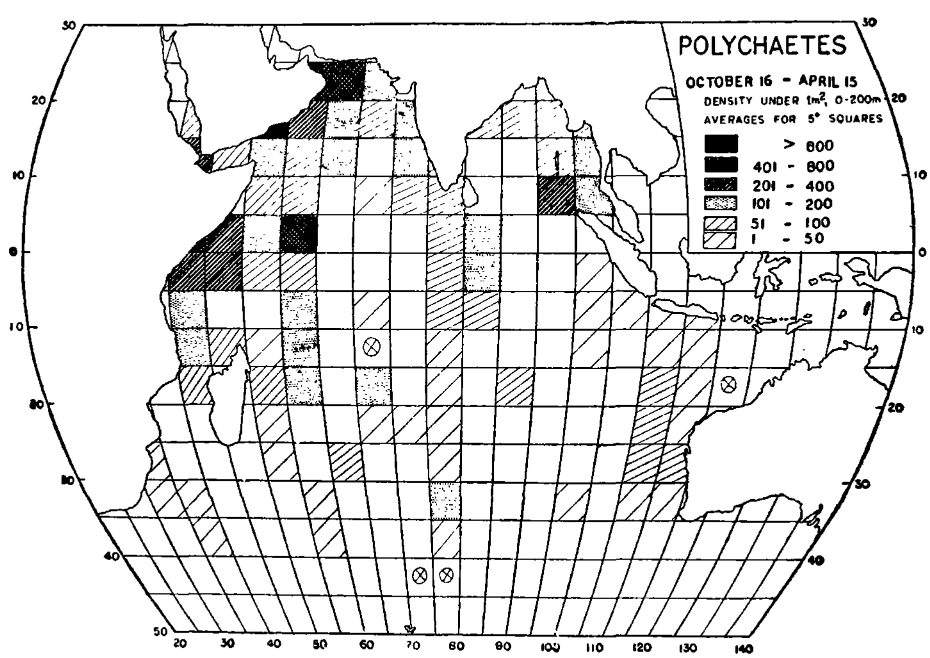

FIG. 4. Distribution of planktonic polychaetes (Excluding Tomopetridae) during the north-east monsoon (October 16-April 15) period in the Indian Ocean.

period is less than the number obtained during the south-west monsoon. It is noted that the high densities seen in the central part of the ocean, on the coasts of Madagascar, Andaman coasts, and off the west coast of Australia, does not show any marked change with change of season.

An effort has been made to study the day and night variation in distribution of Tomopteridae and other planktonic polychaetes, both longitudinally and latitudinally. In general this study shows that the observed population size based on the night collections is higher than that based on day collections and this variation is more or less uniform in almost all regions. However a notable difference between the average number of these groups is seen in the zone of 10°S-20°S latitude— where the number obtained from night collections is much higher than that of day collections (Figs. 5, 6). Similar variations are noted in the zones of 40°E-50°E longitude and 100°E-110°E longitude (Fig. 7a, 7b). But in the region between 80°E and 90°E longitude the number obtained from night collections is less than that obtained from day collections. A possible explanation for these patterns of variation can be given only in the light of further observations.

An attempt has been made to compare the distribution of pelagic polychaetes as a whole in different regions of the Indian Ocean. For this purpose the ocean is divided into six parts as follows :

1. Western part of Arabian Sea, including the regions north of latitude 5° S, and west of longitude 65° E.

2. Eastern part of Arabian Sea, including the regions north of latitude 5° S, and east of longitude 65° E.

3. Western part of Bay of Bengal, including the regions north of latitude 5° S and west of longitude 90° E.

4. Eastern part of Bay of Bengal, including the regions north of latitude 5° S and east of longitude 90° E.

5. South-western part of the Indian Ocean, including the regions west of longitude 75° E and south of latitude 5° S.

6. South-eastern part of the Indian Ocean including the regions south of latitude 5° S and east of longitude 75° E.

It is evident from the year-round collections that the western part of the Arabian Sea is the richest as far as the pelagic polychaetes are concerned. This area provides 43 per cent (computed from averages) of the total number collected. The western part of the Bay of Bengal yields 19 per cent, and the eastern parts of Arabian Sea and Bay of Bengal 14 per cent each. The southern parts of the ocean are comparatively poor, providing only 6 per cent in the south-western part and 4 per cent in the south-eastern part. During the south west monsoon, pelagic polychaetes were at maximum abundance, 36 per cent, in the western part of the Arabian Sea, while 26 per cent were in the western part of Bay of Bengal. But in the north east monsoon period the population peaked at 55 per cent in the western part of the Arabian Sea, and was remarkably less, only 10 per cent, in the western part of Bay of Bengal.

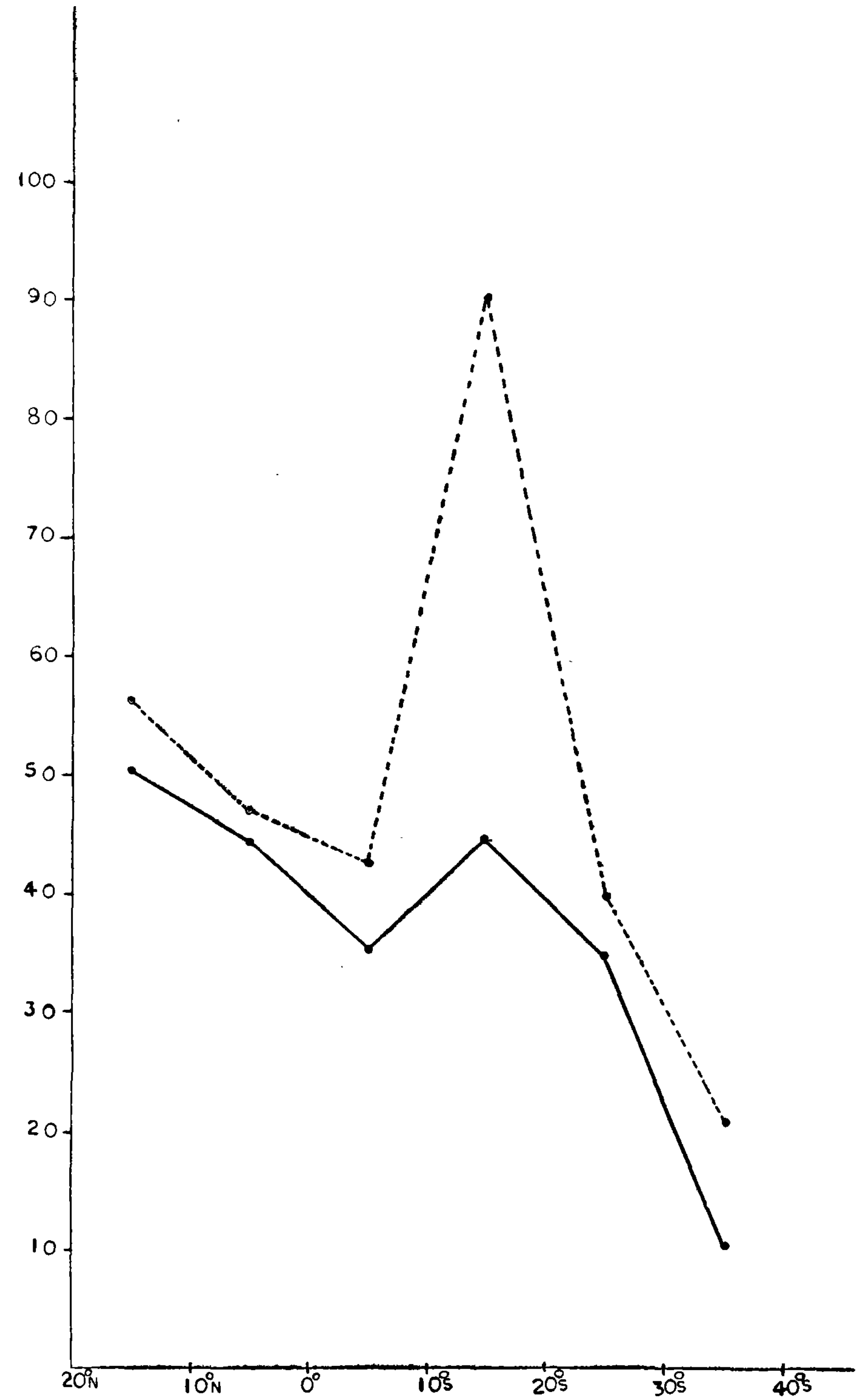

FIG. 5. Day and night variation in the distribution of Tomopteridae per 10° increment of Latitude.

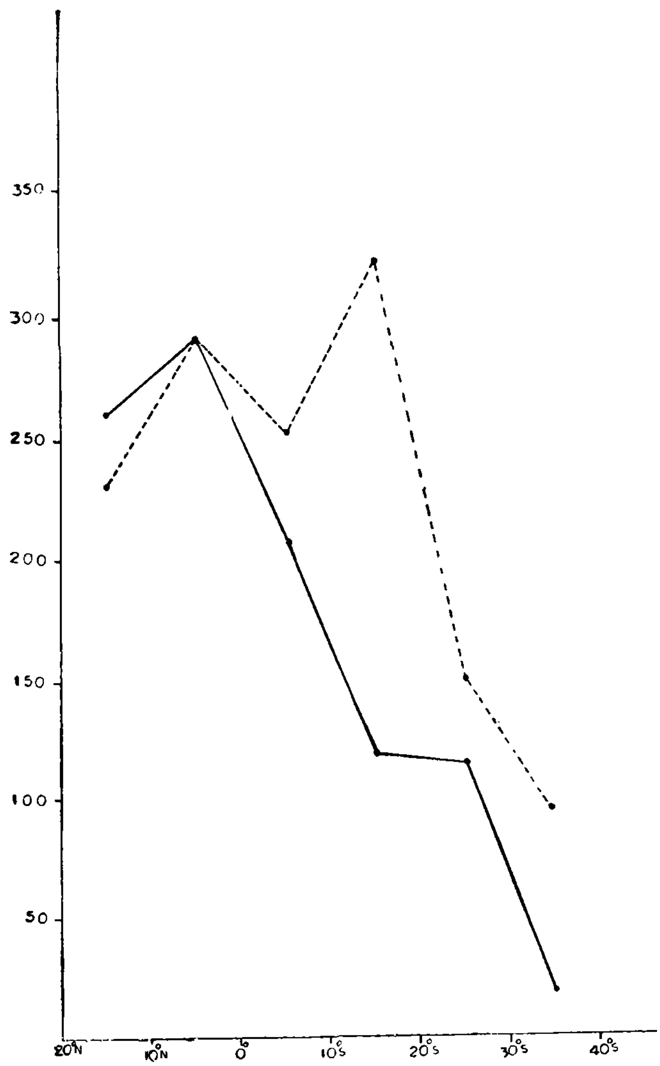

FIG. 6. Day and night variation in the distribution of planktonic polychaetes (excluding Tomopteridae) per 10° increment of latitude. (Straight lines denote day collections and dotted lines night collections).

In general it is observed that pelagic polychaetes are rich in the areas well-known for upwelling. The occurrence of upwelling has been recorded on the Somali coast, Persian Gulf region, east coast of Arabia, west coast of India, and around the Andaman Islands. It is in these regions that the pelagic polychaetes occur in large numbers.

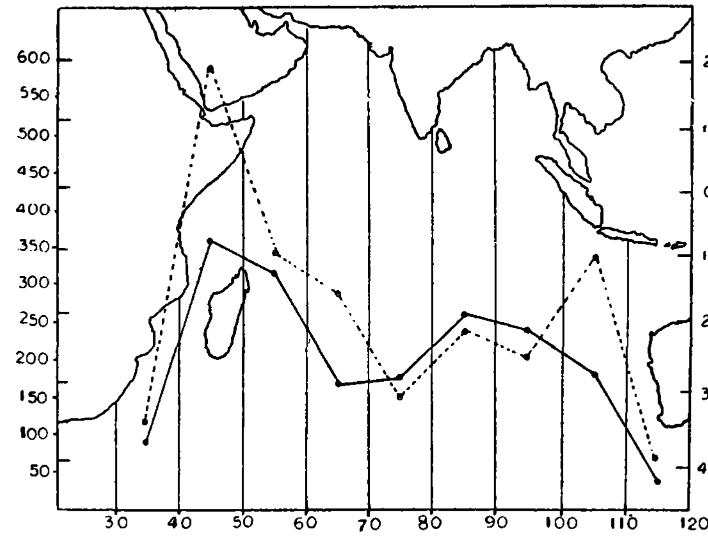

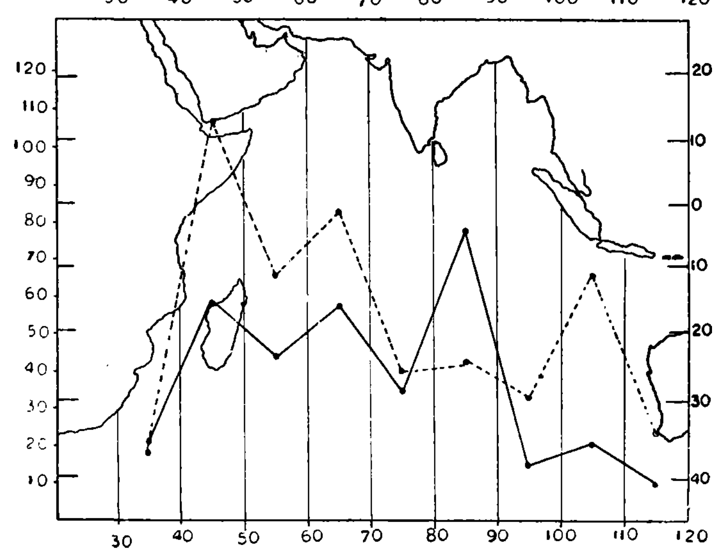

FIG. 7a. Day and night variation in the distribution of planktonic polychaetes (excluding Tomopteridae) per 10° increment of longitude. (Straight lines denote day collections and dotted lines denote night collections.)

FIG. 7b. Day and night variation in the distribution of Tomopteridae per 10° increment of longitude.

ACKNOWLEDGEMENT

I wish to acknowledge my thanks to Dr. N.K. Panikkar, Director, National Institute of Oceanography, for permitting me to present this paper and to Dr. Edward Brinton, for his kind guidance and criticism throughout this study. I am also grateful to Mr. L.R. Kasturirangan, for his valuable suggestions.

REFERENCES

Dales, R. P. (1957). Pelagic Polychaetes of the Pacific Ocean. *Bull. Scripps Inst. Oceanogr., tech. Ser.*, 7, 101-161.

————(1963). Pelagic polychaetes from waters off the coasts of Kenya and Tanganyika. *Ann. Mag. nat. Hist., Ser.* 13, **6**, 501-503.

Fauvel (1953). Fauna of India, including Pakistan, Ceylon, Burma and Malaya; Annelida Polychaeta. Allahabad, The Indian Press (for the Govt. of India).

Stop Bowitz, C. (1948). Polychaeta from the '*Michael Sars*' North-Atlantic Deep Sea Expedition. *Rep. Scient. Results Michael Sars N. Atlant. deep Sea Exped.* 1910 **5**, part 8, 1-91.

Tebble, Norman (1962). The distribution of Pelagic polychaetes across North Pacific Ocean. *Bull. Br. Mus. nat. Hist.*, **7**, 27-407.

Reprinted from *Bull. natn. Inst. Sci. India*, no. 38, 1968, p. 747-752

A PRELIMINARY REPORT ON THE BIOMASS OF CHAETOGNATHS IN THE INDIAN OCEAN COMPARING THE SOUTH-WEST AND NORTH-EAST MONSOON PERIODS

by VIJAYALAKSHMI R. NAIR

Indian Ocean Biological Centre, National Institute of Oceanography, Cochin-16

The data for the present paper have been derived from the analysis of 1276 standard samples of plankton collected during the International Indian Ocean Expedition (1962-65). At the Indian Ocean Biological Centre fractions (3-5 ml) of the samples were sorted and the total number of chaetognaths in the samples were then computed. The average number of chaetognaths for all samples from each 5° Marsden Square is separately estimated for the south-west and north-east monsoon periods. The period mid-April to mid-October (SW monsoon) shows a comparatively higher density of chaetognaths for all areas except the eastern half of the Arabian Sea. In both the periods the areas of highest density are in the western part of the Arabian Sea. The region 40°-60°E between the equator and the northern limit of the ocean is richest in Chaetognaths during both seasons.

INTRODUCTION

Chaetognaths are extremely abundant in the sea and constitute an important part of the marine plankton. There is a substantial amount of published information about the distribution and systematics of Chaetognaths of other oceans but comparatively little on chaetognaths of the Indian Ocean. Mention may be made of the systematic account of chaetognatha of Indian coastal waters by George (1952), of Tokioka's publications (1955-1956) on Chaetognaths of the north-eastern and central areas of the Indian Ocean, of the publications of Rao (1958) and Rao and Ganapati (1958) on chaetognaths of the Bay of Bengal and lastly of the work of Alvariño (1964*b*) on chaetognaths of the "Monsoon Expedition" of the *Argo* during 1960-61. The *Siboga* (Fowler 1906), *Gazelle* (Ritter-Zahony 1909), *Sealark* (Burfield 1926) and *Snellius* (Schilp 1941) expeditions covered only parts of the Indian Ocean. The International Indian Ocean Expedition has, however, achieved a much wider coverage.

The majority of chaetognath species live in warm waters but it is not necessarily anticipated that their greatest abundance would be found in the tropical and subtropical zones. They occur from the surface to depths below 1000 m. Some species are restricted to one geographical region, whereas others are cosmopolitan in distribution. A total of about 52 species is widely accepted for the six pelagic genera (Alvariño 1965). Nearly 28 species have been heretofore recorded from the Indian Ocean. Taxonomic studies on the chaetognaths of the International Indian Ocean Expedition Collections are only just beginning but as a provisional estimate it may be said that at least 22 species occur in these collections. As most of the samples are from 200-0 m depth, mesoplanktonic chaetognaths (200-1000 m, Alvariño 1964*a*) are not expected to comprise a significant part of the material. In this preliminary presentation, the chaetognath component of the plankton would be treated as a whole leaving the distribution of individual species to be studied separately.

Material and Methods

The data presented in this paper have been derived from the analysis of 1276 standard samples collected during the International Indian Ocean Expedition (1962-65). Standard samples are those obtained by a vertical haul of the Indian Ocean Standard Net from approximately 200 m depth to the surface. Samples obtained from shoal water are considered as standard if the depth of haul and depth of water are in close agreement. At the Indian Ocean Biological Centre, fractions (3 to 5 ml) of the samples were sorted and the total number of chaetognaths, as well as numbers of individuals in all major taxa, were computed for each sample. The average number of chaetognaths for all samples from each 5° Marsden square is separately estimated for each of two six-month seasons, that is, the south-west monsoon (taken as 16th April to 15 October) and the north-east monsoon (taken as 16th October to 15th April). For mapping, the contour intervals were chosen so as to reduce the effect of patchiness and at the same time provide five population density ranges. In figures 2 and 3, each 5°-square with a dot in the centre represents a square for which data are available. The figures 2 and 3 give a general picture of the biomass of chaetognaths in the Indian Ocean. The distribution of population density is illustrated for the south-west and north-east monsoon periods.

Discussion

Mean values for day-time and night-time densities (Table I), were calculated for ten randomly chosen 5°- squares, for each of the two seasons. These averages show that there is no significant difference between day and night in the estimated abundance of chaetognaths in the standard samples.

The period mid-April to mid-October shows a comparatively higher density of chaetognaths for all areas except the eastern part of the Arabian Sea and the south-western quadrant of the Ocean. (In the latter region, however, the mean values

Table I

5°-Square	SW Monsoon		NE Monsoon	
	Day	Night	Day	Night
331—1	1790(2)*	2166(3)	3954(8)	2953(8)
032—2	4769(5)	3569(6)	2874(5)	5357(6)
067—1	2627(6)	2130(12)	4004(11)	4053(4)
067—4	3158(9)	2312(5)	3146(2)	3899(2)
102—2	577(3)	187(7)	1191(14)	1373(15)
065—3	792(16)	684(9)	1265(8)	1293(5)
029—4	4905(2)	2176(4)	2490(8)	2910(4)
064—4	4254(7)	2841(12)	1899(8)	1687(3)
027—4	1574(8)	1894(7)	1784(4)	1254(4)
327—1	630(2)	1594(3)	2708(1)	1264(3)
Average	2508	2055	2532	2404

*Numbers in brackets indicate number of collections in each 5°-square.

for the two seasons are nearly equal). In both periods the areas of highest density are the western part of the Arabian Sea, including waters of the Somalia region. Values for the average number of chaetognaths in all standard samples from different geographical regions are as follows:

Area	16th April-15th October	16th October-15th April
Western Arabian Sea (W of 65° E, N of 5° S)	3107	2544
Eastern Arabian Sea (65-80° E, N of 5° S)	1287	1480
Arabian Sea (above two regions combined)	2369	2166
Bay of Bengal (E of 80° W, N of 5°)	2502	1859
SW quarter of the Indian Ocean (W of 80° E, S of 5° S)	693	715
SE quarter of the Indian Ocean (E of 80° W, S of 5° S)	773	495

East-west (Fig. 1*a*) and north-south (Fig. 1*b*) plots of the average number of chaetognaths for all standard samples, are drawn according to 10 increments of longitude and latitude respectively. These show diagrammatically that the region 40°-60°E between the equator and the northern limit of the ocean is richest in chaetognaths during both seasons. Lowest values are at the eastern and western sides of the southern half of the ocean.

For the south-west monsoon there is a maximum peak between 50° E and 60° E and a lesser peak between 80° E and 100° E. Similarly for the north-east monsoon the maximum is between 40° E and 50° E and a lesser one between 80° and 90° E, but the peaks are observed to be shifted a little to the west. It is interesting to note that the north-east monsoon shows a comparatively higher density peak in the Arabian sea and the peak in the Bay of Bengal in the north-east monsoon period is the least prominent of all.

Along the north-south axis it is observed there is an almost uniform rate of decrease in density as we proceed from the north to the south up to 45° south, which is the limit of the IIOE sampling. This is particularly true south of the equator with the values for population density being somewhat lower for the north-east monsoon than for the south-west monsoon in almost all the south latitudes. North of the equator the major peaks for the two seasons occur. But whereas for the north-east monsoon period, the single peak density is observed between 10° N and 20° N, with lower but nearly equal values for the belts both above (20° to 30° N) and below it (0° to 10° N), the exact opposite is observed for the south-west monsoon period, with two peaks, nearly equal to each other occurring between 20° to 30° N and again between 0° to 10° N, with a considerably lower value in the intermediate belt, 10° to 20° N.

The surface salinity is at a minimum near the equator, reaches a maximum in about latitude 20° N and 20° S again decreases toward high latitudes (Sverdrup *et al.* 1942). A majority of chaetognaths appear to show a preference for high salinity and high temperature. Rao and Ganapati (1958), after a study of the distribution of chaetognaths of the Visakhapatnam coast in relation to the salinity and tempera-

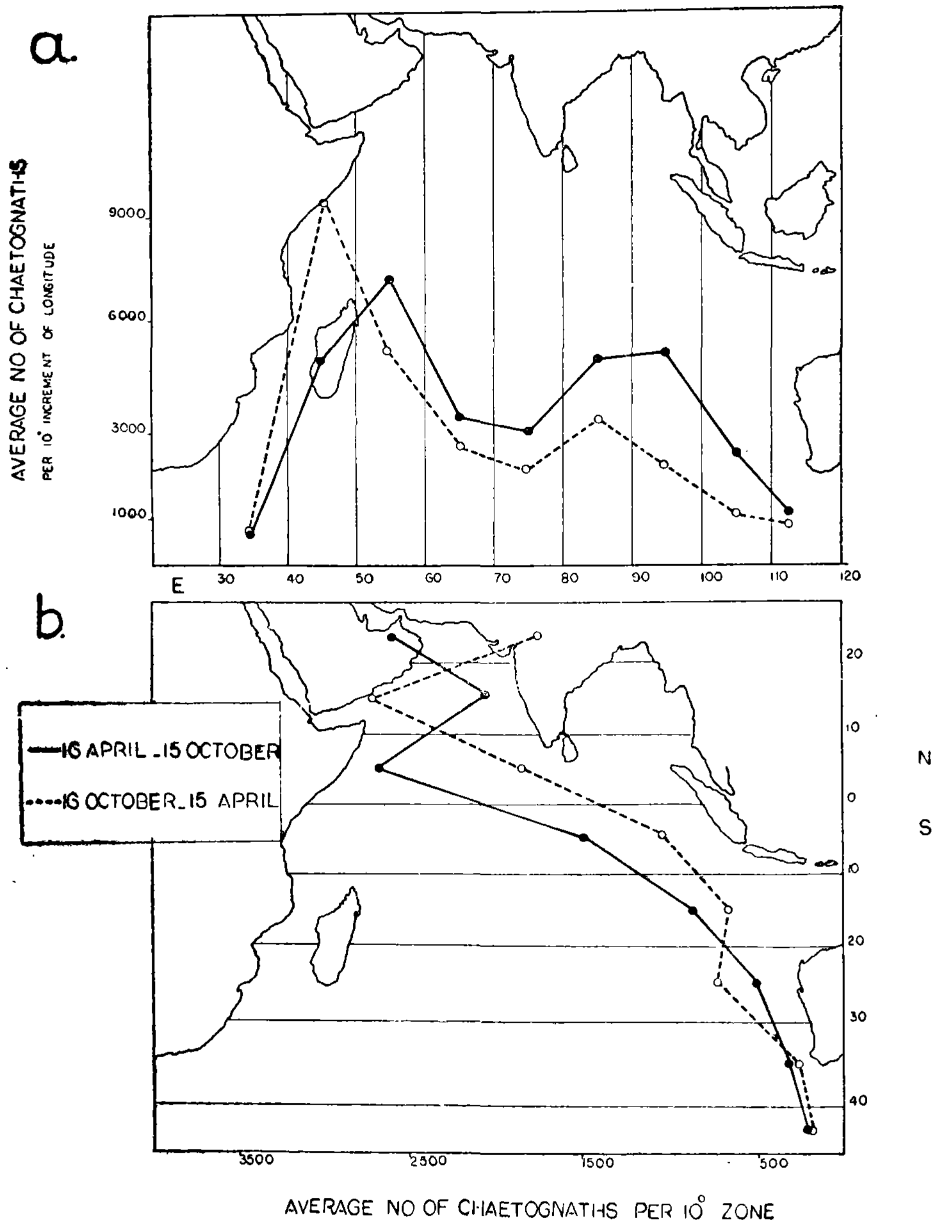

FIG. 1. Average number of chaetognaths beneath 1m², 0-200 m depth, plotted against (*a*) longitude, and (*b*) latitude.

ture, concluded that, apart from *Sagitta enflata* and *Krohnitta pacifica*, the species show aversion to low salinity and temperature. This may account, in part, for the highest density of chaetognaths in the zone 0-20° N. Doubtless, the enrichment process prevailing along the coasts of tropical east Africa and the Asian land mass are also contributing factors. During the south-west monsoon, the highest density

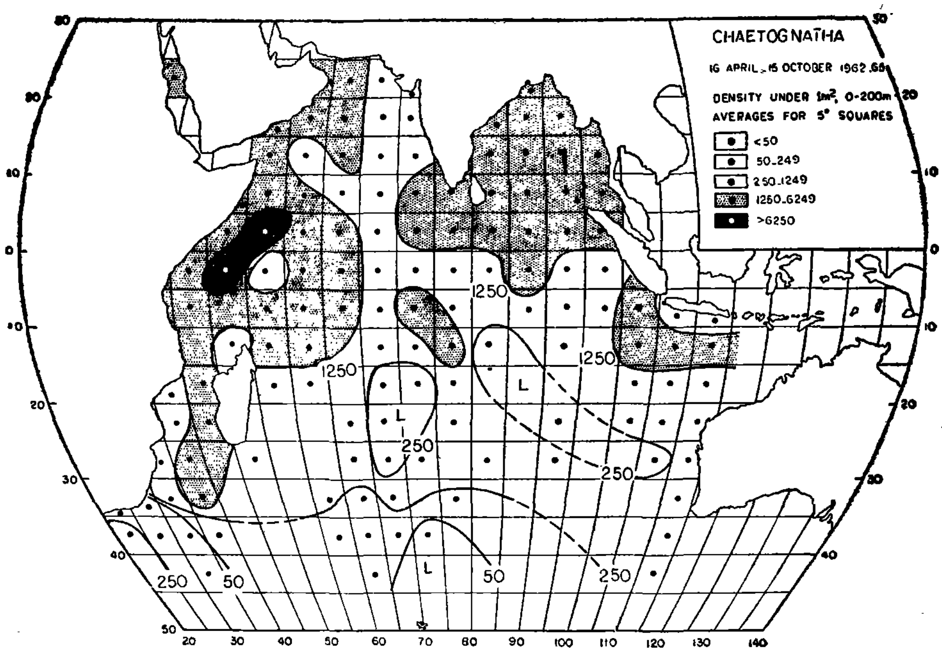

FIG. 2. Population densities of chaetognaths April-October. Dots indicate squares for which data are available. L indicates areas of low density.

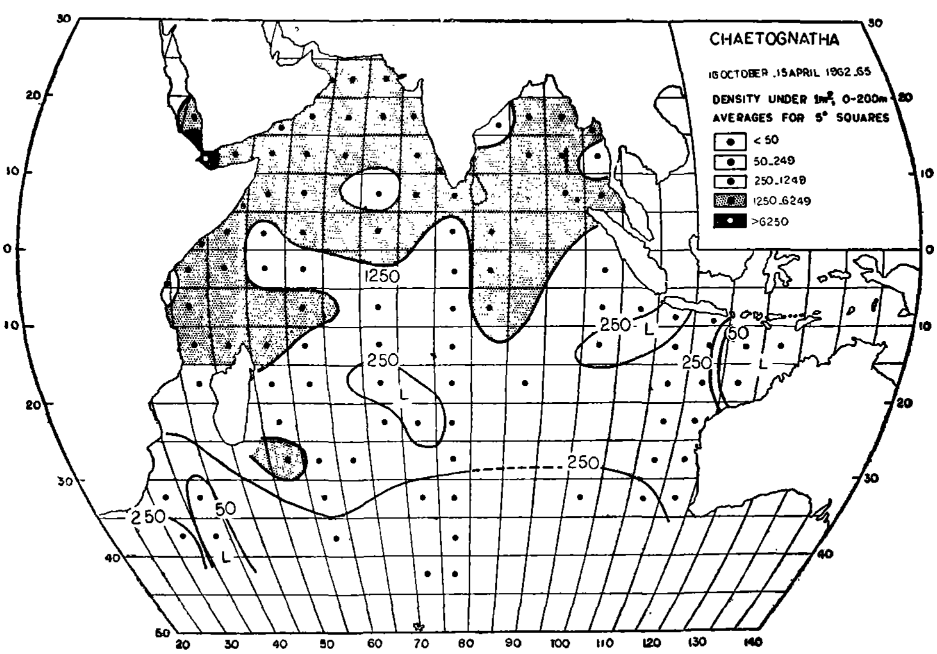

FIG. 3. Population densities of chaetognaths October-April. Dots indicate squares for which data are available. L indicates areas of low density.

is near the Somalia region (Fig. 2). On the western margins of the ocean where the prevailing seasonal winds carry the surface waters away from the coast, an overturn of the upper layers takes place. During the same season the westerly North Equatorial Current disappears and is replaced by the Monsoon Current which flows from the west to east. Along the African coast the current is then directed north from lat. 10° S. Water deriving in part from the Equatorial Current crosses the equator and considerable upwelling takes place off the Somali coast (Sverdrup *et al.* 1942). During upwelling the nutrient content of the surface water increases and this results in an increase in primary production which in turn accelerates the secondary production. It is noteworthy, however, that the 5°-squares showing population maxima during April-October were *not* adjacent to the African coast, but at some distance from it. This suggests that chaetognaths, as a whole, develop and aggregate optimally along the fringe of the enriched area. During the period October to April (Fig. 3) an equatorial maximum east of Africa was not noted, but high population densities occurred throughout the northern part of the Indian Ocean. Highest densities were at the mouth of the Red Sea.

Acknowledgement

I wish to express my sincere thanks to Dr. N.K. Panikkar, Director of National Institute of Oceanography, for encouraging me to write this paper. I am greatly indebted to Dr. Edward Brinton, for his kind advice and guidance. I am also grateful to Mr. L.R. Kasturirangan, for his helpful suggestions.

References

Alvarino, A. (1964*a*). Bathymetric distribution of Chaetognaths. *Pacif. Sci.*, **18**, 64-80.

——————(1964*b*). The Chaetognatha of the Monsoon Expedition in the Indian Ocean. *Pacif. Sci.*, **18**, 336-346.

——————(1965). Chaetognaths. *Oceanogr. mar. biol., Ann. Rev.*, 3, 115-194. George Allen and Unwin Ltd. London.

Burfield, S.T., and Harvey, E.J.W. (1926). The Chaetognatha of the Sealark Expedition. *Trans. Linn. Soc. Lond., Zool., ser.* 2, **19**, 93-119.

Fowler, G.H. (1906). The Chaetognatha of the Siboga Expedition. *Siboga Exped. Monogr.*, **21**, 1-86.

George, P.C. (1952). A systematic account of the Chaetognatha....Malabar Coast. *Proc. natn. Inst. Sci. India*, **18**, 657-689.

Rao, T.S.S. (1958). Studies on Chaetognatha in the Indian Seas, Part II. *Andhra Univ., Mem. Oceanogr.*, **2**, 137-146.

Rao, T.S.S., and Ganapati, P.N. (1958). Studies on Chaetognatha in the Indian Seas, Part III. *Andhra Univ., Mem. Oceanogr.*, **2**, 147-163.

Ritter-Zahony, R. (1909). Die Chaetognathen der Gazelle Expedition. *Zool. Anz.*, **34** 787-793.

Schilp, H. (1941). Biological results of the Snellius Expedition. IX. The Chaetognatha of the Snellius Expedition. *Temminckia*, **6**, 1-99.

Sverdrup, H.U., Johnson, M.W., and Fleming, R.H. (1942). The Oceans. Prentice-Hall, Inc., New York.

Tokioka, T. (1955). A small collection of Chaetognaths and pelagic tunicates from the north eastern part of the Indian Ocean. *Publ. Seto mar. biol. Lab.*, **5**, 75-80.

——————(1965). On chaetognaths and appendicularians collected in the central part of the Indian Ocean. *Publ. Seto mar. biol. Lab.*, **5**, 197-199.

Reprinted from *Bull. natn. Inst. Sci. India*, no. 38, 1968, p. 753-757

PRELIMINARY NOTES ON THE DECAPOD LARVAE OF THE ARABIAN SEA

by M. KRISHNA MENON, P. GOPALA MENON *and* V.T. PAULINOSE
Indian Ocean Biological Centre, National Institute of Oceanography, Cochin-16

The note presents some general facts regarding the distribution of some of the larger groups of decapod larvae in the Arabian Sea. Their relative numbers and the families and subfamilies, so far as can be recognized, represented within each group are also indicated. Suitable charts to illustrate distribution are provided. The data collected on the distribution of larvae of the family Penaeidae are presented separately in this note. Their general distribution in the Arabian Sea and the stations at which fairly good numbers were captured are described and illustrated with suitable charts. The possible effect of the time of haul and the season on the number of larvae caught is explained. The probable parentage of the more commonly encountered types of larvae is indicated.

1. A GENERAL SURVEY OF ALL MAJOR GROUPS EXCEPTING SERGESTIDS AND PHYLLOSOMA

The following notes are based on a preliminary examination of the decapod larvae obtained from the plankton samples collected during the course of the International Indian Ocean Expedition, from the Arabian Sea. The material is not complete since during the initial sorting of the entire sample the Sergestids and Phyllosoma larvae were removed. The rest of the collection from each station is being subsorted into a number of smaller groups, families or sub-families in order to facilitate their detailed study later by specialists. As the subsorting progressed some amount of data relating to their distribution, composition, numbers etc. accumulated and they have been made use of in the preparation of these notes. In the circumstances the notes could not be anything other than purely preliminary in character and may require to be modified in part or supplemented in the light of the results of further study.

Though decapod larvae form an important constituent of the plankton they seldom occur in these collections in large numbers. Possibly the method of collection of plankton (vertical hauls) may be partly responsible for it. Another peculiarity of the present collection is the absence of the early larval stages e.g. nauplii and early protozoeae of Penaeids. This is true of most of the other groups also excepting a few Carideans belonging to 2-3 families such as Pasiphaeidae and Pandalidae and some crabs. Swarms of larvae of various species in different stages of development have been noticed in the sea by previous expeditions (Gurney 1924) and the presence of only 1 or 2 stages of a species in most of the present collections is, in all likelihood, the result of the method adopted. Complete series of larvae may not thus be available in regard to most of the species. Nevertheless it may be possible to establish the probable parentage of several with the help of published descriptions of similar larvae and post larvae. The value of the collection, assessed from the point of view of their biology suffers therefore to some extent.

Material collected by earlier expeditions has served to establish a relationship between the numbers of larvae and the proximity to land of the stations at which they have been collected (Ortmann 1893). This implies that larvae of littoral species usually remain in the neighbourhood without moving out into the open sea. The positions of some of the stations in the Arabian Sea occupied during the course of I.I.O.E. that have yielded fairly good numbers of larvae are shown in Fig. 1. At stations 2005 (Varuna), 2004 (Varuna), 194 (A. Bruun cruise No. 4) and 47 (Argo, Dodo cruise), the numbers of larvae caught are remarkably large, varying between 1460 to 680. It would seem that the relationship generally holds good in regard to the present collections also. Gurney (1924) has stated that the 'Terra Nova' collections, "so far as they permit conclusions to be drawn, fully confirm Ortmann's result." It is true not only in regard to the total number of larvae collected but also to the variety i.e. the number of species represented. Occasionally as many as a dozen species have been secured at some stations around the Minicoy and Maldive Islands (Station 102, cruise No. 4 and Station 104 on the same cruise of I.N.S. Kistna). It should be added however that these collections, though rich in variety, are not always equally rich in numbers.

Larvae belonging to all the main groups of decapods are present in the collection excepting those mentioned earlier; but their numbers vary widely. It may be stated in general that caridean and crab larvae occur in much larger numbers than any other group at quite a number of stations. Figures 1—4 furnish information on the distribution of the larvae of the Penaeidae and two other major groups namely the Anomura and the Brachyura. The Caridea has been left out of consideration here because the subsorting into families or subfamilies is somewhat unsatisfactory owing to the difficulty experienced in recognizing some of the families, especially their early stages, during the course of subsorting when it was not possible to dissect out and study appendages.

The Penaeids will be dealt with in a separate note since a start may be said to have been made towards a more detailed study of the family and some additional data collected. This was done in view of the economic value of the adults of a number of species and in the hope that the study might yield useful information regarding the life histories of some that still remain imperfectly known. A few Stenopid larvae and Amphion have been secured but their numbers are inadequate for studying their distribution.

In regard to the distribution of the Anomuran larvae (Fig. 4) a general resemblance to that of Penaeids is quite evident. They however seem to occur in comparatively larger numbers in the Gulf of Cambay and neighbourhood than the Penaeids. Among them those of the family Axiidae belonging to the Thalassinidea and the Galatheids have been obtained at more stations than some of the other families. Callianassidae (Thalassinidea), Paguridae and Albuneidae have also been obtained from several stations; but Porcellanidae and other families have been taken only rarely. Except Pagurids the number of larvae belonging to any Anomuran group has not been large at any station.

In contrast to the Anomura, Crab zoeae and megalopae (Fig. 5) are noticed in much larger numbers, the greatest numbers occurring in the regions surrounding the southern tip of the Indian Peninsula (a common feature in the distribution of all the 3 groups dealt with here), off the Maharashtra Coast and the northern part of the Somali Coast of Africa. Further away from the two latter regions in the same latitudes there are considerable areas which are apparently barren and from which hardly any larvae have been caught. Larvae provisionally ascribed to the primitive Brachyuran group. Dromiacea have been frequently noticed, but only in small numbers. They seem to belong to more than one genus. Nothing can be ventured here in regard to the comparative numbers and stations of capture of any of the other groups of crabs without further detailed study of the material.

2. PENAEIDAE

The data collected during the subsorting of the plankton samples, and supplemented by what could be obtained in the course of a subsequent rapid re-examination of some of the Penaeid larvae from a few stations are presented in this brief note. The reason for selecting the Penaeids first for further study have been explained in the previous note. The pattern of distribution of Penaeid larvae conforms in a general way with that of the entire order (minus Sergestids and Phyllosoma) and is illustrated in Fig. 2. The maximum average number from a 5°-square area (Marsden square) has been obtained around the southern extremity of the Indian peninsula (1) and off the Somali Coast of Africa (2). Immediately outside these regions the average catch is much less, below 50%. Minimum numbers have usually been recorded from areas situated far away from land. An exception however is the area adjoining the Gulf of Kutch. This is rather strange in view of the fact that the prawn fishery of the area has been reported to be fairly good. It may be that the breeding period of Penaeids here does not happen to coincide with the time of collection (the first half of November). South of it, there is a barren stretch of sea from which apparently no larvae have been caught. A similar area lies midway between the two zones of maximum occurrence (Lat. 5°-10° N, Long. 60°-65° E).

When the actual numbers secured from individual stations are taken into consideration it becomes apparent that the averages calculated are far below them in respect of several stations. Fig. 3 shows the positions of most of such stations At three of them the number obtained is one over hundred. Two of the three stations are included in region No.1. The third, however lies far to the north of region No. 2, off the Coast of Arabia and at a comparatively greater distance from land. A number of other stations at which fairly good numbers of larvae are recorded, as shown in Fig. 3, located in the western part of the Arabian Sea are not also close to the coast. They could be larvae of littoral species that have drifted away from the coast. Or they may be larvae of deep water species; but the point could be settled only after further study of the material.

An attempt was made to discover if there is any relation between the numbers caught and the time of haul. Hauls which yielded 20 or more larvae were alone taken into consideration in this connection. Of the three hauls that brought up

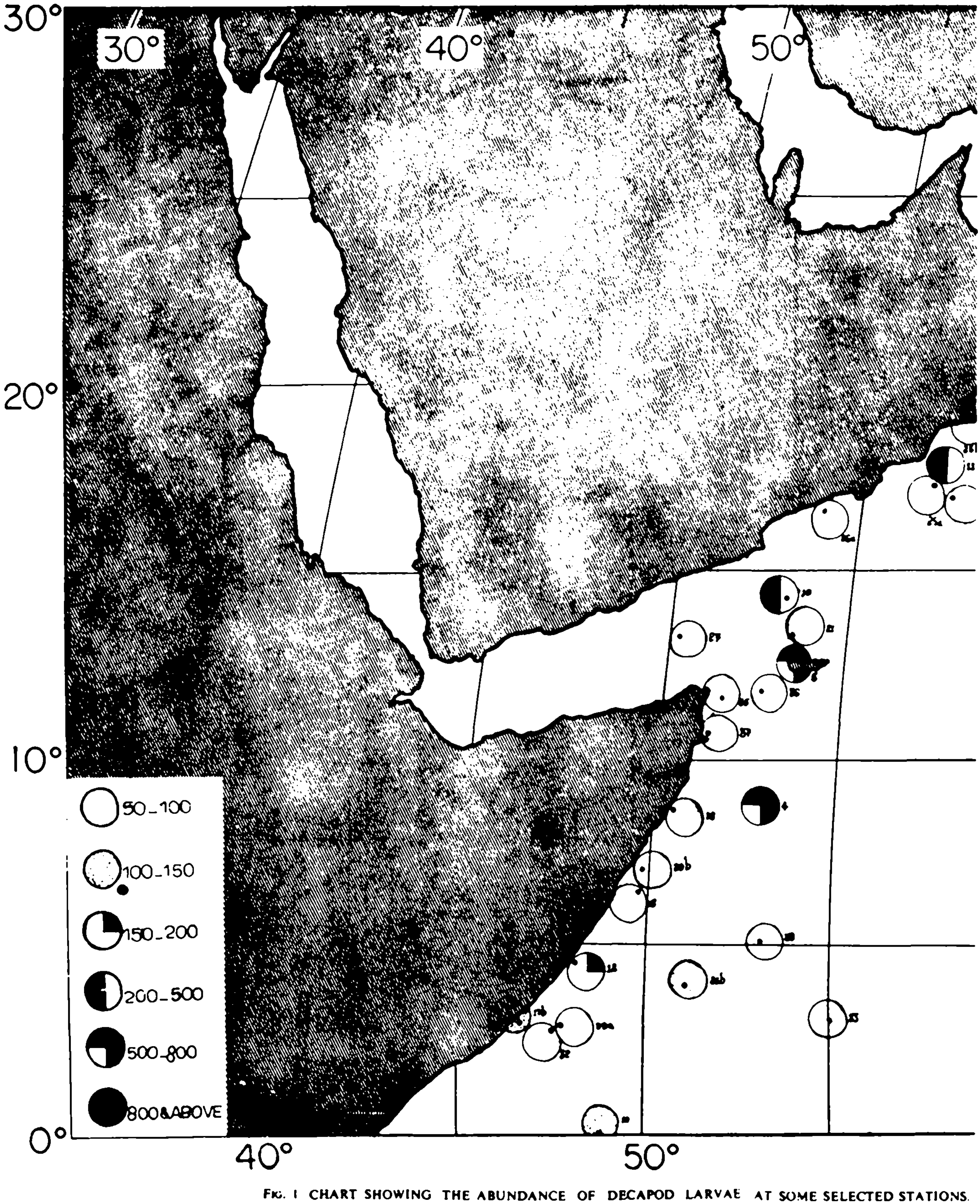

FIG. 1 CHART SHOWING THE ABUNDANCE OF DECAPOD LARVAE AT SOME SELECTED STATIONS.

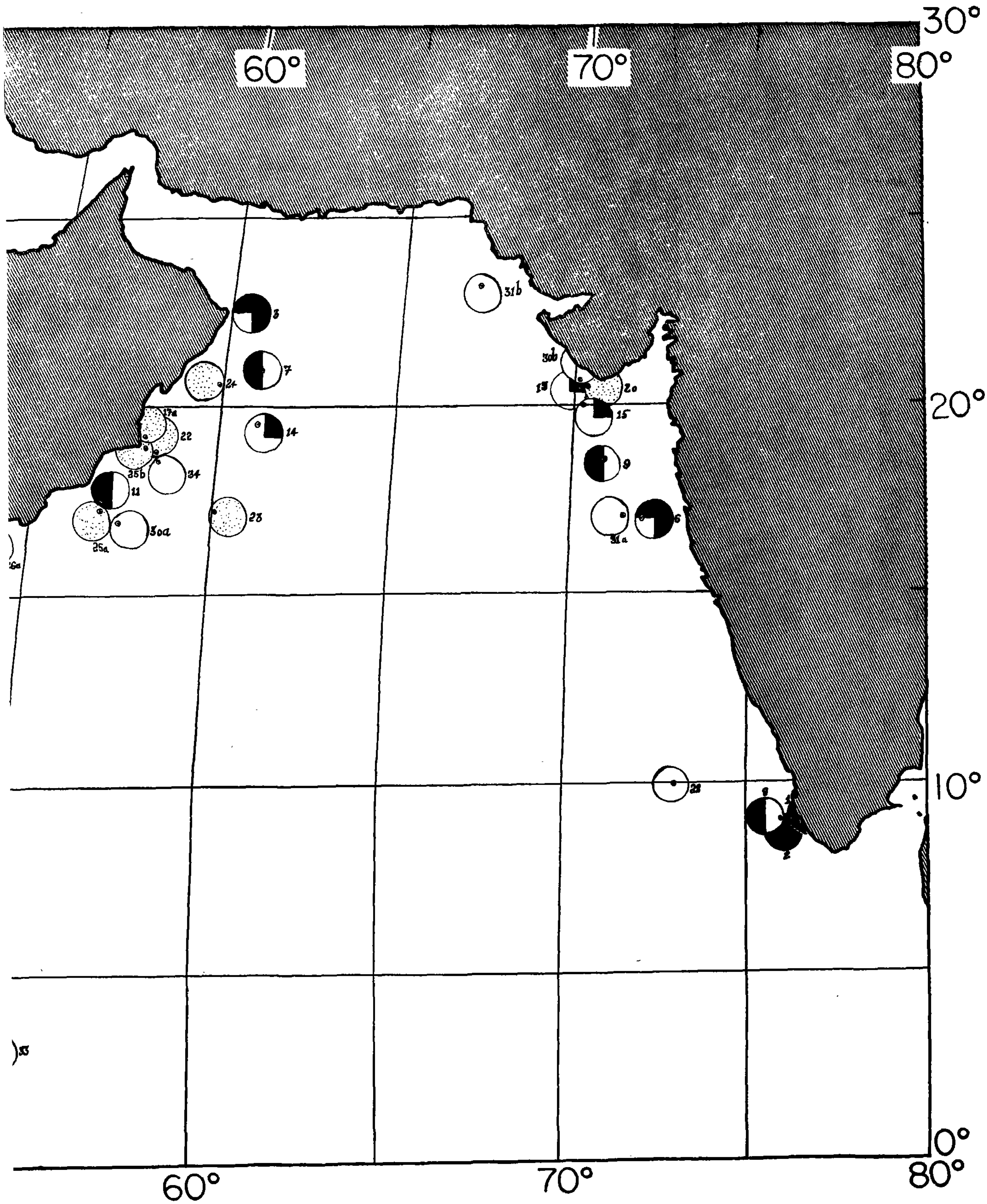

30°
60°
70°
80°
20°
10°
0°
60°
70°
80°
31b
3
7
24
14
22
34
11
23
30a
30b
20
15
9
6
31a
28
2

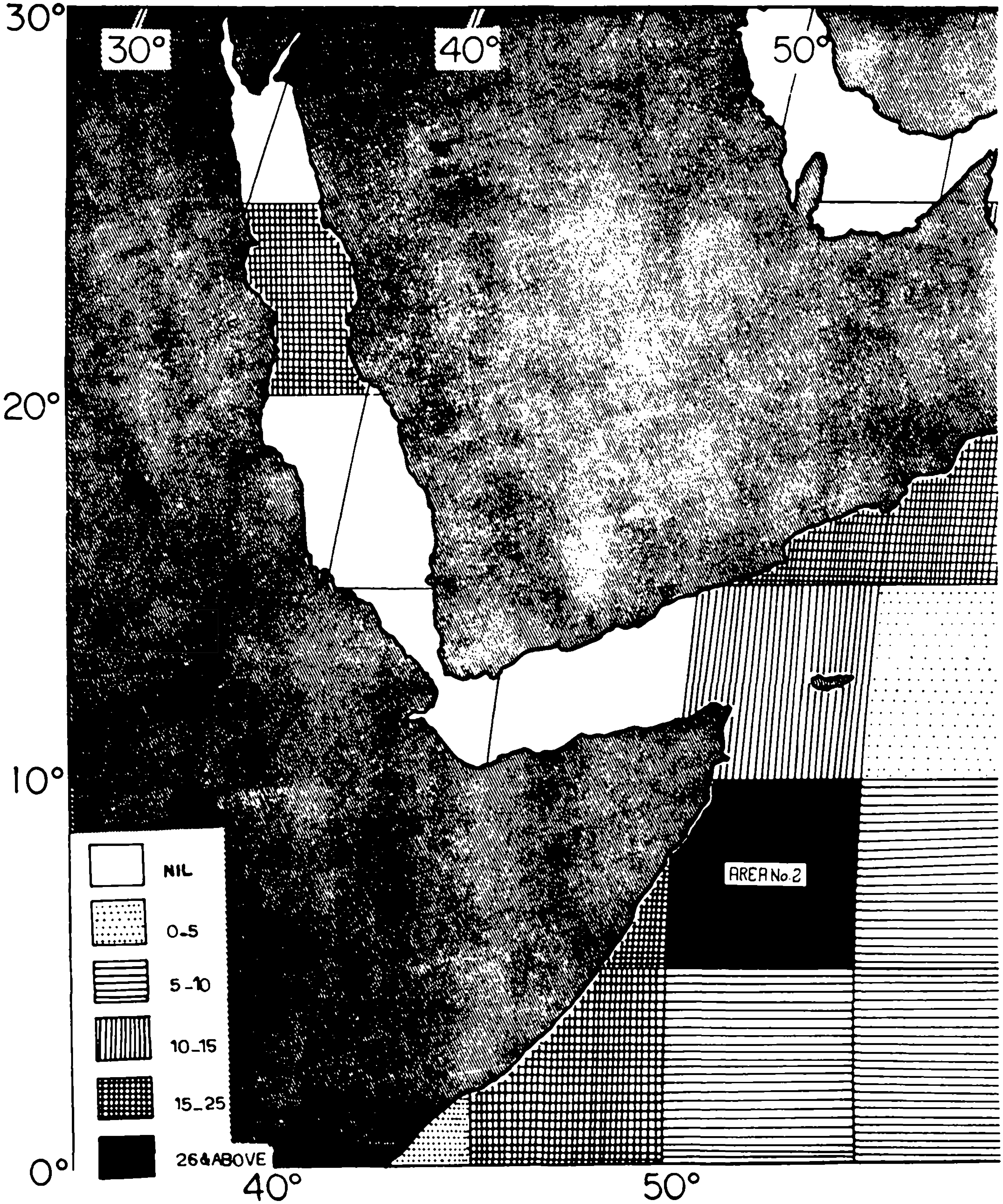

FIG. 2. DISTRIBUTION OF PENAEIDS IN THE ARABIAN SEA (FOR 5° SQUARE)

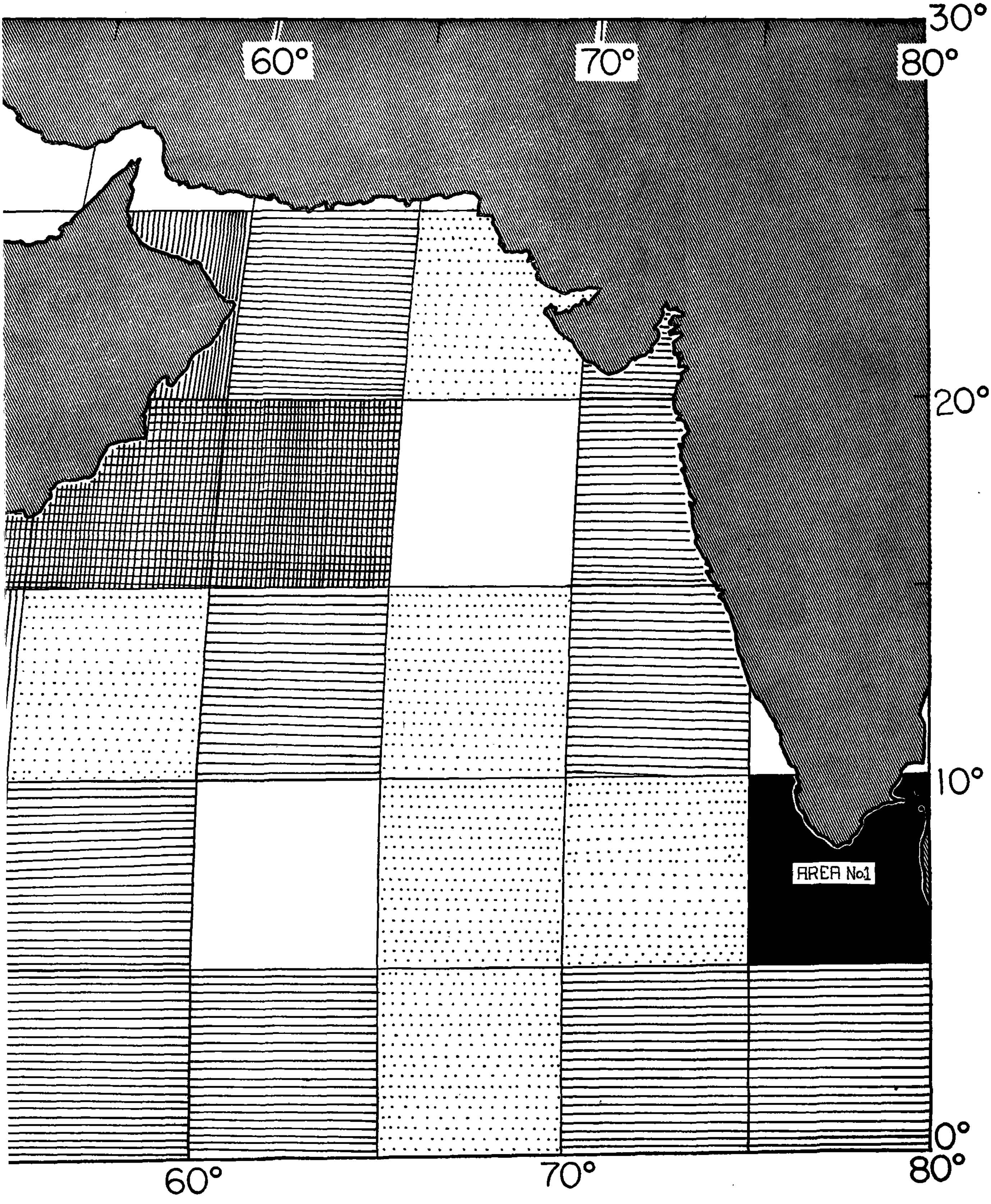
30°
60°
70°
80°
20°
10°
AREA No1
0°
80°
60°
70°

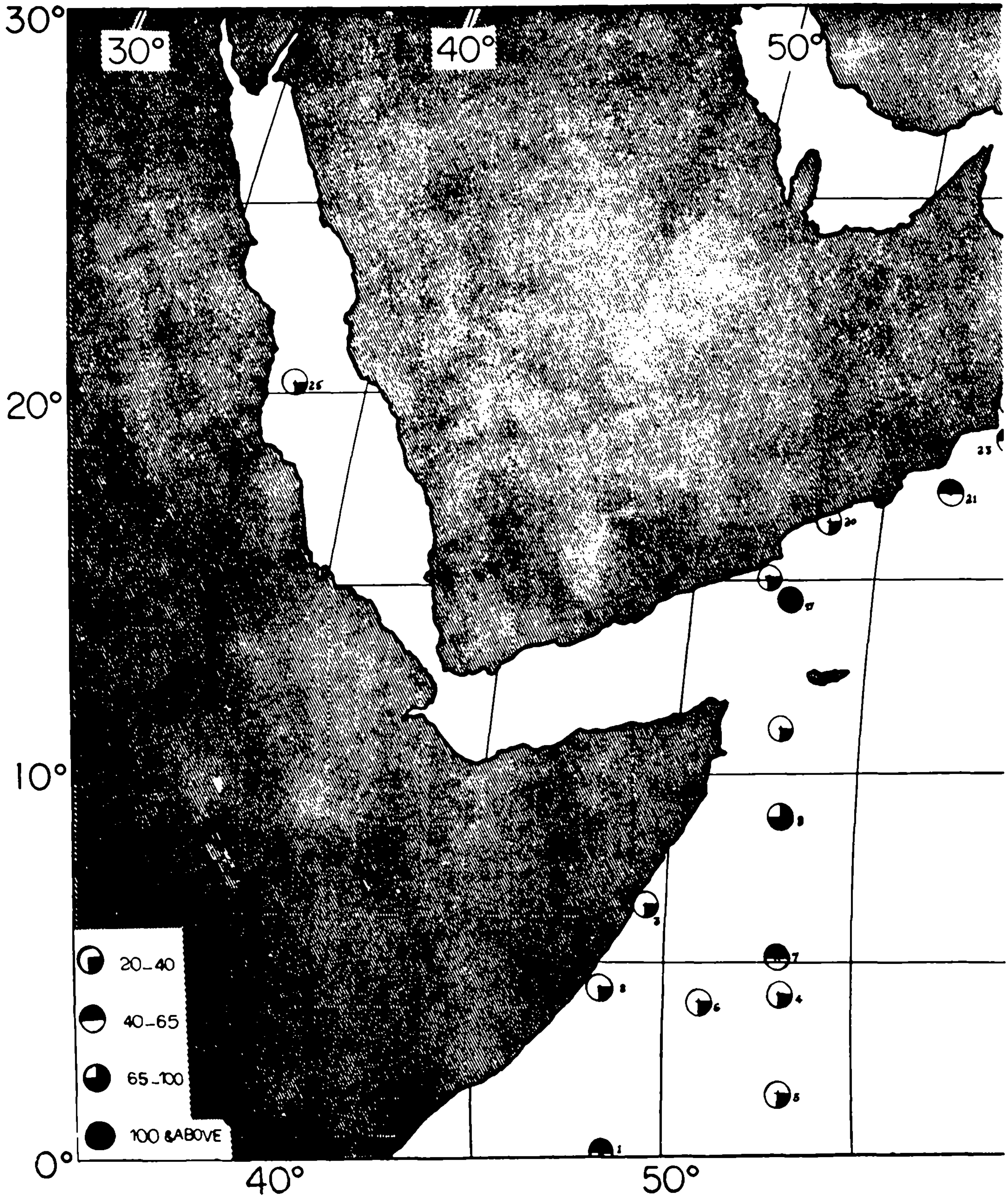

FIG. 3. CHART SHOWING THE NUMBER OF PENAEID LARVAE AT SOME SELECTED STATIONS.

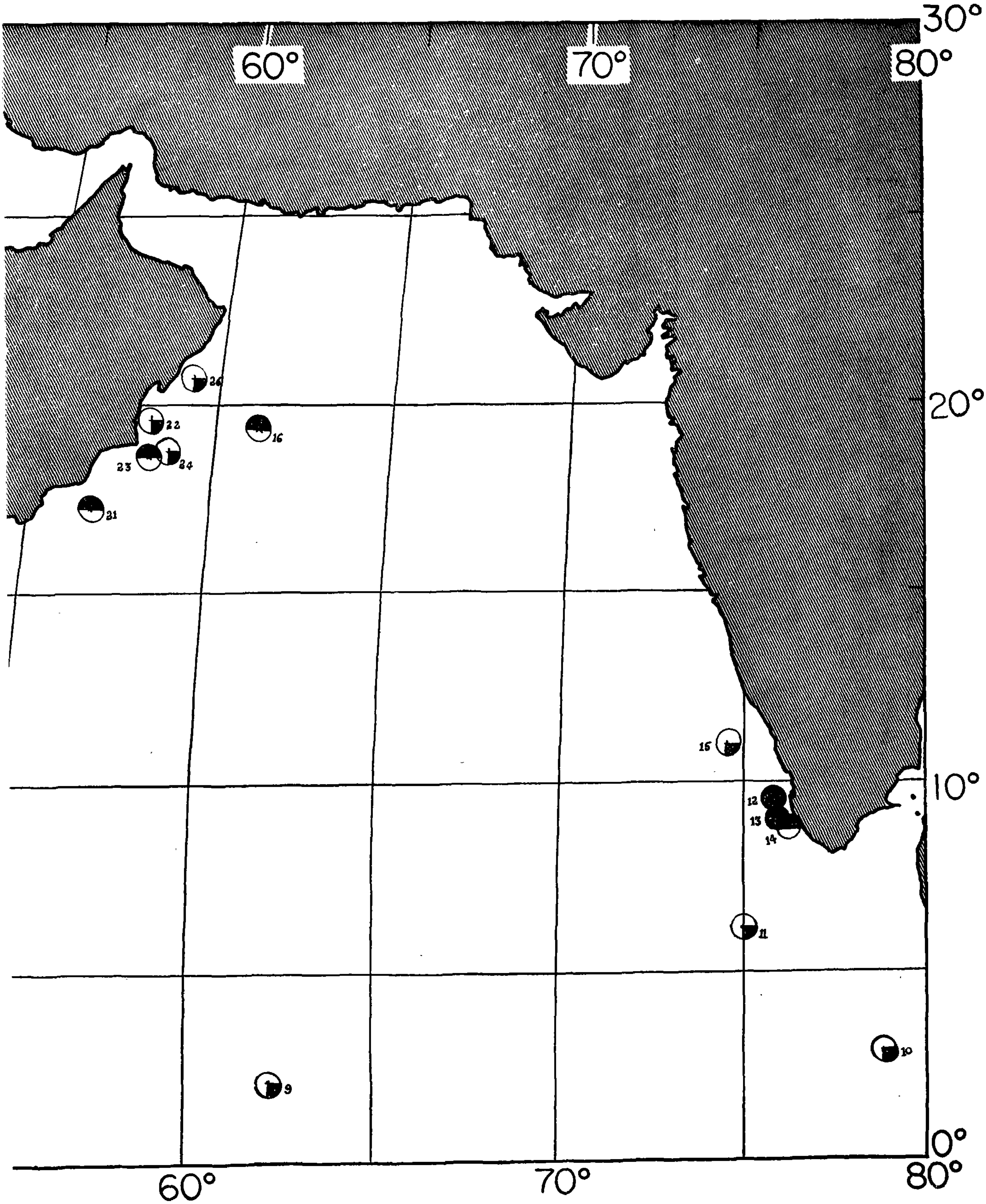
30°
60°
70°
80°
20°
10°
0°
80°
60°
70°
80°
26
22
16
23
24
21
15
12
13
14
11
10
9

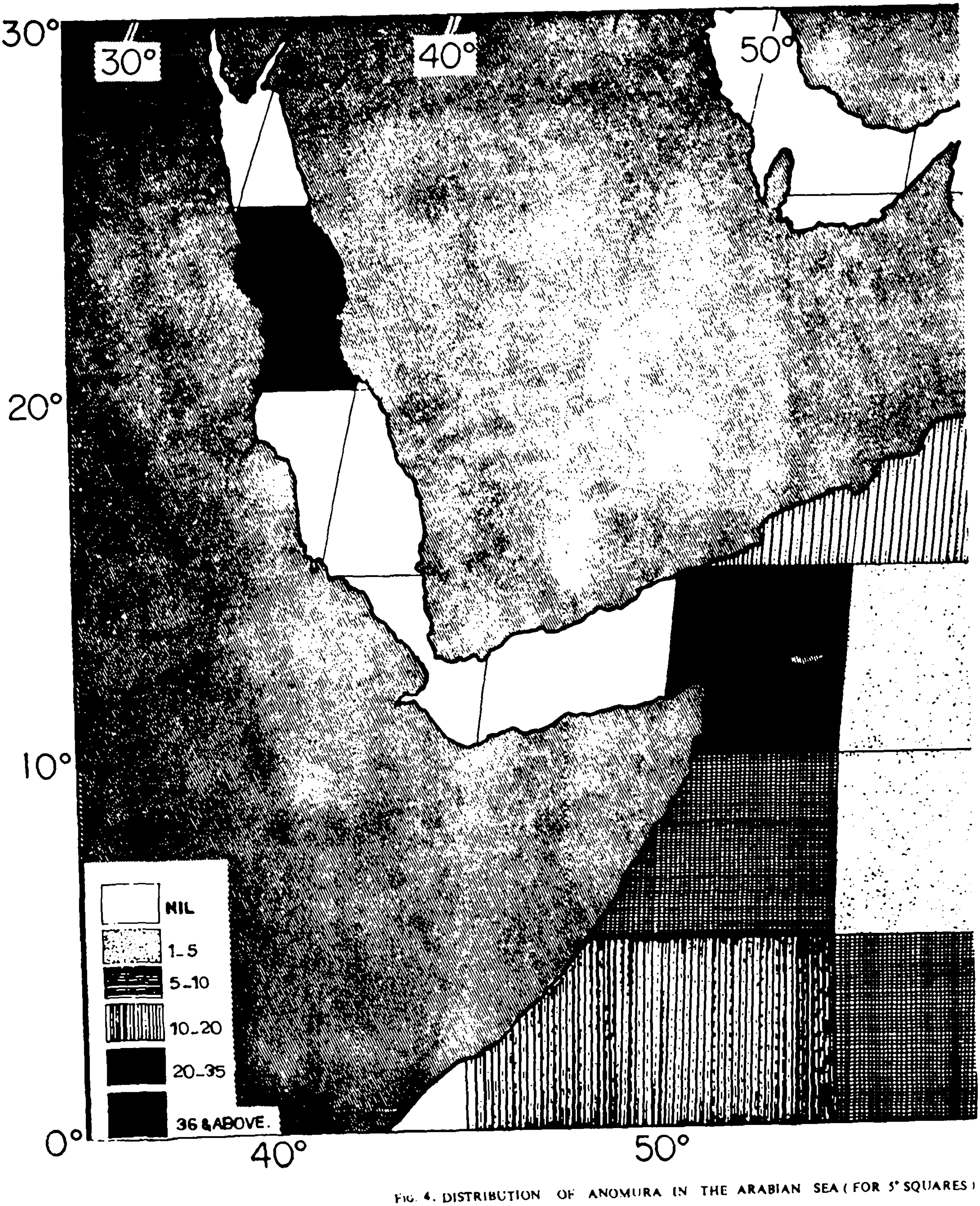

FIG. 4. DISTRIBUTION OF ANOMURA IN THE ARABIAN SEA (FOR 5° SQUARES)

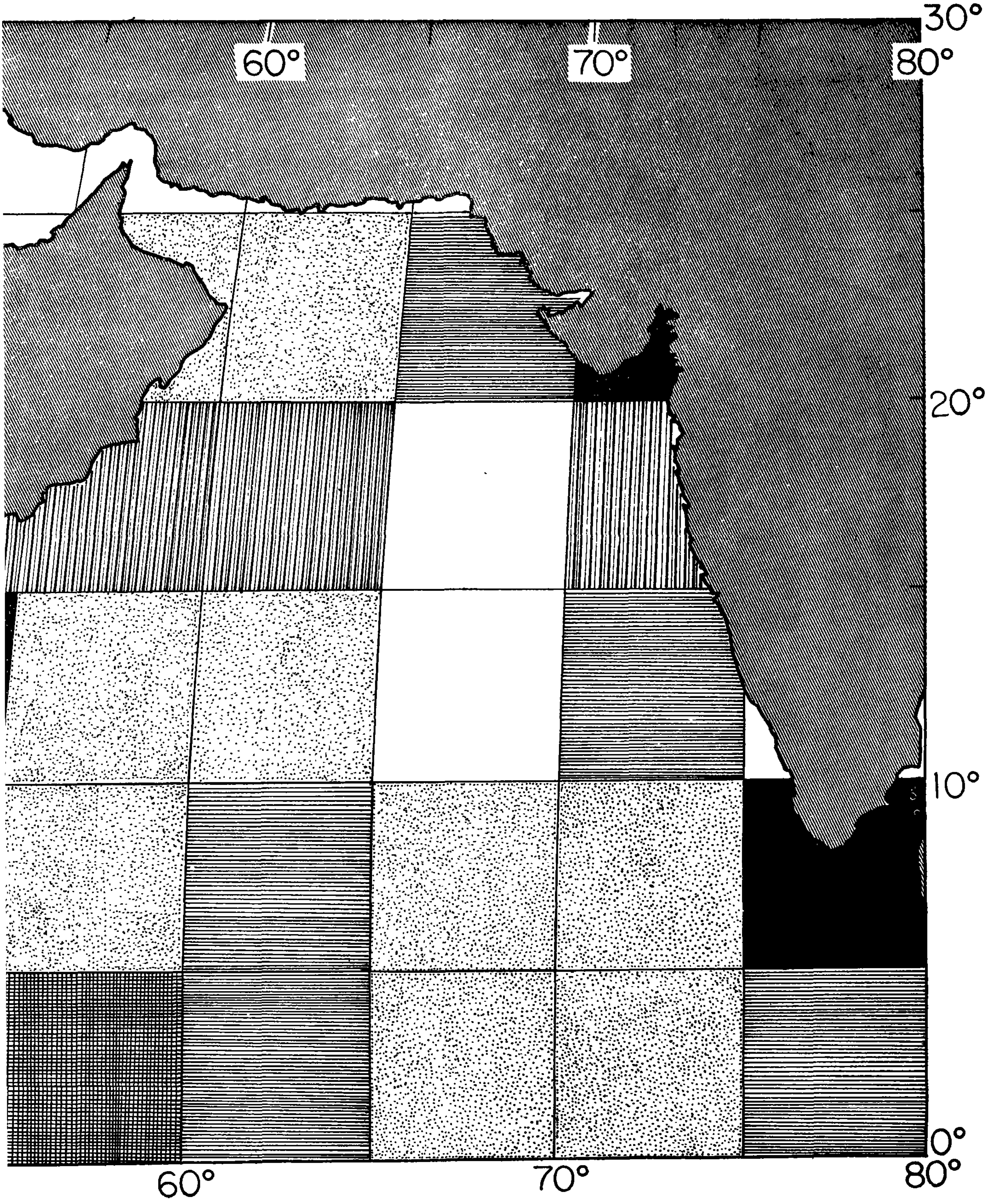
30°
60°
70°
80°
20°
10°
0°
60°
70°
80°

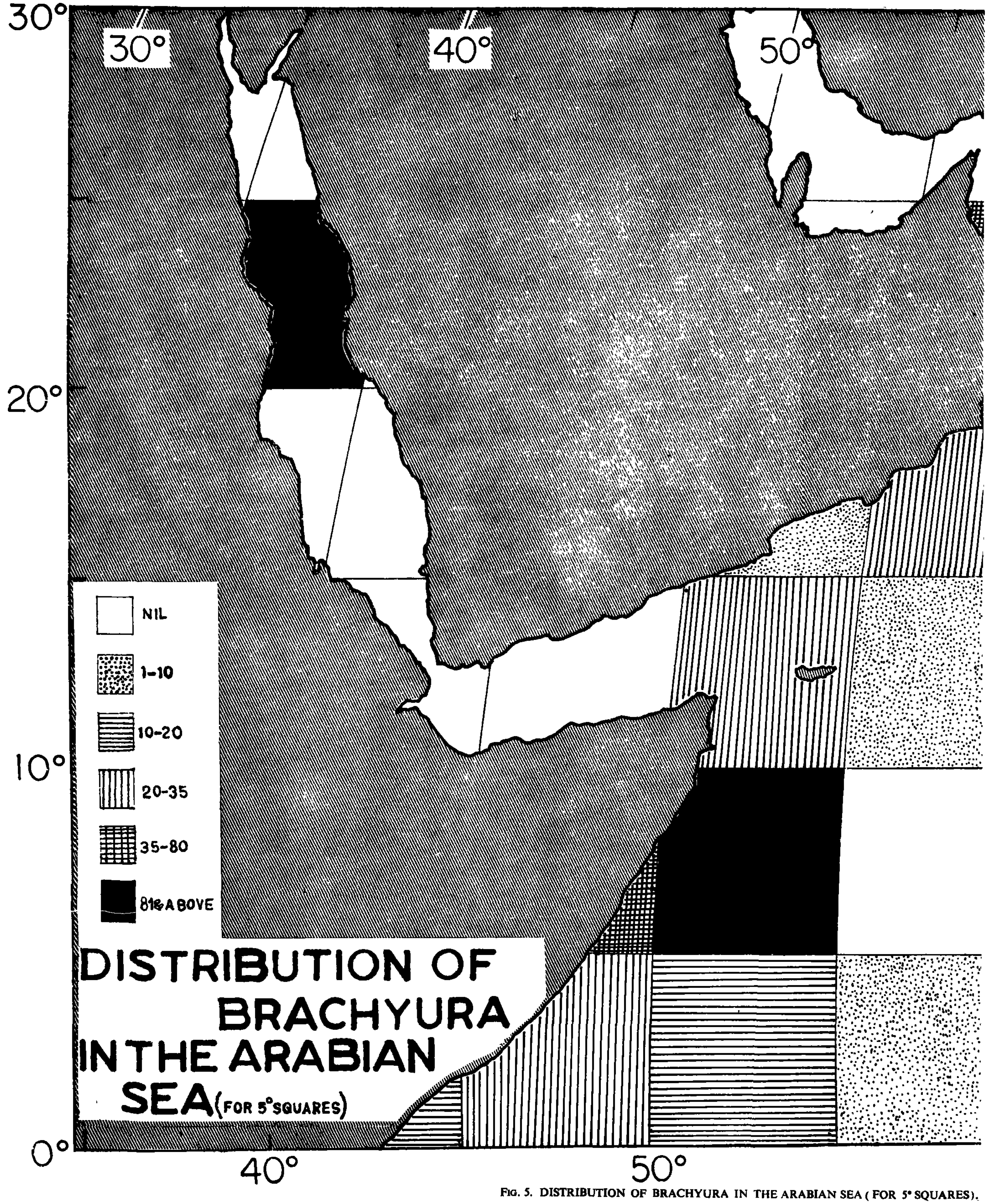

FIG. 5. DISTRIBUTION OF BRACHYURA IN THE ARABIAN SEA (FOR 5° SQUARES).

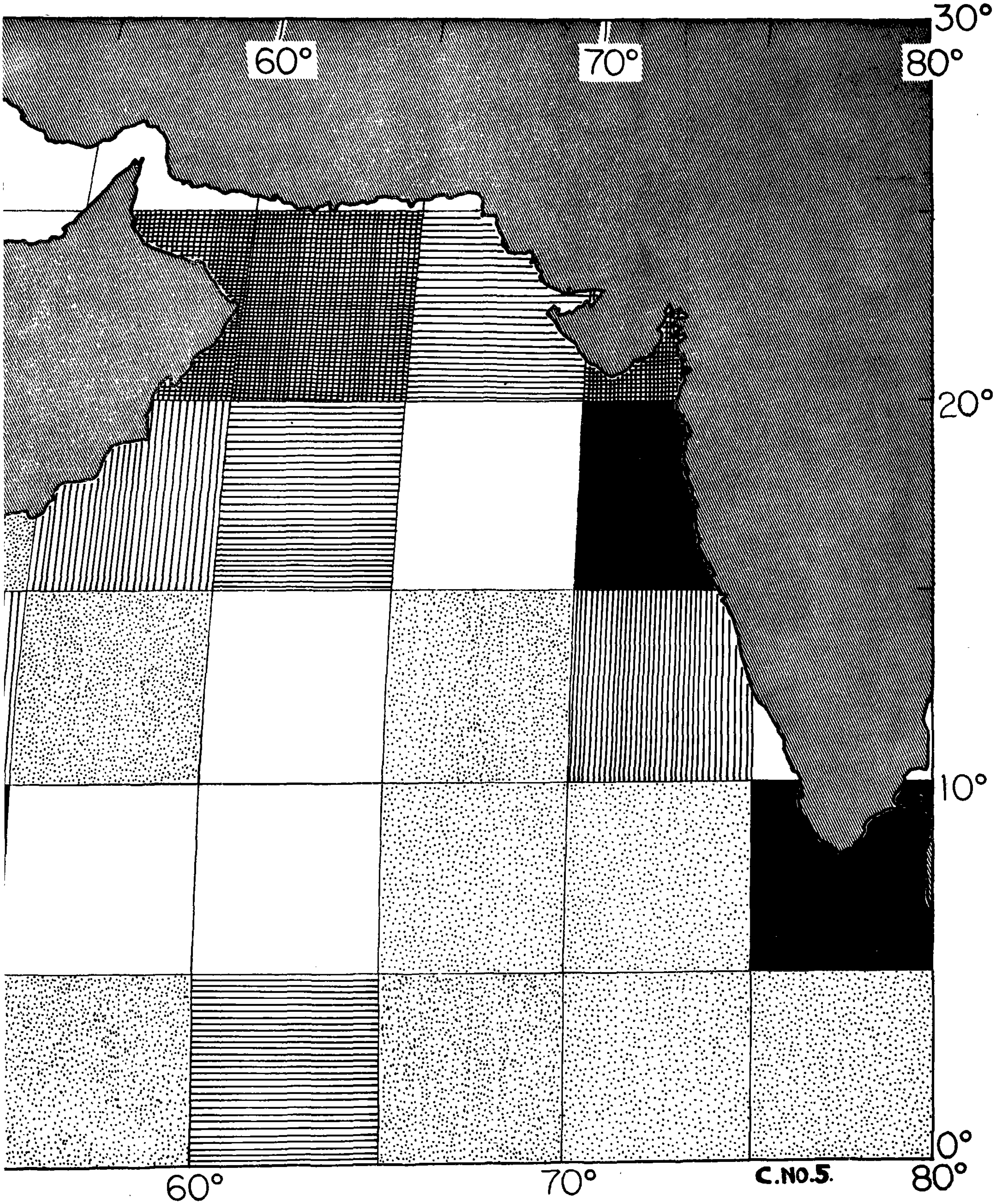

30°
60°
70°
80°
20°
10°
0°
60°
70°
C. NO. 5.
80°

over a hundred larvae in each (referred to in the previous para) two were made during the day and one at night. The data seem to indicate that night hauls in general do not have any marked effect on the number captured. It may be of interest to note here that previous workers on the group such as Dakin (1938) and Racek (1959) have recorded that late stages of *P. plebejus* and other species were obtained in sufficient numbers only in night hauls. Racek assumes that larvae rose to the surface at night and went down during the day. Heldt has reported that larvae of *Gennadas* and *Solenocera* are unaffected by variations of light intensity. Hall (1962) is not inclined to accept this observation as fully valid since he considers evidence on which it is based as insufficient.

The dates on which these hauls were made were also noted. All of them happened to be made during what may be called the monsoon period i.e. May-June to October-November. Collections made during the remaining months were generally much smaller. Equally small collections have been recorded, it is true, on a number of occasions during the monsoon period also. Nevertheless it is justifiable to infer that Penaeid larvae occur in good number in the plankton of the Arabian Sea in the monsoon months and that adult prawns breed in these months (vide Panikkar and Menon 1955).

Without detailed study of the material it is impossible to make any remarks on its composition i.e. on the genera and species represented. One of the more frequently encountered types of larvae at a majority of stations is that of *Gennadas*. Most of those seen are in the mysis stage of development; but a few late Protozoeae taken at some stations also seem to belong to this genus. More than one species seem to be represented, since they exhibit several small differences in their size, character of rostrum, spines on the abdominal somites etc. A few juveniles and adults have also been obtained from some collections; but no attempt was made to identify them beyond determining definitely the genus they belong to. The adult prawns are stated to be mostly pelagic in habits and this may account for the occurrence of the larvae at so many stations (Barnard 1950; Ramadan 1938).

Larvae of the subfamily Solenocerinae are also quite common. The Protozoeae stages have seldom been noticed, only the mysis stages occurring in practically all samples. In regard to the armature of the abdominal segments and carapace they exhibit a number of differences from the typical Solenocera larva (Heegaard 1966) and it is likely that they belong to different species of the genus. Some of them in all probability may even belong to some other closely related genus. The exact parentage will be indicated when systematic study of the group is taken up later.

It is not possible to state anything definite in regard to the parentage of other Penaeid larvae observed. Most of them are in the mysis stage of development and one or two early post-larvae have also been noticed in a very small number of collections. Though resemblances between these larvae and the figures of various species of the subfamily Penaeinae furnished by previous authors have been noticed they could not with any degree of certainty be ascribed to any of these species without further study of appendages, gills and other parts. No useful purpose would be served by indicating such superficial resemblances here. It can only be stated that various species of Penaeinae seem also to be represented frequently in the collections.

References

Barnard, K. H. (1950). Descriptive catalogue of South African Crustacea (crabs and shrimps). *Ann. S. Afr. Mus.*, **38**, 1-837.

Dakin, W. (1938). The habits and life-history of a Penaeid Prawn (Penaeus plebejus Hesse). *Proc. zool. Soc. Lond.*, **108**, 163-183.

Gurney, R. (1924). Decapod Larvae. Terra Nova Expedition. Zoology, VIII, No. 2, Crustacea, Part IX.

Hall, D. N. F. (1962). Observations on the taxonomy and biology of some Indo-West-Pacific Penaeidae (Crustacea, Decapoda). *Fishery Publs colon. Off.*, **17**, 1-229.

Heegaard, P. (1966). Larvae of Decapod Crustacea—The Oceanic Penaeids. *Dana Rep.*, No. 67, 1-147.

Heldt, J. H. (1938). La reproduction chez les Crustaces Decapodes de la famille des peneides. *Ann. Inst. oceanogr., Monaco*, **18**, 31-306.

Kemp, I. S. (1910). Notes on Decapoda in the Indian Museum. *Rec. Indian Mus.*, **5**, 173-181.

Ortmann, A. (1893). Plankton-Expedition der Humboldt-Stiftung, Decapoden und Schizopoden. Kiel and Leipzig.

Panikkar, N. K., and Menon, M. K. (1955). Prawn fisheries of India. *Proc. Indo-Pacific. Fish. Coun.*, 6th session (III), 328-344.

Racek, A. A. (1959). Prawn investigations in Eastern Australia. *Res. Bull. N. S. W. Stn Fish.*, No. 6, pp. 57.

Ramadan, M. M. (1938). Crustacea: Penaeidae. *Scient. Rep. John Murray Exped.*, **5**, No. 3.

Reprinted from *Bull. natn. Inst. Sci. India*, no. 38, 1968, p. 771-777

LARVAE OF *RASTRELLIGER* (MACKEREL) FROM THE INDIAN OCEAN

by K. J. PETER
Indian Ocean Biological Centre,
National Institute of Oceanography,
Ernakulam, Cochin

Three early larval stages of mackerel, probably *Rastrelliger kanagurta* collected during the International Indian Ocean Expedition, have been described and illustrated. These records of larvae of such early stages from the Indian Ocean are made for the first time. The area and time of capture of larvae throw some light on their possible breeding season and spawning grounds.

INTRODUCTION

Mackerel belonging to the genus *Rastrelliger* is very widely distributed in the Indian Ocean, and the mackerel fishery of India is constituted very largely by *R. kanagurta.* But very little is known about its spawning and early larval stages. The published records of young specimens are only of a few juvenile stages. Larvae described by Delsman (1926) as *Rastrelliger kanagurta* were later found to be of another species. The available records on the reported capture of larvae of *Rastrelliger kanagurta* are from Vizhingham near Trivandrum (Balakrishnan 1957), and from Madras (Kuthalingam 1956). But neither publication includes illustrations or descriptions. Another record of larvae of *Rastrelliger kanagurta* is from Gulf of Tonkin (Gorbunova 1965). There are several records of the capture of larvae of the genus *Rastrelliger* from Gulf of Thailand during the Naga Expedition (Matsui 1963). A review of the literature of the records of the capture of young stages of *Rastrelliger* (Rao 1962) shows that they are only occasionally caught from the east and west coast of India.

OBSERVATIONS

This paper deals with the records of occurrence and descriptions of three early larval stages of *Rastrelliger* from the Indian Ocean plankton, collected by the vertical hauls of the Indian Ocean Standard Net from 200 m to the surface, during International Indian Ocean Expedition. These three early larvae (represented by three specimens only) measured 2.7 mm, 3.1 mm, and 5.3 mm, in total length, and were collected respectively from Persian Gulf, Red Sea and Bay of Bengal (Fig. 1). It is noteworthy that such very early stages have not been reported from the Indian Ocean hitherto. Details of the station data are given below (Table I).

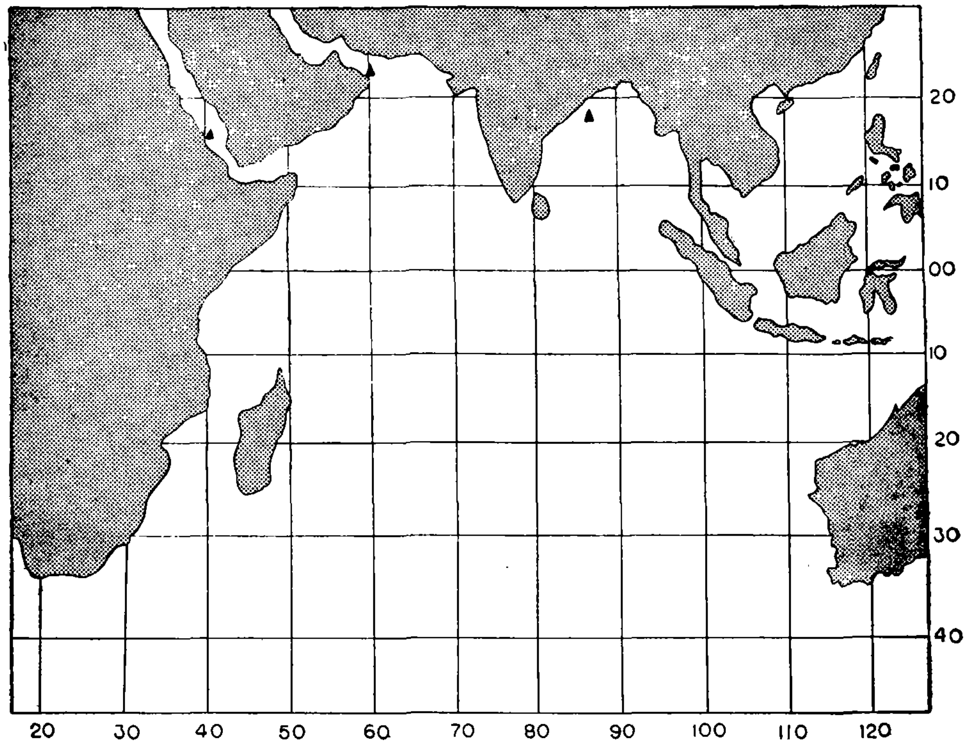

FIG. 1. Localities showing the capture of larvae of *Rastrelliger*.

TABLE I

Details showing the station data regarding the capture of larvae of Rastrelliger

Name of vessel	Station No.	Position Lat.	Position Long.	Date	Time (Local)	Length of specimen (mm)
R. V. Anton Bruun	194	22°22′N	60°05′E	3-11-1963	0450	2.7
R. S. Meteor	73	16°37′N	41°09′E	7-12-1964	2145	3.1
R. V. Pioneer	16	18°15′N	87°48′E	8-5-1964	2000	5.3

The developmental stages of the larvae (Figs. 2, 3, 4 and 5) very closely resemble in general pattern, the Pacific mackerel, *Pneumatophorus diego* (Ayres), the embryonic and larval development of which has been worked out by Kramer (1960). Further, these stages show a high degree of resemblance to the larvae of *Rastrelliger* described by Matsui (1963). The larvae under description have a fairly stubby body, with thirty myomeres, big eyes, wide mouth, coiled intestine and a large head devoid of opercular spines. They differ from the larvae of *Scomber* and *Pneumatophorus* in having a lesser degree of pigmentation and a comparatively deep body.

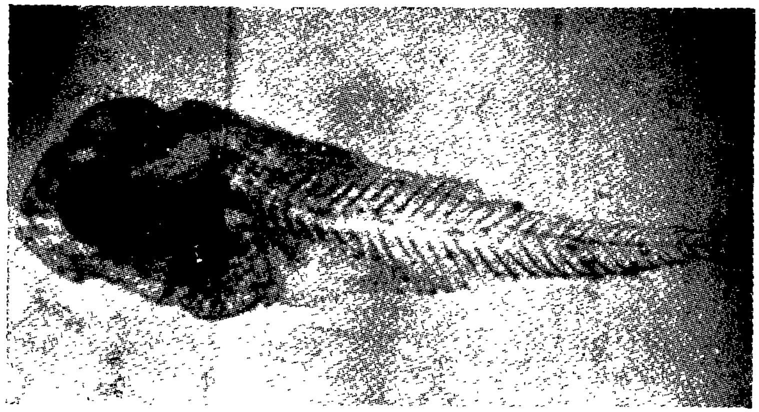

1

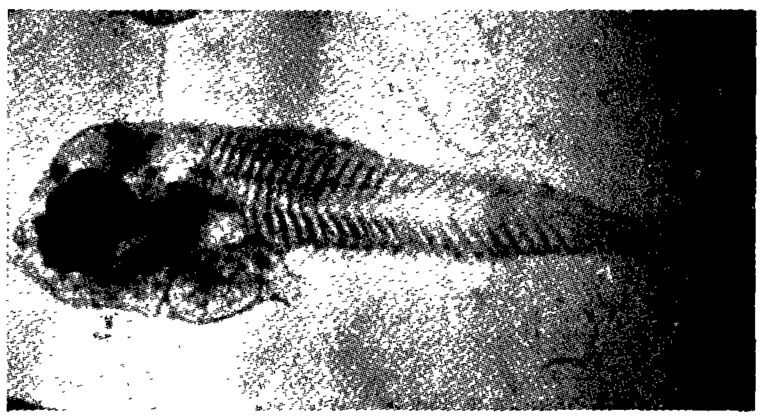

2

3

FIG. 2. Development of *Rastrelliger*—three different stages.

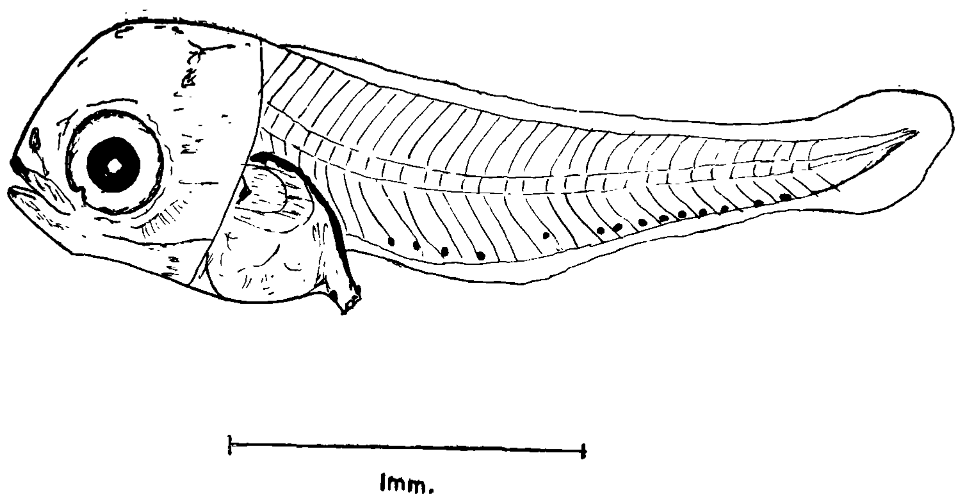

FIG. 3. Larva of *Rastrelliger* (2.7 mm).

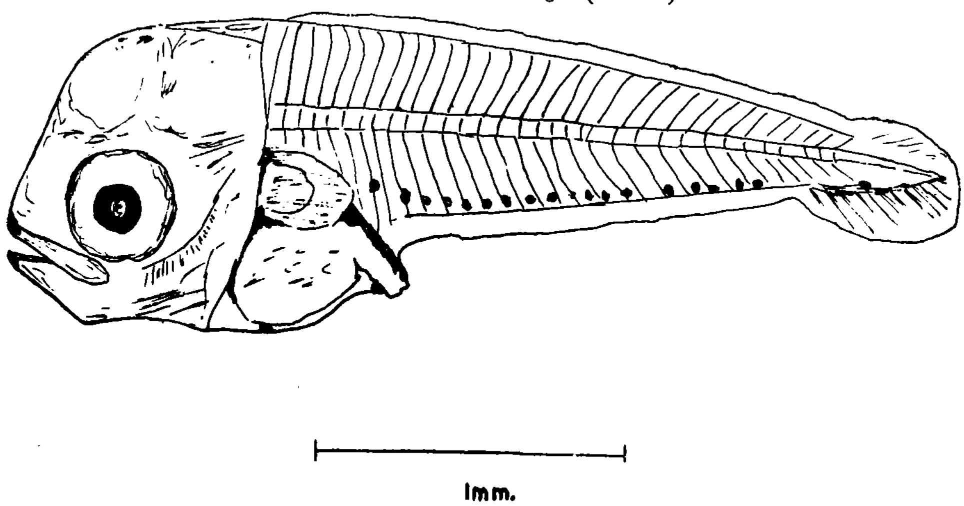

FIG. 4. Larva of *Rastrelliger* (3.1 mm).

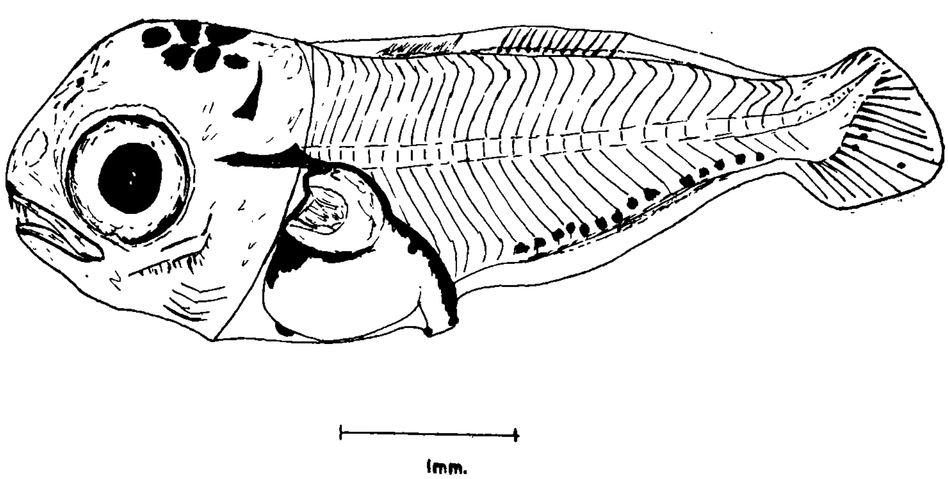

FIG. 5. Larva of *Rastrelliger* (5.3 mm)

The earliest of the stages collected (Fig. 3) measures 2.7 mm in total length. It has thirty well defined myomeres, of which seven are abdominal and thirteen are caudal. The alimentary canal is short and single coiled, the coiling being through the right side. The length of head measures 1.4 mm, and height 1.3 mm. The depth of the body at the region of the stomach is 1.5 mm. The mandibles, maxillae, cleithra and opercula are ossified to a greater degree than the rest of the skeletal elements. The notochord is straight, and partly ossified. Mouth is rather wide, and the inner corner of mouth extending up to the base of middle of eye. The diameter of eye measures 0.5 mm. The eyes are pigmented. The dorsal and anal fins are represented by the long finfold that extends throughout the length of the body. The pectoral fins are represented by two flattened membranous finfolds one on either side. The caudal has a symmetrical appearance with the tip of notochord passing through the centre. The dorsal part of the larva is quite unpigmented, whereas ventral part exhibits certain definite pattern of pigmentation. There are two pigment spots just below the stomach. Located at the anterior and posterior margins of the anal opening two pigment spots are also noticeable. Posterior to the anal opening, a row of melanophores numbering up to fifteen are seen on the ventrolateral margin of the myomeres. They extend from 8th to 29th myomeres. But the 14th, 15th, 18th and 30th myomeres lack this pigmentation. The caudal also does not show any sign of pigmentation.

The next stage in this series (Fig. 4) measures 3.1 mm. The larva has a more stubby-bodied appearance. The length of the head measures 1.5 mm and the height, 1.6 mm. The myomeres could be separated into seven abdominal and thirteen caudals. Some of the anterior myomeres have developed a zig-zag pattern. The processes of branchiostegal rays and gill arches are noticeable. The eyes also show proportional increase in size, having a diameter of 0.6 mm. The mouth lacks teeth at this stage. The notochord is still straight. The pectorals show a certain degree of advancement in their growth. They measure 0.5 mm in length and are very conspicuous. At this stage the larva might be capable of swimming fast. The dorsal parts of stomach and alimentary canal are well-pigmented. The pigmentation in the gut region is confined to the peritoneal cavity. On the top of the head are noticed two small pigment spots. The stomach and intestine retain the same pattern of pigmentation. Posterior to the anal opening as many as eighteen pigment spots could be counted. In the caudal region one pigment spot is noticed at the base of the hypural plates and another at the distal margin of the caudal rays.

The 5.3 mm long larvae (Fig. 5) looks very deep bodied and short. In relation to the greater size of the head, the eyes also show a proportional increase in size (0.7 mm in diameter). A lengthening of the intestine is also observed at this stage. The myomeres appear very compact and exhibit a high degree of zig-zagging, indicating further advancement in the muscle differentiation towards the adult condition. Nine abdominal and twenty-one caudal myomeres could be demarcated. Ossification of principal caudal rays is already noticed. The vertebral column and urostyle are almost completely ossified. The second dorsal, though appearing like a membranous finfold, shows signs of ossification of rays especially at the positions of the basals. Even though the entire finfold uniformly, exhibits a thickened margin towards the base throughout its length, the future position of the second dorsal is clearly indicated. On close examination as many as twelve thickened basals and an equal number of very thin supporting rays could be noticed. Even though the first dorsal is not yet formed, its future site is demarcated by the thickening noticed just anterior to the second dorsal. The anal also is almost in the same stage of development as the second dorsal. It is located just opposite to the second dorsal, having about twelve thickned basals. The dorsal and anal finlets are not developed at this stage. The caudal has undergone a higher degree of ossification than the dorsal and anal and up to fifteen caudal rays could be counted. The tip of the urostyle is curved upwards. Of all the fins, the pectorals are the most conspicuous with a high degree of muscular support. The total length of the fin including the stalk measures 0.6 mm. Six teeth are noticed in the upper jaw and four in the lower. Gill rakers are better developed. Four branchiostegal rays are clearly visible. The dorsal side of the head and the tip of the snout are pigmented. Pigmentation is also seen all over the stomach, especially in the peritoneal cavity. Pigment spots present at the anterior and posterior margins of the anal opening as in the previous stages, are noticed in this stage too, but they appear to be more dark. Two other pigment spots are also noticed just below the stomach. The ventro-lateral row of pigment spots start from the 13th myomere onwards. The 23rd myomere is found to be unpigmented. On the caudal region three conspicuous pigment spots are present on the caudal fin also, of which two are below the hypurals and one towards the distal end of the fin rays. The melanophores on the occipital region and top of head form a more or less circular pattern. The number of ventral pigment spots is limited to fourteen, and they exhibit some degree of fading

Discussion

The above larvae represent three important stages in the life history of *Rastrelliger*. In fact, they form a very significant link in the chain of mackerel fisheries research, as they give some clue regarding the location of spawning grounds of this commercially important fish. A comparative study of the material, with that of the illustrations and descriptions of *Pneumatophorus diego* (Kramer 1960) and of genus *Rastrelliger* (Matsui 1963) proves beyond doubt, that the larvae under description belong to the genus *Rastrelliger*. The larva of *Rastrelliger* is found to be in a more advanced stage of development, than all its nearest scombrid relatives of the same length size so far described. But the stages of larvae described here differ from the *Rastrelliger* collected from the Gulf of Thailand (Matsui 1963) in the following respects: Matsui observed the splitting of the ventral melanophores into right and left components only from the 4.5 mm long (standard length) larvae onwards. But such splitting of ventral melanophores has been observed even in the earliest stage referred in this paper. Similarly, the presence of dorsal pigmentation along each side of the base of the second dorsal and finlets are not seen in the corresponding stages described here. Further, the pigmentation on the top of head and at the tip of the snout is very conspicuous and it appears at an earlier stage than in the specimens described by Matsui. So these changes in the development of pigmentation pattern can be considered as a species character. Matsui does not consider the larvae from the Gulf of Thiland, as belonging to the species *kanagurta* as the fish catch records prove otherwise. But *Rastrelliger kanagurta* is the dominant species in Indian waters. It is therefore to be expected that the present series belong to *Rastrelliger kanagurta.*

Literature regarding the breeding periodicity of mackerel (Rao 1962) shows that on the west coast the spawning is supposed to take place between March and September, and the data for the east coast are too meagre to draw any definite conclusion. In this connection, it is interesting to note that the present record of capture of larvae from the Arabian Sea area is during November-December and from Bay of Bengal, during May. The data based on the capture of eggs and early stages of larvae (whose power of locomotion is very limited) will give a definite clue for the location and time of spawning, than that based on fish catches. The indication of spawning grounds, by catching juveniles, or even adults with spent gonads will not always give a corrrect picture of such areas, because by the time they are caught they might have travelled long distances away from the actual spawning grounds.

ACKNOWLEDGEMENTS

I am deeply indebted to Dr. N. K. Panikkar, Director, National Institute of Oceanography, for permitting me to work on the above material. I am thankful to Dr. Edward Brinton and Mr. L. R. Kasturirangan, Indian Ocean Biological Centre, for reviewing in the manuscript. My thanks are also due to Dr. E. H. Ahlstrom, Fishery-Oceanography Centre, Bureau of Commercial Fisheries, California, for examining the above larvae and confirming the identification.

REFERENCES

Balakrishnan, V. (1957). Occurrence of larvae and young mackerel (*Rastrelliger kanagurta* Cuvier) off Vizhingham, near Trivandrum. *Curr. Sci.*, **26**, 57-58.

Delsman, H. C. (1926). Fish eggs and larvae from the Java Sea. *Treubia*, **8**, 395-399.

Gorbunova, N. N. (1965). On the spawning of scombroid fishes (Pisces, Scombroidei) in Gulf of Tonkin (South China Sea). *Trudy Inst. Okeanol.*, **80**, 167-176.

Kramer, D. (1960). Development of eggs and larvae of Pacific mackerel and distribution and abundance of larvae 1952-56. *Fishery Bull. Fish Wildl. Surv. U. S.*, **174**, 60, 393-438,

Kuthalingam, M. D. (1956). Observations on the food and feeding habits of the Indian mackerel, *Rastrelliger kanagurta* (Russell). *J. zool. soc. India*, **8**, 99-106.

Matsui, T. (1963). The larvae of *Rastrelliger*, in "*Ecology of the Gulf of Thailand and the South China Sea*". Report on Results of Naga Expedition, Scrips Institute of Oceanography. 59-69.

Rao, K. V. (1962). Distribution of young stages of mackerel, *Rastrelliger kanagurta* (Cuvier) in the Indian inshore waters. Symposium on *Scombroid Fishes*. (Pub. by Marine Biological Association of India, Mandapam Camp) Part 1, 469-482.

Reprinted from *Bull. natn. Inst. Sci. India*, no. 38, 1968, p. 785-796

STUDIES ON THE MATURITY AND SPAWNING OF SILVER POMFRET, *PAMPUS ARGENTEUS* (EUPHR.) IN THE ARABIAN SEA

by U.K. GOPALAN*

National Institute of Oceanography, New Delhi

Maturity and spawning of the Silver Pomfret, *Pampus argenteus* (Euphr.) have been studied in an area between the Gulf of Kutch and the Gulf of Cambay. The method of studying were: direct observation on the occurrence of maturity stages, measurements of the diameter frequency of oocytes, seasonal variation in the condition factor and the gonadosomatic index. The results have indicated that the species has a prolonged spawning season-commencing from February and lasting till August. This has been verified by the seasonal abundance of post-larvae and juveniles. A general tendency amongst the fish to migrate from the northern waters of Gujarat towards the Gulf of Cambay has also been noticed.

INTRODUCTION

Pomfrets form one of the principal groups of edible fishes of India. They are caught in considerable quantities from all along the east and west coasts and form a major fishery in the states of Gujarat and Maharashtra. This fishery is contributed by three species viz. the Silver Pomfret, *Pampus argenteus* (Euphr.), Brown Pomfret, *Parastromateus niger* (Bloch) and the Chinese Pomfret, *Pampus Chinensis* (Euphr). Of these, the Silver Pomfret constitutes the main bulk of India's total pomfret landings which in 1962 was 25678 metric tons.

Based on several years of observation on the fishery in Gujarat, certain specific problems which require special attention have been pointed out by Gokhale (1960) and Lakumb (1961). One of the main features of their findings is the occurrence of large numbers of undersized fishes (juveniles) in the commercial catches in recent years when the fishing effort has become many-folds by the introduction of modern gears and techniques. The exploited range of this fishery along Gujarat and Maharashtra continues to remain almost the same—the conventional pomfret grounds extending between the depths of 25 and 50 metres. Some possibilities of a separate fishery of large sized pomfrets beyond the present exploited radius in deeper waters have been expressed by Kewalramani and Pathak in 1964. These observations suggest the need for a systematic investigation on the biology and fishery of this species.

Till now, we have very little information on the Indian Pomfrets. Short accounts of a general nature have been given by Spence and Prater (1931), Chidambaram and Venkataraman (1946), Moses (1947) and Devanesan and Chidambaram (1948). Preliminary attempts to study the biology of *Pampus argenteus* in Maharashtra waters have been made by Rege (1958) and Kewalramani and Pathak (1964). Sivaprakasam (1965) has made a study of the maturity and spawning of *Parastromateus*

**Present Address:* National Institute of Oceanography, Karikkamuri Cross Road, Cochin-11.

niger in Saurashtra waters. In the Arabian Sea, the richest Silver Pomfret grounds are in the coastal waters extending between the Gulf of Kutch and the Gulf of Cambay. The present communication forms part of the author's studies on the fishery and biology of the Silver Pomfret in this area during the period 1961-64.

Materials and Methods

Fortnightly samples collected from Veraval (Lat. 20°54′ N; Long. 70°22′ E) and other representative samples collected from various fishing centres between the Gulf of Kutch and Gulf of Cambay formed the material for the present study. Most of the samples came from the catches of a traditional gear, *Dhakkal* (bottom drift net) whose operational range was limited to 30-50 metres depth. A few samples were also obtained from the *Dol* (bag net) operated off Nawabundar and Jafarabad.

After making various morphometric measurements and counts, the fishes were weighed on a single-pan Salter balance and then dissected to remove the gonads. In fresh condition the gonads were examined to determine the sex and the stages of maturity. They were then weighed on a sensitive balance, their volumes noted by displacement method and finally these were preserved in 5% formalin for subsequent studies.

Samples could not be made available for the months of June and July because of the suspension of fishing, due to the onset of south-west monsoon, which is a usual feature. Occasionally a few samples collected from the market were also used for the study of the condition of gonads. More details regarding the methods adopted for studying the various aspects have been given under pertinent sections of this paper. Total length referred to here is the length from the tip of the snout to the end of the upper caudal lobe.

Description of Gonads

The ovaries of ***Pampus argenteus*** are paired L-shaped organs and occupy a postero-dorsal position in the viscera, underneath the kidneys. The two lobes lie close together with their posterior ends extending very near the cloaca. The ovaries are fused together at their posterior ends from where a short oviduct runs forward and opens into the cloaca. The testes are relatively small, paired and elongated organs occupying a similar position in the viscera. They become milky white on attaining maturity. The ovaries and testes could be distinguished easily by the naked eye in fishes measuring 14 cm and above.

Classification of Maturity Stages

The macroscopic and microscopic variations in the ovaries caused by seasonal changes in the degree of maturity gave clear indications to draw the following seven arbitrary stages of maturity. Similar classification could not be made in males because of difficulties in assigning correct maturity stages to testes. The macroscopic appearance of various maturity stages of ovaries have been diagrammatically shown in Fig. 1.

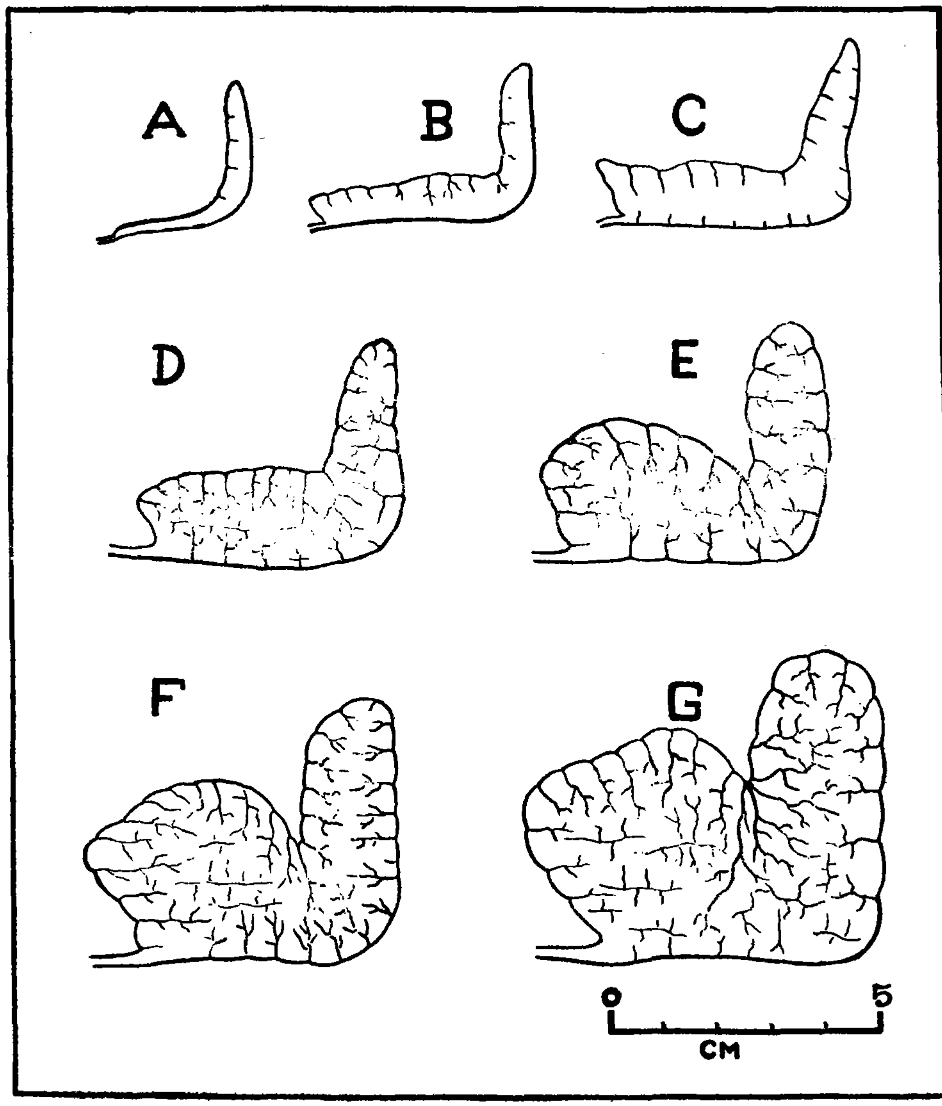

FIG. 1. Macroscopic appearance of ovaries of *Pampus argenteus* in various stages of maturity.

A. Immature virgin 24 cm in length
B. Maturing virgin 26.5 cm in length
C. Recovering spent 30 cm in length
D. Maturing (intermediate) „ „
E. Mature „ „
F. Ripening „ „
G. Ripe „ „

Stage I (Immature)

Ovaries thin, translucent strips of tissue weighing less than 0.5 g. Microscopic and transparent ova with nucleus at the centre and having diameters less than 5 md (1 md-0.021 mm).

Stage II (Maturing virgin and recovering spent)

Creamy to pale yellow ovaries, weight not exceeding 4 g. Maturing group of ova not sharply separated from the immature (reserve stock). Largest ova with diameters 12-15 md. Recovering spent ovaries could be distinguished from the newly maturing by the presence of a lumen and their flaccid nature.

Stage III (Intermediate)

Ovaries slightly swollen, light yellow with a reddish hue due to branching blood vessels. Weighing 4-8 g and having large ova with diameters 24-27 md.

Stage IV (Mature)

Ovaries large, bright yellow, with conspicuous blood vessels and weighing between 8 and 16 g. Diameter of the largest ova 33-36 md.

Stage V (Ripening)

Ovaries very much enlarged, yellowish or speckled, weighing 16-30 g Largest eggs vacuolated, with diameters 42-45 md.

Stage VI (Ripe and Running)

Ovaries very much distended and jelly like weighing up to 45 g Large ripe ova seen through the thin tunica. Transparent ova having oil globules are extruded with a slight pressure. Largest ova have diameter between 60 and 63 md.

Stage VII (spent)

Ovaries blood shot, shrunken and flaccid, weighing less than 2.5 g with some residual eggs, empty follicles and some oocytes in stage II.

Ova Diameter Measurements

Maturation and spawning habits were studied by the method of ova diameter measurements as given by Clark (1934) and Hickling and Rutenberg (1936). This method has been previously applied to several Indian species by Palekar and Karandi kar (1950, 1952 and 1953), Prabhu (1956) and others.

The eggs from a portion of the preserved ovary was separated on a microscopic slide and their diameters were measured indiscriminately with the help of an occular micrometer having a magnification of 1 md-0.021 mm. Ova measurements from various individuals having the same stage of maturity showed no significant difference in the frequency distribution. Measurements from various parts of the ovary revealed similar frequencies which indicate that these were uniformly distributed throughout the ovaries. Immature oocytes of diameter less than 5 md were not measured. Approximately 500 ova were measured from the ovaries of each of the four individuals which were taken to account for a typical condition at each stage. Percentage frequencies of each 3 md interval have been presented in separate polygons in Figure 2. It can be seen from the figure that in stage II there is single batch of eggs represented by the mode at 5-8 md. The biggest ova of this stage have traces of yolk granules in the cytoplasm. As the eggs get more and more ladened with yolk the mode A shifts to the position of mode B_1 in stage III and thereafter to mode B_2 in stage IV. A fully mature batch of eggs likely to be spawned during the ensuing spawning season gets very sharply differentiated into a distinct mode B_3 in stage V. About half of this mature stock of ova suddenly increases in size and becomes completely transparent as the ovary ripens fully (stage VI). Thus the mode C, at this stage, represents the first batch of eggs to be spawned. The other mature eggs represented by the mode B_4 are shifted to the position of mode C after the withdrawal of mode C, and are spawned. The interval between these two spawnings does not seem to be more than a few weeks since the ova at mode B_4 are already in vacuolated condition. A small batch of eggs which gets differentiated from the general egg stock is represented at mode B. But owing to the fact that this remains far separated from the mature stock and does not show much progression it is most likely that this may not be spawned.

Thus from the withdrawal of eggs in successive batches it seems that the fish has a succession of spawnings but, as the fully mature eggs get very sharply differentiated soon from the smaller eggs, the spawning in this species may be restricted to a definite period. Since only half of the mature eggs attain complete ripeness at a time, it can be inferred that each individual has at least two spawnings. Prabhu (1956) observed that in some species which have prolonged spawning seasons the range in the size of mature ova is much larger than what has been noted here. Qasim (1956) while studying the spawning habits of *Blennius pholis* confirmed by aquarium studies that the presence of multiple batches of ova in the unspawned ovary gives rise to more than one spawning.

Spawning Season

Direct observations on the occurrence of fishes at various stages of maturity during the fishing seasons of 1962-63 and 63-64 have been made in order to determine the spawning season. The distribution of 537 females of various maturity stages in different months is expressed quantitatively in Table I.

Table I

Percentage frequency of the number of females in the various maturity stages during the period 1962-64

Maturity stages	Aug.	Sept.	Oct.	Nov.	Dec.	Jan.	Feb.	March	April	May	Number Examined
I*											
II	47.5	73.8	88.4	85.8	44.5	41.6	34.0	10.0	14.1	10.6	273
III	37.5	17.8	5.7	12.6	55.5	44.4	37.2	31.0	22.4	21.1	116
IV	10.0	8.2	2.8	1.2		13.8	29.5	41.3	18.9	20.4	80
V	2.5						9.0	17.2	29.3	32.8	50
VI									3.4	6.6	8
VII	2.5						2.0		11.7	8.2	10

*Immature fishes in stage I occur throughout the year and not included in this table.

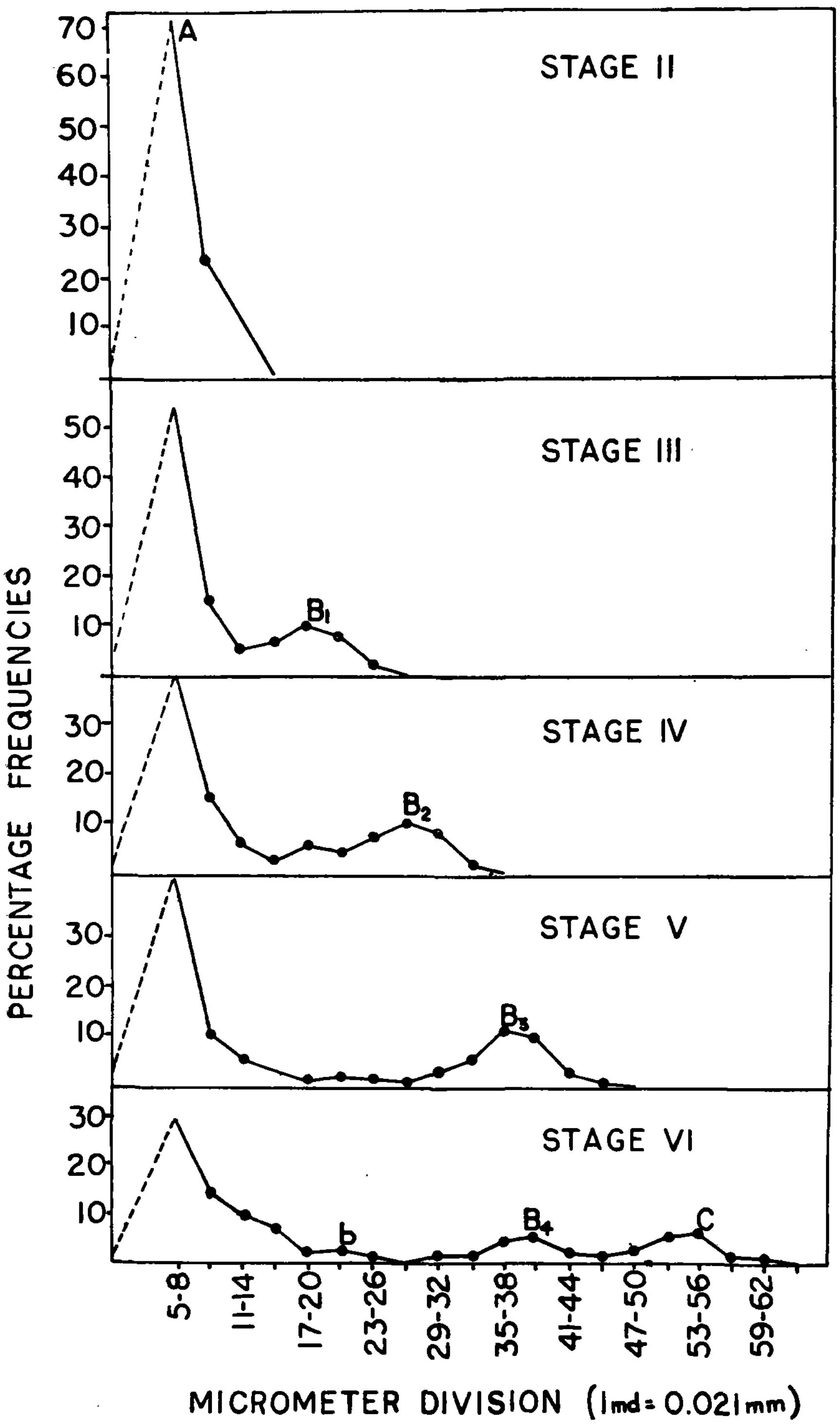

FIG. 2. Frequency polygons of ova diameters at various maturity stages of *Pampus argenteus*.

It can be seen from the table that maturity stages II and III occur throughout the year. From August to November there is a steady increase in the percentage of fishes of stage II. This gradually declines from December when the fishes of stage III become more predominant. By January, fully mature fishes of stage IV are common in the catches and their percentage gradually increases and reaches the maximum in March. The fishes with ripening ovaries begin to appear from February onwards and their frequency of occurrence continues to increase until May when the fishing season comes to a close. A few fishes with ovaries fully ripe and in running condition were collected from Nawabundar and Jafarabad, during April and May.

When the fishing season starts in August, spent fishes in stray numbers are seen in the catches, and thereafter they are not found till February when they start re-appearing. They become common in the catches in April-May. Some of the fishes in seemingly advanced stages of maturity examined during August showed that their ovaries contained mature ova in various stages of resorption indicating that they are not likely to be spawned in the current season. They may be similar to the matured non-spawners of Norway Pout with resorbing eggs described by Gokhale (1957).

It becomes apparent from the increasing occurrence of ripe and spent fishes during April and May that the spawning activity is in progress in these months. Stray numbers of spent fishes observed in late February indicate that the spawning has already started in this month. The appearance of a large number of recovering spent fishes along with a few spent ones in August suggests that the spawning season extends as far as August. Thus the spawning in this species seems to be considerably prolonged, extending between February and August with a peak between April-June.

It has also been observed that larger fishes attain maturity earlier than the smaller ones.

Condition Factor and Seasonal Cycle in Gonad Weight

The fluctuations in the condition factor or the ponderal index has been attributed to various biological features such as fatness, suitability of an environment or the gonad maturity and spawning. It has also been used as an index of the spawning season of fish by many earlier investigators. The ponderal index is calculated by using the following formula (*see* Hart 1946; Menon 1950).

$$K = \frac{W}{L^3} \times 100$$

where W = average weight of fish in g

L = mean length in cm

K = condition factor to be calculated

Average weight for each cm group was worked out in each month and from this the average ponderal index was calculated. Fishes measuring less than 25 cm were found to be immature and hence not considered in this study. The monthly average 'K' values for females have been plotted (Fig. 3).

The curve shows that the condition factor is poorest in September. From October onwards it gradually ascends and reaches its maximum in February. A sudden decline from the peak condition occurs in March. This point of inflexion of the curve coincides with the beginning of spawning which agrees with the direct

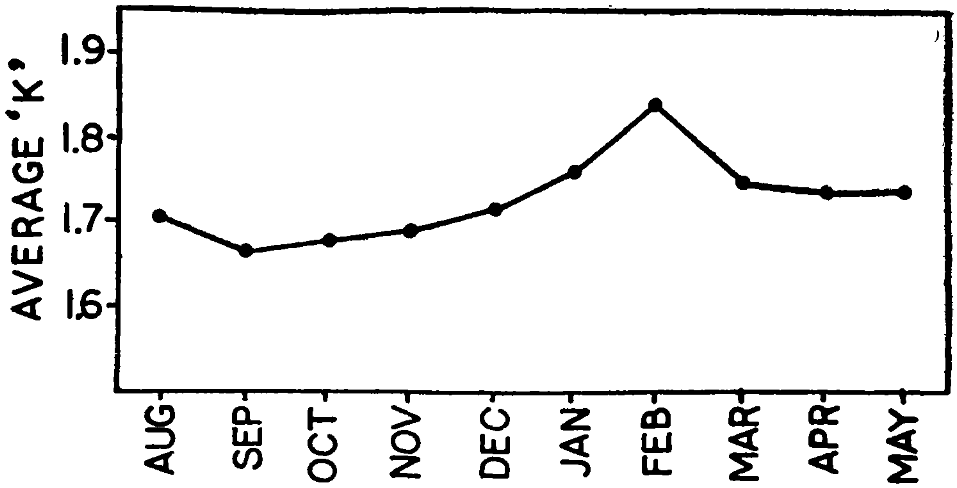

FIG. 3. Seasonal variation in the condition factor "K" of females of *Pampus argenteus.*

observations of gonads. From the values obtained in April and May it can be assumed that no drastic change in the condition of fish is brought about in these months. The values in August also indicate that the downward trend in the curve is not sharp as has been found in fishes with short duration of spawning season.

Gonad weight expressed as percentage of body weight (gonadosomatic index) was calculated and the mean percentage for females in each month is presented in the Table II. Gonadosomatic index of females below 25 cm long was found to be fairly constant throughout the year and therefore these were not included here. It can be seen from the table that the minimum values occur in November when more than 85% of the fishes are in Stage II. From the quiescent stage, the gonads start developing from December onwards till the maximum value (2.38) is reached in March. The downward trend in the gonadosomatic index from March onwards probably indicates the loss of gonad weight due to spawning. As has been found in the condition factor, the decline in the gonadosomatic index is also not sharp. The descending values of the index from August to November can be attributed to the loss of ovary weight due to the progressive resorption of unspawned eggs in the ovaries during this period.

TABLE II

Seasonal variation in the Gonadosomatic Index

Month	Average length of fish in mm	Average weight in g	Average weight of ovary in g	Gonado-somatic index*
August	310.0	512.0	5.57	1.080
September	311.6	523.0	5.12	0.970
October	313.2	542.9	2.98	0.548
November	313.0	509.0	2.14	0.420
December	319.0	559.0	2.77	0.495
January	309.0	518.0	4.65	0.897
February	306.0	473.0	8.63	1.820
March	322.0	590.0	14.05	2.380
April	314	544.0	12.03	2.210
May	310	547.0	11.54	2.10

*Gonadosomatic index= $\frac{\text{Wt. of ovary}}{\text{Wt. of body}} \times 100$

A close relation between the cycle of the gonad weight and the seasonal changes in the relative condition has been observed by Le Cren (1951) in his study on *Perca fluviatilis*. A similar trend is seen in the present study of *Pampus argenteus* also.

SIZE AT FIRST MATURITY

To determine the size at first maturity, data pertaining to 394 fishes caught in the trawl during February-March were used. The appearance of milt in the testes and the yolk granules in the ova of females, were taken as an indication of their maturation. Percentages of maturing individuals in each cm size group have been plotted in Fig. 4.

It can be seen that 5.5% of the male fishes mature at 20 cm, and all the males above 24 cm were either mature or in maturing condition. Maturing females first appear in 24 cm group and their percentage increases thereafter. All of them were found to be maturing or mature at length between 26 and 27 cm, minimum length of the spent female observed was 27 cm. Thus the males seem to mature at a size smaller than that of the females.

LARVAE AND JUVENILES

Large numbers of juveniles of *Pampus argenteus* with length ranging between 5 and 19 cm were available throughout the fishing season in the bag net catches from Diu Head (20°43'N, 70° 59'E) and Jafarabad (20° 52'N, 71 22'E). Pillai (1948) while

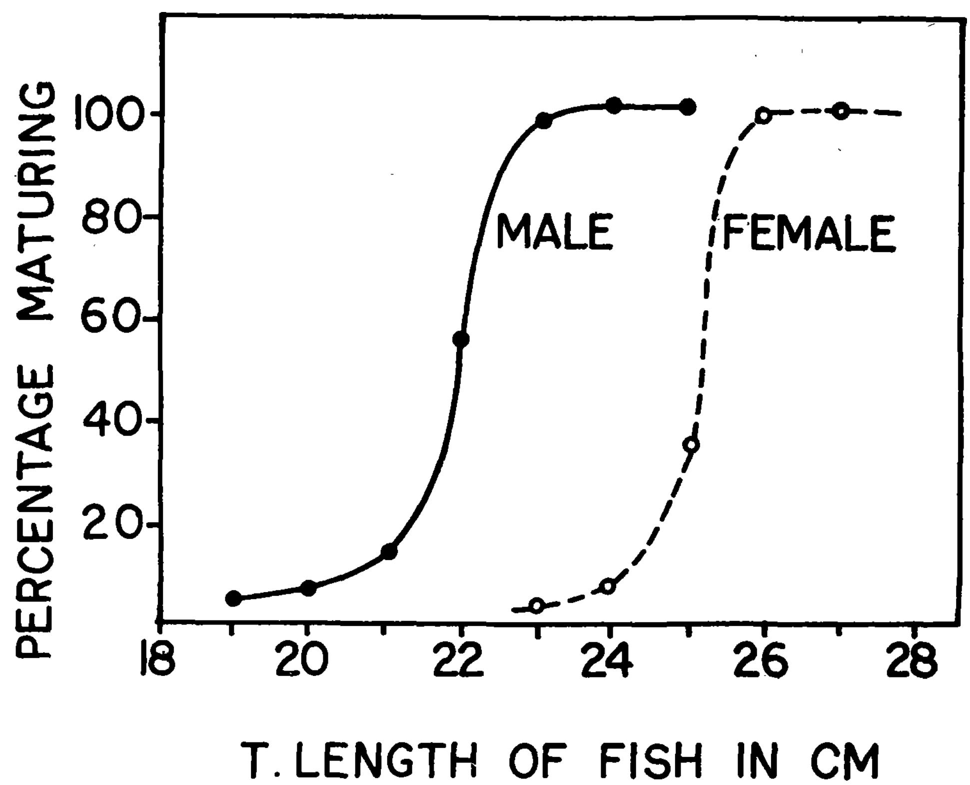

FIG. 4. Size at first maturity of *Pampus argenteus* as indicated by the percentage of maturing fishes in every 1 cm in length.

mentioning about the destructive effect of the bag net on the fishery of this region has pointed out that enormous quantities of young ones of pomfrets, measuring 2"-3" in length are landed regularly along with juveniles of other food fishes.

Examination of the trawl catches during 1961-64 showed that immature pomfrets are caught in grounds off Gujarat and Maharashtra, especially during December-March. Minimum size recorded in the trawl catch was 5 cm long. Monthly observation on the bag net catches at Madhwad, Nawabundar and Jafarabad reveal that post-larvae of Silver Pomfret measuring 2-4 cm appear in large numbers from March onwards. The field identification of these post-larvae were not difficult as fishes of almost all sizes ranging from 5-19 cm were available in the collections (Fig. 5). In the post-larvae, pre-dorsal and pre-anal spines were absent and no dissimilarity between the upper and lower caudal lobes was observed. In the juveniles these characters were conspicuous. The occurrence of the post-larvae in March gives a further indication of the spawning season of the fish noted earlier. The wide range in the size of young ones *i.e.* from 2 to 19 cm, may be because the spawning season is highly protracted.

MIGRATION AND SPAWNING GROUNDS

Landing statistics of the past several years reveal that in the northern parts of the Kathiawar Peninsula, pomfret landing is at its peak between October and December. Fishermen from various parts of Gujarat and Maharashtra migrate to Porbundar and nearby places to take advantage of the fishery during this period. A sharp rise in the catch rate is recorded at Veraval during December-February. In the southern most part of the Peninsula the fishery is relatively more in early March and the peak landings are recorded in April-May.

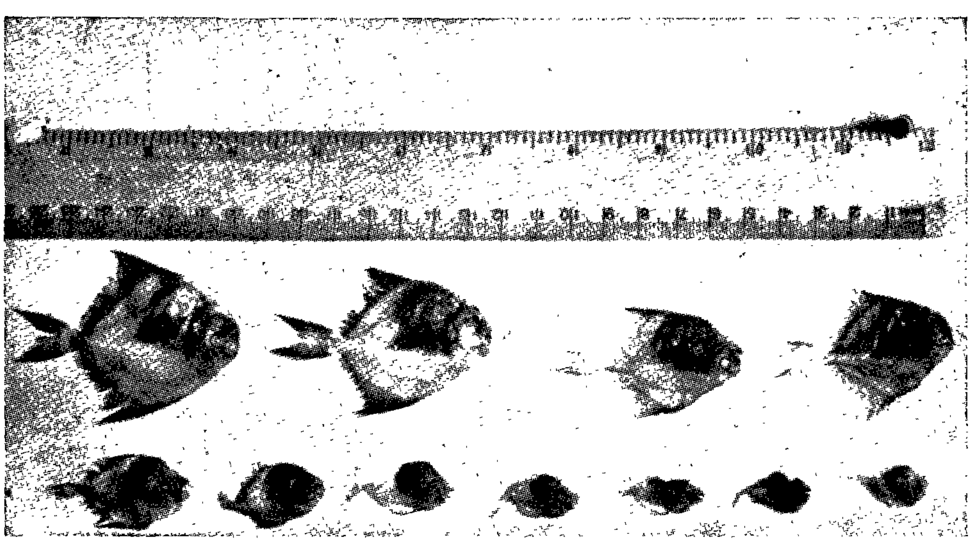

FIG. 5. Post-larvae and juveniles of *Pampus argenteus*.

There seems a general tendency of migration amongst the fish from the northern waters of Gujarat towards the mouth of the Gulf of Cambay. The period of congregation of fish in this region coincides with the period of ripening of gonads. Fully ripe and running females were available only in small numbers in the commercial landings between Diu Head (20° 43′ N, 70° 59′ E) and Jafarabad (20° 52′ N, 71° 22′E). This might be because of the migration of the fully ripe and running fishes into deeper waters of this region for spawning. The availability of large quantities of post-larvae and juveniles of *Pampus argenteus* along with those of many other fishes like Polynemids, Sciaenids and *Harpodon* in the more inshore waters of this region indicates the suitability of this area as a breeding and nursery ground of many species.

The most striking hydrological feature in the mouth of the Gulf of Cambay during this period is the low values of salinity which was 28.35‰ off Jafarabad (*INS DARTHAK* cruise, March 1966). Interior in the Gulf, the values fall below 25‰. Temperature structure in the inshore waters showed no significant variation from surface to bottom. It varied between 28.61 and 25.20° C at different stations in the Gulf. In the fishing ground off Jafarabad it was 25.5° C in March 1966.

Density of plankton was found to be fairly high in this region during March-May.

Summary and Conclusion

Results of investigation on the maturation and spawning of Silver Pomfret, *Pampus argenteus* (Euphr.) in an area between the Gulf of Kutch and Gulf of Cambay indicate that the fish has a prolonged spawning season lasting from February to August with peak spawning occurring during April-June. The minimum size at first maturity is 22 cm in males and 26 mm in females.

There is a general tendency in the fish to migrate from the northern waters of Gujarat towards the Gulf of Cambay during February-May. In this season large numbers of post-larvae and juveniles occur in the inshore waters of Jafarabad and Nawabundar. This indicates that the spawning ground of this fish is somewhere in this area.

Acknowledgements

I am grateful to the Director of Fisheries, Gujarat, for providing the facilities and to Dr. S. V. Gokhale, former Assistant Director of Fisheries, for his keen interest and guidance during the course of this work. Thanks are also due to Dr. N. K. Panikkar, Director, National Institute of Oceanography, for the encouragement offered during the preparation of this paper and to Dr. S. Z. Qasim, for reading through the manuscript offering useful suggestions.

References

Chidambaram, K., and Venkataraman, R. S. (1946). Tabular statement of the natural history of certain marine food fishes of the Madras Presidency, West Coast. *Madras Govt. Publication*, No. 15.

Clark, F. N. (1934). Maturity of California Sardine (*Sardinella Caerulea*) determined by ova diameter measurements. *Fish. Bull.*, Sacramento No. 42.

Devanesan, D. W., and Chidambaram, K. (1948). The common food fishes of the Madras Presidency. *Madras Govt. Publication*, No. 38.

Gokhale, S. V. (1957). Seasonal histological changes in the gonads of the whiting (*Gadus merlangus L.*) and the Norway pout (*G. esmarkii* Nilsson). *Indian J. Fish.*, **4**, 92-112.

————(1960). Need for Fisheries Research in Gujarat. The Fishing Industry of Gujarat, Ahmedabad.

Hart, T. J. (1946). Report on trawling surveys on the Petagonian continental shelf. '*Discovery*' *Rep.*, **13**, 223-408.

Hickling, C. F., and Rutenberg, E. (1936). The ovary as an indicator of spawning period in fishes. *J. mar. biol. Ass. U. K.*, **21**, 331-417.

Karandikar, K. R., and Palekar, V. C. (1950). Studies on the ovaries of *Polynemus tetradactylus* in relation to its spawning habits. *J. Univ. Bombay*, **19**, 21-24.

Kewalramani, H. G., and Pathak, S. D. (1964). A note on silver pomfret fishery. *Bull. Indo-Pacif. Fish. Coun.*, **40**, 5-6.

Lakumb, N. C. (1961). Need for Research on Fishing Gear of Gujarat. Souvenir Fish. of Gujarat, Ahmedabad 70.

Le Cren, E. D. (1951). The length-weight relationship and seasonal cycle in the gonad weight and condition in the perch (*Perca fluviatlis*). *J. Anim. Ecol.*, **20**, 201-219.

Menon, M. D. (1950). Bionomics of the poor-cod (*Gadus minutus*) in the Plymouth area. *J. mar. biol. Ass. U. K.*, **29**, 185-229.

Palekar, V. C., and Karandikar, K. R. (1952). Maturity and spawning period of *Thrissocles purava* (Ham.) as determined by ova diameter measurements. *Proc. Indian Acad. Sci.*, **35, B** 143-154.

————(1953). Maturity of *Coilia dussumieri* (Cuv. and Val.) in Bombay waters during different months of the year. *J. zool. Soc. India*, **5**, 217-226.

Prabhu, M.S. (1956). Maturation of intra-ovarian eggs and spawning periodicities in some fishes *Indian J. Fish*, **3**, 59-90.

Qasim, S.Z. (1957). Biology of *Blennius pholis* L. (Teleostei). *Proc. zool. Soc. Lond.*, **128**, 161-208.

Rege, M. S (1958). A study of the stromateid fishes of Bombay. Ph. D. thesis, University of Bombay.

Sivaprakasam, T. (1965). Observation on the maturation and spawning of Brown Pomfret, *Parastromateus niger* (Bloch) in Saurashtra Waters. *J. Bombay nat. Hist. Soc.*, **62**, 245-253.

Spence, R., and Prater, S. H. (1931). Fish supply of the West coast of India. *J. Bombay nat. Hist. Soc.*, **34**, 973-991.

Reprinted from *Bull. natn. Inst. Sci. India*, no. 38, 1968, p. 854-863

PRELIMINARY REPORT ON THE DENSITY OF FISH EGGS AND LARVAE OF THE INDIAN OCEAN

by K. J. PETER

Indian Ocean Biological Centre, National Institute of Oceanography, Ernakulam, Cochin-18

An estimation of the fish eggs and larvae of the Indian Ocean has been made, based on the calculation of their average number in each 5°-square. Figures are presented to show the numerical abundance of fish eggs and larvae for April-October and October-April periods, and also during day and night times. The areas of occurrence of eggs and larvae are contoured, showing the different grades in the density of distribution. This distinguishes the various areas of spawning and larval development. The highest degree of concentration of eggs is observed during the October-April period, and in the following period, for fish larvae. Further, the dominance of fish eggs in day collections, and of larvae in the night collections is also noticed. The volumetric ratio of fish larvae to the total biomass is also represented graphically. The relationship between them is neither very close, nor uniformly proportional in all zones.

INTRODUCTION

Though fishes exhibit a very wide complexity in their ecological and biological aspects, the investigations on their population sizes or geographical ranges are generally based on fish catches. But a thorough estimation of the fish eggs and larvae will help to a great extent in the evaluation of marine fisheries resources, as most of the marine fishes have pelagic larvae and many of them spawn in the open sea. The observations based on eggs and larvae do give a general picture of the abundance and variety of fish populations. The data pertaining to the distribution and abundance of fish eggs and larvae dealt with here, are based on the 1352 standard samples (collected with the Indian Ocean Standard Net, from 200-0 m depth to the surface) taken from different parts of the Indian Ocean covering oceanic, coastal and intermediate zones, at different times. The average number of fish eggs and larvae, and the volume of fish larvae and total biomass calculated for each 5°-square and 10°-zones are represented in the text figures and graphs. These average values give a general picture of the relative abundance of the fish eggs and larvae in different areas.

OBSERVATIONS

The composition of fish larvae from the plankton samples processed, has been analysed mainly up to the family level. Table I gives the percentage composition of the various families represented in the collection. Since the collections are made by vertical hauls, the qualitative representation of larvae of pelagic groups are not well indicated.

TABLE I

Composition of fish larvae in the IIOE collections based on 1352 samples

Family	Percentage of the sample in which the various families are represented
Albulidae	*
Clupeidae	*
Engraulidae	**
Bathylagidae	*
Stomiatidae	***
Idiacanthidae	**
Chauliodontidae	**
Astronesthidae	*
Melanostomidae	*
Gonostomidae	****
Sternoptychidae	*
Synodontidae	*
Paralepididae	**
Myctophidae	****
Scopelarchidae	*
Leptocephalii of Anguilliformes	*
Exocoetidae	*
Hemirhamphidae	*
Bregmacerotidae	*
Syngnathidae	*
Fistulariidae	*
Melamphidae	*
Holocentridae	*
Sphyraenidae	*
Mugilidae	*
Serranidae	***
Carangidae	***
Stromateidae	***
Coryphaenidae	*
Pomocentridae	*
Labridae	***
Gempylidae	**
Scombridae	*
Scomberomoridae	**
Thunnidae	**
Gobiidae	***
Scorpaenidae	***
Triglidae	**
Blenniidae	*
Bothidae	**
Pleuronectidae	*
Cynoglossidae	*
Balistidae	*
Monacanthidae	*
Diodontidae	*
Tetrodontidae	*
Lophiidae	*
Antennariidae	*
Ceratiidae	*

*Represented in approximately up to 5% of the samples
**Represented in approximately up to 10% of the samples
***Represented in approximately up to 25% of the samples
****Represented in approximately up to 55% of the samples

Approximately 5% of the samples include larvae that have not been yet assigned to any of the above families.

The various families are separated based on the classification of Berg (1947).

The concentration in the distribution of these, has been graded broadly into four density intervals and they are contoured as shown in the text figures (Figs. 1, 2, 3, 4, 5& 6). In the case of fish eggs for the year round period (Fig. 1) the differences in the abundance are as follows. The first or highest degree of concentration is noticed in two regions, one off the east of Socotra Island and the other in Persian Gulf. The second grade of concentration is noticed in between these two regions and also in the middle of the Red Sea. The third level of abundance is observed near the above areas, and also off the Somali coast and the west coast of south India, north of 10° N.

When the data are separated into April-October and October-April periods, there is a change in the picture. For the first period (Fig. 2), the concentrations in the places of the year round maxima appeared somewhat lower near the Persian Gulf, whereas the total absence of fish eggs is noticed to the east of Socotra Island. For the second period, the highest average density is retained only at one place, i.e. east of the Socotra Island (Fig. 3).

An estimation of fish larvae gives a similar picture of distribution of abundance (Fig. 4). Here the highest degree of concentration is noticed at four regions, one at the middle of the Red Sea, another around the Persian Gulf, the third in the central part of the west coast of India and the fourth, off the Bengal coast. The next lower degree of concentration is noticed in Bay of Bengal (excluding the central area south of 15° N) near and off Somali Coast, off the Arabian coast and in the north eastern portion of the Chagos Archipelago.

The pattern of distribution observed during April-October period is almost similar to that of the year round average or the dense area near Chagos. Archipelago (Fig. 5). In the October-April period (Fig. 6) a general fall in the abundance is noticed. The highest degree of concentration of larvae as in the previous case is not seen during this period. The next lower density is found only off the Andhra coast.

Graphical representations made to show the day and night variations in the distribution of fish eggs and larvae, based on the average number in total hauls for each 10°-zone present the following facts: Graph showing the average number of eggs under 1 m^2 (200-0 m) for each 10°-zone (Fig 7) indicates that the maximum abundance of eggs is (at the 15°N which represents the midpoint of) the 10°-20° zone. Further, the relationship between the day and night collections gives certain interesting data. The maximum abundance is noticed during day time, as compared with the night. This relationship is true for all the zones. In the case of fish larvae the graph showing the day and night relationship (Fig. 8) also indicates that the maximum concentration is in the 10°-20°N zone and as in the previous case, shows the same relationship for all the other zones.

Similarly, the relationship between the volume of fish larvae and the total biomass has been represented (Fig. 9) based on their average volume in total hauls for each 10°-zone. The relationship between them is neither close nor uniformly proportional for all the zones.

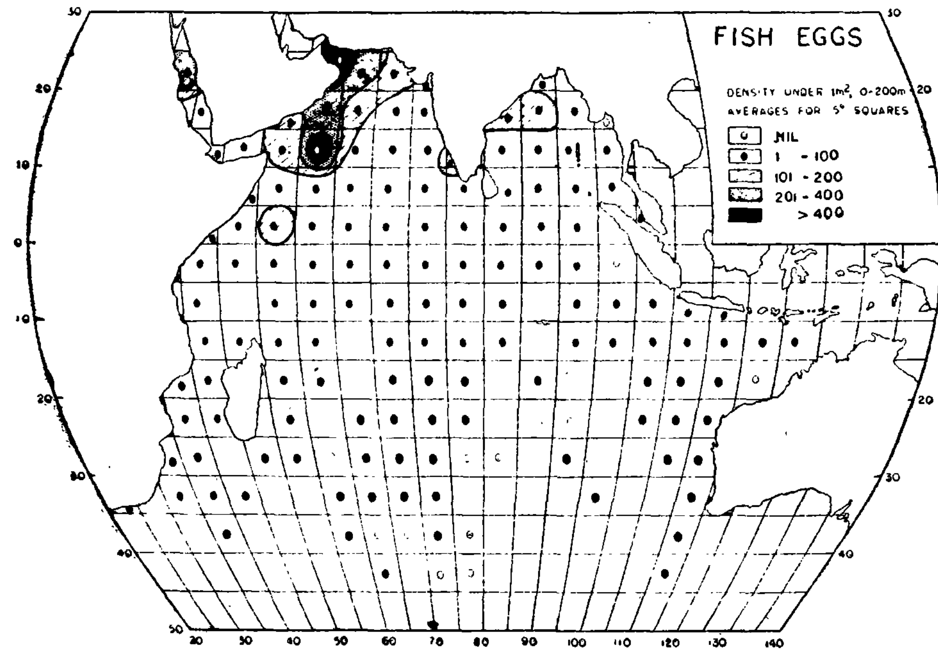

FIG. 1. Distribution and abundance of the total fish eggs for the year round period.

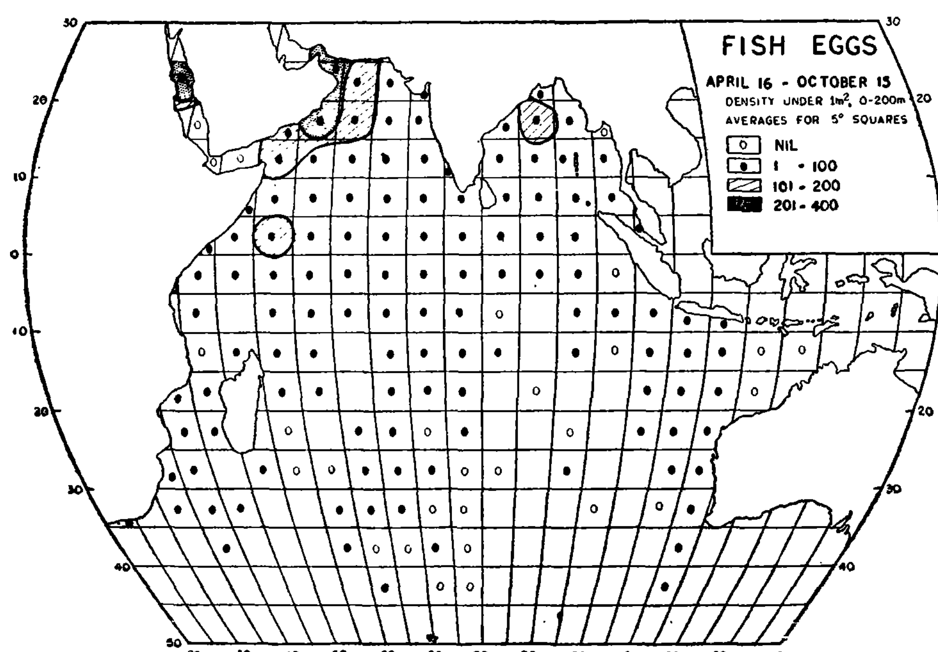

FIG. 2. Distribution and abundance of fish eggs for the April-October period.

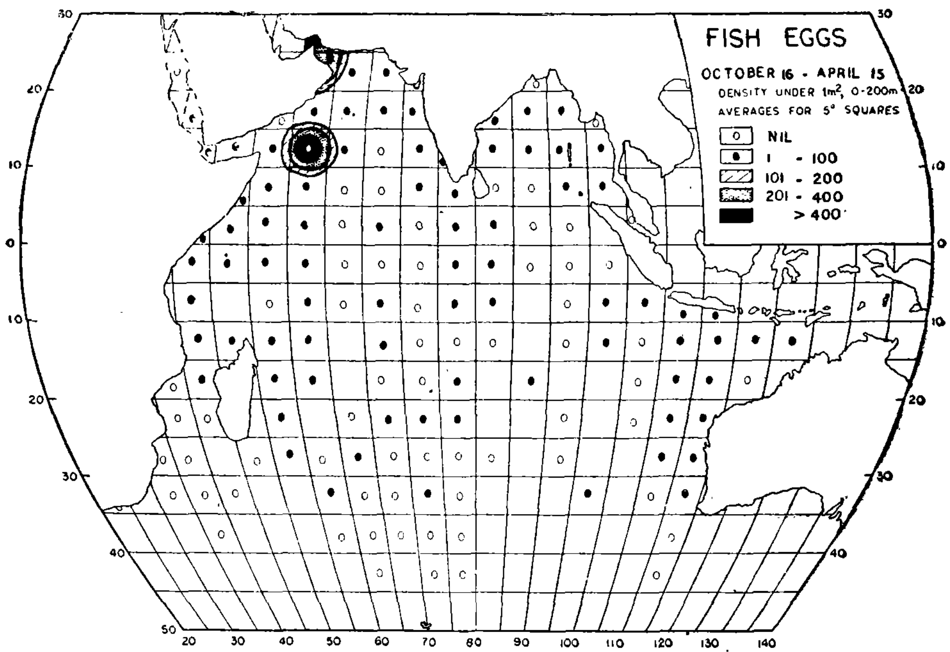

FIG. 3. Distribution and abundance of fish eggs for the October-April period.

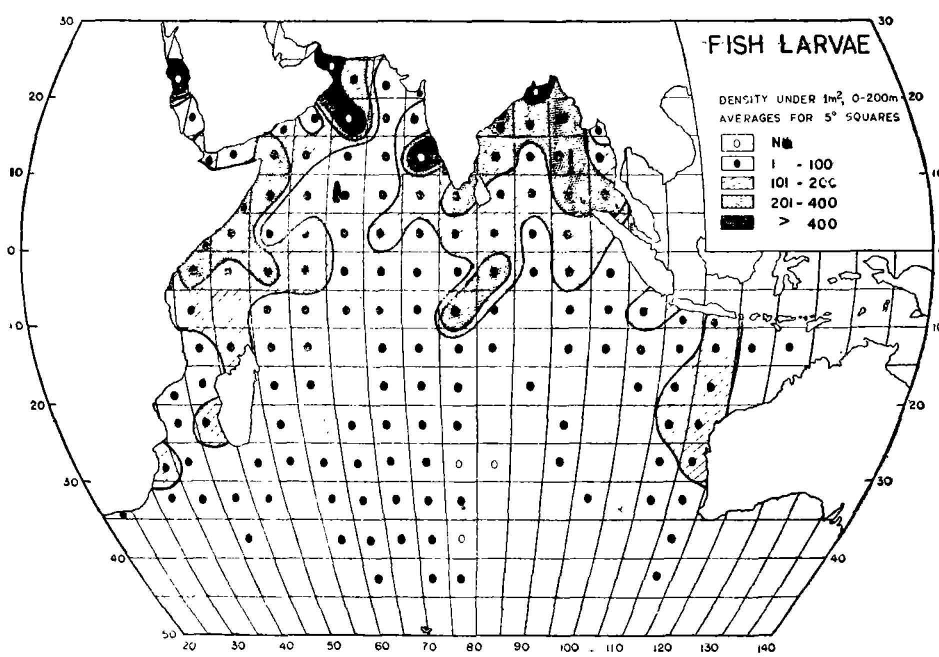

FIG. 4. Distribution and abundance of total fish larvae for the year round period.

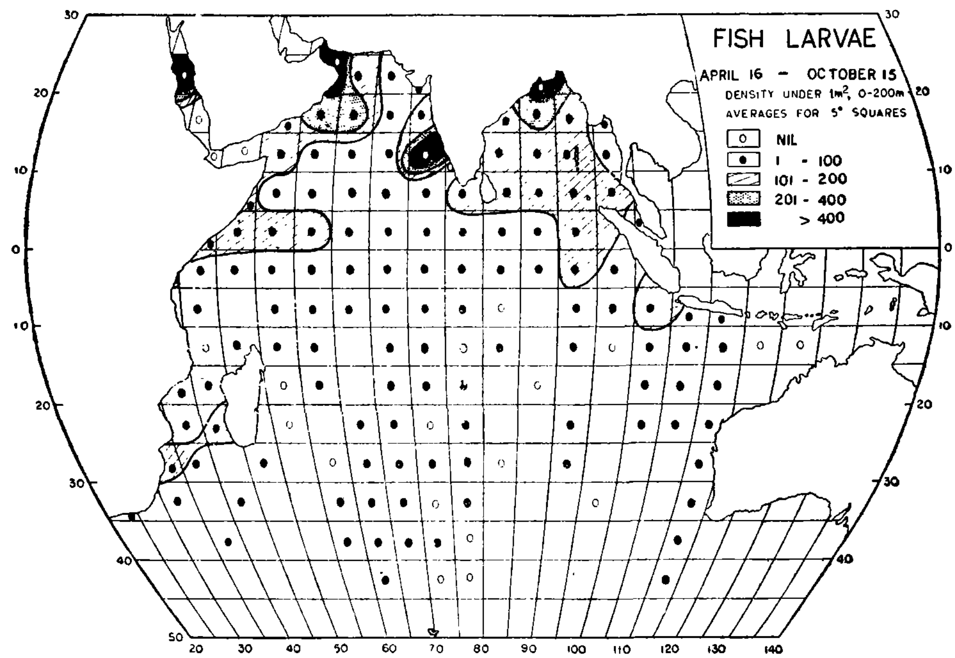

FIG. 5. Distribution and abundance of fish larvae for the April-October period.

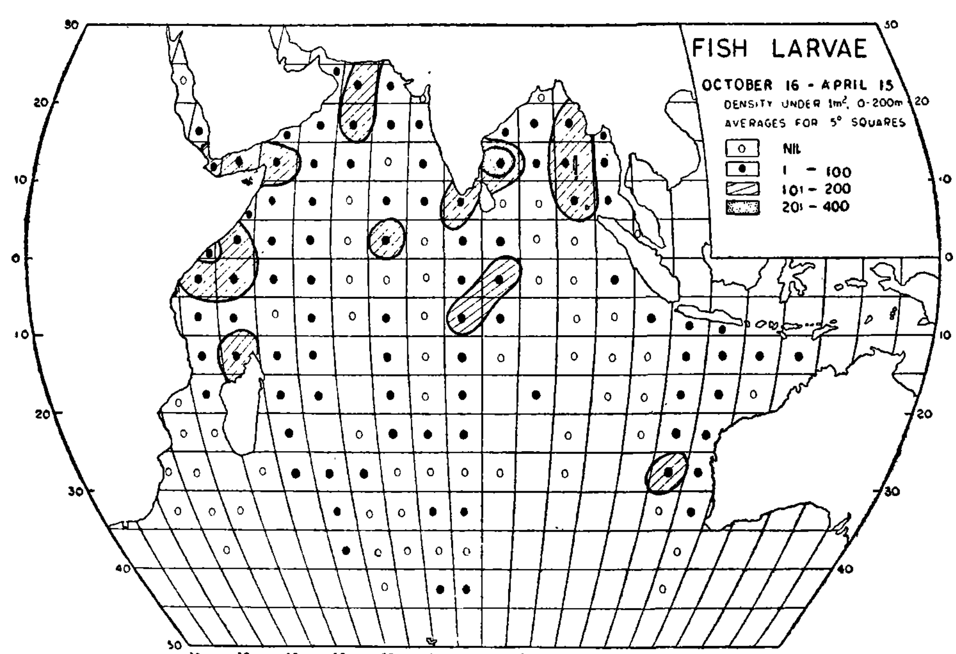

FIG. 6. Distribution and abundance of fish larvae for the October-April period.

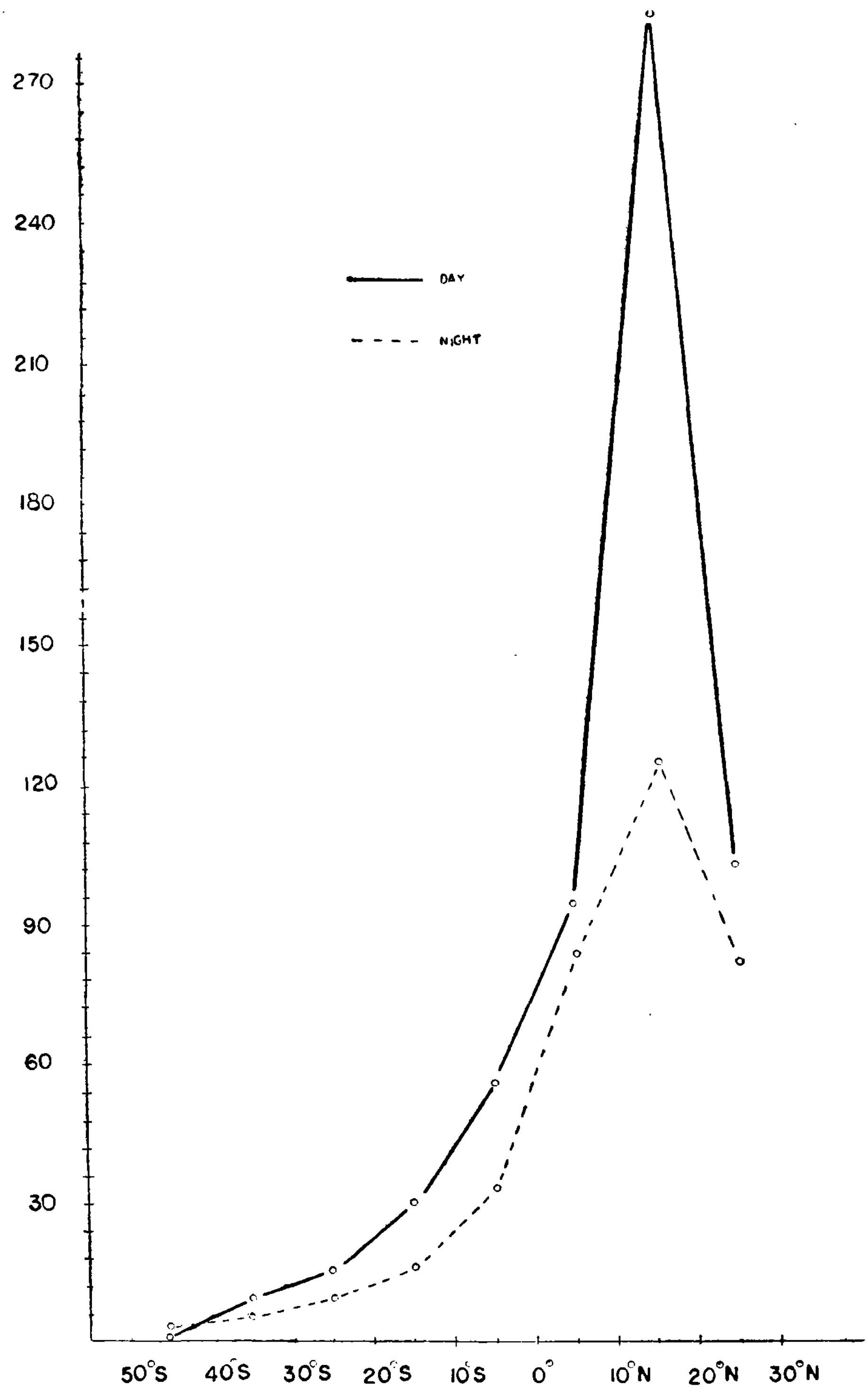

FIG. 7. Average number of fish eggs under 1m² (200-0 m) for each 10°-zone and their variation in number during day and night.

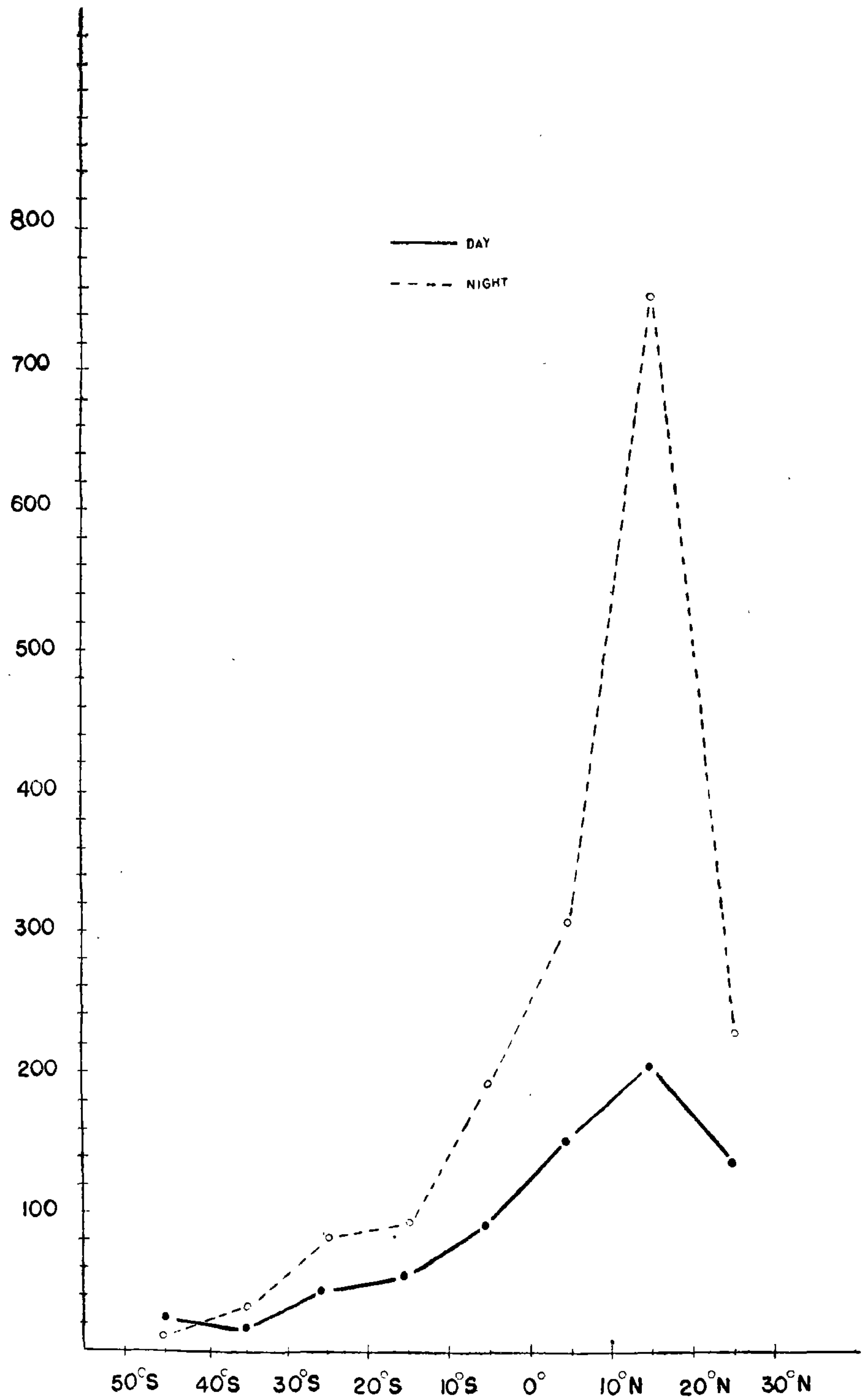

FIG. 8. Average number of fish larvae under 1 m² (200-0 m) for each 10°-zone and their variation in number during day and night.

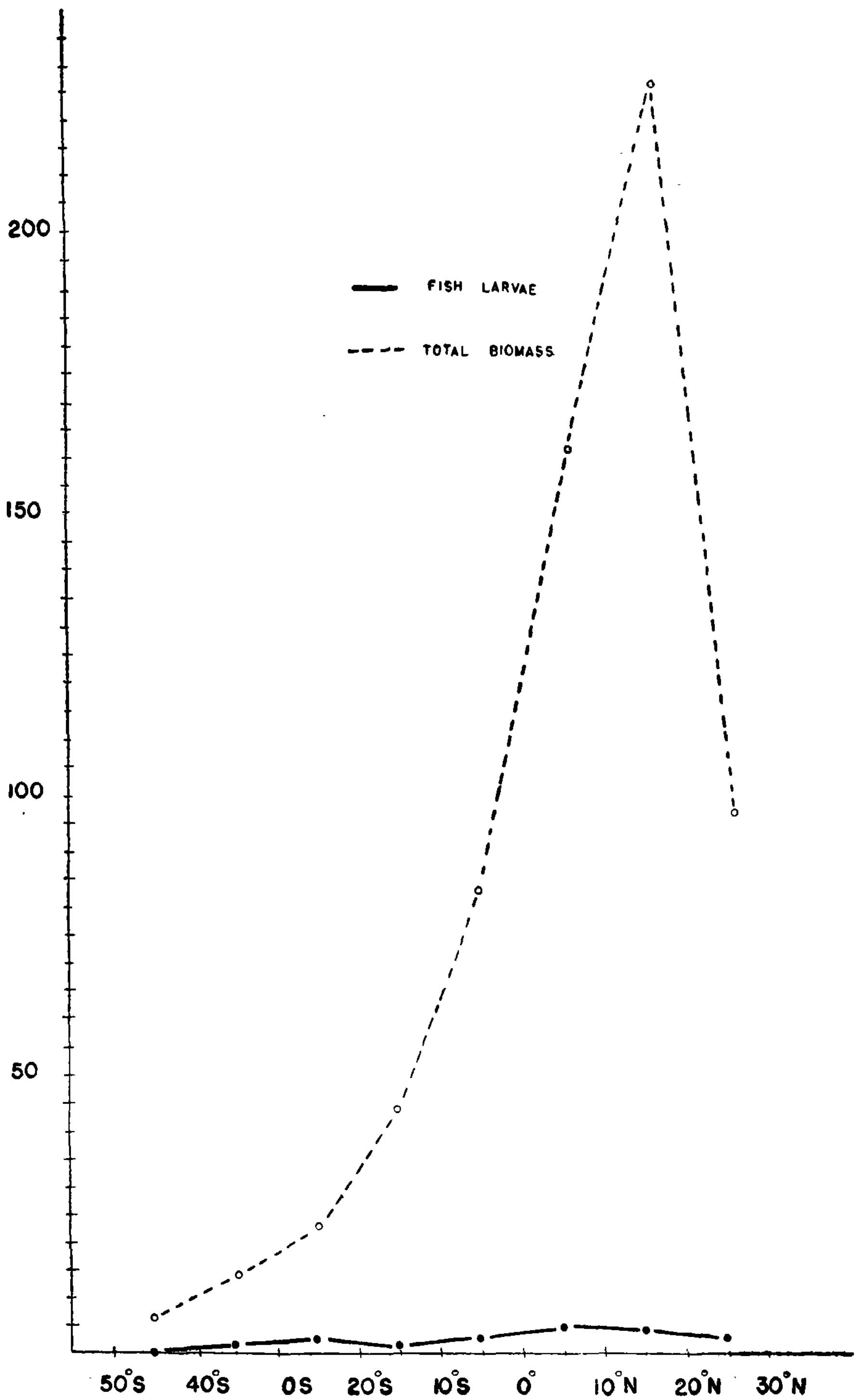

FIG. 9. Relationship between the volume of fish larvae and the total biomass.

Discussion

Figures 1, 2, 3, 4, 5 and 6 show the concentration of fish eggs and larvae during different periods. So it is possible to distinguish certain areas of intensive spawning and larval development, as well as other localities where they are less or at a minimum. But those areas, where the maximum density of eggs or larvae is noticed, can be looked upon as the possible spawning grounds for a good number of species of fish. The eggs collected consisted of those with embryos in different stages of development. Eggs that are in a very early stage of embryonic development are likely to be nearer to the spawning grounds, than those in the advanced stage. The dominance of eggs in the day collections is one of the most interesting observations made. The reason for such an abundance of eggs in the day collections may probably be that, at least in some groups of fishes, spawning might be taking place during day time. In the case of fish larvae, the highest degree of abundance is noticed during the night collections, a condition that is usually observed for plankton in general. But here it is probably due to the ability of larval fishes to avoid plankton nets in the day time, for which evidence has been published in recent years (Ahlstrom 1954, 1959; Silliman 1943). Information on vertical migrations of fish larvae is very scanty in literature of the subject.

Acknowledgements

I wish to express my deep sense of gratitude to Dr. N. K. Panikkar, Director, National Institute of Oceanography, for permitting me to work on the above material. I am thankful to Dr. Edward Brinton and Mr. L. R. Kasturirangan, Indian Ocean Biological Centre, for scrutinizing the manuscript.

References

Ahlstrom, E. H. (1954). Distribution and abundance of eggs and larval populations of the Pacific sardine. *Fishery Bull. Fish Wildl. Serv. U. S.*, **93**, 56, 83-140.

———(1959). Vertical distribution of pelagic fish eggs and larvae off California. *Fishery Bull. Fish Wildl. Serv. U.S.*, **93**, 60, 107-146.

Berg, L. S. (1947). Classification of fishes, both recent and fossil. *Trudy Zool. Inst., Leningr.*, **5**, 87-517.

Silliman, R. P. (1943). Studies on the pacific pilchard or sardine (*Sardinops caerulea*) 6. Thermal and diurnal changes in the vertical distribution of eggs and larvae. *U. S. Fish Wildl. Serv. Spec. Sci. Rept. No.* **22**, 1-17.

Reprinted from *Morning Review Lectures of the second International Oceanographic Congress, Moscow*, 1966. Paris, Unesco, 1969, p. 239-248

R. Raghu Prasad
Central Marine Fisheries Research Sub-Station Ernakulam, India

Recent advances in the study of production in the Indian Ocean

Acknowledgements

The author is grateful to the oceanographic section of the Central Marine Fisheries Research Institute and Indian Ocean Biological Centre for making available some of the data presented in this paper. Thanks are also due to Messrs. P. V. Ramachandran Nair, C P. Ramamirtham and P. A. Abraham for the help rendered in the preparation of the paper and the figures.

Introduction

Prior to the recent international co-operative exploration of the Indian Ocean, several expeditions tried to evaluate production in that ocean. The earliest of these was the *John Murray* expedition which used nitrate data to compute the production of algae in wet weight (Gilson, 1937), but the Danish *Galathea* expedition made the most significant contribution to the investigation of production by introducing the C^{14} technique in the study of marine photosynthesis (Steemann Nielsen, 1952). The *Galathea* made single observations on the western part of the Indian Ocean at middle latitudes, in the equatorial part as a section from Mombasa to Ceylon, the Bay of Bengal and the Indo-Malayan waters (Steemann Nielsen and Jensen, 1957).

Hydrographic features

Available information on the hydrography of the Indian Ocean indicates that there is a south equatorial current during all seasons starting from Australia and flowing across the ocean south of the equator. On reaching the African coast it turns south and continues as the Agulhas current. Another current originates from the south of Africa and proceeds east, and in between the two is the westward north equatorial current which is neutralized or replaced by an eastward current during the south-west monsoon. Between the north and south equatorial currents runs the countercurrent. The Swedish Deep Sea Expedition made a special study of the equatorial currents and countercurrents in the Indian Ocean (Jerlov, 1953).

Quite recently, a considerable amount of information has been gathered on the hydrography of the south-eastern part of the Arabian Sea, partly through the work of scientists in India attached to the Central Marine Fisheries Research Institute. It should, however, be mentioned that this work has been confined to classical hydrography and that nutrient analysis and direct current measurements have not been carried out.

The hydrographic features of the Arabian Sea show pronounced seasonal variations especially along the Indian coast. Four seasons can be arbitrarily postulated, viz., monsoon (June, July, August), post-monsoon (September, October, November), winter (December, January, February) and summer (March, April, May). Along the coast the currents are mainly southerly during the monsoon and immediate post-monsoon periods, whereas they are northerly during winter. During the summer months, however, stagnant conditions prevail along the coast. During the monsoon and immediate post-monsoon periods upwelling occurs along the entire west coast with regional variations in intensity (Fig. 1). This brings up nutrients from the deeper layers which enrich the surface layers. The top of the thermocline is found between 75-100 m at all seasons except during the monsoon and immediate post-monsoon period when the thermocline is drawn

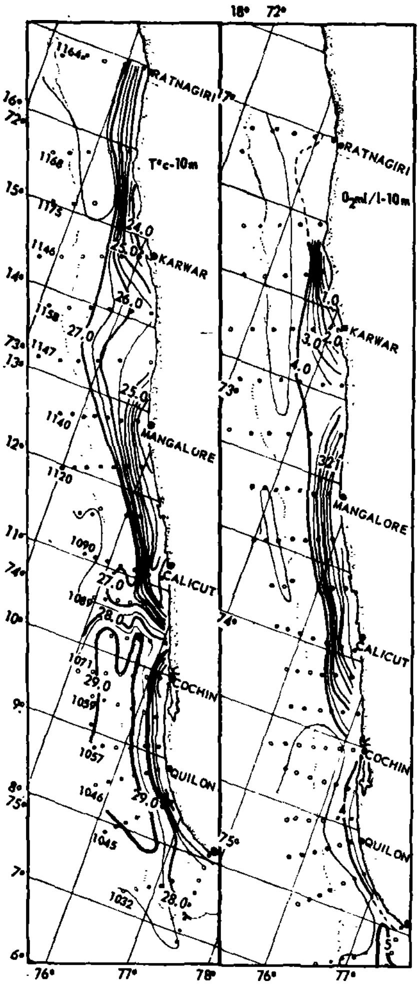

FIG. 1. Distribution of temperature and dissolved oxygen at the 10 m level along the south-west coast of India during the monsoon period of 1962. Note the intense upwelling zones off Mangalore and Karwar.

up to the shallower layers, and the temperature discontinuity has even been found to start at the surface near the coast.

Observations have been made during the winter in the open part of the Arabian Sea. More or less uniform temperature distribution is found up to about 50 m (Figs. 2-4) but at 75 m there are intense thermal gradients (Fig. 5) leading to strong northward currents. Such current patterns have been confirmed from dynamical studies (Figs. 6-8). One large divergence zone between 70°-72° E and 8°-11° N has been inferred and a convergence zone with an axis roughly along 74° E longitude has also been found. The oxygen distribution at 75 m depth further confirms the area and extent of the divergence zone (Fig. 9). In addition it may be mentioned here that recent investigations by the *Vityaz* have indicated an equatorial divergence in the central Indian Ocean between 2° and 3° S, a southern equatorial divergence at 8° S, a tropical convergence at 20° S and a subtropical divergence between 29° and 33° S (Bezrukov, 1963). All these have a marked influence on the production of this region since we must expect a relatively higher phytoplankton production in the regions of divergence and zooplankton abundance in the regions of convergence.

Investigations conducted around the Laccadive Islands have indicated that a fairly pronounced anticyclonic motion is present around the islands from the surface down to the discontinuity layer. At the deeper levels the circulation is completely reversed, the motion being cyclonic in most of the stations. It has also been found that in these waters the oxygen minimum layer is several metres thick and the upper level of this layer is present at 150 m. The observations conclusively point to a high level of production in the Laccadive waters. The circulatory movements help to maintain the highly productive waters in the vicinity of the islands for a considerable length of time (Jayaraman *et al.*, 1960).

Our present knowledge of the distribution of nutrients derives mainly from the *Dana*, *John Murray*, *Discovery*, Swedish Deep-Sea and *Galathea* expeditions. The *Discovery* investigations indicated that in the lower latitudes on the western part of the ocean near Africa there is only a shallow surface layer poor in inorganic phosphate, and since the nutrient-rich water occurs in the lower part of the photosynthetic zone the productive capacity is high. From the profiles of nutrients in the region of equatorial currents based mostly on data from the *Dana* and partly from the *John Murray* and Swedish Deep-Sea expeditions, divergences have been inferred at about 7° S and 2° N between 40° and 45° E, at about 5° S between 50° and 60° E, at 8° S near 88° E and at about 5° S and 2° N near 95° E meridians (cf. Steemann Nielsen and Jensen, op. cit.). In all these zones of divergence, the nutrient-rich water is found within 100 m and hence provides good conditions for production. Even in the zones of convergence in the equatorial region of the Indian Ocean the nutrient-rich water is fairly near the surface. On the other hand in the western part of the ocean, in the middle latitudes (20°-35° S), the surface layer is poor in nutrients and the nutrient-rich water is found far below the lower boundary of the euphotic zone.

The most recent studies seem to indicate that the Arabian Sea has by far the highest concentration of nutrients at or near the base of the photosynthetic zone. The *Vityaz* expedition observed a maximum quantity of nitrite nitrogen over a large area equalling 5.4 μg.at./l (75 mg/m^3) which is a very high value (Bezrukov, op. cit.). Investigations carried out from the *Anton Bruun* also showed that the concentration of nutrients in the Arabian Sea is roughly twice that in the North Atlantic (Ryther and Menzel, 1965).

Primary production

The recently established values of primary production and the data from the *Galathea* and *Vityaz* expeditions give a general idea of the area and extent of the zones of production in the Indian Ocean, since these values are directly comparable. However, it should be borne in mind that the rates given by the *Galathea* are about 30 per cent lower, whereas those given by the Russian scientists since 1960 and those computed by the scintillation method are presumed to be correct (Steemann Nielsen, 1965). Near the shelf, in the south-eastern part of the Arabian Sea, the lower boundary of the photosynthetic zone as determined by light penetration is at a depth of about 50 m. The rate of photosynthesis is high in the surface waters towards the coast ($>$10 mg C/m^3/hour) suggesting a fairly constant supply of nutrients. The rate of production amounts to over 2,000 mg C/m^2/day near the coast off Cape Comorin. Outside the continental shelf the rate of production is moderately high—between 200 to 500 mg C/m^2/day. Very high production rates exceeding 5,000 mg C/m^2/day have been obtained off the south-eastern coast of India in the Gulf of Mannar (Prasad and Nair, 1963) and 2,000 mg C/m^3/day in the surface waters of Palk Bay (unpublished data). Recent reports from the *Anton Bruun* (Ryther and Menzel, loc. cit.) show that at two stations off the Gulf of Oman extremely high rates of 5,700 and 6,400 mg C/m^2/day have been obtained. Though these values may be due to bloom conditions, the mean production rate for the Arabian Sea stations was found to be 1,800 mg C/m^2/day. The *Vityaz* expedition results also indicate that, though production in the open part of the ocean is low and does not exceed 10-30 mg C/m^3/day, it is high in the coastal waters and in the zones of deep water ascent. In the region of Madagascar and in the Arabian Sea region, where there is deep water ascent, the values of primary production increase and the daily rate is between 50 and 120 mg C/m^3/day (Kabanova, 1961).

Though the data cannot be directly compared, the estimate of production in terms of wet weight of algae worked out from nitrate consumption by the *John Murray* expedition in the Arabian Sea was 14.4 g/m^2/day (Gilson, 1937). The carbon equivalents of this value compare very favourably with the results we have obtained so far for the same region with the C^{14} technique.

The *Galathea*'s coverage of the Indian Ocean shows that middle latitudes in the western part of the ocean outside the continental shelf are characterized by a production rate between 100 and 200 mg C/m^2/day, which is the normal value found in tropical and subtropical oceanic regions where there is no constant replenishment of nutrients from below (Steemann Nielsen and Jensen, loc. cit.). Over the shelf the production is high practically anywhere in the tropics. In the region of the Agulhas, current water from the lowest part of the euphotic zone showed a higher production rate, about three and a half times higher, at constant light intensity, than the surface water—indicating the productive potential of the lower regions. In the equatorial current systems, the measurements made by the *Galathea* show that the rate of production on the whole is moderately high with restricted areas of very high production. In the section from Mombasa to Ceylon a pronounced maximum of production is seen between 57° and 72° E longitudes. The production rate in the equatorial part of the Indian Ocean is thus significantly higher than that of tropical waters in general. Quite clearly, the ascent of nutrient high bottom water is the most important factor governing the production rate.

In the Bay of Bengal, although the subsurface water rich in nutrients is found fairly close to the surface, the rate of production is reduced by the low transparency of the water near the subcontinent caused by the influx of organic and inorganic material through the big river systems. However, the Andaman Sea shows a higher production, presumably because of the increase in the depth of the photosynthetic

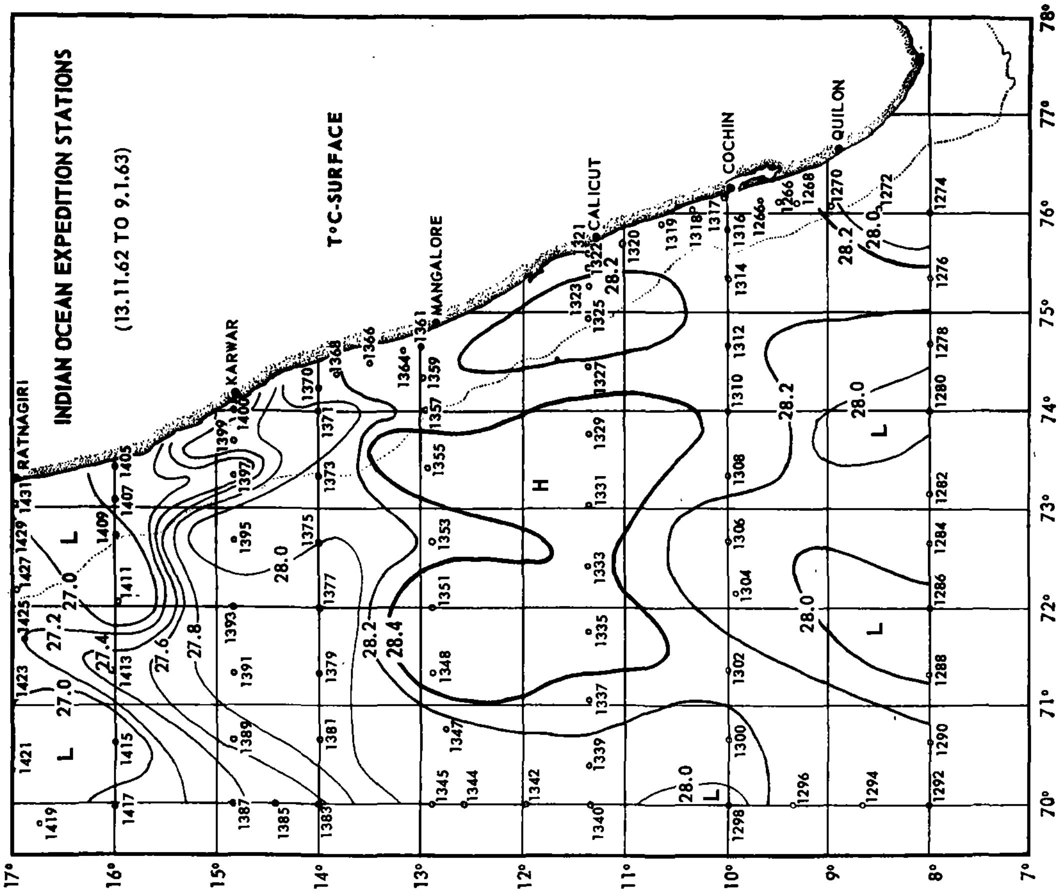

FIG. 2.

zone and possibly the 'island mass effect'. In the northern and eastern Bay of Bengal, the *Anton Bruun* has recently observed a winter upwelling area and a higher primary and secondary production related to it (LaFond, 1965).

Quantitative distribution of plankton

Eight hundred and thirty-three standard samples taken with the Indian Ocean Standard Net, covering the major part of the Indian Ocean up to 45° S, have been estimated volumetrically in the Indian Ocean Biological Centre. Average displacement volume for every five degree square of the ocean has been determined and shows considerable variations in the different regions (Fig. 10). High plankton concentration is observed on the northern and western part of the Arabian Sea and south of Cape Guardafui where the average volume is over 30 ml. The highest, exceeding 50 ml, has been found near the Gulf of Oman and the Saurashtra coast. The south-west coast of India and the waters surrounding Ceylon, the Andaman Sea and the Bengal coast are found to have fairly high quantities of plankton, exceeding 20 ml. The equatorial region on the average has only 10 ml of plankton, except near the coastal regions. But the observations by Japanese ships during both 1962-63 and 1963-64 in connexion with the International Indian Ocean programme consistently showed a high plankton concentration in mean displacement volume as well as in wet weight for the equatorial region between 77° and 79° E (Motoda and Osawa, 1964). This phenomenon of a greater zooplankton abundance in the centre of a vast area of low abundance has been observed in the western and central Pacific by a number of authors. South of the equator, plankton is comparatively more sparse, dwindling in quantity towards the south. It is normally

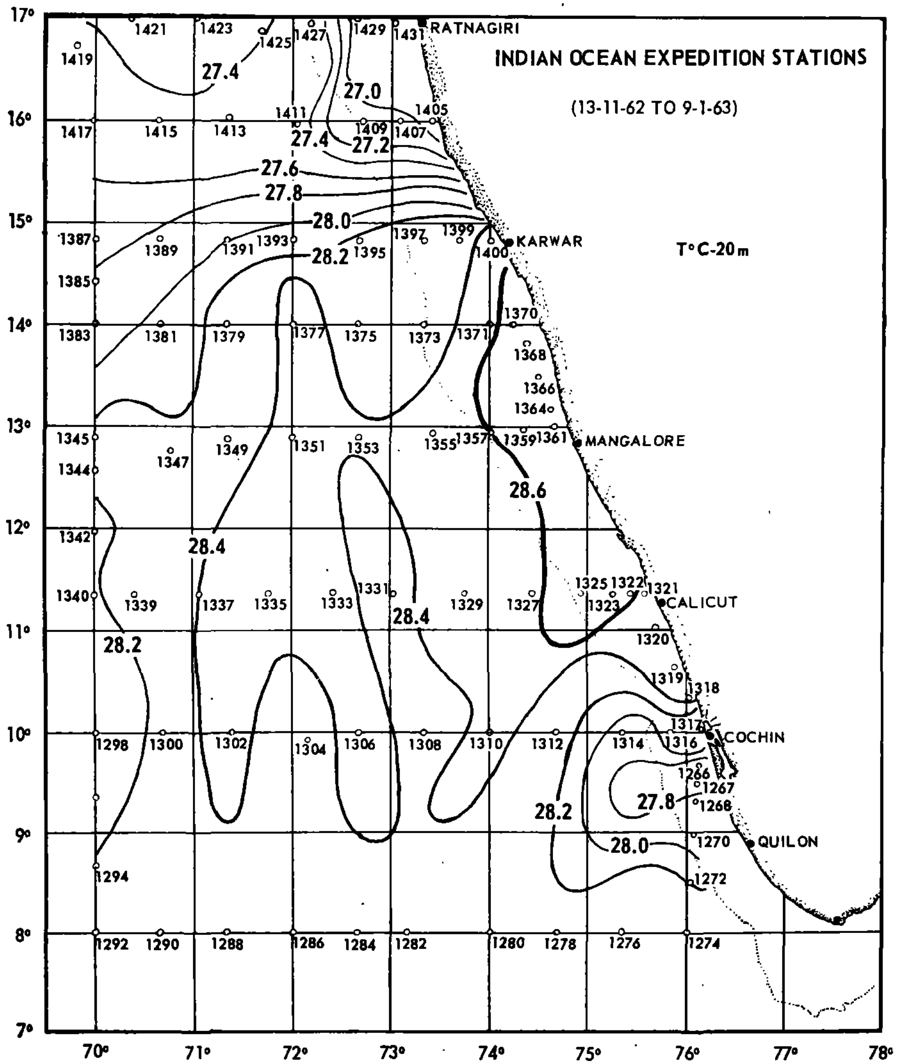

FIG. 3.

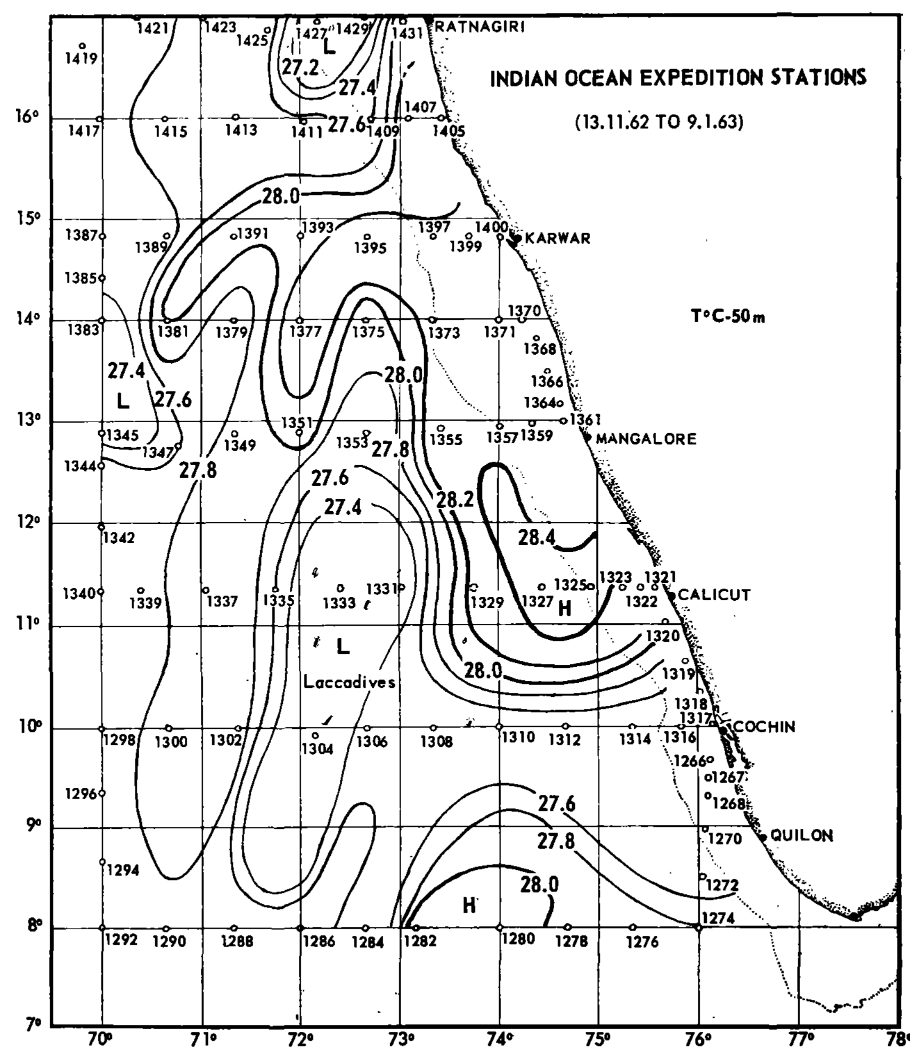

FIG. 4.

FIGS. 2-4. Distribution of temperature at the sea surface, 20 m and 50 m levels during the winter period. Note the more or less uniform distribution in space at all the above levels.

FIG. 5. Distribution of temperature at the 75 m level during the winter period showing intense westward gradient just south of 10° N and the cold-water zone in the Laccadive region.

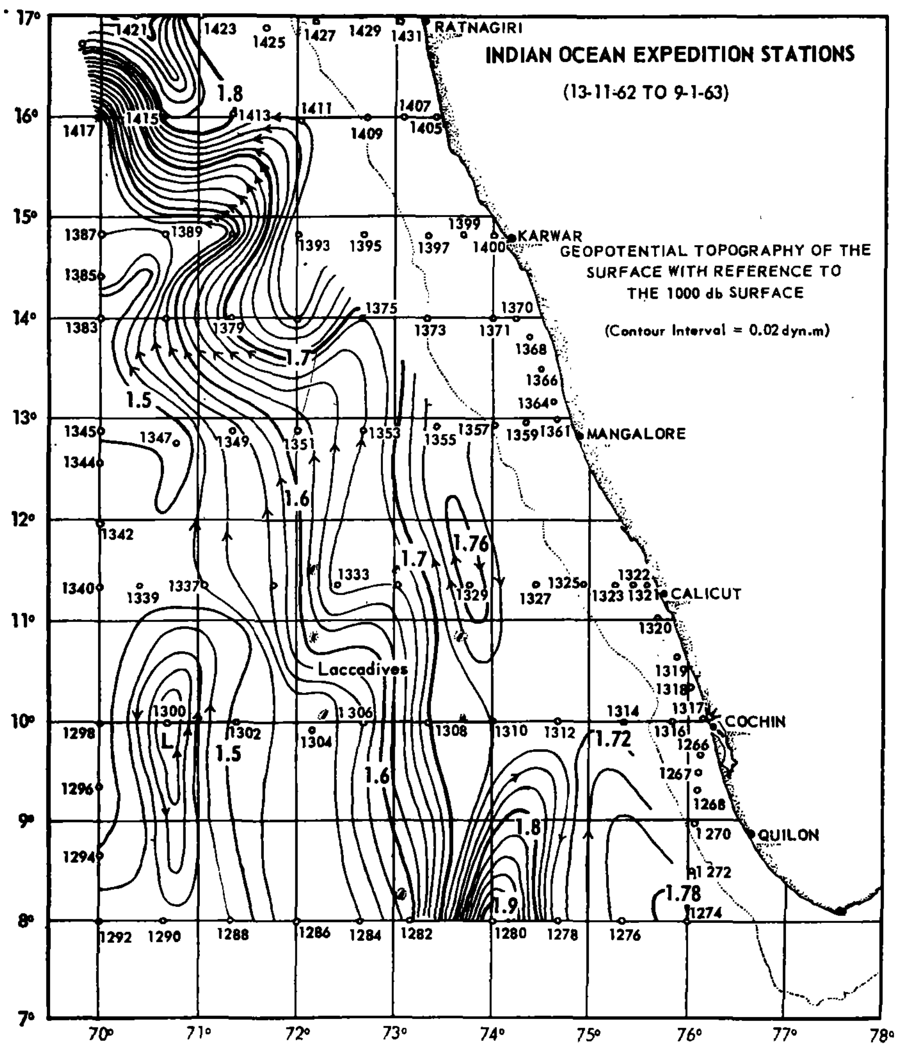

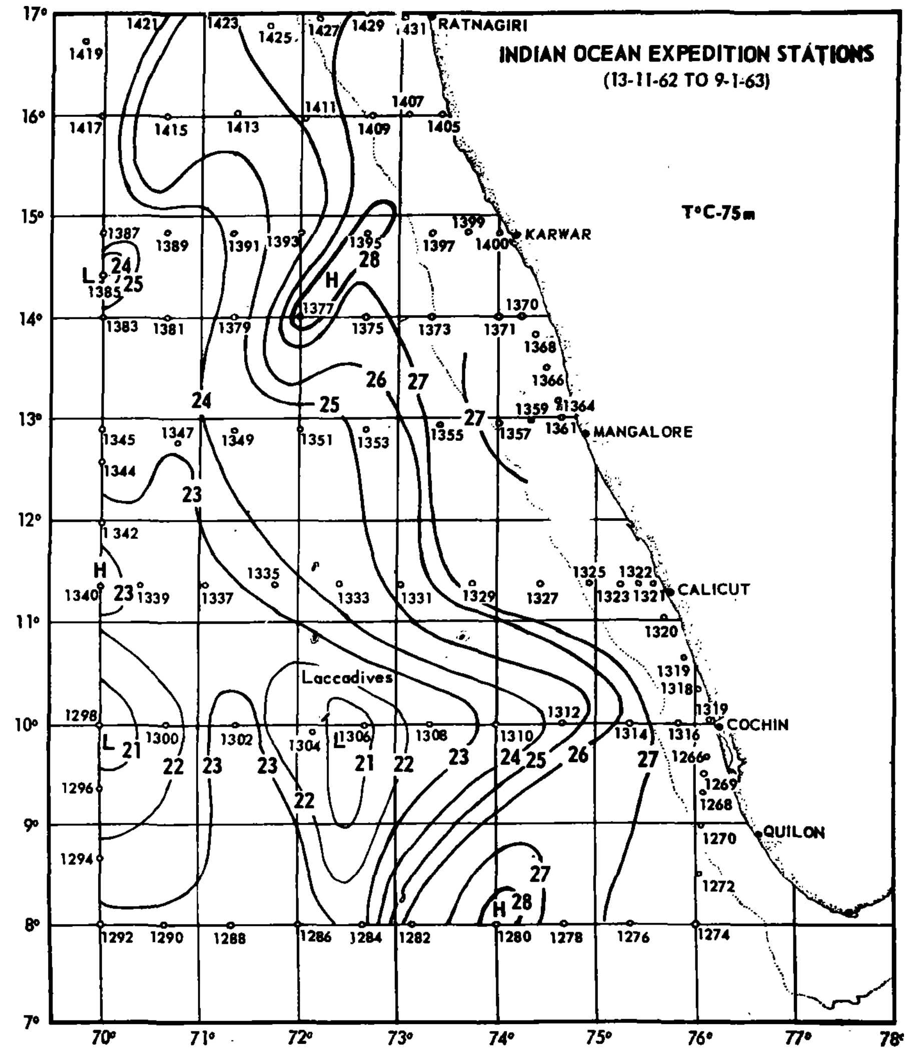

FIG. 6.

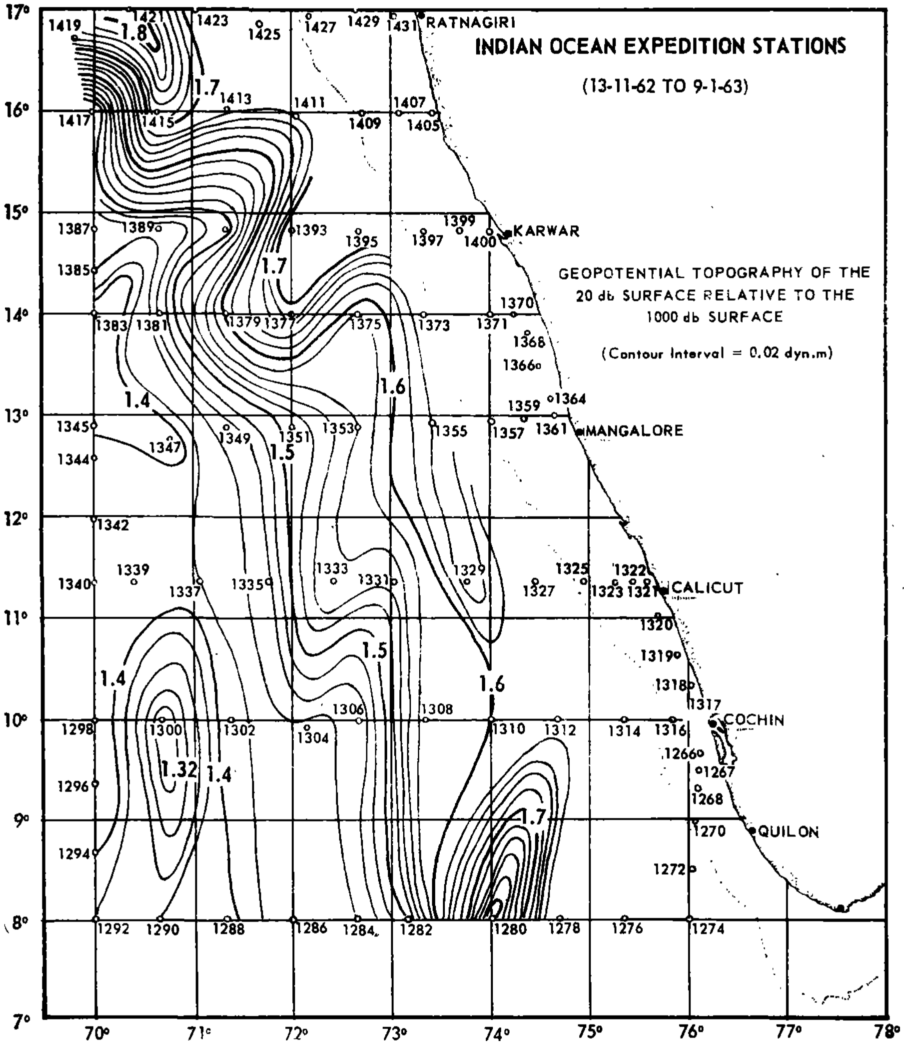

FIG. 7.

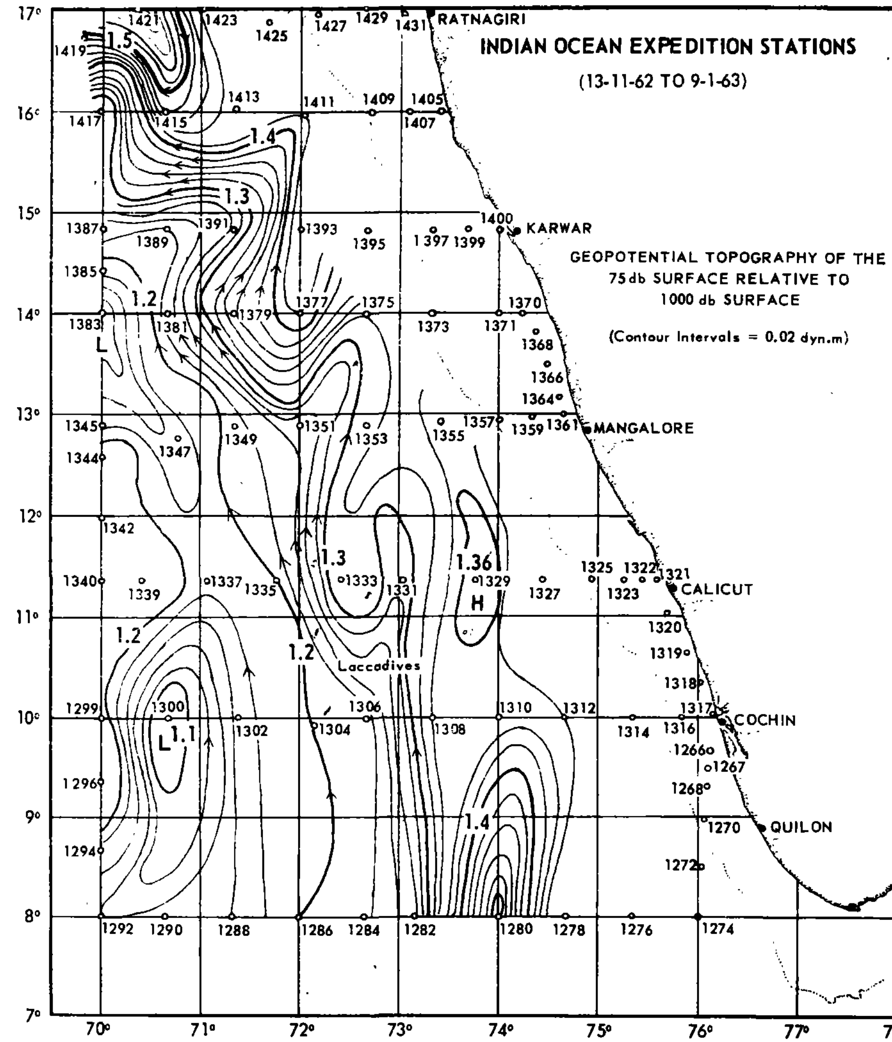

FIG. 8.

FIGS 6-8. Geopotential topography of the sea surface, 20 db surface and 75 db surface relative to 1,000 db surface. Note the swift current north of 13° N, the convergence zone around 74° E and 8° N, and the divergence zone around 71° E and 9° 30′ N in Fig. 6. Also note the similarity in the current distribution at all these layers.

Fig. 9. Distribution of dissolved oxygen content at 75 m level. Note the westward decrease and the low oxygen zone around the divergence zone.

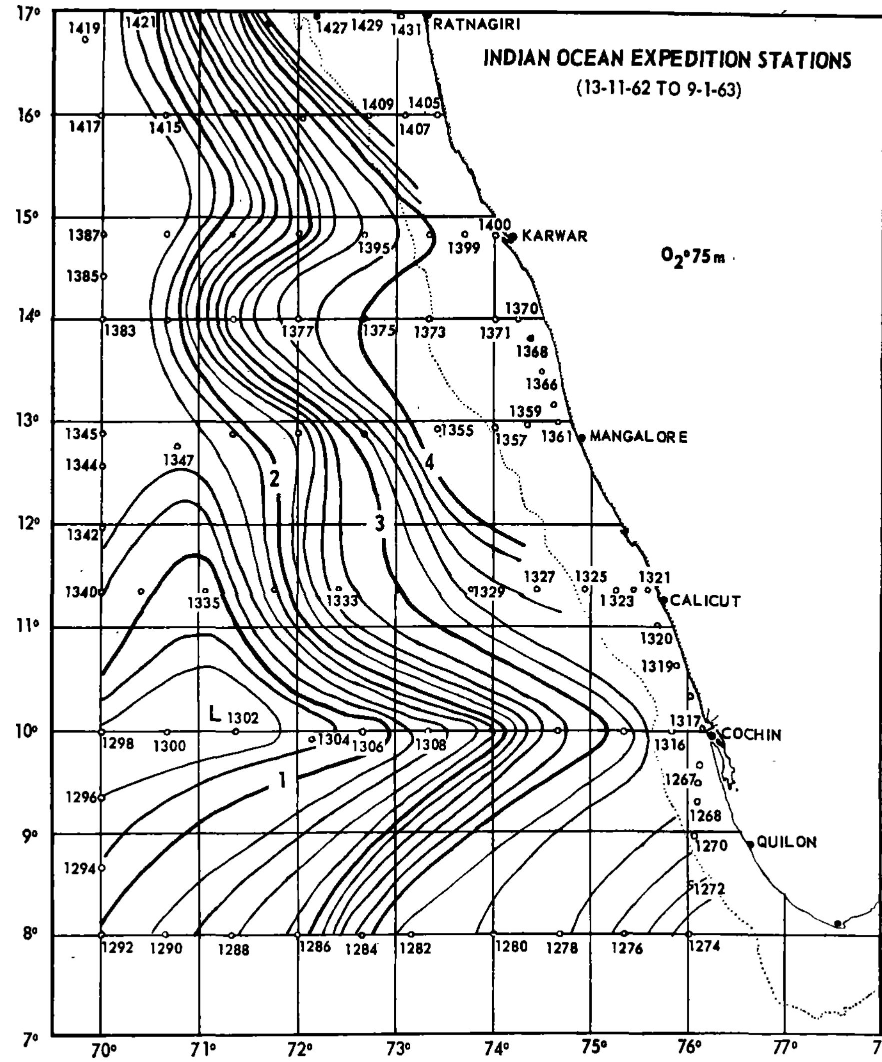

less than 5 ml in almost all the stations south of 15° S. The waters along the west coast of Australia have a low plankton biomass. This observation is in agreement with that of Tranter (1962) who points out that the biomass of zooplankton in the open ocean is no higher than in the Sargasso Sea; but on the continental shelf and in the upwelling area, south of Java, he observed a higher zooplankton biomass. In general, a northward increase of plankton is found in the Indian Ocean from 40° S.

The dry weight of plankton collected during the *Vityaz* expedition from the upper 100 m layers shows areas of high plankton production in the central part of the Arabian Sea from Aden Bay to Bombay between the Seychelles and the Maldives, off Zanzibar and the Comoro Islands to the north-east of Madagascar, off Chagos Bank, off Ceylon, to the south of Indonesia and north-west of Australia (Bogorov and Rass, 1961). It will be seen that there is substantial agreement between the two sets of data, while the differences may be partly due to seasonal variations, sampling differences, etc.

According to LaFond (1965) the highest production rate yet recorded was observed by U.S. and British ships in the summer upwelling areas on the western

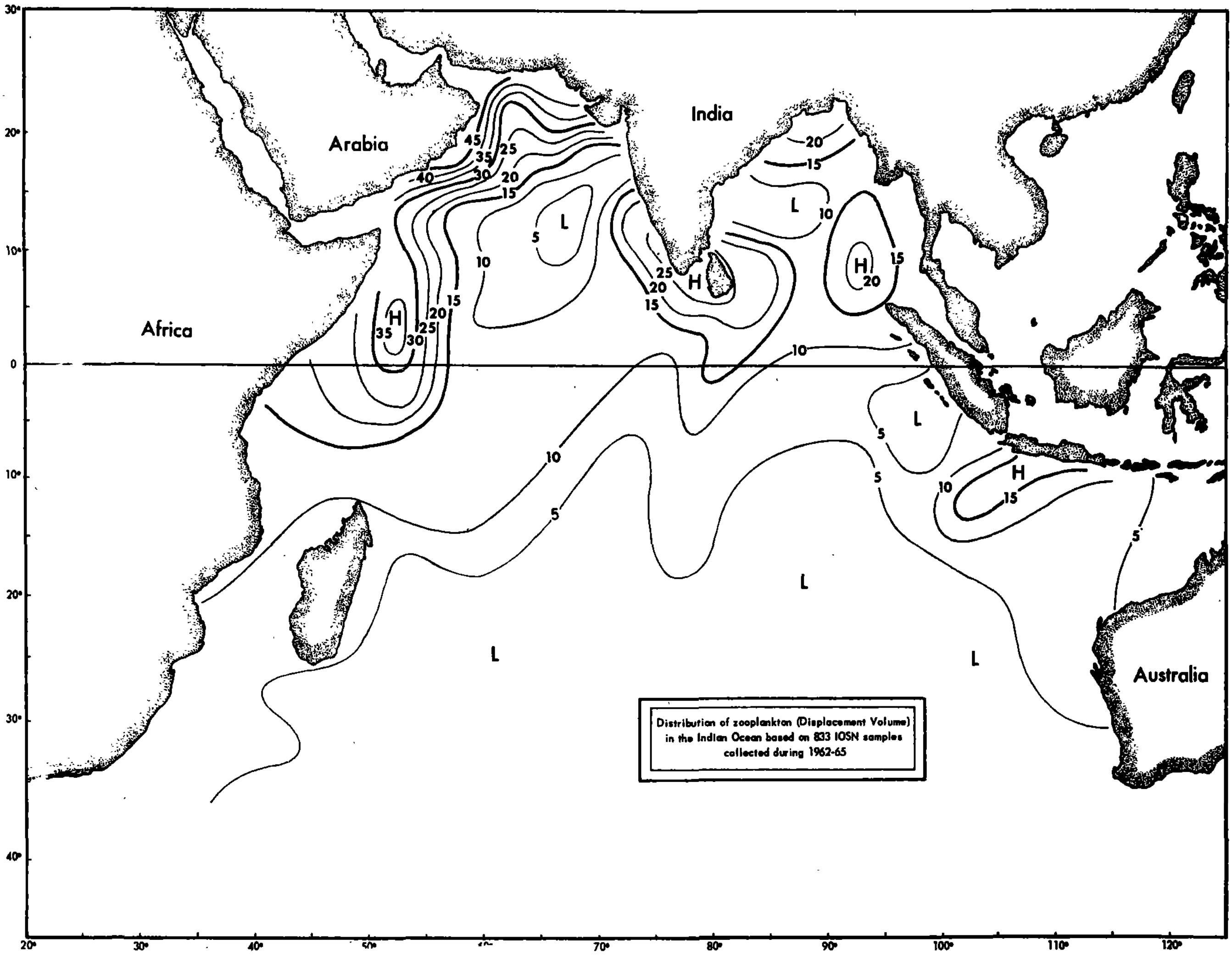

side of the Arabian Sea where the plankton nets were clogged with organisms. They have also detected large quantities of organisms with echo sounders in layers up to 250 m.

FIG. 10. Distribution of plankton in the Indian Ocean, based on the volumetric analysis of 833 Indian Ocean Standard Net samples. Isolines drawn for every 5 ml.

Production in relation to fish mortality

This account would not be complete without mention of the deleterious side effects brought about by the explosive production of plankton in certain regions of the Indian Ocean. Ships have reported extensive mass mortality of fish, sometimes covering enormous areas about 1,000 km long and 200 km wide (Jones, 1962). One such instance reported by the Polish ship *Baltiisk* amounted to an estimated 20 million tons, almost half of the world's total annual catch! Many theories have been put forward (Brongersma-Sanders, 1957) but the most likely cause would seem to lie in factors consequent on high plankton production. According to the investigations conducted by International Indian Ocean Expedition scientists (Vinogradov and Voronina, 1962; Ryther, 1964), the presence of a very high concentration of nutrients at or near the base of the euphotic zone indicates a potentially very productive and biologically unstable situation. Because of the intensive phytoplankton production, zooplankton increases and fish move into these regions. Due to the subsequent death and decay of this enormous quantity of sinking plankton the already low oxygen concentration in the bottom layers is further depleted. The presence of such very low oxygen councentrations has been noticed by Indian scientists in the south-eastern Arabian Sea between 8°-17° N and 70°-76° E at depths of 150-1,000 m (unpublished data), and by the *Vityaz* in the north-eastern region between 125-200 to 1,000-1,250 m (Vinogradov and Voronina, loc. cit.). In the region from Cochin to Karachi, the R.V. *Meteor* has found the oxygen content of the waters within 200-900 m to be extremely low with a minimum of 0.04 ml/1, but nowhere has H_2S occurred. More recently the U.S.S.R. Expedition ship *Akademik Knipovich* is reported to have made somewhat similar observations. The shifting of the oxygen minimum layer is supposed to be primarily responsible for the mass mortality even though hydrogen sulphide poisoning, red tide, sudden changes of temperature, etc., may also be causes (Brongersma-Sanders, op. cit.).

In conclusion it may be mentioned that the subject of production in the Indian Ocean has only been touched on and, as the vast amount of data gathered during the International Indian Ocean Expedition are analysed, the mosaic of partial results will form a complete picture of this hitherto little known ocean, marking an era of fruitful collaboration between nations.

References

BEZRUKOV, P. L. 1961. Research in the Indian Ocean by the survey vessel *Vitiaz* on its thirty-third voyage. *Okeanologia*, **1** (4), p. 745-53. (*Deep-sea Res.*, 1963, **10** (1-2), p. 59-66.)

BOGOROV, V. G.; RASS, T. 1961. On the productivity and prospects of fishing in waters of the Indian Ocean. *Okeanologia*, **1** (1), p. 107-9. (In Russian.)

BRONGERSMA-SANDERS, M. 1957. Mass mortality in the sea. *Geol. Soc. America, Memoir 67*, **1**, p. 941-1010.

GILSON, H. C. 1937. The nitrogen cycle. *John Murray Expedition, 1933-34. Sci. Rep.*, **2** (2), p. 21-81.

JAYARAMAN, R.; RAMAMIRTHAM, C. P.; SUNDARARAMAM, K. V.; ARAVINDAKSHAN NAIR, C. P. 1960. Hydrography of the Laccadives offshore waters. *J. Mar. biol. Ass. India*, **2** (1), p. 24-34.

JERLOV, N. G. 1953. The equatorial currents in the Indian Ocean. *Rep. Swedish Deep-sea Exped.*, **3**, p. 113.

JONES, S. 1962. The phenomenal fish mortality in the Arabian Sea in 1957. A speculation on the possible identity of the species concerned. *Proc. Symposium on Scombroid Fishes Pt. II, Mandapam Camp*, p. 713-19.

KABANOVA, Y. G. 1961. Primary production and nutrients in the Indian Ocean. *Acad. des Sci. de l'URSS Comité de l'Année Geophysique Internationale.* Section X of the IGY programme (Oceanology), No. 4, Moscow, p. 72-5.

LAFOND, E. C. 1965. Indian Ocean. *McGraw-Hill Yearbook of Science and Technology*, p. 213-16.

MOTODA, S.; OSAWA, K. 1964. Filtration ratio, variance of samples and estimated distance of haul in vertical hauls with Indian Ocean Standard Net. *Information Bulletin on Planktology in Japan*, **11**, p. 11-24.

PRASAD, R. R.; NAIR, P. V. R. 1963. Studies on organic production. I: Gulf of Mannar. *J. Mar. biol. Ass. India*, **5** (1), p. 1-26.

RYTHER, J. H. 1964. *Mass fish deaths due to asphyxiation.* IOC information paper, no. 8, p. 36-7.

——; MENZEL, D. W. 1965. On the production, composition, and distribution of organic matter in the western Arabian Sea. *Deep-sea Res.*, **12** (2), p. 199-209.

STEEMANN NIELSEN, E. 1952. The use of radioactive carbon (C^{14}) for measuring organic production in the sea. *J. d. Cons.*, **18**, p. 117-40.

——. 1965. On the determination of the activity in C^{14} ampoule for measuring primary production. *Limnol. Oceanogr.*, **10**. In press.

——; JENSEN, E. A. 1957. Primary oceanic production. *Galathea Repts.*, **1**, p. 49-176.

TRANTER, D. J. 1962. Zooplankton abundance in Australasian waters. *Austral. J. Mar. Freshwater Res.*, **13** (2), p. 106-42.

VINOGRADOV, M.; VORONINA, N. M. 1965. Influence of the oxygen deficit on the distribution of plankton in the Arabian Sea. *Deep-sea Res.*, **9**, p. 523-30.

Reprinted from *Proceed. Indian Acad. Sci.*, vol. LXX, B, no. 4, 1969, p. 178-186

OCCURRENCE OF LARVAE OF *PSEUDORHOMBUS ELEVATUS* OGILBY (HETEROSOMATA—PISCES) ALONG THE SOUTH-WEST COAST OF INDIA

BY C. B. LALITHAMBIKA DEVI

(*Indian Ocean Biological Centre, National Institute of Oceanography, Cochin*-16, *India*)

Received February 17, 1969

(Communicated by Dr. N. K. Panikkar, F.A.SC.)

ABSTRACT

Larvae of *Pseudorhombus elevatus* Ogilby ranging in standard length from 3·47 to 7·76 mm. are described. These were brought on board R. V. VARUNA in the vertical plankton haul collected during the international Indian Ocean Expedition 1962–65 from two stations off the South-West Coast of India. Larvae slightly less than 8 mm. had developed the full complement of dorsal, anal, caudal and pelvic rays but lacked pectoral rays and a few gill rakers. Metamorphosis must take place at a small size, probably at less than 10 mm. standard length. The most notable character of middle and late stage larvae is the pronounced elongation of the nine anteriormost dorsal fin rays. Adults of *P. elevatus* Ogilby with mature gonads were sub equently collected from the same region. The identification of the larva to species is based mainly on meristic characters.

INTRODUCTION

ALTHOUGH the distribution of the adults of the genus *Pseudorhombus* has been frequently described (Norman, 1928, 1934; Whitley, 1934; Ginsburg, 1936; Herre, 1950; Smith, 1955; Silva, 1956; Kuroda, 1957; Kamohara, 1959; Matsuura, 1962; Smith and Smith, 1963; Abraham, 1963 and Pradhan, 1964) little has been published to date on larvae of *Pseudorhombus*. Gopinath (1946) referred specimens of flat-fish post-larvae to *P. arsius* and *P. triocellatus*; Jones and Pantulu (1958) illustrated a late post-larval specimen of *P. oligodon* (10·56 mm. total length) and illustrated a recently transformed individual of *P. arsius* from a collection of specimens ranging in size from 10·28 to 13·53 mm. total length; while Pertseva-Ostroumova (1965) illustrated an 8·2 mm. specimen of *Pseudorhombus* sp.

Material and Methods

From the processed plankton samples of R. V. Varuna of the International Indian Ocean Expedition (IOBC, 1968), 19 post-larvae of *Pseudorhombus* species (Table I) were studied. All these were preserved in 5 per cent. neutral formaldehyde. Body proportions were taken using ocular and stage micrometers. Measurements were made from the tip of the lower jaw and are included in *Appendix* I along with meristic characters. Drawings of larvae were made by using Projectina-Optik, Switzerland.

The composition of the catches of the fishing vessels near Quilon (09° 00′ N, 76° 22′ E) from a depth of 27 to 50 m. showed that *P. elevatus* Ogilby were present in large numbers in September, October and November, 1967. Random samples were preserved in 5 per cent. formaldehyde. Alizarin preparations of the adults were made to ascertain the meristic characters.

Table I

Data for the stations from which Pseudorhombus elevatus *Ogilby larvae were collected*

Name of vessel	Cruise No.	Station No.	Year	Month	Day	Latitude N	Longitude E	Local time	Day/night	Depth of haul	Depth at station	Sampler	No. of specimens
R. V. Varuna	104	2004	1963	11	4	09° 00′	76° 22′	0510	Night	45·0	50 m	IOSN	18
,,	,,	2005	,,	,,	,,	,,	76° 16′	0630	Day	54·0	58	IOSN	1

Results

1. *Description of Larval Stages*

Larva 3·99 *mm* (*Fig.* 1).—The thin transparent body of the larva is symmetrical and laterally compressed. Length of the body is about eight times its depth. Eyes are symmetrical and black. Notochord is vacuolated at the caudal end. There are 29 myotomes, of which 10 are pre-anal. Mouth is small and terminal. Jaws carry small conical teeth. Intestine has a single circular coil. Liver is small and is not as massive as in *Arnoglossus* or *Bothus* species. At the postero-lateral aspect of the operculum there are sets of irregularly arranged spinules. Another set of spinules is also present on the head near the dorsal profile, above the level of the eye. The dorsal fin fold commences just behind the level of the spinules. It is continuous and confluent with the caudal and anal fin folds. At its anterior end a tentacular process is seen in which four interneural spines are faintly marked out. The cleithrum is well differentiated. Embryonic rays are seen in the caudal fin. Pectoral rays are not differentiated. Brown stellate pigment spots are seen in the dorsal and ventral border of each myotome and on the skin covering the tentacular process.

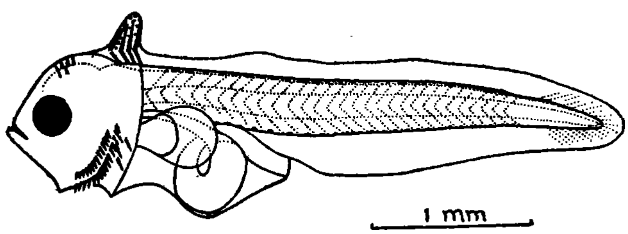

FIG. 1. *Pseudorhombus elevatus* Ogilby—Larva (SL. 3·99 mm).

Larva 4·26 *mm* (*Fig.* 2).—The length is more than 5·5 times its depth. Thirty myotomes are countable. Four elongated dorsal rays are differentiated in the place of the tentacular process. The first ray is more flat and club-shaped than the rest. Rudiment of the fifth ray is seen behind the fourth one. The nature and distribution of pigments and spinules are as in the previous stage.

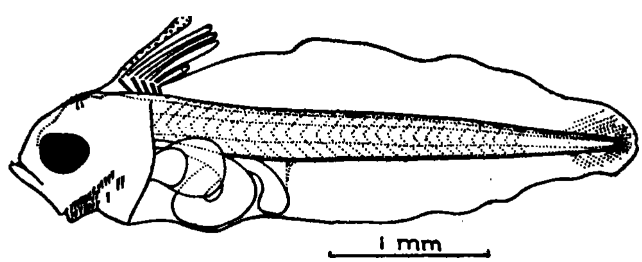

FIG. 2. *Pseudorhombus elevatus* Ogilby—Larva (SL. 4·26 mm).

Larva 4·72 *mm*.—Length of the body is less than 5·5 times its depth. The lower jaw projects beyond the upper. Anterior five rays are elongated. Rudiment of sixth ray is marked out. Thirty-one vertebral segments are differentiated corresponding to the number of myotomes, except at the posterior end where the notochord still remains vacuolated. Gill buds are present. Brown stellate pigment spots are also found along the middle of each myotome.

Larva 5·48 *mm* (*Fig.* 3).—The length of the body is slightly more than four times its depth. Five branchiostegal rays are differentiated. There are five gill rakers on the lower limb. Thirty-two vertebral segments are differentiated. Anterior seven dorsal rays are elongated. Along the dorsal and ventral body wall interneural and interhaemal complexes are differentiated as in *Cynoglossus semifasciatus* Day (Balakrishnan, 1961). Ventral fin radials are differentiated. Rudiments of ventral fins are also seen. Hypural elements are in the process of formation. The opercular spinules have increased in number. Nature and distribution of pigments are same as in the preceding stages.

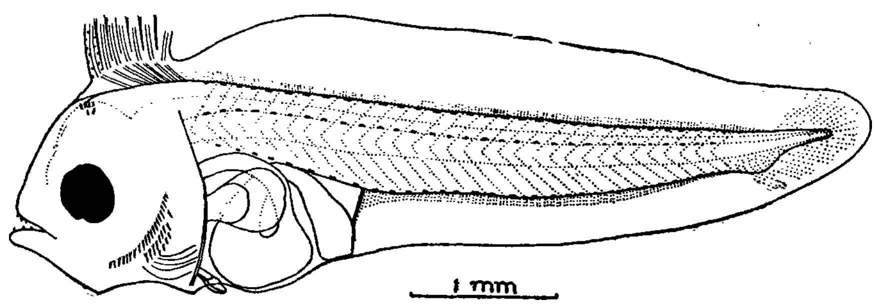

FIG. 3. *Pseudorhombus elevatus* Ogilby—Larva (SL. 5·48 mm).

Larva 6·01 *mm.*—Six branchiostegal rays and seven gill rakers on the lower limb are developed. Rudiments of 10 caudal rays are seen. Isolated brown pigment spots are found on the abdomen.

Larva 6·37 *mm* (*Fig.* 4).—The length of the body is 3·5 times its depth. There are 34 vertebral segments including the urostyle. Anterior eight dorsal rays are elongated and the ninth one is faintly marked. Anteriorly only four interneural spines are differentiated following the first nine ones while 19 of them are differentiated near the caudal end. In the anal fin fold 15 interhaemal spines are differentiated all of them are found near the caudal end. Differentiation of interneural and interhaemal spines near the caudal end earlier than the anterior caudal portion has also been observed in *Cynoglossus monopus* Bleeker (Balakrishnan, 1963). Twelve caudal rays are differentiated. The nature and distribution of pigments and spinules are as in the earlier stages.

Larva 6·86 *mm.*—The length of the body is nearly thrice its depth. Seven branchiostegal rays and eight gill rakers on the lower limb are present. There are vertebral segments including the urostyle. Sixty-six interneural and 52 interhaemal spines are well marked out, but the rays are not fully formed. The anterior nine dorsal rays are elongated. The hypural elements are well differentiated and consequently the urostyle gets pushed dorsalwards. There are 17 caudal rays of which the middle one is the longest. Six ventral rays are faintly marked out. The ventral fin radials are symmetrical and short based. The pectoral fin still remains unrayed. In addition to the pigmentation found in the earlier stages, isolated stellate pigments could be seen on the abdomen and between 24th and 27th vertebral segments.

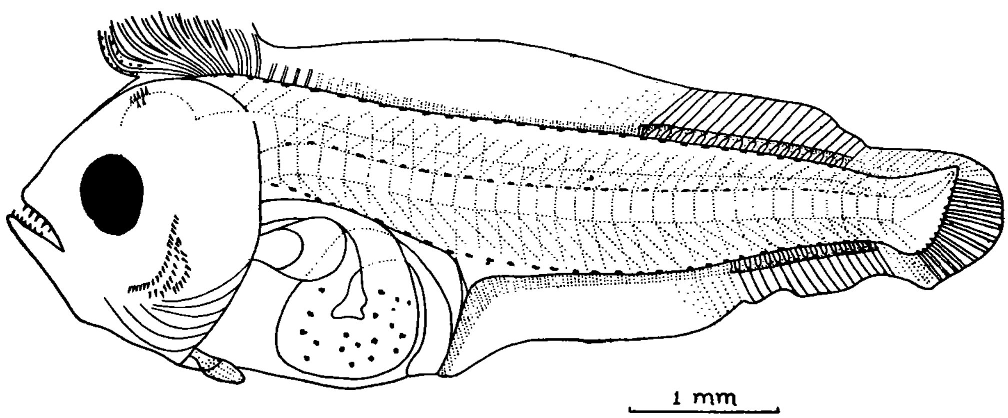

FIG. 4. *Pseudorhombus elevatus* Ogilby—Larva (SL. 6·37 mm).

Larva 7·76 *mm* (*Fig*. 5).—The length of the body is less than three times its depth. The eyes are still symmetrical. Seven branchiostegal rays and nine gill rakers on the lower limb are well differentiated. There are 34 vertebral segments including the urostyle. The dorsal fin rays commence from the very extremity of the dorsal fin fold. The anterior nine dorsal rays are elongated. The first dorsal ray is especially flat and leaf-like and is directed obliquely forwards. Sixty-eight interneural and 54 interhaemal spines are well differentiated. The fin rays are faintly marked out. Ventral fins have short bases and bear six rays. The pectorals still remain unrayed. The nature and distribution of the pigments and spinules are the same as in the preceding stage.

2. *Distinctive Characters of Adult* P. elevatus *Ogilby*.

The adults of *P. elevatus* Ogilby are characterised by the presence of 34 vertebrae including the urostyle, 66–69 dorsal, 50–55 anal, 17 caudal, six ventral rays and 13 gill rakers on the lower limb. These characters agree with those described by Norman (1934).

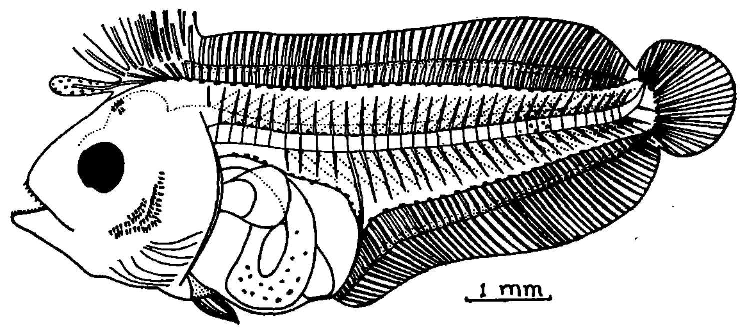

FIG. 5. *Pseudorhombus elevatus* Ogilby—Larva (SL. 7·76 mm).
(The anterior elongated rays of the larvae are broken. Hence their relative lengths are not shown in figures.)

DISCUSSION

The thin, flat body, large numbers of soft continuous fin rays in the dorsal and anal fins, the absence of procurrent rays in the caudal fin, and the relatively few (10) abdominal vertebrae help to distinguish the larvae as those of flat-fish. The presence of precocious elongated anterior rays in the dorsal fin together with symmetrical short-based ventral fins, place this larva in the *Paralichthys-Pseudorhombus* group of bothid flat-fish. Meristic characters support the assignment to *Pseudorhombus elevatus* Ogilby. Gopinath (1946), Jones and Pantulu (1958) and Pertseva-Ostroumova (1965) do not give indication of the presence of a group of elongated anterior dorsal rays on their specimens—although this character is one of the most diagnostic features of *Pseudorhombus* larvae. Larvae of the closely allied genus *Paralichthys*, develop a precocious group of five elongated anterior dorsal rays (Okiyama, 1967). It is probable that the two specimens identified and illustrated as *Samaris macrolepis* Norman by Jones and Pantulu (1958, pp. 131–33, Figs. 22–23) are larvae of *Pseudorhombus*.

The presence of adult *P. elevatus*, with maturing gonads in the locality from where the larvae had been obtained previously, at the same season of the year, strengthens the assignment to this species.

The largest larvae studied, slightly less than 8 mm standard length, possessed a full complement of dorsal, anal, caudal and pelvic fin rays, and lacked only the pectoral rays. The number of gill rakers on the lower limb is also incomplete. This stage of development of flat-fish larvae usually immediately precedes metamorphosis; hence, metamorphosis probably occurs at a length of 10 mm or less in this species.

ACKNOWLEDGEMENTS

The author is grateful to Dr. N. K. Panikkar, Director, National Institute of Oceanography; to Professor T. S. Rass, Senior Specialist (Fish eggs and larvae) and to the members of the Consultative Committee, International Indian Ocean Expedition for permitting her to study the eggs and larvae of Pleuronectiformes collected during the Expedition. The author also wishes to thank Dr. N. Balakrishnan Nair, Professor of Marine Biology and Fisheries, University of Kerala; Mr. D. J. Tranter, Curator, Indian Ocean Biological Centre; Professor E. H. Ahlstrom, Senior Scientist, U.S. Department of the Interior Fish and Wild Life Service, California and Dr. R. R. Prasad, Deputy Animal Husbandry Commissioner (Fisheries), for critically reading through the manuscript and suggesting improvements.

REFERENCES

Abraham, D. S. .. "Bottom fishes collected by the Research Vessel Conch off the Kerala Coast during 1958-63—Heterosomata," *Bull. Dept. Mar. Biol. Oceanogr. Univ. Kerala*, 1963, **1**, 57-80.

Balakrishnan, K. P. .. "Fish eggs and larvae collected by the Research Vessel Conch during 1958-61. 1. Larvae of *Cynoglossus semifasciatus* Day," *Bull. Cent. Res. Inst. Univ. Kerala*, 1961, **8C**, 131-39.

——— .. "Fish eggs and larvae collected by the Research Vessel Conch: 2. Larvae of *Arnoglossus tapeinosoma* (Blkr.), *Bothus ocellatus* (Agassiz), *Laeops güentheri* Alc., *Solea ovata* Rich. and *Cynoglossus monopus* Blkr," *Bull. Dept. Mar. Biol. Oceanogr. Univ. Kerala*, 1963, **1**, 81-96.

Ginsburg, I. .. "Descriptions of a new flat-fish, with notes on related species." *J. Wash. Acad. Sci.*, 1936, **26**, 128-33.

Gopinath, K. .. "Notes on the larval and post-larval stages of fishes found along the Trivandrum Coast," *Proc. nat. Inst. Sci. India*, 1946, **12**, 7-21.

Herre, A. W. C. T. .. "Twenty-six noteworthy Philippine fishes," *Philipp. J. Sci.*, 1950, **79**, 137-54.

IOBC Hand-book to the International Zooplankton Collections Station list. *N.I.O.*, 1968, **1**, 1-133.

Jones, S. and Pantulu, V. R. .. "On some larval and juvenile fishes from the Bengal and Orissa Coasts," *Indian J. Fish.*, 1958, **5**, 118-43.

Kamohara, T. .. "New records of fishes from Kochi Prefecture Japan," *Rep. Usa mar. biol. Stn. Kochi Univ.*, 1959, **6**, 1–8.

Kuroda, N. .. "Additions and corrections to the fishes of Suruga Bay," *Zool. Mag. Tokyo*, 1957, **66**, 461–63.

Matsuura, S. .. "On the maturation of the flat-fish, Ganžo-Birame, *Pseudorhombus cinnamoneus* (Temminck et Schlegel)," *Rec. Oceanogr. Wks. Japan Spec.*, 1962, **6**, 31–39.

Norman, J. R. .. "Flat-fishes (Heterosomata) of India, with a list of specimens in the Indian Museum, Part II," *Rec. Ind. Mus.*, 1928, **30**, 173–215.

——— .. "A systematic monograph of flat-fishes (Heterosomata)," *British Museum Natural History*, 1934, **1**, 459 pp.

Okiyama, M. .. "Study on the early life-history of a flounder, *Paralichthys olivaceus* (Temminck et Schlegel). 1. Descriptions of post-larvae," *Bull. Jap. Sea Reg. Fish. Lab.*, 1967, **17**, 1–12.

Pertseva-Ostroumova, T. A. .. "Flat-fish larvae of the Gulf of Tonkin," *Trudy Inst. Okeenologoii*, 1965, **80**, 177–220.

Pradhan, M. J. .. "A preliminary account of the flat-fishes (Heterosomata) found along the Bombay Coast," *J. Bombay nat. Hist. Soc.*, 1964, **61**, 456–59.

Silva, P.H.D.H. de "A note on the fishes of the families Syngnathidae and Pegasidae and the order Heterosomata in the Colombo Museum," *Ibid.*, 1956, **53**, 477–78.

Smith, J. L. B. .. "The fishes of Aldabra—Part I," *Ann. Mag. nat. Hist.*, 1955, **8** (12), 304–12.

——— and Smith, M. M. "The fishes of Sychelles Grahamstown (Dept. of Ichthyology, Rhodes University), 1963, **215**, viii.

Whitley, G. P. .. "Studies in ichthyology No. 8," *Rec. Aust. Mus.*, 1934, **19**, 153–63.

APPENDIX I

Measurement and meristic counts of Pseudorhombus elevatus *Ogilby larvae*

Sl. No.	Standard length mm.	Total length mm.	Eye diameter maximum mm.	Eye diameter minimum mm.	Snout length mm.	Head length mm.	Length up to Cleithra mm.	Length up to anus mm.	Depth at anus mm.	Depth at caudal peduncle mm.	Vertebrae without urostyle	Branchiostegals	Dorsal rays	Anal rays	Caudal rays	Gill rakers	Remarks
1	3·47	3·56	0·26	0·26	0·30	0·79	0·89	1·95	0·50	0·17	23	..	..	..	..	..	Damaged. 3 interneural spines in the tentacular process
2	3·99	4·13	0·26	0·25	0·17	0·76	0·86	1·91	0·50	0·23	29	..	..	..	..	..	
3	4·26	4·39	0·26	0·26	0·20	0·83	0·92	1·85	0·76	0·17	30	..	4	..	..	..	
4	4·72	4·85	0·30	0·26	0·13	0·76	0·92	2·15	0·86	0·20	31	..	5	..	..	..	
5	4·72	4·85	0·30	0·30	0·26	0·92	1·06	2·01	0·89	0·23	31	..	5	..	..	..	
6	4·85	4·98	0·30	0·30	0·26	0·96	1·06	2·18	0·89	0·23	31	..	5	..	..	..	
7	4·98	5·08	0·36	0·33	0·33	1·16	1·22	2·18	1·25	0·46	31	..	5	..	..	..	
8	5·15	5·25	0·36	0·33	0·40	1·12	1·22	2·28	0·99	0·23	32	3	6	..	..	5	
9	5·31	5·45	0·40	0·33	0·30	0·89	1·19	2·31	1·09	0·30	32	4	7	..	..	5	
10	5·35	5·51	0·36	0·33	0·36	1·19	1·32	2·38	1·02	0·30	32	4	7	..	..	7	
11	5·48	5·58	0·40	0·40	0·33	1·02	1·22	2·34	1·32	0·33	32	5	7	..	..	5	
12	5·61	5·71	0·36	0·33	0·36	1·09	1·29	2·31	1·19	0·26	32	5	7	..	8	5	
13	5·78	5·87	0·43	0·36	0·36	1·09	1·49	2·54	1·35	0·43	32	6	7	..	9	5	
14	6·01	6·14	0·46	0·36	0·43	1·39	1·52	2·74	1·49	0·40	32	6	7	..	10	7	
15	6·04	6·11	0·40	0·40	0·40	1·42	1·49	2·71	1·49	0·36	32	6	7	..	10	7	Damaged and distorted
16	6·14	6·30	0·40	0·36	0·33	1·22	1·45	2·51	1·35	0·40	32	6	7	..	11	7	
17	6·37	6·90	0·50	0·40	0·46	1·55	1·58	2·84	1·82	0·53	33	7	8	..	12	7	
18	6·86	7·99	0·53	0·50	0·46	1·82	2·01	3·23	2·41	0·69	33	7	9+57	52	17	8	
19	7·76	8·98	0·59	0·50	0·59	2·01	2·31	3·76	2·74	0·76	33	7	9+59	54	17	9	

Reprinted from *Oceanographic Research Inst. Durban, Investig. Report no. 23*, 1969, p. 2-24

Phytoplankton studies in the Agulhas Current Region off the Natal Coast

by Margaret Thorrington-Smith

Introduction

A survey of the Agulhas current region off Natal was conducted by the vessel *RSA* during June 1965. This survey was a collaborative effort between the National Physical Research Laboratory (Oceanography Division) of the Council for Scientific and Industrial Research and the Oceanographic Research Institute Durban, and represents part of the Republic of South Africa's contribution to the I.I.O.E. programme. Representatives of the Oceanographic Research Institute participated in the cruise to investigate productivity and species composition of phytoplankton communities. An account of productivity studies is given by Burchall (1968).

Phytoplankton was collected from stations on five transects, A, B, C, D, and E, extending off the Natal coast (Fig. 1) from the Tugela river mouth in the north to Green Point just south of Durban. These stations were located in the Agulhas current area of the south-west Indian Ocean. The boundaries of the current as indicated in Figs. 1 and 2 are approximate since the edges of the current may fluctuate according to prevailing weather conditions.

Phytoplankton samples were collected with a Discovery type N50V plankton net and with a Van Dorn water sampler. Unfortunately the formalin used for preserving the latter samples had not been neutralised adequately. This resulted in a certain amount of damage to the samples by accumulated formic acid and flocculent precipitate (Walker 1944). They could therefore only be used qualitatively and an assessment of relative abundance became dependent on material collected with the net samples. In discussing the results it has been necessary, in the absence of more adequate quantitative sampling techniques, to assume that these hauls give comparable values of relative abundance of species. Limitations imposed by factors such as ship's drift causing variations in the length and depth of the water column sampled or inconsistencies in the filtration rate of the net must therefore be considered in the evaluation of the results obtained.

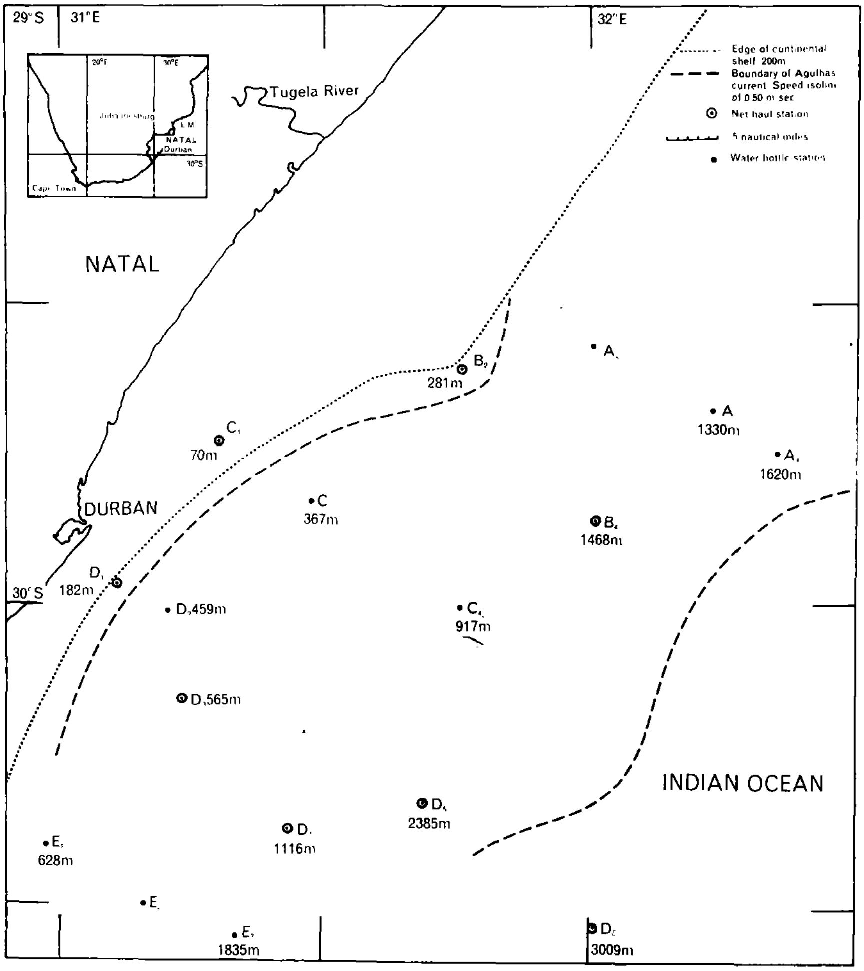

Fig. 1 The Sampling area showing stations where phytoplankton was sampled.

4

Sampling methods and microscopic examination of plankton samples

Concentrated net samples

Concentrated samples were collected with the Discovery type N50V net, hauled from 50 metres to the surface at eight stations: B_2, B_4, C_1, D_1, D_3, D_4, D_5 and D_6. Station depths are indicated in Fig. 1. The material was preserved in 5 per cent formalin.

These samples were used in identification of the species, and the assessment of relative abundance. The net has 200 meshes to a linear inch and consequently does not retain nannoplankton.

A drop from the well-shaken sample was placed on a microscope slide with a grid of 2 mm squares etched on its surface. The preparation was sealed around the coverslip to prevent evaporation. All species observed on the slide were identified using a Zeiss research microscope fitted with phase contrast.

In addition, all phytoplankton cells in a row of ten squares were counted. The count for each species was recorded as a percentage of the total numbers of cells counted in the sample and is presented in Table 1. A cell which was not present in the ten squares counted, but which was present on the slide is represented by a + sign, and a species present as less than 0.5 per cent is represented by a ++.

Unconcentrated bottle samples

Unconcentrated water samples were collected with a Van Dorn water sampler from stations A_2, A_3, A_4, B_2, B_4, C_1, C_2, C_4, D_2, D_3, D_4, D_5, E_1, E_2 and E_3. Stations B_4, C_4 and D_3 were sampled twice. No bottle samples were obtained from D_1 or D_6. The samples were preserved in 5 per cent formalin. It is recommended that formalin always be neutralised with sodium potassium tartrate and calcium carbonate (Armstrong and Wickstead, 1962) in future, to overcome the effects of acidity of the formalin.

Volumes of 50 ml and 100 ml were concentrated by sedimentation for identification with the plankton microscope according to the method described by Utermöhl (1958). All phytoplankton species observed in the sample were identified. These data were used to supplement the species list (Table 1).

Results

The two main classes of algae represented in the samples were the Bacillariophyceae and the Dinophyceae. In addition, two species of Cyanophyceae and one species of the Chrysophyceae were also present.

Table 1 is a list of all the species identified in the samples collected on the *RSA* cruise with their relative abundance in the net-haul samples.

Species composition

Fig. 2 shows the total number of species identified in the net hauls for the eight stations, with diatom and dinoflagellate species differentiated. B_2 situated off the Tugela River mouth is noteworthy for the variety of species found while D_6 has the fewest different species. The dinoflagellates were never present in an abundance greater than 2.3 per cent or less than 0.1 per cent of the total number of cells counted in a sample. They attained their maximum concentrations at Station D_5.

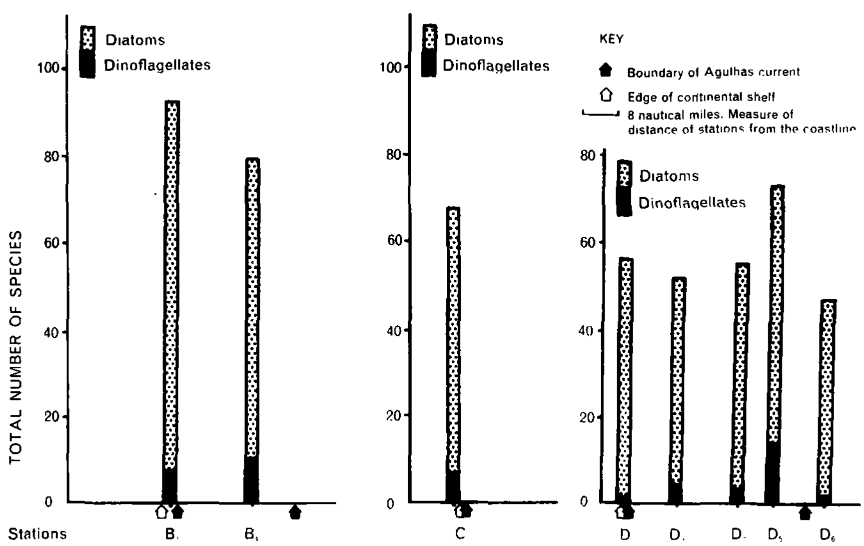

Fig. 2 Numbers of Diatom and Dinoflagellate species at the net haul stations studied.

The range of the most common species as calculated by their percentage relative abundance in the samples is expressed graphically in Fig. 3.

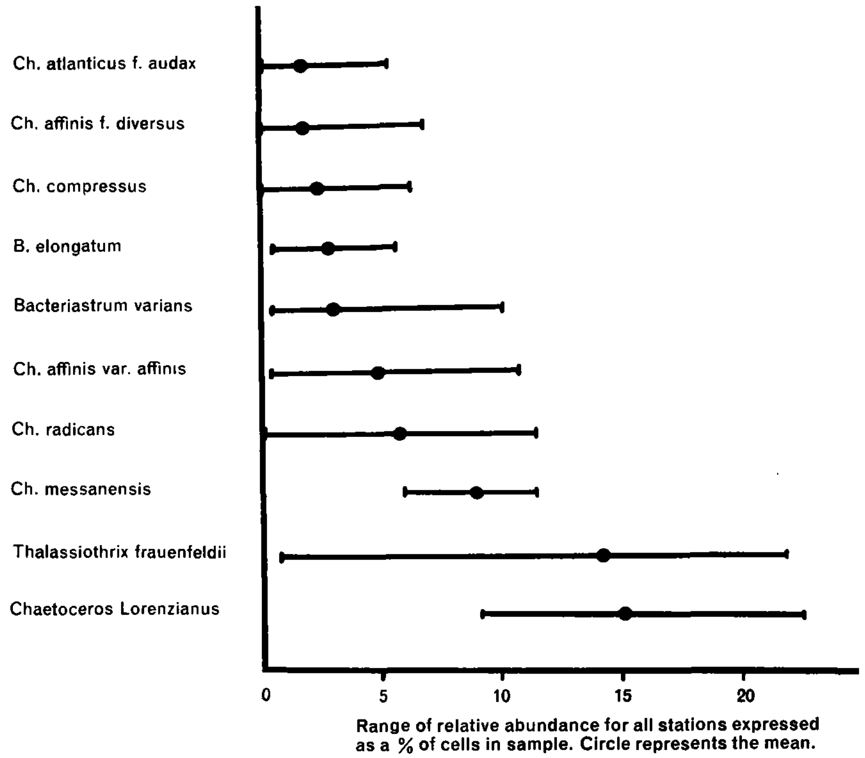

Fig. 3 Diagram showing the range of relative abundance of the ten most common species in the samples.

Affinity of the different stations in relation to ocean currents

The similarity between two stations is a function of the summation of the actual species common to both, and is affected also by the relative abundance of the different species in the two samples.

Two methods were used to show the affinity between stations.

The first does not take into account the abundance of the species but merely the species composition.

7

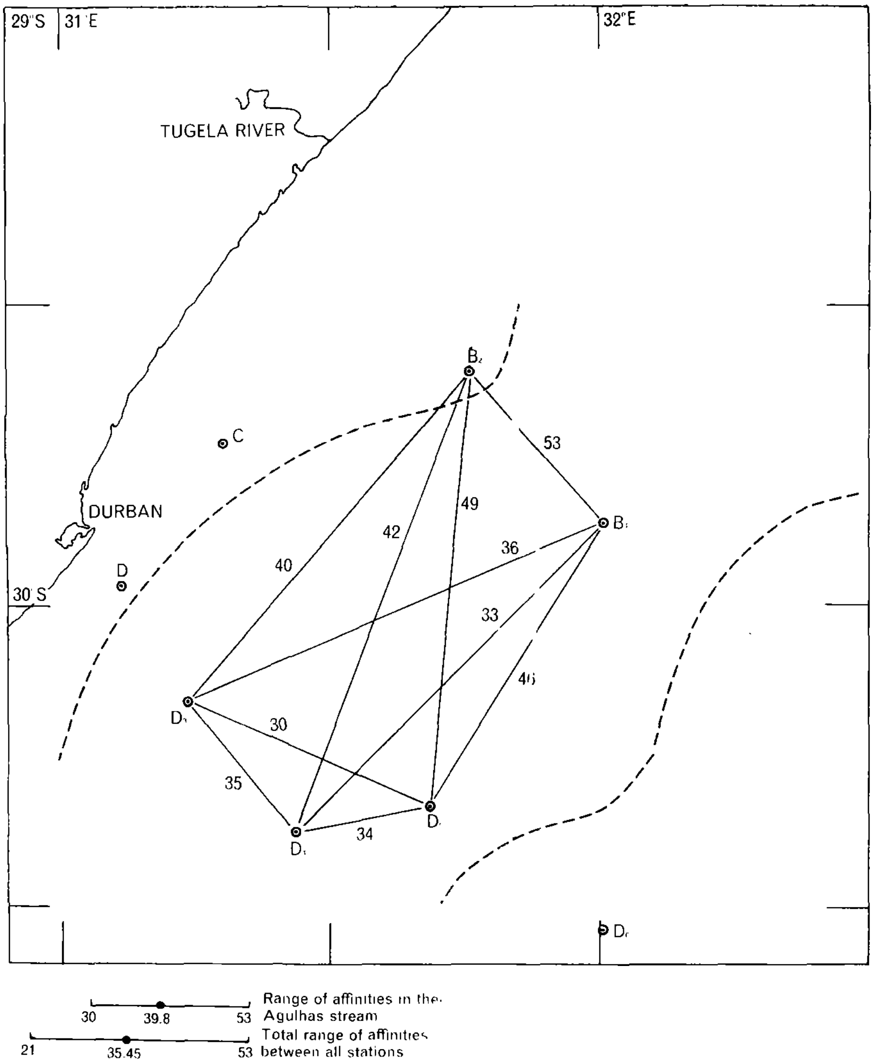

Fig. 4 Diagram to show, by means of numbers of shared species, the affinities between stations in **the Agulhas Stream.**

All species common to any two stations were recorded as such, and summed (Figs. 4, 5 and 6). The lines connecting two stations may be termed lines of affinity. The number of species common to both stations is inserted on the line. Only data from net haul samples were used for this as there were no bottle samples from D_1 and D_6.

8

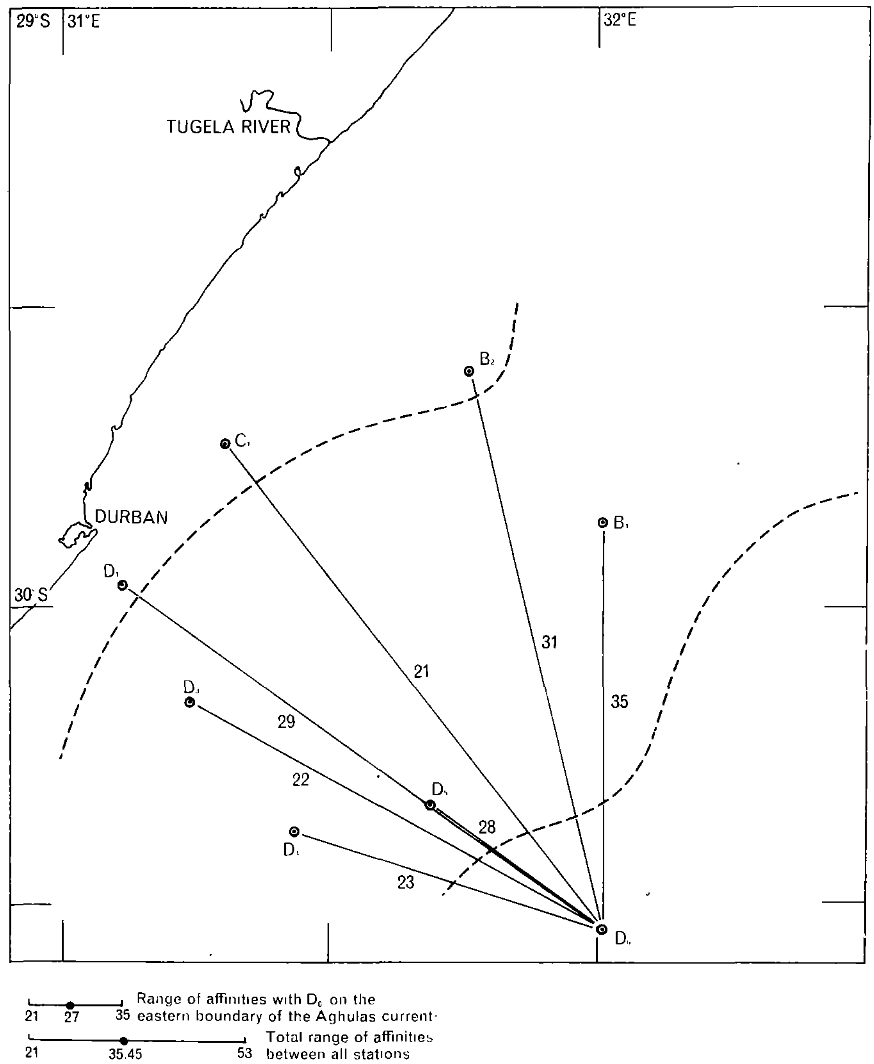

Fig. 5 Diagram to show relative lack of affinity of station D6 on the **eastern boundary** of the Agulhas Stream, with the other stations.

Fig. 4 includes all stations in the Agulhas current; Fig. 5 shows the relationship between D_6 on the eastern boundary and all other phytoplankton stations; and Fig. 6 shows the affinities between the coastal stations and the others.

It is possible to express the similarity or affinity between two stations by a similarity index. This takes into account the relative abundance of species.

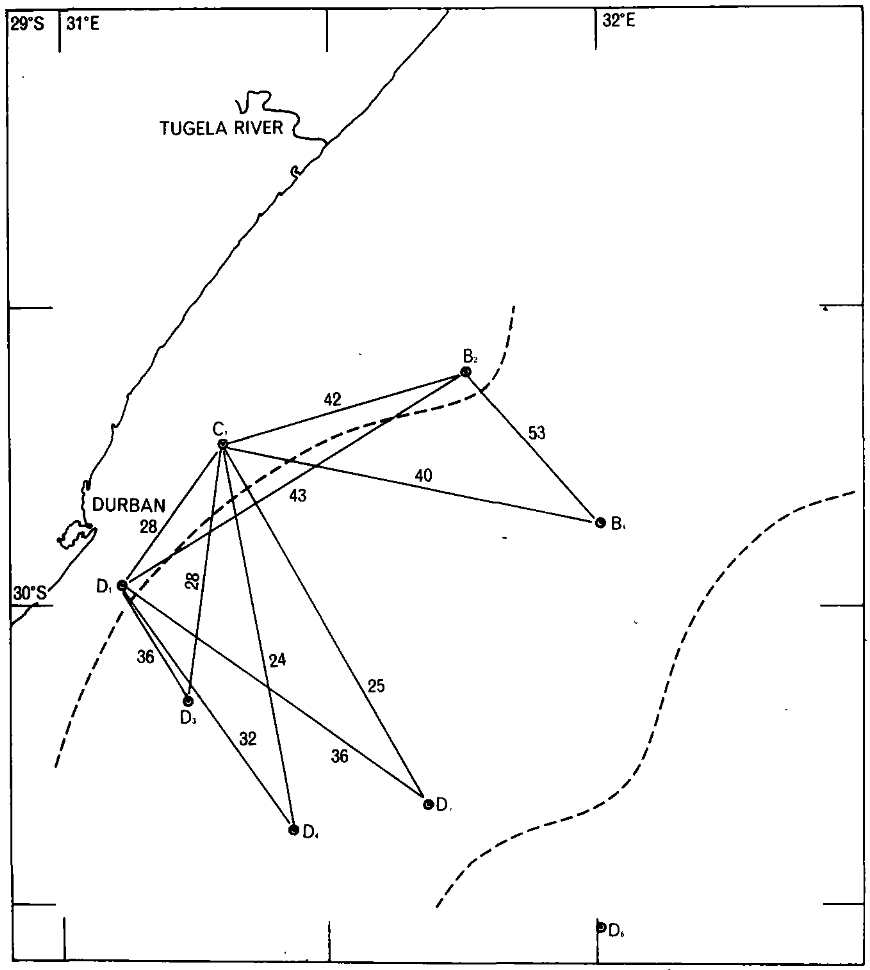

Fig. 6 Diagram to show, by means of numbers of shared species, the affinities of the phytoplankton at **coastal stations** both to each other and to those in the Agulhas Stream.

The index recommended by McIntosh (1967) was used to measure the 'distance' between every pair of stations. The term distance is a measure of the ecological relationship suggested by the resemblance or similarity of two communities or samples. The distance between two communities is the square root of the sum of the squared differences between the measures of each species. The distance between two stations j and h is calculated by the formula

$$D_{jh} = \sqrt{\sum_{i=1}^{S} (X_{ij} - X_{ih})^2}$$

X_{ij}, X_{ih} are the measures of the i^{th} species in stands j and h respectively and S is the number of species.

The similarity of a set of stations is represented by the matrix of distance values between the stations.

If the stations have the same species in equal quantities, i.e., they are identical, the similarity index value will be zero. Thus the lower the value the closer the resemblance.

The similarity index was computed for all combinations of stations using the relative abundance values obtained in the counts. The results are shown in Figs. 7, 8 and 9, the values of the index being inserted on the lines between stations. Fig. 7 includes all stations in the Agulhas stream; Fig. 8 shows the relationship of D_6 on the eastern boundary to all other phytoplankton stations; and Fig. 9 shows the affinities between the coastal stations and the others.

Agulhas current (Figs. 4 and 7)

There is close affinity between stations B_2, B_4, D_3, D_4, and D_5, as shown by a high number of species shared and a low similarity index.

The ocean current date (Anderson, personal communication) show that B_4, D_3, D_4 and D_5 are in the core of the Agulhas current and B_2 is on the western boundary. The following species composition appears to be typical of the Agulhas stream: *Skeletonema costatum*, *Gosslieriella tropica*, *Lauderia annulata*, *Leptocylindrus danicus*, *Guinardia flaccida*, *Rhizosolenia fragilissima*, *Rhizosolenia stolterfothii*, *Bacteriastrum minus*, *Chaetoceros pelagicus*, *Ch. radicans* and *Ceratium tripos*.

These findings are in agreement with Nel (1968) except that she uses the synonym of *L.annulata* (*L.borealis*) Sournia (1968), and found *Ch.pelagicus* at only a few scattered stations.

Western sub-tropical water (Figs. 5 and 8)

D_6 has little affinity with any of the other stations, as shown by the relatively few species shared and the relatively high similarity index. This is to be expected as it is in a different water system, being situated in western sub-tropical waters which appear to flow in from the east. It is interesting to note that, although there are only 29 common species between D_1 and D_6 on opposite boundaries of the Agulhas current, there is a low similarity index (17.73) indicating an above average affinity. This similarity is a function of similar abundance. Both stations are dominated by the common species (Table 1). There is an indication that this is an effect of mixing along the boundaries of the different water masses, and it is possible that only the common species flourish in this region of contact and stress (Margalef, 1967).

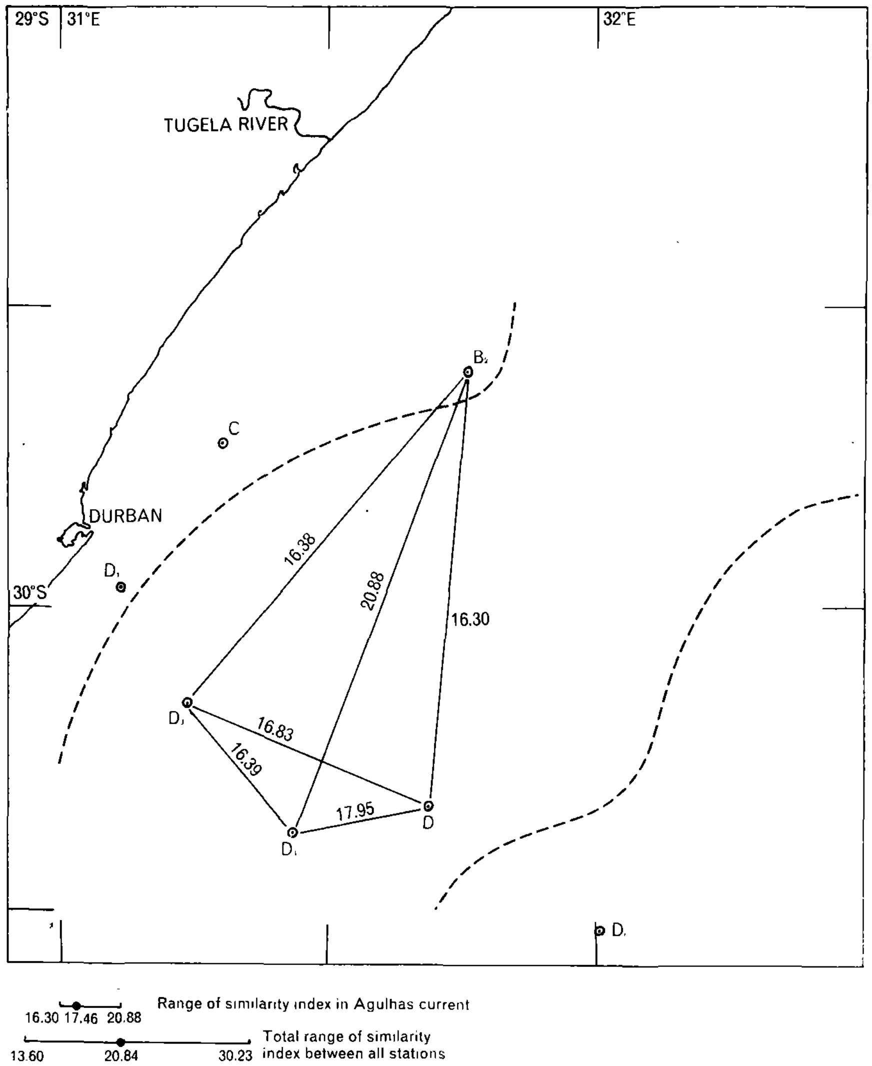

Fig. 7 Diagram to show affinities of phytoplankton at stations **within the Agulhas Stream** by means of a similarity index.

There were only two species unique to D_6 (*Asteromphalus van heurckii* and *Bacillaria paxillifer*) and these were not present in the count. There were 12 species recorded at all stations but two, and eight of these were absent from D_6. These data would suggest that D_6 differs from the other stations in its paucity of species rather than in the species present (Fig. 2).

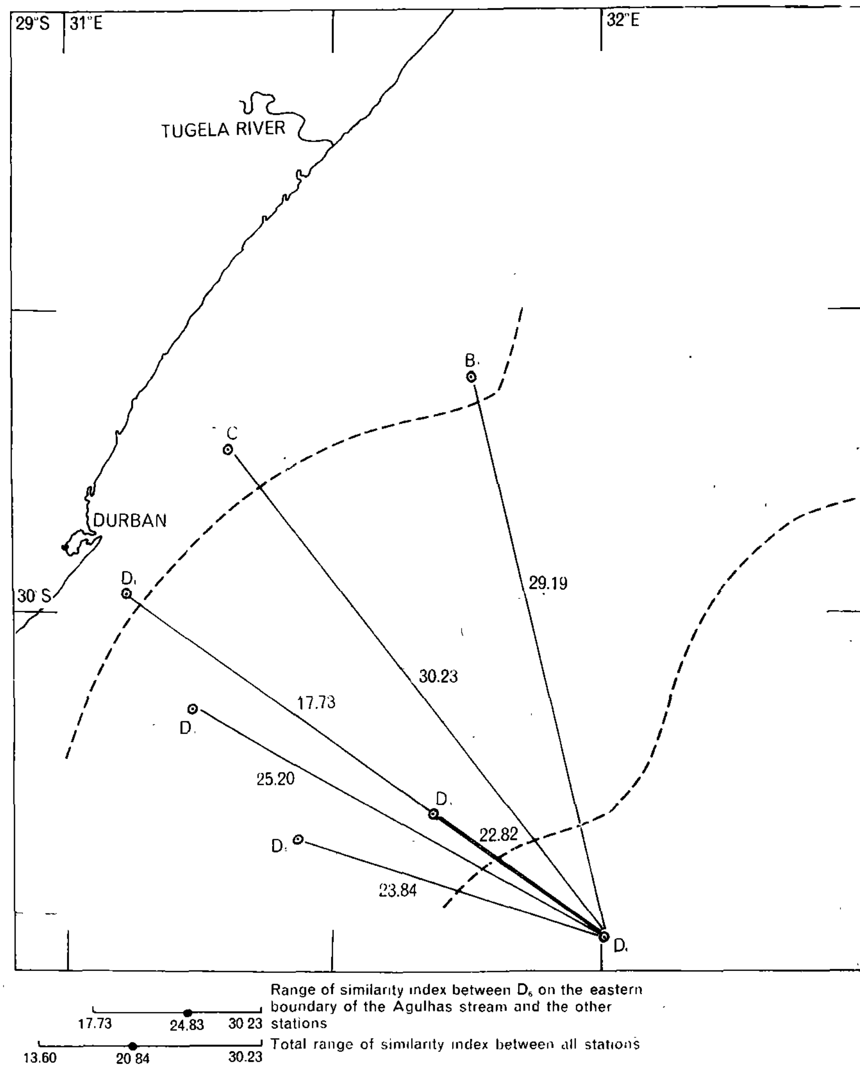

Fig. 8 Diagram to show, by means of numbers of shared species, the relative lack of affinity of phytoplankton at all stations to **D6** on the **eastern boundary** of the Agulhas Stream.

Coastal stations (Figs. 6 and 9).

The relatively shallow coastal stations sampled were D_1, C_1, and B_2. Their affinities are more difficult to interpret. Eddy currents develop to the west of the Agulhas Current and contain north-flowing components. This water originates in the Agulhas stream. These eddies are particularly variable and a station which one week is part of an eddy system may become part of the

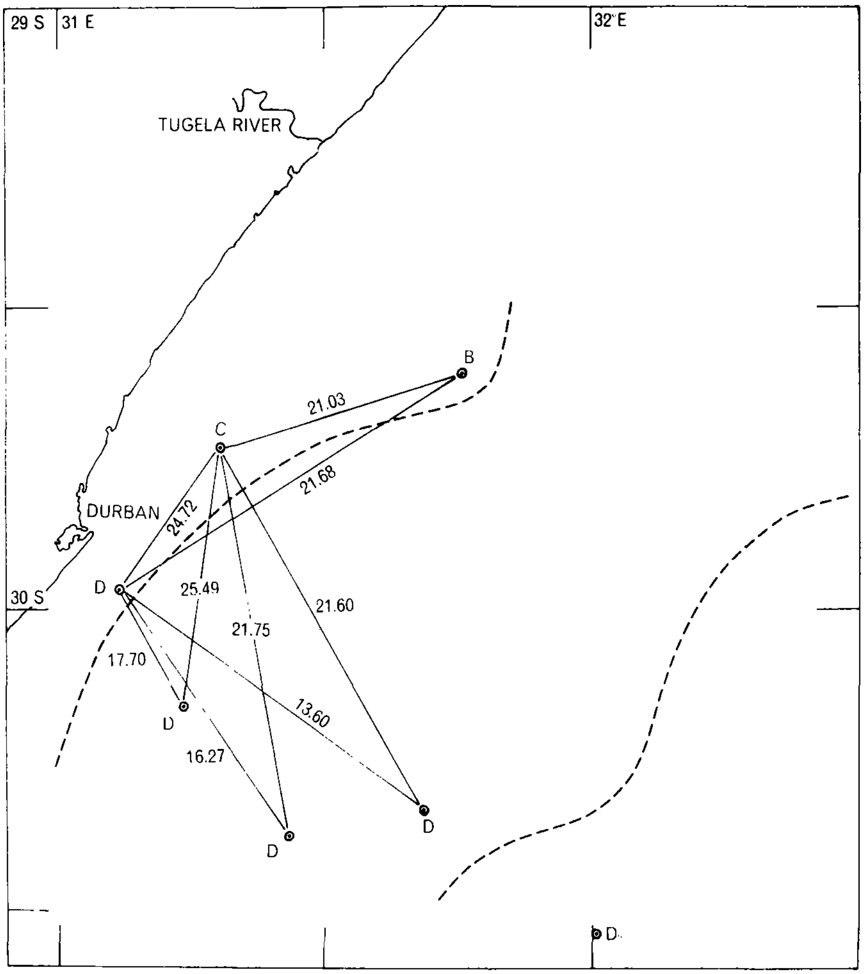

Fig. 9 Diagram to show, by means of a similarity index, the relationship of the **coastal stations** to each other and to the Agulhas Stream stations.

Agulhas stream the following week (Anderson, personal communication).

When C_1 was sampled, it was part of an eddy system and it is understandable that it should have affinities with B_2 further north, rather than D_1 in the south. Species which appear to be typical of this counter current caused by the eddy system are: *Stephanopyxis palmeriana*, *Rhizosolenia alata* f. *indica*, *Chaetoceros dadayii*, *Ch.danicus*, *Ch.affinis*, f.*inaequale*, *Streptotheca tamesis*, *Hemiaulus chinensis* and *Ceratium trichoceros*. It is interesting to note that *S.palmeriana*, *Ch.dadayii*, *S.tamesis* and *H.chinensis* were found in a strong cyclonic eddy south of Cape Town and north of the sub-tropical Convergence (Nel, 1968). She considers upwelling of this kind to have an important

14

bearing on not only the amount of plankton present but also the presence or absence of species.

There are no hydrographic data for D_1. D_1 has affinities with the Agulhas stream, however, and it is suspected that it was on the western boundary of this current.

B_2 on the western boundary of the Agulhas current has greatest affinity with both the central core and the coastal stations. It is a very rich area and would appear to be a source of many large actively dividing phytoplankton species.

Species diversity

In analysing the results, it was necessary to compare the phytoplankton standing crop at stations where both the number of species and the abundance of any particular species vary. Individual stations had up to 95 species in varying quantities. It is useful to be able to reduce these data to a single index in order to compare the diversity at the different stations. Margalef (1958), working on phytoplankton in Mediterranean waters, has used a diversity index as an indication of water masses.

For the present study, an index of diversity was calculated using the formula described by Simpson (1949).

$$\text{If } d = \text{diversity index, then } d = \sum_{i=1}^{s} \frac{n_i(n_i-1)}{N(N-1)}$$

N is the total number of cells counted in a phytoplankton population and $n_1, n_2 \ldots\ldots n_s$ were the numbers of individuals of the species.
Hence, $\Sigma n_i = N$, i.e., total number of cells.

Then d is a measure of the diversity of the concentration and can take any value between 0 and 1. An index of 0 represents the smallest concentration, or largest possible diversity. An index of 1 represents a case of the lowest diversity where all individuals belong to a single species. Then d represents the probability of two individuals, chosen at random, belonging to the same species.

In order to ascertain whether the sample size affected the resultant diversity index, it was computed twice for station D_4. Firstly, the total number of squares was counted (N = 1144) and secondly, only half the squares were counted (N = 535). The resultant diversity indices were .05422 and .05137 respectively. It was concluded that the effect of sample size was negligible.

In Fig. 10, the diversity indices are plotted against station numbers. There is only one transect crossing the Agulhas Current region and this is line D. From this, it appears that the core of the Agulhas current is characterised by a high diversity of phytoplankton at stations D_3 and D_4 (also see B_4) and that the diversity is lower at the eastern boundary of the Agulhas current at stations D_5 and D_6. Stations D_1 and B_2 have relatively low diversity and station C_1 a very low diversity.

Hence, these are signs of three different groups:

1 The stations off the coast, viz. B_2, C_1 and D_1 with low diversity of species.
2 The stations in the core of the Agulhas current with a high diversity of species, viz. D_3 and D_4.
3 The stations on the eastern fringe of the Agulhas current with low diversity of species, viz. D_5 and D_6.

Margalef (1958) found a relationship between species diversity and primary productivity. The primary productivity calculations per column of water beneath $1m^2$ sea surface (Burchall, 1968) have been plotted against station numbers (Fig. 11). Considering productivity and diversity from these three groups, there appears to be an inverse correlation, a finding which is in accordance with the conclusion reached by Margalef in his work on Mediterranean waters.

The enhanced productivity and low diversity may well be a result of mixing along the boundaries of different water masses. Margalef (1968) states that such places of contact and stress often harbour a population of lower diversity, and are frequently found in surfaces of discontinuity where there is an enhancement of productivity.

The hydrographic data available for the stations sampled on the *RSA* cruise include salinity, temperature, phosphorus, nitrate-nitrogen and silica values (Burchall 1968). The mean value of any of these factors for a water column has been calculated from the values for the different depths. The mean value was used in order to make it comparable with the diversity index which was calculated from net haul samples which sample the whole column. The mean values have been plotted against the station numbers (Figs. 12-16).

The Agulhas current has typically a relatively high temperature and low salinity (Orren 1966), in relation to western sub-tropical surface water to the east of the current (Figs. 12 and 13). D_6 in the western sub-tropical water also has enhanced productivity and a low diversity (Figs. 10 and 11).

C_1 has the lowest diversity index of the cruise but this is not correlated with the highest productivity. The productivity is 240 $mgC/m^2/day$, which is nevertheless relatively high. The productivity is probably limited by nutrients as NO_3—N, SiO_3—Si and PO_4—P are low. It is regrettable that no cell counts per litre were possible.

No data other than species composition and diversity are available from D_1.

B_2, however, off the Tugela River, is situated in an extremely interesting area. There are exceptionally high values of nutrients, NO_3—N (Fig. 14), PO_4—P (Fig. 15) and a high silica value (Fig. 16). The salinity is high (Fig. 12), and the temperature is low (Fig. 13). The fact that nutrients are high and that the cold water of high salinity is at the surface is probably explained by upwelling brought about by an eddy current over the continental shelf.

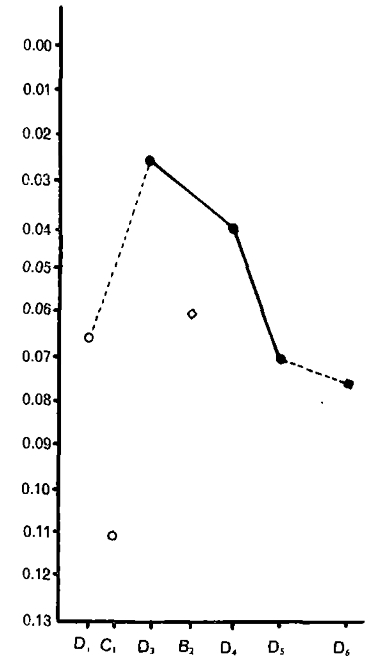

Fig. 10 Diversity index calculated at the net haul stations.

Key for Figs. 10-16

- ■ Boundary station in western sub-tropical water
- ● Agulhas stream station
- ◇ Coastal station off Tugela River
- ○ Coastal station
- ⌴ = 8 nautical miles. Measure of distance of stations from the coastline

Stations on transect D have been linked by a solid line —where they are situated in the Agulhas Stream and by a dotted line to D6 in the western sub-tropical water and to D_1, a coastal station.

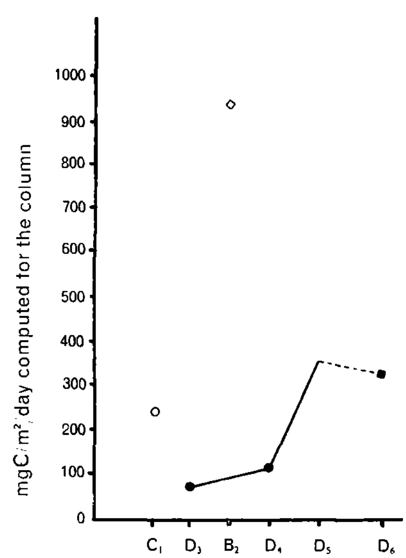

Fig. 11 Primary Productivity Measurements at the net haul stations

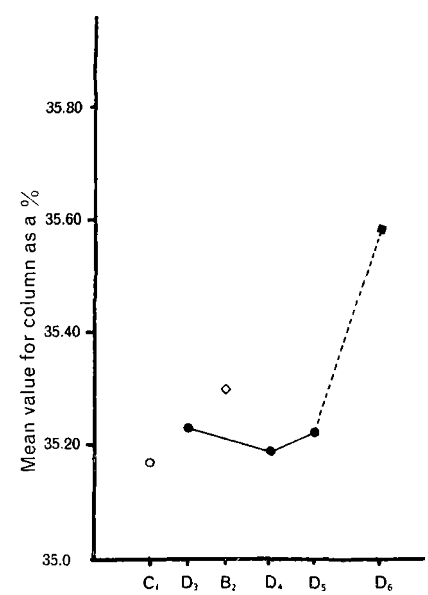

Fig. 12 Salinity at net haul stations.

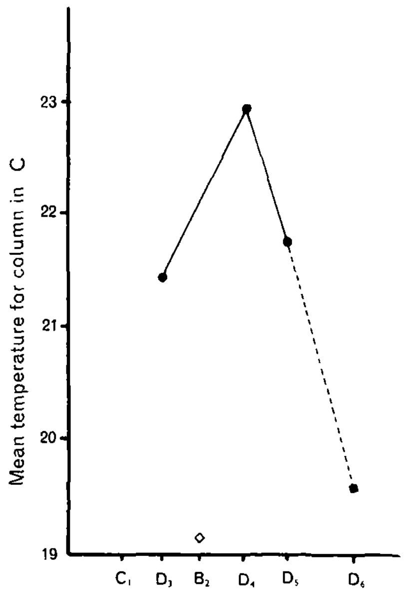

Fig. 13 Temperature at net haul stations.

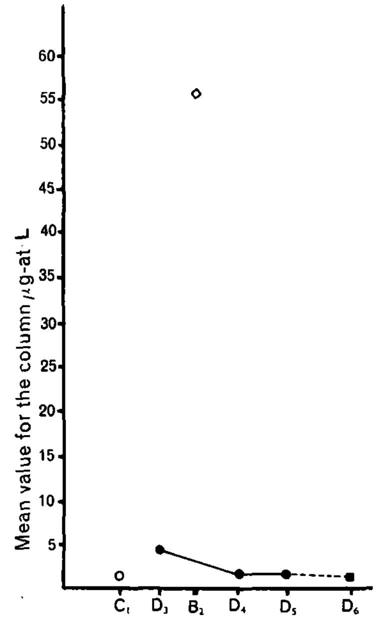

Fig. 14 Nitrate Nitrogen at the net haul stations.

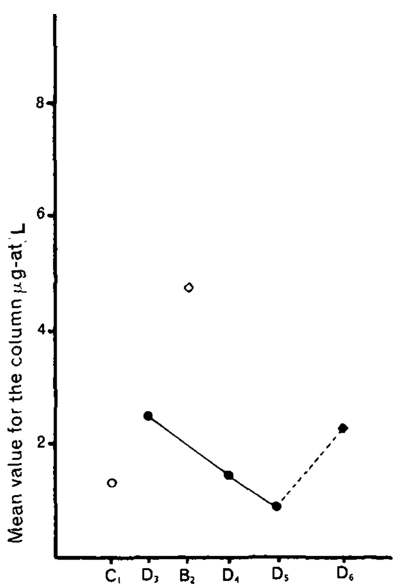

Fig. 15 Silica at the net haul stations.

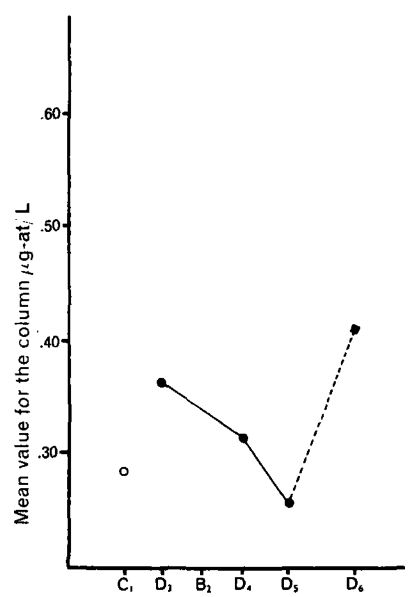

Fig. 16 Phosphate at the net haul stations.

18

which is broad here. The source of nutrients may also be the Tugela River, which is the largest river in Natal, draining fertile farm areas. It is not surprising, therefore, that B_2 is situated in a region of high productivity (Fig. 11). The cells were observed to be large and actively growing and dividing.

The productivity was calculated as 950 mgC/m²/day (Burchall 1968), and is the highest recorded on the cruise, the next highest being 360 mgC/m²/day from station D_5. A previous record of productivity from this region off the Tugela River has also been very high (*Anton Bruun* Cruise, 1964, 3000 mgC/m²/day).

The greatest variety of species was found at station B_2. There were 14 more than B_4 on the same transect and 20 more than D_5, which has 75 different species and the greatest number apart from those on line B (Fig. 2). It is also interesting to note that two new taxa have been described from B_2 (Thorrington-Smith, 1969).

B_2 has great affinities with all stations except D_6, and, as stated before, it is suspected that this station off the Tugela River is an important source of actively growing and dividing species.

Summary and conclusions

Samples of phytoplankton were collected at stations in the Agulhas stream area in the vicinity of Durban. A Discovery type N50 V net and a Van Dorn water sampler were used.

The species present in the samples were identified and counted to give an estimate of relative abundance of species at each station.

Using these results the affinities between all combinations of pairs of stations were worked out in two ways. Firstly from a value based on the number of species shared between the stations under comparison; and secondly by using a similarity index which also takes into account the relative abundance of species at the two stations. This indicated on the limited data available that the Agulhas current stations have greater affinity with each other than with those stations outside the Agulhas stream.

However diversity indices were also calculated for all stations. This index gives a single value for each station based on the numbers of species present and their relative abundance in the sample. The stations within the Agulhas stream had a high diversity of species relative to the coastal stations, and the station in western sub-tropical water.

The greatest number of different species were found at a station situated off the Tugela River. These included two new taxa. The cells were actively dividing and the primary productivity was exceptionally high as were the nutrients.

Phytoplankton has not been sampled extensively in this area before, and most species identified are new locality records. The method of combining expressions of similarity and diversity is considered to be valuable in summarising the confusion of large complex species lists.

Acknowledgments

Thanks are due to the Council for Scientific and Industrial Research of South Africa who invited the Oceanographic Research Institute to participate in this cruise. I am grateful to Miss B. Mitchell-Innes, Miss J. Burchall and Mr. B. Roets for collecting the samples; and am particularly grateful to Miss J. Burchall for making available the hydrographic and primary productivity data from the cruise.

I am indebted to Professor Lutjeharms of the Botany Department of the University of Cape Town for making available facilities for the microscopic examination of the samples; and am very grateful to Mrs. P. Reinecke of the same department for valuable advice on taxonomic problems.

I also wish to thank Professor Linhardt of the University of Natal for his statistical advice; and Mr. F. Anderson of the Council for Scientific and Industrial Research for help with the hydrology; as well as Dr. A. Alexander, Dr. J. R. Grindley, Dr. M. Angel and Mr. J. Wallace for their valuable suggestions and constructive criticisms of the manuscript, and my colleagues at the Oceanographic Research Institute for their assistance.

I also wish to acknowledge the financial support for this research programme provided by the Marine Research Unit of the Council for Scientific and Industrial Research, Pretoria.

Literature cited

ARMSTRONG, F. A. J. and WICKSTEAD, J. H., 1962. A note on the preservation of plankton samples with formalin. *J. Cons. perm. int. Explor. Mer.*, **27** (2): 129-130

BURCHALL, JOAN, 1968. Primary production studies in the Agulhas current region off Natal — June, 1965. *Invest. Rep. oceanogr. Res. Inst.*, (20): 1-16

MARGALEF, R., 1958. Temporal succession and spatial heterogeneity in phytoplankton. Buzzati-Traverso, A. A. Ed. Perspectives in Marine Biology. Berkeley, University of California Press, p. 323-349

MARGALEF, R., 1967. Some concepts relative to the organisation of plankton. *Oceanogr. Mar. Biol. Ann. Rev.*, **5**: 257-289

MCINTOSH, R. P., 1967. An index of diversity and the relation of certain concepts to diversity. *Ecology*, **48** (3): 392-404

NEL, E. A., 1968. The microplankton of the South-West Indian Ocean. *Investl Rep. Div. Fish. S. Afr.*, (62): 1-40 Tables VI-IX

ORREN, M. J., 1966. Hydrology of the South-West Indian Ocean. *Investl Rep. Div. Sea Fish. S. Afr.*, (55): 1-35

SIMPSON, E. H., 1949. Measurement of diversity. *Nature Lond.*, **163**, 688

SOURNIA, A., 1968. Diatomées planctoniques du Canal Mozambique et de l'Ile Maurice. *Mém. O.R.S.T.O.M.*, (31): 1-120

THORRINGTON-SMITH, M., 1969. Descriptions of two new diatoms from the South West Indian Ocean. *Nova Hedwigia* (In Press).

UTERMÖHL, H., 1958. Zur utervolkumnung der quantitativen phytoplankton *Methodik Mitt. Int. Ver. Limnol.*, **9**: 1-38

WALKER, J. R., 1944. Formaldehyde. New York, Reinhold Publishing Corp.

TABLE I SPECIES LIST OF PHYTOPLANKTON COLLECTED ON THE *RSA* CRUISE, JUNE 1965

Samples collected with an N50 V plankton net (stations D1–B4, first group). Each species is expressed as a % of the total number of cells counted in the sample. A + represents a species present in the sample but not present in the count. A ++represents a species present as less than 0.50% in the count. Percentages have beencorrected to the nearest whole number.

Samples collected with a Van Dorn bottle sampler (stations E1–A4, second group). Presence of a species represented by a +. (Three stations were sampled twice; this is indicated as (1) and (2)).

STATIONS	D 1	D 3	D 4	D 5	D 6	C 1	B 2	B 4	E 1	E 2	E 3	D 2	D 3(1)	D 3(2)	D 4	D 5	C 1	C 2	C 4(1)	C 4(2)	B 2	B 4(1)	B 4(2)	A 2	A 3	A 4
SPECIES																										
BACILLARIOPHYCEAE (diatoms)																										
Coscinodiscineae																										
COSCINODISCACEAE																										
Coscinodiscus argus Ehr.			++																							
C.concinnus Smith							++																			
C.divisus Grun.							+																			
C.eccentricus Ehr.						+																				
C.granii Gough							+																			
C.lineatus Ehr.							+	+																		+
C.nodulifera Schmidt							++																			
C.oculis-iridis Ehr.							+																			
C.radiatus Ehr.	1					++		+																		
Coscinosira polychorda Hust.																					+					
Cyclotella sp.								+																		
Gosslieriella tropica Schütt			++	+	+			+																		
Planktoniella sol (Wall.) Schütt		++		++	+	+	1	+													+					
Skeletonema costatum (Grev.) Cleve		3	3	+			++					+					+									
Stephanopyxis palmeriana (Grev.) Grun.						1	1	+																		
Thalassiosira subtilis (Ostenf.) Gran								+													+					
Th. sp.								+								+					+					
ACTINODISCACEAE																										
Asterolampra marylandica Ehr.				++	+			+												+						
A.van heurckii Grun.					+																					
Asteromphalus heptactis (Bréb.) Ralfs in Pritch.				++	+		+	+																		
A.indicus Silva	++				+																					
A.robustus Castr.						++		+																		
Biddulphineae																										
BIDDULPHIACEAE																										
Biddulphia mobiliensis Bail.				+																						
Cerataulina pelagica (Cleve) Hendey	++	1	++	1	++	1	++	+				+	+	+	+	+	+	+	+	+	+					
Climacodium frauenfeldianum Grun.	1	2	1	1			2	+					+		+			+		+	+					
Ditylum sol (Grun.) de Toni	++	++					++					+														
Eucampia cornuta (Cleve) Grun.	++	++						+	+			+									+					
E.zoodiacus Ehr.			++	++		1	++																			
Hemialus chinensis Grev.						++	+																			
H.hauckii Grun.	1	3	++	4	1		2	+	+						+	+	+		+	+	+					+
H.membranaceus Cleve	1	2	++			+	+	+				+				+										+
Streptotheca tamesis Shrubs.	++					1	1					+				+										
Chaetoceraceae																										
Chaetoceros affine Laud. f. *affine*	3	3	1	3	12	3	2	+				+		+	+			+	+	+	+	+				+
Ch.affine Laud.f. *Inaequale* Thorr.-Sm.						3	9	+	+	+	+								+		+			+		
Ch.affine Laud. f. femur (Schütt) Taylor																					+					

Stations	D 1	D 3	D 4	D 5	D 6	C 1	B 2	B 4	E 1	E 2	E 3	D 2	D 3(1)	D 3(2)	D 4	D 5	C 1	C 2	C 4(1)	C 4(2)	B 2	B 4(1)	B 4(2)	A 2	A 3	A 4
Ch.affine var. *willei* (Gran) Hust.	2			++	5		1	+	+	+		+	+			+			+	+	+				+	+
Ch.anastomosans Grun.	3	1	++	1	1		1		+			+	+								+					+
Ch.atlanticum Cleve var. *atlanticum*		3					+												+						+	
Ch.atlanticum Cleve f. *audax* Schütt				5		4	3									+										
Ch.atlanticum Cleve var. *neopolitanum* Schröd.				2		+	+									+					+					
Ch.atlanticum Cleve var. *skeleton* (Schütt) Hust.	2		1		6		+	+				+			+		+			+			+			+
Ch.aurivillii Cleve						1										+										
Ch.breve Schütt	1	5				1	4	+				+			+	+		+	+	+	+					
Ch.ceratosporum Ost.				+																						
Ch.compressum Laud.	1	5	7			2	1	+	+				+	+	+		+	+	+	+	+			+		
Ch.concavicorne Mang.																									+	
Ch.constrictum Gran	1	++	1				1																			
Ch.convolutum Castr.	++										+									+						
Ch.costatum Pavill.	++	++	2				+																			
Ch.curvisetum Cleve				1			1											+			+					
Ch.dadayii Pavill.						3	++												+							
Ch.danicum Cleve						++	++						+	+							+					
Ch.decipiens Cleve					÷			+													+					
Ch.denticulatum Laud.		++	++				+					+														
Ch.didymum Ehr. var. *didymum*	++		++	+		1	+	+	+																	
Ch.difficile Cleve	1			1				+													+					
Ch.distans Van Heurck							5													+	+					
Ch.diversum Cleve	++						+																			
Ch.eibenii (Grun.) Meun.				++	+			+																		
Ch.filiferum Karst.							1																			
Ch.gracile Schütt	++					+																				
Ch.imbricatum Mang.	++				1																+					
Ch.laciniosum Schütt f. *laciniosum*		1		1		1	+	+				+	+		+	+		+		+	+	+				+
Ch.laciniosum Schütt f. *protuberans* Thorr.-Sm.	1			2	+		2	+				+					+		+	+						
Ch.laeve Leud.-Fort.					1		+	+				+					+									
Ch.lorenzianum Gran	14	8	14	13	20	26	11	+	+	+		+	+	+	+	+	+	+	+	+	+	+	+	+		+
Ch.messanense Castr.	13	11	8	9	11	10	7	+	+			+			+	+	+	+	+	+	+		+			+
Ch.neglectum Karst.													+	+	+	+										
Ch.pelagicum Cleve	+	5	1	1			++	+	+						+			+	+		+	+				
Ch.pendulum Karst.					+	+	+																			
Ch.peruvianum Brightw. *f.peruvianum*	1	++	1	1	3	2		+				+		+			+		+	+	+					+
Ch.pseudocurvisetum Mang.	++	2	1	++	+	1	1	+				+	+			+	+									
Ch.radicans Schütt	13	1	7	10	9		+	+	+			+		+		+				+						+
Ch.rostratum Laud. f. *glandazii* (Meun) Taylor	1	2	++	1	+	++	++								+	+	+			+	+		+			
Ch.teres Cleve							+					+					+									
Ch.wighamii Brightw.				1																						
Rhizosoleniineae																										
BACTERIASTRACEAE																										
Bacteriastrum comosum Pavill.	2	1	++	1	++	1	+	+						+	+	+			+			+				+
B.elongatum Cleve	6	3	1	1	2	3	3	+	+			+	+		+	+	+	+	+	+	+	+			+	+
B.tenue Steemann Nielsen							++																			
B.furcatum Shadb.	4			2	5	++	1	+	+			+	+	+	+	+	+	+	+	+	+	+		+		+
B.hyalinum Laud. f. *hyalinum*	1	2	2		++	1	1	+				+			+	+		+			+					+
B.hyalinum Laud. f. *princeps* Cleve							+																			
B.minus Karst.	++	2	++	++		1	3	+	+			+		+	+	+		+	+		+					
B.varians Laud.	4	3	10	++	1	10	1	+				+	+		+	+	+	+						+		+
CORETHRONACEAE																										
Corethron criophyllum Castr.	++	++	++		++	++	1	+	+	+		+	+	+	+	+	+	+	+	+	+		+		+	
LEPTOCYLINDRACEAE																										
Dactyliosolen antarcticus Castr.			2														+									
D.mediterraneus Perag.	1	3		2		+	1	+																		

Stations	D 1	D 3	D 4	D 5	D 6	C 1	B 2	B 4	E 1	E 2	E 3	D 2	D 3(1)	D 3(2)	D 4	D 5	C 1	C 2	C 4(1)	C 4(2)	B 2	B 4(1)	B 4(2)	A 2	A 3	A 4
Detonula moseleyana (Castr.) Gran			1				++	+																		
Guinardia flaccida (Castr.) Perag.		2	++	1			1	+					+		+			+			+					
Lauderia annulata Cleve (Syn. *L.borealis* (Gran))			1	1			++		+			+						+			+					
Leptocylindrus sp.				++			++																			
Leptocylindrus danicus Cleve	++	1	++	++			++	+	+			+	+	+		+	+	+	+	+						+
Schroederella delicatula (Perag.) Pavill.	1	3	1	2		2	+	+					+			+	+				+				+	+
RHIZOSOLENIACEAE																										
Rhizosolenia acuminata (Perag.) Gran																	+		+							
Rh.alata Brightw. f. *alata*												+	+		+				+	+						
Rh.alata Brightw. f. *gracillima* (Cleve) Gran	1			++	++		++	+				+	+													
Rh.alata Brightw. f. *indica* (Perag.) Hust.						+	+																			
Rh.bergonii Perag.						++																				
Rh.calcar-avis Schultze			++	++			++	+							+						+					
Rh.castracanei Perag.												+						+								
Rh.cylindrus Cleve	++	++		++	++		+	+												+						
Rh.fragilissima Bergon	++		++	+			+	+	+			+	+	+		+	+	+	+		+			+		+
Rh.hebetata Bail. f. *hiemalis* Gran	++	++		++	+			+							+					+	+					
Rh.hebetata Bail. f. *semispina* (Hansen) Gran																				+						
Rh.hyalinum Ostenf.									+									+								
Rh.imbricata Brightw. var. *shrubsolei* (Cleve) Schrod.	1	1		1		++	+	+						+	+			+		+	+					+
Rh.robusta Norman															+											
Rh.setigera Brightw.	++	1	1		+	+	++	+				+			+		+		+	+	+			+		
Rh.styliformis Brightw. var. *latissima* Brightw.			++				+																			
Rh.styliformis Brightw. var. *longispina* Hust.							++															+				
Rh.styliformis Brightw. var. *styliformis*	++		++			1	++	+																		
Fragilariineae																										
FRAGILARIACEAE																										
Asterionella japonica Cleve		1	2				+					+			+						+					
Fragilaria leptostauron (Ehr.) Hust.																+										
Licmophora ehrenbergii (Kutz.) Grun.						+																				
Striatella sp.								+																		
Synedra pelagica Hendey				+	5	++		+			+									+		+				+
Synedra sp.A				++	1																					
Synedra sp.B				++		+		+																		
Synedra sp.C					1	+		+																		
Thalassionema nitzschoides Grun.	1	2	1	2	+	3	3	+	+			+	+	+	+	+		+	+		+				+	+
Thalassiothrix acuta Karst.					++	++	++	+								+		+	+	+	+					
Th.delicatula Cupp			++		+																					
Th.frauenfeldii Grun.	11	13	12	18	2	24	20	+	+	+	+	+	+	+	+	+	+	+	+	+	+	+		+	+	+
Th.longissima Cleve and Grun.					++	+		+			+		+	+		+	+	+				+	+			
Th.vanhoeffenii Heid. and Kolbe						1	++	+																		
Acnanthineae																										
ACNANTHACEAE																										
Acnanthes longipes Agardh								+																		
Naviculineae																										
BACILARIACEAE																										
Bacillaria paxillifer (Müller) Hendey					+																					
Nitzschia closterium (Ehr.) Smith		++	++	+		+	+	+	+	+		+					+				+				+	
N.delicatula Hasle		+	5				+									+										
N.pungens Cleve		+	2			+																				
N.seriata group																+	+	+	+						+	
N.longissima (Bréb) Ralfs in Pritch.																	+									
NAVICULACEAE																										
Navicula gigantea Hust.											+		+			+	+		+						+	+

Stations	D 1	D 3	D 4	D 5	D 6	C 1	B 2	B 4	E 1	E 2	E 3	D 2	D 3(1)	D 3(2)	D 4	D 5	C 1	C 2	C 4(1)	C 4(2)	B 2	B 4(1)	B 4(2)	A 2	A 3	A 4
N.membranacea Cleve	++	++		++		+	+	+				+									+					+
N. sp.			++																							
Tropidoneis lepidoptera (Greg.) Cleve			++																							
CHRYSOPHYCEAE																										
DICTYOCHACEAE																										
Dictyocha fibula Ehr.								+																		
CYANOPHYCEAE																										
NOSTOCACEAE																										
Nostoc sp.													+			+				+	+					
OSCILLATORIACEAE																										
Trichodesmium hildebrandtii Gomont		++				+																				
DINOPHYCEAE																										
PROROCENTRACEAE																										
Phalacroma argus Stein							+																			
AMPHISOLENIACEAE																										
Amphisolenia bidentata Schröd.			++	+			+	+																		
DINOPHYSIACEAE																										
Dinophysis tripos Gourr.						++																				
ORNITHOCERCACEAE																										
Histioneis pietschmanni Böhm				++																						
Ornithocercus steinii Schütt						++																				
O.thurnii (Schmidt) Kof. and Scogs.			++																							
PERIDINIACEAE																										
Glenodinium penardeforme (Lindern) Schill.						++																				
Peridinium globosum Dang.				++																						
P.oceanicum Vanhoffen	++			I	+		++																			
P.solidicorne Mang.				++																						
P. sp.		++																								
CERATOCORYACEAE																										
Ceratocorys horrida Stein								+																		
CERATIACEAE																										
Ceratium breve (Ost. and Schmidt) Schröd.							++																			
C.buceros Zach. f. *denticulatum* Jörg.	++																									
C.buceros Zach. f. *tenue* (Ost.) Schmidt				+																						
C.carriense Gourr.				+												+										
C.contortum (Gourr.) Cleve								+																		
C.extensum (Gourr.) Cleve								+														+				
C.fusus (Ehr.) Dujardin													+													
C.inflatum (Kof.) Jörg.						+		+																		
C.limulus Gourr.				+																						
C.macroceros (Ehr.) Cleve								+																		
C.pentagonum Gourr.				++			++																			
C.platycorne von Paday						++																				
C.ranipes Cleve							++																			
C.setacium Jörg		++																								
C.teres Kof.		++						+										+								
C.trichoceros (Ehr.) Kof.						+	+	+																		
C.tripos (Müller) Nitzsch			++	++	++		++	+									+									
OXYTOXACEAE																										
Oxytoxum sp.																	+									
PHYTODINIACEAE																										
Pyrocystis lunula (Schütt) Schütt																+										
P.pseudonoctiluca Thomson				++																						

Reprinted from *Deep-Sea Research*, 1970, vol. 17, p. 595-601

Globorotalia menardii flexuosa (Koch): An 'extinct' foraminiferal subspecies living in the northern Indian Ocean*

ALLAN W. H. BÉ* and ANDREW MCINTYRE†

(*Received* 3 *September* 1969)

Abstract—*Globorotalia menardii flexuosa* is still living in the northern Indian Ocean. This planktonic foraminiferal subspecies was believed to have become extinct after having thrived in a circumtropical belt in the Atlantic, Indian and Pacific oceans during the warm interstadial of the Wisconsin and the Sangamon Interglacial. A total of about 1103 specimens have been collected at 47 plankton stations.

INTRODUCTION

PLANKTON samples collected during the International Indian Ocean Expedition in the Bay of Bengal, the Arabian Sea and the north-equatorial Indian Ocean have yielded many living specimens of *Globorotalia menardii flexuosa* (Koch) (Table 1). ERICSON *et al.* (1964) considered this subspecies extinct after having flourished 90,000 to 125,000 years ago during the Sangamon Interglacial (= *V* zone) and the warm interstadial of the last ice age (= *X* zone). The discovery that this form is still living in the northern Indian Ocean has interesting biological implications and may present clues to the paleo-oceanographic conditions when it was prevalent on a global scale.

MORPHOLOGY AND STRATIGRAPHIC DISTRIBUTION

The foraminiferal tests with chambers twisted towards the umbilical side were first recognized by KOCH (1923), for his *Pulvinulina tumida* Brady, var. *flexuosa*, which was later renamed *Globorotalia tumida flexuosa* (Koch). Subsequent workers have noted that the flexuose forms appear in both *Globorotalia tumida* (Brady) and *G. menardii* (d'Orbigny) and have considered them as subspecific characters. PARKER (1967; personal communication) believes that the flexuose condition is probably restricted to *G. tumida*, but our specimens almost invariably belonged to *G. menardii* (Fig. 1).

The earliest abundant occurrence of *G. tumida flexuosa* is in the *Globorotalia margaritae* zone of late Miocene age (BOLLI, 1966). This zone is now considered to be of early Pliocene age by Saito (in HAYS *et al.*, 1969). ERICSON, EWING and WOLLIN (1964) observed *Globorotalia menardii flexuosa* in large numbers with normal *G. menardii* and *G. tumida* at certain Quaternary levels of tropical and subtropical North Atlantic deep-sea cores. These three varieties were often associated with each other, although *G. m. flexuosa* was restricted to the Sangamon interglacial (*V* Zone) and the warm interstadial of the Wisconsin glacial age (*X* or Flexuosa Zone). *G. m. flexuosa*

*Contribution Number 1476 of the Lamont–Doherty Geological Observatory.
*Lamont–Doherty Geological Observatory of Columbia University, Palisades, New York 10964, U.S.A. and Department of Biology, City College of the City University of New York.
†Department of Geology, Queens College of the City University of New York.

Table 1. *Plankton samples containing* Globorotalia menardii flexuosa *and* Globorotalia menardii sensu stricto *in the northern Indian Ocean. See Fig.* 3 *for their locations.*

Ship	*Cruise Station Sample*	*Lat. North*	*Long. East*	*Date*	*Depth range* (m)	*Surface temperature* (°C)	*Volume of water filtered* (m³)	*Number of* G. menardii flexuosa	*Number of* G. menardii sensu stricto	*Percentage of* flexuosa *specimens*
Bruun	A-12-69	17° 41′	68° 03′	3 Mar. 1963	125– 250	28·0	222	1	2	33
Bruun	I-52-264	18° 55′	91° 59′	6 Apr. 1963	0– 250	28·8	365	4	3	57
Bruun	I-53-268	18° 33′	91° 16′	7 Apr. 1963	0– 250	28·2	555	5	4	55
Bruun	I-53-267	18° 33′	91° 16′	7 Apr. 1963	0– 125	28·2	81	1	5	16
Bruun	I-53-269	18° 33′	91° 16′	7 Apr. 1963	0– 200	28·2	—	20	57	26
Bruun	I-54-271	18° 24′	90° 45′	7 Apr. 1963	0– 250	28·4	316	1	—	100
Bruun	I-54-272	18° 24′	90° 45′	7 Apr. 1963	0– 125	28·4	148	2	4	33
Bruun	I-55-277	18° 20′	90° 06′	8 Apr. 1963	0– 250	28·1	350	1	—	100
Bruun	I-56-281	18° 15′	89° 20′	8 Apr. 1963	0– 125	28·3	175	8	1	88
Bruun	I-56-282	18° 15′	89° 20′	8 Apr. 1963	0– 250	28·3	426	3	2	60
Bruun	I-57-286	18° 13′	88° 42′	8 Apr. 1963	0– 125	29·0	210	3	6	33
Bruun	I-57-287	18° 13′	88° 42′	8 Apr. 1963	0– 250	29·0	291	3	5	37
Bruun	I-57-288	18° 13′	88° 42′	8 Apr. 1963	0–1000	29·0	650	3	6	33
Bruun	I-58-293	18° 11′	88° 04′	9 Apr. 1963	0– 125	28·3	224	22	28	46
Bruun	I-58-294	18° 11′	88° 04′	9 Apr. 1963	0– 250	28·3	247	2	8	20
Bruun	I-58-296	18° 11′	88° 04′	9 Apr. 1963	0– 200	28·3	—	43	120	26
Bruun	I-59-298	18° 00′	87° 16′	9 Apr. 1963	0– 125	28·1	191	6	3	66
Bruun	I-59-301	18° 00′	87° 16′	9 Apr. 1963	0– 250	28·1	291	5	8	38
Bruun	I-60-304	17° 54′	86° 31′	9 Apr. 1963	0– 125	28·2	209	1	1	50
Bruun	I-60-305	17° 54′	86° 31′	9 Apr. 1963	0– 250	28·2	368	22	9	71
Bruun	I-60-306	17° 54′	86° 31′	9 Apr. 1963	0–1000	28·2	850	14	13	52
Bruun	I-61-310	17° 53′	85° 56′	9 Apr. 1963	0– 125	28·2	203	3	2	60
Bruun	I-61-311	17° 53′	85° 56′	9 Apr. 1963	0– 250	28·2	277	6	2	75
Bruun	I-62-316	17° 52′	85° 12′	10 Apr. 1963	0– 300	28·6	296	1	2	33
Bruun	I-63-322	17° 56′	84° 37′	10 Apr. 1963	0–1000	29·2	1060	5	10	33
Bruun	I-64-326	17° 48′	84° 02′	10 Apr. 1963	0– 25	28·5	86	1	2	33
Bruun	I-75-361	13° 16′	91° 34′	18 Apr. 1963	0– 250	29·5	268	1	0	100
Bruun	2-141-817	03° 13′	80° 02′	14 July 1963	0– 125	28·5	—	1	0	100
Bruun	2-142-813	00° 33′	80° 08′	15 July 1963	0– 250	29·0	506	5	50	9
Bruun	2-144-832	04° 18′	80° 08′	17 July 1963	0– 250	28·1	—	6	54	10
Bruun	3-146-7008	10° 09′	59° 55′	15 Aug. 1963	0– 150	26·7	—	5	162	3
Bruun	5-282-1678	16° 13′	63° 29′	29 Jan. 1964	0– 200	25·2	—	270	613	31
Bruun	5-283-1686	15° 42′	60° 52′	30 Jan. 1964	125– 250	25·1	—	11	40	21
Bruun	5-284-1698	15° 22′	58° 12′	31 Jan. 1964	0– 200	23·9	—	1	30	3
Bruun	6-335B-7195	03° 46′	65° 05′	26 May 1964	275–2575	28·9	—	23	115	17
Bruun	6-335B-7197	03° 46′	65° 05′	26 May 1964	0– 275	28·9	—	52	92	36
Bruun	6-336A-7207	02° 03′	65° 04′	26 May 1964	275– 817	29·2	—	1	5	16
Bruun	6-336A-7209	02° 03′	65° 04′	26 May 1964	0– 275	29·2	—	7	87	7
Bruun	6-336B-7203	01° 50′	65° 07′	27 May 1964	0– 275	29·2	—	23	71	24
Bruun	6-337A-7211	00° 03′	65° 00′	27 May 1964	0– 275	29·9	—	6	109	5
Bruun	6-338A-7220	02° 00′S	64° 54′	28 May 1964	0– 528	29·3	—	6	200	3
Bruun	6-334A-7189	06° 01′	64° 59′	24 May 1964	0– 275	29·2	—	1	2	33
Bruun	6-334A-7190	06° 01′	64° 59′	24 May 1964	275– 700	29·2	—	4	6	40
Bruun	6-334B-7186	05° 48′	64° 57′	24 May 1964	275–2868	29·2	—	1	10	9
Bruun	6-335A-7201	04° 02′	65° 03′	25 May 1964	0– 275	28·9	—	68	161	30
Conrad	9-127	06° 38′	76° 25′	14 June 1965	0– 300	—	171	20	191	9
Conrad	9-128	07° 21′	72° 40′	15 June 1965	0– 290	28·3	138	8	140	5
Conrad	9-129	06° 03′	69° 47′	16 June 1965	0–1000	28·9	529	4	201	2
Conrad	9-130	05° 47′	66° 34′	17 June 1965	0–2000	29·5	1169	1	7	12
Kistna	16-383-0634	13° 00′	81° 00′	23 June 1964	0– 200	—	—	203	202	50
Kistna	16-384-0614	13° 00′	82° 00′	24 June 1964	0– 200	—	—	32	80	29
Kistna	16-387-0640	13° 00′	85° 00′	24 June 1964	0– 140	—	—	11	18	38
Kistna	16-388-0619	13° 00′	86° 00′	25 June 1964	0– 140	—	—	60	68	47

Table 1. *continued.*

Ship	*Cruise Station Sample*	*Lat. North*	*Long. East*	*Date*	*Depth range* (m)	*Surface temperature* (°C)	*Volume of water filtered* (m³)	*Number of* G. menardii flexuosa	*Number of* G. menardii sensu stricto	*Percentage of* flexuosa *specimens*
Kistna	16–390–0639	14° 04′	87° 52′	25 June 1964	0– 181	—	—	13	30	30
Kistna	16–392–0626	14° 04′	85° 45′	26 June 1964	0– 129	—	—	13	32	29
Kistna	16–393–0631	14° 07′	85° 45′	26 June 1964	0– 200	—	—	34	49	41
Kistna	16–394–0611	14° 10′	84° 20′	27 June 1964	0– 181	—	—	2	4	33
Kistna	19–513	09° 57′	95° 03′	22 Aug. 1964	0– 153	—	—	P*	P*	—
Meteor	*I*–101–0864	12° 13′	51° 48′	19 Dec. 1964	0– 200	—	—	P*	P*	—
Meteor	*I*–197–0665	14° 18′	72° 44′	16 Feb. 1965	0– 200	—	—	16	60	21
Meteor	*I*–198–0658	14° 14′	72° 19′	17 Feb. 1965	0– 200	—	—	P*	P*	—
Vitijaz	35–5229–0033	07° 08′	91° 31′	14 Sept. 1962	0 –200	—	—	8	53	13
							Total	1103†	3245	

*P equals present.
†Eight hundred and thirty-eight ' medium-flexed ' and 265 are ' strongly flexed '.

became extinct during the following interval of cold climate, but *G. menardii* and *G. tumida* survived to the present.

DISTRIBUTION IN RECENT DEEP-SEA SEDIMENTS OF THE INDIAN OCEAN

There has been no previous report of the occurrence of *Globorotalia menardii flexuosa* in Recent deep-sea sediments of the Indian Ocean or any other ocean. *G. menardii* is the dominant species in the surface sediments of the Bay of Bengal, but no flexuose forms were found (Belyaeva, 1967). *G. m. flexuosa* was not recorded in the tops of two equatorial deep-sea cores obtained along 78°E. (Oba, 1967)* nor in the sediments of the Andaman Sea and eastern Bay of Bengal (Frerichs, 1968). This may have been due to the general sparsity of *G. menardii* in the latter region as was also noted in the living population. On the other hand, Bhatt (1969) found forms resembling *G. menardii flexuosa* in the sediments off the Vishakhapatnam coast in the western Bay of Bengal and Kameswara Rao (personal communication) has noted the occurrence of *G. m. flexuosa* in sediments of the eastern Arabian Sea (Table 2).

DISTRIBUTION OF LIVING POPULATIONS

Globorotalia menardii is a common species in tropical and subtropical waters of the Indian Ocean and appears in two main regions of maximum abundance where it exceeds 20% of the total foraminiferal population (Fig. 2). According to Belyaeva (1964) it occurs in low concentrations in the northwestern Indian Ocean and Arabian Sea and south of 20°S, but it is more frequent in the central waters. However,

*It did occur at 160 cm in core KA-18, correlated with the upper part of the last glacial (Wisconsin).

Table 2. Sediment samples of core tops containing G. menardii flexuosa *from the Arabian Sea. (Data from Mr. K. Kameswara Rao).*

Cruise and Sta.	*Lat.*	*Long.*	*Water depth*	*No. of specimens of* G. m. flexuosa *in top centimetre of core*
Darshak 4–42	18°36·0′N	70°39·4′E	96 m	3
43	18°33·5′N	70°21·6′E	204 m	13
44	18°35·0′N	70°03·0′E	1820 m	176
45	18°49·0′N	69°47·5′E	1660 m	33
46	19°03·0′N	69°30·4′E	1460 m	78
Darshak 5–52	19°02·0′N	69°34·0′E	2240 m	83
54	18°47·0′N	70°08·5′E	800 m	102

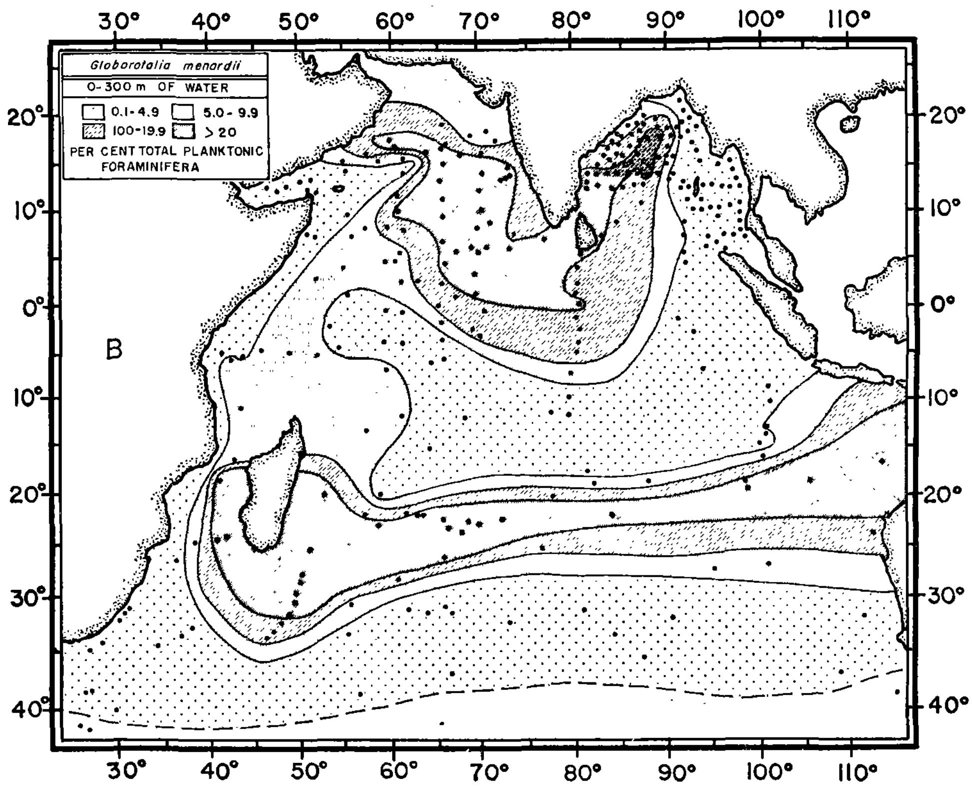

Fig. 2. Distribution of living populations of *Globorotalia menardii* (d'Orbigny) *sensu stricto*, pieced together from samples collected during different seasons. Since the northwest and southeast monsoons cause reversals in oceanic circulation, the distribution may well deviate from the actual seasonal conditions in the Bay of Bengal and the Arabian Sea.

G.menardii flexuosa has not been reported in the plankton of the Indian Ocean or Bay of Bengal (Belyaeva, 1964 and 1967) nor among the living planktonic Foraminifera in the southeast Indian Ocean and along 90°E between the equator and Antarctica (Ujiié, 1968; Boltovskoy*, 1969).

The distribution and abundance of flexuose *Globorotalia menardii* in the northern Indian Ocean closely parallel those of the normal populations. In the plankton

*Boltovsky (1968) discovered in the eastern tropical Atlantic three specimens of *G. menardii* whose " last chambers were situated at an angle with respect to whole coil ", typical of *G. menardii flexuosa* (Koch).

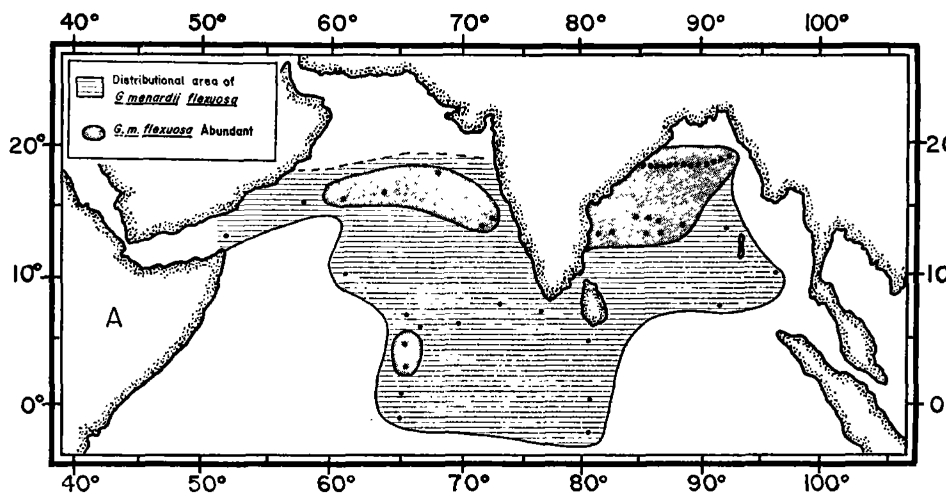

Fig. 3. Distribution of living populations of *Globorotalia menardii flexuosa* (Koch).

collections of the International Indian Ocean Expedition, sorted at the Indian Ocean Biological Centre, at the Smithsonian Oceanographic Sorting Center and in our laboratory, *G. m. flexuosa* appeared in 47 out of 285 plankton stations where *G. menardii* was present (Fig. 3, Table 1). The absence of the flexuose form in the majority of the Indian Ocean plankton stations points to its rarity. Almost all specimens had protoplasm in their tests, so that contamination from sediment samples can be ruled out.

Globorotalia menardii flexuosa appears most numerous, but sporadically, in the Bay of Bengal. For instance, typical *flexuosa* was common between *Bruun* Stas. 53 and 63, but it was virtually absent a week or two later from Stas. 65 to 75 along a transect from Vishakhapatnam to the Andaman Islands. *G. menardii* (including *flexuosa*) was very rare in the eastern Bay of Bengal and the Andaman Sea, as was also noted in the bottom sediments by Frerichs (1968). We believe that *G. m. flexuosa* is more likely to be encountered in the western and central regions of the Bay of Bengal during the dry season and that it does not favor the very low salinities and turbid, epipelagic waters caused by high river discharge during the southeast monsoon.

Globorotalia menardii flexuosa is present all-year round in the northern Indian Ocean, as we have found it in all months except between October and December. Since it is more frequent in 0–200 m or deeper tows and none have been found in surface hauls (0–10 m), *G. m. flexuosa* may be considered a subsurface dweller. Its temperature and salinity tolerances can not be precisely determined due to inadequate information on their vertical distribution. The temperature in the upper 250 m in the Bay of Bengal samples (*Bruun* Stas. 53–75) ranged between 12 and 29·5°C. It ranged between 14 and 25·2°C for the central Arabian Sea samples (*Bruun* Stas. 282 and 284).

G. m. flexuosa is found in regions varying widely in salinities, ranging from the low values in the Bay of Bengal to high salinities in the Arabian Sea. The salinity in the upper 250 m in the Bay of Bengal ranged between 32·1 and 35·1‰, while the relatively high salinity in the upper 200 m of the Arabian Sea ranged from 35·7 to 36·3‰.

DISCUSSION

The flexuose forms in the northern Indian Ocean were almost always related to *G. menardii* rather than *G. tumida*. The degree of flexing depends largely on test size, i.e. strongly flexuose forms tended to be very large, while the smaller specimens appeared to be more like the normal *G. menardii*. In other words, unless the flexing occurred in an early growth stage it would be difficult to recognize whether *G. menardii* would eventually develop into a *flexuosa*. The flexuose condition seemed to develop in specimens that are generally at least 500 μ in length.

The question might be raised whether the flexuose form of twisted final chambers is a subspecific or an ecophenotypic variation of *G. menardii*? Is it genetically or environmentally controlled? There are arguments in favor of each. The ' subspecies ' concept is supported by the observation that it is a ' relict ' population in a comparatively restricted region of the northern Indian Ocean, while it is absent (or not yet observed) in the southern region of abundant *G. menardii* between Australia and Madagascar. In fact, there seem to be slight but noticeable differences between the northern and southern groups—the latter having a more strongly convex spiral side than the former. Moreover, *G. m. flexuosa* is generally considered absent today in the Atlantic Ocean and probably in the Pacific Ocean.

The other argument that *flexuosa* is merely a variant of *G. menardii* induced by some environmental factor is supported by the fact that many aberrant specimens of *G. menardii* occurred in the samples containing *G. m. flexuosa*, especially in the Bay of Bengal. There were an unusually large percentage of distorted and plastogamic specimens of *G. menardii*. LIDZ (1966, Fig. 4) inferred that such aberrant forms were caused by high water temperatures. But high temperature alone would not explain the restriction of *G. m. flexuosa* in the northern Indian Ocean (Table 1).

Another point in favor of the environmental influence rather than a genetic or evolutionary product is that the flexuose form is unlikely to have developed simultaneously in *G. menardii* and *G. tumida* and co-existed during several discontinuous intervals from the Miocene to the present.

Acknowledgements—We are indebted to Drs. N. K. PANIKKAR, T. S. S. RAO, Mr. K. KAMESWARA RAO of the National Institute of Oceanography of India; Mr. D. TRANTER, then curator of the Indian Ocean Biological Centre; Dr. I. E. WALLEN and Mr. D. DAMKAER of the Smithsonian Oceanographic Sorting Center, for their aid in making available the foraminiferal material in their respective plankton and sediment collections. Mrs. GRACE I. IRVING assisted in the sample analysis and LILLIAN CAVALLERO produced the scanning electron micrographs. We are grateful for the helpful discussions and communications with Miss F. L. PARKER, Drs. W. E. FRERICHS, D. B. ERICSON and T. SAITO. This work was supported by the National Science Foundation grants GB-6991 and GA-1205.

REFERENCES

BÉ A. W. H. and D. S. TOLDERLUND (In press) Distribution and ecology of living planktonic Foraminifera in surface waters of the Atlantic and Indian Oceans. In: *Micropaleontology of Oceans* (B. M. FUNNELL and W. R. RIEDEL, eds.). Cambridge Univ. Press, London.

BELYAEVA N. V. (1964) Distribution of planktonic Foraminifera in the water and on the floor of the Indian Ocean. (In Russian). *Trudy, Inst. Okeanol., Akad. Nauk SSSR*, **68**, 12–83.

BELYAEVA N. V. (1967) Distribution of the shells of planktonic Foraminifera on the floor of the Bay of Bengal and some methodological aspects of the analysis of Foraminifera. (In Russian). *Okeanologiia*, **7** (4), 645–654.

BHATT D. K. (1969) Planktonic Foraminifera from sediments off the Vishakhapatnam Coast, India. *Contrib. Cushman Fdn. foramin. Res.*, **20** (1), 30–35.

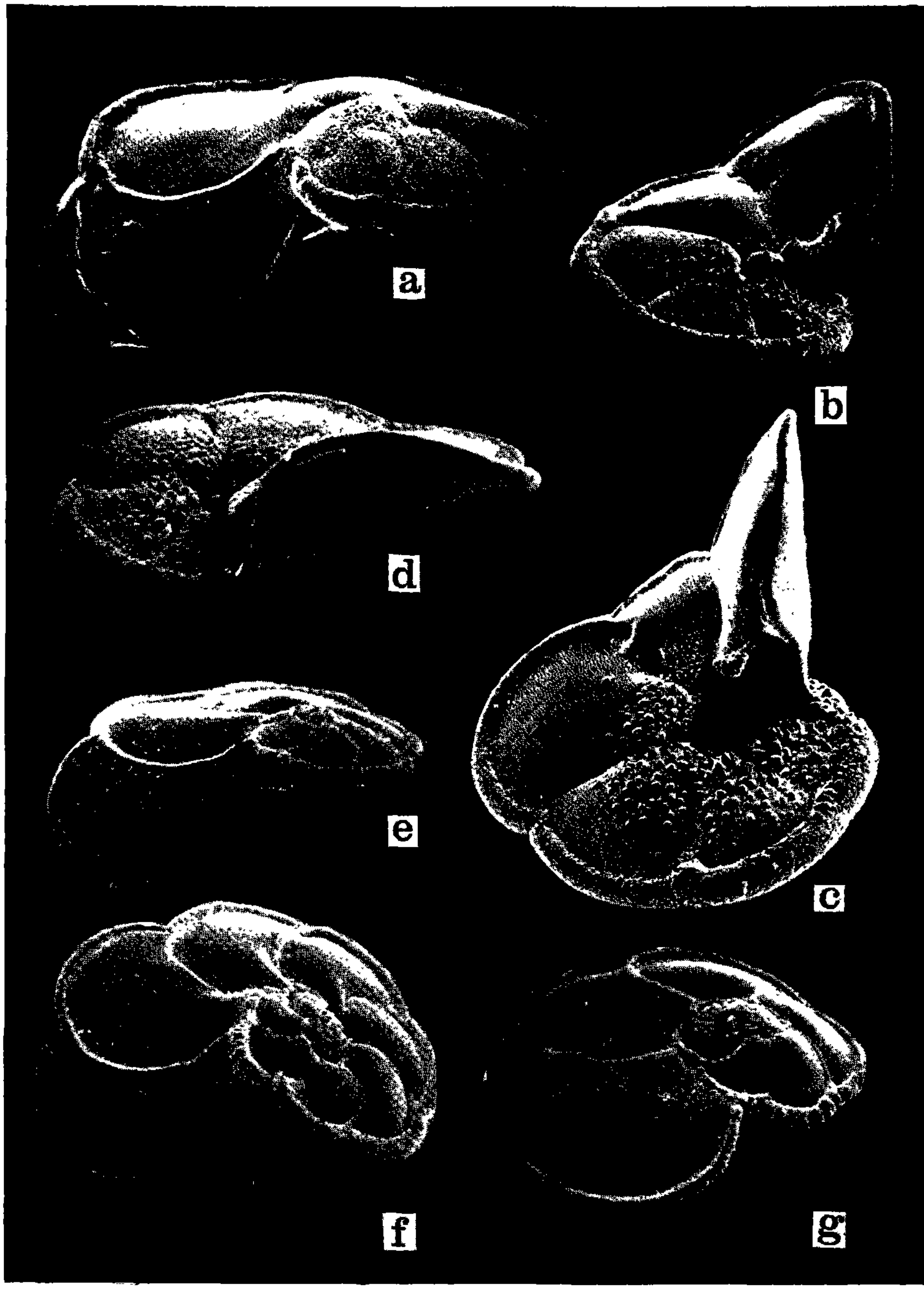

Fig. 1.

(a) and (b) Medium-flexed *Globorotalia menardii flexuosa* (Koch), collected alive in 0–1000 m plankton sample, *Bruun* cruise 1–60–306 (17° 54′N, 86° 31′E). The final chamber is gently, but noticeably twisted and curved to the umbilical side, and is significantly different from the normal curvature of the spiral side of *G. menardii sensu stricto*. (a, × 59; b, × 59).

(c) Strongly-flexed *Globorotalia menardii flexuosa* (Koch), collected alive in same plankton sample as (a) and (b). The final chamber is curved in a position nearly perpendicular to the umbilical side (× 59).

(d) and (f) Strongly-flexed *Globorotalia menardii flexuosa* (Koch), collected alive in 0–275 m plankton sample, *Bruun* cruise 6–335A–7201 (04° 02′N, 65° 03′E) (d, × 59; f, × 42).

(e) Medium-flexed *Globorotalia menardii flexuosa* (Koch), collected alive in same sample as (d) and (f). (× 45).

(g) *Globorotalia menardii* (d'Orbigny) *sensu stricto*, collected alive in 0–863 m plankton sample, *Bruun* cruise 3–145–7002 (12° 00′N, 60° 54′E). (× 50).

Bolli H. M. (1966) The planktonic Foraminifera in Well Bodjonegoro-1 of Java. *Eclog. geol. Helv.*, **59** (1), 449–465.
Boltovskoy E. (1968) Living planktonic Foraminifera of the eastern part of the tropical Atlantic. *Rev. Miciopaléont.*, **11** (2), 85–98.
Boltovskoy E. (1969) Living planktonic Foraminifera at the 90° meridian from the equator to the Antarctic. *Micropaleontology*, **15** (2), 237–255.
Ericson D. B., M. Ewing and G. Wollin (1964) The Pleistocene epoch in deep-sea sediments. *Science*, **146** (3645), 723–732.
Frerichs W. E. (1968) Pleistocene–Recent boundary and Wisconsin glacial biostratigraphy in the northern Indian Ocean. *Science*, **159** (3822), 1456–1458.
Hays J. D., T. Saito, N. D. Opdyke and L. H. Burckle (1969) Pliocene–Pleistocene sediments of the equatorial Pacific—their paleomagnetic, biostratigraphic and climatic record. *Bull. geol. Soc. Am.*, **80** (8), 1481–1514.
Koch R. (1923) Die jungtertiäre Foraminiferenfauna von Kabu (Res. Surabaja, Java). *Eclog. geol. Helv.*, **18** (2), 342–357.
Lidz L. (1966) Deep-sea Pleistocene biostratigraphy. *Science*, **154** (3755), 1448–1452.
Oba T. (1967) Planktonic Foraminifera from the deep-sea cores of the Indian Ocean. *Scient. Rep. Tohoku Univ.*, (Geol.) (2) **38** (2), 193–219.
Parker F. L. (1967) Late Tertiary biostratigraphy (planktonic Foraminifera) of tropical Indo–Pacific deep-sea cores. *Bull. Am. Paleont.*, **52** (235), 111–208.
Ujiié H. (1968) Distribution of living planktonic Foraminifera in the southeast Indian Ocean. *Bull. natn. Sci. Mus.* Tokyo, **11** (1), 97–125.

Reprinted from the *Proceed. natn. Inst. Sci. India*, vol. 35, B, no. 5, 1969, p. 399-437

ZOOPLANKTON BIOMASS IN THE ARABIAN SEA AND THE BAY OF BENGAL WITH A DISCUSSION ON THE FISHERIES OF THE REGIONS

by R. RAGHU PRASAD, *Deputy Commissioner (Fisheries Research), I.C.A.R., Krishi Bhavan, New Delhi*

(Communicated by N. K. Panikkar, F.N.I.)

(Received 25 May 1968; after revision 11 September 1968)

Quantitative analysis of zooplankton samples collected during the IIOE from the Arabian Sea and the Bay of Bengal has been made seasonwise and relative productivity of the two regions has been discussed in the light of hydrographic features and organic production. The distribution of zooplankton biomass in the Arabian Sea shows marked variation during the south-west and north-east monsoons, whereas in the Bay of Bengal there is no definite variation. The Arabian Sea is found to have a richer zooplankton biomass during the south-west monsoon with high concentration towards the coasts of Somalia, Arabian Peninsula, Iran and the south-western part of India with a low-production zone in the central and north-eastern regions. During the north-east monsoon a diffuse distribution of a comparatively lower magnitude is observed throughout the Arabian Sea.

A comparative account of the fisheries of the two regions has been given with information on the regionwise availability, categorized analysis of species composition and catch per unit effort and percentage yield for the different areas.

The relative productivity of the Arabian Sea and the Bay of Bengal has been assessed as observed by the zooplankton biomass, and the fishery resources have been correlated and the scope for increasing the exploitation of the resources in both regions has been indicated.

INTRODUCTION

The fishery resources of the Arabian Sea and the Bay of Bengal show qualitative as well as quantitative differences. Based on investigations carried out at restricted areas along the coasts of India it is believed that these differences are partly due to the inherent differences in the productivity and partly to the differences in the nature and extent of the continental shelf of the two regions. Excepting for a short account by Ponomareva and Naumov (1962) for the period of monsoon change no comprehensive account on the plankton biomass of these two regions covering all the seasons is available. In a broad sense plankton is considered as an index of fertility not only of the water column but also of the sea bottom and so it was thought that a comparative study of the zooplankton biomass* distribution would throw some light on the relative fertility and indirectly the fishery potential of the two regions. Such a study became possible with the data on the displacement volumes of the large number of samples collected during the International Indian Ocean Expedition (IIOE). The following account, therefore, deals with the seasonal variations in the density of the standing crop of zooplankton in the Arabian Sea and the Bay of Bengal. A discussion on the relation between the zooplankton biomass and the fisheries of the two regions with special reference to the coasts of India is also given.

The paper is based on the zooplankton samples collected during 1962–65. Only the standard samples have been used and all the estimations of displacement volume were carried out at the Indian Ocean Biological Centre, Ernakulam. According to the definition, the standard sample is one taken with an Indian Ocean Standard Net (Currie 1963) hauled vertically from 200 m (depth of water permitting) or from as close to the sea bottom as was practical to the sea surface, the net being hauled up at a speed of 1 m/sec. In general, the samples were collected in a uniform manner. Where the depths did not permit sampling from 200 m, samples were taken from as close to the bottom as possible. It should also be mentioned that from the available data some ships would appear to have paid out consistently just 200 m of wire without regard for the wire angle, while others seem to have paid out sufficient length of wire to allow for the wire angle, but unfortunately information on the wire angle has not been given in all cases. Because of these, data are insufficient to estimate the exact depth of sampling and apply correction factors in the estimation of the displacement volumes. Therefore, it is assumed that the samples were either collected from as close to 200 m as possible wherever the depth would permit or from as close to the sea bottom as was practical. These samples have been pooled together in this study on the presumption that at least over 95 per cent of the zooplankton population under a square metre of the sea surface was sampled in all cases. For preparing the figures showing the distribution of zooplankton biomass, the average displacement volume for each 5° square has been calculated and reckoning this as the value at the centre of the square isolines have been drawn for every 5 ml difference in volume.

General Features of the Regions

The northern part of the Indian Ocean is divided into the Arabian Sea and the Bay of Bengal. Each of these is again subdivided into a main and a subsidiary region by a range of islands, the Andaman-Nicobar islands in

* Although the values discussed in this paper represent displacement volume in millilitres, assuming that the specific gravity of plankton will be unity, the displacement weight will be equal to the displacement volume and hence the term biomass has been used in this paper.

the Bay of Bengal and the Laccadive-Maldive islands in the Arabian Sea. Another topographical feature of the Arabian Sea, which is of importance, is the Carlsburg-Murray Ridge which is believed to play a vital role in the process of upwelling.

The Arabian Sea* including the Gulf of Oman, the Persian Gulf and the Red Sea is about 1·8 times the area of the Bay of Bengal. In general, the Bay of Bengal is shallower although the continental shelf area will be greater in the Arabian Sea.

The influence of land drainage is considerably greater in the Bay of Bengal because of the influx of river discharge from a number of large rivers. No less than seven large rivers and a number of smaller ones open into the Bay of Bengal. Consequent on this the surface salinity is considerably lower in the Bay of Bengal. It should, however, be mentioned that the higher surface salinity in the Arabian Sea is also due to the influx of very high saline water of the Persian Gulf and the Red Sea and the intense evaporation in the northern Arabian Sea.

The waters of the Bay of Bengal are warmer than those of the Arabian Sea, whereas the fluctuations in the surface temperature are greater in the Arabian Sea compared to the Bay of Bengal. In the vertical distribution of temperature also the two regions show differences. The thermocline level is usually below 50–55 m in the Bay of Bengal but occasionally it goes down to 100–125 m, whereas in the Arabian Sea during the cold months the thermocline is at about 100–125 m, then it comes up to 75–90 m during the stable period between the cold months and the south-west monsoon and with the progress of the south-west monsoon it moves still further up reaching 20–30 m. The observations of Robinson (1966) show that the temperature cycle at the surface in the Arabian Sea and the Bay of Bengal is bimodal. The annual ranges vary from 2 °C in the south to 6 °C in the north. In the north the spring maxima are generally higher than those in the fall, but both these maxima are approximately the same between 5° and 10° N. The maxima occur in April and October in the north and May and November-December in the south. The spring maximum is during the period when the sun is almost directly overhead while the fall maximum coincides with the period of the weak winds at the time of the onset of the monsoons. The minima occur in January–March and August-September; the winter minimum being when the sun is farthest south and the summer minimum when the south-west monsoon winds are strongest. She further adds that 'the magnitude of the annual range at 100 m is 6 to 7 °C in areas of upwelling and divergence. In other regions investigated, the range was as low as 4 °C, yet always greater than at the surface. In cases where the range is high, the annual cycle is unimodal;

* For computations here the eastern boundary has been fixed at 78° E and the equator as the southern boundary.

where the range is low, it is bimodal, but out of phase with the bimodal cycle at the surface.'

The two regions show some differences in the pattern and speed of the surface currents. During the south-west monsoon season the surface currents in the equatorial regions of the north Indian Ocean are driven by the south-west monsoon winds and are therefore easterlies.

In the Arabian Sea region too the surface currents are essentially easterlies. There is a strong current parallel to the coast of Somaliland, the Somali current flowing north-east with a weak surface counter-current bordering to the right of this. On the western half of the Arabian Sea the meridional components of the currents are northerly while on the eastern half they are southerly. Thus, the currents along the coasts of Arabia and West Pakistan and along the west coast of India constitute a clockwise circulation and in the central part of the Arabian Sea the currents cease to contain the meridional components. The south-easterly currents off the west coast of India after leaving the peninsular region merge with the eastward flowing south-west monsoon current. In the Arabian Sea the speed of the currents is generally about one knot except in the central part where it is only about half of this. In the southern region currents as strong as two knots are found while in the actual core of the Somali current speed up to about six knots are encountered.

The surface currents in the Bay of Bengal also are essentially easterly during the south-west monsoon period but they are very weak compared to the currents in the Arabian Sea, the speed not exceeding 0·5 to 1·0 knot.

During the season of the north-east monsoon a complete reversal of the surface currents takes place and the currents are essentially westerlies both in the Arabian Sea and the Bay of Bengal.

The Somali current prevalent during the south-west monsoon period disappears and instead a reverse current flowing down the coast is set up. The meridional components of the surface currents become southerly in the Arabian Sea and except in the very coastal region along the west coast of India the coast-parallel current is down the coast both on the eastern and western halves. These southerly components vanish in the southern region of the Arabian Sea and the flow merges with the North Equatorial Current which flows westward. Along the west coast of India, however, currents very near the coast are northerly during November to January. In general, the currents are feeble in the Arabian Sea during this season except in the neighbourhood of the equatorial current where the speed is over one knot.

As against this there is a clockwise circulation cell in the Bay of Bengal during this season and consequently the currents along the east coast of India are northerly while they are southerly along the coast of Burma. However, the very coast-parallel currents along the east coast of India are southerly during November-December and northerly along the coasts of Thailand and

Malaya. The surface currents of the southern part of the circulation cell merge with the westerly flow of the North Equatorial Current. The currents are feeble throughout the Bay during this period.

Data at present available, although insufficient, are indicative of the fact that nutrient concentrations in the Bay of Bengal are of a lower order compared to the Arabian Sea. The integral concentration of phosphates in a 100 m column below a square metre of sea surface, reported by Panikkar (1966), shows that (*a*) the concentrations in the Somali-Arabian upwelling region range between 75 and 132 μg-at. PO_4–P below a square metre with a mean value of 100 μg-at. P/m^2, (*b*) along the Pakistan coast west of Karachi up to areas off Muscat and Oman, where upwelling is in evidence especially during September, the values range from 94 to 153 μg-at. P/m^2, and (*c*) between Ratnagiri and Cape Comorin along the west coast of India the mean value is 100 μg-at. P/m^2 with a range of 70–130 μg-at. P/m^2. As against this the only regions in the Bay of Bengal where high concentrations were noticed are the Thailand-Burma coasts and east of the Andaman-Nicobar islands where the values varied between 60 and 88 μg-at. P/m^2 with a mean of 75 μg-at. P/m^2. Several factors contribute to this low nutrient concentrations of which the absence of large-scale upwelling is presumed to be the main cause. Upwelling as a regular seasonal phenomenon has been reported for certain restricted areas in the Bay of Bengal but it would appear that even in such regions the waters do not contain high concentrations of nutrients as compared to the Arabian Sea.

Distribution of Biomass

During the IIOE, 480 and 335 standard plankton samples were collected from the Arabian Sea and the Bay of Bengal respectively. These samples were divided arbitrarily into two seasonal groups, one collected during April 16 to October 15, which corresponds to the period of the south-west monsoon with approximately one month preceding and succeeding it, and the other during October 16 to April 15 corresponding to a similar six-month period of the north-east monsoon.

For the south-west monsoon period April 16 to October 15, volumetric analyses of 137 day samples and 104 night samples from the Arabian Sea and 98 day samples and 108 night samples from the Bay of Bengal have been considered.

In the day samples from the Arabian Sea (Fig. 1) it is found that there is a higher plankton biomass towards the western half. The highest concentration of > 60 ml is recorded on the south-eastern coast of the Arabian Peninsula. Somali coast comes next with a concentration of > 45 ml. The south-western coast of India is also having a fairly high concentration with > 30 ml of plankton. The central region of the Arabian Sea extending from the equator

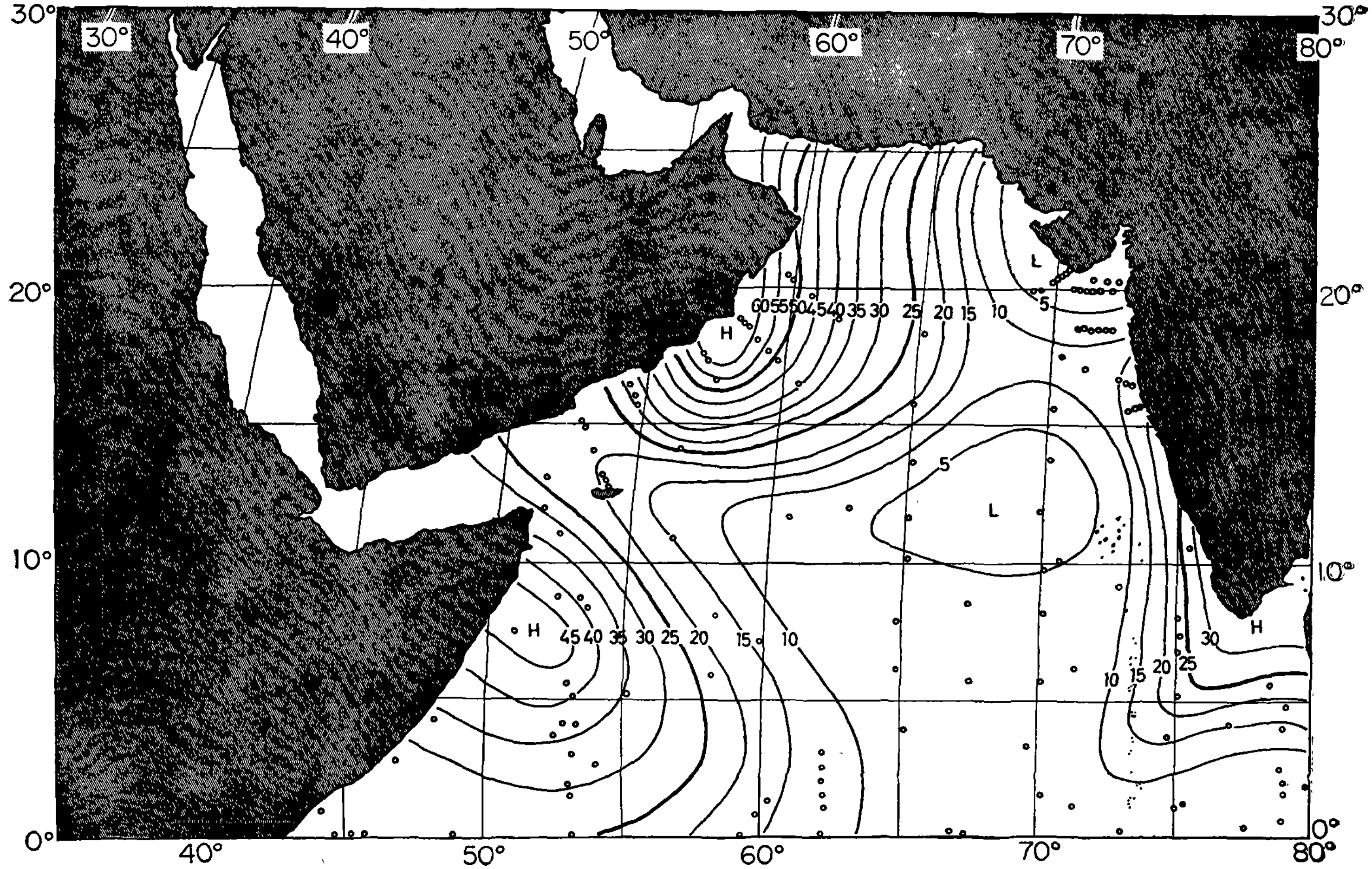

FIG. 1. Density of zooplankton based on 137 day samples collected during April 16 to October 15. In Figs. 1 to 18 average zooplankton volumes have been calculated for each 5° square and isolines drawn for every 5 ml difference in volume. All samples were taken with the Indian Ocean Standard Net. Open and black circles represent day and night stations respectively. (L—low and H—high.)

up to 15° N latitude and between 65° and 75° E longitudes and Gujarat coast from the Gulf of Kutch to the Gulf of Cambay seem to have a low plankton biomass.

During the night also the general picture of plankton distribution does not alter much from that of the day samples. Somali coast, south-eastern coast of Arabian Peninsula and south-west coast of India continue to exhibit a higher concentration of plankton (Fig. 2). In the open part of the Arabian Sea there is altogether an increase in biomass in the night samples. The large central zone of poor plankton production has shrunk to a comparatively smaller area around 65° E and 5° N. Though Gujarat coast continues to have a low concentration, there is progressive increase in biomass towards the outer rim of the continental shelf. The average volume on the south-western coast of India increases twofold from that of the day samples. But there is no significant difference on the Somali and Arabian coasts between day and night samples.

The averages of 241 day and night samples for the above period also exhibit the same pattern of distribution of biomass. The western half of the Arabian Sea and south-western coast of India are having higher density while the central zone and Gulf of Kutch to Gulf of Cambay off Gujarat show a low density of plankton. In all the high density areas the coastal regions possess an average volume exceeding 50 ml with gradual decrease towards the open sea (Fig. 3).

Thus in the Arabian Sea, during the south-west monsoon period the pattern of distribution of plankton biomass is the same for day and night samples though there is a higher density of plankton in most of the areas in the night samples. The isoline for 50 ml remains constant both in day and night samples for the coastal region of the Arabian Peninsula. But there is a slight decrease in the day samples in the Somali coast and south-western coast of India. Both these regions record the maximum density in the night samples.

On the other hand, for the same period the average plankton volume is considerably less in the Bay of Bengal. It is only 10–20 ml on the average in almost all parts of the Bay of Bengal. During day (Fig. 4) the east coast of India shows a very poor plankton biomass and the Andaman Sea and the eastern coast of Ceylon exhibit a feeble increase. But the density is distinctly higher in the Gulf of Manaar and the region between Cape Comorin and 5° N latitude. During night biomass increases towards the eastern coasts of India and Ceylon (Fig. 5). There is a conspicuous increase in the night samples (40 ml) towards the upper reaches of the Bay. The Andaman Sea maintains a medium density of 20 ml. The averaging of 206 day and night samples also underlines the lower plankton biomass in the Bay of Bengal during the south-west monsoon period as compared to the Arabian Sea. Throughout the Bay it is almost a uniform distribution consisting 10–20 ml of plankton (Fig. 6).

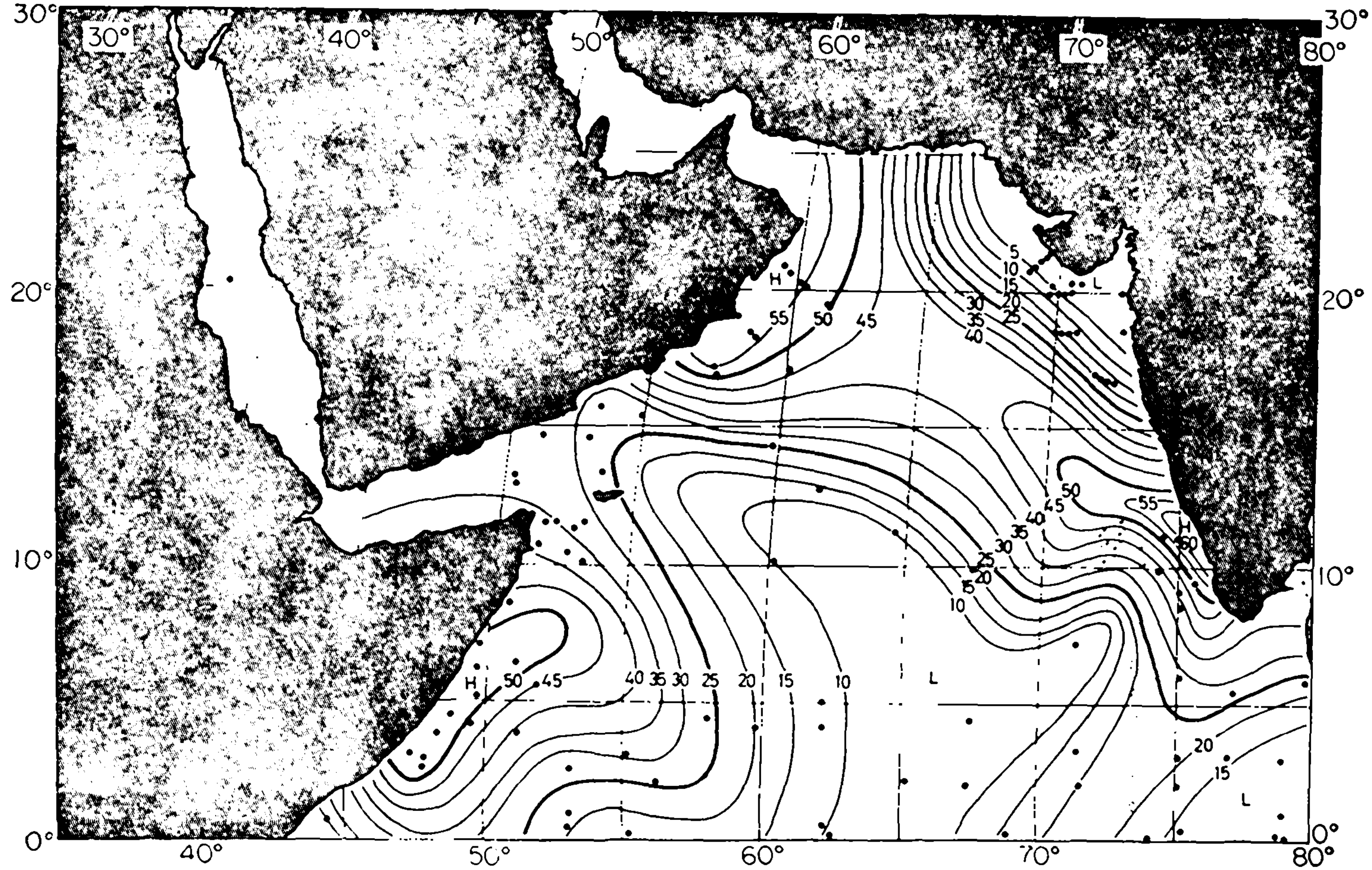

Fig. 2. Density of zooplankton based on 104 night samples collected during April 16 to October 15.

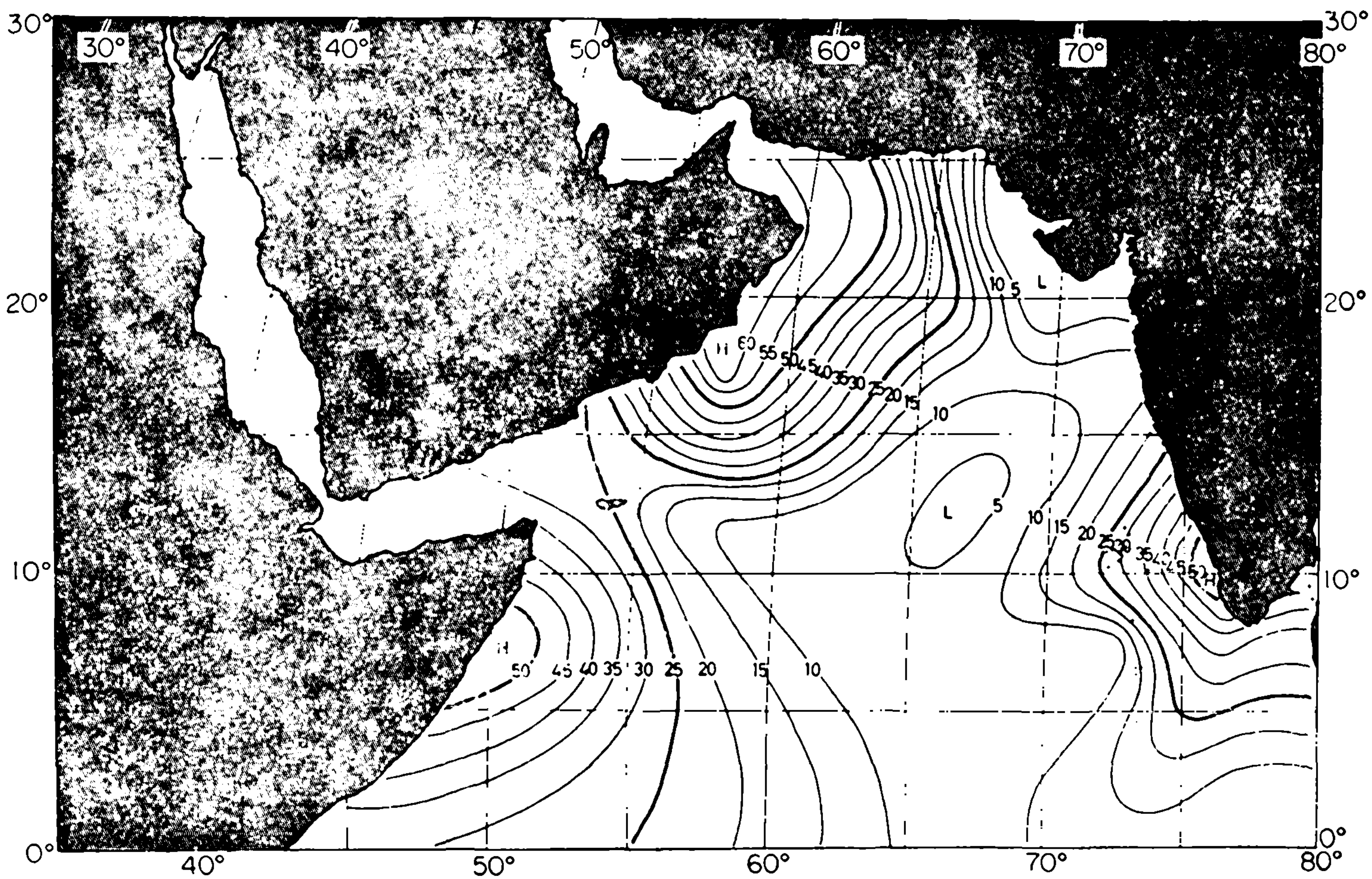

Fig. 3. Density of zooplankton based on 241 day and night samples collected during April 16 to October 15.

For the north-east monsoon period (October 16–April 15) 131 day samples and 108 night samples from the Arabian Sea and 61 day samples and 68 night samples from the Bay of Bengal have been considered for determining the distribution of plankton density.

Notably in the Arabian Sea, it can be found that the picture changes considerably from that of the south-west monsoon period. The plankton

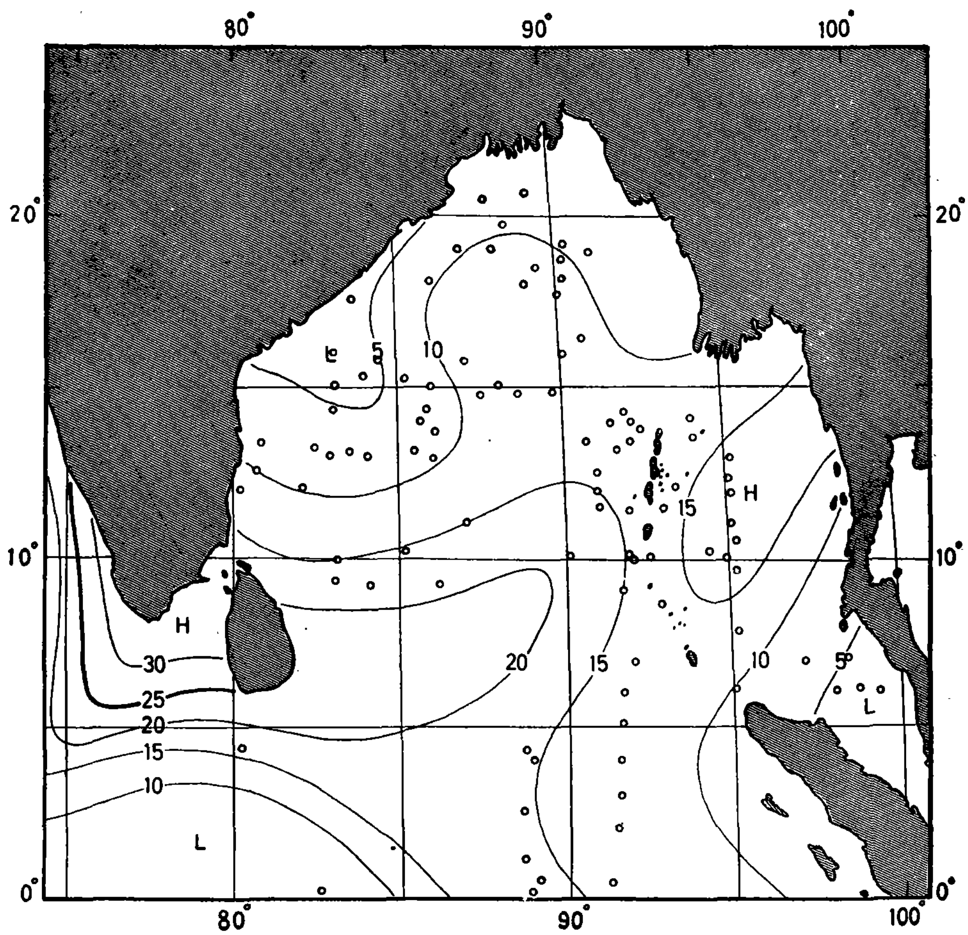

FIG. 4. Density of zooplankton based on 98 day samples collected during April 16 to October 15.

distribution in the Arabian Sea becomes somewhat diffuse. In day samples (Fig. 7) there is no appreciable concentration anywhere excepting in Qamr Bay and surrounding areas on the southern coast of Arabian Peninsula. Even this single concentration is due to a local and isolated occurrence and so cannot be considered as a general feature. The marked low production zone in the central part of the Arabian Sea, too, disappears during this period. The coastal region of Somalia towards the equator registers a small increase in plankton biomass. In day samples of the north-east monsoon period for the major part of the Arabian Sea the volume of plankton is only 10–15 ml.

During the night (Fig. 8) there is a slight rise in density and excepting in the central region towards the equator the major part indicates a volume of 15–30 ml, almost double that of the day volume. The Gujarat coast registers a higher biomass both in day and night samples during this period as compared

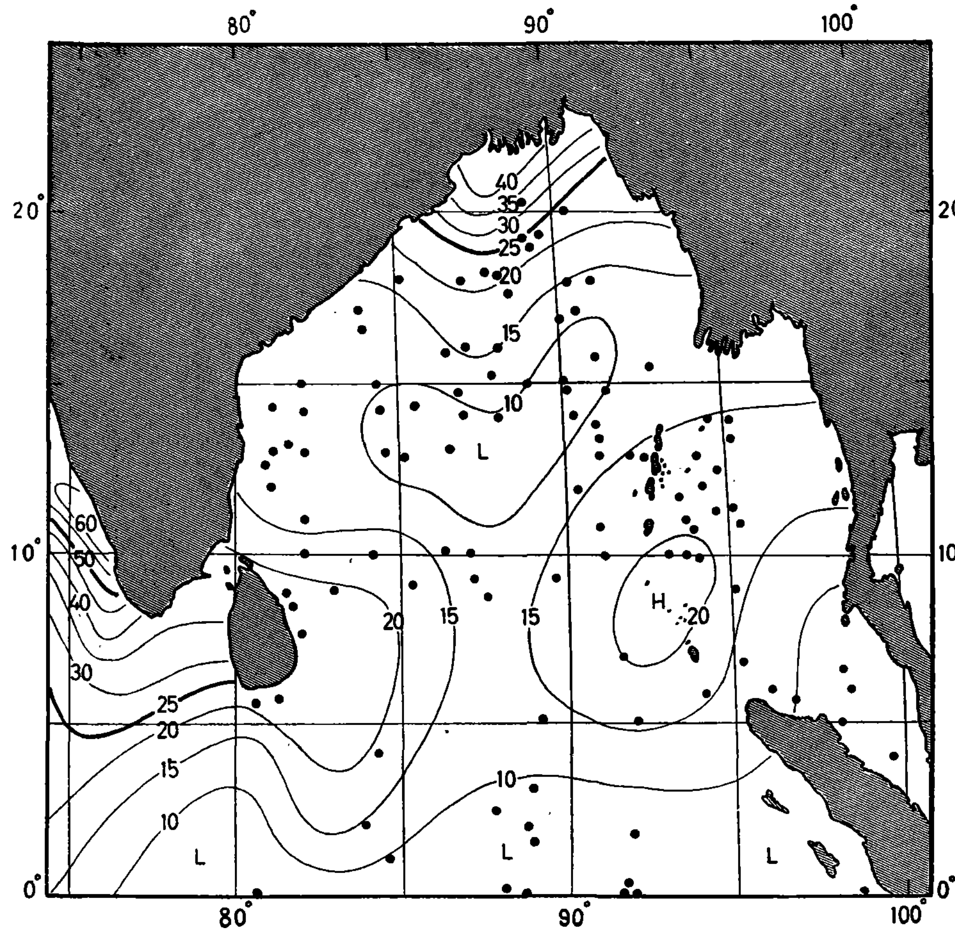

FIG. 5. Density of zooplankton based on 108 night samples collected during April 16 to October 15.

to the south-west monsoon period. Fairly high biomass is seen only around the Gulfs of Aden and Oman and the coastal region of Somalia. Even though there is increase in density in night samples it does not demarcate any particular zone of high production as during the south-west monsoon half. The high density isolines found to concentrate around Qamr Bay disappear, giving way to a completely diffuse distribution.

The averaging of the 239 day and night samples collected during the north-east monsoon period from the Arabian Sea (Fig. 9) also suggests the same diffuse distribution pattern with an average volume of 15–30 ml for almost the whole of Arabian Sea. The local concentration around Qamr Bay on the southern coast of the Arabian Peninsula is still maintained. However, it cannot be attributed as a delineation of a zone of a high production as indicated earlier. The Somali coast also shows a low biomass excepting the southernmost region. The equatorial region up to 5° N and the Malabar coast indicates a faint increase.

During the north-east monsoon period in day samples the biomass in the Bay of Bengal is not appreciably different from that of the south-west monsoon half (Fig. 10). The southern region of the Bay of Bengal is having only a very low concentration. On the other hand, the equatorial region towards the

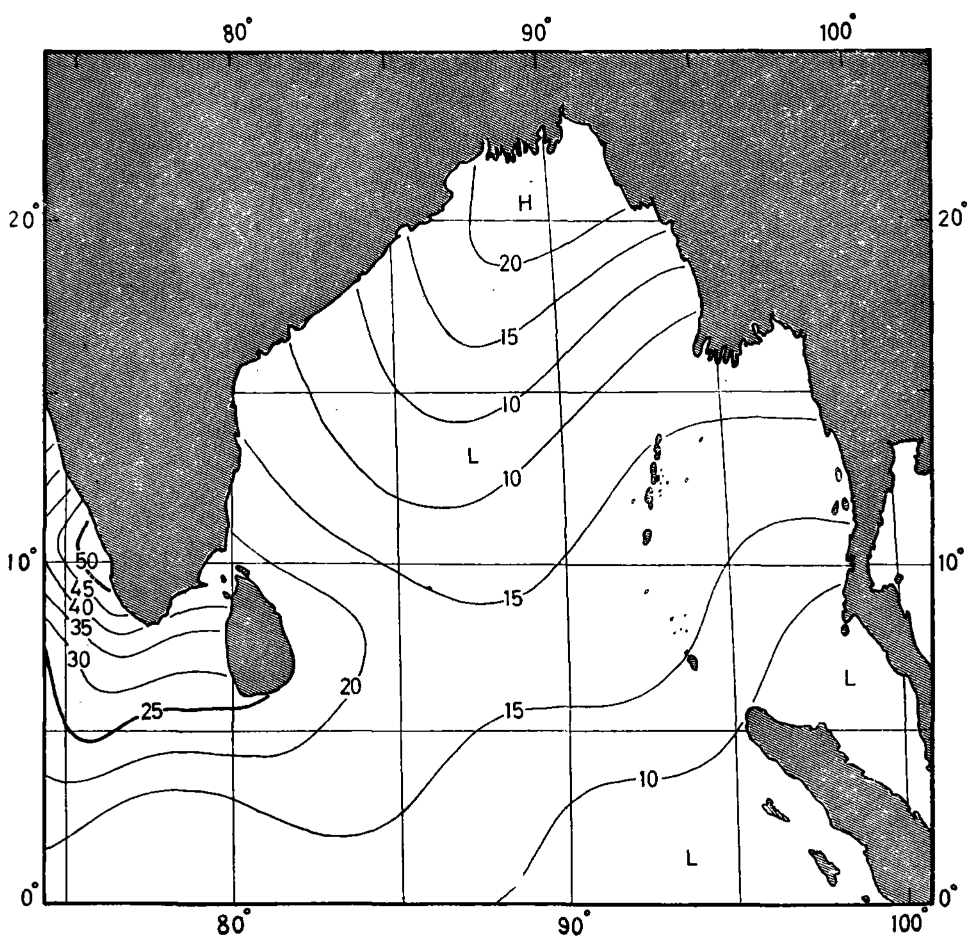

Fig. 6. Density of zooplankton based on 206 day and night samples collected during April 16 to October 15.

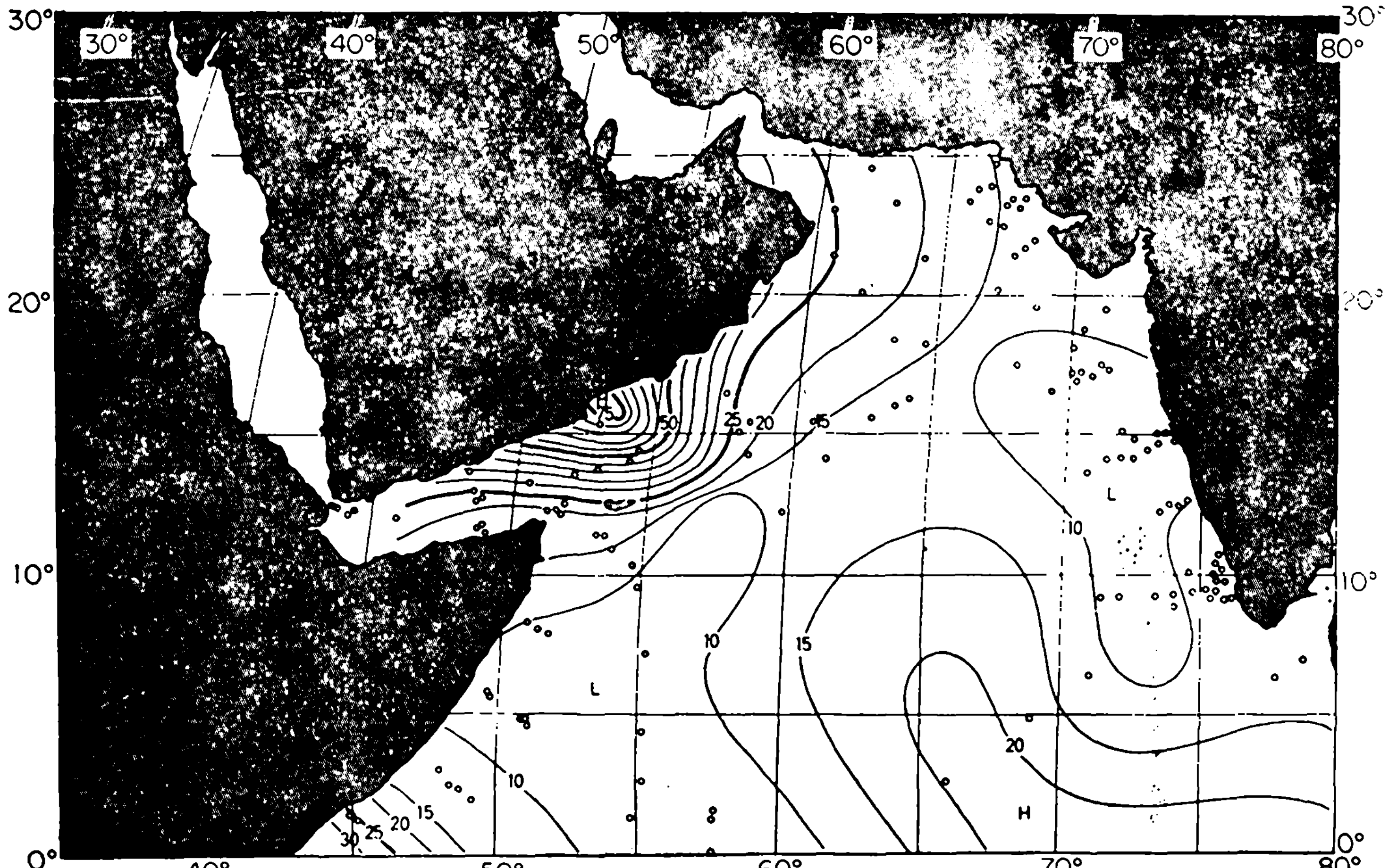

FIG. 7. Density of zooplankton based on 131 day samples collected during October 16 to April 15.

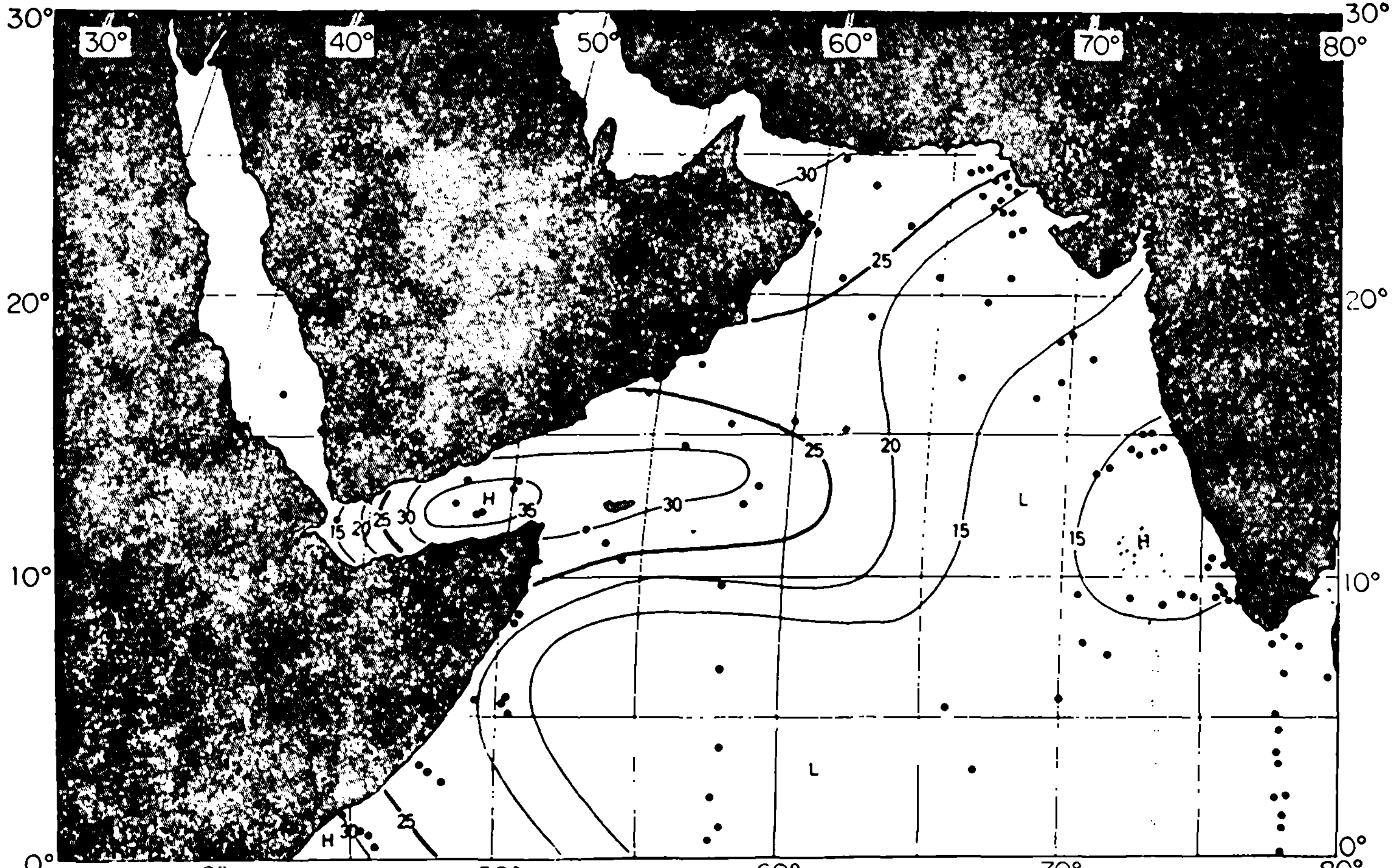

Fig. 8. Density of zooplankton based on 108 night samples collected during October 16 to April 15.

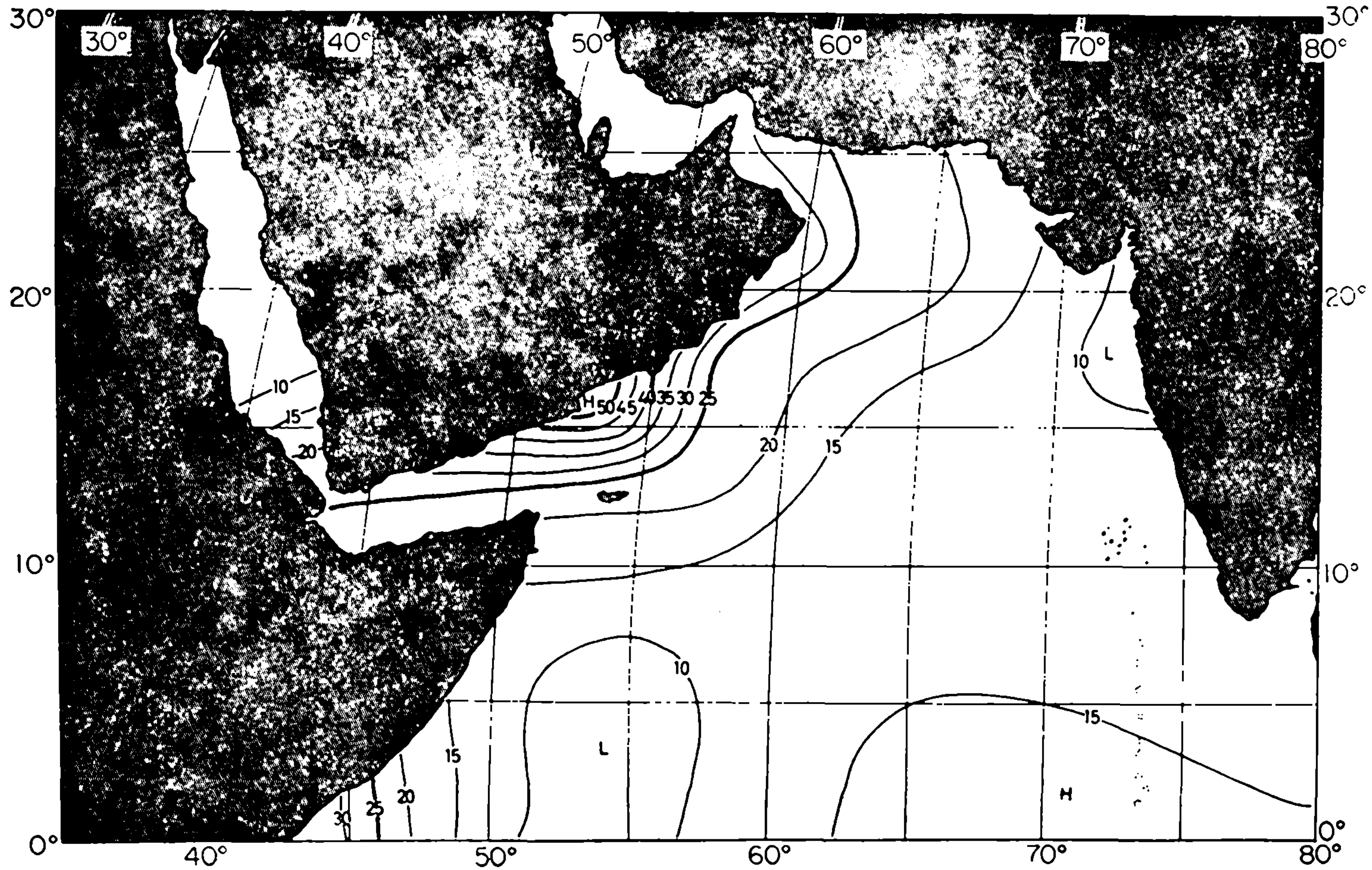

FIG. 9. Density of zooplankton based on 239 day and night samples collected during October 16 to April 15.

80° E longitude is having a higher biomass. The upper reaches of the bay, especially towards the coast of Burma, are also having a slightly higher concentration. Thus, there is a progressive increase towards the northern region. This trend is reversed in the night samples for the same period (Fig. 11). From a low concentration of < 5 ml in the north-eastern part of the Bay the biomass progressively increases towards the south-west. A fairly high concentration of > 25 ml is thus seen towards the east coast of Ceylon. The equatorial region on the western side of Sumatra exhibits a low biomass.

The averaging of 129 day and night samples from the Bay of Bengal for the north-east monsoon period (Fig. 12) does not show any appreciable concentration anywhere. In the major part of the bay the average volume varies from 10 to 20 ml. Off Rangoon in the Gulf of Martaban and in the equatorial region the density is even less than 5 ml.

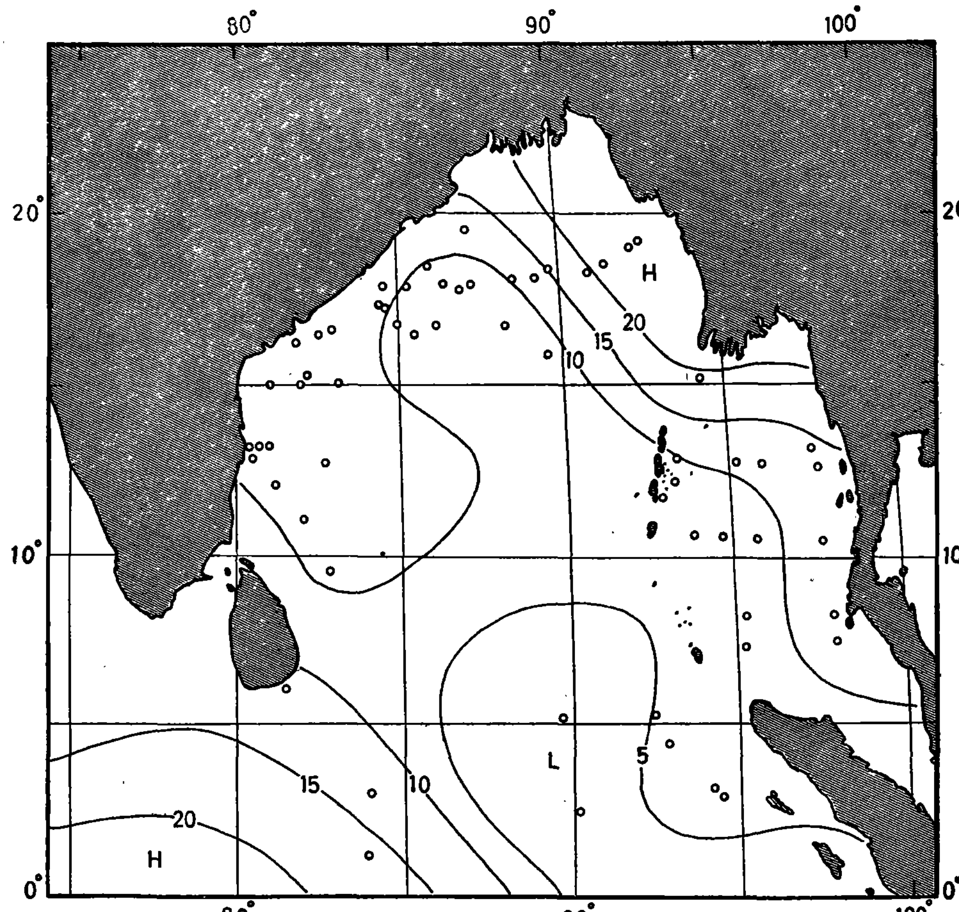

FIG. 10. Density of zooplankton based on 61 day samples collected during October 16 to April 15.

Averages have been calculated and the distribution of plankton biomass has been determined for the entire IIOE period with 268 day samples and 212 night samples from the Arabian Sea and 159 day samples and 176 night samples from the Bay of Bengal.

For the entire IIOE period in the Arabian Sea distribution of plankton biomass as seen from the day samples (Fig. 13) is basically similar to that of the south-west monsoon period with a larger increasing trend towards the

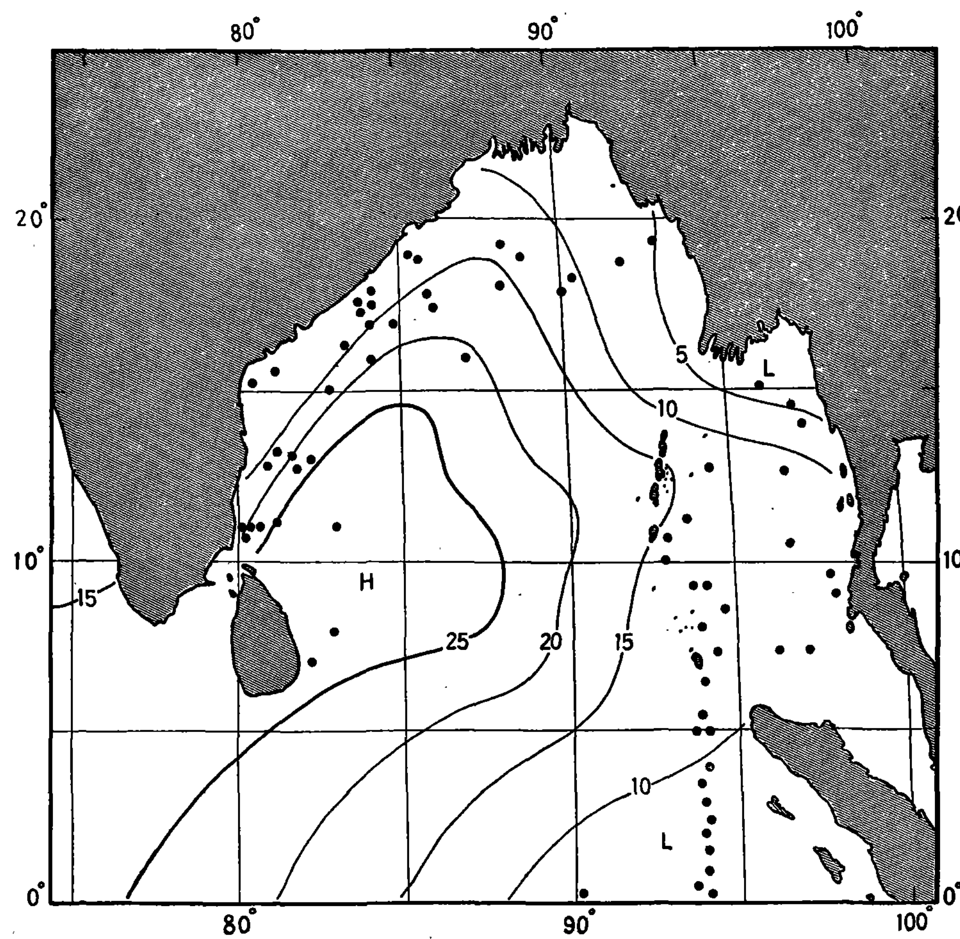

FIG. 11. Density of zooplankton based on 68 night samples collected during October 16 to April 15.

coasts of Somalia and Arabia and a moderate increase towards the south-western coast of India. The central area of the Arabian Sea again exhibits a large zone of poor plankton biomass. There is also a faint increase towards the equatorial regions.

The averaging of the 212 night samples (Fig. 14) presents the same basic picture of distribution pattern. But there is a slight increase in the night samples, especially in the central low productive region and also towards the south-western coast of India. The averages for the Somalia and Arabian coasts do not alter much. The low production zone in the central Arabian Sea also seems to shrink in its extent considerably.

The averaging of the day samples for the entire IIOE period emphasizes the low plankton biomass of the Bay of Bengal (Fig. 15). The whole Bay does not show anything more than 10 ml on the average. But the night

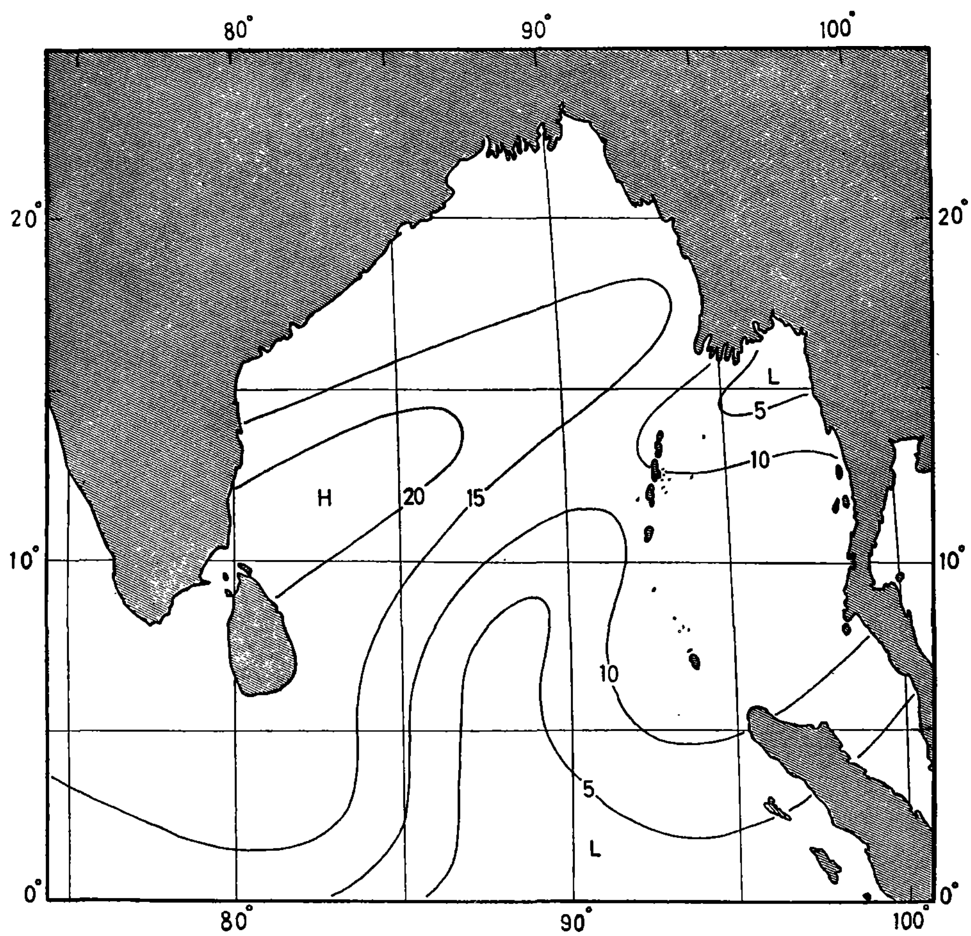

FIG. 12. Density of zooplankton based on 129 day and night samples collected during October 16 to April 15

sample of the entire IIOE period gives some delineations of high and low productive areas. The upper reaches of the bay are found to have a higher biomass reaching a maximum of 40 ml towards the Bengal coast. The Gulf of Martaban with a volume of < 5 ml is having the lowest biomass. For the rest of the Bay it is between 10 and 20 ml which is the normal value for most part of the year (Fig. 16).

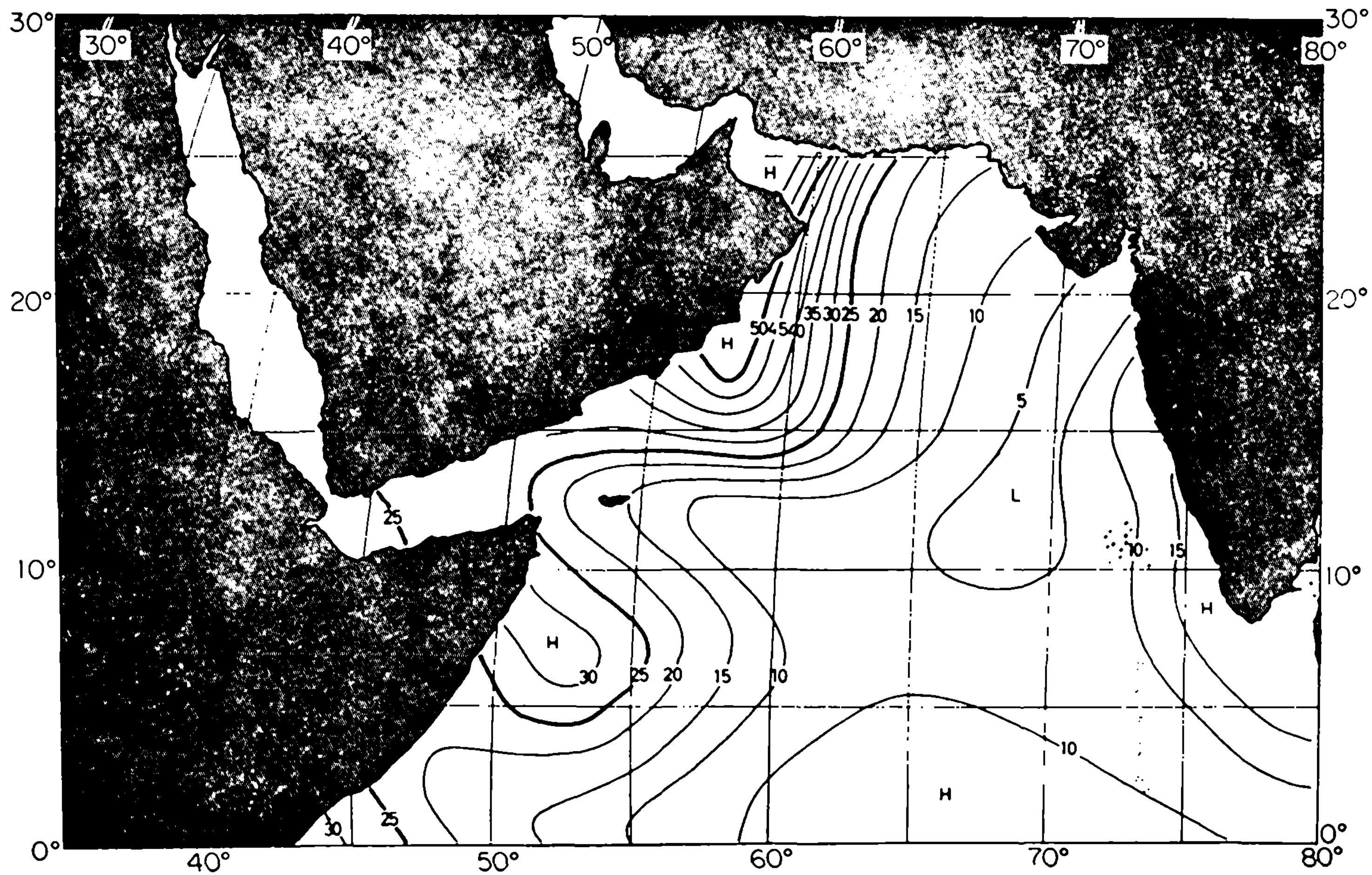

FIG. 13. Density of zooplankton based on 268 day samples collected during the entire IIOE period.

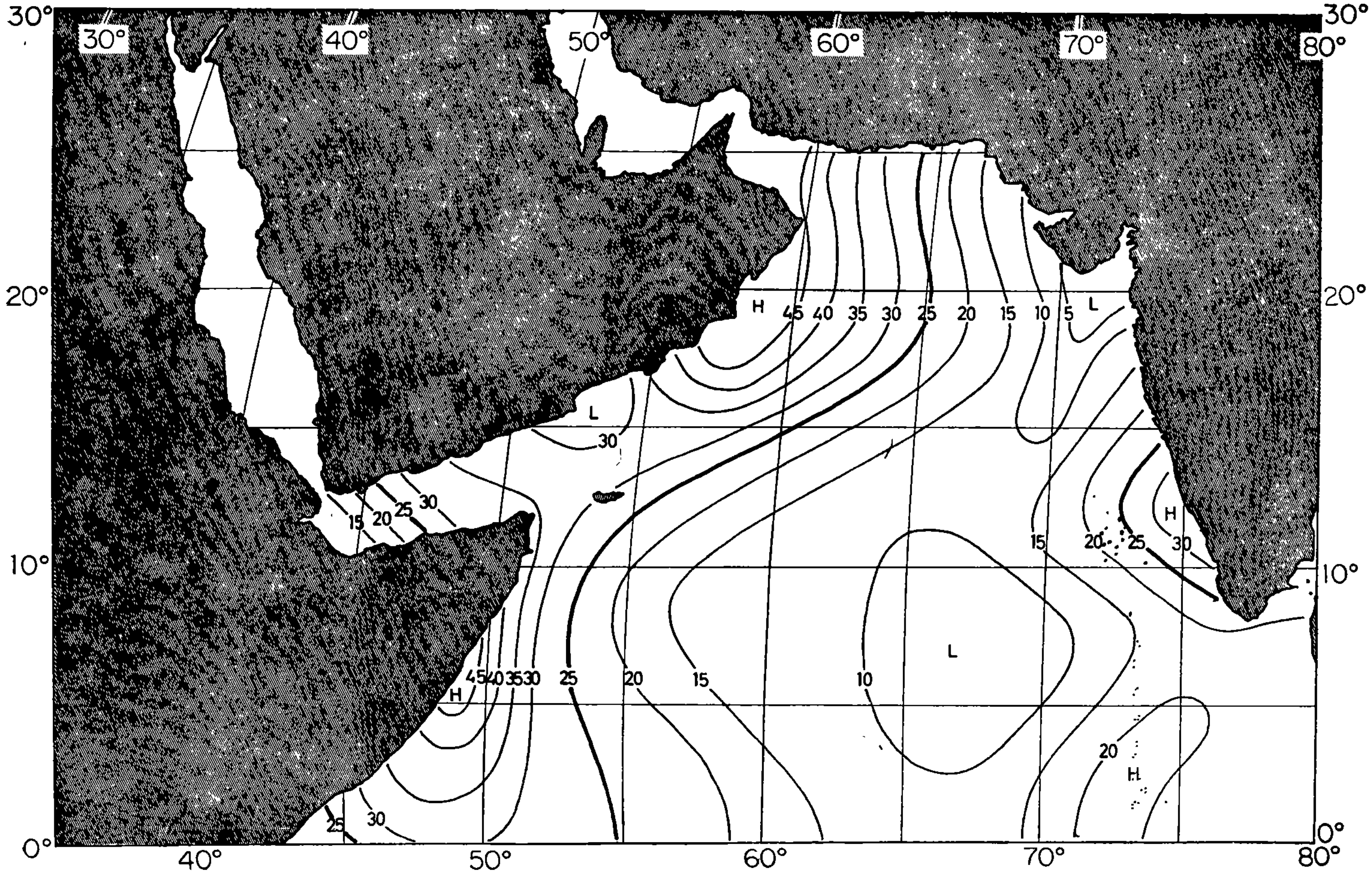

FIG. 14. Density of zooplankton based on 212 night samples collected during the entire IIOE period.

All the total 480 day and night samples collected from the Arabian Sea for the entire IIOE period when averaged (Fig. 17) also exhibit the same picture characteristic of the Arabian Sea for the south-west monsoon period with the maximum concentration in the western half—the high production areas surrounding the Somali and Arabian coasts and to a certain extent on the south-western coast of India and the low production zones occupying the central

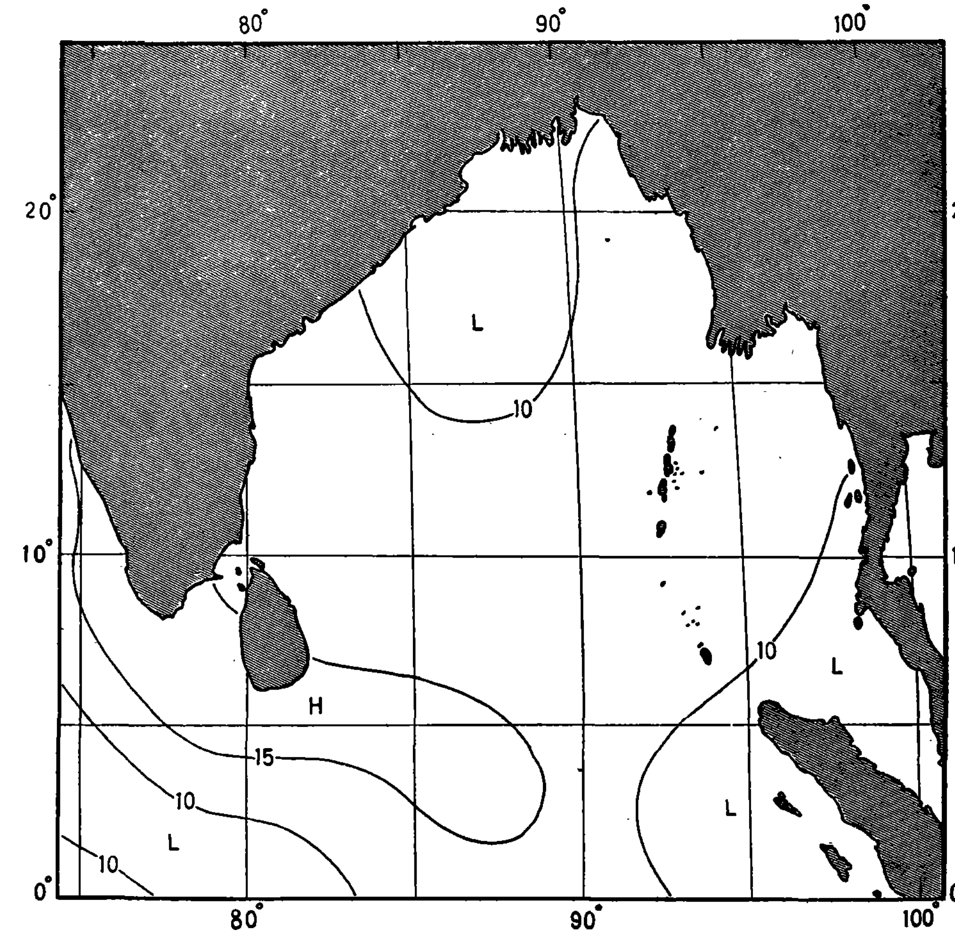

FIG. 15. Density of zooplankton based on 159 day samples collected during the entire IIOE period.

part of the Arabian Sea and the precincts of the Gujarat coast. The distribution of plankton biomass as determined during the cruise of R.V. *Vitiaz* (Bogorov and Rass 1961) compares well with the pattern of distribution observed now. For the Bay of Bengal there is no distinct variation in distribution either between the two monsoon halves or with the entire IIOE period (Fig. 18), almost the whole of the Bay showing a rather low biomass (10–20 ml) with still lower values for the Gulf of Martaban and western region off Sumatra and moderately higher values on the Bengal coast. The averaged isolines for the entire period further stress the sparse distribution and lower biomass in the Bay of Bengal as compared to the Arabian Sea.

It is relevant to consider here the distribution of plankton in the north Indian Ocean in the light of available information on the vergence field and

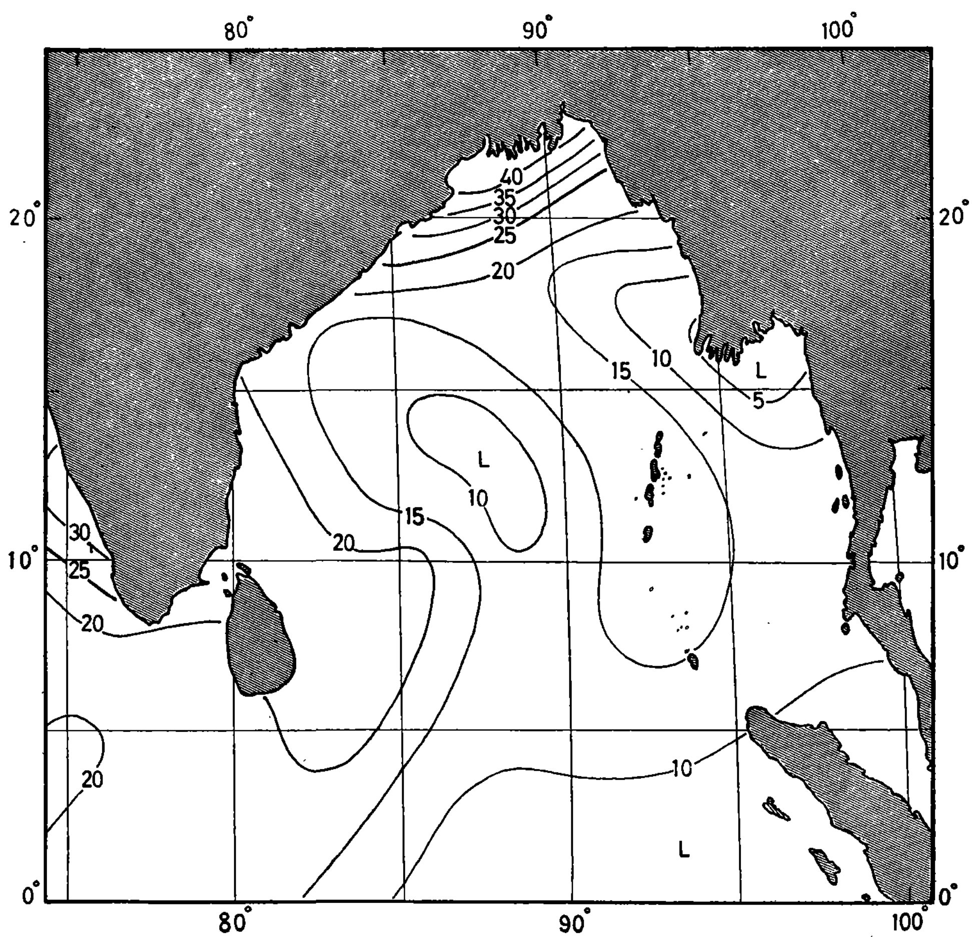

FIG. 16. Density of zooplankton based on 176 night samples collected during the entire IIOE period.

circulation of the surface waters, organic productivity and chlorophyll concentrations.

Varadachari and Sharma (1964, 1967) have presented results of investigations on the divergence and oonvergence and circulation pattern of the surface waters in the north Indian Ocean for different months of the year. According to these authors the divergence pattern shows considerable seasonal and spatial variations. In the equatorial region several centres of strong divergence and convergence occur in the open ocean almost throughout the

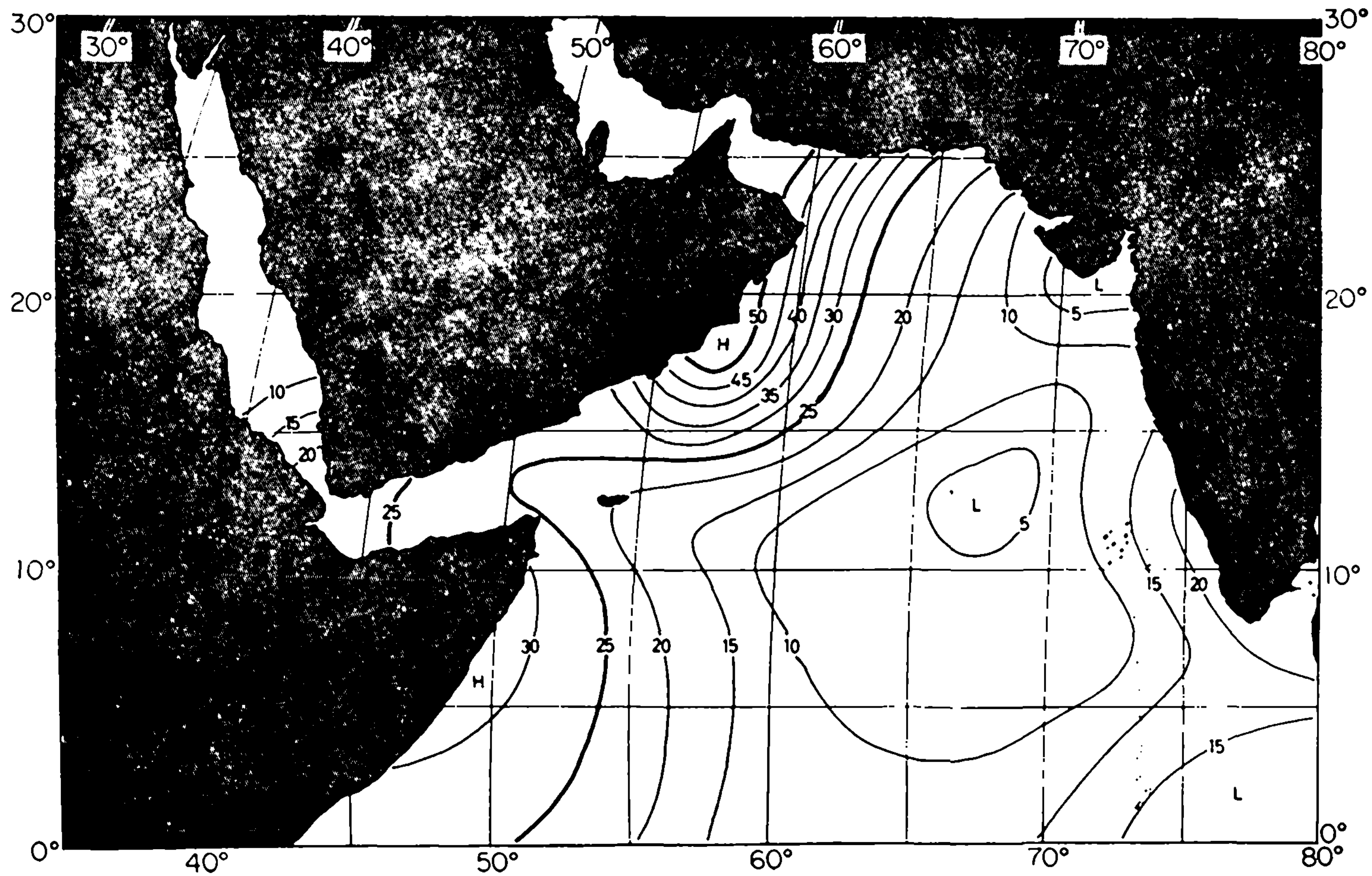

FIG. 17. Density of zooplankton based on 480 day and night samples collected during the entire IIOE period.

year while in the nearshore regions strong divergences and convergences occur only during certain periods of the year. Along the Somali coast divergence is prevalent from January to October and along the west coast of India from January to September and convergence during the rest of the year. The monsoon months, especially June, July and August, are the months of intense divergence of surface currents when central values of divergences and convergences exceed 60 units. In the Somali coast during June the value exceeds

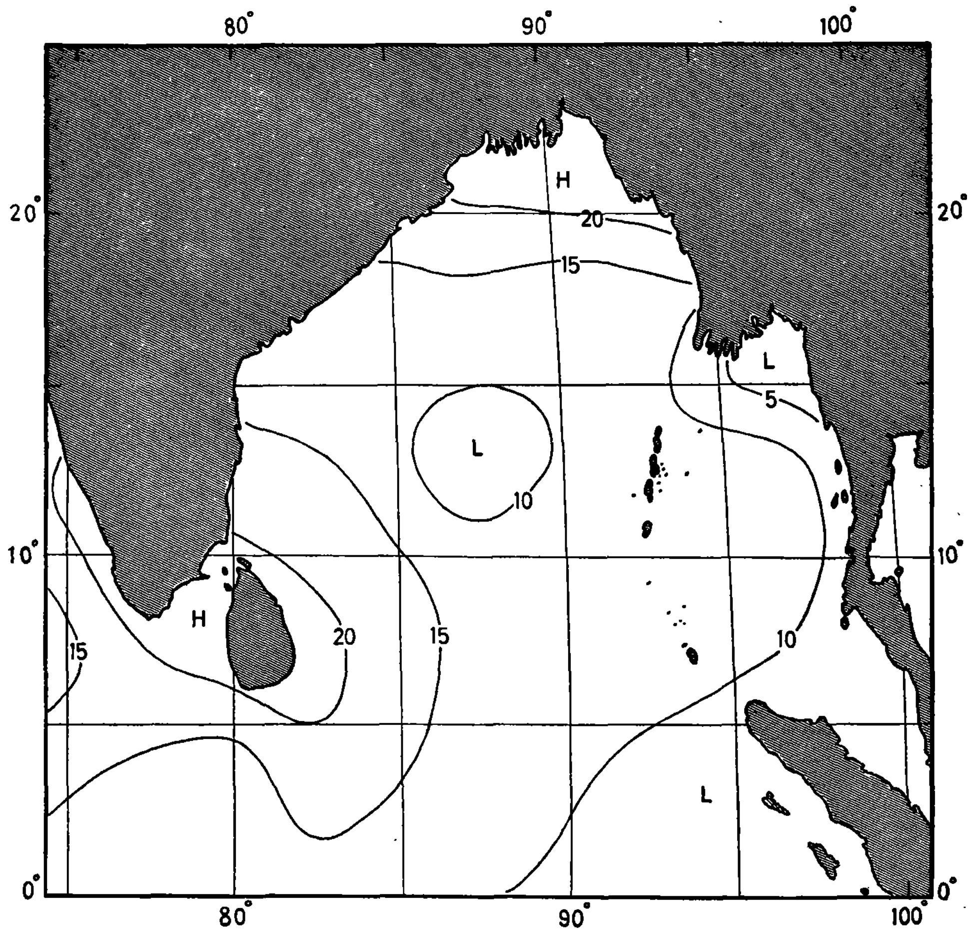

FIG. 18. Density of zooplankton based on 335 day and night samples collected during the entire IIOE period.

even 80 units indicating heavy upwelling. This region is unique as strong divergences or convergences occur almost throughout the year. The convergences cause dynamically a concentration of zooplankton and in divergences a higher production of organic matter takes place. The distribution of zooplankton broadly agrees to the vergence pattern of these areas brought about by the seasonal shift of the monsoons.

The surface currents in the northern Indian Ocean have been discussed briefly earlier. A comparison of the circulation maps (*cf.* Varadachari and Sharma 1967) with the plankton density charts also indicates that the distribution of zooplankton in the north Indian Ocean has a close relation to the surface currents which are directly connected with oceanic circulation. During the south-west monsoon period on the Somali coast the current flows northward and part of it flows along the Arabian coast. In May–September these currents are strongly offshore currents inducing upwelling all along the Somali and Arabian coast up to the Gulf of Oman. Further, the winds also blow parallel to the coast, as a result of which the surface waters are transported away from the coast, giving rise to upwelling, and thereby bring about the chain of events resulting in a high zooplankton standing crop. Thus it may be seen that the high concentration of plankton in the western part of the Arabian Sea generally comes within the orbit of the clockwise circulation developed during the south-west monsoon period and passing through several vergence fields. During this period the central region of the Arabian Sea and the regions off Kutch do not show any appreciable vertical movements. This may account for the low plankton biomass in these areas during the south-west monsoon months.

During the north-east monsoon period, though fairly strong convergences develop on the east coast of India, coast of Ceylon and Andaman Sea, it does not seem to cause a high zooplankton concentration in the Bay of Bengal. The reason for the variation in production between the two areas may be found in the difference in distribution of the nutrients.

In the Arabian Sea the nutrient levels increase sharply with depth (*cf.* McGill 1966) beginning very near the surface and fertile waters lie close to if not within the limits of the euphotic zone (Ryther and Menzel 1965). High level of nutrients in close proximity to the surface is a potentially productive condition and any vertical movement can turn the potential productivity into reality. The monsoons provide the required energy for these biological processes. The vertical distribution of oxygen is a mirror image of the nutrient distribution—dropping sharply below the euphotic zone which further indicates the high productivity. Hence for the variation in the quantity of plankton biomass between the two regions the availability of nutrients near the euphotic zone could be one of the determining factors.

A general picture of the organic productivity of the Indian Ocean is now available through the cruises of *Galathea* (Steemann Nielsen and Jensen 1957), *Vitiaz* (Kabanova 1961) and *Anton Bruun* (Ryther *et al.* 1966). Apart from these, much data have been collected from the coastal regions of the Indian subcontinent by the Central Marine Fisheries Research Institute (Prasad and Nair 1963 and Central Marine Fisheries Research Institute, Annual Reports 1965-66). The *Galathea's* coverage is on the western part of the Indian Ocean off the coast of South Africa, the equatorial region from Mombasa to Ceylon, Ceylon coast, some stations in the Bay of Bengal and the Indo-Malayan waters. The *Vitiaz* and *Anton Bruun* cruises cover a major part of the Arabian Sea. The results achieved during these investigations enable us to draw certain conclusions regarding the comparative productivity of the Arabian Sea and the Bay of Bengal.

It is found that over the continental shelf in the tropical regions the production rate is usually very high. The surface waters generally have a production rate of over 0·2 gC/m^3/day and for the entire column it is found to exceed 0·5 gC/m^2/day and sometimes reach exceptionally high values of over 5·0 gC/m^2/day (Prasad and Nair 1963).

In the Arabian Sea the level of organic production increases to the north and west reaching extremely high values off the coast of Saudi Arabia, Somalia and West Pakistan. Kabanova (1961) observed that the Arabian Sea water was characterized by an especially high productivity connected with the presence of regions of deep-water ascent. Twenty-three measurements made recently in the Arabian Sea by Ryther *et al.* (1966) gave values in excess of 1·0 gC/m^2/day with a maximum of 6·4 gC/m^2/day observed off the south-eastern tip of Arabia. These authors have calculated a total production of 3×10^{12} kg for an area of 23×10^6 km^2. Out of this more than one-fifth is from the western Arabian Sea where the mean production is approximately 10 times that of the world oceans. The data collected at the Central Marine Fisheries Research Institute indicate that the west coast of India is also equally productive. Coastal upwelling along the Somali coast, Arabian coast and off the west coast of India play an important part in the fertilization of the surface waters of the regions which induce high organic production. On the other hand in the Bay of Bengal even though stations located on the shelf were all characterized by a high rate of production, the average for the whole Bay is only 0·19 gC/m^2/day which is only a little more than the rate usually found in tropical oceanic water (Steemann Nielsen and Jensen 1957). Hence it seems reasonable to conclude that the level of organic production in the Arabian Sea should be at least three times that of the Bay of Bengal.

Further evidence of this higher productivity in the Arabian Sea is seen from the chlorophyll measurements made recently by Laird *et al.* (1964). They found during the south-west monsoon period along the Somali coast to the left of the main portion of the Somali Current values greater than 150 mg/m^2. In terms of carbon fixed per square metre per day this would amount to about 4-5 grams. If it is assumed that this is a steady production, during the monsoon period this would amount to 350–450 g/m^2. In terms of dry algae this will be 800 g/m^2 which ranks this area among the most productive. On the other hand, in the Bay of Bengal the chlorophyll concentrations are of a very low order, being less than 10 mg/m^2. The highest value of 20 mg/m^2 has been recorded off the northern part of the Arakan coast of Burma (Panikkar 1966). In this connection a special feature characteristic of the Arabian Sea indicated by Ryther and Menzel (1965) has to be mentioned. They noticed, when the ship drifts, areas of extremely dense plankton blooms which vary in size from 100 yards or less to several miles in diameter and often sharply delineated by extremely clear and unproductive water. Because of such extreme patchiness in the distribution of plankton the Arabian Sea is a region of the greatest contrast containing some of the richest and some of the most infertile areas.

Plankton Biomass and Fisheries of the Regions

General

Several attempts have been made to study the relationship between the organic and/or plankton production and their relation to fisheries along the coasts of India. These attempts, however, have been on a rather restricted scale in the sense that they relate mostly to specified areas along the east or west coast of India.

The investigations of Chidambaram and Menon (1945) on the co-relation of the fisheries of the Malabar and South Kanara coasts with plankton have shown that the landings of fish are directly proportionate to the quantity of plankton. The fishery in general coincides with the major peak in plankton production. Subrahmanyan (1959) observed a close relationship between the standing crop of phyto- and zoo-plankton with the total quantity of fish landed, particularly the landings of oil sardine (*Sardinella longiceps*) and the Indian mackerel (*Rastrelliger kanagurta*). He also estimated (Subrahmanyan 1967) the phytoplankton production for a potential fishing area of 155,400 square km of 100 m depth on the west coast of India and remarked that the fish landings of the west coast represented only 0·029 per cent of the phytoplankton production. As a result of the investigations carried out in the Indian Ocean, Bogorov and Rass (1961) have stated that in the Indian Ocean there exists a number of areas with much plankton biomass, these being mostly in the regions of upwelling. In some areas the amount of plankton exceeds 15 mg of dry matter per m^3 in the 0 to 100 m layer of water. These areas of high plankton production have been noticed by them in the central part of the Arabian Sea from Aden Bay to Bombay; between Seychelles and Maldive Islands; off Zanzibar and Comoro Islands; to the north-east from Madagascar; off Chagos Bank; off Ceylon; to the south of Java and to the north-west from Australia. According to their observations the congregations of tunas and other pelagic fishes are seen in the regions of the ocean where plankton is most abundant. Prasad and Nair (1963) studied the organic production in relation to the local fishery of the east coast extending from Dhanushkodi to Cape Comorin. These investigations showed that the percentage of yield in relation to the organic production is only on an average 0·03 as compared to

0·2 to 0·3 per cent in intensively exploited waters. The seasonal rhythm in organic production was well reflected in the trend of fishery, the peak periods of production corresponding with the low periods in fishery and *vice versa* suggesting an inverse relationship. A high fishery was noticed to follow after a peak production of organic matter in regular sequence with more or less uniform time lag, this time lag being presumably the time taken for the conversion of the organic matter synthesized to form fish protein. Sudarsan (1964) concluded that trawler catches at Bombay showed 'two peaks in the year, one following the period of plankton maximum in March and the other coinciding with the period of very high plankton standing crop in the post-monsoon months (October-November)'. According to Longhurst (1966) areas of high fisheries potential are more localized in the tropics than in the higher latitudes and less dependent upon the conformation and width of the continental shelf. While the level of production in the higher latitudes depends largely upon the annual turnover of the mixed layer during winter, an effect which is uniform over large areas, in the low latitudes production is largely dependent upon processes which result in local enrichment such as divergence, coastal upwelling, doming, frontal shearing and topographical wind intensification. In the tropical high seas fisheries for tunas and other predatory fishes depend mostly upon the aggregation of the fish in areas of localized enrichment and within the migrating temperature fronts, whereas fisheries for shoaling clupeids are situated principally in regions of coastal upwelling and to a lesser extent in the estuarine areas where riverine nutrients create conditions of phytoplankton bloom. The demersal fisheries in the intertropical areas seem to be localized mostly in regions where deposition of riverine organic material occurs and it is this material rather than the results of primary production in the ocean that determines their level of production. However, where the shelf is narrow at the mouth of a great river much of the material for potential production is lost by slumping to great depths. Uda (1966) observed conspicuous upwelling area of cold, fertile waters south of Sunda Islands and the most favourable tuna fishing grounds were located in the marginal area of this upwelling zone. Similar situation of oceanographic and fisheries conditions were recognized in the Arabian Sea. Panikkar and Jayaraman (1966) while discussing the biological and oceanographical differences between the Arabian Sea and the Bay of Bengal, as observed from the Indian region, have drawn attention to the extremely complex nature of the oil sardine and mackerel fisheries along the west coast of India which accounts for the bulk of the fish landing. They made an attempt to provide a suitable explanation for these on the basis of nutrient distribution pattern associated with the occurrence of the seasonal upwelling. They have concluded that the part of the Indian coast known to support a very rich fishery for the oil sardine and mackerel is a region of great biological and oceanographical complexity, almost of biological instability and have pointed out that a thorough understanding of the various factors is essential for finding a satisfactory solution to the major problem of the differences in the fishery productivity of the east and west coasts of India.

From the investigations mentioned above and from other available information it would appear that invariably high concentrations of fish, particularly the pelagic ones, occur in areas of high plankton production which in turn will be areas of upwelling or local enrichment in the tropical oceans. It is also known that in the tropics, areas where there is no constant replenishment of nutrients are poor in plankton production because of the rapid utilization of the nutrients present in the euphotic zone.

Although in area the Arabian Sea is only about 1·8 times that of the Bay of Bengal, the yield of fish from the former region is nearly 2·4 times. Compared to this the total fish landings from the western half of the Indian Ocean (approximately 78° E long. as the line of demarcation) are about 1·6 times those of the eastern half. Considering the fish production of the east and west coasts of India this difference is found to be still magnified, the landings along the west coast being almost three times those of the east coast. On the whole the fisheries of the western and eastern seaboards of the Indian subcontinent reflect the features of the fisheries of the northern Indian Ocean (Figs. 19 and 20) with the pelagic and mid-pelagic species dominating in both cases.

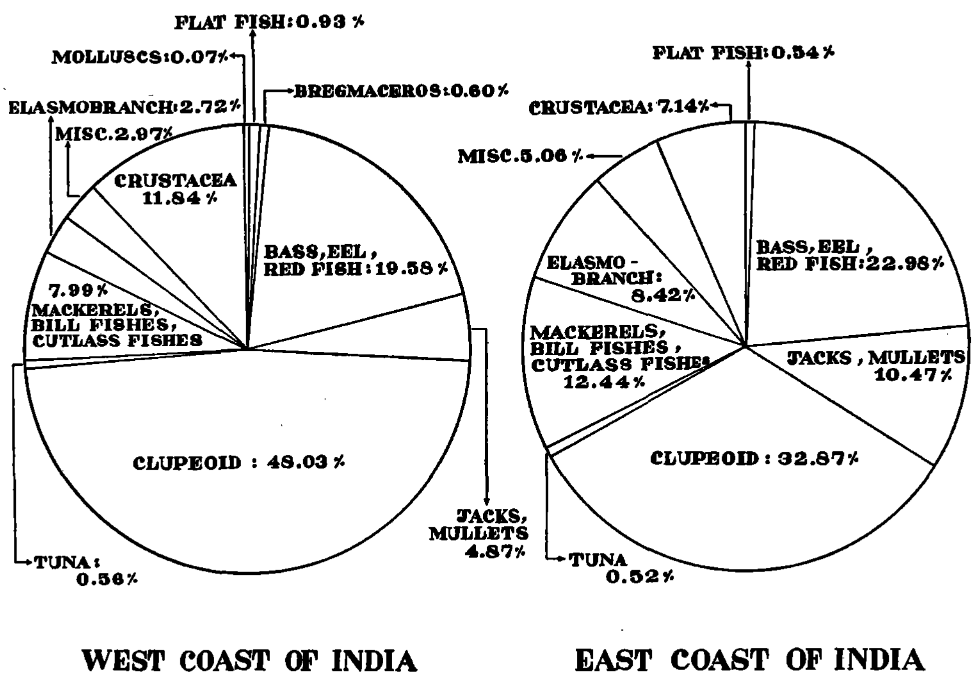

FIG. 19. The catch composition of the west and east coasts of India.

The trend of fish production along the coasts of India for periods approximating to those taken into account for plankton (October–March and April–September) is considered below. The months of October to March coincide with a period of seasonal abundance of fish and intensive fishing activity along the west coast of India and over 80 per cent of the marine fish landed in India during this time is from the west coast. On the east coast in the other half of the year (April to September) the fish landings are comparatively high forming 30 per cent of the total for the Indian coasts. The abundance of the fish along the west coast coincides with the post-south-west monsoon period when a large section of the waters of the region has been enriched by

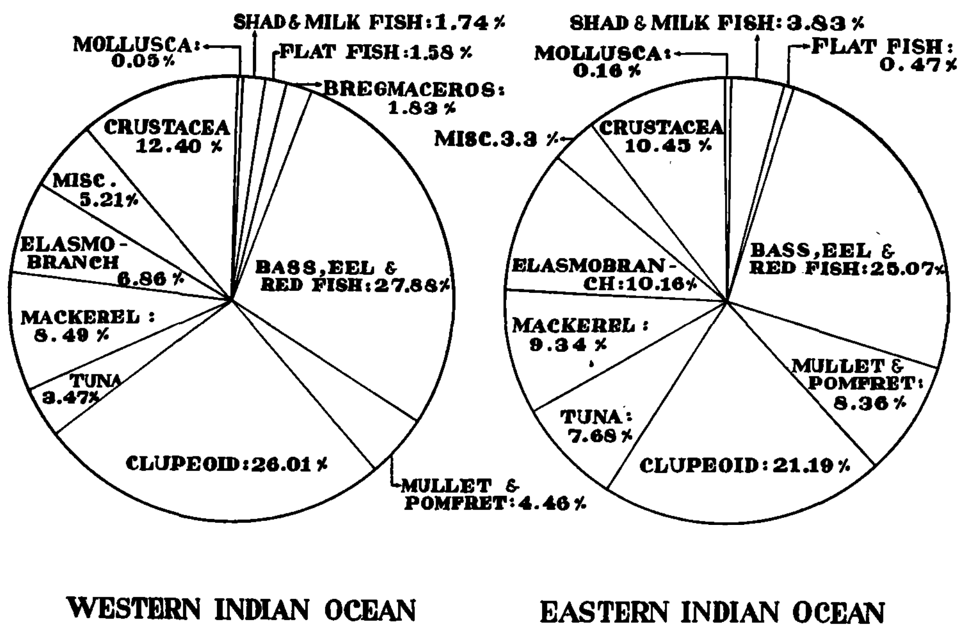

FIG. 20. The catch composition of the western and eastern halves of the Indian Ocean.

upwellings and favourable conditions for production of plankton have been established along the region. The weather is also settled without the effects of any monsoon conditions which hamper fishing activities. The annual appearance of densely shoaling species like the oil sardine, mackerel, prawns, flat-fishes and Bombay-duck start from August/September and these species are the mainstay of the fisheries of the region. April to September is a period of comparative calmness and is favourable for fishing activities on the east coast.

Some salient features of the regionwise availability of different groups of fish are evident from a categorized analysis of the species landed along the coasts of India during 1964–66. Over 80 per cent of the crustaceans, flat-fishes, Indian mackerel and clupeids and 70 per cent of the tunas are caught along the west coast. The elasmobranchs are the only group which makes a substantial contribution to the all-India landings along the east coast. They contribute about 48 per cent of the total for the country. Catch composition for the west coast (1964–66) shows (Fig. 19) that 48 per cent are composed of clupeids, the dominant element being the oil sardine *Sardinella longiceps*, 20 per cent by the 'red fishes, basses and congers' group represented by *Harpodon nehereus*, sciaenids, goat-fishes, lizard-fishes, marine catfishes, eels, perches and silver-bellies. Crustaceans, mainly penaeid and non-penaeid prawns, constitute 12 per cent and the 'mackerels, bill-fishes and cutlass fishes' category (of which the Indian mackerel *Rastrelliger kanagurta* forms the major portion) forms 8 per cent. The 'jacks, mullets' group comprising barracudas, pomfrets, flying fishes, half-beaks, mullets, carangids and polynemids forms about 5 per cent. Elasmobranchs contribute about 3 per cent and flatfishes about 1 per cent. Gadidae represented by a single genus *Bregmaceros* and the 'tunas, skipjack and bonitos' constitute less than 1 per cent each.

On the east coast the clupeids which form about 33 per cent of the catches have the lesser sardines (mainly *Sardinella albella* and *S. jussieu*) and white-baits (*Anchoviella* spp.) as the dominant elements. The 'red fishes, basses, congers' group forms about 23 per cent and the 'mackerels, bill-fishes, cutlass fishes' group dominated by the genus *Trichiurus* about 12 per cent. 'Jacks, mullets' group contributes about 10 per cent, elasmobranchs 8 per cent and crustaceans about 7 per cent.

A generalized picture of the fishery resources of the coasts of India has been given above based on the results of random sampling of fish catches along the areas concerned. This over-all picture highlights the higher productivity of fish along the western coast of India bordered by the Arabian Sea where higher plankton production has also been consistently recorded. In terms of zooplankton biomass the west coast of India, particularly the southern half, is invariably about 2·5 times more productive than the east coast and this is well reflected in the fish landings also since the landings along the west coast are about three times those of the east coast.

Pelagic fisheries

In attempting to study the relation between the zooplankton biomass and fisheries of a region it will be the pelagic fisheries which will show direct relationship. Even then the quantitative relation is valid only in general terms. As mentioned earlier the dominant components of the fishes caught off the coasts of India are either pelagic or mid-pelagic amounting to almost 75 per cent. The truly pelagic fishes are the sardines, mackerel, anchovies, seer, ribbon fishes, carangids, silver-bellies, flying fishes, tunas, sail and sword fishes, etc. While these are common along both the coasts of India large-scale shoaling of pelagic fishes like the oil sardines and mackerel occurs only along the west coast and that too along the southern half of the coast. From the distribution of zooplankton biomass it was seen that during the south-west monsoon period there is a region of comparatively high-standing crop between Cape Comorin and north of Karwar. During the season of the north-east monsoon, although there is a reduction in the extent of area as well as the quantity of production, the Cochin-Mangalore region remains a relatively high production belt. This area coincides with the region of the most important pelagic fisheries of the west coast, the oil sardines and the mackerel which alone account for nearly 28 per cent of the landings of this coast. Considering all fisheries it could be said that almost 70 per cent of the landings are from this zone. It will be seen from the distribution of zooplankton biomass that the northern half of the west coast is comparatively poor and in this region there is a conspicuous absence of large shoals of pelagic fishes and a lower over-all fish production.

The magnitude of zooplankton biomass along the east coast is decidedly low and the scarcity of pelagic shoaling fishes like the oil sardines and mackerel is conspicuous. However, occasional shoals of mackerel are caught off Mandapam, Porto Novo, Madras, Kakinada, Waltair and certain parts of Orissa and of oil sardines from the coasts of Madras, Andhra and Orissa States. The mackerel *Rastrelliger brachysoma* forms a good fishery in the neighbourhood of the Andaman Islands. Pelagic fishes such as anchovies, seer, the lesser sardines, ribbon fishes, silver-bellies, flying fish, etc., constitute a significant percentage of the inshore catches and good tuna fisheries are known to exist in the Andaman Sea where there is a moderately high concentration of zooplankton during April–October period. Prasad and Nair (1963) based on their study of organic production along a stretch of the south-east coast of India (Gulf of Manaar) suggested the possibility of increasing the rate of exploitation. Of late a large number of mechanized vessels have started operating in the area resulting in a substantial increase in the fish landings the bulk of which constitute the silver-bellies.

Ground fisheries

The trawlable ground fish resources along the Indian coasts remained little exploited till recently. However, efforts have been made during the last two decades to initiate and expand trawl fishing and significant advances in this direction have been made during the last one decade. The results of exploratory as well as commercial trawling indicate the existence of rich grounds for different demersal species along the Indian coasts and it has been possible to suggest with the available information (Malpas 1926; Gravely 1929; Sundara Raj 1930; Hefford 1949; Chidambaram and Rajendran 1951; Gopinath 1954; Sivalingam and Medcof 1957; John 1959; Jayaraman *et al.* 1959; Poliakov 1962; Sivalingam 1964; Pruter 1964; Rao 1967; Annual

Reports of the C.M.F.R. Institute, Mandapam Camp, etc.) that the yield of ground fish from the west coast of India is comparatively more than from the east coast.

The percentage composition by weight of trawl catches along the coasts is presented in Fig. 21 based on exploratory fishing operations conducted by the Government of India (Rao 1967, Tholasilingam *et al.* 1967, *unpublished*, Central Marine Fisheries Research Institute, Annual Reports, 1957–66). Miscellaneous fish comprising small sciaenids, lizard-fishes, flatheads, carangids, etc., to the extent of 40–50 per cent and elasmobranchs 5–25 per cent are common to all areas on the west coast. In the Bombay region sciaenids form about 43 per cent of the catch which include good table fishes like *Pseudosciaena diacanthus* and *Otolithoides brunneus* which by themselves form about 5 per cent of the total catch from the region. Among other groups elasmobranchs contribute 25 per cent, catfish 7 per cent, eels and polynemids 3 per cent, *Pomadasys hasta* 3 per cent, prawns about 2 per cent and miscellaneous fish 17 per cent.

At Karwar medium-sized trawlers land mostly Leiognathids (25 per cent), clupeids, mainly *Opisthopterus tardoore* (21 per cent) and miscellaneous small fish (40 per cent). Elasmobranch component is much reduced (5 per cent). There is similarity with the Bombay region in the negligible amount of prawns in the catches. *Lactarius lactarius* is probably the only table fish available from the area.

Mangalore-Quilon region is known for the substantial prawn component in the trawl catches and full-scale commercial shrimp trawling by medium-sized boats has got established at many centres along the region. Generally prawns constitute 25–35 per cent by weight of the trawl catches along the region, mostly caught at intermediate (20–35 m) and shallow (within 20 m) depths. Elasmobranchs constitute 6–14 per cent of the catch and miscellaneous small fishes about 50 per cent. A new fishery, struck by the medium boats at intermediate depths and beyond, in the region is based on the threadfin breams (kilimeen), mainly one species, *Nemipterus japonicus*. 'Kilimeen' contributes 8–14 per cent of the catches of these vessels at Cochin.

Larger vessels which operated in deeper grounds on the continental shelf (1957–61) in the Cannanore-Cape Comorin region using 'Bull trawls' or fish trawls showed the trend of availability of the demersal fish in the region. Elasmobranchs and miscellaneous small fish have been common all along the region. In the northern section (Cannanore-Calicut) a significant catfish component was noticed, whereas in the southern sector (south of Alleppey and Cape Comorin grounds) a dominant perch component was observed. The middle sector (Cochin-Alleppey) appears to be a transition zone with small quantities of catfish and perches but more of the miscellaneous fish.

On the east coast at Tuticorin, trawl catches showed dominance of Leiognathids and sciaenids, together constituting nearly 60 per cent.

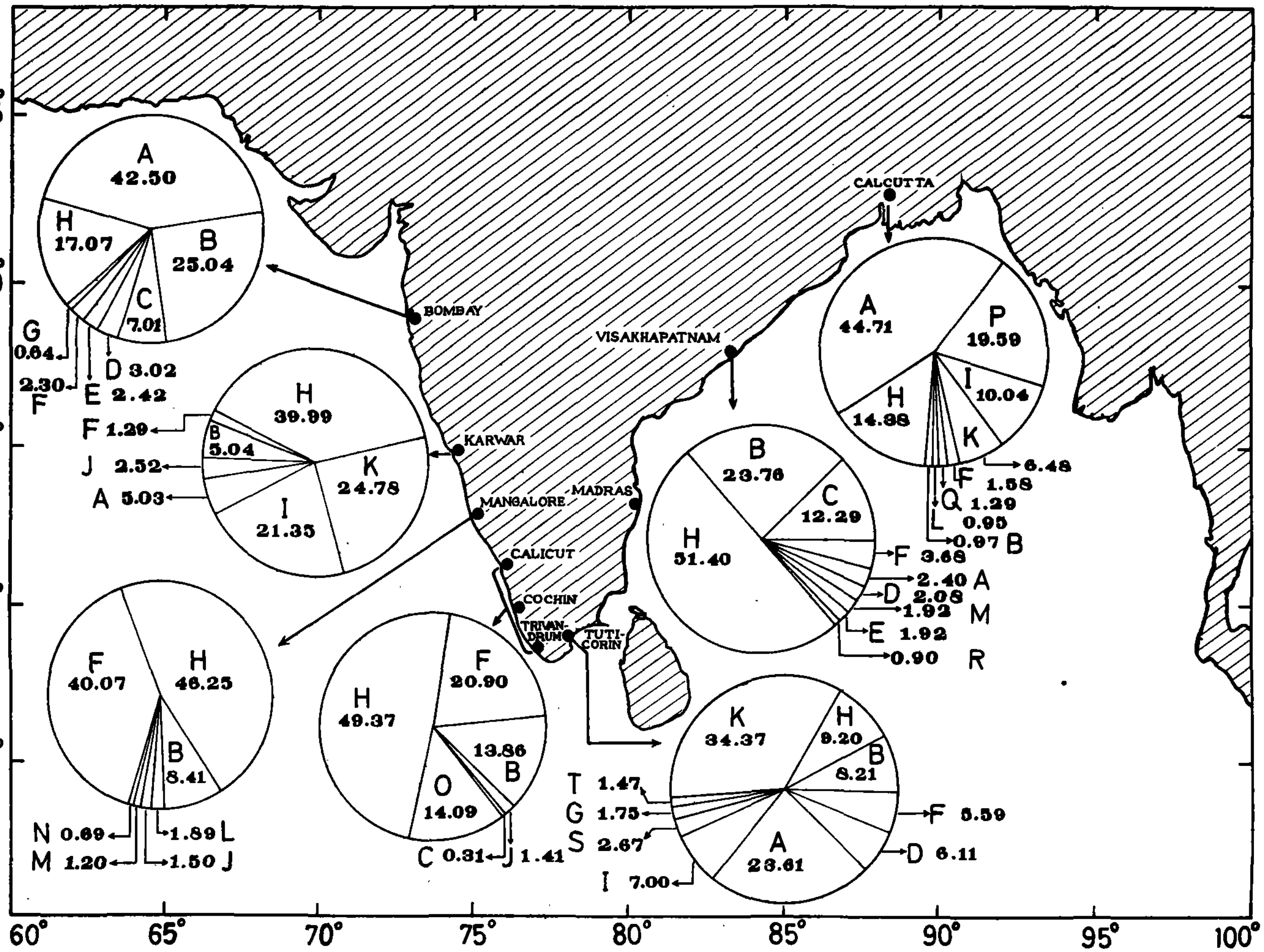

FIG. 21. The percentage composition by weight of trawl catches along the west and east coasts of India. A, sciaenids; B, elasmobranchs; C, catfishes; D, *Pomadasys hasta*; E, eels; F, prawns; G, polynemids; H, miscellaneous; I, clupeids; J, *Lactarius lactarius*; K, *Leiognathus* spp.; L, pomfrets; M, *Trichiurus* spp.; N, lobsters; O, *Nemipterus japonicus*; P, *Kurtus indicus*; Q, *Harpodon nehereus*; R, carangids; S, *Saurida* spp.; T, *Upeneus* spp.

Elasmobranchs (8 per cent), clupeids (7 per cent), *Pomadasys* sp. (6 per cent), prawns (6 per cent) and few other miscellaneous species constituted the rest. Trawl catches in the Mandapam area consisted mainly of silver-bellies (90 per cent), catfishes, *Lactarius lactarius*, rays, prawns and mixed fish.

At Visakhapatnam about 50 per cent of the catch consisted of miscellaneous small fish. Elasmobranchs (24 per cent) and catfish (12 per cent) are the dominant individual items from the region. Prawns constituted a small percentage of the catch (4 per cent). Others were sciaenids about 2 per cent, *Pomadasys hasta* (2 per cent), *Trichiurus* spp. (2 per cent), eels (2 per cent) and carangids about 1 per cent.

Ground fish catches along the Orissa-West Bengal coasts showed dominance of sciaenids (45 per cent). Other items of importance being *Kurtus indicus* (20 per cent), *Leiognathus* spp. (6 per cent), clupeids (10 per cent) and miscellaneous small fish. Hardly 2 per cent of the catch consisted of prawns.

Data available now from exploratory fishing operations enable a general assessment of the productivity of different trawling grounds along the Indian coasts.

The north-western ground from Bombay to Kutch is found to yield on an average a catch 747 kg/hour of 'Bull trawling' (1957–62). Otter trawling during recent years (1961–65) showed a catch rate of 198 kg/hour from the Malvan-Kutch region. At Karwar medium-sized vessels showed a catch rate of 150–219 kg/hour (1963–66). At Mangalore the same type of vessels landed 178–206 kg of fish per hour during 1959–61 and 99–255 kg/hour during 1962–65. Bull trawling yielded 591 kg/hour from the Cannanore area (1957-58), while medium vessels operating shrimp trawls returned 268 kg/hour (1960-61). The yield of smaller shrimp trawlers during 1965-66 was less, being only about 83 kg/hour. High returns ranging from 717 to 2,033 kg/hour were recorded by Bull trawlers (1957–59) from the Calicut area. Otter trawling by the same vessels yielded 136 kg/hour (1960-61).

Bull trawling in the Cochin area showed a catch rate of 1,015–1,184 kg/hour (1957–59). Shrimp trawlers yielded 91–250 kg/hour in 1957–61 period and 111–216 kg/hour during 1961–65 period. In the Alleppey-Quilon area catch rates of 583–1,025 kg/hour was recorded for Bull trawl (1957–59) and 158–187 kg for otter trawling by the same vessels in 1959–61 period. Shrimp trawling yielded 105–220 kg/hour during 1958–60.

In the Trivandrum area Bull trawling yielded 509 kg/hour and on the Cape Comorin banks 352 kg/hour (1957-58). Otter trawling in the latter grounds yielded much less, the rate being 69–83 kg/hour (1959–61).

On the east coast off Tuticorin trawl operations (1963–65) yielded 122–153 kg/hour and in the Mandapam area average catch in 1965-66 amounted to 223 kg/hour. Off Pondicherry catch rate of 76 kg/hour was recorded during 1965-66.

The area between Godavari and Mahanadi estuaries covered from Visakhapatnam during 1959-60 yielded on an average 90 kg of fish per hour. Catches at the rate of 78–115 kg/hour were recorded during 1964 and 1965. Experimental catch with 15 m Russian trawl yielded 192 kg of fish per hour (Poliakov 1962). Catches at the rate of 2,450 kg/day's absence were recorded from the Orissa-West Bengal coasts during 1961 (300 h.p. trawler) and 151 kg/hour during 1962-63.

Pruter (1964) has given the trawling results of R.V. *Anton Bruun* at different stations of the Arabian Sea and the Bay of Bengal during 1963. Fishing in the Arabian Sea was conducted along the coasts of north-west India, West Pakistan, Gulf of Oman and Arabia. In the Bay of Bengal, Andaman Island region, coasts of Thailand, Burma and East Pakistan were covered. Catch per hour for Arabian Sea and Bay of Bengal, worked out separately from these operations, showed yields of 123 kg and 48 kg respectively, indicating about 2·5 times productivity in the Arabian Sea. Based on the indices of productivity of demersal fishes along the coasts of India mentioned above it could be suggested that the grounds on the west coast are comparatively richer.

Conclusion

In conclusion it may be stated that the data on the chlorophyll concentrations, primary organic production and the distribution of zooplankton biomass presented in the earlier section clearly show that the level of fertility is noticeably higher in the Arabian Sea as compared to the Bay of Bengal. This high organic production, however, need not necessarily be converted fully into fish protein of commercially exploitable nature and unusually high organic production could also sometimes lead to untoward results. Thus, several instances of mass mortality of fish resulting from the very high plankton production in the northern half of the Arabian Sea have been reported. While these mass mortalities should be considered as major catastrophes they have proved beyond doubt the existence of large populations of fish in the Arabian Sea. According to Bogorov and Rass (1961) there is evidence of significant fishing resources in the open parts of the Indian Ocean, first of all in the waters of the Arabian Sea.

There are apparently several factors contributing to the low fish production in the Bay of Bengal. Although seven big rivers open into the Bay which would deposit large quantities of riverine organic material for creating conditions favourable for good demersal fisheries, much of this material is presumed to be retained on the land itself because of the longer run of these rivers along the plains compared to those rivers emptying into the Arabian Sea. Also, owing to the narrow continental shelf at the mouths of most of these rivers along the east coast much of the riverine material reaching the sea is lost to great depths. Added to this is the fact that there is lack of large-scale upwelling in the region. This absence of extensive upwelling along the coastal regions is presumably the reason for the absence of shoaling fishes like the oil sardine and the Indian mackerel which are mostly found in regions of coastal upwelling. The unfavourable condition of the grounds for trawling along the shelf in many areas restricts the scope of large-scale expansion of ground fisheries.

The fisheries of India are now almost entirely dependent on the coastal resources though there is a gradual trend to exploit new grounds both along the coast as well as in the deeper and the open ocean. If the density of zooplankton biomass is an indication of the potential fishery resources of an area, the data presented in the foregoing pages suggest the possibility of substantial increase in the rate of exploitation, particularly in the areas such as the south-eastern coast of India, West Pakistan and Iran in the Arabian Sea region and the coasts of Burma, East Pakistan, West Bengal, Orissa and west coast of Ceylon and the Andaman Sea in the Bay of Bengal. The increase is not only possible from the pelagic mid-pelagic complex of fishes but also to a certain extent from the ground fish resources. There are already indications from the recent trends in the exploratory and commercial fishing activities that these areas of high plankton production are indeed potentially rich fishing grounds. Thus, the data on zooplankton biomass fully support the hope and optimism in the further expansion of the fisheries of the two regions.

Acknowledgements

The author wishes to record his grateful thanks to Dr. N. K. Panikkar, Director, National Institute of Oceanography, for allowing the use of the data and to Dr. E. Brinton, the UNESCO Curator, for many courtesies and discussions. To the scientific staff of the Indian Ocean Biological Centre and to some of his colleagues in the Central Marine Fisheries Research Institute the author is grateful for various assistance rendered.

References

Bogorov, V. G., and Rass, T. S. (1961). On the productivity and prospects of fishing in waters of the Indian Ocean. *Okeanol.*, 1961, **1**, 107–109 (*in Russian*).

Central Marine Fisheries Research Institute (1965-66). Annual Reports of the Director, C.M.F.R.I., for the years 1957–1966. *Central Marine Fish. Res. Inst., Mandapam Camp.*

Chidambaram, K., and Menon, M. D. (1945). The co-relation of the west coast (Malabar and South Kanara) fisheries with plankton and certain oceanographical factors. *Proc. Indian Acad. Sci.*, 31B, 252–286.

Chidambaram, K., and Rajendran, A. D., Issac (1951). On the hydrobiological data collected on the Wadge Bank early in 1949. *J. Bombay nat. Hist. Soc.*, 49, 738–748.

Currie, R. I. (1963). The Indian Ocean Standard Net. *Deep Sea Res.*, **10**, 27–32.

Gopinath, K. (1954). A note on some deep sea fishing experiments off the south-western coast of India. *Indian J. Fish.*, **1**, 163–177.

Gravely, F. H. (1929). A systematic survey of the Madras deep sea fishing grounds by steam trawler *Lady Goschen*, 1927-28. Report No. 3 of 1929. *Madras Fish. Bull.*, **23**, 153–187.

Hefford, A. E. (1949). Report on the work of the steam trawler *William Carrick*, Govt. of Bombay, Dept. of Industries. 110 pp.

Jayaraman, R., Seshappa, G., Mohamed, K. H., and Bapat, S. V. (1959). Observations on the trawl fisheries of Bombay and Sourashtra waters, 1949-50 to 1954-55. *Indian J. Fish.*, **6**, 58–144.

John, C. C. (1959). Fishes and Fisheries of the Cape Comorin Bank. *Bull. Res. Inst. Univ. Kerala, Ser.* C, **7**, 65–145.

Kabanova, Yu. G. (1961). Primary production and nutrients in the Indian Ocean. *Acad. des Sci. de L'URSS Comite de l'Annee. Geophysique Internationale*, X Section of the IGY programme (Oceanology), No. 4, 72–75 (*in Russian*).

Laird, J., Breivogel, B. B., and Yentsch, C. S. (1964). The distribution of chlorophyll in the western Indian Ocean during the south-west monsoon period, July 30–November 12, 1963. Woods Hole Oceanographic Institution, Ref. No. 64–33 : 1–52 (Mimeo.).

Longhurst, A. R. (1966). Biological basis of tropical fisheries. *Second Int. Ocean. Congr., Moscow, Abstracts of Papers*, No. 262–SIIe : 230-231.

Malpas, A. H. (1926). The Marine Biological Survey of the littoral waters of Ceylon. *Ceylon J. Sci.* (C), **11**, 13-165.

McGill, D. A. (1966). Chemical and biological observations in the western Indian Ocean during the south-west monsoon, 1963. *Second Int. Ocean. Congr., Moscow, Abstracts of Papers*, **284**, 248-249.

Panikkar, N. K. (1966). Fishery resources of the Indian Ocean. *Second Int. Ocean. Congr., Moscow, Sec.*; oceanography of the Indian Ocean and Antarctic. 1–27 (Mimeo.).

Panikkar, N. K., and Dwivedi, S. N. (1966). Fisheries of the Asian countries bordering the Indian Ocean. *Proceedings of the Seventh International Congress of Nutrition, Hamburg*, 4, 1–24.

Panikkar, N. K., and Jayaraman, R. (1966). Biological and oceanographic differences between the Arabian Sea and the Bay of Bengal as observed from the Indian region. *Proc. Indian Acad. Sci.*, **64B**, 231–240.

Poliakov, M. P. (1962). Report to the Government of India on exploratory trawling in the Bay of Bengal. *Rep. FAO/EPTA–1573*, 31 pp.

Ponomareva, L. A., and Naumov, A. G. (1962). Distribution of zooplankton biomass in the Arabian Sea and Bay of Bengal during the period of monsoon change. *Dokl. Akad. Nauk. SSR.*, **142**, 449–452 (*in Russian*).

Prasad, R. R., and Ramachandran Nair, P. V. (1963). Studies on organic production—I. Gulf of Manaar. *J. mar. biol. Ass. India*, **5** (1), 1–26.

Pruter, A. T. (1964). Trawling results of R.V. *Anton Brunn* in the Bay of Bengal and Arabian Sea. *Comm. Fish. Rev.*, **26** (11*a*), 27–35.

Rao, K. V. (1967). Exploratory fishing. *Souvenir, Twentieth Anniversary, Central Marine Fisheries Research Institute, Mandapam Camp*, 25–36.

Robinson, Margaret K. (1966). Seasonal variation of temperature in the upper 100 metres of the Indian Ocean, Arabian Sea, Bay of Bengal and Red Sea. *Second Int. Ocean. Congr., Moscow, Abstracts of Papers*, No. 357–SIVa : 303-304.

Ryther, J. H., Hall, J. R., Pease, A. K., Bakun, A., and Jones, M. M. (1966). Primary organic production in relation to the chemistry and hydrography of the western Indian Ocean. *Limnol. Oceanogr.*, **11** (3), 371–380.

Ryther, J. H., and Menzel, D. W. (1965). On the production, composition and distribution of organic matter in the western Arabian Sea. *Deep Sea Res.*, **12** (2), 199–209.

Sivalingam, S. (1964). Assessment and possible development of the fishery resources of the Pedro Bank. *Bull. Fish. Res. Stn. Ceylon*, **17** (1), 133–150.

Sivalingam, S., and Medcof, J. C. (1957). General features and productivity of the Wadge Bank Trawl fishery. *Bull. Fish. Res. Stn. Ceylon*, 6, 1–23.

Steemann Nielsen, E., and Jensen, E. A. (1957). Primary organic production. The autotrophic production of organic matter in the oceans. *Galathea Rep.*, **1**, 49–136.

Subrahmanyan, R. (1959). Studies on the phytoplankton of the west coast of India, Pts. I and II. *Proc. Indian Acad. Sci.*, **50**, 115–252.

——— (1967). Phytoplankton. *Souvenir Twentieth Anniversary, Central Marine Fisheries Research Institute, Mandapam Camp*, **89–93**.

Sudarsan, D. (1964). Observations on the plankton and trawler catches off Bombay. *J. mar. biol. Ass. India*, **6** (2), 222–225.

Sundara Raj, B. (1930). Report on a systematic survey of deep sea fishing grounds by steam trawler *Lady Goschen*, 1928-29. Report No. 3 of 1930. *Madras Fish. Bull.*, No. 24, 199–232.

Tholasilingam, T., George, K. C., Dayanandan, M. G., Karunakaran Nair, P., and Nandakumaran, K. (1967). Exploratory trawl fishing and ground fish resources along the Kerala coast and adjacent waters (*unpublished*).

Uda, M. (1966). Upwelling of the subpolar intermediate waters in the tropical world ocean in relation to the highly-productive zone including favourable tuna fishing grounds. *Second Int. Ocean. Congr., Moscow, Abstracts of Papers*, **438**, 373-374.

Varadachari, V. V. R., and Sharma, G. S. (1964). On the vergence field in the north Indian Ocean. *Bull. N.G.R.I.*, **2**, 1–14.

——— (1967). Circulation of the surface waters in the north Indian Ocean. *J. Indian Geophys. Union*, **4**, 61–73.

Reprinted from *Cah. O.R.S.T.O.M., Sér. Océanogr.* vol. VIII, no. 1, 1970, p. 47-57

SUR DES PHRONIMIDAE DE L'OCÉAN INDIEN ET DE L'OCÉAN PACIFIQUE, AVEC LA VALIDATION DE *Phronima bucephala* GILES, 1887 COMME ESPÈCE DISTINCTE DE *P. colletti* BOV., 1887 (CRUSTACÉS AMPHIPODES)

par Ph. LAVAL*

RÉSUMÉ

La découverte de Phronima colletti *(forme « Atlantique ») dans l'océan Indien et le Pacifique Ouest conduit à réexaminer le cas de la « forme Indo-Ouest Pacifique » de cette espèce décrite par* SHIH *(1969). Une étude morphologique détaillée permet de conclure que cette forme constitue une espèce distincte, déjà connue sous le nom de* P. bucephala *et mise à tort en synonymie avec* P. colletti. *Des renseignements supplémentaires sont donnés sur la morphologie et la distribution de l'espèce voisine* P. pacifica.

SUMMARY

The discovery of Phronima colletti *(« Atlantic form ») in the Indian Ocean and the West Pacific leads to a re-examination of the « Indo-W. Pacific form » described by* SHIH *(1969). From a morphological study of this form, it is concluded that it belongs to a separate species, already known as* P. bucephala *but erroneously included in the synonymy of* P. colletti. *Supplementary data are given on the morphology and distribution of the related species* P. pacifica.

INTRODUCTION

Dans sa récente révision des Phronimidae du « Dana », SHIH (1969) a décrit trois variétés géographiques de *Phronima colletti* Bov., 1887 : une forme Atlantique, une forme Indo-Ouest Pacifique et une forme du Pacifique Est. En examinant une collection de Phronimidae aimablement confiée par R. REPELIN (Centre O.R.S.T.O.M. de Nouméa), j'ai pu constater que la « forme Atlantique » de *P. colletti* était présente dans le sud-est de l'océan Indien et dans le Pacifique Ouest. De plus, un examen approfondi de la « forme Indo-Ouest Pacifique » de SHIH, que j'ai retrouvée à Madagascar dans le matériel mis obligeamment à ma disposition par S. FRONTIER

* Station zoologique, 06 — Villefranche-sur-Mer, France.

(Centre O.R.S.T.O.M. de Nosy-Bé), montre que les différences entre cette forme et la forme « Atlantique » sont de valeur spécifique. La juxtaposition géographique et les différences morphologiques permettent de conclure que cette « forme Indo-Ouest Pacifique » est en réalité une espèce distincte, qui a été sommairement décrite par GILES en 1887 sous le nom de *P. bucephala*, et mise à tort depuis en synonymie avec *P. colletti*.

Matériel.

Les exemplaires de Madagascar ont été récoltés dans la région de Nosy-Bé (*cf.* FRONTIER, 1966, pour l'emplacement des stations). Pour ce travail, 38 *P. bucephala* (23 ♂ et 15 ♀) ont été examinées, ainsi que 56 *P. pacifica* (25 ♂ et 31 ♀) et 4 *P. curvipes* (3 ♂, 1 ♀).

Les Phronimes du sud-est de l'océan Indien proviennent d'une radiale effectuée le long du 110e méridien E, de 9°30′ S à 32° S, par la division d'Océanographie du C.S.I.R.O., en accord avec le Centre O.R.S.T.O.M. de Nouméa. J'ai pu étudier 39 *P. colletti* (11 ♂ et 28 ♀), 79 ♂ de *P. pacifica* et 62 ♂ de *P. curvipes*.

Les individus du Pacifique ont été capturés le long du 170e méridien E, entre 5° N et 20° S. Ce matériel comprend 1 *P. colletti* (♀ adulte), 1 *P. bucephala* (♀ adulte), 110 *P. pacifica* ♂ et 14 *P. curvipes* ♂.

La répartition détaillée sera publiée avec les études écologiques entreprises par S. FRONTIER (Nosy-Bé) et R. REPELIN (Nouméa). Je signale toutefois que les individus utilisés pour les illustrations proviennent des stations suivantes :

P. bucephala ♀ : 13°34′ S-47°44′ E ; 15 nov. 1965 ; 23 h 30 ; 10 m.
P. bucephala ♂ : 13°34′ S-47°44′ E ; 20 sept. 1965 ; 23 h 50 ; 10 m.
P. colletti ♀ : 29°00′ S-110°00′ E ; 10 nov. 1962 ; 21 h 14-22 h 58 ; chalut Isaacs-Kidd, 200 m.
P. colletti ♂ : 32°02′ S-110°00′ E ; 11 nov. 1962 ; 21 h 35-23 h 08 ; chalut Isaacs-Kidd, 200 m.
P. pacifica ♂ : 2°31′ S-169°53′ E ; 29 sept. 1966 ; 13 h 40 ; chalut Isaacs-Kidd, 1250 m.

I. COMPARAISON DE P. colletti ET P. bucephala

La littérature n'apportant pas d'illustrations assez précises des appendices de *P. colletti*, j'ai redessiné les plus importants, avec en regard les appendices correspondants de *P. bucephala* (fig. 1, 2 et 3). Les proportions de ces dessins sont suffisamment exactes pour me dispenser d'un texte descriptif. J'insisterai seulement sur les différences entre les deux espèces et les caractères non figurés.

1. Différences entre les femelles.

Certaines ont déjà été soulignées par SHIH (1969) pour distinguer l'« Atlantic form » (= *P. colletti*) de l'« Indo-W. Pacific form » (= *P. bucephala*) : taille à maturité beaucoup plus faible pour *P. bucephala* que pour *P. colletti* (ainsi les femelles dessinées ici mesurent respectivement 5,7 et 10,1 mm); partie supérieure de la tête fortement bombée chez *P. colletti;* article basal du péréiopode V au moins un quart plus court que celui du péréiopode III chez *P. colletti*, plus long que l'article basal du péréiopode III chez *P. bucephala.*

Ces caractères ne sont pas les seuls à différencier les femelles des deux espèces. Le trait le plus commode à observer concerne la forme de la pince : le carpe du péréiopode V est chez *P. colletti* de forme rectangulaire, avec l'angle postérieur proximal remontant au-dessus de l'insertion de l'article méral; celui-ci est aussi long que large. Chez *P. bucephala* le carpe est de forme triangulaire, l'angle postérieur non remontant, et l'article méral beaucoup plus long que large. L'article basal est nettement plus court que l'article basal du péréiopode IV chez *P. colletti*, de même taille chez *P. bucephala.*

L'article basal des péréiopodes III et IV s'élargit à l'extrémité distale chez *P. colletti*, et leurs carpes sont un peu plus dilatés que chez *P. bucephala.* Une garniture dense de courtes soies triangulaires est présente sur la face *interne* du carpe et du propode du péréiopode IV ainsi que sur celle des articles ischial, méral, du carpe et du propode du péréiopode III chez *P. colletti.* Cette ornementation se réduit à une ligne de soies sur le carpe et le propode de ces péréiopodes chez *P. bucephala.*

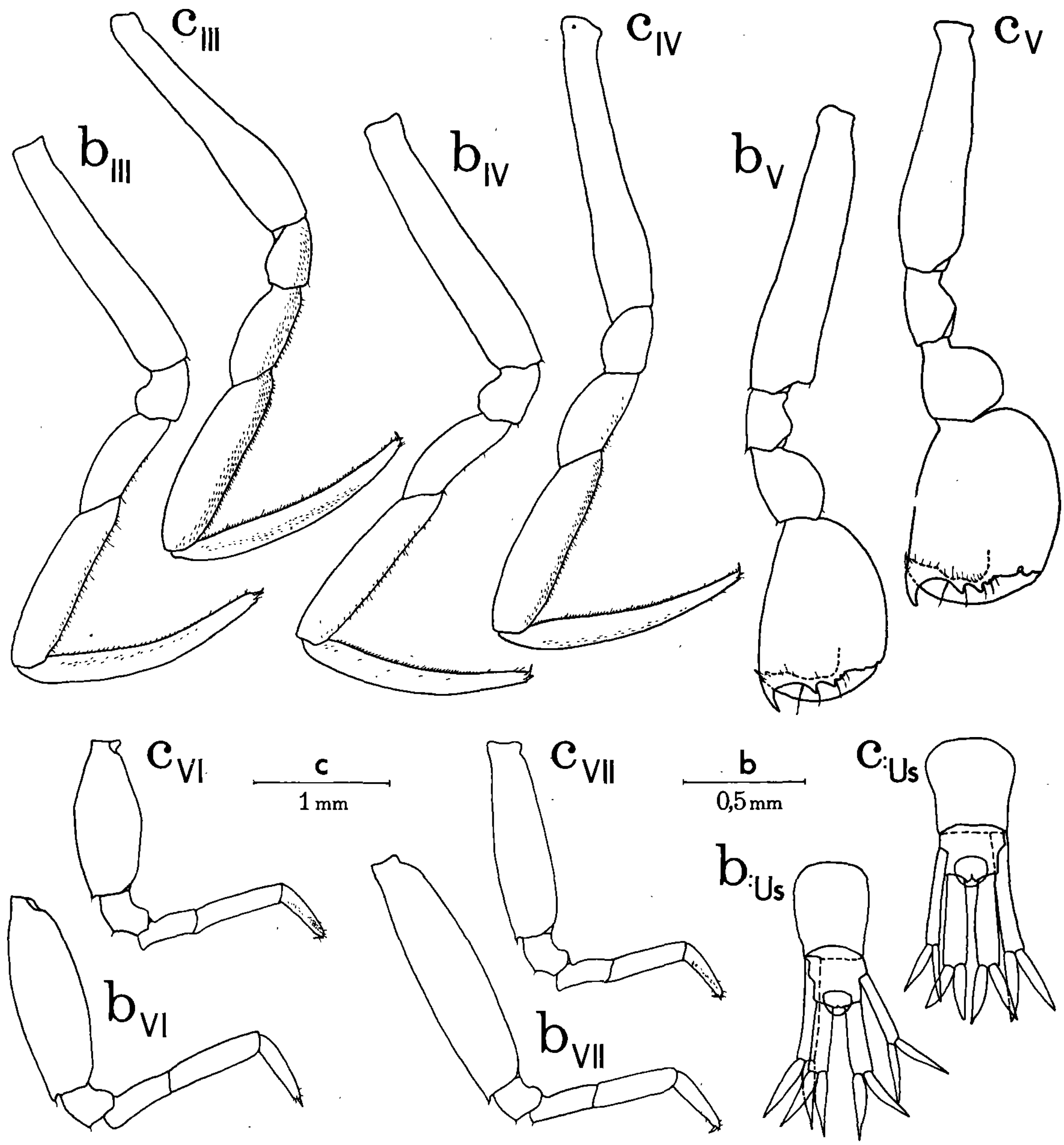

Fig. 1. — c : *Phronima colletti*, femelle adulte de l'océan Indien ; c_{III}-c_{VII} : péréiopodes III à VII ; Us : urosome. — b : *Phronima bucephala*, femelle adulte de l'océan Indien ; b_{III}-b_{VII} : péréiopodes III à VII ; Us : urosome. Les garnitures de petites soies sont situées sur la face *interne* des appendices (remarque valable également pour les fig. 2 et 3).

La première branchie (celle du segment IV) est très réduite chez *P. colletti:* elle est égale à la moitié, en longueur et en largeur, de la branchie V. Elle est beaucoup plus grande chez *P. bucephala:* elle atteint les 3/4 de la longueur et les 4/5 de la largeur de la branchie V. Ce caractère est constant chez tous les individus que j'ai examinés, y compris chez quelques exemplaires de la Méditerranée et de l'Atlantique N. en ma possession.

La fig. 1 montre que les péréiopodes VI et VII sont différents chez les deux espèces. Leurs articles basaux sont beaucoup plus petits par rapport aux autres péréiopodes chez *P. colletti:*

l'article basal du péréiopode VI est égal à 1/2 de celui du péréiopode IV chez *P. colletti*, aux 2/3 chez *P. bucephala;* pour les péréiopodes VII, ces rapports sont respectivement de 2/3 et 7/8. Le propode est garni sur la face interne de soies assez nombreuses chez *P. colletti;* ces soies sont pratiquement absentes chez *P. bucephala.*

Enfin les pédoncules de tous les uropodes sont beaucoup plus longs par rapport aux branches chez *P. colletti.*

Il faut remarquer pour terminer que les femelles de *P. colletti* de l'océan Indien diffèrent légèrement de celles de l'Atlantique. Par exemple, SHIH (1969) note que « chez la forme Atlantique le péréiopode V est remarquablement court, plus court que la longueur du péréion. Son article basal est au moins un quart plus court que celui du péréiopode III ». Chez mes exemplaires de *P. colletti* de l'océan Indien, le péréiopode V est de même taille que le péréïon, l'article basal à peine (1/12) plus court que celui du péréiopode III.

2. Différences entre les mâles.

Comme on peut l'observer pour les espèces voisines, les mâles sont plus difficiles à distinguer que les femelles.

Les différences les plus remarquables concernent les péréiopodes V. SHIH (1969) a déjà noté la forme du carpe, dont l'angle postérieur proximal remonte largement au-dessus de l'insertion de l'article méral chez *P. colletti;* cet angle n'est pas remontant (ou très peu) chez *P. bucephala.* La plus grande largeur de l'article méral est située au tiers proximal chez *P. colletti*, au milieu chez *P. bucephala.* Le tubercule terminal du propode est plus marqué chez cette dernière espèce. L'article basal est plus étroit proximalement chez *P. colletti;* le bord antérieur est fortement convexe, comme l'a souligné SHIH (1969). L'article basal de l'individu de l'Atlantique dessiné par cet auteur montre une petite dent distale postérieure qui est absente chez tous mes exemplaires de *P. colletti* de l'océan Indien (cette dent est bien marquée chez *P. bucephala*). SHIH (1969) indique également que l'article basal du péréiopode V est plus court que celui du péréiopode III chez la forme Atlantique; il est de même taille chez mes exemplaires de l'océan Indien. Il est un peu plus long chez *P. bucephala.*

L'article basal du péréiopode IV est plus étroit proximalement chez *P. colletti.* Les petites soies denses qui garnissent la face interne de l'article méral, du carpe et du propode sont plus nombreuses chez *P. colletti;* le péréiopode III montre également cette différence.

Un bon caractère est donné par la taille de la branchie IV (première paire). Elle est nettement plus petite que la moitié de l'article basal du péréiopode IV chez *P. colletti*, nettement plus grande chez *P. bucephala.* Elle est aussi beaucoup plus petite (environ les 2/3 de la longueur et la moitié de la largeur) que la branchie V chez la première espèce et à peine plus petite chez la seconde.

Comparé à l'article basal du péréiopode IV, celui des péréiopodes VI et VII est plus petit chez *P. colletti*, comme chez la femelle, mais la différence est beaucoup moins accentuée que pour celle-ci. Cet article est plus dilaté chez *P. bucephala.* La garniture de petites soies est un peu plus dense sur la face interne du propode chez *P. colletti.*

Les individus dessinés ici mesurent 7,8 mm pour *P. colletti* et 5,9 mm pour *P. bucephala*, ce qui correspond aux tailles données par SHIH (1969).

En ce qui concerne les antennes, il faut noter que si le dernier article du flagellum des antennes I est à peine plus long que l'avant-dernier chez *P. colletti*, il est en général beaucoup plus long (1,5 à 3 fois) chez *P. bucephala.*

SHIH (1969) utilise le nombre d'articles du flagellum des antennes I pour différencier les deux « formes ». En fait ce nombre est variable, et si 6 semble être le nombre prédominant d'articles chez *P. colletti* contre 5 chez *P. bucephala*, j'ai trouvé quelques individus de *P. bucephala* à 6 articles; vraisemblablement seul le faible nombre d'individus examinés m'a empêché de trouver des variations plus étendues chez les deux espèces. En effet, un dénombrement effectué

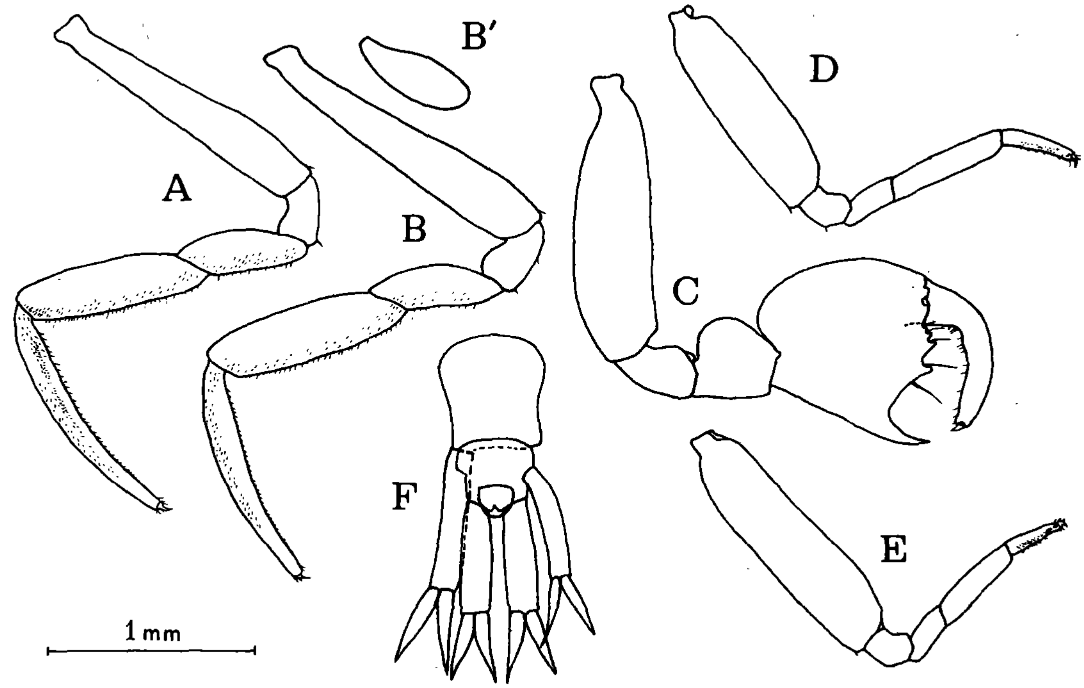

Fig. 2. — *Phronima colletti*, mâle adulte de l'océan Indien ; A-E : péréiopodes III à VII ; F : urosome.

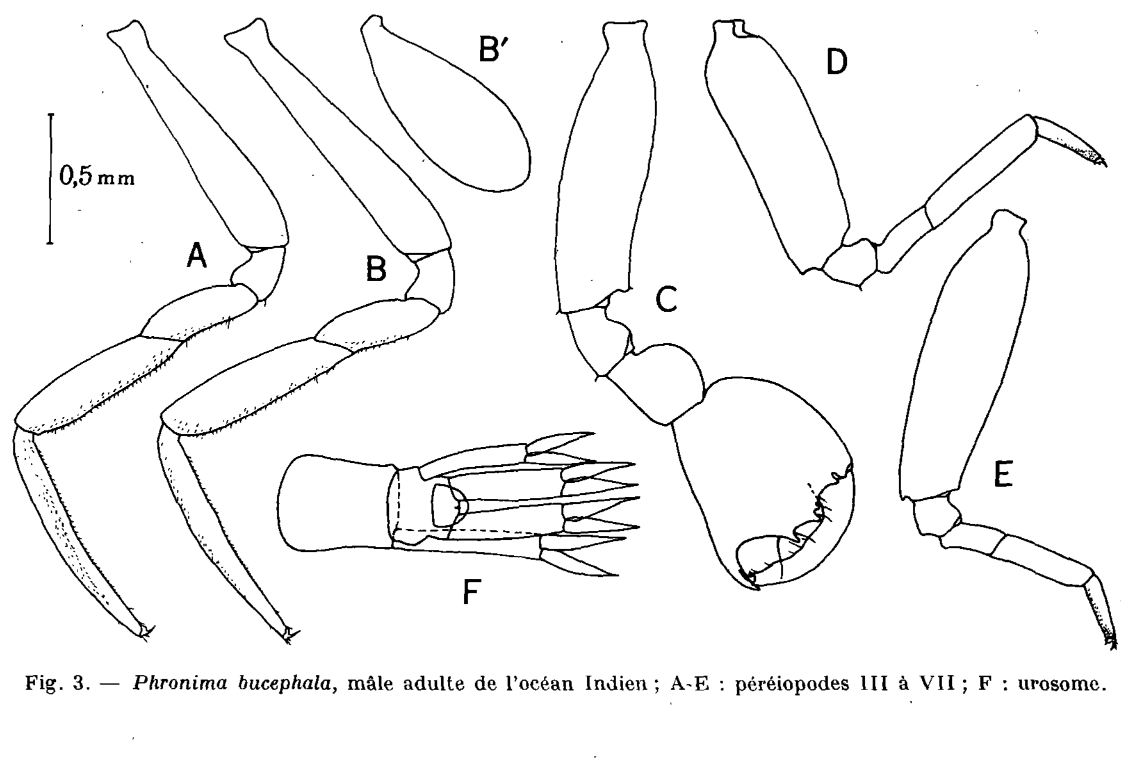

Fig. 3. — *Phronima bucephala*, mâle adulte de l'océan Indien ; A-E : péréiopodes III à VII ; F : urosome.

sur un plus grand nombre d'individus chez *P. pacifica* montre, à côté du nombre 6 indiqué par Shih pour cette espèce et trouvé pour 108 antennes I, six antennes à 5 articles et huit antennes à 7 articles (chaque antenne est comptée séparément pour ne pas perdre l'information apportée par les individus à une seule antenne intacte ou à nombre d'articles différent à droite et à gauche). De même, pour 61 antennes I de *P. curvipes* à 6 articles, nombre donné comme caractéristique par SHIH, on trouve cinq antennes à 5 articles et deux à 7 articles. Les variations encore plus considérables des antennes II (fig. 4) seront étudiées plus loin.

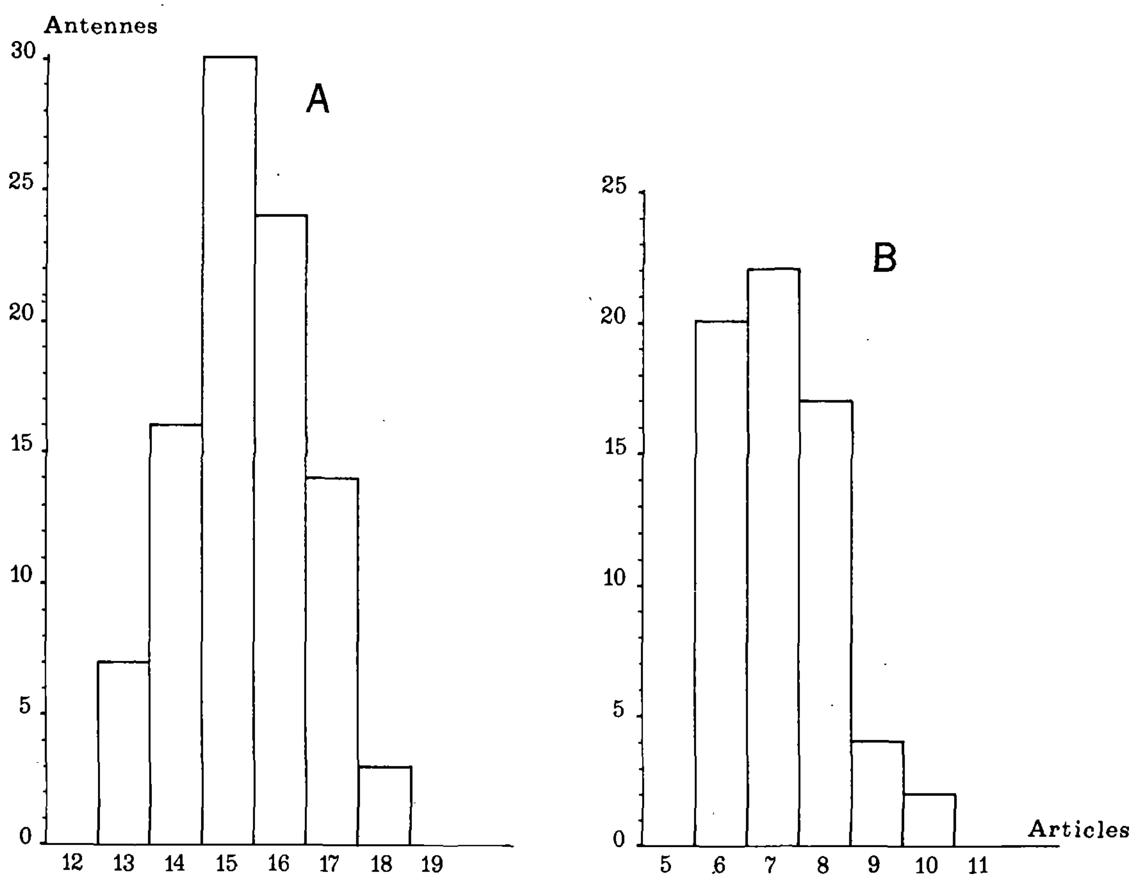

Fig. 4. — Histogrammes du nombre d'articles du flagellum des antennes II du mâle adulte ; chaque antenne est comptée séparément. — A : *Phronima pacifica* (sud-est de l'océan Indien et océan Pacifique). — B : *Phronima curvipes* (sud-est de l'océan Indien et océan Pacifique).

Enfin je n'attache pas la même importance que SHIH (1969) aux mesures faisant intervenir des segments du corps (H_h, H_1, P/A, Pl_1/Per_7). Le rapport des mesures de deux segments ne peut être estimé qu'à environ 1/20 près avec une bonne loupe binoculaire ; les résultats généralement différents obtenus en répétant les mesures (après un intervalle de temps suffisant pour ne plus avoir en mémoire les résultats précédents) prouvent que cette limite d'erreur peut être dépassée. La structure des articulations empêche également de trouver des repères comparables d'un individu à l'autre. Les mesures faisant intervenir plusieurs segments, plus ou moins courbés et rentrant les uns dans les autres, sont encore moins précises. Les rapports intéressant les appendices, qui peuvent être mesurés à plat au microscope, sont moins sujets à caution. Finalement le test *t*, employé par SHIH pour séparer les différentes formes, ne peut être utilisé pour comparer des rapports de mesures; c'est l'analyse de covariance qui est indiquée dans ce cas (voir sur ce point LISON, 1958, p. 236).

3. Discussion.

Il existe certainement des races locales de *P. colletti*, ce qui ne saurait surprendre chez une espèce répartie dans les trois océans. J'ai relevé au passage certaines différences entre des spécimens de l'Atlantique et d'autres de l'océan Indien; des populations à caractéristiques biométriques distinctes seraient sans doute mises en évidence par une étude plus approfondie. Malgré ces variations, *P. colletti* garde son faciès caractéristique dans toute son aire de répartition, où son identification est aisée. Dans l'océan Indien et le Pacifique Ouest, elle coexiste avec la « forme Indo-Ouest Pacifique » décrite par SHIH (1969), avec laquelle elle présente des différences beaucoup plus importantes, qui sont d'ordre spécifique.

Une comparaison avec les dessins et la description d'une femelle de l'océan Indien par GILES (1887) sous le nom de *P. bucephala* montre qu'il s'agit d'une forme identique à la « forme Indo-Ouest Pacifique » de SHIH (1969); les caractères du péréiopode V sont à eux-seuls suffisants pour permettre l'identification.

La validation de *P. bucephala* entraîne une révision de la synonymie de *P. colletti*.

Phronima colletti Bovallius

Phronima colletti BOVALLIUS, *1887*, K. svenska VetenskAkad. Handl., **11**, n° 16, p. 25. BOVALLIUS, *1889*, *Ibid.*, **22**, n° 7, p. 378, pl. 26, fig. 27-47. CHUN, *1895*, Bibl. zool., **19**, p. 109, pl. 8, fig. 1-6. VOSSELER, *1901*, Ergebn. Atlant. Planktonexped., **2**, p. 32, pl. 3, fig. 8-12 [♂ = *P. pacifica*]. CHEVREUX et FAGE, *1925*, Faune de Fr., **9**, p. 396, fig. 395 et 398 [♂ = *P. pacifica*]. MOGK, *1927*, Intern. Rev. Hydrobiol., **17**, p. 60, fig. 31. SHIH et DUNBAR, *1963*, Fich. Ident. Zoopl., **104**, p. 3, fig. 3 a, b et d [fig. 3 c = *P. pacifica* ♂].

Phronima diogenes CHUN, *1889*, S. b. k. preuss. Akad. Wiss. Berl., **30**, p. 527, pl. 3, fig. 5.

Phronima colletti Bov. Atlantic form SHIH, *1969*, Dana-Rep., **74**, p. 21, fig. 5 a-f.

[non] *Phronima colletti* Bov. IRIE, *1957*, Compil. Fish. Sci. (Suisan Gaku Syûsei), **3**, p. 348, fig. 8 [= *P. pacifica*].

[non] *Phronima colletti* Bov. ♂. LAVAL, *1968*, Cah. Biol. mar., **9**, p. 354, fig. 3 B [= *P. pacifica* ♂].

Les autres références citées par SHIH (1969) ne s'accompagnent pas d'une description assez précise pour identifier *P. colletti*, ou s'appliquent à d'autres espèces.

La synonymie de *P. bucephala* est la suivante :

Phronima bucephala Giles

Phronima bucephala GILES, *1887*, J. Asiatic Soc. Beng., **56**, n° 2, p. 215, pl. 3, fig. 1-2.

Phronima colletti Bov. Indo-W. Pacific form SHIH, *1969*, Dana-Rep., **74**, p. 21, fig. 5 g-m.

4. Répartition géographique.

En dehors de l'Atlantique, où elle est répandue entre 45° de lat. N. et 35° de lat. S. (SHIH, 1969), les seules stations se rapportant de façon certaine à *P. colletti* sont celles de la présente étude. Dans l'océan Indien, elle a été récoltée à 8 stations toutes localisées entre 27°30′ S et 32° S le long du 110ᵉ méridien E., c'est-à-dire au sud-ouest de l'Australie. Dans le Pacifique, *P. colletti* n'a été trouvée qu'à une station (16°22′ S-170°00′ E).

Le « Dana » a capturé *P. bucephala* au nord et à l'ouest de l'océan Indien, ainsi qu'à 3 stations situées en Mer de Java orientale, en Mer de Sulu et au nord de la Nouvelle-Guinée (SHIH, 1969). Un individu (femelle adulte de 6,2 mm) présent dans mon matériel de l'océan Pacifique (8°38′ S-169°52′ E) étend plus à l'est cette répartition. Il faut y ajouter l'exemplaire de GILES (1887) du Golfe du Bengale, et les spécimens provenant de la région de Nosy-Bé (Madagascar) utilisés dans ce travail.

Il est évident que de nouvelles investigations sont nécessaires pour préciser la répartition de ces deux espèces dans l'océan Indien et l'océan Pacifique.

II. DONNÉES COMPLÉMENTAIRES SUR P. pacifica STREETS, 1877

Si le mâle et la femelle de *P. bucephala* ne peuvent être confondus avec ceux de *P. pacifica* (la forme du péréiopode V est déjà suffisante pour éviter toute confusion), il n'en est pas de même pour les mâles de *P. colletti* et de *P. pacifica* qui sont très semblables et se trouvent fréquemment dans les mêmes pêches. Il n'est donc pas inutile d'insister ici sur les caractères qui les séparent.

1. Différences entre les mâles de P. colletti et de P. pacifica.

Le mâle de *P. pacifica* a été découvert par Shih (1969) qui en a donné une description détaillée. Cet auteur mentionne certains caractères qui le différencient de celui de *P. colletti* (rapport largeur/longueur du carpe du péréiopode V, forme du pédoncule de l'uropode II, processus carpal). Il existe d'autres caractères qui sont plus faciles à observer. Auparavant il convient de faire une remarque à propos du tubercule carpal du péréiopode V.

Ce processus est de forme triangulaire chez *P. colletti*, avec les dents proches les unes des autres. Chez *P. pacifica* les dents plus espacées forment un processus arrondi, mais il existe des variations individuelles. Comme je l'ai montré chez *Hyperia schizogeneios* (Laval, 1968 a), la mue de puberté peut survenir plus ou moins tôt par rapport à la croissance de l'animal. C'est pourquoi on peut observer chez *Phronima pacifica* des variations depuis une condition proche de celle de la femelle, qui est celle du mâle sub-adulte (c'est-à-dire des dents peu espacées formant un processus arrondi) jusqu'à la condition que j'ai figurée dans un travail précédent (Laval, 1968 b : *P.* « *colletti* », fig. 3 B) avec des dents très espacées les unes des autres.

Les caractères permettant une distinction aisée des deux espèces concernent la forme du propode du péréiopode V, la plaque épimérale I, la branchie IV, le péréiopode IV et, dans certains cas, le nombre d'articles du flagellum des antennes II.

Le propode du péréiopode V de *P. pacifica* est plus mince près de la base qu'au niveau du tubercule terminal; qui est bien marqué car le propode se rétrécit brusquement à l'extrémité. En revanche, chez *P. colletti* on observe un net tubercule proximal, alors que le tubercule terminal est peu apparent (fig. 5, D et H). Cette différence se voit même chez les individus jeunes.

La plaque épimérale I (fig. 5, A et E) a son bord inférieur fortement échancré chez *P. pacifica*, alors qu'il est seulement infléchi chez *P. colletti*. Cependant comme ce bord est droit chez le mâle sub-adulte de *P. pacifica*, selon la date de la mue de puberté on peut trouver certains individus à plaque épimérale I assez peu échancrée.

La branchie IV (première paire) est très petite chez *P. colletti* (voir plus haut) et beaucoup plus grande chez *P. pacifica:* elle atteint ou dépasse les 2/3 de l'article basal du péréiopode IV, et sa largeur est au moins les 3/4 de celle de la branchie V.

Le propode du péréiopode IV (fig. 5, C et G) est nettement plus dilaté chez *P. pacifica* que chez *P. colletti*. Le revêtement de petites soies qui garnissent la face interne est beaucoup plus développé sur le propode des péréiopodes III et IV chez *P. pacifica*, donnant, à l'observation au binoculaire, un aspect sombre caractéristique. Cette garniture de soies est également plus dense sur la face interne des propodes des gnathopodes et des péréiopodes VI et VII de *P. pacifica*.

Shih (1969) note des variations de 15 à 17 pour le nombre d'articles du flagellum des antennes II de *P. pacifica*, et considère que ce nombre permet de différencier cette espèce de *P. colletti* (12-13 articles, « Atlantic form »). En réalité ce nombre varie de 13 à 18 chez *P. pacifica* (fig. 4 A). J'ai observé des variations de 11 à 12 chez les *P. colletti* de l'océan Indien, mais le petit nombre d'individus à ma disposition ne m'a pas permis de déterminer l'étendue réelle des variations, qui est sans doute plus grande. De même le nombre d'articles varie plus largement que ne l'indique Shih chez *P. curvipes:* 6 à 10 au lieu de 7 à 9 (fig. 4 B). Il existe souvent des variations chez un

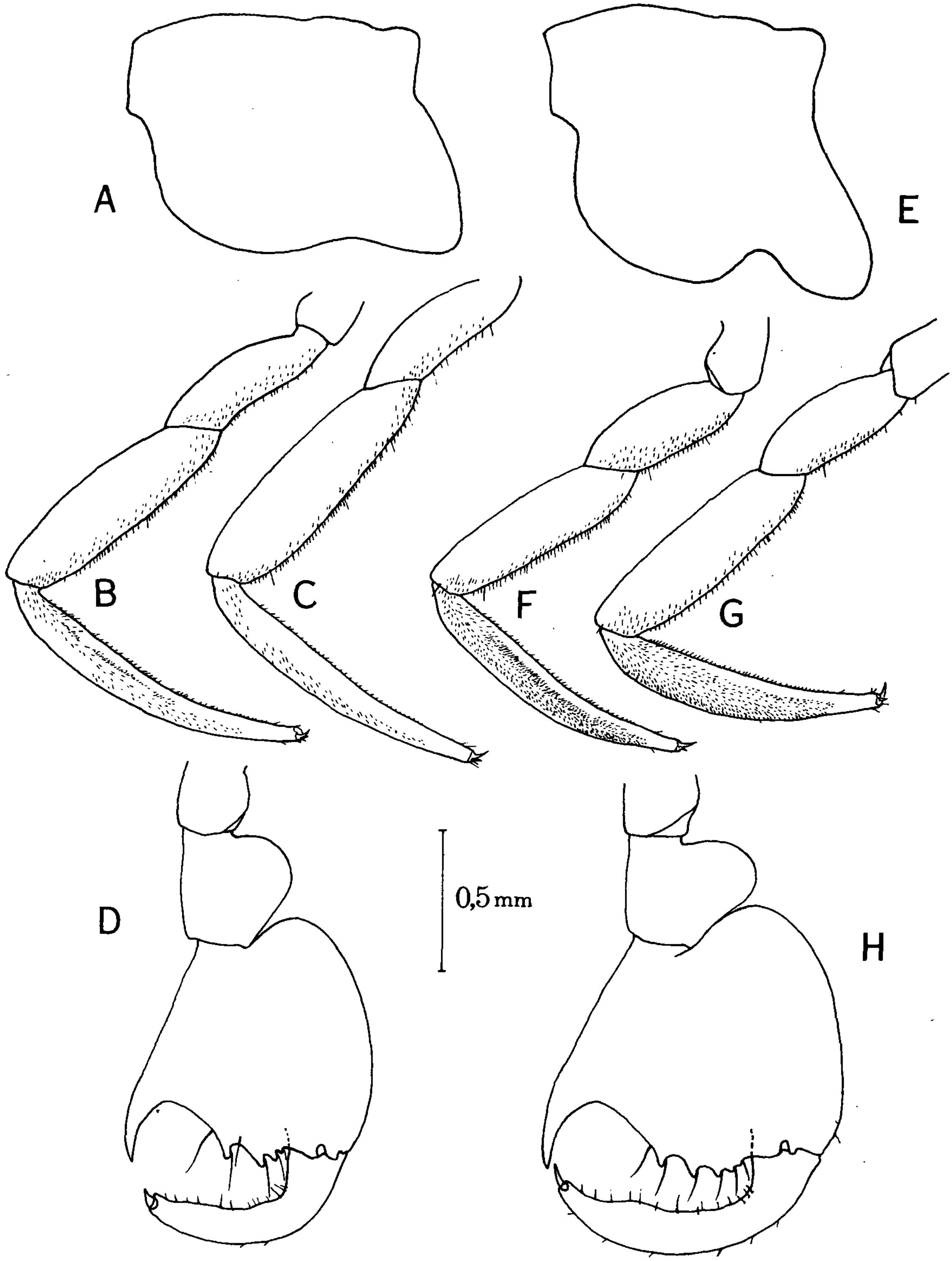

Fig. 5. — A-D : *Phronima colletti*, mâle adulte de l'océan Indien ; A : plaque épimérale I (l'avant dirigé vers la gauche) ; B-C : péréiopodes III et IV, vus par la face interne ; D : péréiopode V. — E-H : *Phronima pacifica*, mâle adulte de l'océan Pacifique ; E : plaque épimérale I ; F-G : péréiopodes III et IV (face interne) ; H : péréiopode V.

même individu : sur 40 mâles adultes de *P. pacifica* dont les deux antennes sont intactes, 8 n'ont pas le même nombre d'articles (différence d'une unité) à gauche et à droite. La même proportion (6 mâles sur 30) se retrouve chez *P. curvipes*. Le nombre d'articles des antennes II est donc trop variable pour permettre une détermination certaine. On peut toutefois affirmer qu'il y a une forte probabilité pour qu'un individu à plus de 15 articles soit *P. pacifica*.

2. Synonymie de P. pacifica.

La prise en considération des caractères précédents permet d'établir ainsi la synonymie de cette espèce :

Phronima pacifica Streets

[?] *Phronima sedentaria* Forsk. CLAUS, *1872*, Z. wiss. Zool., **22**, p. 335, fig. 1; pl. 26, fig. 3; pl. 27, fig. 11.

Phronima pacifica STREETS, *1877*, Bull. U.S. nat. Mus., **7**, p. 128. STREETS, *1882*, Proc. U.S. nat. Mus., **5**, p. 6, pl. 1, fig. 3-3 a. VOSSELER, *1901*, Ergebn. Atlant. Planktonexped., **2**, p. 29, pl. 3, fig. 4-7. MOGK, *1927*, Intern. Rev. Hydrobiol., **17**, p. 60, fig. 31. SHIH et DUNBAR, *1963*, Fich. Ident. Zoopl., **104**, p. 3, fig. 6. SHIH, *1969*, Dana-Rep., **74**, p. 18, fig. 4.

Phronima colletti Bov. VOSSELER, *1901*, *loc. cit.*, p. 29 [♂ seulement], pl. 4, fig. 1-3. CHEVREUX et FAGE, *1925*, Faune de Fr., **9**, p. 396, fig. 398 [♂ seulement]. IRIE, *1957*, Compil. Fish. Sci. (Suisan Gaku Syûsei), **3**, p. 348, fig. 8. SHIH et DUNBAR, *1963*, *loc. cit.*, p. 3, fig. 3 c [♂ seulement]. LAVAL, *1968*, Cah. Biol. mar., **9**, p. 354, fig. 3 B [♂ seulement].

[non] *Phronima pacifica* Streets. STEBBING, *1888*, Rep. Voy. Challenger 1873-76, **29**, p. 1348, pl. 159 [= *P. stebbingii*].

[non] *Phronima pacifica* Streets. BOVALLIUS, *1889*, K. svenska VetenskAkad. Handl., **22**, nº 7, p. 382, pl. 16, fig. 48-50 [= *P. stebbingii* ou *P. curvipes*].

3. Distribution.

La quasi-absence de *P. pacifica* dans l'océan Pacifique indiquée par SHIH (1969) doit être révisée en fonction du matériel étudié ici. *P. pacifica* a été récoltée en grand nombre par R. REPELIN sur la radiale effectuée le long du 170ᵉ méridien E. D'autre part SHIH se réfère aux travaux japonais (c'est-à-dire ceux d'IRIE) pour affirmer que cette espèce ne dépasse pas 20º N dans le Pacifique Ouest. Mais la figure de *P. colletti* donnée par IRIE (1957) montre qu'il s'agit en réalité de *P. pacifica*. L'aire de répartition de cette espèce dans cette partie du Pacifique pourrait ainsi s'étendre jusqu'à 41º N.

Dans l'océan Indien oriental, *P. pacifica* est présente jusqu'à 32º S, soit une limite sud comparable à celle trouvée par SHIH (1969) pour la partie occidentale.

CONCLUSION

Près de 70 ans après la monographie de VOSSELER (1901), le nombre des espèces du genre *Phronima* semblait bien établi (à l'exception de *P. affinis* qui a peut-être été décrite d'après un individu anormal de *P. sedentaria*). C'est pourquoi SHIH (1969), découvrant une forme proche de *P. colletti* dans l'océan Indien, a sans doute hésité à en faire une espèce distincte, d'autant que l'absence de *P. colletti* dans le matériel du « Dana » de l'océan Indien et la présence d'une autre forme dans le Pacifique Est rendaient vraisemblable l'hypothèse de variétés géographiques. La découverte de *P. colletti* dans l'océan Indien et l'océan Pacifique m'a conduit à réviser cette interprétation et à montrer que la forme de l'océan Indien au moins est bien distincte spécifiquement. Les variations géographiques de *P. colletti* dans les trois océans existent bien, mais sont de beaucoup plus faible amplitude.

Il reste le cas de la forme du Pacifique Est décrite par Shih (1969). Cette forme, qui est proche de *P. bucephala*, n'est visiblement pas une variété de *P. colletti*. Plusieurs caractères parmi ceux donnés par Shih (grande taille, nombre élevé des articles du flagellum des antennes II du mâle, proportions différentes du péréiopode V) font cependant hésiter à en faire une variété de *P. bucephala*. Une étude détaillée de la morphologie et la répartition de cette forme, fondée sur un matériel plus abondant, s'impose pour résoudre ce problème.

OUVRAGES CITÉS

Frontier (S.), 1966. — Zooplancton de la région de Nosy Bé. *Cah. O.R.S.T.O.M. sér. Océanogr.*, **IV** (3), pp. 3-36.

Giles (G. M.), 1887. — Natural History notes from H. M. S indian marine survey steamer « Investigator », no. 6 : on 6 new Amphipods from the Bay of Bengal. *J. Asiat. Soc. Beng.*, **56** (2), pp. 212-229.

Irie (H.), 1957. — 25 species of pelagic amphipods, Hyperiidea, in the adjacent seas of Japan. *Compil. Fish. Sci. (Suisan Gaku Syûsei)*, **3**, pp. 345-355 *(en japonais)*.

Laval (Ph.), 1968 a. — Développement en élevage et systématique d'*Hyperia schizogeneios* Stebb. (Amphipode Hypéride). *Arch. Zool. exp. gén.*, **109** (1), pp. 25-67.

— 1968 b. — Observations sur la biologie de *Phronima curvipes* Voss. (Amphipode Hypéride) et description du mâle adulte. *Cah. Biol. mar.*, **9**, pp. 347-362.

Lison (L.), 1958. — Statistique appliquée à la biologie expérimentale. 346 p. Paris, Gauthier-Villars.

Shih (C.-T.), 1969. — The systematics and biology of the family Phronimidae (Crustacea : Amphipoda). *Dana Rep.*, **74**, pp. 1-100.

Vosseler (J.), 1901. — Die Amphipoden der Plankton-Expedition. I Teil : Hyperiidea 1. *Ergebn. Atlant. Planktonexped.*, **2**, G. e., pp. 1-129.

Reprinted from *Cah. O.R.S.T.O.M., Sér. Océanogr.* vol. VIII, no. 2, 1970, p. 3-17

ZOOPLANCTON DE LA RÉGION DE NOSY-BÉ
IV. PLANCTON DE SURFACE AUX STATIONS 3, 4 ET 11.*

par S. FRONTIER**

RÉSUMÉ

L'auteur analyse les données recueillies dans le zooplancton de trois stations néritiques de la région de Nosy-Bé pendant près de trois ans. Une des stations est typique de la zone néritique interne (baies), les deux autres de la zone néritique externe.

Les variations saisonnières sur le plateau continental se caractérisent par une alternance de l'influence côtière en saison chaude, océanique en saison fraîche. La station néritique interne étudiée se trouve à la limite de l'extension vers la côte du peuplement néritique externe en saison fraîche. Le peuplement des stations néritiques externes est assez voisin du peuplement néritique interne en saison chaude, et prend ses caractères spécifiques à partir de mai, à mesure que les apports du large vident le plateau continental de l'eau douce qui s'y est accumulée pendant la saison des pluies. Le maximum de l'influence océanique sur le plateau a lieu entre août et octobre. L'extension vers le large du peuplement néritique interne commence à se faire sentir aux deux stations néritiques externes avec environ un mois de décalage par rapport au début des pluies.

Pour la plupart des groupes zoologiques étudiés, la saison chaude correspond à une période d'abondance, et la saison fraîche à une période de pauvreté. Les variations sont en général beaucoup plus sensibles en zone néritique externe qu'interne; cela doit être mis en relation avec les mouvements de masses d'eau se superposant en saison fraîche, dans la première zone, à l'évolution propre des peuplements.

Outre les variations saisonnières, il apparaît des variations d'une année sur l'autre. La troisième saison sèche étudiée se caractérise sur l'ensemble du plateau par une influence océanique moindre que lors des deux précédentes, ayant pour corollaire le maintien de caractères néritiques internes aux deux stations externes. Lors de la saison humide suivante, certains groupes zoologiques montrent des abondances dépassant celles des années précédentes à époque comparable.

ABSTRACT

The author is analyzing the information collected on the zooplankton of the three neritic stations of the Nosy Be region over three years. One of the stations is characteristic of the inner (bays) zone, the two others of the outer neritic zone.

Seasonal variations on the continental shelf are distinguished by an alternation of coastal

* Voir Cah. Océanogr.. vol. IV, n° 3, 1966 (I et II).

** Océanographe biologiste, Centre O.R.S.T.O.M. de NOSY-BÉ (Madagascar).

influence in warm seasons and oceanic influence in cool seasons. The inner neritic station studied is to be found at the boundary of the area towards the outer neritic population in cool seasons. The population of the outer neritic stations is fairly related to the inner neritic population during warm seasons and takes on its specific characteristics from May onwards in proportion as the alluvial deposits of the sea empty the continental shelf of soft water which becomes accumulated there during the rainy seasons. Maximum oceanic influence on the shelf occurs between August and October. The area towards the inner neritic population begins to establish itself at the two outer neritic stations with about one month of adjustment in relation to the beginning of the rains.

For most of the zoological groups studied, the warm season corresponds to a period of abundance and the cool season to a poor period. The variations are generally far more appreciable in the outer neritic zone than the inner; the latter must be compared to the movements of water masses superposing, during cool seasons in the first zone, on the proper development of the populations.

Beyond seasonal variations, variations crop up from one year to the next. The third dry season studied is distinguished from the shelf as a whole by less oceanic influence than during the two previous seasons, having as corollary the maintenance of inner neritic characteristics at the two outer stations. At the time of the following wet season, certain zoological groups show abundances exceeding those of previous years at comparable times.

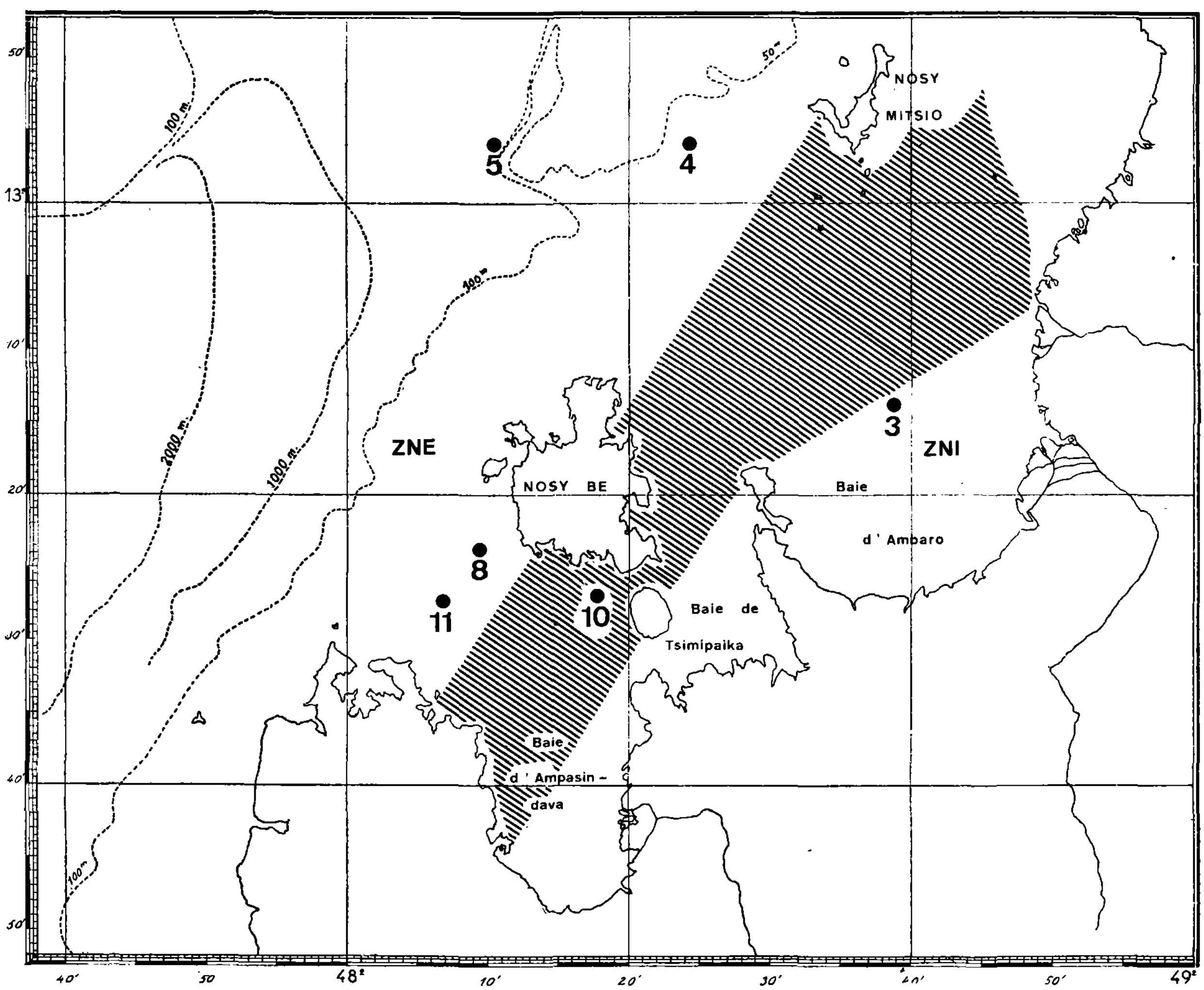

Fig. 1. — Carte des stations (ZNE : zone néritique externe ; ZNI : zone néritique interne ; aire hachurée : zone de balancement saisonnier de la limite ZNE-ZNI).

Les données exposées ci-dessous concernent la période d'avril 1963 à janvier 1966.

La station 3, située à l'ouverture de la Baie d'Ambaro (fig. 1) s'est révélée typique de la zone néritique interne, n'étant que sporadiquement atteinte en saison sèche par des éléments du peuplement néritique externe.

Les stations 4 et 11 sont néritiques externes. La station 4 a été occupée jusqu'en août 1964 ; à partir de septembre, l'intérêt s'étant porté sur le sud de la zone prospectée, elle a été remplacée par la station 11 située approximativement à la même distance que la 4 du talus continental. La station 8, proche de la station 11 et occupée d'avril 1963 à mars 1964, servira parfois de référence pour savoir si des différences constatées aux mêmes mois entre les stations 4 et 11 sont plus probablement à attribuer à la différence de latitude ou à des variations d'une année sur l'autre.

Le rythme des sorties était mensuel.

A. *LE MILIEU HYDROLOGIQUE*

Les données hydrologiques (température et salinité) recueillies aux immersions 2 et 10 m ont été portées, pour chaque station, sur des diagrammes T/S annuels semblables à ceux publiés précédemment (stations 5 et 10 : Frontier, 1966). L'allure de ces diagrammes aux stations 4 et 11 est la même qu'à la station 10, la température descendant toutefois en août-septembre au-dessous de 25 °C, alors qu'elle dépassait toujours 25,3 °C à la station 10 (fig. 2).

La station 3 se distingue des précédentes par :

— l'existence, en saison humide, d'importantes dessalures de surface, avec une forte stratification (maximale en février-mars : suivant les années 28,0 à 32,7 ‰ à 2 m ; 33,7 à 34,5 ‰ à 10 m) ;

— une température de saison fraîche supérieure d'au moins 0,5 °C à celle des stations néritiques externes.

La poursuite des observations sur près de trois ans a permis de constater qu'à ces *variations saisonnières* s'ajoutent des *variations annuelles* c'est-à-dire d'une année sur l'autre*.

La figure 3 reproduit les branches descendantes (mai à août) et ascendantes (septembre à décembre) des diagrammes T/S aux stations 3, 4 et 11, pendant les trois années étudiées, à l'immersion 10 m.

Les branches descendantes pour 1963 et 1964 coïncident presque, alors que celle de 1965 se trouve décalée de 0,2 à 0,5 ‰ vers les faibles salinités. D'autre part le refroidissement hivernal est moins important lors de la troisième année : aux stations 4 et 11, la température d'août reste en 1965 supérieure de 0,5 °C à celle du large alors qu'elle atteint cette dernière (inférieure à 25 °C) en 1963 et 1964. A la station 3, la température ne s'abaisse qu'à 25,65 °C en 1965, contre 25,33 en 1963 et 1964.

Pour la période septembre-décembre (branches ascendantes des diagrammes T/S), ce sont au contraire les deuxième et troisième années qui coïncident, décalées d'environ 0,2 ‰ vers les faibles salinités par rapport à la première.

Une rupture de l'évolution hydrologique est donc apparue entre août et septembre 1964. Il paraît maintenant fâcheux qu'à cette époque, la station néritique externe de référence ait été déportée d'un demi-degré vers le sud. Toutefois, de mai à décembre 1963, l'hydrologie est presque superposable aux stations 4 et 8, cette dernière étant très proche de la station 11, ce qui suggère que le phénomène est indépendant du changement de station. D'autre part, les mêmes faits apparaissent à la station 3, occupée sans interruption pendant les trois ans. Il s'agit donc d'une rupture ayant intéressé l'ensemble du plateau continental pendant la saison fraîche 1965.

* Pour la terminologie des phénomènes liés au temps en écologie : voir Sournia et Frontier, 1967.

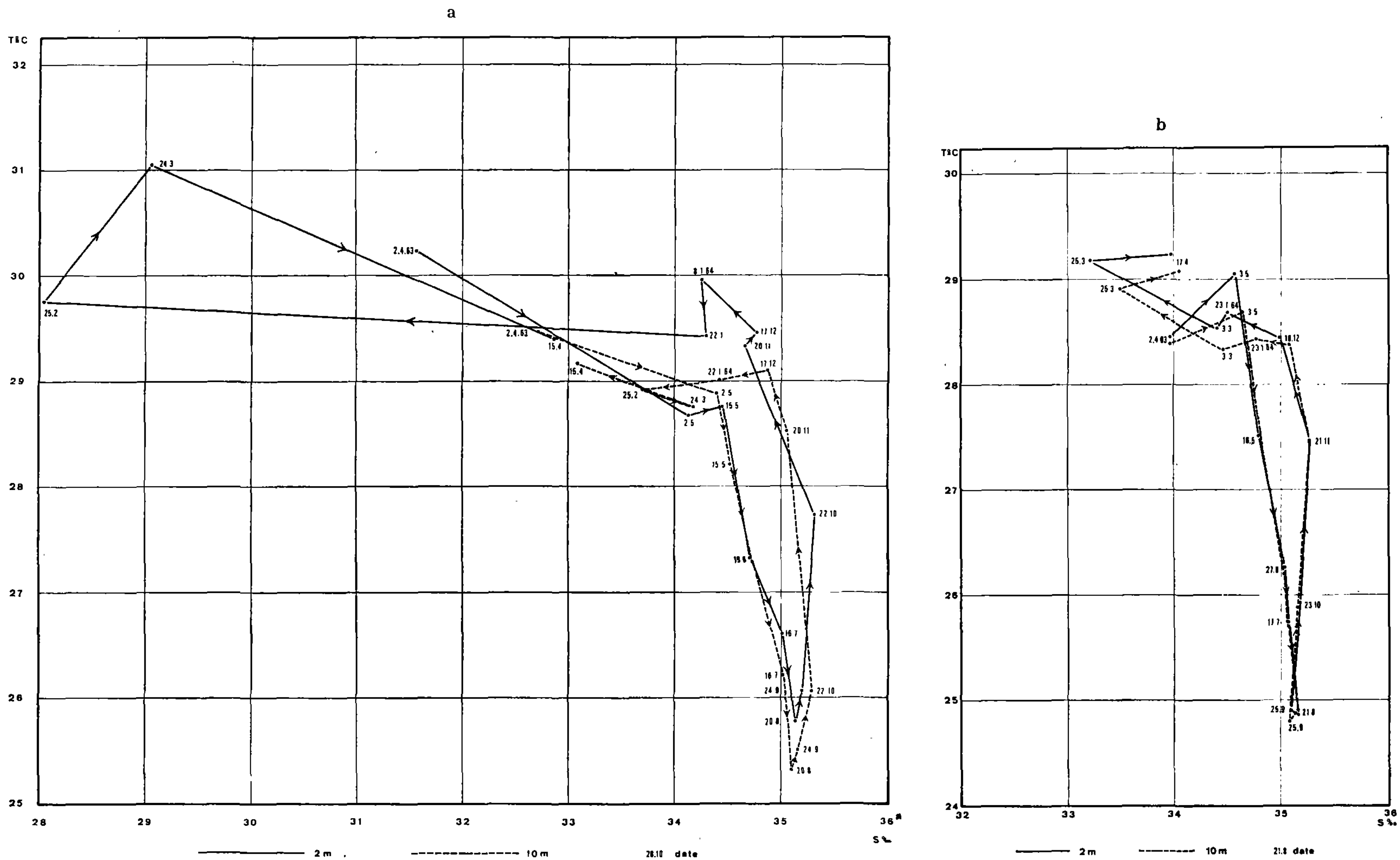

Fig. 2. — Diagrammes T/S d'avril 1963 à mars 1964 pour les stations 3 (a) et 4 (b).

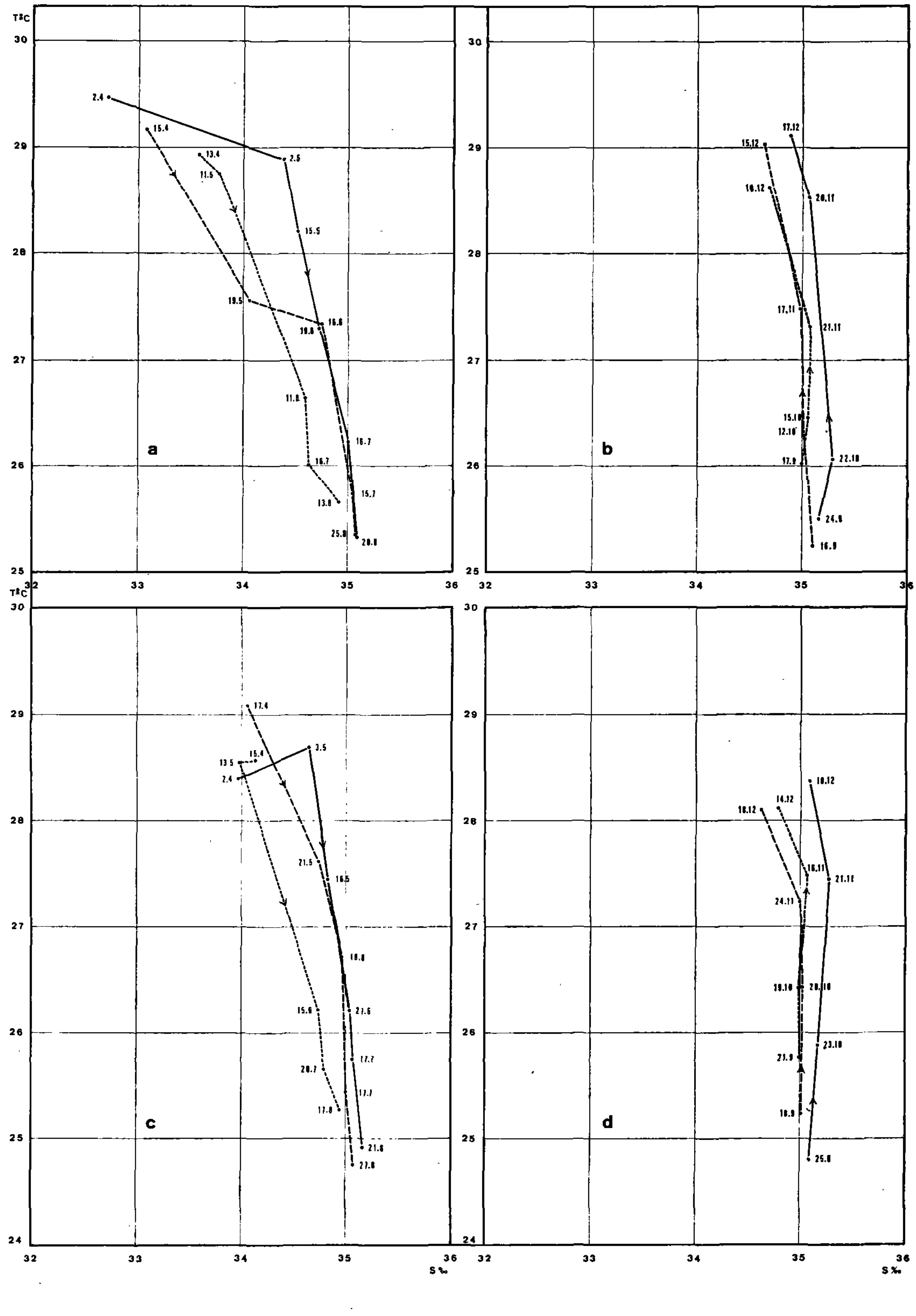

Fig. 3. — Branches descendantes (mai-août) (a, c) et montantes (septembre-décembre) (b, d) des diagrammes T/S aux stations 3 (a, b), 4 et 11 (c, d). Immersion 10 m.

La dessalure de saison humide trouve son origine, pour une part (non encore exactement estimée) dans les précipitations affectant directement la surface de la mer, d'autre part et surtout, dans les arrivées d'eau douce drainant des bassins versants importants vers les baies intérieures du plateau continental constituant la zone néritique interne. Au plus fort de la saison humide, l'influence côtière s'étend en surface au-delà de la ligne des 100 m, l'ensemble du plateau continental présentant une circulation de type estuaire (Piton, comm. person.). A partir du milieu de mai l'influence terrigène régresse graduellement, le plateau se vidant de son eau douce par l'effet d'arrivées de masses d'eau du large, ainsi qu'en témoigne le changement de composition du plancton.

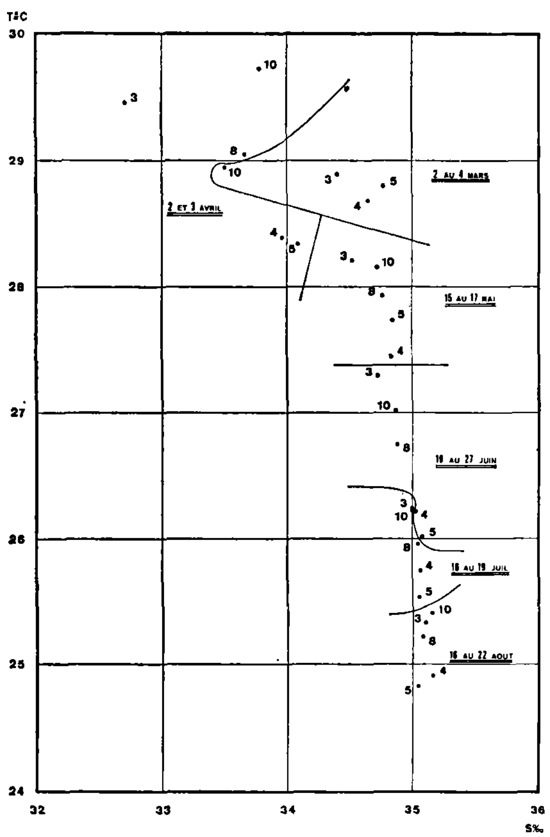

Fig. 4. — Branches descendantes (mai-août) des diagrammes T/S aux stations 3, 4, 5, 8, 10. Immersion 10 m.

Il est possible de suivre approximativement, en comparant les diagrammes T/S aux différentes stations, l'avancée de l'influence océanique vers la côte au cours de l'« automne austral ». Sur le diagramme T/S de la figure 4 sont portées les données hydrologiques obtenues aux stations 3, 4, 5, 8, 10 de mai à août 1963 (branches descendantes), ainsi qu'à titre indicatif les données d'avril (fin de la saison humide). L'évolution presque rectiligne constatée entre mai et août traduit le remplacement d'une eau à caractères très néritiques par une eau voisine de l'eau océanique de surface. On constate un retard permanent, d'un mois en juillet, entre les stations 3 et 10 (à influence côtière prépondérante) et les stations 4, 5 et 8 (zone néritique externe), ces trois dernières montrant entre elles des décalages moins importants et de sens variable, traduisant probablement des fluctuations aléatoires. On constate également que le retard de la station 3 sur la station 11 ou la 4 est moins accentué la troisième année que les deux premières (fig. 3a et c).

Il apparaît donc qu'au cours de la saison sèche 1965, l'eau recouvrant le plateau continental a gardé des caractères nettement plus néritiques que les deux années précédentes (nous verrons plus loin que cette particularité a eu un profond retentissement sur les peuplements planctoniques). Aucun phénomène physique ni météorologique n'a encore pu être mis en parallèle avec ces fluctuations. Les précipitations ne semblent pas être en cause, car les courbes pluviométriques obtenues ces trois années à Nosy-Bé sont presque superposables. Les caractères du peuplement planctonique suggèrent des variations dans l'intensité du refoulement de l'eau néritique par l'eau océanique à partir de mai ; les variations annuelles relèveraient alors de la dynamique (encore mal connue) des eaux du Canal de Mozambique.

B. *VARIATIONS D'ABONDANCE DE QUELQUES GROUPES ZOOLOGIQUES*

La cotation d'abondance introduite dans la première partie de ce travail (FRONTIER, 1966) puis complétée (FRONTIER, 1969) est la suivante :

Cotes	Effectifs	Cotes	Effectifs
0	0	1,5	3 ou 4
1	1 à 3		
2	4 à 17	2,5	environ 18
3	18 à 80	3,5	— 80
4	80 à 350	4,5	— 350
5	350 à 1500	5,5	— 1500
6	1500 à 6500	6,5	— 6500
7	6500 à 27000	7,5	— 27000
8	27000 à 120000	8,5	— 120000
9	120000 à 500000	9,5	— 500000
10	500000 à 2000000		

C'est, comme précédemment, le carré de la cote qui est porté en ordonnées sur les graphiques de variations d'abondance (transformation $\log^2$) — et plus précisément dans ce chapitre, la moyenne des valeurs trouvées à 2 et 10 m.

Les résultats exposés ci-après ainsi que d'autres publiés en partie (BINET et DESSIER, 1967, 1969 ; FRONTIER, 1963, 1966 ; PETIT et *al.*, en préparation) montrent l'existence sur le plateau continental de deux types de peuplements planctoniques nommés (FRONTIER, 1966) néritique interne et néritique externe. Une limite précise entre les deux zones ne peut évidemment être établie. On peut toutefois indiquer (fig. 1) la limite sud-est du peuplement néritique externe en saison sèche, coïncidant avec l'entrée des baies intérieures du plateau ; et la limite nord-ouest du peuplement néritique interne en saison humide, coïncidant grossièrement avec la ligne Nosy-Bé-Nosy Mitsio (bien que des éléments néritiques internes se rencontrent couramment, à l'époque du maximum de dessalure, au-delà de la ligne des 100 m en surface). La région (hachurée sur la carte) située entre ces deux limites est une zone de balancement saisonnier du contact néritique interne-néritique externe ; elle comprend, entre autres, la station 10.

La station 3 était occupée de jour (entre 12 h 30 et 15 h), les stations 4 et 11 de nuit (entre 19 h 30 et 03 h 45). Des études postérieures à cette série de récoltes et menées dans le but de mettre en évidence des variations nycthémérales feront l'objet d'un exposé ultérieur, mais j'en indique dès maintenant quelques conclusions :

— le phénomène de migration verticale nycthémérale est, tout au moins en ce qui concerne le milieu néritique, loin de présenter la généralité habituellement décrite ;

— les déplacements verticaux périodiques varient de nature non seulement avec l'espèce mais pour une même espèce avec le stade de développement (BHAUD, 1969) et peut-être l'époque de l'année ou d'autres circonstances non discernées, en sorte que le phénomène se trouve généralement très estompé au niveau du groupe zoologique ;

— enfin, l'hétérogénéité de la répartition horizontale est telle en milieu néritique qu'il est souvent impossible de distinguer, dans des variations d'abondances en un point fixe, ce qui revient aux migrations verticales des organismes et aux déplacements latéraux de la masse d'eau.

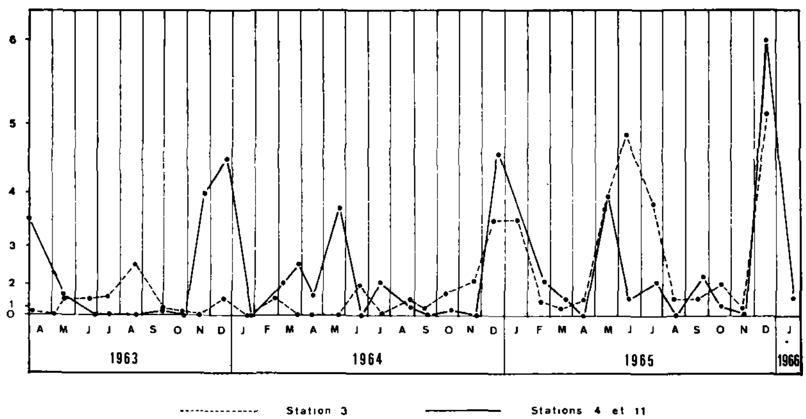

Fig. 5. — Variations d'abondance des Dolioles.

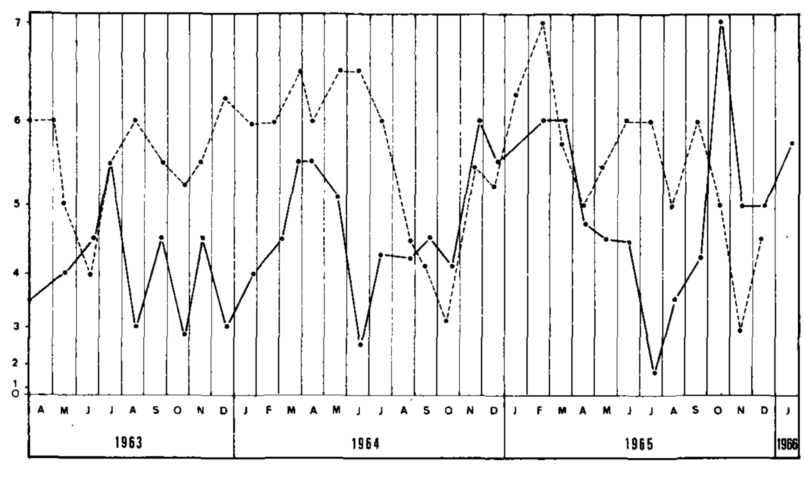

Fig. 6. — Variations d'abondance des Appendiculaires.

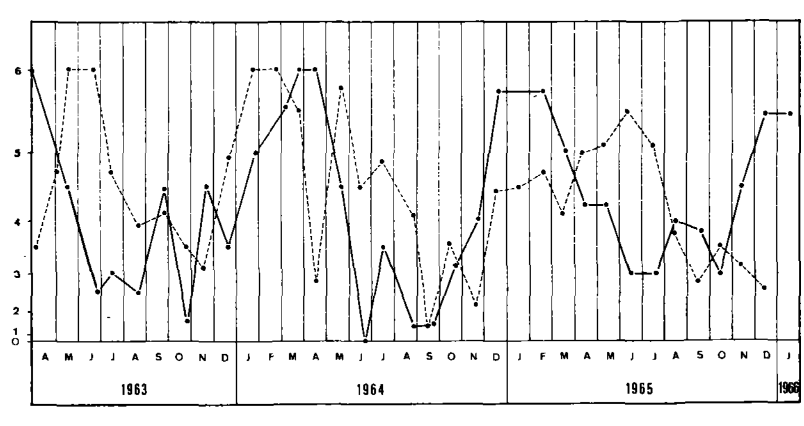

Fig. 7. — Variations d'abondance des Lucifer.

La littérature est très pauvre en ce qui concerne les migrations verticales du plancton néritique — surtout du plancton tropical. Un récent travail sur le plateau continental néo-zélandais (GRACE, 1968) rejoint toutefois nos conclusions.

L'aspect négatif de ces conclusions a une conséquence méthodologique : des résultats recueillis mensuellement, en des stations éloignées les unes des autres, et concernant un groupe zoologique (espèce au moins) pris dans son ensemble, seront comparables indépendamment des heures de prélèvement. Dès lors, variations verticales et hétérogénéité horizontale, indiscernables, constitueront dans nos séries de récoltes un bruit de fond qui, pour important qu'il soit (comme le montreront les graphiques de variations d'abondance) ne masquera pas entièrement les variations dues à l'alternance saisonnière ou au gradient côte-océan.

Dolioles (fig. 5). — Aucune périodicité n'apparaît à la station 3 où les Dolioles sont absentes ou rares, mises à part quelques récoltes exceptionnelles. Aux stations néritiques externes, on observe (comme aux stations 5 et 10 : FRONTIER, 1966), une période de quasi-absence, située ici entre juin et octobre ou novembre, alors qu'elle se situait en janvier-mars à la station 5 et en août-février à la 10 ; ces décalages n'ont pas encore pu être interprétés. On remarque, lors de la troisième saison sèche étudiée, un appauvrissement moins net que lors des deux premières années. La saison humide se caractérise par deux maxima (décembre et avril-mai) séparés par une période de moindre abondance.

Appendiculaires (fig. 6). — Variations de grande amplitude, mais sans caractère saisonnier net, aux stations 4 et 11. Forte abondance à la station 3 avec quelques périodes de raréfaction apparente (peut-être simplement dues à l'hétérogénéité de la répartition spatiale) : mai-juin 1963 août-octobre 1964, novembre-décembre 1965.

Lucifer (fig. 7). — Un cycle annuel d'abondance apparaît de façon nette aux trois stations étudiées : maximum de saison humide, minimum de saison sèche, avec un décalage entre les deux zones néritiques : une chute d'abondance brutale se manifeste en mai (début de saison sèche, c'est-à-dire début du refoulement de l'eau néritique par l'eau océanique) aux stations 4 et 11, alors que le genre reste abondant jusqu'en juillet à la station 3*. La troisième saison sèche se marque en zone néritique externe par un appauvrissement un peu moins accusé que les deux années précédentes.

Larves de Crustacés Décapodes (fig. 8). — Les abondances des larves de Brachyoures, Anomoures et Natantia ont été estimées séparément ; les fluctuations saisonnières des trois groupes présentent un grand parallélisme. La figure 8 représente les enveloppes supérieure et inférieure des trois graphiques d'abondance, pour les stations 4 et 11. On constate un maximum de saison humide et un minimum de saison sèche, les très faibles abondances observées lors des deux premières saisons sèches ne se reproduisant pas la troisième année. La station 3 ne montre que des fluctuations non périodiques autour d'une moyenne plus faible qu'en zone néritique externe.

Euphausiacées (fig. 9). — La grande masse des Euphausiacées rencontrées au-dessus du plateau continental est constituée par l'espèce *Pseudeuphausia latifrons* SARS, qui est l'un des constituants essentiels du peuplement néritique externe. La répartition spatiale est très surdispersée, la tendance à constituer des essaims étant très accusée à tous les stades de développement ; l'abondance aux stations 4 et 11 varie entre les cotes 4 et 6 indépendamment de toute périodicité saisonnière. A la station 3, l'espèce n'apparaît qu'exceptionnellement (et, en général, en très

* A la station 10 (FRONTIER, 1966) on n'observait que des variations de grande amplitude sans périodicité, et à la station 5 un maximum de septembre à décembre. Ainsi qu'il sera exposé ultérieurement (PETIT, en préparation), plusieurs espèces s'étagent entre la côte et le large, et des différences dues aux exigences écologiques spécifiques interfèrent avec celles dues aux variations des masses d'eau dans les zones de transition.

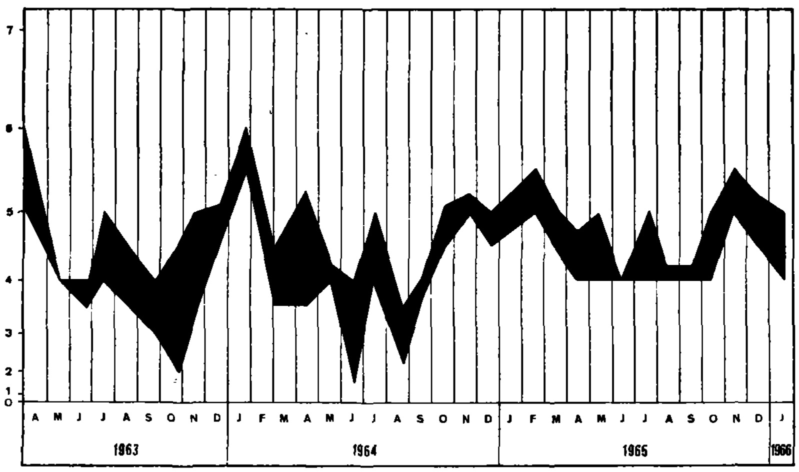

Fig. 8. — Variations d'abondance des larves de Crustacés Décapodes (enveloppes des courbes obtenues pour les larves de Brachyoures, d'Anomoures et de Macroures).

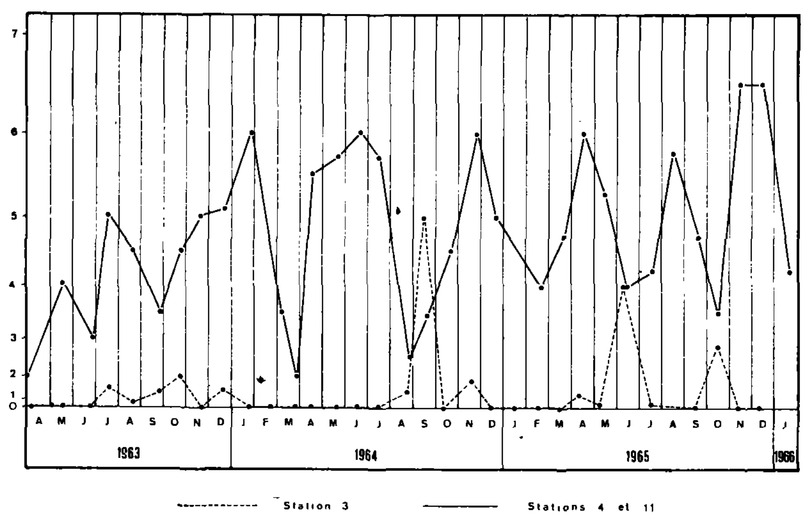

Fig. 9. — Variations d'abondance des Euphausiacés.

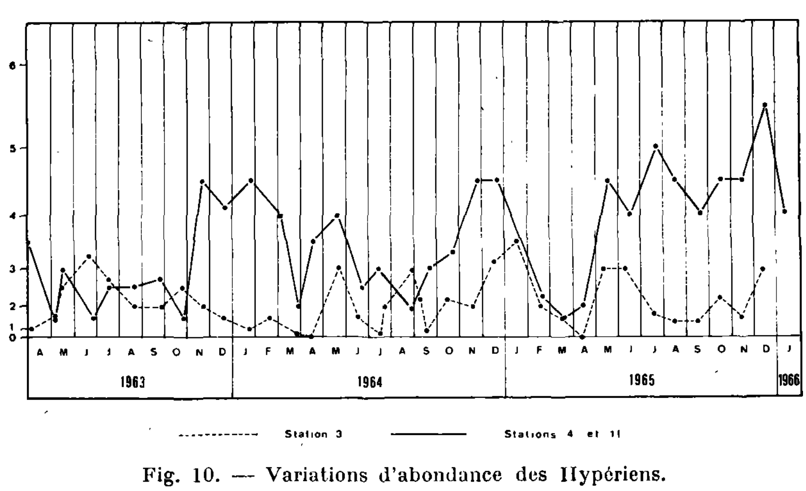

Fig. 10. — Variations d'abondance des Hypériens.

petit nombre) entre juin et novembre, c'est-à-dire pendant la seconde moitié de la saison sèche ; les abondances notables rencontrées en juin, septembre et octobre indiquent des avancées de l'eau néritique externe jusqu'à l'entrée de la Baie d'Ambaro.

Des récoltes de plancton ont été effectuées en divers points de la Baie d'Ambaro en 1966 et 1967 : station 3, et au-dessus des fonds de 5 et 10 m. L'espèce n'apparaît que de juillet à octobre, et principalement au voisinage du fond, à la station 3 et très exceptionnellement au-dessus des petits fonds (5 individus en 25 récoltes effectuées en septembre-octobre) ; en outre il ne s'agit jamais d'adultes (LE RESTE, communication personnelle)*.

Hypériens (fig. 10). — Les stations 4 et 11 sont marquées par un cycle annuel avec un maximum de saison humide s'établissant assez brusquement en novembre, et minimum étalé sur toute la saison sèche. Par ailleurs, la singularité déjà signalée pour la troisième saison sèche apparaît nettement : après une chute d'abondance en février-avril, le groupe devient extrêmement abondant et le demeure jusqu'à la saison humide suivante, où il atteint des effectifs encore jamais rencontrés. Ces fluctuations quantitatives se rapprochent beaucoup de celles constatées pour les Siphonophores Calycophores (on sait que de nombreuses espèces d'Hypériens sont commensales de ce groupe). A la station 3, où le groupe est bien moins nombreux, les variations sont plus confuses et sans parallélisme avec celles des Calycophores. Des remontées d'abondance semblent se produire en mai-juin et en décembre**.

Cladocères (fig. 11). — Aux stations néritiques externes, les Cladocères (seule espèce rencontrée : *Evadne tergestina* Claus) n'apparaissent qu'en octobre et avril, les maxima se situant en mars et décembre 1964 et décembre 1965. L'abondance diminue brusquement en avril 1963, avril 1964, janvier 1965, janvier 1966, et l'espèce est pratiquement absente des récoltes de mai à septembre ou à octobre. L'allure des variations saisonnières coïncide donc avec celles décrites à la station 10. A la station 3, la période d'abondance pour les Cladocères s'étend d'octobre-novembre à juin-juillet ; mais les individus rencontrés en juin et juillet appartiennent en majorité à l'espèce *Penilia avirostris* Dana, non récoltée aux stations 4 et 11.

Ainsi qu'il sera précisé dans une note ultérieure, il existe une vicariance entre les deux espèces de Cladocères. La population de *Penilia*, plus côtière que celle d'*Evadne*, atteint son développement maximum dans les baies intérieures entre juin et août ; elle ne dépasse alors que peu la station 3. La seconde espèce est au contraire une espèce de saison humide qui s'étend entre novembre et avril jusqu'en zone néritique externe.

La fig. 11 montre en outre que la population de Cladocères de la station 3 s'établit en 1964 dès le mois d'octobre, c'est-à-dire avec un mois d'avance sur la station 4 ; en 1965, c'est au contraire la station 3 qui est en retard sur la station 11, ce qui semble contredire l'origine néritique-interne de la population. En fait, la position des stations (fig. 1) suggère que le peuplement planctonique de la station 11 dépend, pour ses éléments néritiques-internes, de celui de la Baie d'Ampasindava plutôt que de la Baie d'Ambaro. Le décalage constaté entre les stations 3 et 11 en 1965 semble refléter, comme il sera montré ultérieurement, un décalage dans le temps entre l'évolution planctologique des Baies d'Ambaro et d'Ampasindava.

Hétéropodes et Ptéropodes. — Ces deux groupes seront l'objet d'une étude ultérieure détaillée.

Polychètes (fig. 12 et 13). — Les *Lopadorhynchidae*, *Alciopidae*, *Tomopteridae*, *Typhloscolecidae* et « autres » (essentiellement formes épigames, et à l'exclusion des formes larvaires) ont été comptés séparément. Les variations d'abondance des *quatre familles holoplanctoniques*

---

* A la station 10, située dans la zone d'alternance des deux types de peuplements néritiques, on observe une grande abondance de *Pseudeuphausia latifrons* en septembre-octobre, une raréfaction de l'espèce de novembre à février, et le reste de l'année des fluctuations entre les cotes 0 et 4, ce qui représente une situation intermédiaire entre celles rencontrées aux stations 3 et 11.

** Aucune périodicité d'abondance n'apparaissait aux stations 5 et 10.

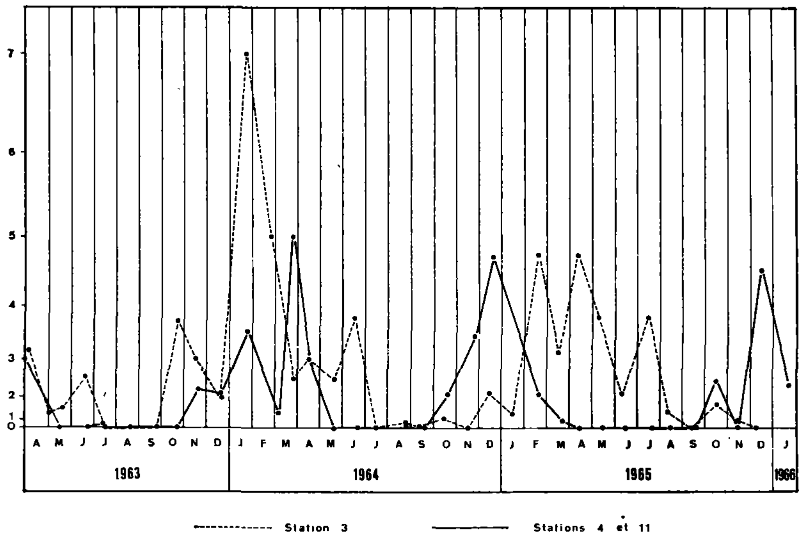

Fig. 11. — Variations d'abondance des Cladocères.

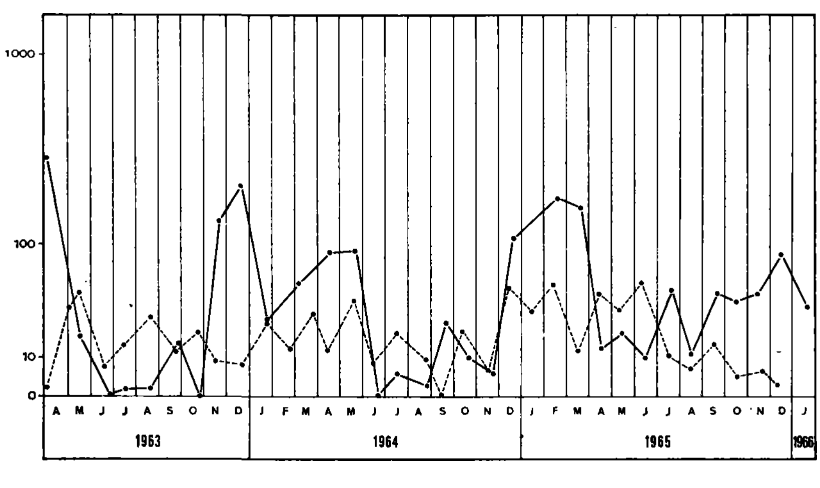

Fig. 12. — Variations d'abondance des Polychètes holoplanctoniques.

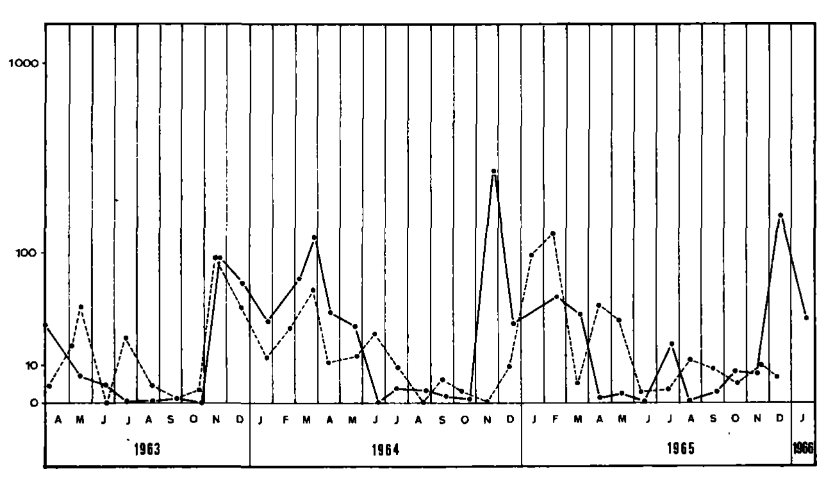

Fig. 13. — Variations d'abondance des Polychètes méroplanctoniques (larves exclues).

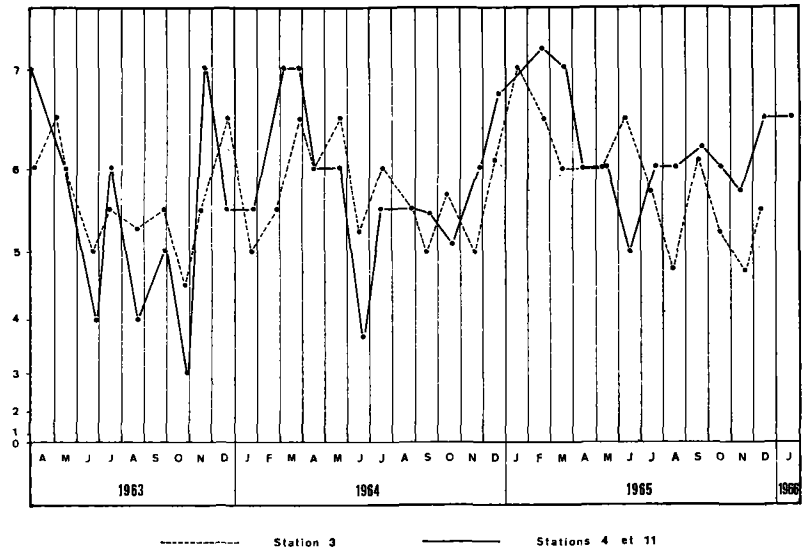

Fig. 14. — Variations d'abondance des Chaetognathes.

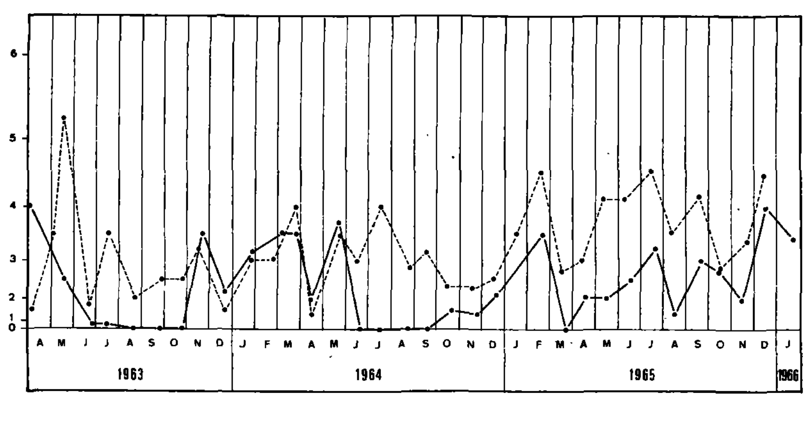

Fig. 15. — Variations d'abondance des Cténaires.,

étant sensiblement parallèles, ce sont les effectifs totaux qui sont portés figure 12. On constate en zone néritique externe un cycle annuel très accusé, avec une période d'abondance de novembre ou décembre à avril, le reste de l'année étant pauvre. La saison sèche 1965 se marque par un appauvrissement moins accentué que les deux années précédentes. En zone néritique interne, on n'observe que des fluctuations sans périodicité nette autour d'une moyenne faible (de l'ordre de 20 individus par récolte — même ordre de grandeur qu'aux stations 4 et 11 pendant la troisième saison sèche).

Les *formes méroplanctoniques* (larves exclues) montrent dans les deux types de stations une augmentation brusque d'abondance située entre novembre et janvier, suivie d'une diminution assez progressive à la station 3, plus brutale en zone néritique externe (avril-mai). On constate un pic en mars 1964 à la station 4. L'abondance est très faible pendant la saison sèche ; on observe cependant un petit nombre d'individus en juillet et octobre 1965.

Chaetognathes (fig. 14). — Cycle annuel très marqué, identique à celui observé à la station 10 : minimum de juin à octobre, maximum de novembre à mai. De faibles effectifs (moins de 350 indi-

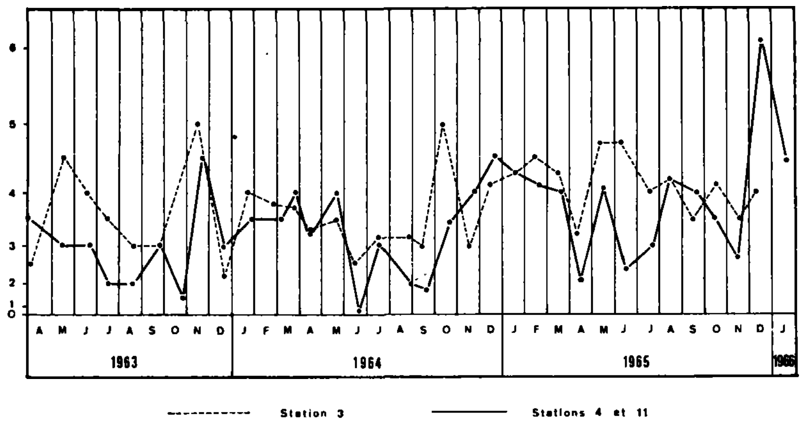

Fig. 16. — Variations d'abondance des Méduses.

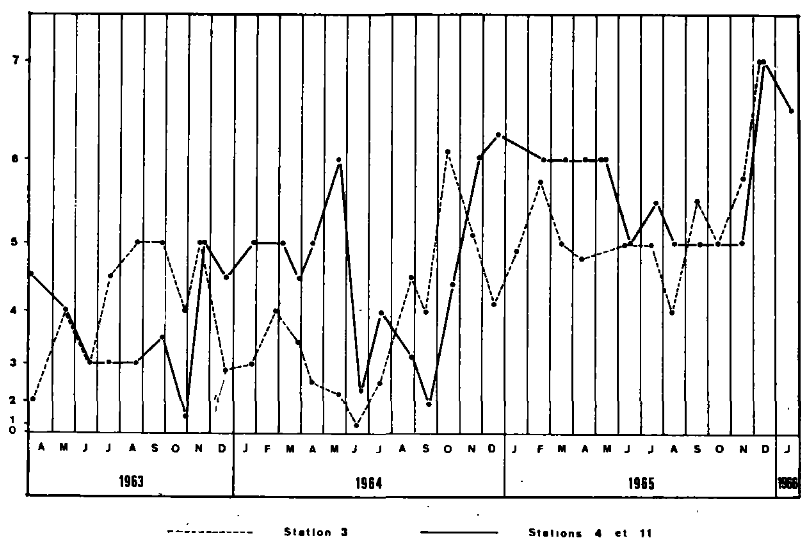

Fig. 17. — Variations d'abondance des Siphonophores.

vidus par récolte) se rencontrent en zone néritique externe pendant les deux premières saisons sèches ; la troisième saison sèche maintient des effectifs de l'ordre de 1500 à 6500 par récolte. A la station 3, le cycle annuel est légèrement moins marqué, les très faibles effectifs rencontrés en saison sèche aux stations 4 et 11 n'étant jamais réalisés.

Pterosagitta draco Krohn, indicatrice d'un peuplement en provenance du talus continental, se rencontre aux stations 4 et 11 essentiellement entre mai et novembre, avec un maximum en juillet-septembre ; sporadiquement et en très petit nombre le reste de l'année. Les captures maximales sont de 20 à 50 individus par récolte. L'espèce apparaît sporadiquement et en très petit nombre à la station 3, entre mai et novembre (captures maximales : 7 à 10 individus par récolte en août).

Cténaires Cydippoïdes (fig. 15). — Aucune périodicité nette n'apparaît à la station 3 où les Cténaires sont moyennement abondants toute l'année. Aux stations 4 et 11 par contre, les variations saisonnières d'abondance sont nettes (plus nettes qu'à la station 10) : le groupe est absent ou presque entre juin et octobre les deux premières années, et le reste de l'année d'une abondance comparable à celle de la station 3. Pendant la saison sèche 1965, les effectifs de Cténaires ne font, à la station 11, que s'appauvrir sans disparaître, illustrant une fois de plus le maintien de caractères néritiques sur l'ensemble du plateau durant ce troisième hiver austral.

Les variations d'abondance des Cténaires semblent faire apparaître un facteur écologique non identifié tenant sous sa dépendance l'ensemble du peuplement planctonique du plateau continental. Un parallélisme frappant apparaît entre les courbes des stations 3 d'une part, 4 et 11 d'autre part, chaque fois que ces dernières présentent un peuplement de caractère néritique, c'est-à-dire en saisons humides, et à la troisième saison sèche. Il y a quasi-superposition des courbes pendant la période novembre 1963-mai 1964, et décalage (la station néritique externe étant plus pauvre que la station néritique interne) d'octobre 1964 à décembre 1965. Vu l'éloignement mutuel des stations, qui exclut un simple phénomène de dérive du peuplement vers le large, (on observerait dans ce cas un temps de latence non négligeable) on est obligé d'avancer l'hypothèse d'un facteur autre que le facteur saisonnier et que le gradient côte-océan. Une comparaison avec la périodicité des marées n'a donné aucun résultat ; il n'est pas impossible que les conditions météorologiques participent à ce facteur, mais rien de certain ne peut encore être avancé.

Méduses (fig. 16). — On observe aux stations néritiques externes un maximum de saison humide et un minimum de saison sèche, ce dernier très accentué les deux premières années et plus estompé la troisième. A la station 3, les variations quantitatives montrent un certain parallélisme avec les stations précédentes, mais l'ampleur du bruit de fond masque toute périodicité.

Siphonophores Calycophores (fig. 17). — Parallélisme assez marqué avec le cycle annuel des Méduses aux stations 4 et 11. Cycle également très net à la station 3, mais décalé par rapport au précédent (2 à 4 mois d'avance). La troisième année se marque, pour les deux zones, par un appauvrissement hivernal moins accentué, suivi à la saison humide suivante par l'apparition d'effectifs encore jamais atteints. La parenté de ces variations avec celles manifestées par les Hypériens a été signalée plus haut.

Manuscrit reçu le 24 mars 1970.

BIBLIOGRAPHIE

BHAUD (M.), 1969. — Étude de la migration verticale quotidienne des larves de *Mesochaetopterus sagittarius* à Nosy-Bé (Madagascar). *Mar. Biol.* IV (1) : 28-35.

BINET (D.) et DESSIER (A.), 1967. — Contribution à l'étude du zooplancton et plus particulièrement des Copépodes de la région de Nosy-Bé. *Centre O.R.S.T.O.M. de Pointe-Noire,* rapp. 362 S.R., multigr. 52 p., 26 pl.

BINET (D.) et DESSIER (A.), 1968. — Zooplancton de la région de Nosy-Bé. III. Premières données sur les Copépodes du plancton de Nosy-Bé (Madagascar). *Cah. O.R.S.T.O.M., sér. Océanogr.,* VI (3/4) : 3-26.

FRONTIER (S.), 1963. — Hétéropodes et Ptéropodes du plancton de Nosy-Bé. *Cah. O.R.S.T.O.M., sér. Océanogr.,* I (6) : 213-227.

FRONTIER (S.), 1966. — Zooplancton de la région de Nosy-Bé. I. Programme des récoltes et techniques d'étude. II. Plancton de surface aux stations 5 et 10. *Cah. O.R.S.T.O.M., sér. Océanogr.,* IV (3) : 3-37.

FRONTIER (S.), 1969. — Sur une méthode d'analyse faunistique rapide du zooplancton. *J. exp. mar. Biol.,* III (1) : 18-26.

GRACE (R. V.), 1968. — The vertical distribution and diurnal migration of zooplancton in the Harauki Gulf. *Th. Univ. Auckland,* multigr. 76 p.

LE RESTE (L.), 1969. — Contribution à l'étude du zooplancton et plus particulièrement des Euphausiacea au large de Nosy-Bé (Madagascar). *Cah. O.R.S.T.O.M., sér Océanogr ,* VII (4) : 39-50.

PETIT (D.), BOUR (W.) et FRONTIER (S.), 1970. — Zooplancton sur une radiale côte-océan de la région de Nosy-Bé (Madagascar). *(En préparation).*

SOURNIA (A.) et FRONTIER (S.), 1967 (1968). — Terminologie des phénomènes liés au temps en écologie. *Bull. Mus. Hist. nat. Paris,* 2e série, V : 1001-1002.

Part II

Physical oceanography and marine meteorology

Reprinted from *Bull. natn. geophys. res. Inst. India*, 1963, vol. 1, no. 3, p. 175-178

NOTE ON THE SEA SURFACE CURRENTS OF THE WESTERN PART OF THE INDIAN OCEAN

by

V. S. RAMA RAJU,
Oceanographic Research Wing of N.G.R.I., Cochin.

ABSTRACT

During the February-March 1960 part of the 31st cruise of the Soviet Research Vessel VITIAZ, the sea surface currents in the western part of the Indian Ocean are computed from the observations on the drift of the vessel at different oceanographic stations when its propellers were not working. An analysis of these surface currents is presented in this note.

INTRODUCTION

When a ship is adrift, it moves under the influence of surface currents and wind. The effect of wind force in dragging the ship along its direction depends on the strength of wind, and the shape and orientation of the ship. The limitations and reliability of direct current measurements under various meteorological and oceanographic conditions have been summarised by BOHNECKE in one of his recent papers (1955). When the surface current is weak and the wind force high, the drift of the ship might largely be influenced by the wind. However, considering the stream-lined shape of the ship and the very high density of sea water compared to that of air (nearly 1,000 times), one can neglect the wind effect (say below Beaufort 4) and assume, under favourable conditions, that the drift of the ship is mainly due to current alone for the purpose of obtaining the general pattern of surface currents. This means that the ship itself can be used as a current-meter while adrift under favourable conditions. The currents, however, may not be reliable in cases where tidal currents prevail and the swell is strong.

DATA

Observation data on the initial and final positions of the Soviet Research Ship VITIAZ while drifting at the oceanographic stations in the western part of the Indian Ocean, during February-March 1960, are utilised for determining the surface currents. The position fixing of the ship is done by celestial method. In the analysis of the data all the doubtful values of the positions taken in cloudy weather are eliminated to minimize errors. Further, stations at which free drifting was not allowed by heavy operations like deep and bottom trawling, etc. are excluded in the computations. The distance through which the ship has drifted is computed from the construction of a right-angled triangle with the latitude and longitude differences between the initial and final positions as the two sides and the hypotenuse as the drifting path. This assumption is justified as the drift distances are not very large. The direction of drift is determined with respect to geographical north. The magnitude of the average current is then equal to the ratio of the drift distance to the drift time. The currents thus evaluated are represented by means of vectors at the initial position of the stations and are shown in Fig. 1. It would be interesting to compare the drift currents thus evaluated with those determined by current-meters at these stations to judge the reliability of this method. It must, however, be noted that currents are not generally measured by this method because of many reasons, but useful

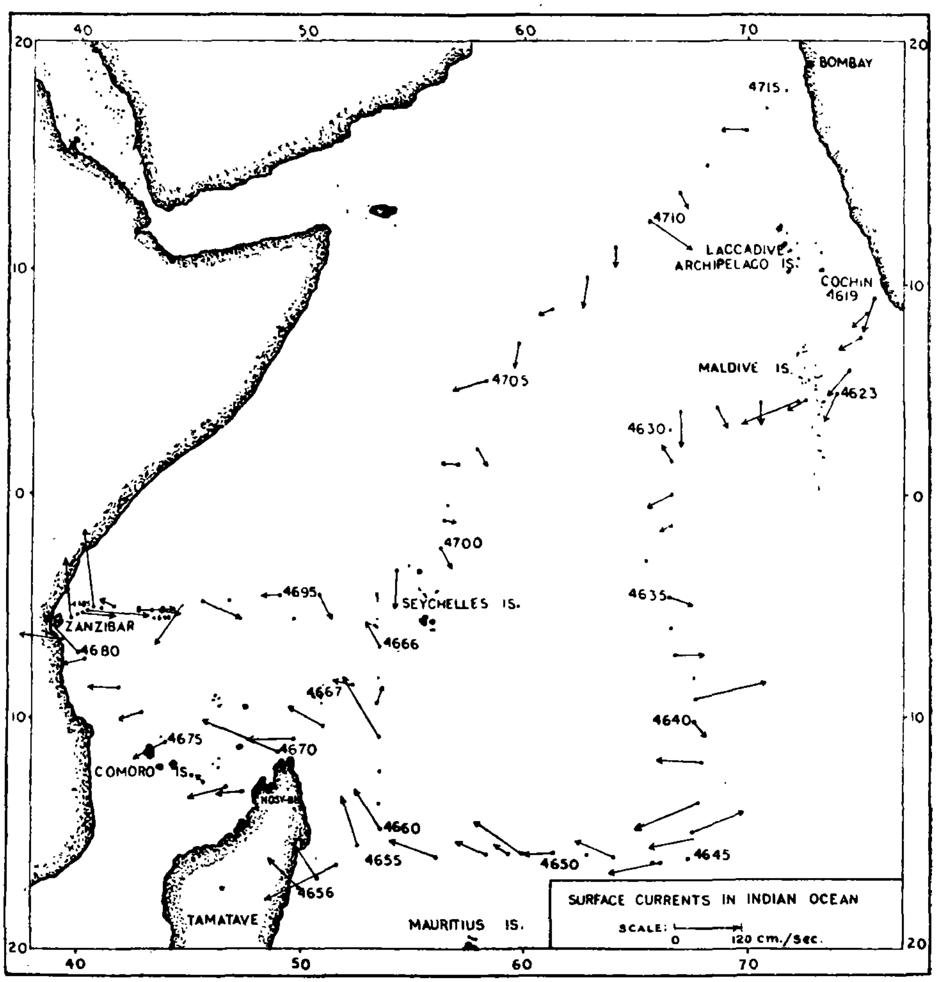

Fig. 1

inferences on surface currents could be derived from drifting oceanographic vessels while on station.

Surface Currents in the Western Part of the Indian Ocean

The period during which the present investigations are carried out forms part of the winter in the northern hemisphere, and during this season strong north-west to north-east winds prevail over the north-western parts of the Indian Ocean.

The surface currents shown in Fig. 1 clearly indicate the presence of North Equatorial Current, Equatorial Counter Current and the South Equatorial Current during February-March 1960.

The current pattern is compared with the surface currents of this region shown in " Plate 8—World Chart of Oceanic Sea-surface Currents for the Northern Hemisphere Winter " by DEFANT (1961).

An examination of the currents along the 68°E meridian gives some indication to the boundaries of the three equatorial circulations in the Indian Ocean. The southern limit of the westward flowing North Equatorial Current extends right upto the equator. The Equatorial Counter Current is well developed and has its axis very near to 9°S latitude. This agrees fairly well with the mean position indicated by SVERDRUP (1942). Further, it can be observed that the Equatorial Counter Current, which starts from the region off Zanzibar, widens as it moves farther and farther from the coast, and at 68°E meridian it appears to extend from about 3°S to 10°S latitude. The South Equatorial Current moving across the east coast of Madagascar can clearly be seen to branch off into north and south flowing currents along the coast. The northern branch moves north and then westward feeding the south flowing surface current in the Mozambique channel. Off Zanzibar, the surface currents show a strong flow towards east, indicating that upwelling might be taking place during this period.

The surface currents in the Arabian Sea do not show any distinct pattern, but a more or less southward and south-westward flow can be observed. Off the west coast of India, the surface current is weak during this period and is directed southwards along the coast.

ACKNOWLEDGEMENTS

The author takes this opportunity to express his gratefulness to Prof. B. G. Bogorov, Chief Scientist, and all other scientists on board VITIAZ during her 31st cruise in the Indian Ocean, for their several courtesies.

The assistance rendered by Shri. V. Hariharan in the computations is greatly appreciated.

REFERENCES

BOHNECKE, G.—Remarks about the Method of Investigation into Oceanic Circulation, *Proc. UNESCO Symposium on Physical Oceanography, Tokyo,* 1955, 17-19.

DEFANT, A.—*Physical Oceanography,* Vol. 1, Pergamon Press, 1961.

SVERDRUP, H. U. *et al—The Oceans—Their Physics, Chemistry and General Biology,* Prentice-Hall Inc., 1942, 1087.

ADDENDUM

Subsequent to the submission of the above note, the author has come across the initial results of the 31st cruise of VITIAZ published in " Results of Researches of IGY Programme, Section X—Oceanological Researches, No. 4, 1962 (in Russian)".

In the paper " Circulation of Waters in the Northern Indian Ocean during the Winter Monsoon " by I. M. OVCHINNIKOV, the surface currents as determined by direct observations are described along with sub-surface currents.

The surface current pattern in the western part of the Indian Ocean obtained from the ' drift method ' is compared with that given in the above paper. The general pattern of surface currents obtained by the ' drift method ' agrees fairly well with the current pattern obtained by direct measurement. However, north of equator, there is some disagreement in the current patterns. The cyclonic circulation observed in the Arabian Sea by direct measurements is not clearly brought out in the 'drift method.' The salient features that are in agreement can be summarised as follows :

1. The three equatorial circulations are well established in the western part of the Indian Ocean during the northern hemisphere winter as is already well known.

2. The current pattern as a whole is displaced to the south in comparison with the equatorial circulations in the Atlantic and Pacific Oceans.

3. The boundary between the North Equatorial Current and the Equatorial Counter Current lies to the south of the equator at 68°E meridian (according to OVCHINNIKOV it lies at 3°S on 56°E longitude and at 2°N on 86°E longitude).

4. The Equatorial Counter Current widens as it flows farther and farther from the east coast of Africa.

5. The South Equatorial Current moving across the east coast of Madagascar divides into north flowing and south flowing branches.

6. Near the west coast of India, the surface current flows southward along the coast.

Reprinted from *J. Mar. Biol. Ass. India*, 1964, vol. 6, no. 2, p. 207-216

THE HYDROGRAPHICAL FEATURES OF THE WATERS OF PALK BAY DURING MARCH, 1963

By A. V. S. MURTY & P. UDAYA VARMA
Central Marine Fisheries Research Sub-Station, Ernakulam-6

INTRODUCTION

DURING the 26th cruise of the Research Vessel *VARUNA*, the Palk Bay has been covered from 18th to 20th March, 1963. The location of the Stations (Nos. 1631 to 1681) occupied during this cruise are shown in Fig. 1.

The Bay is a very shallow and flat basin, nowhere exceeding 15 metres deep. On an average its depth hardly exceeds 9 metres. Temperature, salinity and dissolved oxygen are the parameters of which the data have been collected during the cruise. Samples were taken from the surface at every station and from 5 metre depth at many stations and also from 10 metre depth at a few stations depended on the sonic depth of the station. These data have been used for bringing out the hydrographic features of the Palk Bay. The prevailing winds are also considering in the analysis, the relevant wind date being taken from the daily weather reports of the Indian Mateorological Department. The Palk Bay is divided into four different zones based on the nature of the data collected and the distributions of different parameters in these four zones are also presented.

DISTRIBUTION OF SURFACE TEMPERATURE

The surface waters are subjected to diurnal variations of temperature due to the heating by day and cooling by night. The variations are much more appreciable in case of shallow basins due to the less thermal capacity of the basin waters. It will be possible to compare the temperatures over different regions, only when the diurnal variations of temperature are minimised so that they can be neglected. Since the data of the Palk Bay are collected for three days, it is necessary to eliminate or minimise the diurnal variations from the observed surface temperatures. This may be achieved from shore-station observations. The observations at a shore station near Waltair (17° 41′N, 83° 17′ E) on the diurnal variations of surface temperature, connect the amplitude of temperature with hour of observation for the month of March 1960. The amplitude of temperature α (in °C) about the daily mean temperature is given by

$$\alpha = -0.58 \text{ Cos } \frac{\pi}{12} t + 0.15 \text{ Cos } \frac{2\pi}{12} t - 0.02 \text{ Cos } \frac{3\pi}{12} t - 0.72 \text{ Sin } \frac{\pi}{12} t - 0.10 \text{ Sin } \frac{2\pi}{12} t - 0.07 \text{ Sin } \frac{3\pi}{12} t,$$

where t is measured in hours starting from midnight (Ramanadham and Murty—unpublished). The corrections for diurnal variation ($-\alpha$°C) have been applied for the observed temperatures of the surface waters of the Palk Bay.

1

The distribution of temperature of the surface, after being corrected for daily variations, is shown in Fig. 2. Temperature is less in the southern region as compared to the coastal region of the west and north-west of the Bay. They are moderate in the neighbourhood of the Palk Strait (north eastern region of the Bay).

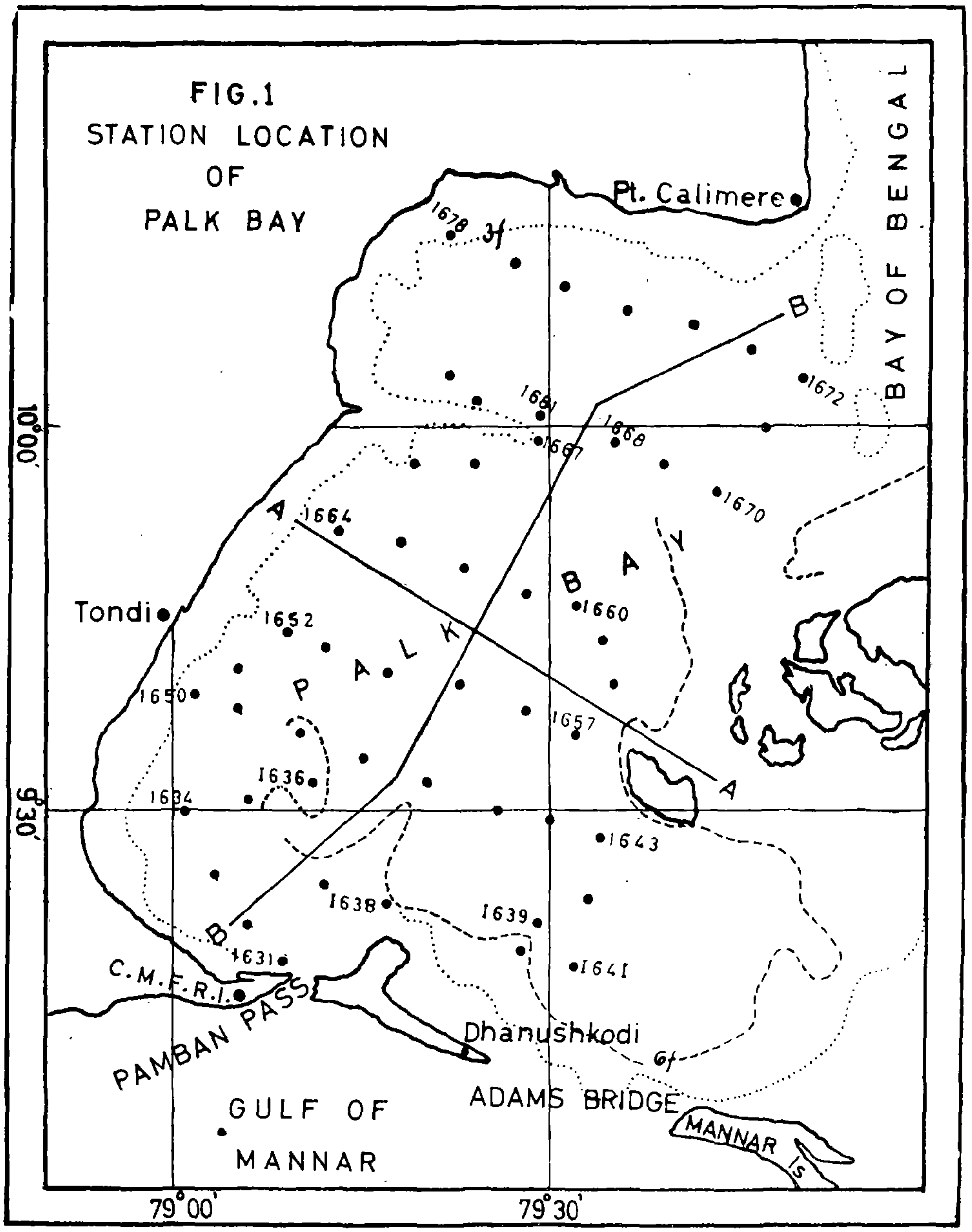

The moderately cool water of the Bay of Bengal after entering the Palk Strait **extends** its influence almost to the middle of the west coast and in doing so, it divides the coastal waters of relatively high temperature into two separate cells. The temperatures of the region west of Pamban Pass are comparable with those of the

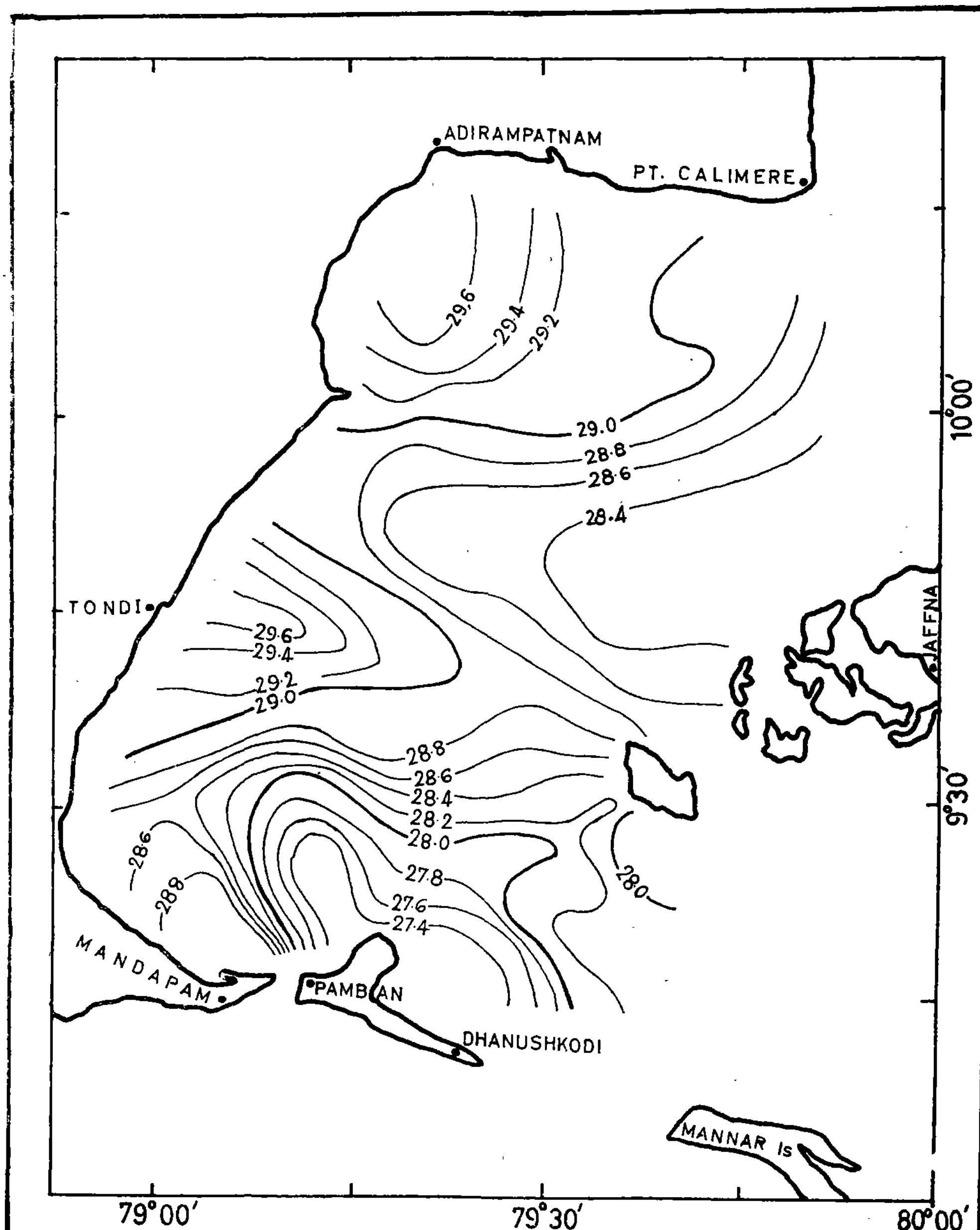

Fig. 2. Distribution of surface temperature (°C) in Palk Bay during March, 1963.

Strait. The thermal gradients are low in the northern region but they are high in the south. There is a very high positive gradient of temperature from the Rameswaram Island (Pamban) to Tondi.

Distribution of Surface Salinity

The distribution of surface salinity is illustrated in Fig. 3. The salinity value depends not only upon the origin of watermass but also on the evaporation from the surface. Unless the factors of evaporation, such as the winds and humidity gradients in the microlayers of air over the surface are known, the effect of evaporation on local salinity values cannot be discussed. Nevertheless, the salinity variations are further complicated by mixing of watermasses brought into effect by currents and turbulent exchanges.

The 32‰ isohaline serves as a line of demarcation between the low saline coastal waters to its left and high saline Bay of Bengal waters to its right. The incursion of the Bay of Bengal water into the Palk Bay through the Strait is such that it splits the coastal water into two separate cells. Except for a weak trough (31‰ isohaline) at the centre of the Bay, the salinity decreases gradually along an axis in the south-west direction running from the Strait. Highly saline water is pocketed in the south-southwestern corner of the Bay. This may be due to the incursion of the Gulf water through the Pamban Pass. The circulation in the south-western region may be weak and the coastal configuration may be hydrodynamically protective constituting the causes for the entrapment of the high saline Gulf water without being mixed with the low saline coastal water in the south. Water having a salinity less than 30‰ may be treated as coastal water. The coastal water in the north is confined to a narrow region near the coast, whereas in the south the coastal water extends even to the middle of the Bay. The west-southwestern region is having the lowest saline water.

Along an axis in the direction of south-west from the Strait the salinity at first decreases gradually and then more rapidly towards the further end of this axis, disregarding the shallow dip at the middle. The gradient is very strong in the south-west, as in the case of temperature.

Distribution of Surface Density (σ_t)

The values of surface density (σ_t) have been computed by making use of the data presented in Figs. 2 & 3. The density distribution of the surface of the Palk Bay is illustrated in Fig. 4. The isopycnal of the value $\sigma_t=20$ in the north may be treated as a forward boundary of the Bay of Bengal water. Similarly, the isopycnal $\sigma_t=19$ may be the limiting contour for coastal water. As in the case of salinity, it is also clear from the orientation of the isopycnal $\sigma_t=19$ that the coastal water is limited to a narrow region in the north-west and to a wider area in the south-west. It is also clear that the Gulf water near the Pamban Pass in the south is locked under the protective configuration of the coast.

The sharp gradients of density of the south-western region indicate that mixing of the coastal water with the sea (Gulf) water is not prominent in this region. It can be further inferred from the orientation of the isopycnal $\sigma_t=20$ that the influence of the Bay of Bengal water on the Palk Bay is much more extensive and

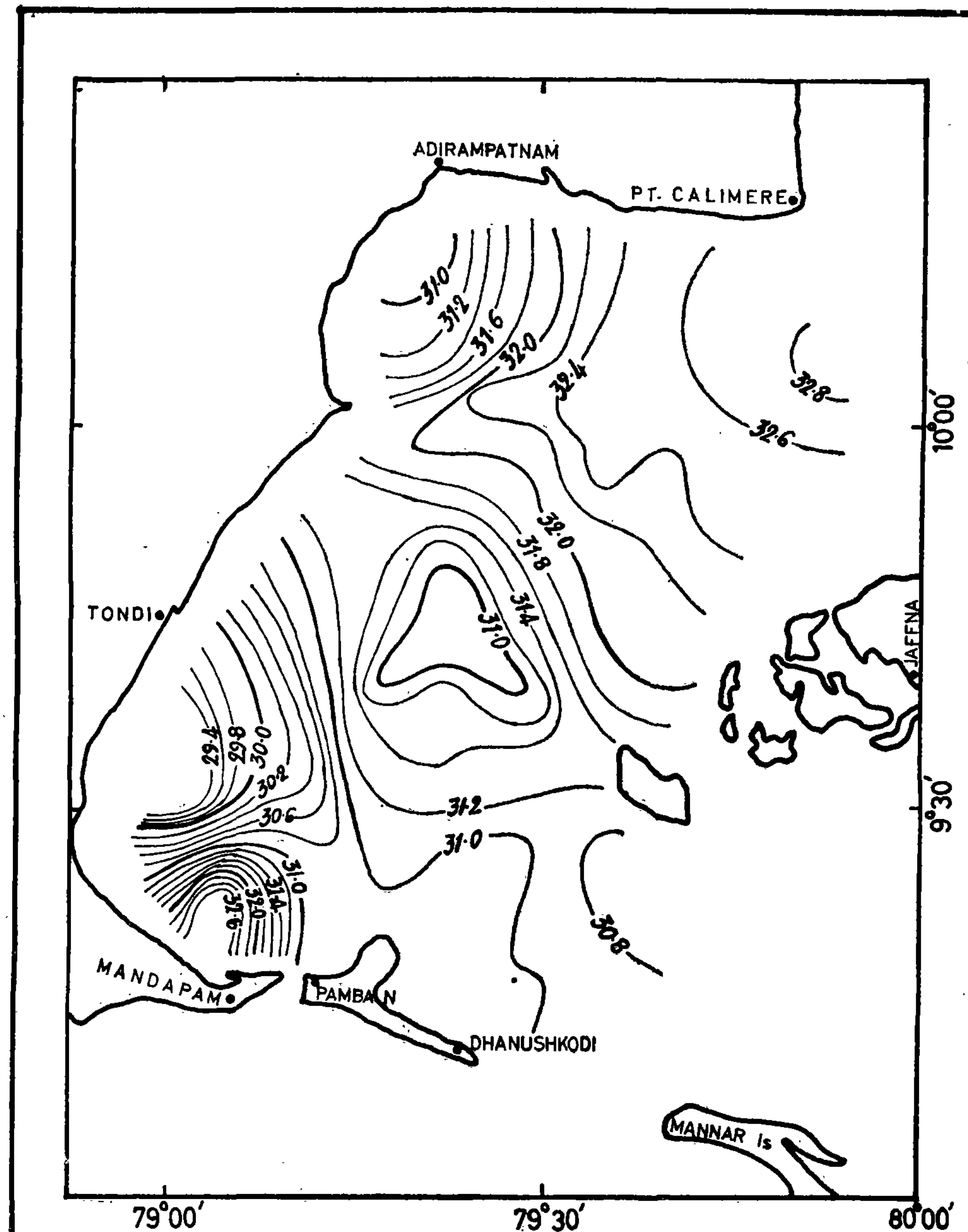

Fig. 3. Distribution of surface salinity (‰) in Palk Bay during March, 1963.

intensive than the Gulf waters. The density decreases along an axis in the south-western direction from the Strait, the waters being more of sea origin at the beginning and more of coastal origin towards its further end.

Distribution of Dissolved Oxygen

The distribution of dissolved oxygen (ml/l) in the surface waters of the Palk Bay is shown in Fig. 5. This being a shallow body of water, the effect of wind

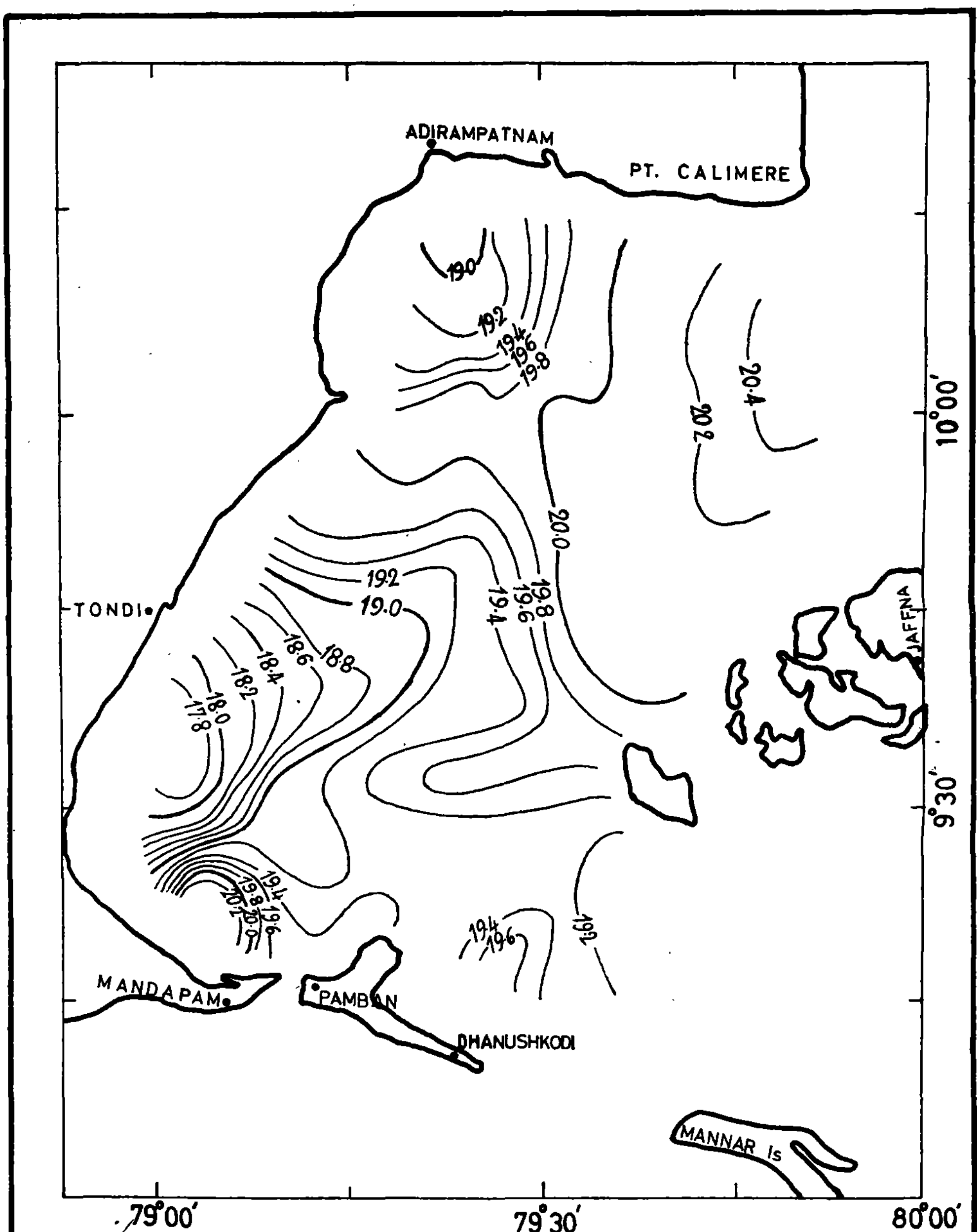

Fig. 4. Distribution of surface density (σt) in Palk Bay during March, 1963.

mixing, apart from the biochemical factors, in the horizontal and vertical distribution of oxygen is suspected. Hence the speed and direction of the wind over the Bay were computed from the daily Weather Reports of the shore stations of Nagapattinam and Pamban obtained from the Indian Meteorological Department. These

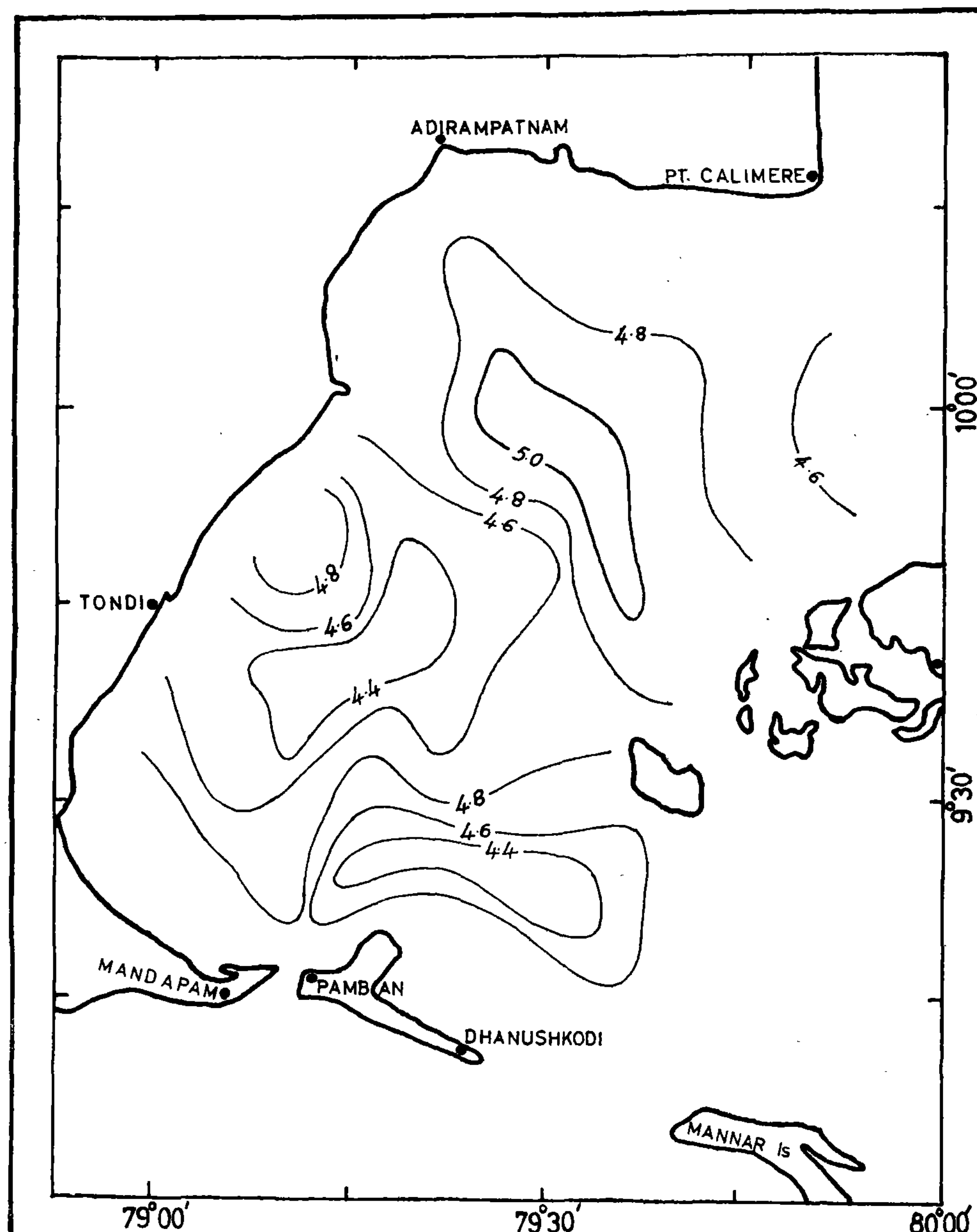

Fig. 5. Distribution of surface dissolved oxygen (ml/l) in Palk Bay during March, 1963

computations show that the North-East winds are more frequent during this period. The wind strength at Nagapattinam is about 8 to 10 knots on an average for the month, and at Pamban it is only 2 to 4 knots. It means that the wind blows over the Palk Bay in the same direction over the northern and the southern region, but with different strength. The winds over the Palk Strait are considerably strong and they decrease along the axis in the south-western direction to attain a minimum speed at the lower end of the axis.

The oxygen content in the surface waters at the Strait is less when compared to that of the waters a little further inside the Palk Bay, in spite of the strong winds at the former region. In the open sea (the Bay of Bengal) the surface oxygen is distributed over a considerable length of water column in the vertical. On the contrary, only a very short column of water shares the oxygen from the surface a little left of the Strait since the depth is hardly 5 fathoms. Therefore, the oxygen content is slightly higher towards left of Palk Strait though the winds are stronger towards its right. As the winds are weakened along the axis of the Bay in the south-western direction, so is the distribution of oxygen content in this direction.

It is noteworthy that the waters everywhere in the Palk Bay are almost saturated with dissolved oxygen. They sometimes even exceed the saturation limit by a small percentage, especially in the northern region.

Zonal Distribution of Physical and Chemical Properties

In view of the nature of observations, the Palk Bay is divided into four different zones by the lines AA and BB as shown in Fig. 1. The division is such that each zone contains the data partly covered by night and partly by day. The diurnal changes, within certain limitations, can therefore be expected to affect all the four zones in a similar way.

The distribution of the physical and chemical properties are represented in the Table for all these zones. The Table gives a summary of the regional differences of properties of the Bay waters. It differentiates the warm, low saline and low oxygen and light waters of the south-western zone from the moderately cool but highly saline and rich oxygen and denser sea waters of the diagonally opposite north-eastern zone.

At least some of the properties are similar for all the four zones. With all that, the south-western zone remains distinctly separate from the rest of the four zones.

Summary

The Palk Bay is a shallow and flat basin; the depth of which being on an average 9 metres and nowhere exceeding 15 metres. The hydrography and dissolved oxygen conditions of the Bay waters are studied during the month of March 1963.

The distributions of temperature, salinity, density and dissolved oxygen of the surface waters of the Palk Bay indicate that the Bay of Bengal waters entering through the Palk Strait have major influence on the hydrographic conditions of the Palk Bay. The Gulf waters influence the Palk Bay to a minor extent only.

TABLE

Zonal Distribution of Physico-Chemical Properties of the Palk Bay

Zone	Surface Temperature °C		Temperature °C		Salinity ‰			Surface Density σ_t	Dissolved Oxygen ml/l			Percentage saturation of Dissolved Oxygen		
	Corrected for daily variations	Uncorrected for daily variations	5m.	10m.	Surface	5m.	10m.	(*t*)	Surface	5m.	10m.	Surface	5m.	10m.
North-West	29.1	29.0	28.8	..	31.85	31.86	..	19.71	4.7	4.7	..	106	105	..
North-East	28.6	28.8	28.7	..	32.29	32.24	..	20.19	4.7	4.6	..	106	103	..
South-East	28.4	28.5	28.7	28.4	31.10	31.02	31.23	19.50	4.6	4.8	4.6	102	105	102
South-West	29.0	28.6	28.6	..	30.26	30.24	..	18.70	4.6	4.5	..	100	100	..

Winds blow over the Palk Bay from the north-east. They are strong at the Palk Strait and weak towards the south-western end of the Bay.

The dissolved oxygen reaches nearly its saturation value over the entire Bay. Sometimes it exceeds its saturation limit by a small percentage. The general pattern of distribution of dissolved oxygen of the surface layers is in accordance with the wind conditions over the Bay.

The waters adjacent to the coast have high temperature, low salinity and low density. The Bay of Bengal water extends its influence almost to the middle of the coast and hence separates the coastal water into two cells.

Denser sea water is pocketed near the coast at the south-western region of the Bay. The south-western zone is the least disturbed area under the protective configuration of the coast and the non-disturbing atmosphere. The coastline of the north-western region is similarly protective. But the waters in this region are disturbed by the strong north-easterly winds and the associated circulation of water through the Strait.

Reprinted from *J. Geophys. Res.*, vol. 70, no. 10, 1965, p. 2319-2324

Large-Amplitude Internal Waves Observed off the Northwest Coast of Sumatra

RICHARD B. PERRY AND GERALD R. SCHIMKE

U. S. Coast and Geodetic Survey, Washington, D. C.

Abstract. Internal waves of large amplitude were observed north of Sumatra by the U. S. Coast & Geodetic Survey ship *Pioneer* in June 1964. The bathythermograph investigation which defined these waves was initiated after observation of curious periodic surface phenomena resembling tide rips. Analysis of bathythermograph records indicates that internal waves with a maximum observed wave height of 82 meters are the probable cause of the surface disturbances.

Introduction. The existence of internal waves in the sea, along surfaces separating layers of contrasting density, has been inferred from oceanographic observations for many years. A better understanding of these waves is important because of their effect on dynamic height computations, current measurements, marine life, undersea navigation, and submarine warfare. Large internal waves, and surface disturbances believed to be associated with these waves, were observed in the Andaman Sea area between Great Nicobar Island and Sumatra by the U. S. Coast & Geodetic Survey ship *Pioneer* in June 1964 during the vessel's participation in the International Indian Ocean Expedition.

Setting. The Andaman Sea is separated from the Bay of Bengal by the Andaman and Nicobar islands (see Figure 1) and a submerged, north-south trending ridge from which the exposed island peaks rise, the Andaman-Nicobar ridge (see Figure 2). The sea is bordered by Burma, Thailand, the northern end of the Strait of Malacca, and the northwest coast of Sumatra. Between Great Nicobar Island, the southernmost island of the group, and Sumatra, the waters of the Andaman Sea connect with those of the Indian Ocean through the Great Channel, a passage in the submerged ridge characterized by rugged sea-bottom topography and depths greater than 2000 m.

General summaries of meteorological and oceanographic conditions in the Bay of Bengal–Andaman Sea area are given in *U. S. Navy Hydrographic Office Special Publication 53* [1960] and by *Sewell* [1932]. They indicate that in June a well-mixed surface layer of water, having lower salinity and higher temperature than the surface waters in the Bay of Bengal, flows southwest through the Great Channel. Temperature profiles taken by the *Pioneer* in June 1964 showed a well-mixed layer extending to a depth of about 100 m. A recent analysis of oceanographic conditions in the area indicates that surface currents in the Great Channel set to the west at about 0.8 m/sec during much of the year and that a subsurface flow sets to the east, into the Andaman Sea, below the thermocline depth (R. H. Sullivan, Jr., U. S. Navy Fleet Weather Service, personal communication).

Observations. On the morning of June 12, 1964, distinct zones of whitecaps ranging from 200 to 800 m in width and stretching from horizon to horizon (approximately 30 km) in a north-south direction were observed in the Andaman Sea north of Sumatra (see Figure 2). At least five of these zones, with a spacing of about 3200 m between each zone, were observed. The observed zones or bands of choppy water had short, steep, randomly oriented waves with heights of about 0.3 to 0.6 m. Each band stood out distinctly in an otherwise undisturbed sea. A 4-m/sec NNW wind and a surface water temperature of 29°C were observed, but neither changed significantly as the ship crossed the bands of choppy water. Detailed salinity measurements were not made while crossing the bands; however, routine bi-hourly salinity samples showed a maximum regional salinity gradient of 0.03‰ per km. Later in the day, several other bands of similar dimensions, but having smaller waves, were observed.

On June 13, similar north-south trending

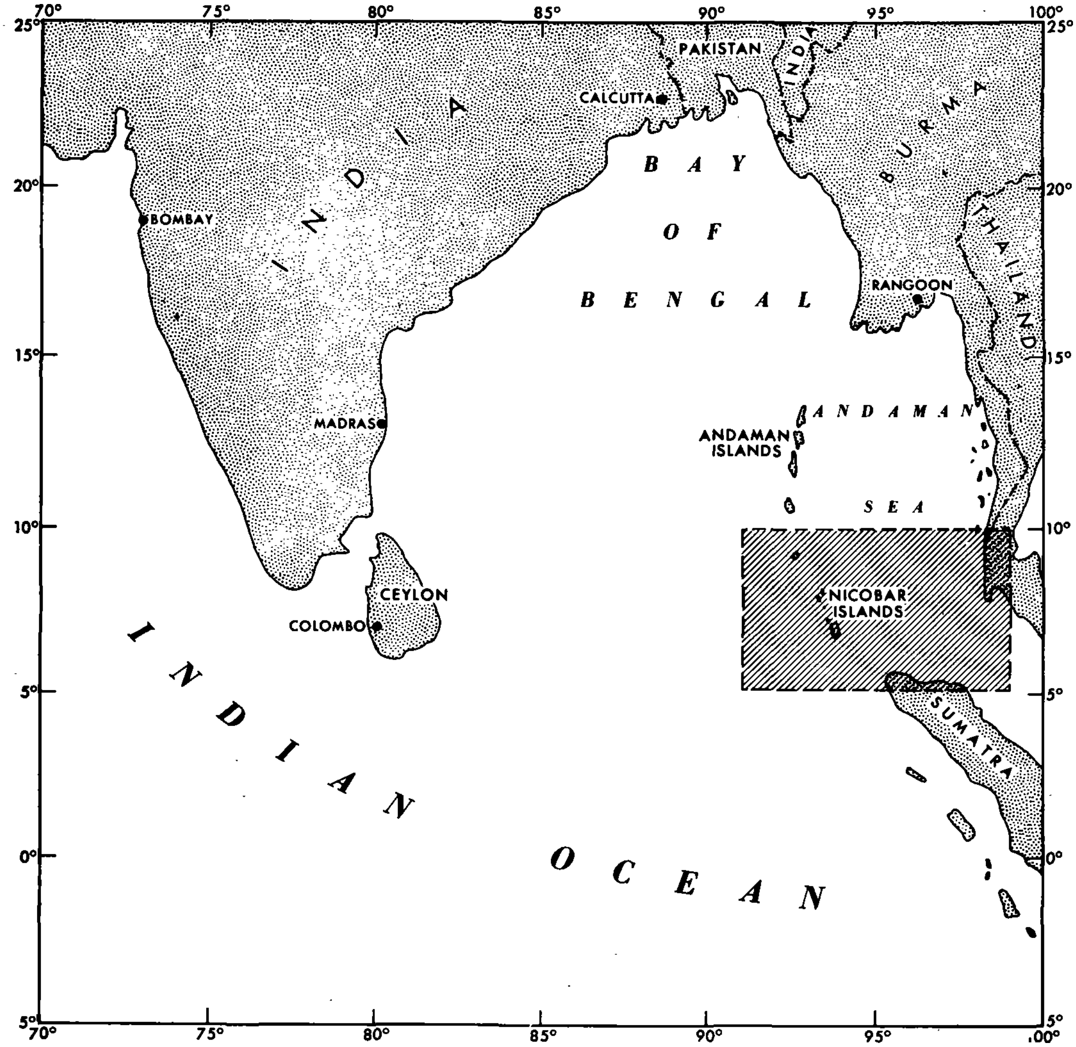

Fig. 1. Indian Ocean area.

bands of choppy water were seen farther to the west in the Great Channel, near 06°09′N, 94° 37′E. Ten bands, each approximately 200 m wide and 800 m apart, were observed. In some instances, the water between the bands of choppy water had a slicked appearance despite a 9-m/sec SSW wind. Similar slicks were not apparent on the preceding day when the bands of choppy water were farther apart. Boundaries of the choppy water were all well defined. After crossing a number of the bands, the ship changed course to an easterly direction to initiate a bathythermograph (BT) investigation of the observed phenomenon. The time at which the bow of the ship entered a chop line and the time the stern entered the same line was observed. By using the ship's course and average speed as determined by visual fixes on land, it was possible to compute the rate at which the bands were moving, assuming their direction of progress to be perpendicular to their long axis. The bands were computed to be moving eastward at 2.6 m/sec. A series of five BT observations was obtained by repeatedly lowering the instrument while the ship steamed west at 4.7 m/sec, approximately perpendicular to the long axis of the chop lines. Four well-defined bands of choppy water were crossed during the BT

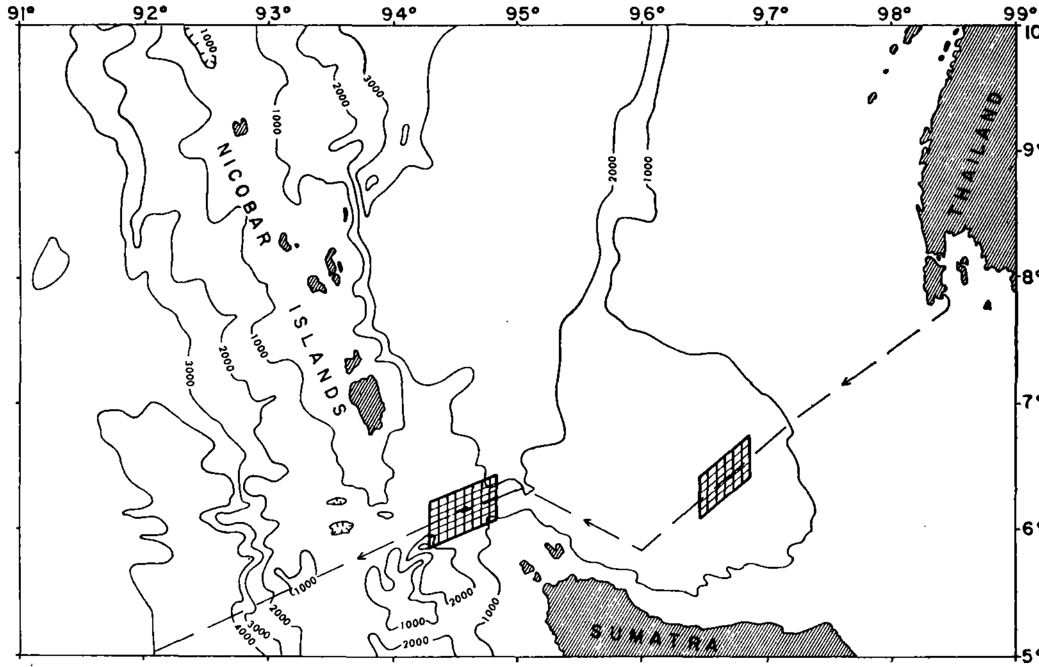

Fig. 2. Trackline of USC&GS ship *Pioneer,* June 12–13, 1964. Crosshatched areas indicate places where surface disturbances were observed. Depth contours in meters.

observations (see Figure 3). Each BT record taken while crossing the chop lines showed a split trace in the thermocline region. A maximum separation of nearly 15 m was recorded on one lowering. Since the bathythermograph functioned properly on previous and subsequent measurements, the cause of the split trace was attributed to pronounced horizontal temperature gradients, possibly associated with internal waves.

The temperature profile in Figure 3 was derived by plotting the depth of the isotherms from the five BT traces against the time elapsed during the observations. The temperatures recorded during the descent of the BT are separated from those recorded during the ascent. In the resulting profile the periodic undulations of the closely spaced isotherms, which depict the depth of the thermocline, strongly suggest the presence of internal waves. The maximum height of the apparent waves is approximately 80 m. If they are indeed internal waves, and moving at the same speed and in the same direction as the surface chop lines, then the wavelength is calculated to be about 2000 m.

Upon completing the special BT observations, the *Pioneer* resumed its westward course through the Great Channel into the Bay of Bengal. As the ship proceeded westward, the surface waves in the bands of choppy water were observed to increase in size. The last and westernmost chop line sighted, at 06°03′N, 94° 21′E, was a very choppy north-south zone characterized by seas of 1.8 to 2.1 m and extending from horizon to horizon.

During the ship's westward course through the area where the internal waves were found, the routine bi-hourly BT observations indicated an intensification of the temperature gradient in and a rising of the thermocline. From the point where the last line of surface chop was observed, and westward into the Bay of Bengal, the thermocline depth gradually increased and its temperature gradient became somewhat less intense.

Discussion. In the Bay of Bengal and adjacent waters, surface phenomena similar to that observed aboard the *Pioneer* have been previously observed and variously described as current rips, tide rips, lines of demarcation, and disturbed and rippled water [*Marine Observer,* 1958, 1959, 1962*a*, 1962*b*, 1963, 1964]. Alternate

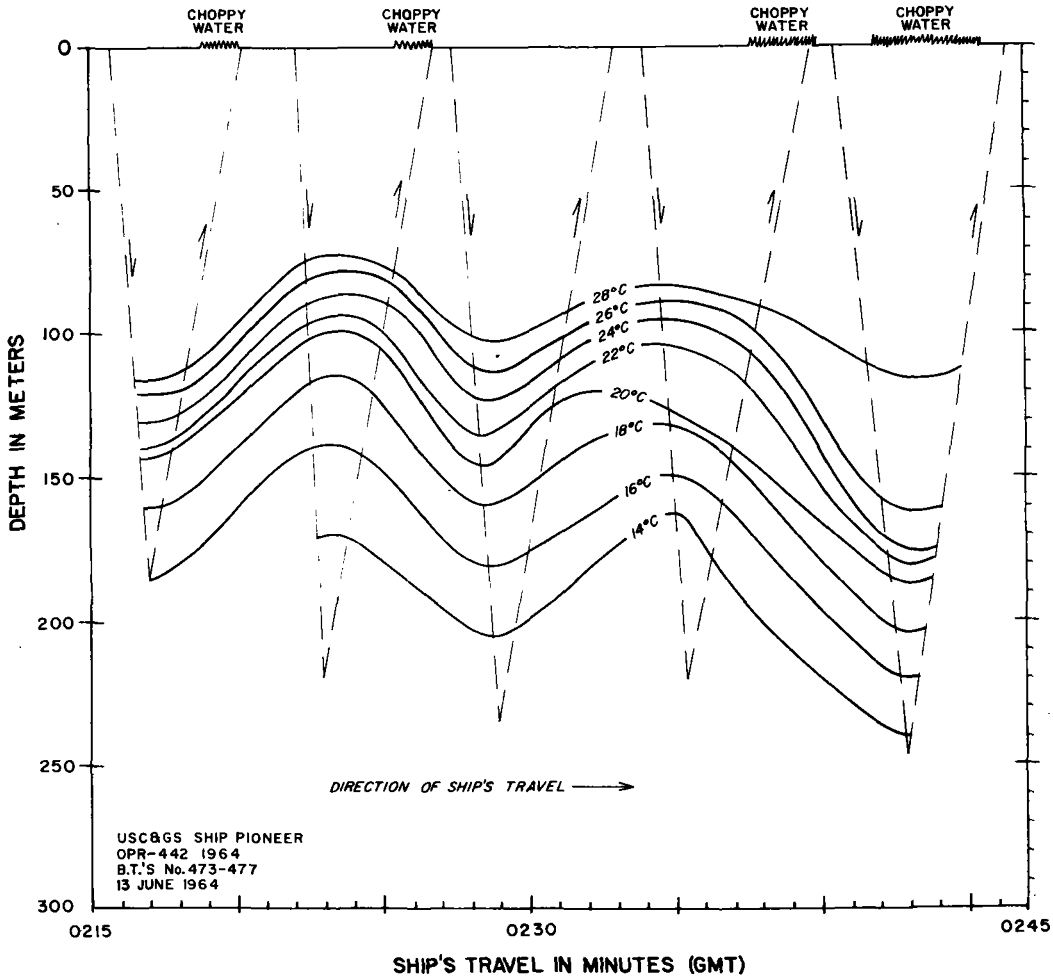

Fig. 3. Temperature profile as defined by bathythermograph. Dashed lines indicate path followed by bathythermograph.

bands of rough and smooth water passed the R.V. *Anton Bruun* at four oceanographic stations in the Andaman Sea in March 1963 while that ship was operating under the National Science Foundation Program in Biology for the International Indian Ocean Expedition. At one of these stations a low roar accompanied by breaking whitecaps was observed as the bands passed the ship in a flat calm sea (E. C. LaFond, U. S. N. Electronics Laboratory, 1965, written communication).

In more restricted areas similar but smaller-scale, elongated surface features occasionally are caused by converging currents, by tide rips, or by the influence of bottom topography. *Pickard* [1961] has observed similar surface phenomena on a much reduced scale in certain inlets along the British Columbia mainland. His surface phenomena were related to progressive internal waves associated with a shear zone between inflowing bottom water and outflowing surface water in a positive estuarine situation.

Bands of surface chop have also been associated with oceanic fronts. Such fronts are generally characterized by strong horizontal temperature gradients at the surface and by marked faunal and color changes [*Knauss*, 1963]. A pronounced lateral shear in the surface flow is often in evidence as the observing ship crosses the disturbed band of water. The *Pioneer* experienced no difficulty in maintaining a true course while crossing the bands of disturbed water. There were no noticeable horizontal temperature or salinity gradients at the surface for a distance of more than 145 km on either side of the five special BT observations taken on June 13. Therefore, the possibility that the observed phenomena were directly associated with an oceanic front can be dismissed.

The possibility of bottom topographical influence as a causative factor has been considered because remarkable correlations have been made between sightings of disturbed water and sharp rises in the bottom topography at relatively great depths. Such a correlation was noted aboard the *Pioneer* earlier in the expedition while in the Andaman Sea. However, the jumbled and rugged topographical features and great depth of the sea floor in the immediate vicinity of the chop lines (Figure 2) make it hard to conceive of the bottom features giving rise to long, straight, narrow surface disturbances stretching from horizon to horizon.

Surface slicks have been related to internal waves in shallow water areas [*Ewing,* 1950; *Dietz and LaFond,* 1950]. In many cases, slicks are particularly noticeable in waters close to shore, where they usually are associated with wave heights of 10 m or less. *Pickard* [1961] pointed out the basic difference between these slicks and the bands of choppy water which we observed.

Internal waves of greater height than 10 m have been observed in the deep oceans by means of Nansen bottles with reversing thermometers, BT's, and, more recently, thermistor chains. Generally, these internal waves have been long waves with periods of the same order of magnitude as the tidal period. Slicks or disturbed surface conditions have not been associated with internal waves in deep water far from shore before these observations.

The mechanism for generating internal waves is frequently in question. In coastal areas the rise and fall of the tides over the continental shelf [*Rattray,* 1960] and shear caused by one mass of water flowing over another [*Proudman,* 1953] are among the mechanisms proposed for the generation of internal waves. The internal waves observed by the *Pioneer* were of such short wavelength that tidal generation hardly seems to be a reasonable explanation. On the other hand, because of their large amplitude, it seems somewhat speculative in the absence of direct current measurements to propose that shear flow was the generating mechanism. However, investigations by R. H. Sullivan, Jr. U. S. Navy Fleet Weather Service, personal communication, 1964), indicate that a strong shear flow may occur in the vicinity of the observed phenomena during most of the year. If this is the case, the situation seems directly analogous to that observed by *Pickard* [1961].

Defant [1961] wrote, 'the appearance of waves at the boundary surface between two water layers has for a long time escaped the attention of observers because, even when the amplitude of the oscillation at the boundary surface is large, the free surface of the upper layer is only slightly disturbed and remains practically at rest.' In the case at hand, the density of ρ' the upper well-mixed layer was 1.021 g/cm^3. From the previous observations of *Sewell* [1932] and *USN H. O. Special Publication 53* [1960], the density ρ of the lower layer can be reckoned as 1.026 g/cm^3. Using 40 m for the amplitude of the internal wave, and the formula $\eta_0 = -Z(\rho - \rho')/\rho$ [*Defant,* 1961], where η_0 is the amplitude of the wave at the free surface and Z is the amplitude of the internal wave, we compute a 0.2-m amplitude for the wave at the free surface.

The generating mechanism of the highly agitated bands of chop is not clear, but they probably are caused by a redistribution of mass that takes place with the passage of the internal wave. Pickard's observations in Canadian waters indicate that his 'ruffled bands' are associated with the convergence taking place at the surface just behind the advancing internal wave crest. As seen in Figure 3, it was not possible to establish a clear relationship between the bands of chop at the surface and a particular phase of the wave.

There is no direct correlation of wind effects and the observed phenomena since they were observed on June 12 in a relatively calm sea. Also the waves of the chop zone showed variable heights under relatively constant wind conditions on June 13. A topographic influence seems unlikely because of the irregular character and depth of the bottom.

Owing to the prevailing oceanographic conditions north of Sumatra during much of the year, and reported sightings of disturbed bands of water stretching from horizon to horizon, we believe that the existence of the phenomenon reported herein may be common in this part of the world, and its occurrence on June 13, 1964, probably was not unique.

More comprehensive investigations of this phenomenon might include the use of aircraft for aerial reconnaissance and aerial photography to chart the extent and periodicity of the surface disturbances. Current measurements and detailed thermal investigations should also be made using at least two ships equipped with thermistor chains.

Conclusions. The zones or narrow bands of choppy water sighted by the USC&GS ship *Pioneer* in the Andaman Sea area are believed to have been caused by internal waves. Internal waves, which were observed to occur simultaneously with the choppy surface phenomena, had uncommon dimensions of approximately 80 m in height and 2000 m in length.

Although the limited observational data preclude any conclusive demonstrations of a generating mechanism for these waves, the cause may be related to a shear zone resulting from a well-mixed upper layer of warm, low-salinity water flowing westward over cooler, higher-salinity water flowing eastward through Great Channel north of Sumatra.

References

Defant, A., Physical Oceanography, vol. 2, Pergamon Press, New York, 1961.

Dietz, R. S., and E. C. LaFond, Natural slicks on the ocean, *J. Marine Res.*, *9*(2), 69–76, 1950.

Ewing, G., Slicks, surface films, and internal waves, *J. Marine Res.*, *9*(3), 161–187, 1950.

Knauss, J. A., Equatorial current systems, in *The Sea,* vol. 2, edited by M. N. Hill, pp. 235–252, Interscience (Wiley), New York, 1963.

The Marine Observer, Meteorological Office, London: vol. 28, no. 179, p. 5, 1958; vol. 29, no. 183, p. 183, 1959; vol. 32, no. 197, p. 117, 1962; vol. 32, no. 198, p. 178, 1962; vol. 33, no. 200, p. 64, 1963; vol. 33, no. 202, p. 186, 1963.

Pickard, G. L., Oceanographic features of inlets in the British Columbia mainland coast, *J. Fisheries Res. Board Can.*, *18*(6), 907–999, 1961.

Proudman, J., *Dynamical Oceanography,* John Wiley & Sons, New York, 1953.

Rattray, M., Jr., On the coastal generation of internal tides, *Tellus*, *12*(1), 54–62, 1960.

Sewell, R. B. S., Geographic and oceanographic research in Indian waters, *Mem. Asiatic Soc. Bengal,* *9*(6), 357–424, 1932.

U. S. Navy Hydrographic Office, Summary of oceanographic conditions in the Indian Ocean, *Spec. Publ. 53,* 1960.

(Manuscript received January 18, 1965;
revised February 17, 1965.)

Reprinted from *Defence Science Journal (India)*, vol. 16, no. 1, 1966, p. 47-50

OFF SHORE SEA AND SWELL STUDIES IN THE INDIAN SEAS

P. S. SRIVASTAVA, K. JOHN THOMAS AND D. K. NAIR

Indian Naval Physical Laboratory, Cochin

(*Received* 24 *June* 1965)

Off shore sea and swell measurements on board INS KISTNA during the International Indian Ocean Expedition have been presented. Spatial diagrams showing significant height, average period and direction of wave approach have been given. A comparative study of wave hindcasts using Wilson's method with the observed values has been presented.

"Sea" is defined as the waves which are generated locally and in which all the frequencies are present. When the waves pass out of the generating area the low high frequency waves are outstripped by the large waves of low frequency and we get nearly regular waves, which are known as swell. The roughness of the sea surface is a guiding factor in ship movement. Pierson *et al*[1]. have drawn a graph for 'Victory' type ship showing the trend of ship speed with increasing wave height. The speed of the ship decreases from 16 to 10·5 knots as wave height increases from 5 to 15 ft. Hansen and James[2] of the U. S. Oceanographic Office have shown that by careful use of sea state forecast in choosing the ship's course, the time of passage of a ship can be saved up to 10% with increase in safety for the cargo and comfort to passengers and crew. In the last two decades wave studies have revolutionised the design of ships as well as the stabilizers.

The knowledge of the thickness of isothermal water layer is of importance to physical and biological oceanographers. Sea state, to a great extent, decides the variation in the thickness of this layer.

Bathymetric charts of inaccessible coasts can be drawn by taking aerial photographs[3] of the wave pattern.

The landing and taking off of sea planes on which depends the success or failure of search and rescue operations are also decided by the sea state.

Pre-knowledge of sea state can also be used to advantage in coastal constructions beach erosion problems, off-shore drillings, fishing etc.

The study of wind waves in India is still in its infancy. Before 1949 no quantitative measurements of various wave parameters were taken in the Indian seas. Systematic visual observations of sea and swell were the outcome of the International Meteorological Organisation Conference held in Washington in 1947. Based on visual observations, some useful papers have been published by the meteorologists of the India Meteorological Department[4-6]. The monthly averages of significant wave height and period for the Arabian Sea and the Bay of Bengal have been reported in these papers.

COLLECTION OF SEA AND SWELL DATA

Off-shore sea and swell data were collected on board INS KISTNA with the help of a set of buoyant floats tied at every fifty feet to a string floating on the surface, following the technique of Pierson *et al*[1] (Fig. 1). The floats were lowered from the stern of the ship. After stopping the engine of the ship the floats as well as the ship were allowed to drift for about fifteen minutes after which the floats adjusted themselves perpendicular to the crest of the wave. Under these conditions the various wave parameters were easily measured. Thus

(*a*) wave period was observed by noting the time of passage of one full wave at the sixth or seventh float with the help of a stop watch.

(*b*) wave length was observed by sighting one of the floats on the crest of a wave and estimating the distance of the next successive crest.

(*c*) wave speed was calculated by noting the time of travel of a particular wave crest over a distance of 200 ft.

and (*d*) wave height was estimated visually.

For every wave parameter at least twenty five observations were made.

The raw data collected by using the stringed buoyant floats were processed for computing height (significant, average and the highest ten per cent), average period, average wave length and average wave speed. The data for 0—19 cruises of INS KISTNA were issued as departmental reports. The spatial diagrams of the collected data showing significant height, average period and the direction of wave approach are given in Fig. 2—4. Based on the data for 0—14 cruises and also on the data presented in the Atlas

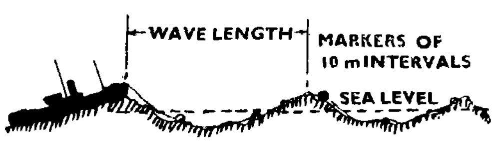

Fig. 1—Measurement of wave parameter.

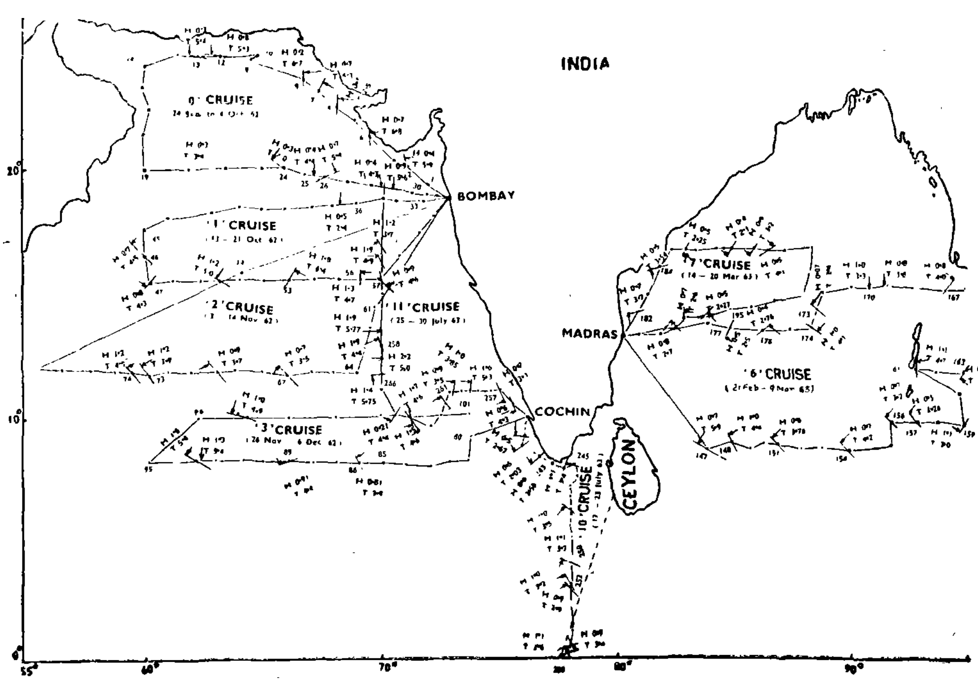

Fig. 2—Spatial diagram [— sea and swell directions; T—average period in seconds and H—significant height in metres]

of sea and Swell issued by the U. S. Oceanographic Office, monthly maps of the areas surrounding India depicting sea state (calm, moderate, moderately rough, rough and very rough) have been published by Srivastava[7].

An instrument using pressure bellows for self recording of wave-height and wave period and capable of being operated from a ship, has been constructed. It will be put to field trials in the future cruises of INS KISTNA.

THEORETICAL COMPUTATIONS OF WAVE PARAMETERS FROM SURFACE SYNOPTIC WEATHER CHARTS

Wave parameters for a few stations of the cruises of INS Kistna, using Wilson's[8] method were calculated. A typical curve showing the comparison of wave hindcasts with observed values is given in Fig. 5 and 6.

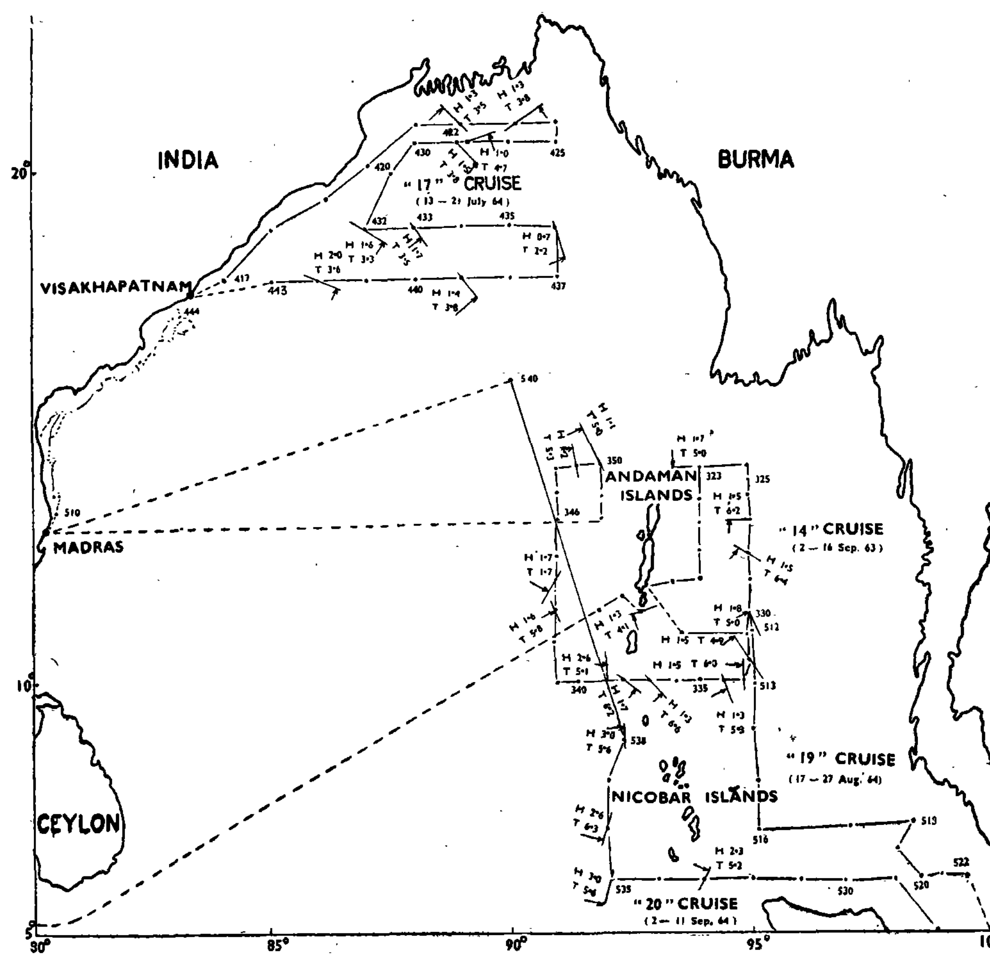

Fig. 3—Spatial diagrams (*—sea and swell directions; T—average period in seconds and H—significant height in metres]

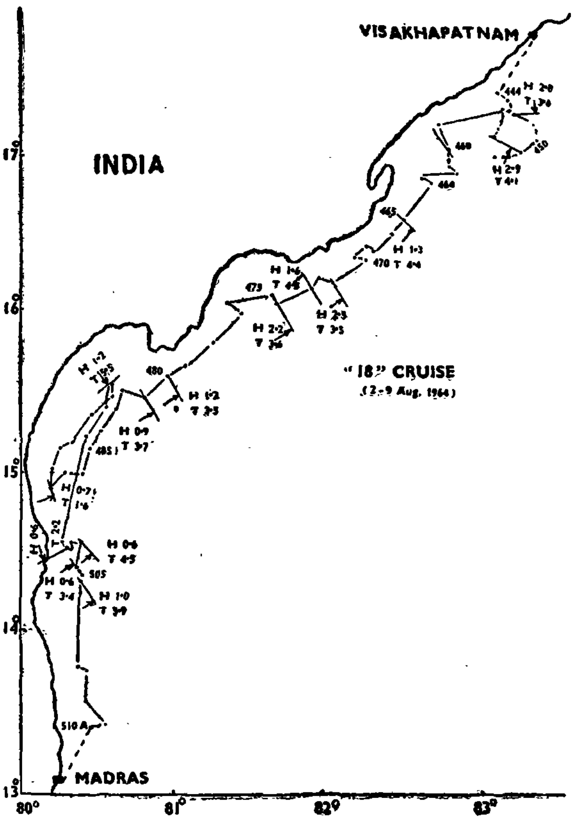

Fig. 4—Spatial diagram

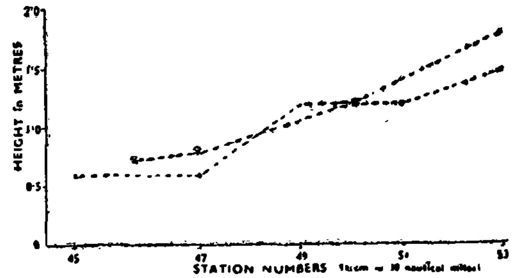

Fig.5-Comparison of wave hindcast with observed values [●—●—hindcasted significant height; ×-×—observed significant height]

The theoretical wave parameters obtained for a few stations fairly agreed with the observed values. The wind velocity in the above situ tions never exceeded 15 knots and hence the above calculations do not represent stormy conditions in the Indian seas.

A wave hindcast study for typical storm conditions both in the Arabian Sea and the Bay of Bengal, using Wilson's method, is also in progress. Wilson's method has been chosen since it takes into account the moving fetches in a simple graphical way. Wind fields have been calculated along the alternate longitudes (*i.e.*, every 2°). It is proposed to hindcast wave parameters over a grid pattern covering the Arabian Sea and the Bay of Bengal. Isopleths of wave height will be prepared for typical storm conditions. These maps will be used to forecast probable quiet lanes for the typical storm conditions.

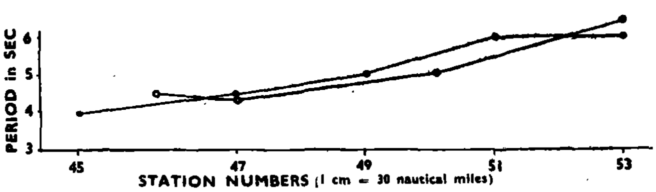

Fig. 6—Comparison of wave hindcasts with observed values [o-o—hincasted significant period; ●-● - observed average period]

ACKNOWLEDGEMENTS

The authors are greatful to Dr. D. Srinivasan for his keen interest. Special thanks are due to Mr. B.M. Agarw.., Mr. P.K. Vijayarajan and Mr. K. V. S. Murti for the initial computations.

REFERENCES

1. Pierson, W. J. Jr., Neumann, G. & James, R. W., "Observing and Forecasting Ocean Waves by Means of Wave Spectra and Statistics" (U. S. Navy H. O. Pubs. No. 603), 1955.
2. Deacon, G.E.R., *J. Roy. Nav. Sci. Service*, **17** (1962), 125.
3. Srivastava, P. S., *ibid.*, **19** (1964), 366.
4. Chakravorty, K. C. & Bhattacharji, R. C., *Indian J. Met. Geophys.*, **8** (1957), 313.
5. Venkataraman, K.S., *ibid.*, **7** (1956), 179.
6. Mukherjee, A. K., Korkhao, J. M. & Srinivasan, V., *ibid.*, **12** (1961), 598.
7. Srivastava, P. S., *J. Roy. Nav. Sci. Service*, (U.K.) **19** (1964), 300.
8. Wilson, B.W., "Graphical Approach to the Forecasting of Waves in Moving Fetches". (Beach Erosion (Board; Deptt. of Army. U.S A. Tech. report No. 95) 1st Jan. (1955).

Reprinted from *Bull. natn. geophys. res. Inst. India*, vol. 5, nos 1 and 2, 1967, p. 11-20

SEA-LEVEL VARIATIONS ALONG THE WEST-COAST OF INDIA*

V S. RAMA RAJU and V. HARIHARAN

*Oceanographic Research Wing of Indian Ocean Expedition, Cochin***

Abstract

The diurnal and seasonal variations of sea-level at Cochin during the years 1958 and 1959 indicate that there is an annual range of 18 inches in sea-level, most of the variation occurring during the period August to December. The short period fluctuations in sea-level observed during south-west monsoon period bear a close association with the rainfall during this season. A deviation of 21° between the surface wind direction and the surface drift is arrived at; the departure from the theoretical value of 45° in the open ocean may be attributed to the shallowness of the region off Cochin.

The general trend of secular variations of sea-level along the west-coast of India indicates that the variations are considerably large for Bhaunagar (1.77 cm/year) and small for Bombay (0.03 cm/year). Studies on the periodicities show that in the case of Bombay and Bhaunagar an 18 years cycle among other periods is also indicated. Further, studies on sea-level variations in relation to precise levelling data at Cochin indicate that the observed sea-level variations are not only due to variations in the water level but also due to variations in the level of the neighbouring land.

Introduction

Tide-gauge records in harbour show that the varying perturbations of sea-level are superimposed over the regular tidal oscillations. The abnormal occurrence of very large deviations from the predicted tides is generally associated with tidal waves generated by earthquakes, submarine landslides, severe cyclones, etc. But the more frequent deviations of observed sea-levels from the predicted tides occur due to the influence of oceanographic and meteorological factors. These factors are mostly dependent on one another and it is rather difficult to study their individual effects as several of them act together. The object of the present study is to (i) investigate the influence of various meteorological and oceanographic factors more favourable and responsible for the frequent deviations of observed sea-level from the predicted values at Cochin,

* Presented at the symposium on "Problems in Geophysics Relating to the Crust of the Earth", held by the Geophysics Research Board in January 1964 at Hyderabad.

** Redesignated as the Physical Oceanography Division of the National Institute of Oceanography, Cochin.

and (ii) understand the secular trends in the mean sea-level at certain stations along the west-coast of India. The various meteorological and oceanographic factors that are considered to be responsible for the short period deviations are (a) rainfall and runoff, (b) atmospheric pressure variations, (c) wind effect, (d) seasonal variations of density in a vertical column of water, and (e) the secondary phenomenon of standing oscillations that may occur during favourable conditions.

Data and Methods

The hourly readings of the actual and predicted tide levels at Cochin recorded for the period of 1st January 1958 to 31st December 1959 are collected from the tide-gauge records of Cochin Port. Data on pressure, winds, rainfall, etc. are taken from the *Indian Daily Weather Reports*. In the study of sea-level variations at Cochin, the meteorological data available at Minicoy Island weather station have been found to be extremely useful.

The ' meteorological effect ' is obtained either by subtracting predicted astronomical tide from the observed sea-level or by computing the average of the hourly heights of observed elevations for a period of twenty four hours. The former method has the drawback that the reliability of the value depends on adequate prediction of tides. Moreover the results include secondary phenomenon such as seiches or surges. This method may not be sound, especially in shallow waters, as the constituents of the tides may be altered. In the present study the latter method is preferred as it eliminates to a large extent the regular astronomical tides and also reduces the transient variations. The meteorological effect thus obtained is called the "non-tidal sea-level".

For the study of the secular variations along the west-coast the continuous mean sea-level data uncorrected for meteorological and eustatic variations available from the publications of IAPO (*Publication Scientifique* Nos. 19 and 20) for Cochin, Bombay (Apollo Bandar,, Bhaunagar and Kandla are utilized. Annual mean sea-levels are calculated from the daily high and low water readings. Although the data are available for Bhaunagar from 1937 to 1958, because for a change in datum from 1956, the latter three years' data are not considered.

Of the several methods now available for the computation of secular trends in geophysical time series, the method of periodogram analysis (KENDALL, 1951) is used for the stations Cochin, Bombay and Bhaunagar from where the data are available for fairly long periods (about 15 years or more). The authors are aware of the limitations involved in this type of study with data of 15 or 20 years. However, an attempt is made here to get some preliminary

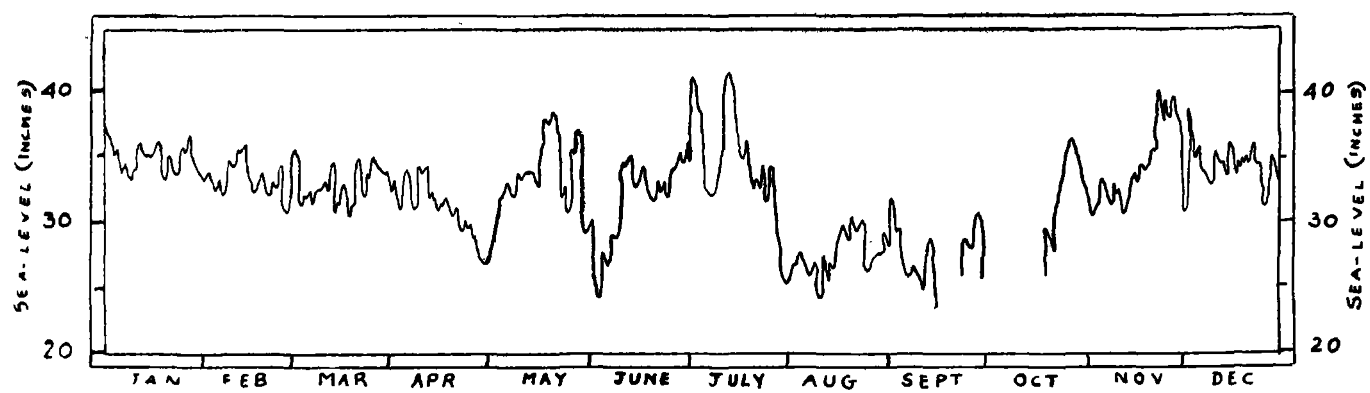

Fig. 1—Non-tidal sea-level at Cochin for each day of 1958

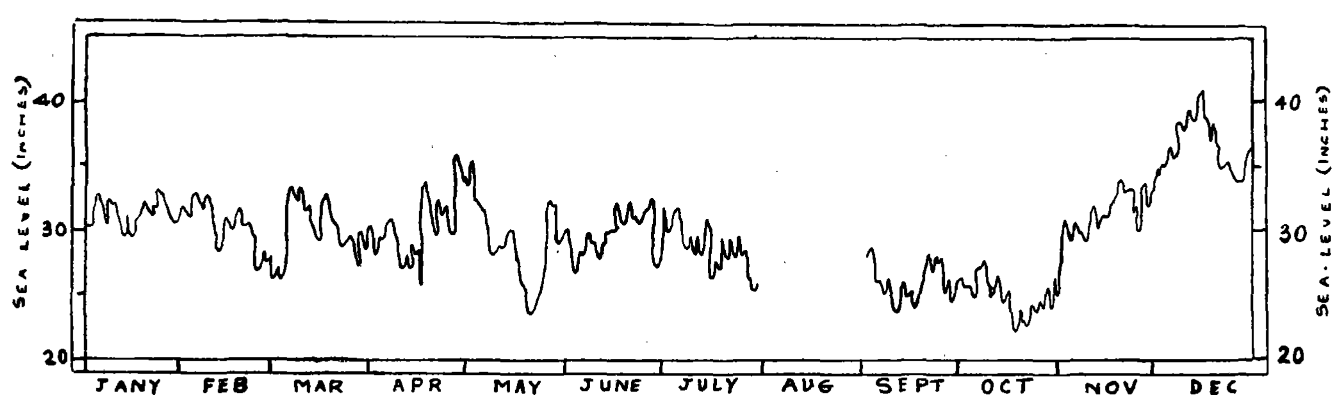

Fig. 2—Non-tidal sea-level at Cochin for each day of 1959

results about the periodicities. The intensities obtained by the periodogram analysis for various trial periods show high values when trial periods coincide with the actual periods present in the series.

Discussion of Results

Diurnal and Seasonal Variations of Sea-level at Cochin

The variations of non-tidal sea-level during 1958 and 1959 are shown in Figs. 1 and 2 respectively. During earlier months of both the years the mean sea-level remained almost steady with minor fluctuations, whereas wide variation in level exists during the period July to December. Further, it is seen that the maximum and minimum values of sea-level exist during the latter half of the year. The mean sea-level during 1958 is 29.9 inches and though there is a rise of 2.5 inches in mean sea-level during 1959, the annual range is 18 inches during both the years and thus the seasonal trend appears to be maintained.

Rainfall and Runoff

At Cochin, out of the average annual rainfall of 115 inches, about 80 inches of rainfall occur during the months of May, June, July and August. Though the direct influence of rainfall and runoff on sea-level is purely temporary there is a clear-cut relationship between the short period fluctuations in non-tidal sea-level and rainfall during south-west monsoon periods. Figs. 3 and

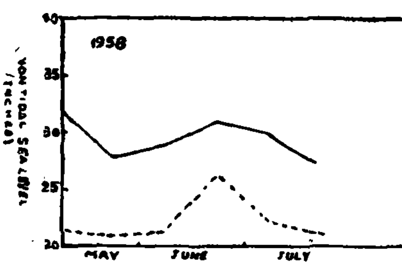

Fig. 3

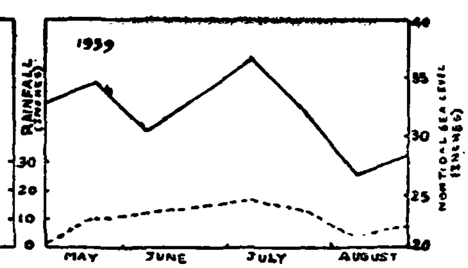

Fig. 4

4 show the variation of fifteen days' mean non-tidal sea-level and fifteen days' total rainfall during the above months. Further, correlation coefficients of 0.94 and 0.97 between these parameters during 1958 and 1959 suggest that apparently during the south-west monsoon period the non-tidal sea-level is closely associated with rainfall.

Barometric Effect

The atmospheric pressure changes in time over a wide area bring out changes in sea-level in accordance with the ratios of densities of air and water.

This sea-level change equals a column of water having the same weight per unit area as the change in atmospheric pressure. The theoretical value is very nearly 1 cm/mb. But the atmospheric pressure variations acting on small areas of water surfaces may not show corresponding changes in sea-level. The ' barometric effect ' is calculated for certain favourable periods of almost negligible winds with weak pressure gradients over the sea surface and when there is no rainfall, assuming for such periods that the sea-level change is primarily due to atmospheric pressure variations. While taking the mean pressure of the day, the pressure values at Cochin and Minicoy at the synoptic hours, namely 0830 hours and 1730 hours IST, have been chosen, and the average of these values is taken to represent the mean pressure of the day fairly well. As the times of synoptic observations are such that the effect of semi-diurnal pressure oscillations is practically eliminated, a fairly representative mean pressure for the day is obtained by taking the average of these values. During the two years there were twelve such occasions when the sea-levels at Cochin and appropriate variations with the atmospheric pressure changes were available. From these it is found that the ' barometric effect ' applicable for sea-level at Cochin is 1.065 cm/mb and is considered to be fairly in agreement with the theoretical value.

Winds and Set-up

According to Ekman's theory of wind currents, winds blowing over the sea-surface drag the surface waters at an angle of 45° to the right of the direction of wind. This was proved by Krummel and the important assumption made in the theory is that the depth of water is great compared to the ' depth of frictional resistance ' (SVEKDRUP *et al*, 1942). But in shallow waters the deflection of surface drift from the wind will be less than 45° and depends on the shallowness of the region. The piling up of water against the coast and consequently the rise of sea-level can be expected to be maximum when the surface drift is normal to and towards the coast and the sea-level expected to be minimum when the drift is normal to and away from the coast (MILLER, 1957). However, the wind currents depend on the steadiness and fetch of the wind and the wind effect on sea-level called "set-up" will be appreciable in central regions of long coast lines.

In order to find out the effect of wind on 'non-tidal sea-level' at Cochin, the surface wind observations of Minicoy Island Station for the complete year 1959 are taken as representative values over the surface, off Cochin. Figs. 5, 6, and 7 show the harmonic analysis of 'non-tidal sea-level' variations with direction of wind at velocity ranges of 0.5 to 3.9, 4.0 to 6.9 and 7.0 to 9.5 knots respectively. The weak winds upto 3.9 knots do not appear to have any appreci-

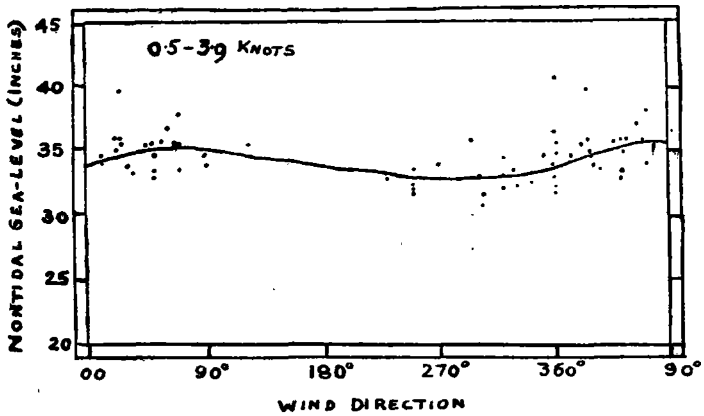

Fig. 5

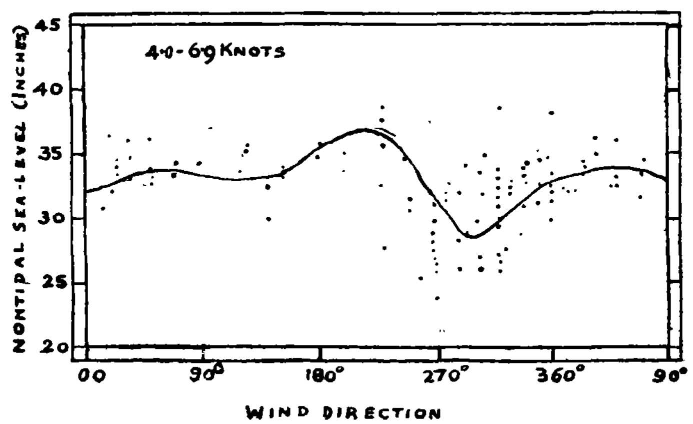

Fig. 6

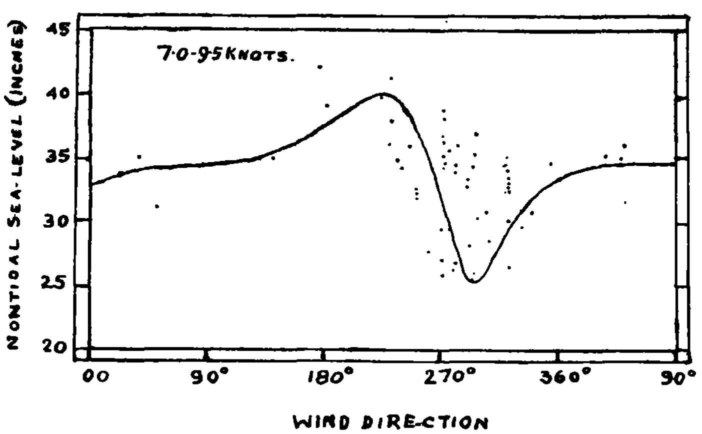

Fig. 7

able effect on sea-level and from Figs. 6 and 7 it can clearly be seen amplitudes increasing with increasing wind speeds. It is also clear that the wind blowing with direction between 210° and 260° are mostly favourable for rise of sea-level at Cochin.

In Fig. 8, the schematic diagram shows the results of favourable conditions for maximum "set-up". The deviation of 21° between the surface wind direction and the surface drift directed towards the coast may represent a

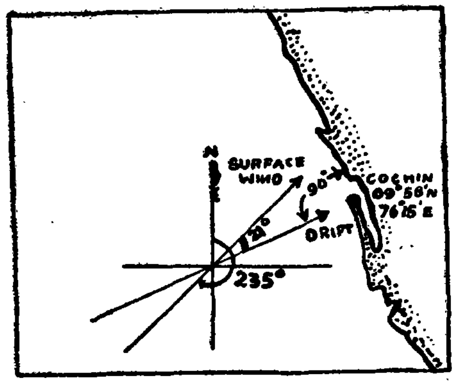

Fig. 8

characteristic feature of the shallowness of the region off Cochin at wind velocities 7.0 to 9.5 knots. However, it is to be noted that in this study only the steady winds to the extent possible are considered.

Secular Variations of Mean Sea-Level

The secular variations of mean sea-level per year and the standard deviations for the four stations Cochin, Bombay (Apollo Bandar), Bhaunagar and Kandla are calculated by the standard least squares method for the purpose of comparison and accuracy and given in the following table (*IAPO Publication Scientifique* No. 13, 1954).

TABLE

Station	Position		Period	Total No. of years	Secular Variation	Standard deviation
	Latitude	Longitude			(0.01 cms/year)	
COCHIN	09°58′N	76°15′E	1939–'58	20	43	± 15
BOMBAY (Apollo Bandar)	18°55′N	72°50′E	1937–'58	22	3	± 6
BHAUNAGAR	21°48′N	72°09′E	1937–'55	19	177	± 53
KANDLA	23°01′N	70°13′E	1950–'58	9	61	± 39

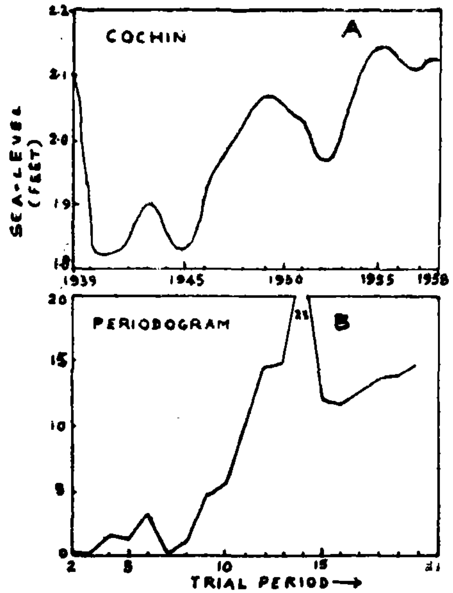

Fig. 9

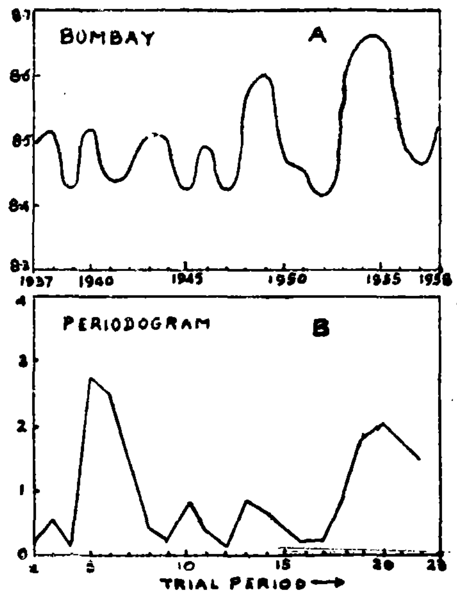

Fig. 10

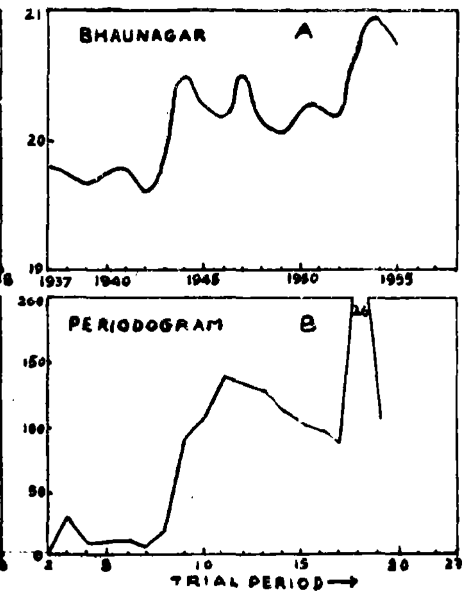

Fig. 11

The yearly mean sea-level variations and periodograms are shown in Figs. 9A and 9B for Cochin, 10A and 10B for Bombay and 11A and 11B for Bhaunagar respectively. The mean sea-level variation for Kandla is shown in Fig. 12. At all the stations, the general trend of secular variation shows an

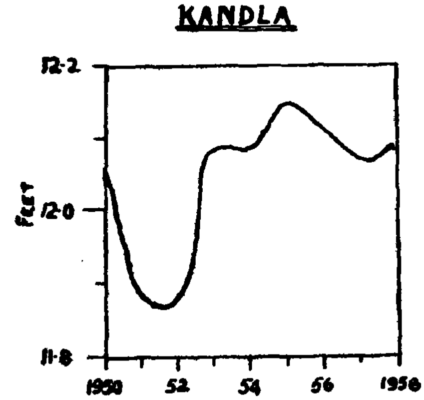

Fig. 12

increase in mean sea-level, the highest value of 177 units (1 unit=0.01 cm) occurring at Bhaunagar in the years considered There does not appear to be any gradual variation in the secular trend as we observe the values from Cochin in the south to Kandla in the north.

The most probable periods as seen from the figure are :

Cochin	—	6 and 14 years
Bombay (Apollo Bandar)	—	5 and 20 years
Bhaunagar	—	3,11 and 18 years

The variation of mean sea-level at any station is either due to the variation in height of the fixed point to which the tidal observations are referred, or due to the changes in the depths of the ocean bottom, or due to eustatic variations by the supply of water by melting ice in the polar region and the precipitation minus evaporation over the sea, and to the material brought to sea by rivers and similar transports to and from sea or due to meteorological and oceanographic factors or a combination of all these factors. Thus the secular variation is a complex phenomenon. However, the subsidence of land is considered to have large effect on secular sea-level variations. Therefore, an attempt is made to find out the relation between the sea-levels and the precise land survey levels available for the Willingdon Island where the Cochin tide-gauge is situated. The correlation coefficient between the mean sea-level and the levelled heights is found to be -0.82 for six values. This clearly indicates that the land subsidence can be an effective agent responsible for the observed secular sea-level variations.

Bhaunagar and Bombay indicated the presence of a periodic variation of 18 and 20 years respectively. The longitude of the Moon's ascending node varies with the 18.6 years period and this is considered to be the origin of 18 and 20 years cycles observed (MIYAZAKI, 1953).

Acknowledgements

The authors wish to express their sincere thanks to Shri M. S. Venkataraman, Administrative Officer, Port of Cochin, for the valuable information made available to them. Their thanks are also due to Shri L. N. Kailasam for his keen interest on the investigations and to Dr. V.V.R Varadachari, Officer-in-charge, Oceanographic Research Wing, for his critical suggestions. They are also thankful to Shri K. V. Sundara Ramam for his help during the work. The research facilities made available by the Directors of the National Geophysical Research Institute, Hyderabad and the Indian Ocean Expedition, New Delhi, are gratefully acknowledged.

References

ASSOCIATION INTERNATIONALE D' OCEANOGRAPHIC PHYSIQUE—Secular Variations of Sea level, *Publication Scientifique* No. 13, 1954

__________ Monthly and Annual Mean Heights of Sea-level, *Publication Scientifique*, No 19, 1958.

__________ Monthly and Annual Mean Heights of Sea-level for the Period of IGY, *Publication Scientifique* No 20, 1959.

KENDALL, M.G. –*The Advance Theory of Statistics*, Charles Griffin & Co, London, 1951

MILLER, ARTHUR R · The Effect of Steady Winds on Sea-level at Atlantic City—Contribution No. 829, *Collected Reprints W.H O.I* 1957.

MIYAZAKI, MASAMORI –Secular Variation of Annual Mean Sea-level along the Japanese Coasts, *Proceedings of the 8th Pacific Science Congress of the Pacific Science Association*, Vol. III—Oceanography, 1953

SVERDRUP, H U., JOHNSON, M. W. and FLEMING—*The Oceans, their Physics, Chemistry and General Biology*, Prentice-Hall, 1942.

Reprinted from *Arch. für Meteorol. Geophys. und Bioklimat.*, Serie B, Band 15, Heft 1-2, 1967, p. 81-98

551.521 : 551.581 (267)

(Meteorological Office, Poona, India)

Distribution of Global and Net Radiation over the Indian Ocean and Its Environments[1]

By

Anna Mani, O. Chacko, V. Krishnamurthy, and V. Desikan

With 10 Figures

(Received July 14, 1966)

Summary. Maps showing the distribution of global solar, net terrestrial and net radiation over the Indian Ocean area have been prepared from available observations, supplemented by calculations based on other meteorological measurements. Annual and monthly maps for four representative months January, April, July and October for global solar and net radiation are presented.

Global solar radiation shows minima over the equatorial and monsoon regions, and maxima over land in the high pressure belts of the northern and southern hemispheres along the tropics of Cancer and Capricorn, the highest values of the order of 220 kcal/cm²/year occuring over North Africa and Arabia. While there is very little latitudinal variation over the ocean during the southern summer, the variations are marked during the northern summer. The geographical distribution is mainly zonal except in the low latitudes, where areas of higher or lower radiation are distributed according to regions of higher or lower amounts of cloudiness.

Net radiation over the ocean is always positive and greater than that on land. The distribution is mainly zonal, maxima occuring over the sea in the tropics, with the highest values in the North Arabian Sea and the ocean areas to the northwest of Australia. Minima occur over land in the arid regions of both hemispheres and in the monsoon areas where global solar radiation itself is low. There is very little variation over the ocean during the southern summer but variations are large during the northern summer.

Zusammenfassung. Auf Grund des verfügbaren Beobachtungsmaterials, das durch Berechnungen an Hand weiterer meteorologischer Messungen ergänzt wurde, wurden Karten über die Verteilung der Globalstrahlung, der effektiven langwelligen Ausstrahlung und der totalen Strahlungsbilanz für das Gebiet des Indischen

[1] Published by permission of the Director General of Observatories, New Delhi, India.

Ozeans und seiner Umgebung entworfen. Im nachfolgenden sind die Jahres- und die Monatskarten für die vier charakteristischen Monate Januar, April, Juli und Oktober für die Globalstrahlung und die totale Strahlungsbilanz wiedergegeben.

Die *Globalstrahlung* zeigt Minima in den Äquatorial- und den Monsungegenden, Maxima über Land in den Hochdruckgürteln der Nord- und der Südhalbkugel in der Gegend der Wendekreise, wobei die höchsten Werte von etwa 220 kcal/cm² und Jahr über Nordafrika und Arabien auftreten. Während im Südsommer die Breitenvariation über dem Ozean nur sehr klein ist, ist sie im Nordsommer stärker betont. Die geographische Verbreitung ist in der Hauptsache zonal gegliedert, mit Ausnahme der niederen Breiten, wo die Gebiete höherer oder niedererer Globalstrahlungssummen entsprechend den Unterschieden der Bewölkungsverhältnisse verteilt sind.

Die *totale Strahlungsbilanz* ist über dem Ozean durchwegs positiv und größer als über Land. Die Verteilung ist in der Hauptsache zonal, wobei die Maxima über dem Meer in den Tropen auftreten mit Höchstwerten in der Nordarabischen See und in den Meeresgebieten nordwestlich von Australien. Minima liegen über Land in den Trockenregionen beider Hemisphären sowie in den Monsungebieten, wo die Globalstrahlung vermindert ist. Über dem Ozean sind die Unterschiede der Strahlungsbilanz während des Südsommers nur gering, während des Nordsommers dagegen größer.

Résumé. Au vu des observations disponibles complétées de valeurs calculées en partant d'autres données météorologiques, on a établi des cartes de la répartition du rayonnement global, du rayonnement effectif émis à grandes longueurs d'ondes et du bilan radiatif total, et cela pour la région de l'Océan Indien et ses environs. On donne maintenant des cartes du rayonnement global et du bilan radiatif total pour l'année entière et pour quatre mois caractéristiques, à savoir janvier, avril, juillet et octobre.

Le *rayonnement global* présente des minimums dans les régions équatoriales et de moussons. Les maximums en sont concentrés sur terre dans les zones à hautes pressions des hémisphères nord et sud situées dans le voisinage des tropiques du Cancer et du Capricorne. Les plus hautes valeurs, de l'ordre de 220 kcal/cm² par année, se trouvent sur l'Afrique du Nord et sur l'Arabie. Alors que les variations dues à la latitude sont très faibles sur l'océan durant l'été austral, elles sont plus prononcées durant l'été boréal. La répartition géographique est en général zonale à l'exception des basses latitudes où les régions à plus faibles ou plus fortes quantités de rayonnement global sont réparties selon les différences de la nébulosité.

Le *bilan radiatif total* est toujours positif sur les océans et plus grand que sur terre. La répartition en est avant tout zonale Les maximums se trouvent sur la mer sous les regions tropicales et les plus hautes valeurs s'enregistrent dans le nord de la Mer d'Oman ainsi que sur la mer au nord-ouest de l'Australie. Les minimums se recontrent sur les terres dans les régions arides des deux hemisphères ainsi que dans les régions à mousson où le rayonnement global est réduit. Au-dessus des océans, les différences du bilan radiatif sont faibles durant l'été austral, plus importantes durant l'été boréal.

1. Introduction

Studies of net radiation on the earth's surface and in the atmosphere, are of vital importance in an understanding of the general balance of the energy on the earth and the processes of heat and moisture exchange between the earth's surface and the atmosphere. Information on net radiation has been very scanty in the past, but recent studies during the IGY and after, particularly in the USSR, have resulted in increasing knowledge of the magnitude and geographical distribution of the components of radiation and heat balance over the earth.

Direct measurements of net radiation over the oceans are understandably meagre. A number of indirect studies of the radiation balance of the oceans have been made by MOSBY [9], JACOBS [7], SVERDRUP [13] and SAUBERER and DIRMHIRN [11], who compiled radiation balance data and maps for the latitudinal zones, mainly of the Atlantic and Pacific oceans. ALBRECHT [1] computed the components of heat balance for the Indian Ocean and constructed a series of maps showing the distribution of the components of radiation balance for four single months and for the year. ROBINSON [10] has tabulated the annual and seasonal zonal means of net radiation at the surface of the earth from the IGY/IGC radiation data. BUDYKO's [6] World Atlas of radiation climate is the most comprehensive of recent studies of the heat balance of the earth's surface and contains maps of global and net radiation for the whole earth based partly on direct observations and partly on estimates.

One of the meteorological objectives of the International Indian Ocean Expedition 1962—65 (IIOE) was to obtain an increased understanding of the energy exchange between the sea and the atmosphere and of energy transport and transformation in the atmosphere over the oceans. For this, it was necessary to have extended measurements of the energy input viz., separate measurements or critical estimates of the upward and downward fluxes of shortwave and longwave radiation over the whole Indian Ocean, both at the earth's surface and in the atmosphere. All nations taking part in the IIOE had programmes large or small, for the measurement of one or more of the components of the net radiation. India had 13 radiation stations for surface radiation measurements and one for measurement of the infra-red radiative fluxes in the atmosphere with radiometersondes. The University of Michigan programme of radiation observations in the Indian Ocean was the largest, with a network of 13 coastal and island stations in the Indian Ocean to measure global solar and total radiation at the surface and a number of oceanographic ships. Despite the co-ordinated effort of many nations which took part in the IIOE, the data actually obtained are too meagre for any reliable climatological studies.

This should have been anticipated from the sheer magnitude of the problem itself and the difficulty of making reliable, accurate, large-scale observations over the oceans. Even on land, these measurements are difficult. Tested and proved instruments for continuous measurement of solar and terrestrial net radiation at the earth's surface and in the free atmosphere are still not commercially available. Fairly precise instruments for the continuous measurements of global solar radiation are available and are in regular use at over 100 stations in the Indian Ocean area. But these again are very unevenly distributed and mainly located on the surrounding continents. Net terrestrial radiation measurements at the surface are made at only 16 stations, net radiation measurements at only 6 and infra-red radiation measurements in the atmosphere at only one station in the region.

Although it soon became clear that the various components of the radiative budget of the ocean and the atmosphere could not be extracted from the IIOE measurements, it was felt that an attempt to derive the spatial distribution of the components of radiation balance from available observations, supplemented by empirical calculations, based on other meteorological measurements, would still be worthwhile. In the present study a critical evaluation of the available radiation data over the Indian Ocean has been made and where such data are not available, estimates have been made from meteorological data using empirical relationships. Annual and monthly charts showing the geographical distribution of global solar radiation and net radiation over the Indian Ocean have been prepared and are presented.

2. Availability of Data

2.1. Global Radiation

Since global solar radiation observations were available for only 107 land stations, and none over the oceans, it was necessary to resort to empirical calculations to obtain estimates of global radiation for the remaining areas. For stations for which duration of sunshine data were available, global radiation T was calculated from values of sunshine S using Ångström's well known formula:

$$T = T_0\,[K_1 + (1 - K_1)\,S], \tag{1}$$

in which T_0 is the total radiation with a clear sky, S is the ratio of observed sunshine hours to the possible amount for the given period, and K_1 is a constant, determining what portion of the possible radiation consists of actual radiation with overcast sky conditions. Values of the coefficient K_1 are taken as 0.35.

For the remaining 200 locations, global radiation was computed from cloudiness data using the Angström-Savinov formula (Budyko, 1956)

$$T = T_0 [1 - (1 - k_2) n], \tag{2}$$

in which n is the mean cloud amount in tenths and k_2 a coefficient indicating the effect of clouds on the radiation. The coefficient k_2 representing the ratio between the actual radiation under overcast conditions and the possible radiation, depends on the mean altitude of the sun, the characteristics of the clouds and the value of albedo. Thus the mean value of k_2 varies from region to region and also shows annual and diurnal variations. Values of k_2 are taken from tables prepared by Berliand and given in Budyko's book on the heat balance of the earth's surface. These methods have limitations since they do not include changes in the transparency of the atmosphere and of the heights and types of clouds.

The observed values of global radiation, other than those for Indian and Michigan University radiation stations for the IIOE period, were taken from the IGY/IGC Radiation Data published by WMO [16] and the Actinometric Reference Book by Berliand [3]. Data of sunshine and cloudiness for the Indian Ocean area were taken from IGY data published by WMO and monthly charts for the Indian Ocean published in German [15] and USA [14] Marine Climatic Atlases. Observations made in the Indian Ocean area during the 28 scientific cruises of the Indian oceanographic ship INS Kistna during 1962—1965 have also been used, wherever available.

2.2. Net Radiation

Net radiation Q is expressed by

$$Q = (R_s\downarrow - R_s\uparrow) + (R_L\downarrow - R_L\uparrow),$$

where the first two terms give the net solar radiation Q_1 and the second two, the net terrestrial radiation Q_2. $R_s\downarrow$ is the downward shortwave flux or global solar radiation T. $R_s\uparrow$ is the reflected solar radiation given by Ta where a is the albedo. $R_L\uparrow$ is the longwave radiation emitted by the earth's surface and $R_L\downarrow$ the longwave counter radiation from the atmosphere.

Direct observations of net radiation Q being made at only 3 stations in the Indian Ocean area, large-scale estimates based on empirical calculations had to be resorted to, for obtaining values of the net solar, net terrestrial and net radiation.

2.2.1. *Net Solar Radiation* Q_1

Observations of albedo were available at only 7 stations in the area. Monthly values of albedo were therefore calculated for land surfaces from mean values given by BUDYKO [5] for various underlying surfaces, varying from 0.30 for desert areas to 0.10 for moist grey soil. The albedo of water surfaces is very low, compared to that of natural land surfaces. It depends on the altitude of the sun and varies from a few per cent at noon to 100 per cent with the sun near the horizon, for direct solar radiation. For diffuse radiation the albedo is fairly constant and about 8—10 per cent. The albedo for total radiation thus shows definite diurnal and annual variations. Albedo for 41 locations in the Indian Ocean area was calculated using Savinov's formula (BUDYKO [5]) for direct radiation. Assuming 0.10 for diffuse radiation, albedo for total radiation for water surfaces for all these locations was computed. Using observed and computed values of T and α, values of net solar radiation $Q_1 = T(1-\alpha)$ for 163 locations, 122 on land and 41 on sea, were calculated.

2.2.2. *Net Terrestrial Radiation*

The outgoing longwave radiation $R_L\uparrow$ from the underlying surface follows Stefan's law and is equal to $s\sigma\Theta_w^4$ where σ is the Stefan-Boltzmann constant. Θ_w is the temperature of the surface and s is a coefficient, characterising the departure of the radiation from that of a blackbody and varies from 0.85—1.00 for natural surfaces. Much of the outgoing longwave radiation is re-radiated by the atmosphere, depending on its water content, air temperature and cloud type and amount. The net terrestrial radiation is given by the two formulae:

$$Q_2' = s\sigma\Theta^4(0.39 - 0.058\sqrt{e}), \tag{3}$$

$$Q_2 = I_0(1 - c\,n^2) + 4\,s\sigma\Theta^3(\Theta_w - \Theta), \tag{4}$$

where Q_2 is the effective outgoing or net terrestrial radiation,
Q_2' the net terrestrial radiation with clear skies,
e the vapour pressure in mm of mercury,
n the cloud amount in tenths,
Θ the air temperature in degrees C,
Θ_w the temperature of the surface in degrees C. and
c a numerical coefficient.

The first formula gives the value of the net terrestrial radiation under a cloudless sky and the second allows for the amount of clouds and the difference in temperatures between the soil surface and the air. Since regular net terrestrial radiation values are available for only 10 stations in India and 6 elsewhere in the Indian Ocean area, net terrestrial radition Q_2 was calculated from values of water vapour content, air and soil temperatures and cloud amounts using the above formulae for 134 locations, evenly distributed over the Indian Ocean and the adjoining continents.

3. Distribution of Global Radiation *T*

Global solar radiation is the principal component of the radiation balance, determining as it does the amount of solar energy received by a unit area of the earth's surface and used later by various natural processes originating near the surface. Maps showing the monthly and annual distribution of global radiation from 10^0 E to 160^0 E and

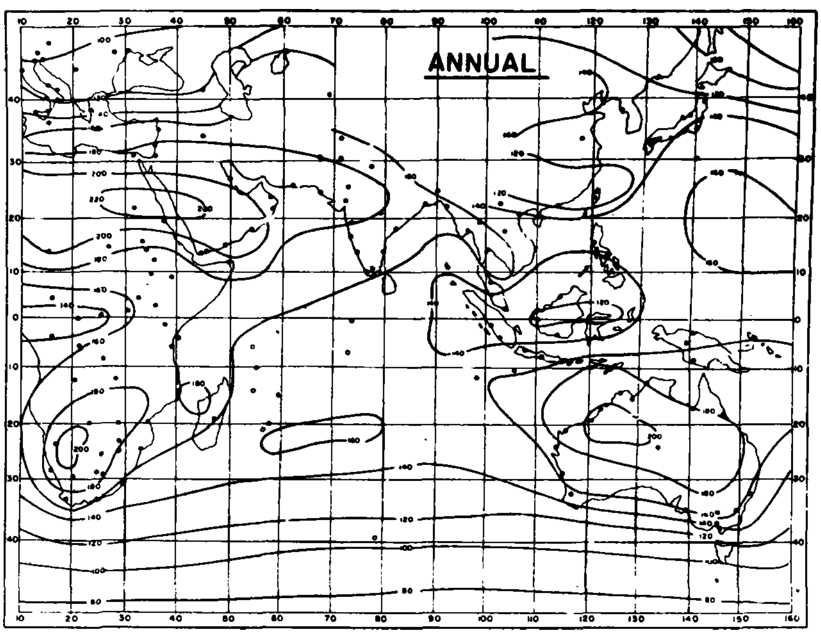

Fig. 1. Global solar radiation in kcal/cm²/year

50^0 N to 50^0 S have been prepared from observed data at 107 stations and computed data from 203 locations on land and sea. Only the maps showing the annual distribution and those for 4 representative months January, April, July and October, are presented in Figures 1, 2, 3, 4 and 5.

Fig. 1 shows the annual values of global solar radiation in kilocalories/cm²/year. Isolines are drawn every 20 kcal/cm²/year. The total shortwave radiation flux varies from 100—220 kcal/cm²/year over the Indian Ocean and its adjacent areas. High values of T

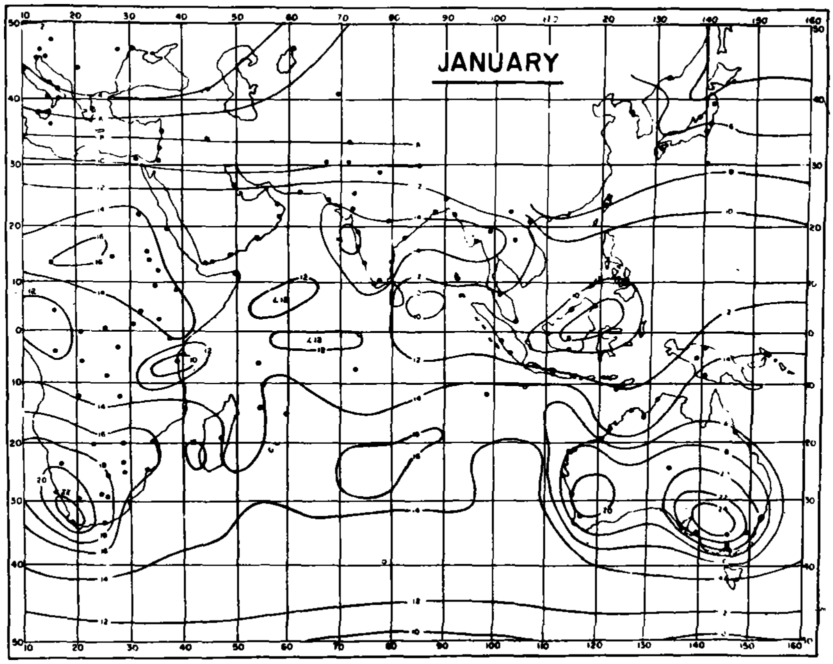

Fig. 2. Global solar radiation in kcal/cm²/month: January

are found over the high pressure belts of the northern and southern hemispheres, especially over the deserts of West Asia, Africa and Australia, where yearly totals exceeding 200 kcal/cm² are received. The highest values reached are 220 kcal/cm² over North East Africa and Arabia. The particular distribution of the land masses in the two hemispheres is clearly responsible for the greater radiation input in the northern sub-tropics compared to that in the southern sub-tropics.

The lowest amounts of global solar radiation are received over the equatorial belts and the monsoon regions of Asia. The equatorial zone in general receives less than 140 kcal/cm² annually and in South-East Asia, it is as low as 120 kcal/cm².

The distribution of global radiation shows on the whole a zonal pattern, except in the low latitudes. In the southern hemisphere, it increases with decreasing latitude till maxima are reached about 20—30° S with markedly higher values over land, decreases near the equator, increasing again with latitude northwards, reaching a maximum about 25° N, except over south and South-East Asia, and decreases again with latitude. Cloud amount is the main control of global radiation, although it is affected to a lesser extent by atmospheric aerosols (haze and dust) and by atmospheric absorption, the main variable absorber being water vapour. The decrease in the equatorial and monsoon regions is thus caused by the greater cloudiness in these areas.

Fig. 2, 3, 4 and 5 show the distribution of global solar radiation during roughly the winter and summer solstices and during the two

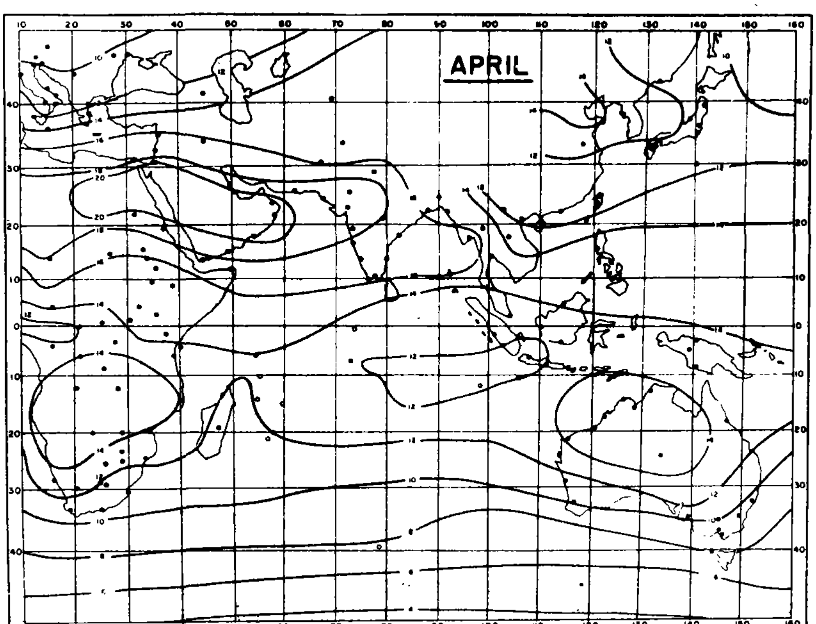

Fig. 3. Global solar radiation in kcal/cm² month: April

equinoxes. In January or the southern summer, global radiation increases southward mainly zonally, with the maximum values of the order of 22 kcal/cm² occuring in the southern hemisphere around 30° S, over the desert regions of South Africa and Australia, with a secondary maximum about 20° N. The pattern is broken up in regions of cloudiness, minima occuring around the equator; the lower values coincide with the low pressure areas on either side of the equator, where the clouding is maximum. Over the Indian Ocean itself, global radiation shows very little zonal change and does not decrease with

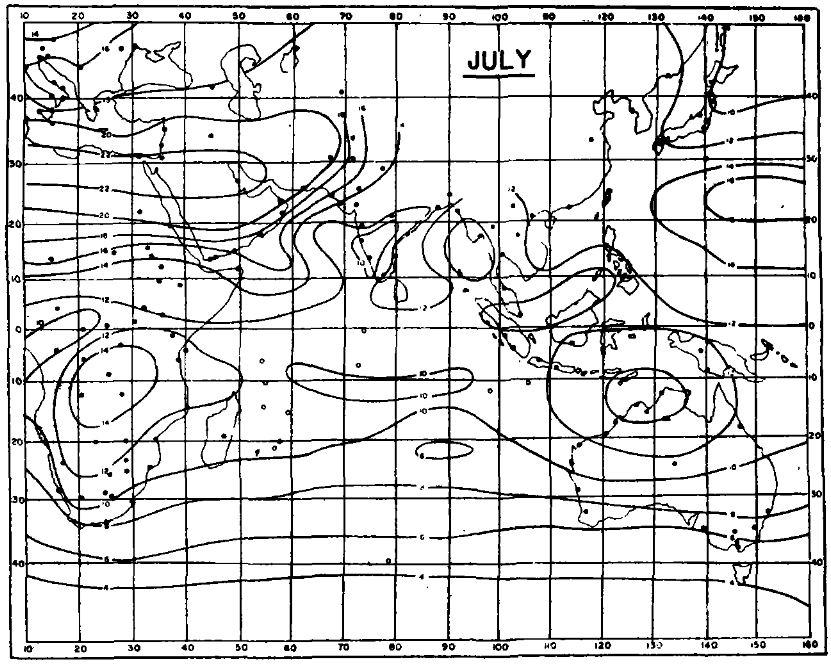

Fig. 4. Global solar radiation in kcal/cm²/month: July

increasing latitude, because of the compensating effect of the increasing length of the day in the southern latitudes.

The pattern changes gradually as the sun moves north, till in April—May, the pattern is reversed with high values along 25° N. Secondary maxima are again present along 20° S and minima as usual in the equatorial belts. In June—July the pattern abruptly changes with the establishment of the monsoon and corresponding marked minima in radiation occur in the monsoon areas along the west coast of India and South-East Asia. The highest values of 22 kcal/cm²/month occur over the deserts of North Africa and Asia. Over the oceans, the distribution of global solar radiation in July is quite different from that in January, with values decreasing rapidly with increasing latitudes in the southern hemispheres.

The distribution of global radiation in April and October resemble qualitatively the annual pattern and other months have intermediate patterns of distribution between those described earlier. Basically, maxima in global solar radiation occur in the regions of the tropical deserts and minima over the equatorial and monsoon regions.

Earlier world maps of global solar radition by BLACK [4], ASHBEL [2], LANDSBERG [8] and SCHULZE [12], showed very little or

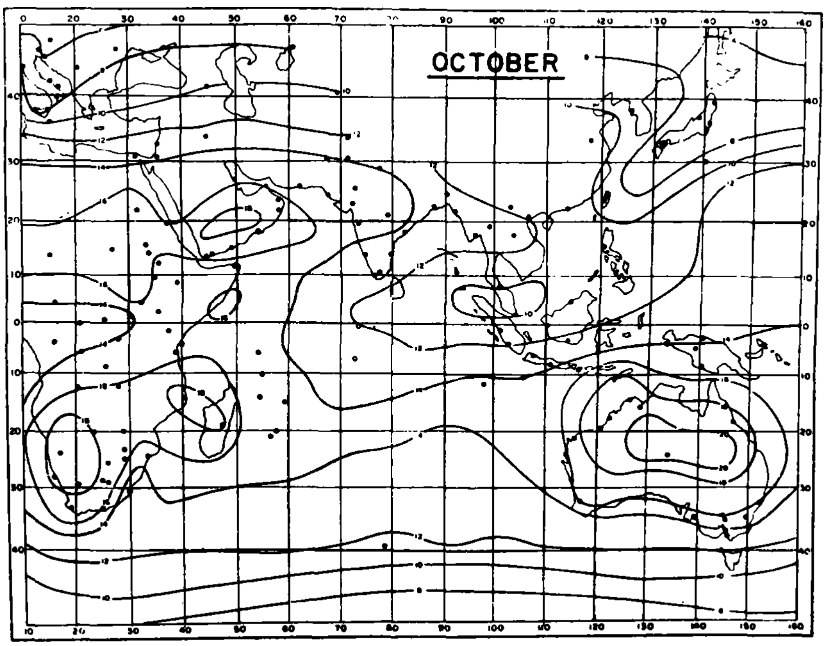

Fig. 5. Global solar radiation in kcal/cm²/month: October

practically no detail over the Indian Ocean area. The maps presented in Fig. 1 to 5 are, however, not very different from those given by BUDYKO in his Atlas of Heat Balance [6], though more detailed.

4. Distribution of Net Radiation

The annual distribution of net radiation Q is shown in Fig. 6. It is less complex than that of global radiation, the latitudinal variation of Q being much less than that of T. The distribution over the sea is mainly zonal, except in regions affected by warm or cold sea currents. These deviations may have different signs for the same type of ocean currents, because of the complexity of relations between the values of heat balance components, the air and water temperatures, humidity of the air and cloudiness.

The distortion of the zonal pattern over land is mainly due to the effect of differential moistening. There are well marked regions

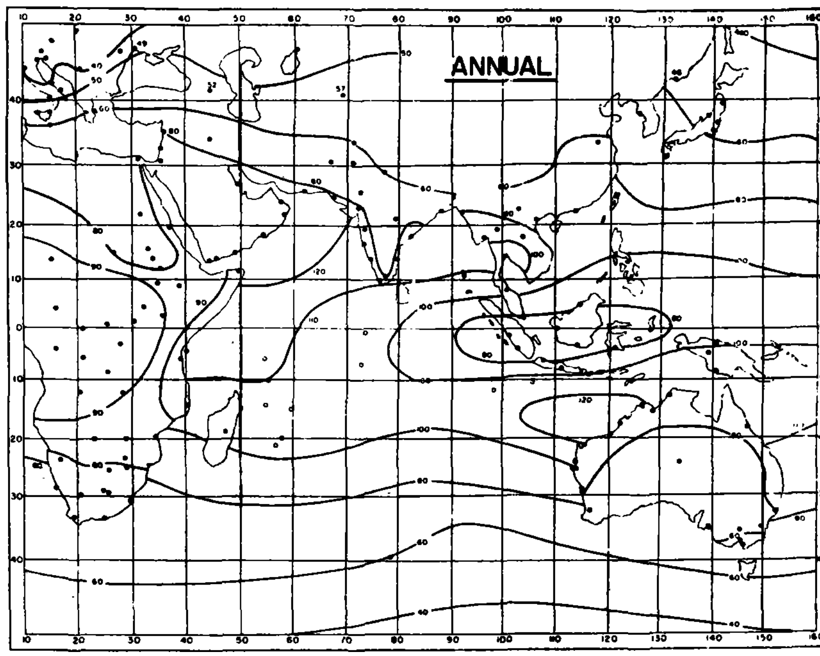

Fig. 6. Amount of net radiation in kcal/cm²/year

of low net radiation associated with arid climates. This is particularly pronounced in the deserts of Central Asia, Africa and Australia where net radiation is very low. In the monsoon areas, the annual amounts of net radiation are also somewhat lower, because of the reduced global solar radiation resulting from greater cloudiness, during the warm seasons.

Unlike the distribution of global solar radiation pattern, the net radiation values over the sea are always higher than those over land, because of the lower albedo of ocean surfaces. And the maximum values, about 120 kcal/cm²/year occur about 20° S and 20° N over the ocean, in the north Arabian sea and the ocean areas to the north-west of Australia. Due to the large net terrestrial radiation over land in these sub-tropical areas, the net radiation over land remains low, despite the large values of global radiation. The net terrestrial radiation over sea being low, net radiation remains high.

During winter (Fig. 7) with low solar altitudes over the northern hemisphere and high over the southern hemisphere. the net radiation is low over the northern hemispere and negative above 40° N. It increases with latitude till it reaches 8 kcal/cm² over the equator. Southwards from the equator the net radiation on the oceans changes very little, and the greatest values are mainly recorded in the regions of the Tropic of Capricorn (10—12 kcal/cm²). Still further south, it

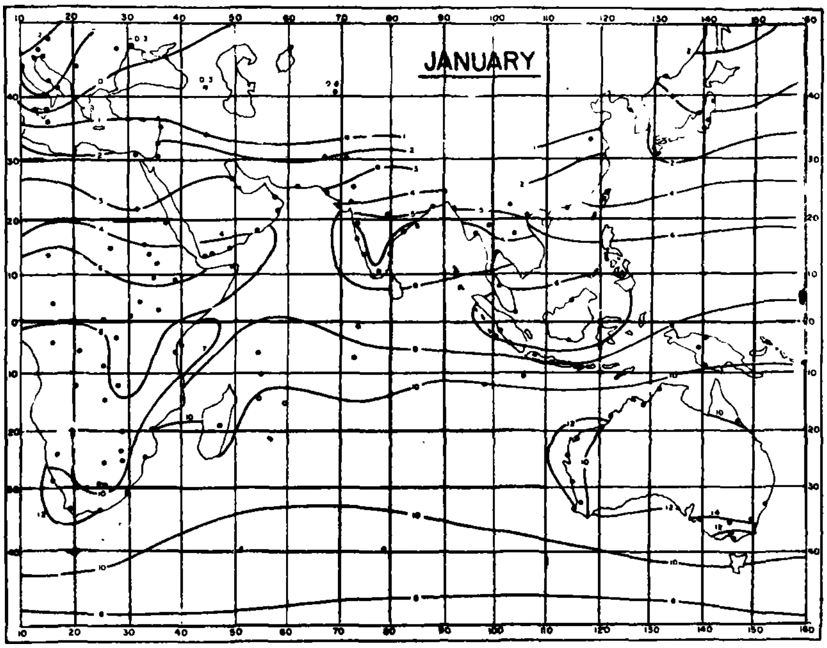

Fig. 7. Amount of net radiation in kcal/cm²/month: January

decreases slightly. Over land, in the northern hemisphere it increases steadily southwards and in the southern hemisphere, it changes very little, lying between 6—9 kcal/cm²/month. .

During summer (Fig. 8) the features in the north and south hemispheres are reversed. The zero line lies about 45° S. North of this line, the net radiation increases, till it reaches the greatest amount over the ocean in the region of the Tropic of Cancer with peak values of 12 kcal/cm² over the north Arabian sea. On land in the southern hemisphere it increases in a northerly direction up to the equator. Northward it changes only slightly over the vast expanses of land. Over almost the whole of North Africa and Asia it fluctuates only between 6—8 kcal/cm^2. The net radiation in the Arabian sea and the Bay of Bengal are basically different, both for the year

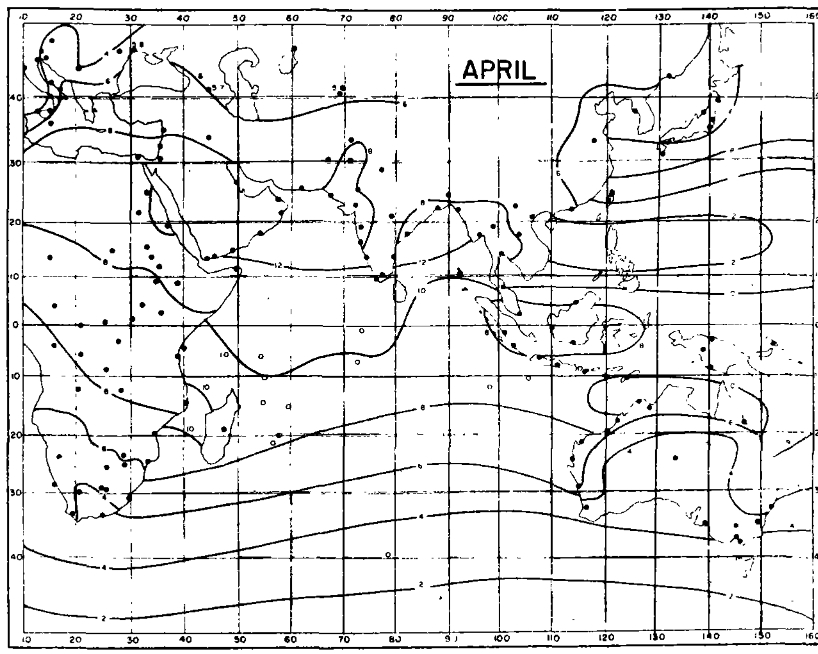

Fig. 8. Amount of net radiation in kcal/cm^2/month: April

and from month to month. It is also evident that large amounts of radiation energy are available in the Arabian sea for the genesis of the Indian monsoon and its movement.

5. Distribution of Net Terrestrial Radiation

A study of the spatial variations of net terrestrial radiation over the Indian ocean area showed that they are also generally smaller than those of global solar radiation. The reason lies in the fact that in the majority of the climatic zones, changes of temperature and absolute humidity are associated with each other: with increase in temperature, absolute humidity also increases. Since an increase in temperature and absolute humidity affect the net terrestrial radiation in opposite ways, the changes are comparatively small.

The greatest amounts of net terrestrial radiation are observed in the tropical desert, where they reach values of 80 kcal/cm^2/year. This is mainly the result of the high temperature of the underlying surface compared with that of the air above. Near the equator, the net terrestrial radiation is only about 30 kcal/cm^2/year and differs little between land and sea.

6. Errors in Observations and Computation

The possible error of measurement of global solar radiation using thermoelectric pyranometers is of the order of 5—10 per cent and for net radiation using net pyrradiometers is about 15 per cent, if the instruments used are basically accurate and are well maintained and

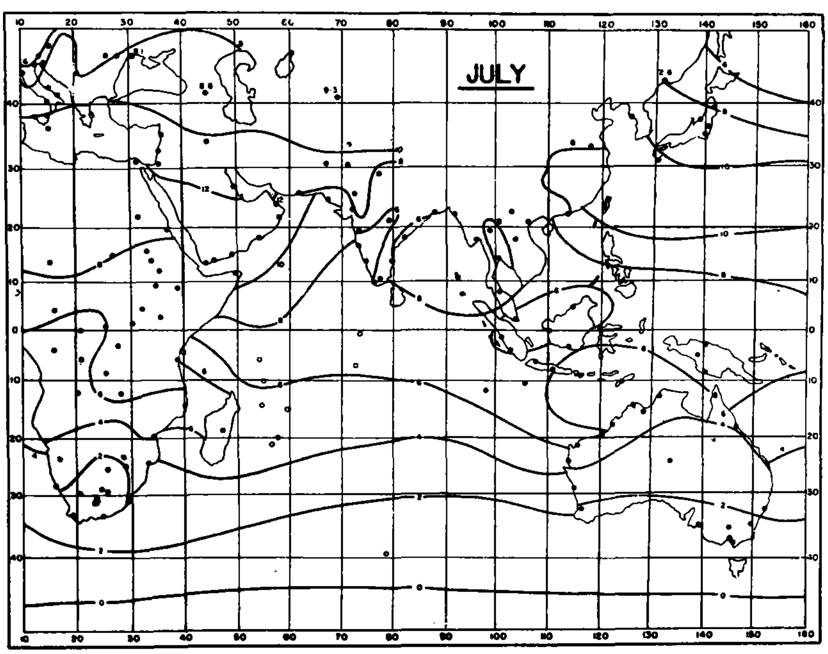

Fig. 9. Amount of net radiation in kcal/cm^2/month: July

standardized regularly against acknowledged standards. This is, however, not the case with most of the radiation records over the region. Large variations are noticed in T from country to country and errors of the order of 20 per cent or more exist. The intercomparisons of pyranometers and net pyrradiometers used in various countries and the reduction of the data to a common level will facilitate the preparation of more accurate radiation maps of the region.

In the computations, errors in T will average 10 per cent while that of Q can vary by 20 per cent or more depending on the nature of the underlying surface. According to ROBINSON [10] estimates of

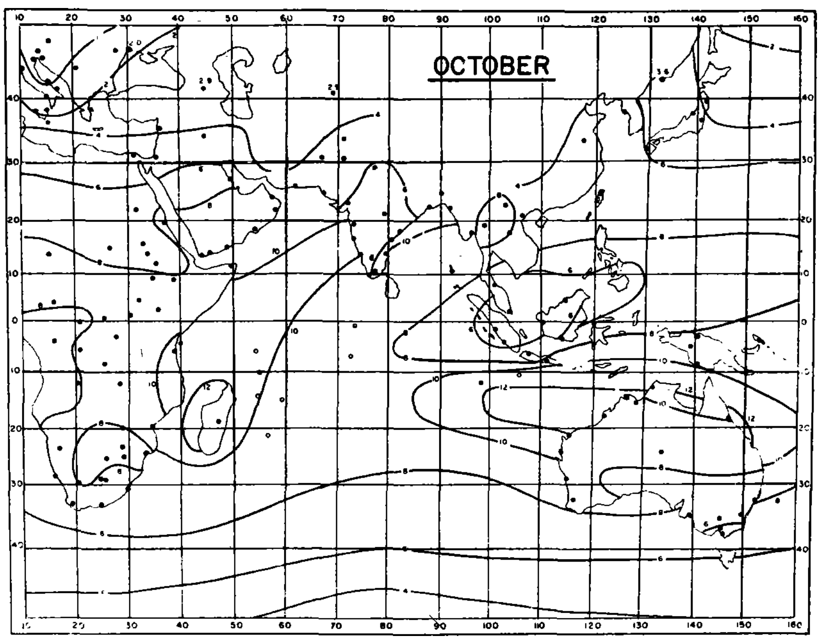

Fig. 10. Amount of net radiation in kcal/cm²/month: October

monthly and annual means of the radiation balance and the global radiation are generally within 25 per cent of the measurements, estimates being lower than observations and the differences systematic.

7. Conclusion

The need for strengthening the network of radiation stations in the Indian Ocean area, for systematic recording of all components of the radiation balance, particularly over the sea remains urgent. India has plans to extend its network of stations to measure all components of the radiation balance at the surface of the earth and to carry out regular atmospheric soundings with radiometersondes at a number of stations. Radiation measurements from weather ships and automatic weather stations at sea are, however, difficult and expensive. Radiation measurements from satellites should be expected to contribute in some measure towards a solution of this basic problem.

References

1. Albrecht, F.: Strahlung und Wärmehaushaltsuntersuchungen während einer Seereise durch den Indischen Ozean im Juni 1949. Ber. Deutsch. Wetterd. U. S. Zone **7**, No. 42, 5—10 (1952).
2. Ashbel, D.: New World Maps of Global Solar Radiation during IGY 1957—58. Hebrew University, Dep. Climatol. Meteorol. Jerusalem, 1961.
3. Berliand, T. G.: Actinometric Reference Book. Hydro-meteorol. Publ. Off., Leningrad, 1964.
4. Black, J. N.: Distribution of Solar Radiation Over the Earth's Surface. Arch. Met. Geoph. Biokl., Ser. B, **7**, 165—189 (1956).
5. Budyko, M. I.: The Heat Balance of the Earth's Surface. Gidro-meteorologicheskoe izdatel 'stvo, Leningrad, 1956.
6. Budyko, M. I.: Atlas of Heat Balance, Moscow, 1963.
7. Jacobs, W. C.: Sources of Atmospheric Heat and Moisture over the North Pacific and North Atlantic Oceans. Ann. N. Y. Acad. Sci., **44**, 19—40, 1943.
8. Landsberg, H. E., H. Lippmann, Kh. Paffen, and C. Troll: Weltkarten zur Klimakunde. Springer-Verlag, Berlin, 1963.
9. Mosby, H.: Verdunstung und Strahlung auf dem Meere. Ann. Hydr. Marit. Met. **7**, 64 (1936).
10. Robinson, G. D.: Surface Measurements of Solar and Terrestrial Radiation during the IGY and IGC. Annals IGY, Pergamon Press **32**, Meteorology II, Radiation 17—61 (1964).
11. Sauberer, F., and I. Dirmhirn: Über den Strahlungshaushalt der Ozeane auf der Nordhalbkugel. Arch. Met. Geoph. Biokl., Ser. B, **6**, 113—127 (1954).
12. Schulze, R.: Zum Strahlungsklima der Erde. Arch. Met. Geoph. Biokl., Ser. B, **12**, 185 (1963).
13. Sverdrup, H. U.: Oceanography for Meteorologists. New York, 1945.
14. U. S. Navy Marine Climatic Atlas of the World. Vol. III. Indian Ocean, 1957.
15. Monatskarten für den Indischen Ozean, 3. Aufl., Deutsch. Hydrograph. Inst., Hamburg, 1960.
16. World Meteorological Organization, Catalogue of IGY/IGC Meteorological Data WMO, No. 135, IGY 4, 1962.

Authors' address: Dir. A. Mani, Meteorological Office, Ganeshkhind Road, Poona 5, India.

Reprinted from *Indian J. Meteorol. and Geophys.* vol. 19, no. 3, 1968, p. 329-330

Monthly Wave Characteristics of the Arabian Sea

P. S. SRIVASTAVA, D. K. NAIR and K. R. RAMAN KARTHA

I. N. Physical Laboratory, Cochin

(*Received 22 November 1967*)

ABSTRACT. The monthly wave characteristics of the Arabian Sea are reported, based on an analysis of the wave data published in the *Indian Daily Weather Reports* of the India Meteorological Department for the period 1960-1964. June and July are the roughest months in the Arabian Sea and October the calmest. The maximum height of the highest ten per cent wave which has actually occurred in the month of June is 12·6 m. The direction of approach of such waves ranges between W and SW.

1. Introduction

The knowledge of the sea state will be of use in problems related to naval architecture, navigation and naval warfare (Srivastava 1964). No map giving the detailed monthly sea state conditions for the Arabian Sea and the Bay of Bengal has been published so far. The presently available publications (Bigelow and Edmondson 1952 and U.S. Navy Hydrogr. Office 1948, Mar. Div., Lond. Met. Office 1958) give only the qualitative picture of the wave conditions.

Quantitative wave data are published since the last few years in the *Indian Daily Weather Reports* of the Meteorological Department and a preliminary analysis for a short period was made earlier relating to Bay of Bengal (Chakravortty and Bhattacharjee 1957). An analysis of the wave data reported for the five-year period 1960—1964 and monthly charts of wave characteristics are presented in the paper.

2. Analysis of the data

The data presented in the *Indian Daily Weather Reports* are based on visual estimates reported by naval and merchant vessels. The data are not likely to represent the roughest sea conditions since these vessels will normally avoid rough weather areas not to say the eyes of hurricanes and typhoons.

In the present analysis the wave data for each month was grouped for each 2°-square. It is assumed for the purpose of this analysis that the height reported is the significant height and the periods and directions of wave the average. The average of the significant wave height, the standard deviation of the significant wave height, predominant wave period and direction were determined for each group. Maps depicting the average significant wave height, the standard deviation of the significant wave height, the predominant wave period and predominant wave direction were prepared for each month. A typical map for the month of June is presented in Fig. 1.

It has been shown by Longuet-Higgins (1952) that the ratio of the average height of the highest 10 per cent waves to the significant wave height is 1·27. An estimate of the maximum of highest 10 per cent waves which could possibly occur in 2°-square can be obtained by multiplying the maximum significant height reported in each 2°-square for each month by 1·27. The maximum of the highest 10 per cent waves thus found were plotted for each zone for each month and contoured. A typical map for the month of June is presented in Fig. 2. The areas shown by dots in the map represent the low wave activity and the value given therein represents the lowest value recorded. Similarly, the areas shown by dash represent the high wave activity and the value given therein represents the highest value recorded.

3. Conclusion

A complete set of 24 maps depicting the monthly wave characteristics of the Arabian Sea has appeared in the INPL Departmental Report (*see* Ref.).

A study of the maps shows that June and July (Figs. 1 and 3) are the roughest months. The direction of approach of waves during these period ranges between W and SW. The maximum highest 10 per cent wave which could have probably occurred has a height of 12·6 metres (Fig. 2), October appears to be the calmest month in the Arabian Sea and the direction of waves, if any present, is of a random pattern (Fig. 4).

The area bounded by latitudes (5°N to 10°N) and longitudes (75°E to 79°E) is mostly rough throughout the year. The gulf of Cambay is calm almost all the year round. The coastal area of the West Coast of India is characterised by a number of alternate zones of calm and rough seas.

4. Acknowledgement

The authors are grateful to Dr. D. Srinivasan, Director, I. N. Physical Laboratory, for his keen interest in the present study.

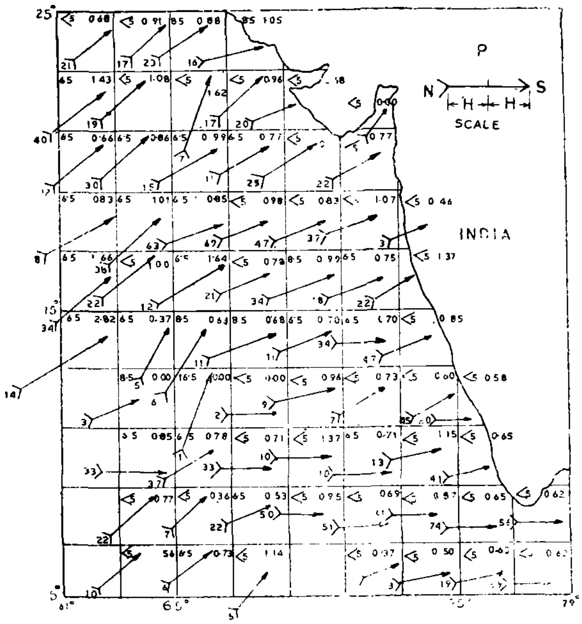

Fig. 1. Wave characteristics — June

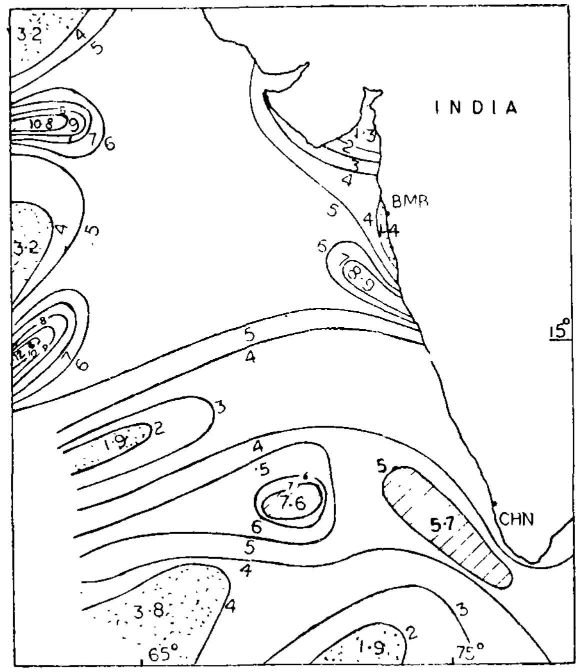

Fig. 2. Highest 10 per cent high waves — June

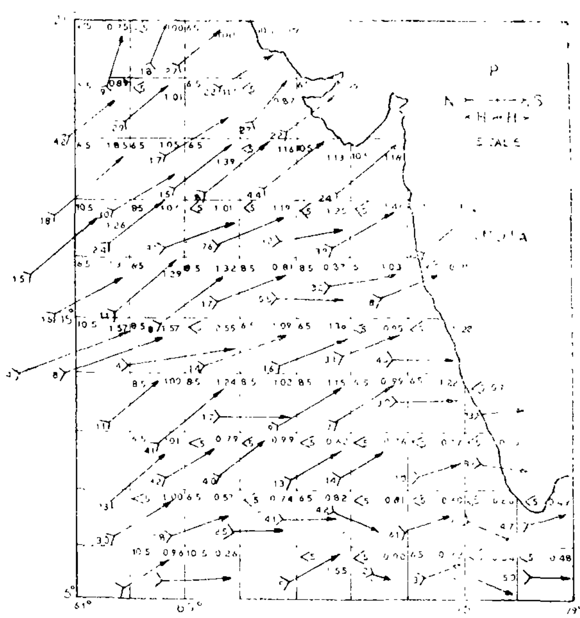

Fig. 3. Wave characteristics — July

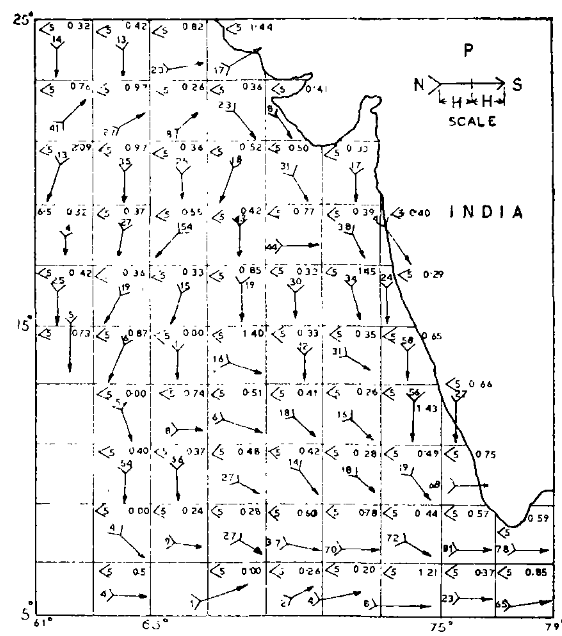

Fig. 4. Wave characteristics — October

REFERENCES

Bigelow, H. B. and Edmondson, W. T.	1952	*Wind Waves at Sea breakers and Surf.*, U.S. Hydrogr. Office Publ. No. 602.
Chakravortty, K. C. and Bhattacharjee, R. C.	1957	*Indian J. Met. Geophys.*, 8, 3, pp. 313-320.
Longuet-Higgins, M. S.	1952	*J. Mar. Res.*, 11, pp. 245-266.
Mar. Div., Lond. Met. Office	1958	*Monthly Meteorological Charts of the Indian Ocean*, M.O. 519, Air Ministry, London.
Srivastava, P. S.	1964	*Sea and Swell Studies versus Naval Warfare*, J. R. N.S.S. (U.K), 19, 6, pp. 366-369.
Srivastava, P. S., Nair, D. K. and Ramankartha, K. R.	—	INPL Departmental Report (Unpublished).
U. S. Navy Hydrogr. Office	1948	*Atlas of Sea and Swell Charts, Indian Ocean.*

Reprinted from *Bull. natn. Inst. Sci. India*, no. 38, 1968, p. 289-293

A NOTE ON CURRENT MEASUREMENTS AT ANGRIA BANK IN THE ARABIAN SEA

by K.V.K. NAIR *and* P.M.A. BHATTATHIRI*

Health Physics Division, Bhabha Atomic Research Centre, Trombay, Bombay-74

Current measurements were carried out at two stations (1:16°34'N, 72°01'E; 2:16°25'N, 72°06'E) in the Angria Bank in the Arabian Sea. An Ekman-Merz current meter was used for measuring the currents over a period of 24 hours at each station, covering the full cycle of semidiurnal tide. An analysis of the data indicated residual currents with average velocities of 0.23 knots and 0.29 knots respectively at Stations 1 and 2. The current directions were West Southwest at Station 1 and West at Station 2. This was in accord with the inference on water movements based on salinity temperature data at the Bank.

INTRODUCTION

In studies on the distribution of radioactivity in the sea, a knowledge of the sea currents is an essential prerequisite since the currents transport radioactivity, both dissolved and particulate. In a programme of work on radioactivity along the West Coast of India, an expedition was undertaken to Angria Bank, a shallow coralline bank situated 70 miles west of Ratnagiri. Between 28th and 30th November 1964, current measurements were carried out at two stations in the Bank (Fig. 1) at hourly intervals for 24 hours at three depths, viz. near the surface, mid-depth and near the bottom.

At Stations 1 and 2 the observations were begun respectively 154h 40m and 125h 31m before New Moon Spring High Water (December 5, 1964). An Ekman-Merz current meter (Ogawa Seiki) was used for the measurements each of which was for a duration of 3 minutes. Simultaneously estimates were made of wind speed and direction. All observations were made from the vessel JANJIRA (Maharashtra Fisheries Department) lying at two anchors. The vessel was reasonably stable throughout and the sea was slight to moderate.

RESULTS

Current speeds were computed from the dial readings of the current meter using the calibration certificate and the current directions were inferred from the distribution of the balls in the various compartments of the compass box. The observed currents were resolved into North and East components and are given along with the wind and current vectors in Figures 2A and 2B.

* Present Address: Biological Oceanography Division, National Institute of Oceanography, Ernakulam,

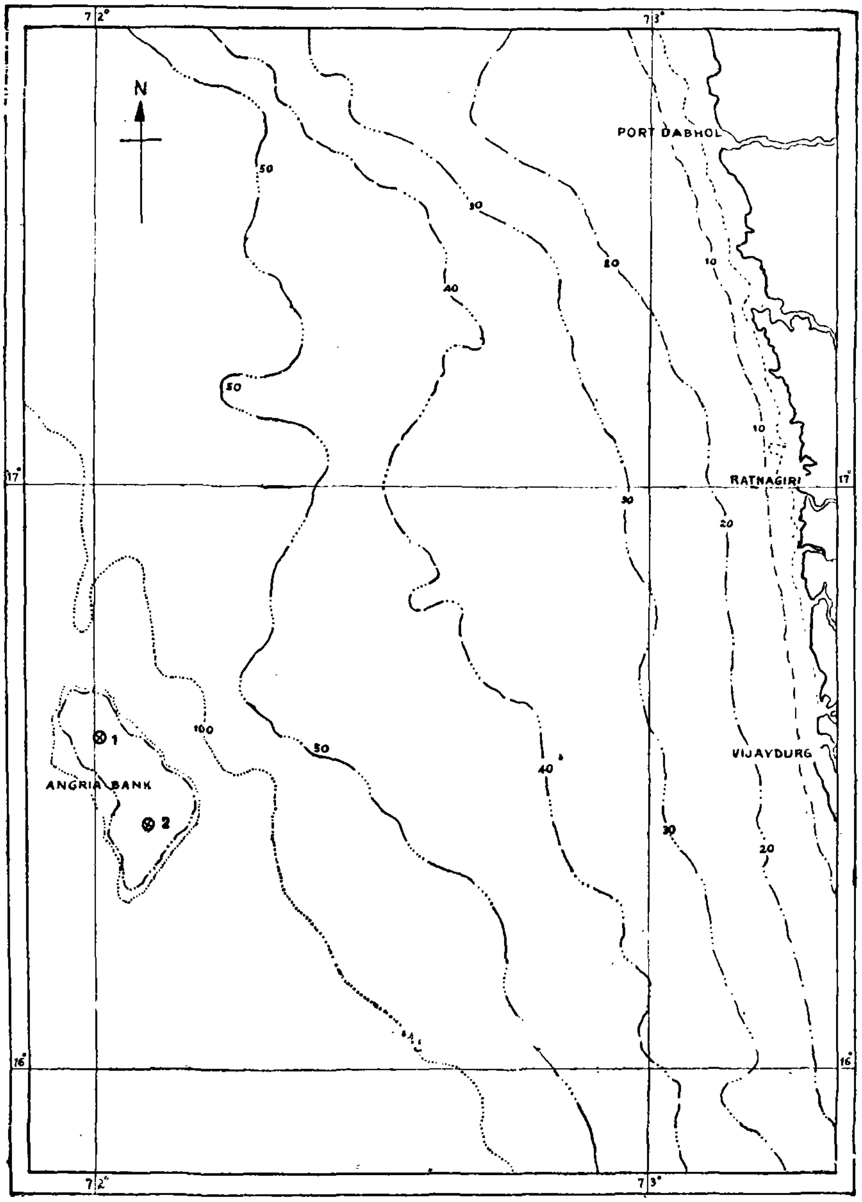

FIG. 1. Current Stations on the Angria Bank.

The current ranges at the three depths at Stations 1 and 2 are given in Table I.

TABLE I

Current ranges at different depths

Station No.	Depth (m) (below the surface)	Range (Knots)
1	1	0.17-0.63
	10	0.30-0.68
	20	0.36-0.74
2	1	0.16-0.68
	12	0.32-0.75
	24	0.24-0.75

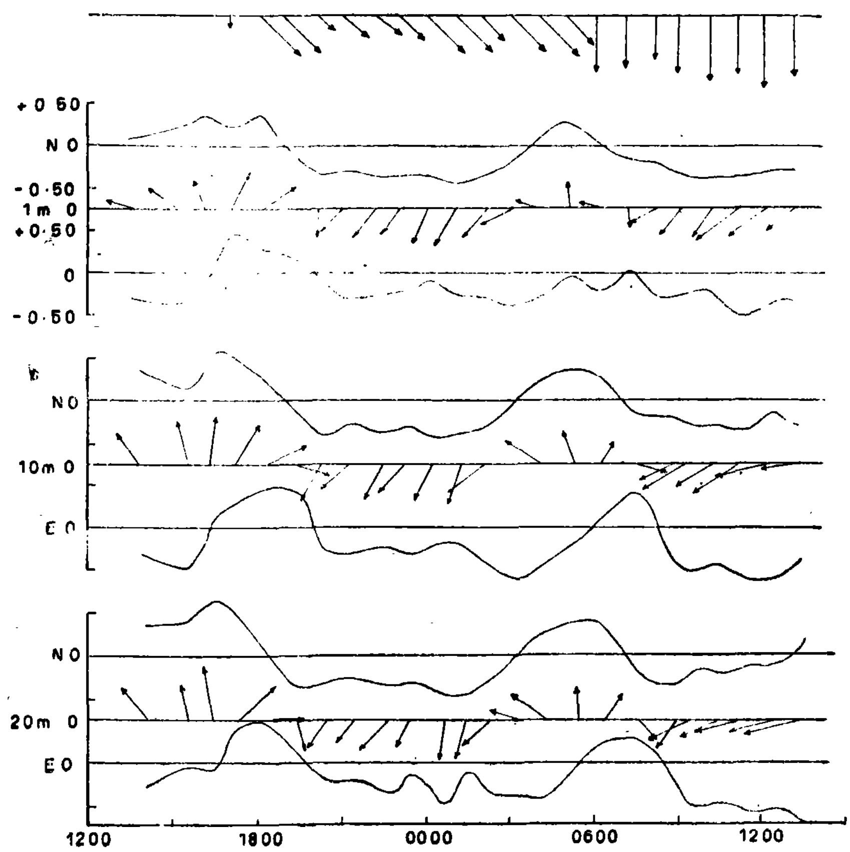

FIG. 2A WIND AND CURRENT VECTORS AND NORTH AND EAST CURRENT VELOCITY COMPONENTS AT STATION- 1

WIND VECTORS — CURRENT VECTORS

NORTH-EAST COMPONENTS

SCALE - 0 10 20 30 KTS WIND; 0 0.5 1.0 KTS CURRENTS

Residual currents (Table II) over the period of observation were calculated by vectorially adding the individual hourly observations.

TABLE II
Residual currents at the two stations

Station No.	Depth (m) (below the surface)	Residual currents	
		Speed (Kts.)	Direction
1	0	0.15	23° W of S
	10	0.22	72° W of S
	20	0.21	76° W of S
2	0	0.31	75° W of N
	12	0.33	88° W of N
	24	0.22	41° W of N

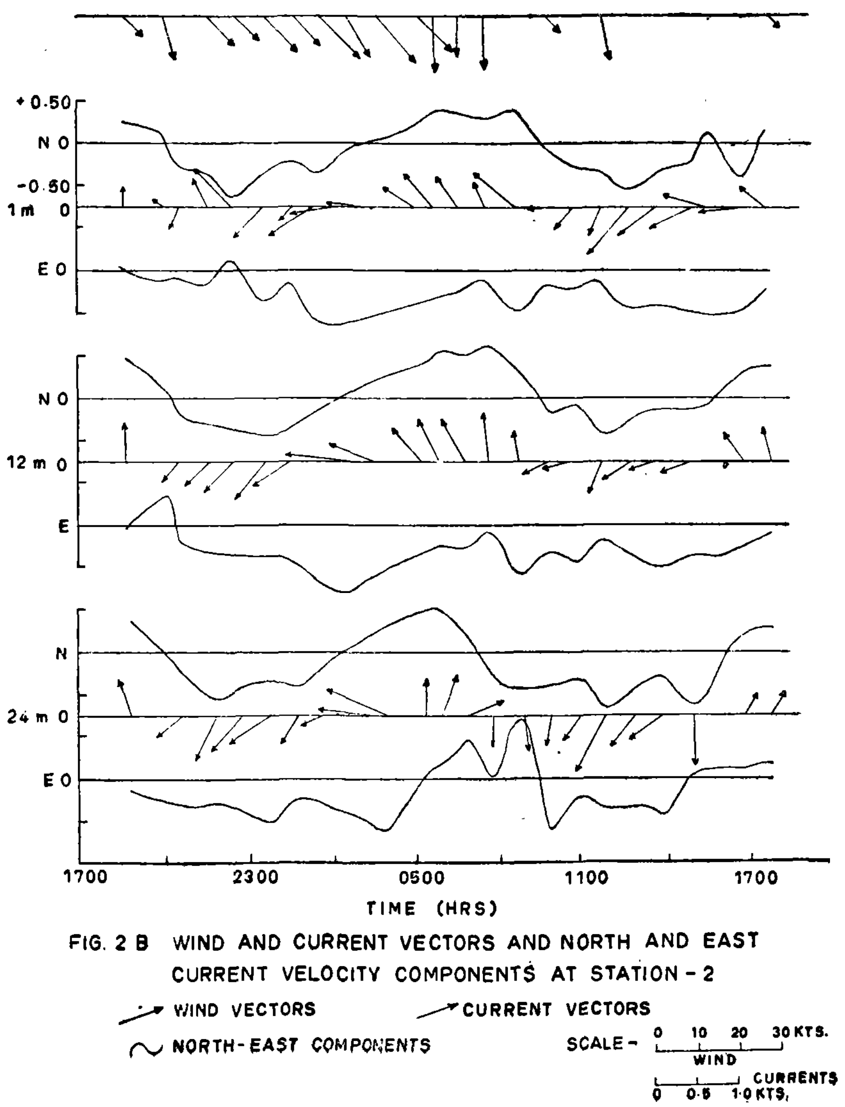

FIG. 2 B WIND AND CURRENT VECTORS AND NORTH AND EAST CURRENT VELOCITY COMPONENTS AT STATION - 2

Discussion

The observed current speed maxima of 0.74 and 0.75 knots at Stations 1 and 2 respectively may be considered minimal values since the observations were made during the neap tide period. The current vectors (Figs. 2A, 2B) suggest that the tidal currents are more oscillatory than rotational in character. At both the stations, the current was directed SSW to WSW during low tide. At high tide the directions were predominantly NNW to NNE at Station 1 while at Station 2 the current was NNW at the surface and 12 m depths and variable from W to E at a depth of 24 metres. The North and East components at Station 1 showed a definite periodicity. At Station 2 however, the periodicity was less prominent and the West component was predominant at all the three depths investigated.

The residual currents (Table II) were directed SSW at O m depth and WSW at 10 and 20 m depths at Station 1. At Station 2 the residual current directions were NNW at 0 and 12 m depths and W at 24 m depth. The pattern of water movements suggested by the current measurements is similar to the one indicated by data on salinity and temperature at the Bank (Nair, Bhattathiri and Chhapgar 1965).

Acknowledgements

We are thankful to the International Atomic Energy Agency, Vienna, for their generous assistance under Research Contract No. 155/RB (Project Marina.) Our thanks are also due to Dr. C.V. Kulkarni, Director of Fisheries, Maharashtra State and Dr. A. K. Ganguly, Head, Health Physics Division, Bhabha Atomic Research Centre, who facilitated the expedition to Angria Bank.

References

Vijayakrishnan Nair, K., Bhattathiri, P.M.A., and Chhapgar, B.F. (1965). Angria Bank Expedition, General Hydrographic and Chemical Features. AEET/HP/PM-3, Bhabha Atomic Research Centre, Bombay.

Reprinted from *Bull. natn. Inst. Sci. India*, no. 38, 1968, p. 301-307

ON THE LEVEL OF LEAST MOTION AND THE CIRCULATION IN THE UPPER LAYERS OF THE BAY OF BENGAL

by V. V. R. VARADACHARI, C. S. MURTY *and* PIYUSH KANTI DAS
Physical Oceanography Division, National Institute of Oceanography, Ernakulam

The paper presents the circulation pattern in the upper 500 metres of the western Bay of Bengal between 9°N and 16°N during the south-west monsoon period, based on the geo-potential anomalies computed from the hydrographic data. The circulation is characterised by two anti-cyclonic cells centred at 11°N 83°E and 16°N 85E with a zone of strong cyclonic shear between them. The strength of the circulation decreases with depth and it becomes feeble below a depth of 400 metres. The level of least motion is situated around 500 metres depth. The methodology in choosing the reference level is discussed.

INTRODUCTION

Studies on the circulation in the Bay of Bengal based on the dynamic computations are quite meagre. Mention may be made of the dynamic computations of currents off the Visakhapatnam Coast, by Poornachandra Rao (1956), and the investigations on the winter circulation in certain parts of the Bay by the dynamic method, by Fomicev (1964), with the data obtained on the 33rd cruise of R. V. "VITYAZ". Before the advent of the IIOE, practically no dynamic computations of currents in the Bay of Bengal were carried out for the southwest monsoon season. The data collected during the 15th and 16th cruises of I.N.S. "KISTNA" under the Indian Programme of the International Indian Ocean Expedition along a close network of stations in the western Bay of Bengal, enabled a detailed investigation of the level of least motion in the Bay and the circulation at different levels in the upper 500 metres, during the southwest monsoon period.

MATERIAL AND METHODS

The region of study and the location of stations are shown in Fig. 1. The area extends from 9°N to 16°N and from the East Coast of India to 90°E. The period of study is from 8th June to 4th July, 1964. The hydrographic data was collected down to a depth of 1000 metres at most of the stations and at a few stations the data was available down to 2000 metres or more. The data was processed using standard techniques and from the processed data of temperature and salinity at standard depths for each station, the anomalies of dynamic height between different standard levels were calculated. The total dynamic height anomaly for each station is obtained by adding the anomalies of dynamic height from a selected reference level of no motion (or least motion) to the level at which the relative currents are to be computed (LaFond 1951). Using these values at different stations, charts showing the dynamic topography of the sea surface (zero decibar surface), as well as 100, 200 and 400 decibar surfaces relative to 500 decibar surface (which is found to be the

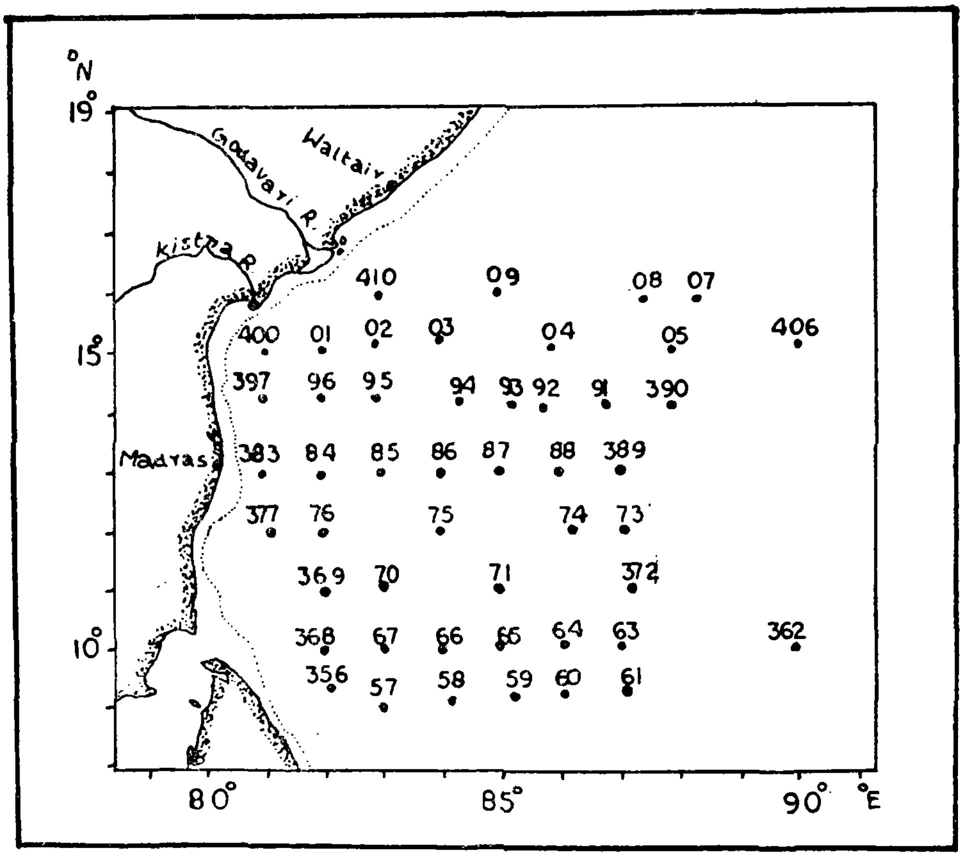

FIG. 1. Map showing the location of stations.

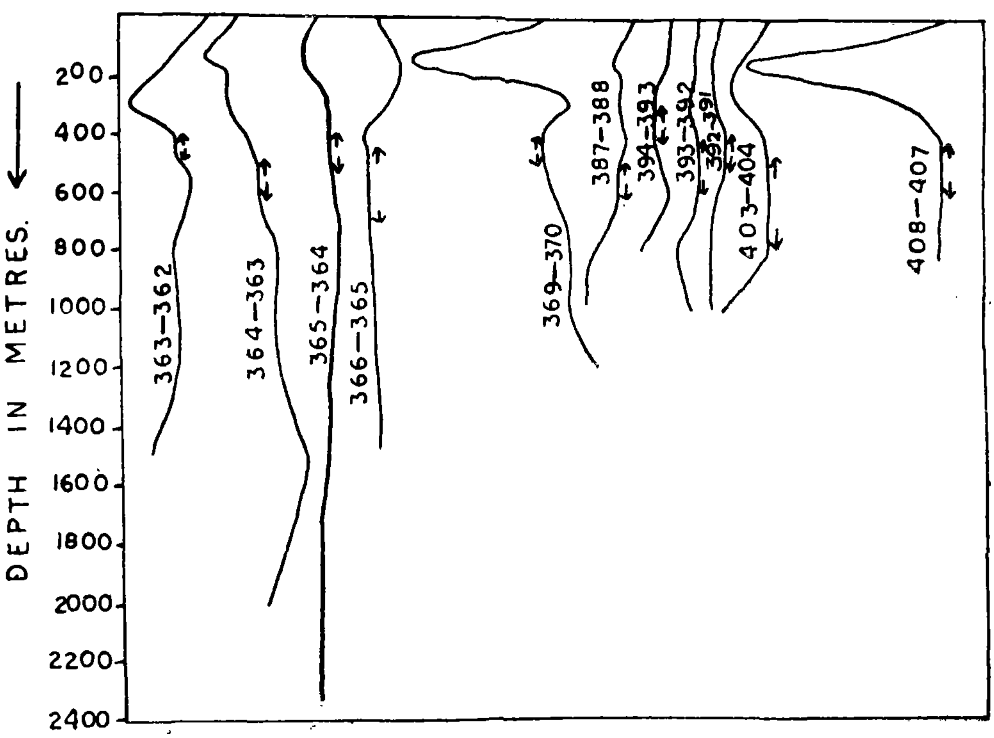

FIG. 2. Dynamic depth differences between selected stations pairs.

reference surface), are constructed and these charts are shown in Figures 3, 4, 5 and 6. The inset diagram in each of these figures gives the current velocity for different values of contour spacing on the charts, for different latitudes.

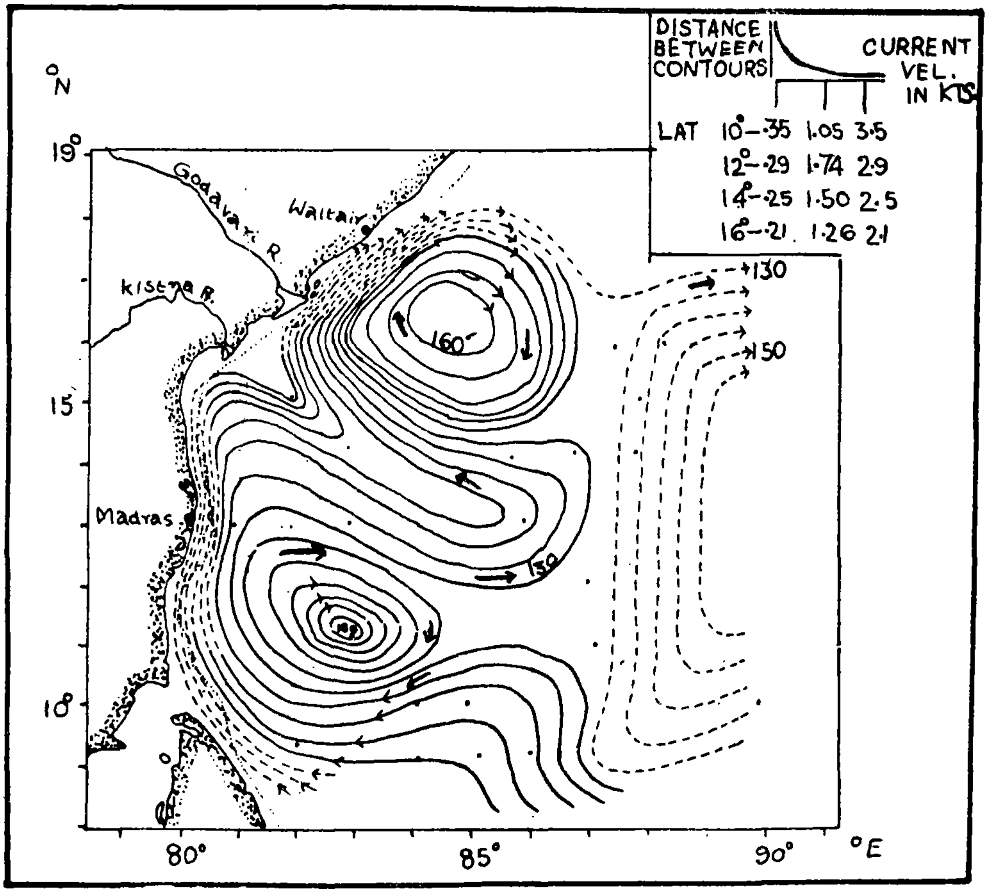

FIG. 3. Geopotential topography of the sea surface relative to 500 decibars in centidynamic metres.

CHOICE OF THE REFERENCE LEVEL

The current velocities computed by the dynamic method indicated above, describe the motion of water relative to water particles at some reference level. If these velocities are to be representative, the reference surface should be placed where the horizontal pressure gradient and geostropic component of of the velocity are equal to zero or are insignificantly small. The computation of the current velocities by the dynamic method, depends on the correct choice of this surface of "no motion" or "least motion". The depth of this surface depends essentially on the

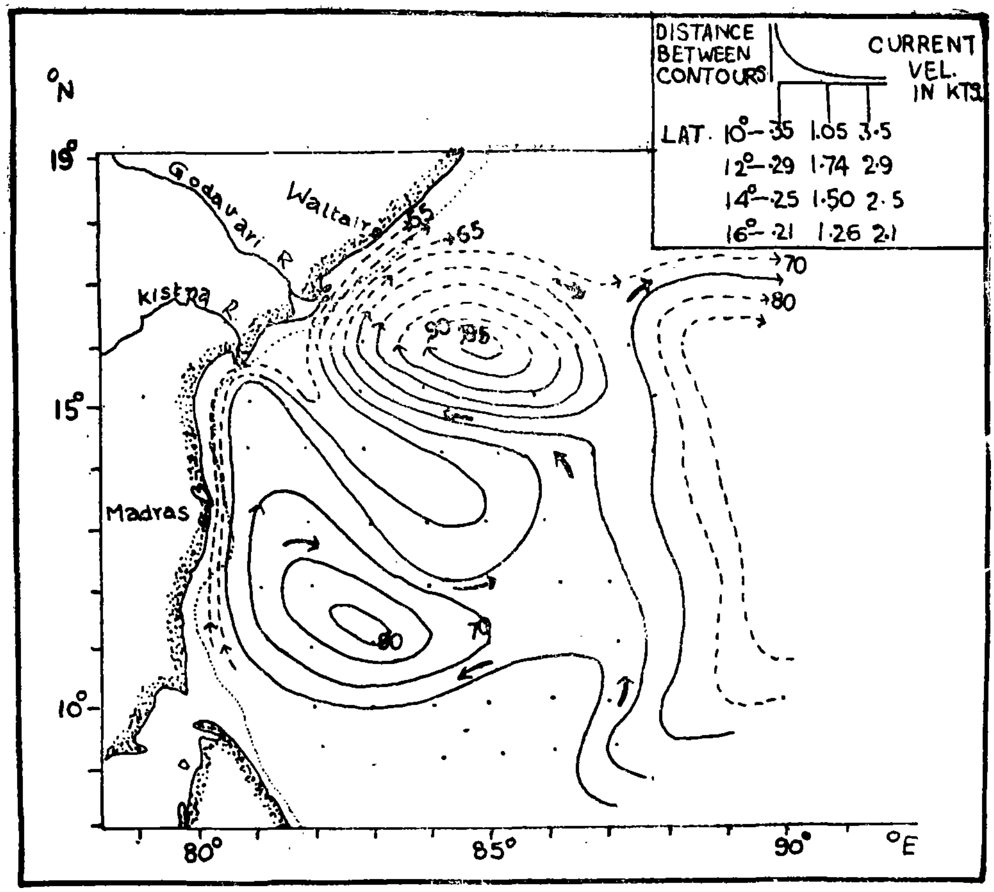

FIG. 4.
Geopotential topography of the 100 decibaric surface relative to 500 decibars in centidynamic metres.

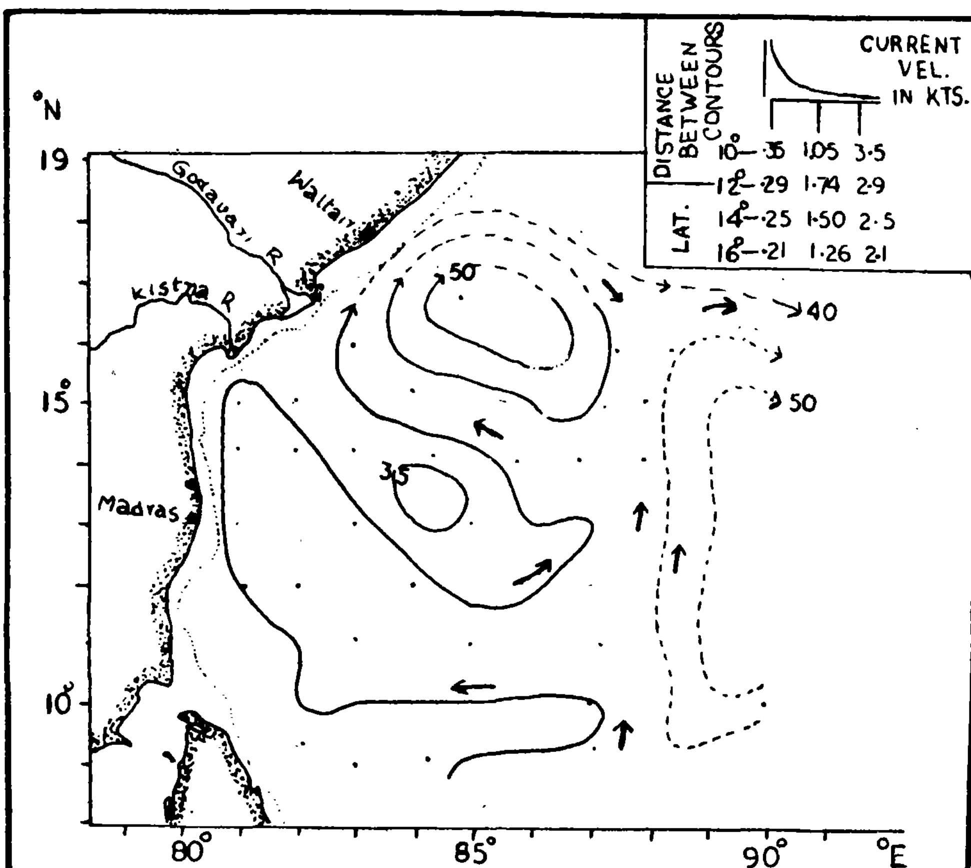

FIG. 5.
Geopotential topography of the 200 decibaric surface relative to 500 decibars in centidynamic metres.

horizontal density difference between two stations and on the slope of the sea surface between the stations. If the ocean is very weakly stratified, the depth of this reference level becomes very deep (Neumann *et al.* 1966). So far, oceanographers tried to find this level by indirect evidence. A good amount of uncertainity exists in choosing a proper reference surface for computing the ocean currents to arrive at a close approximation to the absolute values, by this method. Many investigators established this surface by considering the hydrological parameters such as oxygen, sigma-t, salinity etc. A discussion of the merits and demerits of these methods is presented by Sverdrup (1942) and Fomin (1964).

A more direct attempt to determine the depth of the layer of no horizontal motion was made by Defant (1941). Although, this method may not always lead to unique results, in regions of weak and variable currents it seems to be consistent and reliable for moderately or strongly stratified water bodies (Neumann *et al.* 1966). This technique was adopted in the present study for determing the level of 'least motion'. It involves the analysis of the difference in the dynamic depths of the isobaric surfaces between station pairs. An examination of Fig.2 representing the plot of the dynamic depth difference of the isobaric surfaces versus the geometric depth, for a number of station pairs, indicates the constancy in the dynamic depth differences between 400 and 600 metres in a majority of the cases and between 800 and 1000 metres in a few cases. Since the present observations are limited mostly to 1000 metres and since in the majority of the cases the dynamic depth differences between the station pairs, are constant between 400 and 600 metres, 500 metres depth (500 decibar surface) is considered as the reference level or the level of 'least motion'.

Discussion of Results

The circulation patterns for the western Bay of Bengal for the southwest monsoon period, as deduced from the geopotential topography for surface, 100, 200 and 400 metres depth with respect to 500 decibar surface (the level of least motion) is shown in Figures 3, 4, 5 and 6 respectively. The current follows the geopotential contours indicated in the figures and the strength of the current is inversely proportional to the spacing of the contours. While the contours are shown at intervals of 5 geopotential centimetres for the surface, 100 and 200 metre levels, they are shown at intervals of 1 geopotential centimetre on the 400 metre depth chart as the contour gradients and consequently the currents are very weak at this level. The following are some of the important features of the circulation pattern.

(a) The circulation is characterised by two anticyclonic cells centred at 11°N 83° E and 16°N 85°E with a zone of strong cyclonic shear between them extending towards the southeast from the region of Godavari and Krishna river mouths to about 87°E longitude. Another anticyclonic circulation shows up beyond 90°E longitude.

(b) The strength of the current decreases with depth. The strongest currents obtained at the surface have speeds of about 3 knots. At 400 metres depth, the currents are very feeble with speeds not exceeding 0.1 knot.

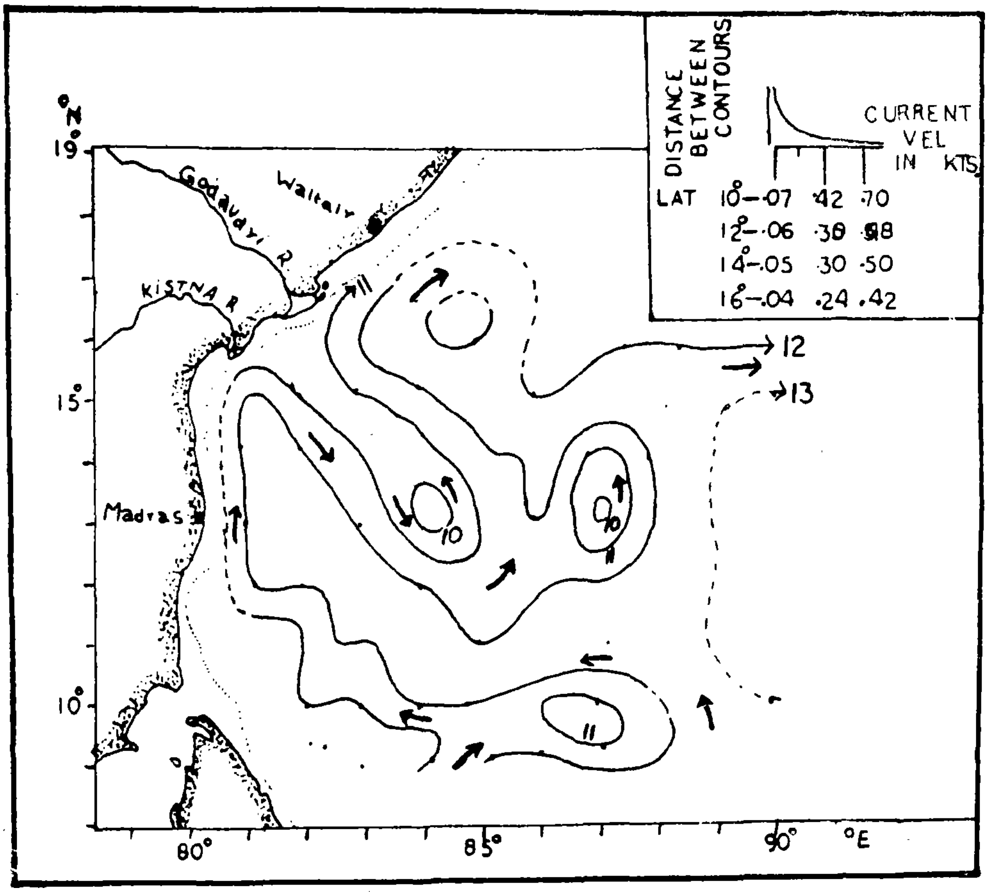

FIG. 6. Geopotential topography of the 400 decibaric surface relative to 500 decibars in centidynamic metres.

(c) The current follows the coast line in the continental margins. Strongest currents are noticed along the western boundary of the Bay of Bengal.

While the dynamic topographic charts show anticyclonic motion in general agreement with the mean circulation pattern in the Bay of Bengal for the month of June (Bay of Bengal Pilot 1953; Varadachari and Sharma 1967), the dynamic computations reveal that the circulation is more complex than that shown in the mean maps. While the general clockwise circulation in the Bay of Bengal during the southwest monsoon is attributable to the general wind system, the more complex and cellular nature of the flow pattern seems to be partly the result of river discharges and strong shears in the wind field. The importance of internal waves as a factor affecting the dynamic computations was considered and it was found that their effect was negligible in the present study, Detailed investigations are required for a better understanding of the circulation in the area.

ACKNOWLEDGEMENTS

The support of the Indian National Committee on Oceanic Research and Dr. N. K. Panikkar, Director, Indian Programme of the International Indian Ocean Expedition and National Institute of Oceanography (CSIR), and the cooperation and assistance of the Captain, Crew and the participating Scientists of the 15th and 16th cruises of I.N.S. "KISTNA" are gratefully acknowledged.

REFERENCES

Anonymous. (1953). Bay of Bengal Pilot. Admirality, London, pp. 1-527.

Defant, A. (1941). Die absolute topographie des Physikalischen Meeresmiveaus und der Druckflachen, Sowie die Wasserbewegangen im Atlantischen Ozean., Meteor work, **6**, 191-260, (Berlin).

Fomin, L.M. (1964). A Dynamic Method in Oceanography, Elsevier Oceanography Series.

Fomicev, A.V. (1964). Study of the currents in the Northern part of the Indian Ocean. *Trudy Inst. Okeanol.*, **64**, 43-50.

LaFond, E.C. (1951). Processing Oceanographic Data. H.O. Publ. No. 614., U.S. Navy Hydrography Office, pp. 1-114.

Neumann, G., and Pierson, W. J. (Jr.) (1966). Principles of Physical Oceanography, Prentice-Hall, Inc., N.Y.

Poornachandra Rao, C. (1956). Currents off Visakhapatnam Coast in March. *Indian J. Met. Geophys.*, **7**, 377-379.

Sverdrup, H.U., Johnson, M.W., and Fleming, R.H. (1942). The Oceans, Their Physics, Chemistry and General Biology. Prentice Hall, New York.

Varadachari, V.V.R., and Sharma, G.S. (1967). Circulation of the surface waters in the north Indian Ocean. *Indian Geophys. Un.*, **4**, 2, 61-73.

SALINITY MAXIMA ASSOCIATED WITH SOME SUB-SURFACE WATER MASSES IN THE UPPER LAYERS OF THE BAY OF BENGAL

by V. V. R. VARADACHARI, C. S. MURTY *and* C. V. GANGADHARA REDDY

Reprinted from *Bull. natn. Inst. Sci. India*, no. 38, 1968, p. 338-343

SALINITY MAXIMA ASSOCIATED WITH SOME SUB-SURFACE WATER MASSES IN THE UPPER LAYERS OF THE BAY OF BENGAL

by V. V. R. VARADACHARI, C. S. MURTY *and* C. V. GANGADHARA REDDY

Physical Oceanography Division, National Institute of Oceanography, Ernakulam

The distribution of some sub-surface water masses in the western Bay of Bengal during the south-west monsoon period is presented. Based on the salinity maxima and σt values the existence of waters of Persian Gulf and Red Sea origin could be established. The studies show that the Persian Gulf and Red Sea waters enter the Bay at depths of about 200 m and 400 m respectively, and follow the circulation pattern at the respective depths of entry. The probable paths of entry are indicated. These waters sink to different depths subsequent to their entry into the Bay. The Persian Gulf water could be traced down to a depth of about 350 m while the Red Sea water could be traced down to 900 m depth.

INTRODUCTION

Attempts were made in the past to identify and describe some of the water masses in the top layers of the Bay of Bengal (LaFond 1958; Poornachandra Rao 1956; Balaramamurty 1957) but due to lack of extensive oceanographic data, these studies had to be confined mostly to the region of the continental shelf on the East Coast of India. An attempt was made by Gallagher (1966) to make a preliminary study of the variability of water masses in the Indian Ocean and to designate the broad areal limits of some sub-surface water masses of the Indian Ocean. The surveys conducted on I.N.S. KISTNA during the International Indian Ocean Expedition, afforded an opportunity for a detailed study of some of the sub-surface water masses in the upper 1000 metres of the western Bay of Bengal.

Water masses can be identified by one or more characteristic indicators such as relative maximum of salinity, oxygen or temperature or a combination of such factors. Rochford (1964), while identifying the water masses following the salinity maxima in the upper 1000 metres in the north Indian Ocean, indicated the existence of two water masses of Persian Gulf and Red Sea origin at depths of 300 to 400 metres and 400 to 500 metres respectively, in the Bay of Bengal, based on the inferences drawn from the oceanographic data collected by the Russian Research Vessel "Ob" in 1958. Since the stations of "Ob" were located only along 88°E long. in the Bay of Bengal, the presence of these waters over wide areas and the paths of their entry into the Bay could not be ascertained.

The present study, covering a considerable area in the Bay, revealed more information regarding the entry paths and pattern of distribution.

MATERIAL AND METHOD

Figure 1 shows the distribution of stations occupied during the 15th and 16th cruises of I.N.S. "KISTNA" in the southwest monsoon season, under the Indian

Programme of International Indian Ocean Expedition. Treatment of the data in classifying and tracing the water masses is, as described by Rochford (1964), on the basis of salinity maxima.

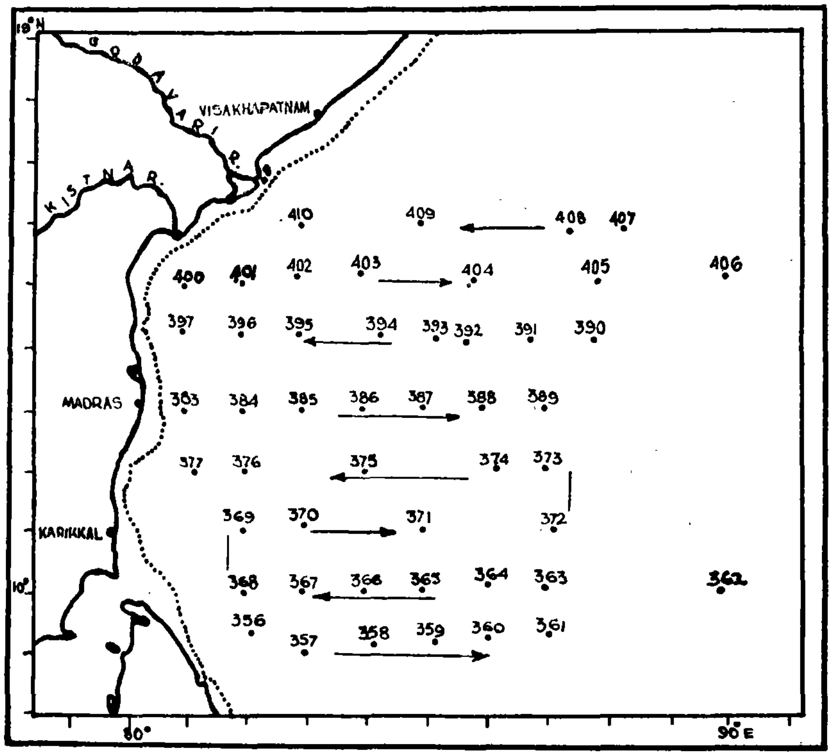

FIG. 1. Map showing the station locations.

RESULTS AND DISCUSSION

Two distinct salinity maxima could be traced in the majority of the stations during the southwest monsoon season. Significant regional variations in the intensities of these maxima and the depths of their occurrence are noticeable. The σ_t limits of these water masses agree with those described by Rochford (σ_t=26.2 to 26.9 for Persian Gulf water and σ_t=26.95 to 27.4 for the Red Sea water).

(a) *First Salinity Maximum:*

This salinity maximum lying between σ_t limits 26.2 to 26.9 and salinity limits 35.03‰ to 35.35‰ exists at depths of about 200 to 350 m excepting at station 357, where the depth is 140 m. According to Rochford (1964) this high salinity water was absent around the Gulf of Aden. Hence, he considered Persian Gulf as the origin for this maximum. During its spread to the southwest and to the east, its average depth was found to be 200 m. Since the data is inadequate, he could not show by which route it enters the Bay. An examination of the distributional charts of salinity maxima (Fig. 2) and the depths at which the maxima are noticed (Fig. 3) shows that

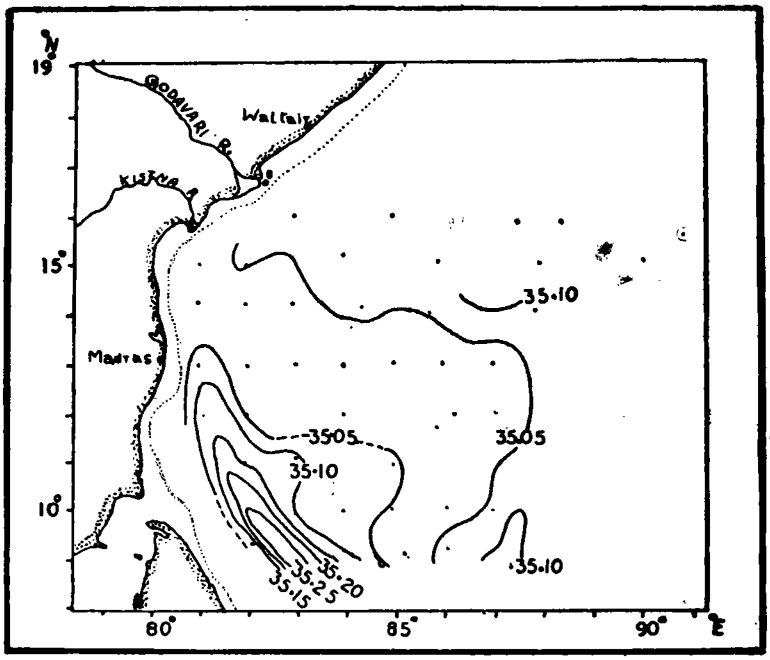

FIG 2. Isoline of first Salinity maximum (Persian Gulf water).

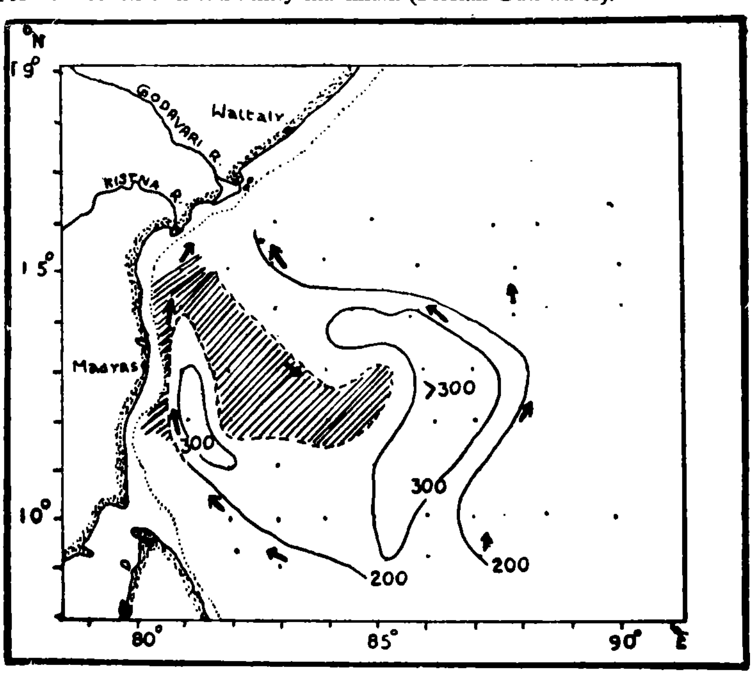

FIG. 3. Depth contours of first salinity maximum (Persian Gulf water).

the high salinity core appears at about 200 m depth south of 9°N lat. and the water enters the Bay of Bengal at least through two main paths, one around Long. 84°E and the other around Long. 87°E, following more or less the general circulation pattern at that level (Varadachari *et al.* 1967). Along the western side, the path of water appears to be north-north-westerly up to Lat. 11°N beyond which it could not be traced (shaded region in Fig. 3), perhaps because of excessive mixing with low salinity water in the region. However, in view of the existing circulation pattern, it is likely to take a turn towards the east around Lat. 15°N. The second entrance path appears to be mainly northerly. This northerly flow around 87°E meridian extends up to Lat. 14°N and then turns westerly following the circulation pattern. Between the two main paths of entry, this water could be traced at depths greater than 200 metres. From the available data, it may be said that the general spread tends to be more towards north-westerly. The progressive reduction of the salinity values in the salinity core from south to north, is indicative of lateral mixing and perhaps some vertical mixing.

Phosphate concentrations corresponding to the salinity maxima show some variations. According to Rochford (1964), the phosphate content at the depths of location of the Persian Gulf water is about 3 μg at/l. In the present study, most of the stations show phosphate values between 1.0 to 1.9 μg at/l. at the level of occurrence of the Persian Gulf water. High values (2.5 to 3.0 μg at/l.) are encountered only between Lat. 10°N and 11°N (station numbers 368 to 371). Corresponding salinity maxima also are high. The station 357 which is the western-most station of the southern-most section of these cruises, is also characterized by the highest value for salinity maximum and extremely high phosphate content, suggestive of a discrete water body, perhaps having a very long residence time. The high phosphate content may be due to oxidative regeneration of the suspended organic matter. It is interesting to note that the Persian Gulf water, at its source, contains high phytoplankton (Zernova 1962). The high values of salinity and phosphate at stations 368 to 371 could be traced to the waters at station 357 (Fig. 1).

(b) *Second Salinity Maximum :*

This core of high salinity, characteristic of Red Sea water (Rochford 1964), is found to be within the salinity and σ_t limits of 35.00‰ to 35.33‰ and 26.95 to 27.40 respectively. This water mass also appears to enter through two paths, south of 9°N around 84°E and 87°E Long. between 500 and 400 m level (Figs. 4, 5). Studies on the circulation for the same period in the area, show that the level of least motion is around 500 metres depth (Varadachari *et al.* 1967) and even at 400 meters depth the speed of the current is mostly less than 0.1 knot. Hence, the Red Sea water is likely to spread northward more slowly. But it may sink to different depths under the influence of the clockwise circulation or shoal up under counterclockwise circulation. It could be traced as far as 16°N. However, west of 82°E Long. the salinity maximum could not be located except at 14°N, 81°E. The maximum depth of occurrence is about 900 metres. The intense sinking region roughly coincides with that for Persian Gulf water (Lat. 11 N). At a few stations two salinity maxima within the σ_t range of Red Sea water, appear at depths ranging from 400 to 900 m (Stations 356, 368, 394, 396 and 404). Low values of salinity

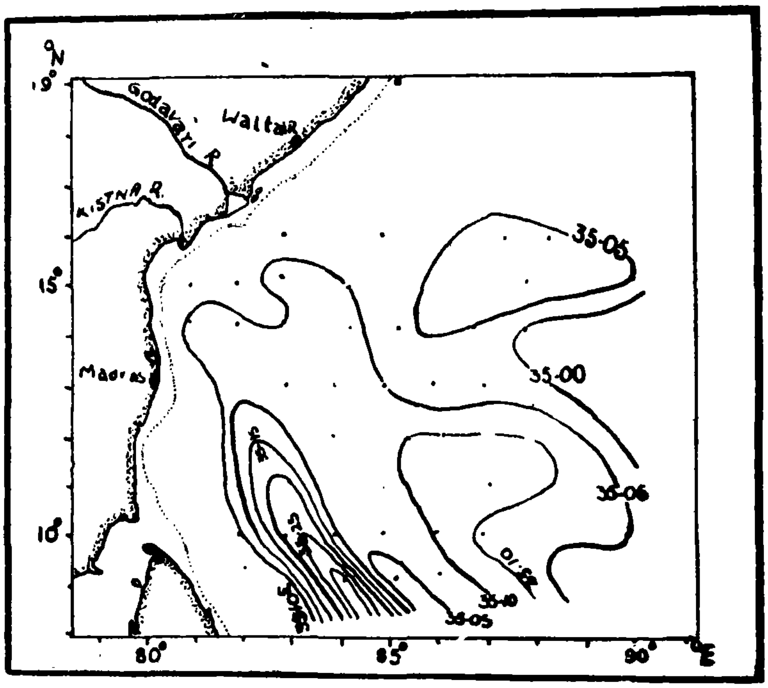

FIG. 4. Isolines of second salinity maximum (Red Sea water).

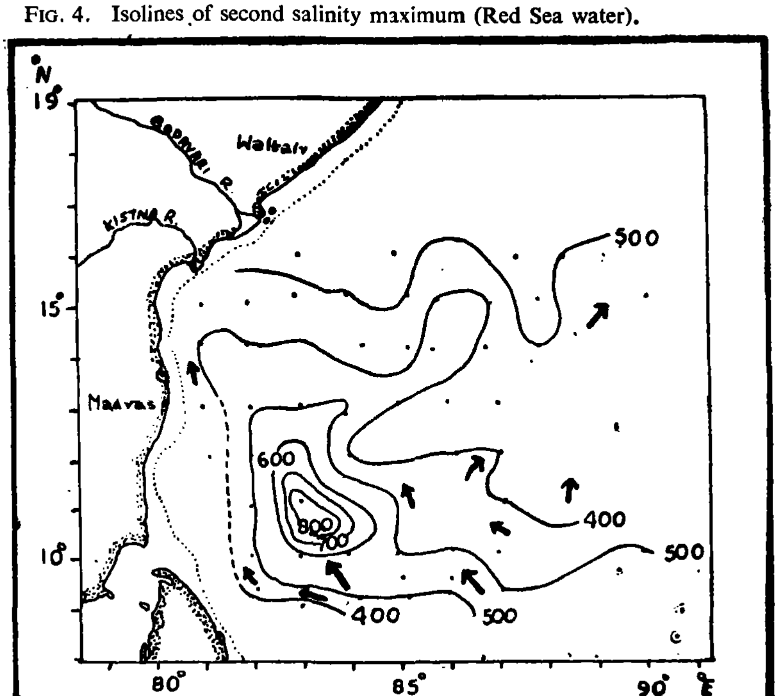

FIG. 5. Depth contours of second salinity maximum (Red Sea water).

maxima, in the northern part, indicate that the Red Sea water mixes and gradually loses its identity during its northerly spread. Inorganic phosphate concentrations associated with the salinity maxima are found to be predominantly between 1.0 and 1.9 μg at/l. Higher values of phosphates (2.0 to 3.8μg at/l.) are found at stations 370 to 374. It may be pointed out here that around the same region the Persian Gulf water also shows maximum phosphate concentrations, excepting that the high phosphate region is slightly extended towards the east for the Red Sea water.

Conclusions

Two water masses could be identified in the upper 1000 m of the Bay of Bengal with distinct salinity and σ_t characteristics. The upper water mass has the characteristics of Persian Gulf water and the lower one, that of Red Sea water. Both the water masses enter the Bay south of 9°N Lat. through two distinct paths. They move northward, sink and spread following the circulation pattern. From the available data ("Ob", 1958 and the present data), it appears that the two waters may be flushing in during the southwest monsoon period and retreating during the northeast monsoon period. The high phosphate concentrations of Persian Gulf water (3.0 μg at/l.) as reported by Rochford (1964) during the northeast monsoon period are higher than those found during the present investigation (1.0—1.8 μg at/l.) for the southwest monsoon period. The high values encountered during the northeast monsoon might be due to the oxidation of organic matter of planktonic origin and such conditions are favourable only for waters having long residence time. However, the retreat during the northeast monsoon appears to be far from complete before fresh influx commences during the southwest monsoon. The general high phosphate content of the Red Sea water as compared to the Persian Gulf water indicates the longer residence time of the former in the Bay.

Acknowledgements

The authors wish to express their thanks to the Indian National Committee on Oceanic Research and Dr. N. K. Panikkar, Director, Indian Programme of International Indian Ocean Expedition and National Institute of Oceanography (C.S.I.R.), for their support and to the Captain, crew and the participating Scientists of the 15th and 16th cruises of I.N.S. "KISTNA", for their cooperation and assistance in the research programme.

References

Balaramamurty, C. (1957). Water masses of the western central Bay of Bengal during November. *Curr. Sci.*, **26**, 80.

Gallagher, J.F. (1966). The variability of water masses in the Indian Ocean. *N. O. D. C. Publ. G*-11, Washington; U.S. Naval Oceanographic Office, pp. 1-74.

LaFond, E.C. (1958). On the circulation of the surface layers off the East Coast of India. *Andhra Univ. Mem. Oceanogr.*, **2**, 1-11.

Poornachandra Rao, C. (1956). Water masses in the Bay of Bengal. *Curr. Sci.*, **25**, 51-53.

Rochford, D. J. (1964). Salinity maxima in the upper 1000 metres of the north Indian Ocean. *Aust. J. mar. Freshwat. Res.*, **15**, 1-24.

Sabinin, K.D. (1964). Layers of increased salinity in the northern part of the Indian Ocean. *Trudy Inst. Okeanol.*, **64**, 51-58.

Varadachari, V. V. R., Murty, C.S., and Das , P.K. (1967). On the level of least motion and the circulation in the upper layers of the Bay of Bengal. *Proc. natn. Inst. Sci. India* (In Press).

Zernova, V. V. (1962). Quantitative distribution of the phyto plankton in the northern Indian Ocean. *Trudy Inst. Okeanol.*, **58**, 45-53.

THE INFLUENCE OF SOME HYDROGRAPHICAL FACTORS ON THE FISHERIES OF COCHIN AREA

by V. N. SANKARANARAYANAN *and* S. Z. QASIM

Reprinted from *Bull. natn. Inst. Sci. India*, no. 38, 1968, p. 846-853

THE INFLUENCE OF SOME HYDROGRAPHICAL FACTORS ON THE FISHERIES OF COCHIN AREA

by V. N. SANKARANARAYANAN *and* S. Z. QASIM

Biological Oceanography Division, National Institute of Oceanography, Cochin-11

From the seasonal changes in the hydrographical features of Cochin area during the year 1965-66, it is possible to deduce that a shore-ward influx of upwelled water occurs from about June to October. The effect of this water is felt in very shallow areas. During this period the bottom layers become cold, markedly saline, poorly oxygenated and rich in nutrients. Minimum oxygen of less than 0.5 ml/L is recorded at 10 m in August. The fish populations are not very abundant during this season and tend to avoid the oxygen-deficient water. Both fish and prawn catches are poor from June to September. The available evidences show that the enrichment of the euphotic zone with nutrients in the post-upwelling period produces an intense phytoplankton bloom. The red-tide phenomenon which acts as a further threat to fish life is of common occurrence during this season. From November onwards there is a reappearance of fish shoals in coastal waters and a resumption of large scale fishing activity.

INTRODUCTION

Many of the accounts which have appeared in recent years on the Indian Ocean, as parts of various programmes of the I.I.O.E., clearly indicate that the Arabian Sea is characterized by a relatively lower temperature, higher salinity, higher nutrient content, greater primary productivity, richer phytoplankton and zooplankton biomass and a greater fish yield than those of the Bay of Bengal (Panikkar and Jayaraman 1966; Reddy and Sankaranarayanan 1968; Ryther and Menzel 1965; Prasad 1966; Ryther *et al.* 1966; Panikkar 1968, *See* pp. 811-832). The high level of primary productivity though restricted to certain areas, particularly to the coastal regions, has been attributed to higher nutrient contents brought to the euphotic zone by upwelling (Ryther and Menzel 1965; Ryther *et al.* 1966). The fishery resources of the west coast, rich as they are, amounting to 75% of the total marine catch of India (700-900 thousand tons annually), are subjected to wide fluctuations from year to year (Panikkar 1968).

Several earlier studies carried out on the hydrography of various parts of the Arabian Sea and the Bay of Bengal have been primarily directed to find an answer to the fluctuation of fisheries (LaFond 1954; Jayaraman and Gogate 1957; Subrahmanyan 1954; Pradhan and Reddy 1962; Prasad and Nair 1959). In most of these studies it has been pointed out that the highly complex and changing conditions of the Arabian Sea seem to be responsible for the seasonal and annual fluctuations of the fish catches. For instance, in the Bombay area, rather sudden and pronounced variations in temperature, salinity and oxygen, resulting from upwelling, influence the availability of fish (Carruther *et al.* 1959). Similarly from Cochin to Calicut, Banse (1959, 1966) by making use of the earlier informations and from his own data collected during September/October 1958, has laid special emphasis on the phenomenon of upwelling on the west coast and its possible influence on trawl catches.

From these accounts it is clear that the phenomenon of upwelling is fairly widespread in the Arabian Sea and that it has a direct influence on the fisheries of the West Indian coast. More specific information on upwelling can be obtained from the accounts given by Ramamirtham and Jayaraman (1960), Sastry and Myrland (1959), Rao and Jayaraman (1966) and from a paper by Sharma presented at this symposium (1968). Published accounts, however, relating hydrography to parallel fish and prawn catches are very few.

METHODS

Two stations were fixed in the inshore region of Cochin during the year 1965-66. Station 1 was very close to the shore at a depth of 10 m, while the station 2 was a few miles away and had a depth of 30 m. Water samples collected at fortnightly intervals from these stations were analysed for various hydrographical features indicated in Fig. 1. For all estimations the working instructions of Strickland and Parsons (1960) were largely followed. Data on fish and prawn catches were obtained from such vessels of the Indo-Norwegian Project which continue to fish throughout the year in coastal waters.

RESULTS AND DISCUSSION

The immediate aim of this paper is to direct the informations on the hydrography of the inshore waters, which have been primarily collected for some other purpose, to fish catches of the Cochin area. Fig. 1 shows some of the main features at station 1. It can be seen from the figure that almost all parameters *viz.* temperature, salinity, dissolved oxygen, alkalinity, *p*H and nutrients are adapted to an annual rhythm and that the maximum and minimum values of these parameters alternate with each other. Temperature variations are more pronounced at the bottom than at the surface. Maximum temperature is recorded in the month of April and minimum in August and September. From December to May the temperature differences from surface to the bottom were less than 1°C, but in the monsoon months (June-October) normal variations were about 1.5-5°C. Salinity changes from surface to the bottom were also very wide. In the pre-monsoon months, January to May, when the salinity is at about its maximum, practically no change is encountered from surface to the bottom. But from June to August when there is a sharp decline in the surface salinity, the bottom salinity remains high. This indicates that wide fluctuations in the salinity due to the influx of freshwater during the monsoon months are only confined to the top-most layers and that the sharp decrease in temperature is not associated with a similar decrease in salinity at the bottom. Total alkalinity shows a direct correlation with the salinity and so has the *p*H. In marked contrast to the alkalinity, the oxygen values show an inverse correlation with the salinity, i.e. from May onwards when the surface oxygen is increasing, the bottom oxygen shows a sharp decline, reaching its minimum of less than 0.5 ml/L in August. During this period the phosphates show high values and same is the case with other

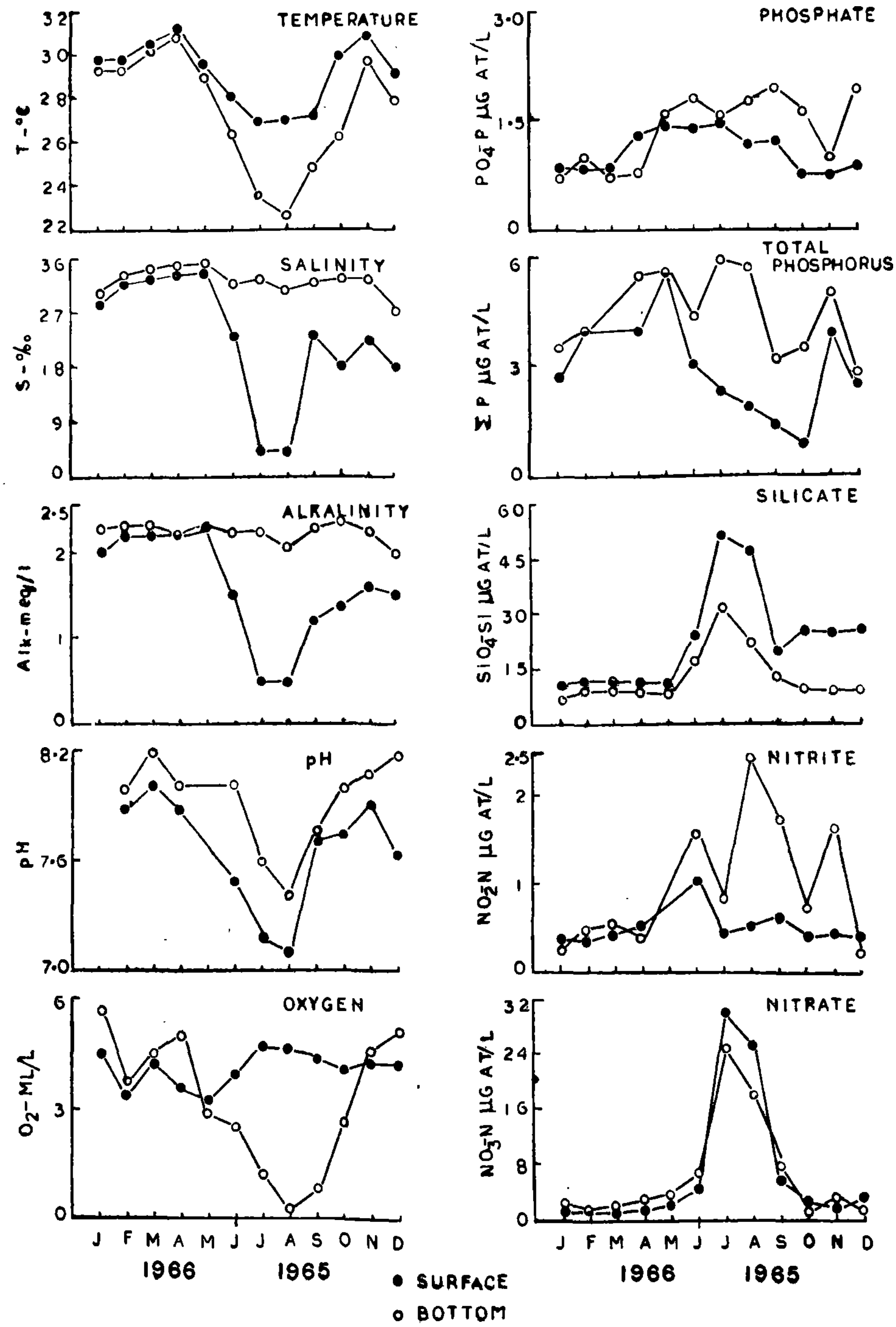

FIG. 1. Hydrographical features during the year 1965-66 at Station 1 fixed in the inshore regions of Cochin. Closed circles refer to the values at the surface and open circles to the bottom.

TABLE I

Values of temperature, salinity and oxygen at station 2 in some months of the year 1965-66

	Months						
	1966				1965		
	February	March	April	May	October	November	December
Temperature °C							
Surface	28.80	30.00	31.00	29.50	28.10	29.00	29.00
Bottom (30 M)	28.00	29.25	29.50	29.00	24.52	28.40	28.00
Salinity ‰							
Surface	33.13	34.21	34.54	35.34	27.35	35.23	32.83
Bottom (30 M)	33.89	34.57	35.24	35.39	35.35	35.41	33.51
Oxygen ml/L							
Surface	4.34	3.68	4.92	4.77	5.43	5.16	4.78
Bottom (30 M)	3.31	4.05	4.24	3.77	0.28	4.21	3.56

nutrients (silicate, nitrite and nitrate). Almost all nutrients record peak values from June to August (Fig. 1).

Unfortunately, at station 2 similar data on all related parameters could not be obtained throughout the year. However, the values of temperature, salinity and oxygen for both surface and bottom are given in Table I for a period of seven months. It can be seen from the table that within the limits of the available data, the changes in temperature, salinity and oxygen are very similar to what has been shown at Station 1, except that the variations in salinity at the two depths (surface and bottom) are not very pronounced.

From the hydrographic conditions at the two stations presented above it is clear that if temperature, salinity, oxygen and nutrients are taken as the chief criteria, the inshore region begins to reflect the characteristics of upwelled water from June to October. Probably in June there seems an influx of cold, saline and poorly-oxygenated water, rich in nutrient, towards the shore which continues with varying degrees till about October.

Figure 2 shows the catches of fish and prawns. It can be seen from the figure that, neglecting random variations, the catches of both fish and prawns were minimum from June to September. This cannot be attributed to poor fishing effort as the data presented in Figure 2 are only related to such vessels which operate throughout the year and which allow a fair comparison of monthly hauls. Seasonal changes in temperature and oxygen when plotted along with the fish and prawn catches (Fig. 2) fell in accordance with each other i.e., minimum values of temperature and oxygen at the bottom coincided with lowest fish and prawn catches.

The main fishing season along the west coast, (leaving aside the bigger fishing boats of 50 ft and above which operate throughout the year) generally starts in October and ends in May. The termination of the fishing season is partly because the sea becomes rough and the weather due to heavy rain is unfavourable for fishing; and partly because of a general feeling amongst the fishermen that due to lack of fish, fishing in the inshore waters is not very economical.

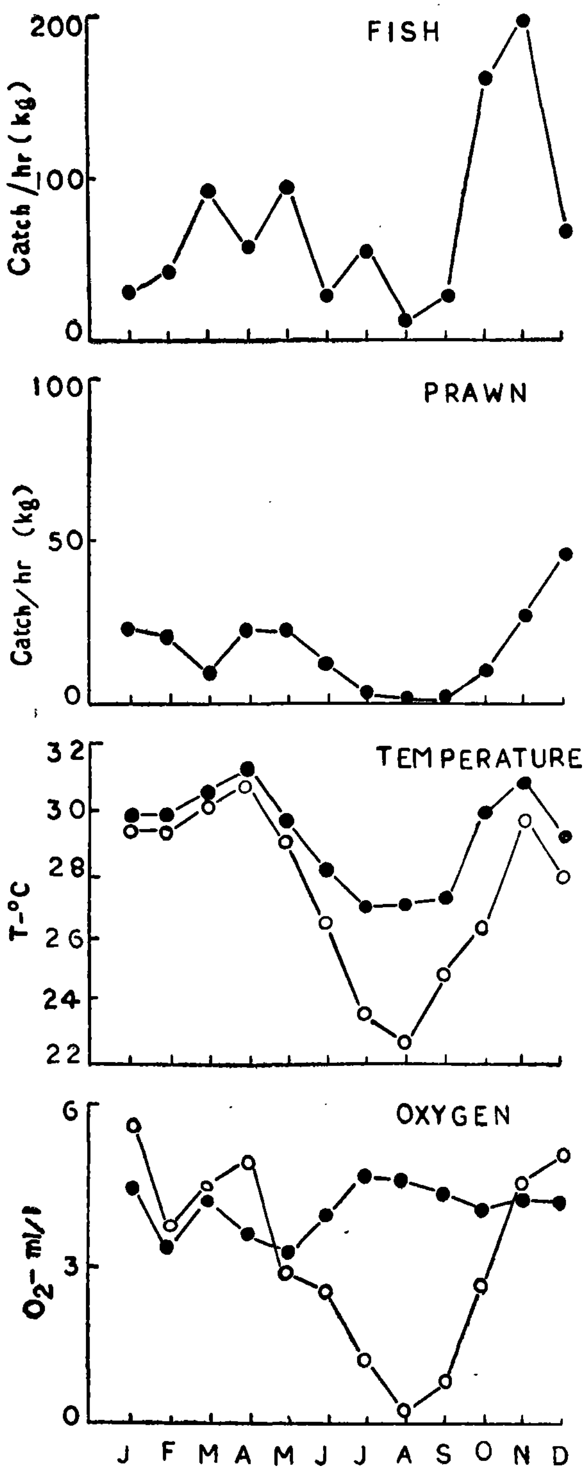

FIG. 2. Seasonal variations in fish and prawn catches of Cochin area during the year 1965-66. The seasonal changes in temperature and oxygen have also been included in the figure to show their possible influence on fish and prawn catches. For temperature and oxygen, see Fig. 1.

One of the important characteristics of the Arabian Sea is that it is greatly influenced by the monsoon cycle. The south-west Indian coast gets the full force of both S.W. and N.E. monsoons. The total annual rainfall in the Cochin area is about 3200 mm, of which nearly 75% occurs from May-September. Many complex and dynamical changes of water circulation and mixing processes have been reported in the Arabian Sea during the two monsoon periods. Although the period when widespread upwelling has been reported seems to be the two monsoons, from the available data it appears that the phenomenon is not well synchronized throughout the west coast at the same time. It seems to be delayed in latitudes further north. Thus, around Ceylon and the southern-most parts of India, from Cape Comorin to Calicut, it occurs during the S.W. monsoon, August to October (Schott 1935; Banse 1959) and more specifically in the Cochin area from late August to October (Ramamirtham and Jayaraman 1960). Around Bombay it has been shown to occur during the period of N. E. monsoon, October-December (Carruthers *et al.* 1959) and along the Bombay and Saurashtra coasts, the possibility of upwelling has been indicated during December to February (Jayaraman and Gogate 1957).

The seasonal upwelling and the associated upward movement of oxygen-deficient water seem to regulate the local fisheries. The termination of the fishing season towards the end of May, therefore, seems to coincide with a decrease in fish abundance from the inshore regions. In the Bombay region the fish, in order to avoid low oxygen concentration, has been reported to migrate towards the shallow regions, near the coast (Carruthers *et al.* 1959). This is because the influx of poorly-oxygenated water does not reach very close to the shore. But in the Cochin area the upwelled water not only reaches the near-shore waters (10 m depth), but its effect is even felt in the lower reaches of the backwaters (Ramamirtham and Jayaraman 1963). This may probably be due to the shelf region being narrow in the Cochin area and very wide along the Bombay region, and presumably for this reason the fish migration does not occur towards the inshore waters of the Cochin area. There is, however, an interesting instance on record by the present authors (during one of the cruises of 'R V. Varuna' in early October), when the poorly-oxygenated water was still prevalent at the bottom (Table I), repeated trawling near Cochin resulted in very poor catches. But during the same cruise, about 50 miles down south, near Quilon, trawling was most encouraging. An examination of water taken from 30 m and below showed the oxygen content to be appreciably higher than at Cochin. This confirms that the disappearance of fish shoals from one locality is to avoid the poorly-oxygenated water and that their migration seems to be either directed towards other coastal regions or towards deeper water, probably in such areas where dissolved oxygen is not very low. It may even be directed towards the surface, in which case, the operation of non-mechanised country-crafts, which invloves the use of various indigenous gears whose working range is limited to a few metres near the surface, would be more useful than trawling, particularly for prawns and soles which have a limited migratory power.

To sum up it seems that the seasonal fluctuations of the fisheries of the west Indian coast are governed, to some extent, by the intensity of upwelling, and since its time and duration vary from one region to the other and these may not be repeated with utmost accuracy and intensity year after year, it may eventually prove to be one of the main factors controlling the seasonal abundance of fish in a particular region. In other words, while the phenomenon of upwelling is very important in replenishing the nutrients of the impoverished euphotic zone and increasing the phytoplankton productivity and finally the fish catches, its influence during the season initially becomes a deterrent to fish life in many ways. Firstly, it very often leads to mass fish mortality by sudden changes in temperature, salinity or due to the influx of oxygen-deficient water which is well-known in the Arabian Sea (Brongersma-Sanders 1957; Foxton 1965). Secondly, the enrichment of water with nutrients produces an intense outburst of phytoplankton bloom whose rapid growth in the absence of secondary consumers such as zooplankton and fish, leads to anaerobiosis which becomes a further threat to animal life (Ryther and Menzel 1965). Finally, it gives rise to an accelerated growth of a few organisms or the red-tide — a phenomenon of common occurrence along the south-west coast (Bhimachar and George 1950; Subrahmanyan 1954; Prakash and Sarma 1964). It is interesting to note that the period when the red-tides have generally been reported, September to November, coincides with the end of the upwelling season, when the weather is warmer with far greater sunshine hours than during the monsoon months. Very often, mass mortalities of fish and invertebrates have been found associated with the blooms during this season.

From November onwards the changes reported in the sea have been termed as "sinking" which are followed by stable conditions till April (Ramamirtham and Jayaraman 1960). It may be recalled that fishing season starts from October when both fish and prawns begin to reappear in large numbers in coastal waters. It is gradually intensified and the peak season approaches during a period when stable conditions begin to prevail in the sea.

Acknowledgement

We wish to thank Dr. N. K. Panikkar, for many helpful discussions on this problem.

References

Banse, K. (1959). On upwelling and bottom-trawling off the south-west coast of India. *J. mar. biol. Ass. India*, **1**, 33-49.

——— (1966). Further observations on the upwelling off the west coast of India, and its biological effects. Paper presented in the *Second Int. Oceanogr. Congr., Moscow.*

Bhimachar, B. S., and George, P. C. (1950). Abrupt set-backs in the fisheries of the Malabar and Kanara coasts and "Red water" phenomenon as their probable cause. *Proc. Indian Acad. Sci.*, **31**, 339-350.

Brongersma-Sanders, M. (1957). Mass mortality in the sea. *Geol. Soc. Am. Mem.*, **67**, 941-1010.

Carruthers, J. N., Gogate, S. S., Naidu, J. R., and Laevastu, T. (1959). Shorewards upslope of the layer of minimum oxygen off Bombay; its influence on marine biology, especially fisheries. *Nature, Lond.*, **183**, 1084-1087.

Foxton, P. (1965). A mass fish mortality on the Somali coast. *Deep-Sea Res.*, **12**, 17-19.

Jayaraman, R., and Gogate, S. S. (1957). Salinity and temperature variations in the surface waters of the Arabian Sea off the Bombay and Saurashtra coasts. *Proc. Indian Acad. Sci.*, **45**, 151-164.

Jayaraman, R., and Seshappa, G. (1957). Phosphorus cycle in the sea with particular reference to tropical inshore waters. *Proc. Indian Acad. Sci.*, **46**, 110-125.

LaFond, E. C. (1955). On upwelling and fisheries. *Curr. Sci.*, **24**, 253-255.

Panikkar, N. K., and Jayaraman, R. (1966). Biological and oceanographic differences between the Arabian Sea and the Bay of Bengal as observed from the Indian region. *Proc. Indian Acad. Sci.*, **54**, 231-240.

Pradhan, L. B., and Reddy, C. V. G. (1962). Fluctuations in mackerel landings at Calicut in relation to hydrographical factors. *Indian J. Fish.*, **1**, 100-109.

Prakash, A., and Sarma, A. H. V. (1964). The occurrence of red water phenomenon on the west coast of India. *Curr. Sci.*, **33**, 168-170.

Prasad, R. R. (1966). Recent advances in the study of production in the Indian Ocean. Paper presented in the *Second Int. Oceanogr. Congr., Moscow.*

Prasad, R. R., and Nair, P.V. R. (1963). Studies on organic production—1. Gulf of Mannar. *J. mar. biol. Ass. India*, **5**, 1-26.

Ramamirtham, C. P., and Jayaraman, R. (1960). Hydrographical features of the continental shelf waters off Cochin during the years 1958 and 1959. *J. mar. biol. Ass. India*, **2**, 199-207.

————(1963). Some aspects of the hydrographical conditions of the backwater around Wellington Island (Cochin). *J. mar. biol. Ass. India*, **5**, 170-177.

Rao, L. V. G., and Jayaraman, R. (1966). Upwelling in the Minicoy region of the Arabian Sea *Curr. Sci.*, **35**, 378-380.

Reddy, C. V. G., and Sankaranarayanan, V. N. (1968). Distribution of nutrients in the shelf waters of the Arabian Sea along the west coast of India. *Proc. Symp. Indian Ocean, Bull. natn. Inst. Sci. India*, No. 38, Part 1, 206-220.

Ryther, J.H., and Menzel, D. W. (1965). On the production, composition and distribution of organic matter in the Western Arabian Sea. *Deep-Sea Res.*, **12**, 199-209.

Ryther, J. H., Pease, A. K., Bakun, A., and Jones, M. M. (1966). Primary organic production in relation to the chemistry and hydrography of Western Indian Ocean. *Limnol. Oceanogr.*, **11**, 371-380.

Sastry, A. A. R., and Myrland, P. (1959). Distribution of temperature, salinity and density in the Arabian Sea along the South Malabar Coast (South India) during the post-monsoon season. *Indian J. Fish.*, **2**, 223-255.

Schott, G. (1935). Geographie des Indischen and Stillen Ozeans. Boysen, Hamburg.

Strickland, J. D. H., and Parsons, T. R. (1960). A manual of sea water analysis. *Fish. Res. Bd Can.*, Bull. No. 125, 185 pp.

Subrahmanyan, R. (1954). On the life-history and ecology of *Hornellia marina* Gen. et sp. nov., (Chloromonadineae) causing green discoloration of the sea and mortality among marine organisms off the Malabar coast. *Indian J. Fish.*, **1**, 182-203.

————(1959). Studies on the phytoplankton of the West Coast of India, Parts I and II. *Proc. Indian Acad. Sci.*, **50**, 113-252.

SEASONAL VARIATION IN HEAT FLUX FROM THE SEA SURFACE OVER THE BAY OF BENGAL

by R. RAMANADHAM, G. R. LAKSHMANA RAO *and* D. P. RAO

Reprinted from *Bull. natn. Inst. Sci. India*, no. 38, 1968, p. 1004-1010

SEASONAL VARIATION IN HEAT FLUX FROM THE SEA SURFACE OVER THE BAY OF BENGAL

by R. RAMANADHAM, G. R. LAKSHMANA RAO *and* D. P. RAO*

Department of Meteorology & Oceanography, Andhra University, Waltair

The seasonal variations in the flow of heat flux from the sea surface to the atmosphere over the Bay of Bengal are studied using the data, Dry and Wet bulb temperatures, wind speed and sea surface temperature, supplied by India Meteorological Department. Sensible and latent heat transfer, evaporation and Bowen's ratio are evaluated using turbulance transfer formulae for each two-degree-square area of the Bay of Bengal. The evaporation exhibits a double maxima one in winter and the other in south-west monsoon period with a minimum in the summer (hot season). The sensible heat transfer from the sea surface to the atmosphere, taken as positive is found all over the Bay during the winter season and the retreating period of south-west monsoon. In the earlier period of south-west monsoon also the sensible heat transfer is positive except over south-west part of the Bay. In the summer season the sensible heat transfer is reversed over the central and northern parts of the Bay. The Bowen's ratio is computed all over the Bay. The results are discussed in relation to climatic factors.

INTRODUCTION

A knowledge of the rate of energy exchange between sea and atmosphere is an essential requirement for a proper study of general circulation of atmosphere and ocean. Water vapour, having energy of latent heat which it can supply to its environment when it condenses, plays a prominent part in the initiation and development of weather systems.

Direct measurements of evaporation were made from pans placed on board of German expedition vessels during 1890-1900. But Schmidt and other workers proved that the evaporation from pan was not representative of sea surface. Evaporation and magnitude of the pan coefficient were found uncertain.

The classical work was carried out during 1930-40, by Rossby and Montgomery (1935, 1936) and Montgomery (1940). Their aims were a quantitative formulation of the turbulent structures at the air-sea interface and method of deducing thereby the fluxes of heat, moisture and momentum transfer from the ocean surface through the lowest layers of air above. In the intervening years, this approach has been refined and tested critically by Priestely (1959), Sheppard (1958) and Deacon, Sheppard and Webb (1956).

Sverdrup (1937) suggested a mass transfer equation for computing evaporation which is followed by many research workers in this field. Later Jacobs studied extensively evaporation over North Pacific and North Atlantic Oceans and discussed all the theoretical methods and arrived at a mean evaporation factor in a semi-empirical fashion. Budyko (1956) used transfer formulae with a coefficient for evaporation study, differing only a few per cent than that used by Jacobs.

*Present Address: National Institute of Oceanography, (CSIR), Panjim, Goa.

Investigation on energy transfer over North Indian ocean is very limited. Wust (1936) published the annual latitudinal evaporation values and Albrecht (1949) prepared charts for February and August. In his Atlas of Heat Balance for the oceans, Budyko (1955) gave charts of heat balances parameteres for all the twelve months using climatic data for areas of size 5° lat. and 10° Long. Venkateswaran (1956) studied seasonal variation of evaporation and annual sensible heat transfer by interpolating 5-degree-square values for the wet bulb depression from the Atlas of climatic charts of the ocean and similar values for the air and sea surface temperatures from Monthly Meteorological Charts of the Indian Ocean. In his study of evaporation from North Indian Ocean including the Red-sea and Persian Gulf, Prevett (1959) published monthly charts of evaporation for each 5-degree-square by using a modified form of Jacob's formula and climatic data supplied by the Metrological Office, London.

Methods and Data

The details of the method (Malkus 1962) by means of which evaporation and sensible heat transfer have been determined for the region under study are given briefly. The useful forms of the exchange formulae for each property of interest are:

$$\tau = K_m \frac{du}{dz} \qquad \text{........(1)}$$

$$Q_s = C_p \, K_s \frac{T}{\theta} \frac{d\theta}{dz} \approx - C_p \, K_s \frac{dT}{dz} \qquad \text{........(2)}$$

and

$$Q_e = L\,E = - L\,K_e \frac{dQ}{dz} \qquad \text{........(3)}$$

Here standard notation is followed. It will be now assumed, that the height above the sea at which all the three atmospheric properties are measured, is identical and that

$$K_m = K_s = K_e = K \qquad \text{........(4)}$$

so that $K = \tau / \frac{du}{dz}$ ....(5)

Substituting (5) into (2) and (3) and further using

$$\tau_o = \rho \, C_D \, u_a^2 \qquad \text{........... (6)}$$

where the subscript '*o*' refers to the surface and 'a' to the anemometer height. C_D is the drag coefficient which can be expressed in terms of surface roughness, anemometer height and Von Karman's constant.

We express the derivatives in terms of finite differences for the vertical intervals $\Delta z = z_a - z_o$, so that

$$\left.\begin{aligned} \Delta u &= (u_a - o) = u_a \\ \Delta T &= (T_a - T_o) = -(T_o - T_a) \\ \Delta Q &= (Q_a - Q_o) = -(Q_o - Q_a) \end{aligned}\right\} \qquad \text{............(7)}$$

Substituting (4), (5), (6) and (7) into (1)-(3), we obtain three transfer equations.

$$\tau_o = \rho \, C_D \, u_a^2 \qquad \text{........(8)}$$

$$Q_s = \rho \, C_D \, C_p \, (T_o - T_a) \, u_a \qquad \text{............(9)}$$

$$Q_e = LE = \rho L C_D \, (Q_o - Q_a) \, u_a \qquad \text{............(10)}$$

The value of C_D is taken as 1.4×10^{-3} for a mean wind speed of 15 knots from the graph given by Deacon, Sheppard and Webb (1956). In eqn (10) the specific humidity gradient is replaced by vapour pressure gradient and the wind speed is used in knots and substituting the values of ρ, L and C_p in eqns (9) and (10).

$$Q_s = 1.85\ (t_o - T_a)\ u_a\ gm.cal/cm^2/day \qquad \ldots\ldots\ldots\ldots(11)$$

and

$$E = 4.73 \times 10^{-3}\ (e_o - e_a)\ u_a\ cm/day \qquad \ldots\ldots\ldots\ldots(12)$$

The meteorological data used in this investigation is supplied by Marine Section, India Meteorological Department, Poona. The average values of the meteorological parameters, dry and wet bulb temperatures, sea surface temperature and wind speed are computed for each two-degree-square of the Bay of Bengal between 0-20° Lat. and 80-100° Long. From the sea surface temperature T_0 the saturated vapour pressure is obtained from the formula $e_0 = 0.98\ e_d$ where e_d is the saturated vapour pressure at temperature T_0 and 0.98 is a correction due to presence of dissolved salts in the sea water. January, April, July and October are selected for winter, summer, south-west monsoon and retreating south-west monsoon respectively. Monthly values of sensible heat transfer and evaporation from each 2-degree-square area of the Bay are estimated by using above eqn (11) and (12) respectively. In the present investigation results of the preliminary analysis are discussed.

SENSIBLE HEAT TRANSFER : Q_s

In the month of January, the north-east monsoon prevails over the Bay. The sensible heat transfer is from the sea surface to the atmosphere all over the Bay except the eastern parts of the Bay and a small patch of area over North-west Bay where it is reversed (Fig. 1). The Q_s values are maximum in the southern parts of the Bay and gradually decrease with latitude towards north. Near the head of the Bay again the magnitude of Q_s is increased. The same trend is maintained with an increase in magnitude over the southern Bay during the month of April and a reversal of Q_s over the northern Bay. The atmosphere receives the sensible heat energy in the Southern Bay and the same is partly returned to the ocean surface in the Northern Bay and the variation of Q_s appears to be latitudinal. With the advent of south-west monsoon reaching its maximum in July there is complete transformation of sensible heat field all over the Bay. With consistent strong winds blowing over northern parts of the Bay, having sufficient sea-air temperature difference maintained, the sensible heat transfer reaches its maximum value for all seasons exceeding 35 g cal/cm²/day. In the south there is a secondary maximum over the eastern parts of the Bay and the value of Q_s decreases towards west where the flow of Q_s is reversed. During the month of October, with the retreat of south-west monsoon the Q_s maximum is shifted to the southern parts of the Bay having minimum over the central parts. During this month practically all over the Bay the atmosphere receives the energy across sea-air interface.

Even though the sensible heat transfer is mainly governed by the incoming solar radiation and the characteristics of the prevailing air-masses in different seasons, the ocean circulation is considered to be one of the important parameters when similar studies are made in other oceans. The circulation in the Bay of Bengal

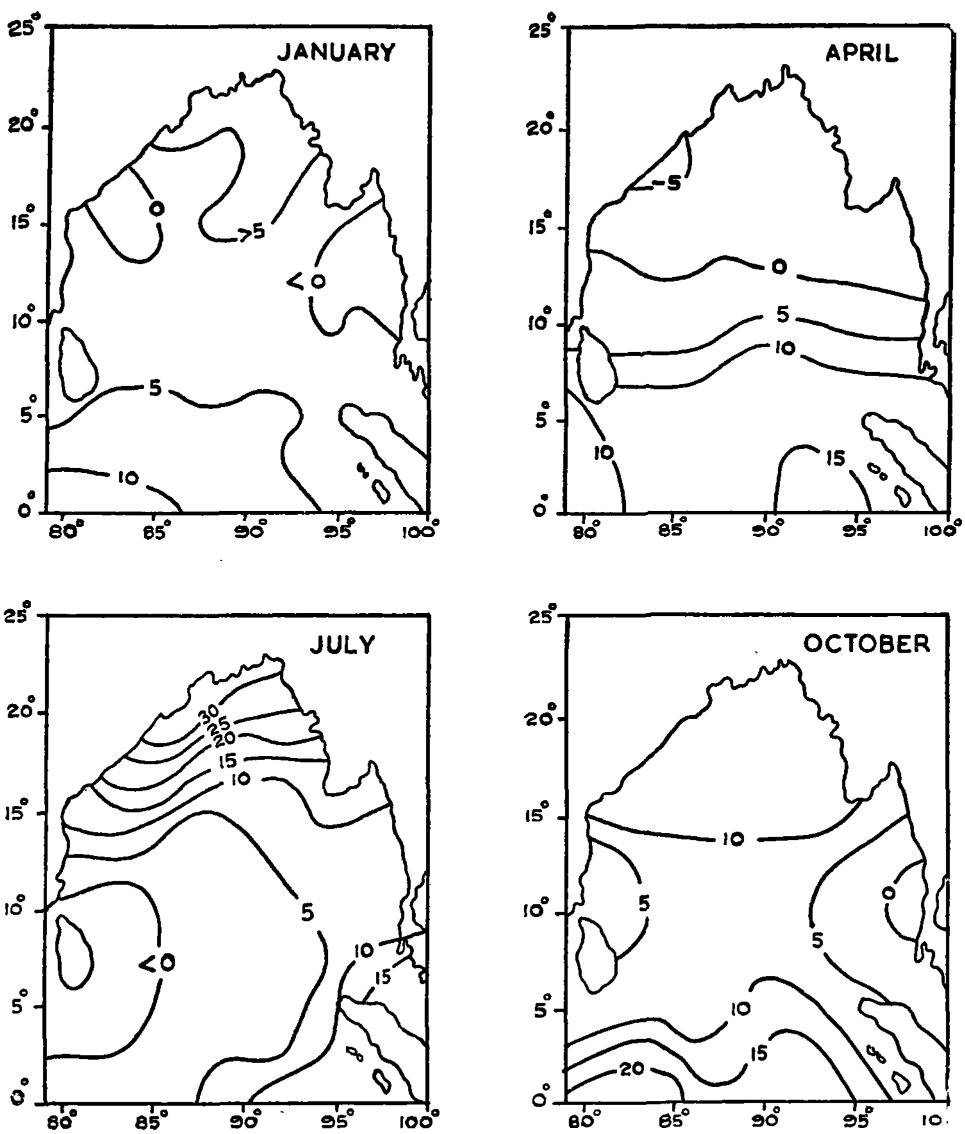

FIG. 1. Sensible Heat Transfer over the Bay of Bengal.

is greatly influenced by the monsoonal winds. During south-west monsoon season, the general flow in the central and southern Bay is from west to east and during north-east monsoon the flow is east to west. In both cases the flow is directed northerly on one side of the Bay and southerly on the other side. This type of circulation continuously renews the cold waters of the Bay by the inflowing warm equatorial waters and maintained reasonably high average sea surface temperature over the whole Bay during winter. The cold continental air flowing over the Bay gives rise to strong positive temperature gradients which show a gradual increase from south to north. During the south-west monsoon period the sea surface temperature increases towards north due to incoming solar radiation. Further the seasonal low pressure system produces high winds at the heat of the Bay which contributes for the increased sensible heat transfer towards the head of the Bay. The warm waters of Red Sea origin which are flowing from Arabian Sea into the equatorial Bay and Southern Bay may be responsible to certain extent for the high sensible heat transfer in the month of October.

EVAPORATION: E

The isopleths for all the four months are shown in figure 2. In the month of April generally the evaporation over the Bay is low compared with the other months owing to warm and indeterminate winds prevailing over most parts of the Bay. The evaporation is high in the Southern Bay and decreased towards the head of the Bay. By the month of July the S-W monsoon is active all over the Bay with consistently strong winds prevailing. The evaporation reached its maximum value over the southern Bay for all the four seasons and the minimum is maintained over N-W and N-E parts of the Bay. During the month of October when the S-W monsoon is retreating, the rate of evaporation is practically uniform over most parts of the Bay except over the N-E Bay where the minimum is maintained. By January, the evaporation decreases all over the Bay except from a small area over the central Bay.

BOWEN'S RATIO : R

The ratio between the amounts of heat given off to the atmosphere as sensible heat and that used for evaporation is called Bowen Ratio (R) and is given by $R = Q_s/Q_e$ or Q_s/LE where L is the latent heat of vapourisation of water. The general trend of Bowen Ratio is small in low latitudes and practically it remains constant throughout the year, but is greater in middle latitudes. The negative value indicates that heat is conducted from the atmosphere to the sea. On an average, the value for all oceans is about 0.1, i.e. about 10% of heat surplus is given off as sensible heat, whereas about 90% is used for evaporation.

The space distribution of the Bowen's Ratio has shown similar trends to that of sensible heat transfer. Hence only the latitudinal variation of the ratio is given in Table I. In all the four months excluding April month 'R' is minimum over the central parts of the Bay, i.e. the available energy received by the atmosphere is in the form of latent heat transfer. In the month of April, the ratio is negative over the northern Bay. In all the months the ratio is less than 10% all over the Bay except during the month of July it reached 13% over the head of the Bay.

ACKNOWLEDGEMENTS

The authors thank the India Meteorological Department for providing the marine meteorological data which is used in this investigation. The authors (G.R.L. and D.P.R.) thank the Council of Scientific & Industrial Research, New Delhi, for providing research fellowships for carrying out the above investigations.

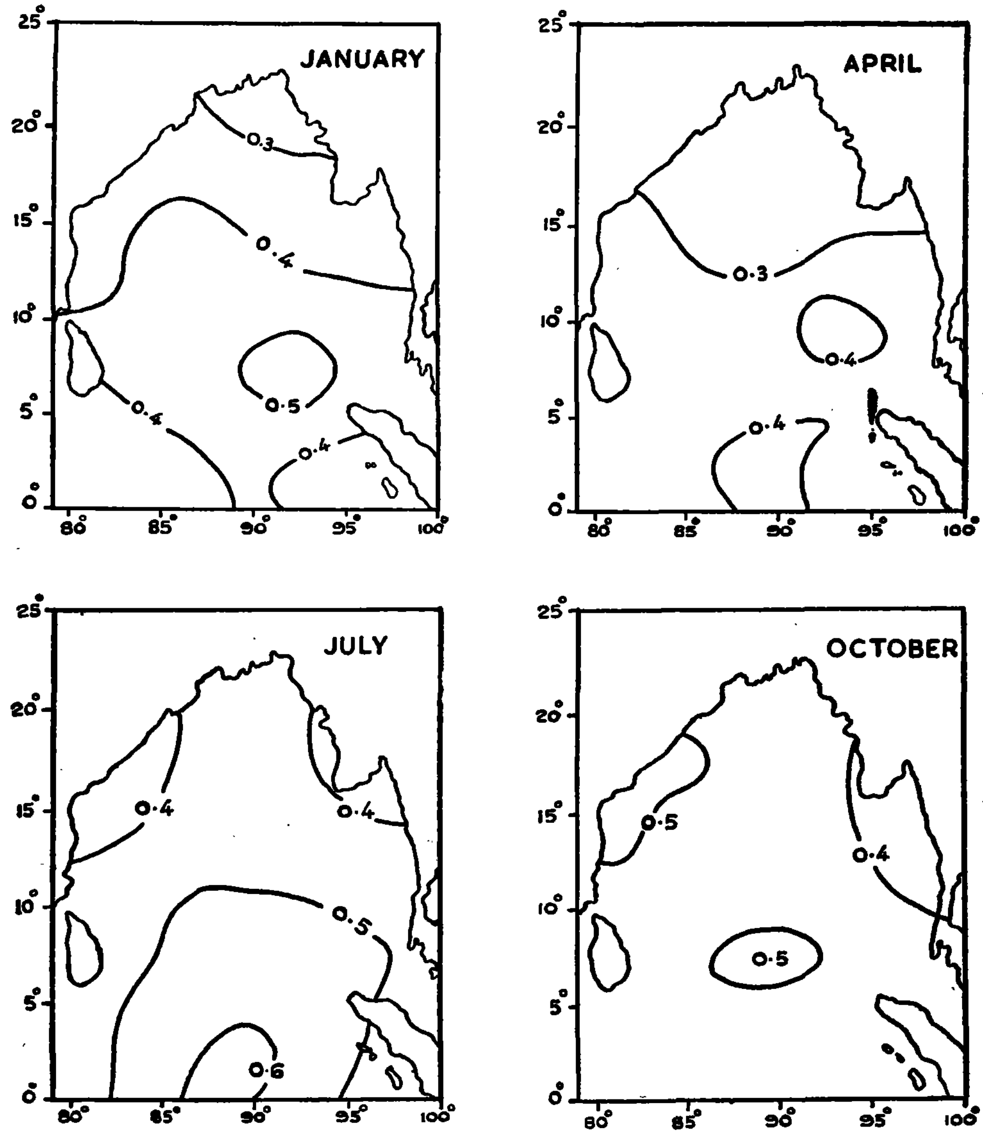

FIG. 2. Evaporation over the Bay of Bengal.

TABLE I
Bowen's Ratio

Latitude	January	April	July	October
1	0.038	0.060	0.023	0.070
3	0.027	0.054	0.005	0.048
5	0.020	0.053	0.006	0.031
7	0.015	0.050	0.020	0.020
9	0.008	0.026	0.012	0.014
11	0.005	0.008	0.003	0.017
13	0.003	0.008	0.020	0.028
15	0.012	0.016	0.044	0.044
17	0.022	0.021	0.068	0.047
19	0·400	0.018	0.130	0.084

REFERENCES

Albrecht, F. (1949). *Ber. dt. Wetterd U. S. Zone*, **29**.

Budyko, M. I. (1955). Atlas of the Heat Balance of the Earth's Surface, Leningrad, pp. 41.

————(1956). Heat Balance of the earth's surface Gidrometeorologicheskoe izdatel'stvo, Leningrad, 255 pp. (Translated by Mina A. Stepanova; translation distributed by the U. S. Weather Bureau, Washington D. C. 1958).

Deacon, E. L., Sheppard, P. A., and Webb, E. K. (1956). Wind profiles over the sea and the drag at the sea surface. *Aust. J. Phys.*, **9**, 511-541.

Jacobs, W. C. (1942). On the energy exchange between the sea and atmosphere. *J. mar. Res.*, **5** 37-66.

Miyazaki, M. (1949). Oceanographical Mag. 1, pp. 37.

Malkus, J. S. (1962). Large-scale Interactions in: "*The sea*" Vol. I, 88-294.

Montgomery, R. B. (1940). Observations of vertical humidity distribution above the ocean surface and their relation to evaporation. *Pap. phys. Oceanogr. Met.*, **7**, 30.

Priestly, C. H. B. (1959). Turbulent transfer in the Lower Atmosphere. Univ. of Chicago Press, pp. 130.

Privett, D. W. (1959). Monthly charts of evaporation from the N. Indian Ocean (including the Red Sea and Persian Gulf). *J. R. met. Soc.*, **85**, 424-428.

Rossby, C. G., and Montgomery, R. B. (1935). The layer of frictional influence in wind and ocean currents. *Pap. phys. Oceanogr. Met.*, **3**, 101.

Rossby, C. G., and Montgomery, R. B. (1936). On the momentum transfer at the sea surface. *Pap. phys. Oceanogr. Met.*, **1**, 30.

Schmidt, W. (1915). *Ann. Hydrol. mar. Met.*, **43**, 111, 169.

Sheppard, P. A. (1958). Transfer across the earth's surface and through the air above. *Q. Jl R. met. Soc.*, **84**, 205-224.

Sverdrup, H. U. (1937). On the evaporation from the Ocean. *J. mar. Res.*, **1**, 3-14.

Venkateswaran, S. V. (1956). On the evaporation from the Indian Ocean. *Indian J. Met. Geophys.*, **7**, 265-284.

Wust, G. (1936). Veroff. Inst. F. Muresh, Univ. Berl. N. F. A. Georgr. Nature Reiche—Heff,. **6**, 95.

Reprinted from *Earth and planetary science letters (Amsterdam)*, no. 6, 1969, p. 56-60

MONSOON CIRCULATION FROM OBSERVATIONS OF NATURAL RADON

RAMA
Tata Institute of Fundamental Research, Bombay 5

Received 28 March 1969

Radon concentrations have been measured in the surface air over the Indian Ocean and the Arabian Sea. The concentrations in the equatorial maritime air over the Indian Ocean are found to be low (1–4 dpm/m^3). Those in the monsoon air over the West Arabian Sea are similar but gradually increase to higher values (20–30 dpm/m^3) as the monsoon approaches the west coast of India, indicating a gradual mixing between the lower maritime air and the continental air aloft. There appears to be a significant contribution of moisture to the monsoon current by evaporation over the east Arabian Sea.

1. INTRODUCTION

During the months of June, July, August and September, a moist homogenous south westerly current of air (south west monsoon), about 5 km thick, passes over the west coast of India. Early investigations [1] led to the belief that this moist current comes from the southern latitudes of the Indian Ocean, i.e., it is a part of the southeast trades which, on crossing the equator, gets deflected into south westerly to westerly current. But, the meteorological observations made during the recent International Indian Ocean Expedition cast serious doubts on this view. These observations indicate that over the west Arabian Sea the monsoon current consists of two very distinct air masses; the lower maritime moist air mass; from the surface to about 1 km level, coming from the southern hemisphere (deflected south east trades); and the upper relatively dry continental air mass (from 1 km to about 5 km level) coming from north Africa and Saudi Arabia [2,3], with a temperature inversion between the two. As the two masses approach the west coast of India, the temperature inversion between them is destroyed and the entire 5–6 km thick layer appears as one homogenous moist air mass. The moisture content of this 5–6 km thick layer over the west coast of India exceeds 1.5 times that of its two constituent layers over the west Arabian Sea as can be seen from table 1 (the moisture contents are computed from data referred to by Desai [4]). The extra moisture in the current near the coast is of prime importance from the point of view of rainfall over the subcontinent. Two views have been advanced for the origin of this extra moisture:

(1) The moisture is introduced into the air current during its traverse over the Arabian Sea. As the two constituent air masses move eastward, there is a gradual mixing between the two and the inversion level gets lifted from 1 km upwards, till at some distance from the Indian coast the inversion completely disappears and the whole 5 km thick layer appears as single homogenous air mass. Moisture evaporated from the Arabian Sea is transported upwards as a result of mixing between the two air masses [2,5,6].

(2) The contribution of moisture by evaporation from the Arabian Sea in negligible; the moisture is fed upwards from the lower moist current itself near the west coast of India. This can result when the lower moist current is forced upwards by orography through obstruction by west coast hills. The increase is therefore only apparent [4].

It should be possible to establish the validity of either of these views if sufficient meteorological data were available to permit a study of mass balance of air and moisture in the two components of the current. A simple check is, however, possible just from a study of the interaction between the two components. According to the first view, the mixing between the two components is necessary to transport moisture from the sea surface upwards; this would obviously

Table 1
Moisture content of monsoon current over the Arabian Sea.

West Arabian Sea		West coast of India (East Arabian Sea)	
Lower Layer Surface to 900 mb	Upper Layer 900 mb to 600 mb	Homogenous Layer Surface to 900 mb	900 mb to 600 mb
1.5 g/cm^2	1.4 g/cm^2	1.7 g/cm^2	3 g/cm^2

result in bringing continental air from upper layer to lower layer. According to the second view, the air from lower layer moves upwards into the upper layer and increases its moisture content; but prominent intrusions of upper dry hot air into the lower layer are not allowed since such intrusions would reduce the water content of the lower layer in the absence of contribution of moisture from the sea surface. Thus the two views lead to quite different predictions as to the amount of continental air in the low level air over the east Arabian Sea and near the west coast of India.

Our preliminary investigation [7] revealed that the radon content of equatorial maritime air over the Indian ocean is low (1–4 dpm/m^3) while that of recent continental air such as is supposed to constitute the upper layer can be expected to be 10 to 20 times as much. Therefore, any mixing of this air downwards can be detected in an increase in the radon content of the lower layer. A study of vertical radon profiles should thus be diagnostic in studying the interaction and the consequential moisture transport between the air masses. As a first step, a study of radon content of the surface air alone, which can be carried out far more easily, should provide fair indication of the phenomenon. With this end in view, the radon contents of the surface air over the Arabian Sea and the Indian Ocean were measured during the summer monsoon of 1967 and are reported here.

2. EXPERIMENTAL

For measuring the concentrations of radon in air, a

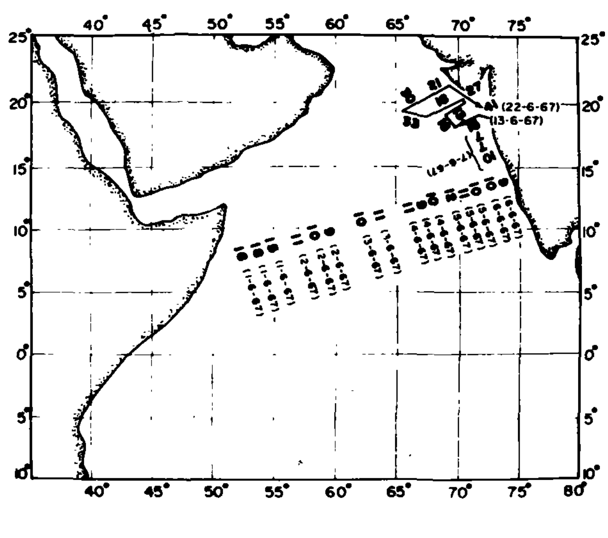

Fig. 1. Concentration of radon in surface air over the Arabian Sea and the Indian Ocean. Units (dpm/m^3).

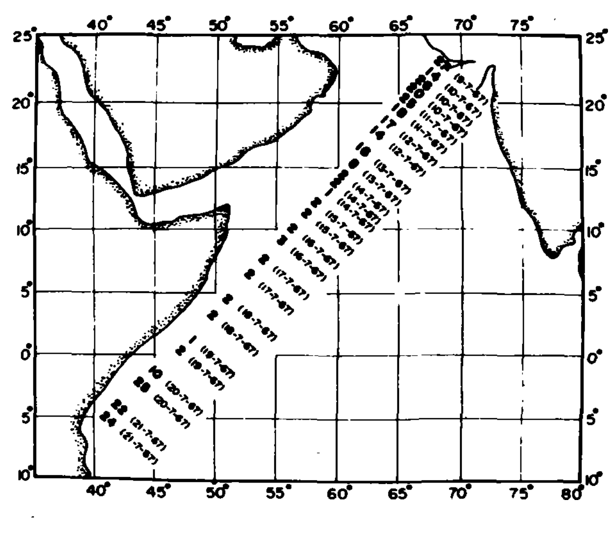

Fig. 2. Concentration of radon in surface air over the Arabian Sea and the Indian Ocean. Units (dpm/m^3).

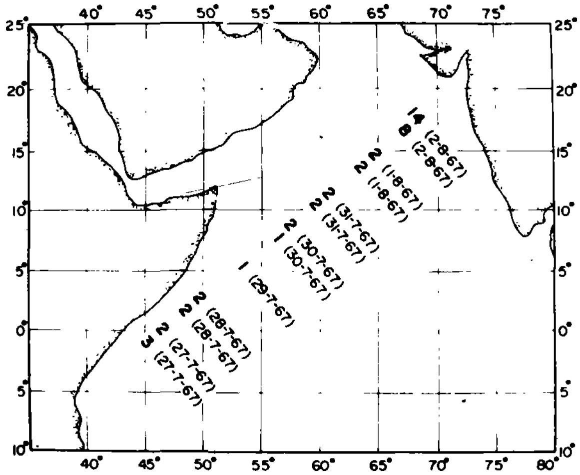

Fig. 3. Concentration of radon in surface air over the Arabian Sea and the Indian Ocean. Units (dpm/m^3).

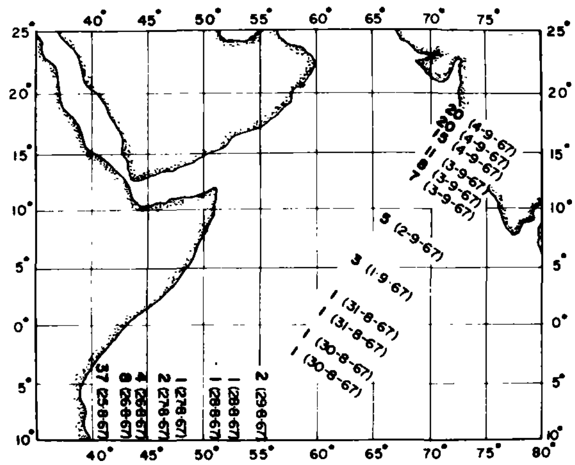

Fig. 5. Concentration of radon in surface air over the Arabian Sea and the Indian Ocean. Units (dpm/m^3).

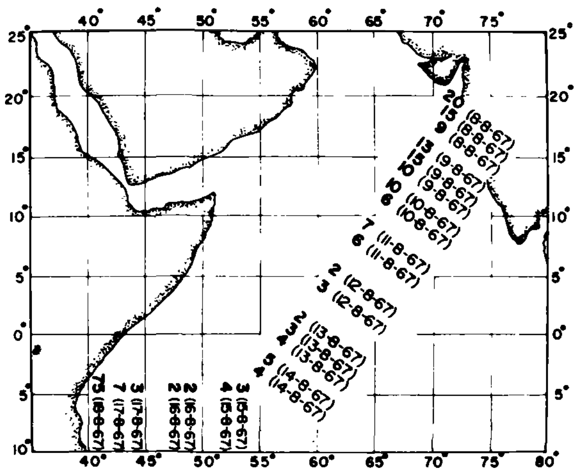

Fig. 4. Concentration of radon in surface air over the Arabian Sea and the Indian Ocean. Units (dpm/m^3).

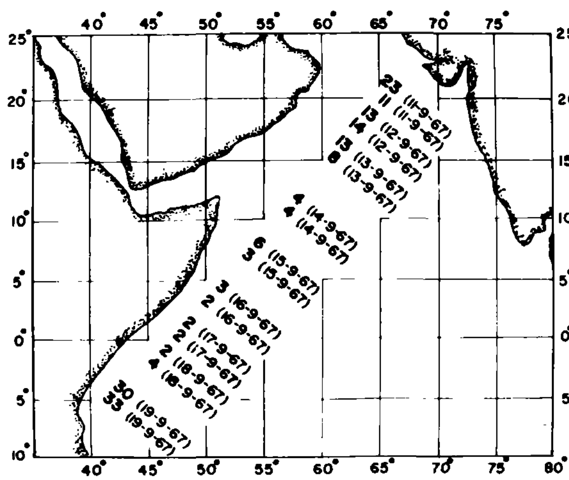

Fig. 6. Concentration of radon in surface air over the Arabian Sea and the Indian Ocean. Units (dpm/m^3).

simple and convenient method was employed. The air was filtered at constant speed (using a positive displacement pump) through a glass fibre filter for a few hours, and the decay products of radon thus collected on the filter were assayed on an end window Geiger counter. This technique was previously compared with the method of direct extraction and of counting of radon and its decay products inside a hollow scintillation counter as adopted by Moses et al. [8].

The measurements were made at deck level aboard 'State of Haryana' and 'Oceanographer' during several cruises over the Arabian Sea and the Indian Ocean. The accuracy of most measurements is better than ten percent, except in cases where the activities are ex-

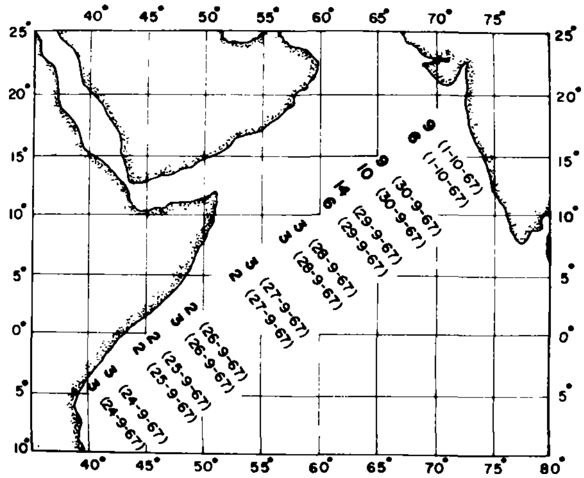

Fig. 7. Concentration of radon in surface air over the Arabian Sea and the Indian Ocean. Units (dpm/m^3).

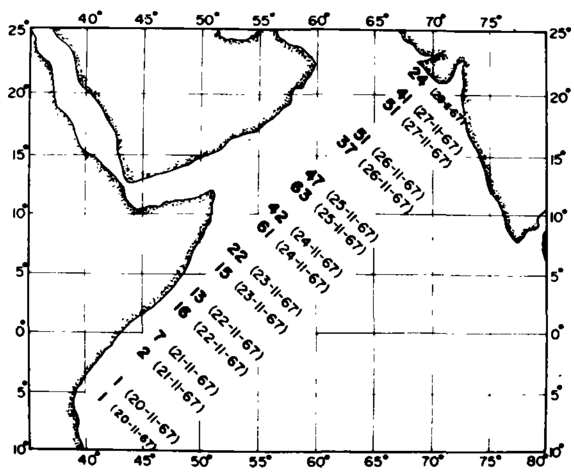

Fig. 8. Concentration of radon in surface air over the Arabian Sea and the Indian Ocean. Units (dpm/m^3).

tremely low and the counting error then may be as large as fifty percent. The accuracy of measurements is considered quite adequate for the problem in hand where we are looking for variations by large factors. A systematic error of about twenty percent in calibration may also exist but does not affect the considerations based on relative variation of concentrations.

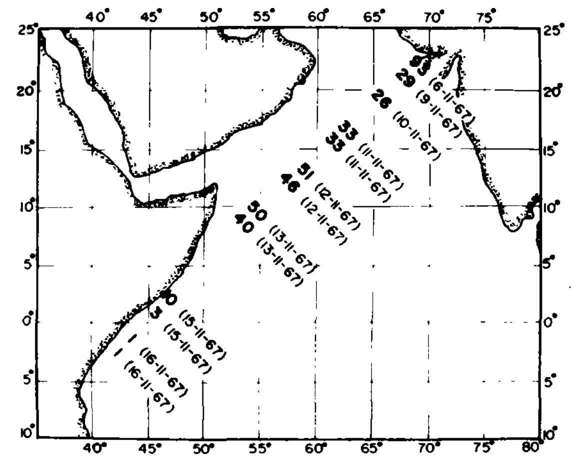

Fig. 9. Concentration of radon in surface air over the Arabian Sea and the Indian Ocean. Units (dpm/m^3).

3. RESULTS

The results of measurements made over the Arabian Sea and the Indian Ocean are shown in figs. 1–9; the radon concentrations (dpm/m^3) are shown in bold letters printed at the approximate location of sampling; the date of sampling is also indicated.

4. DISCUSSION

The observations made during the monsoon period (figs. 2 to 7) show that the radon concentration in low level air over the equatorial Indian Ocean and West Arabian Sea were very low (1–4 dpm/m^3), indicating the presence of pure maritime air mass over these regions. The low values were occasionally observed over the central Arabian Sea also but rarely over the eastern Arabian Sea. The radon concentration usually started increasing at about 65°E and reached a value of 20–30 dpm/m^3 near the west coast of India. The increase of radon in the lower current implies the introduction of continental air in it probably as a consequence of mixing from above. The component of continental air in the lower current can be correctly assessed if the radon content of the continental air in the upper layer is accurately known. The measurements at high altitudes have not yet been made, but we may obtain an indirect approximation as follows.

The air from the Indian subcontinent is known to pervade over the Arabian Sea during winter months. Its radon content in the month of November ranged from 25 to 65 dpm/m^3 (figs. 8 and 9) and averaged around 40 dpm/m^3. It may likewise be expected that the radon content of the air coming from the African continent would be about 40 dpm/m^3 at the surface and somewhat lower at higher altitudes.

The radon contents of the surface monsoon air over the east Arabian Sea range between 5 and 30 dpm/m^3. The values near the western coast of India average around 20 dpm/m^3. Comparing these with a value of $\sim$ 40 dpm/m^3 deduced for continental air in the upper current, one arrives at the conclusion that the component of the continental air in the surface air exceeds 50 percent near the coast, pointing to vigorous vertical mixing between the two air masses. In spite of a large component of continental air at the lower levels, the moisture content (and humidity mixing ratio) of the lower current does not decrease (see table 1). This is evidently possible if an adequate amount of water is introduced by evaporation from the sea surface. The data show that at least about forty percent of the extra moisture observed in the monsoon current near the coast originates from evaporation over the Arabian Sea. This appears to be appropriate interpretation of the data in terms of two-air-mass picture of the monsoon current which however needs to be verified by measuring radon in vertical profiles.

Fig. 1 shows the radon concentrations measured in a west-east traverse across the Arabian Sea just before the onset of monsoon rains, and off the Saurashtra coast just after the onset. The high concentrations in the latter arise as a consequence of mixing of continental air from above; the continental air originating from North Africa or possible in the mid-tropospheric circulation [9].

5. CONCLUSIONS

The radon measurements in the monsoon current provide a convenient method for studying the interaction and moisture transport between its two constituent air masses i.e. maritime equatorial air mass and continental African air mass. The limited data indicate that a significant amount of moisture is introduced into the current by evaporation over the east Arabian Sea.

ACKNOWLEDGEMENTS

I am grateful to Prof. M.G.K.Menon, Prof. D.Lal and Dr. F.Ostapoff for their interest in this experiment. The skillful assistance of Mr. S.G.Patil and Mr. B.I. Shaikh is greatly appreciated. I take this opportunity to express my sincere thanks for the cooperation of the captain, crew and Management of S.S.Haryana and U.S.C. and G.S.S. Oceanographer.

REFERENCES

[1] G.C.Simpson, The south west monsoon, Quart. J. Roy. Met. Soc. 47 (1921) 152.

[2] J.A.Colon, On the low level thermal stratification of. monsoon air over the Arabian Sea and its connection to the water temperature field, Technical Note 9-SAIL-1, U.S.Dept. of Commerce (1965) p. 209.

[3] C.R.V.Raman, Cyclonic vortices on either side of the equator and their implications, Proc. Symp. Met. Results of International Indian Ocean Expedition, Bombay (1965) p. 155.

[4] B.N.Desai, Relation between moisture transported across the equator and the west coast of the peninsula during the south west monsoon season, Indian J. Met. Geophys. 17 (1966) 559.

[5] A.F.Bunker, Interaction of summer monsoon air with the Arabian sea, Proc. Symp. Met. Results of International Indian Ocean Expedition, Bombay (1965) p. 3.

[6] P.R.Pisharoty, Evaporation from the Arabian Sea and the Indian Southwest monsoon, Proc. Symp. Met. Results of International Indian Ocean Expedition, Bombay (1965) p. 43.

[7] Rama, An attempt to trace the monsoon flow using natural radon, Indian J. Met. Geophys. 19 (1968) 167.

[8] H.Mosses, A.Stehney and H.F.Lucas Jr., The effect of meteorological variables upon the vertical and temporal distribution of radon, J. Geophys. Res. 65 (1960) 1223.

[9] F.R.Miller and R.N.Keshavmurty, The Arabian sea summer monsoon, Proc. Symp. Met. Results of International Indian Ocean Expedition, Bombay (1965) p. 337.

Reprinted from *Oceanogr. Mar. Biol. Ann. Rev.*, vol. 7, 1969, p. 11-30

INDIAN OCEAN SURFACE METEOROLOGY*

C. S. RAMAGE
University of Hawaii, Honolulu

The surface layers of the atmosphere are inextricably meshed with the surface layers of the ocean. Winds make waves and cause horizontal and vertical currents; heat of evaporation, released to the atmosphere when rain falls, provides most of the energy for driving the winds. Thus, in such a complex region as the Indian Ocean knowledge of the meteorology is essential in order to understand the oceanography.

The many survey papers written on the International Indian Ocean Expedition have already familiarized readers with a simplified climatological model of that ocean's monsoon circulations (see for example, Ramage, 1965). However, since this is applicable for only part of the ocean and I shall be treating the whole ocean, it would be useful to attempt first to differentiate the regions dominated by the monsoons from those not influenced by the monsoons.

In the monsoon regions the annual shift in wind direction is used by sailors and fishermen as a monsoon criterion. Therefore, one way of defining a monsoon regime over the ocean is to consider as monsoonal those areas where the directions of mean resultant winds change by more than 90° between winter and summer. This involves excluding the regions of very light winds or calms—the doldrums, where directions fluctuate widely and rapidly (Figure 1). By this criterion, the monsoons are essentially a northern hemisphere phenomenon. Only off the tropical east coast of Africa and around northern Australia is the overwhelming modifying influence of the vast southern Indian Ocean overcome by the ocean-continent interaction which produces the monsoons.

To the land-bound inhabitants of the continents bordering the Indian Ocean, monsoons signify weather changes associated with the annual changes in wind direction. Summers are wet and winters are dry (Figure 2). A comparison of Figures 1 and 2 reveals within the monsoon-wind regime double maxima of rainfall in a band extending from equatorial Africa to Cambodia. These maxima result from double maxima of heating corresponding roughly to the passage of the Sun northwards across the equator on March 21st and southwards across the equator on September 23rd. North

* Hawaii Institute of Geophysics Contribution No. 225. Supported by the Atmospheric Sciences Section, U.S. National Science Foundation, NSF Grant GA-386.

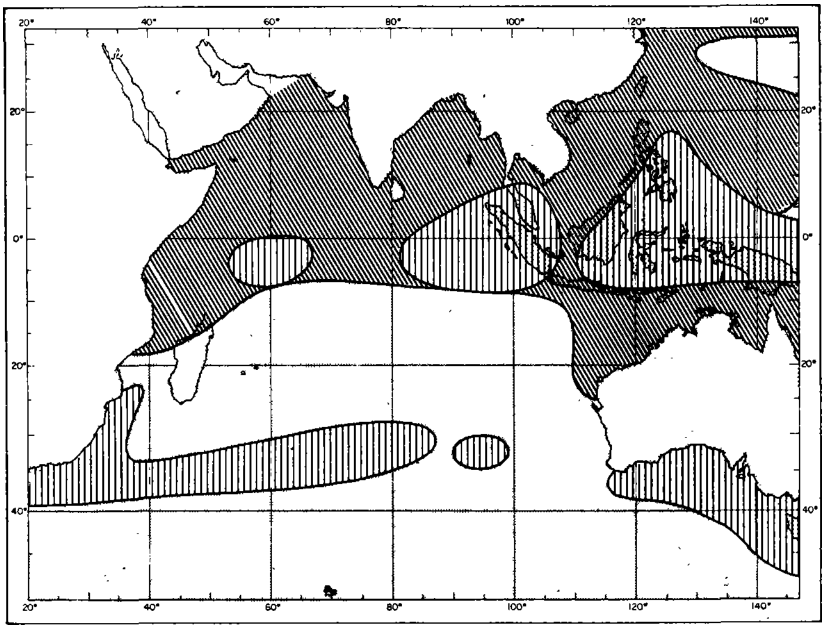

Fig. 1.—Wind direction as a monsoon criterion. A change in the mean resultant wind direction between January and July of more than 90° indicates that the ocean area possesses a monsoonal climate (diagonally hatched); direction change less than 90° (stippled); winds in both January and July less than 2·5 m sec $^{-1}$ (vertically hatched).

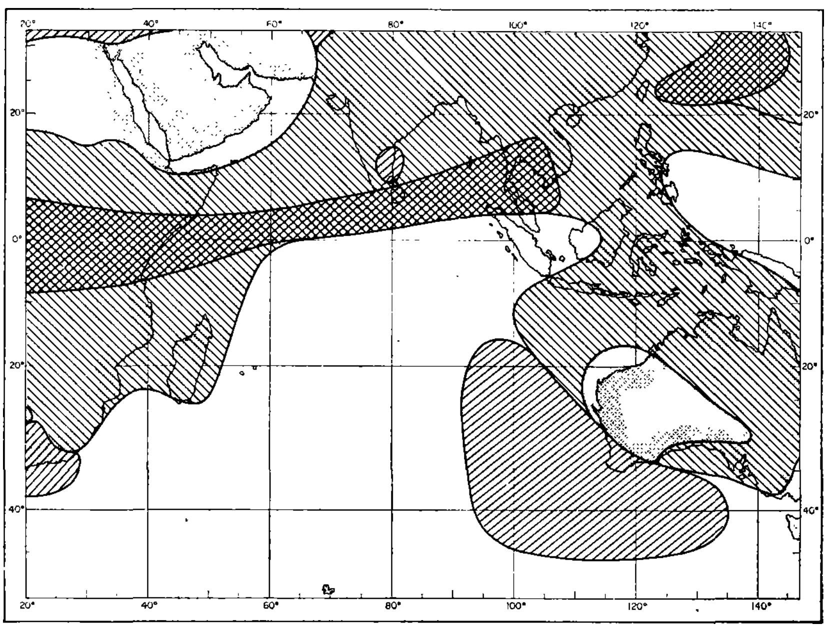

Fig. 2.—Rainfall as a monsoon criterion. Periods during which more than 75% of the annual rain falls are regionally delineated; regions with winter rainfall maximum (diagonally hatched, upward to right); regions with summer rainfall maximum (diagonally hatched, upward to left); regions with double rainfall maximum (cross hatched); regions with less than 250 mm per year are classed as deserts (stippled); regions accumulating 75% of the annual rainfall in over seven months are considered to have no seasonal maximum.

and south of this zone, around the continental periphery, rainfall possesses a single summer maximum. The region dominated by the double and summer maxima roughly coincides with the region of monsoon winds.

Since monsoon summers are cloudy and wet, and monsoon winters are fine, one would expect the difference between the winter and the summer net heat balance at the ocean surface to reflect this (Figure 3). Except for the western Arabian Sea and the western Bay of Bengal, the northern Indian Ocean gains more heat in January than in July. Strong winds and cloudy skies in July and light winds and clear skies in January outweigh greater solar radiation in July. In the monsoon regions of the southern hemisphere the effect is scarcely perceptible; however, somewhat cloudier skies and more rain in the west and stronger winds in the east, in January than in July, reduce the summer–winter difference in the net heat balance. In the doldrums, between the equator and 10° S, where skies are generally cloudy and winds light throughout the year, differences are also small.

The largest differences occur in the regions of trade winds and polar westerlies, reflecting the constancy of winds and weather and the annual change in solar radiation. Throughout the monsoon region, the annual curve of heat exchange at the sea surface is bimodal with maxima in spring and autumn and minima in summer and winter. As Wooster, Schaefer and Robinson (1967) have shown in detail for the Arabian Sea, the annual curves of sea-surface temperatures in monsoonal regions are similarly bimodal (La Violette and Mason, 1967).

In the remainder of this paper I shall distinguish between the monsoon and non-monsoon regimes. Conditions in January and conditions in July will first be described and then linked in an annual sequence using material from Van Duijnen Montijn (1952) and the U.S. Weather Bureau (1957).

Tropical cyclones, although locally and sporadically important, can be ignored as 'noise' in the large-scale circulations.

Research reports from the International Indian Ocean Expedition are already pouring out (UNESCO, 1965–onwards; Ramage, 1968a) and extensive data compilations are under way. In the final sections of this paper, I briefly discuss three topics selected from a wealth of material, namely (1) Inter-annual changes at the sea surface; (2) The Somali Current; (3) Near-equatorial and heat troughs.

CONDITIONS IN JANUARY

MONSOON REGION

North-east Monsoon

Radiational cooling over Asia exceeding that over the neighbouring ocean establishes shallow continental highs and a seaward-directed pressure

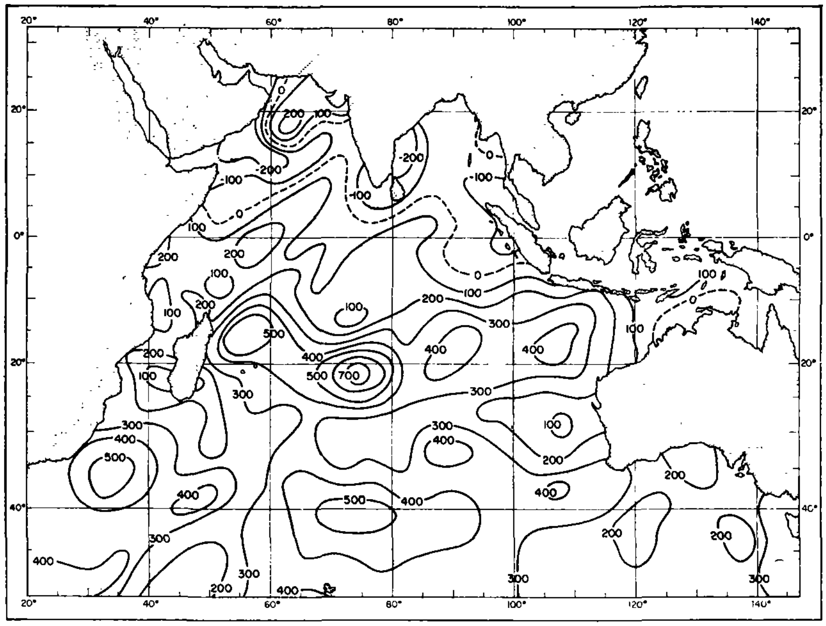

Fig. 3.—Net heat balance at the sea surface as a monsoon criterion. The difference, January minus July, is shown in units of langleys per day; computations based on Budyko (1956); away from the equator, small changes between January and July are confined to regions with wet or cloudy summers and dry sunny winters.

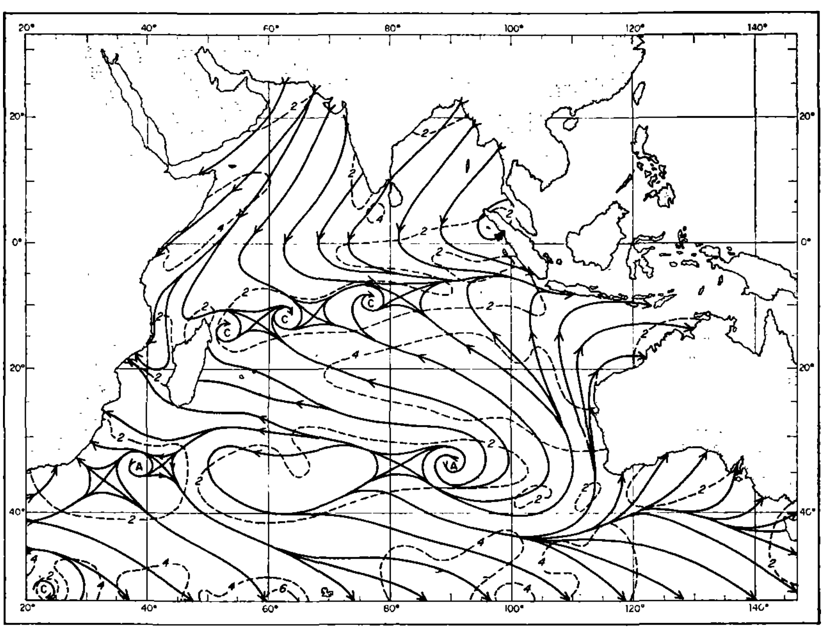

Fig. 4.—January, mean resultant surface winds. Streamlines (full lines); isotachs (broken lines) in Beaufort Force numbers; the circulation as represented by mean resultant winds is closely related to average pressure distribution; centres of average anticyclonic and cyclonic flow coincide with centres of average highs and lows; friction causes streamlines to angle across isobars toward lower pressures.

gradient. The huge Siberian polar anticyclone, source of chilling gale-force outbreaks which sweep southward across the China Seas, is effectively cut off from the Indian Ocean by the Himalayas and the contiguous mountain ranges of Afghanistan and Iran. Thus the Indian winter monsoon is a gentle phenomenon—prevailing moderate northeast winds (Figure 4) are temporarily freshened in the rear of depressions moving eastward south of the massif. Air over the continent is dry and as it flows out across the Arabian Sea and the Bay of Bengal it absorbs both heat and moisture from the ocean surface. Continuing clear skies and light winds combine to favour insolational heating over evaporative cooling so that even in mid-winter the ocean gains heat except for the central Arabian Sea and the southern Bay of Bengal (Figure 6).

Over Africa, cooling in the north and heating in the south have established a significant trans-equatorial pressure gradient, affecting the circulation 800 km to the east and extending the north-east monsoon well into the southern hemisphere (Figure 4).

Northern Hemisphere Near-equatorial Trough

Over the southern Bay of Bengal convergence, cloudiness, and squally thundery showers occur (Figure 5), generally north of a weak east–west oriented pressure trough. It is here that much of the moisture, evaporated earlier from the sea-surface by the north-east monsoon, is condensed and the released latent heat goes to warm the troposphere. The rain-shadowing of India and Ceylon weakens the trough's effectiveness over the Arabian Sea.

Southern Hemisphere Near-equatorial Trough

Anchored by heat lows over the Kalahari and Australian deserts, the pressure trough arcs northward to near 13° S over the central ocean (Figure 4). It is associated with considerable cloudiness and precipitation (Figure 5), and is the birthplace of tropical cyclones. In the trough region the ocean gains heat (Figure 6), for although clouds may significantly reduce incoming radiation and the ocean loses sensible heat to the atmosphere, light winds and high humidity minimize evaporational cooling.

The northern and southern hemisphere near-equatorial troughs and the intermediate zone of light, predominantly westerly winds comprise the 'doldrums'.

Australian Summer Monsoon

The heat low over Australia draws in trade wind air deflected from the southwest (Figure 4) (see below). Appreciable rain falls in the area of anti-clockwise-turning surface winds west of Sumatra (Figure 5) (Gordon and Taylor, 1969). Farther south, however, the tropical maritime air converging into the Australian heat low is surprisingly deficient in cloud and rain.

NON-MONSOON REGION

The non-monsoon region, south of the summer latitude of the pressure trough includes the trade winds, the subtropical ridge at about 25° S, and the polar westerlies (Figure 4).

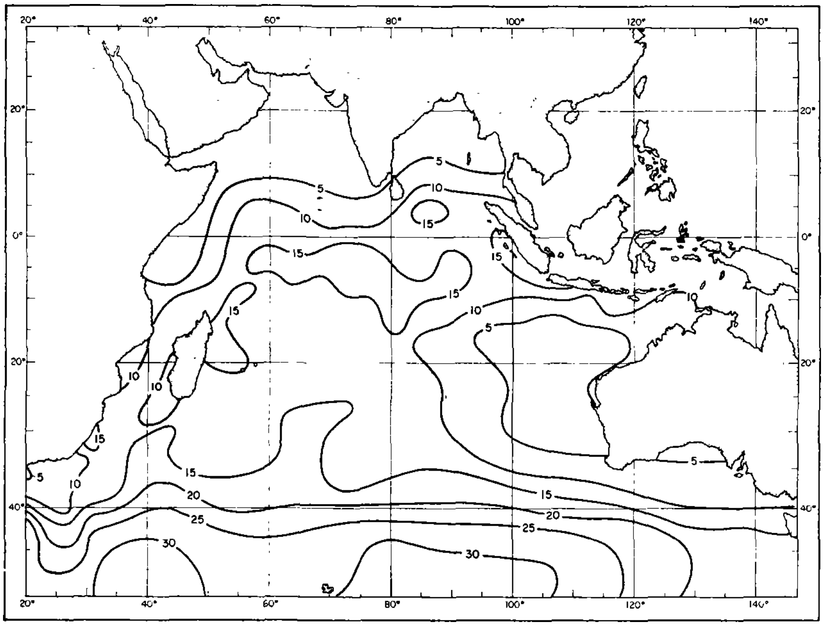

Fig. 5.—January, precipitation. Percentage of observations reporting precipitation (after U.S. Weather Bureau, 1957).

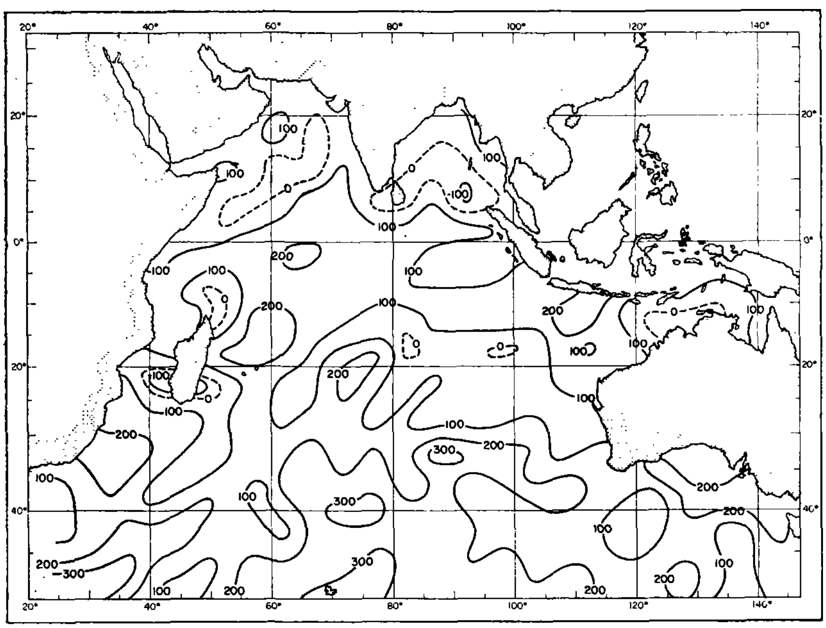

Fig. 6. January, net heat balance at the sea surface in langleys per day.

Between the trough and ridge, where the Trade Winds prevail, temperature is uniform. In the east, between the heat low over Australia and the subtropical ridge to the south-west, the pressure gradient is steep and winds are fresh and divergent, with an eastern branch spiralling inward to the heat low and a western branch sweeping around the subtropical ridge. The divergent southerlies advect and cause cold water to upwell, which in turn affects the distribution of temperature and moisture and presumably accounts for recognizable cold fronts penetrating farther equatorward than is the case in other longitudes.

In the trade wind areas farther west cloudiness is less than in the east, but, because the air is moister and flow converges toward the pressure trough, rain is more frequent (Figure 5).

The Subtropical Ridge lies about 1000 km south of the axis of minimum rainfall frequency (Figures 4 and 5). That this is a significant displacement is borne out by measurements made during the METEOR I Expedition to the South Atlantic (Ficker, 1936) where the base of the trade wind inversion was closest to the surface at 1000 to 1500 km north of the ridge. Presumably, divergence acting for some time on air outflowing from the ridge produces a downstream lowering of the inversion and precipitation decrease. The heated continent of Australia apparently displaces anticyclonic conditions southward, making the Great Australian Bight drier and less cloudy than the open Indian Ocean at the same latitudes. Beneath the ridge, because of light winds and fair weather, the net heat gain by the sea is greatest (Figure 6).

Polar Westerlies (see Palmer, 1942). South of the subtropical ridge, frequencies of fog, mist, haze, cloudy skies and precipitation increase fairly uniformly with latitude (Figure 5). Although cloud interrupts much of the incoming radiation, enough is received from the sun in this midsummer month to produce a net heating at the surface (Figure 6).

CONDITIONS IN JULY

MONSOON REGION

South-west Monsoon

Intense heating over southern Asia, particularly the desert arc extending from Somalia to north-west India, maintains vigorous heat lows and a landward-directed pressure gradient (Figure 7).

South-west winds off the coasts of Arabia and Somalia force cold water to upwell, which in turn modifies the overlying air (Figure 9) (see pages 24 and 25). Fair weather over the northern and western Arabian Sea can only be explained in terms of middle tropospheric subsidence (see page 26). Frequent heavy rains off the west coast of India, where in the mean, surface winds neither converge nor diverge, can be accounted for by development of subtropical cyclones (Miller and Keshavamurthy, 1968).

'Monsoon depressions' (having the thermal properties of tropical cyclones but seldom reaching storm intensity) develop near the head of the Bay of Bengal and, moving slowly west-north-west, merge with and reinforce the pressure trough lying along the Ganges Valley. Over the northern Bay of Bengal, these depressions maintain south-westerlies, which are weaker than those over the Arabian Sea (Figure 7). Cloudiness and considerable rain

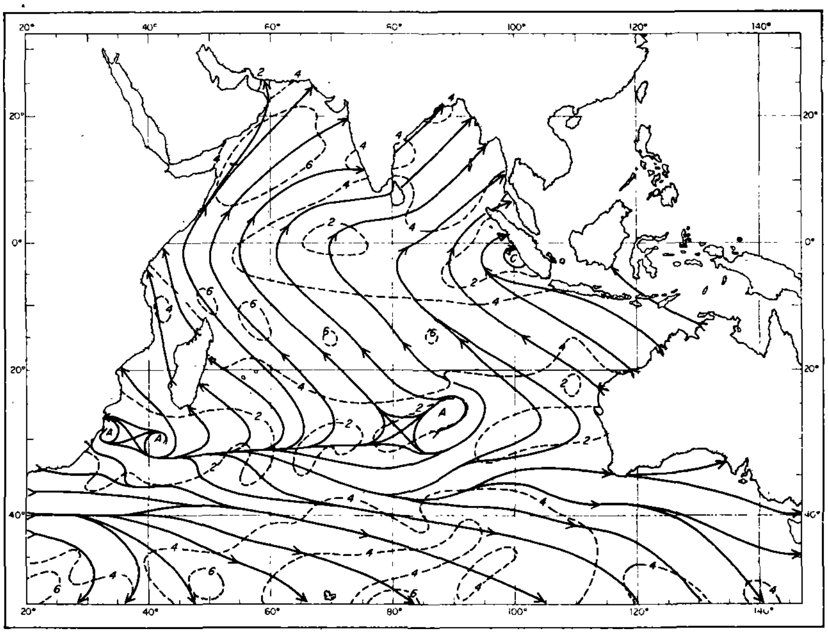

Fig. 7.—July, mean resultant surface winds. Streamlines (full lines); isotachs (broken lines) in Beaufort Force numbers.

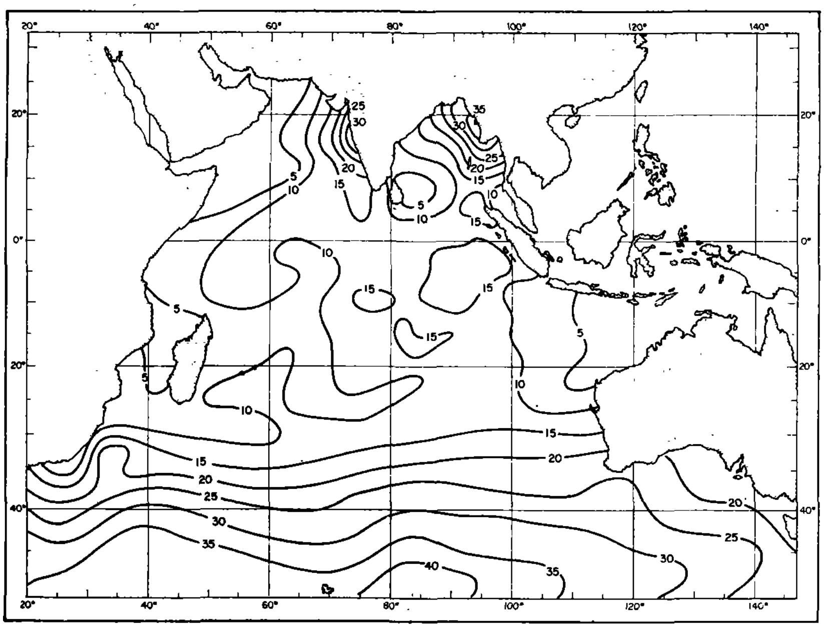

Fig. 8.—July, precipitation. Percentage of observations reporting precipitation (after U.S. Weather Bureau, 1957).

result (Figure 8). Over the southern Bay of Bengal the rain-shadowing effect of peninsular India and Ceylon extends a great distance downstream (see Figure 14). Over the north-eastern Arabian Sea and the central Bay of Bengal, evaporational cooling by strong monsoon winds and reduction of incoming solar radiation by clouds result in a net cooling of the sea surface (Figure 9) (Colon, 1964).

To the west, high pressure in the cool south and low pressure in the warm north extend the monsoon over Africa south to 20° S (Figure 7). Blowing SSE rather than SW this monsoon branch belongs in effect to the wintertime trade winds of the southern hemisphere (see page 20).

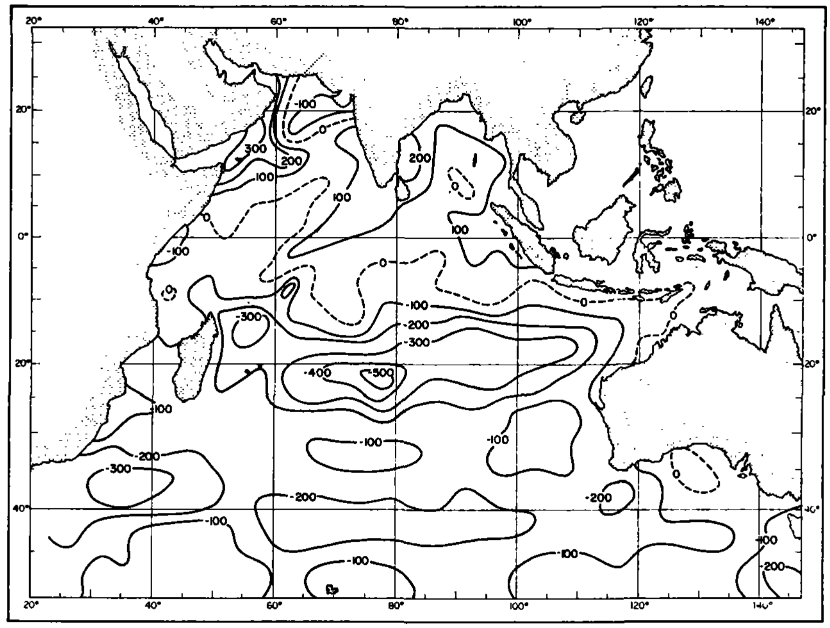

Fig. 9. July, net heat balance at the sea surface in langleys per day.

Southern Hemisphere Near-equatorial Trough

A pressure trough lies just south of the equator with bad weather occurring somewhat farther south (Figures 7 and 8). Doubtless the orientation of the Somali coast, the effect of upwelling in restricting inflow to the heat low, and the circulation around the subtropical ridge to the south contribute to extending this trough across the width of the ocean, although west of 55° E, where winds are strong and steady from the south, cyclonic circulations are unknown. Over the central and eastern ocean, in the doldrums, weak clockwise eddies prevail, appearing and disappearing and occasionally drifting across the equator.

As in January, the ocean beneath the trough gains heat (Figure 9).

Australian Winter Monsoon

Between Indonesia and western Australia an outflow from the continental anticyclone contributes to coastal upwelling (Figure 7) (Wyrtki, 1962). The continental air, already dry, tends to be stabilized by the relatively cool underlying surface. Cloudiness and rainfall are scanty but increase downstream as warmer waters modify the air mass (Figure 8). As in the west, the monsoon between 5° and 25° S is in effect an extension of the winter trade winds.

Both over the north-east Timor Sea and north-west of Madagascar the sea gains some heat (Figure 9), probably because usually clear skies allow a significant fraction of the solar radiation to reach the surface. But because of the stronger winds, the effect is similar to but not as marked as the January heating of the northern Indian Ocean (Figure 6).

NON-MONSOON REGION

Trade Winds

The Trade winds (Figure 7) are characterized by even temperature. Weather is fair in the east, where the air is predominantly of continental origin and in the west where divergence develops as air accelerates northward under the influence of the north–south pressure gradient across Africa (Figure 8). In July, evaporative cooling of the sea surface by the trade winds is only slightly greater than in January but incoming solar radiation is much less because of the change in season. Thus surface cooling exceeding 300 langleys per day (Figure 9) contrasts with a slight net warming in the summer (Figure 6).

The Subtropical Ridge. This, 500 km farther north, but now closer to the belt of minimum rainfall than in January (Figures 7 and 8) is marked by fair weather. Outflow from the Australian anticyclone keeps skies over the Great Australian Bight less cloudy than the latitudinal average (Figure 8). Beneath the ridge line, winter cooling of the surface waters is minimal owing to the clear skies and light winds (Figure 9).

Polar Westerlies. In these the distributions resemble those of January except that winds are less variable (Figures 7 and 4). The Sun's low zenithal angle, considerable cloudiness, and strong winds combine to cool the sea surface (Figure 9).

SEQUENCE THROUGH THE YEAR

During spring and autumn transition months the circulation over the Indian Ocean often closely resembles circulations over the other oceans. Gentle land-ocean temperature gradients muffle monsoonal effects.

Means for a transition month are seldom widely observed on any day, for they average complex combinations and sequences in which winter-like situations border on, or alternate with, summer-like situations. For example, twice between April 1st and 15th, 1963, circulations typical of winter developed over the western Indian Ocean on *both* sides of the equator. The south-east trades of the southern hemisphere and the north-east monsoon of the northern hemisphere merged into equatorial easterlies. This situation strikingly resembled normal conditions over the east central Pacific.

Although a day in March is more likely to resemble a day in January than a day in July, and the converse applies to May, nevertheless, in some years over some parts of the ocean the resemblances may be reversed.

NORTHERN HEMISPHERE MONSOON REGION

November to April

North of 6° to 8° N, rainfall decreases through the period. North or north-east winds flow outward from the continental anticyclone (Figure 4). In February, however, warming over Burma, peninsular India and Arabia weakens the ridge and anticyclonic cells appear over the northern parts of the Arabian Sea and Bay of Bengal and shift southward as the season advances.

In April rain increases. On an average in this month the high cells are located near 12° to 13° N over the Arabian Sea and Bay of Bengal, while a weak heat low prevails over central India. North of the highs, south-westerlies have set in, although farther south northerlies still prevail.

In November the sea surface soon begins to lose more heat to the dry cold northerlies than it gains by radiation through nearly cloudless skies. Cooling reaches a maximum in December (Figure 6). Thereafter, as the north-east monsoon weakens, sea and air temperatures come into equilibrium and insolation increases, net heat gain to the surface rising rapidly to a maximum in April.

South of 6° to 8° N, the northern hemisphere near-equatorial pressure trough is well marked over the Bay of Bengal but after November it becomes very weak over the eastern Arabian Sea and is non-existent in the western Arabian Sea (Figure 4) where air flows across the equator into the summer-time low pressure over south-central Africa. During March, heating over north-east Africa reverses the transequatorial pressure gradient and winds off Somalia veer from north-east to south-east in response.

May to mid-September

During May heating increases over the continental arc from the Sudan to Burma, intensifying the heat trough. By the middle of this month the anti-cyclones only occasionally appear in the Arabian Sea and Bay of Bengal and flow typical of the south-west monsoon prevails. A remnant of the near-equatorial pressure trough also comes and goes between 5° and 10° N; and cloud and rainfall are greatest along about 5° N.

The considerable rain shadowing effect of the southern Indian peninsular and Ceylon, a feature of the summer monsoon, first appears in May.

In May and June, interaction between the advancing tropical maritime air of the south-west monsoon and modified continental air, which is rather less stable in the middle and upper troposphere, probably accounts for the fact that thunderstorms are commonest in these months.

In June, the trend established in May continues until by the last week the summer monsoon dominates, to persist without significant interruption until mid-September (Figures 7–9). The average surface circulation changes little from that in May, except for strengthening winds. Onset of heavy rain stems from monsoon depressions over the northern Bay of Bengal or from subtropical cyclones (Ramage, 1968a) over the north-eastern Arabian

Sea (Figure 8) which make their appearance some weeks after the moist surface south-westerlies have set in (Meteorological Office, 1943). Along the west coast of India, the rains may start any time from early May in the south to the second half of June in the north with an average standard deviation of six days (Ramdas, Jagannathan and Gopal Rao, 1954).

Beginning in May, strengthening south-westerlies combine with increased cloud to counteract heating of a sun at its zenith, even leading to a net cooling of the sea surface where the winds are strongest (Figure 9). The north-central Arabian Sea loses more heat in August than in any other month.

Mid-September to October

The weather of the second half of September resembles the weather of May. Although south-west winds prevail they are becoming weaker and less steady as the continental heat trough weakens and the monsoon rains of the eastern Arabian Sea and north-eastern Bay of Bengal also diminish. Small anticyclones appear over the central Arabian Sea and Bay of Bengal and the net heat gain at the ocean surface increases to a secondary maximum. The near-equatorial pressure trough between 5° and 10° N once more begins to effect an increase in cloud and rain.

Transition to the winter monsoon is rapidly completed in October. A weak secondary maximum of thunderstorm frequency results from interaction between maritime and continental air masses. By the end of the month anticyclonic cells over the Arabian Sea and Bay of Bengal give way to the continental high and northerlies prevail. The near-equatorial pressure trough is the birthplace of depressions which travel northward and occasionally intensify into cyclones. Maximum precipitation is usually found somewhat south of the trough.

EQUATORIAL REGION

During the transition seasons, a bewildering variety of circulations and weather occurs in the region of the equatorial doldrums which extends across the width of the ocean. Clockwise and counter-clockwise eddies may coexist or, if the near-equatorial pressure troughs are active in both hemispheres, moderate or fresh westerlies prevail. Little net trans-equatorial exchange takes place.

SOUTHERN HEMISPHERE MONSOON REGION

Western Indian Ocean

By December, typical summer conditions prevail with trans-equatorial flow becoming most intense in January (Figure 4). In March as the heat low over the Kalahari Desert and the high over the Sahara weaken, a near-equatorial pressure trough develops over Africa but becomes diffuse during May as the northern hemisphere heat lows take over; southerlies set in along the equator, and trade winds extend to the coast of Africa between 5° and 25° S (Figure 7) (see page 19). In the second half of the year the sequence is reversed.

Central Indian Ocean

Over the central Indian Ocean, the near-equatorial pressure trough appears to move more or less continuously between 13° S (Figure 4) (in February) and 3° S (Figure 7) (in July and August). Most of such displacement takes place in the transition months. The ocean always gains heat at the trough with values ranging from less than 100 langleys per day in winter to more than 200 in other months (Figures 6 and 9). The trough does not usually coincide with the areas of maximum rainfall (Figures 5 and 8).

SOUTHERN HEMISPHERE NON-MONSOON REGION

Trade Winds

Between 14° and 24° S and 60° and 110° E, the trade winds prevail throughout the year. They are most extensive and strongest in winter, dominating the width of the ocean between 5° and 25° S (Figure 7), and least extensive and weakest in summer (Figure 4) when the near-equatorial pressure trough and the African and Australian monsoons restrict them on the north, west and east.

Although some interseasonal differences can be detected in the trades the changes are gradual. The most significant is the annual variation of net heat exchange at the ocean surface; its range averages about 400 langleys per day (Figure 3) which is accounted for almost entirely by the march of the Sun, and is not exceeded anywhere else in the Indian Ocean.

Western Trade Winds. The conditions described for January (see page 17) prevail from October to April and July conditions (see page 20) typify the period May–September.

Eastern Trade Winds. The combination of considerable cloudiness, subsidence inversion and little rain (see page 17) persists from November to March (Figure 5). From then until August the rainfall minimum shifts north-east toward the Timor Sea and the cloud maximum shifts westward to coincide with a rainfall maximum along about 90° E (Figure 8), while probably changing from predominantly stratiform to predominantly cumuliform types. During September and October the sequence is rapidly reversed.

INTER-ANNUAL CHANGES AT THE SEA SURFACE

Until now data have been considered too scanty to allow any but long-term means to be computed. During 1963 and 1964, however, we collected 194,000 weather observations made by merchant ships and research vessels, checked them for errors and determined five-degree-square averages for the 24 individual months of the two years (Ramage, Miller and Jeffries, 1969). Along two well-travelled routes—north-east and east-south-east from the Gulf of Aden—80–400 observations were made each month in each square giving sufficient data to provide stable, representative averages.

Figure 10 depicts the changes in net heat balance at the sea surface between corresponding months in 1963 and 1964. These were two fairly normal years meteorologically and yet the differences, averaged without regard to sign, amount to 45% of the long-term means along the two sections. Thus the usefulness of long-term means probably suffers less from the crude empirical methods used in their computation than from considerable inter-annual variations. The changes in sea surface temperatures between corresponding months in 1963 and 1964 (Figure 11) cannot be simply related to the changes shown in Figure 10, although comparing the two can provide insight into interaction processes. Near Arabia the sea surface was colder

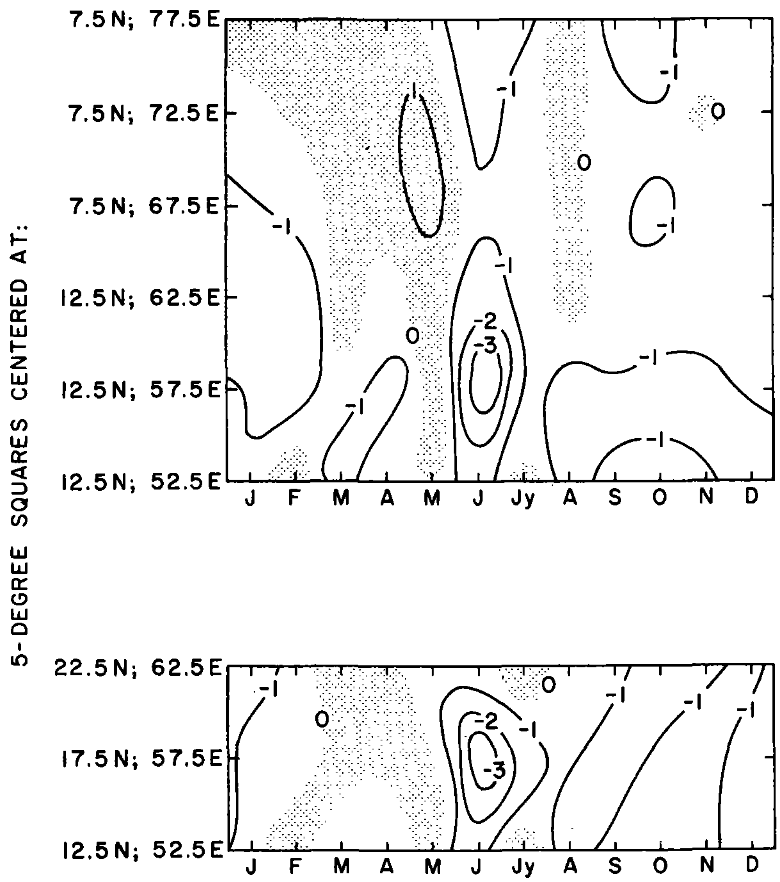

Fig. 10.—Changes in monthly average net heat balance at the ocean surface between corresponding months of 1963 and 1964. Computations based on Budyko (1956); isopleths labelled in hundreds of langleys per day; stippled areas, 1963 received less heat than 1964.

and gained considerably more heat in June 1963 than in June 1964, a combination which could result only from more vigorous upwelling in the earlier month.

A rather different combination appears from September to December and January to April. In these months, changes in net heat balance and in temperatures at the sea surface between 1963 and 1964 have the same sign, indicating that the surface temperature is probably largely controlled by evaporative cooling. From September to December, over most of both sections, the sea was colder and gained less heat in 1964 than in 1963. The most important factor in evaporational cooling, the wind, averaged 4·9 m sec^{-1} in 1963 and 5·7 m sec^{-1} in 1964.

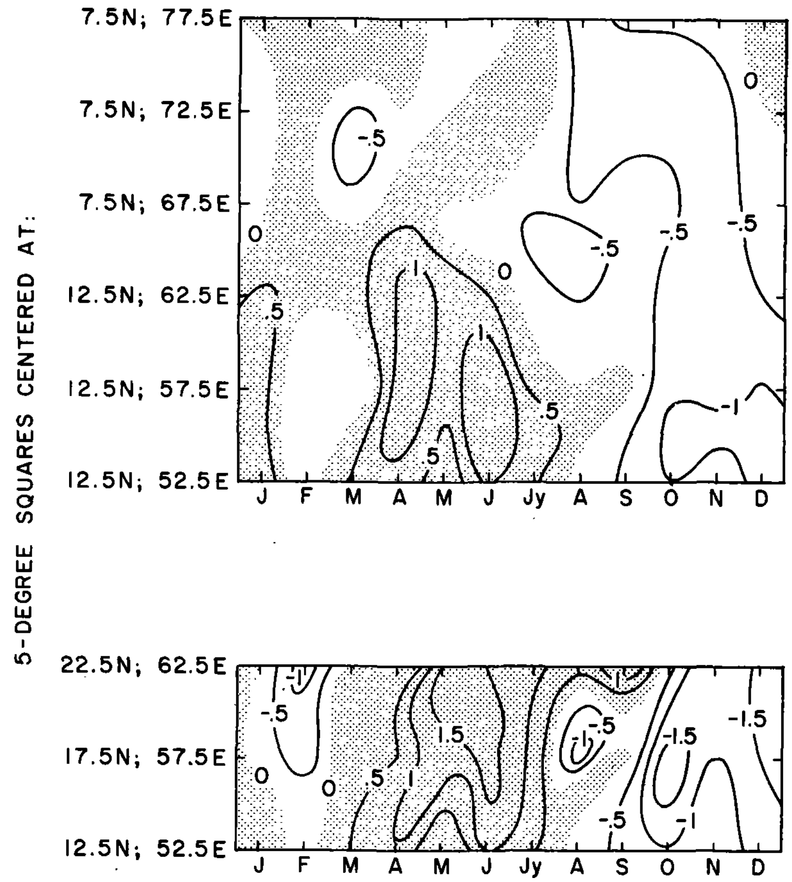

Fig. 11.—Same as Figure 10 but for sea-surface temperature. Isopleths labelled in °C; stippled areas, 1963 colder than 1964.

SOMALI CURRENT

The region of intense summertime upwelling off the coast of Somalia was surveyed by IIOE research vessels (see for example, Royal Society, 1965; Stommel and Wooster, 1965). How did their findings tally with observations of upwelling elsewhere?

Hart and Currie (1960) point out, "There are . . . four *extensive* areas of coastal upwelling, all on the western coasts of the continents of North and South America and Africa. . . . These currents have certain visible features in common—a negative surface-temperature anomaly, characteristic coastal winds, frequent fogs over the cold water and arid or desert conditions over the adjacent land." Strangely enough, fog is unknown off Somalia in summer, despite the fact that air moving from the south over the cold water is rapidly cooled to its dew point. Ramage (1968a) has suggested that an explanation may be found in the character of the summer circulation over the Arabian Sea. In the vertical plane, air moves at low levels across the Arabian Sea from south-west, rises over India in the region of heavy monsoon rains, returns toward the south-west in the layer between 6 and 12 km and sinks over the western Arabian Sea to close the circulation. The sinking air, warmed by compression, provides, through turbulent transfer, sufficient heat to the surface layers to counteract the fog-forming effect of the cold underlying surface.

Foxton (1965) observed large numbers of dead fish near Ras Mabber on the coast of Somalia during the summer 1964 DISCOVERY Expedition. He ascribed the mortality to extreme coldness of the upwelled water (minimum temperature 13·2° C). In this same area, Swallow (1965) and Bailey (1965) saw remarkably few sea birds, although Swallow pointed out that the water was relatively rich in nutrients though poor in plankton. It is my impression that ample nutrients, scarce plankton, dead fish and few birds struck the oceanographers as quite unexpected in a region of upwelling. If one accepts for the moment Foxton's suggestion that mass fish mortality might be an annual event off Somalia in contrast to its being most unusual in other upwelling regions, then corresponding peculiarities in the Somali upwelling must be sought.

Off the west coasts of North and South America and Africa, winds and wind-driven currents causing upwelling are directed toward the equator, so that there is a continuous, though often narrow, cold surface current extending from higher latitudes to the area of maximum upwelling. Fish can move along this ribbon, benefiting from increased food but not being subjected to severe or fatal temperature changes. Off Somalia, on the other hand, winds and wind-driven currents directed *away* from the equator suddenly set in at the beginning of summer. Very cold water appears at the surface, *unconnected* in space or time with correspondingly cold surface water elsewhere. Fish (and presumably plankton) in the area are subject to sudden

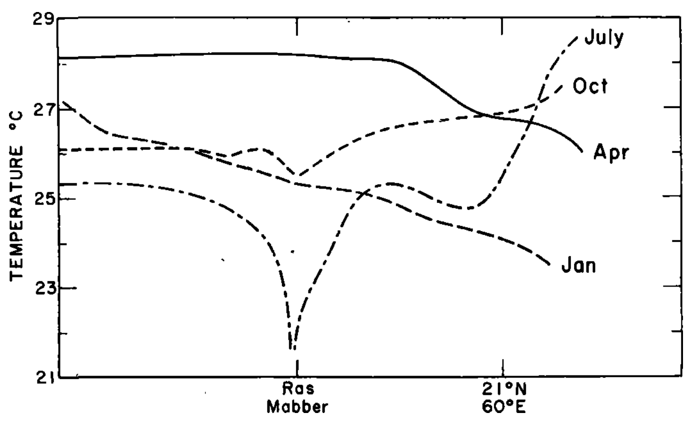

Fig. 12.—Profiles of mean sea-surface temperatures northeastwards from, and along the coast to the south of Ras Mabber, Somalia.

cold stress and many die. Fish accustomed to such temperatures are 'walled' off from the upwelling by surrounding very warm waters (Figure 12).

Should this explanation be valid, then evaluations of the unexploited fishing potential off Somalia and possibly to some extent off Arabia (Wooster, Schaefer and Robinson, 1967) might prove to be over-optimistic. Perhaps fishermen have not missed too much by being harbour-bound during the height of the summer monsoon.

NEAR-EQUATORIAL AND HEAT TROUGHS

In January a weak pressure trough lies just north of the equator east of 70° E (see Figure 4) while in July, an intense pressure trough extends from Somalia across Arabia and northern India (see Figure 7). Until recently, meteorologists assumed that the trough followed the march of the sun between these winter and summer positions, with the south-west monsoon circulation on the south side of the trough correspondingly advancing and retreating. Rain is associated rather complexly with the trough and so it was also thought to advance and retreat (onset and withdrawal of the monsoon).

In fact, although the dominant pressure trough is located near the equator in spring and autumn and near 30° N in midsummer, Figure 2 (p. 12) reveals that the double rainfall maximum is confined to latitudes below 15° N. Furthermore, south-westerlies set in over the northern Arabian Sea and northern Bay of Bengal in early April while northerlies still prevail to the south. This may be accounted for by the fact that not one trough moves continuously between latitudinal extremes but, rather, *two* distinct troughs

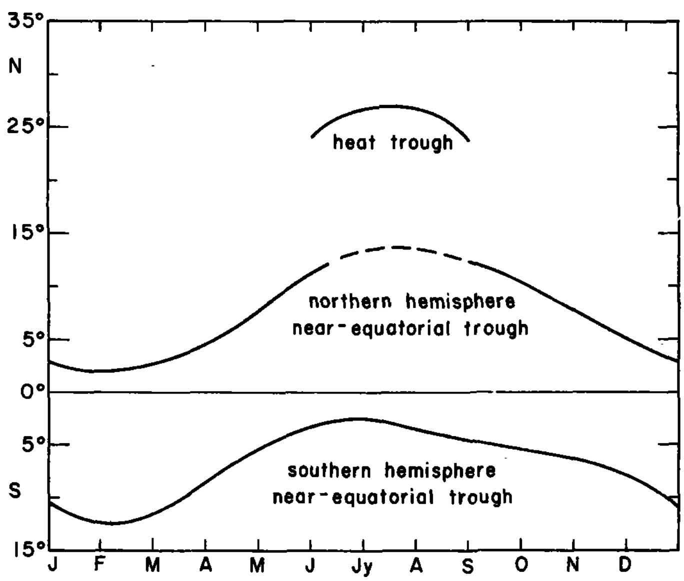

Fig. 13.—Annual latitudinal variation of lower tropospheric (1·5 km) pressure troughs over the Indian Ocean (after Raman, 1969).

are involed (Ramage, 1968a). The near-equatorial trough exists alone during the winter months. Then, as Raman (1969) has discovered, it moves to about 11° N and becomes very weak during the height of summer. Farther north the continental heat trough develops in May and dominates the circulation during June through September, when it begins to dissipate as the near-equatorial trough once more becomes dominant (Figure 13).

In spring, as the near-equatorial trough intensifies, rainfall in the vicinity increases, but diminishes when the continental heat trough becomes dominant. Then, redevelopment of the near-equatorial trough in autumn is accompanied by a second rain enhancement. A second diminution follows in winter as the southern hemisphere summer trough draws air across the equator. Latitudes above 10° to 15° N are not traversed by a trough (in the climatological sense) and therefore experience only a single rainfall maximum as the continental heat trough develops and intensifies to the north.

CONCLUDING REMARKS

Throughout our investigation of Indian Ocean meteorology we obtain tantalizing glimpses of what may be important feedback mechanisms. Bunker (1967) found that an intense summertime low-level jet is caused by, and overlies, steep thermal gradients associated with the Somali current. The jet in turn acts to enhance upwelling and so further to steepen thermal gradients in the surface air layers. Ramage (1968b) suggested that conditions associated with a protracted break in the summer monsoon rains of western India can modify the atmospheric circulation so as to increase the chances of the break continuing and of a drought developing.

Only sophisticated numerical modelling techniques are likely to give us a grip on quantitative aspects of these problems. Provided sufficient data were available, we could then hope to determine the significant variables contributing to the phenomena and to estimate their magnitudes.

Although meteorologists have been analysing daily weather charts for a century, only recently have oceanographers moved toward synoptic studies (Seckel, 1968). More needs to be done (although the cost could be quite staggering) to see what responses the ocean might make to short-period meteorological fluctuations, such as sea breezes (Figure 14), katabatic winds, or tropical cyclones.

The problem of surveying weather and of measuring circulations over vast uninhabited regions is being tackled by a variety of new techniques. Orbiting (Pyle, 1965) and synchronous (McQuain, 1967) weather satellites, equipped with television cameras and infra-red detectors are photographing clouds and recording temperatures of emitting surfaces with increasing detail and frequency. Satellite sensing of many other meteorological variables will soon be undertaken (Bolin, 1967) while the ATS-3 satellite is already transmitting colour pictures of clouds (Warnecke and Suderlin, 1968). For the past two years balloons made of the new synthetic, Mylar, have been flying at constant pressure levels (usually about 12 km above MSL) around the Southern Hemisphere (Lally, Litchfield and Solot, 1966). One balloon stayed aloft for 315 days while making 22 circuits. Information concerning the direction of winds obtained from tracking the balloons (Solot, 1967) has

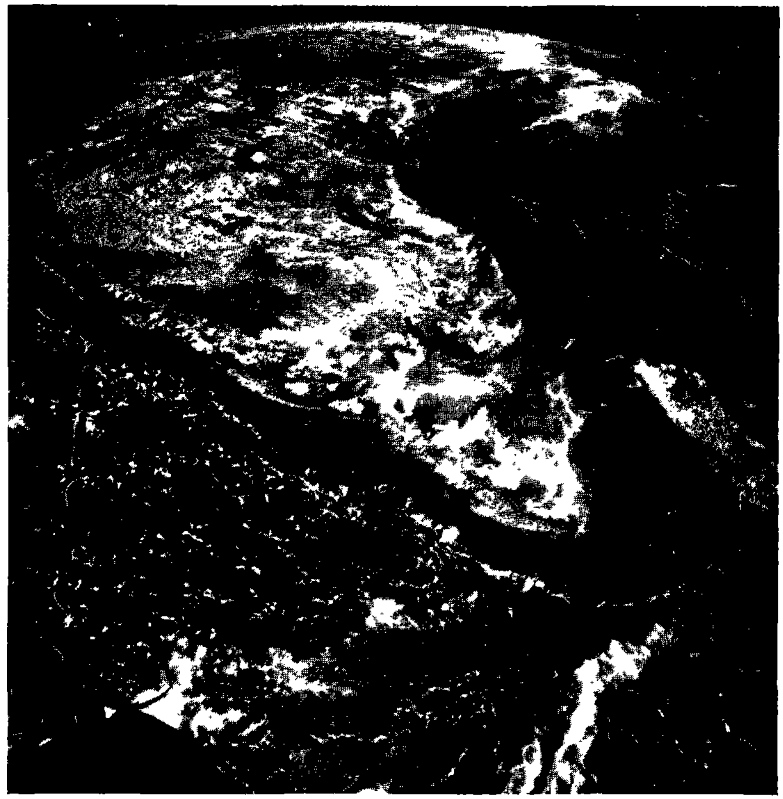

Fig. 14.—The Indian sea-breeze. On the afternoon of September 14, 1966, clouds reveal the magnitude of the circulation; in the vertical plane, air near the surface moves inland where it rises and cools and clouds are formed; at a height of about 1 km a return current, which is warming by subsidence, evaporates the clouds along the coast and up to 100 km offshore; in the Gulf of Mannar the south Indian and Ceylon sea breezes reinforce each other. (Photo—National Aeronautics and Space Administration.)

already added significantly to our knowledge of the atmospheric circulation over the southern oceans and there is no scientific reason why this powerful and relatively inexpensive technique could not be extended over the whole globe.

To render these new methods most effective, spot soundings must continually be made over land and sea in order properly to calibrate instruments, which although capable of accurately determining *gradients*, are less than satisfactory in making absolute measurements. For this a research vessel as completely equipped as METEOR II (Brocks, 1967) is essential. To meteorologists, the value of complete hydrographic and aerological soundings is about proportional to the square of the number of ships making simultaneous measurements! Thus I strongly favour closely coordinated multi-vessel expeditions of which the International Indian Ocean Expedition was an appetizing foretaste. Perhaps costs could be reduced by using a small aircraft carrier as a mother ship or by integrating aircraft and ship operations.

But first of all, scientists must want to work together. The most ambitious expedition ever conceived would collapse into a dusty file of unread records if the investigators did not enthusiastically participate from first plans to final publications.

REFERENCES

Bailey, R. S., 1965. *Sea Swallow*, **17**, 52–56.

Bolin, B. (Chairman), 1967. *Report of the study conference held at Stockholm*, 28 *June*–11 *July* 1967 *on the global atmospheric research programme* (*GARP*). 70 pp., and appendices.

Brocks, K., 1967. *Meteor Forschungs.*, B, **1**, v–x.

Budyko, M. I., 1956. *The Heat Balance of the Earth's Surface*. Gidrometeorologicheskoe izdatel'stvo. Leningrad, 255 pp. Translated by Nina A. Stepanova and distributed by the U.S. Weather Bureau, Washington, D.C., 1958.

Bunker, A. F., 1967. In, *Proceedings of Symposium on Meteorological Results of the International Indian Ocean Expedition*, edited by P. R. Pisharoty, India Meteorological Department, New Delhi, 3–16.

Colon, J. A., 1964. *Indian J. Met. Geophys.*, **15**, 183–200.

Ficker, H. von., 1936. *Veröff. met. Inst. Univ. Berl.*, **1**, (4), 33 pp.

Foxton, P., 1965. *Deep Sea Res.*, **12**, 17–19.

Gordon, A. H. and Taylor, R. C., 1969. *Int. Ind. Ocean Exped. Meteor. Monogr.*, **7**, (in press).

Hart, T. J. and Currie, R. I., 1960. '*Discovery*' *Rep.*, **31**, 123–298.

La Violette, P. E. and Mason, C., 1967. *Monthly Charts of Mean, Minimum and Maximum Sea Surface Temperature of the Indian Ocean*. Naval Oceanographic Office, Washington, D.C., 48 pp.

Lally, V. E., Litchfield, E. W. and Solot, S. B., 1966. *WMO Bull.*, **15**, 124–128.

McQuain, R. H., 1967. *Bull. Am. met. Soc.*, **48**, 74–79.

Meteorological Office, 1943. *Weather in the Indian Ocean. Volume I, General information*, 52 pp. *Volume II, Local information*, Parts 1–9, H.M. Stationery Office, London.

Miller, F. R. and R. N. Keshavamurthy, 1968. *Int. Ind. Ocean Exped. Meteor. Monogr.*, **1**, 94 pp.

Palmer, C. E., 1942. *Prof. Notes Wellington met. Off.*, **1**, 38 pp.

Pyle, R. L., 1965. *Bull. Am. met. Soc.*, **46**, 707–713.

Ramage, C. S., 1965, *WMO Bull.*, 166. TP 81, 31 pp.

Ramage, C. S., 1968a. *Weather*, **28,** 28–37.
Ramage, C. S., 1968b. In, *Eclectic Climatology*, edited by A. Court, Oregon State University Press, Corvallis, Oregon, 41–54.
Ramage, C. S., Miller, F. R. and Jefferies, C., 1969. *International Indian Ocean Expedition Meteorological Atlas*, **1**, *The Surface Climate of 1963 and 1964*. East–West Center Press, Honolulu (in press).
Raman, C. R. V., 1969. *Int. Ind. Ocean Exped. Meteor. Monogr.*, **7**, (in press).
Ramdas, L. A., Jagannathan, P. and Gopal Rao, S., 1954. *Indian J. Met. Geophys.*, **5**, 1–10.
Royal Society, 1965. *International Indian Ocean expedition, RRS Disovery Cruise* 3 *Report: Oceanographic Work in the Western Indian Ocean* 1964. London, 55 pp.
Seckel, G. R., 1968. *Trans. Am. geophys. Un.*, **49,** 377–387.
Solot, S. B., 1967. *GHOST Atlas of the Southern Hemisphere*. National Center for Atmospheric Research, Boulder, Colorado, 10 plates.
Stommel, H. and Wooster, W. S., 1965. *Proc. natn. Acad. Sci. U.S.A.*, **54,** 8–13.
Swallow, J. C., 1965. *Mar. Obsr.*, **35,** 125–130.
UNESCO, 1965—. *International Indian Ocean Expedition, Collected reprints*. Paris.
U.S. Weather Bureau, 1957. *U.S. Marine Climatic Atlas of the World, Volume III, Indian Ocean*. Chief of Naval Operations, Washington, D.C., 7 pp., 267 charts.
Van Duijnen Montijn, J. A., 1952. *Roy Neth. Meteor. Inst.*, **135,** 31 pp., 24 charts.
Warnecke, G. and Sunderlin, W. W., 1968. *Bull Am. met. Soc.*, **49,** 75–83.
Wooster, W. S., Schaefer, M. B. and Robinson, M. K., 1967. *Atlas of the Arabian Sea for Fishery Oceanography*. Univ. of California, Inst. of Marine Resources, La Jolla, 35 pp. plus charts.
Wyrtki, K., 1962. *Aust. J. mar. Freshwat. Res.*, **13,** 217–225.

Reprinted from *Indian J. Meteorol. and Geophys.*, vol. 21, no. 1, 1970, p. 111-114.

Monthly wave characteristics of the Bay of Bengal

P. S. SRIVASTAVA*, P. K. VIJAYARAJAN and M. X. JOSEPH

Naval Physical and Oceanographic Laboratory, Cochin

(*Received 17 April 1969*)

ABSTRACT. The monthly wave characteristics of the Bay of Bengal are reported, based on an analysis of the wave data published in the *Indian Daily Weather Reports* of the India Meteorological Department for the period 1960–64. March is the calmest and June, the roughest month in the area. In June the average wave height is 1·75 m although the maximum number of depressions and cyclones occur during the month of October.

1. Introduction

In a previous paper (Srivastava *et. al* 1968) the monthly wave characteristics of the Arabian Sea are reported, based on an analysis of the wave data published in the *Indian Daily Weather Reports* of the India Meteorological Department for the period 1960–64. The present paper which is in continuation of the above mentioned paper gives the monthly wave characteristics of the Bay of Bengal. Recently HMSO, U.K. has published ocean wave statistics of the world's ocean (Hogben and Lumb 1967). It does not give any detailed analysis of the waves in the Bay of Bengal as the entire area has been chosen as a single unit for purposes of statistical analysis. In the present analysis the Bay of Bengal has been divided into two-degree square zones. Statistical analysis of waves for each of the zones is presented.

2. Analysis of the data

The details of the procedure followed for the analysis of the data are similar to that of Srivastava *et al. (loc. cit.)*. The wave data for each month were grouped for each 2° square. The average of the significant wave height, the standard deviation of the significant wave height, the predominant wave period and wave direction were determined for each zone. Maps depicting the average significant wave height, the standard deviation of the same, the predominant wave period and wave direction were prepared for each month. A typical map for the month of June is presented in Fig. 1.

The highest 10 per cent waves, which could possibly occur in 2° square were calculated for each month and were plotted for each zone for each month and contoured. A typical map for the month of June is presented in Fig. 2. The areas shown by dots in the map represent the low wave activity areas and the value given therein represents the lowest value reported. The shaded areas represent the high wave activity and the value given therein represents the highest value reported.

The monthwise average wave height taking the whole of Bay of Bengal as a single unit, is presented in Table 1.

3. Results and Discussions

A complete set of 24 maps depicting the monthly wave characteristics of the Bay of Bengal is presented in the NPOL Departmental Report (unpublished).

By studying the average wind pattern for fifty years as presented in the IMD Wind Atlas, the Bay of Bengal can be divided into following four seasons for the study of waves —

(*a*) *Northeast monsoon* (November to February) — Wind mostly northeasterly,

(*b*) *Pre-monsoon* (March-April) — Anticyclonic wind pattern,

(*c*) *Monsoon* (May-September) — Wind mostly southwesterly.

(*d*) *Post monsoon* (October) — Variable wind pattern.

(*a*) *Northeast monsoon* (November to February) — The waves in general follow the northeast direction of the northeasterly wind pattern, except around the Nicobar group of islands, where the wave direction is variable during the month of January and November (Figs. 3 and 4). The wave amplitudes during the northeast monsoon period are in general lower than during the southwest monsoon (Figs. 1, 5 and 6).

*Present address: National Institute of Oceanography, Karikkamuri Road, Ernakulam

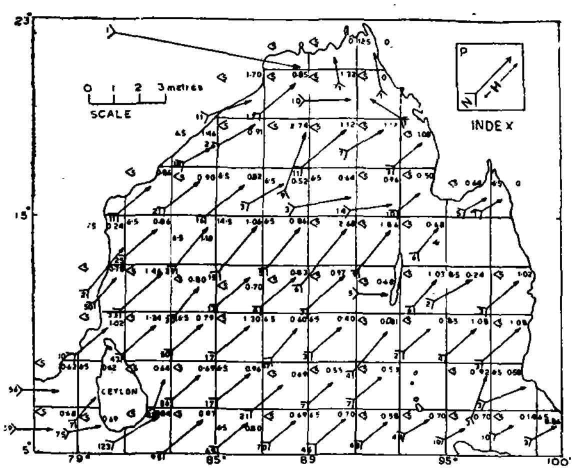

Fig. 1. Wave characteristics — June

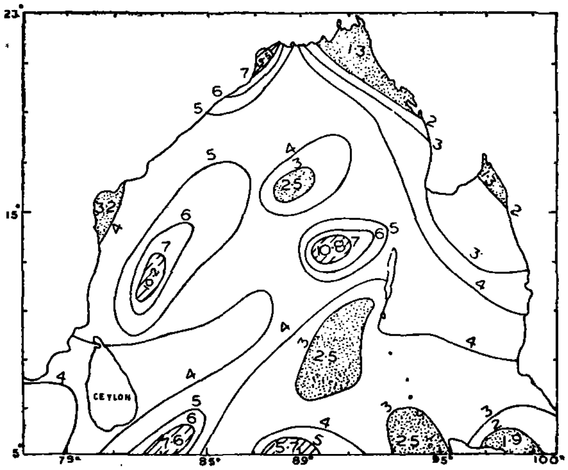

Fig. 2. Highest 10 per cent high waves — June

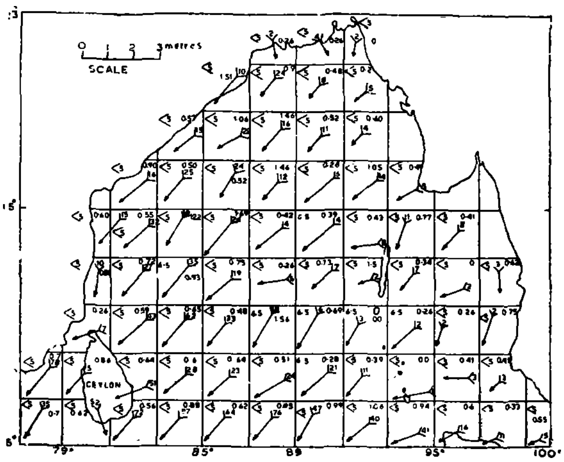

Fig. 3. Wave characteristics—January

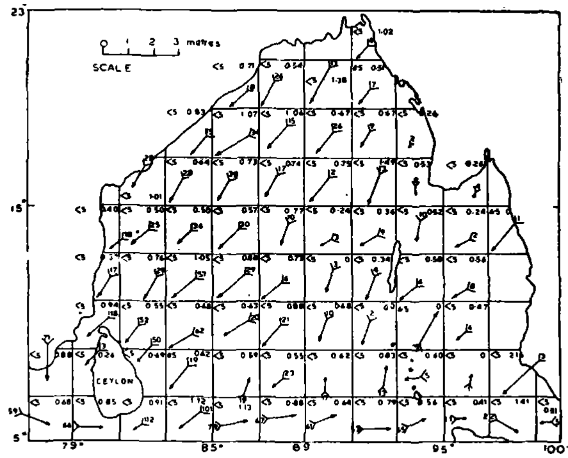

Fig. 4. Wave characteristic—November

H—Average significant wave height in metres; S—Standard deviation of average height; P—Most predominant wave period in seconds N—Number of observations

TABLE 1

Monthly average wave height taking Bay of Bengal as a single unit

Month	Average wove height (m)	Month	Average wave height (m)
January	1·13	July	1·39
February	1·04	August	1·41
March	0·84	September	1·20
April	0·87	October	0·97
May	1·19	November	0·97
June	1·75	December	1·05

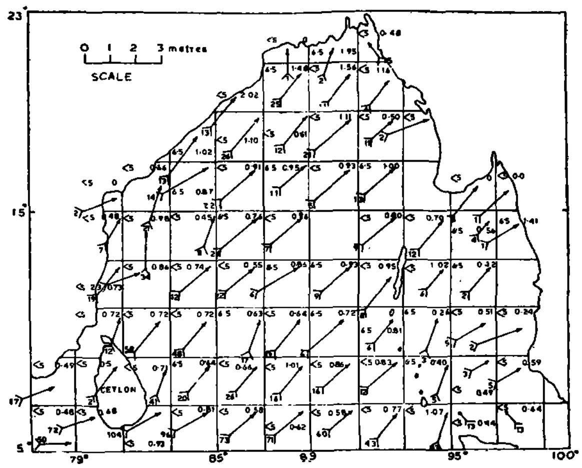

Fig. 5. Wave characteristics — July

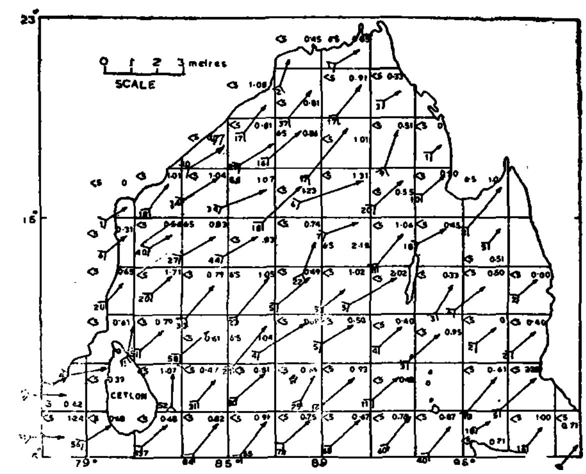

Fig. 6. Wave characteristics — August

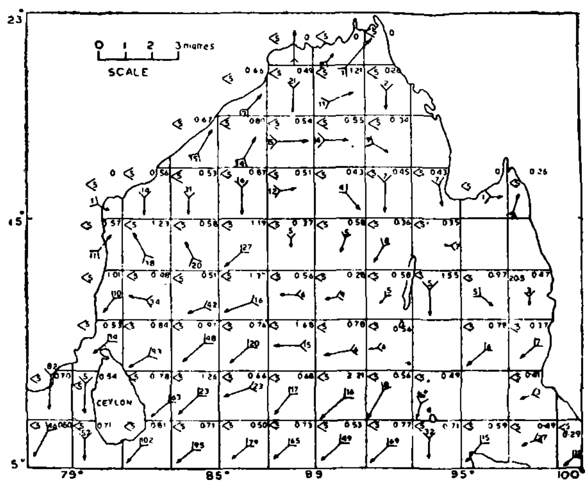

Fig. 7. Wave characterstics — March

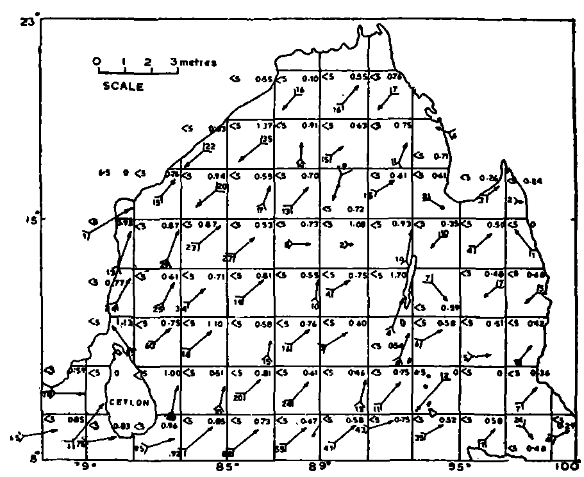

Fig. 8. Wave characterstics — October

H—Average significant wave height in metres,; P—Most predominant wave period in seconds
S—Standard deviation of average height; N—Number of observations

(*b*) *Pre monsoon* (March to April) — The direction of wave is variable throughout the Bay of Bengal. The maps depicting the average wave conditions in the Bay of Bengal show that March (Fig. 7), is the calmest month in the area. The average height, taking Bay of Bengal as a single unit, is 0·84 m.

(*c*) *Monsoon* (May to September) — The direction of wave ranges between W and SW. The waves in the monsoons are in general higher than in any other seasons. June is the roughest month in the area (Fig.1). The average height, taking Bay of Bengal as a single unit, is 1·39 m.

(*d*) *Post monsoon* (October) — The direction of wave is variable. The average height, taking Bay of Bengal as a single unit, is 0·97 m (Fig. 8).

The area southeast of Ceylon is rough throughout the year. The coastal area of East Pakistan is calm for the most part of the year.

A comparative study of the monthwise cyclones and depressions during the period 1960-64 and the monthly average wave height has been made (Fig. 9). It will be seen from the figure that maximum number of depressions and cyclones occur during the month of October, whereas the Bay of Bengal is roughest during the month of June. The reasons for this apparent anomaly are as follows —

(*a*) During the month of June, southwesterly wind is blowing steadily over a longer fetch giving rise to a steady state and this condition prevails

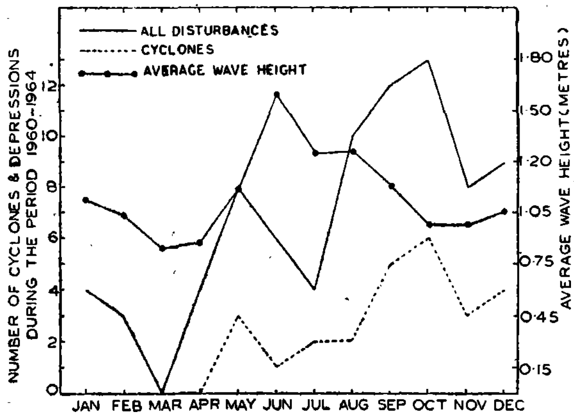

Fig. 9. Comparison of depressions and cyclones with average wave height

for most time of the month. Thus the roughest sea conditions are obtained.

(*b*) Though the wind under a cyclonic condition is of higher velocities, since the fetch is limited, the steady state condition is not reached. Besides the cyclonic pattern exists for a few days only. Hence in spite of the large number of cyclones and depressions, the wave heights are relatively smaller in October than in June.

4. Acknowledgements

The authors are grateful to Dr. D. Srinivasan, Director, NPOL for his keen interest in the present study. Thanks are due to Shri D. K. Nair, JSA for doing the initial computations.

REFERENCES

Hogben, N. and Lumb, F. E.	1967	*Ocean wave statistics*, Her Majesty's Stationary Office, London.
Srivastava, P. S., Nair, D.K. and Ramankartha, K. R.	1968	*Indian J. Met. Geophys.*, **19**, 3, p. 329.

Reprinted from *Pure and Applied Geophysics (Basel)*, vol. 79, 1970/II, p. 98-102

Studies of Evaporation from the Sea at Waltair

By R. RAMANADHAM and A. V. S. MURTY [1])

Summary – The values of evaporation for several months from the sea at Waltair are computed from climatic means of observations made at a near-shore station at Waltair. The simplified equation of evaporation $E = K_a(\bar{e}_s - \bar{e}_a)\,\bar{u}_a$, has been used in the computations.

Introduction

The simplified theoretical form of evaporation which may be written as $E = K_a(\bar{e}_s - \bar{e}_a)\,\bar{u}_a$ – (where K_a is the numerical coefficient of evaporation, $\bar{u}_a$ is the mean wind speed at the level a, $\bar{e}_s$ is the mean water vapour pressure corresponding to the sea surface temperature corrected for salinity value of the water, and $\bar{e}_a$ is the mean water vapour pressure in the air at the level a) – permits the use of climatological data to compute evaporation rates. The theoretical value (2) of K_a for observations at 6 m level from the surface is 8.7×10^{-4} when E is expressed in centimeters of liquid water per hour, u in meters per sec and e in mb. When the climatic means of the observations are used together with the independently calculated values of E, JACOBS found that the value of the numerical coefficient becomes 6×10^{-4} which is about two-thirds of the theoretical value. Corresponding to 10 m level observations, the theoretical value of the numerical coefficient will become 7.5×10^{-4}. The upper limit of the coefficient (7.9×10^{-4}) as given by DEFANT [1][2]) is approximately the same as above. The lower limit (5.0×10^{-4}) given by DEFANT coincides with that of Wüst's data after it is corrected (multiplied by 1.22) in view of Sverdrup's calculations of evaporation making use of the meridional distribution of temperature, relative humidity and wind velocity at the surface of the Atlantic. It is interesting to note that these two values of the coefficient (i.e. the theoretical value 7.5×10^{-4} and the climatic value 5.0×10^{-4}) again bear the same ratio (i.e., 3:2).

The evaporation values may be computed using the climatological means of the meteorological parameters observed from a height of about 12 m from the surface by making use of the equation $E = 4.8 \times 10^{-4}\,(e_s - e_{12})\,u_{12}$ where 4.8 is the numerical value of K_a adjusted for 12 m level of observations.

[2]) Numbers in brackets refer to References, page 102.

[1]) Dept. of Meteorology and Oceanography, Andhra University, Waltair, India. Present address: Central Marine Fisheries Research Sub-Station, Ernakulam, India.

A total number of 115 diurnal cycles of observations were conducted by the authors during the period from February 1960 to January 1961, with the number of cycles varying from 5 to 13 per month. The observations include wind velocity, dry-bulb and wetbulb temperatures in the air from a height of about 12 m from the sea level and the surface temperature and salinity of the shore waters of the sea. The mast holding the equipment for the meteorological observations was situated at a distance of about eighty meters from the shore waters. The observations were made at an interval of two hours in each diurnal cycle.

As it was observed that the wind blows from sea to land during day, the particular period from 09 hr to 19 hr is considered for computing evaporation values, so that the error due to the land influence is minimised.

Results and discussion

The annual march of various parameters relevant to evaporation are discussed below. The monthly mean value of each parameter is represented by circles and the seasonal trend by a continuous curve. The smoothing effect is achieved by making use of the formula $B=(a+2b+c)/4$ where a, b and c are successive terms of a series and B which is the result of $(a+2b+c)/4$ is represented in the place of b.

The sea minus air temperature (shown in Fig. 1) is either positive or less negative during the winter season (December to March) and the winter-transition period (October–November). Its value is lowest (far negative) during the summer transition (April to May) and the beginning of the S.W. Monsoon season. During the S.W. Monsoon season its value gradually reaches zero from the lowest.

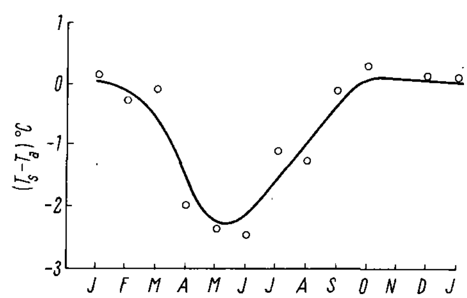

Figure 1
Annual variation of sea minus air temperature

The depression of wet-bulb (shown in Fig. 2) during the hot weather season (April to May) and the S. W. Monsoon (June–September) is of the order of 3.5 °C which is relatively lower when compared to winter season. The depression of wet-bulb is conspicuously much during the transition period from the S.W. Monsoon to the winter.

The difference of water vapour pressure between the sea surface and the 12 meter

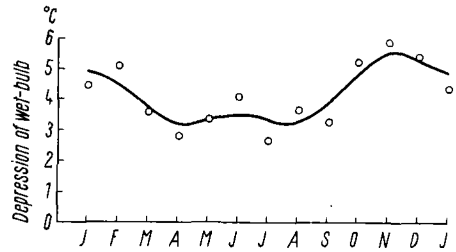

Figure 2
Annual Variation of wet-bulb depression

level which is a complex function of sea minus air temperature and wet-bulb depression in the air, is shown in Fig. 3. Its value is lowest during the hot weather season and at the beginning of the S.W. Monsoon season. It reaches predominantly high value during the winter transition, October–November. There is a gradual rise of the hydrolapse as time advances during the S.W. Monsoon season. Its fall to the minimum is more rapid than its rise to the maximum.

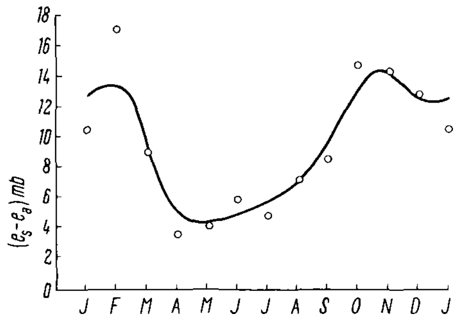

Figure 3
Annual variation of sea minus air-water vapour pressure

Fig. 4 shows the annual variations of wind speed. The annual trend of the wind speed indicates a sharp rise from February to April which is just in opposite to the

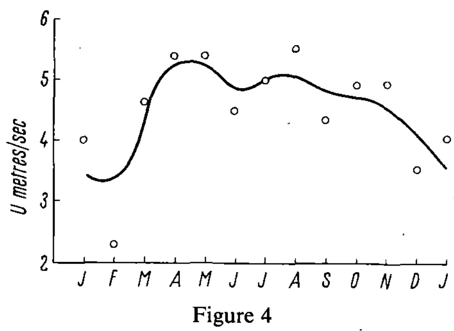

Figure 4
Annual variation of wind speed

hydrolapse conditions. The wind speed is lowered down gradually from April to its winter minimum. It is interesting to note that the wind speed during the winter transition (October–November) is less than that of the summer transition (April–May) only by about 0.5 m/sec.

The mean variations, through different hours of the day, of the rate of evaporation, during different seasons, are shown in Fig. 5. The main feature associated with the diurnal curve of evaporation is a rapid rise to the maximum which occurs about 1400 hrs or earlier and a gradual fall from that time onwards. This feature is less pronounced during the summer transition period (April–May) and is more pronounced during the remaining seasons of the year. The range of the rate of evaporation, during the selected interval of the day, is the largest during the winter transition (October–November) and is the lowest during the summer transition (April–May); and the range during the other two seasons each falls in between.

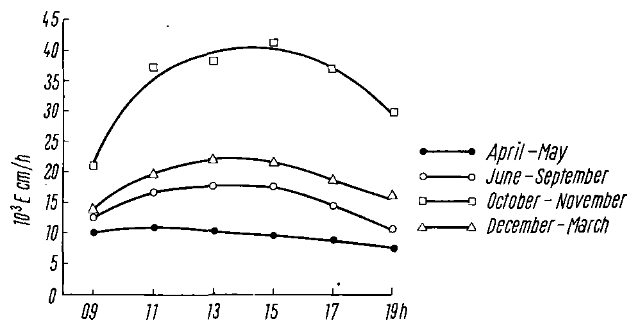

Figure 5
Hourly variations of evaporation during different seasons

The annual march of evaporation is shown in Fig. 6. The individual monthly values in this figure are computed from the trend values of the wind speed and the water vapour pressure difference between the sea surface and the 12 m level, during the respective months. The rate of evaporation is moderate during the winter and the later part of the S.W. Monsoon season. It is minimum during the summer transition period (April–May) and maximum during the winter transition period (October–November). It may be noted that the rate of evaporation is minimum during he summer transition (April–May) even though winds are high, during this season. This is because of the low value of hydrolapse (see Fig. 3) during this period of the year. Wind speed and hydrolapse are both favourable for the occurrence of maximum evaporation rate during the winter transition (October–November). The situation of the sea minus air temperature and the wet-bulb depression further explains the seasonal variations of evaporation rate.

The mean value of evaporation is about 0.012 cm/hr during the summer transition (April–May), about 0.016 cm/hr during the S. W. Monsoon season (June to Sep-

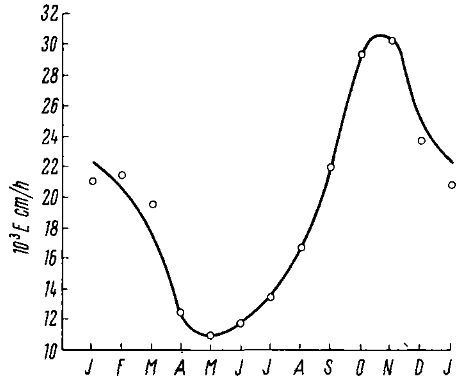

Figure 6
Annual variation of rate of evaporation

tember), about 0.030 cm/hr during the winter transition (October–November) and about 0.021 cm/hr during the winter season (December to March). The annual mean value, during these particular hours of the day, is about 0.019 cm/hr. The contribution of the selected interval of the day (from 09 to 19 hrs) to the total annual evaporation is about 70 cm of liquid water from a square centimeter of the surface.

From a chart of isopleths of evaporation given by VENKATESWARAN [5], it may be noticed that the evaporation over the Bay of Bengal on its western side is about 110 cm per annum per sq. cm. According to PRIVETT [3] the approximate value of the annual evaporation over a square centimeter corresponding to Waltair region of the Bay of Bengal is about 150 cm.

It may be concluded as pointed out by PRIVETT [4] that in addition to divergent views on turbulence, the use of different climatic records can lead to different results of evaporation.

REFERENCES

[1] A. DEFANT, *Physical Oceanography*, Vol. 1 (Pergamon Press Ltd., London 1961), 226–231.

[2] S. L. HESS, *Introduction to Theoretical Meteorology* (Henry Holt & Co., New York 1959), 286–287.

[3] D. W. PRIVETT, *Monthly Charts of Evaporation from the North Indian Ocean (Including the Red Sea and the Persian Gulf)*, Quart. J. Roy. Meteorol. Soc. *85* (1959), 424–428. (See also Coll. Repr. Natl. Inst. Oceanogr. *8*, No. 295.)

[4] D. W. PRIVETT, *The Exchange of Heat Across the Sea Surface*, Marine Observer *28* (1958), 23–28. (See also Coll. Repr. Natl. Inst. Oceanogr. *6*, No. 212.)

[5] S. V. VENKATESWARAN, *On Evaporation from the Indian Ocean*, Indian J. Meteorol. Geophys. *7* (1956), 265–284.

(Received 31st October 1968)

Part III Marine chemistry

Reprinted from *Defence Science Journal (India)*, vol. 15, no. 3, 1965, p. 185-194

STUDIES ON DISTRIBUTION OF OXYGEN IN THE NORTH ARABIAN SEA DURING THE POST MONSOON PERIOD

S. P. ANAND

Directorate of Scientific Research (Navy). Naval Headquarters, New Delhi

(*Received 12. Nov. 64; revised 19 April 65*)

Study on distribution of dissolved oxygen is important from the point of view of productivity and structure of water masses. Water samples at about 60 stations spread over the Northern Arabian Sea were collected and their oxygen conten estimated. The study reveals fairly high oxygen content in Surface waters off the Bombay coast and along latitude 15°N. Progressive lowering in depth of oxygen minimum zone from 24°N Southwards is also noticed. Subsurface upwelling around 60°E, 20°N seems to be in progreess.

Study of distribution of dissolved oxygen in the ocean is important from the point of view of productivity of water masses. It also helps in elucidating the structure of water masses. Earlier work in this field which is of special interest is of Thomsen[1]; Seiwell[2]; Richard[3]; and Myake and Saruhashi[4]. Observations recorded by the Dana and the Swedish Deep Sea Expedition[5] regarding oxygen minimum were made in the Southern part of the Arabian Sea. In the recent years important contributions, however, have been made by Jayaraman and Gogate[6], Jayaraman[7]. Carruthers *et al.*[8] and Ramamirtham and Jayaraman[9]. But their investigations have been mostly in the coastal waters of the Arabian Sea. Thus information available so far is for limited regions only and not based on systematic study. With this object in view an intensive Oceanographic Research programme in the Indian Ocean under the name—'International Indian Ocean Expedition' was started in 1961 by the International Council of Scientific Unions and UNESCO. The programme of the Indian participation in this joint venture was developed by the Indian National Committee on Oceanic Research (INCOR). Active participation by India commenced in the year 1962 when one of our research vessels INS KISTNA made her first four cruises in the Arabian Sea during post monsoon period. On the basis of observations made at about 60 stations spread over the Northern Arabian Sea certain tentative conclusions have been drawn and presented herein.

AREA UNDER INVESTIGATION

The part of the Arabian Sea which is in the North of latitude 15°N and bounded by longitudes 60° and 72·5°E was covered by a net work of 60 observation stations. The distance between two successive stations was approximately 60 miles. Details regarding positions of stations, dates and timings of collection of water samples are given in Appendix 'A'.

ANALYTICAL TECHNIQUE

The classical Winkler procedure[10] has been adopted throughout for the determination of dissolved oxygen in the sea water samples. Tight fit ground glass stoppered bottles of 300 ml capacity were made use of for collection of water samples. Water samples were "pickled" immediately after collection and placed in the dark. Time gap between the first and second stages, pickling and titration, was usually between 6 — 12 hours. An automatic burette graduated to 0·02 ml was used. All the apparatus were calibrated before the start of the cruise.

RESULTS AND DISCUSSION

In order to facilitate the interpretation of observed data all the observation stations were grouped into eight sections as shown in Fig. 1. Oxygen concentration (ml/L) of water samples collected at stations that come under one section were plotted against the corrected depths of sampling and the isopleths were drawn. Thus a section-wise study regarding the structure of water masses in the northern Arabian Sea has become more convenient and feasible.

Section No. 1—(*Stations* 1—9 *along the Gujarat Coast*)

This section mainly represents conditions that existed over the continental shelf off the Gujarat coast. The average depth in this region was about 88 metres. Being the first portion of the maiden cruise of INS KISTNA, very few water samples were collected and analysed. Results of the analysis are presented in Table 1.

The data in Table 1 are inadequate for drawing the oxygen isopleths for the region. Thus a detailed study regarding oxygen distribution in this region in the present state is not possible. However, a look at the data suggests that water from surface down to 30 m. in che coastal region North of Bombay upto latitude 22°N is well mixed up and rich in oxygon tontent (5 — 6 ml/litre). The oxygen distribution suggests that thermocline does not

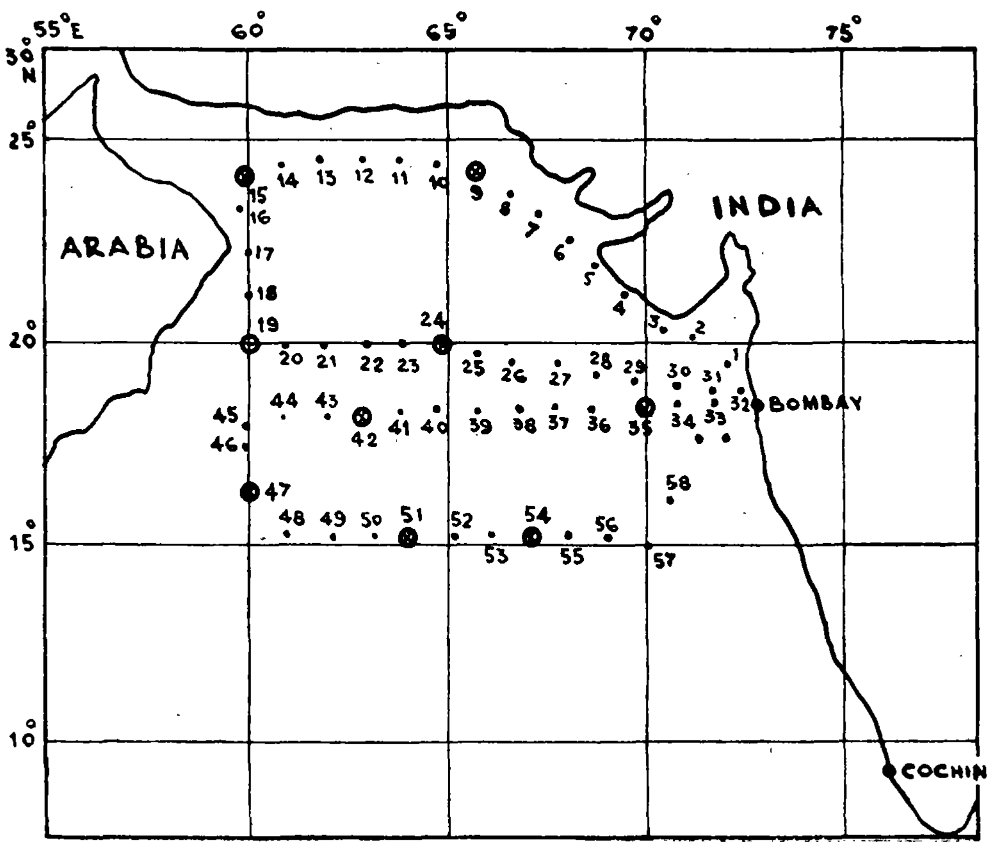

FIG. 1

TABLE 1

OXYGEN CONCENTRATION (Ml/litre)

Depth in m.	Stn. 1	Stn. 3	Stn. 4	Stn. 5	Stn. 7	Stn. 8	Stn. 9
0	6·2	5·5	..	..	..	..	..
10	3·6	4·9	..	..	5·03	4·38	4·2'
20	1·8	5·0	4·4	6·0	4·86	..	..
30	..	5·18	3·4	1·94	..	2·11	2·27
50	..	..	..	..	..	1·30	1·62

seem to be clearly developed here but further North the surface water is com ıaratively poor in oxygen content and marked fall below 30 m. is noticed. This hints that the thermocline in this region is clearly developed. Such a feature of the thermocline along this coast was also reported by Menon and Kurup[11] and Ramam *et al.*[12].

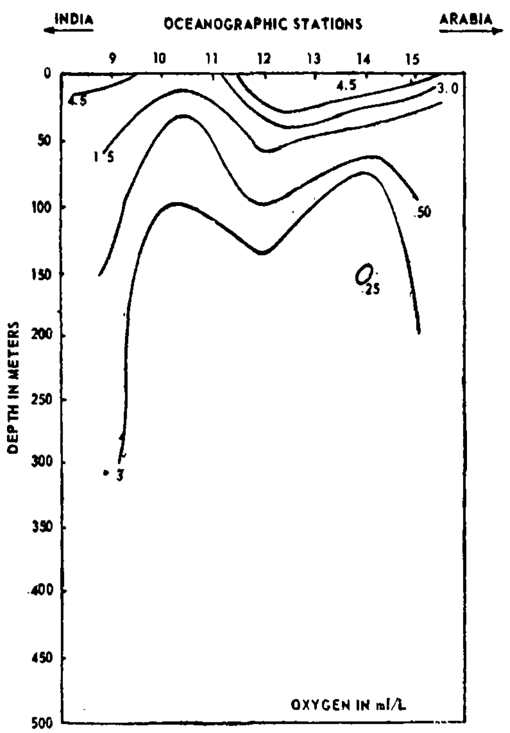

FIG. 2

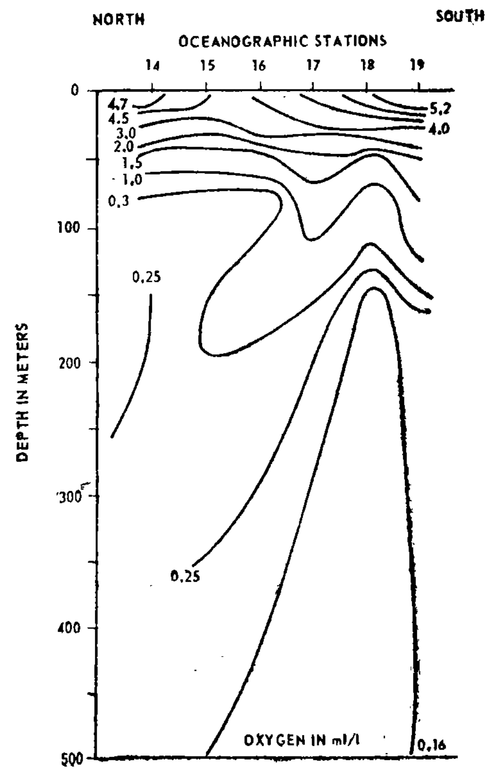

FIG. 3

Section No. 2 (*Stations* 9—14 *along latitude* 24°*N*)

The oxygen isopleths as shown in Fig. 2 indicate that maximum oxygen (4·5 ml/litre) exists in the surface waters at most of the stations except near station Nos. 10 and 11. The 1·5 ml/litre isopleth shows a ridge between station Nos. 10 and 11 and a trough at Station No. 12, west of which it rises towards the surface following the isopleths of higher values in the upper levels. The isopleths at deeper levels show ridges at Station No. 10 and 14 with a trough at station No. 12. Here regular sinking of the isopleths with rise on either side of Station No. 12 below 50 m. depth is maintained. Similar feature is indicated in the thermal structure presented by Menon and Kurup (op. cit.). A water mass with minimum oxygen content (0·25 ml/litre) seems to be localised only near station No. 14 at a depth of about 150 m.

Section No. 3 (*Stations* 15—19 *along longitude* 60°*E*)

This is a meridianal section along 60°E presenting the hydrographic conditions off the Arabian coast. This section was covered in all by 5 observation stations. The oxygen isopleths which are shown in Fig. 3 indicate that oxygen distribution at the surface shows an increase towards South from about 4·5 ml/litre at Station No. 16 to more than 5·2 ml/litre at station No. 19. At all the stations the oxygen concentration decreases with depth indicating a concentration of 2·0 ml/litre at depths of about 40 to 50 m. Below 50 m. the isopleths show appreciable sinking near Station No. 17. Isopleth with minimum oxygen content (0·16 ml/litre) seems to start below 500 m. at station No. 17 and shoots to 150 m. at station No. 18.

Section No. 4 (*Stations* 19—30 *along latitude* 20°*N*)

This section comprises 14 observation stations along latitude 20°N and extends between 60°E to 70°E. Oxygen isopleths as shown in Fig. 4 mark the following features regarding oxygen distribution in this region.

1. Zone of maximum oxygen concentration occurs in surface waters and extends down to 20 m. at most of the stations.

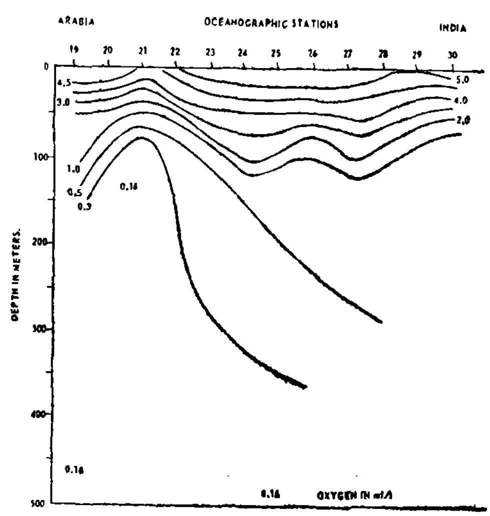

FIG. 4

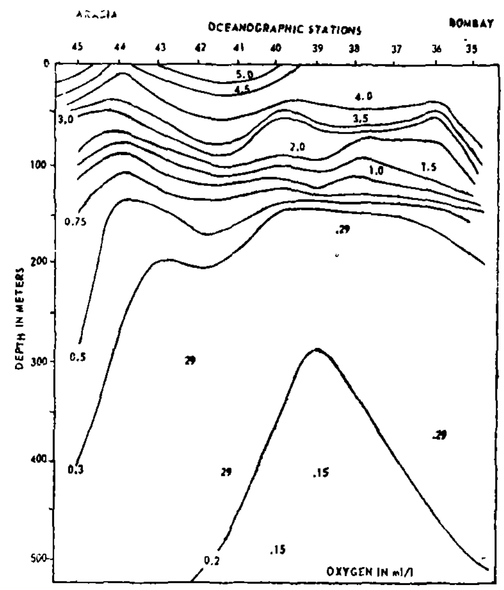

FIG. 5

2. The surface and sub-surface waters at Station No. 21 are comparatively poor in oxygen concentration. Marked 'dooming' of isopleths at these levels near this station is quite noticeable.

3. Area of oxygen minimum (0·3 ml/litre) is well developed between 150 m. to 500 m. in the Western part of the section.

Section No. 5 (*Stations* 35—45 *along latitude* 18°N)

Along this section there were only 11 observation stations spread along latitude 18°N; longitudinal limits of this section are 60°E and 70°E. Fig. 5 presents the vertical distribution of oxygen in this region. Study of these isopleths indicates that a zone of maximum oxygen concentration (4·5—5·0 ml/litre) from surface to 30 m. is confined to the Western flank of the section. At station 44, the isopleths from the surface layers show marked doming, a pattern similar to that near Station No. 21 along 20°N. Existence of almost uniform zone of oxygen minimum (0·15—0·20 ml/litre) is observed at 300 m. and this extends down to 500 m. or more at most of the stations.

Section No. 6 (*Stations* 45—47 *along longitude* 60°*E*)

It is a short meridianal section along 60°E. Latitudes 18°N and 16°N are the upper and lower limits of this section. The section was covered by 3 observation stations. The distribution pattern as shown by the disposition of oxygen isopleths (Fig. 6) indicates that water layers from surface down to 40 m. contains maximum oxygen content. Below50 m. the isopleths show oscillatory behaviour. Appreciable depression in the 0·75 ml/litre isopleth to a depth of about 250 m. near Station No. 45 from a depth of about 160 m. at Station No. 47 is observed. A limited zone of water mass with minimum oxygen content (0·29 ml/litre) is noticed near Station No. 45 at a depth of about 420m.

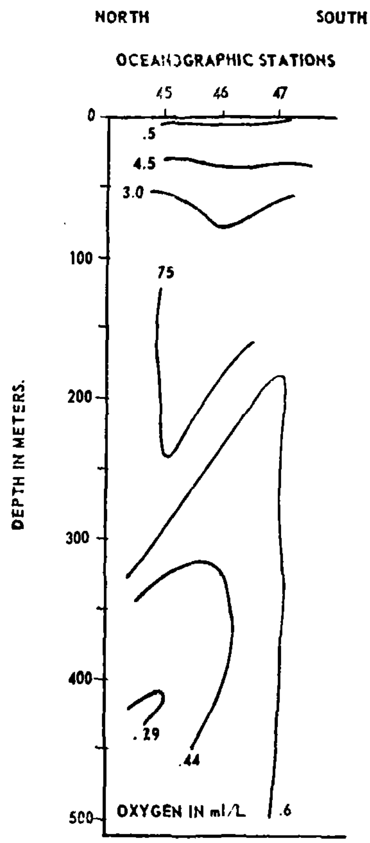

Fig. 6

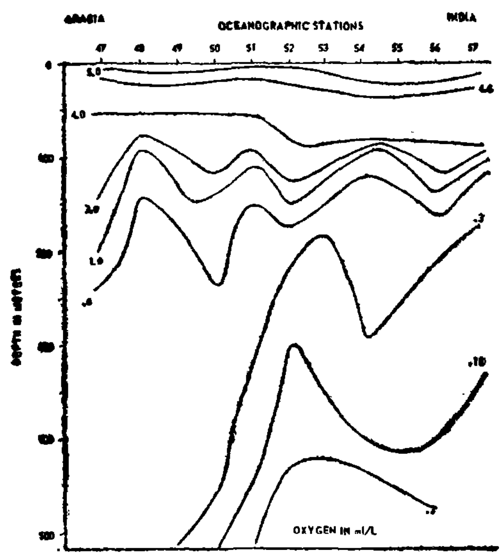

Fig. 7

Section No. 7 (Stations 47-57 along latitude 15°N)

In this section observations were made at 11 stations spread along latitude 15·5°N. Meridional limits of the section are 60°E and 69°E. Study of oxygen isopleths, as shown in Fig. 7, reveals that oxygen distribution from surface down to 40 m. is fairly uniform at all the stations. However, thickness of the well mixed surface waters is slightly reduced in the West. It is also observed that isopleths below 80 m. show wavy trend while the gradients within the layers increase towards the East. This structure within the layer is similar to that of thermocline along this section as indicated by Menon and Kurup[11].

Section No. 8 (Stations 57-60)

It is a diagonal section that runs about 15°N and 70°E in the North-East direction to wards Bombay. The section comprises of 4 observation stations. A close study of the isopleths as shown in Fig. 8 reveals that surface water down to 50 m. contains maximum oxygen 4·27 ml/litre isopleth seems to start from 90 m. depth near Station No. 57 and ascends to 20 m. level near Station No. 60. A sharp decrease in oxygen content in water layers below the said isopleths is noticed. 'Depression' in 0·3 ml/litre isopleth near Station No. 58 at a depth of about 300 m. is quite noticeable. In the same area another isopleth from a depth of about 500 m. shows marked doming but in the reverse order.

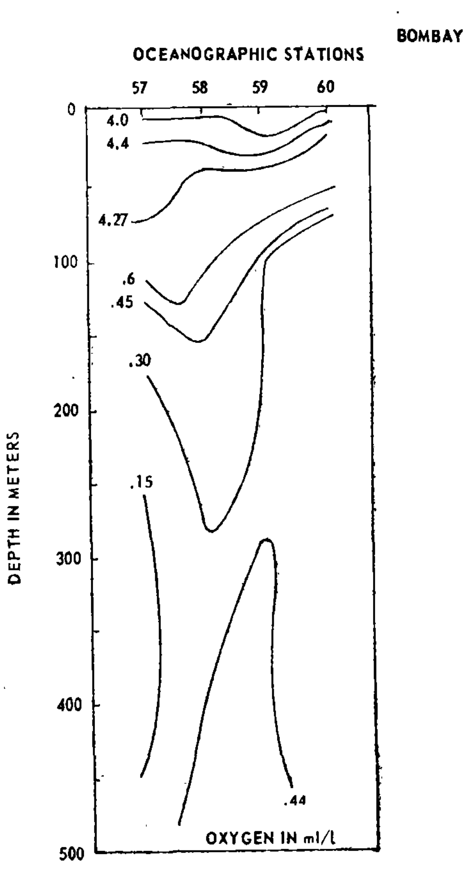

FIG. 8

CONCLUSION

On the basis of observations notice in the preceeding sections following conclusions regarding oxygen distribution in relation to water mass characteristics can be arrived at.

Existence of higher concentration of dissolved oxygen in the surface and sub-surface waters off the Bombay coast (along 20°N upto 22°N) and along latitude 15°N suggests the possibility of higher concentration of phytoplankton in these regions. Upwelling, which was reported to have occurred in the former region[6,8] and record of high temperature values in the surface layer in the latter region[12], are perhaps the main reasons for it.

Zone of low oxygen (0·3 ml/litre) is well developed along latitude 15°N at a depth of about 200 m. and extend down to 500 m. westwards; whereas the same exists at less than 100 m. along 18°N (eastwards only; Stn. No. 60). For want of other biochemical data the existence of low oxygen concentrations at variable depths could not be explained at present.

In the vicinity of meridians 62°E and 63°E along the latitude 24°N the waters of higher density from the Gulf of Oman flow into the Northern Arabian Sea. This water mass of higher density partially mixes with the surface waters and sinks down partially. Existence of zone of oxygen minimum at a depth of 100—150 m. and relatively higher salinity values provide additional support to this deduction.

It is observed that conditions in the Northern Arabian Sea upto latitude 20°N are somewhat less stable in the early post monsoon period. But further down along latitude 15°N the conditions are fairly stable. Whether this can be the cause of progressive lowering in depth of the oxygen miminum zone needs further studies. Menon and Kurup[11] have reported existence of thick isothermal layers and increase vertical stability in the southern part of the Arabian Sea in the month of November.

Near longitude 60°E along latitude 20°N the existence of oxygen minimum zone at a depth less than 100 m. indicates that upwelling to certain extent in the sub-surface layers was in progress at the time of observations. The temperature structure presented by Menon and Kurup[11] suggests an anticlockwise circulation of the water mass. Perhaps this circulation is responsible for divergence and associated upwelling.

Since data on nutrients and plankton density are not available at present, it is emphasised that conclusions drawn should be considered essentially preliminary in character. However, it may be seen that a fairly generalised picture regarding oxygen distribution and structure of water masses in the Northern Arabian Sea during the post monsoon seasons has been obtained.

Rechford[13] has convincingly shown the intrusion of Persian Gulf waters into the Indian Ocean through the Northern Arabian Sea from his study of the salinity maximum in the North Indian Ocean. However, his data (from Vityaz 1960) did not extend North of 20°N. It will be interesting to correlate the results of this present study with a more rigorous study of the hydrographic conditions in this part of the Arabian Sea.

A water mass with characterised poor oxygen content appears to be spreading approximately South-East wards from the region of Gulf of Oman where it appears at a depth of about 120 m. and sinks to a greater depth (300 m.) at its South-Eastern limits.

ACKNOWLEDGEMENTS

The author wishes to express his thankfulness to Dr. S. S. Srivastava, Director, Scientific Research (Navy) and Dr. N. K. Panikkar, Director, Indian Programme for the International Indian Ocean Expedition for due encouragement and kind permission to publish this paper. Thanks are also due to Dr C. B. Murty and Shri R. Jayaraman (I.I.O.E.) for fruitful discussions.

REFERENCES

1. Thomsen, Helge, *Nature* (Lond.), 127 (1931), 489.
2. Seiwell, H. R., *Pap. phys., Oceanogr. Meteor.*, 3(1), (1934), 86.
3. Richards, Francis A. & Redfield, Alfred C., *Deep Sea Res.*, 1 (1954), 279.
4. Miyake, Y. & Saruhashi, K., *Deep Sea Res.*, 3 (1956), 242.
5. Richards, Francis A., *Geol. Soc. Amer. Memoir.*, 67 (1957), 185.
6. Jayaraman, R. & Gogate, S. S., *Proc. Indian Acad. Sci.*, 45B (1957), 151.
7. Jayaraman, R., "The Present State of our Knowledge Concerning Upwelling in the Indian Coastal Waters" (Ms), 1959.
8. Carruthers, J. N., Gogate, S. S., Naidu, J. R. & Laevastu, T., *Nature (Lond.)*, 183 (1959), 1081.

9. Ramamirtham, C. P. & Jayaraman, R., *J. Mar. Biol. Ass. India*, 2 (1960), 199.

10. Strickland & Parsons, "Manual of Sea Water Analysis," Bull. (125), (Publ. of Fisheries Research Board, Canada), 1960, p. 23.

11. Menon, N. R. K. & Kurup, C. B., "Arabian Sea During the Post Monsoon Period (Sept—Nov)", (Deptt Report—RR 11/63, INPL, Cochin), 1963.

12. Ramam, K.V.S., Miss Girija, M.V., Narayana Pillai & Seshagiri Rao, M.G., "A Study of Hydrographic Conditions in the Arabian Sea During the Post Monsoon Period;" (Deptt. Report 13/63 Pt. I, INPL, Cochin), 1963.

13. Rechford, D. J., *Austr. J. Marine & Fresh Water Res.*, 15 (1964), 1.

APPENDIX 'A'

Station No.	Position		Date	Time (1st)
	Lat.°N	Long.°E		
1	19°25′	72°00′	25-9-62	0050
2	20°02′	71°13′	25-9-62	0720
3	20°15′	70°30·5′	25·9-62	1350
4	21°11′	69°46·5′	25-9-62	2020
5	21°46′	69°02·5′	26-9-62	0312
6	22°20′	68°15·5′	26-9-62	0920
7	22°58′	67°27′	26-9-62	2015
8	23°27′	66°41′	27-9-62	2015
9	24°15′	65°45′	27-9-62	1145
10	24°18′	65°00′	27-9-62	2015
11	24°18′	64°00°	28-9-62	0405
12	24°18′	63°00′	28-9-62	1230
13	24°15′	61°58′	28-9-62	1825
14	24°12′	60°58′	29-9-62	0110
15	24°00′	60°00′	29-9-62	0740
16	23°05′	60°00′	29-9-62	2135
17	22°12′	60°11′	30-9-62	0430
18	21°15′	60°00′	30-9-62	1135
19	20°00′	60°00′	30-9-62	1900
20	20°00′	61°00′	1-10-62	0330
21	20°00′	61°59′	1-10-62	0915
22	20°00′	63°00′	1-10-62	1435
23	20°00′	63°55′	1-10-62	2030
24	20°00′	65°00′	2-10-62	0334
25	19°51′	65°57′	2-10-62	1430
26	19°45′	66°50′	2-10-62	2020
27	19°33′	67°42′	8-10-62	0200
28	19°24′	68°50′	3-10-62	0900
29	19°11′	69°50′	3-10-62	1430
30	19°03′	70°44′	3-10-62	2110

Station No.	Position		Date	Time (Ist)
	Lat. °N	Long. °E		
31	18°55′	71°45′	4-10-62	0128
32	18°52′	72°27′	4-10-62	0540
33	18°45′	71°45′	13-10-62	1745
34	18°45′	70°40′	14-10-62	0016
35	18°46′	70°05′	14-10-62	0430
36	18′36′	68°57′	14-10-62	1315
37	18°35′	67′54′	14-10-62	2030
38	18°31′	66°52′	15-10-62	0305
39	18°27·25′	65°52′	15-10-62	0445
40	18°25′	64°47′	15-10-62	1620
41	18°31′	63°55′	15-10-62	2320
42	18°15′	62°52′	16-10-62	0445
43	18°12′	62°00′	16-10-62	1235
44	18°08′	60°56′	16-10-62	1920
45	17°40′	60°00′	17-10-62	0155
46	16°35′	60°00′	17-10-62	0845
47	15°30′	60°00′	17-10-62	1615
48	15°31′	61°00′	18-10-62	0100
49	15°30′	62°00′	18-10-62	0745
50	15°30′	63°00′	18-10-62	1400
51	15°30′	64°00′	18-10-62	2030
52	15°30′	65°00′	19-10-62	0305
53	15°29′	66°00′	19-10-62	0945
54	15°30′	67°00′	19-10-62	1620
55	15°30′	68°00′	20-10-62	0052
56	15°30′	69°00′	20-10-62	0740
57	15′13′	70°00′	20-10-62	1345
58	16°18′	70°28′	20-10-62	1930
59	17°04′	71°17′	21-10-62	0030
60	17°50′	71°55′	21-10-62	0531

Reprinted from *South African Ass. for Marine Biol. Res.–Oceanogr. Res. Inst. Investig. Rep. no. 21*, 1968, p. 1-44

An evaluation of primary productivity studies in the Continental Shelf Region of the Agulhas Current near Durban (1961-1966)

By Joan Burchall

Introduction

As part of the Republic of South Africa's contribution to the International Indian Ocean Expedition, primary productivity studies were undertaken in the continental shelf region of the Agulhas current near Durban during the period 1961 to 1966.

Pioneer studies were begun at a fixed station 29° 54′S and 31° 07′E approximately five miles off Durban in 50 fathoms of water, (Fig. 1). Primary productivity measurements were continued in this position at fortnightly intervals until December 1964, and subsequently also at a second fixed station in 100 fathoms of water. The second station was located on the same compass bearing as for the first station, namely 127°-129°SE, and situated approximately seven miles off Durban, (Fig. 1). Other measurements made were: temperature, salinity, dissolved oxygen, and inorganic phosphorus, nitrate-nitrogen (nitrate-N), nitrite-nitrogen (nitrite-N), and silica.

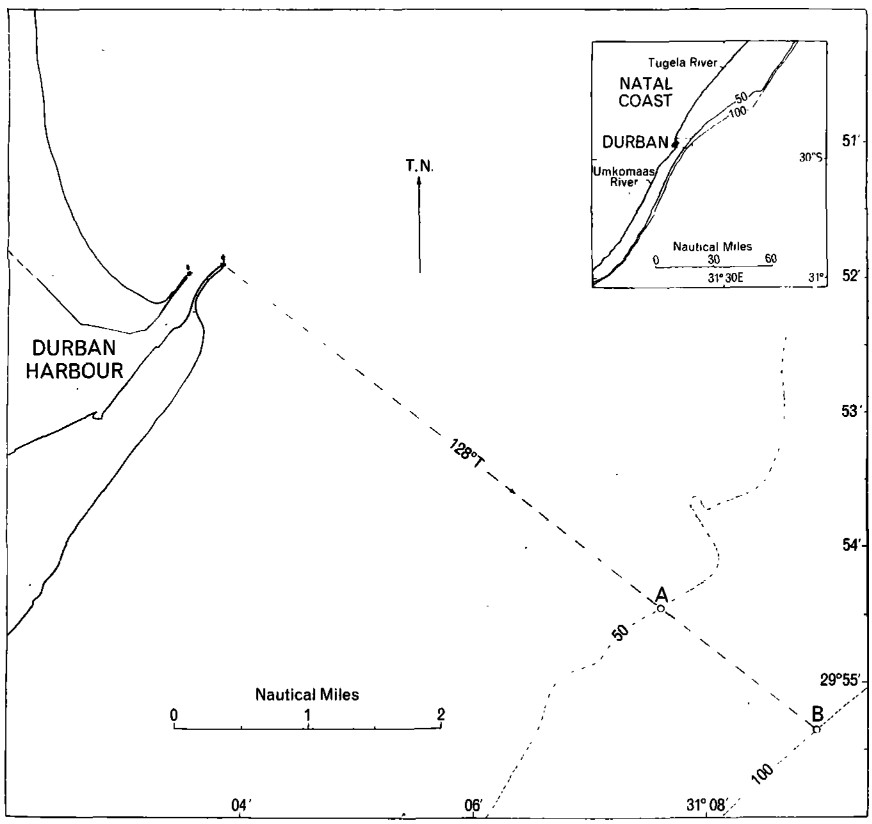

Fig. 1. Station positions relative to depth contours in fathoms.

Measurement of the rate of assimilation of radiocarbon by phytoplankton provides a rather crude index of primary productivity (Jitts, 1957). As the universal adoption of standard techniques and equipment has not yet been achieved, it is important that whenever the radiocarbon method is used, precise details of technique and equipment be given in order that results obtained by different workers may be compared meaningfully. To ensure the validity of such comparisons it is even more important to evaluate the sources of error and bias in individual use of the method. This approach has been adopted as a necessary preliminary to the interpretation of primary productivity measurements obtained at the Durban off-shore stations from 1961 until 1966.

In this paper the sources of error which have been considered are those inherent in the use of the radiocarbon technique, and especially in the methods used to incubate samples during phytoplankton assimilation of carbon-14. When measurements of primary productivity were made from 1961 to 1966, samples were incubated 'in situ' in the ocean, and in three types of shore incubators. These shore incubation techniques have been evaluated in relation to 'in situ' measurements to enable a direct comparison of results obtained using the different techniques. The degree of error of a single primary productivity measurement has also been determined.

Finally there is a brief discussion of primary productivity in relation to available hydrographic information about the off-shore stations.

Methods

Sampling was carried out initially from the R.V. *Lady Theresa* and later from the local shark meshing vessels, *Sea Hound* and *Shark Mesher II*. Water samples were taken at approximately 1000 hours S.A.S.T. depending on other commitments of the vessel.

1. Primary productivity measurements

The rate of carbon assimilation by phytoplankton was measured by means of the carbon-14 technique of Steemann Nielsen (1952). During occupation of stations D1-D69 (Tables 1a, b) water samples were obtained using an insulated non-toxic Nansen-Peterson water bottle of 1 litre capacity. Samples were collected from three depths in the euphotic zone, namely from the surface and from those depths corresponding to 10% and 1% of the surface light intensity. During occupation of D70-D90 (Table 1b) water samples were obtained using van Dorn water samplers with capacities of six litres. Samples were obtained from five depths in the euphotic zone, namely from the surface and from four depths corresponding to 50%, 25%, 10% and 1% of the surface light intensity. These depths were established using a submarine photometer fitted with an Evans electroselenium type photocell, as described by Steemann Nielsen and Jensen (1957). When sea and weather conditions were unfavourable, only surface samples were taken.

Sample water from each depth was dispensed into two 50 cc glass bottles, one of which was darkened, and to each bottle was added 1 cc of $NaHCO_3$ of activity 4 microcurie. Both subsamples were illuminated in an incubator, and the one contained in the darkened bottle was used as control.

1.1 *Sample incubation*

During the period 1961 until 1966, various methods of sample incubation were used for primary productivity measurements. Originally, 'in situ' experiments were carried out, but this proved impractical due to frequent rough seas encountered near Durban, and it became essential to carry out productivity measurements in a laboratory under simulated conditions. Three types of shore incubation techniques were used.

1.1.1 *'In situ' (D1-D8)*

Using this technique, the 'light' and 'dark' bottles for each sample depth were inoculated with radiocarbon and incubated for four hours at sea, usually commencing at noon. On occasions, samples were incubated from noon until sunset. The distance off-shore of the fixed station discouraged incubation of the samples at this position and as a general procedure the samples were incubated at a position closer in-shore, where it was necessary to redetermine the 10% and 1% light intensity depths. The bottles were spaced along a cable, allowance being made for current undertow, and returned to the water, the cable being secured by an anchor and marked by several floats. Throughout the shipboard procedure, the samples were kept in a bucket of sea water and shielded from direct sunlight.

Numerous practical difficulties entered into the above procedure. If there was even a slight swell, there was a danger of the sample bottles smashing against the ship's hull while being lowered into the water, or during recovery. The success of each experiment was dependent on the weather, and if there was any deterioration in conditions during incubation, the experiment would have to be prematurely terminated. In positioning the bottles along the cable, it was difficult to estimate the allowance which should be made for current undertow and impossible to be quite certain that the sample bottles were returned to the level of sampling.

1.1.2 *Incubator-1 (D9-D46(1))*

Using this technique, one 'light' bottle and one 'dark' bottle from each depth sampled were placed on a rotating disc in a water bath at a known temperature and exposed for a measured period to illumination of a known intensity. The samples were exposed for four hours commencing at noon. The design of this incubator was similar to that described by Steemann Nielsen and Jensen (1957).

The phytoplankton was incubated at light saturation values. In the tropics and subtropics these values range from 20,000 to 30,000 lux (see light intensity-photosynthesis graphs; Steemann Nielsen, 1952, p. 131, Fig. 6; and Steemann Nielsen and Jensen, 1957, p. 101-103, Figs. 32-36). The samples were incubated at a light intensity of 25,000 lux. This light intensity was obtained using six lamps — Philips Type 13011 E/99 (220 volt, 150 watt) ES, pressed glass with fittings Type 66254 HE/00. An advantage of using pressed glass was that the light was diffused and illumination more even. The light quality was an approximation of the daylight spectrum, the whole problem of which was discussed by Steemann Nielsen and Hansen (1959, 1961). Two types of filters were placed in front of the bottles during incubation, a light neutral ON 32, and a dark neutral ON 31. The filters were manufactured by Chance Pilkington Optical Works. A light filter was placed in front of the 10% water sample and a light and a dark filter in front of the 1% water sample. No filter was placed in front of the 100% sample. The filters were used to simulate conditions in the sea but the neutral filters have the same rate of absorption in the whole part of the spectrum where photosynthesis takes place. In the sea, light quality changes with depth, and simulation was hence only an approximation.

Sea water was circulated through the incubator during an experiment, maintaining the samples at approximately sea surface temperature.

1.1.3 *Incubator-2 (D46(2)-D69)*

In the design of this incubator use was made of sunlight and glass filters to simulate light conditions at depths in the ocean.

Incubator-2 consisted of six metal compartments coated with dark paint and arranged in two rows of three compartments each. One 'light' bottle and one 'dark' bottle for each of the three depths sampled were placed in these compartments side by side and exposed to sunlight. The 10% sample was covered with a light neutral filter (ON 32) and the 1% sample by a light (ON 32) and a dark (ON 31) neutral filter. No filter was placed over the 100% sample. The samples were incubated from noon until sunset and were maintained at approximately sea surface temperature by a constant flow of sea water. The incubator was mounted on a small platform which was operated by a motor and agitated the samples up and down during incubation (Doty and Oguri, 1957).

1.1.4 *Incubator-3 (D70-D90)*

Experimental bottles from each depth sampled were illuminated by sunlight in incubator-3, whilst the 'dark' bottle, or experimental control, was wrapped in aluminium foil and placed in a light-proof box. Both incubator-3 and the 'dark' box were supplied with circulating sea water which maintained the samples at sea surface temperature. Samples were incubated for 24 hours.

Incubator-3 comprised five cylindrical clear perspex tubes fitted with neutral density metal screens in order to simulate the light intensities of the depths sampled. The incubator was made locally and metal screening was obtained from Perforated Products Inc., 60 Harvard St., Brookline, Mass.

02146, U.S.A. The code numbers were 15G (simulating 50% light intensity), 40/10P (25%), 125P (10%), and 5W (1%). The incubator was similar to those used on the R.V. *Anton Bruun*, which took part in the U.S. Programme in Biology for the International Indian Ocean Expedition (Ryther, Hall, Pease, Bakun and Jones, 1966).

1.2 *Post-incubation treatment of samples*

After incubation all samples were filtered through membrane filters (group 2, Membranfilter, Göttingen). The filters were clamped into special holders in which drying was completed during the following 24 hours (Steemann Nielsen, 1952).

As soon as possible after drying overnight, the filters were placed in a closed container above fuming hydrochloric acid for 20 minutes. The acid removed inorganic carbonate which acts as a beta-emission absorber (Mitchell-Innes, 1967). Immediately afterwards the filters were dried in a desiccator and then removed from the filter holders and stored in plastic boxes inside a desiccator containing silica gel and soda lime. Soda lime mixed with the desiccant removed the atmospheric CO_2 in the desiccator and reduced exchange with the carbonate in the sample (Doty and Oguri, 1957). The filters were then ready for counting.

A Geiger-Müller tube with a Philips scaler (type 111.531) was used to count the number of C^{14}-disintegrations in both the phytoplankton samples and the radiocarbon solution. At each depth the activity of the illuminated sample was corrected for non-photosynthetic uptake of C^{14} by subtracting the 'dark' bottle activity. The carbonate-carbon content of sea water was calculated for each depth using temperature and salinity data, and assuming a pH of 8.20. Primary productivity was calculated as milligrams of carbon assimilated per cubic metre per day (mg C/m^3/day). By integration the production in the water column beneath one square metre surface was calculated and the results expressed as milligrams of carbon assimilated per square metre per day (mg C/m^2/day). The hours of daylight (to the nearest 0.25 hour) between sunrise and sunset were used in the calculations of daily production.

2. **Hydrographic data**

2.1 *Salinity*

All salinity determinations were carried out at the regional laboratory of the Council for Scientific and Industrial Research, Durban. The determinations were carried out using a conductometric technique. The meter was calibrated with standard sea water and the salinity values, expressed as parts per thousand (‰) are considered to have an accuracy of at least 0.01 parts per thousand.

2.2 *Temperature*

Graduated centigrade thermometers were mounted inside the water samplers. Temperatures were read immediately the samplers were brought to the surface.

2.3 *Oxygen*

Winkler's technique was used to determine the dissolved oxygen present in samples (Riley and Skirrow, 1965). The oxygen content of samples was expressed in cc/litre.

2.4 *Inorganic nutrients*

During occupation of D1-D69 only inorganic phosphorus was determined. This determination was done colorimetrically using the standard molybdenum-blue method and subsequent visual comparison with an artificial standard made up in distilled water (Harvey, 1960). The phosphate was expressed as milligram atoms per cubic metre (mg-at/m^3).

During occupation of D70-D90 sample water from each depth was stored in polyethylene bottles in a deep freeze. All analysis was carried out using a Beckman DU spectrophotometer. The method used for the determination of inorganic phosphorus was that given by Murphy and Riley (1962), nitrate-nitrogen as given by Mullin and Riley (1955), nitrite-nitrogen as given by Rider and Mellon (1946), and silica as given by Mullin and Riley (1955). The concentration of inorganic nutrients has been expressed in each case in milligram atoms per cubic metre (mg-at/m^3).

Hydrography

Ocean currents and water masses

The Durban off-shore station where primary productivity studies were begun in 1961 was situated at the outer edge of the continental shelf in fifty fathoms of water. The Agulhas current flows south-west following the edge of the continental shelf; the current is not a steady stream but it varies its position and flow rate from day to day (Anderson, 1967).

It is known that the coast currents within five or ten miles of the coast off Durban reverse direction periodically and it seems likely that these reversals are linked to the variations of the Agulhas current. Adding to the complexity of the system, numerous large eddies are contained in the continental shelf region of the Agulhas current near Durban. Two eddies have been detected at times, one to the north and the other to the south of Durban (Anderson, 1967). These may be semi-permanent. Movement of the water around these eddies was clockwise, and the water in the centre was cooler than round the outside.

It seems possible that the Durban off-shore stations which were sited without prior knowledge of Agulhas current features, may have been situated between these two eddies. This introduces difficulties into the interpretation of results if the eddies move north or south.

Although the entire body of water in the east coast region is said to comprise the Agulhas current, several water masses are represented in this system

(Darbyshire, 1966). Off Durban these water masses comprise surface, subtropical and central water masses, with mixed or boundary water occurring between surface and subtropical water and also between surface and central water; the T-S relationships by which the water masses are characterised are illustrated in Fig. 2 (Anderson, personal communication, 1966).

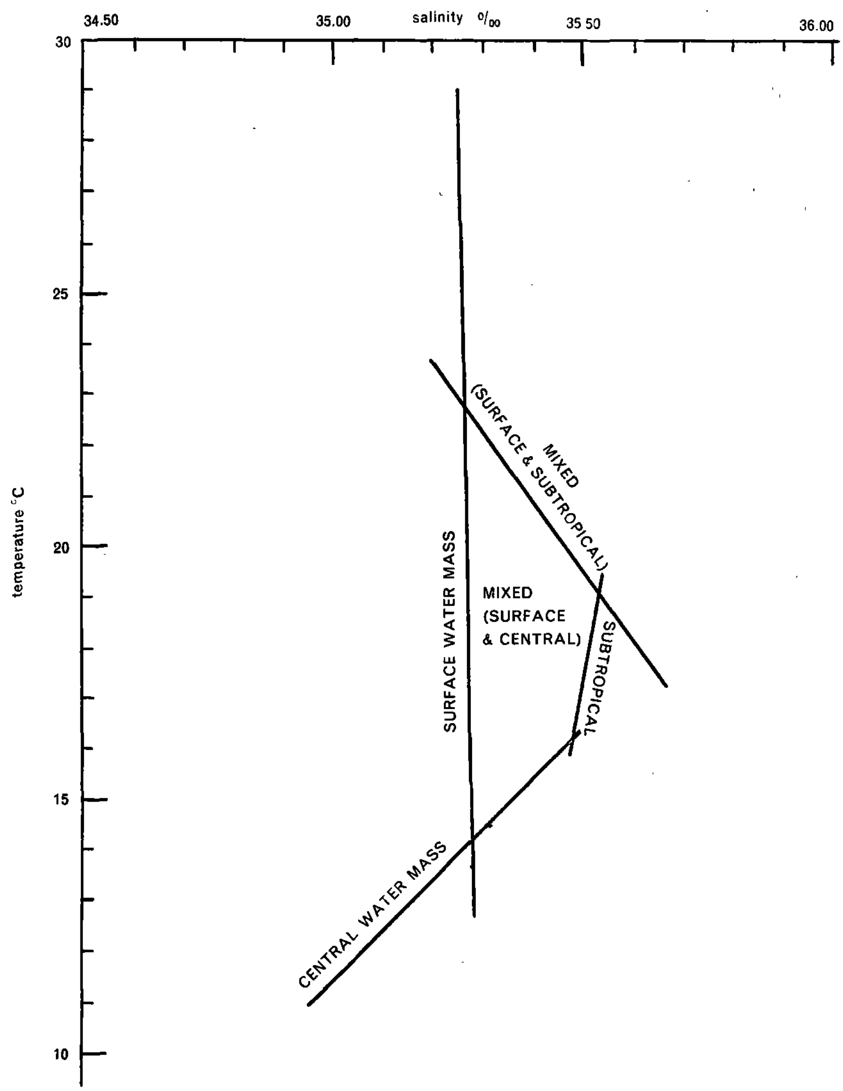

Fig. 2. T-S diagram (water masses comprising the Agulhas current system, F. Anderson personal communication, 1966)

9

The water mass types to be expected near the shore in shallow water are surface and boundary water. To test this idea it was decided to compare the temperature and salinity observations for each sample depth whenever the off-shore stations were occupied (Tables 2a, b), with the temperature and salinity characteristics of the water masses illustrated in Fig. 2.

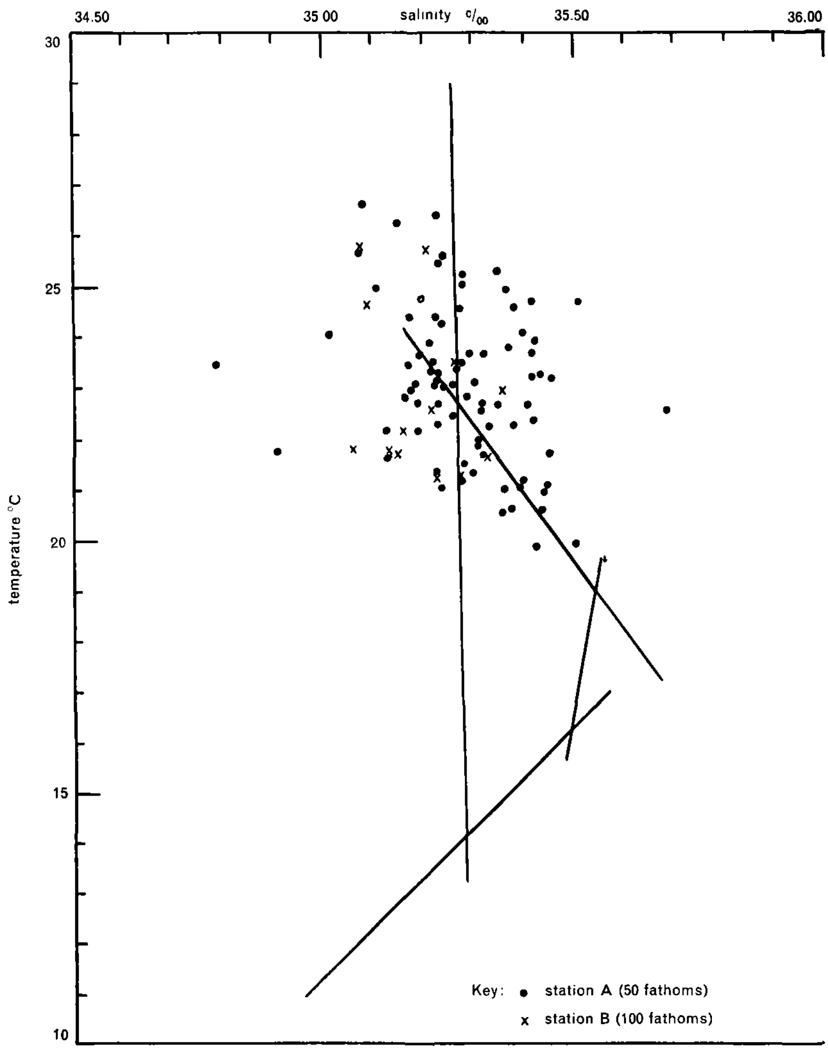

Fig. 3a. T-S diagram compiled from sea surface samples obtained at 100% light depth.

10

Indications are that the continental shelf region of the Agulhas current near Durban comprises essentially surface and boundary water. At the surface or depth representing 100% light intensity, surface water was indicated and also boundary water. The latter type was the mixed layer between surface and subtropical water masses (Fig. 3a). This pattern was repeated at sub-surface

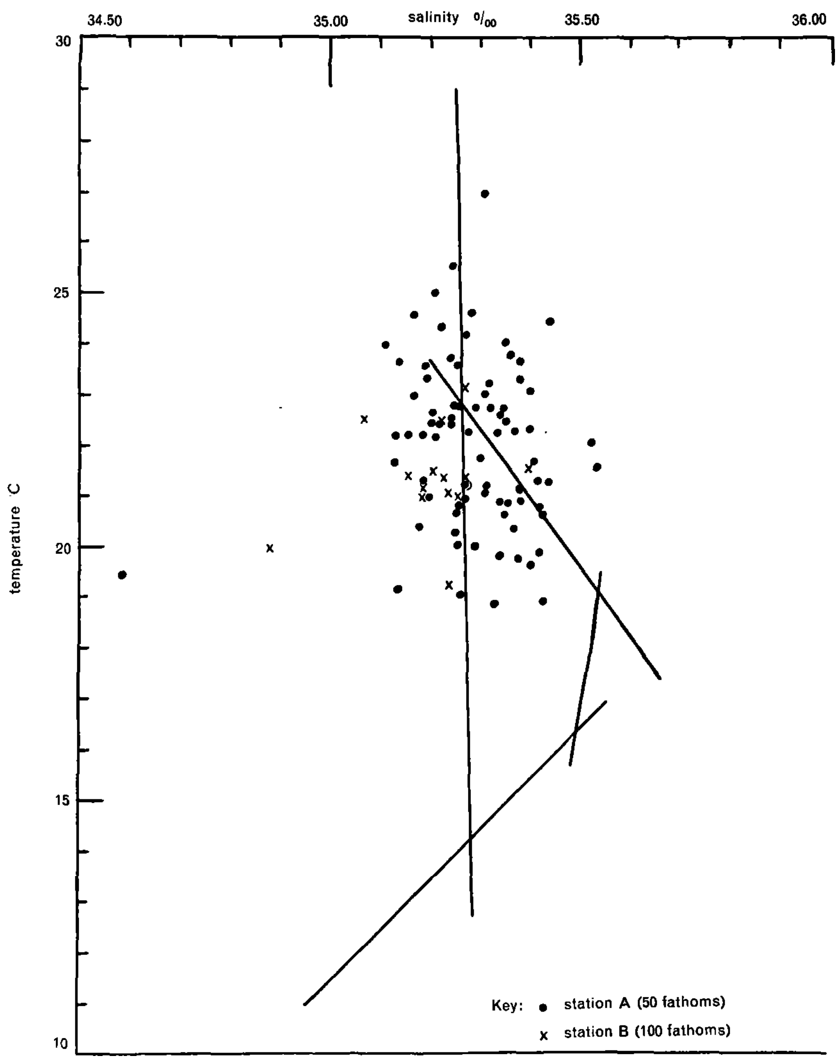

Fig. 3b. T-S diagram compiled from sub-surface samples obtained at 10% light depth.

levels to which 10% and 1% of surface light intensity penetrated, but there was also evidence of the mixed layer between surface and central water masses, especially at the 1% depths (Figs. 3b, c).

Distribution of temperature and salinity

These data are presented in Tables 2a, b.

It has been shown how temperature and salinity data have been used to

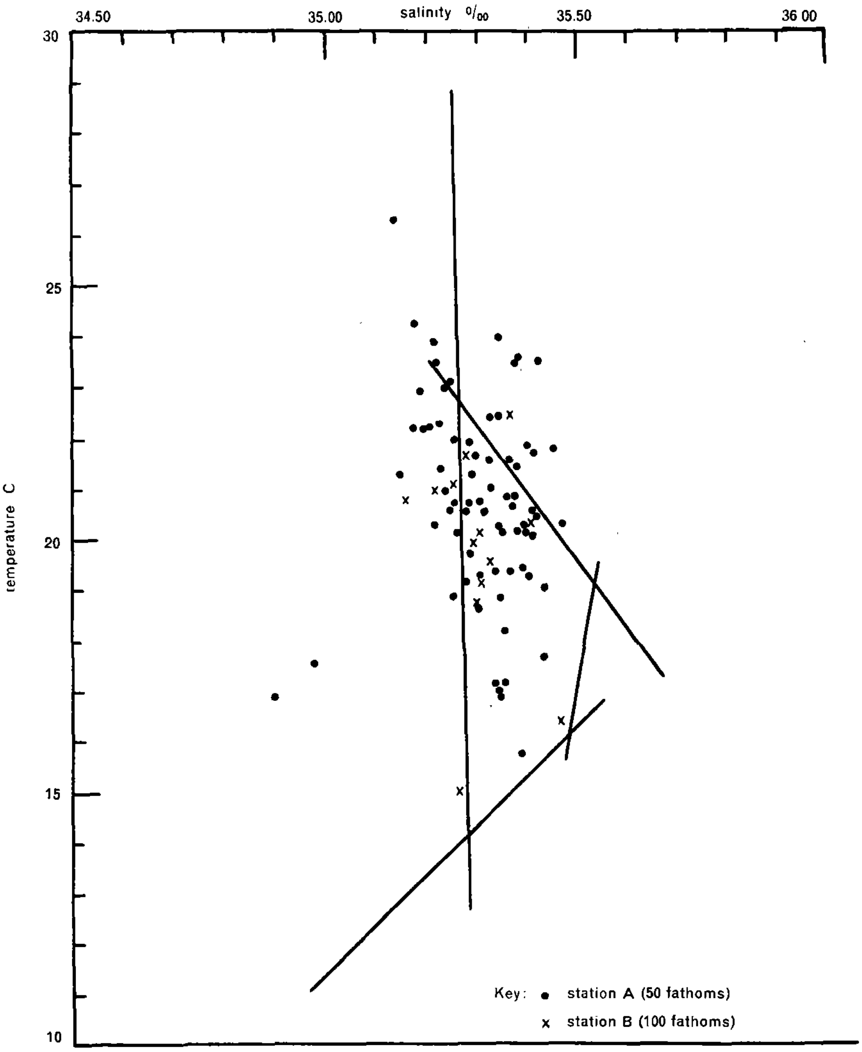

Fig. 3c. T-S diagram compiled from sub-surface samples obtained at 1% light depth.

12

identify the water masses present at the off-shore stations (Figs. 3a, b, c). These water masses are known to comprise a very variable system and work has begun comparatively recently towards monitoring this variability. In view of this fact it would be premature to attempt to construct sections showing seasonal variations of temperature and salinity on the basis of the information obtained at the off-shore stations. Such sections could suggest an entirely fictitious picture.

Distribution of inorganic nutrients and dissolved oxygen

These data are presented in Tables 2a, b.

It was thought that each water mass discerned at the off-shore stations might be characterised by relatively higher or lower concentrations of inorganic nutrients, but no clear distribution was evident on available results (Figs. 4 a, b, c, d).

The distribution of inorganic phosphorus in the surface water mass varied from 0.5-1.5 mg-at/m^3 with approximately the same distribution in the boundary water, which was the mixed layer between the surface and subtropical water masses. Considerably fewer results were available on the distribution of inorganic phosphorus in the boundary water which formed the mixed layer between the surface and central water masses (Figs. 4a, b).

The distribution of inorganic nitrogen and silica in the surface water mass varied from 0-10 mg-at/m^3. Very little information was available on the distribution of either of these elements in the two types of boundary water (Figs. 4c, d).

The distribution of inorganic phosphorus may indicate that the mixed layer between surface and central water masses is generally more fertile with respect to inorganic nutrients, than the other two water masses represented at the off-shore stations, because of the mixing with central water. This cannot be concluded on available evidence, since the water masses represented at the off-shore stations are not adequately characterised by existing data.

Dissolved oxygen was determined as a routine procedure during the course of primary productivity studies. Surface oxygen values did not vary greatly from saturation values (Orren, 1963).

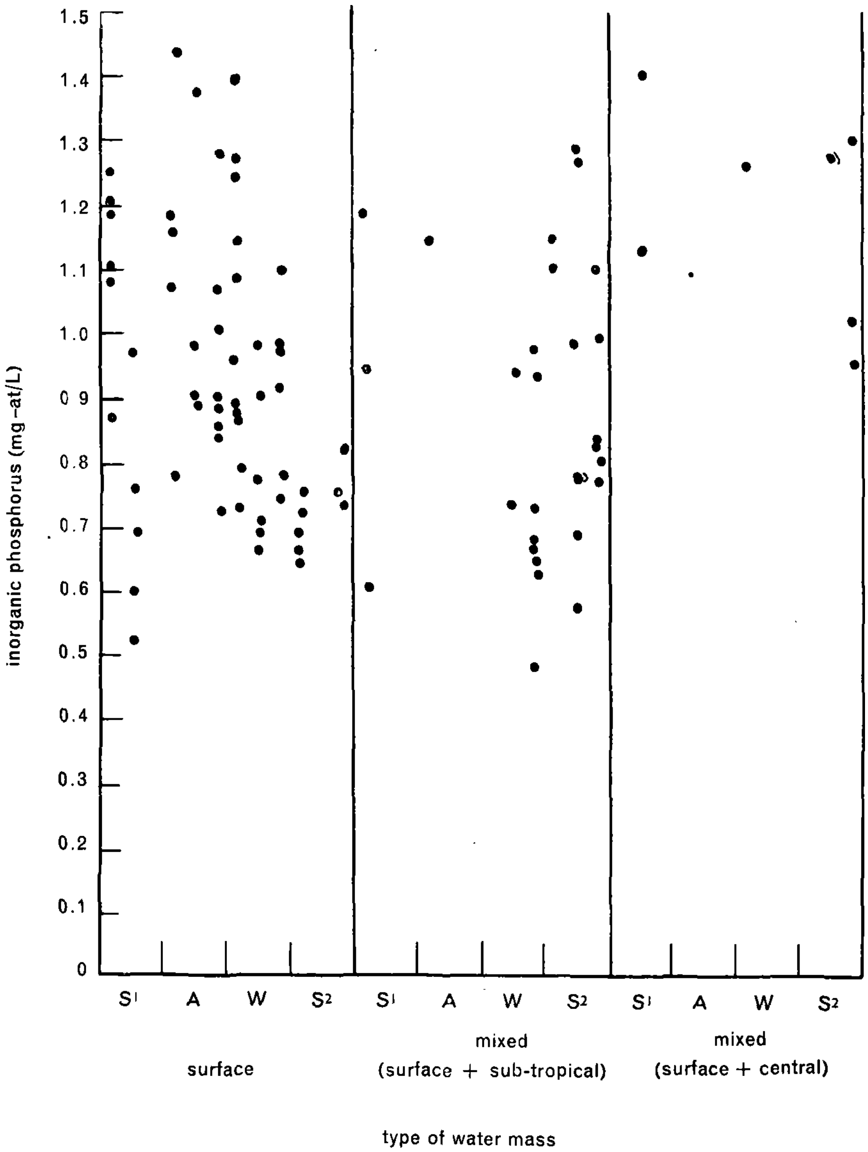

Key: S1 = summer (November, December, January)
A = autumn (February, March, April)
W = winter (May, June, July)
S2 = spring (August, September, October)

Fig. 4a. Distribution of inorganic phosphorus (D1-D69).

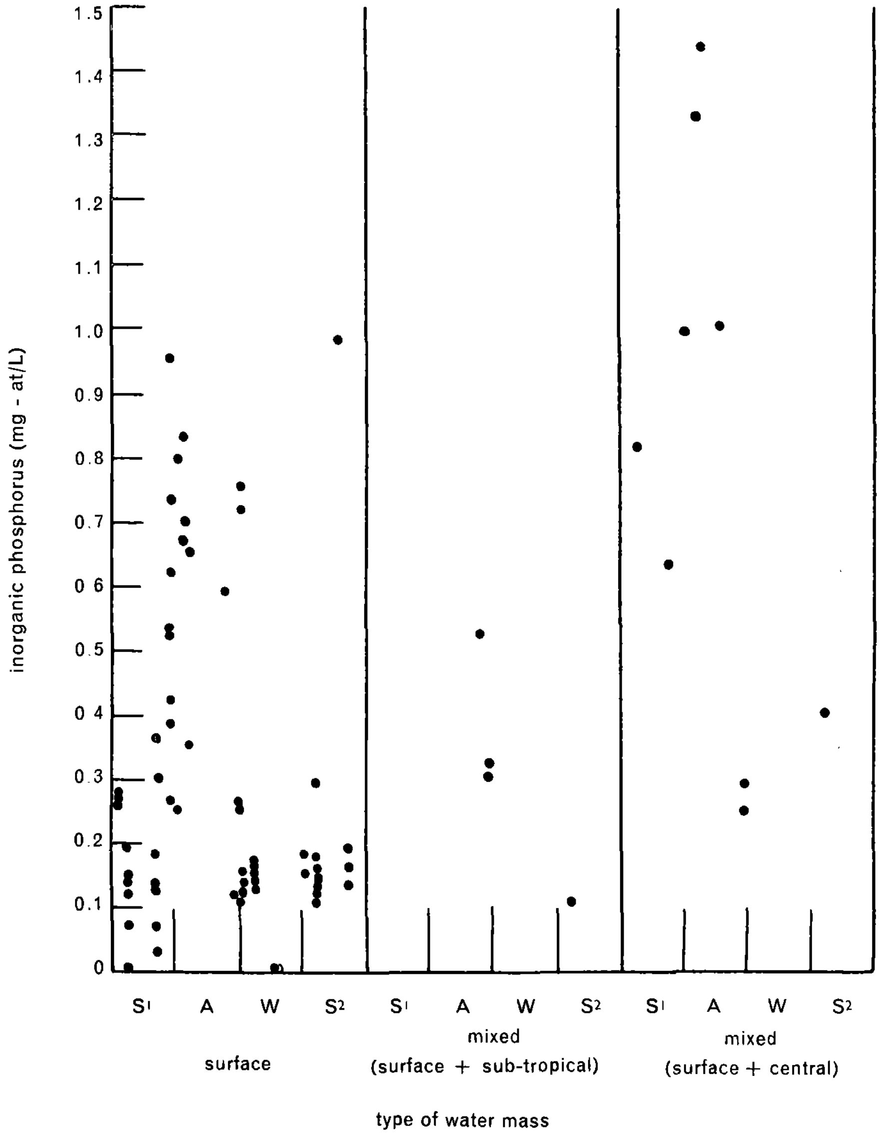

Key: S1 — summer (November, December, January)
A — autumn (February, March, April)
W — winter (May, June, July)
S2 — spring (August, September, October)

Fig. 4b. Distribution of inorganic phosphorus (D70-D90).

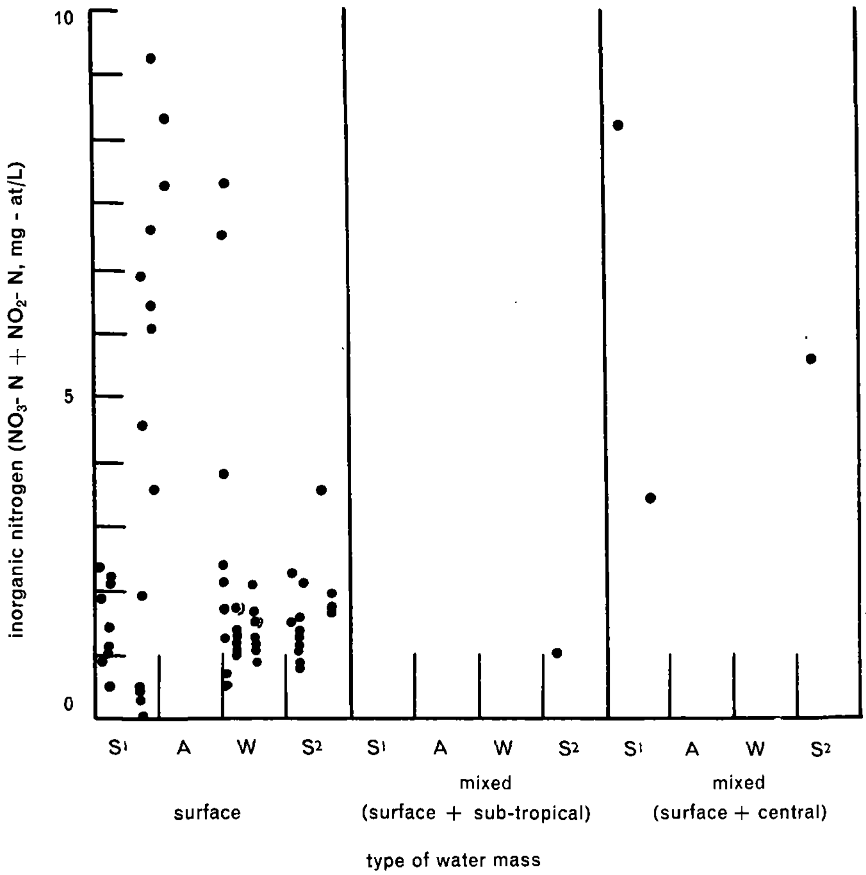

Key: S^1 = summer (November, December, January)
A = autumn (February, March, April)
W = winter (May, June, July)
S^2 = spring (August, September, October)

Fig. 4c. Distribution of inorganic nitrogen (D70-D90).

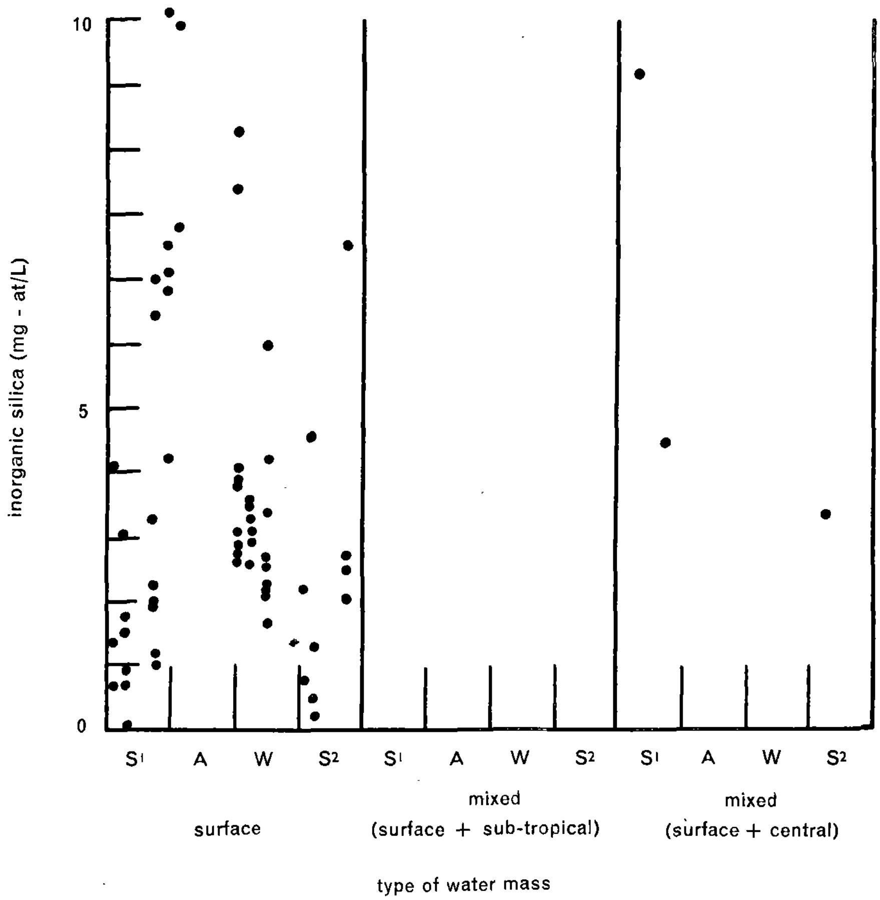

Key: S1 = summer (November, December, January)
A = autumn (February, March, April)
W = winter (May, June, July)
S2 = spring (August, September, October)

Fig. 4d. Distribution of inorganic silica (D70-D90).

Primary productivity results

Evaluation of incubation techniques

The various sample incubation procedures used during Durban off-shore primary productivity studies have been described in section 1.1 of this report. To enable direct comparison of all measurements obtained, a statistical analysis was carried out to evaluate the bias introduced into the results by each experimental procedure.

In carrying out this evaluation of incubation techniques simultaneous measurements of primary productivity using incubator-1 and incubator-2 were made on replicate samples both in the incubators and 'in situ' in the ocean. Measurements were made at five stations off Durban from September 1965 until January 1966. Conditions varied from calm seas and clear skies to choppy seas and overcast skies, and the magnitude of primary production at the five stations varied considerably, e.g. the production in a column beneath $1 m^2$ of sea surface varied from 0.31 to 1.66 grams $C/m^2/day$ (Table 3a).

During the period March 1967 and May 1967, when a total of five stations was occupied, simultaneous measurements of primary productivity were made on replicate samples both in incubator-3 and 'in situ' in the ocean (Table 3b).

On the basis of experimental results, regression equations have been calculated enabling 'in situ' primary production to be predicted from incubator measurements. The linear regression formula as shown below has been used to calculate regression equations:

$$b = \frac{n\Sigma XY - \Sigma X \Sigma Y}{n\Sigma X^2 - (\Sigma X)^2}$$

b = regression co-efficient, or the slope of the regression line
n = number of observations
X = incubator measurements of primary productivity
Y = 'in situ' measurements of primary productivity

$$a = \overline{Y} - b\overline{X}$$

a = the constant term

The regression equations predicting 'in situ' primary production from incubator measurements for each sample depth (mg $C/m^3/day$) are shown (Table 4a, b, c). The regression equations predicting 'in situ' primary productivity (mg $C/m^2/day$) from incubator measurements are as follows:

$$P_{\text{'in situ'}} = 0.55\, P_1 + 96 \qquad (1)$$

$$P_{\text{'in situ'}} = 0.64\, P_2 + 196 \qquad (2)$$

$$P_{\text{'in situ'}} = 0.52\, P_3 + 143 \qquad (3)$$

where P_1 = primary productivity in incubator-1
P_2 = primary productivity in incubator-2
P_3 = primary productivity in incubator-3

(1) is based on four experimental observations, (2) on the results of three experiments, and (3) on the results of five experiments. In relating primary productivity measurements obtained 'in situ' in the ocean to those obtained using incubator-2, the measurement obtained on 25.1.1966 was regarded as aberrent (Table 3a). It was established that during use of the radiocarbon technique the original sample water had been contaminated with radiocarbon solution.

The standard errors of the regression co-efficients and constant terms in equations (1), (2) and (3) were calculated as follows:

Source	*d.f.*	*sum of squares*	*variance estimate*
Regression	1	$(\Sigma XY)^2/\Sigma X^2$	
Error	n — 2	by difference	σ_e^2
Total	n — 1	ΣY^2	

The regression analyses of (1), (2) and (3) have been shown (Tables 5a, b, c). These analyses provided an estimate of σ_e^2 for each equation. The standard errors of the regression co-efficients b_1, b_2, and b_3 were determined as follows:

$$\text{standard error of } b=\sqrt{\frac{\sigma_e^2}{\Sigma X^2}}$$

and for $b_1=0.55$, the standard error$=0.07$
$b_2=0.64$, the standard error$=0.10$
$b_3=0.52$, the standard error$=0.00$

The standard errors of the constant terms a_1, a_2, and a_3 were determined as follows:

$$\text{standard error of } a=\sqrt{\sigma_e^2\left(\frac{1}{n}+\frac{\bar{X}^2}{\Sigma X^2}\right)}$$

and for $a_1=$ 96, the standard error$=186$
$a_2=196$, the standard error$=174$
$a_3=143$, the standard error$=117$

From these results it may be concluded that in predicting primary productivity 'in situ' from incubator measurements, the degree of error to be expected is considerable.

It is also important to realise that in predicting an 'in situ' curve from incubator measurements of primary productivity a second type of error is involved. This is the experimental error or error of technique and regression analysis cannot improve on this.

Error of a single primary productivity measurement

This might be called the error of technique since it is the experimental error that might be expected in any single measurement.

Unfortunately in primary productivity studies, it is not possible to repeat any one measurement because the technique itself seriously alters the sample. A natural biological sample cannot be regarded as completely homogeneous so that the error obtained from measuring sub-samples will contain two components, one due to error of technique and one due to the inherent biological variability of the materials (Cassie, 1961). Samples taken a few feet (or even inches) apart are likely to differ by amounts which are considerably more than the errors of the actual physical techniques of estimation (Cassie, 1962). This means that one cannot be too exact in formal statistical estimates of the error of a single sample and these considerations must be borne in mind when proceeding to the formal aspects.

It is preferable to use a co-efficient of variation rather than the standard deviation itself to set upper and lower limits, because in most biological measurements of this kind, larger numbers tend to vary more than small so that the standard deviation is roughly proportional to the mean and this implies that biological rather than physical factors are the main source of error (Cassie, personal communication, 1966). Doty and Oguri (1959) found that sub-samples drawn from a bucket of sea water gave measurements of productivity with a co-efficient of variation for a single observation of up to 10%. In similar experimental work, Dyason, Jitts and Scott (1965) found that the co-efficient of variation of productivity measurements varied from 13-20% in three tests. On a culture of *Skeletonema*, Cassie (1962) estimated a range of from 9-15%, and pointed out that it is probable that sampling errors contribute a large part of this error of technique errors, even in aliquots from a large well-mixed sample.

In a series of experiments carried out by the author, the errors due to method were determined by measuring the productivity of replicate sub-samples from a large sample of surface sea water. The co-efficients of variation of these measurements varied from 7-17% in three tests (Table 6).

Annual variations in primary productivity

'In situ' predictions of primary productivity measurements ranged from 32-2191 mg C/m^2/day during six years of routine sampling off Durban (Table 1a, b). The vertical distribution of primary productivity (mg C/m^3/day) revealed that the maximum photosynthetic rate occurred between the surface and that depth to which 10% of the surface light intensity penetrated. The 10% depth was generally obtained at depths between 10 metres and 30 metres.

Little is known of the seasonal characteristics of the component water masses of the Agulhas current system. In view of the variability of this system (Anderson, 1967) it is highly probable that short-term variations exceed seasonal variations of primary productivity. For this reason a seasonal interpretation has not been placed on available primary productivity measurements. As an alternative approach, primary productivity has been considered in relation to the water masses present at the off-shore stations, (Fig. 5). It would seem that the surface water mass was generally associated with values of primary productivity of a lower order of magnitude than those generally associated with the presence of boundary water. However, the evidence is

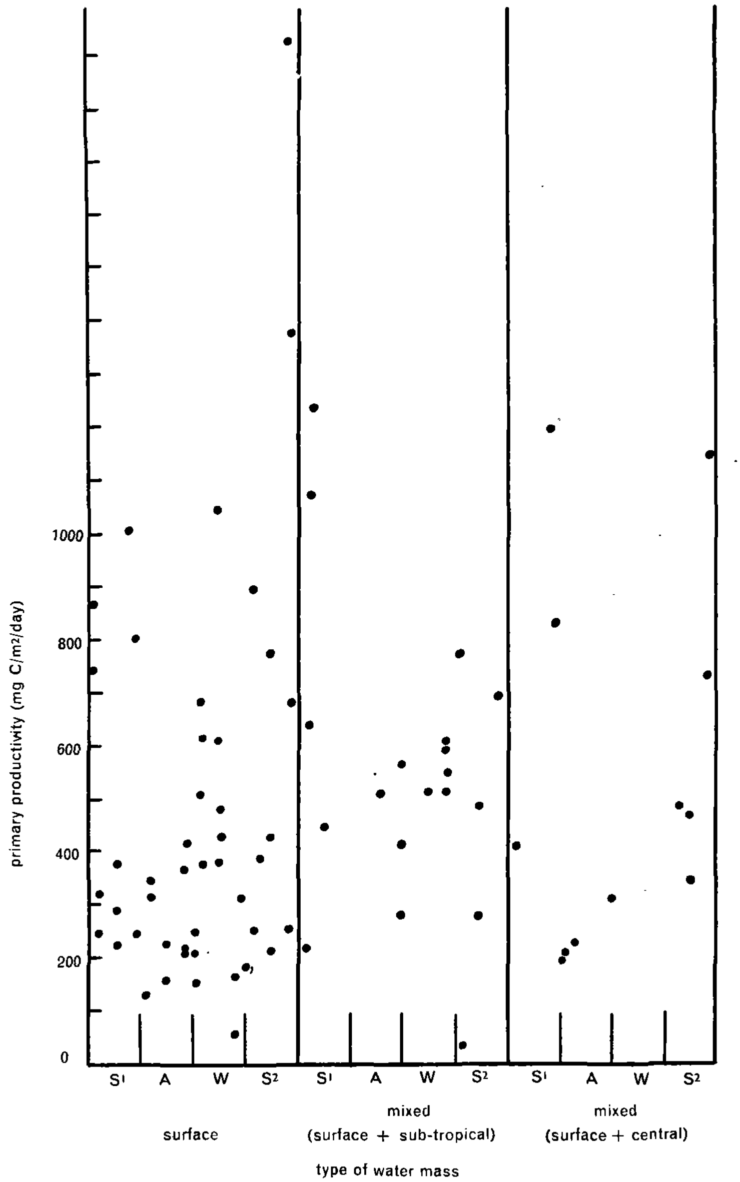

Key: S^1 = summer (November, December, January)
A = autumn (February, March, April)
W = winter (May, June, July)
S^2 = spring (August, September, October)

Fig. 5. Primary productivity in relation to water mass.

21

inconclusive since values of primary productivity which were relatively high were also obtained for the surface water mass.

Primary productivity in relation to environment

An understanding of the processes controlling the primary productivity of the sea near Durban is intimately bound up with knowledge of the behaviour of the water masses comprising the Agulhas current system, and of the associated chemistry and origins of the nutrients in the component water masses of the current system.

The available evidence of the levels of inorganic phosphorus is inconclusive, but is consistent with some apparent greater richness of boundary current water influenced by the central water mass (Figs. 4a, b). Considerably fewer observations are available on the distribution of inorganic nitrogen and silica, and hence the previous statement cannot be supported from these sources. However, in the boundary water where primary productivity was relatively high from May to October, the distribution of inorganic phosphorus actually increased towards the end of spring, whereas in the surface water mass where primary productivity was relatively lower, the distribution of phosphorus showed a decrease from May to October (Figs. 4a, b, and 5). A possible explanation of this feature of the surface distribution of inorganic phosphorus may be that, during winter, the surface water cools and sinks so that an isothermal layer of water is obtained near the surface. In deep ocean, this layer is well established during winter, though in coast waters it is not so apparent. The surface distribution of inorganic phosphorus under such conditions will tend to be depleted as a result of phytoplankton growth, until it is replenished by mixing processes.

The other chemical characteristics of the several distinct water masses comprising the Agulhas current system are virtually unknown at the present time, and it seems probable that the physical variability of the Agulhas current will be reflected in the distribution of inorganic nutrients.

Significance of primary productivity measurements

By means of the radiocarbon technique the rate of transfer of inorganic to organic substances in the sea may be monitored. The technique has therefore been widely used to measure the rate of photosynthesis of natural phytoplankton populations. An important query thus relates to the validity of the method used and the significance of the results obtained. It must be stressed in conclusion that this paper does not attempt a critical evaluation of the actual radiocarbon technique for measuring primary productivity, nor an investigation of the biological sources of error in such studies. This paper represents an evaluation of primary productivity studies in continental shelf waters off Durban. The evaluation of results derived through a routine sampling programme presented particular problems. An attempt has been made to resolve these problems and to present the results obtained mainly for their descriptive value.

Summary

During 1961 primary productivity studies were begun at a fixed station, 29° 54′S, 31° 07′E, approximately five miles off Durban in fifty fathoms of water. Primary productivity measurements were continued in this position at fortnightly intervals until December 1964, and subsequently also at a second fixed station in 100 fathoms of water. Primary productivity was measured using the Steemann Nielsen C^{14} technique. Other measurements made were; temperature, salinity, dissolved oxygen and inorganic phosphorus, nitrate-nitrogen (nitrate-N), nitrite-nitrogen (nitrite-N), and silica.

During the period 1961 until 1966, samples were incubated 'in situ' and in three types of shore incubators. To enable direct comparison of all primary productivity measurements obtained, experiments were carried out to evaluate the bias arising from each incubation procedure. These experiments involved simultaneous determinations of primary productivity using replicate samples from each incubator and 'in situ' in the ocean. Regression equations have been calcaulated so that incubator measurements of primary productivity may be used to predict 'in situ' primary productivity. This prediction is subject to considerable error, however, as revealed by the large standard errors computed. The error of a single primary productivity measurement, or the error of technique, was also determined by measuring the productivity of replicate sub-samples from a large sample of surface sea water. The co-efficient of variation of these measurements ranged from 7-17% in three tests.

From temperature and salinity observations obtained for each sample depth whenever the off-shore stations were occupied, it was shown that the continental shelf region of the Agulhas current near Durban comprises essentially surface and boundary water. Indications are that short-term variations of the current system are considerable. In view of the fact that short-term variations might exceed seasonal variations of primary productivity the measurements were not interpreted on a seasonal basis. Available evidence on the distribution of primary productivity and inorganic nutrients between the component water masses of the Agulhas current system in the in-shore waters is inconclusive, but is consistent with some apparent greater richness of boundary current water influenced by the central water mass.

It seems that an understanding of the processes controlling the primary productivity of the sea is intimately bound up with knowledge of the behaviour of the water masses comprising the Agulhas current system. A real understanding must await the elucidation of the current system, and of the associated chemistry and origins of the nutrients in the component water masses of the current system.

Acknowledgments

I am grateful to the late Dr. David H. Davies for his endeavours in providing facilities for phytoplankton research during his directorship of the Oceanographic Research Institute (O.R.I.).

I would like to acknowledge the following: Miss H. Goddyn, formerly of O.R.I., for collection of data recorded for D1-D28; Miss B. A. Mitchell-Innes, formerly of O.R.I., for collection of data recorded for D29-D69, and for instructing me in the use of the Steemann Nielsen C^{14} technique; Dr. A. J. Alexander, Professor T. A. Villiers, Professor H. Linhart, all of the University of Natal, Mr. F. P. Anderson of the National Physical Research Laboratory, Mr. W. D. Oliff of the National Institute for Water Research, and Dr. A. E. F. Heydorn present Director of O.R.I., for constructive criticism at various stages in the preparation of this paper; and Dr. M. R. Cassie of the University of Auckland for helpful correspondence relating to the statistical treatment of results.

I am also grateful to the City Engineers Department of the Durban Corporation for the use of the local shark meshing vessels *Sea Hound* and *Shark Mesher II*; and similarly to Mr. Douglas Roberts of Murray and Roberts Construction Co., for the use of the *Lady Theresa*.

Finally grateful acknowledgment is made to the Council for Scientific and Industrial Research for financial support through the Marine Research Unit.

Literature cited

ANDERSON, F. P., 1967. Time variations in the Agulhas current near Durban. Unpublished paper read at 'International association of physical oceanographers' Conference, Berne, Switzerland

CASSIE, MORRISON R., 1961. Statistical and sampling problems in primary production. Proc. of the Conference on Primary Productivity Measurement, Marine and Freshwater, University of Hawaii. U.S. Atomic Energy Commission

CASSIE, MORRISON R., 1962. Microdistribution and other error components of carbon-14 primary production estimates. *Limnol. and Oceanogr.*, 7 (2): 121-130

DARBYSHIRE, MOLLIE, 1966. The surface waters near the coasts of southern Africa. *Deep Sea Res.*, **13** (1): 57-81

DOTY, M. S. and OGURI, M., 1957. Selected features of the isotopic carbon primary productivity technique. Contribution to a plankton symposium. *Rapp. P. — v. Réun. Cons. perm. int. Explor. Mer*, **144**: 47-55

DOTY, M. S. and OGURI, M., 1959. The carbon-14 technique for determining primary plankton productivity. *Pubbl. Staz. zool. Napoli*, **31**: 70-94

DYASON, N., JITTS, H. R. and SCOTT, B. D., 1965. Techniques for measuring oceanic primary production using radioactive carbon. *Tech. Pap. Div. Fish. Oceanogr. C.S.I.R.O. Aust.*, (18)

HARVEY, H. W., 1960. The chemistry and fertility of sea waters. Cambridge University Press, p.188

JITTS, H. R., 1957. The carbon-14 method for measuring CO_2 uptake in marine productivity studies. *Rep. Div. Fish. Oceanogr. C.S.I.R.O. Aust.*, (8)

MITCHELL-INNES, BETTY A., 1967. Primary production studies in the south-west Indian Ocean, 1961-1963. *Invest. Rep. oceanogr. Res. Inst.*, (14): 1-20

MULLIN, J. B. and RILEY, J. P., 1955. The spectrophotometric determination of nitrate in natural water with special reference to sea water. *Analytica chim. Acta*, **12**: 464-480

MULLIN, J. B. and RILEY, J. P., 1955. The colorimetric determination of silicate with special reference to sea and natural waters. *Analytica chim. Acta*, **12**: 162-176

MURPHY, J. and RILEY, J. P., 1962. A modified single solution method for the determination of phosphate in natural waters. *Analytica chim. Acta*, **27** (1): 31-36

ORREN, M. J., 1963. Hydrological observations in the south-west Indian Ocean. *Investl Rep. Div. Sea Fish. S. Afr.*, (45): 1-61

RIDER, B. F. with MELLON, M. G., 1946. Colorimetric determination of nitrites. *Ind. Engng Chem. analyt. Edn.*, **18**(2): 96-99

RILEY, J. P. and SKIRROW, G., 1965. Chemical oceanography. London, Academic Press, **2**, p. 313-320

RYTHER, JOHN H., HALL, JOHN R., PEASE, ALLAN K., BAKUN, ANDREW and JONES, MARK M., 1966. Primary organic production in relation to the chemistry and hydrography of the western Indian Ocean. *Limnol. and Oceanogr.*, **11** (3): 371-380

STEEMANN NIELSEN, E., 1952. The use of radioactive carbon (C^{14}) for measuring organic production in the sea. *J. Cons. perm. int. Explor Mer*, **18** (2): 117-140

STEEMANN NIELSEN, E. and JENSEN, E. AABYE, 1957. Primary oceanic production. The autotrophic production of organic matter in the ocean. *Galathea Rep.*, **1**: 49-136

STEEMANN NIELSEN, E. and HANSEN, V., 1959. Light adaption in marine phytoplankton populations and its interrelation with temperature. *Physiologia Pl.*, **12**: 353-370

STEEMANN NIELSEN, E. and HANSEN V., 1961. Influence of surface illumination on plankton photosynthesis in Danish waters (56°N) throughout the year. *Physiologia Pl.*, **14**: 595-613

TABLE 1a 'IN SITU' MEASUREMENTS OF PRIMARY PRODUCTIVITY AT A FIXED STATION (D) OFF DURBAN IN 50 FATHOMS

Station	Date	Sampling Depth metres	Organic Production	
			mg C/m³/day	mg C/m²/day
D 1	17.5.61	0	1.05	49
		17	2.31	
		32	0 38	
D 2	8.6.61	0	1.74	32
		18	0.56	
		36	0.75	
D 4	31.7.61	0	1.51	62
		23	2.04	
		42	0.22	
D 5	30.8.61	0	1.96	45
		13	2.42	
		24	0.58	
D 6	8.9.61	0	31.96	487
		13	18.92	
		28	1.88	
D 7	2.10.61	0	52.25	1188
		43	1.38	
		86	0.25	
D 8	6.11.61	0	9.86	605
		28	14.31	
		53	7.02	
D 23	12.6.62	0	13 02	426
		16	16.20	
		32	7.89	
D 24	21.6.62	0	12.71	385
		22	10.97	
		41	2.15	
D 25	5.7.62	0	17.43	608
		18	17.12	
		37	14.14	

TABLE 1b **'IN SITU' PREDICTIONS OF PRIMARY PRODUCTIVITY AT FIXED STATIONS (D) OFF DURBAN IN 50 FATHOMS (A) AND IN 100 FATHOMS (B)**

Station	Date	Sampling Depth metres	Organic Production		'in situ' prediction
			mg C/m³/day	mg C/m²/day	mg C/m²/day
D 9A	17.11.61	0	8.94	422	328
		30	8.80		
		58	2.34		
D 10A	21.11.61	0	9.49	596	424
		29	13.61		
		49	12.51		
D 11A	30.11.61	U	3.50	1028	661
		23	46.90		
		41	2.94		
D 12A	15.12.61	0	3.92		
D 13A	5.1.62	0	114.24		
D 14A	11.1.62	0	24.22	278	249
		11	12.18		
		23	0.74		
D 15A	19.2.62	0	27.17	415	324
		8	28.47		
		21	1.14		
D 16A	8.3.62	0	88.88		
D 17A	15.3.62	0	5.64		
D 18A	20.3.62	0	18.25	963	626
		14	51.33		
		28	16.66		
D 19A	27.4.62	0	13.75	382	306
		20	8.14		
		40	8.14		
D 20A	4.5.62	0	7.63		
D 21A	15.5.62	0	22.05	572	411
		15	19.95		
		33	8.61		
D 22A	25.5.62	0	3.05	216	215
		24	4.94		
		46	5.99		
D 26A	25.9.62	0	75.00	2744	1605
		33	38.76		
		64	17.16		
D 27A	29.10.62	0	10.40	1081	691
		44	19.63		
		83	1.95		
D 28A	12.12.62	0	5.60	645	451
		32	16.52		
		64	1.68		

TABLE 1b CONTINUED

Station	Date	Sampling Depth metres	Organic Production mg C/m^3/day	Organic Production mg C/m^2/day	'in situ' prediction mg C/m^2/day
D 29A	21.1.63	0	2.90		
D 30A	25.2.63	0	1.04	62	130
		34	0.78		
		62	1.43		
D 31A	1.3.63	0	1.53	119	161
		32	2.81		
		59	0.89		
D 32(1)A	21.3.63	0	76.44	838	557
		7	72.12		
		13	33.96		
D 32(2)A	27.3.63	0	3.50		
D 33A	19.4.63	0	13.73	234	225
		13	7.99		
		26	6.30		
D 34A	24.4.63	0	10.89	214	214
		13	7.81		
		26	6.38		
D 35A	2.5.63	0	58.63	1093	697
		20	18.37		
		42	11.00		
D 36A	21.5.63	0	0.20		
D 37A	29.5.63	0	2.10	118	161
		28	2.63		
		60	0.63		
D 38A	16.7.63	0	1.79	138	172
		38	1.89		
		76	1.68		
D 39A	31.7.63	0	4.41	405	319
		23	12.81		
		42	8.93		
D 40A	8.8.63	0	98.34	1478	909
		9	85.80		
		16	99.77		
D 41A	22.8.63	0	3.38	290	256
		32	7.09		
		52	5.18		
D 42A	24.9.63	0	4.92	234	225
		27	4.08		
		55	3.96		
D 43A	27.11.63	0	1.82	284	252
		24	9.10		
		52	1.82		

TABLE 1b CONTINUED

Station	Date	Sampling Depth metres	Organic Production mg C/m³/day	Organic Production mg C/m²/day	'in situ' prediction mg C/m²/day
D 44A	12.12.63	0	1.54	238	227
		29	6.86		
		55	2.10		
D 45A	17.1.64	0	1.25		
D 46(1)A	31.1.64	0	3.79		
D 46(2)A	25.2.64	0	0.97	240	350
		34	6.33		
		70	0.90		
D 47A	25.3.64	0	0.17	48	227
		20	1.54		
		52	0.42		
D 48A	8.4.64	0	2.37	284	378
		17	12.36		
		33	7.47		
D 49A	21.4.64	0	4.59	528	534
		18	21.25		
		36	11.61		
D 50A	1.5.64	0	4.02	302	389
		21	12.44		
		39	1.86		
D 51A	15.5.64	0	2.29	503	518
		27	18.40		
		45	7.20		
D 52A	27.5.64	0	7.73	680	631
		16	38.97		
		31	1.91		
D 53A	3.6.64	0	8.59	388	444
		20	12.54		
		42	3.53		
D 54A	10.6.64	0	10.38	462	492
		29	10.54		
		50	4.60		
D 55A	17.6.64	0	14.90	516	526
		22	8.86		
		46	12.35		
D 56A	16.7.64	0	5.30	487	508
		22	12.39		
		44	14.22		
D 57A	23.7.64	0	13.62	506	520
		22	10.83		
		50	6.13		
D 58A	12.8.64	0	15.77	933	793
		22	38.31		
		38	3.90		

TABLE 1b CONTINUED

Station	Date	Sampling Depth metres	Organic Production mg C/m³/day	Organic Production mg C/m²/day	'in situ' prediction mg C/m²/day
D 59A	3.9.64	0	11.39	411	459
		22	10.00		
		40	9.47		
D 60A	11.9.64	0	4.08	150	292
		18	6.98		
		26	5.75		
D 61A	18.9.64	0	4.13	469	496
		26	11.77		
		49	11.03		
D 62A	22.9.64	0	6.19	269	366
		38	5.00		
		57	0.91		
D 63A	9.10.64	0	13.92	875	756
		24	34.67		
		36	13.95		
D 64A	22.10.64	0	15.48	717	655
		25	16.75		
		49	9.46		
D 65A	30.10.64	0	1.89	109	266
		29	2.91		
		48	1.20		
D 66A	11.11.64	0	1.08	43	224
		45	0.19		
		77	0.73		
D 67A	25.11.64	0	3.63		
D 68A	9.12.64	0	0.43	158	297
		31	3.76		
		51	5.59		
D 69A	16.12.64	0	3.21	298	387
		23	8.93		
		57	0.41		
D 70A	28.1.65	0	0.64	1325	832
		25	59.98		
		42	6.74		
D 71A	3.2.65	0	0.79	97	193
		38	1.92		
		60	2.23		
D 72A	11.2.65	0	3.91	126	209
		20	3.63		
		48	—		
D 73A	25.2.65	0	0.62	449	233
		27	18.40		
		47	3.05		

TABLE 1b CONTINUED

Station	Date	Sampling Depth metres	Organic Production mg C/m³/day	Organic Production mg C/m²/day	'in situ' prediction mg C/m²/day
D 74A	10.3.65	0	14.81	604	457
		26	12.96		
		48	9.16		
D 75A	30.3.65	0	3.32	702	508
		24	25.73		
		50	1.47		
D 76A	12.4.65	0	4.42	270	283
		25	8.32		
		41	5.53		
D 77A	28.4.65	0	8.65	319	309
		23	3.22		
		49	10.85		
D 77B	28.4.65	0	4.68	814	566
		23	24.42		
		49	12.44		
D 78A	20.5.65	0	1.03	105	198
		21	4.08		
		41	1.01		
D 78B	20.5.65	0	0.98	74	181
		21	2.35		
		41	1.58		
D 79A	4.8.65	0	7.40	80	185
		7	4.06		
		17	1.17		
		29	0.21		
		44	0.58		
D 79B	4.8.65	0	2.65	77	183
		7	2.86		
		17	1.07		
		29	2.08		
		44	0.49		
D 80A	25.8.65	0	13.02	671	492
		7	7.31		
		13	12.44		
		21	30.13		
		39	11.07		
D 80B	25.8.65	0	28.09	471	388
		7	24.49		
		13	10.56		
		21	8.37		
		39	3.52		
D 81A	20.9.65	0	25.13	1220	777
		7	13.95		
		13	96.05		
		24	15.22		
		40	2.44		

TABLE 1b CONTINUED

Station	Date	Sampling Depth metres	Organic Production mg C/m³/day	Organic Production mg C/m²/day	'in situ' prediction mg C/m²/day
D 81B	20.9.65	0	32 34	552	430
		7	39.07		
		13	6.46		
		24	6.20		
		40	5.80		
D 82A	7.10.65	0	92.48	3432	1928
		7	120.55		
		13	121.23		
		23	87.67		
		41	14.09		
D 82B	7.10.65	0	76.03	2377	1379
		7	71.32		
		13	70.72		
		23	76.19		
		41	1.64		
D 83A	2.11.65	0	69.08	1156	744
		5	31.67		
		11	25.07		
		18	45.69		
		36	8.33		
D 83B	2.11.65	0	32.64	1388	865
		5	26.14		
		11	58.93		
		18	57.10		
		36	7.29		
D 84A	29.11.65	0	40.20	2119	1245
		7	65.73		
		13	60.54		
		25	46.96		
		52	6.71		
D 84B	29.11.65	0	64.19	1793	1075
		7	33.38		
		13	53.28		
		25	43.71		
		52	1.43		
D 85A	6.1.66	0	40.75	2031	1199
		9	28.15		
		19	84.10		
		28	45.12		
		50	7.41		
D 85B	6.1.66	0	11.01	1663	1008
		9	23.44		
		19	37.58		
		28	65.09		
		50	2.28		

TABLE 1b CONTINUED

Station	Date	Sampling Depth metres	Organic Production mg C/m³/day	Organic Production mg C/m²/day	'in situ' prediction mg C/m²/day
D 86A	27.1.66	0	44.56	1265	801
		8	83.83		
		13	22.84		
		20	21.27		
		43	7.43		
D 86B	27.1.66	0	56.39	3939	2191
		8	157.84		
		13	163.92		
		20	111.90		
		43	2.20		
D 87A	15.2.66	0	14.62	866	593
		7	20.18		
		15	16.81		
		24	36.26		
		43	1.32		
D 87B	15.2.66	0	15.50	549	428
		7	28.11		
		15	9.59		
		24	14.44		
		43	–		
D 88A	2.5.66	0	2.34	131	211
		10	5.73		
		18	3.23		
		31	0.79		
		54	1.64		
D 88B	2.5.66	0	4.78	211	253
		10	6.73		
		18	5.95		
		31	3.02		
		54	0.85		
D 89A	27.5.66	0	19.06		
D 89B	27.5.66	0	21.14		
D 90A	16.6.66	0	56.92	1743	1049
		7	64.80		
		13	51.65		
		22	34.65		
		41	26.26		
D 90B	16.6.66	0	33.55	903	613
		7	27.82		
		13	33.16		
		22	22.45		
		41	4.44		

TABLE 2a **HYDROLOGY AT A FIXED STATION OFF DURBAN (D) IN 50 FATHOMS**

Station	Date	Sampling Depth metres	Temperature °C	Salinity ‰	PO_4-P mg-at/m³	O_2 cc/1
D 1	17.5.61	0	23.65	35.43	—	4.70
		17	23.60	35.39	—	4.80
		32	23.50	35.40	—	4.60
D 2	8.6.61	0	22.20	35.39	0.88	4.90
		18	22.15	35.38	0 96	5.00
		36	21.65	35.42	1.01	4.60
D 3	26.7.61	0	22.50	35 33	1.00	4.87
		20	22.50	35.35	1.13	4.94
		30	22.30	35.34	1.12	4.76
D 4	31.7.61	0	22.80	35.30	0.99	—
		23	22.10	35.34	0.96	4.92
		42	21.90	35.27	1.10	4.93
D 5	30.8.61	0	21.00	35.46	1.16	4.95
		13	20.60	35.43	1.17	4.91
		24	20 30	35.43	1.22	4.96
D 6	8.9.61	0	19.80	35.52	1.30	4.98
		13	19.45	35.46	1.32	4.93
		28	18.90	35.45	1.40	4.46
D 7	2.10.61	0	20.40	35.37	1.13	5.18
		43	19.90	35.31	0.84	—
		86	16.80	35.36	1.33	4.23
D 8	6.11.61	0	22.60	35.42	0.94	5.13
		28	22.20	35.41	0.98	5.18
		53	21.40	35.38	0.97	4.73
D 9	17.11.61	0	23.70	35.38	1.18	4.89
		30	23.70	35.37	1.11	4.86
		58	20.90	35.34	1.21	4.75
D 10	21.11.61	0	23.20	35.45	1.13	4.97
		29	21.55	35.42	—	—
		49	18 00	35.37	—	—
D 11	30.11.61	0	23 50	35.43	1.13	5.05
		23	22.30	—	—	—
		41	19.90	35.43	1.22	4.67
D 12	15.12.61	0	22.50	35.70	—	—
D 13	5.1.61	0	23.20	35.43	—	—
D 14	11.1.62	0	24.95	—	1.00	5.51
		11	24.95	35.22	—	—
		23	24.65	35.42	—	—
D 15	19.2.62	0	24.35	35.23	—	—
		8	24.25	35.23	—	—
		21	24.20	35.19	—	—
D 16	8.3.62	0	25.30	35.36	—	—

TABLE 2a CONTINUED

Station	Date	Sampling Depth metres	Temperature °C	Salinity ‰	PO_4-P mg-at/m³	0^2 cc/1
D 17	15.3.62	0	24.70	35 43	–	–
D 18	20.3.62	0	24.55	35.39	–	–
		14	23.25	35.39	–	–
		28	21.61	35.43	–	–
D 19	27.4.62	0	24.95	35.38	1.04	4.52
		20	24.35	35.45	1.06	4.52
		40	23.45	35.44	1.27	4.54
D 20	4.5.62	0	24.65	35.52	–	–
D 21	15.5.62	0	23.90	35.44	1.24	4.45
		15	23.90	35.36	–	–
		33	23.85	35.36	–	–
D 22	25.5.62	0	23.20	35.47	1.23	5.03
		24	23.05	35.42	–	–
		46	21.65	35.47	–	–
D 23	12.6.62	0	22.30	35.43	–	–
		16	22.30	35.36	–	–
		32	22.30	35.35	–	–
D 24	21.6.62	0	21.80	35.32	0.93	4.97
		22	21.80	–	–	–
		41	21.70	35.42	–	–
D 25	5.7.62	0	21.60	35.46	0.90	5.14
		18	21.50	–	–	–
		37	21.30	35.40	–	–
D 26	25.9.62	0	21.50	–	–	–
		33	21.20	–	–	–
		64	19.40	–	–	–
D 27	29.10.62	0	23.60	35.33	–	–
		44	22.10	35.29	–	–
		83	20.10	35.23	–	–
D 28	12.12.62	0	24.80	34.57	–	–
		32	21.90	35.53	–	–
		64	20.10	35.40	–	–
D 29	21.1.63	0	–	–	–	4.89
D 30	25.2.63	0	25.20	35.29	1.08	–
		34	24.50	35.27	0.80	–
		62	22.20	35.24	1.17	–
D 31	1.3.63	0	26.60	35.09	0.73	–
		32	24.80	35.27	0.91	–
		59	21.80	35.30	1.18	–
D 32(1)	21.3.63	0	22.90	35.18	0.88	–
		7	22.80	35.17	0.94	–
		13	22.80	35.20	0.83	–

TABLE 2a CONTINUED

Station	Date	Sampling Depth metres	Temperature °C	Salinity °/oo	PO_4-P mg-at/m³	O_2 cc/l
D 32(2)	27.3.63	0	–	34.98	1.16	–
D 33	19.4.63	0	24.00	35.02	0.94	–
		13	23.80	35.12	0.88	–
		26	23.80	35.23	0.76	–
D 34	24.4.63	0	23.60	35.20	1.08	–
		13	23.50	35.21	0.75	–
		26	23.40	35.23	0.87	–
D 35	2.5.63	0	23.10	35.24	0.81	
		20	22.90	35.32	0.72	–
		42	21.15	35.31	0.89	–
D 36	21.5.63	0	22.75	35.17	0.97	–
		50	22.50	35.21	0.75	–
D 37	29.5.63	0	23.01	35.19	0.72	–
		28	22.30	35.21	0.90	–
		60	20.00	35.37	1.29	–
D 38	16.7.63	0	22.60	35.20	–	–
		38	23.20	35.20	–	–
		76	26.30	35.15	–	–
D 39	31.7.63	0	23.00	35.25	0.79	5.14
		23	22.30	35.25	0.76	5.12
		42	20.40	35.26	0.72	5.21
D 40	8.8.63	0	23.90	35.22	0.67	5.09
		9	23.60	35.25	0.70	5.14
		16	22.90	35.25	0.65	5.25
D 41	22.8.63	0	25.60	35.25	0.77	5.05
		32	25.50	35.25	0.74	5.05
		52	24.90	–	0.70	4.94
D 42	24.9.63	0	26.40	35.24	–	5.75
		27	26.90	35.31	–	5.35
		55	–	35.39	–	5.38
D 43	27.11.63	0	23.60	35.30	1.28	4.45
		24	23.50	35.27	1.23	3.70
		52	23.40	35.39	1.51	3.29
D 44	12.12.63	0	23.40	35.18	0.84	4.97
		29	20.70	35.35	0.99	4.22
		55	19.20	35.35	1.43	4.11
D 45(1)	17.1.64	0	22.80	–	0.84	–
D 45(2)	31.1.64	0	24.40	35.17	0.80	–
D 46	25.2.64	0	24.30	35.18	0.79	–
		34	23.10	35.33	1.47	–
		70	18.70	35.27	1.21	–

TABLE 2a CONTINUED

Station	Date	Sampling Depth metres	Temperature °C	Salinity ‰	PO_4-P mg-at/m^3	O^2 cc/1
D 47	25.3.64	0	25.00	35.29	0.92	–
		20	24.00	35.28	1.00	–
		52	20.00	35.28	1.41	–
D 48	8.4.64	0	23.00	35.27	0.90	–
		17	22.00	35.22	0.92	–
		33	19.00	34.91	1.04	–
D 49	21.4.64	0	23.50	35.28	0.86	–
		18	24.50	35.29	1.03	–
		36	23.00	35.26	1.31	–
D 50	1.5.64	0	23.00	35.23	1.11	–
		21	22.60	35.33	1.27	–
		39	20.60	35.30	1.30	–
D 51	15.5.64	0	–	35.21	0.88	–
		27	22.40	35.25	0.98	–
		45	22.00	35.19	1.10	–
D 52	27.5.64	0	23.20	35.24	1.17	–
		16	22.60	35.27	0.91	–
		31	18.60	35.32	1.43	–
D 53	3.6.64	0	21.60	35.33	0.72	–
		20	21.50	35.31	0.72	–
		42	21.50	35.31	0.92	–
D 54	10.6.64	0	21.40	35.29	0.79	–
		29	20.80	35.28	0.67	–
		50	20.60	35.27	1.00	–
D 55	17.6.64	0	20.80	35.36	0.66	–
		22	20.70	35.36	0.76	–
		46	20.40	35.53	0.71	–
D 56	16.7.64	0	21.00	35.40	0.68	–
		22	21.00	35.39	0.70	–
		44	20.40	35.43	0.75	–
D 57	23.7.64	0	21.20	35.36	0.50	–
		22	21.20	35.43	0.66	–
		50	20.70	35.38	0.64	–
D 58	12.8.64	0	19.70	35.44	–	–
		22	19.60	35.44	–	–
		38	19.10	35.42	–	–
D 59	3.9.64	0	19.80	–	–	4.35
		22	19.20	–	–	4.28
		40	18.10	–	–	4.35
D 60	11.9.64	0	20.80	35.45	0.59	4.65
		18	20.50	35.44	0.59	4.96
		26	20.10	35.42	0.71	5.37

TABLE 2a CONTINUED

Station	Date	Sampling Depth metres	Temperature °C	Salinity ‰	PO_4-P mg-at/m^3	O_2 cc/1
D 61	18.9.64	0	21.10	35.41	0.80	4.35
		26	—	35.45	0.80	4.16
		49	20.20	35.49	0.80	4.21
D 62	22.9.64	0	20.50	35.45	1.01	—
		38	18.70	35.49	1.30	—
		57	17.50	35.45	1.30	—
D 63	9.10.64	0	20.50	35.39	0.79	6.24
		24	19.60	35.40	0.97	5.89
		36	19.30	35.41	1.04	5.66
D 64	22.10.64	0	20.90	35.37	0.85	5.31
		25	20.70	35.39	0.86	5.43
		49	20.70	35.39	1.02	5.66
D 65	30.10.64	0	22.20	35.34	0.75	5.20
		29	21.10	35.32	0.77	4.82
		48	20.50	35.39	0.83	5.28
D 66	11.11.64	0	22.10	35.20	0.72	4.91
		45	21.40	35.55	0.75	4.99
		77	20.00	35.42	0.63	4.30
D 67	25.11.64	0	22.60	35.24	0.89	—
D 68	9.12.64	0	23.00	35.31	0.54	3 81
		31	22.60	35.30	0.62	4.97
		51	21.50	35.34	0.71	5.08
D 69	16.12.64	0	24.00	35.28	0 55	4.56
		23	19.90	35.35	0.78	4.16
		57	17.10	35.35	1.15	4.88

TABLE 2b **HYDROLOGY AT FIXED STATIONS OFF DURBAN (D) IN 50 FATHOMS (A) AND IN 100 FATHOMS (B)**

Station	Date	Sampling Depth metres	Temp. °C	Salinity ‰	PO_4-P	NO_3-N	NO_2-N	SiO_3-Si
					mg-at/m^3			
D 70A	28.1.65	0	24 80	35.20	0 26	–	–	–
		25	21.10	35.31	0.39	–	–	–
		42	18.90	35.35	0.74	–	–	–
D 71A	3.2.65	0	23.40	35.22	0.25	–	0.05	–
		38	18.90	35.33	0.79	–	0.36	–
		60	17.20	35.56	1.00	–	0.21	–
D 72A	11.2.65	0	22 50	35.26	0.70	–	0.09	–
		20	19.20	35.14	1.09	–	–	–
		48	15.80	35 39	1.33	–	0.12	–
D 73A	25.2.65	0	24 30	35.24	0.36	–	0.07	–
		27	19.05	35.27	0.65	–	0.46	–
		47	16.90	35.35	1.44	–	0.34	–
D 74A	10.3.65	0	23.50	34.79	–	–	0.10	–
		26	19.47	34.59	0.17	–	0.15	–
		48	16.90	34.90	0.32	–	0.25	–
D 75A	30.3.65	0	22.70	35.32	–	–	0.03	–
		24	19.90	35.42	1.03	–	0.70	–
		50	16.90	35.59	1.02	–	0.08	–
D 76A	12.4.65	0	24.10	35.40	0.36	–	0.05	–
		25	21.30	35.44	0.52	–	0.37	–
		41	20.80	35.31	0.60	–	0.25	–
D 77A	28.4.65	0	22.70	35.35	0.12	–	0.08	–
		23	20.40	35.37	0.25	–	0.17	–
		49	20.30	35.35	0.30	–	0.16	–
D 77B	28.4.65	0	23.00	35.36	0.21	–	0.08	–
		23	21.60	35.40	0.33	–	0.11	–
		49	20 40	35.41	0.30	–	0.16	–
D 78A	20.5.65	0	–	35.34	0.44	–	0.07	–
		21	–	35.37	0.34	–	0.03	–
		41	–	35.33	–	–	0.06	–
D 78B	20.5.65	0	–	35.39	0.53	–	0.12	–
		21	–	35.36	0.39	–	0.10	–
		41	–	35.35	0.43	–	0.27	–
D 79A	4.8.65	0	22.20	35.13	0.13	1.61	0.08	0.80
		7	22.20	35.15	0.20	2.08	0.10	0.80
		17	22.20	35.15	0.18	2.33	0.11	0.57
		29	22.20	35.19	0.20	2.69	0.09	1.14
		44	22.20	35.20	0.15	2.18	0.10	0.80
D 79B	4.8.65	0	22.20	35.16	0.15	–	0.09	0.57
		7	22.20	35.15	0.28	–	0.09	0.57
		17	21.90	35.17	0.17	1.75	0.05	0.57
		29	21.20	35.19	0.18	2.16	0.05	0.57
		44	21.70	35.28	0.19	1.50	0.09	2.28

TABLE 2b CONTINUED

Station	Date	Sampling Depth metres	Temp. C	Salinity °/oo	PO_4-P	NO_3-N	NO_2-N	SiO_3-Si
					mg-at/m³			
D 80A	25.8.65	0	21.25	35.27	0.17	1.27	0 13	0 57
		7	21.20	35.35	0 11	0.99	0 09	μ
		13	21.20	35.29	0 14	0 74	0.10	μ
		21	20.85	35.26	0.19	0.88	0.05	1.37
		39	19.40	35.37	0.40	5.48	0.14	3.42
D 80B	25.8.65	0	21.25	35.27	0.13	1.04	0.08	μ
		7	21.15	35.24	0.13	0.43	1.18	μ
		13	21.10	35.30	0.14	1.20	0 08	μ
		21	21.00	35.26	0.11	0 82	0 06	0 23
		39	20.00	35.30	0.30	2.98	0.17	4.67
D 81A	20.9.65	0	21.70	35.13	0.24	1.20	0 08	1.48
		7	21.70	35.12	0 32	1.03	0 08	0.57
		13	21.10	34.98	0.67	1.98	0.23	6.73
		24	20.40	35.18	0 60	4.44	0.29	6.61
		40	20.60	35.28	0.88	3.29	0.31	7.64
D 81B	20.9.65	0	21.70	35.13	0.32	1.40	0 08	2.28
		7	21.70	35.16	0 22	1.64	0.07	2.51
		13	21.70	35.12	0.37	1.34	0.08	1.37
		24	21.40	35.16	0.37	1.45	0.19	2.62
		40	20.80	35.16	0.45	1.76	0.19	4.22
D 82A	7.10.65	0	21.40	35.23	0.14	1.60	0.13	2.53
		7	21.40	35 27	0.17	1.82	0.14	2.74
		13	21.30	34 95	0.17	1.60	0.14	5.02
		23	21.30	35.19	0.17	1.82	0.16	4 22
		41	21.30	35.15	0.10	1.95	0.16	4.10
D 82B	7.10.65	0	21.75	35.15	0.12	1.60	0.09	2.96
		7	21.70	35.25	0.19	1.59	0.10	2.17
		13	—	35.21	0.14	0.84	0.09	1.14
		23	21.50	35.21	0.13	1.35	0.12	2.39
		41	—	35.17	0.17	1.38	0.10	2.96
D 83A	2.11.65	0	21.80	34.91	0.41	1.89	0.14	3.19
		5	21.80	34.97	0.14	1.78	0.11	1.37
		11	21.40	35.16	0.16	1.23	0.11	3.65
		18	21.00	35.20	0.45	2.23	0.14	4.56
		36	21.40	35.23	0.28	0.84	0.14	1.48
D 83B	2.11.65	0	21.80	35.06	0.21	1.41	0.10	3.08
		5	21.70	34.88	0.21	2.16	0.12	3.42
		11	21.30	35.23	0.29	2.33	0.14	0.80
		18	21.00	35.19	0.31	1.71	0.16	2.74
		36	21.00	35.22	0.26	1.76	0.18	4.10
D 84A	29.11.65	0	22.00	35.31	0.09	1.34	0.14	1.60
		7	21.80	35.24	0.15	0.40	0.14	0.11
		13	21.80	35.24	0.08	1.01	0.11	0.80
		25	20.70	35.25	0.19	2.05	0 21	3.08
		52	17.60	34.98	0.56	8.43	0.17	6.95

TABLE 2b CONTINUED

Station	Date	Sampling Depth metres	Temp. °C	Salinity °/oo	PO_4-P	NO_3-N	NO_2-N	SiO_3-Si
					mg-at/m³			
D 84B	29.11.65	0	21.70	35.33	0.15	1.01	0.10	1.03
		7	21.60	35.23	0.13	1.99	0.13	1.82
		13	21.40	35.08	0.16	1.24	0.14	0.57
		25	20.00	34.88	0.59	3.08	0.23	3.99
		52	16.50	35.47	0.81	8.15	0.14	10.26
D 85A	6.1.66	0	26.30	35.15	μ	1.64	0.09	2.85
		9	23.60	35.25	0.30	μ	0.08	1.25
		19	21.80	35.30	0.04	1.84	0.16	3.31
		28	20.65	35.35	0.63	3.15	0.26	4.56
		50	19.60	35.33	0.37	4.17	0.46	7.07
D 85B	6.1.66	0	25.70	35.21	0.04	0.27	0.09	1.94
		9	23.90	35.33	0.13	0.39	0.06	2.39
		19	22.40	35.28	0.19	0.35	0.09	1.03
		28	21.40	35.27	0.07	0.30	0.11	2.05
		50	20.20	35.31	0.12	6.57	0.36	6.50
D 86A	27.1.66	0	25.00	35.11	0.09	0.35	μ	2.39
		8	23.55	35.12	0.09	0.03	μ	0.68
		13	21.00	35.22	0.43	4.13	0.15	5.59
		20	20.30	35.25	0.54	5.92	0.22	7.64
		43	19.75	35.29	0.63	7.44	0.24	6.84
D 86B	27.1.66	0	24.70	35.09	0.06	0.26	μ	1.71
		8	22.85	35.13	0.19	0.26	0.02	2.17
		13	20.00	35.25	0.43	3.60	0.09	4.22
		20	19.25	35.24	0.52	6.30	0.15	7.18
		43	15.15	35.27	0.95	10.23	0.05	11.17
D 87A	15.2.66	0	25.70	35.07	0.14	0.57	0.12	2.62
		7	25.70	35.04	0.14	0.14	0.11	3.42
		15	25.60	35.05	0.15	0.10	0.12	3.88
		24	23.65	35.14	0.31	2.42	0.43	3.53
		43	19.20	35.29	0.68	8.01	0.40	7.87
D 87B	15.2.66	0	25.80	35.08	0.14	0.19	0.13	2.51
		7	25.50	35.07	0.15	0.38	0.13	1.82
		15	25.45	35.10	0.27	0.96	0.22	2.85
		24	22.50	35.07	0.45	4.08	0.42	5.24
		43	18.70	35.31	0.84	9.10	0.26	10.94
D 88A	2.5.66	0	23.50	35.27	0.13	1.63	0.08	2.38
		10	23.45	35.27	0.12	2.01	0.10	2.74
		18	23.65	35.27	0.15	2.39	0.11	2.62
		31	22.80	35.25	0.27	3.69	0.20	3.88
		54	19.25	35.31	0.72	7.48	0.18	9.35
D 88B	2.5.66	0	23.60	35.27	0.15	0.42	0.08	2.96
		10	23.60	35.30	0.15	0.60	0.10	4.10
		18	23.50	35.21	0.15	1.17	0.10	3.99
		31	23.15	35.27	0.25	1.62	0.14	3.19
		54	19.30	35.31	0.75	8.26	0.14	8.44

TABLE 2b CONTINUED

Station	Date	Sampling Depth metres	Temp. °C	Salinity ‰	PO_4-P	NO_3-N	NO_2-N	SiO_3-Si
					mg-at/m^3			
D 89B	27.5.66	0	22.30	35.23	0.15	1.26	0.12	3.19
		5	22.50	35.20	0.17	1.57	0.13	3.08
		10	22.30	35.21	0.18	1.23	0.12	2.96
		17	22.45	35.22	0.13	1.15	0.14	3.65
		35	22.25	35.21	0.17	1.57	0.21	2.62
D 89B	27.5.66	0	22.60	35.22	0.18	1.67	0.11	3.53
		5	22.50	35.22	0.15	1.34	0.13	3.53
		10	22.55	35.23	0.16	1.11	0.13	3.65
		17	22.45	35.22	0.14	1.07	0.11	3.31
		35	22.50	35.37	0.19	1.48	0.14	2.85
D 90A	16.6.66	0	21.05	35.24	–	2.10	0.05	2.51
		7	21.15	35.23	–	1.53	0.03	2.28
		13	21.10	35.24	–	1.09	0.24	6.04
		22	21.10	35.24	–	1.40	0.18	4.22
		41	21.00	35.24	–	1.50	0.25	2.74
D 90B	16.6.66	0	21.30	35.23	–	0.87	0.15	1.71
		7	21.45	35.24	–	0.99	0.12	2.39
		13	21.35	35.23	–	0.81	0.18	2.17
		22	21.40	35.23	–	0.94	0.21	3.42
		41	21.15	35.26	–	1.06	0.19	2.17

TABLE 3a **MEASUREMENTS OF PRIMARY PRODUCTION OBTAINED FROM REPLICATE SAMPLES INCUBATED SIMULTANEOUSLY IN TWO TYPES OF SHORE INCUBATORS AND 'IN SITU' IN THE OCEAN**

Date	Depth	'in situ'		incubator-1		incubator-2	
	% light intensity	mg C/m^3 /day	mg C/m^2 /day	mg C/m^3 /day	mg C/m^2 /day	mg C/m^3 /day	mg C/m^2 /day
30. 9.65	100%	13.03	311	18.88	897	5.53	186
	10%	4.30		23.42		3.55	
	1%	0.73		4.93		1.75	
27.10.65	100%	72.84	1660	113.10	2577	94.45	2279
	10%	35.75		55.19		51.68	
	1%	0.00		0.53		0.32	
17.11.65	100%	74.36	–	66.40	1022	75.75	1209
	10%	–		14.50		17.57	
	1%	–		1.18		3.27	
13. 1.66	100%	23.77	572	13.49	480	12.61	590
	10%	6.83		8.09		13.13	
	1%	0.65		3.09		5.43	
25. 1.66	100%	20.63	1621	17.95	2920	25.51	4409
	10%	81.88		158.90		224.20	
	1%	8.98		18.33		73.58	

TABLE 3b **MEASUREMENTS OF PRIMARY PRODUCTION OBTAINED FROM REPLICATE SAMPLES INCUBATED SIMULTANEOUSLY IN INCUBATOR-3 AND 'IN SITU' IN THE OCEAN**

Date	Depth	'in situ'		incubator-3	
	% light intensity	mg C/m^3/day	mg C/m^2/day	mg C/m^3/day	mg C/m^2/day
6.3.67	100%	227.00	1145	200.50	2302
	10%	12.00		127.75	
	1%	3.50		55.50	
23.3.67	100%	36.36	556	17.16	543
	10%	6.24		10.68	
	1%	1.08		14.04	
30.3.67	100%	63 24	117	105.72	1860
	10%	75.24		89.40	
	1%	9.60		87.48	
1.5.67	100%	34.87	349	32.67	598
	10%	14.96		34.43	
	1%	1.65		9.24	
15.5.67	100%	93.50	1652	103.07	2591
	10%	31.35		63.47	
	1%	4.51		25.19	

TABLE 4a **CORRELATION CO-EFFICIENTS AND REGRESSION EQUATIONS FOR CARBON-14 UPTAKE 'IN SITU' IN THE OCEAN VERSUS CARBON-14 UPTAKE IN INCUBATOR-1(P_1)**

Depth % light intensity	correlation co-efficient (r)	significance	regression equations
100%	0.90	significant at 5% level	$P_{\text{'in situ'}}=0.63\,P_1+12.00$
10%	0.98	significant at 5% level	$P_{\text{'in situ'}}=0.52\,P_1+0.25$
1%	0.99	significant at 1% level	$P_{\text{'in situ'}}=0.55\,P_1-1.25$

TABLE 4b **CORRELATION CO-EFFICIENTS AND REGRESSION EQUATIONS FOR CARBON-14 UPTAKE 'IN SITU' IN THE OCEAN VERSUS CARBON-14 UPTAKE IN INCUBATOR-2 (P_2)**

Depth % light intensity	correlation co-efficient (r)	significance	regression equations
100%	0.97	significant at 5% level	$P_{\text{'in situ'}}=0.70\,P_2+8.00$
10%	0.993	not significant	$P_{\text{'in situ'}}=0.68\,P_2+0.33$
1%	0.65	not significant	$P_{\text{'in situ'}}=0.20\,P_2+0.20$

TABLE 4c **CORRELATION CO-EFFICIENTS AND REGRESSION EQUATIONS FOR CARBON-14 UPTAKE 'IN SITU' IN THE OCEAN VERSUS CARBON-14 UPTAKE IN INCUBATOR-3 (P_3)**

Depth % light intensity	correlation co-efficient (r)	significance	regression equations
100%	0.94	significant at 5% level	$P_{\text{'in sitn'}}=1.03\,P_3-3.58$
10%	0 33	not significant	$P_{\text{'in situ'}}=0.20\,P_3+14.96$
1%	0.896	significant at 5% level	$P_{\text{'in situ'}}=0.10\,P_3+0.24$

TABLE 5a **ANALYSIS OF REGRESSION OF 'IN SITU' VALUES (Y) ON INCUBATOR-1 VALUES (X)**

Source	**Sum of squares**	**d.f.**	**Variance estimate**
regression	5647100	1	5647100
residual error (σ_e^2)	160279	2	80139
TOTAL	5807379	3	

TABLE 5b **ANALYSIS OF REGRESSION OF 'IN SITU' VALUES (Y) ON INCUBATOR-2 VALUES (X)**

Source	**Sum of squares**	**d.f.**	**Variance estimate**
regression	3120200	1	3120200
residual error (σ_e^2)	57981	1	57981
TOTAL	3178181	2	

TABLE 5c **ANALYSIS OF REGRESSION OF 'IN SITU' VALUES (Y) ON INCUBATOR-3 VALUES (X)**

Source	**Sum of squares**	**d.f.**	**Variance estimate**
regression	5600400	1	5600400
residual error (σ_e^2)	116335	3	38778
TOTAL	5716735	4	

TABLE 6 **ERROR OF TECHNIQUE IN THREE TESTS OF CARBON-14 UPTAKE BY REPLICATE SURFACE SAMPLES**

Test	**Mean activity (counts/minute)**	**No. of samples**	**Std. dev. (s)**	**Co-eff. of variation**
1	699	8	121	17.31
2	1546	6	111	7.18
3	1020	6	104	10 20

Reprinted from *Bull. Instit. Océanogr. Monaco*, vol. 69, no. 1407, 1970, p. 1-15

Some trace metal analyses in the Mediterranean, the Red Sea and the Arabian Sea

by

Stig H. FONSELIUS

International Laboratory of Marine Radioactivity,
International Atomic Energy Agency, Monaco

(present address : *Hydrographic Department, Fishery Board of Sweden, Göteborg)*

Abstract

Earlier results for chromium in sea water, marine organisms and sediments, reported in the literature, are briefly discussed. The sampling technique and methods of analyses of Cr, Zn and Cu used in the present paper are described. The results of the analyses are given and discussed.

Résumé

Les données, publiées jusqu'ici, sur le Chrome dans l'eau de mer, les organismes et les sédiments marins, sont discutées brièvement. La technique de prélèvement et les méthodes d'analyse du Chrome, du Zinc et du Cuivre, utilisées pour le présent travail, sont décrites. Les résultats des analyses sont donnés et discutés.

Некоторые индикаторные анализы металлов в Средиземном, Красном и Аравийском морях

Краткое содержание

Кратко рассматриваются первые результаты анализов на хром в морской воде, в морских организмах и отложениях, опубликованные в литературе.

В настоящем докладе дается описание используемых способов взятия проб и методов анализов Cr, Zn и Cu. Даются и обсуждаются результаты этих анализов.

Descripteurs retenus pour cette étude :

Chrome, eau de mer — Cuivre, eau de mer — Zinc, eau de mer — Missions *Winnaretta-Singer* — Mission *Atlantis II.*

[2]

Introduction

Very few analyses of the chromium content of sea water have been reported in the literature. RILEY [1965] gives six references, which show a variation between 0.04 and 2.2 μg Cr/l sea water. Of these references some can be discarded by different reasons. The analyses by NODDACK and NODDACK [1939] were carried out spectrographically on water from the Gullmarfjord at the Swedish west coast. This water is shallow coastal water and should not be considered representative for sea water. The spectrographic analyses by BLACK and MITCHELL [1952] on several trace elements in sea water, are generally considered to give too high results and this seems to be true also for their Cr values. SCHUTZ and TUREKIAN [1963] report the very high result of 2.2 μg Cr/l, but in a later paper [1965] they admit that their chromium values might be too high due to contamination. Then there are only three references left, all using co-precipitation methods and photometric analysis with di-phenyl carbazide. The remaining values lie now between 0.04 and 0.6 μg/l. The co-precipitation method with spectrophotometric analysis was first used by ISHIBASHI [1953].

Textbooks and abstracts wich give tables of trace elements in sea water, generally quote values around 0.05 μg Cr/l, always originating from ISHIBASHI, or NODDACK and NODDACK values from the Gullmarfjord.

Almost nothing seems to be known about the form in which chromium exists in sea water, if it is present as particulate matter or in solution, if it is attached to an organic molecule or if it is an inorganic ion. SILLÉN [1962] has studied theoretically the equilibrium constants of several trace elements in sea water. According to SILLÉN the most probable form for chromium should be the hydroxy form. Therefore, if chromium exists in inorganic form in sea water, it very likely should be as $Cr(OH)_3$.

Chromium is known to be present in marine organisms. FUKAI and BROQUET [1965] have given the standard abundance of chromium in various groups of marine organisms, computed from the results of several authors. The values vary between 0.1 and 10 μg Cr/g dry matter.

FUKAI [1965] has analyzed trace metals in marine sediments from the Bay of Roquebrune. He showed that chromium and iron were leached from the sediments in the proportion 1.3×10^{-3}. These analyses were made from shallow water sediments, but the proportion Cr : Fe is anyhow not too far from the crustal average according to TAYLOR [1964], which is 1.8×10^{-3}. FUKAI found in his two samples 33 resp. 15 μg Cr/g material.

The variations of iron in sea water are so great and the values of chromium so few, that it is not possible at present to state any Cr : Fe relations in sea water.

MANHEIM [1965] gives chromium values for several sediments from different parts of the world. These values agree with the values of FUKAI *(loc. cit.)*. MANHEIM values vary from 5 to 32 μg Cr/g sediment.

Chromium is brought to the oceans by river water. DURUM and HAFFTY [1963] give some chromium values for river water in the U.S. The variation range is 0.72-84 μg Cr/l river water and the median value is 5.8 μg/l.

The occurrence and accumulation of chromium in marine organisms indicate the possibility of variations of the chromium content in sea water. Cr may be removed from the water by accumulation in organisms and it may be brought back into the water phase through decay of dead organisms directly, or indirectly via the sediments, or it may also be retained in the sediment.

GOLDBERG [1963] has calculated the residence time for different elements in the ocean. He estimates the residence time for Cr to be 3.5×10^2 years.

Another source for Cr might be the fallout from nuclear explosions. All nuclear explosions produce large amounts of radio isotopes through the release of neutrons which cause nuclear reactions with e.g. the bomb shell. In this reaction Cr-51 is formed among other products. This fallout reaches the sea either by direct deposition on the sea surface or with river water. MIYAKE [1963] has calculated that about 61 per cent of the stratospheric fallout is deposited directly into the sea. Even with radioactive wastes some Cr is brought into the oceans. Cr-51 is formed among the corrosion products in nuclear power plants [WALLAUSCHEK & LÜTZEN, 1964]. This source is probably of importance only in coastal areas.

Zinc and copper values reported in the literature for sea water, have earlier been reviewed by FONSELIUS and KOROLEFF [1963].

Stations and sampling technique

Sea water for chromium analyses was collected in the Ligurian Sea close to Monaco, in the spring 1963 during the author's assignment to the Laboratory of Marine Radioactivity, IAEA. The surface samples, about 60 l each, were collected in polyethylene barrels by help of a plastic bucket and a nylon rope. The deep samples were taken with a 100 l stainless steel sampler sprayed with colourless Krylon spray on the inside and the outside. This method was later abandoned due to the great risk of contamination from the sampler. The spraying had to be renewed before each sampling. The work was carried out at the IAEA stations 1 and 2 on board the *Winnaretta Singer* from the Musée océanographique in Monaco.

The coordinates of the stations are given in table I.

During the International Indian Ocean Expedition, samples for chromium, zinc and copper analysis were taken in July-August 1963 on board *Atlantis II* from the Woods Hole Oceanographic Institution, on the cruise from Monaco to Colombo. All the surface samples were taken with a plastic bucket and a nylon rope directly over the ship's side. The deep samples for chromium were taken with 10 l Van Dorn samplers made of polyethylene. Five samplers were attached to the hydrographic wire 5 m apart and the series was closed from deck by help of a messenger exactly as the hydrographic series. The big 50 l plastic sampler originally intended for the work, had unfortunately been broken during the transport and could not be properly repaired on board during the cruise. All samples were filled into polyethylene barrels for further treatment.

The water for zinc and copper analyses was taken with plastic type " Mecabolier " samplers.

There is always the danger of contamination of surface samples taken close to the ship's side, but that can unfortunately hardly be avoided. The deep samples again may be contaminated by the metallic wire used. If possible, nylon wire should be used for sampling of trace metals, but it is very difficult to get time for " extra " hydrographic casts with special gear on long cruises with a fixed time schedule. The ship will be delayed too much and therefore one is forced to use the ordinary wire in spite of the risk for contamination.

Seven samples for chromium analysis were taken, one surface and one 350 m sample in the Mediterranean west of Crete, one surface and one deep sample in the middle part of the Red Sea and two surface samples and one 100 m sample in the Arabian Sea.

69 zinc and 63 copper samples were analyzed on board *Atlantis II.* The water was sampled on nine stations, one in the Mediterranean off Crete, one in the Great Bitter Lake in the Suez Canal, three in the Red Sea and four in the Arabian Sea.

The location of the stations and the depths sampled are given in table II.

Chemical methods and results of the analyses

Chromium was analyzed according to Ishibashi *(loc. cit.)*. On board the ship the samples were co-precipitated with $Al(OH)_3$, the precipitate was allowed to settle for 24 hours, the main bulk of the water was removed with a siphon, the rest was filtered through quantitative filter paper tested for chromium and the precipitate was washed with distilled water and air dried. The dry filter paper was folded together and stored in a plastic jar for further treatment after the cruise. In the shore laboratory the filter paper was ignited and fused with sodium carbonate and potassium nitrate in a platinum crucible and interfering elements were removed as described by Sandell [1944]. The di-phenyl carbazide colour was measured at 540 mμ in a Beckman DU spectrophotometer. The chromium values were evaluated by help of a standard curve.

Zinc and copper were analyzed on board according to Fonselius and Koroleff *(loc. cit.)*. For zinc the " monocolour " method was used. 100 ml of sea water were shaken with dithizone dissolved in carbon tetrachloride, the CCl_4 was shaken with an ammonia solution and the dithizone colour of the tetrachloride phase was measured at 524 mμ in the Beckman DU spectrophotometer. For copper the "mixed colour" method was used. 1000 ml of sea water were shaken 30 minutes in a flask after addition of 1.2 ml acetic acid and dithizone dissolved in carbon tetrachloride. The interfering zinc was removed by shaking the organic phase with 0.01-N sulfuric acid. The extinction of the tetrachloride extract was measured in the spectrophotometer at 620 mμ. Standard curves were prepared for evaluation of the zinc and copper concentrations.

The results are given in tables I and II. Table II contains also the temperatures and salinities at the corresponding depths. The depths given in the table refer to the temperature and salinity from the ordinary hydrographic cast at the station. The depths of the trace metal samples are only approximative because the plastic samplers had to be attached to the wire between the ordinary Nansen bottles.

TABLE I

Ship, Station number, date and co-ordinates	*Sample* Nô	*Depth* (m)	Cr (μg/l)	*Remarks*
Winnaretta-Singer	1	0	0.092	Unfiltered 60 l
IAEA Sta No 1 off Monaco	2	0	0.076	Total (2a + 2b) 60 l
24-IV-1963	2a		0.058	Particulate
43°39.5′N 07°37′E	2b		0.018	Soluble
Winnaretta-Singer	3	0	0.005	Unfiltered 60 l
IAEA Sta No 2 off Monaco	4	200	1.25?	Unfiltered 60 l
May 1963	5	600	0.212	Unfiltered 60 l
43°31.5′N 08°03.5′E	6	1 500	0.004	Unfiltered 60 l

TABLE II

Stations	*Depth* (m)	*Temp.* (°C)	*Sal.* (°/₀₀)	Zn (μg/l)	Cu (μg/l)	Cr (μg/l)
Atlantis II, Sta.No 30, 25-VII-63	0	25.93	38.55	24.7	0.65	0.02
36°34.5′N 21°04.5′E 5084 m	10	26.71	38.54	22.8	1.53	..
Mediterranean, off Crete	20	24.81	38.50	17.6	1.89	..
	50	17.19	38.58	0.1?	0.44	..
	99	15.07	38.75	16.2	0.67	..
	149	14.70	38.79	0.8?	0.48	..
	198	(14.60)	38.80	17.6	0.38	..
	297	14.55	38.88	18.8	0.34	..
	396	14.35	38.87	29.4	2.86	0.49
	495	14.09	(38.82)	10.6	0.00	..
Atlantis II, Sta. No 33, 29-VII-63	0	29.07	46.38	40.0	3.86	..
30°20.6′N 32°24.7′E 11 m	10	29.05	46.60	19.4	2.66	—
Great Bitter Lake, Suez Canal						
Atlantis II, Sta. No 39, 30-VII-63	0	28.29	40.45	20.6	0.24	..
27°28′N 34°14′E 1150 m	10	28.30	40.33	22.3	0.44	..
Red Sea, northern part	20	28.07	40.49	12.4	2.00	..
	30	26.34	40.62	14.3	0.75	..
	50	24.48	40.70	17.7	1.46	..
	100	22.84	40.77	15.9	2.24	..
	498	21.68	41.04	9.5	1.02	..
	734	21.72	41.11	12.9	1.26	..
	1031	21.76	41.14	18.0	1.17	..
	1131	21.78	40.99	17.4	1.56	..

Stations	*Depth* (m)	*Temp.* (°C)	*Sal.* (°/oo)	Zn (μg/l)	Cu (μg/l)	Cr (μg/l)
Atlantis II, Sta. No 42, 1-VIII-63	0	30.12	38.26	2.4	0.40	0.02
21°21.5′N 38°04.5′E 1959 m	20	30.06	38.67	17.3	..	..
Red Sea, middle part	49	28.44	39.08	20.0	0.57	..
	99	23.79	39.98	17.4	1.00	..
	199	21.94	40.57	13.2	0.00	..
	496	21.70	40.68	23.2	0.10	..
	991	21.72	40.69	24.8	0.00	..
	1336	21.80	40.66	..	..	0.06
	1632	21.89	40.59	15.0	0.34	..
	1781	21.93	40.76	11.6	0.00	..
Atlantis II, Sta. No 45, 3-VIII-63	0	32.73	37.14	24.8	0.32	..
14°28′N 42°22′E 419 m	50	23.02	36.32	13.6	0.52	..
Red Sea, Bab el Mandeb	99	18.42	37.11	8.1	0.93	..
	198	21.99	40.37	6.8	0.12	..
	297	21.75	40.70	7.5	0.52	..
	397	21.72	40.63	8.4	0.57	..
Atlantis II, Sta. No 53, 8-VIII-63	0	29.83	36.37	26.7	..	0.13
13°15′N 50°36.5′E 2506 m	49	24.15	35.91	11.1	0.93	..
Gulf of Aden	99	17.16	35.50	7.2	1.28	..
	198	14.02	35.33	10.1	0.94	..
	497	13.32	36.02	19.2	0.68	..
	987	11.46	36.00	7.9	0.00	..
	1268	7.58	35.36	11.5	0.45	..
	1463	5.75	35.11	8.0	0.30	..
	1857	3.61	34.90	11.6	0.57	..
	2045	3.12	34.85	9.7	0.00	..
	2300	..	..	9.0	0.62	..
Atlantis II, Sta. No 61, 11-VIII-63	0	25.10	35.10	10.5	..	..
14°56.5′N 56°59′E 3195 m	384	11.72	35.38	21.5	0.50	..
Gulf of Aden, off Socotra	771	10.38	35,53	19.4	0.00	..
	1370	6.27	35.16	11.6	0.00	..
	2284	2.45	34.80	19.4	0.12	..
	3121	1.82	34.75	11.4	1.32	..
Atlantis II, Sta. No 77, 22-VIII-63	0	26.79	36.37	33.6	2.38	0.02
19°58.5′N 64°58′E 3166 m	10	26.79	36.37	18.2	..	..
Arabian Sea, northern part	100	20.90	35.90	6.8	1.20	0.07
	496	12.39	35.72	11.6	0.08	..
	993	8.65	35.40	7.0	..	..
	1975	3.04	34.84	10.4	..	..
Atlantis II, Sta. No 98, 2-IX-63	0	28.05	36.23	19.4	0.10	..
09°58′N 63°40′E 4439 m	10	28.05	36.24	8.6	0.13	..
Arabian Sea, southern part	50	27.08	36.24	7.0	0.06	..
	99	25.96	36.16	7.0	0.14	..
	497	11.17	35.37	5.0	0.14	..
	988	8.02	35.24	3.7	0.43	..
	2060	2.59	34.80	2.7	0.32	..
	3235	1.73	34.75	0.4	0.20	..
	4393	1.59	34.73	1.0	0.11	..

(1407)

Discussion of the results

Chromium. Filtering of the chromium samples showed that most of the Cr is retained on the filter paper. In table I the sample 1 shows the chromium content of an unfiltered sample. Sample 2a in the same table shows the amount of chromium retained on the filter paper after filtering a 60 l sample and 2b the amount left in the filtrate. The sum of 2a and 2b is sample 2 and the value, 0.076 μg Cr/l is fairly close to the result of the unfiltered sample 1, 0.092 μg Cr/l. The filtering of large amounts of sea water is a laborious and slow task and therefore it was decided to omit it in the future. The main part of the chromium will anyhow be retained on the filter paper.

It is not possible to draw any definite conclusion regarding the distribution and variations of chromium in sea water from the few analyses carried out. Obviously the high value of 1.25 μg/l in table I, sample no 4 is due to contamination from the sampler. If the Cr values at station 2 in table I are compared to the values at station 30 in table II, which is also in the Mediterranean, there is an indication that the " intermediate Levantine water " [WÜST, 1961] has a higher Cr content than the surface water. The core of this water is at around 600 m in the Ligurian Sea [FONSELIUS & KOROLEFF, *loc. cit.*], and at this depth the Cr concentration is 0.212 μg/l while it is only 0.005 μg/l at the surface (table I). Fig. 1 shows the distribution of trace metals, temperature and salinity at the *Atlantis II* station No. 30 west of Crete. The salinity maximum, which indicates the " intermediate Levantine water " is found between 300 and 400 m. At 400 m the Cr concentration is 0.49 μg/l while the surface concentration is 0.02 μg/l. The Cr values from the Red Sea and the Indian Ocean are too few to allow any kind of conclusions. They, however, support ISHIBASHI result [1955] that the chromium concentration in the open sea is around 0.05 μg/l.

Zinc and copper. From Fig. 1 it can be seen that both elements at station 30, have a maximum in the core of the " intermediate Levantine water ", which supports the earlier results of FONSELIUS and KOROLEFF *(loc. cit.)* from the Ligurian Sea. The Zn values at 50 m and 149 m are extremely low, possibly due to faulty analyses and have been regarded as questionable.

Station No. 33 in table II shows Zn and Cu values in the Great Bitter Lake in the Suez Canal. This water is of course not sea water, but the high values for trace elements there may be an indication of the origin of the high Zn and Cu values in some parts of the Red Sea.

In the northern Red Sea the Cu values seem to be extremely high except close to the surface. The Zn values are slightly higher than in the Mediterranean. In the middle part of the Red Sea the Cu values are low, close to 0 or 0 at some depths. The Zn values are like the values in the northern part except at the surface where the value was 2.4 µg/l. In the strait of Bab el Mandeb, the Zn values from 100 m down to the bottom are low. In the Gulf of Aden the highest Cu values are found in the surface water. At around 1000 m and also at 2000 m the Cu concentration was 0. The water in the Gulf of Aden and also in the northern part of the Arabian Sea seems to be much influenced by local conditions. The layers of Red Sea and Persian Gulf water between layers of Indian Ocean water makes the picture of the trace element distribution very complicated and much more measurements are needed in order to understand the figures obtained.

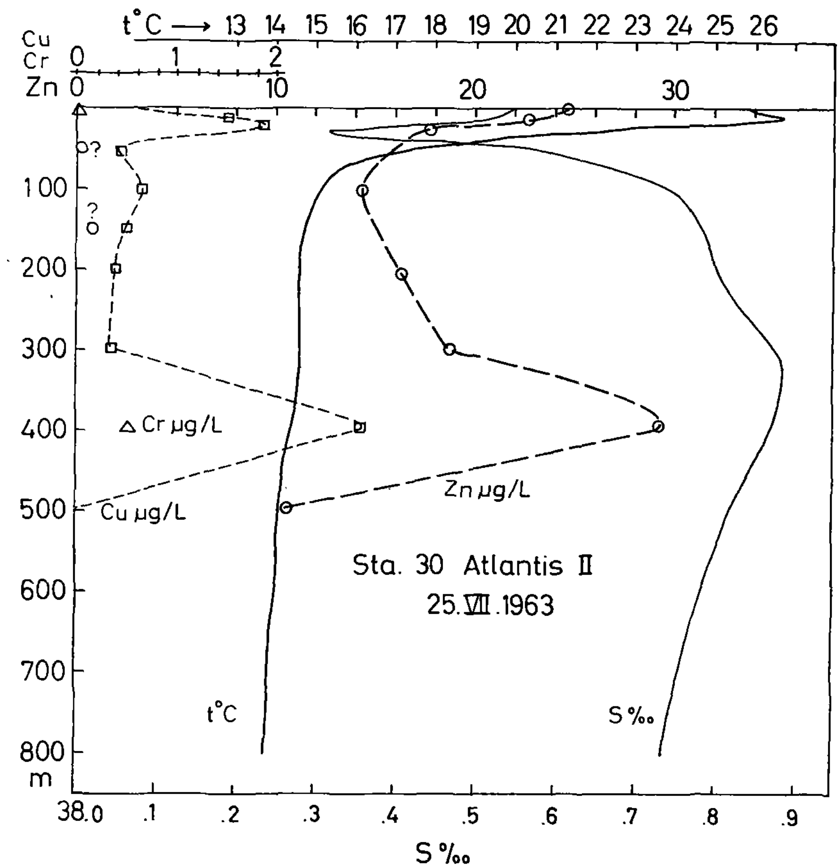

FIGURE 1

The station 98 in the middle of the Arabian Sea shows an even distribution of Zn and Cu, with concentrations decreasing downward (Fig. 2). Generally the surface values for Zn in the oceans seem to be higher than the deep values. The surface Zn values in the Indian Ocean agree fairly well with the surface values found by DOSHI et *al.* [1965] while the Cu values are much lower than the values found by DOSHI and co-workers in the same area.

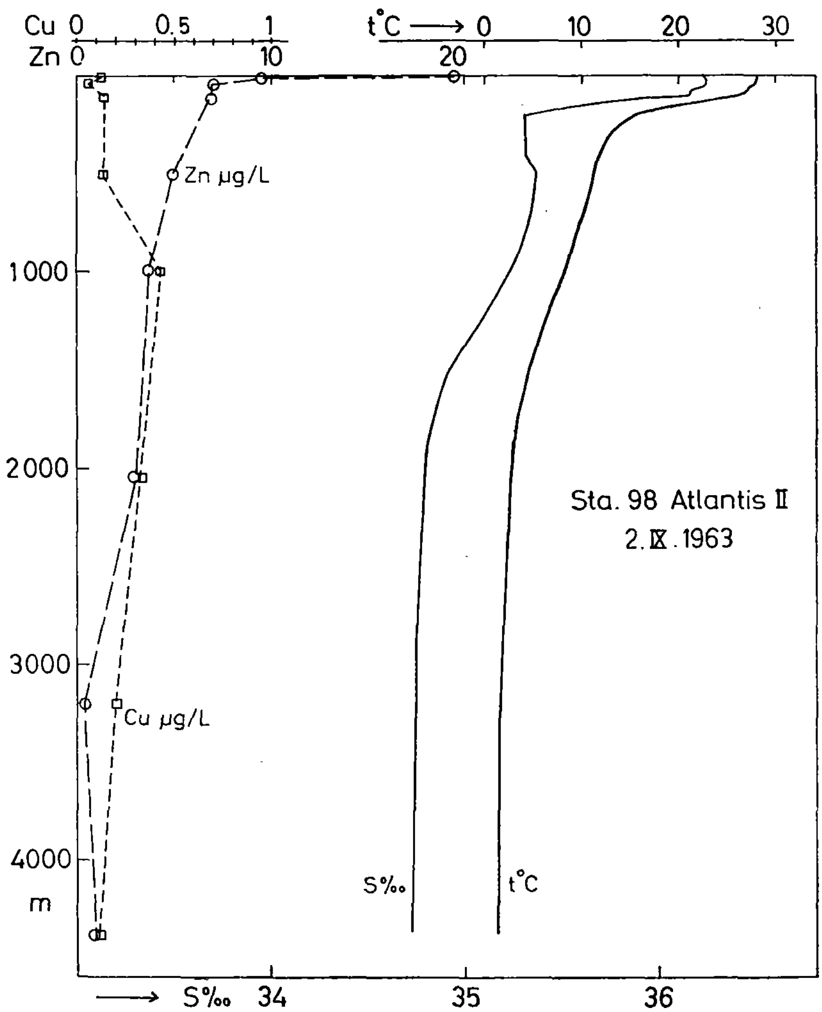

FIGURE 2

Acknowledgments

The author wishes to express his sincere thanks to Mr. R. MILLER, from the Woods Hole Oceanographic Institution, chief scientist on *Atlantis II*, for providing the possibilities to participate in the International Indian Ocean Expedition, and to the scientific staff and the crew of *Atlantis II* for kind assistance in the work and for the hospitality on board. Further, thanks are due to the director of the Musée océanographique in Monaco for the use of the *Winnaretta Singer* and to Dr. R. FUKAI at the IAEA laboratory for valuable discussions and suggestions regarding the chromium analysis. Thanks are also due to Mr. D. MALEAS, who assisted at the work on board the ships and in the laboratory.

*
* *

References

BLACK (W.A.P.) & MITCHELL (R.L.), 1952. — Trace elements in the common brown algae and in sea water. *J. mar. biol. Ass. U.K.*, **30**, 3, pp. 575-584.

DOSHI (G.R.), SEN GUPTA (R.), SHAH (S.M.), SASTRY (V.N.), NAIDU (J.R.) & VISWANATHAN (R.), 1965. — *Trace element content of the marine environment. Report of project marina.* — Trombay (India), Atomic energy establishment. 11 p. multigr.

DURUM (W.H.) & HAFFTY (J.), 1963. — Implications of the minor element content of some major streams of the world. *Geochim. et cosmoch. Acta*, **27**, 1, pp. 1-11.

FONSELIUS (S.H.) & KOROLEFF (F.), 1963. — Copper and zinc content of the water in the Ligurian Sea. *Bull. Inst. océanogr. Monaco*, **61**, n° 1281, 15 p. [*Radioactiv. Sea*, 7].

FUKAI (R.), 1965. — Chemical composition of shallow-water sediments in the Bay of Roquebrune. *Bull. Inst. océanogr. Monaco*, **65**, n° 1337, 15 p. [*Radioactiv. Sea*, 17].

FUKAI (R.) & BROQUET (D.), 1965. — Distribution of chromium in marine organisms. *Bull. Inst. océanogr. Monaco*, **65**, n° 1336, 19 p. [*Radioactiv. Sea*, 16].

GOLDBERG (E.D.), 1963. — The oceans as a chemical system, *in : The sea*, ed. by M.N. Hill, **2**, pp. 3-25. — London, New York, Interscience publishers.

ISHIBASHI (M.), 1953. — Studies on minute elements in sea-water. *Rec. oceanogr. Wks Jap.*, (N.S.) **1**, 1, pp. 88-92.

ISHIBASHI (M.), 1955. — Quantitative distribution of chemical elements in the sea water, *in : Proceedings of the Unesco symposium on physical oceanography, 1955, Tokyo*, pp. 175-178. — Paris, Unesco; Tokyo, Japan society for the promotion of science.

MANHEIM (F.T.), 1965. — Manganese-iron accumulations in the shallow marine environment. *Occ. Publ. Narragansett mar. Lab.*, **3** [Symposium on marine geochemistry], pp. 217-276.

MIYAKE (Y.), 1963. — Artificial radioactivity in the sea, *in : The sea*, ed. by M.N. Hill, **2**, pp. 78-87. — London, New York, Interscience publishers.

NODDACK (I.) & NODDACK (W.), 1939. — Die Häufigkeiten der Schwermetalle in Meerestieren. *Ark. Zool.*, **32** A, 4, 35 p.

RILEY (J.P.), 1965. — Analytical chemistry of sea water, *in : Chemical oceanography*, ed. by J.P. Riley and G. Skirrow, **2**, pp. 295-424. — London, New York, Academic press.

SANDELL (E.B.), 1944. — Chemical analysis III, *in : Colorimetric determination of traces of metals*, pp. 189-199. — New York, Interscience publishers.

SCHUTZ (D.F.) & TUREKIAN (K.K.), 1963. — *Abstr. Pap. Gen. Assembly IUGG.* **13**, F 23.

SCHUTZ (D.F.) & TUREKIAN (K.K.), 1965. — The investigation of the geographical and vertical distribution of several trace elements in sea water using neutron activation analysis. *Geochim. et cosmoch. Acta*, **29**, 4, pp. 259-313.

SILLÉN (L.), 1962. — *Fysikalisk-kemiska orsaker till havsvattnets nuvarande sammansättning* [Physical-chemical grounds of the present constitution of sea water]. — Åbo, 11 nordiska kemistmötet. 16 p.

TAYLOR (S.R.), 1964. — Abundance of chemical elements in the continental crust : a new table. *Geochim. et cosmosch. Acta*, **28**, 8, pp. 1273-1285.

WALLAUSCHEK (E.) & LÜTZEN (J.), 1964. — *Study of problems relating to radioactive waste disposal into the North Sea II. General survey on radioactivity in sea water and marine organisms.* — Paris, O.E.C.D., European nuclear energy agency. 96 p .

WÜST (G.), 1961. — On the vertical circulation of the Mediterranean Sea. *J. geophys. Res.*, **66**, 10, pp. 3261-3271.

Reprinted from *Bull. natn. Inst. Sci. India*, no. 38, 1968, p. 103-122

DISTRIBUTION OF PHOSPHATES AND SILICATES IN THE CENTRAL WESTERN NORTH INDIAN OCEAN, IN RELATION TO SOME HYDROGRAPHICAL FACTORS

by C. V. GANGADHARA REDDY *and* V. N. SANKARANARAYANAN
National Institute of Oceanography, Ernakulam

The paper presents a descriptive account of the distribution of phosphates and silicates of the Central region of the Western North Indian Ocean in the upper 200 m during the south west monsoon period. The relationship of the nutrients with temperature, salinity, oxygen and also zooplankton is shown. Vertical distribution of the nutrients indicates low concentrations at the surface layers up to 50 or 75 m. This is followed by higher concentration layers down to 200 m. Considerable meridional and zonal variations in the concentrations and the thickness of these layers have been noticed. The distributional features of the oceanographic properties indicate the distinctness of the North Equatorial Indian Ocean from the geographically similar regions of the Pacific and Atlantic Oceans. The disposition of the isopleths shows an equatorial upslope of the waters which is associated with the equatorial divergences. However, the ascent appears to be weaker near and along the equator as compared to the equatorial regions of the Pacific and Atlantic. The spreading of the isolines near and along the equator is probably due to the equatorial undercurrent. Three regions of convergence (i) between Lat. 15°30' and 16°30' along 68°E, (ii) around 8°N and 71°30'E, and (iii) around 5°N and 75°E have been noticed. The variations in zooplankton volumes seem related to the changes in hydrographical features.

INTRODUCTION

Before the International Indian Ocean Expedition began, our knowledge about the Oceanographic Conditions of the Indian Ocean was mainly based on reports of the Dana Expedition (1928—1930), the John Murray Expedition (1933—1934), the Discovery Expedition (1934), the Swedish Deep Sea Expedition (1947—1948) and the Galathea Expedition (1950—1952) and more recently from the data collected by the Russian Ship "Ob" (1956) and Vityaz (1958).

As part of the Indian Programme of the International Indian Ocean Expedition, the vessel, I.N.S. KISTNA carried out many cruises in the Arabian Sea and the Bay of Bengal. The present paper which deals mainly with distribution of nutrients (phosphates and silicates) in the Central Western North Indian Ocean, is based on the observations made during the XII and XIII monsoon cruises of the I.N.S. KISTNA undertaken in August 1963. Until recently most of the investigations on nutrients were made in the Arabian Sea, along the West Coast of India and these were limited to shelf waters only (Reddy and Sankaranarayanan 1966). The present data from the open ocean may give a better understanding to the problem of possible influence of the oceanic waters on the inshore waters.

METHODS

Cruise tracks with the station locations are given in Fig. 1. The cruise XII covers 68°E meridian from Lat. 19° to 14°N in August 1963. Cruise XIII covers a composite section of the following three legs: (1) A meridional section along 71° 30′F

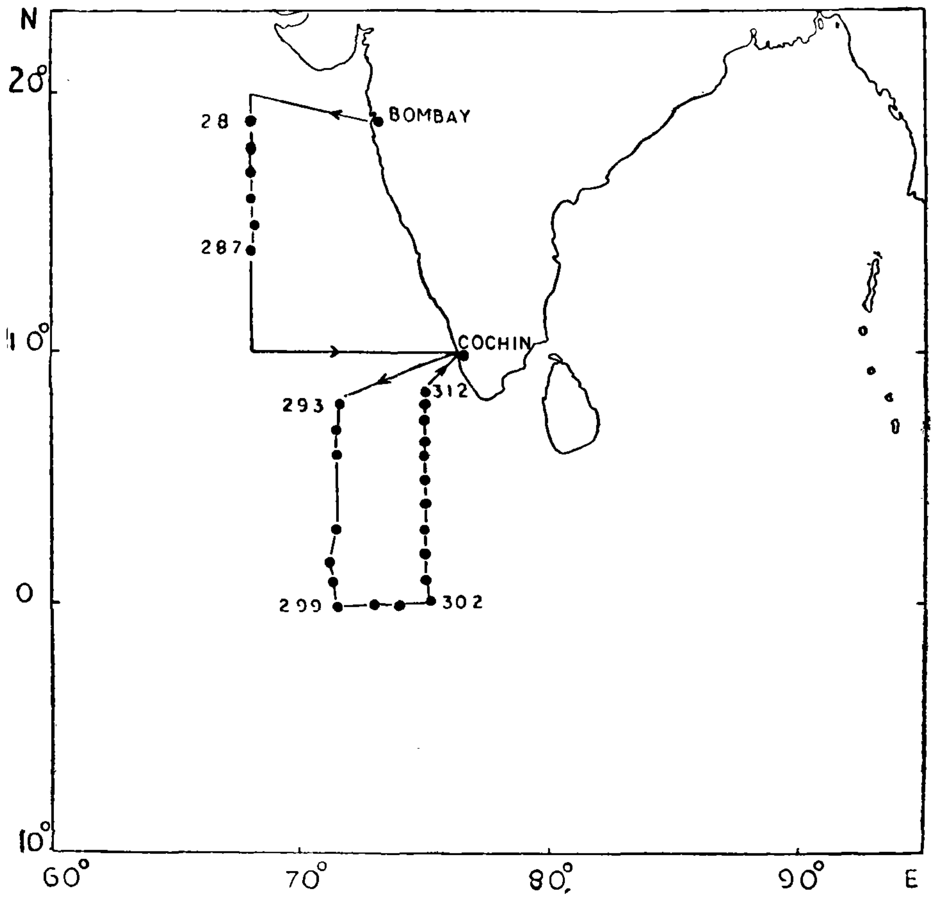

FIG. 1. Map showing the cruise tracks and station locations.

from Lat. 8°N to Equator, (2) Zonal section along the equator through 71°30′ to 75°E, and (3) Meridional section along 75° across Lat. 0° to 8°24.5′ N.

Sea water samples were collected at all standard depths up to 200 m. Samples were preserved at—10°C. on board the ship and analysed in the Indian Ocean Biological Centre, Cochin soon after the cruises.

Inorganic phosphates were estimated by the method given by Wooster and Rakestraw (1951). The values are not corrected for salt error. Silicates were estimated by the method outlined by Robinson and Thompson (1948). Absorbance was measured at 404 mμ as suggested by Barnes (1960) and comparisons were made with potassium chromate standard solutions, buffered with borax.

Results

1. *Section along 68°E meridian, between Lat. 19° and 14°N*

Figure 2A shows the phosphate distribution in surface layers. It can be seen from the figure that phosphate in surface layers down to 50 m is more or less uniformly distributed (Fig. 2A). The values are generally low (0.4 μg at/l.).

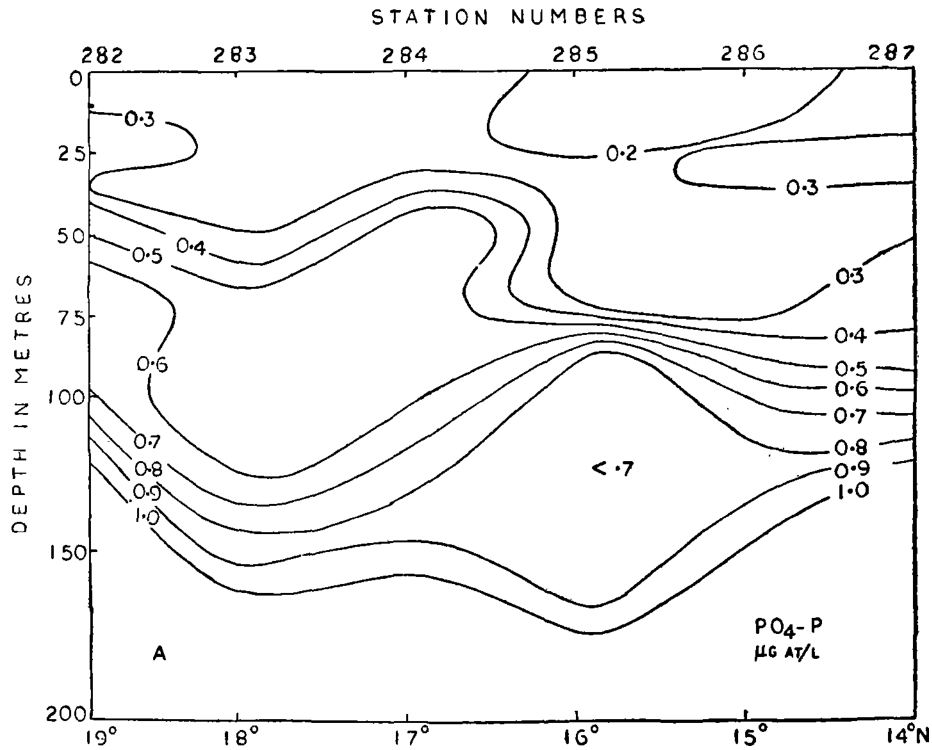

FIG. 2A.

FIG. 2(A-E). Vertical distribution of properties along 68° E meridian between Lat. 19° and 14° N

Vertical profiles indicate that the values tend to increase slightly depthwise up to 100 m. This is followed by a sharp increase at deeper levels reaching maximum concentrations of 1 to 1.5 μg at/l. at about 200 m. Phosphate gradient is not well defined in the first half of the section. The gradient which is weak in the northern part, tends to become strong towards the mid section and further south the gradient again weakens. The phosphate values are relatively high in the northern end of the section. Between Lat. 16° and 15°N the concentrations are remarkably low at all depths.

Silicate values (Fig. 2B) down to 75 m are also low. They show more or less the same pattern of distribution as that of phosphates. The surface values ranged from 0.2 to 4 μg at/l. Relatively higher values are found at deeper layers, reaching maximum values up to 14 μg at/l. A strong gradient of silicate is noticeable in the northern most part between Lat. 19°and 17°N at 100 and 200 m. The presence of the strong silicate gradient in the northern end is in contrast to that of phosphates which is noticeable only in the mid section, running at a higher level.

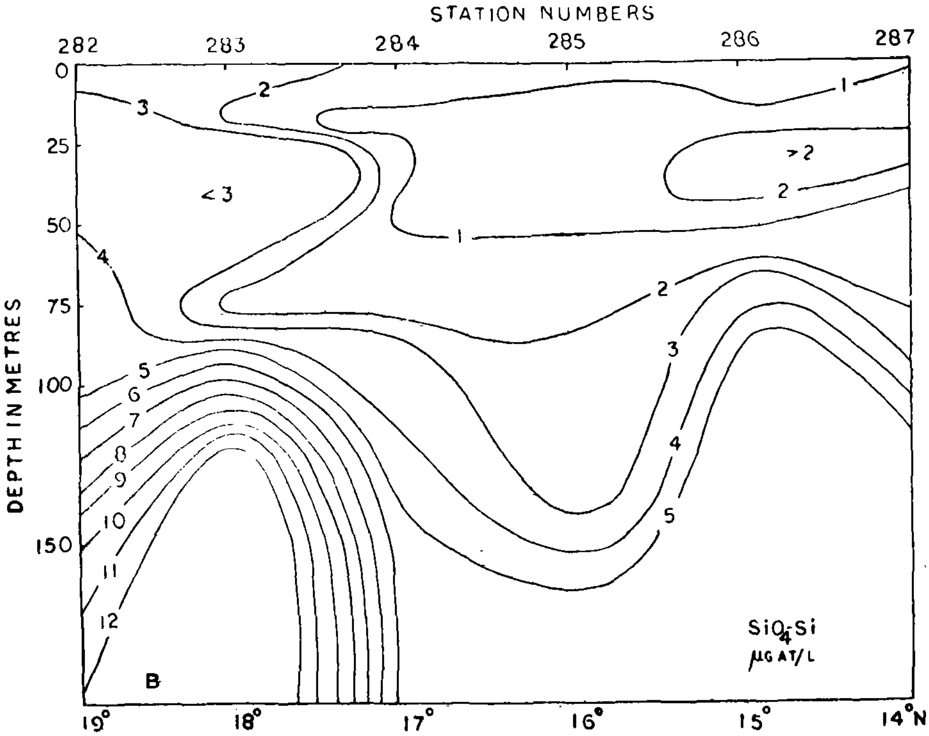

FIG. 2B

Temperature distribution (Fig. 2C) shows that the depth of mixed layer increases towards the South (from about 40 to 50 m in northern section to about 60 to 90 m towards South). The down slope of the isotherms towards south is significant enough to indicate the presence of an easterly current which is in accordance with the general current pattern described in the Admiralty (1950). Thermocline (gradient 2°/25 m) layer found between 45 and 75 m in the northern part up to 17°N Lat. penetrates gradually to deeper levels further south, setting between 75 and 130 m.

Salinity distribution shows more uniform variation with depth showing a decreasing trend down to 200 m (Fig. 2D). Distinct gradients are absent. Salinities decrease slightly towards south. The isohalines show a general reverse pattern to that of isotherms.

Oxygen distribution (Fig. 2E) within the upper 50 m shows little variation. Oxygen discontinuity is noticeable within the thermocline extending down to 200 m. The gradients are rather strong in the southern half. Minimum values of 0.5 ml/l. or less are normally found below 150 m. Along the north-south direction, values were found to be more or less constant, but the southern end of the section is marked by a decrease in Oxygen. Oxygen isopleths follow more or less the same trend as those of salinity and silicates.

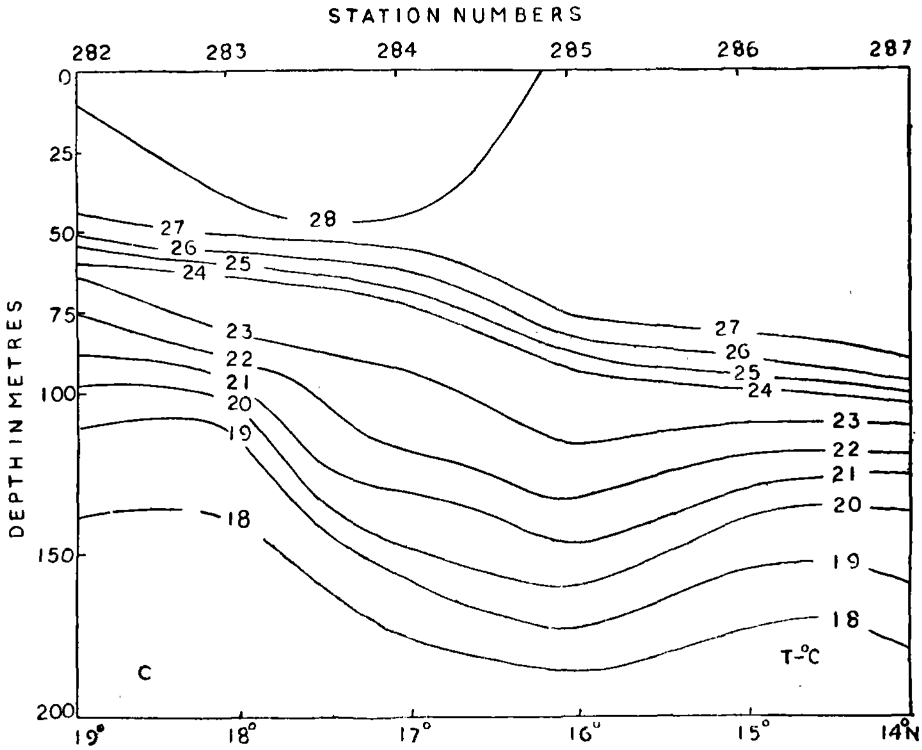

STATION NUMBERS
282
283
284
285
286
287
0
25
50
75
100
150
200
DEPTH IN METRES
28
27
26
25
24
23
22
21
20
19
18
C
T-°C
19°
18°
17°
16°
15°
14°N

FIG. 2C.

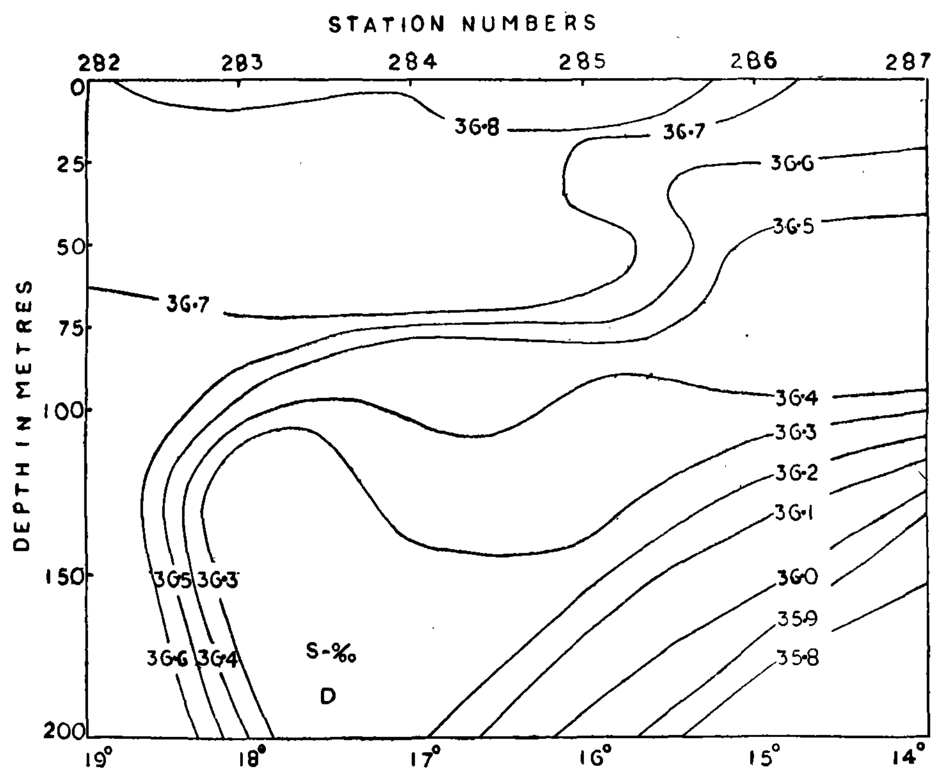

STATION NUMBERS
282
283
284
285
286
287
0
25
50
75
100
150
200
DEPTH IN METRES
36·8
36·7
36·6
36·5
36·4
36·3
36·2
36·1
36·0
35·9
35·8
36·5
36·3
36·6
36·4
S-‰
D
19°
18°
17°
16°
15°
14°

FIG. 2D.

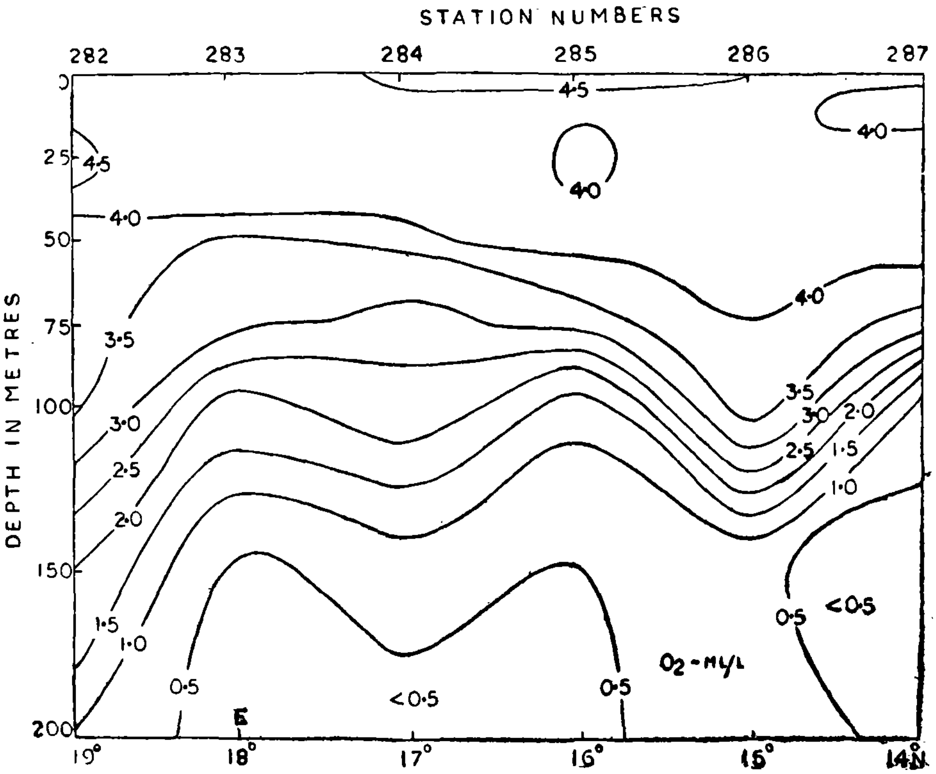

FIG. 2E.

Section along 71°30′*E meridian between Lat.* 8°*N and* 0°:

Phosphate levels in the upper 75 m are generally low (0.3 μg at/l.) and further south the low phosphate zone is limited to upper 50 m only (Fig. 3A). The isopleths at deeper levels (below 120 m) in the northern end of the section (Station 293), show a significant upslope towards south (up to station 294). Beyond that, the isolines converge and constitute a steep gradient delimited between 75 and 100 m. This gradient is maintained at the same level between 75 and 100 m up to Lat. 0°58′N (Station 298). Near the equator the gradient weakens. A core of high phosphate (2 to 2.5 μg at/l.) water is present between Lat. 6° and 1° 42.5′N., just below the phosphate discontinuity layer (below 100 m) extending down to 200 m.

Silicates in the upper 75 m in the northern part up to about 6°N Lat., in general, are low, the values ranging between 0.9 and 2 μg at/l. (Fig. 3B). Like phosphates, the silicates also exhibit a weak gradient (varying from 2 to 7 μg at/l.) in the northern most station below 75 m and the isolines slope upwards towards south with simultaneous steepening of the gradient, setting between 80 and 130 m. Towards the equator the gradient tends to be weak and loses its identity near about the equator. Low silicate concentrations are observed just below the gradient layer, in contrast to the higher phosphate values found in the same region (between Lat. 6° and 2°N).

Temperature profiles (Fig. 3C) indicate that the mixed zone is maintained down to 50 m along the entire section excepting in the northern end where it reaches

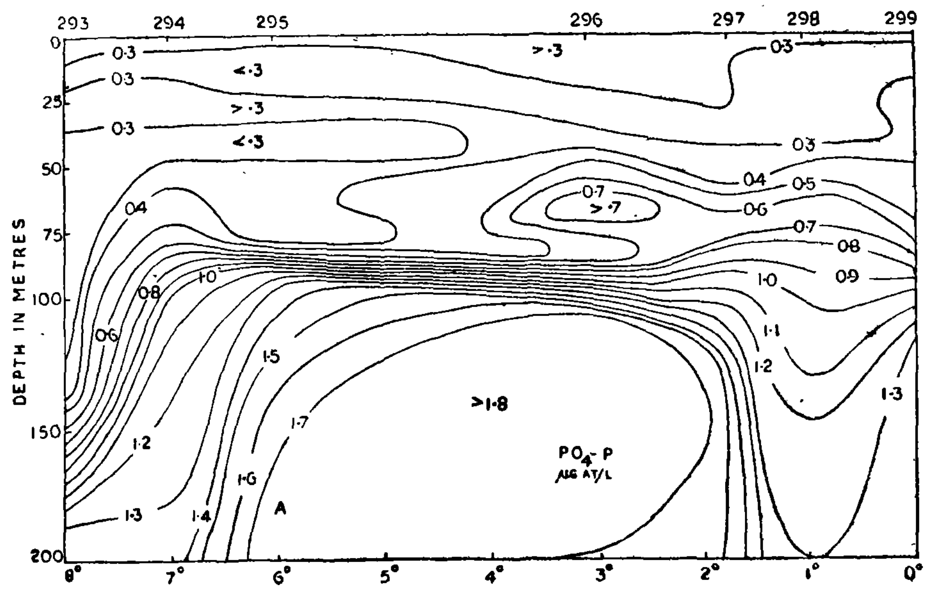

FIG. 3A.

FIG. 3(A-E). Vertical distribution of properties along 71° 30'E meridian between 8° N and 0°.

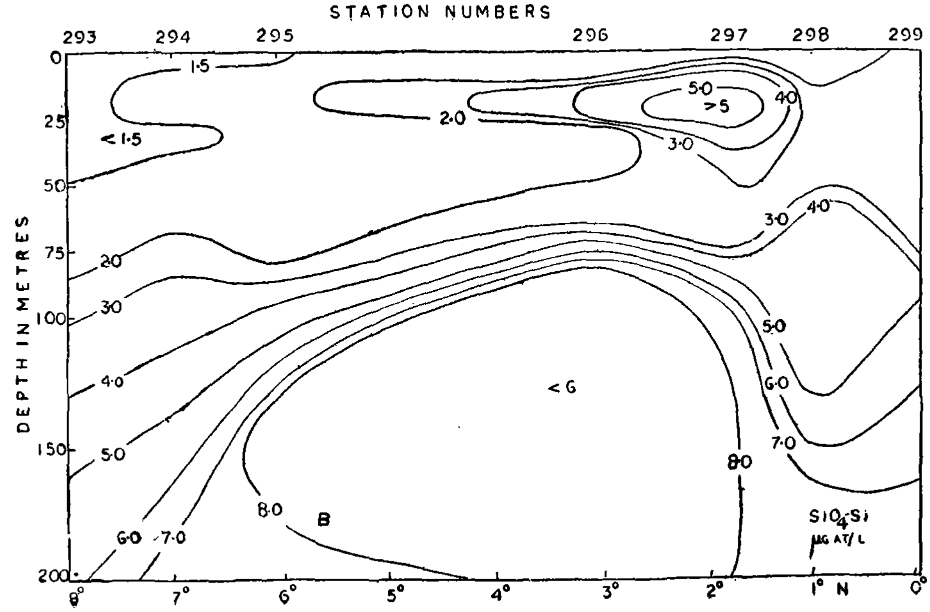

FIG. 3B.

down to 75 m. Isotherms slope upwards in the north-south direction up to 3°N. Lat. similar to those of phosphates and silicates. Thermocline layer varies between 100 and 150 m in the northern end. It migrates to upper levels between 50 and 100 m towards south and at the equator the thermocline tends to spread.

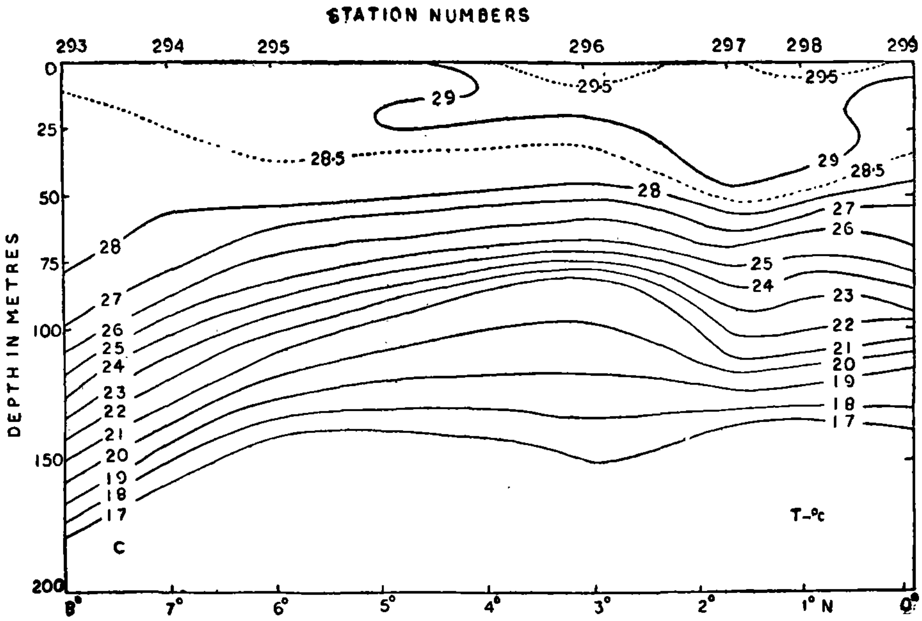

FIG. 3C.

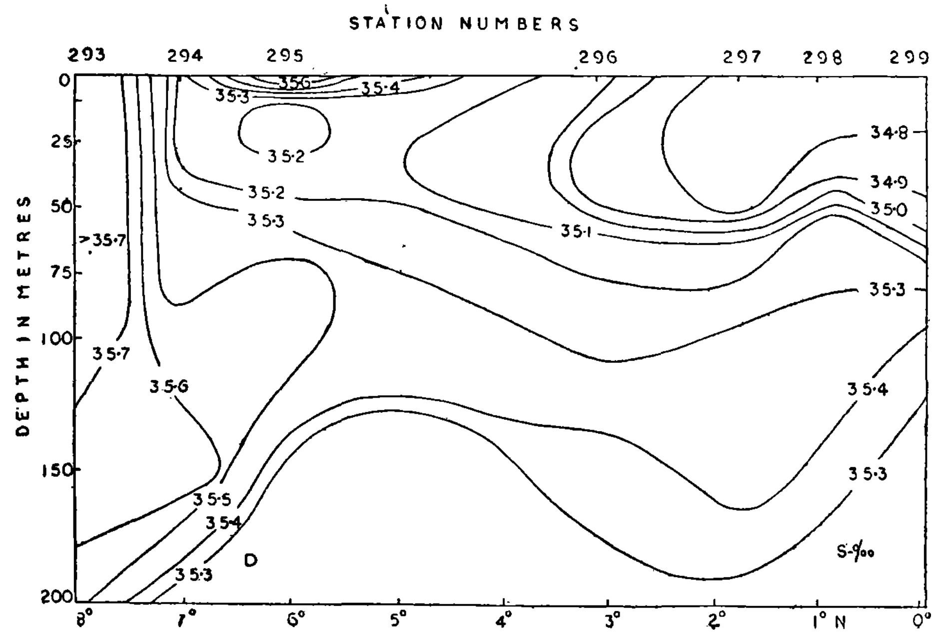

FIG. 3D.

Salinity profiles (Fig. 3D) do not bear any relationship with those of temperature. There is no marked variation with depth, except for a slight decrease from surface to 50 or 75 m. Below this depth a thin layer of relatively high salinity zone exists which is followed again by a gradual decrease in salinity down to 200 m. Northern part of the section is generally associated with higher salinities.

Oxygen values in the upper mixed zone show uniform distribution (Fig. 3E). Along the section towards the south, the surface values remain more or less uniform

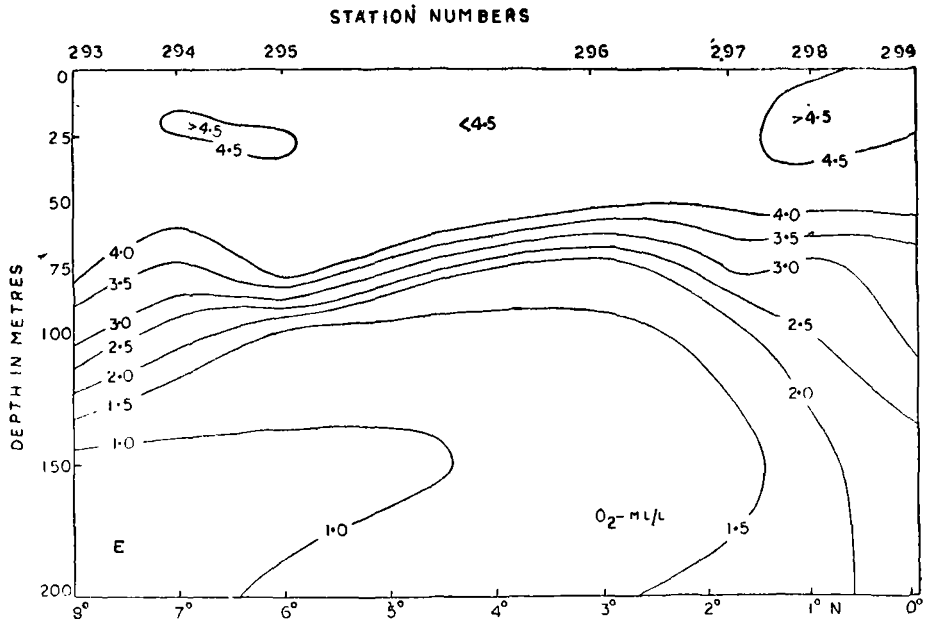

FIG. 3E.

up to 3°N Lat. and beyond that, the values tend to increase reaching maximum at the equator. Oxygen discontinuity layer coincides with the thermocline depth. Isolines show an upward extension towards south, tending to spread near the equator. Lowest values of less than 1 ml/l. are found below 150 m in the northern end of the section. But near the equator at almost the same levels, relatively more oxygenated waters occur (2-3 ml/l.).

Section along the Equator between 71°30′ and 75°E:

Phosphate values of the surface layers (about 75 m) are particularly low and more or less uniformly distributed (ranging from 0.19 to 0.56 μg at/l.) (Fig. 4A). Little variations have been found along the west to east direction. Below 75 m the layer of phosphate gradient (varying from 0.6 to 1.5 μg at/l.) extending down to 150 m is present along the entire section. Below that the values tend to increase slightly and remain more or less constant (1.5 μg at/l.) to about 200 m.

Silicate concentrations (Fig. 4B) also are in general of lower magnitude in the surface, excepting that they are more variable than phosphates in the west to east direction and slightly higher concentrations are found in the mid section. Progressive increase towards deeper levels becomes apparent. Surface values vary from 2 to 5 μg at/l. and higher values of about 9 μg at/l. are recorded at about 200 m.

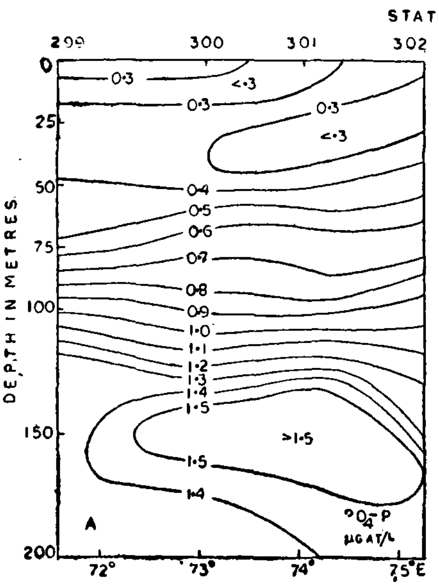

FIG. 4A.

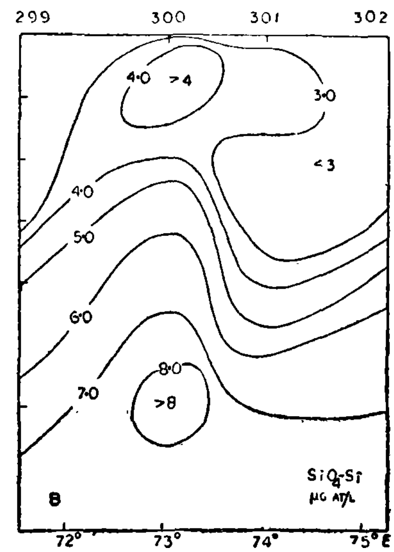

FIG. 4B.

FIG. 4(A-E). Vertical distribution of properties along the equator between 71° 30′ and 75′ E.

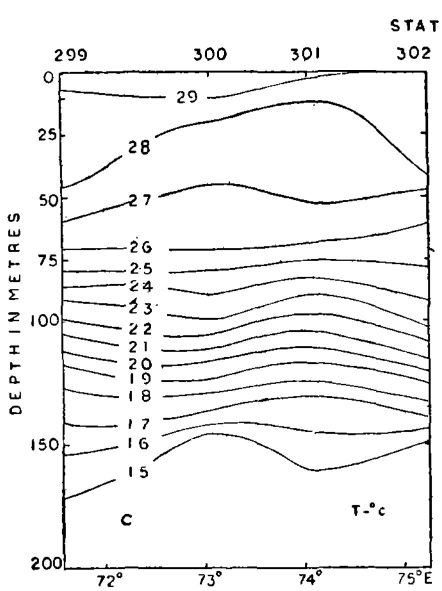

FIG. 4C.

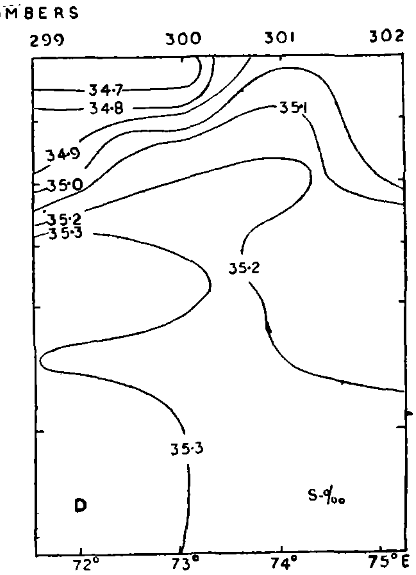

FIG. 4D.

Temperature distribution is uniform in the upper 75 m (Fig. 4C). The thermocline is present just below 75 m, spreading down to 150 m. Surface temperatures are slightly low towards east indicating an uplift of the subsurface layers within 50 m.

Salinity profiles also indicate a uniform vertical distribution (Fig. 4D). Progressive increase up to 75 m is noticeable, which is followed by isohaline conditions down to 200 m. Isohalines within 50 m show an upward tilt towards east resulting in the formation of relatively higher salinities as compared to the western part.

Distribution of oxygen (Fig. 4E) is relatively more uniform vertically and

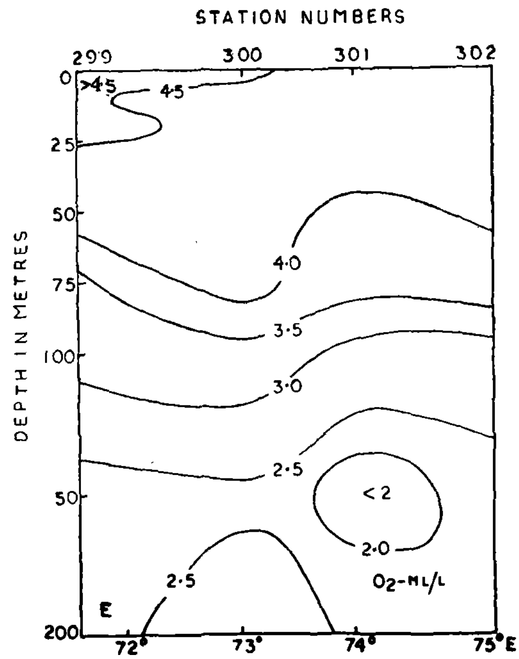

FIG. 4E.

horizontally as compared to the previous sections. Oxygen discontinuity is noticeable below 50 m and the gradient is weak. Lowest oxygen values of the order 2 ml/l. are found below 150 m. The oxygen isopleths tend to slope upwards in eastern part, similar to salinity and silicate profiles.

Section along 75°E meridian from 0° to 8°24.5′ N:

Uniformly low phosphate levels are present down to 75 m along the entire section (Fig. 5A). The values being generally less than 0.5 μg at/l. Values of phosphate varying between 0.5 and 1.1 μg at/l. are found between 75 and 120 m near the equator which are continued up to 3°N Lat. wherein there is a slight increase

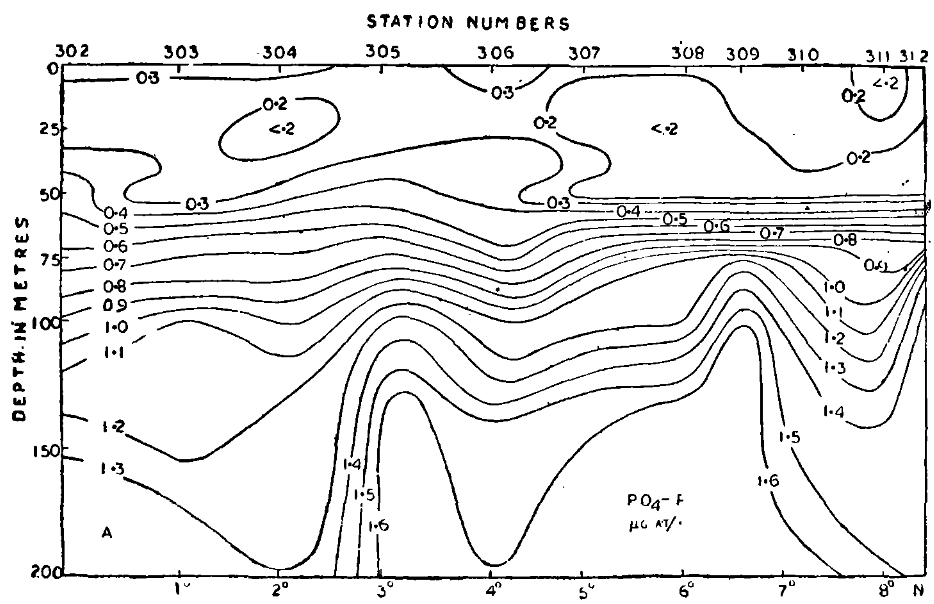

FIG. 5A.

FIG. 5(A-E). Vertical distribution of properties along 75° E meridian between 0° and 8° 24.5'N.

in the range (from 0.5 to 1.5 μg at/l.) with corresponding increase in the lower depth limit to 130 m. The general disposition of the profiles indicate a certain amount of instability below 75 m.

Surface silicates down to 75 m at both ends of the section are low varying between 1.2 and 3 μg at/l. (Fig. 5B). In the mid section between Lat. 4° and 5°N a slight increase in the values (3-5 μg at/l.) is noticeable due to upslope of the layers between 75 and 100 m. Values greater than 9 μg at/l. are present below 150 m. However, it may be mentioned that the profiles present an irregular pattern, suggesting the existence of eddies.

Temperature variations in the upper 10 m along the section are interesting (Fig. 5C). Near the equator the values are lower and northwards up to 5°N Lat., the temperature increases, and beyond a fall in temperature is again noticeable. The same trend is reflected down to about 40 m excepting that the intensity of variation is less marked between Lat. 3° and 6°N; there appears to be an upslope of waters from 30-40 m towards the surface thus causing the transition from higher to lower temperatures towards higher latitudes. Thermocline begins just below 75 m extending down to 150 m near the equator and breaks up towards 1°N Lat. limiting between 40 and 68 m only, and further north it extends down to 80 m. It

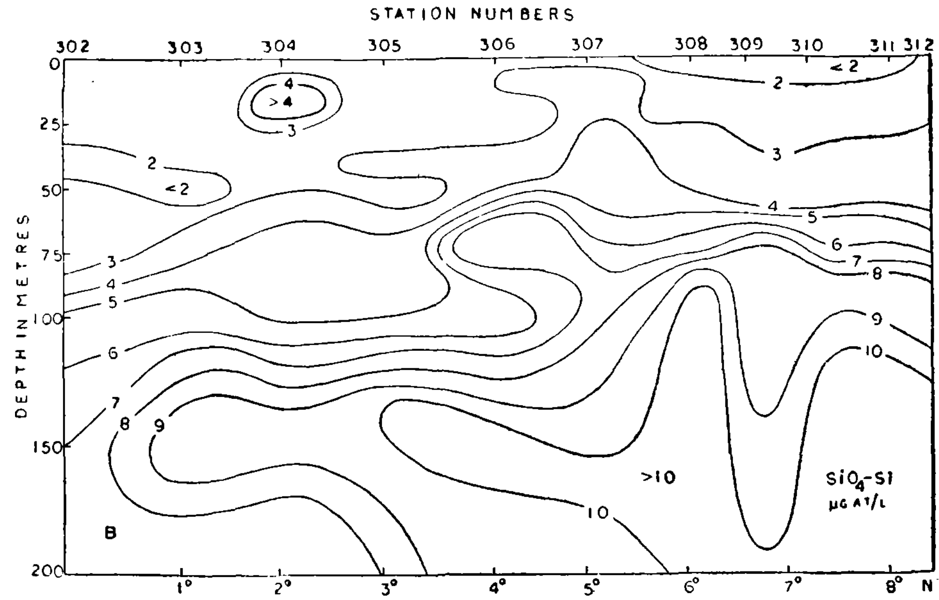

FIG. 5B.

may be mentioned here that meridionally the thermocline is tending to be weak from west to east direction. At deeper levels the vertical temperatures show relatively a uniform distribution; the general pattern of the isotherms suggest considerable movement of waters.

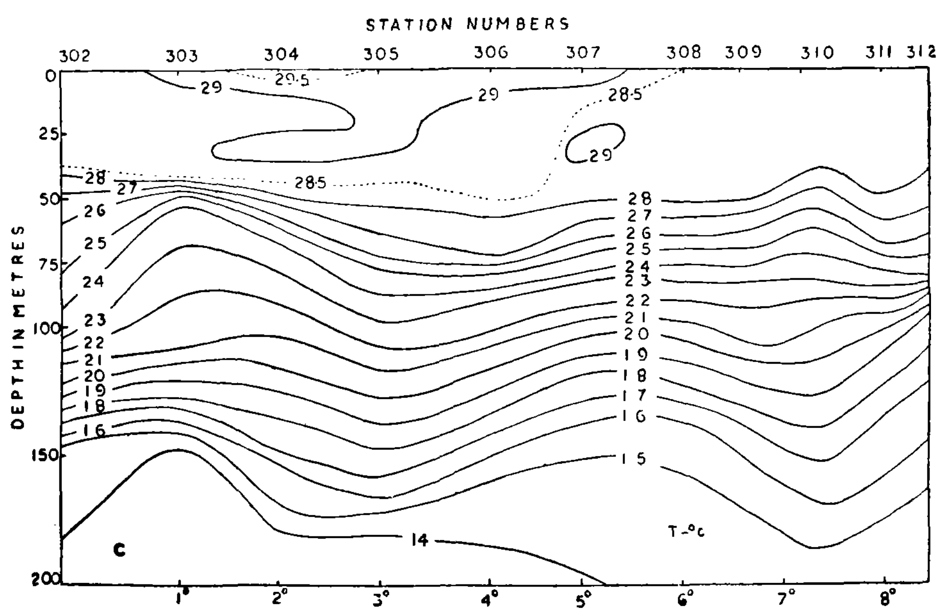

FIG. 5C.

Salinity distribution of the upper 75 m (Fig. 5D) presents an irregular pattern which might be the result of eddies as is also indicated while examining the distribution of the other parameters. There appears to be a general increasing trend from

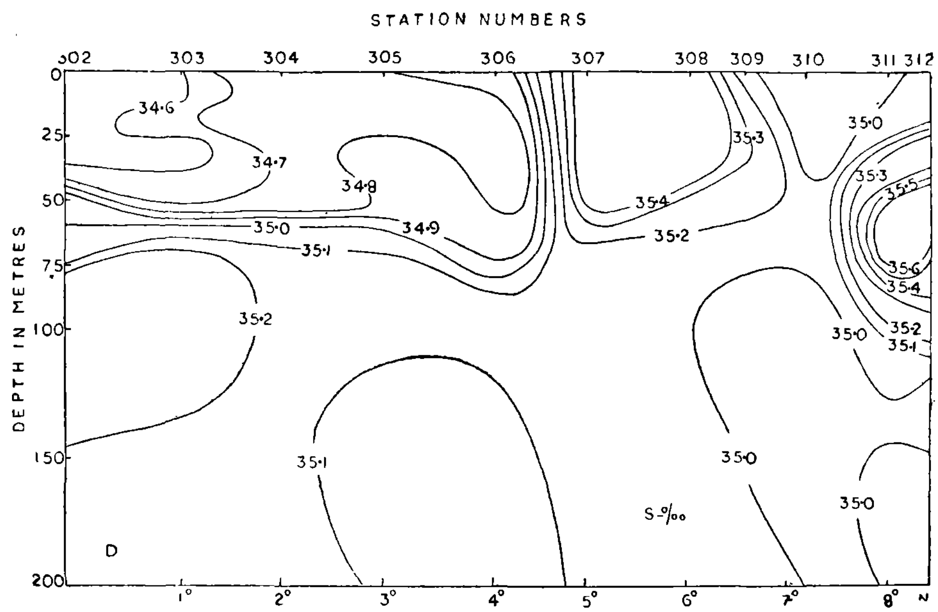

FIG. 5D.

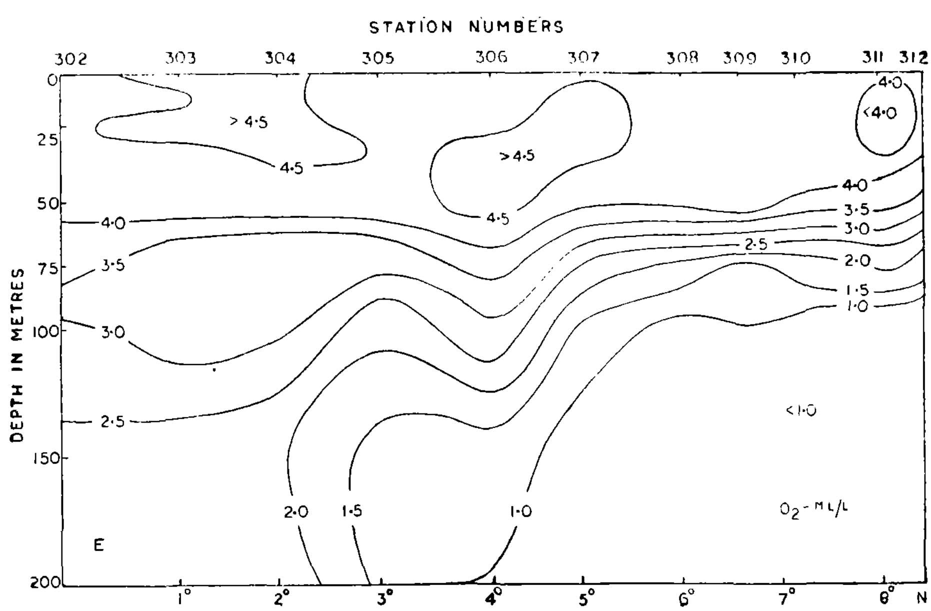

FIG. 5E.

south to north direction up to 2° Lat. followed by a fall up to 4° Lat.; rather a sharp increase is again noticeable up to about 7°N. Lat. and beyond a general lowering of the values are observed. Below 75 m the vertical variations are very little and remained more or less constant. In the northern end of the section a tongue of high saline water between 20 and 100 m appear to be moving northwards (the axis points slightly downwards). A layer of salinity maximum at about 100 m level extends all along the section excepting that the level shoals up towards north coinciding with the tongue of high saline water.

Vertical variations of the oxygen in the upper 50 m are little (Fig. 5E) and a general decrease in the values towards north is noticeable. Oxygen discontinuity begins below 50 m and the gradient which is weak near the equator tends to become stronger towards north. Oxygen poor layer (<1 ml/l.) is present at 4° N at 200 m level and towards further north it extends to shallow depths, reaching up to about 80 m.

Discussion

Distribution of nutrients and other parameters like temperature and salinity in the open oceanic waters seems to be more uniform and regular than those in the inshore waters where the proximity of land introduces complexity in the nature of distribution of these parameters. Nutrients of the oceanic waters appear to be more dependent on the general current pattern and sources of origin of distinct moving water masses. Greater accumulation of nutrients at deeper levels and their consistancy, irrespective of seasons and places may have far reaching significance in determining the fertility of surface waters. The deep nutrient rich waters seem to act as inexhaustible reservoirs and these may replenish the losses of nutrients of the surface layers caused by physical or biological factors. A knowledge of the spatial and temporal distributions of the nutrients in the oceanic regions is valuable in understanding their influence on the shelf waters which are more productive.

Present investigations are mainly related to the distributional aspects of nutrient salts in relation to some hydrographical factors of the upper 200 m waters in the Central Western North Indian Ocean during the south-west monsoon season in the month of August. The great impact of the south-west monsoon on the North Indian Ocean, resulting in the extensive movements and exchange of water masses in determining the biological productivity of the shelf waters of the Arabian and West Indian coasts are well established and as such the information on spatial variations of these important factors in the oceanic waters during this period may also aid in understanding the fertility of different regions.

Monsoon winds over the north Indian Ocean change the current pattern into two distinct types of circulations. During the south-west monsoon period the coastal circulation is clockwise and in the open ocean the current is easterly. But during the north-east monsoon period the entire pattern reverses. The current system becomes strong and stable during the south-east monsoon period in contrast to that during the north-east monsoon. The effect of north-west monsoon is relatively weak over the North Indian Ocean. Towards the equator the general west going North Equatorial Current is replaced by stronger east going monsoon current during south-west monsoon season.

Water masses of the North Indian Ocean have the general characteristics of mid-latitudes and equatorial region and the main surface water mass extending to moderate depths is demarcated as North Indian Equatorial Water mass (Sverdrup *et al.* 1942). Present observations on the hydrographic characteristics are limited to the upper 200 m of this water mass.

Examination of the vertical profiles of nutrients reveal broadly two distinct features; a surface layer of low nutrient content extending down to 50 or 75 m followed by a region of higher and fairly steep gradient of nutrient concentrations down to 200 m. Considerable meridional and zonal variations in the thickness of these layers are apparent which may be mainly due to variable intensities of the current velocities and consequent vertical movements of the waters. These broad features in general, correspond to those observed in Pacific and Atlantic Oceans. Present investigations indicate that the nutrient levels in the regions of the North Indian Ocean under review, generally fall between those in the similar regions of Pacific (highest) and Atlantic (lowest). The major exception being the region north of 10° N in the Indian Ocean where in the surface values are observed to be higher than in Pacific. Temperature, salinity and oxygen profiles are consistent with the variations in the nutrient profiles. A scrutiny of the nutrient profiles with those of temperature, salinity and oxygen indicates a closer relationship of phosphates with temperature, while silicates with salinity and oxygen. This feature, perhaps is characteristic of the upper layers of the Oceanic waters of this region, in view of the relatively more labile nature of phosphates and temperature in the surface layers than the silicates, salinity and oxygen which are rather more stable, and which may often characterise the distinctness of a surface water body.

Phosphate distribution along the North-South direction presents some striking features; along 68° E meridian, even though the surface values are of low order along the entire section, concentrations tend to decrease further towards south up to 14°N Lat. This feature is in contrast to the conditions prevailing in the shelf waters along the West Coast of India wherein the phosphate levels tend to increase towards south (Reddy and Sankaranarayanan 1965). At deeper levels also, the increase in phosphate is not marked; the maximum of about 1 μg at/l. is found only at about 200 m. The probability of the existence of low phosphate levels in this region, might be due to the easterly transport of nutrient depleted surface layers off the Arabian Coast caused by the prevailing southerly component of south-west monsoon winds and these waters are continuously transported across the sea by the large eastward current. The general high salinity of the region is also in agreement with the above explanation. The secondary effect of these impoverished waters in lowering the phosphate content towards deeper levels (down to 200 m) might have been thus indicated as a result of progressive mixing. The general disposition of the isopleths also indicate considerable amount of water movements along the entire section.

Silicate distribution also corroborates the inferences drawn from those of phosphate data. It is significant to note that in the northern region between 19° and 17° N Lat., below 100 m, the formation of silicate isolines of relatively higher concentrations suggest an apparent streaming up of silicate rich waters. While salinity and oxygen profiles are in agreement with the above observation, those of phosphate and temperature do not indicate this feature. Possibly this might be due to relatively small vertical variations of phosphate or temperature as compared with the silicate or salinity.

Remarkably low nutrients between stations 284 and 285 (Lat. 16°30′ to 15°30 N) with corresponding increase in depth of mixed zone is noticeable indicating marked convergence which may possibly be due to the influence of horizontal eddies.

The southern section along 71°30′ E from Lat. 8°N extending to the equator, is characterised by deeper mixed zone extending down to 75 m. Generally phosphates and silicates, even though continued to be low show slightly increasing trend towards the south and this feature is more distinct near the equatorial region. A core of high phosphate layer containing relatively lower silicate and oxygen concentrations, is found below 100 m, in the region extending approximately between 2° and 6°N along 71°E meridian. The indications suggest a distinct water body with longer residence time and thus perhaps accounts for higher phosphate and lower oxygen contents due to biochemical oxidation. The strong discontinuity layer in the area might be impeding vertical mixing and thus promoting regenerative processes. Around 8°N along 71°E a rather abrupt variation in all the parameters, particularly in salinity and temperature is noticeable towards south. Temperature and nutrients show an increase while salinity and oxygen show a decrease. The salinity and temperature magnitudes at either sides of the transition region are suggestive of sinking process. Towards the equator, nutrients, temperature, salinity and Oxygen profiles show a slight and gradual uplift of the waters from about 75 m to the upper levels. This phenomenon may be attributed to the natural sequences associated with the equatorial divergences. Varadachari and Sharma (1964) presenting the seasonal distribution of vergence field of the surface waters in the north Indian Ocean, showed the occurrence of several centres of divergence and convergence in the open ocean regions throughout the year, more intense field being in the south-west monsoon period, particularly in equatorial regions. The general pattern of equatorial divergences and centres of convergences in regions north of equator in the south-west monsoon period as could be inferred from the present observations, are in broad agreement with their findings. However it may be mentioned that the nutrient levels at the surface layers near the equator are continued to be of low order inspite of the divergences and consequent upwelling. From the vertical profiles of nutrients, it is seen that the uplift of waters is restricted to within the shallow depths wherein the nutrient concentrations are not high and thus indicating that intensities of divergences in the equatorial Indian Ocean may be of lower magnitude than in the counterparts of the other Oceans. Possibly this difference between the equatorial Indian and the equatorial Pacific and Atlantic Oceans, appears to be somewhat related to the absence of the regular west going North Equatorial Current in the Indian Ocean during this period and instead the presence of east going monsoon current. In the Pacific and Atlantic the general equatorial current systems remain unchanged throughout.

However, the situation in the North of equator (beyond 10°N) presents a different picture in the Indian Ocean, wherein higher surface nutrient concentrations are found to exist, compared with the same regions of other Oceans. Armstrong (1965) while discussing the phosphate distribution in the oceans, mentions that in the Central Pacific region between 40° and 10°N and away from the coast, lower surface concentrations of less than 0.16 μg at/l. were encountered. Present investigations in Central North Indian Ocean show relatively high surface concentrations (0.3 μg at/l.) of phosphate between 20° and 10° N as compared with the same region of the Pacific.

Another notable feature in the Central North Indian Ocean is the presence of relatively shallow zone of phosphate low layer extending from surface to only 75 m as compared with the similar zones which are generally thicker, extending down to 100 m or more in North Pacific and Atlantic. This featural difference may have an important bearing in rapid exchange of nutrients to the surface layers from the nutrient rich sub-surface layers, and thus may explain the existence of relatively higher surface concentrations in the Central North Indian Ocean than in the same regions of the Pacific and Atlantic.

Nutrient concentrations along the equator between 71° and 75° E do not show the expected higher levels. Phosphates and temperature profiles (Fig. 4 A & C) exhibit more or less a normal pattern while the silicates, salinity and oxygen profiles (Fg. 4 B, D & E) indicate fairly a marked divergence pattern in the upper 70 m between 72° and 73° E meridians. Phosphate and temperature profiles also do agree to some extent with the above feature, though not strongly indicative and this is obviosly due to more uniform vertical characteristics of both the parameters within that layer. Thermocline is present at deeper level (70 m) spreading down to 150 m and is maintained throughout at the same level. Phosphate gradient coincide with the thermocline. Salinity gradients are limited to upper 70 m only while the silicate and oxygen profiles do not exhibit strong gradients. The characteristic spreading of the thermocline, nutrient and oxygen isolines at the equator was also reported by Knauss (1964) and Gangadhara Rao and Jayaraman (in press) and related to the presence of an undercurrent. How ever the discussion relating to the presence of this current is beyond the scope of the present paper.

The section running south to north along 75°E gives some idea in the meridional variation in the distribution of nutrients, running parallel to the North-South section along 71°E. However, the observed meridional and zonal differences appear to be more influenced by the Maldive Islands positioned between these two sections (at 73°E). The nutrients register an increasing trend towards south along both the sections. In the northern half, the concentrations are in general, slightly higher on the western side, while along the southern half, only the surface waters show slightly higher concentrations towards east. The nutrient values in the eastern equatorial region and the distribution might be associated with the monsoon current augmented by the island effect. In the northern half, the observed low values on the eastern section could possibly be related to the diffusion of the southerly current, contributing the nutrient depleted waters. Another notable feature is the relatively low stability of the waters towards east, as could be seen from the thermocline structures and the disposition of nutrient isopleths (Fig. 5 A-E). Around 5°N Lat. along 75°E a marked transition in the water properties could be noticed (Fig. 5 A-E). The indications point to boundary conditions. Investigations by Varadachari and Sharma (paper under publication) on the circulation of surface waters in the north Indian Ocean, showing some point similarities and line similarities in the streamline pattern of the circulation, documented a line convergence around the same region. It may be mentioned here that this region may be limiting the extent of the spread of southerly flow and thus forming a boundary with the easterly monsoon drift current.

A brief comment on the abundance of zooplankton in some parts of the ocean during the cruise may reveal some interesting features related to nutrients and other oceanographic features. Zooplankton samples were collected from some regions covered during the 13th cruise. Several earlier workers have reported a correlation between zooplankton and Po_4-P, and other oceanic features such as thermocline, and pycnocline topographies in the Pacific and Atlantic Oceans (King and Hida 1957; Holmes *et al.* 1957; Brondhorst 1958; Reid 1962).

Zooplankton organisms (in terms of displacement volumes collected from the upper 200 m using IOSN) between Lat. 8° and 0° N along 71°E show a general increase towards the equator and along the equator between 71° and 75°E. Along 75°E there was a sharp decrease towards north of equator up to 3°N and beyond this position a short increase in zooplankton organisms (3 to 6 fold, became noticeable). The increase of zooplankton toward the equator along 71°E coincided with the general upslope of the isopleths. Higher zooplankton content along the equator also seem to be associated with divergences. However the sharp decline in zooplankton along 75°E towards north of equator up to 3°N presents a complex situation. Since the nutrient concentrations in this region are more or less same as those along the equator and relatively higher than further north (between 3°N and 8°N), the sharp reduction in zooplankton might be associated with hydrographical conditions or may be related to natural sequences of the food cycle. It is also possible that in this region a greater intensity of easterly current and the presence of large eddies might be responsible for the low plankton content. The very high incidence of zooplankton between 3° and 8°N along 75°E is in close correspondence with the boundary conditions observed (loc. cit.) between eastward monsoon current and the spread of the southerly flow. The waters of the southerly flow along the West Coast of India might be contributing to the extremely high plankton concentration of this region. Synchronously the low nutrient content of the same region suggests that the waters brought in by the southerly current were stripped off their nutrients during their sojourn along the West Coast of India due to high biological productivity and thus contributing to the observed increase in the biomass of the region.

ACKNOWLEDGMENT

The authors wish to express their grateful thanks to Dr. N. K. Panikkar, Director, National Institute of Oceanography (C.S.I.R.), for his guidance and keen interest in the present study; to Dr. S. Z. Qasim, Shri R. Jayaraman and Dr. V. V. R. Varadachari for valuable suggestions.

REFERENCES

Admiralty. (1950). West Coast of India Pilot, London.

Amstrong, F.A.J. (1965). Phosphorus. Chemical Oceanography 1. Academic Press, London, 323-364.

Brarnes, H. (1959). Apparatus and Methods of Oceanography. Part I. Chemical. George Allen and Unwin Ltd., London.

Brandhorst, W. (1958). Thermocline topography, zooplankton standing crop, and mechanisms of fertilisation in the eastern tropical Pacific. *J. Cons. Inst. Explor. Mer.*, **24**, 16-31.

Grangadhara Rao, L.V., and Jayaraman, R. (1967). Vertical distribution of temperature, salinity and density in the upper 500 metres of the North Equatorial Indian Ocean during the North-east monsoon period. (in press).

Joseph, E. King., and Jhon Demond (1953). Zooplankton abundance in the Central Pacific. *U.S.F.W.S. Fish. Bull.*, **54**, 111-144.

Joseph, L. Reid Jr. (1962). On Circulation, Phosphate—Phosphorus Content and zooplankton volumes in the upper part of the Pacific. *Limnol. Oceanogr.*, **7**, 287-306.

King, J.E., and Hida, T.S. (1957). Zooplankton abundance in the Central Pacific. Part II. *U.S.F.W.S. Fish. Bull.*, **57**, 365-395.

Knauss, J.A., and Taft, B.A. (1964). Equatorial undercurrent of the Indian Ocean. *Science*, **143**, 354-356.

Robinson, R.J., and Thompson, T.J. (1948). Determination of Silicates in Sea Water. *J. mar. Res.*, **7**, 49-55.

Rozanov, A.C. (1964), Distribution of phosphates and silicates in the Northern part of the Indian Ocean. *Trudy-Inst. Okeanol.*, **64**, 102-114.

Ryther, J.H., and Menzel, D.W. (1965). On the production, composition and distribution of organic matter in the western Arabian Sea. *Deep Sea Res.*, **12**, 199-209.

Sverdrup, H.U., Johnson, M.W., and Fleming, R.H. (1942). The Oceans, Their Physics, Chemistry and General Biology. Prentice Hall, New York.

Thomas, S. Austin (1958). Variations with depth of oceanographic properties along the Equator in the Pacific. *Trans. Am. Geophys. Un*, **39**, 1055-1063.

Varadachari, V.V.R., and Sharma, G.S. (1964). On the vergence field in the North Indian Ocean. *Bull. N.G.R.I.*, **2**, 1-14.

——— (1965). Circulation of surface waters in the North Indian Ocean. *Bull. N.G.R.I.* (in press)

Wooster, W.S., and Rakestraw, N.W. (1951). The estimation of dissolved phosphates in Sea water. *J. mar. Res.*, **10**, 91-100.

Reprinted from *Bull. natn. Inst. Sci. India*, no. 38, 1968, p. 148-163

NUTRIENTS OF THE NORTH-WESTERN BAY OF BENGAL

by V. N. SANKARANARAYANAN *and* C. V. GANGADHARA REDDY
National Institute of Oceanography, Ernakulam

Studies on the distribution of phosphates, silicates and nitrates in relation to some hydrographical features of the north-western Bay between latitudes 16° and 19°N during the month of January showed marked regional variations. The distribution is found to be related to the prevailing currents. The chief feature of the region investigated is the commencement of coastal upwelling. The ascent of the sub-surface waters is weak and extends only up to 20 m below the surface. rom the disposition of the isolines it appears that the vertical movement of the waters extends down to 500 m. Phosphate maximum is found between 600 800 m and the nitrate maximum between 300 and 800 m. The silicates, on the other hand, continue to increase with depth. The factors influencing the distribution of nutrients over the entire region have been discussed.

INTRODUCTION

While considerable information is available on the general oceanographic conditions in the Bay of Bengal, very little is known regarding the distribution of nutrient salts. Even the available data is centred around few regions, particularly off Waltair and Madras and most of the studies limit to near-shore areas (Jayaraman 1952; Ganapathy and Sarma 1958; Bhavanarayana and LaFond 1957; Varma and Reddy 1959). The Bay of Bengal especially the northern region is influenced by the discharge of large rivers and complex current patterns varying with monsoons. Since the distribution of nutrients and other hydrographical features are affected more by the dilution and currents, the general estuarine character of the Bay of Bengal limits the generalisation of characteristics based on meagre regional and seasonal studies. This feature is in contrast to the Arabian Sea, in which the riverine inflow is considerably less and the conditions are predominantly oceanic and relatively more stable. Therefore it is imperative that several distinctive small regional studies through different seasons are necessary to assess the hydrological characteristics of the Bay of Bengal as a whole.

During the International Indian Ocean Expedition (1962-1965) it was possible to cover several regions in the Bay of Bengal in different seasons and the present account on the nutrients in the north-western Bay of Bengal in relation to hydrographical factors, is based on the data collected during the 21st Cruise of I.N.S. Kistna in the month of January, 1965.

MATERIAL AND METHODS

Figure 1 shows station locations along the sections normal to the coast. Stations were selected from the regions (1) off False point (between Lat. 20°08′ and 18°N and Long. 86°54′ and 90°E), (2) off Gopalpur (between Lat. 19°09′ and

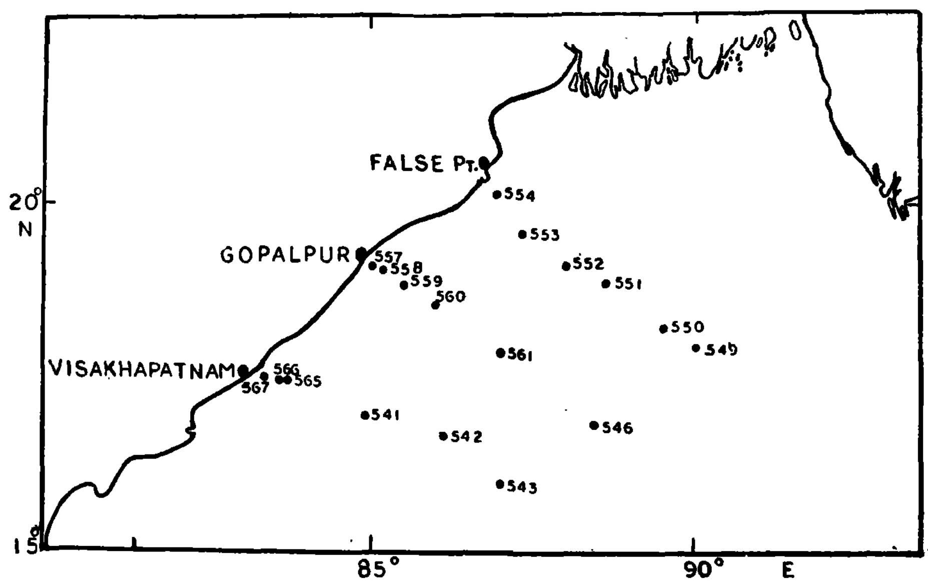

FIG. 1. Map showing the station locations.

16°53′N and Long. 85°02′ and 88°20′E) and (3) off Visakhapatnam (between Lat. 17°32′ and 16°N and Long. 83°29′ and 87°N). Methods of chemical analysis of the water samples for phosphates and silicates were the same as reported earlier (Reddy and Sankaranarayanan 1966). Nitrates were estimated as described by Strickland and Parsons (1960) using Sulphanilamide and N-(1-naphthyl) ethylene diamine for the azodye formation and the extinction was measured at 543 mμ. Observations between depths 0-1000 m are presented.

RESULTS

Fugures 2A, 3A and 4A show the vertical profiles of phosphates along the three sections. Phosphates in the mixed layer (upper 60 m), show some meridional and latitudinal variations. The concentrations are relatively higher in the shelf waters ranging from 0.3 to 1.1 μg at/l. The values tend to decrease towards the east registering less than 0.5 μg at/l with the only exception in the northern part of the section (off False point) wherein the values show a rise at the eastern end of the section. Along the north-south direction, high values (0.5 to 1.1 μg at/l) exist in the south (off Visakhapatnam) and low values (0.3 to 0.58) in the mid-region (off Gopalpur). Phosphate discontinuity layer coincides with the thermocline topography and a common feature of the entire region is that the phosphate discontinuity layer shows a gradual coastward upslope from the mid section with varying intensities. In the north (off False point) the phosphate gradient layer tends to slope up towards shallower depths at the eastern end also. This feature is absent in the remaining

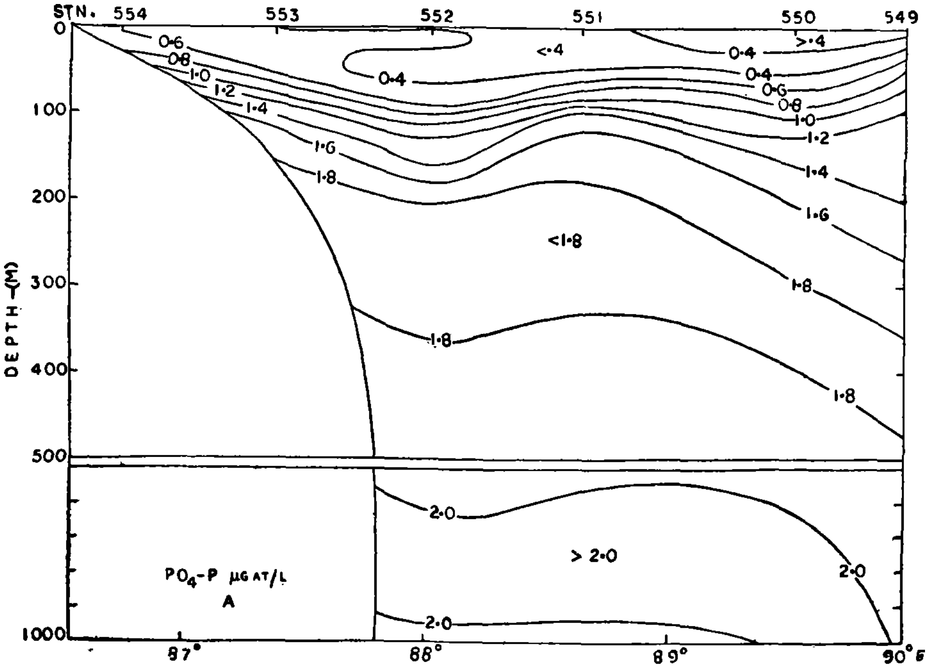

FIG. 2A.

FIG. 2 (A-F). Vertical profiles of properties along the section off False Point.

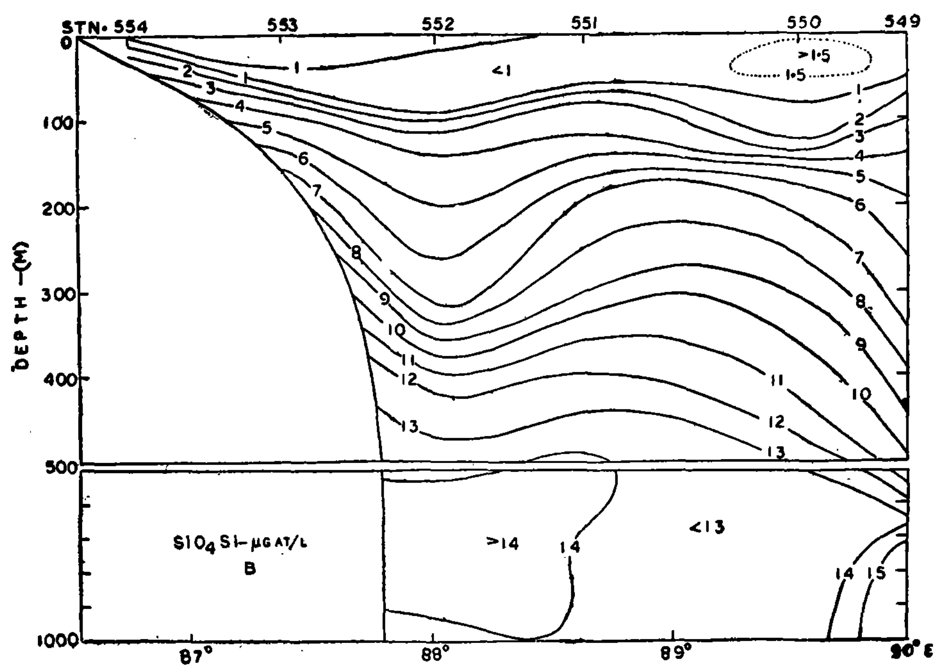

FIG. 2B.

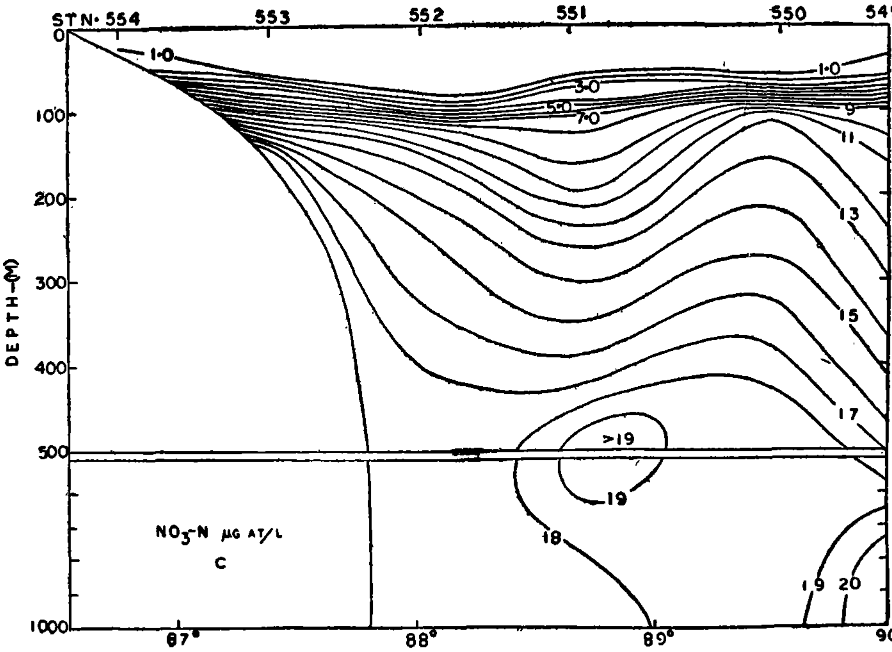
STN·554
553
552
551
550
549
DEPTH—(M)
0
100
200
300
400
500
1000
87°
88°
89°
90°E
1·0
3·0
5·0
7·0
9
11
13
15
17
>19
19
18
19
20
NO_3-N μG AT/L
C

FIG. 2C.

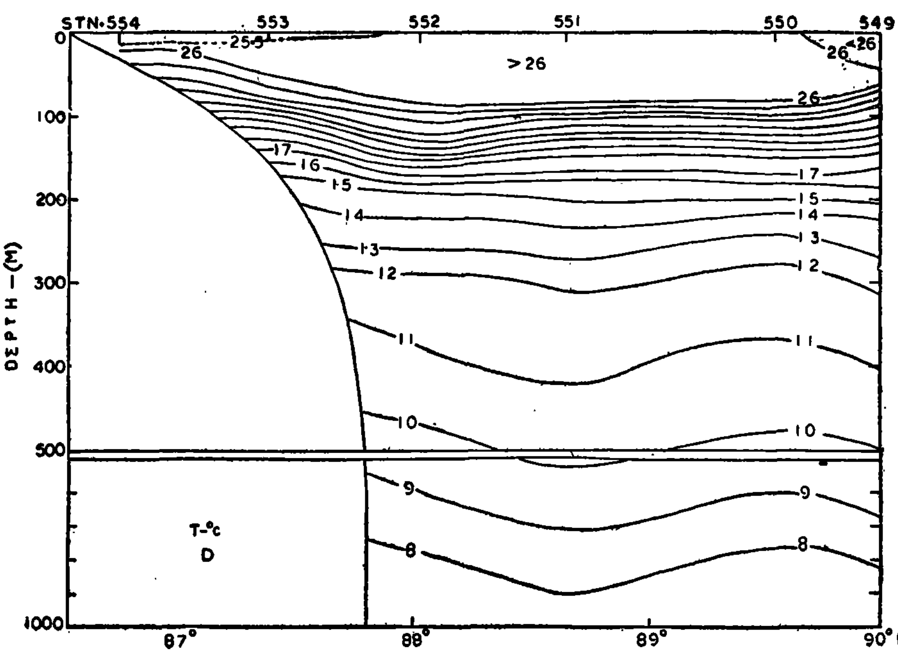
STN·554
553
552
551
550
549
DEPTH—(M)
0
100
200
300
400
500
1000
87°
88°
89°
90°E
25·5
26
>26
<26
17
16
15
14
13
12
11
10
9
8
T-°C
D

FIG. 2D.

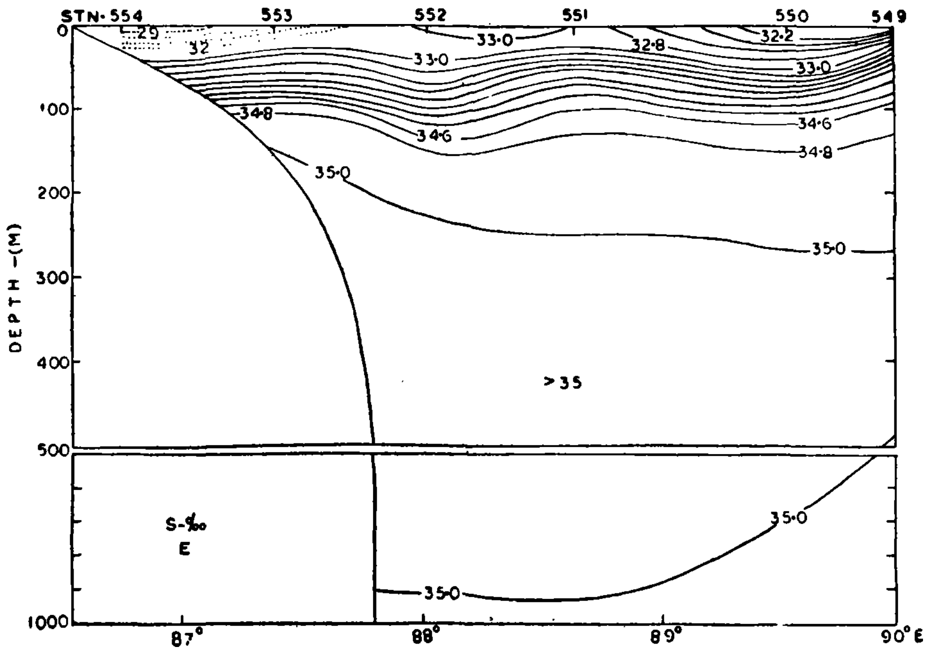
STN· 554
553
552
551
550
549
DEPTH –(M)
0
100
200
300
400
500
1000
29
32
33·0
32·8
32·2
34·8
34·6
35·0
>35
S-‰
E
87°
88°
89°
90°E

FIG. 2E.

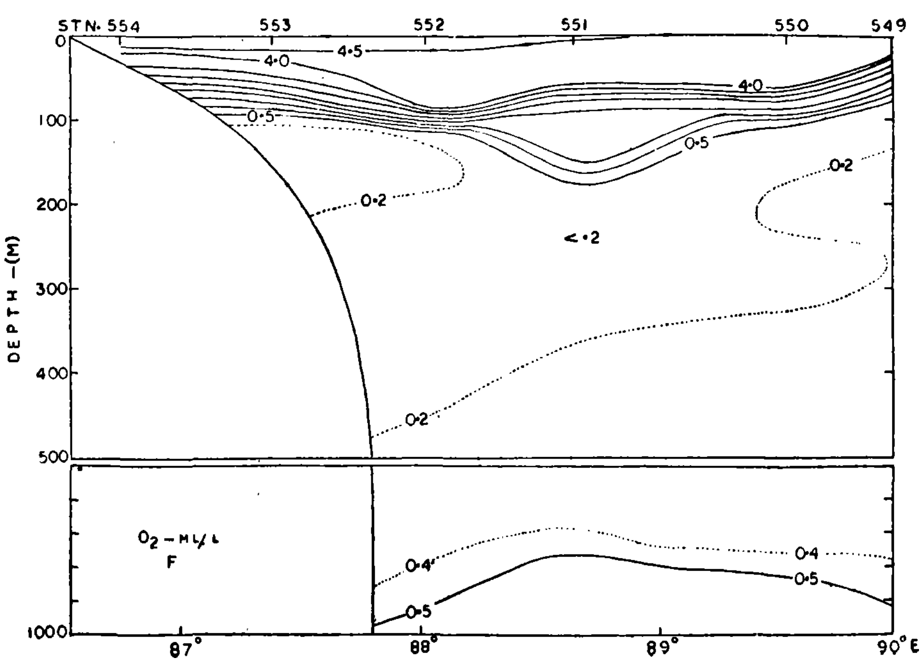
STN· 554
553
552
551
550
549
DEPTH –(M)
0
100
200
300
400
500
1000
4·0
4·5
0·5
0·2
<·2
0·4
O2 – ML/L
F
87°
88°
89°
90°E

FIG. 2F.

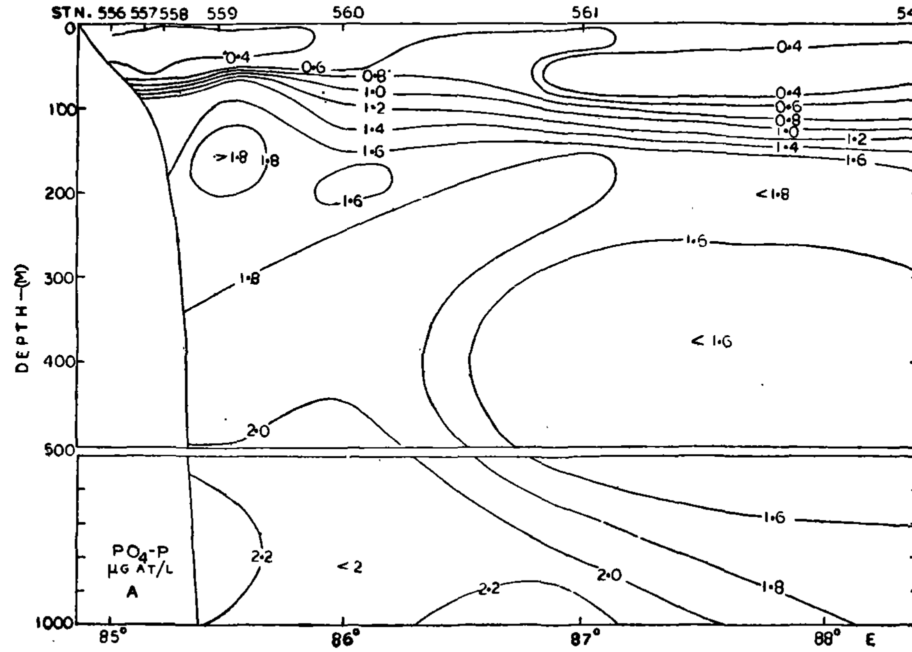

FIG. 3A.

FIG. 3 (A-E). Vertical profiles of properties along the section off Gopalpur.

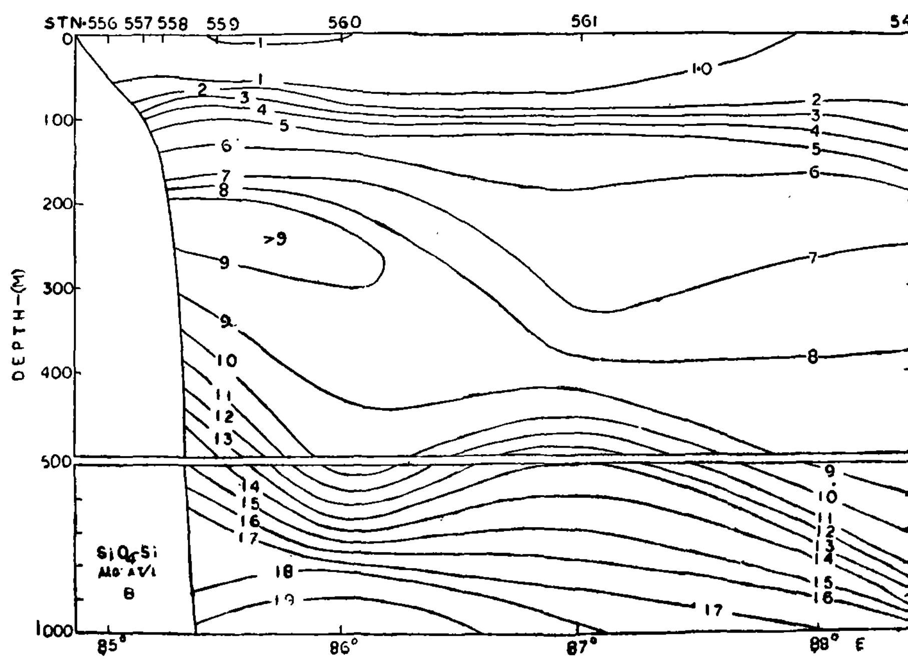

FIG. 3B.

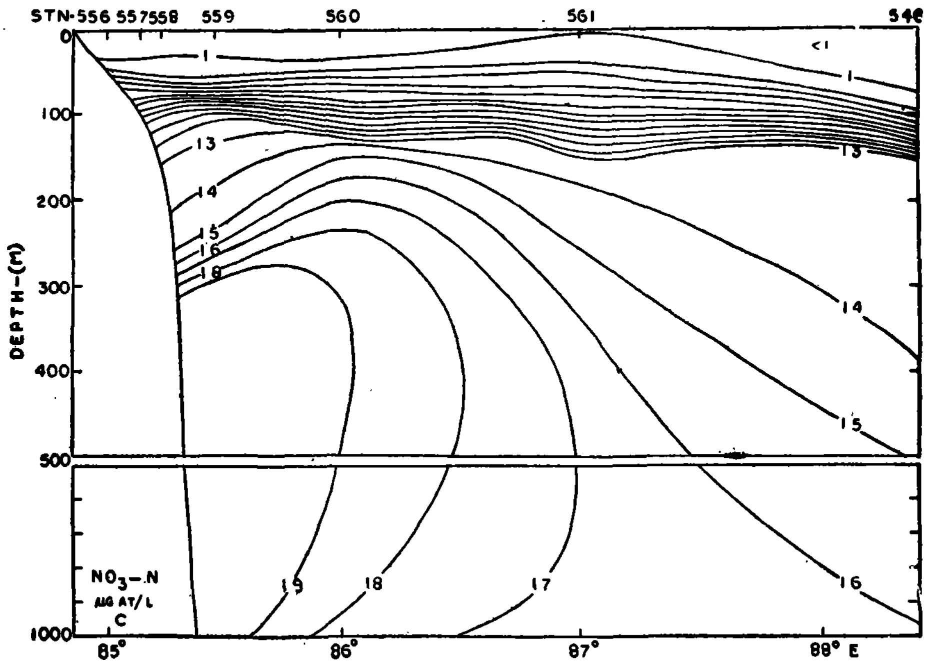
STN-556 557 558 559 560 561 546
DEPTH-(M)
NO3-N
μG AT/L
C
85° 86° 87° 88° E

Fig. 3C.

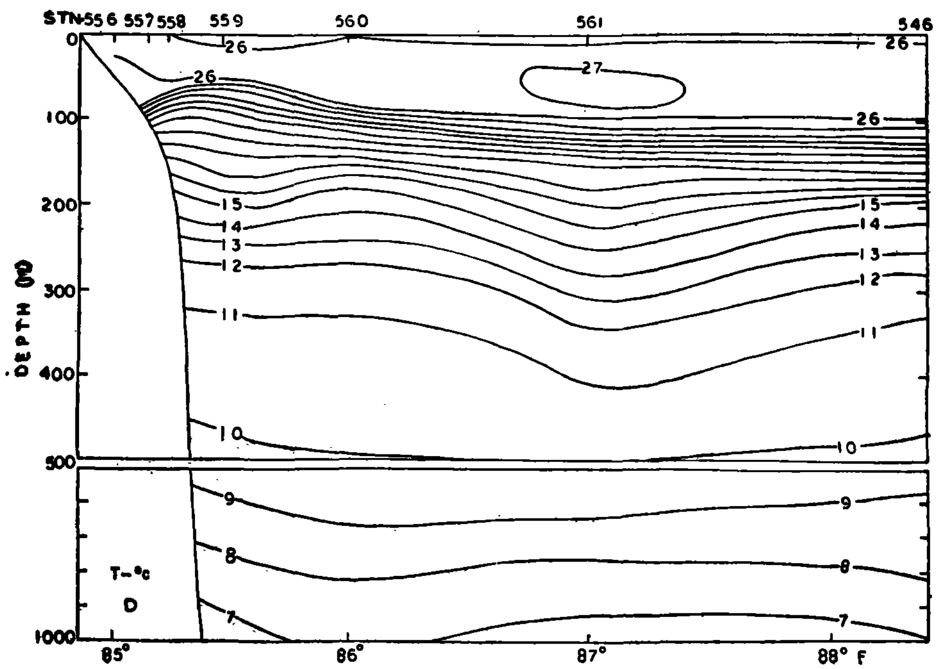
STN-556 557 558 559 560 561 546
DEPTH (M)
T-°C
D
85° 86° 87° 88° F

Fig. 3D.

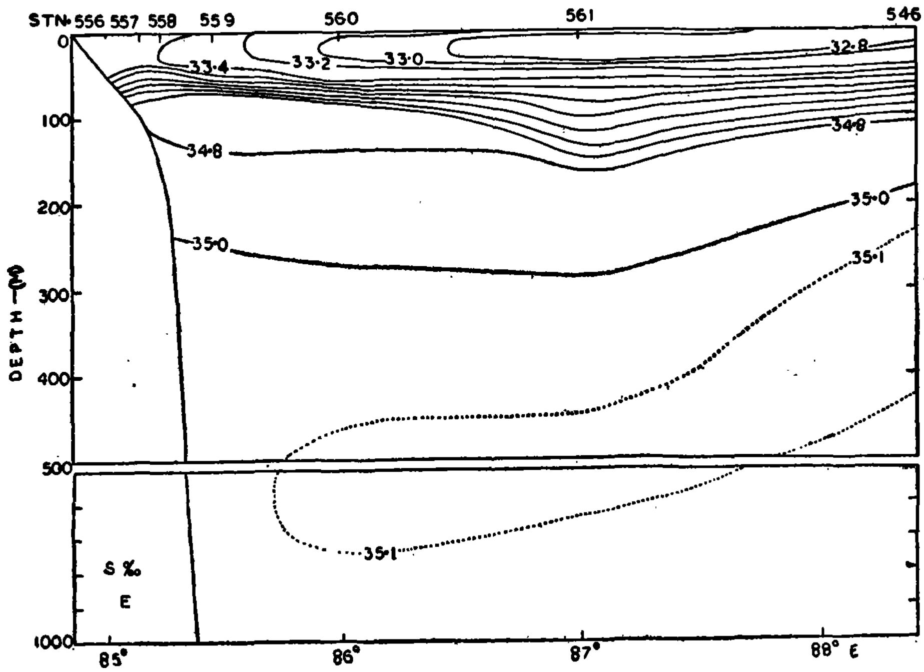

FIG. 3E .

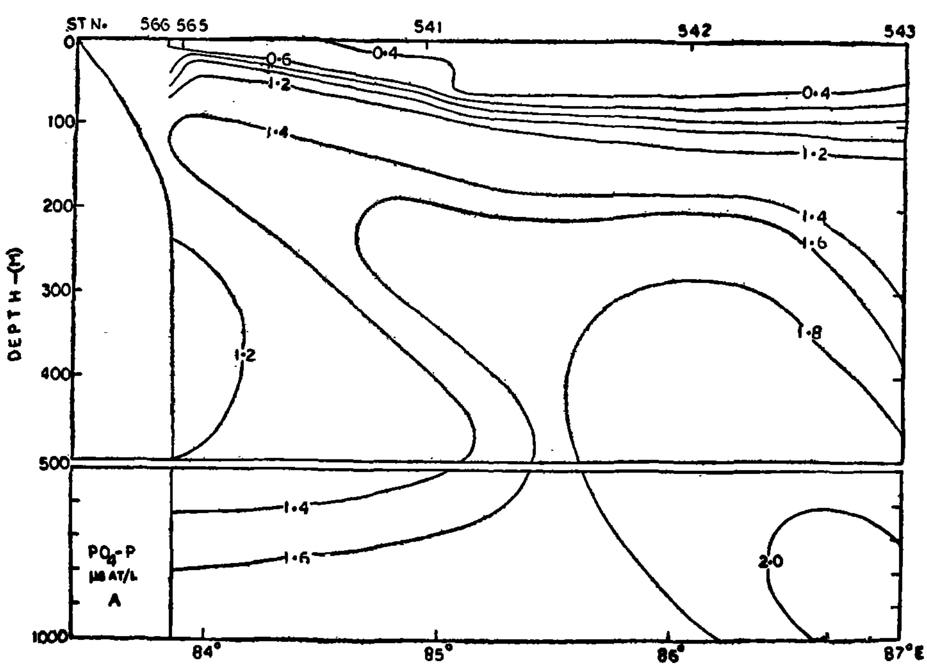

FIG. 4A.

FIG. 4 (A-F). Vertical profiles of properties along the section off Visakhapatnam.

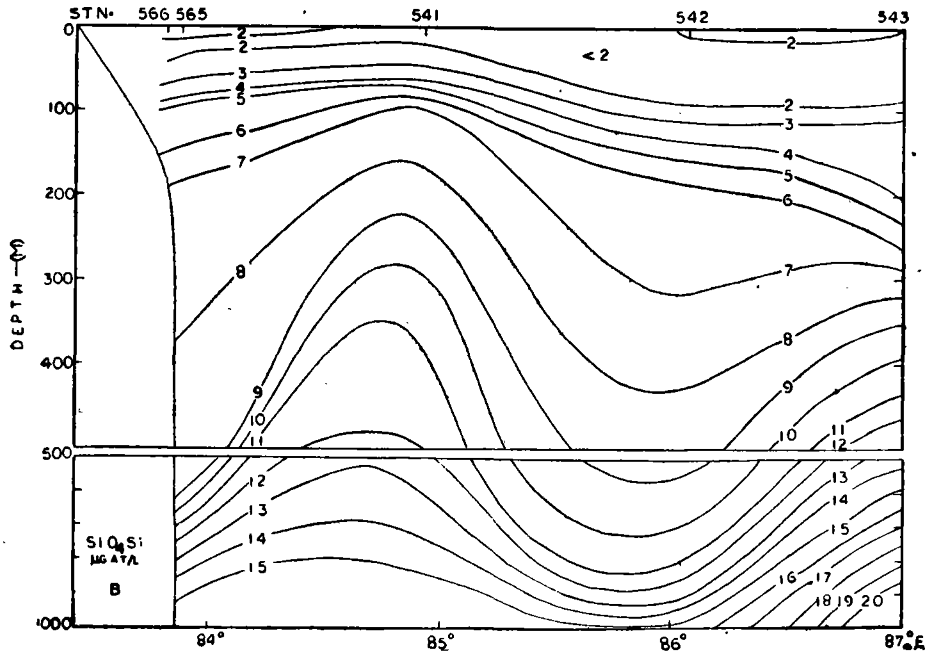
STN. 566 565 541 542 543
DEPTH —(M)
0
100
200
300
400
500
1000
<2
SIO4-Si
μG AT/L
B
84°
85°
86°
87°E

FIG. 4B.

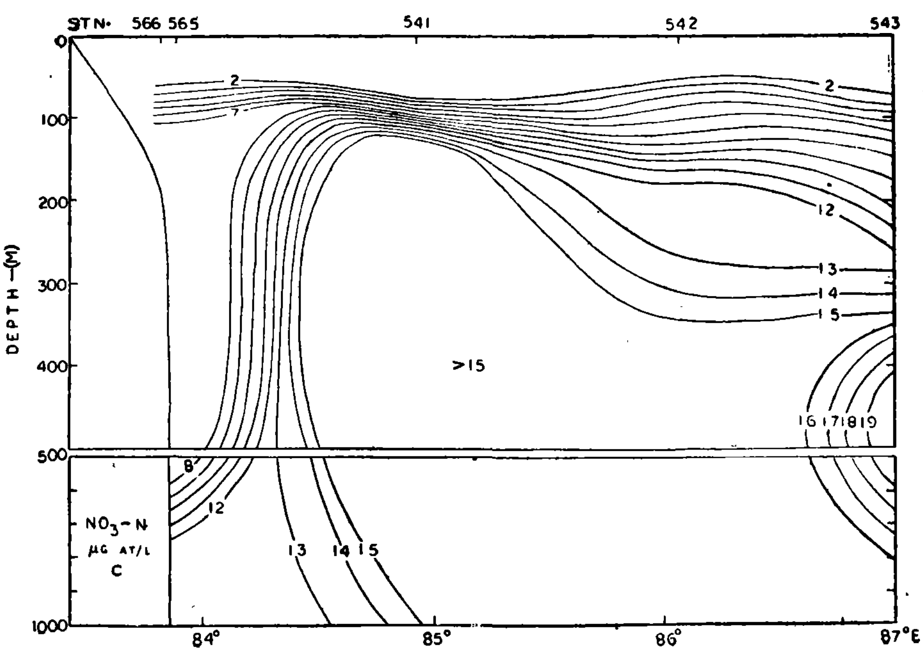
STN. 566 565 541 542 543
DEPTH —(M)
0
100
200
300
400
500
1000
>15
NO3-N
μG AT/L
C
84°
85°
86°
87°E

FIG. 4C.

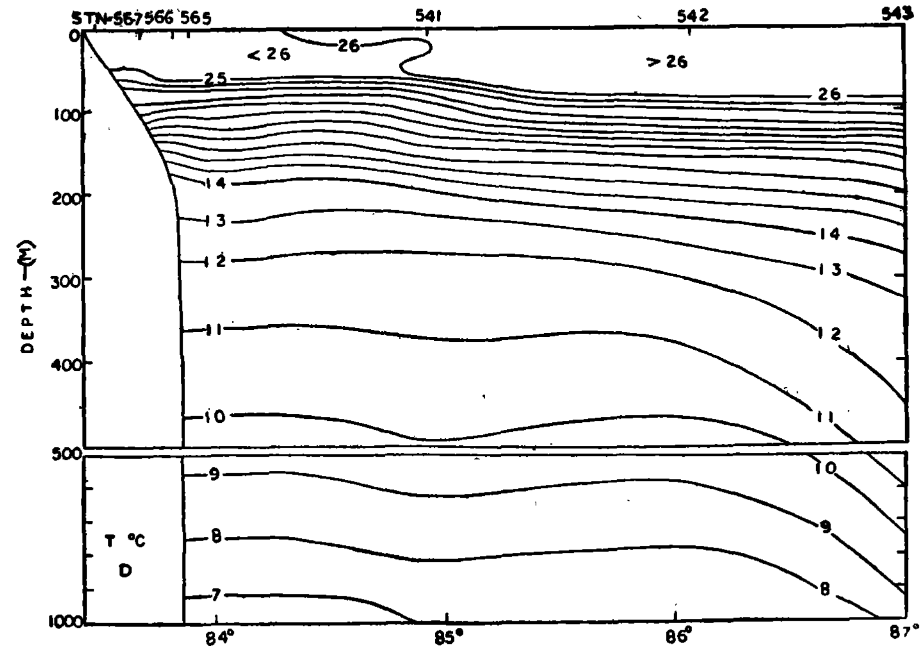
STN-567 566 565
541
542
543
< 26
26
> 26
25
26
14
13
12
14
13
11
12
10
11
9
10
9
8
8
7
8
T °C
D
DEPTH—(M)
0
100
200
300
400
500
1000
84°
85°
86°
87°E

FIG. 4D.

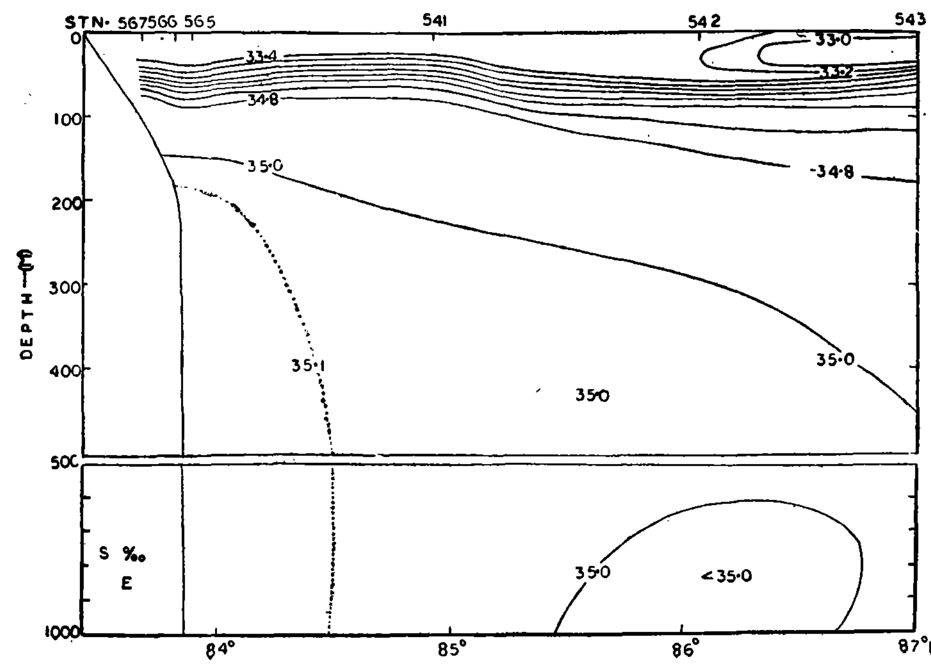
STN- 567566 565
541
542
543
33·0
33·4
33·2
34·8
35·0
-34·8
35·1
35·0
35·0
35·0
<35·0
S ‰
E
DEPTH—(M)
0
100
200
300
400
500
1000
84°
85°
86°
87°E

FIG. 4E

southern sections. However, it may be noted that the subsurface waters do not reach the surface over the shelf excepting in the region off False point. The general ascent of the subsurface waters extends up to only 20 m in the southern sections. Below 200 m the distribution is more uniform, but the upward trend of the isolines is noticeable down to 500 m also and this feature is more pronounced in the south, off Visakhapatnam. Depth of phosphate maximum is found to be varying between 600 and 800 m.

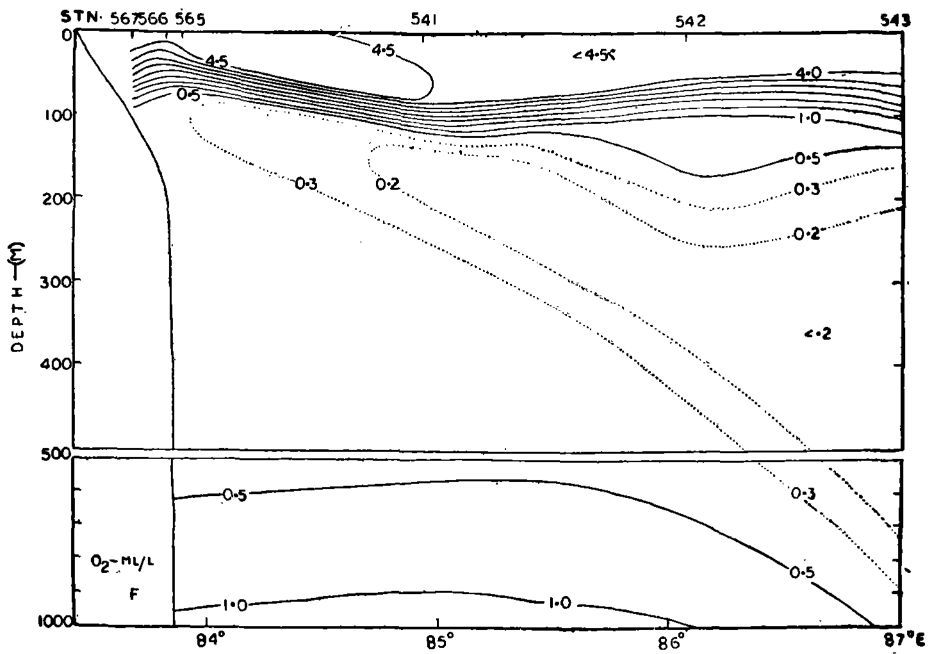

Fig. 4F.

Silicate distribution (Figs. 2B, 3B and 4B) corresponds well with that of phosphate. Surface concentrations range from 0.1 to 4 μg at/l. Higher values are found to occur in the southern section and lowest in the mid section. Within the thermocline the concentrations register a rapid increase extending down to 200 m; at deeper levels the values increase continuously with depth reaching a maximum of 21 μg at/l in the south. Similar to phosphates, silicate isolines also show a strong upslope towards the coast.

Nitrates (Figs. 2C, 3C and 4C) also follow more or less the same pattern of distribution as the other nutrients, excepting that the subsurface gradients are stronger and extending to deeper levels. Surface nitrates are low over the entire region varying between 0.1 to 2 μg at/l. An increase in the concentration towards south is noticeable. The variations towards east appear to be non-uniform with alternate bands of highs and lows with minimum concentrations around 90 E. The nitrate discontinuity layer is located within the thermocline in both the north and south sections, but in the mid section it commences a little above the thermocline (50 m). Below 150 m the variations with depth are rather more uniform. The layer of maximum nitrate content appears to be varying between depths 300 and 800 m and in general it may be said that the nitrate maximum is at a higher level than that of phosphate over major portion of the region. From the configuration of the isolines it is apparent that significant vertical motion of the waters occur at subsurface levels.

HYDROGRAPHICAL FEATURES

Temperature profiles, (Figs. 2D, 3D and 4D) show an uniform feature along the western end of the whole region, characterised by the presence of a layer (15 m thick) of cold surface water extending to a maximum distance of 75 miles off the coast. The stretch of the cold layer decreases towards south with a simultaneous rise in temperature. In the mid section (off Gopalpur) the cold surface layer is intercepted by a significant band of warm water around 20 miles off the coast. A close examination of the thermocline layer reveals its shoaling nature towards west. The disposition of the isolines below 200 m also indicate the existence of vertical movements in deeper waters.

Salinity profiles (Figs. 2E, 3E and 4E) show that the cold surface waters near the coast off False point and Gopalpur are of low salinities whereas in the souths off Visakhapatnam are of higher salinity. In the case of former the influence of river flow is still felt. The westward upslope of the isohalines at subsurface level, is indicated with a lesser degree over the entire region. In the northern section at its eastern end (around 90°E) the ridging up of the isohalines of the upper 100 m point to an apparent divergence region. This feature is also reflected in the nutrient and temperature profiles, but to a lesser extent. Along the entire region around 90° E the salinities are low and these low salinity values appear to be associated with the prevailing gyral circulation.

Oxygen distribution is presented only for the two sections, off False point and off Visakhapatnam (Figs. 2F and 4F). The cold and low saline waters are associated with higher Oxygen content. A notable feature is that the Oxygen discontinuity layer commences at a higher level than the thermocline. However the Oxygen minimum layer (<0.5 ml/l) starts in the middle of the thermocline extending down to 800 m coinciding more or less with the depth of phosphate maximum. The sloping up of the Oxygen minimum layer towards west is well seen. This feature appears to be more pronounced in the south (off Visakhapatnam). Significant increase in the Oxygen levels could be noted only below 800 or 900 m. In general the Oxygen distribution closely follows those of salinity and phosphates.

DISCUSSION

The distributions of the hydrographical factors in the Bay of Bengal, are primarily influenced by the immense land drainage and complex current patterns associated with the changing monsoons. The highly estuarine charactei of the Bay, narrows the biological influence on the nutrients. The suspended organic and inorganic particulate matters are believed to be more responsible for the observed irregular variance of nutrient distributions through the processes of adsorption, sedimentation, regeneration by chemical and bacterial agencies and finally diffusion by vertical and horizontal circulations. A cursory examination of the recent data collected on I.N.S. Kistna reveal that the effects of land drainage are evident over a wider area in the Bay, during major part of the year following the circulation patterns. The property distributions show considerable variations within narrow regional and time limits. Thus the conditions in the Bay necessitates the use of extensive small regional and temporal observations to obtain an integrated picture of the propeity distributions. The present report gives a descriptive account of nutrients in relation to other hydrographical features in the North-Western Bay in the month of January.

During the period of observations the general current pattern can be differentiated into (1) anticyclonic circulation at the head of the Bay extending to about 15°N and (2) the west drift in the open parts of the Bay.

A significant observation in the region under study is the beginning of coastal upwelling which is evident from all the sections, as one of the factors governing the distribution of nutrients. It is clear from the trend of the profiles (Figs. 2-4) that this feature appears to be relatively more advanced in the north and least in the mid region (off Gopalpur). LaFond (1954) while discussing upwelling off the East Coast of India, observed a marked increase in temperature and salinity at the end of January and throughout February. This is attributed largely to the reversal of the current direction during this season of the year, which brings in warm high saline water from the equatorial region. At the same time the south south-west winds cause an offshore drift of the surface water. As colder subsurface water rises to take its place, upwelling staits. Further investigations by LaFond (1954) indicate that the upwelling develops fully, off Visakhapatnam in March, extending up to April. The offshore transport of water fits with the prevailing wind direction (SW) and the northerly current along the coast. Present investigations confined to the 3rd week of January when the conditions (LaFond 1954) are favourable for the commencement of the observed upwelling. The observations show that this feature extends only up to the mid-shelf limiting the ascent up to about 20 m below the surface in the southern sections, whereas in the northern section (off False point) it extends almost to the surface towards the inner shelf. It is obvious that the resultant operative force responsible for the upwelling is weak and of variable strength over the entire region. As mentioned earlier the characteristic feature of the prevailing current system is the anticyclonic gyre at the head of the Bay extending down to about 15°N. The centre of the gyre is in proximity to the northern section (off False point). It is felt that this circulation may be playing a significant role in the upwelling processes towards the coast. The convergence at the centie of the anticyclonic gyre may be drawing the surface waters around, and therefore it is highly probable that the magnitude of transport of the surface waters towards east could be increased tending the upwelling to be more conspicuous near the coast. This feature is well reflected in the northern section off False point. Decreasing intensity of the process towards south could be due to the increasing distances from the centre of the gyre. Local changes in the prevailing wind may also equally affect the intensities of upwelling.

The general surface nutrient levels in the upper 60 m (Figs. 2-4) reveal that the trends of variation in the east-west and north-south directions show some regional differences. These variations run parallel with those of temperature and salinity. In the north (off False point) near the coast the posphate values are high (0.65 μg at/l) and progressively decrease towards off-shore up to 88°E and beyond this a significant rise to maximum (1.13 μg at/l) is noticeable. The higher values are associated with cold and low saline waters while the lower values with warm and high saline waters. The existence of cold and low saline surface waters near the coast may be due to the effect of discharge from the river Mahanadi. The progressive increase in salinity towards south supports this view. These waters normally extend over a thin surface layer (20 m thick) spreading to about 120 km forming a boundary with the warm high saline and low phosphate waters; these in turn form another boundary around Long. 89°30′E with another cold, low saline and high phosphate layer. At this end the disposition of the profiles indicate an uplift. The cold and low saline surface waters appears to be caused by a part of the surface gyres weeping from north to south-west direction, bringing in cold and dilute waters from the head of the bay. The conspicuous upslope of the same may be coinciding with a local divergence zone probably extending further east. This particular ridging feature is not found in the southern sections. But the presence of cold and low saline waters is evident, suggesting the southward extension of the gyre. The gradual rise in the temperature and salinity with a fall in phosphate level in the east indicate the weakening of the gyral circulation towards south; the sharp fall in the phosphate content perhaps suggests the influence of the westerly drift, bringing in warm high saline and phosphate poor waters from east and south-east. The phosphate concentrations over the shelf show maximum values off Visakhapatnam and minimum off Gopalpur. The intermediate concentrations off False point may be reflecting the relatively weaker upwelling trend as could be inferred from the vertical profiles. The maximum surface values in the shelf off Visakhapatnam are believed to be very local caused by regeneration processes. Ganapati and Sarma (1958) observed the phosphate peak in the surface waters off Visakhapatnam during the month of January. They attributed this to the nutrient rich Antarctic bottom water, entering the bay to compensate the loss of water due to evaporation. However, in the present case the authors consider that the high level of phosphates are due to local regeneration processes, as the present observations indicate only the beginning of upwelling which is not affecting the surface waters.

The silicate and nitrate concentrations in the upper mixed layer are low. Nevertheless they also exhibit some variations; phosphates and silicates agree fairly well while the nitrates show certain amount of inverse relation with the other nutrients regionally. Since the concentrations and the differences are of lower order no special emphasis can be made on the factors governing the silicate and nitrate distribution excepting that the minor variations may be more of regenerative character.

At deeper levels (below 60 m) the concentration gradients of the nutrients coincide with the thermocline. The characteristic slight upslope of the gradient layers could be noticed in the east-west direction in all the profiles. The concentrations of silicates and especially nitrates show strong gradients with depth even extending down to 500-600 m. This property is obviously related to the differential rates of regeneration and some physical processes determining the accumulation. The maximum variations in the concentrations coincide with very low oxygen content. Highest accumulation of phosphates is between 600 and 800 m and the nitrate between 300 and 800 m. Silicates show a continuous increase with depth.

It is apparent from the vertical profiles that the vertical motion of the waters extend to deeper levels also. Nutrients conform well with the inference while the temperature shows wavy patterns suggesting the effect of internal waves promoting vertical eddies. It is believed that the characteristic upslope of the strong gradients of the subsurface nutrients especially that of silicates and nitrates are believed to be due to the differential rates of regeneration and disposal by eddy diffusion. Another feature of importance to be mentioned in this context is the presence of salinity maximum between 300 and 500 m. Rochford (1964) discussing the salinity maxima in the upper 1000 m of the North Indian Ocean indicated the incursion of Persian Gulf and Red Sea waters (300 to 450 m) into the Bay. The incursion of new water mass may favour the formation of internal waves at the boundary enhancing eddy diffusion, and perhaps this may explain the observed peculiar patterns of the vertical distribution of the nutrients below 200 m.

ACKNOWLEDGEMENTS

We acknowledge our grateful thanks to Dr. N. K. Panikkar, Director, National Institute of Oceanography (C.S.I.R.), for his inspiring guidance, to Dr. S. Z. Qasim, Mr. R. Jayaraman and Dr. V. V. R. Varadachari, for helpful criticism and suggestions.

REFERENCES

Bhavanarayana, P.V., and LaFond, E.C. (1957). On the replenishment of some plant nutrients during the upwelling period on the East Coast of India. *Indian J. Fish.*, **4**, 75-79.

Ganapati, P.N., LaFond, E.C., and Bhavanarayana, P.V. (1956). On the vertical distribution of chemical constituents in the shelf waters off Waltair. *Proc. Indian Acad. Sci.*, **33**, 68-72.

Ganapati, P.N., and Venkata Rama Sarma, D. (1958). Hydrography in relation to the production of plankton off Waltair Coast. *Andhra Univ. Mem. Oceanogr.*, **2**, 168-192.

Gangadhara Reddy, C.V., and Sankaranarayanan, V.N. (1966). Distribution of nutrients in the shelf-waters of the Arabian Sea along the West Coast of India. (*Mss.*)

Harvey, H.W. (1955). The Chemistry and Fertility of Sea waters. Cambridge Univ. Press.

Jayaraman, R. (1951). Observations on the Chemistry of the waters of the Bay of Bengal off Madras City during 1948-49. *Proc. Indian Acad. Sci.*, **33**, 92-99.

LaFond, E.C. (1954). On upwelling and sinking off the East Coast of India. *Andhra Univ. Mem. Oceanogr.*, **1**, 117-121.

——— (1957). Oceanographic studies in the Bay of Bengal. *Proc. Indian Acad. Sci.*, **46**, 1-46.

Rochford, D. (1964). Salinity maxima in the upper 1000 metres of the North Indian Ocean. *Aust. J. mar. Freshwat. Res.*, **15**, 1-24.

Udayavarma Thirupad, and Gangadhara Reddy, C.V. (1959). Seasonal variations of the hydrographical factors of Madras Coastal Waters. *Indian J. Fish.*, **2**, 298-304.

Reprinted from *Bull. natn. Inst. Sci. India*, no. 38, 1968, p. 206-220

DISTRIBUTION OF NUTRIENTS IN THE SHELF WATERS OF THE ARABIAN SEA ALONG THE WEST COAST OF INDIA*

by C. V. GANGADHARA REDDY *and* V. N. SANKARANARAYANAN

Biological Oceanography Division, National Institute of Oceanography, Ernakulam, S. India

The paper presents a descriptive account of the distribution of phosphates, silicates and nitrates in the shelf waters of Arabian Sea along the West Coast of India including a brief mention about the hydrographical features and their relationship with the former during the period September to December 1963. The results indicate marked variations through different periods, in nutrients and other hydrographical features. Two distinct environmental conditions are apparent in the shelf waters from the nutrients point of view, characterised by nutrient deficient surface layers in the post-monsoon period and nutrient rich surface layers in the south-west monsoon period. These conditions are well reflected in the corresponding variations of the hydrographical features. It is also observed that the concentrations of the nutrients show a general decreasing trend from south to north. The distribution of the elements are more influenced by a phenomenon similar to upwelling, occurring during the closing phase of the south-west monsoon. The regional differences in the concentrations of the nutrients along the coast during this period, are attributed to the varying intensities of this upwelling like phenomenon. Post-monsoon period is characterised by more vertical stability of the waters and uniform distribution of the properties. A significant feature of the nutrient components of the near shore environment (less than 15 miles) is their constancy through different periods; the value are relatively high throughout. Probable factors controlling the vertical and horizontal distribution of nutrients are indicated.

INTRODUCTION

The significance of the nutrients in the sea, especially of phosphates, silicates and nitrates, is well recognised, in understanding the diversities exhibited in the distribution of marine populations in space and time and also in characterizing the water masses and their movements in conjunction with other physical oceanographic parameters. West Coast of India supports a rich fishery of varied intensities in different seasons and in view of this fact it is felt that the study of the nutrient levels in different periods of the year, apart from the regular hydrographic conditions (temperature, salinity and oxygen) may also help in understanding the seasonal changes in fisheries. The present work was undertaken as part of the studies on the nutrient distribution in the Indian Ocean under the Indian Programme of the International Indian Ocean Expedition.

The present paper deals with the results based mainly on the nutrient data of the shelf waters along the West Coast of India within which the major fisheries

*This paper was presented at the Second International Oceanographic Congress, Moscow on 8th June, 1966.

of sardine and mackerel are known to occur. The relationship of the nutrients to other hydrographical features has also been briefly discussed. Among the previous investigations on nutrients, especially in the inshore waters, mention may be made of studies by George (1953), Rao (1957), Subramanian (1959), Seshappa and Jayaraman (1956), Jayaraman and Seshappa (1957). The present work covers three regions along the West Coast from Quilon to Ratnagiri giving the variations in monsoon and post monsoon seasons in 1963.

Material and Methods

Collections were obtained during the regular oceanographic cruises of R. V. VARUNA from three selected regions: 1. Off Quilon, 2. Off Mangalore, 3. Off Ratnagiri across the continental shelf falling in line with oceanographic programme of the Central Marine Fisheries Research Institute. Collections were mostly made up to the edge of the continental shelf except on some occasions when a few samples were collected beyond the shelf. Sections covered and station locations and periods are given in Fig. 1. Only parts of the sections comprising the station locations wherein water sampled for nutrients are represented in the map. The water samples were preserved by freezing at —10°C for subsequent analysis at the shore laboratory at Cochin. In the laboratory the samples were brought to the room temperature quickly with the aid of a thermostatic water bath, before analysis.

Inorganic phosphates:—Phosphates were estimated by the method of Deniges as adopted by Wooster and Rakestraw (1951). Absorbance was measured at 700 mμ using SP 500 Unicam Spectrophotometer. Phosphate values are not corrected for salt error.

Silicates:—The method of Wandenbulcke (1923) as adopted by Robinson and Thompson (1948) was used. Absorbance was measured at 404 mμ as suggested by Barnes (1960). Comparisons were made with potassium chromate standards buffered with borax.

Nitrates:—Nitrates were estimated by the technique of Mullin and Riley (1955) as described by Barnes (1960). The absorbance of the resulting azo-dye was measured at 524 mμ.

Results

The sections covered in a particular region during the two different periods (monsoon and post-monsoon) are designated as 'a' and 'b'.

Sections Off Quilon:

Section 'a':—(Between Lat. 8°59′ N, Long. 75°59′ E and Lat. 9°11′ N, Long. 76°22′ E) covered in the month of September 1963.

During this period, the phosphate content of the upper 10 m in the inshore region (less than 20 miles from the coast) is high ranging from 0.54 to 1.4 μg. at/L

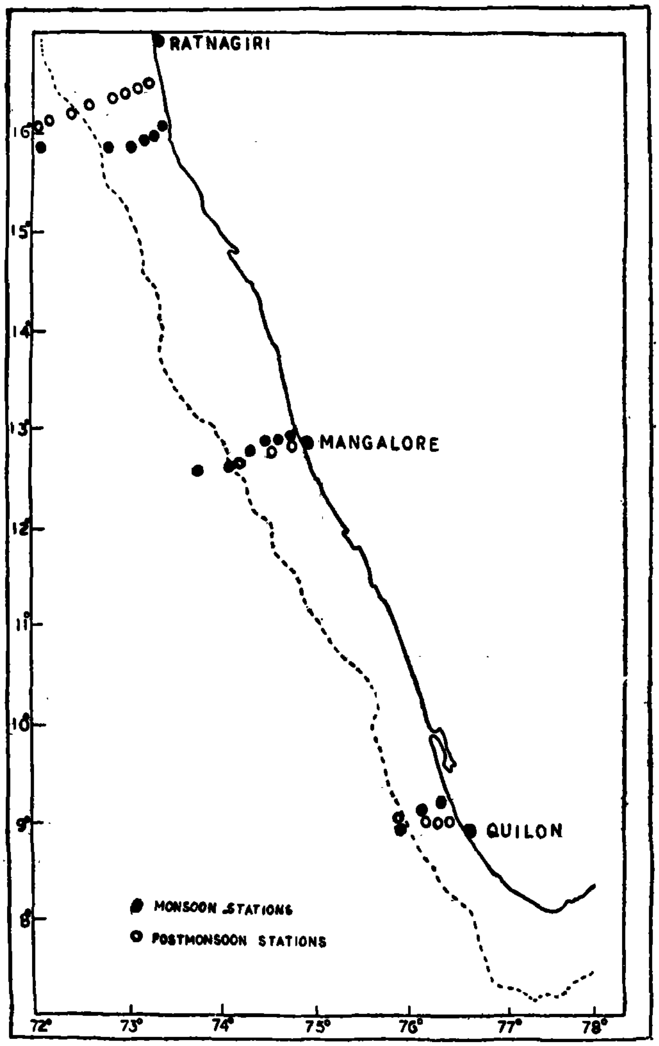

FIG. 1. Map showing the locations wherein collections were made.

and towards the offshore region, it becomes lower ranging from 0.6 to 1.2 μg. at/L (Fig. 2a). In general, throughout the section it is interesting to note that the phosphate concentration dropped from surface to 10 m or 20 m level and the values show a gradual increase up to 50 m, followed by a sharp rise towards the bottom layers; the values reach as high as 2.7 μg. at/L. It could be seen from the figure that the isopleths form into a tongue like projection towards the coast suggesting the incursion of offshore waters towards the coast.

Silicate content especially in the inshore stations (Nos. 1914 and 1916; Fig. 2a) shows erratic distribution, but a general trend of increase is evident towards the bottom layers. Farther off, at station No. 1918 near the edge of the continental shelf, the silicate distribution generally parallels with that of phosphate. From the trend of isolines there is also an indication of the influx of offshore waters towards the coast. The values of the upper 10 m varied between 1.7 and 3.1 μg. at/L. Bottom layers in the inshore region contain generally more than 5 μg. at/L and reach as high as 14 μg. at/L towards offshore region.

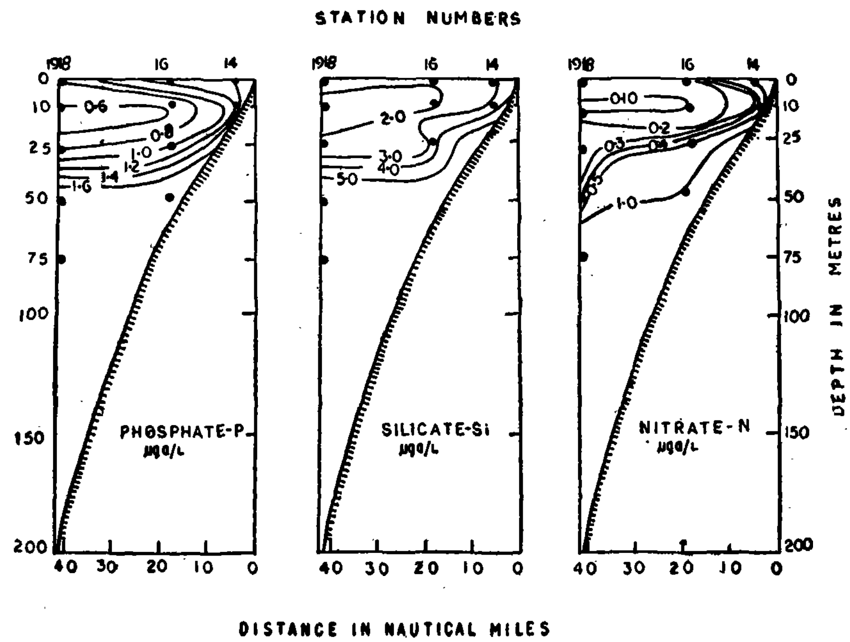

FIG. 2(a) Vertical distribution of phosphates, silicates and nitrates in the section off Quilon in September.

Nitrate distribution is similar to that of phosphate in the upper 10 m. The values tend to decrease towards the offshore region, ranging between 0.1 and 2.8 μg. at/L; values greater than 1 μg. at/L are usually found below 20 m and the highest of 4.4 μg. at/L is recorded near the edge of continental shelf at about 100 m. Below this depth the values again tend to decrease to about 1 μg. at/L.

Section 'b':—(Along Lat. 9°00′ N between Long. 75°58′ E and 76°28′ E) covered in December 1963. Phosphates in the surface waters remained high (1 μg. at/L) in the near shore region and towards the middle of the section they decreased to about 0.4 μg. at/L and thereafter the values tend to increase up to the edge of the shelf reaching 1.8 μg. at/L. As compared to the monsoon period the values in the offshore region show an increase. The subsurface isolines (Fig. 2b) show a slight upward tilt from the offshore region towards the mid section and further there is no indication of the upslope of the contours towards the coast.

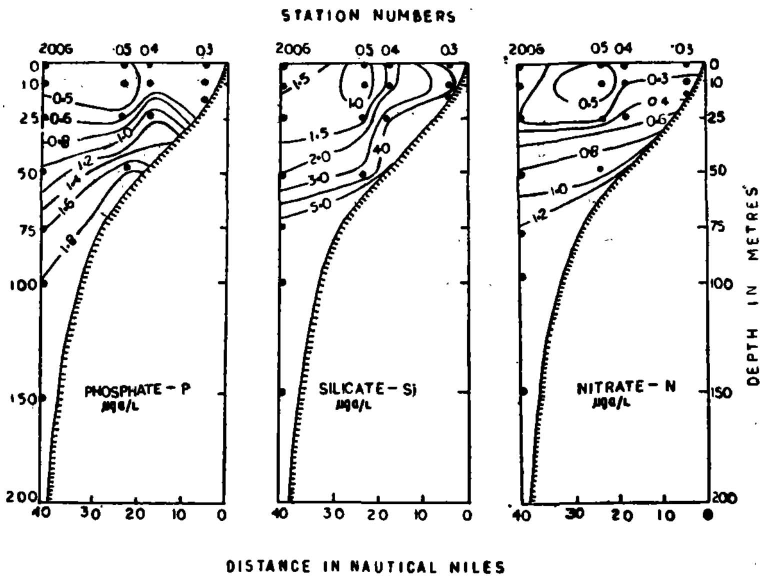

FIG. 2(b) Vertical distribution of phosphates, silicates and nitrates in the section off Quilon in November.

Silicates are generally poor in December relative to the monsoon period except in the nearshore station No. 2003 wherein a slight increase is noticeable, Surface values varied from 0.73 to 4.8 µg. at/L. The values decreased to minimum in the mid region from the coast and thereafter gradually increased towards the shelfedge. Silicate accumulation is significant only below 100 m, the order being 8 to 12 µg. at/L.

The trend of nitrate distribution is similar to that of phosphate. Except the first station near the coast, in general, nitrates show a slight increase in the rest of the section. The values ranged from 0.2 to 3.2 µg. at/L.

Section Off Mangalore:

Section 'a':—(Between Lat. 12°52′ N, Long. 74°54′ E and Lat. 12°33′ N Long. 73°48′ E) covered during October 1963. October represents the month of transition between south-west monsoon is still active, but weak, a gradual reversal of the current system takes place.

Surface phosphates are high (0.8 to 1.5 µg. at/L) in the near shore stations within 15 miles and decrease further offshore to below 0.4 µg. at/L. The isopleths at the depths between 25 to 50 m (0.5 to 1.5 µg. at/L; Fig. 3 a) in the offshore region show a downward trend towards the mid section and again a sharp rise towards the coast reaching the surface. Vertical variation up to about 25 m is not uniform in most of the stations, but there is a sharp increase towards bottom layers below this depth. Values greater than 2 µg. at /L are found below 100 m, particularly in the offshore region, Silicates also show a trend of distribution similar to phosphates. Surface silicates in the nearshore stations range between 4 and 10 μg. at/L, while in the off-

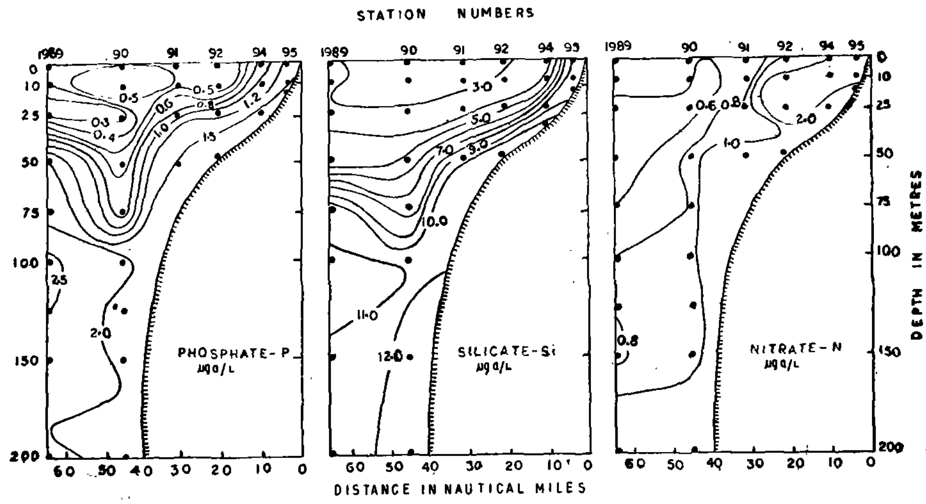

FIG. 3(a) Vertical distribution of phosphates, silicates and nitrates in the section off Mangalore in October.

shore region the values are in general less than 4 μg. at/L. Concentrations as high as 12 μg. at/L are found below 100 m.

The pattern of nitrate distribution also shows a strong upslope of the isoliness towards the surface near the coast. The values are relatively high in the near shore area, ranging from 1 to 4.5 μg. at/L. The concentration is low in the offshore region ranging between 0.4 and 1 μg. at/L. Unlike phosphates and silicates, nitrates are generally low down to 150 m. Nitrate accumulation is apparant only below this level.

Section 'b':—(Between Lat. 12°49′ N, Long. 74°45′ E and Lat. 12°00′ N, Long. 72°30′ E) covered during the month of December.

In December the phosphate content was very low as compared to October all along the section; the values range from 0.09 to 0.4 μg. at/L (Fig. 3b). This depletion extends up to 100 m and only a slight increase is observed below this level.

Silicates show a similar trend as those of phosphates; the values are between 3 and 5 μg. at/L, and higher concentrations (>6 μg. at/L) are found only below 100 m.

Nitrate distribution corresponds more or less to that of phosphates and silicates. Surface values near the coast range from 0.7 to 1.8 μg. at/L and further off the coast the values drop to 0.6 μg. at/L. Higher concentrations up to 6 μg at/L are found below 10 m in the increasing order with depth.

Section off Ratnagiri:

Section 'a':—(Between Lat. 16°03′ N, Long. 73°25′ E and Lat. 15°50′ N, Long. 72°45′ E) covered during the month of September.

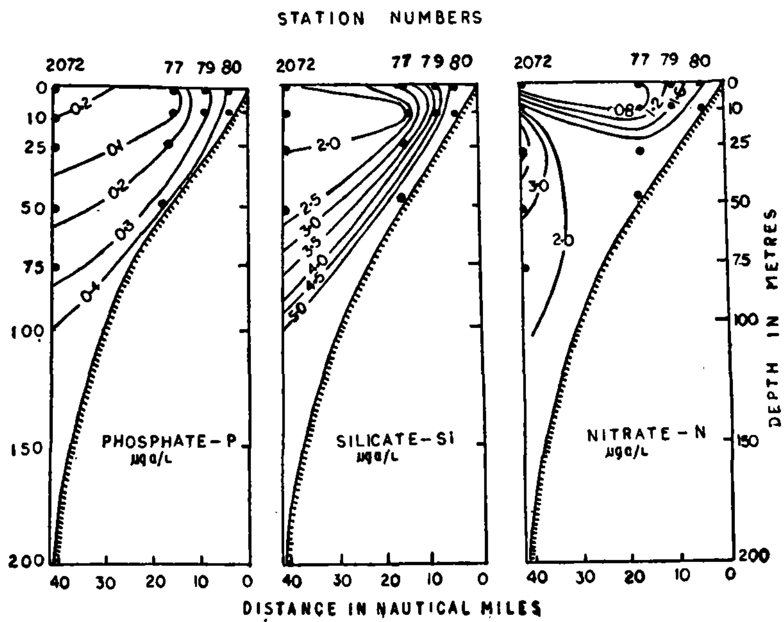

FIG. 3(b) Vertical distribution of phosphates, silicates and nitrates in the section off Mangalore in December.

Surface layers of the inshore area are found to have higher phosphate concentrations (0.8 to 1.3 μg. at/L) and lower (0.6 to 0.8 μg. at/L) towards offshore. Isopleths (Fig. 4a) between the depths 30 and 75 m in the offshore region show a

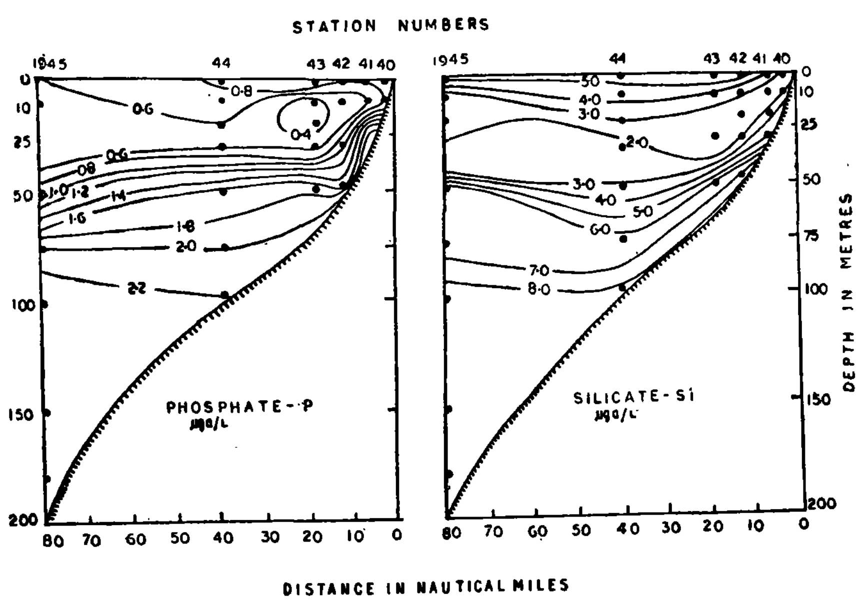

FIG. 4(a) Vertical distribution of phosphates and silicates in the section off Ratnagiri in September.

gradual upslope towards the coast, ascending to levels between 10 and 25 m. In general the concentration is observed to be in decrease from surface to 20 m along the entire section and below this depth, it increases gradually reaching maximum of 2.7 μg. at/L near the bottom.

Silicate distribution is quite similar to that of phosphate. Horizontal variation along the section shows that the surface values near the shore are between 2.8 and 9.6 μg. at/L and those of offshore between 5.6 and 6 μg. at/L. Below 40 m there is uniform increase; maximum values up to 12 μg. at/L are recorded at the bottom layers near the edge of the shelf.

Section 'b':—(Between Lat. 16°28′ N, Long. 73°16′ E and Lat. 16°01′ N, Long. 71°56′ E) covered during the month of December.

Surface phosphates are in general lower relative to the monsoon period, The values are between 0.2 and 0.6 μg. at/L. It could be seen from the Fig. 4b that

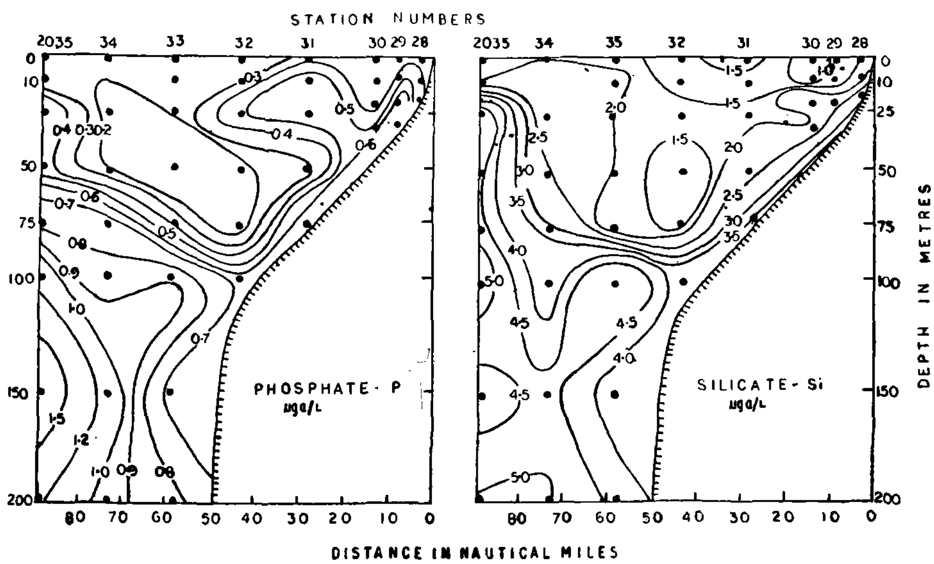

FIG. 4(b) Vertical distribution of phosphates and silicates in the section off Ratnagiri in December.

the isolines between the depths 20 and 95 m of the offshore region show a tendency of down-slope towards the middle of the section, followed by a strong deviation near the coast; the isolines of lower concentrations (0.7 to 0.9 μg. at/L) shift upwards while those of higher concentrations downward. Concentrations below 100 m are constant at deeper stations up to 200 m.

Silicate distribution in general closely follows that of phosphate. The values are relatively lower than those of monsoon period. Surface silicates range from 0.5 to 2 μg. at/L and are in the increasing order towards offshore waters. Vertical variation is not significant either in the inshore region or in the offshore one; the values in the former range from 0.5 to 3.5 μg. at/L and in the latter 2 to 5 μg. at/L, *Hydrographical conditions and their relation to nutrients*:

Data of a few stations have been selected to study the general depthwise variation of the hydrographical features (temperature, salinity and oxygen) and their relation to nutrients. This procedure is adopted for all the sections.

Quilon section:

In September the thermocline is at 20 m extending almost to the bottom in the inshore area and in the offshore region it is present at 30 m (Fig. 5). Salinity does not bear any relationship to temperature above the thermocline; below the

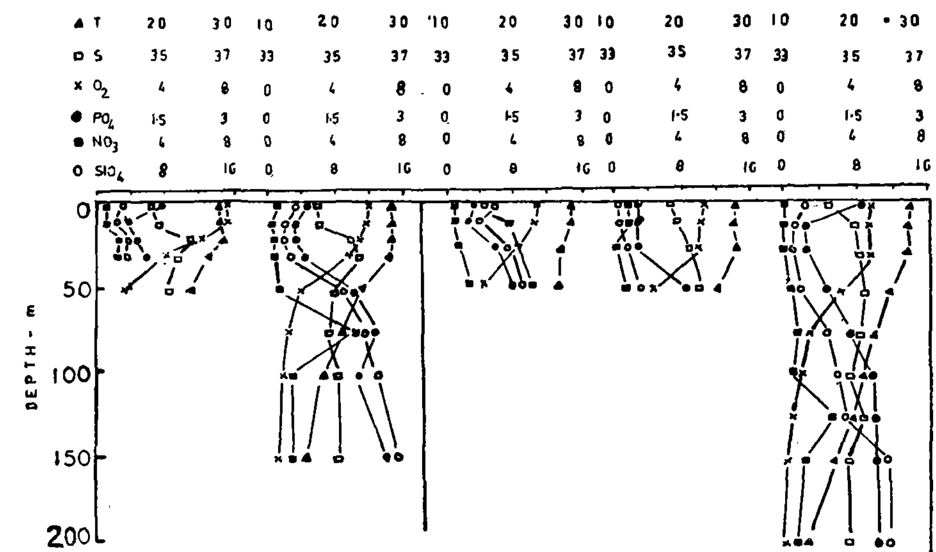

FIG. 5. Depthwise variations of the hydrographical factors and the nutrients at selected stations (Nos. 1916, 1918, 2004, 2005 and 2006) off Quilon in September, and November. Oxygen in ml/litre, nutrients in μg at/litre, salinity in °/₀₀ and temperature in °C.

thermocline in the inshore region it shows direct relationship and in the offshore region salinity remains more or less constant. The distribution patterns of phosphates, silicates and nitrates are almost identical above the thermocline, whereas, within the thermocline layer they show some deviation. In the offshore region high values of nutrients are generally associated with low oxygen and low temperatures. Oxygen minimum layer (0.5 and less) is present only near the continental shelf edge at the bottom. Rapid fall in the oxygen concentration is generally noticed just below the thermocline along the entire section. In November the thermocline is absent in the inshore region (within 20 miles) and is present at 25 m in the offshore region extending almost to the bottom and further off, near the shelf edge, it is present at 75 m. The gradient is strong in December as compared to September. Salinity exhibited a general inverse relationship with the temperature. Salinity discontinuity coincides with the thermocline. Nutrients show a good

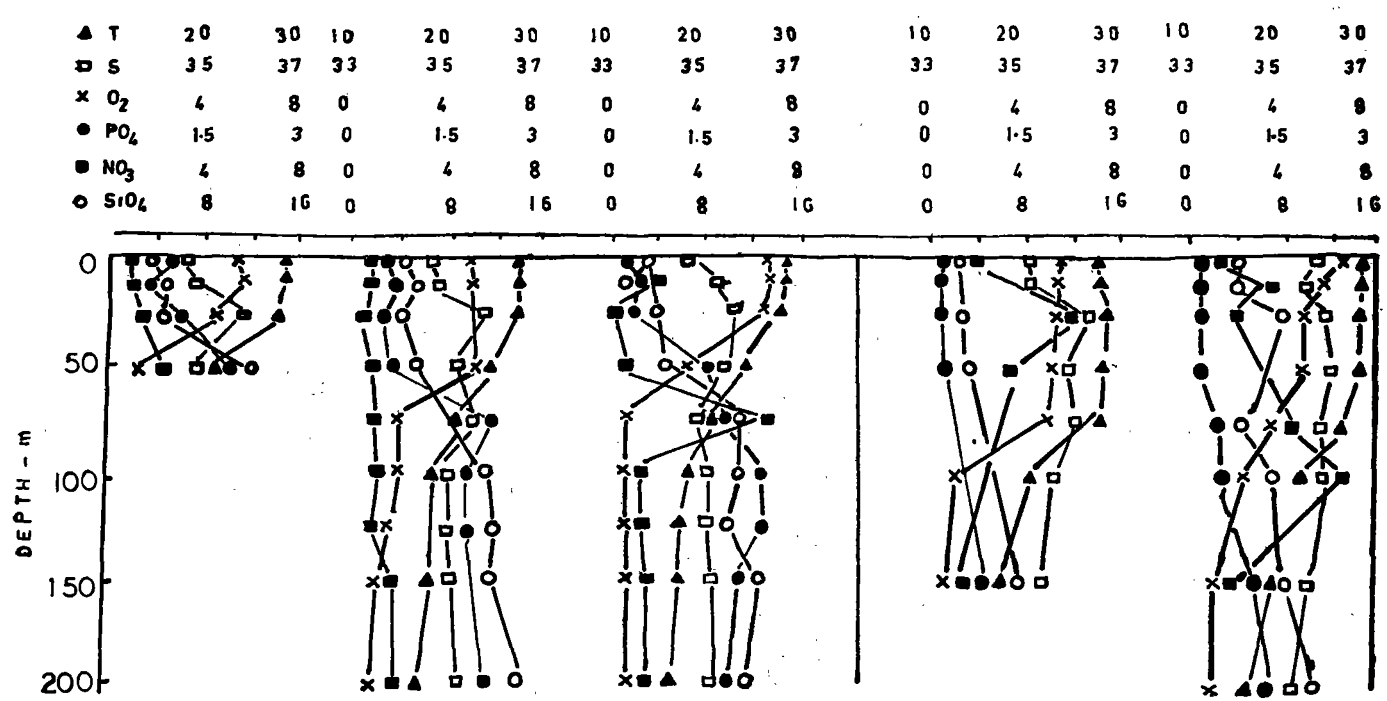

FIG. 6. Depthwise variations of the hydrographical factors and the nutrients at selected stations (Nos. 1989, 1990, 1991, 2077 and 2072) off Mangalore in October and December. Oxygen in ml/litre, nutrients in μg at/litre, salinity in °/₀₀ and temperature in °C.

correlation *inter alia* above and below the thermocline. High nutrient concentrations are associated with lower temperatures and oxygen and higher salinities. Nitrates showed comparatively little variation than phosphates and silicates. Oxygen minimum layer reaches up to the shelf edge, being present at about 160 m. It does not extend over the shelf and the oxygen shows more uniform distribution in contrast to conditions in September.

Off Mangalore:

In October the thermocline in the offshore waters is at 25 m with a thickness of 100 m which slopes gradually towards the inshore region presenting itself at 10 m (Fig. 6). Salinity discontinuity coincides with the thermocline. Waters above the thermocline are more or less isohaline and within the thermocline the salinity variation is irregular and below it is again stable. The top of the oxygen minimum layer which varied between 75 and 145 m in the offshore region showed a strong upslope towards the shelf over which it is present at about 35 m. High nutrient concentrations are as usual accompanied by low temperatures and oxygen, while salinity does not bear any regular relationship with the nutrients.

In December the thermocline in the offshore region, begins at 75 m with thickness extending to 150 m. The spread of the thermocline is limited to the edge of the continental shelf and over the shelf the waters are isothermal. While the temperature pattern shows a fairly good mixed layer above the thermocline, salinity gradients are observed within this layer, sometimes extending down to 100 m. Oxygen minimum layer is present neaı the edge of the shelf where it is found at about 150 m; over the shelf, the waters are nearly saturated. Phosphate and silicate variations, in general, are consistant with those of temperature, salinity and oxygen. Nitrate concentration, particularly below 25 m, appears to be independent of the hydrographical factors.

Off Ratnagiri:

In September the thermocline is generally present below 30 m with a thickness of 75-150 m in the offshore region, and shows strong upslope towards the coast presenting below 10 m or 20 m, extending down to bottom (Fig. 7). Significantly low salinity (32-33$^{\circ}/_{oo}$) water is present at the surface all along the section excepting in the near shore region, wherein the waters are of higher salinity. Salinity increase is sharp below 10 m reaching maximum at about 30 m and below once again observed to be in decrease. Oxygen minimum layer is present at about 86 m within the thermocline in the offshore waters and in the inshore region it is limited to bottom layers only. Above the thermocline the phosphates and silicates are observed to be decreasing from surface up to the thermocline top and below they show a general increase. Relatively high surface concentrations are associated with the observed low surface salinities. In Sub-surface waters, high nutrient concentrations are generally found to be related with low temperatures and oxygen contents and high salinities.

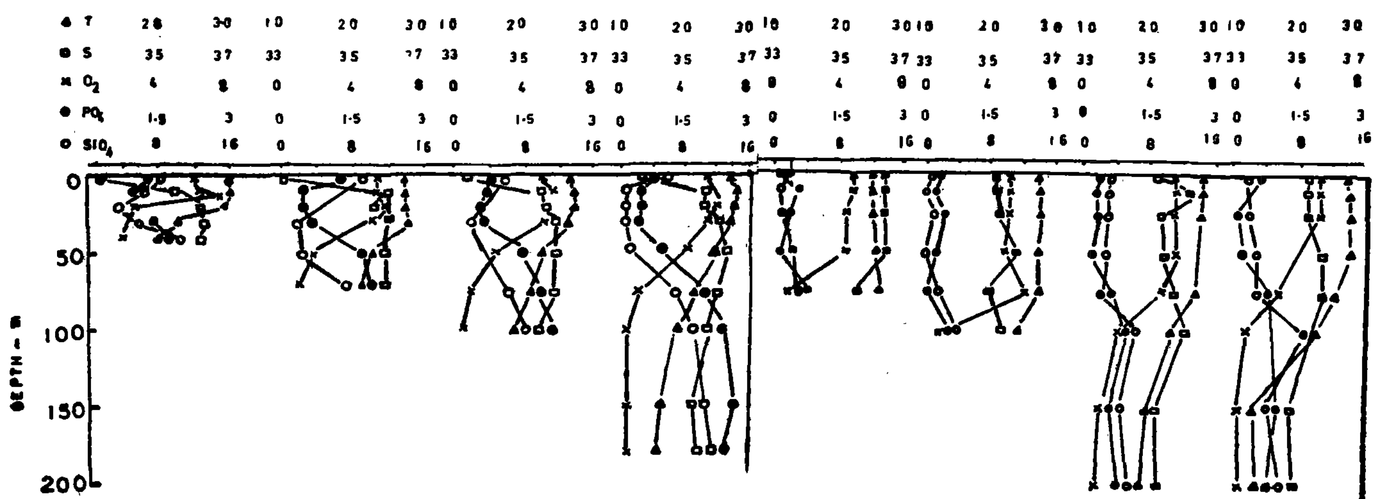

FIG. 7. Depthwise variations of the hydrographical factors and the nutrients at selected stations (Nos. 1942, 1943, 1944, 1945, 2031, 2032, 2033 and 2034) off Ratnagiri in September and December. Oxygen in ml/litre, nutrients in μg at/litre, salinity in ‰ and Temperature in °C.

As compared with the monsoon period, in December the waters ore isothermal near the coast and thermocline is present at deeper levels (between 75 and 150 m) towards offshore. In the inshore area waters are more or less isohaline, Salinity discontinuity is significant generally below 25 m in the offshore region and the distribution is irregular. Surface salinity values are relatively higher than in September. Oxygen minimum layer is absent over the shelf region and beyond, in is present at deeper levels (120-185 m). In the near shore waters nutrients showed little vertical variation, which is in conformity with the isothermal and isohaline conditions. Seawards the distribution appears to be independent of the thermocline conditions. However, the accumulation is significant below the thermocline.

Discussion

The present studies at three selected regions across the West Coast covering the shelf waters provide some picture of the distribution of nutrients on the West Coast of India.

The vertical profiles of nutrients during the monsoon months indicate the enrichment of coastal waters by the nutrients brought up from the sub-surface levels. This gives a picture of upwelling which is further corroborated by the distribution of salinity and temperature. Along the south-west coast of India, the presence of a distinct band of water which has all the characteristics of an upwelled water is evident. It is possible that this enrichment could be the result of certain dynamic factors associated with the prevailing southerly drift during the monsoon months. The degree of enrichment may vary from year to year and from region to region and these could be attributed probably to varying intensities of the southerly flow. During the post-monsoon months this phenomenon is absent and the waters are more or less stable. This feature is consistent with the reversal of the current system observed during the period which favours the opposite conditions i.e. sinking (Ramamritham and Jayaraman 1960).

The present nutrient studies suggest that the processes of enrichment are more intense towards southern part of the West Coast of India. The decrease in the concentration of nutrients following the period of enrichment is to be attributed to possible utilization by the phytoplankton. Increased vertical stability of the waters particularly in the post-monsoon period keeps the nutrient levels low. The nutrient concentrations in the near shore region are relatively less affected through different seasons as compared with the major part of the shelf waters. These concentrations are generally very high, possibly due to the rapid regeneration of nutrients by bacterial oxidation and chemical decomposition. The effect of constant mixing of the entire water column due to turbulence prevailing throughout the year is felt more near shallow regions. Further offshore, marked variations in the nutrient levels are observed in different seasons. The observed low nutrient levels in the more offshore regions as compared with the near shore regions might be due to the fact that consumption exceeds regeneration and lack of active replenishment of nutrients; in the nearshore region the converse is true.

Regarding the nutrient relationship *inter alia*, it is noted that at all sections (Figs. 5-7) phosphate and silicate values show similar trends. Nitrates in general show an inverse relationship with the other nutrients particularly in the surface at a sligthly deeper level than those of phosphate and silicate. These differences in maxima of respective nutrients might be, as suggested by Redfield *et al.* (1963), due to more rapid release of certain nutrients earlier than others and it provides a mechanism by which nitrogen and phosphorus may be fractionated and this may explain the variation in the ratio of these elements in the sea water. The ratio between elements Si, N, and P as observed in the present context, is highly variable unlike that of the temperate region. This variation may presumably be due to the differential and rapid rates of regeneration and consumption of the nutrients accompanied by extensive mixing of water masses which seems a characteristic feature of tropical waters.

Hydrographical features like temperature, salinity and dissolved oxygen also lend support to some of the conclusions drawn from the distribution of the various nutrients. A brief mention of these features during the period of investigation and their relationship with nutrients would be pertinent for the present discussion.

Thermocline is rather weak during the monsoon months and strong during the post-monsoon months. The nutrients are present in very high concentrations below the thermocline. The steep temperature gradient in the post-monsoon months, prevents the vertical mixing of the waters and thus hinders the replenishment of the nutrients to the upper layers. Salinity unlike temperature and oxygen does not bear marked relationship with nutrients. It is noted from the salinity and nutrient data off Quilon and Ratnagiri sections in September, that the effect of land drainage is not very significant. This is unlike in the East Coast of India where many large rivers flow into the Bay of Bengal. One of the significant points in the hydrographical features, is that the surface salinities in the more northern Ratnagiri section are somewhat lower than those in the more southern Mangalore and Quilon sections in September. This gives some evidence of a greater intensity of upwelling in the southern part of the West Coast. Another important feature worth mentioning particularly in the deeper parts of the shelf is that during monsoon months, a distinct salinity maximum is noted between 20 and 30 meters and in the post-monsoon months between 50 and 100 meters and these layers are seen just above or to coincide with the depth of oxygen discontinuity layer. Nutrients, especially phosphates and silicates show a rather abrupt increase at this depth and below. This layer of salinity maximum probably has its source in the offshore region, but during the monsoon months influences the salinity of the near shore region. Oxygen discontinuity shows the same trend of variations as thermocline through the different seasons. The low oxygen values and the associated high nutrients at these levels are indicative of active regenerative process leading to consumption of oxygen with ultimate concentrations reaching as low as 0.5 ml/L.

ACKNOWLEDGMENT

We are grateful to Dr. N. K. Panikkar, Director, National Institute of Oceanography (C.S.I.R.), for his valuable guidance and keen interest in the present work; to the staff of the Central Marine Fisheries Research Institute and the Indo-Norwegian Project, for their help during the cruises of R.V. VARUNA; to Dr. S. Z. Qasim and Shri R. Jayaraman of the National Institute of Oceanography, for offering helpful suggestions and to Shri M. Krishna Menon, Indian Ocean Biological Centre, for providing all laboratory facilities.

REFERENCES

Admiralty. (1960) West Coast of India Pilot, London.

Banse, K. (1959). On upwelling and bottom trawling off the southwest coast of India. *J. mar biol. Ass. India*, **1**, 33-49.

Barnes, H. (1960). Apparatus and Methods of Oceanography. Part I, Chemical, London.

Broenkow, W.W. (1965). The distribution of nutrients in the Costa Rica Dome in the Eastern Tropical Pacific Ocean. *Limnol. Oceanogr.*, **10**, 40-52.

George, P.C. (1953). The marine plankton of the coastal waters of Calicut with observations on the hydrological conditions. *J. zool. Soc. India*, **5**, 76-107.

Jayaraman, R., and Seshappa, G. (1957). Phosphorus cycle in the sea with particular reference to tropical inshore waters. *Proc. Indian Acad. Sci.*, **46**, 110-125.

Panikkar, N.K., and Jayaraman, R. (1956). Some aspects of productivity in relation to fisheries of Indian neritic waters. Oceanography & Zoology. *Proc. 8th Pacific. Sci. Congr.*, **34**, 1111-1122.

Ramamritham, C.P., and Jayaraman, R. (1960). Hydrographical features of the continental shelf waters off Cochin during the years 1958 and 1959. *J. mar. biol. Ass. India*, **11**, 199-207.

Redfield, A.C., Ketchum, B.H., and Richards, F.A. (1963). The influence of organisms on the composition of seawater. *The Sea*, **2**, 26-77.

————————(1958). Dissolved silicates and related properties of some western North Atlantic and Caribbean Waters. *J. mar. Res.*, **17**.

Richards, F.A. (1960). Some chemical and hydrographic observations along the north coast of South America. *Deep Sea Res.*, **7**, 163-182.

Robinson, R.J., and Thompson, T.G. (1948). The determination of silicates in sea water. *J. mar. Res.*, **7**, 49-55.

Ryther, J.H. (1963). Geographic variations in productivity. *The Sea*, **2**, 347-380.

Sastry, A.A.R., and Myrland, P. (1960). Distribution of temperature, salinity and density in the Arabian Sea along the south Kerala Coast (S. India) during the post-monsoon season. *Indian J. Fish.*, **6**, 223-255.

Seshappa, G., and Jayaraman, R. (1956). Observations on the composition of bottom muds in relation to the phosphate cycle in inshore waters of the Malabar Coast. *Proc. Indian Acad. Sci.*, **43**, 288-301.

Subrahmanyan, R. (1959). Studies on the phytoplankton of the West Coast of India. Part I. *Proc. Indian Acad. Sci.*, **50B**, 113-187.

————————(1959). Studies on the phytoplankton of the West Coast of India. Part II. *Proc. Indian Acad. Sci.*, **50B**, 189-252.

Suryanarayana Rao, S.V. (1957). Preliminary observations on the total phosphorus content of the inshore waters of the Malabar Coast off Calicut. *Proc. Indian Acad. Sci.*, **45B**, 77-85.

Sverdrup, H.U., Johnson, M.W., and Fleming, R.H. (1942). The Oceans, Their Physics, Chemistry and Biology. New York.

Vinogradov, M., and Voronina, N.H. (1960). Influence of the oxygen deficit on the distribution of plankton in the Arabian Sea. *Deep Sea Res.*, **9**, 523-530.

Wooster, W.S., and Rakestraw, N.W. (1951). The estimation of dissolved phosphates in sea water. *J. mar. Res.*, 49-55.

Reprinted from *Bull. natn. Inst. Sci. India*, no. 38, 1968, p. 324-333

SPECIFIC ALKALINITY IN THE NORTHERN INDIAN OCEAN DURING THE SOUTH WEST MONSOON

by R. SEN GUPTA[1] *and* ABRAHAM PYLEE[2]

Titration alkalinity was measured for a total of 500 water samples from the northern Indian Ocean during the south-west monsoon cruises of I.N.S. KISTNA in 1963 and the specific alkalinity were calculated from the chlorinity values. Results are represented along two sections in the Indian Ocean, two in the Arabian Sea and three in the Andaman Sea. Observations were restricted to a depth of 200 metres in the Indian Ocean and to about 500 metres in the Arabian and the Andaman Seas. In the Indian Ocean the values decreased between 25 and 50 metres where the optimal conditions for the lime secreting organisms seem to exist. The values then increase to about 100 metres and then show a slight decrease to 200 metres. The higher values appear to be in the core of the equatorial under-current, which has been found to exist in the Indian Ocean, as well. In the Arabian Sea the values vary little with depth and slightly higher values are found below 150 meters. These higher values may be due to the high salinity intermediate water in the Arabian Sea whose origin has been traced to the Persian Gulf. The values in the Andaman Sea are comparatively lower at the surface than at the depths slightly below it (between 20 and 40 metres). This may either be due to the 'island effect' or this area being in a zone where precipitation exceeds evaporation, and the observations were taken at the time of almost the highest precipitation. The surface values at the eastern section is in general higher than those at the western part, which may be due to the effect of the discharges from the River Irawaddy and its tributaries. The values gradually decrease towards the depth which may also be due to the fact that this is an area of intense south-west monsoon upwelling.

INTRODUCTION

The alkalinity of sea water is a measure of the quantity of anions of weak acids present in it and of the cations balanced against them (Sverdrup *et al.* 1942). In most sea water, the cations of weak bases are present in negligible concentration and the only anions that need be considered are those of carbonic and boric acids, and in a sea water sample, the alkalinity (defined as 'titration alkalinity' by Harvey 1955) is the sum, in terms of equivalent per litre, of the analytical concentrations of these anions. This can be expressed as:

$$\text{alkalinity (eq./l)} = C_{HCO_3^-} + 2C_{CO_3^{2-}} + C_{H_2BO_3^-} + \left(C_{OH^-} - C_{H^+}\right)$$

Wattenberg (1933) used the term 'specific alkalinity' in the Atlantic waters, which can be defined as:

$$\text{Specific alkalinity} = \frac{\text{Alkalinity} \times 10^3}{\text{Chlorinity}}$$

and found a constant value of 0.123. Koczy (1956) found that this value varies between 0.119 and 0.130 in all the oceans. The specific alkalinity indicates the changes due to the calcium precipitation or dissolution, but should not be affected by the mixture of water masses with different salinities, if not the history of the water in respect of the geochemistry of calcium carbonate is different. With rising pres-

1. Oceanografiska Institutionen, Göteborg, Sweden.
2. Physical Oceanographic Division, National Institute of Oceanography, Ernakulam-1, India.

sure of carbon dioxide, increasing depth and decreasing temperature the solubility of carbonate increases. Therefore, the specific alkalinity increases with depth. Depending on the state of the calcium carbonate system at the origin, the specific alkalinity can be used as a tracer for the flow of different water masses.

Materials and Methods

As part of the Indian programme for the International Indian Ocean Expedition, titration alkalinity was measured in samples from the northern Indian Ocean, during the south-west monsoon cruises of I.N.S. KISTNA in 1963 (Fig. 1), and the specific alkalinity was calculated from the chlorinity values. The titration alkalinity was measured according to the method of Gripenberg (1937). 10 ml of N/20 HCl

KISTNA
Cruises in 1963 (Monsoon)

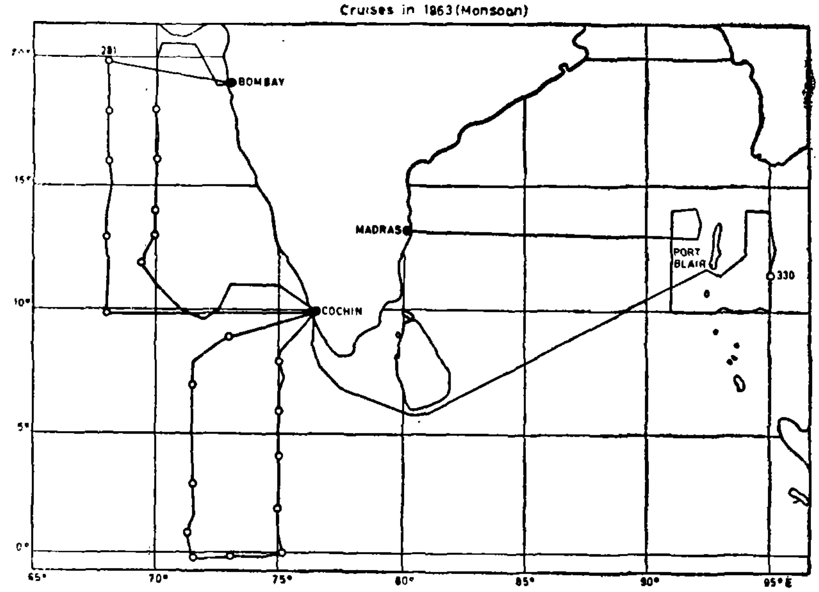

Fig. 1

was put in a polyethylene bottle (ca. 200 ml volume) and it was then filled up with sea water. When the ship reached the harbour the samples were boiled, on board, for 5 minutes in order to drive off all the carbon dioxide set free by the acid. The hot liquid was then back-titrated with a N/20 carbonate-free sodium hydroxide solution to a pH of 7 using a mixture of 3 parts of Brom-cresol green and 2 parts of Methyl red as indicator. During the titration carbon dioxide-free air was bubbled through the sample.

Results and Discussion

The values for the same depths at all the stations along the sections are represented as scatter in the diagrams. The mean values have been drawn as a line to show the variations of the values around the mean.

(i) *Indian Ocean*: Figure 2 represents two sections in the Indian Ocean. Line 1 is for a section along the equator between 71° and 75°E longitude and line 2 is for a meridional section between 4° and 8° N latitude along the 75° E longitude. Observations along both the sections represent values down to the depth of 300 metres.

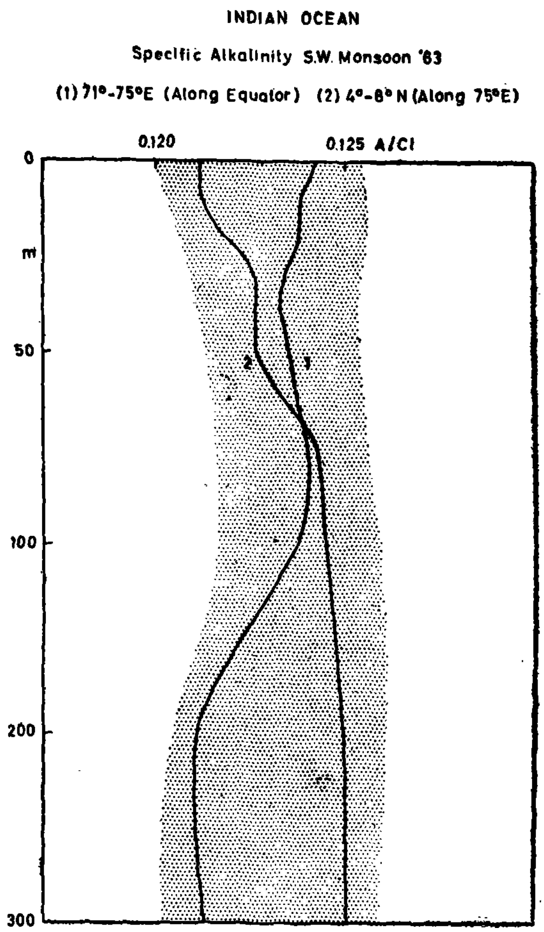

Fig. 2.

A look at line 1 will show a decrease in the values to about 50 metres, followed by an increase to about 100 metres and a slow decrease to about 200 metres, below which it becomes almost steady. The equatorial surface waters, in which the main production of calcareous shells goes on, show a low specific alkalinity and the depth between 25 and 50 metres, is the region where the optimal conditions for lime-secreting organisms exist (Koczy 1956) as a result of the oversaturation in the carbonate content by the increased temperature, which is the reason for the lowering of the specific alkalinity values.

Line 2 of the Fig. 2 shows a steady increase in the values of specific alkalinity in the surface layers associated with lower salinity values. Such higher values have also been reported in the northern part of the Indian Ocean near Ceylon (Koczy 1956), and also around the New Hebrides and Fiji Island in the Pacific Ocean (Rotschi 1965). This increase may not be representative of general conditions in the Indian Ocean but may be an 'island effect', where the surface waters have been modified by a variety of runoff products (Waterman 1964).

Figure 3 shows the horizontal distribution of specific alkalinity along the equatorial section. It can be seen that there is an increase in the values in the surface layers from the west to the east. Similar observations have been recorded by Bruneau *et al.* (1953) who have noted changes in specific alkalinity values in the surface layers from 0.120 at 66° 16′E to 0.123 at 77° 28′E almost along the equator. Figure 3 also illustrates the gradual increase of the specific alkalinity values to about 100 metres and then a slow decrease. The same nature of variation has also been observed during the Swedish Deep Sea Expedition (Bruneau *et al.* 1953). One of the reasons for this increase in specific alkalinity values can be correlated with the change in the slope of the surface of the Indian Ocean from west to east, which has been observed to be of opposite sign from that in other oceans (Knauss and Taft 1964). Figure 4, which has been taken from their observations, illustrates this. Ivanenkov (1964) has also reported a gradual increase in values of the surface specific alkalinity along the equator in the Indian Ocean from west to east.

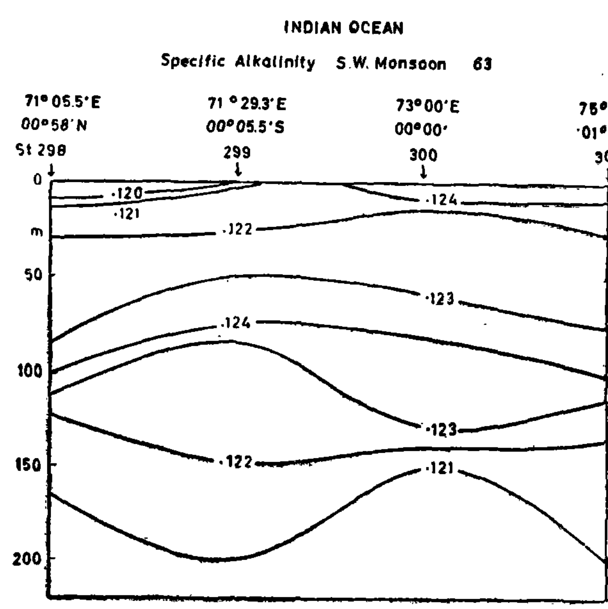

Fig. 3.

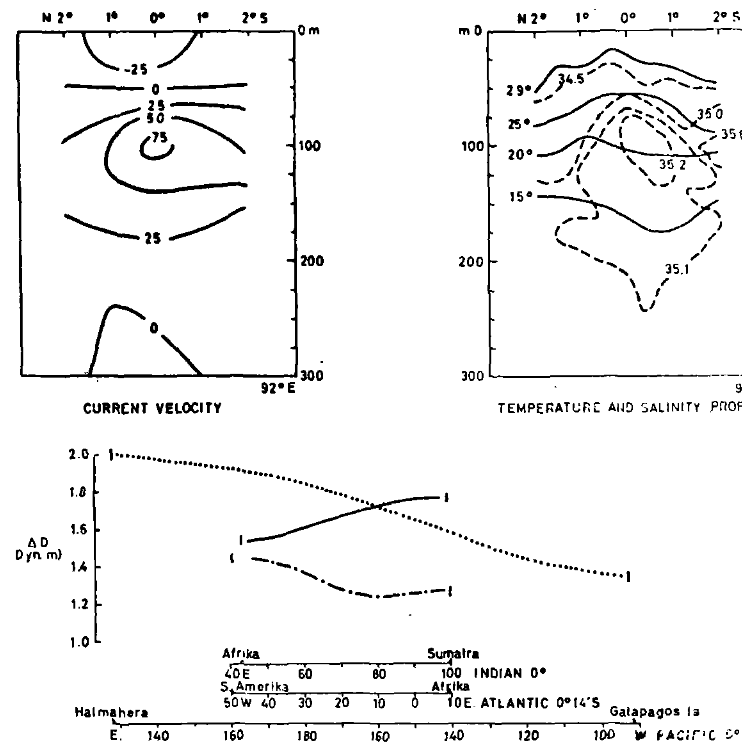

FIG. 4

A comparison of Figs. 3 and 4 shows that the region of the maximum specific alkalinity almost coincides with regions of high salinity and with the core of the weakly developed equatorial under-current in the Indian Ocean, which has been observed to exist by Knauss and Taft (1964).

(ii) *Arabian Sea*: Figure 5 represents two sections in the Arabian Sea. Line 1 represents a section along 70°E and line 2 along 68°E. Both the sections represent values between 10° and 20°N, the first to a depth of 100 metres and the second to 500 metres.

Line 1 shows the slight increase of the values to about 25 metres below which it becomes steady. A comparison between these values and those at station 4890 (Ivanenkov 1964) show an almost identical nature of variation. Since the present observations were taken during the south-west monsoon and the latter observations during the north-east monsoon, though at different years, it may be assumed that the values of specific alkalinity are slightly increased during the south-west monsoon but the nature of variations remains the same.

Line 2 shows a gradual increase from the surface values to the deeper ones, which becomes almost steady at about 100 m. Figure 6 shows an attempt at correlating the specific alkalinity values with the corresponding σt surfaces. In general,

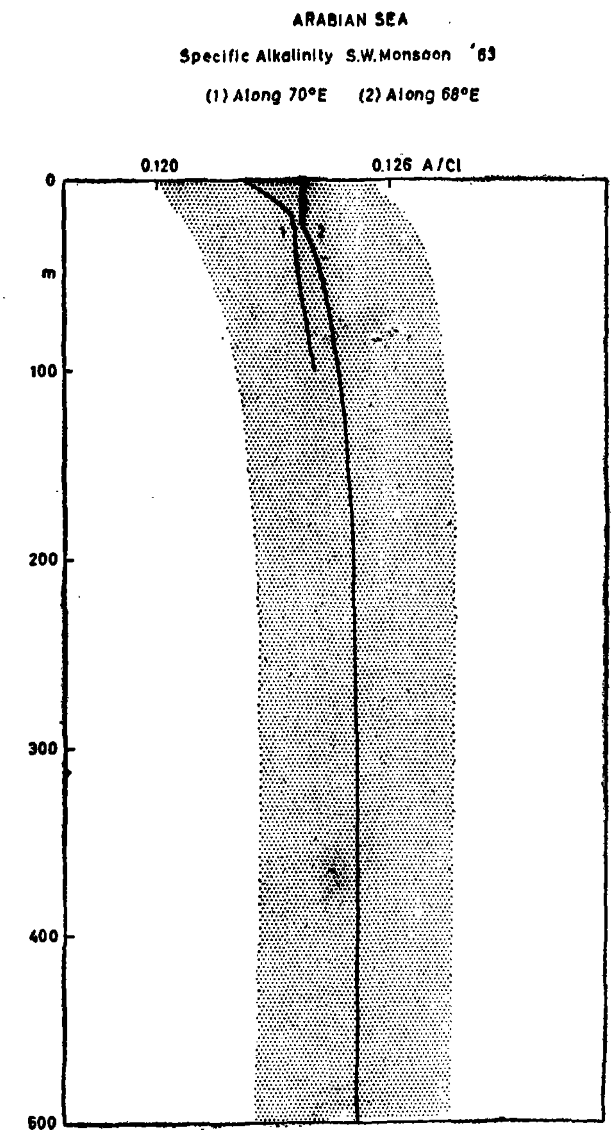

FIG. 5.

it is seen that they agree within a fair amount of approximation. Three different water masses are apparent from the figure, the first, the surface and the sub-surface layers to about 100 metres, coinciding with σt 25 surface, the second, to about 200 metres, coinciding with σt 26 surface, and the third, to about 500 metres, coinciding with σt 27 surface. All the surfaces are found to slope downward from north to south. The surface layer may be said to be originated in the Arabian Sea itself

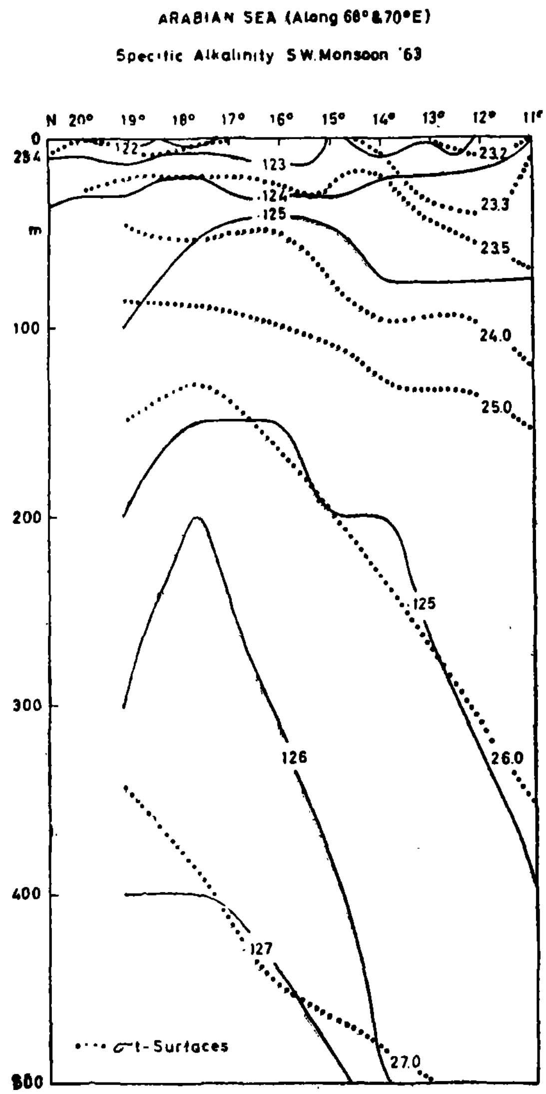

FIG. 6.

(Sabinin 1964). The intermediate layer is formed by the tributary of the high salinity water of the Persian Gulf—the salinity maximum of this water is found to lie between 150 and 300 metres (Sabinin 1964). The specific alkalinity values, characteristic of this water (0.125) is observed between 200 and 300 metres in the section along 75°E (Fig. 2). Hence, from these observations, it can be said that the waters of the Persian Gulf-origin has been traced down to 4°N latitude. The lower layer of σ_t 27 (specific alkalinity 0.125—0.126) can be said to be of the Red

Sea origin—the salinity maximum of which is observed between 400 and 800 metres in the Arabian Sea. It is apparent from the Fig. 6 that this layer extends below 500 metres as both the specific alkalinity and the σt values show a gradual increase southwards from about 13°N latitude. The Red Sea water seems to have a higher specific alkalinity associated with higher salinity and calcium contents.

(iii) *Andaman Sea*: Figure 7 represents the specific alkalinity values from three sections covered around the Andaman Islands. Line 1 represents the eastern section between 11° and 14°N and 93° and 95°E; line 2 represents the western

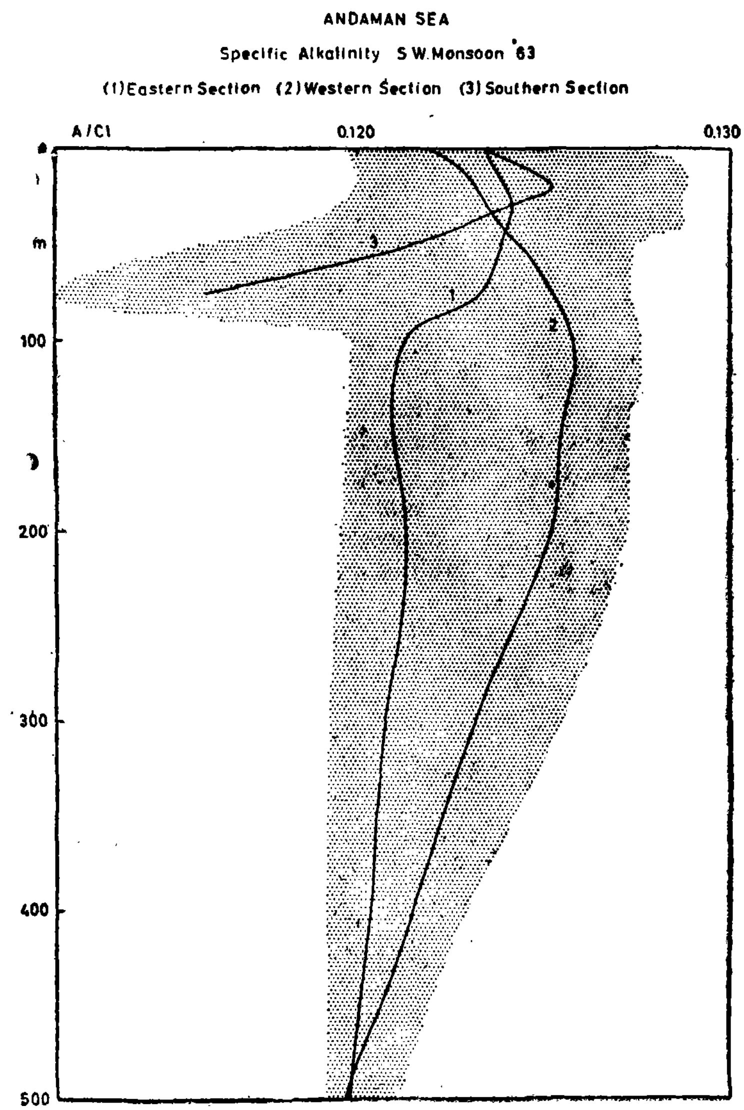

FIG. 7.

section between 11° and 14°N and 91° and 92°E; and line 3 along 10°N between 91° and 95°E. Observations were confined to 500 metres in the eastern and the western sections while in the southern it was only to 75 metres. The wide scatter of the values in the figure is the cumulative result of observations at all the stations along the three sections.

In the north-eastern Indian Ocean precipitation exceeds evaporation (Ivanenkov 1964) and it is an area of intense upwelling, specially during the monsoons (LaFond 1963).

The high surface values in all the sections in this area may be correlated with this factor. Also, the observations were taken at the time of very high precipitation, if not the highest (early September). In the eastern section of this area, the River Irawaddy from Burma discharges, and hence, it can be said that, in general the recently mixed river water and the rain of continental origin enhances the specific alkalinity values in the surface layers, associated with low salinity values lying between 31‰—33‰. The gradual increase in the specific alkalinity values with depth to (ca. 200 m) in the western section (line 2) probably indicates that upwelling is more intense in this part of the Andaman Sea than in the others. The gradual lowering of the values in the southern section with depth probably indicates that the water masses in this region are influenced more by the waters of oceanic origin.

General Remarks

It can be noted from these observations that: (1) the specific alkalinity behaves as a conservative property of sea water and with certain limitations, the mean values can be used approximately as a tracer for the flow of water masses of different origin, and (2) the specific alkalinity values along the equator in the Indian Ocean during the monsoon follows fairly well the modulations of the equatorial under-current, the high values almost coinciding with its core, and the dynamic topography of the ocean surface.

Acknowledgements

The authors wish to record their gratefulness to Dr. N. K. Panikkar, Director, National Institute of Oceanography, India, for his kind approval of the programme and for permission to present the paper at the Second International Oceanographic Congress at Moscow. The help and cooperation of the Officers and men on board I.N.S. KISTNA in the collection of the samples is gratefully acknowledged. Sincere thanks are also due to Dr. John A. Knauss of the Graduate School of Oceanography, University of Rhode Island, U.S.A., for helpful discussion and kind permission to reproduce the diagram of the equatorial under-current and dynamic topography of the Indian Ocean, and to Mrs. Elna Juhlin of Oceanografiska Institutionen, Göteborg, Sweden, for her painstaking care in drawing the figures.

REFERENCES

Bruneau, L., Jerlov, N.G., and Koczy, F.F. (1953). Physical and chemical methods. *Rep. Swed. deep Sea Exped.*, **3**, pp.

Gripenberg, S. (1937). On the determination of excess base in sea water. Com. 10B, Vth Hydrol. Conf. Helsingfors.

Harvey, H.W. (1955). The Chemistry and Fertility of Sea Waters. Cambridge.

Ivanenkov, V.N. (1964). Distribution of PCO_2, pH, alk/cl in the northern part of the Indian Ocean. *Trudy Inst. Okeanol.*, **64**, (*In Russian*).

Knauss, J.A., and Taft, B.A. (1964). Equatorial undercurrent of the Indian Ocean. *Science*, **143**, 3604.

Koczy, F.F. (1956). The specific alkalinity. *Deep Sea Res.*, **3**. pp.

LaFond, E.C. (1963). Preliminary reports of the first cruise of USRV. ANTON BRUUN.

Rotschi, H. (1965). Le pH et l'alcalinite des eaux profondes de la fosse des Hebrides et du bassin des Fidji. Progress in Oceanography. Mary Sears (ed.), 3.

Sabinin, K.D. (1964). The layers of high salinity in the North Indian Ocean. *Trudy-Inst. Okeanol.*, **64**, (*In Russian*).

Sverdrup, H.U., Johnson, M.W., and Fleming, R.H. (1942). The Oceans, Their Physics, Chemistry and General Biology. Prentice Hall.

Waterman, L.S. (1964). Indian Ocean Expedition—investigations by members of the SIO carbon dioxide project—*Lusiad* Expedition. Preliminary results of SIO investigations in Indian Ocean during 1960-1963.

Wattenberg, H. (1933). Kalzium Karbonat—und Kohlensäuregehalt des Meerwassers. *Wiss. Ergebn. dt. atlant. Exped. 'Meteor'*, **8**.

Reprinted from *Proceed. natn. Inst. Sci. India (New Delhi)*, vol. 36, B, no. 2, 1970, p. 71-79

TOTAL PHOSPHORUS CONTENT IN THE WATERS OF THE ARABIAN SEA ALONG THE WEST COAST OF INDIA

by V. N. Sankaranarayanan *and* C. V. Gangadhara Reddy, *Biological Oceanography Division, National Institute of Oceanography, Ernakulam*

(Communicated by Dr. N. K. Panikkar, F.N.I.)

(*Received 14 November 1968*)

Total phosphorus estimations are made on samples collected along four sections, perpendicular to the coast between Bombay and Cochin, during the 25th cruise of INS *Kistna* in March 1965. The results reveal considerable variability in the regional and depthwise distribution of the same. Higher concentrations are encountered in the upper 800 m in the northern sections (off Bombay and Karwar) than in the southern ones (off Mangalore and Cochin) while at deeper levels (> 800 m) the trend is reverse. Off Cochin greater concentrations (> 10 μg-at/l) are found below 800 m as compared with 2–4 μg-at/l found at the same depths in the other regions. Percentage of organic phosphorus is in general very high in the surface (upper 200 m). Even at 1,000 m mineralization of organic phosphorus is not complete and at majority of the stations the composition amounted to 20–30 per cent of the total phosphorus. Distinct convergence of the waters is indicated almost all along the coast over the mid-shelf, extending towards the slope region. Probable factors governing the distribution of total phosphorus are discussed.

Introduction

The significance of the total phosphorus concentration in the sea as an index of potential fertility of waters and for identifying different water masses as tracer has been emphasized earlier (Redfield *et al.* 1937; Armstrong and Harvey 1950; Bush *et al.* 1955; Rochford 1958). While considerable information is available on inorganic phosphate content of the waters in the Arabian Sea, very little is known on the distribution of total phosphorus. Earlier studies on the total phosphorus of the west coast of India were made by Seshappa and Jayaraman (1956) and Rao (1957). The present account is based on the observations made in March 1965 during the 25th cruise of INS *Kistna* which was undertaken as part of the Indian Programme of the International Indian Ocean Expedition.

Methods

Location of the stations from where samples of water were collected for the analysis of nutrients has been indicated in Fig. 1. The four sections, perpendicular to the coast, run approximately (1) off Bombay, (2) off Karwar,

(3) off Mangalore and (4) off Cochin. Water samples were collected in clean heavy polythene bottles and were preserved by freezing at −10 °C for subsequent analysis at the shore laboratory.

Total phosphorus was estimated by the method described by Hansen and Robinson (1953), digesting the organic matter with perchloric acid. Inorganic phosphates were estimated by the method adopted by Wooster and Rakestraw (1951).

Results and Discussion

The distribution of total and inorganic phosphorus along the four sections has been represented in Figs. 2–7. Detailed discussion of inorganic phosphates

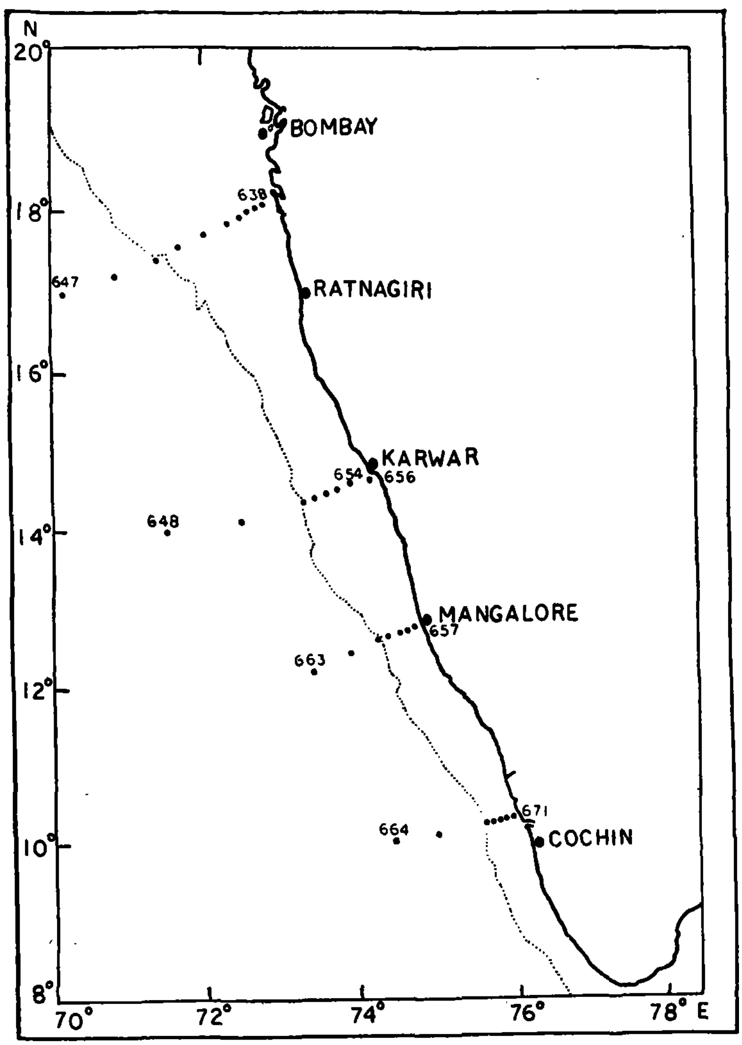

Fig. 1. Showing station locations.

IB

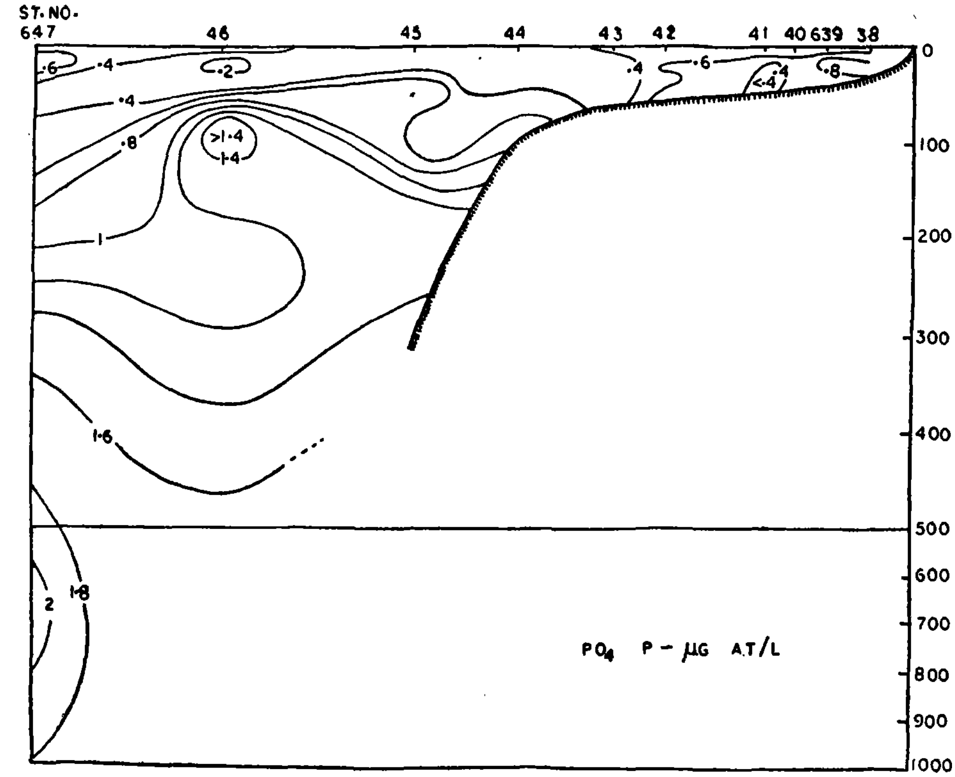

FIG. 2. Showing distribution of phosphate-phosphorus off the Bombay Coast.

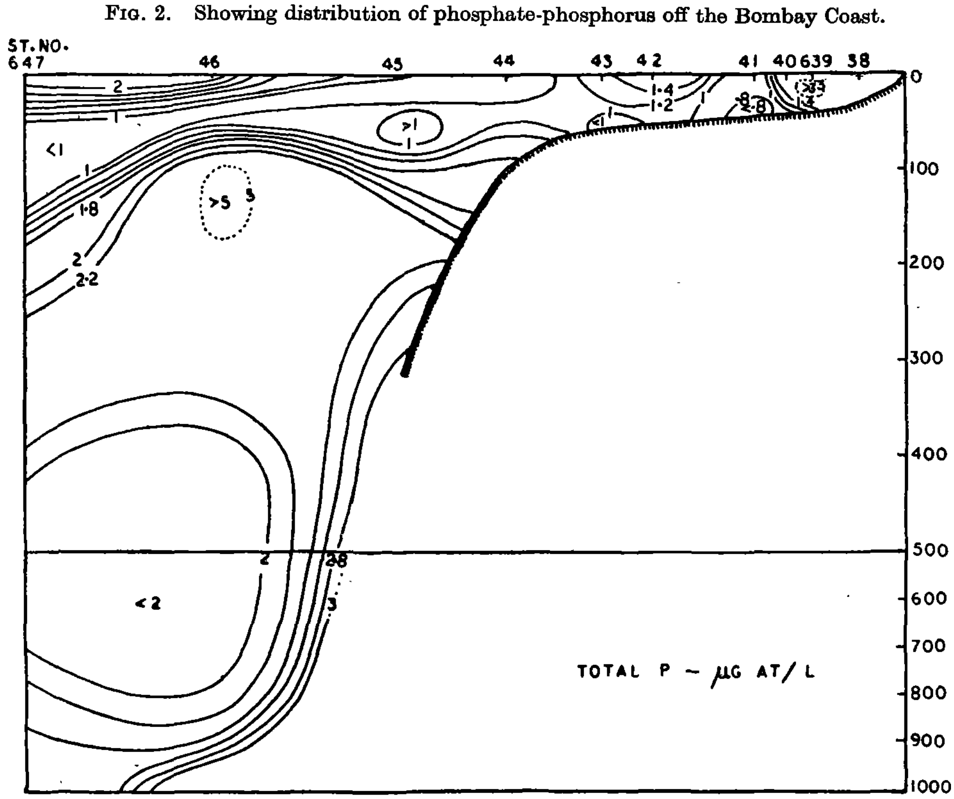

FIG. 3. Showing the distribution of total phosphorus off the Bombay Coast.

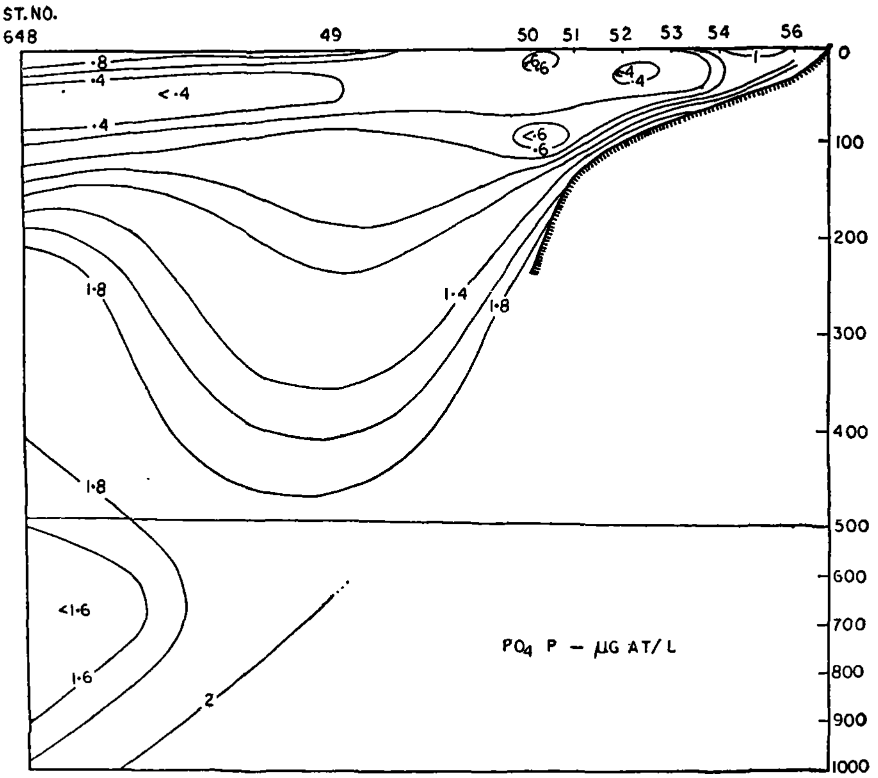

FIG. 4. Showing the distribution of phosphate-phosphorus off the Karwar Coast.

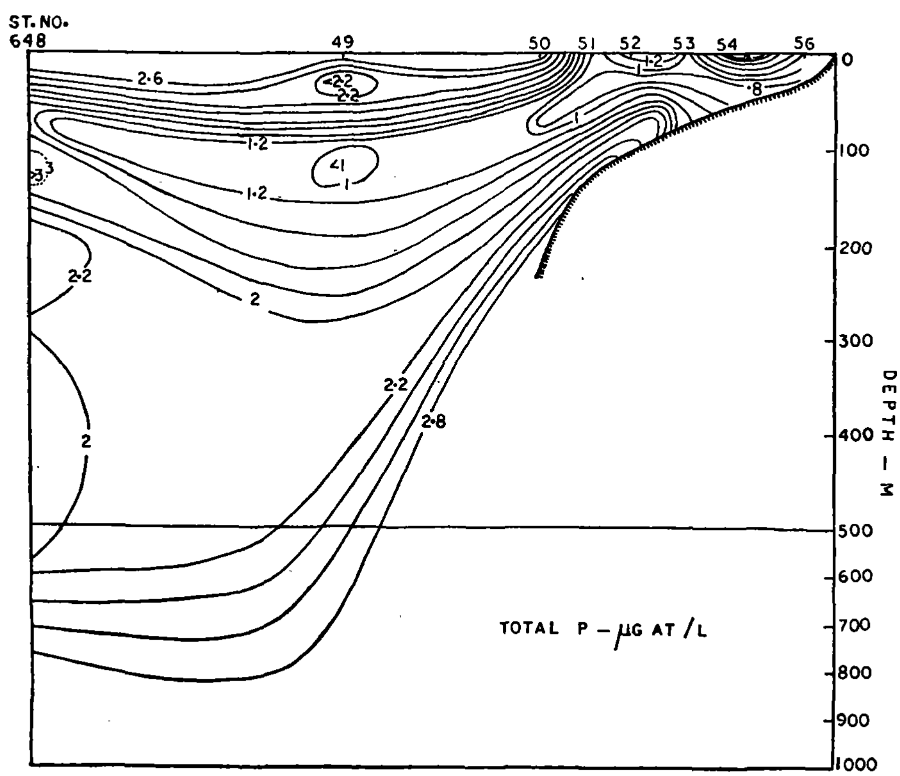

FIG. 5. Showing the distribution of total phosphorus off the Karwar Coast.

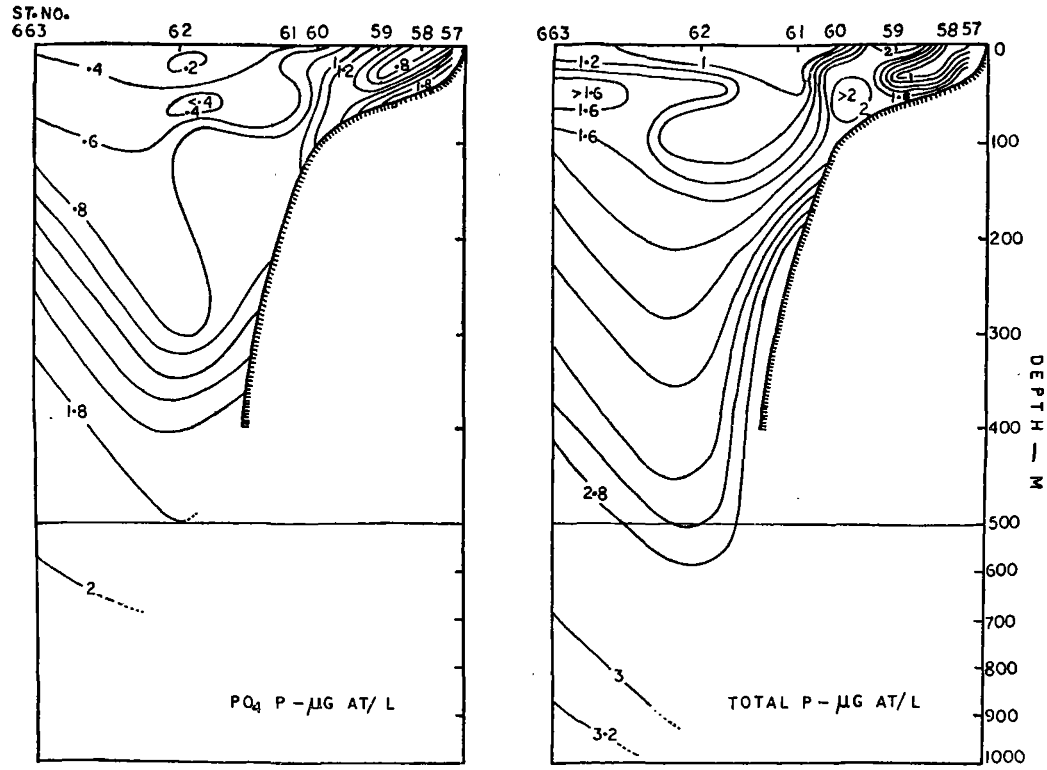

FIG. 6. Showing the distribution of phosphate-phosphorus and total phosphorus off the Mangalore Coast.

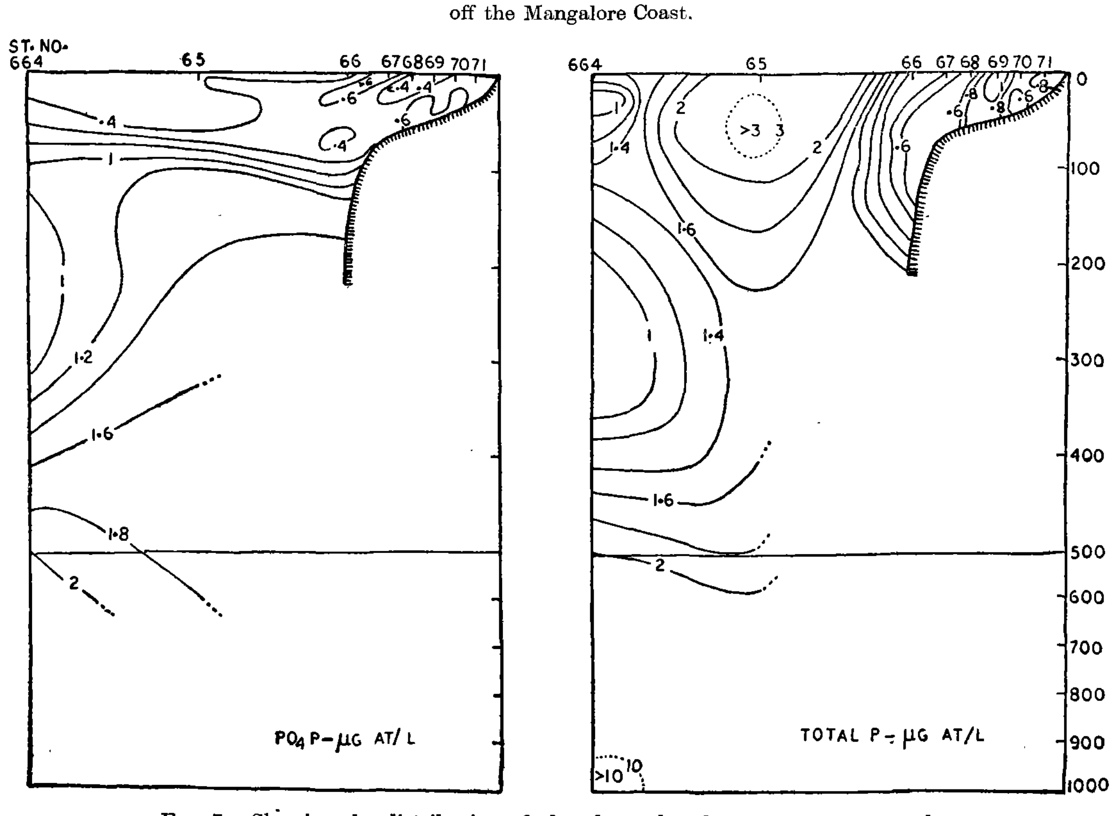

FIG. 7. Showing the distribution of phosphate-phosphorus and total phosphorus off the Kerala Coast.

will be presented along with other nutrients elsewhere. An examination of the profiles will indicate that there is a close similarity between inorganic and total phosphorus distributions in the three sections except along Cochin where similar distribution is restricted to the shelf region only. Total phosphorus values in the upper 1,000 m show wide variations. The range in the concentrations in the upper 500 m is 0·44–8·2 μg-at/l and at deeper levels it is 1·4–16·7 μg-at/l. It may, however, be mentioned here that concentrations exceeding 6 μg-at/l were recorded only off Cochin. Higher concentrations are normally encountered in the surface waters (upper 10 m) and in deep waters (below 500 m) with maximum in the latter. One characteristic feature in all the sections is the random cellular distribution of total phosphorus in the mixed zone (upper 100 m), containing either high or low concentrations. This feature can possibly arise due to entrapment of water bodies containing widely different concentrations of living and dead organic matter including soluble fractions during the process of mixing. This type of distribution is more pronounced in the shallow regions of the shelf.

Depthwise distribution of total phosphorus is irregular particularly in the upper 100 m and is more uniform below 500 m. Surface concentrations are generally increasing towards offshore. Clear maximum of total phosphorus is absent in the upper 1,000 m and from the available data of deeper levels (below 1,000 m) at few stations, it appears that its greater accumulation may be in between 1,000 m and 1,500 m.

Regional variation of the total phosphorus concentrations shows diverse trends. The concentrations in the upper 800 m are higher in the northern sections (off Bombay and Karwar) than those in the southern sections (off Mangalore and Cochin), but at deeper levels the trend seems to be reversed. Maximum surface concentration (4 μg-at/l) is found off Karwar in the offshore region. Off Cochin a greater concentration (> 10 μg-at/l) is found below 800 m as compared to the 2–4 μg-at/l found at the same depths in the other regions.

In the surface waters of the offshore region generally organic phosphorus forms the major fraction of the total. Apart from some random values of very high concentrations at few depths the organic phosphorus generally tends to decrease from 100 to 1,000 m. Even at 1,000 m the inorganic phosphorus was never equivalent to that of total phosphorus and the organic phosphorus amounted to 20–30 per cent of the total phosphorus. A comparison of the average organic phosphorus values in the shelf waters of different regions will reveal that maximum levels occur around Bombay (64 per cent of the total phosphorus). Along the Cochin area, it comes next (40 per cent) and off Karwar and Mangalore the concentrations are low, about 36–37 per cent of the total phosphorus. In waters beyond the shelf the percentage of organic phosphorus tends to increase gradually towards the south and the delineation becomes fairly marked between the northern and southern sections. The average contents of organic phosphorus in the slope waters off Bombay and Karwar are 46 and 48 per cent of total phosphorus and off Mangalore and Cochin these are 54 and 56 per cent respectively.

The foregoing account indicates considerable variation in the regional distribution of the total phosphorus and its major fractions and even in a particular section the variations in the horizontal and vertical distributions are quite significant. Contrary to the fact that total phosphorus may serve as a useful index to identify water masses in general, the present data suggest that the total phosphorus loses its true conservative nature in the shallow and productive regions (shelf and slope) of the sea. Rochford (1958) during his investigations on the East Australian water masses in relation to total phosphorus observed that, in the region of turbulence extending to the bottom, anomalies in the distribution of total phosphorus occur. The high productive nature of the shelf and slope waters along the west coast of India perhaps renders the total phosphorus more a non-conservative property due to irregular distribution of all forms of organic matter aided perhaps by the random movement of the waters. Nevertheless the distribution of total phosphorus in the present instance broadly indicates only certain very distinct water movements and the fertility of the regions.

An examination of the total phosphorus data will reveal that the waters of the upper 800 m in the northern sections (off Bombay and Karwar) have a very high concentration of total phosphorus, much of which is in the organic form. In the southern sections (off Mangalore and Cochin) on the other hand the total phosphorus concentrations are relatively low and, excepting for the inshore region, the organic phosphorus remains predominant. Another notable feature is the total phosphorus concentrations in the slope region being consistently higher than those of the shelf and very high accumulation of total phosphorus (>10 μg-at/l) is found off Cochin at 1,000 m and below. This high accumulation of total phosphorus (organic phosphorus 80 per cent) in the slope waters below 300 m is quite significant and it appears to have a good bearing on the fertility of the region in general (McGill 1964; Ryther and Menzel 1965). The high concentrations seem to be consistent with higher productivity of the region as a result of upwelling occurring during the southwest monsoon period. The particulate organic matter produced in the surface waters seems to be sinking to deeper layers without being mineralized completely. Total mineralization may be obliterated, perhaps, by the relatively lower oxidative nature of the water column. The high total phosphorus values in the upper 800 m in the northern section might also be related to the abundance of plankton and fish generally reported to be occurring during this period suggesting the probable sources for the standing levels of high phosphorus concentrations. Moreover the shelf, which is wide and shallow in the north, permits mixing to a considerable extent, distributing phosphorus components from the sediments over a wide area. Examination of the vertical profiles indicates distinct convergence of the surface waters from the mid-shelf region extending over to a large area towards the slope region all along the coast. This feature is also in accordance with the distribution of other hydrographical factors. A general feature noticeable in the convergence regions is the presence of cells of high total phosphorus, comprising 60–80 per cent of organic phosphorus indicating the concentration of phosphorus of planktonic or detrital origin. From the standing levels of low inorganic and high total phosphorus in the surface layers, it could be inferred that the rate of regeneration is perhaps slow at least during the period under report and much of the regeneration activity appears to be limited to deeper layers as evidenced by greater accumulation of inorganic phosphates at these levels. However, mineralization is not complete even to 1,000 m at majority of the stations indicating the presence of significant quantities of organic phosphorus, which seems to be relatively more resistant to oxidation. This feature corresponds to some extent with those of recent investigations in the Pacific (Strickland and Austin 1960) and Atlantic (McGill 1964). Former authors suggest the presence of 'microstructure' of organic phosphorus distribution: a residuum which is highly resistant to process of mineralization. However, in the present instance, the presence of relatively high proportion of organic phosphorus at some locations suggests the possibility that the entire portion may not be the microstructure, but perhaps reflects on the general physical, chemical and bacteriological conditions of the upper 1,000 m controlling the rate of regeneration. The standing oxygen levels at these deeper layers are also too low to meet the oxygen demand for complete mineralization of the organic phosphorus and it is considered that some factors including the observed sinking phenomenon of the waters might be largely responsible in aiding faster sinking rate of particulate matter through the active regeneration zone (approximately between 200 m and 500 m characterized by low percentage of organic matter, Rochford 1962). More detailed investigations on the vertical distribution of different forms of phosphorus as a function of time may throw more light on this aspect.

Acknowledgements

The authors wish to express their grateful thanks to Dr. N. K. Panikkar, Director, National Institute of Oceanography, for his guidance and encouragement and to Shri R. Jayaraman and Dr. S. Z. Qasim, Scientists, National Institute of Oceanography, for helpful discussion.

References

Armstrong, F. A. J., and Harvey, H. W. (1950). The cycle of phosphorus in the waters of the English Channel. *J. mar. biol. Ass. U.K.*, **29**, 145–162.

Bush, A. J., Lenczar, R. E., Murray, J. E., and Soule, F. M. (1955). International ice observation and ice patrol service in the North Atlantic Ocean Season of 1953. *Bull. U. S. Cst. Guard*, 39, 138.

Hansen, A. L., and Robinson, R. J. (1953). The determination of organic phosphorus with perchloric acid oxidation. *J. mar. Res.*, **12**, 31–42.

McGill, D. A. (1964). The distribution of phosphorus and oxygen in the Atlantic Ocean, as observed during the I.G.Y., 1957–1958. Progress in Oceanography. Vol. 2. Pergamon Press, London.

Rao, S. V. S. (1957). Preliminary observations on the total phosphorous content of the inshore waters off Calicut. *Proc. Indian Acad. Sci.*, **45**, 77–85.

Redfield, A. C., Smith, H. P., and Ketchum, B. H. (1937). The cycle of organic phosphorus in the Gulf of Maine. *Biol. Bull., mar. biol. Lab., Woods Hole*, **73**, 421–423.

Rochford, D. J. (1958). Total phosphorus as a means of identifying East Australian water masses. *Deep Sea Res.*, **5**, 89–110.

——(1962). Hydrology of the Indian Ocean. II. The surface waters of the South-east Indian Ocean and Arafura Sea in the spring and summer. *Aust. J. mar. freshwat. Res.*, **13**, 226–251.

Ryther, J. H., and Menzel, D. W. (1965). On the production, composition and distribution of organic matter in Western Arabian Sea. *Deep Sea Res.*, **12**, 199–209.

Seshappa, G., and Jayaraman, R. (1956). Observations on the composition of bottom muds in relation to phosphate cycles in the waters of the Malabar Coast. *Proc. Indian Acad. Sci.*, **43**, 288–301.

Strickland, J. D. H., and Austin, K. H. (1960). Forms of phosphorus in NE Pacific waters. *J. Fish. Res. Bd Can*, **17**.

Wooster, W. S., and Rakestraw, N. W. (1951). The estimation of dissolved phosphates in sea water. *J. mar. Res.*, **7**, 49–55.

ON THE OCCURRENCE OF OXYGEN MAXIMA AND MINIMA IN THE UPPER 500 METERS OF THE NORTH-WESTERN INDIAN OCEAN

By D. Panakala Rao and R. Jayaraman

Reprinted from *Proceed. Indian Acad. Sci. (Bangalore)*, vol. LXXI, B, no. 6, 1970, p. 230-246

ON THE OCCURRENCE OF OXYGEN MAXIMA AND MINIMA IN THE UPPER 500 METERS OF THE NORTH-WESTERN INDIAN OCEAN

By D. Panakala Rao and R. Jayaraman

(Indian National Oceanographic Data Centre, National Institute of Oceanography Miramar, Panaji, Goa)

Received September 23, 1969

(Communicated by Dr. N. K. Panikkar, F.A.SC.)

Abstract

The depths of occurrence of oxygen maxima and minima have been studied in the upper 500 meters of the north-western Indian Ocean (including Arabian Sea and Laccadive Sea). The data collected by various ships during the International Indian Ocean Expedition were pooled into one degree grids and analysed for getting patterns of distribution—seasonally and regionally.

The studies reveal that there is much variation in the depths of occurrence of oxygen maxima and minima in different areas and different seasons in the north-western Indian Ocean. Along the continental shelf all over the Arabian Sea, biological activity appears to play a predominant role in controlling the oxygen content, while in the open parts of the ocean the depths of occurrence of oxygen maxima and minima mainly appear to be governed by the water movements, circulation and mixing. one of the important observations is the existence of stagnant or near-stagnant conditions in the more central part of the Arabian Sea, restricting the exchange of water masses with the adjoining seas.

Introduction

During the International Indian Ocean Expedition (1960–65) a considerable amount of data has been collected by most of the participating ships on the distribution of dissolved oxygen in the different areas of the Indian Ocean. While these studies involve the general pattern of distribution both in the vertical and horizontal and the occurrence of oxygen minima, no detailed work has yet been undertaken on the occurrence of layers of oxygen maxima and minima and their seasonal variations. This type of study, while giving a general pattern of seasonal and regional variations in oxygen maxima and minima, will also help in an understanding of water movements and mixing processes, and potential productivity in the different regions of the Indian Ocean, as the oxygen content of the upper layers is intimately related to biological activities. The present paper deals with the surface and sub-surface layers of the north-west Indian Ocean in the upper 500 metres.

The oxygen maxima in the Arabian Sea in the upper layers has been discussed by Rochford (1966) and Khimitsa (1968). The oxygen minimum in the sub-surface layers in the tropical marginal seas of the world oceans was reported in the Pacific and Atlantic Oceans (Wust, 1935; Dietrich, 1937; Seiwell, 1937) and has been attributed to several factors such as limited circulation in the basins and oxidative processes of the organic matter (Sverdrup, 1938; Kawamoto, 1935; Wattenberg, 1939; Redfield, 1942). During the John Murray Expedition of 1933–34 (Gilson, 1937) well-defined oxygen minima were observed in the central and northern Arabian Sea. Clowes and Deacon (1935) reported oxygen minimum between the 300–100 meter layers with oxygen concentration of less than 0·8 ml/L at 8° N and further stated that at 11° S this minimum with oxygen content of 2·0 ml/L is found at 1,200 meters. Schott (1935) pointed out that the sub-surface oxygen minimum is most prominent at about 50 meters off Bombay, while Carruthers *et al.* (1959) found the oxygen minimum at a depth of 18 meters at a distance of 18 nautical miles off Bombay and stated that the oxygen minimum lies below the salinity maxima and occasionally reaches surface layers. Neyman (1961) referring to the presence of oxygen minima along the entire west coast of India states that both the oxygen content and the thickness of the layer are sharply heterogeneous. Vinogradov and Voronina (1961) correlated the minimum values for oxygen in the sub-surface layers with plankton in the Arabian Sea. According to their studies the oxygen below 150 meters dropped suddenly to 0·15 ml/L or sometimes below this value. Further studies by Gallagher (1966), Warren *et al.* (1967), Elizarov (1968), Timofeev (1968) and Khimitsa (1968) confirmed the above results. The sub-surface oxygen minimum was generally correlated with high phosphates (Timofeev, 1968; Reddy and Sankaranarayanan, 1968). Khimitsa (1968) attributed oxygen minimum in the north-western Indian Ocean, especially in the north and north-eastern parts of Arabian Sea to the aging of the Red Sea waters introduced through the Gulf of Aden into the subsurface and intermediate depths and to limited circulation in the area.

Area of investigation, data and analysis.—The observations presented here relate to the depths of occurrence of oxygen maximum and minimum in the north-western Indian Ocean, including the Arabian Sea and the Lacca-dive Sea (Special Publication No. 23 of International Hydrographic Bureau) covering the grid between the equator and the northern-most part of the Arabian Sea, *i.e.*, upto Pakistan and Iran coasts and 45°-80° E longitude.

For convenience and ease of interpretation, the following seasona classification has been adopted:

(1) Summer or hot weather season—March, April and May;

(2) South-west monsoon season—June, July and August;

(3) Post-monsoon season—September, October and November; and

(4) North-east monsoon season or winter monsoon—December, January and February.

All the available data on oxygen maxima and minima with corresponding depths of occurrence collected by different ships during the IIOE period in the region have been taken into consideration. The data were pooled into one degree squares seasonally and the averages taken as the representative values for that square. In selecting the depths for oxygen maxima and minima certain arbitrary limits were fixed for the maximum and minimum concentrations of oxygen. All values of oxygen which fell between 4·5 and 5·5 ml/L or above have been included as maxima and the values of oxygen which fell between 0 and 1·0 ml/L. were taken as minimum. These limits were chosen because the occurrence of the respective values have the 80–90% probability.

After pooling the data, the depths were plotted on maps for oxygen maxima and minima for each season. Contours were drawn at the intervals of 5–10 meters in the case of maxima and 25–50 metres in the case of minima, depending on the extent of variation of the values (Figs. 1 to 8).

RESULTS

Summer season.—Figures 1 and 2 show the depths of oxygen maximum and minimum respectively during the summer months. In regard to the oxygen maximum it is seen that in the shelf waters along the west coast of India (eastern Arabian Sea) oxygen maximum occurs between 1 and 12 meters except at 9° N latitude where the maximum is seen to exist at 30 meters. Taking the whole of the north Indian Ocean, west of the Indian Peninsula, it is observed that there is a central zone extending north to south and comprising of a number of cells (A to J in Fig. 1) where the oxygen maxima occur fairly deep at depths exceeding in most of the cases 50 metres and sometimes going down to as much as 86 meters (H). On either side of this central zone extending eastwards to the coast of India and westwards to the coast of Arabia, including the Gulf of Aden, oxygen maxima invariably exist in the upper layers often reaching the surface as the coast is approached. Thus the central part of the Arabian Sea is characterized by having deep oxygen maximum during this season.

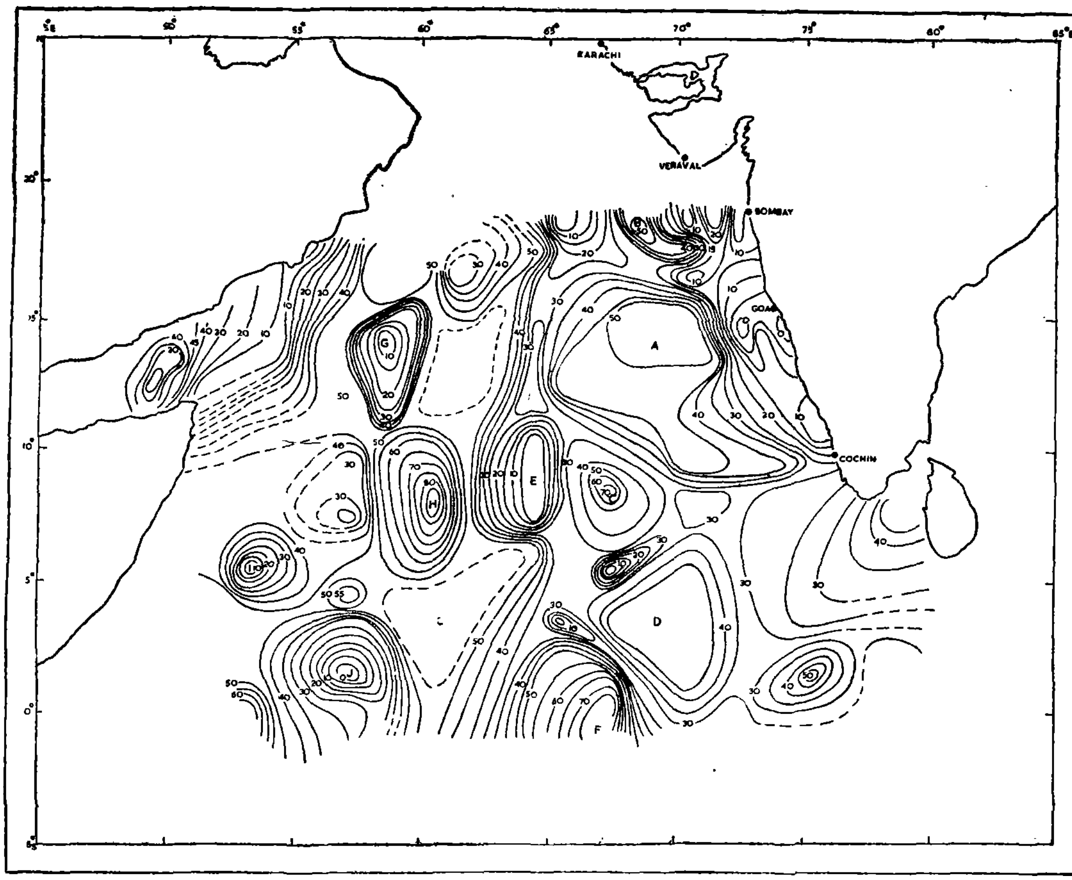

FIG. 1. Depths of occurrence of oxygen maximum during summer season (March, April and May).

'A and B' represent the areas of occurrence of oxygen maxima at about 50 meters. 'C' represents the area of occurrence of oxygen maxima at about 70 meters. 'D' represents the area of occurrence of oxygen maxima below 75 meters. 'E and J' represent the areas of occurrence of oxygen maxima in the surface waters. 'F' represents the area of occurrence of oxygen maxima around 75 meters. 'G and I' represent the areas of occurrence of oxygen maxima in the first 10 meters. 'H' represents the area of occurrence of oxygen maxima around 85 meters.

While the depths of occurrence of oxygen minimum show a similar cellular pattern, the comparison with the depths of oxygen maximum ends here. In general, there is no regularity in the pattern of distribution. The highest value for depth of minimum is 522 meters and that is observed in the area bounded by 14° and 15° N latitude and 72° and 73° E longitude (that is to say in the eastern Arabian Sea nearer the Indian west coast off Goa). North and south of this area oxygen minimum comes up to 200 meters. As the equator is approached in this eastern part, there is shoaling with the oxygen minimum layer reaching up to 120 meters. Proceeding westwards towards western and central parts of the Arabian Sea, the oxygen

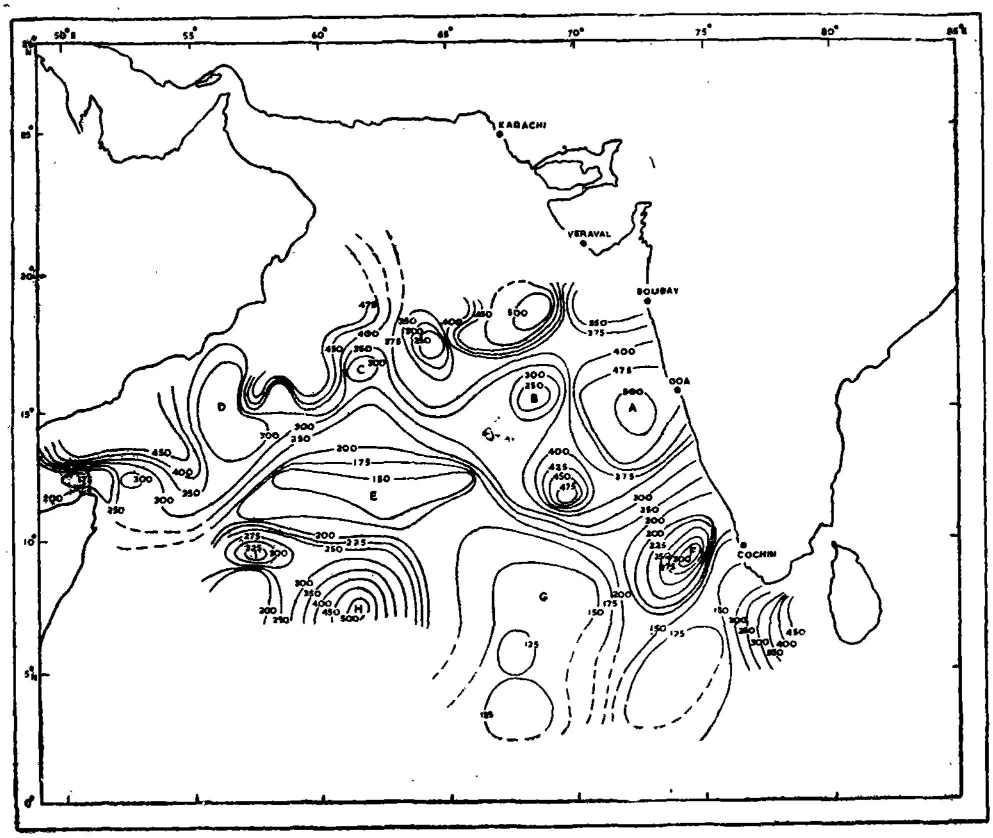

FIG. 2. Depths of occurrence of oxygen minimum during summer season (March, April and May).

'A and H' represent the areas of occurrence of oxygen minimum around 500 meters. 'B' represents the area of occurrence of oxygen minimum at about 250 meters. 'C, D, F and I' represent the areas of occurrence of oxygen minimum at about 300 meters. 'E' represents the area of occurrence of oxygen minimum at about 150 meters. 'G' represents the area of occurrence of oxygen minimum at less than 150 meters.

minimum is seen to exist between 130 and 500 meters; often there is an alternation of deepening and shoaling resembling a sine wave.

South-west monsoon season.—Figure 3 shows the distribution of oxygen maximum during south-west monsoon season. The oxygen maxima in the eastern and western fringes of the Arabian Sea are observed in depths ranging from 0 to 10 metres. In the Central Arabian Sea deep occurrences of oxygen maxima are seen but not to that extent as during summer months.

From the east coast of Arabia down to the Gulf of Aden, maximum values are seen mostly at the surface while at the mouth of the Gulf of Aden

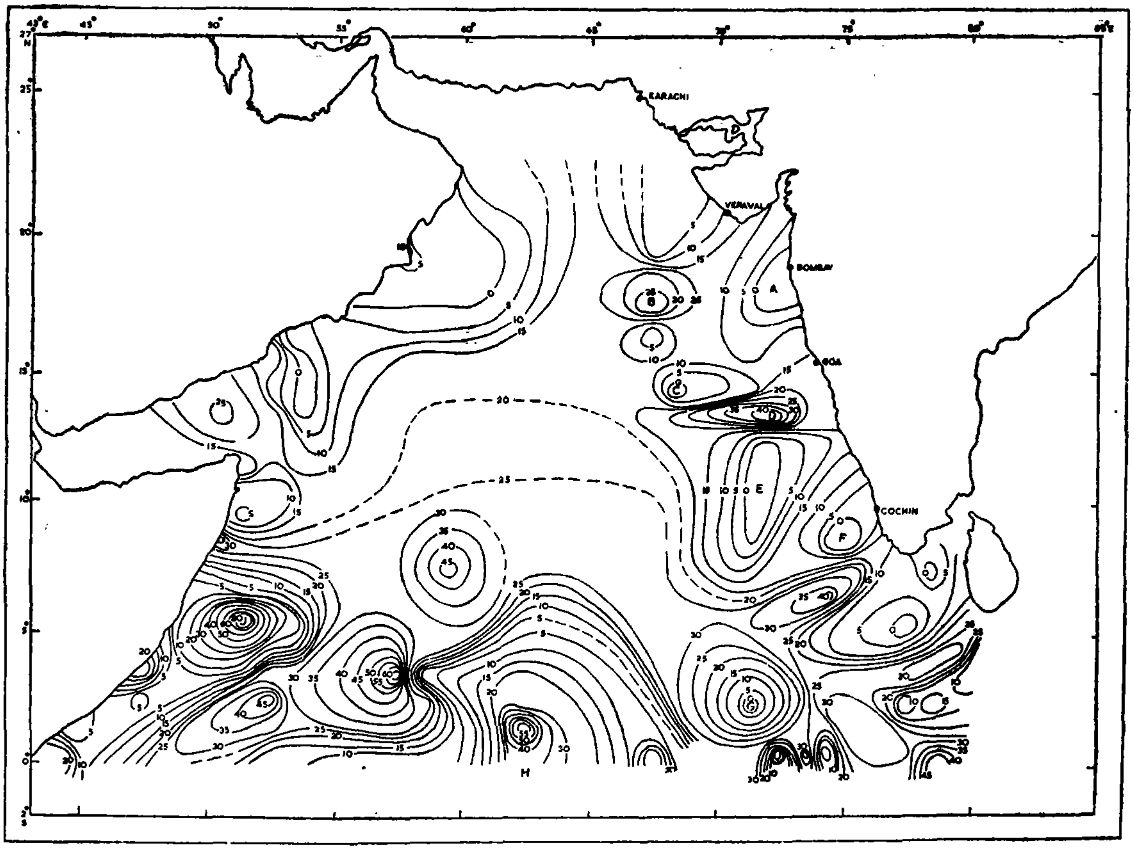

FIG. 3. Depths of occurrence of oxygen maximum during south-west monsoon season (June, July and August).

'A, B, E, F and G' represent the areas of occurrence of oxygen maximum in the surface. 'B' represents the area of occurrence of oxygen maximum at about 25 meters. 'D' represents the area of occurrence of oxygen maximum at about 40 meters. 'H' represents the area of occurrence of oxygen maximum at about 55–60 meters. 'I' represents the area of occurrence of oxygen maximum at about 60 meters. 'J' represents the area of occurrence of oxygen maximum at about 80 meters.

it is at 25 meters. Off the eastern Somali coast at 51–52° E longitude and 5–6° N latitude a closed cell (J) is formed where the oxygen maximum is seen to occur at a depth of 83 meters with steep gradients around this grid. In the northern-most and the open regions away from the coastal influences, the depth of oxygen maximum ranges between 20 and 25 meters.

Figure 4 shows the distribution of oxygen minimum. Off Bombay in the northern Arabian Sea, oxygen minimum is seen at 400 meters, but towards west (in the grid 17–18° N and 67–68° E) it occurs higher up at 150 meters (cells 'A' and 'B'). In the southern part, off Cape Comorin, the

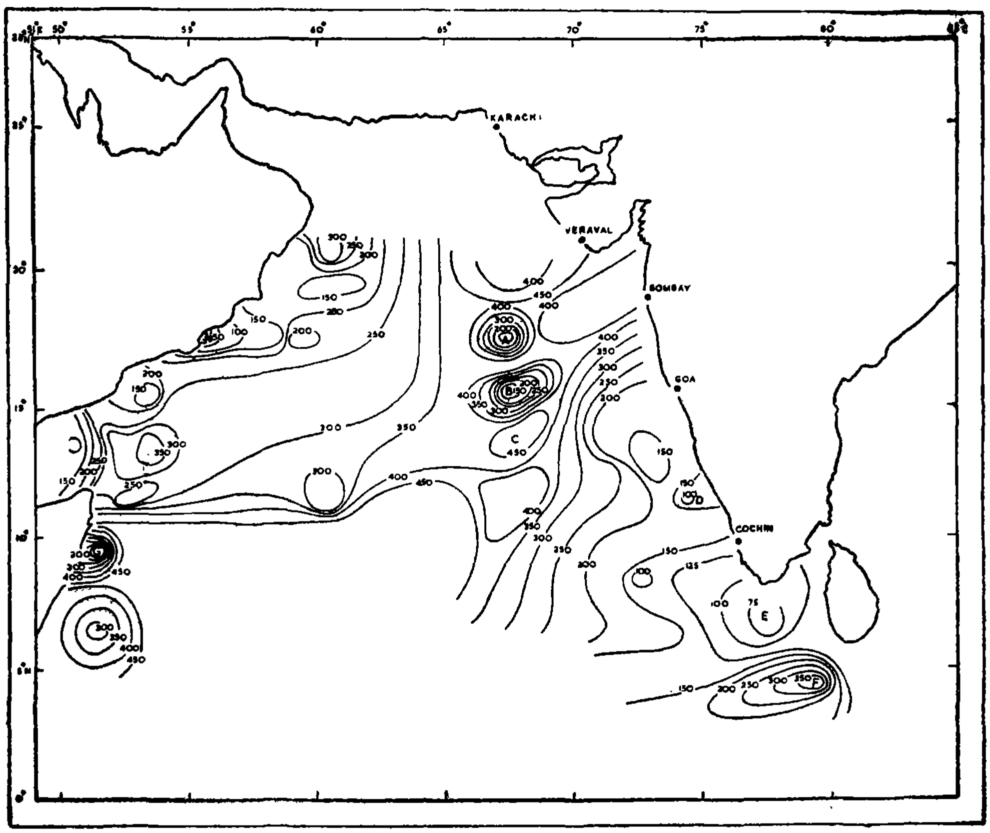

FIG. 4. Depths of occurrence of oxygen minimum during south-west monsoon season (June, July and August).

'A, B and G' represent the areas of occurrence of oxygen minimum at about 150 meters. 'C' represents the area of occurrence of oxygen minimum at about 450 meters. 'D' represents the area of occurrence of oxygen minimum at about 100 meters. 'E' represents the area of occurrence of oxygen minimum at about 75 meters. 'F represents the area of occurrence of oxygen minimum at about 250 meters.

oxygen minimum layer has come up to 75 meters (Cell E). Further south it deepens and goes down to 370 meters (Cell F).

Off eastern Arabian coast the depths of oxygen minimum vary between 30 and 200 meters, the lowest value being at the south-eastern part of Arabian Peninsula. Towards the Gulf of Aden and around Socotra Island, the depth increases. Off the Somali coast the minimum is found at a depth of 130 meters.

Post-monsoon season.—The distribution of oxygen maxima and minima for the post-monsoon season is shown in Figs. 5 and 6 respectively. In

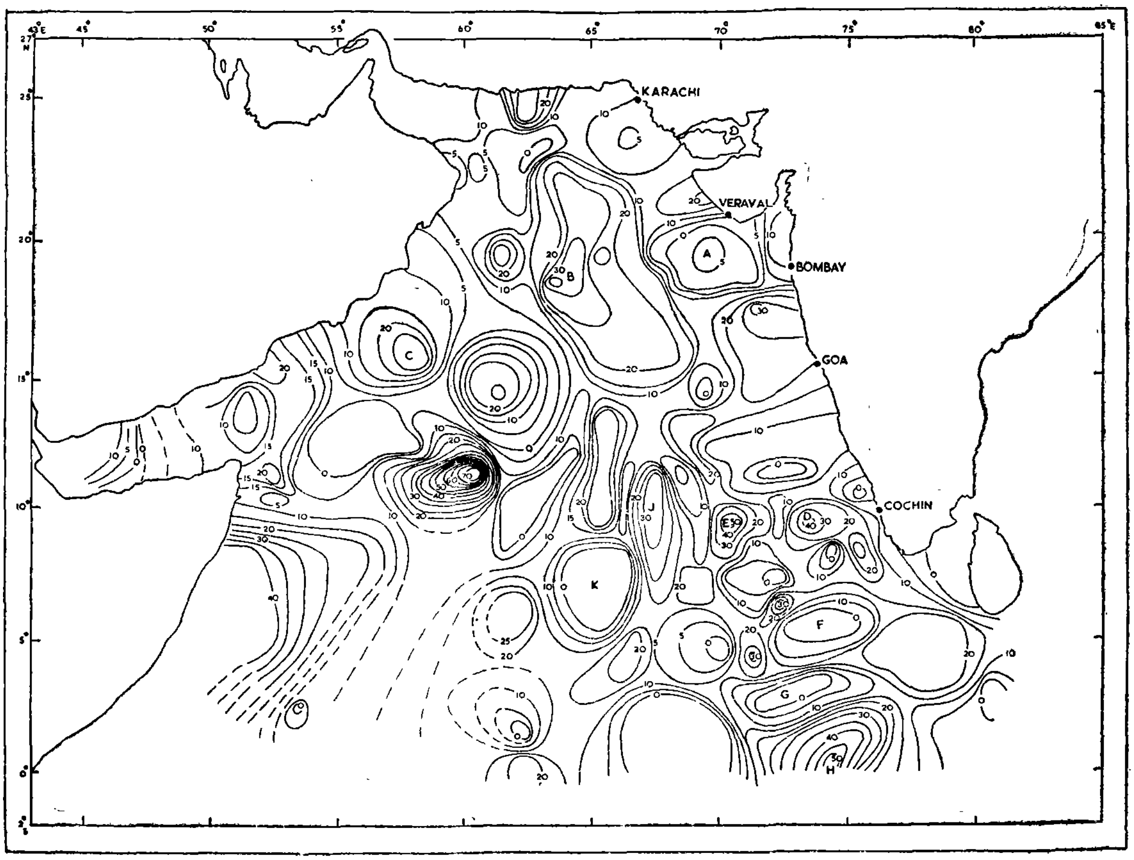

FIG. 5. Depths of occurrence of oxygen maximum during post-monsoon season (September, October and November).

'A' represents the area of occurrence of oxygen maximum between 0–5 meters. 'B' represents the area of occurrence of oxygen maximum at about 35 meters. 'C' represents the area of occurrence of oxygen maximum at about 25 meters. 'D' represents the area of occurrence of oxygen maximum at about 50 meters. 'F, G, I and K' represents the area of occurrence of oxygen maximum in the surface. 'J' represents the area of occurrence of oxygen maximum at about 30 meters. 'L' represents the area of occurrence of oxygen maximum below 70 meters.

B2

both the cases, the distribution pattern appears to be ' cellular '. The oxygen maxima are present off the west coast of India almost at the surface, the depths of occurrence oscillating in general between zero and 30 meters. Surface oxygen maximum is more common along the east coast of Arabia and southern Arabian Sea, going to deeper layers such as 30 metres along the northern-most parts of the sea and to 50 metres at ' H '. South of 10° N off the Somali coast the maximum exists between 0 and 25 meters with steep-gradients (Cell L).

FIG. 6. Depths of occurrence of oxygen minimum during post-monsoon season (September, October and November).

'A, B, C, E and K' represent the areas of occurrence of oxygen minimum between 150–200 meters. 'D, G and I' represent the areas of occurrence of oxygen minimum at about 500 meters. 'F' represents the area of occurrence of oxygen minimum at about 400 meters. 'H' represents the area of occurrence of oxygen minimum at about 300 meters. 'J' represents the area of occurrence of oxygen minimum at less than 100 meters.

North-east monsoon season.—Figures 7 and 8 show the depths of occurrences of oxygen maximum and minimum respectively during north-east monsoon season.

The oxygen maximum is found in the upper layers along the west coast of India between 5–10 meters, sinking to 30 meters at a few places. But in the central Arabian Sea, in the area bounded by 63–64° E longitude and 16–17° N latitude the oxygen maximum sinks to 100 meters (at 'A') and rises to upper levels both in the southern and northern parts of the Arabian Sea. At the mouth of the Gulf of Aden, the oxygen maximum reaches a depth of about 30 meters. South of 5° N, the maximum occurs at 45 meters.

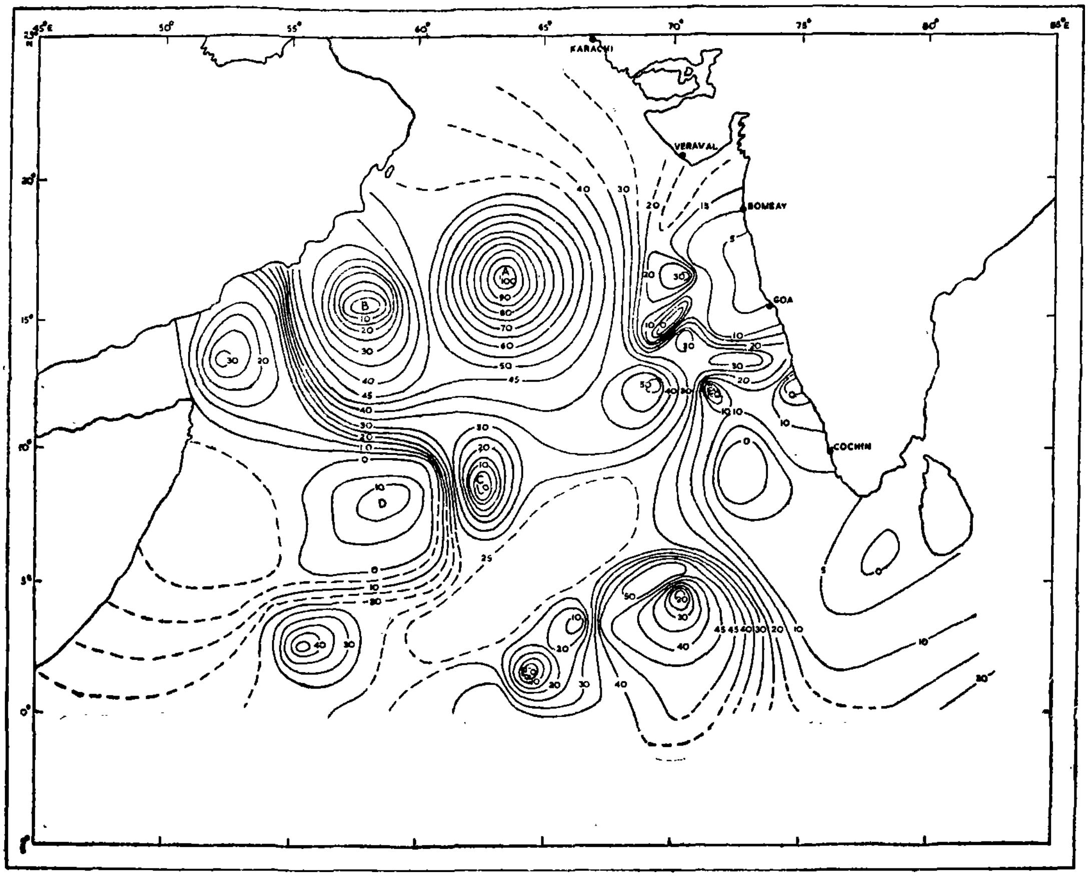

FIG. 7. Depths of occurrence of oxygen maximum during north-east monsoon or winter monsoon (December, January and February).

'A' represents the area of occurrence of oxygen maximum at about 100 meters. 'B, C, E and F' represent the areas of occurrence of oxygen maximum at the surface, 'D' represents the area of occurrence of oxygen maximum at about 10 meters.

The main features (Fig. 8) of the occurrence of oxygen minimum along the west coast of India are that from the southern tip to the Gujarat coast, the minimum occurs in the deeper layers when compared to the south-west monsoon season, occurring between 300–500 meters, but not less than 300 meters deep. In the open Arabian Sea the minimum shoals up and found at depths between 120–150 meters along 70° E longitude (Cells A and B). Off Cochin, it is found to sink to 500 meters (Cell C) and thereafter to shoal to 150 meters towards the open sea (Cell D). South of the Indian Peninsula also the oxygen minimum sinks to 500 meters. In the central Arabian Sea the minimum is found at 400 meters deep shoaling to 150 meters in the southern part of the sea. In the mouth of Gulf of Aden, it reaches to 350 meters and rises up to upper levels towards the Gulf of Aden. Increasing trend of depths of oxygen minimum is also found south of Somali coast.

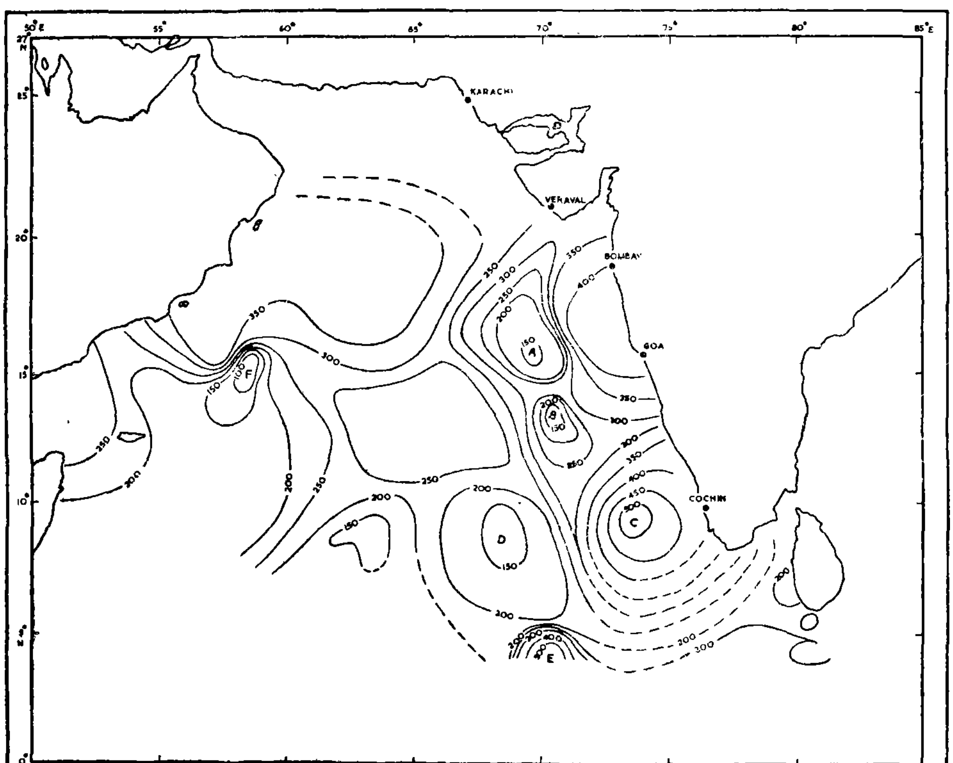

FIG. 8. Depths of occurrence of oxygen minimum during north-east monsoon or winter monsoon (December, January and February).

'A, B and D' represent the areas of occurrence of oxygen minimum at about 150 metres. 'C and E' represent the area of occurrence of oxygen minimum at about 500 meters. 'F' represents the area of occurrence of oxygen minimum at about 100 metres,

Discussion

The results presented in the earlier section make it abundantly clear that there are considerable seasonal and regional variations in the distribution of oxygen in the upper 500 meters of the North-western Indian Ocean, which includes mainly the Arabian Sea, the Laccadive Sea, the Gulf of Aden and the Persian Gulf. The most important factor controlling the distribution of oxygen is physical, such as exchanges across the sea surface, oceanic circulation and water movements, although biological conditions such as photosynthetic production and respiratory activities of the organisms gain importance in certain selected regions, particularly along the coasts. On the other hand, in the open parts of the ocean we have to take into account the circulation pattern and water movements as the major contributing factor.

During the months constituting the south-west monsoon the south-east trades from the southern hemisphere cross the equator and blow as south-westerly winds along the Somali coast. The winds are rather steady in this region and they blow mainly towards north and north-east along the Somali-Arabian coasts, then take an easterly course in the more open parts of the ocean (Swallow, 1965, Swallow and Bruce, 1966, Warren, B., 1965, Warren *et al.*, 1966, Gallagher, 1966). Under the influence of these winds the high speed Somali current crosses the equator bringing with it the oxygen-rich Indian Equatorial waters. The turning of the current away from the coast north of 6° N latitude gives rise to intense upwelling nearer the Somali coast. Thus an ' oxygen front ' is created with low oxygen water nearer the coast and a high oxygen water away from the coast, the axis of the Somali current forming some kind of a boundary between these two types of waters. The current travelling away from the coast gives rise to convergence cells north of 5° N and along 60° E. The northern limits of these convergence cells are sometimes seen as far as 10° N. The oxygen maximum sinks here to depths of about 90 meters with values ranging from 4·5 to 4·35 ml/L.

Along the Arabian coast the upwelling processes reduce the oxygen content in the surface layers but soon this is compensated by high organic production-photosynthetic activity leading to oxygen enrichment of the upper layers. The Arabian shelf is narrow and the highly productive waters are carried farther and farther off-shore, where the transparency is high. It is thus possible that the column production is high resulting in deepening of the layers of oxygen maxima. Oxygen maxima are observed at about 50 meters in this area.

Coming nearer the Indian coast, the large influx of river-water, the high degree of turbulence due to monsoonal winds, give rise to increased turbidity of the waters, thereby reducing considerably the thickness of the photic zone. Thus very often, the oxygen maxima are seen in the surface layers only.

One of the noteworthy features during the south-west monsoon is that the circulation and water movements are predominantly meridional and hence a greater part of the north-western Indian Ocean, including the Arabian Sea, is occupied by water spread northwards from the equatorial Indian Ocean. The equatorial Indian Ocean being a region of strong currents and consequently high degree of ventilation, the spreading of these waters to the northern part of the Arabian Sea results in a considerable degree of oxygenation of these waters with the exception of upwelling areas near the Somali-Arabian coast and the south-west coast of India. This factor should therefore determine to a large extent the depths of occurrence of oxygen maxima and minima in the different areas in this part of the Indian Ocean.

When we consider, on the other hand, the conditions during the north-east monsoon, when there is a reversal of winds, oceanic circulation and water movements, it is seen that the predominant flow becomes zonal—the North Equatorial Current system gaining in intensity and becoming important. Due to opposing forces the Somali current becomes insignificant. The coastal current off the west coast of India becomes northerly. Again compared to the southerly drift along this coast during the south-west monsoon months, the northerly drift is somewhat weaker, intensifying perhaps only north of Bombay where this takes a north-westerly turn conforming to the coastal configuration and in line with the general circulation pattern. As a result of this circulation pattern, in a greater part of the central and northern Arabian Sea, there are no appreciable water movements—a near stagnation condition prevailing in certain areas. The sub-surface conditions, however, reflect to some extent the characteristics of Red Sea and Persian Gulf waters.

The southern part of the Arabian Sea is, however, influenced to a considerable extent by the waters brought in by the North Equatorial Current system from the eastern Indian Ocean and the Bay of Bengal. Thus oxygen distribution pattern in the southern Arabian Sea conforms to the conditions prevailing in the eastern Indian Ocean and the Bay of Bengal.

In discussing the depths of occurrence of oxygen minima in the upper 500 metres of the northern Indian Ocean, one has to consider the source of oxygen minima in relation to biochemical cycles as well as the pattern of circulation. Of course the most essential data required for this purpose are the depths of occurrence of oxygen minimum layer, the minimum oxygen concentration and also the thickness of this layer. The last-mentioned parameter will give the necessary clue to the biological and biochemical activities in the upper surface layers. The importance of biological and biochemical activities leading to the oxidation of organic matter with consequent consumption of oxygen as the organic materials sink to deeper levels, has been fully highlighted by earlier workers (Richards, 1957). The respiratory activities of the organisms leading to reduction of oxygen concentration in oxygen-poor layer has also been mentioned by Harvey (Harvey, 1963). The application of these ideas to the conditions in the Arabian Sea and other open parts of the northern Indian Ocean requires a detailed knowledge of the biological productivity and distribution of organisms in this region of the Indian Ocean. A fairly good picture of the plankton biomass has been brought out in the detailed and interesting paper by Prasad (under publication).

One of the most interesting and detailed accounts on the oxygen distribution in the Arabian Sea containing an explanation for the formation of oxygen minimum in the region is that of Khimitsa (1968). This author has summarised the observations of Smetanin (1959) and Neyman (1961) besides stating his own views. Khimitsa mentions that the views of Smetanin are more or less in accord with those of Seiwell (1937). Seiwell has mentioned that the oxygen minimum may appear and re-appear with a continuous decrease in both the horizontal current velocity, or maximum oxygen consumption may, perhaps, coincide with the depth of oxygen minimum layer. He has also noted that the vertical distribution of oxygen results from development history of the water masses and that the effects of infinitely small processes may be considerably increased by their manifold repetitions.

Neyman (1961) relates the formation of oxygen minimum to the regions of formation of deeper water masses in the Arabian Sea. Referring to the Gulf of Aden and the Persian Gulf as the main source regions, Neyman states that 'the surface waters of these regions with high salinity and temperature (with consequent low concentration of oxygen) sink and spread to the sub-surface levels contributing to the oxygen minimum in the whole of the Arabian Sea'. But there is some difficulty in our accepting Neyman's hypothesis because in the Gulf of Aden, which has been shown to be a very high productive zone where oxygen saturation is known to reach as high as 110–115% and in the Persian Gulf, which is comparatively shallow, thermohaline convection leads to thorough mixing and consequent enrichment of oxygen in the entire column. The sinking and spreading of these waters is more likely to enrich the sub-surface layers rather than deplete them of oxygen. Thus the formation of layer of oxygen minima with extremely low concentrations of oxygen is more likely to be attributed to the near-stagnant conditions in the central and northern parts of the Arabian Sea.

The Soviet oceanographers who had carried out investigations in this region have reported the occurrence of hydrogen sulphide in the intermediate depths in the northern Arabian Sea (Ivanenkov and Rozanov, 1961) which is an indication of stagnant or near-stagnant conditions. In this connection a reference to the interesting paper by Mokievskaya (1961) would be pertinent, as she discusses the hydrochemical conditions at the intermediate layer leading to the formation of hydrogen sulphide.

In concluding this discussion on the occurrence of oxygen minimum, it is particularly emphasized that the studies on the intermediate water masses of the Indian Ocean, with particular reference to occurrence of oxygen minima—sometimes alternating with layers of oxygen maxima—would be a most fruitful line of research and this would solve some of the most complicated problems of circulation and sub-surface water movements in this part of the Indian Ocean.

ACKNOWLEDGEMENTS

The authors wish to express their grateful thanks to Dr. N. K. Panikkar, Director, National Institute of Oceanography, for his interest and valuable suggestions in the preparation of this paper and his kind permission for its publication. Thanks are also due to Shri Des Raj Mongia for his invaluable help in preparing the illustrations for publication.

REFERENCES

Carruthers, J. N., Gogate, S. S., Naidu, J. R. and Laevastu, T. — "Shorewards upwelling of the layer of minimum oxygen off Bombay: Its influence on marine biology, especially fisheries," *Nature, London*, 1959, **183** (4668), 1084–87.

Clowes, A. J. and Deacon, G. E. R. — "The deep water circulation of the Indian Ocean," *Ibid.*, 1935, **136** (3450), 936–38.

Dietrich, G. — "Uber Bewegung und Herkunff des Golfstromwassers inst," *Merresk, Univ. Berl. Veroff, N.F. Ser. A*, 1937, **33**, Tiel 2: 53–91.

Elizarov, A. A. .. "Oceanological researches off the west coast of India," (In Russian), *Proc. Sov. Fish Invest. in the Indian Ocean and Adjacent Waters*, 1968, **64** (1), 94–101.

Gallegher, J. F. .. *The Variability of Water Masses in the Indian Ocean*, National Oceanographic Data Centre, General Series, 1966, Publication G-11, pp. 74.

Gilson, H. C. .. "The nitrogen cycle," John Murray Exped. of 1933–34, *Sci. Repts.*, London, 1937, **2** (8), 21–81.

Harvey, H. W. .. *Chemistry and Fertility of Sea-waters*, Cambridge University Press, 1963, pp. 240.

Kawamoto, T. .. "On the distribution of the dissolved oxygen in the Pacific Ocean, Part I," *U.M.I. to Gora Kobe Marine Observatory*, 1935, **32**, 23–37.

Khimitsa, V. A. .. "On the vertical and horizontal distribution of oxygen off the western coast of India during the north-eastern monsoon," (In Russian), *Proc. Sov. Fish Invest. in the Indian Ocean and Adjacent Waters*, 1968, **64** (1), 162–80.

Mokievskaya, V. V. .. *Certain Hydrochemical Features of the Northern Part of the Indian Ocean*, Oceanological Research, Publication A.N. SSSR, Moscow, 1961, No. 4.

Neyman, V. G. .. "Formation of oxygen minima in the surface waters of the Arabian Sea," *Okeanol., Akad Nauk, SSSR*, Moscow, 1961, **4**, 62–65.

Redfield, A. C. .. "The processes determining concentration oxygen, phosl phates and other organic derivatives within the depths of the Atlantic Ocean," Papers in *Phy. Oceanogr. Meteorol.*, 1942, **9** (2), 1–22.

Reddy, C. V. G. and Sankaranarayanan, V. N. "Distribution of phosphates and silicates in the centra, western north Indian Ocean in relation to some hydrographical factors," *Bulletin of the National Institute of Sciences of India*, 1968, **38**, 103–22.

Richards, A. C. .. "Oxygen in the oceans," *Amer. Geol. Soc. Memoirs*, **67**, 1957, Vol. I, 185–238.

Rochford, D. J. .. "Source regions of oxygen maxima in intermediate depths of Arabian Sea," *Aust. J. Mar. Freshwater Res.*, 1966, **16** (2), 129–49.

Schott, G. .. *Geographic des Indischen und stilten Ozeans*, Hamburg-1935, pp. 413.

Seiwell, D. A. .. "The minimum oxygen concentration in the western basin of the north Atlantic," Papers in *Phy. Oceanogr. Meteorol.*, 1937, **5** (3), 24.

Smetanin, D. A. .. "On the causes of formation of the oxygen minimum layer and the laws of their disposition in the oceans," (In Russian), *Trudy Inst. Okeanol, Akad Nauk, SSSR*, Moscow, 1959, **33**.

Sverdrup, H. U. .. "On the explanation of oxygen minima and maxima in the oceans," *Jour. du conseil.*, 1938, **13**, 162–72.

Swallow, J. C. .. *Some Observations Made Aboard R.R.S. Discovery during August* 1964," Marine Obsr., London, July 1965.

———, and Bruce, J. G. Jr. .. "Current measurements off the Somali coast during the south-west monsoon of 1964," *Deep-Sea Res.*, 1966, **13** (5), 861–88.

Timofeev, N. A. .. "Distribution of oxygen and phosphorus in the Red Sea," (In Russian), *Proc. Sov. Fish Invest. in thê Indian Ocean, and Adiacent Waters*, 1968, **64** (1), 152–61.

Vinogradov, M. E. and Voronina, M. M. "Influence of the oxygen deficit on plankton distribution in the Arabian Sea (In Russian), *Okeanol.*, Vol I, No. 4, 670–78.

Warren, B. .. "The Somali Current," *Oceanus*, **12** (1), 2–7.

———, Stommel, H., and Swallow, J. C. "Water masses and pattern of flow in the Somali basin during the south-west monsoon of 1964," *Deep-See Res.*, 1966, **13** (5), 825–60.

Wooster, W. S., Schaefer, M. B. and Robinson, N. K. *Atlas of Arabian Sea for Fishery Oceanography*, University of California, Institute of Marine Resources, IMR Reference No. 67–12, May 1967.

Wattenberg, H. .. "Die entstchung der sauerstoffarmen zwischenschicht im Ozean," *Ann. Hydrogr. Bul.*, 1939, **67**, 257–66.

Wust, G. .. "Schlichtung und Zirculation des Atlantischen Ozean," Tiel 2, Die stratosphere. *Dtsch. Atlant. Expd. Meteorol.*, 1925–27, Wiss., Ergebn., 1935.

Part IV

Marine geology and geophysics

Reprinted from *Bull. natn. geophys. res. Inst. India*, vol. 1, 1963, p. 48-51

NOTE ON THE BOTTOM PROFILES OF THE WESTERN PART OF THE INDIAN OCEAN

by

V. S. RAMA RAJU,

Oceanographic Research Wing of N. G. R. I., Cochin.

The oceans and seas cover 70.8 per cent of the Earth's surface. The area of the Indian Ocean including its adjacent seas is nearly 75 million sq. km and equals approximately one-fifth of the total water cover or one-seventh of the total area of the globe. Its mean depth is very nearly 3,900 m. Although the Indian Ocean does not appear to lack in marine resources in comparison with the Atlantic and Pacific oceans, it has received very little attention in systematic oceanographic studies.

In the past, several oceanographic expeditions have been conducted in the Indian Ocean by various countries covering some areas starting with that by NOVARA in 1857-59 to the present (31st) cruise of VITIAZ (1959-60) conducted by the Academy of Sciences of U.S.S.R., in which the author participated during a part of the expedition. Most of the earlier expeditions were conducted when the equipment and methods of observation were not standardised, but they certainly created interest in furthering the knowledge of oceanography by many startling discoveries.

During its 31st cruise, the VITIAZ covered nearly 30,000 miles in the northern and central parts of the Indian Ocean over which systematic data collection was carried out in hydrology, hydrometeorology, marine biology and chemical oceanography. In the geological laboratory on board the ship, continuous recording of the ocean bottom was one of the main activities. For this purpose, six precision echo-sounders were put in operation throughout the period of the ship's traverses in relays and records were taken on special paper (this preserves the tracing for a fairly long period). The soundings were logged at one minute intervals of time.

Fig. 1 shows the route of the expedition from Cochin to Bombay. From the data collected during this part of the cruise, the bottom profiles of the western part of the Indian Ocean are shown in Figs. 2A to 2I, along the various sections. The vertical exaggeration of the profiles is 270:1. The position fixing of the stations is made by celestial methods and no corrections are applied to the echo-sounder observations. The depth of each station is the mean of the depths noted at start and end of

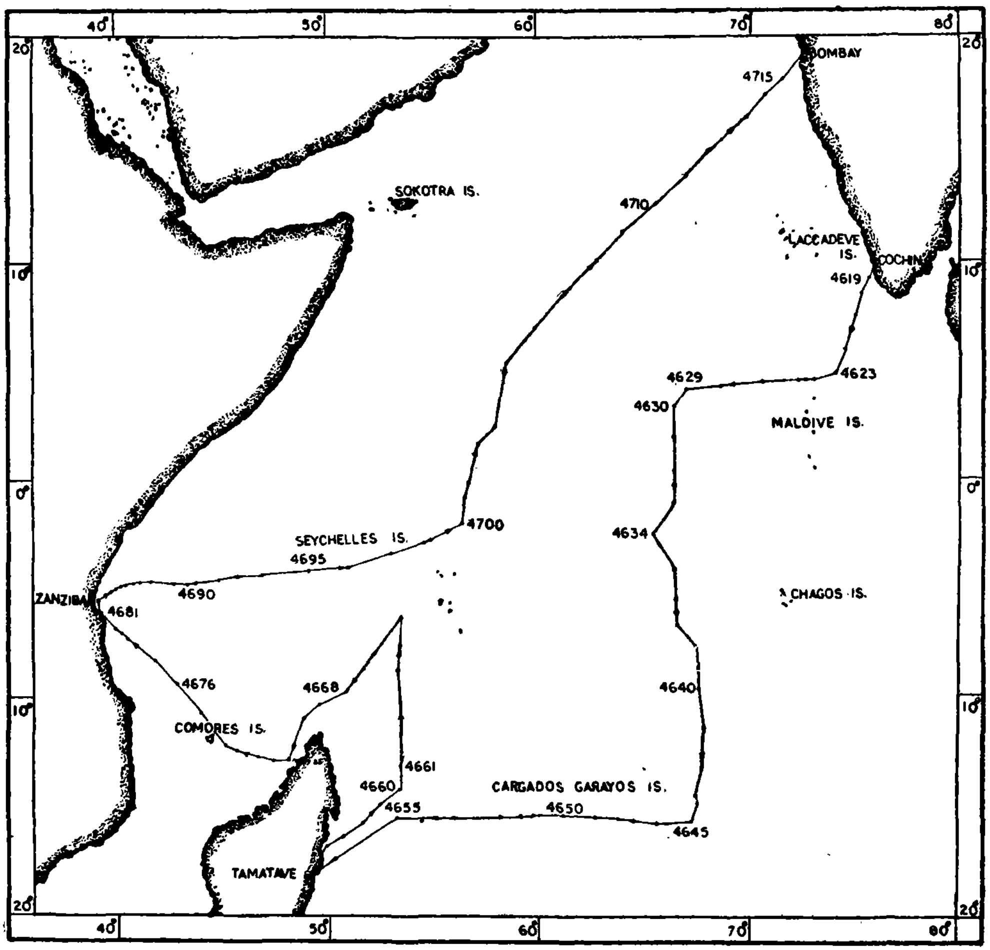

FIG. I STATION POSITIONS OF 31 ST CRUISE OF 'VITIAZ' (4 FEB-4 APRIL 1960)

station. The latitude and longitude are the mean positions of the ship while on station.

All the identified major features of the bottom profiles are noted and the figures are self-explanatory. In Fig. 2E at station 4661 is shown a newly discovered sea-mount (not shown in Admiralty charts) which

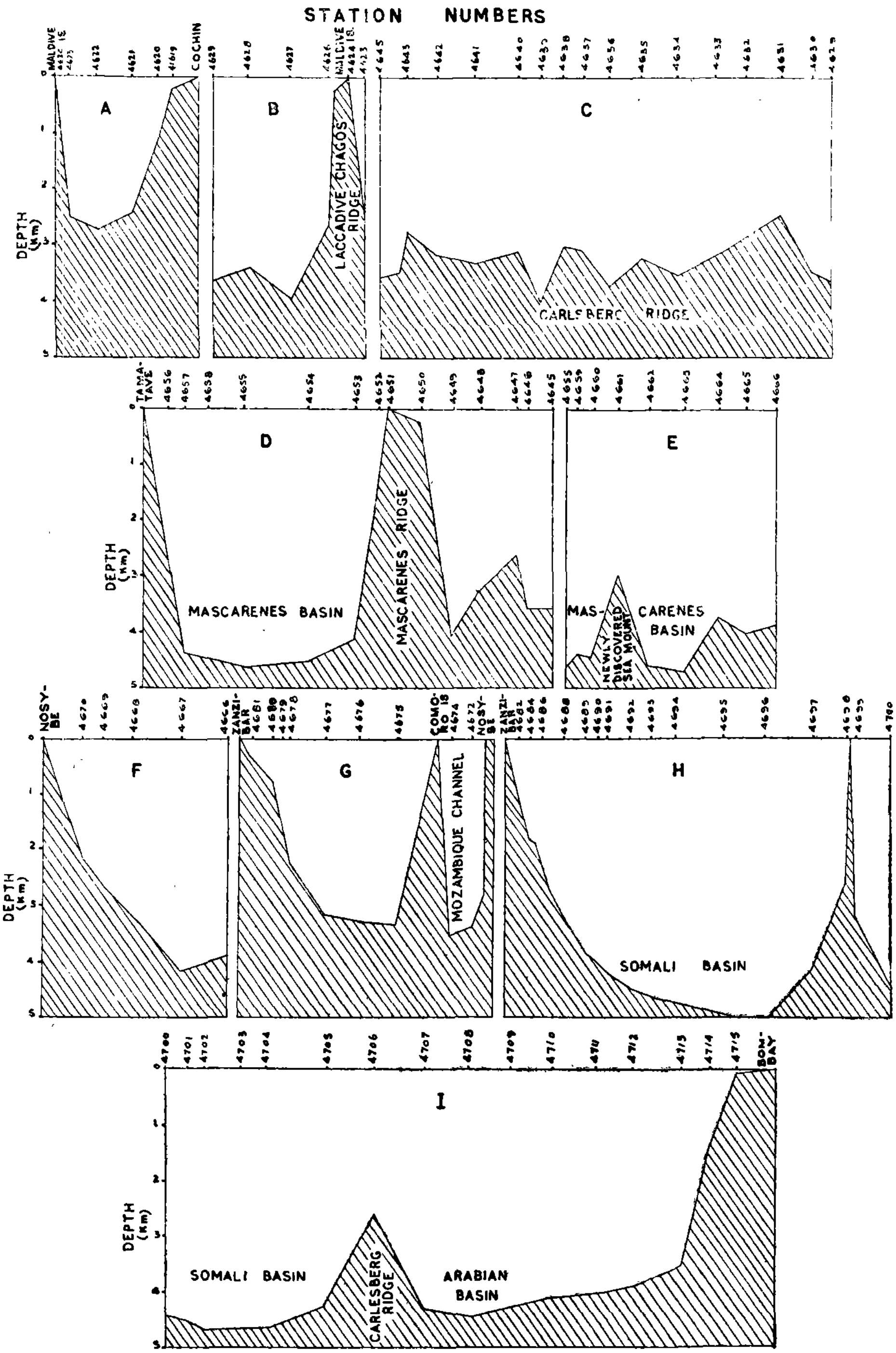

FIG.2 BOTTOM PROFILES OF WESTERN PART OF INDIAN OCEAN

rose from a mean depth of 4.5 to 3 km, and a detailed survey across the mountain has revealed that the shape of the mountain is conical. Further, preliminary studies of the nature and structure of the ocean bed from the collections of bottom grab and hydrostatic corer have revealed some very interesting features. At station 4660 in the region off Madagascar, both 'grab' and corer brought up large nodules of manganese which might be present in large quantities for economic exploitation. At station 4694 off Zanzibar, a core sample 10 m long taken from a depth of 4,720 m, contained 1.8 m of red clay and blackish-green mud in the top layer and the rest was clear sand. This appears to be the first observation of its kind in Indian Ocean, although similar reports of the presence of sands in the abyssal basins were first discovered in the Gazelle expedition (ANDRE 1920) in the South Atlantic and in recent years by ATLANTIS (1947) in the Hudson submarine canyon. Several theories of transport of material from the continents to the deep ocean basins by strong winds, by ice rafting, by turbidity currents, etc. have been put forward to explain deep-sea sands. But the theory of transport by turbidity currents appears to gain support from the observed good sorting and grading of the materials. These are only a few preliminary remarks on the initial results of the expedition and the detailed investigations will bring many new facts about the Indian Ocean.

From the physical oceanographic point of view, the knowledge of bottom topography of the oceans is vital in understanding the circulation of water.

ACKNOWLEDGEMENTS

I wish to express my thanks to Captain I. V. SERGEEV and Prof. Dr. B. G. BOGOROV, Leader of the expedition and all the members of the expedition for kindness and many courtesies extended on board VITIAZ.

REFERENCES

ERICSON, D. B., EWING, M. and HEEZEN, BRUCE C.—Deep-Sea Sands and Submarine Canyons *WHOI Collected Reprints*, 1951.

SVERDRUP, H. U., JOHNSON, M.W. and FLEMING, R.H.—*The Oceans, their Physics, Chemistry and General Biology*, 1087, Prentice—Hall Inc., 1942.

Reprinted from *Okeanologija*, vol. V, fasc. 4, 1965, p. 684-691

The structure of the terrestrial crust of the Indian Ocean, based upon geophysical studies

by P. A. Stroev and A. G. Gaïnanov

П. А. СТРОЕВ, А. Г. ГАЙНАНОВ

О СТРОЕНИИ ЗЕМНОЙ КОРЫ ИНДИЙСКОГО ОКЕАНА ПО ДАННЫМ ГЕОФИЗИЧЕСКИХ ИССЛЕДОВАНИЙ

Московский государственный университет им. М. В. Ломоносова

Обширные комплексные геофизические исследования строения земной коры к настоящему времени проведены в Атлантическом и Тихом океанах; Индийский океан наименее изучен в этом отношении, и сведения о строении земной коры являются весьма схематичными и недостаточно точными [11].

Первые геофизические исследования на акватории Индийского океана были проведены Венинг-Мейнесом в 1923 г. Результаты измерений силы тяжести были использованы для установления изостатического состояния и особенностей строения земной коры Индонезийских переходных зон [2]. В последующие годы гравиметрические исследования в Индийском океане были продолжены Венинг-Мейнесом, а также американскими и английскими геофизиками [24, 26—28].

Первые сейсмические исследования методом преломленных волн в Индийском океане были проведены Гаскеллом и Своллоу в районе Сейшельских о-вов и в восточной части океана [23]. На Сейшельских о-вах под слоем коралловых рифов мощностью 30 *м*, имеющих скорость продольных волн 2,1—2,7 *км/сек*, был обнаружен слой толщиной около 2,4 *км*, в котором скорость волн составляла 5,5—6,0 *км/сек*. Недостаточная протяженность профилей не позволила изучить структуру более глубоких горизонтов. К юго-западу от о. Суматра и к юго-востоку от о. Цейлон, в области глубин океана от 3 до 5 *км* были выявлены рыхлые осадочные отложения мощностью 0,2—0,8 *км*, скорость распространения продольных волн в которых составила 2,1 *км/сек*. Под этим слоем почти во всех пунктах устанавливается верхний слой мощностью 1,4—2,0 *км*, в котором скорости продольных волн 4,2—5,0 *км/сек*, подстилаемый слоем, вероятно «базальтовым», более плотных пород, где скорости 5,9—6,6 *км/сек*. В наиболее глубоководной части котловины «базальтовый» слой, где скорость 6,54 *км/сек*, начинается непосредственно под маломощным слоем осадков на глубине 0,46—0,76 *км* от дна океана.

В течение МГГ началось планомерное комплексное изучение Индийского океана, включающее различные геофизические исследования с целью выяснения особенностей глубинного строения земной коры [3, 12, 16 и др.].

В настоящее время интерес к изучению Индийского океана значительно возрос. Для координации океанологических исследований создана Международная Индо-океанская экспедиция, по программе которой выполнялись комплексные работы в 1959—1962 гг. английскими и американскими исследователями, а также 31—33 и 35 рейсы э/с «Витязь» в 1959—1962 гг. [13, 17—18, 22].

Первые советские геофизические исследования в Индийском океане были проведены во время плавания сотрудников ГАИШ и геологического факультета МГУ на дизель-электроходе «Обь» в составе Советских антарктических экспедиций. Производились измерения силы тяжести при помощи морских маятниковых приборов и морских гравиметров [3, 7—8, 19—21].

Во время МГГ Индийский океан был пересечен пятью рейсами советского немагнитного судна «Заря» [12]. На основании этих работ выявилось, что в океане существуют довольно четко различимые области относительно спокойного и аномального магнитных полей. Как правило, степень аномальности магнитного поля увеличивается в областях крупнейших поднятий дна океана, таких как плато Крозе, Центрально-Индийский хребет и др. Однако в целом аномальность не зависит от тех или иных частных форм рельефа дна океана, а определяется неоднородностью магнитных свойств пород, слагающих кристаллический фундамент дна. Очевидно, так называемый базальтовый слой, подстилающий осадочные отложения в океанах, крайне неоднороден по составу, и степень этой неоднородности может быть выявлена геофизическими методами только при весьма частых точечных или непрерывных маршрутных измерениях.

В 31-м рейсе э/с «Витязь» в 1959 г. были проведены первые советские сейсмоакустические исследования в Индийском океане методом отраженных волн [13]. Были выполнены два профиля: первый — через Яванский глубоководный желоб, второй — к востоку от Африки в районе о. Занзибар. Общая протяженность профилей более 500 миль. Кроме того, в центральной части океана была определена мощность донных отложений на двух станциях. Скорости звука в верхней пачке осадочных отложений равны 1,8—2,5 *км/сек*.

На подводном склоне о. Ява на глубине 1530 *м* мощность осадочной толщи около 450 *м*. По мере удаления на юг вниз по склону происходит увеличение мощности осадков. Максимальной величины, более 1200 *м*, мощность осадочного слоя достигает в Балийской впадине, лежащей между внутренним и внешним хребтами Яванской дуги. На внешнем подводном хребте Яванского желоба мощность осадков уменьшается до 700 *м*. На склоне его она снова увеличивается и достигает на дне желоба около 1000 *м*. По мере движения в сторону океана происходит постепенное уменьшение мощности осадочного слоя до 600 *м*, а на дне котловины, расположенной на ложе океана в 350 милях от о. Бали, до 500 *м*.

На материковом склоне Африки мощность донных осадков на разрезе не превышает 500 *м* и очень медленно уменьшается по мере продвижения в сторону океанического ложа. В центральной части Индийского океана мощность донных осадков, определенная на двух станциях, не превышает 300 *м*. В конце 1960 г. в 33-м рейсе э/с «Витязь» в Аравийском море были проведены сейсмические работы методом отраженных волн с целью изучения мощности и строения донных отложений [17]. Всего выполнено 23 станции. В результате проведенных работ выяснено, что в исследованном районе мощность осадков колеблется от 0,5 до 2,5 *км*. Наименьшие мощности приурочены к южной, самой глубоководной части Аравийской котловины. Значения скоростей в осадках изменяются от 1,5 до 2,3 *км/сек*.

В 1961 г. во время 33-го рейса э/с «Витязь» были проведены сейсмические исследования методом преломленных волн в западной части Индийско-Австралийской котловины с использованием радиобуев [18]. В результате этих исследований впервые для Индийского океана были получены сейсмические данные о строении земной коры вплоть до поверхности Мохоровичича. Мощность земной коры в исследованном районе равна $7{,}0 \pm 1{,}5$ *км*. Кора имеет типично океаническое строение и состоит из следующих слоев: 1) осадочный слой, $V_г = 2{,}0$ *км/сек*, мощность $H = 0{,}3 — 0{,}5$ *км*; 2) базальтовый слой, $V = 6{,}4$ *км/сек*, $H = 6{,}5 \pm 1{,}5$ *км*; 3) подкоровый слой, $V_г = 8{,}0$ *км/сек*.

Многими исследователями было показано, что на основании данных гравиметрии можно достаточно успешно определять общую мощность земной коры до поверхности Мохоровичича [1, 6, 10, 11].

Если принять значение средней плотности земной коры σ_1, а плотности подстилающих пород верхней мантии σ_2, то получим разность плотностей на границе Мохоровичича $\Delta\sigma = \sigma_2 - \sigma_1$. При этом изменение мощности земной коры ΔH вызовет изменение аномалии силы тяжести в редукции Буге на величину $\delta\Delta g$. Пользуясь формулой притяжения для бесконечного плоскопараллельного слоя, получим:

$$H_i = H_0 - \frac{\delta i \Delta g}{2\pi k \Delta\sigma}, \qquad (1)$$

где

$$\sigma_i \Delta g = \Delta g_i - \Delta g_0.$$

Таким образом, зная глубину поверхности Мохоровичича H_0 и аномалию Буге Δg_0 в какой-либо опорной точке океана, можно по этой формуле вычислить глубину H_i для любой точки, если известны аномалии Буге в этих точках. Значения H_0 в опорных точках определяются методом сейсмических зондирований. Необходимо, однако, иметь в виду, что в действительности наблюдаемые аномалии силы тяжести обусловлены не только изменением мощности земной коры, но и изменением мощности рыхлых и уплотненных осадочных отложений, а также изменением плотности «базальтового» слоя и плотности подкорового вещества в горизонтальном направлении. В неблагоприятных областях, особенно в переходных зонах от материков к океанам, эти факторы могут значительно снизить точность определения мощности земной коры по гравиметрическим данным. Некоторыми исследователями на основании сопоставления мощности земной коры, полученной по сейсмическим данным, с соответствующими для этих участков осредненными аномалиями Буге, составлены корреляционные графики зависимости между толщиной земной коры и осредненными аномалиями Буге [1, 6, 9—11, 29].

Данные геофизических исследований позволили дать некоторое представление о строении земной коры под дном Индийского океана. Нами построены схематические разрезы земной коры по двум профилям (рис. 1); определение мощности земной коры производилось по аномалиям Буге с разностью плотностей вещества коры и верхней мантии 0,4 *г/см*³, определение глубины *М* производилось по формуле плоскопараллельного слоя.

Профиль I. Кейптаун (Африка) — Земля Королевы Мод (Антарктида). Так как в западной части Индийского океана данных сейсмозондирования не имеется, мощность земной коры определялась по корреляционным соотношениям между аномалиями силы тяжести и мощностью земной коры. Принято, что нулевым аномалиям Буге соответствует кора мощностью 33 *км* и изменение аномалии на 20 *мгл* соответствует изменению мощности коры на 1 *км* [4, 5].

Профиль II О. Цейлон — шельфовый ледник Шеклтона (Антарктида). Мощность земной коры вычислялась по формуле (1). В качестве известного опорного пункта H_0 был использован сейсмический профиль э/с «Витязь» [18].

Первый профиль пересекает западную часть Индийского океана от Кейптауна до Антарктиды. Дно океана здесь ровное, спокойное. Профиль проходит через котловину мыса Игольного и Африканско-Антарктическую котловину, а также плато Крозе. Области океанических котловин (собственно океаническое дно) характеризуются спокойным

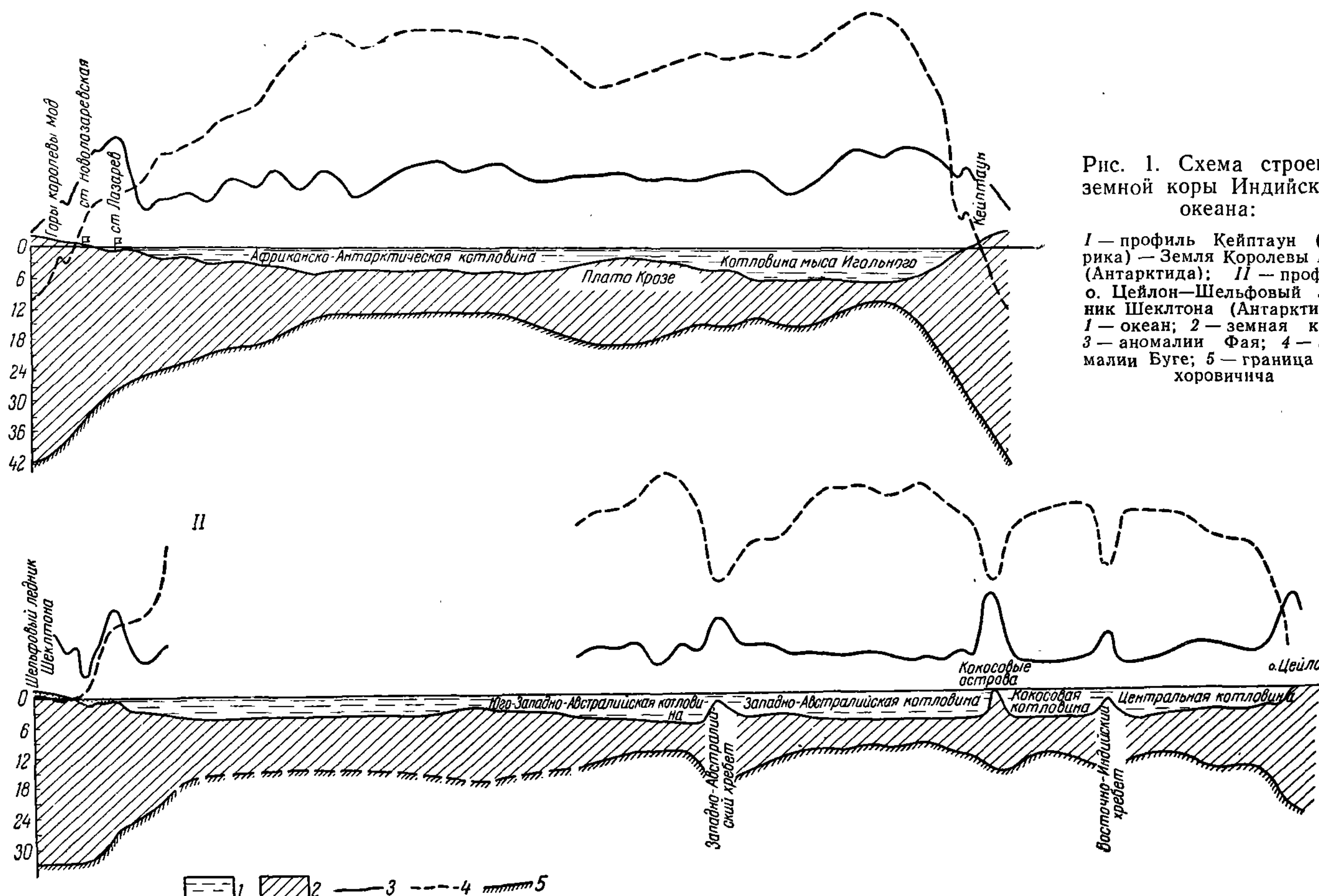

Рис. 1. Схема строения земной коры Индийского океана:

I — профиль Кейптаун (Африка) — Земля Королевы Мод (Антарктида); *II* — профиль о. Цейлон—Шельфовый ледник Шеклтона (Антарктида); *1* — океан; *2* — земная кора; *3* — аномалии Фая; *4* — аномалии Буге; *5* — граница Мохоровичича полем силы тяжести, с небольшими положительными или близкими к нулю аномалиями Фая и значительными положительными аномалиями Буге (до $+400 \div 450$ *мгл*). Над плато Крозе аномалии Фая заметно не изменяются; аномалии Буге здесь уменьшаются до $+250$ *мгл*. При переходе от океана к Африканскому материку положительные аномалии Фая постепенно убывают до -30 *мгл*; аномалии Буге резко убывают до -120 *мгл*, создавая значительный гравитационный градиент (15 этвеш). При переходе от океана к Антарктическому материку аномалии Фая убывают и носят переменный характер. В районе континентального склона преобладают отрицательные аномалии Фая. В районе шельфового ледника аномалии Фая резко возрастают, переходя снова к отрицательным величинам в Горах Королевы Мод. Аномалии Буге убывают от океана к материку от $+400$ до -100 *мгл*. Такая широкая переходная зона объясняется значительным погружением шельфа антарктического материка под действием ледовой нагрузки.

Мощность земной коры на этом разрезе меняется от 5—7 *км* (в районе котловин) до 15—17 *км* на плато Крозе и при переходе к материкам увеличивается до 40—43 *км*.

Второй профиль пересекает океан от о. Цейлон до шельфового ледника Шеклтона в Антарктиде. За отсутствием фактических данных (кроме глубин дна) профиль имеет разрыв протяженностью 1000 миль. Поверхность *M* на этом участке проведена ориентировочно по рельефу дна океана.

Рельеф океанского дна на этом профиле значительно сложнее. Он представлен рядом океанских котловин (Кокосовая, Центральная, Западно-Австралийская и др.), несколькими хребтами (Центрально-Индийский, Западно-Австралийский, Восточно-Индийский), о. Цейлон и архипелагом Кокосовых о-вов. И на этом профиле океанские котловины характеризуются сравнительно спокойным полем аномалий Фая с небольшими отрицательными значениями (до $-30 \div 40$ *мгл*) и значительными положительными аномалиями Буге (до $+400 \div 420$ *мгл*). Со стороны антарктического материка профиль уходит в океан лишь на 350—400 миль. Поэтому о ширине переходной зоны трудно что-либо сказать. Однако и тут в районе континентального склона аномалии Фая имеют отрицательные значения и резко возрастают в районе шельфового мелководья, переходя опять к значительным отрицательным величинам, обусловленным наличием здесь глубоких желобов под шельфовым ледником. Аномалии Буге резко убывают от океана к берегу, уменьшаясь от $+300 \div 350$ *мгл* до нуля.

Мощность земной коры в океанских котловинах колеблется в пределах 5—12 *км*. При переходе к антарктическому берегу мощность коры возрастает до 33—35 *км*, т. е. переходит в типичную материковую кору.

Кокосовые о-ва и о. Цейлон отличаются значительным увеличением аномалий Фая (до $+50 \div 60$ *мгл*) и резким уменьшением аномалий Буге (до $+80 \div 150$ *мгл*). Мощность земной коры увеличивается под островами до 15 *км* (Кокосовые о-ва) и до 24 *км* (о. Цейлон).

Следует отметить, что для Индийского океана, так же как и для других океанов, характерно наличие выдающихся океанических хребтов [15, 25]. Средне-Индийский хребет начинается у берегов Аравии. У о. Сокотра он раздваивается: одна ветвь идет в северо-восточном направлении (к Пакистану), другая образует Аравийско-Индийский хребет, переходящий в Центрально-Индийский. На широте 25° ю. ш. Центрально-Индийский хребет раздваивается: одна ветвь уходит через плато Крозе в Атланто-Индийский порог, соединяясь со Средне-Атлантическим валом, другая ветвь хребта через Гаусс-Кергеленское поднятие уходит в Антарктиду, а также через о-ва Амстердам и Святого Павла — в Тихий океан к о-вам Новой Зеландии. От берегов Индии до

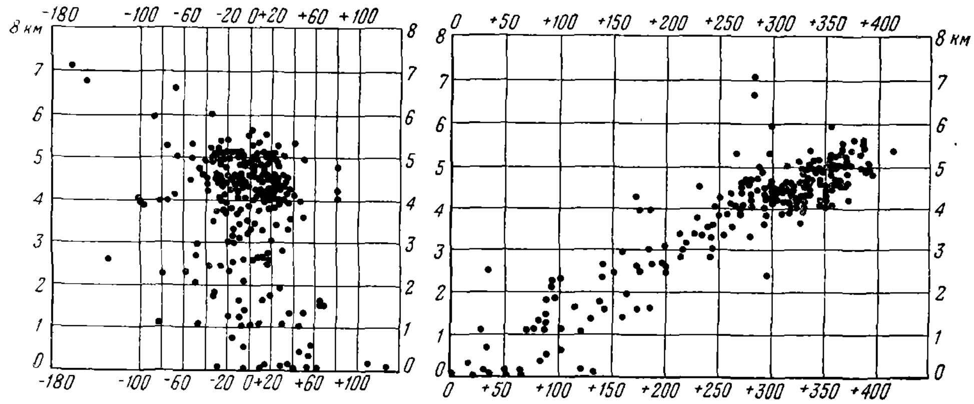

а *б*

Рис. 2. Зависимость аномалий Фея и Буге от глубин дна Индийского океана:
а — аномалии Фая (*мгл*); *б* — аномалии Буге (*мгл*)

сороковых широт южного полушария в меридиональном направлении протянулся Восточно-Индийский хребет, который между 30° и 40° ю. ш. почти под прямым углом переходит в широтный Западно-Австралийский хребет.

Важной особенностью хребтов Индийского океана является наличие глубоких трещинных (рифтовых) долин, совпадающих с размещением эпицентров землетрясений (корреляция, хорошо установленная и для других океанов) [14, 25, 26]. Эти долины проходят вдоль хребтов, глубина их достигает 5—6 *км*, а ширина не превосходит десятка километров (Восточно-Индийский желоб).

Хребты Индийского океана так же, как и острова, выделяются положительными аномалиями Фая (до $+30 \div 50$ *мгл*), на фоне спокойных отрицательных аномалий над котловинами. Для Центрально-Индийского хребта получен непрерывный профиль, указывающий на большую изменчивость аномалий в окрестностях гребня хребта [26]; причем над рифтовой долиной значение аномалии Фая равно -67 *мгл*, в то время как над самим хребтом аномалии равны $+50 \div 60$ *мгл*. Мощность земной коры под хребтами увеличивается до 15 *км*.

Непрерывные гравитационные профили через Северо-Атлантический хребет [14—15, 26] указывают на коррелляцию аномалий Фая и топографии дна, т. е. на большую изменчивость $\Delta g_{Фая}$ в окрестности хребтов. В частности, аномалии Фая над самими хребтами имеют значение $+30 \div 60$ *мгл*, рифтовые долины отмечаются значительными отрицательными (до $-50 \div 60$ *мгл*) аномалиями.

Характер гравитационных полей над хребтами Индийского и Атлантического океанов и строение земной коры под ними указывают на их сходство. Это подтверждает мнение многих исследователей о существовании единой цепи океанских хребтов, опоясывающих весь земной шар. Эти хребты сопровождаются глубокими каньонообразными трещинами, к которым приурочены пояса эпицентров землетрясений, проявления вулканической деятельности. Эти трещины имеют, очевидно, тектоническое происхождение и рассматриваются как проявление медленного расширения Земли.

Для того, чтобы качественно сопоставить региональные особенности в строении земной коры Индийского, Атлантического и Тихого океанов, нами были составлены графики (рис. 2) зависимости аномалии Фая и Буге от глубин дна Индийского океана, а полученные результаты сравнены с аналогичными соотношениями, построенными для Атлантического и Тихого океанов Вуллардом и Странжем [29].

По имеющимся к настоящему времени данным можно указать, что как по разбросу величин аномалий Фая и Буге для одних и тех же интервалов глубин, так и по среднему значению этих аномалий на соответствующих интервалах глубин Индийский океан ближе к Тихому океану. Разброс аномалий Фая и Буге для соответствующих интервалов глубин Атлантического больше, чем для Тихого и Индийского океанов. Среднее значение аномалий Фая и Буге, в интервале глубин 4000—5000 и 5000—6000 *м* (где имеется наибольшее количество определений силы тяжести) для Атлантического океана примерно на 20 *мгл* ниже, чем для Тихого и Индийского океанов. Возможно, эти различия обусловлены большей неоднородностью вещества земной коры и верхней мантии в области Атлантического океана по сравнению с Тихим и Индийским. Вариации скоростей продольных сейсмических волн на поверхности Мохоровичича под Атлантическим и Тихим океанами показывают, что вероятно верхние слои мантии менее однородны по плотности под Атлантическим океаном, нежели под Тихим [9].

ЛИТЕРАТУРА

1. Андреев Б. А. 1958. Гравитационные аномалии и мощность земной коры континентальных областей, Докл. АН СССР, **119**, № 2.
2. Венинг-Мейнес Ф. А. 1940. Гравиметрические наблюдения на море. Геодезиздат, М.
3. Гайнанов А. Г. 1961. Гравиметрические определения на дизель-электроходе «Обь» в первом антарктическом рейсе. Вып. 1. Морские гравиметрич. исслед. Сб. статей, Изд. МГУ.
4. Гладун В. А., Строев П. А., Ушаков С. А., Фролов А. И. 1963. Геофизические исследования строения земной коры в переходной зоне от Антарктического континента к Индийскому океану на участке между 55° и 100° в. д. Докл. АН СССР, **153**, № 2.
5. Гладун В. А., Деменицкая Р. М., Строев П. А., Ушаков С. А., Фролов А. И. 1963. Некоторые результаты геофизических исследований строения земной коры Антарктики к северу от ст. Новолазаревская. Докл. АН СССР, **153**, № 6.
6. Грушинский Н. П. 1961. О связи поверхности Мохоровичича с рельефом и аномалиями силы тяжести. Сообщ. Гос. астроном. ин-та им. П. К. Штернберга, № 119.
7. Грушинский Н. П. 1961. Морские определения силы тяжести в Антарктике в 1956—1957 гг. Морские гравиметрич. исслед., вып. 1. Изд. МГУ.
8. Грушинский Н. П. 1961. Опыт применения гравиметра на надводном корабле. Морские гравиметрич. исслед., вып. 1. Изд. МГУ.
9. Гурарий Г. З., Соловьева И. А. 1963. Строение земной коры по геофизическим данным. Изд. АН СССР.
10. Деменицкая Р. М. 1958. Планетарные структуры земной коры и их отображение в аномалиях. Буге. Сов. геология, № 8.
11. Деменицкая Р. М. 1961. Основные черты строения коры Земли по геофизическим данным. Тр. Ин-та геол. Арктики, **115**.
12. Иванов М. М. 1963. Некоторые вопросы строения дна Атлантического и Индийского океанов по магнитным данным. Геомагнетизм и аэрономия, III, № 1.
13. Ковылин В. М. 1961. Сейсмоакустические исследования в океане методом отраженных волн с многоканальной приемной системой. Океанол. исслед. Изд. АН СССР, № 4.
14. Корякин Е. Д. 1963. Гравитационное поле Атлантического океана и его связь с глубинным строением земной коры. Морские гравиметрич. исслед., вып. 2. Изд. МГУ.
15. Корякин Е. Д. 1958. О глубинном строении земной коры в области Атлантического океана. Изв. АН СССР. Сер. геофиз., № 12.
16. Максимов И. В. 1958. Океанографические исследования советских антарктических экспедиций. Информ. бюл. САЭ, № 1.
17. Непрочнов Ю. П. 1961. Мощность осадков котловины Аравийского моря. Докл. АН СССР, **139**, № 1.
18. Непрочнов Ю. П. 1962. Новые данные о строении земной коры под дном Индийского океана. Докл. АН СССР, **144**, № 2.
19. Строев П. А. 1963. Методика морских гравиметрических измерений в VI рейсе дизель-электрохода «Обь». Информ. бюл. САЭ, № 43.
20. Фролов А. И. 1963. Гравиметрические работы ГАИШ в 3-й Советской Антарктической экспедиции в 1957—1958 гг. Морские гравиметрич. исслед., вып. 2. Изд. МГУ.

21. Фролов А. И. 1963. Гравиметрические работы ГАИШ в 5-й Советской антарктической экспедиции в 1959—1960 гг. Морские гравиметрич. исслед., вып. 2. Изд. МГУ.
22. Bathymetric, Magnetic and Gravity investigation H. M. S. 1963. Wuen 1961—1962. London, Hydrographic department, Admiralty Marine Science publication, No 4, part. 1.
23. Gaskell T. F., Hill M., Swallow I. 1958. Seismic measurements made by H. M. S., «Challenger» in the Atlantic, Pacivic and Indian Oceans and in the Mediterranean sea. 1950—1953. Philos. Trans. Roy. Soc. London, A, **251,** No 988.
24. Girdler R. W., Harrison Y. C. 1957. Submarine gravity measurements in the Atlantic Ocean, Indian Ocean. Red sea and Mediterranean sea Proc. Roy. Soc. A, **239.**
25. Ewing M., Heezen B. C. 1960. Continuity of mid oceanic ridge and rift valley, in the Sorth-Western Indian Ocean confirmed Science, 131.
26. Talwani M. 1962. Gravity measurements on H. M. S. «Acheron» in South Atlantic and Indian Oceans Bull. Geol. Soc. America, **73,** No 9.
27. Vening-Meiness F. A. 1938. Theory and Practice of Pendulum Observations at sea, part II. Delft, 1941.
28. Vening-Meiness F. A. 1948. Gravity Expeditions at Sea, 1923. IV Publications of the Netherlands Geodetic Comission, Delft.
29. Wollard G. P., Strange W. E. 1962. Gravity anomalies and the crust of the Earth in Pacific Basin. Geophysical Monography, No 6, Amer. Geophys. Un.

Поступила в редакцию
19.VI.1964

Reprinted from *J. Geophys. Res.*, vol. 71, no. 2, 1966, p. 495-509

A Reconnaissance Geophysical Survey in the Andaman Sea and across the Andaman-Nicobar Island Arc

G. Peter, L. A. Weeks, and R. E. Burns

U. S. Coast and Geodetic Survey, Rockville, Maryland

Abstract. A marine geophysical study of the Andaman Sea has been conducted as part of the International Indian Ocean Expedition. A combination of magnetic, gravity, bathymetric, and sea-floor heat-flux measurements, seismic sparker reflection profiles, and bottom sediment samples has been used in a study of the seaward continuity of major subaerial tectonic trends. The data indicate positive continuity of the structural trend of the Barisan Range of northern Sumatra and the Burma Range. It was found that the central graben of the Barisan Range of northern Sumatra extends into the Andaman Sea north to latitude 10°N. A previously unreported interdeep has been observed between the outer sedimentary island arc and the inner igneous trend of the major primary arc which forms the western boundary of the Andaman Sea. Continental thickness of the crust is indicated under the sedimentary island platform. In the area of the backdeep, the north-northeast trends of the Malaysian peninsula are prominent.

Introduction. As part of its participation in the International Indian Ocean Expedition, the U. S. Coast and Geodetic Survey Ship *Pioneer* conducted a reconnaissance geophysical survey in the Andaman Sea and across the Andaman-Nicobar island arc (Figure 1). The basic survey consisted of a major series of simultaneous measurements (with the ship underway) of the earth's magnetic and gravity fields. These were supplemented by the continuous recording of water depth, a series of sub-bottom seismic reflection profiles, and associated programs of sea-floor heat-flux measurements and bottom sediment sampling.

Measurements of the magnetic field were made with a towed Varian proton-precession magnetometer which measures the total intensity of the earth's magnetic field with a sensitivity of $\pm 1\ \gamma$. The sensing unit was towed far enough behind the ship to keep the ship's influence smaller than $\pm 5\ \gamma$. Because of the location of the survey area on the geomagnetic equator, the measurements were subject to diurnal variation as high as $\pm 35\ \gamma$. On the other hand, short-period variations related to magnetic storms appear to be absent from the record, since the U. S. Coast and Geodetic Survey Honolulu Magnetic Observatory records indicate that the survey was conducted during a quiet period.

The gravity measurements were made with a LaCoste-Romberg air-sea gravity meter. The performance of the gravity meter was checked at the San Francisco gravity meter evaluation range both before and after the Indian Ocean operations. These checks indicate that rms errors are smaller than ± 5 mgal when the seas are calm (Browne corrections smaller than 100 mgal). Because the average Browne correction during the Andaman Sea operations was approximately 50 mgal and frequently was smaller than 10 mgal, the data are considered to be accurate within the ± 5 mgal limit.

A continuous record of water depth was obtained with the precision depth recorder (PDR) during all underway operations. The bathymetric profiles in this report represent uncorrected soundings obtained from the PDR record for points of inflection and gradient changes in the indicated bottom slopes.

The seismic reflection profiles were obtained with a Rayflex sparker, using a 20,000-joule electrical spark as a sound source. The spark source was towed about 100 m behind the ship and was energized every 4 sec. The hydrophone array consisted of 20 hydrophones spaced about 4.5 m apart and enclosed in a long plastic tube filled with diesel oil. The oil-filled tube provided neutral buoyancy during towing, and minimized the water noise around the hydrophones. The reflected signal received by the hydrophone array was recorded both on paper strip chart and on magnetic tape. On the reflection profiles presented in this report, the

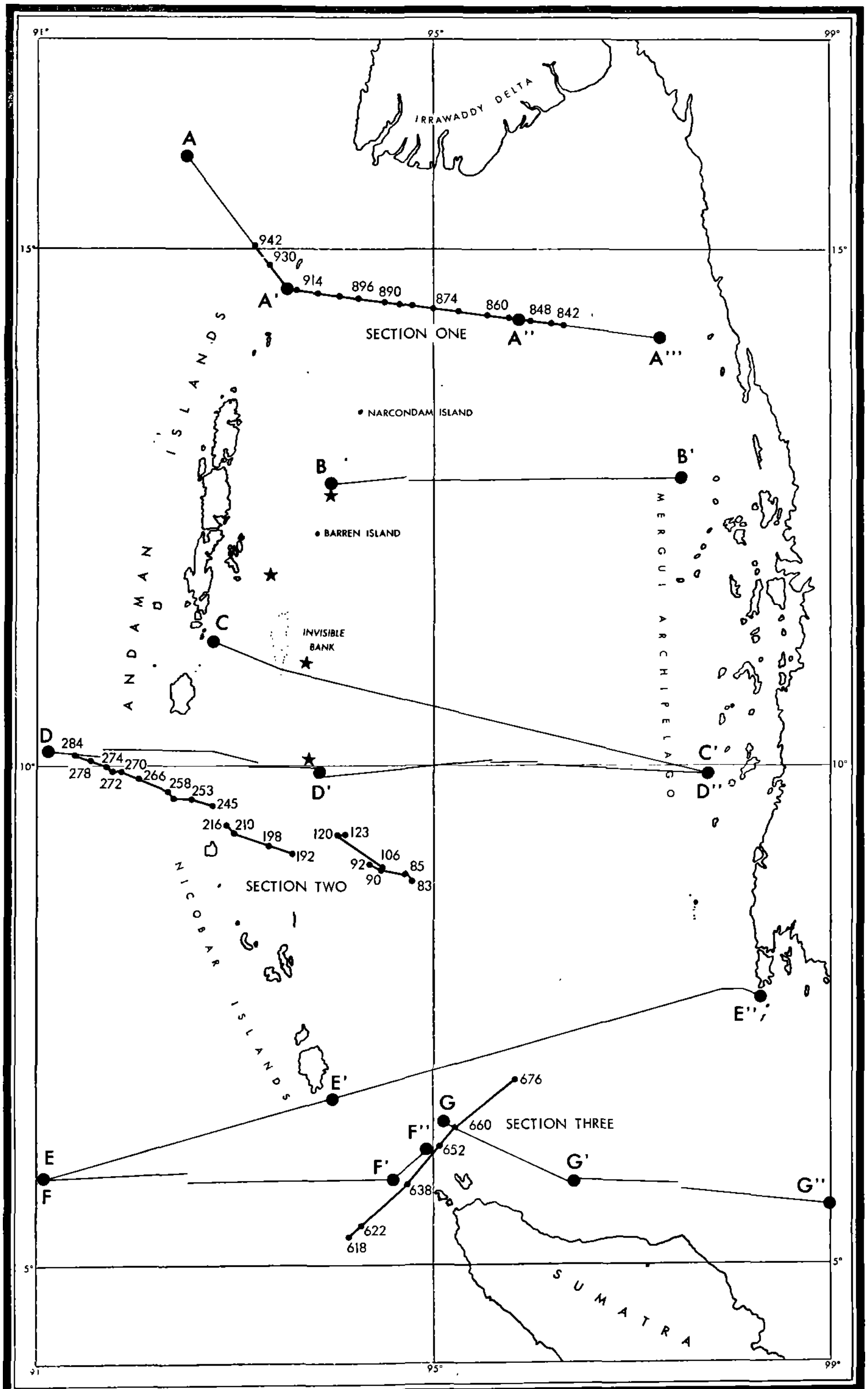

Fig. 1. General location chart.

form lines of structures and faults were interpreted from the original records. The horizontal scale on the sections is based on 30-min fix positions at a ship's speed of about 10 km/hr. Each fix point marked on the sections is 30 min from the adjacent fix regardless of the specific number assigned to it. Because of the small speed changes in the various parts of the sections, the assigned distance scale must be considered only approximate. The vertical scale is in meters, so the first reflection can be related directly to bathymetric profiles. This scale was based on an assumed sound velocity of 1.6 km/sec, and the depths indicated for the subbottom horizons are probably deeper by as much as 40%.

The measurements of sea-floor heat flux were made in association with the bottom sediment sampling program. Bottom sediment samples were collected with several types of coring, grab, and dredge sampling devices. The results of the heat-flux measurements have been reported separately [*Burns* 1964], and the detailed description of the bottom sediment composition and distribution will be the topic of another paper.

Geologic and tectonic framework. The principal objective of the reconnaissance geophysical survey in the Andaman Sea was to examine the seaward continuity of the major geologic trends of this area. These trends are schematically indicated in Figure 2, which is based on a geologic map prepared by the Geological Survey

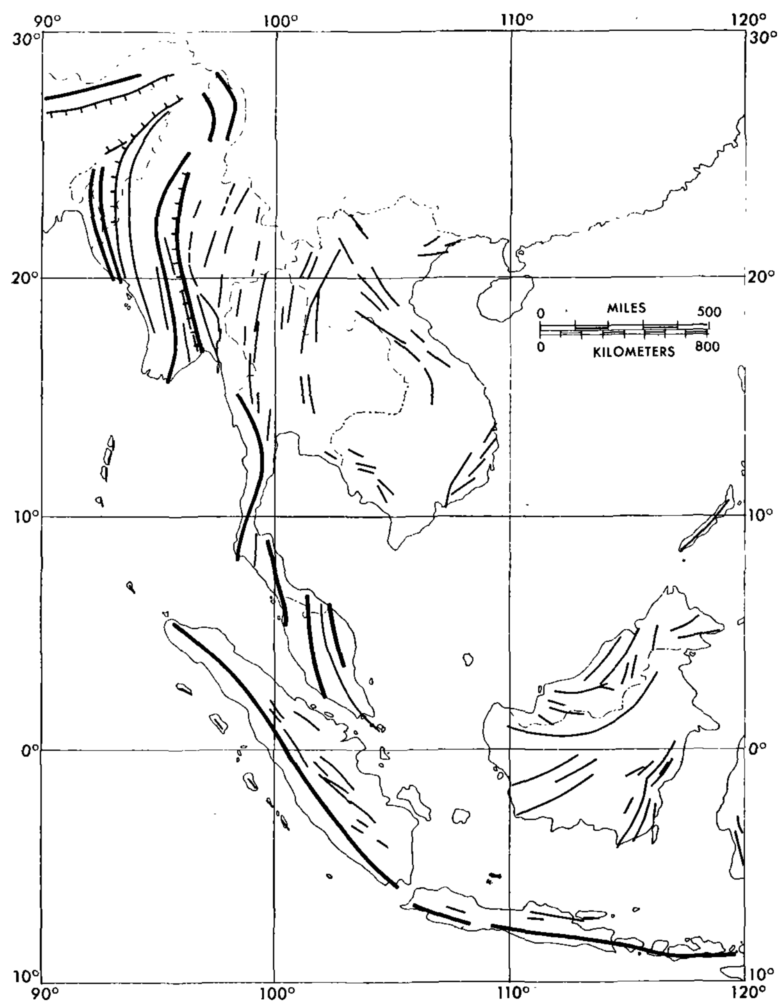

Fig. 2. Major geologic trends around the Andaman Sea.

of the Federation of Malaya [*Alexander*, 1962]. A generalized representation of the principal bathymetric features of the area (Figure 3) has been compiled from several sources, including the bathymetric program of the *Pioneer*.

The dominant structural features in this area are related to the Indonesian arc, which is part of the system of young primary arcs of Southeast Asia. The field program of the *Pioneer* was designed to provide a series of traverses of the Andaman Sea from the Mergui archipelago in the east and extending westward across the Andaman-Nicobar island arc.

To the east of the Andaman Sea, the geologic structure belongs to the fold-mountain system which extends from Burma, through Thailand and Malaysia, and eastward into Borneo. The major orogeny of this eastern folded belt occurred during the Triassic and Jurassic periods.

The Indonesian arc in this area consists of a primary double arc with a recognized inner volcanic trend and an outer sedimentary arc. The inner volcanic trend is well defined in central Burma and also in Sumatra. It consists of a belt, originally folded during the Cretaceous, which developed during the late Tertiary and Quaternary into a volcanic arc system that is still marked by active volcanism. In Sumatra this volcanic trend is represented by the Barisan Range, which is split longitudinally by the Semangko fault, a garben or rift valley extending the full length of Sumatra (Figure 2). In northern Sumatra the trend of the fault zone is identified by the Atjeh garben which extends offshore into the Andaman Sea. On both sides of the garben there are members of the pre-Tertiary and Lower Tertiary block mountain system, composed mainly of metamorphic rocks with diabase and serpentine. On the northeast side of the graben there are additional young volcanic rocks, which are generally identified as andesite effusives. On the basis of reports of recent volcanic activity in the Barren and Narcondam Islands, it has been postulated that this volcanic trend extends through these islands northward to Burma. In Burma, a major fault zone separates the Triassic-Jurassic fold-mountain system of eastern Burma from the Cretaceous Burma Range.

The only clear subaerial indication of the outer sedimentary arc is the island arc formed by the Andaman and Nicobar Islands, which form the western border of the Andaman Sea. Orogenic activity in this belt began as early as the Cretaceous, but the elevation of the islands did not occur until the Oligocene-Miocene [*Karunakaran et al.*, 1964].

Bemmelen [1949] proposes that the geologic development of the area has been from east to west. The relationship of a rapidly developing outer sedimentary arc to an inner volcanic arc has not changed, although the double arc system has shifted progressively to the west. The inner volcanic arc of today was the sedimentary arc of an earlier period, and what is now an uplifted platform started as an outer depressed belt.

Trends paralleling the island arc. The Cretaceous to Oligocene-Miocene orogenic belt is represented in this area by major trends which are generally indicated by the morphologic trends in Figure 3. The basic elements of a primary double island arc can be identified. The inner igneous arc runs east of the Andaman and Nicobar Islands, through Narcondam Island, Barren Island, and Invisible Bank and connects the Cretaceous orogenic ranges of Burma and Sumatra. A structurally depressed belt separates the inner igneous arc from the outer sedimentary arc. The trend of the sedimentary island arc is represented by the Andaman-Nicobar platform, which passes south of Sumatra through Simalure and Nias Islands (outside the area of the base map). The fourth trend is indicated by the northern extension of the Java-Sumatra trench, which is locally a weak trough west of the sedimentary island platform with depths in excess of 4000 m at the south and greater than 2500 m at the north.

The free-air gravity anomalies are presented in chart form (Figure 4) and may be compared with the general trends indicated above. The inner igneous arc is indicated by generally high, positive free-air anomalies, specifically prominent at the northern tip of Sumatra, Invisible Bank, and near Barren and Narcodam Islands. A parallel belt of negative anomalies indicates the trend of the sedimentary island platform, and the axis of this belt passes through the Nicobar Islands but shifts to the inner (eastern) side of the Andaman Islands. A belt of slightly positive free-air anomalies in the west is generally associated with the outer limit of the

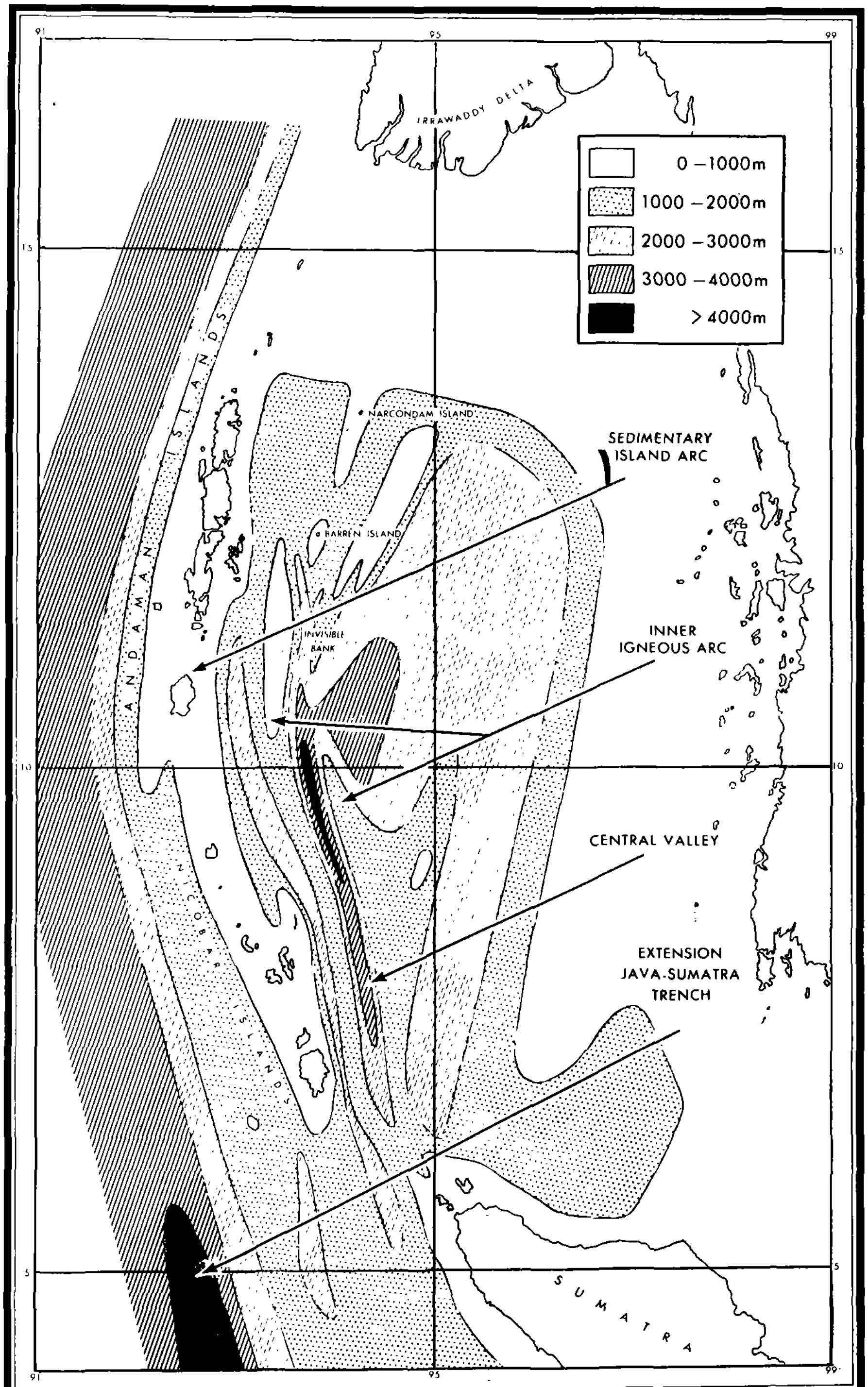

Fig. 3. Schematic presentation of principal bathymetric features.

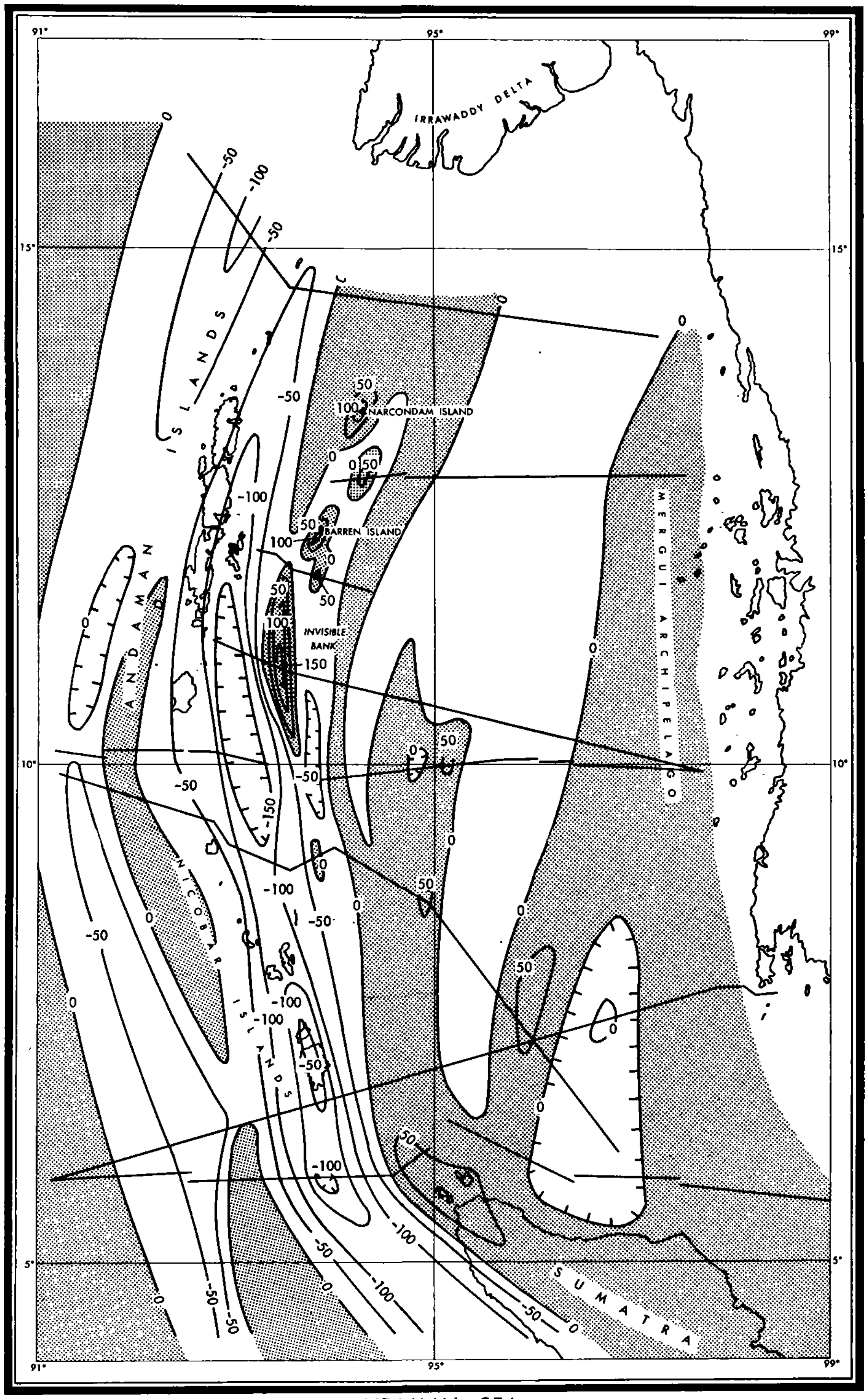

ANDAMAN SEA

Fig. 4. Free-air anomalies, Andaman Sea (contour interval 50 mgal; control lines indicated).

island arc in the southern part of the area, but it moves up onto the insular shelf and disappears just north of 10°N. The westernmost belt of negative anomalies is coincident with the axis of the foredeep.

Four profiles based on simultaneous measurement of gravity, magnetic field, and water depth cross the entire arc system and are shown in Figure 5. The magnetic field measurements generally indicate minor anomalies associated with the extension of the Java-Sumatra trench. The magnetic field is relatively smooth over the sedimentary island platform, and the relatively large and sharp anomalies are clear indications of the igneous belt to the east. Most of the magnetic anomalies associated with the igneous belt are negative, indicating induced magnetization of the rocks in this equatorial region. Several sharp positive peaks suggest reverse remanent magnetization [*Girdler and Peter*, 1960].

The postulated continuity of the igneous belts of Burma and Sumatra is strengthened by this set of profiles. Although on profile *A′-A″* there is complete lack of bathymetric indication because of burial due to the encroachment of the Irrawaddy delta from the north, the igneous trend is clearly indicated by both the positive free-air anomaly and the magnetic anomalies. In the south, the igneous trend is best indicated by the magnetic anomalies. Seismic reflection profile section 3 (Figure 6) indicates an almost direct correlation with the subaerial geological trends of northern Sumatra, and section 2 (Figure 7), farther to the north, also shows significant similarity. The continuity is further strengthened by the very high sea-floor heat flux measured in the deepest part of the Andaman basin (Figure 8), which is directly on the axis of the igneous trend (cf. the deep area near the eastern end of profile *D-D′*). Two other measurements of the heat flux along the axis of the igneous trend are also somewhat higher than world average, and the only low value was measured in a sediment-filled basin (interdeep) between the sedimentary island arc and the igneous belt.

The extension of this igneous belt with its known seismicity, high heat flux, volcanic activity, and central graben appears to be somewhat similar to the extension of the East-Afri-

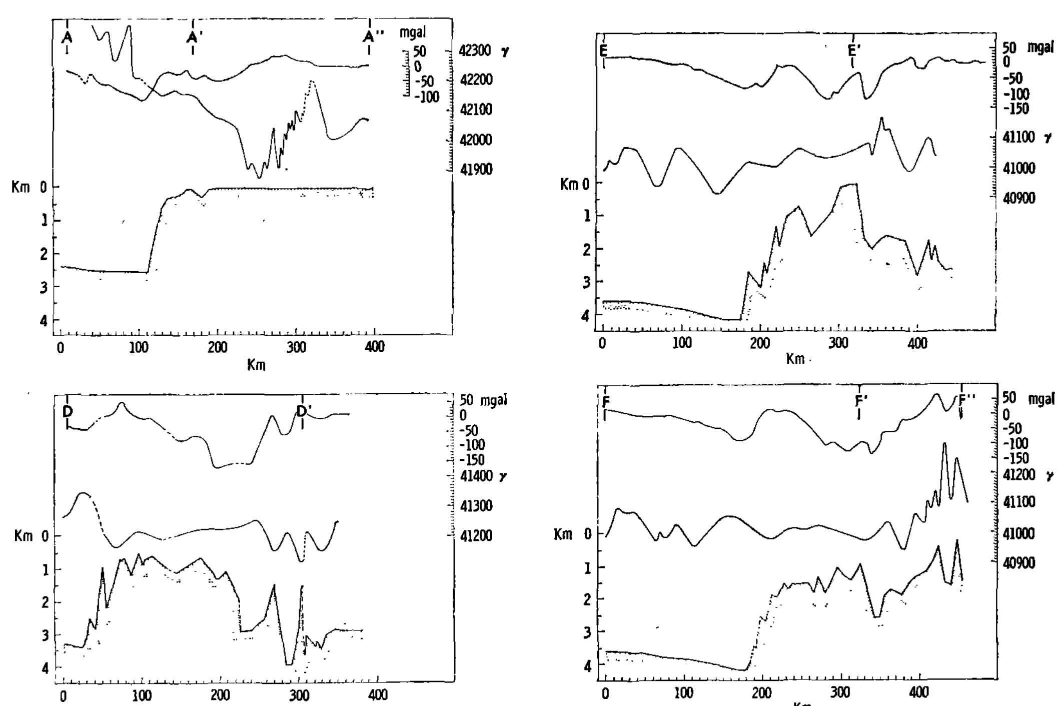

Fig. 5. Bathymetric, magnetic, and free-air anomaly profiles (profiles *A-A′-A″*, *D-D′*, *E-E′*, and *F-F′-F″* as shown in Figure 1).

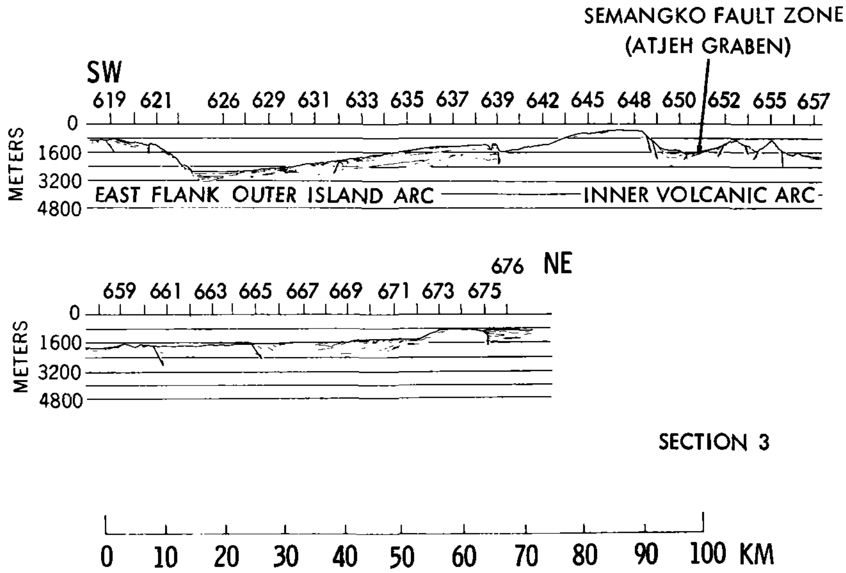

Fig. 6. Sub-bottom profiles based on seismic reflection measurements (section 3 near profile F'-F'').

can rift system into the Gulf of Aden, the extension of the Iceland graben into the mid-Atlantic ridge, or possibly the extension of the great Alpine fault of New Zealand into the Tonga-Kermadec ridge. In each case, it appears that the same tectonic forces operate both on land and at sea. The Iceland and the East-African graben systems are established as tensional weakness zones of the earth's crust that are connected to the mid-oceanic ridge systems. The central graben of the Barisan Range, which has been discussed by *Bemmelen* [1949] as a tensional relaxation feature, may indicate through some of these similarities that the island arc sys-

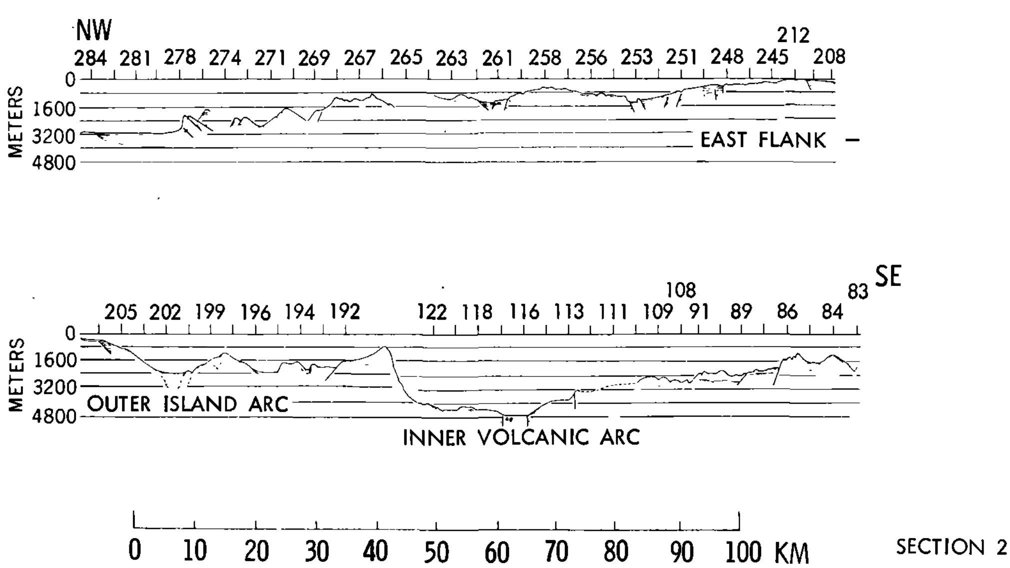

Fig. 7. Sub-bottom profiles based on seismic reflection measurements (section 2 near profile D-D').

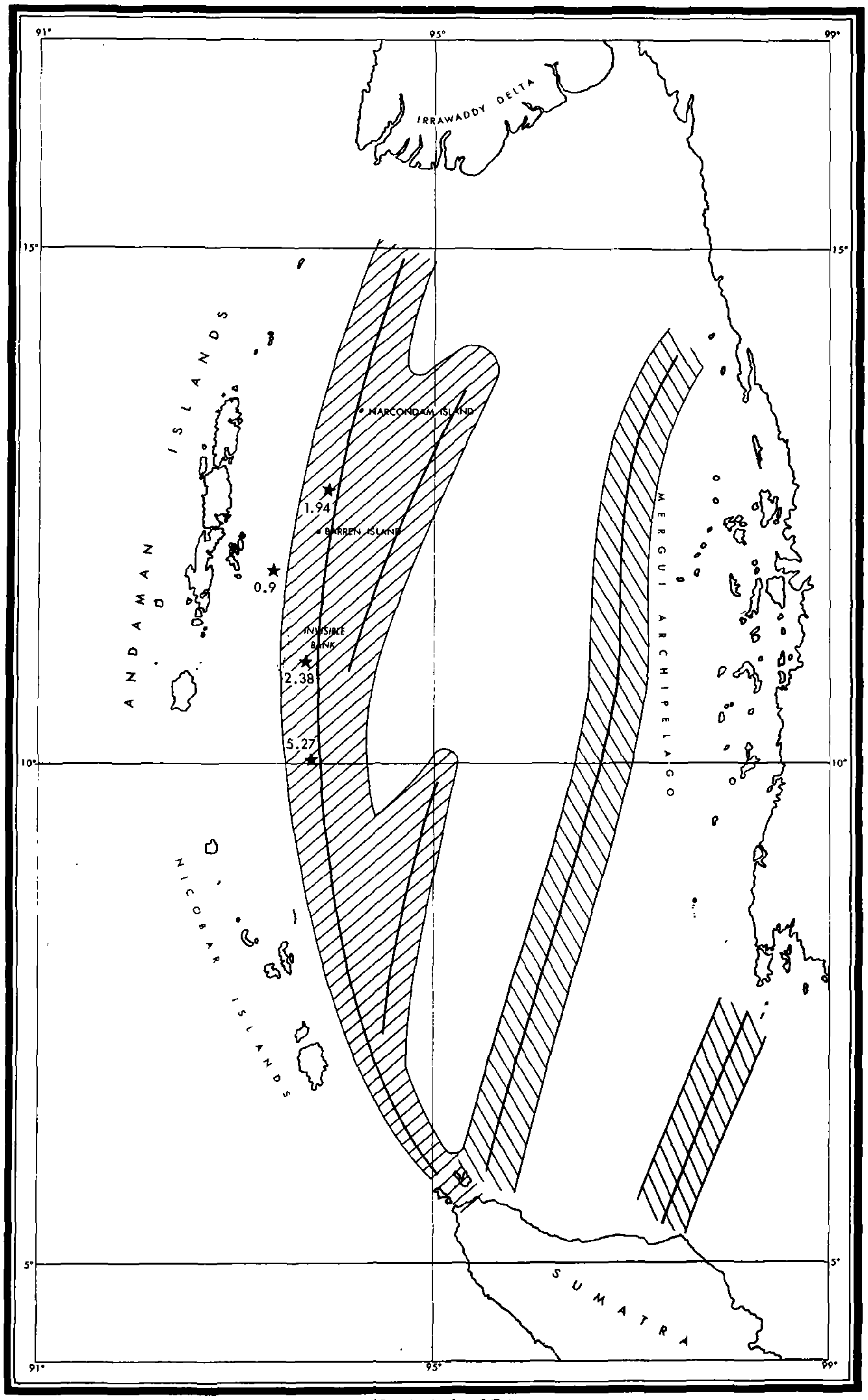

Fig. 8. Magnetic anomaly trends and measured sea-floor heat flux (10^{-6} cal cm^{-2} sec^{-1}).

tems represent another manifestation of global crustal tension.

North-northeast trends. With the exception of the major trends of the arc system which have already been discussed, the trends in the Andaman basin itself tend to strike north-northeast. The most prominent north-northeast trend indicated in Figure 8 is formed by continuity of magnetic and positive free-air anomalies with the shelf break along the Malaysian peninsula in the northern half of the Andaman Sea. The profiles shown in Figure 9 indicate that this trend was detected on each crossing of the basin. In the northern part of the basin, the trend was detected a few kilometers south of point *A‴* in Figure 1 (on a section not included in this report), and profiles *B-B′*, *C-C′*, and *D′-D″* indicate similar associations with the shelf immediately to the east of the shelf break. In the southern part of the basin, profile *E′-E″* shows the trend in deeper water about 250 km west of the poorly defined shelf break and associated with a minor rise that may be a slope terrace. Still farther south, profile *G-G′* (Figure 10) indicates that similar anomalies were detected in deeper water (>1000 m) off the northern tip of Sumatra. The anomalies may reflect the underlying Triassic-Jurassic tectonic trends of the Malaysian peninsula, or may be similar to anomaly trends of this type frequently associated with intrusive and effusive rocks along the shelf break in other parts of the world [*Drake et al.*, 1958; *Peter et al.*, 1965]. This latter interpretation is partially supported by the fact that igneous rocks were brought up in several dredge hauls made from the *Pioneer*.

In the southern half of the Andaman Sea, while crossing the 200-m shelf break, we found indications of normal faulting. On profile *G′-G″* (Figure 10) there is a distinct change in the magnetic field character from smooth to moderately active at the shelf break over the inferred fault. These geophysical anomalies, together with the fault observed near fix position 675 on the southernmost seismic reflection profile (Figure 6 and Figure 11), seem to support our second conclusion and to suggest that the shallow southeastern part of the Andaman Sea is underlain by a downfaulted part of the west Malaysian shelf.

There is an abrupt change in the depth of the sea floor (from 2700 to 3000 m) indicated in

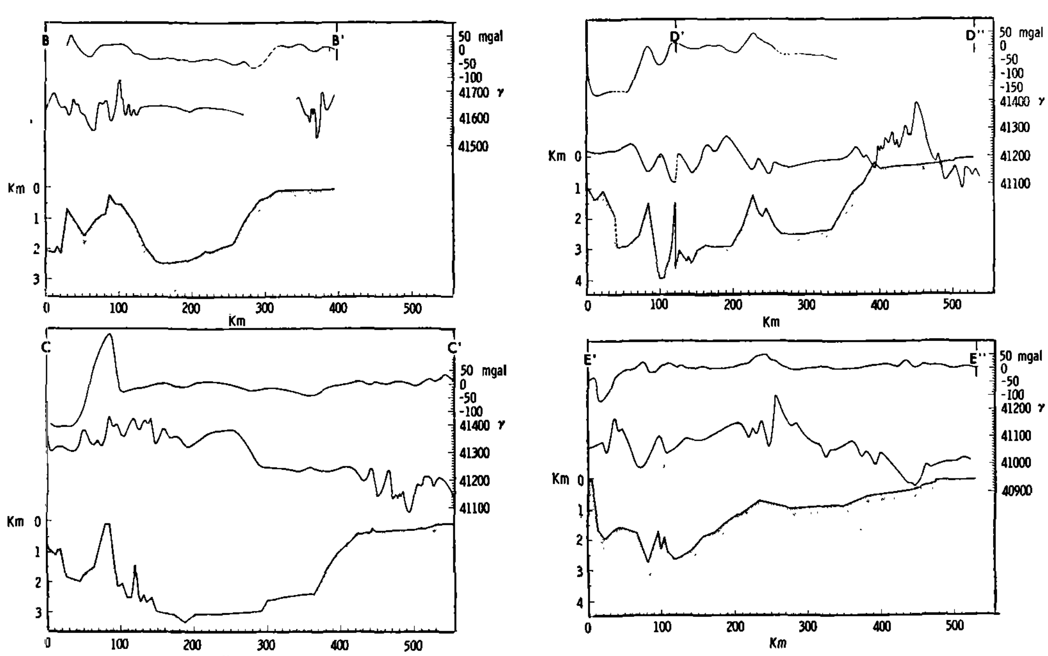

Fig. 9. Bathymetric, magnetic, and free-air anomaly profiles, (profiles *B-B′*, *C-C′*, *D′-D″*, *E′-E″*).

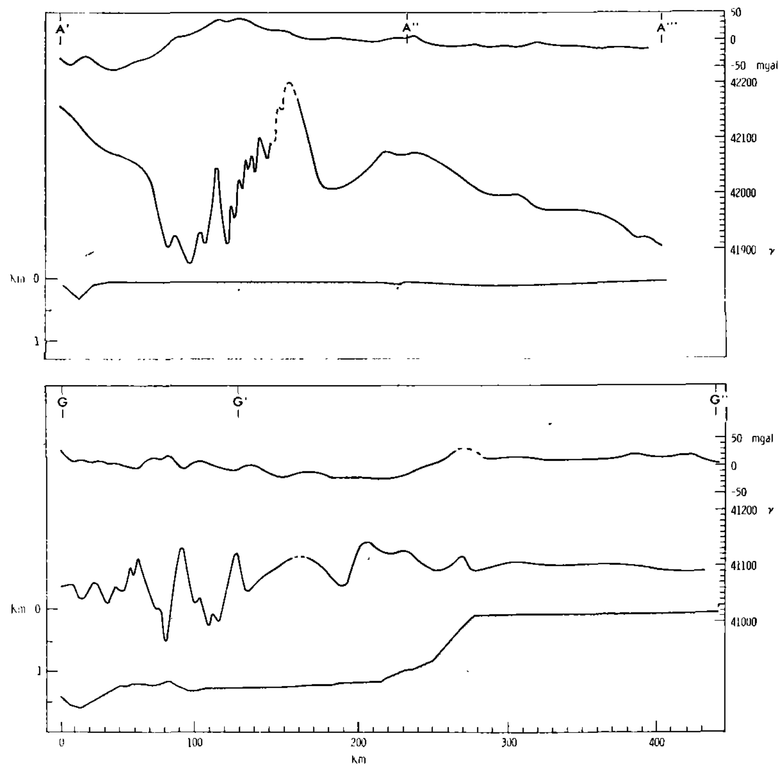

Fig. 10. Bathymetric, magnetic, and free-air anomaly profiles (profiles A′-A″-A‴, G-G′-G″).

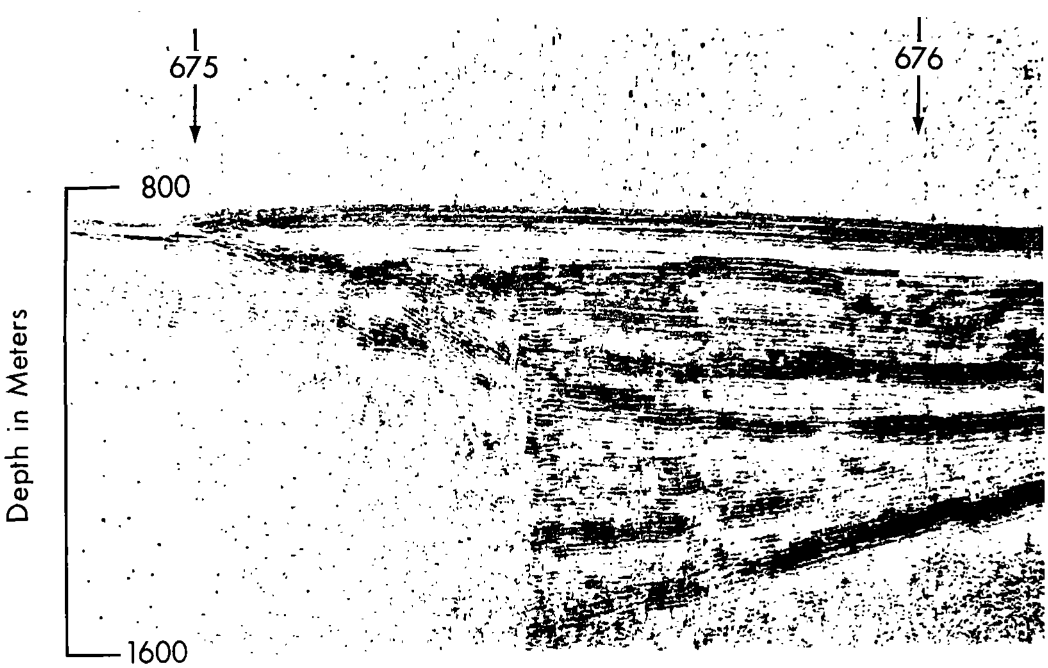

Fig. 11. Sub-bottom profile based on seismic reflection measurements (detail of Figure 6).

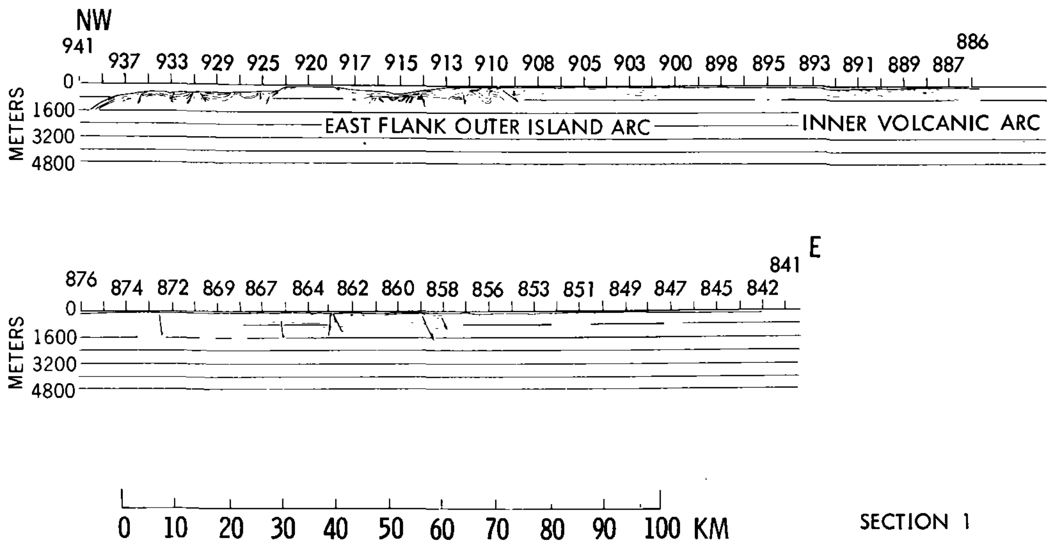

Fig. 12. Sub-bottom profile based on seismic reflection measurements (section 1 along profile A'-A'').

profiles C-C' and D'-D'' (Figure 9), which may be an indication of another fault zone. The associated step-like change in the magnetic anomaly also appears to support this conclusion. The trend of the inferred fault is also north-northeast, and it is parallel to the shelf-break anomaly trend mentioned above.

South of profile C-C' the actual fault plane cannot be observed. Profile D'-D'' indicates that it is overlain by the mountain range which merges with the igneous inner arc at the latitude of the south Nicobar Islands (Figure 3).

Toward the north there is no indication of this fault on profile B-B' (Figure 9). The fault indications in profile section 1 (Figure 12) are probably due to sediment settling, since A''-A''' (Figure 10) lacks the significant geophysical anomalies which usually indicate deep-seated tectonic control.

Northeast of Invisible Bank another north-northeast trend, a mountain range, merges with the igneous arc. The range is less than 250 km long, and the geophysical data along profile A''-A''' indicate that no other mountains are buried under the Irrawaddy delta along this trend.

Bouguer and isostatic anomalies. Bouguer anomalies have been calculated for sections C-C' and E-E'-E'' (Figures 13 and 14). The calculations are based on an assumed crustal density of 2.84 g/cm³ and a two-dimensional model of the bottom topography [*Talwani et al.,* 1959]. The 2.84-g/cm³ density is the average density of the combined 'low-velocity basement' and 'high-velocity basement' as derived by marine seismic refraction measurements [*Talwani et al.,* 1959; *Peter et al.,* 1965]. Similar high values can be obtained by averaging the densities in that part of the crust which lies below sea level [*Woollard,* 1959]. Because the local sections are primarily marine areas below sea level, it is appropriate to use the 2.84-g/cm³ density for Bouguer corrections rather than the customary 2.67-g/cm³ density, which is more appropriate for the average density of continental rocks above sea level.

In Figure 13, the Bouguer anomaly over Invisible Bank indicates that the bank may be composed of rocks of higher density than the assumed 2.84 g/cm³ and that a large density contrast exists deep in the crust in the area along the trend of the igneous arc.

In Figure 14, a crustal cross section, which has been calculated from the Bouguer anomalies, is shown. In this calculation, the mantle density was assumed to be 3.3 g/cm³ and the depth to the mantle surface was adjusted until its gravitational attraction matched the Bouguer anomalies. Besides the assumptions that the structure is two-dimensional and perpendicular to the profile, it was assumed that at the point where the free-air anomaly and the Bouguer

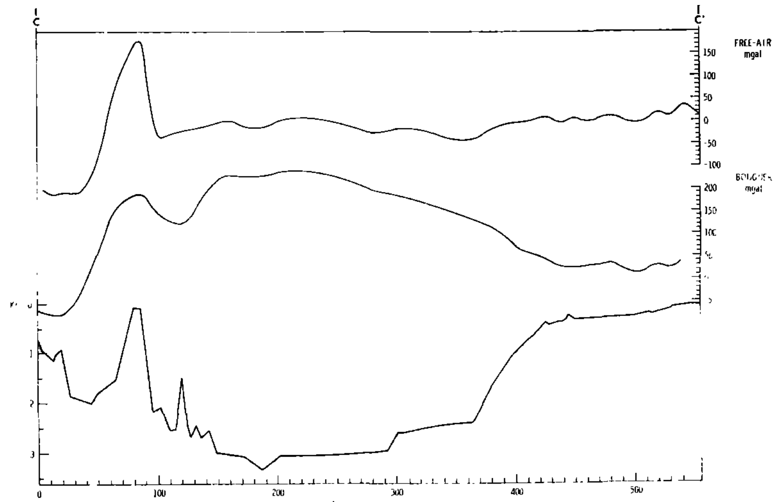

Fig. 13. Bathymetric, free-air, and Bouguer anomaly profile (profile C-C').

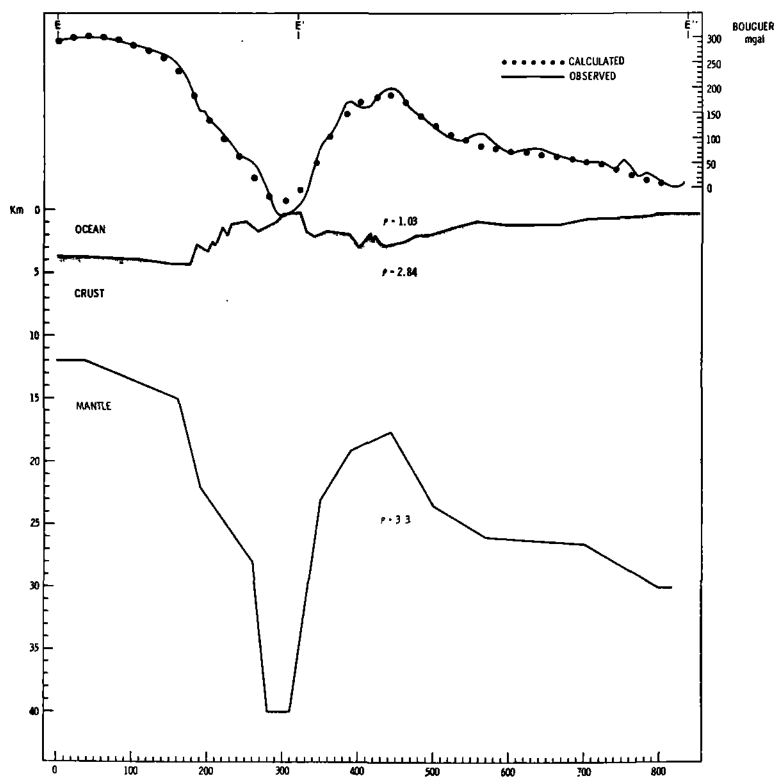

Fig. 14. Bathymetric and Bouguer anomaly profile (profile E-E'-E'' includes calculated crustal model).

anomaly are each zero (the continental shelf) the crustal thickness is 30 km. Through successive calculations, the crust under the Andaman Islands was lowered to 40 km, and the mismatch between the calculated and the observed curves was reduced to only 30 mgal. In additional calculations the crust-mantle interface was lowered to below 40 km, but the computed curve had started to broaden, indicating a shallow rather than a deep source for the anomaly.

Generally, the fit between the gravitational attraction of the mantle in the calculated crustal section and the Bouguer anomalies is good. The departures at the eastern flank of the outer (sedimentary) island arc and over the igneous arc are within the errors caused by the assumptions of the model. This is certainly true for the sedimentary island platform (area west of *E′* on Figure 14), where the use of the 2.84-g/cm^3 density in the Bouguer corrections was obviously too high.

The derived crustal cross section, because it is based solely on the gravity data, does not represent a unique solution. On the basis of similar calculations by *Woollard* [1959], the estimated error in the crustal thickness of the model is $\pm 10\%$. It is entirely possible that sedimentary material has a much greater role in the Bouguer anomalies than is implied in Figure 14 (a mismatch of only 30 mgal). However, more detailed treatment of this possibility would be purely speculative without additional seismic information. Regardless of the possible magnitude of these corrections for a thick accumulation of sedimentary material, the present conclusions should still be applicable; the crustal thickness under the sedimentary island platform is far in excess of normal oceanic crust and, in fact, appears to be of continental type.

The Airy-Heiskanen two-dimensional isostatic anomalies [*Talwani et al.*, 1959] are shown for profile *E-E′-E″* in Figure 15. These show a close resemblance to the free-air anomalies along the section (Figures 5 and 9). The negative isostatic anomaly includes not only the local extension of the Java-Sumatra trench [*Woollard and Strange,* 1962] but also the sedimentary island arc itself. A similar phenomenon was observed by Lyons (published by *Eardley* [1962]) and Talwani (personal communication) in the Antilles arc, where the large negative anomalies of the Puerto Rico trench continue into the Barbados-Trinidad ridge. Although this phenomenon is still not well understood, it is most likely connected to the relative age or state of development of the different parts of the island arc.

Conclusions. On the basis of the data available from the reconnaissance survey by the *Pioneer,* a detailed quantitative interpretation is impossible. The principal objective of this paper, other than the reporting of the data, has been to indicate the continuity of the subaerial geological and tectonic trends through the Andaman Sea area. This continuity is particularly well supported for the extension of the structural trends of northern Sumatra northward through the igneous belt. The geophysical data verify the connection between the Cretaceous belts of the Barisan Range in Sumatra and the Burma Range which was formerly postulated principally on evidence of bathymetry and of volcanism in the Barren and

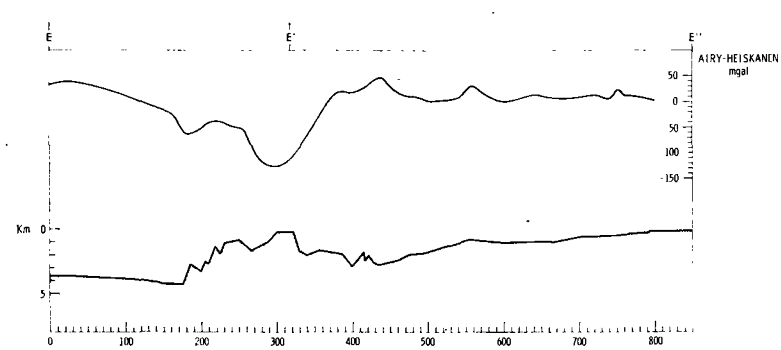

Fig. 15. Bathymetric and Airy-Heiskanen two-dimensional isostatic anomaly profile (profile *E-E′-E″*).

Narcondam Islands. There is strong evidence that the southeast Andaman Sea is underlain by the down-faulted Sunda shelf (west Malaysian shelf).

The Bouguer anomalies indicate continental thickness of the crust under the Andaman-Nicobar island platform, and the Airy-Heiskanen anomalies suggest that future elevation of the islands may be expected.

Acknowledgments. We wish to thank Dr. H. B. Stewart of the Coast and Geodetic Survey for his efforts in incorporating the many measurements required by this study into the scientific program of the *Pioneer* and Dr. J. B. Alexander and his colleagues at the Geological Survey of the Federation of Malaya for their helpful assistance in the program. Dr. Stewart and Captain E. Brown of the *Pioneer* were instrumental in providing needed support during the measurement and data processing phases of this study.

References

Alexander, J. B., A short outline of the geology of Malaya with special reference to Mesozoic orogeny, *The Crust of the Pacific Basin, Geophys. Monograph 6,* pp. 81–86, American Geophysical Union, Washington, D. C., 1962.

Bemmelen, R. W. van, *Geology of Indonesia,* Government Printing Office, The Hague, 1949.

Burns, R. E., Sea bottom heat-flow measurements in the Andaman Sea, *J. Geophys. Res., 69*(22), 4918–4919, 1964.

Drake, C. L., M. Ewing, and G. H. Sutton, Continental margins and geosynclines: The east coast of North America, north of Cape Hatteras, *Phys. Chem. Earth, 3,* 110–198, 1958.

Eardley, A. J., *Structural Geology of North America,* Harper and Row, New York, 1962.

Girdler, R. W., and G. Peter, An example of the importance of natural remanent magnetization in the interpretation of magnetic anomalies, *Geophys. Prospecting, 8*(3), 474–483, 1960.

Karunakaran, C., K. K. Ray, and S. S. Saha, A new probe into the tectonic history of the Andaman and Nicobar Islands, *Intern. Geol. Congr., 22nd, India, 1964, Rept. Session,* edited by B. C. Roy, Volume of Abstracts, section 4, p. 45, New Delhi, 1964.

Peter, G., D. Elvers, and M. Yellin, Geological structure of the Aleutian trench southwest of Kodiak Island, *J. Geophys. Res., 70*(2), 353–366, 1965.

Talwani, M., G. H. Sutton, and J. L. Worzel, A crustal section across the Puerto Rico trench, *J. Geophys. Res., 64*(10), 1545–1555, 1959.

Woollard, G. P., Crustal structure from gravity and seismic measurements, *J. Geophys. Res., 64*(10), 1521–1544, 1959.

Woollard, G. P., and W. E. Strange, Gravity anomalies and the crust of the earth in the Pacific basin, in *The Crust of the Pacific Basin, Geophys. Monograph 6,* pp. 60–80, American Geophysical Union, Washington, D. C., 1962.

(Manuscript received May 22 ,1965;
revised October 27, 1965.)

Reprinted from *Geofizičeskie issledovanija*, Sbornik II, Izdatel'stvo MGU, 1966, p. 231-240

Some particularities of the gravimetric field and of the structure of the terrestrial crust of the Atlantic, Indian and Pacific Oceans

by A. G. Gaĭnanov and P. A. Stroev

ГАЙНАНОВ А. Г., СТРОЕВ П. А.

НЕКОТОРЫЕ ОСОБЕННОСТИ ГРАВИТАЦИОННОГО ПОЛЯ И СТРОЕНИЕ ЗЕМНОЙ КОРЫ АТЛАНТИЧЕСКОГО, ИНДИЙСКОГО И ТИХОГО ОКЕАНОВ

Измерения силы тяжести на морях и океанах в настоящее время производятся морскими маятниковыми приборами и морскими гравиметрами как с подводных лодок, так и с надводных судов.

Использование кварцевых часов для получения отметок времени на фотозаписи колебаний маятников значительно уменьшает величину поправки за ход хронометра и повышает точность морских гравиметрических наблюдений.

Наиболее крупные погрешности при наблюдениях силы тяжести на надводных судах возникают из-за влияния возмущающих ускорений на периоды колебаний маятников и на показания морских гравиметров. Регистрация и учет влияния возмущающих ускорений — одна из самых важных и наиболее трудных задач в морской гравиметрии. В настоящее время морские маятниковые приборы снабжены дополнительными коротко- и длиннопериодическими маятниками для регистрации наклонов и горизонтальных ускорений корабля и вертикальными акселерометрами для записи вертикальных возмущающих ускорений.

При наблюдениях на подводных лодках наибольшие погрешности возникают из-за неучета скорости и направления морских течений, что вносит ошибку в определение поправки Этвеша.

Первые измерения силы тяжести в Атлантическом, Индийском и Тихом океанах были произведены в 1923—1930 гг. в экспедициях на подводной лодке Венинг-Мейнесом. Измерения силы тяжести производились по разработанной Венинг-Мейнесом методике при помощи сконструированного им специального трехмаятникового прибора [30]. В 1937 г. были произведены определения силы тяжести в Охотском и Японском морях Л. В. Сорокиным [16]. С 1951 г. кафедрой геофизических методов исследования земной коры геологического факультета Московского университета им. М. В. Ломоносова совместно с Всесоюзным научно-исследовательским институтом геофизических методов разведки (ВНИИГеофизики) и Государственным астрономическим институтом им. П. К. Штернберга (ГАИШ) с перерывами производились гравиметрические исследования на э/с «Витязь» Института океанологии АН СССР во время плавания судна в Охотском, Японском и Беринговом морях, Курило-Камчатской глубоководной впадине и Тихом океане. Измерения силы тяжести производились как с помощью различных маятниковых приборов, так и с морскими затушенными гравиметрами, разработанными ВНИИГеофизики [2, 3].

Большой объем гравиметрических исследований в переходной области от Азиатского континента к Тихому океану был выполнен в период МГГ в 1957—1958 гг. [1, 7].

В переходной зоне от Японских островов к Тихому океану морские гравиметрические измерения при помощи морского маятникового прибора были выполнены японскими геофизиками [27]. Многочисленные определения силы тяжести в переходных зонах от Американского континента к Тихому океану, от Алеутской гряды к Тихому океану и Берингову морю, а также в открытом океане произведены американскими геофизиками. Измерения силы тяжести производились при помощи усовершенствованного морского маятникового прибора Венинг-Мейнеса на подводной лодке, а также при помощи морских гравиметров, установленных на кораблях на гироскопически стабилизированных платформах. Сводка зарубежных гравиметрических данных по Тихому океану дана в работе Вулларда и Странжа [31]. Ими составлены схематические гравиметрические карты Тихого океана в редукциях Фая и Буге (нормальная формула — международная 1930 г.). В дальнейшем при описании аномалий силы тяжести Тихого океана мы будем пользоваться гравиметрическими картами, составленными Вуллардом и Странжем.

Гравиметрическая изученность Тихого океана к настоящему времени еще совершенно недостаточна. Почти совершенно не освещены в гравиметрическом отношении громадные площади южной части Тихого океана. Относительно хорошо изучено гравитационное поле переходной зоны от Азиатского и Австралийского континентов к Тихому океану.

Аномалии силы тяжести в редукции Буге вычислены при постоянном значении плотности промежуточного слоя $\sigma=2{,}67$ *г/см*^{3}. Некоторые авторы предлагают вычисление поправки Буге производить при переменной плотности промежуточного слоя, а именно для континентов $\sigma=2{,}67$ *г/см*^{3} (плотность «гранитного» слоя земной коры), для океанов $\sigma=2{,}8$ *г/см*^{3} (плотность «базальтового» слоя). При использовании для вычисления мощности земной коры корреляционных зависимостей между мощностью земной коры и аномалиями силы тяжести в редукции Буге возможно использовать поправки Буге с переменной плотностью, однако в этом случае осложняется использование аномалий Буге для выяснения особенностей глубинного строения в переходных зонах от материков к океанам, срединных океанических хребтов, островов, где развиты породы как «гранитного», так и «базальтового» состава. Поэтому при региональных исследованиях особенностей строения земной коры целесообразно вычислять поправку Буге с постоянной плотностью промежуточного слоя, равной средней плотности верхней части земной коры 2,67 *г/см*^{3}.

Первые советские гравиметрические определения в Атлантическом океане были произведены в 1954 г. на борту китобазы «Слава», в IX рейсе китобойной флотили «Слава» в 1954—1955 гг. Измерения силы тяжести производились двумя морскими трехмаятниковыми приборами [4]. В дальнейшем измерения силы тяжести в Атлантическом океане, особенно в Антарктическом секторе Атлантического океана, производились при помощи морских маятниковых приборов и морских затушенных гравиметров, установленных на борту дизель-электрохода «Обь» в составе советских антарктических экспедиций [5, 8, 9, 18, 19, 20]. Большой объем морских маятниковых определений силы тяжести на подводных лодках в Атлантическом океане и в прилегающих морях выполнен американскими, английскими и другими зарубежными исследователями [22, 23, 24, 25, 26, 28, 29 и др.].

Первые советские гравиметрические измерения в Индийском океане были произведены во время плавания сотрудников ГАИШ и геологического факультета МГУ на дизель-электроходе «Обь» в составе советских антарктических экспедиций [5, 8, 9, 17, 18, 19].

После работ Венинг-Мейнеса гравиметрические измерения в Индийском океане проводились американскими и английскими геофизиками [26, 29]. Особенно большой объем гравиметрических измерений в Аравийском море и западной части Индийского океана выполнен английскими геофизиками на экспедиционном судне «Овен» в 1961—1962 гг. Измерения силы тяжести производились при помощи морского набортного гравиметра GSS—2—11 Аскания Верке (Графа), установленного на гиростабилизированной платформе системы «Аншютц» [21]. Одновременно с измерением силы тяжести производились измерения напряженности полного вектора магнитного поля при помощи буксируемого ядерного магнитометра и эхолотные промеры. Точность определения аномалий силы тяжести порядка ±5 *мгл*. Индийский океан до настоящего времени в гравиметрическом отношении является наименее изученным из всех океанов.

По характеру гравитационных аномалий Атлантический, Тихий и Индийский океаны можно разделить на три основные группы областей:

1. Области глубоких океанических котловин, характеризующиеся относительно спокойным полем силы тяжести с небольшими, близкими к нулю, положительными или отрицательными аномалиями Фая и очень большими, до +450 *мгл* положительными аномалиями Буге.

2. Области подводных хребтов и океанических островов, характеризующиеся увеличением аномалий Фая до +100 *мгл* и более и уменьшением аномалий Буге до 0+100 *мгл*. Так, над Срединно-атлантическим хребтом аномалии Фая достигают значений +70, +80 *мгл*, над южной частью Китового хребта до +150 *мгл*.

На островах Буве, Вознесения, Азорских, св. Павла, Тристан-да-Кунья аномалии Буге уменьшаются до +110, +120 *мгл*, на острове Кергелен до +55 *мгл*, на острове Цейлон до +50 *мгл*, на острове Мадагаскар до —100 *мгл*. Другая группа островов отличается сравнительно высокими аномалиями Буге. Так, в районе Бермудских островов аномалия Буге достигает величины +353 *мгл*, в районе Канарских островов +200 *мгл*, у островов Зеленого мыса +271 *мгл*, на острове Мадейра +254 *мгл*, на Гавайских и Каролинских островах до +250 *мгл*, на Маршалловых островах до +200 *мгл* [13, 21, 31].

3. Переходные области от океана к континентам. Эти области выделяются наиболее резкими изменениями аномалий силы тяжести как в редукции Фая и Буге, так и в изостатических редукциях.

Наиболее резкие изменения аномалий силы тяжести наблюдаются в переходной зоне от Азиатского материка к Тихому океану в области развития островных дуг и глубоководных желобов. Так, в районе Японских островов и Японского глубоководного желоба, а также в прилегающих районах Курильской островной дуги и Курильского глубоководного желоба аномалии Фая изменяются от +240 *мгл* до —320 *мгл*, горизонтальный градиент достигает 30 *этвеш*. Аномалии Буге изменяются от —40 *мгл* на острове Хонсю до +420 *мгл* в Японском желобе с горизонтальным градиентом 10—15 *этвеш*. Отчетливо прослеживается вдоль глубоководных Японского, Курило-Камчатского, Алеутского, Перуанско-Чилийского желобов и желоба Тонга и Кермадек пояс интенсивных отрицательных аномалий Фая.

В Северо-Американской переходной зоне этот пояс распадается на отдельные области отрицательных аномалий Фая.

Наиболее обширная область отрицательных аномалий Фая примыкает к Калифорнийскому побережью и ограничена с юга разломом Кларион, а с севера разломами Пионер и Мендосино. Пояс отрицательных аномалий Фая при переходе далее в океан обрамляется менее интенсивным поясом положительных аномалий Фая. В некоторых случаях эти пояса положительных аномалий Фая хорошо коррелируются с краевыми валами глубоководных желобов, однако, как правило, ширина аномальной зоны больше. Наиболее интенсивная и обширная область положительных аномалий Фая примыкает к Алеутскому желобу. Обширная зона повышенных значений аномалий Фая выявлена в районе Соломоновых, Ново-Гебридских островов, островов Фиджи и Новая Каледония [31]. При переходе от Атлантического океана к материкам Северной и Южной Америки, Европы и Африки также прослеживается пояс отрицательных аномалий Фая. Наиболее отчетливо прослеживается этот пояс при переходе от Атлантического океана к материкам Северной Америки и Европы, где ширина его достигает 150—300 *км*. В Африканской и Южноамериканской переходных областях пояс отрицательных аномалий Фая распадается на отдельные пятна. Юго-восточнее Рио-де-Жанейро расположена область большого гравитационного градиента, где на расстоянии около 100 *км* аномалии Фая убывают от +12 до —205 *мгл* (21 *этвеш*), а аномалии Буге изменяются от +268 до +75 *мгл* (19 *этвеш*). При переходе от Атлантического, Индийского и Тихого океанов к Антарктиде также наблюдаются области отрицательных аномалий Фая. Ширина переходной зоны от Атлантического океана к Антарктиде больше, чем ширина переходных зон к другим континентам [13].

Переходные области Индийского океана наименее изучены. Относительно лучше изучены переходные зоны от Австралийского материка к Индийскому океану, Индонезийская переходная зона и переходные зоны Аравийского моря [21]. Еще Венинг-Мейнесом были выявлены пояса интенсивных отрицательных аномалий силы тяжести (в редукциях Фая и изостатических) в Индонезийской переходной зоне, получившие название поясов Венинг-Мейнеса [30]. В переходной зоне от Африки к Индийскому океану и от западного побережья Индии к Индийскому океану также выявляются зоны интенсивных отрицательных аномалий Фая [21].

Многими исследователями показано, что на основании данных гравиметрии достаточно успешно может быть выполнено определение общей мощности земной коры до поверхности Мохоровичича [6, 11, 12, 31 и др.].

Если принять значение средней плотности земной коры для океанических областей $\sigma_1 = 2{,}8$ *г/см*^{3}, а плотности подстилающих пород $\sigma_2 = 3{,}3$ *г/см*^{3}, то получим разность плотностей на границе Мохоровичича $\Delta\sigma = \sigma_2 - \sigma_1 = 0{,}5$ *г/см*^{3}. При такой разности плотностей, естественно, изменение мощности земной коры ΔH и вызовет изменение аномалии силы тяжести в редукции Буге на величину $\delta\Delta g$. Пользуясь формулой притяжения бесконечного плоско-параллельного слоя, получим

$$H_i = H_0 - \frac{\delta_i \Delta g}{2\pi k \Delta\sigma}; \quad \delta_i \Delta g = \Delta g_i - \Delta g_0. \qquad (1)$$

Таким образом, зная глубину поверхности Мохоровичича H_0 в какой-либо опорной точке океана, можно по этой формуле вычислить глубину H_i для любой точки, если известны аномалии Буге в этих точках. Значения H_0 в опорных точках определяются методом сейсмических зондирований. Необходимо, однако, иметь в виду, что в действительности наблюдаемые аномалии силы тяжести обусловлены не только изменением мощности земной коры, но и изменением мощности рыхлых и уплотненных осадочных отложений, а также изменением плотности «базальтового» слоя и плотности подкорового вещества в горизонтальном направлении. Особенно значительные погрешности в определении мощности земной коры по формуле (1) могут получиться в переходных зонах от материков к океанам, в областях развития срединных океанических хребтов, глубоководных впадин, подводных гор и островов, где наблюдаются наиболее резкие изменения мощностей осадочного слоя, соотношения мощностей «гранитного» и «базальтового» слоев, изменения плотностей слоев коры и подкорового вещества в горизонтальном направлении. Обычно для некоторого ослабления влияния локальных неглубоких неоднородностей земной коры на наблюденные аномалии силы тяжести производят усреднение аномалий по площади. Определения силы тяжести, произведенные с борта корабля в открытом океане, где глубины достигают 3—5 *км*, в значительной степени свободны от влияния локальных аномалий силы тяжести вследствие удаленности источников локальных аномалий от уровня наблюдения. Влияние локальных аномалий резко возрастает в переходных зонах, в областях развития подводных хребтов, островов, где источники локальных аномалий приближаются к уровню наблюдения.

Некоторыми исследователями на основании сопоставления мощности земной коры, полученной по сейсмическим данным с соответствующими для этих участков осредненными аномалиями Буге, составлены корреляционные графики зависимости между толщиной земной коры и осредненными аномалиями Буге [11, 31 и др.]. Так как строение земной коры переходных зон от материков к океанам весьма сложное и определение мощности земной коры в этих зонах по гравиметрическим данным получается менее точным, чем в океанических областях, нами были построены разрезы земной коры по гравиметрическим данным по профилям, близким к меридиональным, проходящим через центральные части Атлантического, Индийского и Тихого океанов (рис.). Вычисление глубин поверхности Мохоровичича производилось двумя способами:

1) по корреляционному графику зависимости между толщиной земной коры и осредненными аномалиями Буге, полученному Р. М. Деменицкой;

2) по формуле притяжения бесконечного плоско-параллельного слоя.

Причем для расчета по формуле (1) для участка разреза в Атлантическом океане в качестве опорных значений H_0 и Δg_0 взято среднее значение из 12 точек Северной Атлантики, где достаточно хорошо известно поле силы тяжести в редукции Буге и имеются сравнительно многочисленные сейсмические определения мощности земной коры [10, 12]. Участок профиля в Индийском океане был привязан к опорной сейсмической точке в Тасмановом море [12]. И, наконец, Тихоокеанский участок разреза был привязан к опорным данным ГСЗ в северо-восточной части Тихого океана, полученным в период МГГ советскими исследователями [14].

Рассчитанная по двум методам толщина земной коры не имеет систематической разницы. За окончательный результат было принято среднее значение из двух методов. Оценить точность получения толщины земной коры можно по внутренней сходимости между двумя методами вычисления. Ошибка в этом случае получается равной ±1 *км*. Более реальную оценку точности определения мощности земной коры по гравиметрическим данным можно получить при сопоставлении наших вычислений с сейсмическими данными о

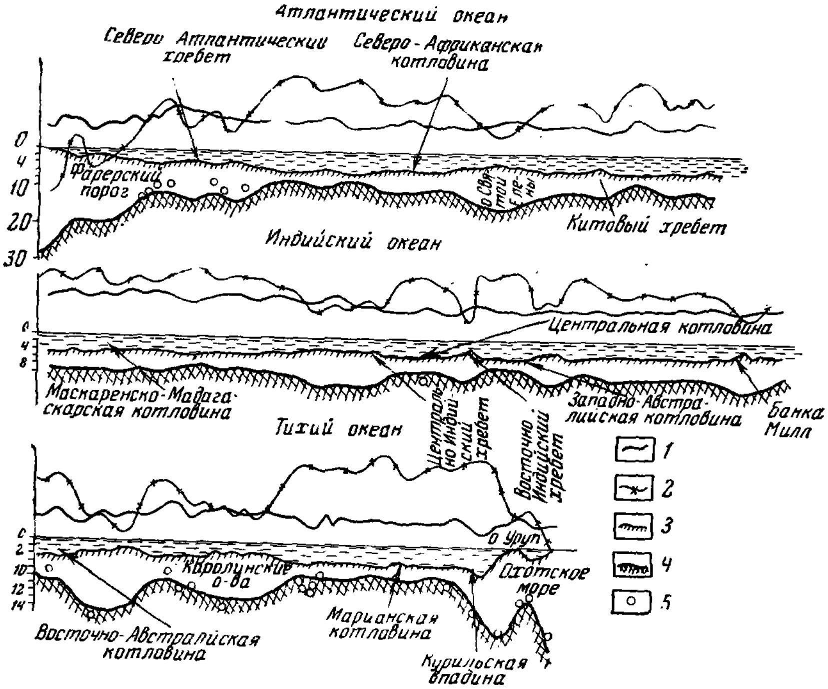

Рис. Схематический разрез земной коры на акваториях Атлантического, Индийского и Тихого океанов:

1 — аномалия Фая, 2 — аномалия Буге, 3 — рельеф дна, 4 — граница Мохоровичича 5 — граница Мохоровичича по сейсмическим данным

глубине границы Мохоровичича. Сводка сейсмических данных о строении земной коры приведена в работах Р. М. Деменицкой, Г. З. Гурария и И. А. Соловьевой [10, 12]. Наиболее изученными в сейсмическом отношении являются Северная Атлантика, а также западная и юго-западная окраины Тихого океана. В Индийском океане к настоящему времени имеется единственный сейсмический профиль, где получены данные о строении земной коры океана вплоть до поверхности Мохоровичича [15]. Наши профили пересекают участки океана, где имеются достаточно близко расположенные сейсмические пункты. Всего таких пунктов 20. В результате сопоставления сейсмических и гравиметрических данных о глубине поверхности Мохоровичича средняя квадратическая ошибка определения мощности земной коры по гравиметрическим данным получилась равной $\pm 2,4$ *км*. Необходимо учесть, что сами сейсмические определения могут содержать ошибки порядка $\pm 1,5$ *км*.

На рис. 1 приведены разрезы земной коры через центральные части Атлантического, Индийского и Тихого океанов. Как видно на этих разрезах, наиболее тонкая кора наблюдается в областях глубоких океанических впадин. Поверхность Мохоровичича под впадинами раполагается на глубинах 7—10 *км* от уровня океана. Если учесть слой воды мощностью 5—6 *км*, то толщина коры под впадинами уменьшается до 2—4 *км*.

Под срединными океанническими н подводными хребтами, а также под островами наблюдается увеличение мощности земной коры до 12—25 *км*. Намечаются некоторые региональные отличия в мощности земной коры различных океанов. Так, под впадинами глубиной 5000—6000 *м* кора в Атлантическом океане несколько тоньше, чем под глубоководными впадинами Тихого океана. По общей мощности земная кора под глубокими котловинами Индийского океана ближе к Тихому океану.

Мощности земной коры, полученные по сейсмическим данным для Северо-Атлантического хребта, как правило, меньше мощности, полученной по гравиметрическим данным. Возможно, эта разница обусловлена изменением плотности вещества верхней мантии под Срединноатлантическим хребтом. Мощность земной коры, полученная по гравиметрическим данным для Тихого океана, лучше согласуется с сейсмическими данными при разности плотностей между веществом земной коры и верхней мантии несколько меньшей, чем 0,5 *г/см*^{3}. Для Индийского океана имеющийся единственный сейсмический пункт лучше согласуется с гравиметрическими определениями мощности земной коры также при меньшей, чем 0,5 *г/см*^{3}, разности плотностей вещества коры и верхней мантии. Дальнейшее накопление гравиметрических и сейсмических данных о строении земной коры Атлантического, Индийского и Тихого океанов и их комплексная интерпретация позволят более определенно судить о намечающихся в настоящее время различиях в строении земной коры и верхней мантии под акваториями Атлантического, Индийского и Тихого океанов.

ЛИТЕРАТУРА

1. Веселов К. Е., Евдокимов Ю. С., Жилин А. В., Телепин М. А. О гравиметрической съемке с морскими статическими гравиметрами на Охотском море и Тихом океане. «Прикладная геофизика», 1961, № 29.

2. Гайнанов А. Г. Маятниковые определения силы тяжести в Охотском море и в северо-западной части Тихого океана. «Тр. Ин-та океанологии АН СССР», 1955, т. XII.

3. Гайнанов А. Г., Смирнов Л. П. Гравиметрические исследования на э/с «Витязь» в Тихом океане в 1957—1958 гг. Сб. «Морские гравиметрические исследования», вып. 1. Изд-во МГУ, 1961.

4. Гайнанов А. Г. Гравиметрические определения в Антарктиде, Атлантическом океане и Средиземном море в IX рейсе китобойной флотилии «Слава». Сб. «Морские гравиметрические исследования», вып. 1. Изд-во МГУ, 1961.

5. Гайнанов А. Г. Гравиметрические определения на дизель-электроходе «Обь» в первом антарктическом рейсе. Сб. «Морские гравиметрические исследования», вып. 1. Изд-во МГУ, 1961.
6. Гайнанов А. Г. О некоторых результатах гравиметрических исследований в Охотском море, Курило-Камчатской впадине и прилегающих частях Тихого океана. Сб. «Морские гравиметрические исследования», вып. 2. Изд-во МГУ, 1963.
7. Гладун В. А., Марчук Г. Д., Пантелеев В. Л., Строев П. А. Гравиметрические исследования в районе Курило-Камчатской впадины и северо-западной части Тихого океана в 1958 году. Сб. «Морские гравиметрические исследования», вып. 2. Изд-во МГУ, 1963.
8. Грушинский Н. П. Морские определения силы тяжести в Антарктике в 1956—1957 гг. Сб. «Морские гравиметрические исследования», вып. 1. Изд-во МГУ, 1961.
9. Грушинский Н. П. Опыт применения гравиметра на надводном корабле. Сб. «Морские гравиметрические исследования», вып. 1. Изд-во МГУ, 1961.
10. Гурарий Г. З., Соловьева И. А. Строение земной коры по геофизическим данным. М., Изд-во АН СССР, 1964.
11. Деменицкая Р. М. Планетарные структуры земной коры и их отображение в аномалиях Буге. «Сов. геология», 1958, № 8.
12. Деменицкая Р. М. Основные черты строения коры Земли по геофизическим данным. «Тр. Ин-та геологии Арктики», 1961, т. 115.
13. Корякин Е. Д. Гравитационное поле Атлантического океана и его связь с глубинным строением земной коры. Сб. «Морские гравиметрические исследования», вып. 2. Изд-во МГУ, 1963.
14. Косминская И. П., Зверев С. М., Вейцман П. С. и др. Основные черты строения земной коры Охотского моря и Курило-Камчатской зоны Тихого океана по данным глубинного сейсмического зондирования. «Изв. АН СССР», сер. геофиз., 1963, № 1.
15. Непрочнов Ю. П. Новые данные о строении земной коры под дном Индийского океана. ДАН СССР, 1962, т. 144, № 2.
16. Сорокин Л. В. Гравиметрия и гравиметрическая разведка. М., Гостоптехиздат, 1953.
17. Строев П. А. Методика морских гравиметрических измерений в VI рейсе дизель-электрохода «Обь». «Инф. бюл. САЭ», № 42. Л., «Морской транспорт», 1963.
18. Фролов А. И. Гравиметрические работы ГАИШ в III Сов. Антарктической экспедиции в 1957—1958 гг. Сб. «Морские гравиметрические исследования», вып. 2. Изд-во МГУ, 1963.
19. Фролов А. И. Гравиметрические работы ГАИШ в V Сов. Антарктической экспедиции в 1959—1960 гг. Сб. «Морские гравиметрические исследования», вып. 2. Изд-во МГУ, 1963.
20. Чеснокова Г. С., Грушинский Н. П. Гравиметрические определения в Гренландском море, проведенные в 1956 г. на дизель-электроходе «Обь». Сб. «Морские гравиметрические исследования», вып. 1. Изд-во МГУ, 1961.
21. Bathymetric, Magnetic and Gravity investigations H. M. S. Owen 1961—1962. London, Hydrographic department, Admiralty Marine Science publication. No. 4, 1963.
22. Browne B. C. Cooper R. Y. The British submarine gravity surveys of 1938 and 1946. «Roy Soc. London, Phylos. Trans.», ser. A, 1950, v. 242, No. 847.
23. Browne B. C. Cooper R. Y. Gravity measurements in the English Channel. «Proc. Roy. Soc.», ser. B, 1952, v. 139, No. 896.
24. Ewing M., Worzel I. L. Gravity anomalies and the structure at the West Indies. «Bull. Geol Soc. America», 1954, v. 65, No. 2.
25. Ewing M., Worzel I. L., Shurbet G. L.' Gravity observation at sea in U. S. submarines. «Barracuda.», «Tusc», «Conger», «Argonaut» and «Medregal». Verhand. Konikl. Neder Geol.— Mijn. Genoot., Geol., ser. 18. (Vening Meinsz commem vol.), v. 49, No. 115, 1957.
26. Girdler R. W. Harrison I. C. Submarine gravity measurements

in the Atlantic Ocean, Indian ocean, Red Sea and Mediterranean sea, «Proc. Roy. Soc.» ser. A, 1957, v. 239, No. 202.
27. Matuyama M. Distribution of gravity over the Nippon Trench and related areas. «Imp. Acad. Tokyo», Pr. 1936.
28. Shurbet G. L., Worzel I. L. Gravity observations at sea in USS «Conger», cruise III (1954), Trans Amer, Geoph. Un, v. 38, No. 1, 1957.
29. Talwani M. Gravity measurements on HMS «Acheron»» in South Atlantic and Indian oceans. «Bull. Geol. Soc. America», 1962, v. 73, No. 9.
30. Vening—Meinesz F. R. Gravity expeditions at sea 1923—1938, v. 4, Delft, 1948.
31. Wollard G. P., Strange W. E. Gravity anomalies and the crust of the Earth in the Pacific Basin. «Am. Geoph. Un», 1962, No. 6.

Reprinted from *Proceed. Indian Acad. Sciences*, vol. LXIV, 1966, p. 192-202

SOME STUDIES ON WAVE REFRACTION IN RELATION TO BEACH EROSION ALONG THE KERALA COAST

By P. K. Das, V. Hariharan and V. V. R. Varadachari

[*Indian Ocean Physical Oceanographic Centre of the Indian Ocean Expedition (C.S.I.R.), Ernakulam*)]

Received June 11, 1965

(Communicated by Dr. N. K. Panikkar, F.A.SC.)

Abstract

Using the British Admiralty bathymetric charts off the West Coast of India and employing the graphical method of constructing wave refraction diagrams, an attempt is made to study the behaviour of the short-period waves (4, 5 and 6 seconds) which are found to affect the coast generally in the neighbourhood of Cochin Port entrance. Nineteen stations, at intervals of roughly one mile, are chosen around the three-fathom line in this area. Considering a probable field of approach of deep-water waves, limited to a cone of 90°, five directions of approach are chosen at intervals of 22½° in the range of 202½° to 292½°. Refraction diagrams are prepared for these directions and periods, and from these, the refraction functions and directional parameters are evaluated for each station. The possible directions of flow of long-shore current and the areas vulnerable to erosion and sedimentation are investigated.

Introduction

The area under investigation is a twenty-mile stretch along the Kerala Coast, the neighbourhood of the entrance to the Cochin Port—which has to be maintained at a constant depth of 6 fathoms by frequent dredging as it often gets chocked with accretion materials. There is evidence of beach erosion at some points that are covered by this study.

The seaward stretch of the area of investigation extends from the coast to the fifty-fathom line. The bathymetric charts used for the purpose are British Admiralty Charts Nos. 749 and 750 (with recent corrections) which have been enlarged for convenience. A preliminary statistical analysis of the wave periods, reported in the *Indian Daily Weather Reports* for the years

1961 and 1963, shows that waves with periods around 5 seconds or less form a large percentage of the waves affecting the coast. Hence, this study is limited to waves of periods 5 and 6 seconds. However, 4-second period waves are also considered as the lower limit. Waves of periods less than 4 seconds are not considered because it is felt that their effect is small. Five directions for deep-water waves approaching the shore are chosen at intervals of $22\frac{1}{2}°$ in the range of $202\frac{1}{2}°$ to $292\frac{1}{2}°$. Angles beyond these limits are left aside due to the involved drafting errors and the possibilities of diffraction.

Nineteen stations marked, alphabetically, A to S are chosen roughly at intervals of one mile along and around the three-fathom line. Stations A to F are to the south of Cochin Port entrance while G to S are on the northern side of it.

METHOD OF STUDY

With the introduction of high speed electronic computers in recent years, the construction of wave refraction diagrams has become much simplified and less time-consuming (Dorrestein, 1960; Griswold, 1963; H. M. Iyer *et al.*, 1963). But the basic procedures remain almost the same as that followed in the present study, where the method suggested by Arthur, Munk and Isaacs (1952) and adopted by Pierson, Neumann and James (1955) is used to prepare refraction diagrams and to evaluate the refraction and direction functions R and θ respectively. These functions have been used to gain an understanding of beach erosion and sedimentation along the coast.

In this study, the ocean waves are represented as simple sine waves. A single wave train is considered at a time in which the crests are parallel in deep water. This is followed up to the coast in all successive refractions at different depths at intervals of one fathom applying Snell's Law—$c_d/c=$ sine α_d/sine α; where c_d and c are the wave celerities in deep and shallow waters and α_d and α are the angles made by the wave ray with the normal to the contour on the deep and shallow sides respectively. A wave ray is a line perpendicular at every point to the successive wave crests and shows the direction of propagation of wave energy which again is supposed not to cross any wave ray. For a particular wave crest, as many wave rays or orthogonals are drawn as practicable, which are equally spaced in deep water where all the orthogonals are parallel to each other. These are followed up to the points of interest (stations A to S here), when, after successive refractions, the spacing between the adjacent wave rays and their directions are changed, depending upon the nature of the bathymetry. The changes in direction and spacing between adjacent wave rays are used to evaluate the refraction

2

TABLE I

Refraction functions

Directions	202½°			225°			247½°			270°			292½°		
Period→ / Stations	4 Sec.	5 Sec.	6 Sec.	4 Sec.	5 Sec.	6 Sec.	4 Sec.	5 Sec.	6 Sec.	4 Sec.	5 Sec.	6 Sec.	4 Sec.	5 Sec.	6 Sec.
A ..	..	..	..	0·8208	..	..	0·8543	0·9871	..	0·8518	0·9727	1·2379	0·8241	0·8084	0·8020
B ..	0·7273	..	..	0·7871	..	..	0·8342	0·7438	0·7317	0·8417	0·7780	0·9120	0·8202	0·7361	0·8846
C ..	0·6861	0·6560	..	0·8302	0·7429	0·8485	0·8470	0·8618	0·9767	0·8374	0·8077	0·9509	0·8017	0·7336	0·8576
D ..	0·7327	0·6544	..	0·8119	0·7668	0·8655	0·8477	0·8292	1·1602	0·8292	0·7846	0·9451	0·7962	0·6709	0·8293
E ..	0·7705	0·7158	..	0·8256	0·8225	1·0187	0·8490	0·8860	0·9060	0·8269	0·9805	1·0538	..	0·7443	1·0305
F ..	0·8307	0·8172	0·9451	0·8946	0·8870	1·0987	0·8973	0·7896	1·0845	..	0·9412	1·2850	0·7752	..	..
G ..	..	..	..	..	..	..	0·7775	..	..	0·7410	0·9152	1·0667	0·6609	0·5784	0·8357
H ..	..	..	..	0·7831	0·8424	1·1175	..	0·7738	0·9898	0·7117	0·7459	0·8302	0·4360	0·4663	0·7642
I ..	0·8167	0·8454	0·9566	0·8541	0·9101	1·0110	0·8295	0·8441	1·0654	0·7646	0·8654	1·1325	0·7747	0·6560	0·8608
J ..	0·8115	0·8226	0·8652	0·8537	0·8412	1·0256	0·8978	0·9894	1·4441	0·9314	0·9687	1·2168	0·8865	1·0055	1·0515
K ..	0·8146	0·7545	1·1153	0·9310	1·1420	1·6192	0·9179	0·9017	1·0732	0·8226	0·7238	1·0233	0·8470	0·7230	0·8010
L ..	0·5617	0·9370	0·7647	0·4875	0·6308	0·6564	0·7121	0·6785	0·5758	0·7644	0·8182	1·1683	0·7170	0·5856	0·8105
M ..	0·8567	0·5152	0·5958	0·7163	0·6193	0·5949	0·8344	0·8291	1·2365	0·7951	0·7294	0·8198	0·6954	0·6680	0·9331
N ..	0·6519	0·5648	0·6138	0·8068	0·7759	0·9093	0·8313	0·7567	0·9357	0·7840	0·8252	0·9836	0·6933	0·7969	0·9501
O ..	0·7871	0·8571	0·7799	0·8355	0·8633	1·3086	0·8765	0·9136	1·1408	0·8511	0·8148	1·0792	0·8074	1·1475	1·0480
P ..	0·6371	0·3728	0·7720	0·7782	0·8334	0·8156	0·7597	0·6942	0·9598	0·8012	0·9442	1·2512	0·7298	0·7058	0·8240
Q ..	1·1225	0·8631	0·7420	0·9380	0·7191	0·8139	0·9483	0·9989	1·5191	0·9053	0·9165	1·1220	0·9273	0·9611	0·8410
R ..	0·9459	1·0070	1·8940	0·8648	0·9425	1·2830	..	0·9882	1·0829	0·7398	0·7033	0·7289	0·7972	0·6864	..
S ..	0·7545	0·8306	..	0·8653	1·0804	1·2310	..	0·7762	0·8950	0·8703	0·8693	1·4460	..	..	..

Table II

Direction functions

Directions	202½°			225°			247½°			270°			292½°		
Period→ / Stations	4 Sec.	5 Sec.	6 Sec.	4 Sec.	5 Sec.	6 Sec.	4 Sec.	5 Sec.	6 Sec.	4 Sec.	5 Sec.	6 Sec.	4 Sec.	5 Sec.	6 Sec.
A ..	..	..	..	+ 4·50	...	...	+8·90	+4·57	..	−0·80	+1·47	+ 0·48	− 2·10	− 3·94	− 6·79
B ..	+ 8·60	..	..	+ 3·40	...	...	+1·60	+3·30	+ 6·63	..	−1·40	− 2·72	− 2·80	− 7·45	−11·24
C ..	+ 7·10	+12·90	..	+ 2·70	+ 8·56	+10·58	+1·16	+2·50	+ 2·46	−2·40	−2·90	− 5·70	− 3·40	− 9·83	−13·80
D ..	+ 6·40	+12·74	..	+ 2·40	+ 6·22	+ 7·65	+0·30	+0·98	+ 0·10	−3·10	−4·72	− 8·60	− 4·60	−12·28	−16·82
E ..	+ 5·26	+10·13	..	+ 1·60	+ 4·33	+ 3·88	−0·70	−0·67	− 1·90	−5·02	−6·60	− 6·80	− 4·80	−12·24	−16·05
F ..	+ 3·56	+ 7·40	+12·05	+ 1·20	+ 3·60	+ 3·30	−0·20	−0·33	− 2·83	..	−5·63	− 8·40	..	..	..
G ..	..	..	..	..	..	..	+4·10	..	..	−1·50	−4·00	− 8·15	− 7·80	−15·73	−18·37
H ..	..	..	..	+ 1·50	+ 3·90	+ 7·14	−3·80	−3·40	− 3·25	−7·30	−6·25	−13·70	−16·80	−23·27	−26·17
I ..	+ 5·00	+ 8·98	+12·40	+ 0·15	+ 3·68	+ 1·92	−3·60	−4·37	− 6·64	−9·42	−7·57	−17·95	−14·80	−21·47	−24·20
J ..	+ 7·70	+10·80	+16·04	+ 3·00	+ 3·08	+ 6·03	−0·30	−2·28	− 0·20	−2·90	−2·37	− 7·76	− 7·00	−11·10	−12·50
K ..	+13·37	+15·47	+28·50	+10·55	+ 9·70	+18·25	+6·60	+5·73	+13·82	+3·10	−3·00	+ 1·72	− 1·90	− 5·60	− 8·30
L ..	+13·40	+24·57	+37·70	+13·60	+15·00	+23·00	+6·30	+3·80	+ 9·10	+0·63	−1·67	− 3·67	− 5·10	−10·27	−15·02
M ..	+11·40	+20·48	+23·60	+ 5·10	+ 9·50	+11·28	−0·40	+0·63	− 1·03	−4·70	−4·42	−10·92	−11·52	−16·75	−21·67
N ..	+ 9·10	+14·75	+20·20	+ 4·44	+ 5·10	+ 6·84	−0·50	−1·00	− 2·12	−6·04	−6·15	−10·02	−11·10	−18·05	−22·67
O ..	+ 9·48	+15·58	+18·50	+ 4·06	+ 3·60	+ 7·60	+1·00	−1·22	− 1·04	−3·30	−4·38	−10·30	− 8·80	−16·07	−17·90
P ..	+11·10	+15·75	+17·10	+ 5·20	+ 5·06	+10·78	+0·08	−1·45	+ 0·87	−4·70	−4·10	−10·76	..	−14·25	−17·25
Q ..	+ 7·40	+10·73	+14·40	+ 5·90	+ 4·25	+ 4·60	+0·06	−1·55	− 2·52	−2·76	−0·30	− 6·30	..	−10·40	−14·35
R ..	+ 8·20	+19·00	+21·60	+ 8·00	+ 4·88	+11·60	+2·50	+1·64	+ 9·83	−1·40	−1·80	− 7·02	..	−11·62	..
S ..	+10·88	+16·95	..	+ 5·90	+ 7·74	+11·70	+0·50	+1·84	+ 3·00	−3·80	−2·12	− 7·50	..	..	..

function R and the direction function θ at the point of interest. The refraction function R is given by

$$R = [K(F, \theta)]^2 = \frac{b_d/b}{\frac{c}{c_d} + \frac{4\pi d}{L} \frac{1}{\sinh \frac{4\pi d}{L} \frac{c_d}{c}}}$$

where L is the wavelength, d the depth at the point of interest, C_d and C the wave velocities in deep water and at depth d respectively, b_d and b the distances between two adjacent orthogonals in deep water and at depth d respectively and F is the frequency of the wave. The refraction parameters are evaluated for each wave period and direction from the refraction diagrams prepared for each individual direction and period.

Discussion

In Tables I and II are presented the refraction and direction functions, worked out at each of the stations for varying directions and periods. Table III presents the angles that the refracted rays make with the normal drawn to the contour at the point of interest. Figures 1 to 5 show the variation of R values from stations A to S with different directions and periods, while the arrow marks at each station show the probable direction of flow of long-shore currents derived from the direction function θ.

The distribution of R values along the stations is directly related to the amount of energy associated with the changed wave height which can be shown to be equal to $\sqrt{R}$ times the deep-water wave height. Hence the convergence and divergence of wave rays, deciding R and θ values at a particular station, speak for the accumulation and dissipation of wave energy as no energy crosses wave rays. The change in wave direction at the station, seen as the change from the deep-water direction, and the angle made by the wave ray with the normal drawn at the station to the mean contour on the landward side, gives us an idea about the direction of flow of the longshore current. The accumulated water, after the breaking of the waves, goes back as rip current and the like, only after an alongshore flow for a certain distance, depending upon the angle at which the wave breaks with the shore line (Per Bruun, 1963). Suggestions are therefore made regarding the longshore drift of beach materials along with the longshore currents at each station. The general pattern of erosion and accumulation of beach material follows from this.

TABLE III

Direction functions

(With respect to the Normal at the Station contour)

Directions	202½°			225°			247½°			270°			292½°		
Period→ / Stations	4 Sec.	5 Sec.	6 Sec.	4 Sec.	5 Sec.	6 Sec.	4 Sec.	5. Sec.	6 Sec.	4 Sec.	5 Sec.	6 Sec.	4 Sec.	5 Sec.	6 Sec.
A ..	..	..	..	+34·50	..	..	+ 7·60	+11·93	..	− 5·20	− 7·47	− 6·48	−26·40	−24·56	−21·71
B ..	+55·90	..	..	+38·60	..	..	+ 7·30	+15·20	+12·87	.	− 4·60	− 0·28	−22·70	−21·05	−14·26
C ..	+47·40	+41·60	..	+29·30	+23·44	+21·42	+ 8·34	+ 7·00	+ 7·04	−10·60	−10·10	− 7·30	−32·10	−25·67	−21·76
D ..	+44·10	+37·76	..	+25·60	+21·78	+20·35	+ 5·20	+ 4·52	+ 5·40	−13·90	−12·28	− 8·40	−34·90	−27·22	−22·68
E ..	+45·24	+40·37	..	+26·40	+23·67	+24·12	+ 6·13	+ 6·17	+ 7·40	−14·98	−10·40	−10·20	−34·70	−27·26	−23·45
F ..	+25·94	+22·10	+17·45	+ 5·80	+ 3·40	+13·70	+ 4·70	−15·17	−12·73	..	−32·37	−29·60	..	..	..
G ..	..	..	..	..	..	..	+19·40	..	..	+ 2·50	+ 5·00	+ 9·15	−13·70	− 5·77	− 3·13
H ..	..	..	..	+17·50	+15·10	+11·86	+ 0·30	− 0·10	− 0·25	−18·70	−19·75	−12·30	−31·70	−25·23	−23·32
I ..	+ 6·50	+ 2·52	− 0·90	−15·15	−14·68	−12·92	−29·90	−29·13	−26·87	−46·58	−48·43	−38·05	−63·70	−57·03	−54·30
J ..	+40·80	+37·70	+32·46	+23·00	+22·92	+19·97	+ 3·80	+ 5·78	+ 3–70	−16·10	−16·63	−11·24	−34·50	−30·40	−29·00
K ..	+73·13	+71·03	+58·00	+53·45	+54·30	+45·75	+34·90	+35·77	+17·68	+15·90	+16·00	+17·28	− 1·60	+ 2·10	+ 4·80
L ..	+58·10	+46·93	+33·80	+35·40	+34·00	+26·00	+20·20	+22·70	+17·40	+ 3·37	+ 5·67	+ 7·67	−13·40	− 8·23	− 3·40
M ..	+23·10	+14·02	+10·90	+ 6·90	+ 2·50	+ 0·72	−10·10	−11·13	− 9·47	−28·30	−28·58	−22·08	−43·98	−38·75	−33·63
N ..	+45·40	+39·75	+34·13	+27·56	+20·90	+25·16	+10·00	+10·50	+11·62	− 6·96	− 6·85	+ 0·02	−24·40	−17·45	−12·83
O ..	+42·02	+35·92	+33·00	+24·94	+25·40	+21·40	+ 5·50	+ 7·72	+ 7·54	−12·70	−11·62	− 5·70	−29·70	−22·43	−20·60
P ..	+57·40	+52·75	+51·40	+40·80	+40·94	+35·22	+23·42	+24·95	+22·63	+ 5–70	+ 5·10	+11·76	..	− 7·25	− 3·25
Q ..	+43·10	+39·77	+36·10	+22·10	+23·75	+23·40	+ 5·44	+ 7·00	+ 8·02	−14·24	−16·70	−10·70	..	−29·10	−25·15
R ..	+56·30	+45·56	+42·90	+34·00	+37·12	+30·40	+17·00	+17·86	+ 9·67	− 1·60	− 1·20	+ 4·02	..	−13·88	..
S ..	+32·62	+26·55	..	+16·10	+13·26	+ 9·30	− 2·30	− 3·34	− 4·50	−20·20	−21·88	−16·50	..	..	..

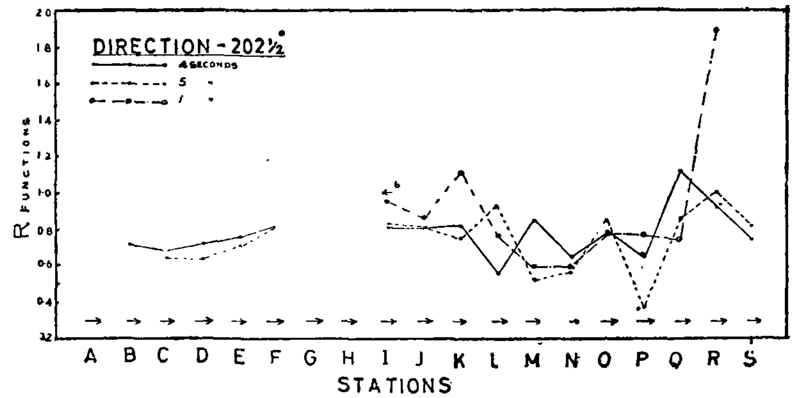

FIG. 1.

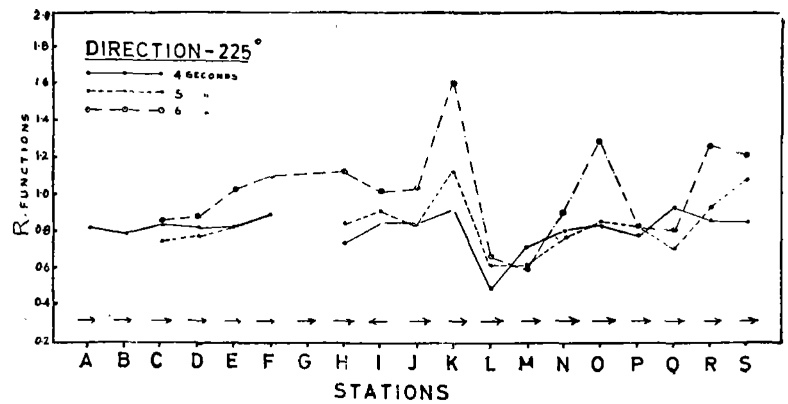

FIG. 2.

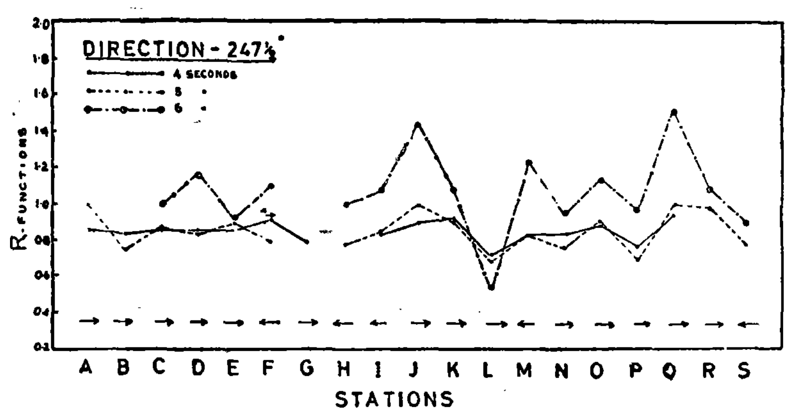

FIG. 3.

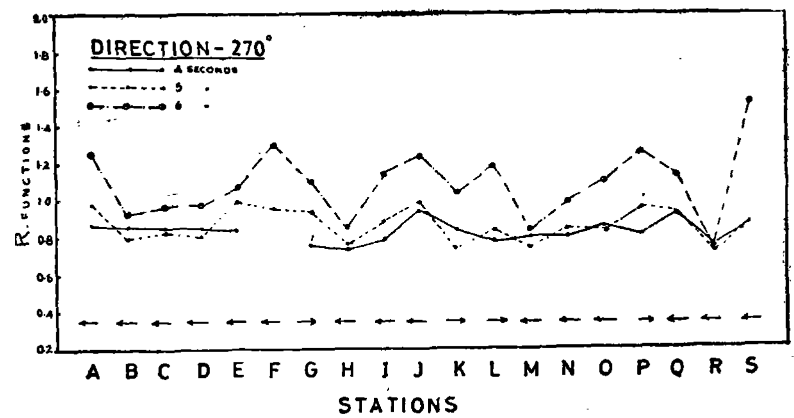

FIG. 4.

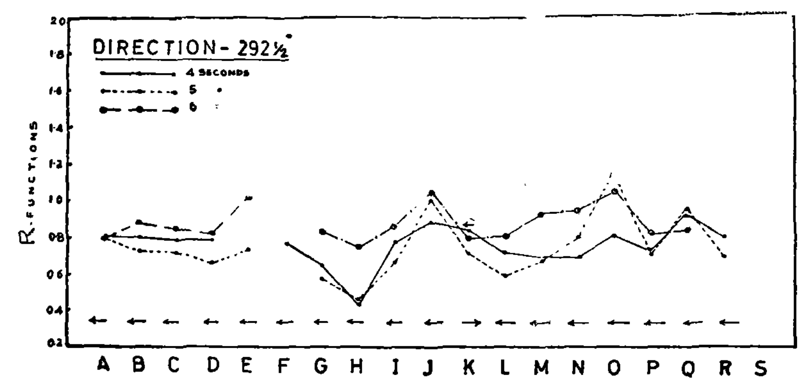

FIG. 5.

As has been reasoned before, the lower period waves, like the one considered in this study, are the most expected to have any continuous action on the shore line, barring the occasional storms that may send swells or long-period waves to make sudden impacts on it. In the latter cases, however, the energy associated with the waves at breaking would be very high, compared with those of the lower periods studied here. The refraction functions therefore would be much higher than those found in the cases of 4, 5 and 6-second waves. The waves however will break at greater depths and the total effect may vary much from those expected from the wave actions of lower periods.

In general, the refraction functions show increasing values from 4-second to 6-second waves as expected. The interesting point, however, is that while this is gradual between 4 to 5 seconds it is abrupt between 5 and 6-second periods. Thus, it is felt that any significant wave action in this region may be due to waves around 5 seconds and above as the energy associated with still lower periods will be too low to have much bearing on this. This is readily verifiable from Figs. 2, 3 and 4 where the R values for 4 and 5 seconds seem to lie close to each other and follow closely for the directions 225°, 247½° and 270°. In the limiting cases, *i.e.*, for angles 202½° and 292½° (as can be seen from Figs. 1 and 5) this trend in R values is not well defined, probably because of the drafting errors asociated with the acute angles of approach of the waves.

The R functions as can be seen from Table I are mostly less than 1·0 for 4 and 5-second waves for all the deep-water directions. This shows a lessening of wave height in general and therefore dissipation of the energy associated, which may be aggravated by local wind actions, bottom percolations and the like. The 5-second waves, however, show R function to be more than the value of 1·0 at certain stations with varying directions such as at K and S for 225° and at J and O for 292½°. This, however, will be discussed later along with the station characteristics. For 6-second period, R mostly shows a value of more than 1·0 for all the five directions of approach and at particular stations (Table I) this is seen to be persistent as at stations E and F on the southern side of the fairway channel and at J, K and O on the northern side of it. The maximum and minimum R values for all the periods and the directions are found to be 1·89 (at station R for period 6 seconds and direction 202½°) and 0·37 (at station P for period 5 seconds and direction 202½°).

In Table II are presented the net changes in directions, brought in by refraction, indicated with positive and negative signs so that when added algebraically to the corresponding deep-water directions, the direction of arrival of the wave at the point of interest is obtained. It is seen from this table that up to a deep-water direction of 225° the changes in direction are positive whereas beyond 270° the changes are negative for all stations, *i.e.*, up to 225° the angles increase and beyond 270° they decrease. The deep-water direction 247½° shows the characteristics of transition and the changes in angles here are mixed indifferently for different periods. There are positive and negative values for each of the periods which vary stationwise. Table III shows the angles that the refracted wave rays make with the landward drawn normals to the depth contours of the station. A rough idea of the alongshore currents can be had from the values given in the table.

In the perspective of the above findingst he following suggestions, regarding the longshore flow, may be offered. For 202½° deep-water direction, the northerly component of longshore current is predominant for all the periods excepting a singular case in station I for 6-second waves. For the direction 292½° the direction of flow of longshore currents is towards south in general excepting at station K where for 5 and 6-second wave periods the flow is found to be northerly. While these are as expected, being the two marginal directions, the refracted wave rays for the other deep water directions show very interesting behaviour as seen from Figs. 2, 3 and 4. Here the longshore current is not northerly or southerly at all stations as in the marginal cases. The changes in longshore currents associated with the changes in peak and trough values of refraction functions give very plausible hints for the erosion and accumulation patterns for different waves.

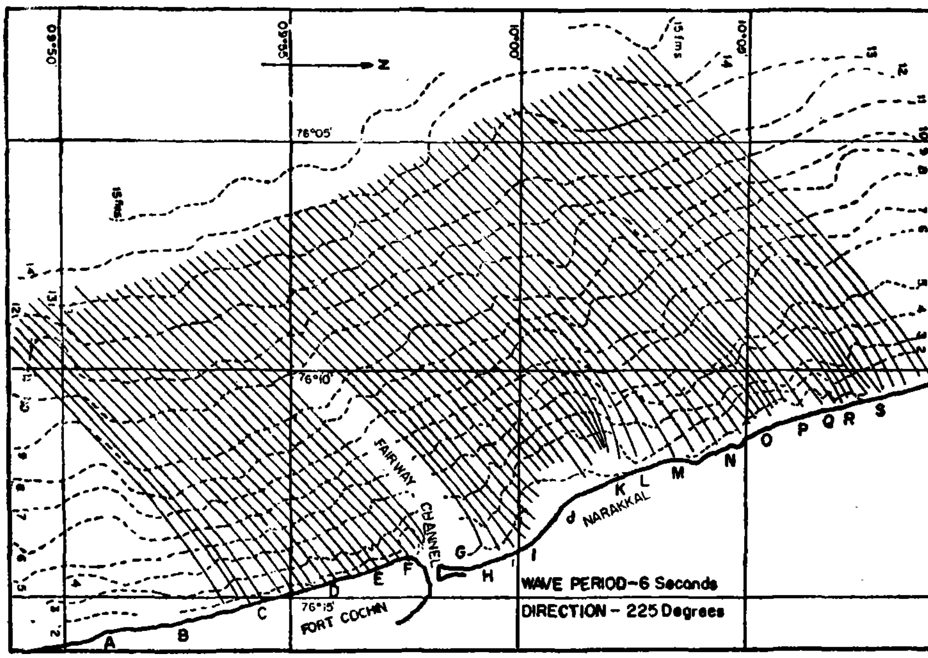

FIG. 6.

As seen from Figs. 1 to 5 there exist alternate peaks and troughs for R in the northern side of the fairway channel, *i.e.*, from stations G to S. This however is less true for the southern side, *i.e.*, for the stations A to F. Thus the southern side is likely to be less disturbed by the wave refraction and this is more so as there are few cases of energy concentration due to convergence of wave rays. The situation at station F is somewhat different and the high value of R here is mostly associated with an increased wave height which is due to the shoal immediately south of the channel (Fig. 6). Considering the directions 225°, 247½° and 270° for stations F to S it is found that the longshore current directions diverge out from certain stations and converge to certain others (Figs. 2 to 4). And this whole process keeps changing with changing deep-water directions and periods. These factors can most presumably be utilised to explain the facts that (i) the fairway channel gets filled up with materials carried in from both sides and (ii) erosion takes place near the stations J and K (Narakkal area). In Fig. 6 it can be seen that at station K the wave rays converge strongly.

Station O is another point where a peak for R exists due to convergence of wave rays for all the directions and periods with the only exception for a deep-water direction of 270°. Hence, this point is also susceptible to denudation due to wave action.

SUMMARY

The investigations on wave refraction along the coast near Cochin reveal the possible existence of areas of concentration of wave energy at certain points and removal of the material of the beach, which is disturbed near areas of concentration of wave energy by diverging longshore currents and the accretion of materials at certain regions due to converging longshore currents. The accretion of material in the fairway channel near Cochin and the reported beach erosion near Narakkal (situated near station K in Fig. 6) could be clearly explained with the help of this investigation.

ACKNOWLEDGEMENT

The authors wish to acknowledge gratefully the facilities extended by Prof. M. S. Krishnan, formerly Director of National Geophysical Research Institute and Dr. N. K. Panikkar, Director, Indian Ocean Expedition. Two of the authors (P. K. Das and V. Hariharan) wish to express their sincere thanks to Shri V. S. Rama Raju for the encouragement given and facilities provided during the work and to Shri K. V. Sundara Ramam for his very helpful suggestions during the initial stages of this study.

REFERENCES

1. Arthur, R. S., *et al.* .. "The direct construction of wave rays," *Transactions of the American Geophysical Union*, 1952, **33**, 855–65.
2. Bruun Per. .. "Longshore currents and longshore troughs," *J. Geophys. Res.*, February 15, 1963, **68** (4).
3. Dorrestein, R. .. "Simplified method of determining refraction coefficients for sea-waves," *Ibid.*, February 1960, **65** (2).
4. Griswold, G. M. .. "Numerical calculation of wave refraction," *Ibid.*, March 1963, **68** (6).
5. Iyer, H. M. and Punton, N. V. W. .. "A computer program for plotting wavefronts and rays from a point source in dispersive mediums," *Ibid.*, June 1, 1963, **68** (11).
6. Pierson, W. J. Jr., *et al.* "Practical methods for observing and forecasting Ocean Waves by means of wave spectra and statistics," *U.S.H.O. Publication No.* 603, 1955.

Reprinted from *Vestnik Moskovskogo Universiteta*, Geology series, no. 6, 1967, p. 3-15

Some aspects of the structure of the terrestrial crust in the Red Sea, Gulf of Aden and the north-western part of the Indian Ocean

by A. G. Gaïnanov and P. A. Stroev

А. Г. ГАЙНАНОВ, П. А. СТРОЕВ

НЕКОТОРЫЕ ЧЕРТЫ СТРОЕНИЯ ЗЕМНОЙ КОРЫ В КРАСНОМ МОРЕ, АДЕНСКОМ ЗАЛИВЕ И СЕВЕРО-ЗАПАДНОЙ ЧАСТИ ИНДИЙСКОГО ОКЕАНА

Первые геофизические исследования в области Красного моря были проведены в 1890—1898 гг., когда Фон Триулзу провел маятниковые определения силы тяжести в различных пунктах побережья, а также на некоторых островах [25].

В 1923 г. Венинг-Мейнес [3] при плавании на подводной лодке к Индонезийскому архипелагу выполнил четыре определения силы тяжести морским маятниковым прибором в различных районах Красного моря. В 1955 г. Гирдлер и Гаррисон провели гравиметрические измерения на подводной лодке в южной части Красного моря между островами Дахлак и Фарсан [26].

В 1958 г. американские экспедиции на исследовательских судах «Вима» и «Атлантик» выполнили комплексные геофизические исследования в Красном море, включающие эхолотирование, сейсмические работы (15 профилей методом преломленных волн), измерения полного вектора напряженности магнитного поля [21]. Всего в 1958 г. выполнено 4500 *км* профилей. В 1959 г. английская экспедиция на судне «Далрампль» отработала 3000 *км* профилей в Красном море, проведя батиметрические и магнитные исследования.

В конце 1961 г. итальянская экспедиция на научно-исследовательском судне «Арагонез» провела эхолотирование, а также магнитную и гравитационную съемку акватории Красного моря на 54 профилях [17].

В 1965 г. немецкое (ФРГ) научно-исследовательское судно «Метеор», работавшее по плану Международной Индоокеанской экспедиции, провело исследования (океанография, морская геология) в южной части Красного моря, в Персидском заливе, Аденском заливе и Аравийском море по маршруту длиной в 44 тыс. *км*. В 1958 г. во время рейса судна «Вима» американскими исследователями были выполнены комплексные геофизические исследования в Аденском заливе, включающие эхолотирование, сейсмические работы (5 профилей методом преломленных волн) и магнитные измерения [28]. В отдельных пунктах Красного моря выполнены измерения теплового потока [19, 29]. Кроме морских геофизических исследований на берегах и островах Красного моря выполнены геофизические работы с геологоразведочными целями.

При плавании подводной лодки «Ачерон» Гирдлер и Гаррисон [26] в 1955 г., а в 1959 г. Тальвани [31] проводили морские маятниковые определения силы тяжести в западной и северо-западной частях Индийского океана. Первые сейсмические исследования методом преломленных волн были проведены на судне «Челленджер» в 1950—1953 гг. Гаскеллом и др. [24].

Обширные комплексные геофизические исследования северо-западной части Индийского океана выполнены в 1961—1962 гг. английскими учеными на экспедиционном судне «Оуэн» [16]. Экспедиция проделала 16 тыс. миль (37 профилей), проводя непрерывные батиметрические, гравиметрические и магнитные исследования. Большой объем сейсмических работ методом преломленных волн в северо-западной части Индийского океана был выполнен американскими и английскими исследователями по программе Международной Индоокеанской экспедиции [15, 22, 23]. В этот же период впервые в Индийском океане были выполнены измерения величины теплового потока [12, 13, 19, 29].

Первые советские геофизические исследования в Красном море и северо-западной части Индийского океана были начаты в 1956 г. во время плавания сотрудников ГАИШ и геологического факультета МГУ на дизель-электроходе «Обь» в составе советских антарктических экспедиций. В этих экспедициях производились измерения силы тяжести при помощи морских маятниковых приборов и морских гравиметров [4, 6, 7].

В период МГГ (1957—1958 гг.) в Красном море и северо-западной части Индийского океана советская немагнитная шхуна «Заря» провела магнитные исследования [8, 9].

В 1959 г. в 31-м рейсе судна «Витязь» были выполнены первые советские сейсмоакустические исследования в Индийском океане методом отраженных волн [11].

В 33-м рейсе «Витязь» (1960—1961 гг.) были проведены сейсмические исследования методами отраженных и преломленных волн в северной части Индийского океана. Наблюдения методом отраженных волн проведены в Аравийском море, на Аравийско-Индийском хребте, а методом преломленных волн — в южной части котловины Аравийского моря [11]. В 1964—1965 гг. в 36-м рейсе судна «Витязь» в Индийском океане выполнен значительный комплекс геолого-геофизических исследований [13]. В частности, проведены детальные полигонные сейсмические (методами МОВ и МПВ), гравиметрические и гидромагнитные исследования, а также измерения теплового потока в рифтовой зоне Срединно-Индоокеанского и других подводных хребтов.

В период подготовки и проведения МГГ и особенно Международной Индоокеанской экспедиции (1959—1962 гг.) выполнен большой объем работ по изучению рельефа дна северо-западной части Индийского океана. На основании обобщения материалов этих исследований в институте океанологии АН СССР составлены новые батиметрические карты северо-западной части Индийского океана [1, 2]. На этих картах выделяются наиболее крупные особенности рельефа дна северо-западной части Индийского океана, такие как Аравийско-Индийский, Маскаренский, Мальдивский хребты, Аравийская, Маскаренская, Сомалийская котловины и другие менее протяженные хребты и желоба (Амирантский, Меррея и др.). На карте эпицентров землетрясений, составленной по материалам Гутенберга, Рихтера, Роте, Дрейка и Гирдлера [2, 21 и др.], хорошо прослеживается приуроченность большинства эпицентров к рифтовой зоне Аравийско-Индийского хребта (рис. 1). Зона резкого изменения простирания Аравийско-Индийского хребта в районе Аденского залива характеризуется усилением сейсмической активности. Примерно на линии предполагаемого соединения рифтовой зоны Аденского залива с зоной восточноафриканских разломов концентрируются эпицентры землетрясений [10]. В Красном море сейсмическая активность выше в южной части; севернее 20° с. ш. отмечено лишь несколько эпицентров. Далее к северу, в Мертвом море и восточной части Средиземного моря,

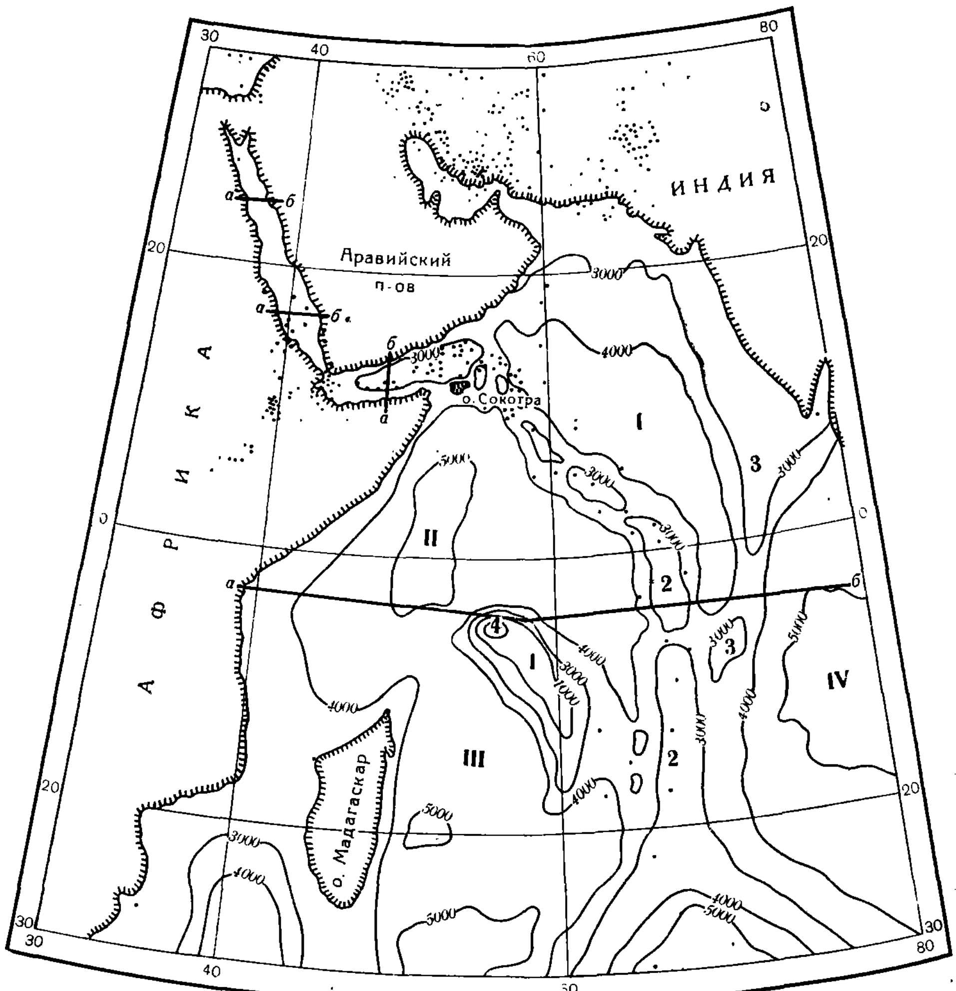

Рис. 1. Карта эпицентров землетрясений и расположение разрезов:
I — Аравийская котловина, II — Сомалийская котловина, III — Маскаренская котловина, IV — Центральная котловина. 1 — Маскаренский хребет, 2 — Аравийско-Индийский хребет, 3 — Мальдивский хребет, 4 — Сейшельские острова. Точками обозначены эпицентры землетрясений: *а—б* — сводные сейсмогравиметрические разрезы

снова отмечаются эпицентры землетрясений. Очень высока сейсмическая активность в Персидском заливе и северо-восточном побережье. Зарегистрированы отдельные эпицентры, приуроченные к хребтам Меррея, Мальдивским, а также к Мозамбикскому проливу.

Полученные к настоящему времени данные позволяют провести комплексную интерпретацию геолого-геофизических материалов с целью выяснения глубинного строения земной коры и верхней мантии в северо-западной части Индийского океана и Красном море.

На основании имеющихся гравиметрических данных нами были составлены для исследуемой области схематические карты аномалий силы тяжести в редукциях Буге с плотностью промежуточного слоя 2,67 и 2,80 *г/см*^{3} и в редукции Фая (нормальная формула международная). На схематической карте аномалий Фая преобладают отрицательные аномалии порядка —30, —40 *мгл.* Только над сильно раздробленной поверхностью подводных хребтов, состоящих из сочетания небольших хребтов и узких грабенообразных депрессий и желобов наблюдается резкая изменчивость аномалий Фая. В частности, аномалии Фая над самими гребнями хребтов имеют значения порядка +50 *мгл* (а над Маскаренским хребтом до +230 *мгл*), а рифтовые долины отмечаются значительными отрицательными аномалиями, порядка —50 *мгл.* Детальное описание гравитационного поля северо-западной части Индийского океана было нами дано ранее [5].

Магнитное поле северо-западной части Индийского океана чрезвычайно неоднородно. Анализ магнитных профилей, выполненных экспедиционными судами «Оуэн» и «Заря», позволяет схематически выделить отдельные области, характеризующиеся степенью аномальности магнитного поля. Для качественной оценки магнитной аномальности нами вычислялась характеристическая величина $N = \frac{(\Delta T_{\max}) \cdot n}{100}$ для равных 150-мильных участков маршрутов «Оуэн». Такие расчеты были впервые выполнены в северо-западной части Индийского океана М. М. Ивановым для Z_a [9].

Наименее аномальные области следующие. Первая — от острова Сокотра к юго-западу, материковый шельф, материковый склон Африки и западная часть Сомалийской котловины. Здесь наблюдаются аномалии $\Delta T \approx \pm 40\ \gamma$ и только в отдельных участках они достигают величины $\pm 100\ \gamma$. Вторая — центральная часть исследуемой области к северу от Сейшельских островов и Аравийское море. Аномалии ΔT в этой области в среднем колеблются в пределах $\pm 100 \div 150\ \gamma$.

Аравийско-Индийский хребет характеризуется типичными для срединно-океанических хребтов магнитными аномалиями [27]. Так, на трех пересечениях в центральной и северной части хребта наблюдаются следующие изменения аномалий ΔT. Если в Сомалийской котловине наблюдаются длиннопериодические магнитные аномалии с амплитудами от —420 γ до +260 γ, то при подходе к склону Аравийско-Индийского хребта длиннопериодные магнитные аномалии затухают и выделяются короткопериодные аномалии с амплитудой $\pm 60 \div 100\ \gamma$. Над рифтовой зоной амплитуда магнитных аномалий возрастает от —360 γ до +400 γ (рис. 2). На материковом склоне к югу от Карачи наблюдаются интенсивные магнитные аномалии с амплитудой от —200 γ до +400 γ, которые у побережья Индостана затухают до $\pm 20\ \gamma$. Цепочка Лаккадивских островов характеризуется интенсивными положительными магнитными аномалиями с амплитудой до +400 γ, а Мальдивских островов — преимущественно отрицательными аномалиями с амплитудой до —400 γ. Сейшельские острова выделяются интенсивными, преимущественно отрицательными магнитными аномалиями с амплитудой в среднем $\pm 300\ \gamma$. Маскаренский хребет характеризуется слабыми магнитными аномалиями с амплитудами $\pm 60\ \gamma$. Северная часть Маскаренской впадины более аномальна ($\pm 150\ \gamma$), чем южная ($\pm 20\ \gamma$).

В Аденском заливе и в зоне поперечного разлома и сдвига Аравийско-Индийского хребта выявлены интенсивные магнитные аномалии с амплитудами от —300 до +400 γ (отдельные максимумы до 2000 γ [16, 28]). В Красном море, особенно в южной части в зоне развития рифта,

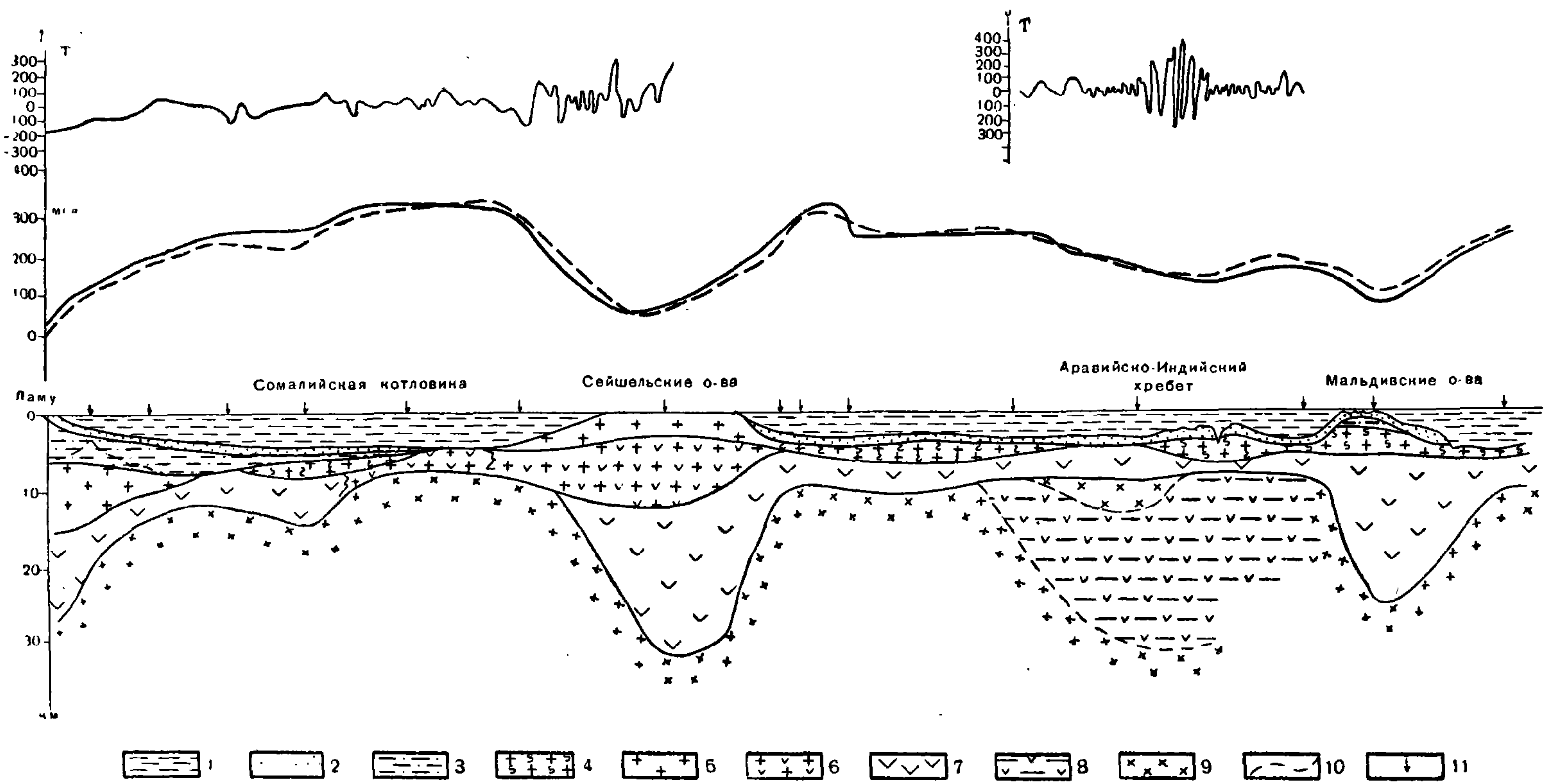

Рис. 2. Сводный разрез земной коры, построенный по сейсмическим и гравиметрическим данным по профилю Африка — Сейшельские острова — Центральная котловина Индийского океана:

1 — слой воды; 2 — неуплотненные осадочные отложения v=1,8—3,2 *км/сек*, σ=2,0—2,3 *г/см*^{3}; 3 — уплотненные осадочные отложения v=3,3—4,8 *км/сек*, σ=2,4—2,5 *г/см*^{3}; 4 — осадочно-вулканогенные отложения («надбазальтовый» слой) v=4,2—5,8 *км/сек*, σ=2,6 *г/см*^{3}; 5 — породы кристаллического щита («гранитный» слой) v=4,7—5,9 *км/сек*, σ=2,7 *г/см*^{3}; 6 — второй «гранитный» слой Сейшельских островов v=6,3 *км/сек*, σ=2,8 *г/см*^{3}; 7 — «базальтовый» слой v=6,4—6,8 *км/сек*, σ=2,9—3,0 *г/см*^{3}; 8—серпентинизированные перидотиты аномальной верхней мантии v=7,3—7,8 *км/сек*, σ=3,1 *г/см*^{3}; 9 — верхняя мантия v=8,0—8,3 *км/сек*, σ=3,3 *г/см*^{3}; 10 — нижняя граница разуплотнения мантии; 11 — пункты сейсмических зондирований. Сплошная линия — Δg наблюденная; пунктирная линия — Δg вычисленная

наблюдаются весьма характерные для рифтовых зон срединных океанических хребтов интенсивные магнитные аномалии с амплитудами в среднем от —500 γ до +500 γ [21].

На основании имеющихся геофизических данных нами были построены схематические разрезы земной коры северо-западной части Индийского океана и Красного моря (рис. 3, 4, 5). При подсчете влияния изменения разреза земной коры на наблюденные аномалии силы тяже-

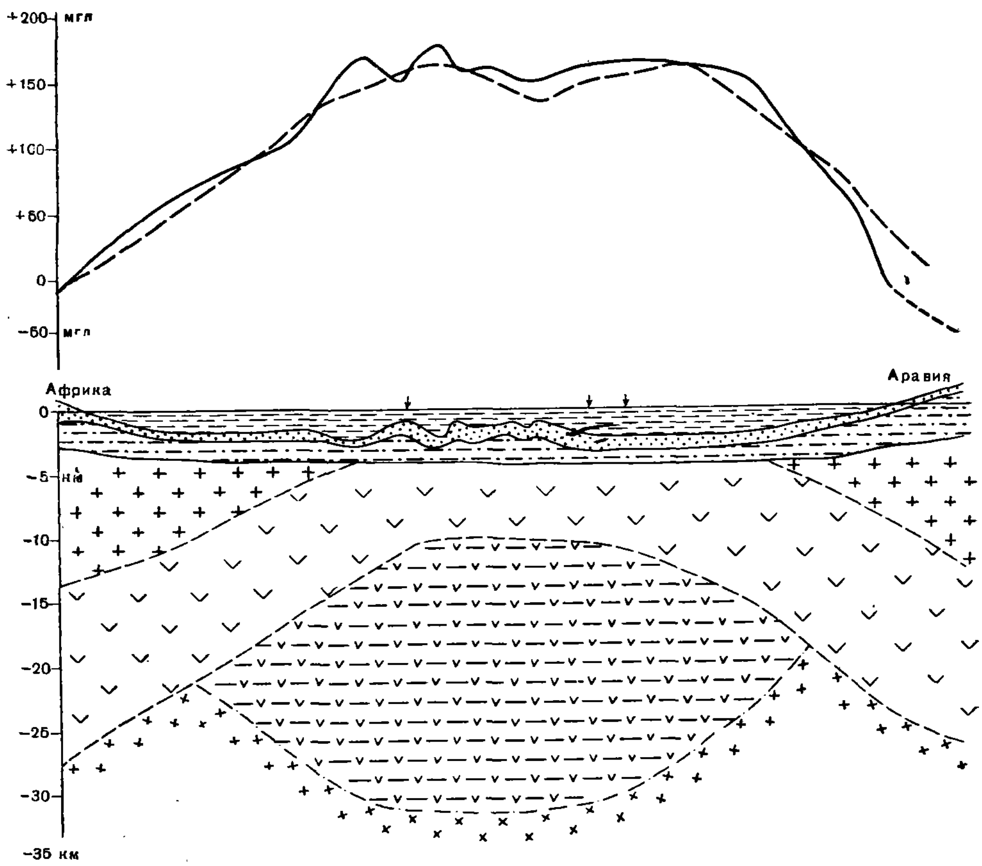

Рис. 3. Сводный разрез земной коры, построенный по сейсмическим и гравиметрическим данным через Аденский залив (по 48°E). Условные обозначения см. рис. 2

сти плотности соответствующих слоев земной коры определялись по значениям граничных скоростей продольных волн, используя эмпирическую зависимость скорости распространения продольных волн от плотности по Нейфу и Дрейку [32]. Разрез через северо-западную часть Индийского океана (см. рис. 2) проходит от Кенийского побережья Африки (порт Ламу), через Сомалийскую котловину к Сейшельским островам, далее примерно по 5° ю. ш., пересекая Аравийско-Индийский хребет, Мальдивский хребет и желоб Чагос. На основании геолого-геофизических исследований на суше установлено, что у побережья Кении в районе Ламу мощность осадочных пород равна 15 *км*, причем нижние 9 *км* осадков представляют собой формацию Карру, состоящую преимущественно из континентальных фаций со скоростью продольных волн около 4,8 *км/сек*. Сейсмические профили в океане хорошо согласуются с результатами исследований на суше [15, 23].

Сейсмическими исследованиями установлено, что Сейшельская банка имеет материковый тип коры. Гранитные породы, выходы которых на поверхность обнаружены на острове Маэ, мощностью до 13 *км* состоят из двух слоев. Первый слой со скоростью продольных волн 5,6—5,7 *км/сек* достигает мощности до 3,5 *км*. Под этим типично «гранитным» слоем залегает слой со скоростью продольных волн 6,3 *км/сек*, который, вероятно, соответствует несколько более уплотненным гранитам.

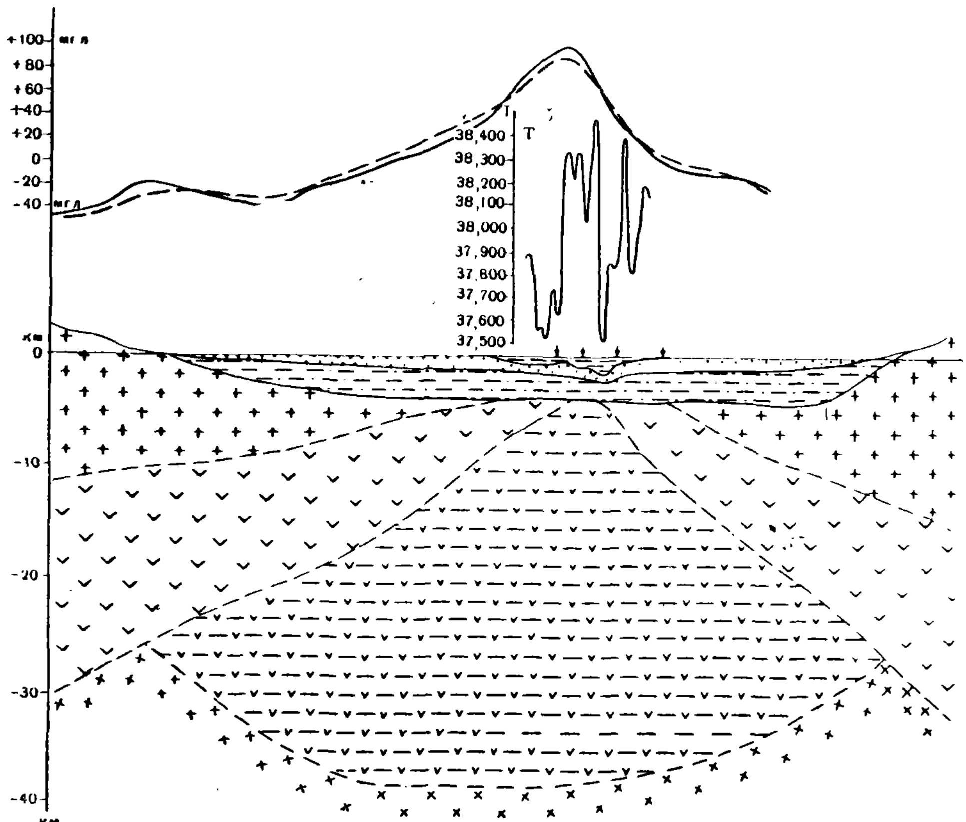

Рис. 4. Сводный разрез земной коры, построенный по сейсмическим и гравиметрическим данным в Красном море (по 16°N). Условные обозначения см. рис. 2

На глубине 13 *км* обнаружен слой со скоростью продольных волн 6,8 *км/сек*, типичный для «базальтового» слоя или, по терминологии американских исследователей, породы океанической коры. Граница М обнаружена на глубине 32 *км* под Сейшельскими островами. Наименьшая мощность земной коры обнаружена непосредственно к западу от Сейшельской банки, где выклинивается «океанический» слой со скоростью 6,8 *км/сек*, а мантия находится на глубине всего лишь 8,5 *км* ниже уровня моря. Далее в западной части Сомалийской котловины в разрезе земной коры снова появляется слой со скоростью 6,8—7,2 *км/сек*, а глубина поверхности М погружается до 13—15 *км* ниже уровня моря.

В районе банки Сойя де Малья, расположенной южнее Сейшельских островов и являющейся частью Маскаренского хребта, гранитный слой не обнаружен. Разрез земной коры на банке Сойя де Малья типичен для океанических островов с вулканическим основанием. Под слоями небольшой мощности (скорости продольных волн 1,72 и 3,25 *км/сек*), представляющими коралловые породы, сходные с породами, найденными на дне Сейшельской банки, обнаружены слои со скоростями 4,4 и 5,4—5,5 *км/сек* мощностью соответственно около 3 и 4 *км*. Эти слои типичны для вулканических островов и подстилаются материалом со ско-

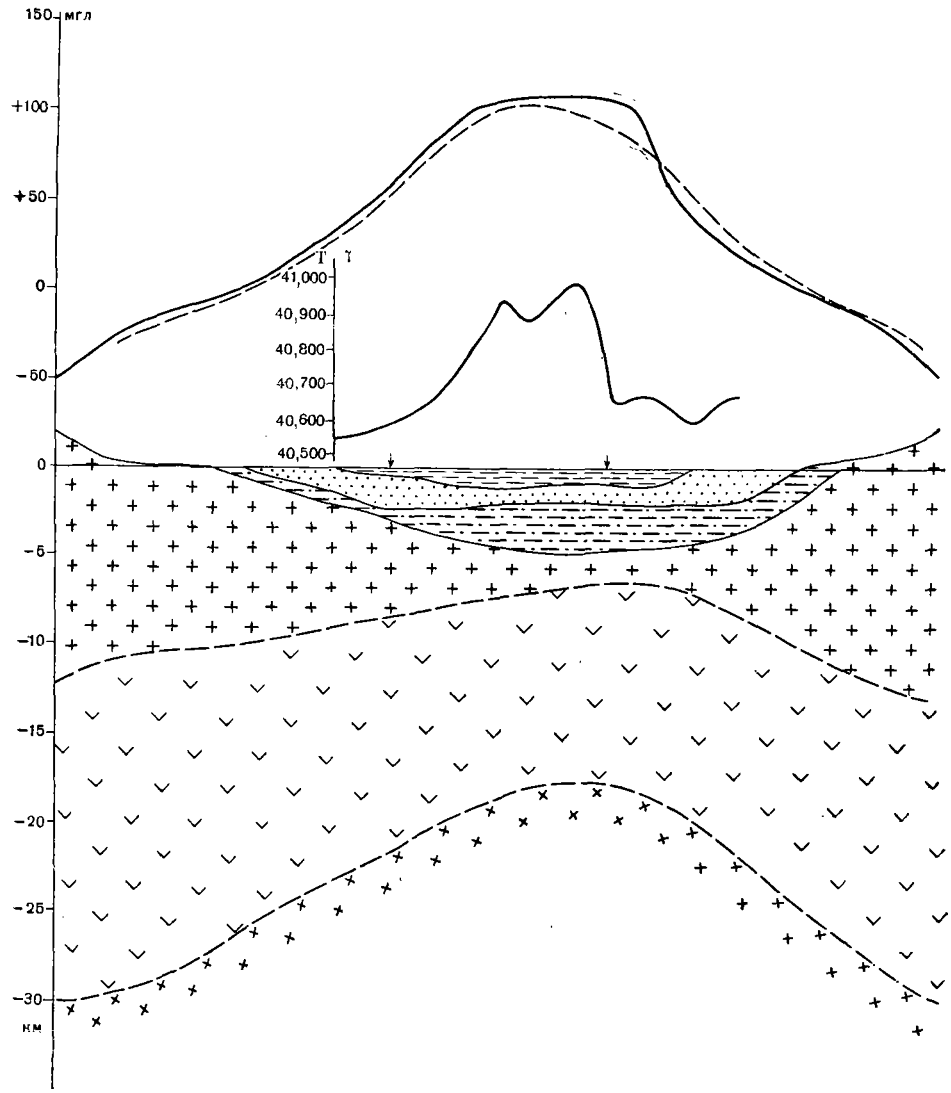

Рис. 5. Сводный разрез земной коры, построенный по сейсмическим и гравиметрическим данным в Красном море (по 25°N). Условные обозначения см. рис. 2

ростью продольных волн 6,8—7,0 *км/сек* [15, 30]. К западу от банки Сойя де Малья обнаружены слои со скоростями продольных волн 6,03 *км/сек* большой протяженности и мощности.

Эти слои, нетипичные для вулканических структур, можно рассматривать как продолжение на юг гранитного массива Сейшельских островов. Американские исследователи Френсис и Шор, опираясь на эти факты, предполагают, что Маскаренский хребет образовался в результате вулканической деятельности вдоль границы массива континентального типа [15, 22]. Под Аравийско-Индийским хребтом, морфологически очень сходным со Срединно-Атлантическим хребтом, американские исследователи не обнаружили аномальной верхней мантии с пониженными скоростями продольных волн, как в Срединно-Атлантическом и Восточно-Тихоокеанском хребтах. Возможно, мантия с аномально низкой скоростью продольных волн в этой области Аравийско-Индийского хребта охватывает область шириной менее 300 *км* и американские сейсмические станции, расположенные на западном и восточном склонах хребта на расстоянии 300 *км* друг от друга, пропустили аномальную зону. Сейсмические исследования в рифтовой зоне Аравийско-Индийского хребта, проведенные в 36-м рейсе «Витязя», обнаружили в этой зоне на глубине 7,5 *км* от уровня моря слой со скоростью продольных волн 7,0 *км/сек*, а американские исследователи под западным подножием Аравийско-Индийского хребта — слой со скоростью продольных волн 7,81 *км/сек*. Возможно, непосредственно под Аравийско-Индийским хребтом аномальная верхняя мантия представляет не единый массив, а чередование вертикальных блоков с нормальными и аномальными физическими свойствами, которые на большой глубине, возможно, имеют общий корень. Однако фактических данных еще недостаточно для однозначного решения этого вопроса. Интенсивные пониженные аномалии силы тяжести в редукции Буге, повышенные значения теплового потока, характерные магнитные аномалии — все эти особенности естественных полей земли в совокупности с повышенной сейсмичностью присущи для всех срединноокеанических хребтов. Для удовлетворительного объяснения интенсивных пониженных аномалий Буге над Аравийско-Индийским хребтом приходится допустить под земной корой мощностью около 8 *км* наличие аномальной верхней мантии с пониженной до 3,1 *г/см*^{3} плотностью, охватывающей область глубиной около 32 *км*. Если же плотность вещества верхней мантии сохраняется постоянной (~3,3 *г/см*^{3}) как под хребтом, так и под примыкающими котловинами, то в этом случае наблюдаемые понижения аномалий Буге над Аравийско-Индийским хребтом возможно объяснить утолщением земной коры под хребтом до 25 *км*. Нам кажется более вероятным вариант интерпретации с разуплотнением вещества верхней мантии, хотя своеобразие Аравийско-Индийского срединного хребта, как бы зажатого между Маскаренским и Мальдивскими хребтами с глубокими корнями в коре, может проявиться и в несколько ином, по сравнению со Срединно-Атлантическим хребтом, глубинном строении Аравийско-Индийского срединного хребта.

По сейсмическим данным, в северной части Мальдивского хребта между Мальдивским и Лаккадивскими островами обнаружен типичный для вулканических островов разрез земной коры — почти 5 *км* вулканогенных пород со скоростями продольных волн 3,8 и 5,0 *км/сек*, подстилаемых основным «океаническим» («базальтовым») слоем земной коры мощностью 10,6 *км* со скоростью продольных волн 6,8 *км/сек*. Граница М обнаружена на глубине 17,3 *км* под уровнем моря. Южнее в разрезе земной коры появляется слой мощностью около 5 *км* со скоростью продольных волн 6,13 *км/сек*, который также можно отнести к вулканическим породам. Граница М расположена, вероятно, на глубине не менее 20 *км*, так как несмотря на то, что сейсмический профиль был длиной более 100 *км*, волны от границы М не зарегистрированы. Граница М на южном конце хребта, вероятно, расположена на большей глубине. Над банкой Чагос выявлены слои со скоростями 3,01; 4,76 и 6,79 *км/сек*, типичные для коралловых и вулканических пород и для основного океанического («базальтового») слоя. На основании сейсмических данных выяснилось, что Мальдивский хребет по всей длине сложен из вулканического слоя мощностью от 4 до 5 *км*, подстилаемого «базальтовым» слоем. Интенсивные магнитные аномалии, выявленные почти на всем протяжении Мальдивского хребта, подтверждают такую точку зрения. Вероятно, образование и развитие Мальдивского хребта происходило вдоль линейного глубинного разлома, причем этот процесс, начавшийся в южной части хребта в районе банки Чагос, в дальнейшем охватывал все более северные районы. Вулканические процессы, приведшие к излияниям лавы и образованию Мальдивского хребта, возможно, захватили на севере примыкающую к Мальдивским хребтам часть Индии, где широко развиты траппы Деккана. Лабораторные измерения скоростей продольных волн в различных образцах траппов дают хорошее согласие со скоростями продольных волн, наблюденными в вулканогенных слоях разреза земной коры Мальдивского хребта [18]. Возраст траппов Деккана как по абсолютным определениям, так и по находкам фауны наиболее вероятен в пределах от верхнего мела до олигоцена. Основная масса траппов, вероятно, изливалась в раннее — эоценовое время. Древний вулканизм в районе банки Чагос, возможно, проявлялся с раннего или среднего мела [22]. Петрография траппов Деккана также подтверждает гипотезу о миграции раннемелового вулканизма с юга, от банки Чагос, на север, к побережию Индии. Как показал Чейз, содержание TiO_2 в лавах является весьма точным индикатором «внутриокеанического» или «внеокеанического» кайнозойского вулканизма [20]. Содержание TiO_2 более 1,75% указывает на «внутриокеанический» вулканизм. Анализы траппов Деккана дают содержание TiO_2 в среднем 1,91%. Для образцов траппов с больших глубин содержание TiO_2 возрастает до 2,34%, а для поверхностных траппов — понижается до 0,63%, т. е. первоначально «внутриокеанический» вулканизм как бы трансформируется во «внеокеанический» вулканизм [22]. Нахождение «внутриокеанической» лавы на континенте, возможно, обусловлено большим объемом океанической магмы и необходимостью весьма длительного воздействия континентальной среды для изменения состава магмы.

Для удовлетворительного объяснения наблюденных аномалий силы тяжести в редукции Буге над Мальдивским хребтом необходимо допустить утолщение земной коры до 25 *км*.

При построении разрезов земной коры в Красном море по широте 16° N (см. рис. 4) и 25° N (см. рис. 5) были использованы сейсмические колонки земной коры для Красного моря, полученные Дрейком и Гирдлером [21]. По сейсмическим данным, в разрезе земной коры Красного моря выделяются: 1) неуплотненные осадочные отложения со скоростями продольных волн 1,7—3,0 *км/сек*, включающие очень пористый материал и частично уплотненные осадки; 2) осадочные отложения и пирокластический материал со скоростями продольных волн от 3,0 до 5,0 *км/сек*; 3) кристаллические породы со скоростями продольных волн 5,5—6,4 *км/сек*; 4) основные ультраосновные породы со скоростями продольных волн 6,7—7,4 *км/сек*.

Выявляется интересная особенность в распространении этих пород по акватории Красного моря. В центральной глубоководной части Красного моря, южнее 25° N, породы со скоростями продольных волн 5,5—6,4 *км/сек*, интерпретируемые как породы кристаллического щита, отсутствуют и замещаются высокоскоростными (6,7—7,4 *км/сек*) породами. Суэцкий залив и залив Акаба характеризуются отрицательными аномалиями в редукции Буге. Переход от отрицательных аномалий Буге северной части Красного моря к положительным аномалиям южной части Красного моря, вероятно, происходит в зоне замещения низкоскоростных кристаллических пород высокоскоростными. Севернее 25° N магнитное поле относительно спокойное, а южнее 25° N, в центральной глубоководной части Красного моря, наблюдаются интенсивные знакопеременные магнитные аномалии, весьма характерные для рифтовых зон срединноокеанических хребтов. С учетом этих данных нами построены наиболее вероятные разрезы земной коры и верхней мантии для северной и южной частей Красного моря. Разрез земной коры южной части Красного моря (см. рис. 4) весьма сходен с разрезом земной коры Аравийско-Индийского срединного хребта.

Вулканогенно-осадочная толща со скоростью продольных волн 3,7—5,0 *км/сек*, мощностью 2—3 *км* залегает непосредственно на ультраосновных породах со скоростью продольных волн 7,0—7,3 *км/сек*. На основании исследований ультраосновных пород, собранных в 36-м рейсе «Витязя» со склонов рифтовых ущелий трех ветвей Срединно-Индоокеанского хребта (Аравийско-Индийского, Западно-Индийского и Центрально-Индийского хребтов), и анализа имеющихся геофизических данных (сейсмических, магнитных, и измерений теплового потока) по Срединно-Индоокеанскому хребту Г. Б. Удинцев и В. И. Чернышева высказывают предположение, что эти породы являются малоизмененными породами верхней мантии Земли [14]. Ведущими процессами формирования коры в этой зоне являются серпентинизация вещества верхней мантии, приводящая к увеличению ее объема, и к горизонтальным и вертикальным растяжениям. Вещество верхней мантии под Срединноокеаническими хребтами находится в условиях пониженного давления, относительно высоких температур и подвергается серпентинизации и динамометаморфизму. Все это, естественно, приводит и к соответствующим изменениям физических свойств вещества верхней мантии, в частности к уменьшению плотности и граничной скорости продольных волн. Повышенные значения теплового потока в Красном море подтверждают правомерность такой интерпретации [19, 29]. Зона аномальной мантии под южной частью Красного моря, вероятно, простирается на 250—300 *км* по ширине и 34—38 *км* в глубину.

Серпентинизация и соответственно расширение такого объема вещества верхней мантии, возможно, и явилось причиной образования рифта Красного моря и поворота Аравийского полуострова против часовой стрелки на 6—9°.

Строение земной коры северной части Красного моря (см. рис. 5) близко к строению коры внутренних и окраинных морей (Средиземного, Черного и др.). Мощность земной коры в прибрежной части изменяется от 25—30 до 18—20 *км*. Кора в центральной части Красного моря имеет нормальную верхнюю мантию как по составу, так и по физическим свойствам. Вероятно, процесс серпентинизации вещества верхней мантии и растяжения и переработки земной коры еще не захватил эту часть Красного моря.

Однако слой кристаллических пород, имеющих мощность около 10 *км* у прибрежной и 2—3 *км* в центральной части моря, является разорванным на блоки вертикальными разломами, заполненными основными интрузивными породами. По всей вероятности, это результат процесса перестройки земной коры. Причем, далее на север процесс перемещается вверх по разрезу. Так, в заливе Акаба рифт выражен наличием грабенов в мощной осадочной толще, и зоны разрывов не захватили слои кристаллических пород. Это подтверждается наличием интенсивных отрицательных аномалий силы тяжести $\Delta g_{\text{Фая}} = -200$ *мгл*, $\Delta g_{\text{Буге}} = -100$ *мгл*) и отсутствием заметных магнитных аномалий [17].

Исследования в Аденском заливе показали продолжение рифтовой долины африканской платформы на восток-северо-восток к острову Со-

13

котра, где подводный хребет и рифтовая долина соединяются с Аравийско-Индийским хребтом. Земная кора здесь имеет строение, сходное с Аравийско-Индийским хребтом и с южной частью Красного моря (см. рис. 3). Сверху по разрезу [28] залегают малоуплотненные осадки мощностью 0,5—1,2 *км* со скоростями 2—3 *км/сек*; ниже располагаются уплотненные осадки и вулканогенные породы со скоростями 4,0—4,5 *км/сек* мощностью 1,2 *км*. Основные и ультраосновные кристаллические породы со скоростями продольных волн 6,4—6,8 *км/сек* залегают на глубине 4—4,5 *км* от поверхности воды. На нескольких станциях были зарегистрированы скорости 7,5—7,8 *км/сек*, которые и характеризуют, по всей вероятности, породы аномальной верхней мантии. Самая глубокая граница со скоростями 7,5—7,8 *км/сек* в районе Аденского залива определена на глубине 10 *км*. Результаты геофизических исследований показали, что, несмотря на различие в деталях строения, структуры Аденского залива и Красного моря (южной части) весьма схожи и являются одна продолжением другой.

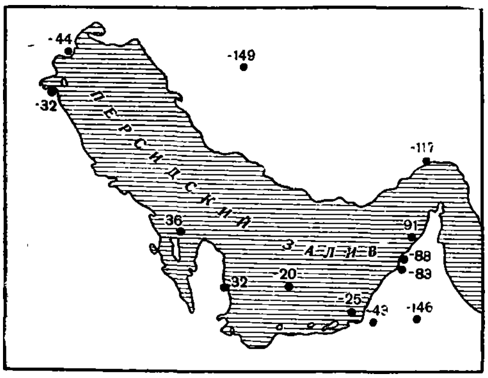

Рис. 6. Аномалии силы тяжести в районе Персидского залива. Редукция Буге ($\sigma = 2{,}67$ *г/см*^{3}). Нормальная формула — международная

Персидский залив характеризуется значительными отрицательными аномалиями силы тяжести (рис. 6). Он, вероятно, образовался на коре материкового типа. По данным иранских исследователей [33], земная кора в районе залива имеет континентальное строение. Верхняя гранитная толща с $\sigma = 2{,}7$ *г/см*^{3} имеет мощность свыше 25 *км*. Ниже залегает базальтовый слой с $\sigma = 3{,}0$ *г/см*^{3}. Эти предположения получены на основании качественной интерпретации гравитационных аномалий. Сейсмических исследований в Персидском заливе, по всей вероятности, пока не проводилось.

Таким образом, в исследованном районе выделяется земная кора четырех основных типов: материковая, океаническая, переходная и кора срединноокеанических хребтов.

ЛИТЕРАТУРА

1. Белоусов И. М. Батиметрическая карта северо-западной части Индийского океана. В сб.: «Океанологические исследования», № 13. М., «Недра», 1965.
2. Белоусов И. М. О рельефе дна северо-западной части Индийского океана. В кн.: «Геология дна океанов и морей». М., «Наука», 1964.
3. Венинг-Мейнес Ф. А. Гравиметрические наблюдения на море. М., Геодезиздат, 1940.
4. Гайнанов А. Г. Гравиметрические определения на дизель-электроходе «Обь» в первом антарктическом рейсе. В сб.: «Морские гравиметрические исследования», вып. 1. Изд-во МГУ, 1961.
5. Гайнанов А. Г., Строев П. А. Гравитационное поле и мощность земной коры северо-западной части Индийского океана. В сб.: «Морские гравиметрические исследования», вып. 3. Изд-во МГУ, 1967.
6. Грушинский Н. П. Морские определения силы тяжести в Антарктике в 1956—1957 гг. В сб.: «Морские гравиметрические исследования», вып. 1. Изд-во МГУ, 1961.

7. Грушинский Н. П. Опыт применения гравиметра на надводном корабле. В сб.: «Морские гравиметрические исследования», вып. 1. Изд-во МГУ, 1961.
8. Иванов М. М. Об особенности распределения магнитного поля в Красном море. «Геомагнетизм и аэрономия», 1962, т. II, № 6.
9. Иванов М. М. Некоторые вопросы строения дна Атлантического и Индийского океанов по магнитным данным. «Геомагн. и аэрономия», 1963, т. III, № 1.
10. Костенко Н. П. Неотектоника Африки и ее связь с сейсмичностью. В сб.: «Сейсмические исследования», № 6. М., «Наука», 1965.
11. Непрочнов Ю. П., Ковылин В. М., Михно М. Ф. Результаты сейсмических исследований строения земной коры и осадочной толщи в Индийском океане. В сб.: «Геология дна океанов и морей». М., «Наука», 1964.
12. Тейлор П. Т. О величине теплового потока через дно Индийского океана. «Тез. докл. 2-ого Международн. океаногр. конгр.». М., Изд-во АН СССР, 1966.
13. Удинцев Г. Б. 36-й рейс научно-исследовательского судна «Витязь». «Океанология», 1965, т. V, № 6.
14. Удинцев Г. Б., Чернышева В. И. Образцы пород верхней мантии Земли из рифтовой зоны Индийского океана. ДАН СССР, 1965, т. 165, № 5.
15. Френсис Т. Дж. Использование сейсмических измерений методом преломленных волн при морских геологических исследованиях в северо-западной части Индийского океана. «Тез. докл. 2-ого Международн. океаногр. конгр.». М., Изд-во АН СССР, 1966.
16. Admiralty Marine Science Publication. Bathymetric magnetic and gravity investigations. H. M. S. Owen, 1961—1962. London, 1963.
17. Allan T. D., Charnock H., Morelli K. Magnetic, gravity and depth surveys in the Mediterranean and Red Sea. «Nature», 1964, vol. 204, No. 4965.
18. Balakrishna S. Velocties of compressional waves in some Indian rocks. «Trans. Am. Geoph. Un.», 1958, vol. 39.
19. Birch F. S., Halunen A. J. Heat flow measurements in the Atlantic ocean, Indian Ocean, Mediterranean Sea, and Red Sea. «J. Geoph. res.», 1966, vol. 71, No. 2.
20. Chayes F. A. A petrographic distinction between Cenozoic volcanics in and around the open oceans. «J. Geoph. res.», 1964, vol. 69, pp. 1573—1588.
21. Drake C. G., Girdler R. W. A Geophysical study of the Red Sea. «The Geophysical journal», 1964, vol. 8, No. 5.
22. Francis T. I. G., Shor G. G. Seismic refraction measurements in the morthwest Indian Ocean. «J. Geoph. res.», 1966, vol. 71, No. 2.
23. Francis T. I. G., Davies D., Hill M. N. Crustal structure between Kenya and the Seychelles «Phil. Trans. Roy. Soc.», London, 1965.
24. Gaskell T. F., Swallow S. C., Hill M. N. Seismic measurements made by H. M. S. «Challenger» in the Atlantic, Pacific and Indian oceans and the Mediterranean Sea 1950—1953. «Philos., Trans. Roy. Soc.» London, 1958.
25. Girdler R. W. The relationship of the Red Sea to the Ecast African rift system. Quart. «J. Geol. Soc.», 1958, vol. 79.
26. Girdler R. W., Harrison J. C. Submarine gravity measurements in the Atlantic ocean, Indian ocean, Red Sea and Mediterranean sea. «Proc. Roy. Soc. Am.», 1957, 239, 202
27. Heirtzler J. R., Pichon X. L. Crustal structure of Mid-ocean ridges, 3. Magnetic anomalies over the Mid-Atlantic ridge «J. Geoph. res.» 1965, vol. 70, No. 16.
28. Nafe I. E., Hennion I. F., Peter G. Geophysical measurements in the Gulf of Aden. Preprints of Jnt. Ocean. Congr, N. Y., 1959.
29. Sclater I. G. Heat flow in the north west Indian Ocean and Red Sea. «Phil. Trans. Roy. Soc.», London, 1966.
30. Shor G. G., Pollard D. D. Seismic investigations of Seychelles and Saya de Malha banks, northwest Indian Ocean. «Science», 1963, vol. 142, No. 3588.
31. Talwani M. Gravity measurements on H. M. S. «Acheron» in South Atlantic and Indian Oceans. «Bull Geol. Soc. Amer.», 1962, vol. 73, No. 9.
32. Talwani M., Sutton G. H., Worzel L. A crustal section across the Puerto — Rico trench. «J. Geoph. res.», 1959. vol. 64, No. 10.
33. Establishment of gravity bases in the Persian Gulf area. «Tehran University Press. Publ.», 1963, No. 11.

Поступила в редакцию
26/IX 1966 г.

Кафедра
геофизики

Reprinted from *Vestnik Moskovskogo Universiteta*, Geology series, no. 6, 1967, p. 16-24

The geotectonic development of the Indian Ocean and the top of the Earth

by E. Kraus

Э. КРАУС

ГЕОТЕКТОНИЧЕСКОЕ РАЗВИТИЕ ИНДИЙСКОГО ОКЕАНА И «КРЫШИ МИРА»*

Теперь, после появления отлично выполненной карты рельефа дна Индийского океана Хейзена и Тарпа (рис. 1), представляется возможным наметить характер и последовательность процесса дрифта материков при мезозойском образовании (приоткрытии) Индийского океана. При этом мы опираемся не только на опубликованные в последнее время представления о главных причинах этого процесса, но также непосредственно на результаты палеомагнитных, палеоклиматических, палеогеографических и сейсмических исследований.

Мы исходим из концепции «Гондваны», т. е. существования гигантского континента, частично располагавшегося в пределах южнополярной области, который вплоть до окончания палеозоя в основном состоял из орогенов, образованных на месте геосинклиналей. Гондвана объединяла домезозойские ядра Антарктики, Южной Америки, Африки, Индии и Австралии. Эту концепцию предложил Вегенер еще в 1912 г. [13] на том основании, что в течение позднекаменноугольного и раннепермского времени обширные части этих ныне так далеко друг от друга отстоящих континентов были перекрыты общим материковым оледенением и находились близ южного полюса [6] (рис. 2).

Ныне мы можем различить в течение мезозоя и кайнозоя около пяти главных фаз этого поразительно грандиозно протекавшего развития участка земной поверхности в области Индийского океана (вплоть до ее нынешнего состояния). В качестве последнего существеннейшего следствия этого развития можно рассматривать возникновение «Крыши мира» к северу и северо-востоку от Индии.

Вероятный характер и последовательность геотектонического развития Индийского океана

В течение первой фазы развития южные континенты (Южная Америка, Африка, Индия и Австралия) отделились от Антарктиды вдоль разлома, расположенного периферически по отношению к обла-

* Доклад, прочитанный 3 июня 1966 г. на заседании коллоквиума по методике картирования дна морей и океанов II Международного океанографического конгресса в Московском университете. Перевод с немецкого языка Е. В. Дорошенко и Д. П. Найдина.

сти, окружающей южный полюс. В пределах первых континентов после позднепалеозойского материкового оледенения к началу триаса климат стал теплее. Они передвигались, будучи еще соединенными вместе, к северу, навстречу другому палеозойскому гигантскому континенту — Лавразии. Упомянутый выше отделивший их от Антарктиды разлом возник как глубинный разлом близ современного 50° ю. ш. и параллельно этой широте. Вдоль него и параллельных ему разломов, по-видимому, в периоды растяжения поднимались огромные массы из расплавленного основания, сальсимической оболочки Земли, а также из лежащей под ней верхней части мантии. При этом зоны разломов все более расширялись,

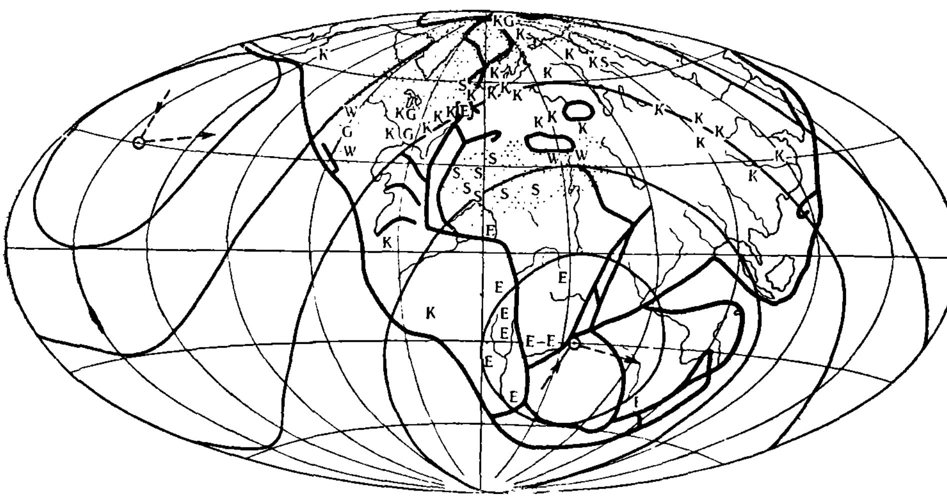

Рис. 2. Положение континентов в позднем карбоне (по Вегенеру, 1924). Представления А. Вегенера о перемещении континентов (эпейрофорезе) основывались на распространении остатков материкового оледенения (Е — только на еще объединенных континентах), размещении местонахождений углей (К), солей (S) в аридных областях (показаны точками), гипса (G) и «песчаников пустыни» (W). Кружочки с точкой обозначают предполагаемое положение южного и северного полюсов; пунктир со стрелкой показывает перемещение полюсов в позднем карбоне и в течение пермского периода

так что части Гондваны, находившиеся ранее вместе, отделились друг от друга.

Этот процесс представляет полную аналогию с процессом, ныне идущим в восточной части Исландии, где он был неоднократно описан [1, 2; подробнее см. 8]. Огромное значение подобного механизма, действующего в центральных частях океанов, можно увидеть из рис. 3.

Общее перемещение четырех континентальных глыб на север происходило, очевидно, неравномерно. Между ними образовывались меридионально направленные горизонтальные зоны сдвигов (Blattverchiebungen, transcurrent faults, décrochements), возможно, выраженные постумно как линеаменты, которые в последующем стали составными частями «медианных зон» [8], т. е. «срединноокеанических хребтов»: Срединно-Индийского и Срединно-Атлантического валов. Эти древнемезозойские разломы разделяли Австралию, Индию, Лемурию, Африку и Южную Америку. На основании только палеомагнитных измерений, которые не определяют современного долготного положения валов, на рис. 4 показаны представления, не подтвержденные еще геологическими данными.

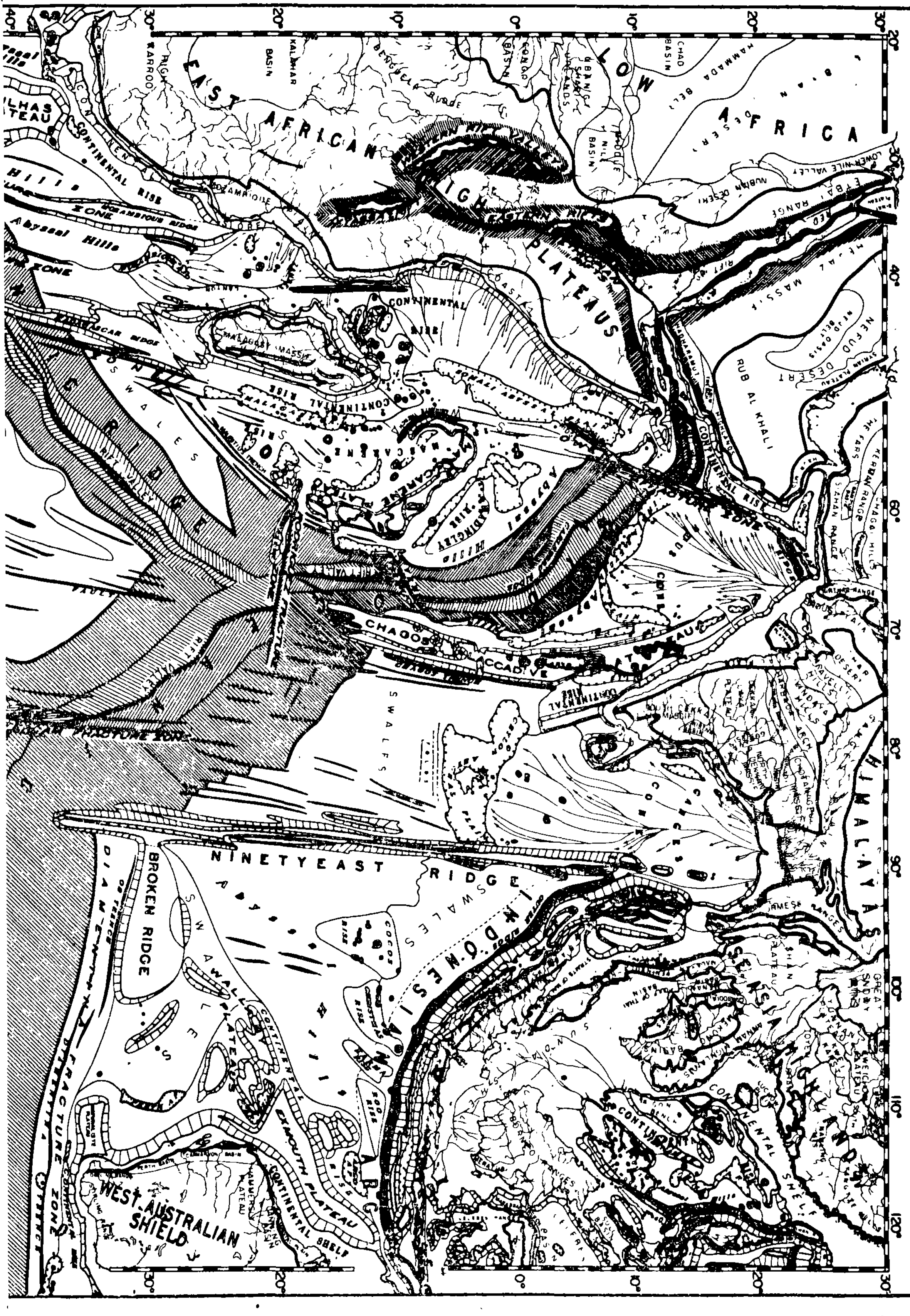
EAST AFRICAN HIGH PLATEAUS
LOW AFRICA
CHAD BASIN
KALAHARI BASIN
KAROO
BENGUELA RIDGE
NUBIAN DESERT
LOWER NILE VALLEY
RUB AL KHALI
NEFUD DESERT
Abyssal Hills
CONTINENTAL RISE
CONTINENTAL SHELF
CHAGOS
LACCADIVE
SWALES
NINETYEAST RIDGE
BROKEN RIDGE
INDONESIA
HIMALAYAS
EXMOUTH PLATEAU
WEST AUSTRALIAN SHIELD
FRACTURE ZONE

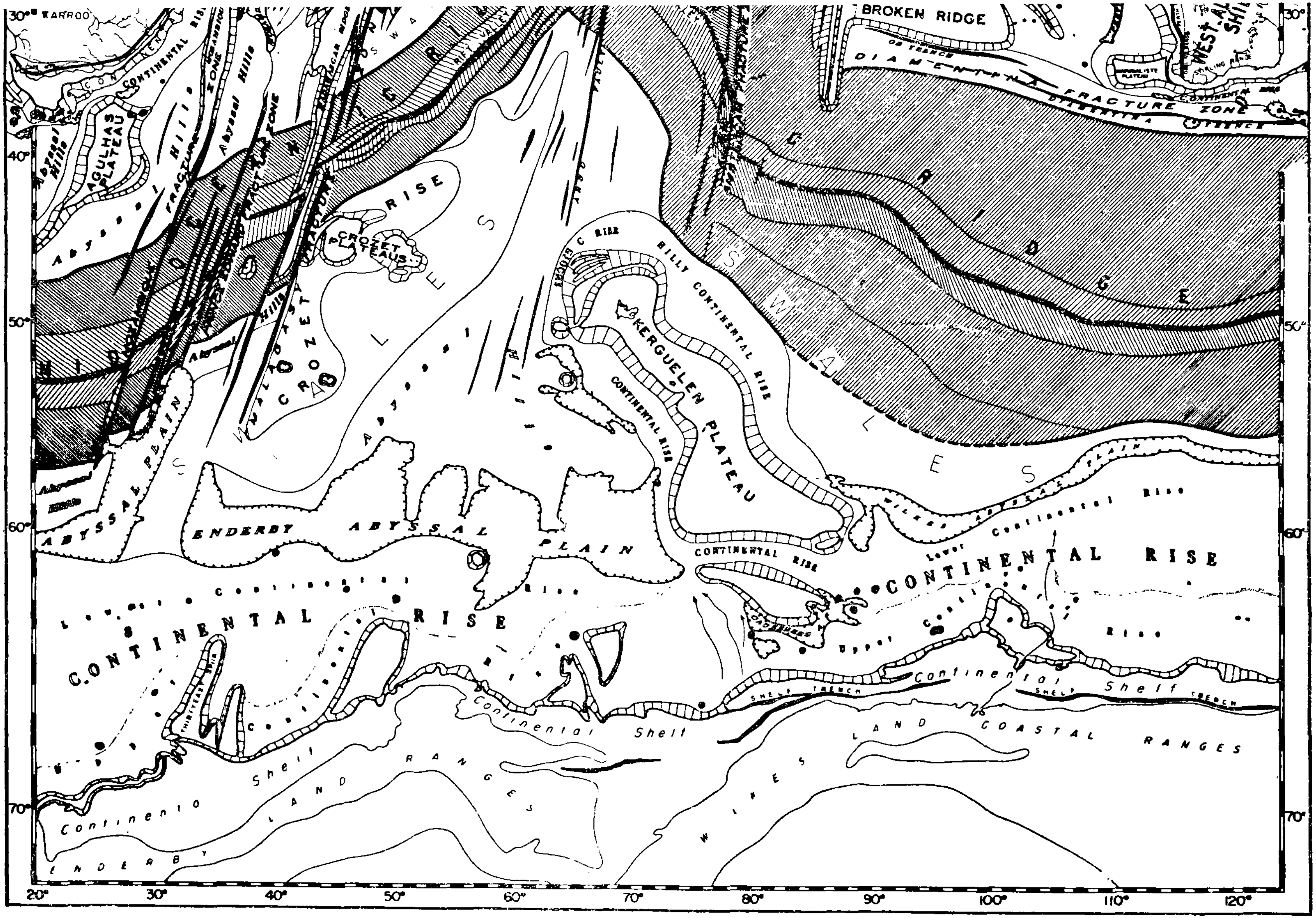

Рис. 1. Физиографическая схема Индийского океана (по Хейзену и Тарпу, 1965). Густая косая штриховка — склоны Срединно-Индийского вала и его продолжения; рифтовая долина показана черным; редкой косой штриховкой показаны участки вала, прилежащие к рифту; полосы с поперечными редкими штрихами — склоны континентов и плато; линии с точками ограничивают абиссальные равнины; длинные тонкие стрелки — подводные каньоны; пунктирные линии — складки; толстые черные заостренные линии — разломы

Зак. 652 стр. 16—17

По мере совместного перемещения этих континентов в триасе на север, они попадали в область более быстрого вращения Земли. При этом, очевидно, большой комплекс, состоявший из Южной Америки, Африки, Индии, вращавшийся медленнее из-за своей большей инерции, несколько отставал от значительно меньшей Австралийской глыбы, которая могла раньше приспособиться к большей скорости вращения эллипсоида несколько севернее 50° ю. ш. Здесь, конечно, нельзя забывать и о действии закона Кориолиса. Таким образом, вероятно, значительно расширилась сдвиговая трещина между Австралийской глыбой и западным комплексом континентов. Этим разломом является современный хребет 90° в. д.*,

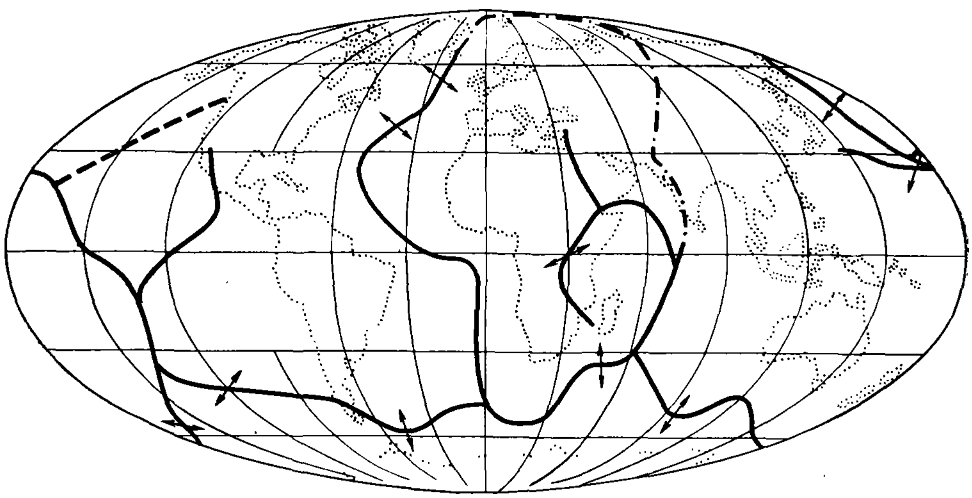

Рис. 3. Мировое распространение медианных зон разломов — срединных океанических валов (по Ранкорну, 1962)

вдоль которого происходили мощные поднятия магматических масс (см. рис. 1 и 5). От него к востоку на морском дне, по-видимому, остались краевые следы, ограничивающие с юга и с севера тот путь, по которому Австралия двигалась на восток. На юге этот путь ограничен зоной разломов Диамантина, а на севере — пучком разломов вдоль Зондской дуги. Континентальные массы к западу от сдвига хребта 90° в. д. и зона срединноокеанического вала передвигались в западном направлении. Различимые ныне препятствия этому передвижению там впервые возникли, как будет показано ниже, впервые лишь после триаса.

Благодаря этому восточному дрифту Австралии к месту ее современного положения и перемещению глыб Индии, Африки, Южной Америки на запад, имевшему место еще в триасе, сначала образовалась южная часть Индийского океана. Это произошло после первой фазы удаления континентальных глыб от полюса во *время второй, позднетриасовой стадии развития.* На рис. 6 показано изменение широтного положения Австралии по палеомагнитным данным с докембрия до кайнозоя, но без поправок на долготу.

Связь Индии с Лемурией, состоявшей из Мадагаскара и большей частью ныне погрузившихся глыб в области Сейшельских островов, доказывается для юрского периода общностью ископаемой фауны. Лемурия в юре уже отделилась от Африки вдоль морского пролива, вероятно, предопределенного примерно меридионально направленной зоной сдви-

* Восточноиндийский хребет на советских картах Индийского океана (*прим. переводчиков*).

гов. Последующее отделение Индийской глыбы от Лемурии в раннемеловую эпоху произошло, вероятно, вдоль поднятий и сдвигов южной части Карлсбергской медианной зоны, а также вдоль северного участка Срединно-Индийского вала. Именно тогда Индия переместилась своим восточным краем несколько на восток до хребта 90° в. д. (который ныне не является активным срединноокеаническим хребтом), а южным краем — примерно до 40 ° ю. ш. Одновременно поднятие масс во время рас-

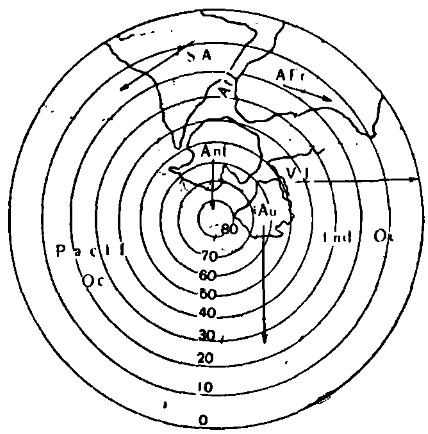

Рис. 4. Перемещение континентов в южном полушарии с середины мезозоя (по Ранкорну, 1962). Сплошные контуры — положение континентов в середине мезозоя; стрелки — направление перемещения континентов; пунктирные контуры — современное положение континентов

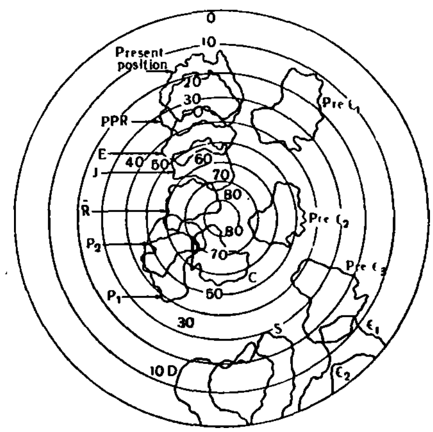

Рис. 6. Положение Австралии, определенное по палеомагнитным данным, от докембрия до кайнозоя (по Ранкорну, 1962)

тяжения Карлсбергского вала обусловило передвижение Лемурии к западу. Такие дрифтовые перемещения произошли в *третью фазу развития*. В течение третьей фазы, по-видимому, окончилось действие механизма процессов растяжения, расширявшего разломы и приводившего к поднятию из глубин огромных магматических масс и таким образом бывшего причиной континентального дрифта и образования (приоткрытия) Индийского океана. Последовавшее затем перемещение Индии к северу уже не может быть объяснено действием этого механизма.

Подкоровое течение под Индийским океаном, направленное к северу, и его последствия

На дне океана, как и на пути триасового дрифта Австралии, прослеживаются следы перемещения Индийской глыбы в меловое время. Эти следы представлены параллельными зонами краевых сдвиговых разломов, ограничивающими с запада и с востока Срединно-Индийскую меридионально вытянутую глыбу и возникшими при перемещении Индии на север. В качестве восточного краевого разлома следует рассматривать линеамент 90° в. д., не являющийся более сейсмически активным. На севере линеамент погружается под дельтовые осадки Бенгальского залива. Его северное продолжение пересекается с восточным краем Индии. Примерно такой же длины западный краевой разлом, а именно хребет Чагос-Лаккадивы. Он имеет северо-северо-западное простирание и исчезает под осадками дельты Инда. Его северное продолжение образует

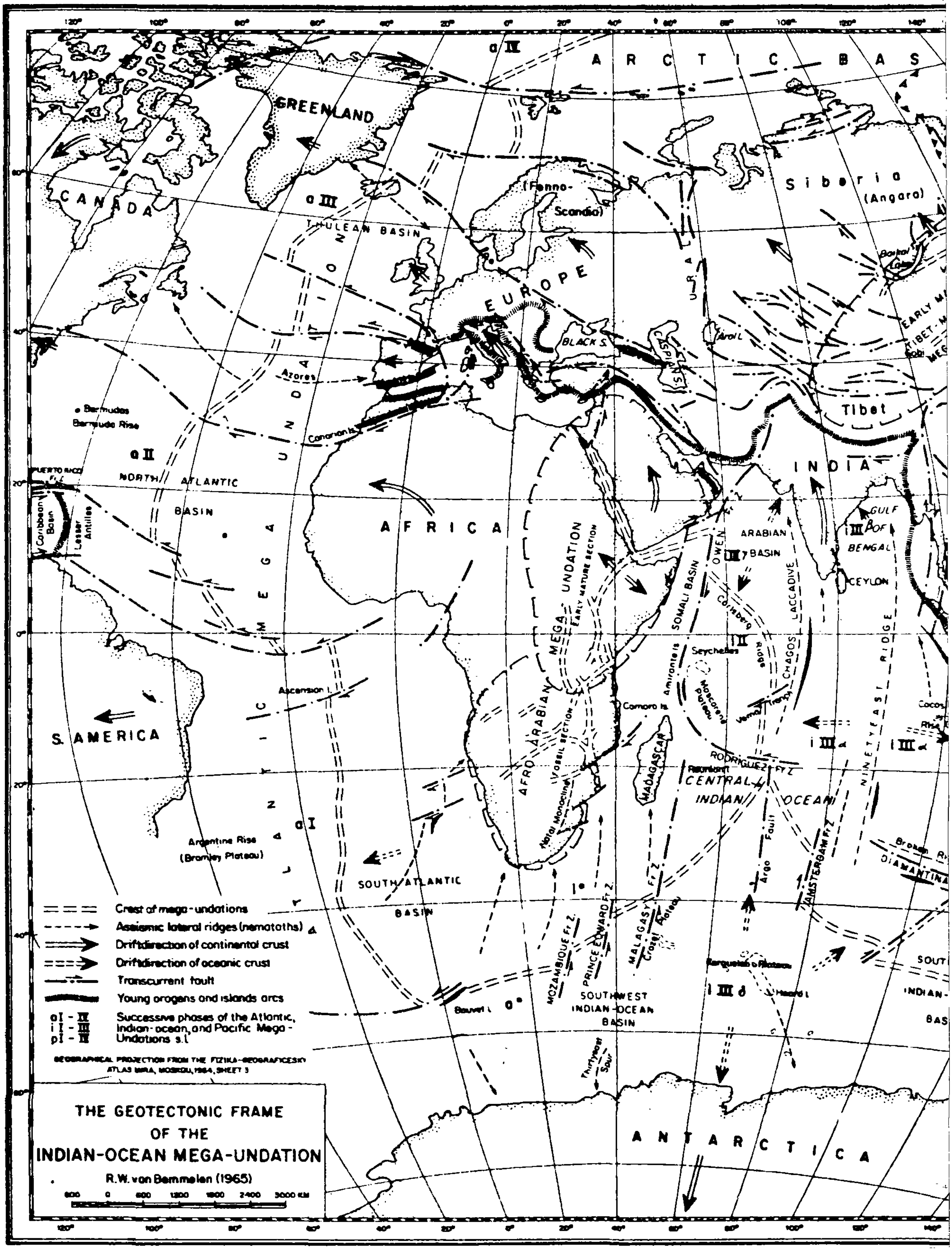

Рис. 5. Тектоническая схема западной части Тихого океана, Индийского и Атлантического
в работе Крауса,

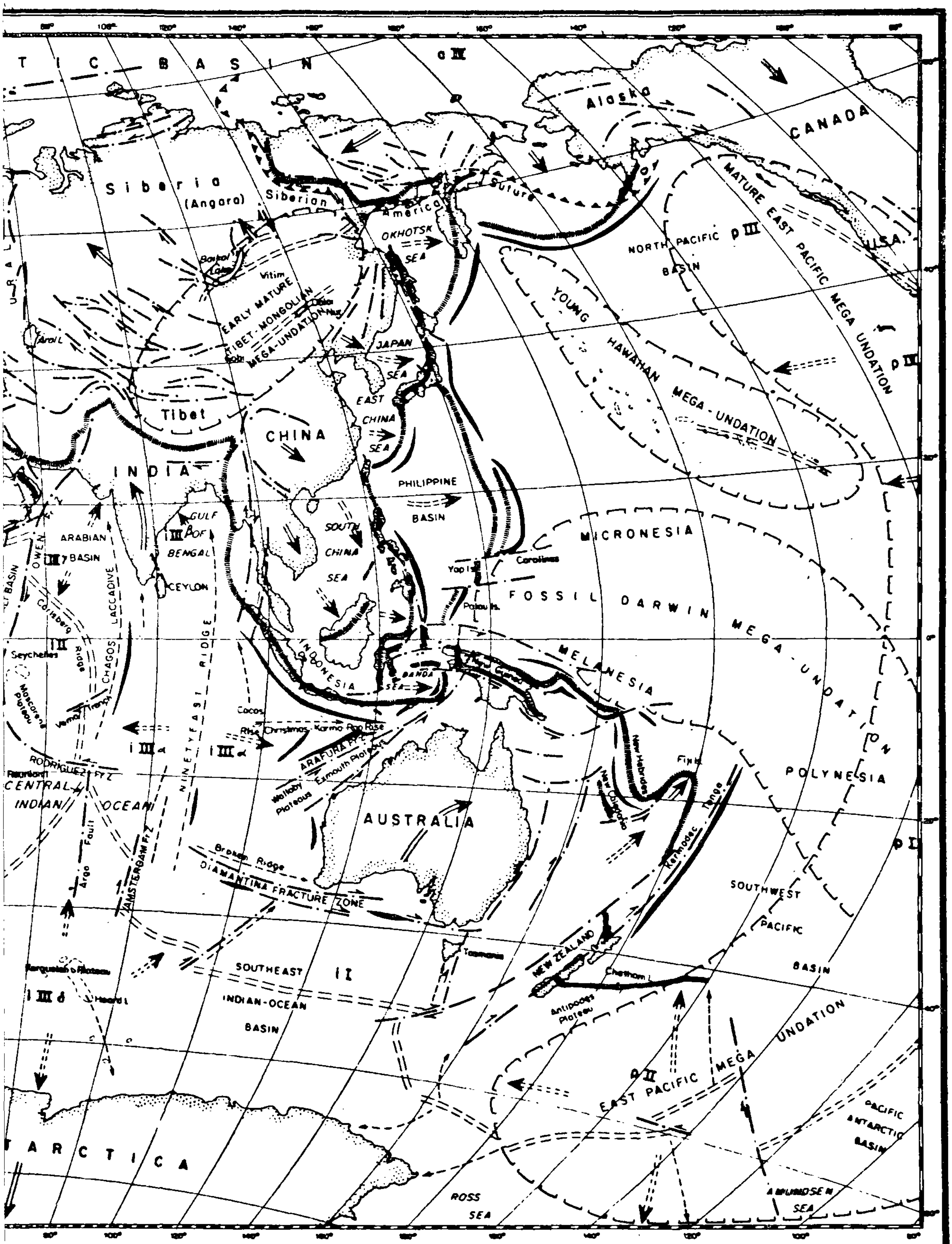

океанов (по Беммелену, 1965). О показанных здесь мегаундациях подробнее сказано
находящейся в печати

Зак. 652 стр. 20—21

западный край Индийского субконтинента. Западный краевой разлом несколько изогнут к востоку. Вероятно, это является результатом действия еще и ныне сейсмически активного Карлсбергского (Срединно-Индийского) вала. Обе эти зоны краевых разломов в настоящее время сейсмически не активны.

Перемещение Индии к северу, вне всякого сомнения, происходило уже после дрифта Австралии на восток в триасе: как видно на рис. 1 и 5, восточное краевое ограничение пути перемещения Индии (хребет 90° в. д.) срезает краевые ограничения пути перемещения Австралии. Точно также у западного краевого ограничения пути перемещения Индии исчезают все неровности рельефа дна, наблюдаемые к западу от Чагос-Лаккадивской зоны разлома.

С другой стороны, Индия уже в позднемеловую эпоху заняла место вблизи своего современного положения. Это доказывается существованием Деканского базальтового плато. Ведь массы покровных базальтов происходят из основания Аравийского моря, дно которого также покрыто базальтами. Базальты прорвались одновременно через Индийскую сиалическую плиту, существовавшую на этом месте уже в позднемеловое время, когда происходило излияние деканских лав.

В позднемеловую эпоху и в палеогене, когда в Гималайской геосинклинали распространилось море Тетис, северный край Индийской плиты был вовлечен в покровные структуры Гималайского орогена. Краевые части плиты ныне можно наблюдать в тектонических окнах этой горной системы.

Движущие силы основания Индийского океана в меловое время

Активный срединноокеанический вал, ориентированный примерно широтно, в меловое время не существовал. Поэтому меридиональный дрифт не может быть объяснен причинами, действовавшими ранее. Лишь в триасе существовал подобный вал, обусловивший перемещение Антарктиды к югу, а остальных континентов — к северу. Этот вал уже не мог обеспечить гораздо более поздний северный дрифт Индии, так как он сам в течение мелового периода был расчленен на всем своем протяжении на юге Индийского океана региональными перемещениями к северу. При этом он был передвинут примерно с 50° ю. ш. до 20° ю. ш., т. е. на место, на котором еще в юре находилась Индия. Рис. 1 и 5 показывают, что потерявший активность триасовый срединноокеанический вал был расчленен правыми сдвигами на юго-востоке и левыми сдвигами на юго-западе. Таким образом, отдельные обломки вала были пассивно перемещены друг относительно друга при всеобщем перемещении к северу. Максимальное перемещение на север испытала вытянутая в меридиональном направлении центральная часть океанического дна, в связи с чем Индия и достигла своего нынешнего положения. Позади этих участков также на север перемещались различные по очертаниям преимущественно подводные глыбы (в частности, глыба Кергеленского плато). Эти глыбы, по крайней мере частично, представляют обломки северного сиалического обрамления Антарктиды. Следовательно, под ними еще и поныне господствует разрушительная глубинная энергия, направленная из южной полярной области.

Таким образом, мы наблюдаем результат действия деструктивного и нараставшего к северу глубинного движения, охватившего в течение мелового периода все основание Индийского океана. Регионально проявлявшийся, направленный к северу глубинный поток расчленял несомое им, а обломки перемещал с собой. Так была создана современная картина, «океанская тектоника» Индийского океана. Действие регионального глубинного потока составляет четвертую фазу развития океана.

Однако этот гигантский глубинный поток продолжал действовать и в третичное время, составляющее пятую фазу развития.

Дрифт Индии к северу и «Крыша мира»

Помимо упомянутого выше вовлечения структур Гондваны в Гималайской ороген существует, вероятно, еще и другая, более широкая связь между появлением Индии в пределах орогена Тетис (на западе в Белуджистане, на севере в Гималаях, на востоке в цепи Бирманских гор), с одной стороны, и гористым нагорьем «Крыши мира», с другой.

Не только самые высокие горы мира возвышаются над индийским форландом. С олигоцена началось постепенное общее воздымание как древних, так и молодых горных систем к северу и востоку от Индии: Гиндукуша, Памира, Каракорума, Куньлуня, Тибета, а далее к востоку далеко за пределами прииндийских горных стран также горных сооружений вплоть до бассейнов Янцзы и Хуанхэ. Несомненно, молодые альпийские орогены Тетиса при этом прошли нормальный путь развития и после преимущественного погружения в течение гипорогенной геосинклинальной стадии вступили в стадию эпиорокинеза *, в фазу образования высокогорного рельефа. Но вместе с ними в третичном периоде поднялись в среднем на высоту от 4000 до 7000 *м,* образовав «Крышу мира», палеозойские сооружения, а также еще более древние, давно пенепленизированные орогенные образования.

Какие же силы создали эти молодые высокие горы, подняли эту «Крышу мира» на высоту, неизвестную нигде более на Земле? К нормальному эпиорогенному поднятию здесь присоединились воздымания гораздо большего масштаба. Следует объяснить, каким образом нагромождались столь высокие молодые горы. Очевидно, необходимо предположить, что под эту «Крышу мира» проникли огромные подкоровые массы, так как представить образование там пустот или необычайное уплотнение пород, естественно, невозможно. Откуда же поступали такие огромные подкоровые массы?

Они не могли прийти с севера, из областей палеозойской и еще более древней консолидации. Не могли они прийти также ни с востока, ни с запада, где также располагались материковые структуры. Они могли прийти только с юга. Литосфера тех областей, из которых переместились подобные огромные массы, должна была в третичном периоде испытать региональные, хотя и медленные опускания. Итак, напрашивается вывод, что эти гигантские массы поставлялись основанием Индийского океана, которое после его образования в мезозое, в позднетретичное время было еще значительно погруженным. Подобная возможность наиболее вероятна.

Также напрашивается предположение, что особенно значительные массы, переместившиеся на север и восток под «Крышу мира», происходят из средней меридионально вытянутой части Индийского океана. Именно под этой частью океана действовало подкоровое течение, перенесшее Индию на север.

Гигантское подкоровое течение, с результатами действия которого мы коротко ознакомились, отнюдь не остановилось перед Гималаями. Этот огромный глубинный магматический поток двигался и далее на север под древние и молодые складчатые участки сиалической коры. Он

* Под орокинезом Э. Краус понимает совокупность движений в геосинклиналях (*прим. ред.*).

распространялся также далеко на восток. Именно он воздвигнул «Крышу мира».

В. Н. Крестникову и И. Л. Нерсесову [10] принадлежит заслуга проведения, по крайней мере, в той части «Крыши мира», которая обрамляет с северо-запада Индию, первых систематических геолого-геофизических наблюдений, а также публикации результатов этих наблюдений. Мы видим здесь крупные блоки, поднятые на различную высоту относительно других, оставшихся неподвижными, блоков, а положение поверхности Мохоровичича сильно меняется в пределах от 30 до 70 *км*. Это проявление поздне- и послеорокинетических импульсов. По времени и особенно по своему пространственному распространению эти импульсы далеко превосходят нормальный масштаб геосинклинально-орогенного процесса.

Столь ясный характер проявления этих процессов дает дополнительное основание для принципиального разделения двух геодинамически различных ярусов движений. Мы выделяем верхний ярус, в пределах которого развиваются геосинклинальные орогены с их частными глубинными течениями и перемещениями магмы, в конце концов превращающиеся в континенты, и нижний ярус, значительно более глубоко расположенный. В этом последнем возникают как горизонтальные, так и вертикальные глубинные течения гораздо бо́льших масштабов и значительно бо́льшей продолжительности. Фазы возрастания энергии этих течений во времени отнюдь не всегда совпадают с этапами роста напряжений в различных в этом отношении локально отличающихся геосинклиналиях. Поэтому часто происходят коллизии между движениями обоих ярусов; в том числе иногда при совпадении направления движений происходит их сложение. Верхний ярус автор в 1950 г. назвал «гипореоном» (Hyporheon), а нижний — «батиреоном» (Bathyrheon). Крупные перемещения в области океанического дна и континентальный дрифт принадлежат к категории батиреонных движений. Батиреонные движения вызывают перемещения крупных глыб, приводящих к образованию прямолинейных поразительно протяженных сдвигов, поднятия колоссальных масс магмы в пределах срединноокеанических валов, а также процессы растяжения огромного масштаба. Сложное сочетание батиреонных и гипореонных процессов и в настоящее время еще проявляется вокруг Тихого океана в пределах андезитового пояса. Подкоровые течения под Индийским океаном, имеющие региональное распространение и с середины мелового периода проникшие под «Крышу мира», представляют хороший пример батиреонных процессов.

На дне океанов мы не распознаем никаких следов геосинклинального развития, за исключением андезитового пояса вокруг Тихого океана. Во внутренних основных частях дна океанов, так же как и в южных океанах, отсутствует тихоокеанская дифференциация (кроме андезитового пояса), а также атлантическая дифференциация. На подробностях здесь нет возможности останавливаться.

Выводы

Характер и последовательность событий, приведших к образованию молодого Индийского океана, мало еще обоснованные наблюдениями, могут быть выяснены с помощью геотектонически достоверных заключений (см. рис. 1 и 5) об основных причинах последних континентальных перемещений.

В позднем палеозое Гондвана́ (см. рис. 2) была расчленена зоной разломов, ориентированной периферически к южнополярной области, на две части: Антарктиду, с одной стороны, и Южную Америку, Африку, Индию и Австралию, с другой. В раннем триасе, вследствие сильного меридионального растяжения подкоровой преимущественно базальтовой сальсимической оболочки Земли, происходил колоссальный подъем расплавленных масс. Упомянутые выше четыре континентальные глыбы составляли в общем единый массив и, вероятно, вместе с их основанием были перемещены за 50° ю. ш. При этом в результате различий в скорости перемещения между глыбами возникли и меридиональные зоны крупных сдвигов.

Крупные участки земной коры, вследствие меньшей скорости вращения в высоких широтах, по-видимому, оказались расположенными далее к западу по сравнению с менее крупным участком — Австралией. Это послужило причиной дальнейшего расширения зоны меридионального разлома (возможно, разлома 90° в. д.) между Австралией и большей частью Гондваны (Индией, Африкой, Южной Америкой). Во всяком случае, в позднем триасе перемещение Австралии на восток осуществлялось как бы на «ленточном транспортере», резко ограниченном от своего окружения как справа (разломом Диамантина), так и слева (частично структурами северо-восточного простирания) (см. рис. 1 и 5). Австралия перемещалась из области, близкой к южному полюсу, к ее современному положению более окольным путем, чем тот, который показан на рис. 6.

Юрские окаменелости показывают, что Индия после восточного дрифта Австралии располагалась на западе вместе с Лемурией (Мадагаскар-Сейшельские острова). Лемурия была отделена от Африки, по всей вероятности, также разломом или, во всяком случае, морским проливом. Лишь к началу мелового периода в результате подъема магмы Карлсбергский разлом расширился, превратившись в участок Срединно-Индийского вала. Вследствие этого Лемурия переместилась к западу от названного вала, а Индия к востоку от него, вероятно, достигнув зоны разломов 90° в. д. с южным ограничением примерно на 20° ю. ш.

К середине мелового периода в области молодого Индийского океана процесс образования срединных валов, связанный с подъемом магмы, очевидно, закончился. После образования большей части Индийского океана вместо этого процесса началось грандиозное перемещение с юга на север. Посредством резких правых и левых сдвиговых перемещений триасовая южноиндоокеанская зона поднятий была продвинута с 50° ю. ш. до 20° ю. ш. Перед нею обособилась (см. рис. 1 и 5) срединноиндийская полоса океанического дна, ограниченная справа, т. е. с востока, разломом 90° в. д., а слева, т. е. с запада, зоной грабенов Чагос-Лаккадивы. На этой меридиональной полосе, простиравшейся, вероятно, вплоть до верхней мантии Земли, располагалась Индийская глыба. Эта глыба была передвинута по меридиональной полосе, как по «ленточному транспортеру», через экватор к ее современному положению. В позднемеловую эпоху к западу от Южной Индии, а также в пределах юго-западной Индии через океаническую земную кору прорвались покровные базальты Деканского плато. Индия в это время была уже «в Индии»! Ее северный край, сложенный гондванскими отложениями, был вовлечен в структуру Гималайской геосинклинали.

Структуры дна Индийского океана в основном сформированы воздействием регионального подкорового течения, действовавшего с юга на север в позднемеловую эпоху и в третичном периоде. Очевидно, будет правильным предположить, что это гигантское подкоровое течение не остановилось под Гималайским орогеном, но проникло под земной корой еще дальше в направлении горных сооружений, показанных на рис. 7, под Тибет и горные сооружения, обрамляющие Индию. В результате действия этих течений «Крыша мира» была поднята на современ-

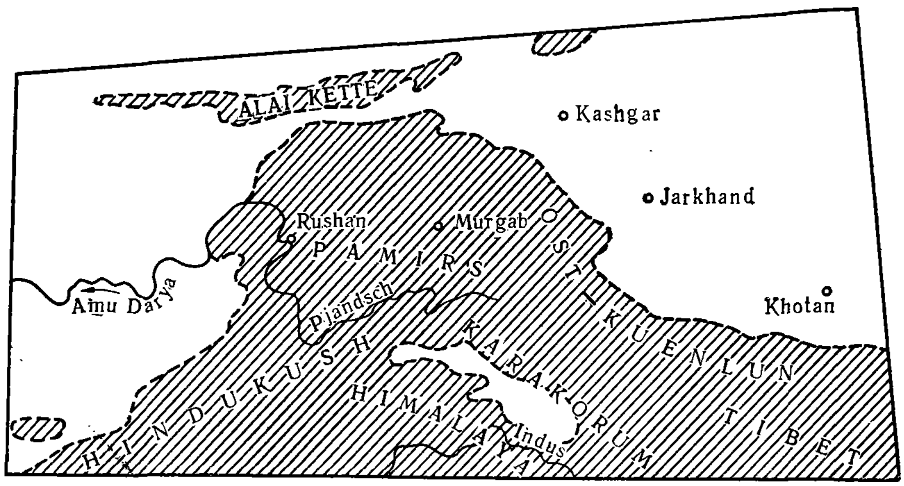

Рис. 7. Схема западной части «Крыши мира». Участки, показанные штриховкой, представляют высоко поднятые (более 4000 *м* над уровнем моря), но глубоко расчлененные горные сооружения. Это гигантское воздымание началось после олигоцена вследствие воздействия подкоровых течений магмы, по-прежнему направленных на север. Расположенная ныне к югу от Гималаев Индийская глыба была перемещена этими течениями к северу от 20—40° ю. ш. до 10—25° с. ш.

ные отметки от 4000 до 7000 *м* над уровнем моря. Гигантская южная виргация Гималаев с их огромными высотами делает это очевидным.

Наша схема, конечно, требует еще многих уточняющих и дополняющих ее наблюдений.

ЛИТЕРАТУРА

1. Bernauer F. Island und die Frage der Kontinentalverschiebungen. «Geol. Rundschau», 1939, Bd. 30.
2. Bernauer F. In Niemczyc «Spalten auf Island». Stuttgart, 1943.
3. Bemmelen van R. W. The evolution of the Indian Ocean Mega-Undation. «Tectonophysics»», 1965, Vol. 2, No. 1.
4. Heezen B. C., Tharp M. Physiographic diagramm of the Indian Ocean. Dept. Geology and Lamont Geol. Observatory. Columbia University N. Y., 1965.
5. Köppen W., Wegener A. Die Klimate der geologischen Vorzeit. Berlin, 1924.
6. Kraus E. Das Wachstum der Kontinente nach der Zyklustherie. «Geol. Rundschau», 1928, Bd. 19.
7. Kraus E. Über Hyporheon und Bathyrheon. «Z. Deutsch. Geol. Ges.», 1950, Bd. 102.
8. Kraus E. Die Entwicklungsgeshichte der Kontinente und Ozeane. Akademieverlag, Berlin, 1959.
9. Kraus E. Über Geotektonik und Ozeantektonik (в печати).
10. Krestnikov V. N., Nersesov I. L. Relation of the Deep Structure of the Pamirs and Tien-Shan to their tectonics. «Tectonophysics», 1964, vol. 2.
11. Runcorn S. K. Paleomagnetic evidence for continental drift and its geophysical cause. In «Continental drift», ed. S. K. Runcorn. Acad. Press, N. Y., 1962.
12. Schwarzbach M. Das Klima der Vorzeit. 2. Aufl., Verlag Enke, Stuttgart, 1961.
13. Wegener A. Die Entstehung der Kontinente. Petermanns Geogr. Mitt., 1912.

Поступила в редакцию
18/XI 1966 г.

Мюнхенский университет,
ФРГ

Reprinted from *Amer. Associat. Petrol. Geol. Bull.*, vol. 51, no. 9, 1967, p. 1803-1815

ISLAND ARC SYSTEM IN ANDAMAN SEA[1]

L. AUSTIN WEEKS,[2] R. N. HARBISON,[2] AND G. PETER[2]
Silver Spring, Maryland

ABSTRACT

A sub-bottom profiler survey of the Andaman Sea was conducted as part of the marine geophysical program of the U. S. Coast and Geodetic Survey during the International Indian Ocean Expedition. The survey lines were run at right angles to the predominantly north-south tectonic lineations of the island arc system.

A 20,000-joule sparker, energized every 4 sec, was used as a sound source and was towed about 100 m behind the ship. A 20-hydrophone array received the reflected signals, which were recorded both on a paper strip chart and magnetic tape.

The sub-bottom profiler sections and the marine gravity and magnetic measurements augmented knowledge of the geology of the island arc system; the linear structural belts on land were traced through the Andaman Sea by geophysical methods. The structural development of the island arc system from east to west can be traced, based on available continental and marine data.

It was possible to delineate the major segments of the island arc system through a distance of 600 nautical mi (1,110 km) in the Andaman Sea, specifically, the foredeep, outer sedimentary island arc, interdeep, inner volcanic arc (and rift valley), and backdeep.

INTRODUCTION

As part of the International Indian Ocean Expedition the U. S. Coast and Geodetic Survey ship *Pioneer* conducted continuous sub-bottom profiler surveys in the Andaman Sea. These surveys were designed to study the nature of the great Indonesian island arc system between Sumatra and Burma, and to show the possible interrelations of these areas as common members of a single great structural geologic province.

GEOLOGIC HISTORY AND TECTONIC DEVELOPMENT

The Indonesian arc developed on the landward side of its associated submarine trench, a feature which is typical of all arc-shaped island chains. For this reason the origin of island arc trenches is believed to be closely related to crustal movement. This view is substantiated further by the facts that earthquakes commonly occur along trenches, and their foci deepen markedly landward to depths greater than 200 mi. Volcanoes also occur in parallel zones along many of the trenches and lie approximately above the zone of intermediate-focus earthquakes (landward of the trenches). In the Andaman Sea volcanoes are present on the landward side of the outer sedimentary island arc.

The tectonic development and patterns of the Andaman Sea region are discussed in an east-to-west direction (Fig. 1).

The Malay Peninsula is the tectonic continuation of the eastern Burma north-south fold-mountain system, which, at the southern end, swings eastward, parallel with the island arc system, into Borneo. The main fold axes in the southern peninsula trend slightly west of north, changing perceptibly to east of north at the Thailand-Burma border. These structural trends are at an acute angle to those of the island arc and are nowhere precisely parallel with them. The Mergui Archipelago along the west coast of Burma is moderately faulted and has been submerged slightly in late geological time (Chhibber, 1934). The Malacca Strait and adjoining Sunda Shelf also were submerged during Recent time.

A large fault, striking north-south through central Burma, extends seaward into the Gulf of Martaban. In the 1964 *Pioneer* survey the sub-bottom profiler sections did not extend far enough east to detect this fault under the Andaman Sea. However, the bathymetry of the eastern Andaman Sea shelf and the magnetic observations suggest that it is present. Differences in structural grain between the Malay Peninsula and trends of the island arc on the west could be explained by such a fault, downthrown toward the west.

The Malay peninsula came into existence during the Mesozoic as a result of a series of diastrophic cycles during Triassic-Jurassic time. The cycles radiated from an older center of

[1] Manuscript received, May 27, 1966; accepted, November 18, 1966.

[2] Institute for Oceanography, Environmental Science Service Administration; formerly with U. S. Coast and Geodetic Survey, Rockville, Maryland.

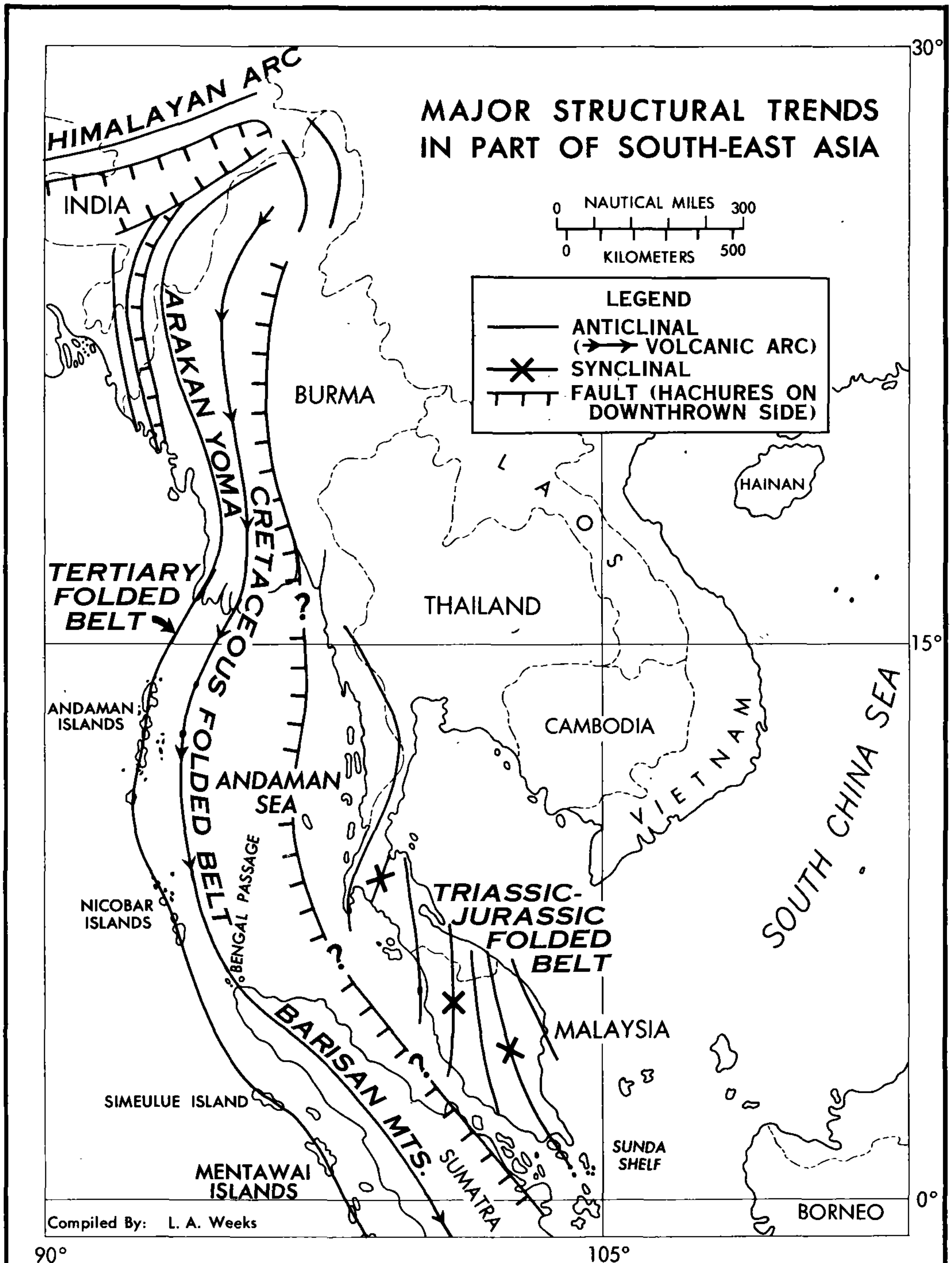

FIG. 1.—Map showing major structural trends in Andaman Sea area, southeast Asia.

orogeny on the east (Van Bemmelen, 1949). Evidence for this Triassic-Jurassic orogeny includes the folding of older sediments and intrusions of granitic rocks during Triassic-Jurassic time.

The sedimentary oil-producing basins of Sumatra and Burma (backdeep) are interconnected through the Andaman Sea, and are terminated on the east by a fault or by the abruptly sloping "basement rocks" of the Malay Peninsula. According to Krishnan (1960) the Andaman Sea probably acquired its present shape at the end of the Cretaceous.

West of the peninsula and the backdeep basin zone is the Cretaceous folded belt or inner volcanic arc. This belt can be traced from central Burma across the Irrawaddy delta, through Narcondam and Barren Islands and Invisible Bank, into the volcanic Barisan Range of Sumatra, thence through Krakatoa and the Indonesian islands. The main orogeny, at the end of the Cretaceous, folded and thrusted the pre-Tertiary sediments toward the southwest. Uplift and emplacement of batholiths followed. In Sumatra, the whole length of the Barisan Range was elevated during the Plio-Pleistocene (Van Bemmelen, 1949). The Semangko graben (rift) zone developed as a post-elevation collapse feature. The whole inner volcanic arc comprises a positive isostatic anomaly.

Across an intervening inner sedimentary trough or interdeep, the next belt on the west is the nonvolcanic outer island arc. It can be traced from the eastern Himalayan arc southward through eastern India, Burma, the Andaman and Nicobar Islands, and the islands west of Sumatra. This is a Tertiary fold belt, and forms the present-day outer island arc. The rocks of this belt are predominantly marine sediments which have been folded, faulted, and uplifted. The belt is isostatically negative, indicating a deficiency of mass—in direct contrast to the inner volcanic arc.

West of the outer island arc is the foredeep or trench. On the south, this feature is called the "Java trench." As a morphological feature the trench does not extend north of Simalur Island (3°N.), nor is it present off the Andaman and Nicobar Islands (Van Bemmelen, 1949). However, the 1964 *Pioneer* survey work indicates that the trench is present as a buried structural feature off these islands. Vertical and (or) horizontal movements in the northern part of the Andamans are believed to have occurred earlier than in the southern part. There is a definite gradation from coarse to fine sediments in Eocene beds from north to south. Therefore, movements in the Andamans and Nicobars are believed to predate the equivalent belt farther south along the Indonesian chain. Westward thrusting of the outer island arc geanticline had more or less ceased prior to the Miocene—as indicated by Miocene sediments that rest unconformably on older rocks and are hardly folded (Van Bemmelen, 1949). Subsequent elevation of the outer island arc during the Quaternary has resulted from vertical uplift combined with a post-glacial rise in sea-level.

Van Bemmelen (1949), in his classic synthesis of the geology of Indonesia, ascribed variations along various parts of the same structural belt to the fact that different orogenic centers or foci were involved. He believed that the Andaman Sea belts developed from a different orogenic focus than did the areas south and north. Van Bemmelen also concluded that northern Sumatra (Atjeh section), near which the *Pioneer* ran several track lines, belonged to the same orogenic system as the Andaman Sea.

Sub-Bottom Profiling Results

Sub-bottom profiling was done along five sections that cross the structural belts of the island arc system in the Andaman Sea (Fig. 2). Figure 3 shows sections 1 and 2. Figure 4 shows sections 3, 4, and 5. Section 5, the southernmost, is confined to the backdeep. Section 4, just north of Sumatra, extends from the backdeep to the axis of the outer island arc. Section 1, a discontinuous profile, extends from the backdeep to the foredeep along the Ten Degree Channel just north of Car Nicobar Island. Section 3, the northernmost, extends from the backdeep in the vicinity of the Tenasserim coast of Burma across the submerged Irrawaddy delta to a point just south of Preparis Island, and then northwest across the outer island arc.

The sections, as interpreted, show form lines of the structure and approximate thicknesses of sedimentary layers. Some of the faults indicated on the sections are clearly observed on the sub-bottom profiler records. Others are inferred because the attitude of the beds and the structurally complex geology of the area make their iden-

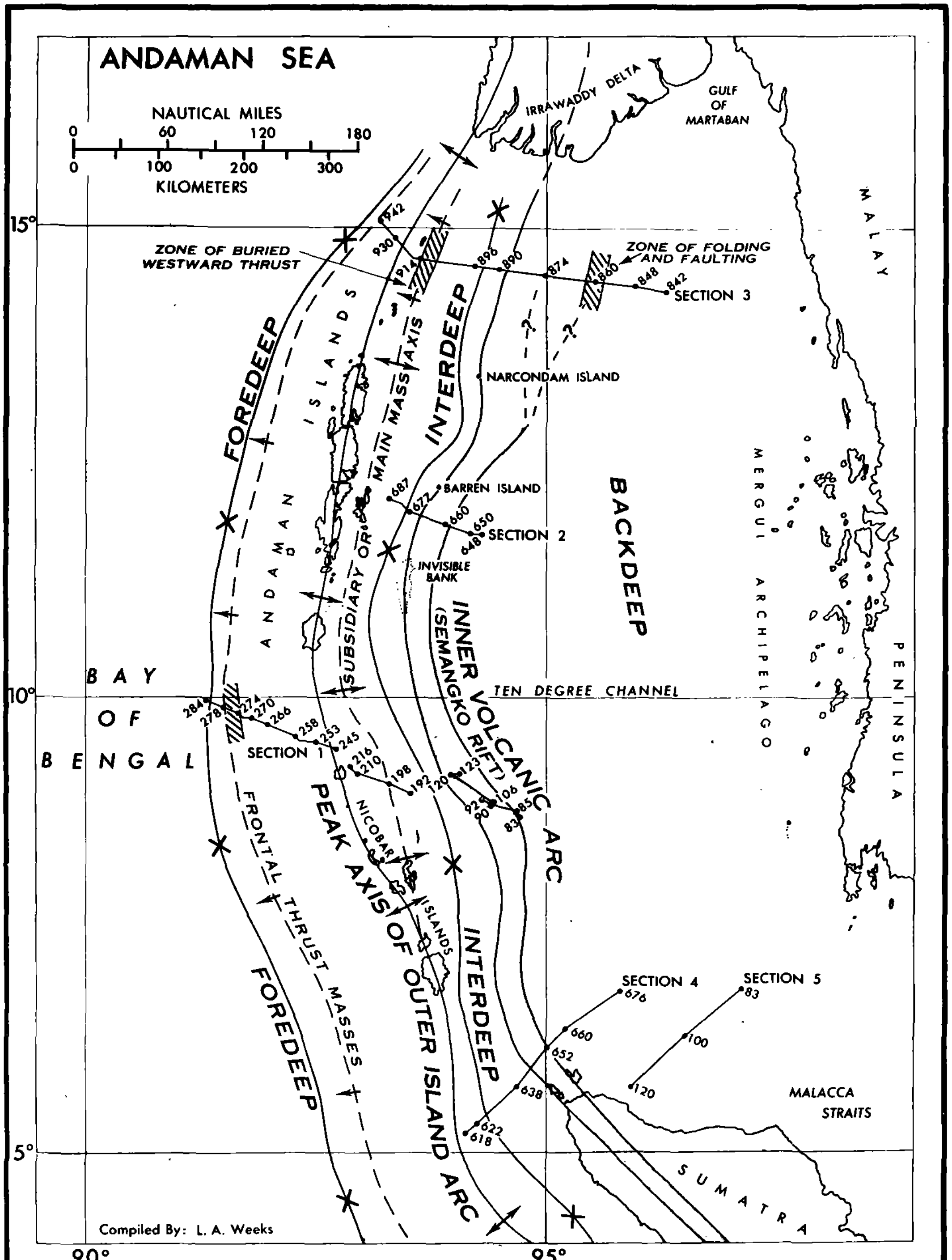

FIG. 2.—Island arc elements of Andaman Sea. Locations of sections 1-5 (Figs. 3, 4) shown. Locations of Figures 5-8 also can be determined from this figure.

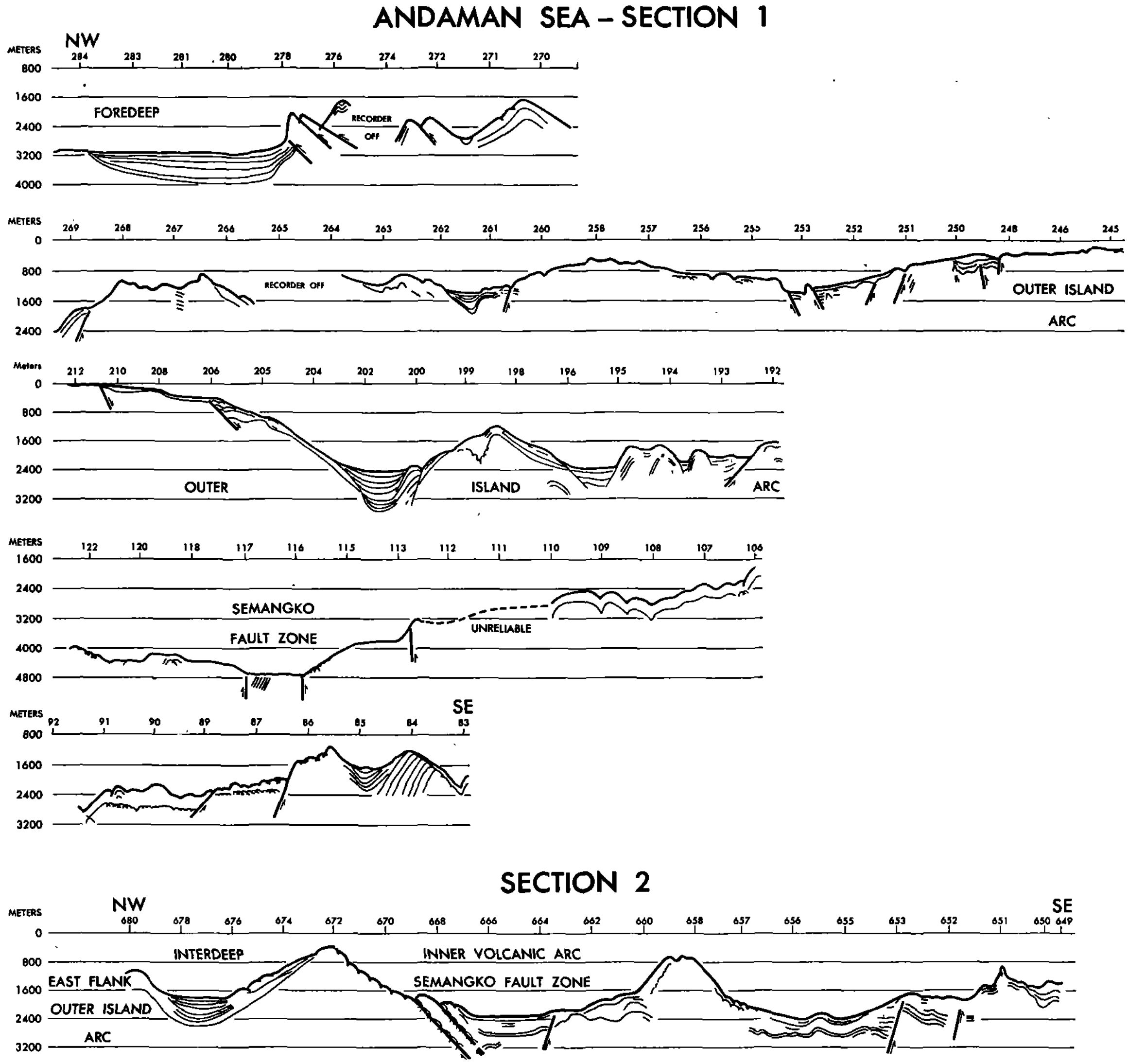

FIG. 3.—Sections 1-2, Andaman Sea island arc system. Locations shown on Figure 2.

tification less certain. Fault planes and the direction of movement along faults commonly are indefinite.

The horizontal scale of the interpreted sections is based on the ship's position fixes. These were made at 30-min intervals while traveling at a speed of about 5 knots. Hence, each fix point marked on the sections is separated from the adjacent fix by a 30-min time interval—regardless of the number assigned to it—and the horizontal scale is approximately 5 nautical mi between every second fix mark. Analysis and interpretation of the results preceded the receipt of adjusted fix locations by many months, but the differences between the true or corrected track line (as on Fig. 2) and the section track lines (Figs. 3, 4) are relatively slight.

Penetration depths are uncorrected for sound velocity. The scale of the sections is based on a velocity of 1,600 m/sec, or 5,248 ft/sec. Where "lower velocity" sediments overlie or are adjacent to "high-velocity" rocks, any particular velocity assumption is incorrect. A higher estimated velocity would increase the thicknesses of sedi-

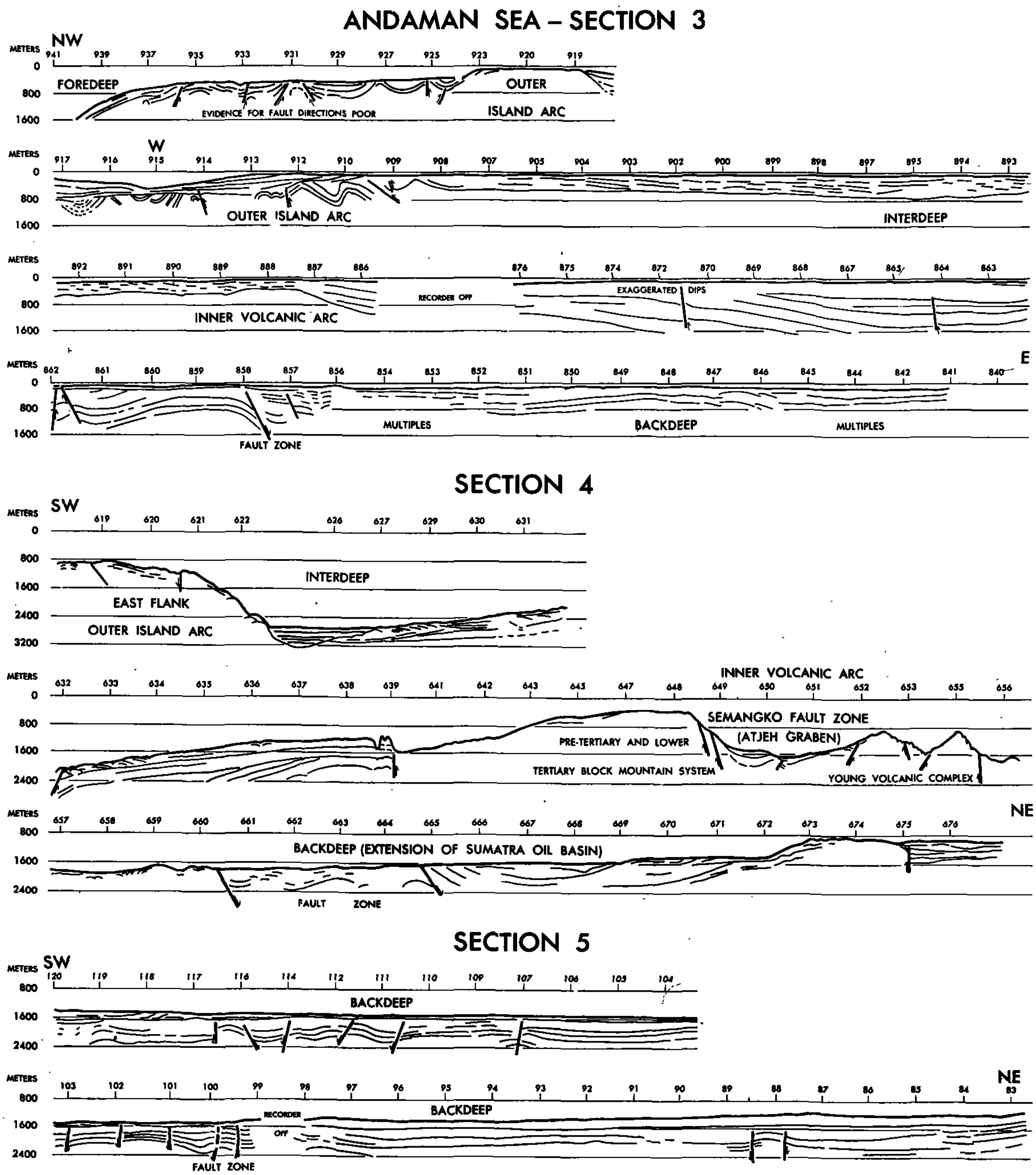

FIG. 4.—Sections 3-5, Andaman Sea island arc system. Locations shown on Figure 2.

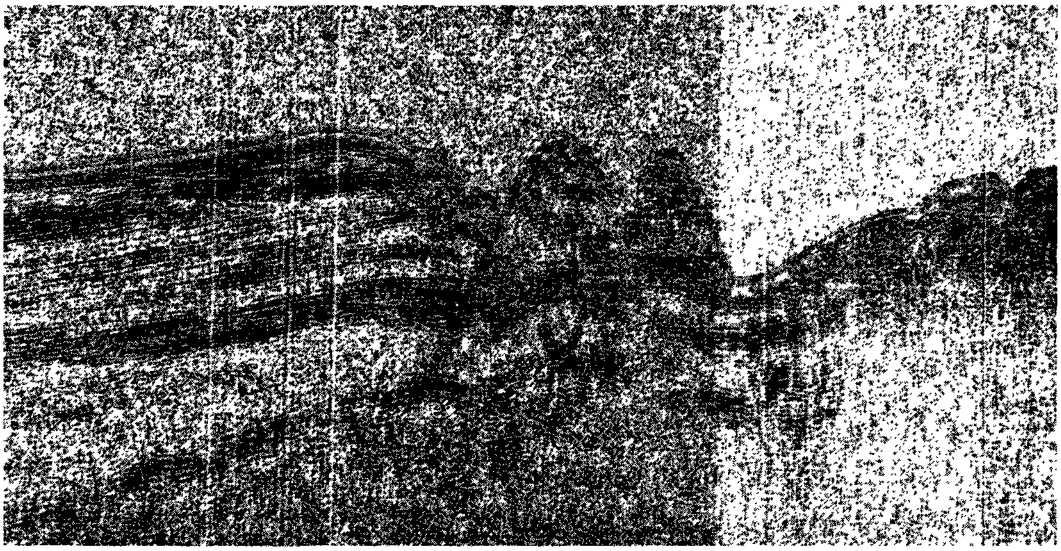

FIG. 5.—Section 4, fix 639, southwest-northeast profile. Sediments on southwest (left) are seen to disappear against hard bedrock or volcanics toward northeast. Mass on northeast is western block of inner volcanic arc, supposedly a horst block. A fault is postulated at right side of picture, upthrown toward northeast. For location, see Figures 2 and 4.

ments penetrated, perhaps as much as 50 per cent in some cases. Bottom depths change greatly throughout the Andaman Sea; therefore instrumental scale shifts were frequent. The results of the sub-bottom profiler surveys are discussed from south to north.

NORTHERN SUMATRA—SECTIONS 4 AND 5

The two profiles just north of Sumatra were made in order to cross known trends of major proportions. Section 4 (Fig. 4) begins on the east flank of the outer island arc, which plunges steeply into the interdeep. Clear evidence of sedimentation is lacking, possibly because of the ruggedness and steepness of the slope. However, bedding and some indications of faulting can be seen at the top of the arc. Simalur Island, on the south, is a geanticline cut by north-south-trending transverse faults (Van Bemmelen, 1949). From the interdeep to fix 639 several unconformities are detectable. Sediments Southwest of fix 639 (section 4, Fig. 4) disappear against hard bedrock or volcanics on the northeast (Fig. 5). The mass on the northeast is the western block of the inner volcanic arc—a horst. A fault is postulated at fix 639, section 4 (Fig. 4), upthrown toward the northeast.

The part of section 4 from fix 639 to 648 is the offshore continuation of the pre-Tertiary and lower Tertiary block-mountain system of northern Sumatra. The block is represented by the western side of the Atjeh graben and the islands west of the Bengal Passage. There is a lack of obvious bedding on the records, probably because the rocks are dense. On Sumatra, these rocks are primarily Permo-Carboniferous sediments (undoubtedly metamorphosed), diabase, and serpentinites (Geologic Maps of Netherlands Indies, 1927). The Atjeh graben, part of the Semangko fault zone which can be traced the entire length of Sumatra, shows up very clearly. It is considered to be a relaxation feature after the Plio-Pleistocene uplift in the Barisan (Van Bemmelen, 1949). On Sumatra the graben is filled with Neogene (Pliocene and Miocene) sediments which are overlain by Quaternary and alluvial deposits, and extends into the Bengal Passage. East of the graben in northern Sumatra the rocks are primarily volcanics (post-lower Tertiary?), identified as andesite effusives, or are block-mountain structures similar to those on the west side. The whole belt from fix 639 to fix 656 represents the inner volcanic arc, including the Semangko fault zone.

Northeast of the inner volcanic arc is the backdeep. This is the Andaman Sea extension of the Sumatra oil basin. Folding and faulting are evi-

FIG. 6.—Section 4, fix 671, southwest-northeast profile. Unconformity, showing bottom beds rising toward northeast and overlying beds wedging out. Bottom beds reflect one side of an arch whose peak reaches bottom surface beyond picture (right). For location, see Figures 2 and 4.

dent. In this area and also in Sumatra, structural complexity tends to decrease away from the inner volcanic arc. The zone between fixed 660 and 665 is more contorted than are zones on the northeast. Fixes 665 to 673 are in a broad synclinal trough, although the bottom rises gradually toward the northeast (Fig. 6). Beyond fix 673 and northeastward to the large fault at fix 675 (Figs. 4, 7), sub-bottom reflections disappear (Fig. 6). The writers interpret this to mean that the "basement" or volcanic rocks are faulted against approximately 1,600 m of sediments. The fault does

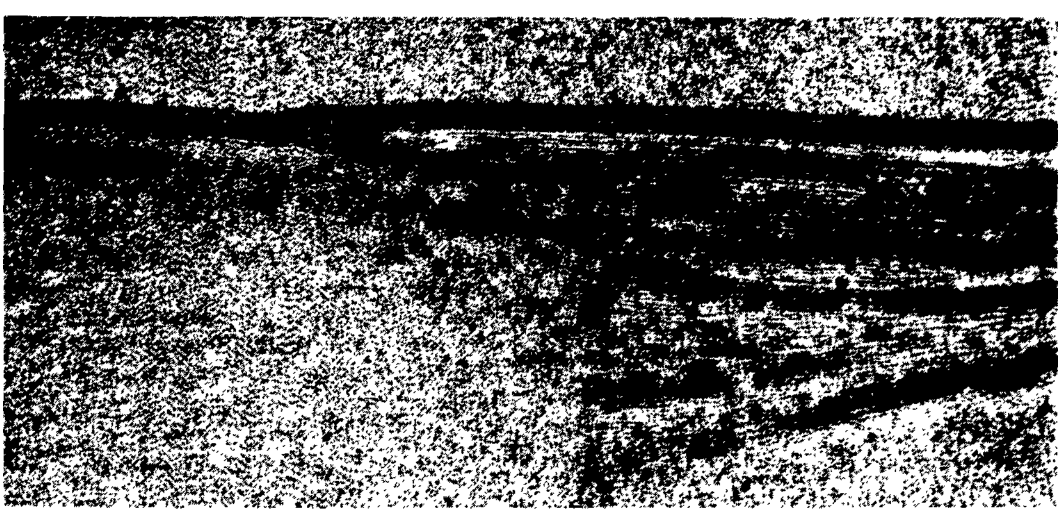

FIG. 7.—Section 4, fix 675, southwest-northeast profile. Large fault downthrown toward northeast (right). Southwestern block consists of "basement" or volcanic rocks faulted against approximately 1,600 m of sediments. Note how basal sediments dip into fault, whereas youngest beds drape across fault and onto "basement" or volcanic block. Small buried channel can be seen above fault plane, as well as larger buried channel on right. For location, see Figures 2 and 4.

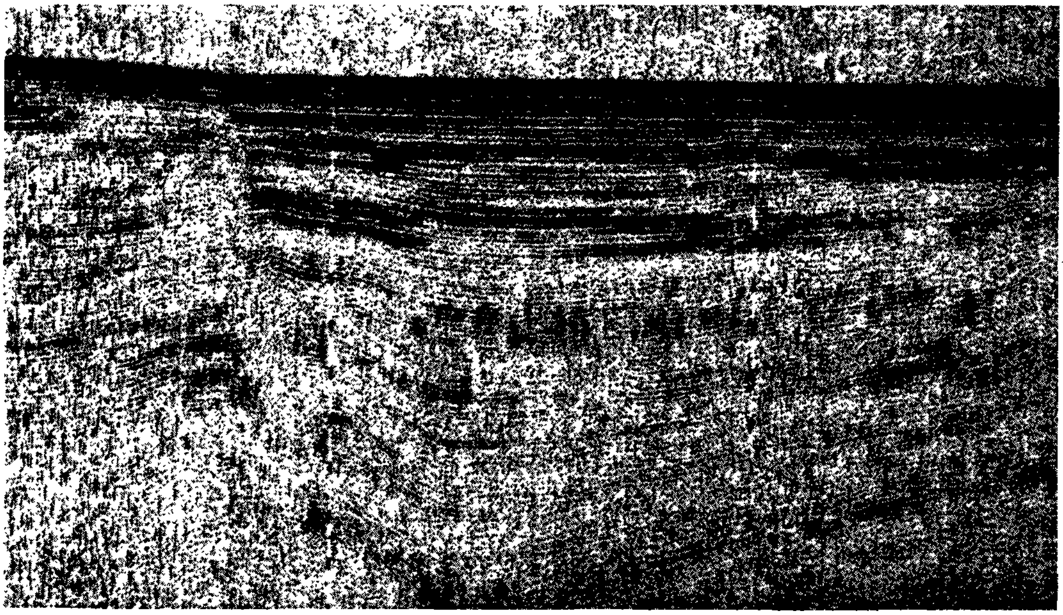

FIG. 8.—Section 5, fix 100, northeast-southwest profile. Fault with about 200 m of displacement, downthrown toward southwest (right). About 1,000 m of penetration can be seen here. Fault plane does not quite reach ocean floor. For location, see Figures 2 and 4.

not reach the sea floor, which commonly is the case within the areas surveyed in the Andaman Sea. Northeast of the fault, the basal sediments dip into the fault, whereas the upper beds overlap the fault and the "basement" or volcanic rocks. The records show an old channel above the fault plane; this channel probably was cut into the softer materials at that place.

Section 5 (Fig. 4) is about 50 mi (92 km) southeast of section 4. The purpose of this section was to investigate the backdeep, to include trends found on section 4, and to search for the fault which occurs at the end of section 4 on the north (fix 675). The southwestern part of the section shows sub-bottom folding and faulting in rocks that lie unconformably beneath a thin veneer of surface deposits. The surface veneer is relatively flat, except at fix 118. Between fixes 99 and 100 a large fault zone was observed (Fig. 8). The large fault found on section 4 (fix 675) does not appear to be present. A similar relationship of "basement" or volcanic rocks to sediments was not found on section 5; consequently its extent and true significance are not known.

Northeast of fix 99 the remainder of the backdeep shows a folded sub-bottom section, in part unconformably overlain by surface deposits. At the northeast end of the section, the bottom and sub-bottom deposits are conformable and rise onto the Andaman Sea shelf.

TEN DEGREE CHANNEL—SECTION 1

Section 1 (Fig. 3), the first profile run in the area, was interrupted frequently in order to make oceanographic observations at various stations. Consequently, this profile is not continuous and some important features were missed. The section from fixes 245 to 284 includes structural features of the western outer island arc (Nicobar Islands), west of the Ten Degree Channel. From fix 272 to fix 284, the records indicate sedimentary blocks that are thrust westward against the ancient foredeep. The bathymetry west of fix 284 indicates gradual shoaling. The greatest depths are adjacent to the thrust blocks. The Java trench (foredeep) terminates considerably south of this area and a deep trench does not appear on any crossings of the foredeep. However, the deepest water is everywhere adjacent to the western limit of the outer island arc. It seems probable that later sedimentation filled the foredeep west of the Andaman and Nicobar Islands.

From fix 245 to the thrusted blocks at fix 278 the nature of the western flank of the outer island arc is evident. The shelf has a rugged and youthful appearance, both structurally and topographically, which one would expect from an island mass which has emerged so recently. Bottom depth increases approximately 2,400 m between fixes 245 and 284, in a distance of 92 nautical mi (170 km).

There is a 16½-mi gap (31 km) in the record between fixes 245 and 212. Both fixes lie in the same structural trend along the outer island arc and can be considered to be in structurally equivalent positions. The youthful and structurally complex area from fix 192 to fix 212 is the eastern flank of the outer island arc. Bathymetric data show its continuation a short distance southeast of fix 192. The total width of the outer island arc in this sector is about 100 mi (185 km). The maximum width of Car Nicobar Island, near which the *Pioneer* passed, is 7 mi (13 km). The sea-floor base of the outer island arc is many times this width. East of the outer island arc the bottom is rough and the sub-bottom structure has a youthful appearance. Just south of this traverse the Nicobar Islands are broken up into several groups with trends that apparently extend northward.

Fixes 192 and 122 are 30 mi (55 km) apart. Sub-bottom profiles were not obtained between these fixes, but continuous depth soundings were made.

Bathymetric data indicate that the bottom rises markedly to less than 180 m depth just southeast of fix 192. The bottom then plunges abruptly toward the interdeep where depths of about 4,100 m were observed. It rises again toward the western block of the inner volcanic arc west of fix 120. The bottom of the graben valley (Semangko rift) is between fixes 116 and 117 at about 4,800 m depth. This is deeper than the interdeep by approximately 700 m. Lack of sub-bottom penetration prevented delimiting the graben valley between the faults. Also, the survey line did not cross structural trends at right angles. The result of this is that the graben has a greater apparent width in this section. The peak of the eastern block of the inner volcanic arc appears at fixes 84–86. The western block lies between fixes 120 and 192, as is the interdeep. The backdeep lies a short distance east of fix 83.

RITCHIE'S ARCHIPELAGO—SECTION 2

Section 2 (Fig. 4) was run south of Barren Island and extends west to Ritchie's Archipelago, just east of the Andaman Islands. This section and section 4 show very well the structure of the inner volcanic arc and associated rift valley. Fix 680 is above the east flank of the outer island arc. The interdeep is evident, with about 800 m of sediment in the structural trough. The peak at fix 672 lies on the western part of the inner volcanic arc and is approximately half way between Invisible Bank and Barren Island. Both the bank and the island are part of the inner volcanic arc (western flank). The area between fix 672 and 658 is a continuation of the Semangko rift valley which occurs both on the island of Sumatra and offshore (section 4). A large fault may be present at fix 660 along the steep slope, but the records are inconclusive. Tipper (1911) believes that Barren and Narcondam Islands have emerged along a master fault zone east of the Andaman Islands. However, both Barren and Narcondam Islands, as well as Invisible Bank, form only the west side of the inner volcanic arc.

Southeast of fix 658, the profiler and bathymetric data indicate the presence of another ridge-like area. Sediments are more abundant than on the flanks of the volcanic arc. Except for a possible small intrusive at fix 651, volcanic or basement-type rocks appear to be lacking. This ridge does not extend very far either north or south of this section.

IRRAWADDY DELTA—SECTION 3

Section 3 (Fig. 4), the northernmost traverse made in the Andaman Sea, crossed the submerged extension of the Irrawaddy delta from the Tenasserim coast of Burma. Just south of Preparis Island the east-west traverse was turned northwest to its termination.

The western part of section 3 shows the western slope of the outer island arc. At the western limit, the slope plunges steeply seaward in the foredeep area. Faulting and folding are not noticeable along the smooth sea floor of this slope. A smooth sea floor is typical of the northern traverse of the Andaman Sea, even where the underlying structure is complex. A small channel at fix 933 is the only indication of sub-bottom structure controlling bottom topography between fixes 923 and 935. Sub-bottom profiling shows the structural complexity of the wide belt from fix 939 to fix 909, a distance of 38 mi (70 km). This is the outer island arc, whose apex apparently is at fix 920. East of fix 919 the sub-bottom features are even more complex. Here, younger sediments lie unconformably on the older folded rocks of the outer island arc. Perhaps this is the pre-Miocene unconformity, described by Van Bemmelen (1949). Thrusting presumably ended before Miocene time in the outer island arc. The younger beds undoubtedly are part of the massive Irrawaddy delta. The Irrawaddy River deposits 670,000 tons of silt per day on its rapidly building delta (Chhibber, 1934). Protection from the open sea and lack of effective longshore currents favor the advance of the delta toward the south.

Fixes 908 to 888 show the gradual descent of the bedrock to the interdeep at about fix 895, and gradual rise of the bedrock to the inner volcanic arc at fix 888. The deepest or basal reflection is a composite, and should not be interpreted as a continuous reflection. Single beds cannot be traced for long distances. The largest free-air gravity value along the entire traverse occurs at fix 888 (plus 40 mgals). The extent of the traverse is covered by deltaic deposits, and lack of sub-bottom penetration beneath the bedrock prevents interpretation of the underlying features.

East of fix 886 equipment failure prevented obtaining data for 16 mi (30 km). Hence it was impossible to identify the rift valley (Semangko fault zone), which may be buried by overlying sediments. The inner volcanic arc does not appear to be as well developed here as it is farther south (sections 2 and 4). Attenuation of sparker energy through the soft overburden masks some features, but the main reason for poor development of island arc structure may be that the volcanic arc has more mature topography at the northern end. There are at least two indications that the island arc becomes younger toward the south: (1) the infilling of the former trench west of the outer island arc to such an extent that it is only barely indicated by the bathymetry, even though structurally apparent in the sub-bottom; and (2) the southward gradation of Eocene sediments on the Andaman and Nicobar Islands from coarse terrestrial to fine marine (Van Bemmelen, 1949).

East of fix 887 the beds appear to dip gently east with a few faults. The surface beds lie unconformably on older sediments. Whether all the reflections are from delta deposits is uncertain. If the basal beds are of deltaic origin, the faults, although older than the surface sediments, must be very recent. Between fixes 857 and 862 an interesting sub-bottom structure was developed. Its interpretation is not clear. The structure may be a folder section of the backdeep or the eastern segment of the inner volcanic arc, whose twin nature was noted on the south. Free-air gravity and magnetic intensity values increase above this feature. Thin surface beds unconformably overlie the folded sediments.

If this folded section is the eastern block of the inner volcanic arc, then there is considerable divergence of structural trends north from the Ritchie's Archipelago traverse (section 2, Fig. 3). Off Sumatra and Ritchie's Archipelago, the distance between segments is about the same, about 20 mi (37 km). On the Irrawaddy delta traverse the segments may be separated by as much as 61 mi (113 km), or three times the separation farther south. However, it appears more likely that the eastern segment, if still in existence, is in the 16-mi (30-km) area of no records between fixes 876 and 886.

The remainder or eastern part of the traverse has no distinctive features, and contains gently folded beds, presumed to be delta deposits. The records contain many multiple reflections which may mask some structural features.

Description of Structural Belts

The study of sub-bottom profiles, bathymetry, gravity, and magnetic measurements in the Andaman Sea makes it possible to describe the various structural belts of the island arc system. Regionally, these are, from east to west, the following.

BACKDEEP

The typical structure of the backdeep is best shown in sections 4 and 5 (Fig. 4). In section 3 (Fig. 4), which also traverses the backdeep, the sub-bottom features are masked by the cover of deltaic sediments. In general, the structural features of the backdeep are less complex than those of the belts on the west, but some large anticlines, synclines, and fault zones are present. The largest anticline was recorded off the Sumatra coast, between fixes 100 and 105 of section 5. Its width is about 14 mi (26 km). This feature could

TABLE I. SIMILARITIES OF ANDAMAN SEA INNER VOLCANIC ARC AND CENTRAL PART OF MID-ATLANTIC RIDGE

Andaman Sea Inner Volcanic Arc	*Mid-Atlantic Ridge*
Volcanic rock types: serpentine, diabase, andesite	Volcanic rock types: serpentine, diabase, basalt
Earthquake belt: zone of epicenters (200 km)	Earthquake belt: zone of epicenters (25 km or less) (G. H. Sutton, pers. comm.)
Prominent rift valley	Prominent rift valley
Adjacent high mountains	Adjacent high mountains
Peaks above sea-level: Narcondam and Barren Islands	Peaks above sea-level: Iceland to Bouvet Island
Considerable relief between rift valley and adjacent peaks	Considerable relief between rift valley and adjacent peaks
Comparable width of rift valley: 20–25 mi, peak to peak	Comparable width of rift valley: 15–30 mi, peak to peak
Depth to floor of valley ranges from 5,000 to 15,000 ft where crossed by profiler	Depth to floor of valley averages 12,000 ft
High length to width ratio	High length to width ratio

be of impressive size—depending on its extent normal to the traverse. Numerous faults were recorded across this anticline, which appears to terminate against a fault on the northeast, at fix 100. A smaller anticline is present between fixes 111 and 115. This feature is about 7 mi (13 km) wide and also is faulted. In the backdeep part of section 3, two anticlinal structures were observed, one 12½ mi (23 km) wide between fixes 845 and 851 and the other 8 mi (15 km) wide between fixes 858 and 861. The rocks in both are unconformably overlain by flat-lying sediments.

The backdeep consists primarily of sedimentary rocks. In most places, the sedimentary sections are thicker than 800 m. Suspected volcanic or "basement" rocks were found only between fixes 673 and 675, section 4. The greatest water depths at which the backdeep complex was observed were at fix 658 of section 4 (about 1,900 m) and fix 656 of section 2 (about 2,400 m), both adjacent to the inner volcanic arc.

INNER VOLCANIC ARC AND SEMANGKO RIFT VALLEY

The inner volcanic arc (with its associated Semangko rift valley) was the most interesting structural feature observed in the Andaman Sea. On land, the rift valley can be traced approximately 1,100 mi (2,040 km), the entire length of Sumatra. During the 1964 *Pioneer* cruise, by means of sub-bottom profiling, it was traced for the first time about 600 mi (1,110 km) farther north through the Andaman Sea. Free-air gravity values also indicated the presence of the volcanic arc beneath the sediments of the Irrawaddy delta (Peter *et al.*, 1966), but the sub-bottom structural detail along the traverse in this area (section 3) could not be resolved beneath some 400 m of sediments.

The width of the rift valley, as determined by the east-west traverses between northern Sumatra and Ritchie's Archipelago, is 5–10 mi (9¼–18½ km) between the bounding ridge crests. The valley relief, between adjacent ridge crest and valley floor, is 1,200 m off Sumatra (section 4) and 2,000 m at section 2. The western ridge of the inner volcanic arc rises higher above the sea floor and is a more massive feature than the eastern ridge. Narcondam and Barren Islands and Invisible Bank are part of the western structural elements of the inner arc system.

The magnetic and gravity results in the Andaman Sea area provide further evidence of the submarine continuation of the inner volcanic arc (Peter *et al.*, 1966). A broad magnetic high belt extends from the tip of Sumatra approximately 600 mi north to the Irrawaddy delta traverse (section 3). This belt broadens northward to Narcondam Island and then narrows before it crosses section 3. Gravity highs in excess of 50 mgal occur off the tip of Sumatra and at Invisible Bank, Barren Island, and Narcondam Island. The largest free-air values, in excess of 100 mgal, were observed at Invisible Bank and Barren and Narcondam Islands—a value of more than 150 mgal being present at the south end of Invisible Bank. Interesting similarities between the Andaman Sea inner volcanic arc and the Mid-Atlantic Ridge are listed in Table I. The Mid-Atlantic Ridge is a much longer structural feature and is not part of an island arc development, but the rift valley and many related tectonic features are common to both the Mid-Atlantic Ridge and the Andaman Sea inner volcanic arc.

INTERDEEP

The interdeep is the structurally depressed belt between the two major uplifts of the island arc system. Its appearance is similar along the north-south extent of the arc except in the extreme north where deltaic deposits have masked many features. Off Sumatra (section 4) approximately 700 m of flat-lying sediments fill the depression (interdeep) between the two arcs. The eastern slope of the outer island arc is steeper than the western slope of the inner volcanic arc and may have been the source of most of the sediment. On the south, the interdeep separates Sumatra and the offshore Mentawai Islands. The interdeep was not profiled in the Ten Degree Channel (section 1), but is indicated by the bathymetry on several other traverses made by the ship.

Off Ritchie's Archipelago on the east flank of the outer island arc in section 2, the narrow and downwarped interdeep is filled with sediments that appear to have been deposited from both flanks and folded in the form of a syncline as the downwarping continued. In section 3 off the Irrawaddy delta, the broad interdeep lies between flanks with very slight slope, and is filled with sediments that mask its topographic expression on the sea floor.

OUTER ISLAND ARC

The outer island arc is composed predominantly of sedimentary rocks. It is the youngest arc of the whole Andaman Sea structural system. It continues north of section 3 as the Arakan Yoma (mountains) of western Burma and finally abuts against the eastern Himalayan arc along the Burma-India border. Toward the south, the outer arc includes the Mentawai Islands off Sumatra and the submarine ridge on the landward side of the Java trench.

The outer arc is structurally complex. It has the overall features of a large anticline. Its width in places exceeds 100 mi (185 km). Near the Irrawaddy delta the outer arc narrows before entering Burma, but toward the south, between Narcondam and Barren Islands, a distinct eastward bulge is indicated by the bathymetric data obtained by the *Pioneer*. The sub-bottom profiles of sections 1 and 3 suggest that westward thrusting of the outer arc took place. The apparent thrust ridges of section 1 can be traced northward by means of the bathymetric data. The presence of other ridges with long, straight, east-dipping slopes suggests westward thrusting.

Gravity measurements show a negative free-air anomaly approximating the peak axis (line of highest elevations) of the outer island arc (Peter *et al.*, 1966). The peak axis of the arc and the negative gravity axis coincide exactly at the south end of the index map (Fig. 2). At 8°00′ N. and 93°30′ E. the negative gravity axis veers east of the Nicobar Islands. It continues east of the islands and rejoins the peak axis of the outer islands where the negative gravity axis enters Burma. The trend labeled "subsidiary or main mass axis" on Figure 2 is the negative gravity axis north of 8° N. A belt as wide as the outer island arc and tilted westward would be expected to have its main mass axis lying east of its surface peaks (Nicobar and Andaman Islands). The zone of westward thrusts on section 3, Ritchie's Archipelago (southwest of Barren Island), and the cluster of islands at 8°00′ N. and 93°30′ E. are considered to be parts of the subsidiary trend, coinciding with the negative free-air anomaly.

Results of Survey

The geologic-geophysical investigations of the 1964 *Pioneer* Indian Ocean Expedition provided much new data and information about the geological features of the Andaman Sea, particularly the submarine tectonic patterns and crustal development of the area. The sub-bottom profiles made it possible to delineate the major segments of the island arc system through a distance of more than 600 mi (1,110 km) and provided information about the structural relations of the basement and overlying rock complexes in the major structural belts—foredeep, outer sedimentary island arc, interdeep, inner volcanic arc and associated rift valley, and backdeep. Continued detailed analysis of the geophysical data obtained in the Andaman Sea area and correlation of the 1964 results with results of other surveys can be expected to yield additional discoveries of scientific significance.

References Cited

Chhibber, H. L., 1934, The geology of Burma: London, Macmillan and Co., 538 p.

Geologic Maps of Netherlands Indies, 1927, Scale 1:1,000,000: compiled by J. V. Scrivenor.

Krishnan, M. S., 1960, Geology of India and Burma, 4th ed.: Madras, Higginbothams (Private), 604 p.

Peter, G., L. A. Weeks, and R. E. Burns, 1966, A reconnaissance geophysical survey in the Andaman Sea and across the Andaman-Nicobar island arc: Jour. Geophys. Research, v. 71, no. 2 (Jan.), p. 495–509.

Tipper, G. H., 1911, Geology of Andaman Islands, with references to Nicobars: Mem. Geol. Survey Ind., v. 35, pt. 4, p. 195–213.

Van Bemmelen, R. W., 1949, Geology of Indonesia, v. 1A: The Hague, Govt. Printing Office, 732 p.

Reprinted from *Morskie gravimetričeskie issledovanija*, vol. 3, Izdatel'stvo MGU, 1967, p. 82-94

The gravimetric field and thickness of the terrestrial crust of the north-western part of the Indian Ocean

by A. G. Gaïnanov and P. A. Stroev

IV. РЕЗУЛЬТАТЫ ГРАВИМЕТРИЧЕСКИХ ИЗМЕРЕНИЙ В МИРОВОМ ОКЕАНЕ И АНТАРКТИДЕ

А. Г. Гайнанов, П. А. Строев

ГРАВИТАЦИОННОЕ ПОЛЕ И МОЩНОСТЬ ЗЕМНОЙ КОРЫ СЕВЕРО-ЗАПАДНОЙ ЧАСТИ ИНДИЙСКОГО ОКЕАНА

Обширные комплексные геофизические исследования строения земной коры к настоящему времени проведены в Атлантическом и Тихом океанах. Индийский океан до недавнего времени оставался наименее изученным геофизическими методами. И только в период Международного геофизического года началось планомерное комплексное изучение Индийского океана, включающее различные геофизические исследования с целью выяснения особенностей глубинного строения земной коры. В настоящее время интерес к изучению Индийского океана значительно возрос. Для координации всех работ создана Международная индо-океанская экспедиция, по программе которой выполнялись комплексные работы в 1959—1962 гг. английскими и американскими исследователями, а также 31—32, 35 рейсы э/с «Витязь» в 1959—1962 гг. [1].

Наиболее изученными в гравитационном отношении в Индийском океане являются его западная (особенно северо-западная) часть, а также приантарктические области [1, 2].

Первые гравиметрические измерения на акватории Индийского океана были проведены Венинг-Мейнесом в 1923 г. [3]. Наблюдения проводили на подводной лодке при следовании ее из Голландии к о. Ява через Суэцкий канал. Измерения силы тяжести производились с помощью морского маятникового прибора. Всего в Индийском океане и Красном море было определено 22 пункта с ошибкой аномалий Фая ±5—6 *мгл*, аномалий Буге около ±10 *мгл*.

В последующие годы Венинг-Мейнес продолжал гравиметрические исследования на подводных лодках в Индийском океане. Так, в экспедиции 1948 г. [4] при плавании между Африкой и Австралией им выполнено несколько десятков гравиметрических пунктов с ошибками аномалий Фая ±5 *мгл*, аномалий Буге ±10 *мгл*. При плавании английской подводной лодки «Ахерон» в 1955 г. [5] в Индийском океане было выполнено 37 пунктов. Наблюдения проводили Р. Гирдлер и Дж. Гаррисон с 3-маятниковым морским прибором Венинг-Мейнеса и кварцевым хронометром. Глубина моря измерялась эхолотом. Координаты пунктов определяли астрономическим способом; точность аномалий Фая ±4—5 *мгл*, аномалий Буге ±6—8 *мгл*.

В 1959 г. Американская экспедиция под руководством М. Тальвани на той же британской подводной лодке «Ахерон» выполнила гравиметрические измерения в западной и северо-западной частях Индийского океана [6]. На маршруте Дурбан—Момбаса через Мозамбикский пролив выполнено 11 пунктов. Весьма интересным оказался профиль из 11 пунктов наблюдений через Аравийско-Индийский хребет к юго-востоку от о. Сокотра. Профиль протяженностью 650 *км* начинается в Сомалийской котловине, пересекает Индийско-Аравийский хребет, заканчивается в Аравийской котловине и дает гравитационную характеристику срединно-океанического хребта и его окрестностей. Измерения силы тяжести проводились с 3-маятниковым прибором Венинг-Мейнеса; служба времени обеспечивалась кварцевыми хронометрами.

Обширные комплексные геофизические исследования северо-западной части Индийского океана были проведены в 1961—1962 гг. английскими учеными на экспедиционном судне «Оуэн» [7]. Экспедиция проделала 16 тыс. миль (37 профилей), проводя непрерывные батиметрические, гравиметрические и магнитные исследования. Измерения силы тяжести на борту «Оуэна» проводились Б. Лонкаревичем с надводным морским гравиметром GSS-2-II фирмы «Askania Werke» (ФРГ). Прибор был установлен на гиростабилизированную платформу фирмы «Анштюц» (ФРГ). Гравиметр имел термостат, смещение нуль-пункта в среднем по рейсу составило 0,9 *мгл/сут*. Нуль-пункт определяли между опорными наблюдениями в портах; калибровка гравиметра проведена на английском опорном профиле от Саутгемптона до Абердина с $\Delta g = 573$ *мгл*. Измерений горизонтальных ускорений не производили, влияние кросс-каплинг эффекта игнорировали, полагая, что ошибки от них не могли быть большими, так как море за все время плавания было спокойным. Средние наклоны корабля были 1—2° в килевой плоскости и 2—4° в бортовой плоскости.

Следует отметить, что результаты геофизических исследований экспедиции на «Оуэне» опубликованы [7] в виде непрерывных профилей с батиметрическими промерами, магнитными и гравитационными (в свободном воздухе) аномалиями. Эти данные представлены без каких-либо комментариев и интерпретации их. Точность полученных значений аномалий Фая можно оценить величиной ± 5 *мгл*. Кроме морских гравиметрических измерений экспедиция выполнила сухопутную съемку на островах Альдабра, Сейшельских и атолле Адду. Съемка выполнена с помощью гравиметра Уордена.

Во всех портах морские гравиметрические профили привязаны к береговым опорным пунктам.

В последнее время в работах [8—9] упоминается об обширных комплексных геофизических исследованиях Индийского океана, проведенных в 1960—1964 гг. американскими экспедициями («Мунсон», «Лунзиад» и др.). В этих работах сообщается, что гравитационные измерения проведены почти в 20 000 пунктах, покрывающих более 45 000 миль маршрутов. Точность этих измерений характеризуется ошибкой $\pm 8 \div 18$ *мгл*. К сожалению, эти данные не опубликованы, за исключением данных по профилю $\Delta g_{Фая}$, приведенных в работе М. Капуто [8]. Профиль проходит по линии экватора от 48° до 100° в. д.

Таким образом, сделанные к настоящему времени гравиметрические исследования (рис. 1) дают возможность составить некоторое представление о характере гравитационного поля северо-западной части океана и в общих чертах выявить строение земной коры в этом районе.

На рис. 2 представлена схематическая гравитационная карта аномалий Буге (нормальная формула международная) северо-западной части Индийского океана. Карта составлена по данным упомянутых экспедиций английских и американских геофизиков и экспедиций Ве-

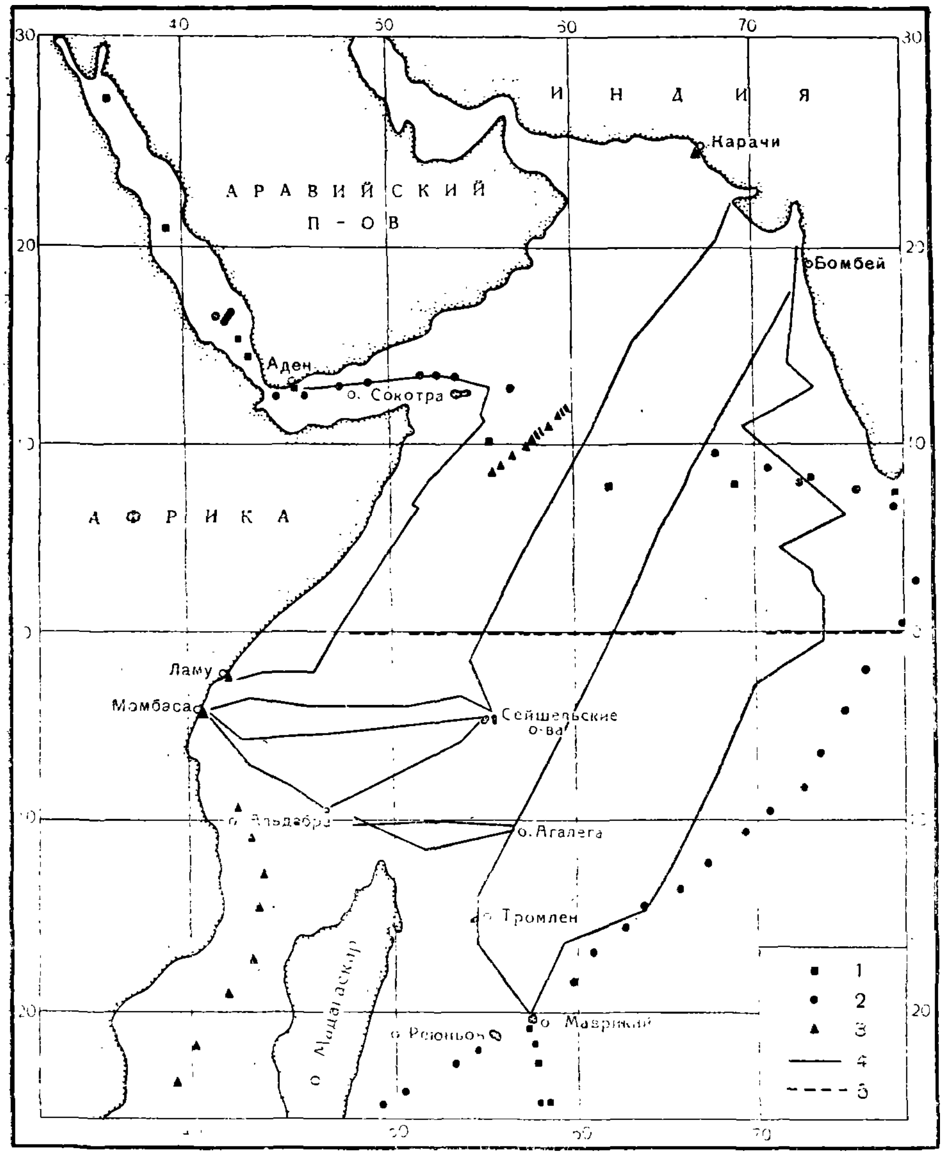

Рис. 1. Схема гравиметрической изученности северо-западной части Индийского океана. Условные обозначения:

1 — маятниковые пункты (Vening-Meinesz 1923—1948); *2* — маятниковые пункты (Girdler and Harrison, 1955); *3* — маятниковые пункты (Talwani, 1959); *4* — маршруты гравиметровой съемки («Owen», 1961—1962); *5* — гравиметровый профиль (Caputo, 1960—1963)

нинг-Мейнеса. Аномалии Буге вычислены с плотностью промежуточного слоя $\sigma_1=2{,}8$ *г/см*^{3} и морской воды $\sigma_2=1{,}03$ *г/см*^{3}. Изоаномалы проведены через 50 *мгл*.

Рассматриваемый район с севера и с запада окаймляется материками Африка и Азия. На востоке эта часть океана ограничивается полуостровом Индостан и далее к югу цепочками островов Мальдивских и Чагос. На юге район ограничен параллелью 25° ю. ш.

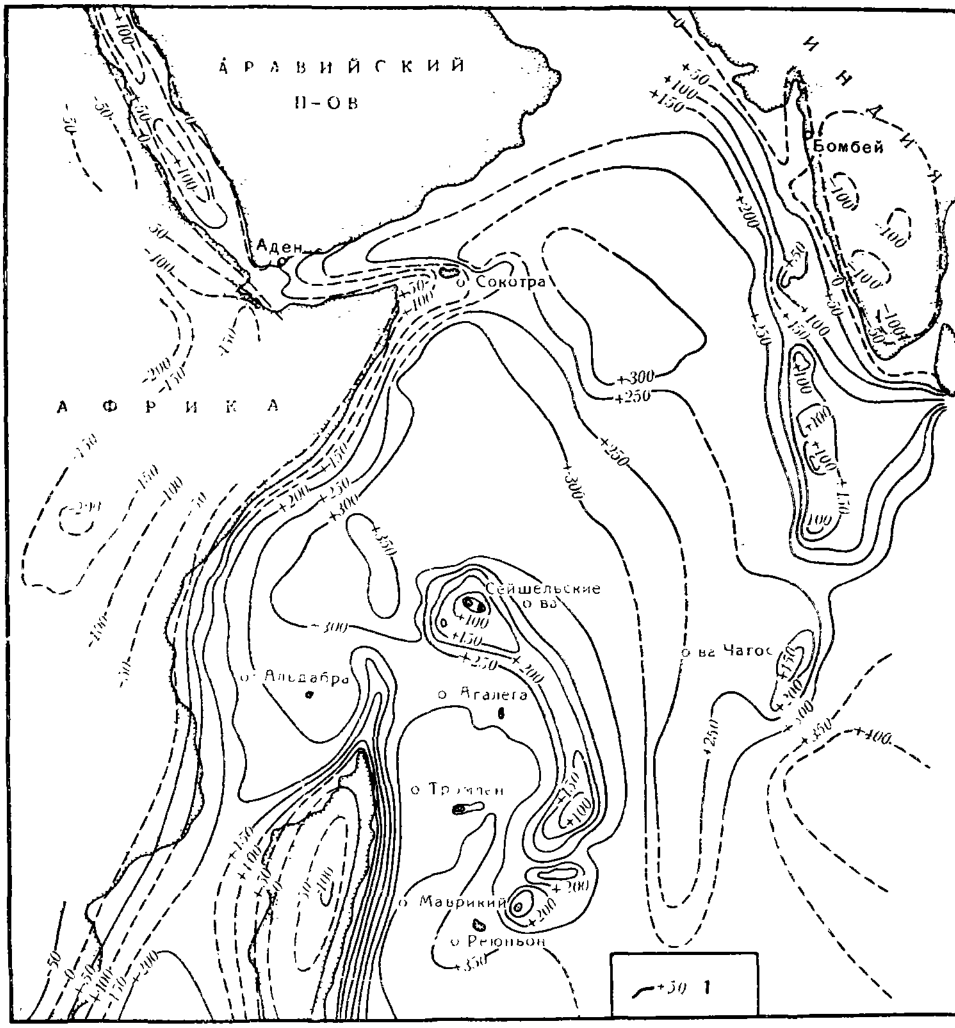

Рис. 2. Схематическая карта аномалий Буге северо-западной части Индийского океана (нормальная формула международная, $\sigma = 2{,}8$ *г/см*^{3}).
Условные обозначения: 1 — изоаномалы, *мгл*

Строение дна северо-западной части Индийского океана определяется системой хребтов, разделяющих ее на ряд котловин [10, 11]. Это Аравийско-Индийский, Мальдивский, Маскаренский, Амирантский хребты, хребет Меррея, хребет Коморских островов, остров Мадагаскар и связанный с ним массив островов Фаркуар. В районе о. Родригес основные хребты соединяются вместе и отсюда уходят в Атлантический и Тихий океаны, составляя единую систему срединных хребтов Мирового океана. Системы хребтов представляют собой, как правило, довольно широкое и очень раздробленное поднятие, подножие которых находится на глубине около 4 *км*. Средняя относительная высота хребтов равна 1500—2000 *м*, но отдельные вершины поднимаются выше, иногда до дневной поверхности, образуя многочисленные коралловые острова: Мальдивские, Чагос, Сейшельские, Коморские и др. Как и для всех срединных океанических хребтов [12], для хребтов Индийского океана характерны глубокие разломы — рифтовые долины. У Аравийско-Индийского хребта этот разлом проходит примерно по его оси; у других хребтов они примыкают с внешней стороны (Амирантский желоб, желоб Чагос и др.).

Подножия хребтов постепенно переходят в менее расчлененное дно океанских котловин с глубинами 4000—5000 *м*. В исследуемом районе — это Аравийская, Сомалийская, Маскаренская, Мадагаскарская, Коморская, Мозамбикская и Центральная котловины. На северо-западе это котловины Аденского залива и Красного моря.

По характеру гравитационных аномалий в северо-западной части Индийского океана можно выделить следующие основные области:

1. Глубокие океанские котловины.
2. Океанические хребты и острова.
3. Переходные зоны от океана к материкам.

Глубоководные океанские впадины характеризуются относительно спокойным полем силы тяжести с отрицательными аномалиями Фая (—30÷—50 *мгл*) и значительными по величине аномалиями Буге (до +350÷+400 *мгл*). Заметной корреляции аномалий Фая с глубиной океанических котловин не наблюдается. Так, для Аравийской котловины со средней глубиной около 4000 *м* аномалии Фая достигают —30÷÷—40 *мгл*, а в области Центральной котловины с глубинами свыше 5000 *м* аномалии Фая также равны —30÷—50 *мгл*. Аномалии же Буге для вышеуказанных котловин отличаются на 80÷100 *мгл*.

Подножия океанических хребтов четко оконтуриваются изоаномалой Буге +250 *мгл*. Это относится ко всем основным хребтам: Аравийско-Индийскому, Мальдивскому и Маскаренскому.

Коралловые атоллы Лаккадивских, Мальдивских островов и архипелага Чагос отмечаются положительными аномалиями Фая (+10÷+15 *мгл*). На карте аномалий Буге эти острова четко прослеживаются уменьшением аномалий до +50÷+100 *мгл*. Сейшельские, Маскаренские, Амирантские острова, Фаркуарский массив, атолл Адду, о. Тромлен характеризуются резко положительными аномалиями Фая (до +100÷+150 *мгл*) и такими же по величине аномалиями Буге.

Группа Маскаренских островов отмечается наиболее интенсивными положительными аномалиями Фая (свыше +200 *мгл*) и значительными аномалиями Буге (+200÷+250 *мгл*).

На островах Мадагаскар и Цейлон по побережью наблюдаются небольшие положительные аномалии Буге (до +50 *мгл*). На о. Мадагаскар изоаномала +50 *мгл* окаймляет остров. В центральной части острова аномалии уменьшаются до —135 *мгл* [13, 14], причем изолинии тянутся параллельно берегу. При переходе от острова к океану с восточной стороны аномалии Буге резко увеличиваются до +350 *мгл*; с западной — этот переход более плавный, где аномалии Буге увеличиваются до +200 *мгл*.

О. Цейлон оконтуривается нулевой изоаномалой Буге. К центру острова аномалии Буге уменьшаются. К югу от острова, в сторону центральной котловины аномалии Буге резко увеличиваются до +300 *мгл* и более [13, 1].

Вблизи всех островов гравитационное поле меняется довольно резко, горизонтальные градиенты достигают 20—30 *этвеш*.

Океанические хребты, как уже отмечалось [1, 6], так же как и острова, выделяются положительными аномалиями Фая (до +30÷

÷+50 *мгл*) на фоне спокойных отрицательных аномалий над котловинами. В окрестностях гребней хребтов наблюдается заметная корреляция топографии дна и аномалий силы тяжести. Сильно раздробленная поверхность срединно-океанических хребтов, состоящая из сочетания небольших хребтов и узких грабенообразных депрессий и желобов характеризуется большой изменчивостью аномалий Фая (рис. 3). В частности, аномалии Фая над самими гребнями хребтов имеют значения +30÷+50 *мгл,* рифтовые долины отмечаются значительными отрицательными (до —50÷—70 *мгл*) аномалиями. Маскаренский хребет отличается чрезвычайно резким изменением аномалий Фая. Вершины хребта со спокойной поверхностью отмечаются значительными положительными аномалиями Фая (до +230 *мгл*). Межгорные впадины с глубинами до 3500 *м* характеризуются значительными отрицательными аномалиями Фая (до —50 *мгл*).

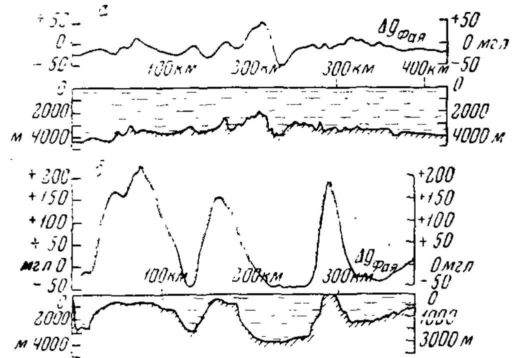

Рис. 3. Профиль аномалий Фая через Аравийско-Индийский (*а*) и Маскаренский (*б*) подводные хребты

В области перехода от Индийского океана к материкам Азии и Африки аномалии Буге значительно уменьшаются. В Мозамбикском проливе положительные аномалии Буге подходят к берегу и сохраняют свой знак и на низменности Мозамбика. Далее к западу на возвышенности аномалии Буге уменьшаются до —50 *мгл.*

В районе Момбасы значительные положительные аномалии Буге резко уменьшаются и далее на запад к озеру Виктория достигают значений —200 *мгл*.

У п-ова Индостан вблизи берега отмечаются небольшие положительные (+50÷+100 *мгл*) и даже отрицательные (до —16 *мгл*) аномалии Буге. Нулевая изоаномала оконтуривает полуостров. К центру Индии аномалии Буге достигают —100 *мгл.*

Красное море характеризуется положительными аномалиями Буге с двумя максимумами (+100 *мгл*) в центре моря. Ось максимумов вытянута вдоль наиболее глубокой средней части моря. На берегах моря отмечаются слабые положительные или отрицательные аномалии (от +40 до —40 *мгл*). При переходе к Африканскому материку отрицательные аномалии Буге уменьшаются до —150÷—200 *мгл* в области Абиссинского нагорья.

Как известно, осредненные гравитационные аномалии в редукции Буге на океанах в основном отображают изменение мощности земной коры. В настоящее время для многих районов земного шара составлены корреляционные графики зависимости между толщиной земной коры и осредненными аномалиями Буге.

При наличии «опорных» мощностей земной коры, полученных глубинными сейсмическими зондированиями (ГСЗ), для океана возможно использование формулы притяжения бесконечного плоскопараллельного слоя [15, 16, 1 и др.]. По этой формуле можно вычислить глубину поверхности Мохоровичича (Мохо) в любой точке, если известна глубина поверхности Мохо в опорной точке и если известны аномалии Буге в этих точках.

Ближайший район, где в настоящее время известна глубина поверхности Мохо, — это Центральная котловина к юго-востоку от островов Чагос, в которой советские геофизики в 1961 г. выполнили профиль методом преломленных волн [17]. Земная кора в этом районе имеет типично океаническое строение (вода, осадки, «базальт»); глубина поверхности Мохо составляет ~11,5 *км*. Используя этот опорный профиль

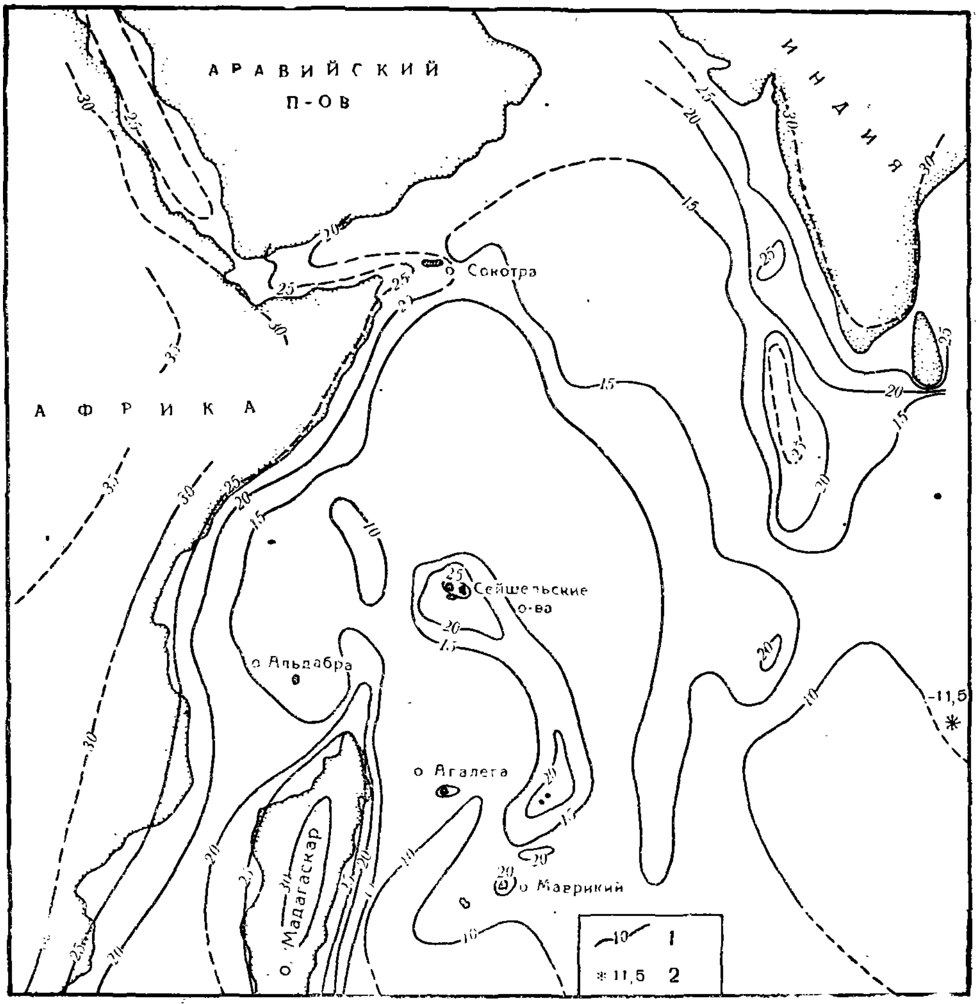

Рис. 4. Схематическая карта глубин поверхности Мохо северо-западной части Индийского океана. Условные обозначения:

1 — изолинии глубин поверхности Мохо (*км*); 2 — глубина Мохо (*км*) по сейсмическим данным.

и карту аномалий Буге, мы рассчитали по формуле плоскопараллельного слоя глубины до поверхности Мохо для всего описываемого района в предположении разности плотностей между корой и верхней мантией, равной 0,5 $г/см^3$. На рис. 4 приведена схема глубин поверхности Мохо, изоглубины проведены через 5 *км*.

Как видно, области океанических котловин имеют сравнительно «тонкую» земную кору. Так, Центральная, Маскаренская, Мадагаскарская и Сомалийская котловины имеют мощность коры 4—6 *км;* Аравийская котловина около 8—10 *км*; Коморская, Мозамбикская котловины, относящиеся к переходной зоне, имеют повышенную мощность коры до 12—15 *км*.

На схеме четко прослеживаются океанические хребты, ограниченные изоглубинами Мохо 15 *км*, где наблюдается, по-видимому, утолщение земной коры до 20 *км* и до 25 *км* на островах этих хребтов. Так Аравийско-Индийский хребет прослеживается от о. Сокотра до о. Родригес. Гребни хребтов характеризуются увеличением мощности коры до 20 *км*.

Маскаренский хребет от Сейшельских до Маскаренских островов также прослеживается изолинией Мохо 15 *км*. На Сейшельских островах и островах Каргадос—Карахос мощность коры увеличивается до 25 *км;* Маскаренские острова отмечаются увеличением толщины коры до 20 *км*. Острова Фаркуар и Альдабра имеют мощность коры более 20 *км*. Мальдивский хребет с его многочисленными островами отмечается повышенной толщиной земной коры. Он весьма четко оконтуривается изолинией Мохо 20 *км*. Мальдивские и Лаккадивские острова характеризуются увеличением мощности коры до 25—27 *км*.

На о. Цейлон мощность коры достигает 25 *км*. О. Мадагаскар отличается значительным утолщением земной коры. Так в центральной высокогорной части острова мощность коры достигает 35 *км*.

В переходных областях от океана к материкам толщина земной коры увеличивается. Так при переходе к Африке в районе Мозамбика и Сомали толщина коры увеличивается до 35 *км*. Е. Буллард по гравиметрическим данным предполагал, что у восточного берега Африки мощность коры примерно равна 30 *км* [18]. В районе п-ова Индостан толщина земной коры увеличивается до 30 *км*.

Впадина Красного моря характеризуется средней толщиной коры около 25 *км*, с уменьшением толщины коры до 20 *км* в центральной, глубоководной ее части. Эти данные подтверждают мнение М. В. Муратова [19], который на основании характера рельефа океанического дна Красного моря и качественного сопоставления аномалий Буге считает, что толщина земной коры в Красном море составляет около 25 *км*. Р. Гирдлер [20] полагает, что мощность (вернее глубина изостатической компенсации) земной коры в Красном море составляет 30 *км*. При переходе к Африканскому высокогорному берегу толщина земной коры увеличивается до 35—40 *км*.

Сопоставление схематической карты глубин поверхности Мохо, составленной нами по гравиметрическим данным с аналогичными схематическими картами, построенными Р. М. Деменицкой [21] и Н. П. Грушинским [22], показывает наличие систематических расхождений между этими тремя картами. Схематическая карта толщины земной коры до поверхности Мохо Индийского океана построена Р. М. Деменицкой по «осредненным графикам» почти исключительно по батиметрическим картам. Наибольшие расхождения с нашей картой, достигающие 10 *км*, наблюдаются в районе Маскаренской котловины и Маскаренского хребта. На карте Р. М. Деменицкой глубина поверхности Мохо в Маскаренской котловине достигает 25 *км*, на нашей карте не более 15 *км*. Схематическая карта толщины земной коры построена Н. П. Грушинским по рельефу, осредненному в пределах трапеций со сторонами, равными 5 экваториальным градусам. При таком осреднении рельефа больших площадей сильно сглаживаются многие примечательные особенности рельефа дна Индийского океана, такие, как Аравийско-Индийский, Маскаренский, Мальдивский подводные хребты. Поэтому на карте Н. П. Грушинского в основном проявляется монотонное уменьшение глубины поверхности Мохо от 35—40 *км* у побережья Африки и Азии до 12—15 *км* в северо-западной части Индийского океана. Расхождения с нашей картой в основном в пределах 5—7 *км*. Такие сравнительно небольшие расхождения вероятно обусловлены тем, что Н. П. Грушинский при составлении схематической карты толщин земной коры по батиметрическим данным использовал коэффициенты линейной связи толщин земной коры с рельефом, полученным не для всей Земли, а для области Тихого, Индийского океанов.

При оценке точности нашей схематической карты глубин поверхности Мохо, построенной по гравиметрическим данным, необходимо оценить хотя бы приближенно порядок систематических и случайных ошибок. Систематические ошибки при определении глубин поверхности Мохо по гравиметрическим данным могут быть обусловлены в основном двумя факторами.

1. Так как мы при расчетах глубин поверхности Мохо по гравиметрическим данным опирались на единственный сейсмический пункт, где граница Мохо определена с погрешностью $\pm 1,5$ *км* [17], то вся наша схема глубин Мохо может быть систематически завышена или занижена в пределах погрешности определения глубины поверхности Мохо сейсмическим методом.

2. Исследования последних лет [23 и др.] показали, что в среднем плотность вещества верхней мантии для всей Земли равна 3,3 *г/см*^{3}. Однако выявляются планетарные плотностные неоднородности в верхней мантии, достигающие 0,1 *г/см*^{3}. Поэтому при неправильном выборе плотности коры и верхней мантии могут в расчетах глубин поверхности Мохо по гравиметрическим данным появиться систематические погрешности. Нами при расчетах принята средняя плотность вещества верхней мантии, равной 3,3 *г/см*^{3}, а средняя плотность коры 2,8 *г/см*^{3}.

Некоторое представление о плотностной неоднородности вещества верхней мантии могут дать карты осредненных аномалий силы тяжести в редукции Фая и графики зависимости аномалий Фая от глубин дна океана. Составленная нами схематическая карта аномалий силы тяжести в редукции Фая для северо-западной части Индийского океана (нормальная формула международная) показывает преобладание на всей рассматриваемой акватории отрицательных аномалий Фая порядка $-30 \div -40$ *мгл*. На карте осредненных аномалий Фая для всей земли, составленной В. М. Каулой, который использовал наиболее полные гравиметрические и спутниковые данные, северо-западная часть Индийского океана характеризуется отрицательными аномалиями Фая -30 *мгл*, в отличие от южной части Индийского океана, для которой наиболее характерны положительные аномалии Фая $+10$ *мгл* [24]. На составленном нами графике (рис. 5) зависимости аномалий Фая от глубин дна северо-западной части Индийского океана достаточно четко проявляется тенденция к преобладанию более отрицательных аномалий Фая для соответствующих интервалов глубин по сравнению с аналогичным графиком, построенным нами для всего Индийского океана [1].

Все эти данные свидетельствуют о том, что плотность вещества верхней мантии в северо-западной части Индийского океана вероятно несколько меньше средней плотности верхней мантии. Некоторое влияние на наблюдаемые отрицательные аномалии Фая северо-западной части Индийского океана может оказать и аномально низкая средняя плотность земной коры. Однако для полного объяснения наблюдаемых отрицательных аномалий Фая необходимо предположить, что плотность земной коры северо-западной части Индийского океана на 0,2 *г/см*^{3} меньше средней плотности земной коры. Однако такое предположение маловероятно, и оно не подтверждается строением земной коры, полученным по сейсмическим данным для отдельных участков северо-западной части Индийского океана [25]. Таким образом, если допустить, что плотность вещества верхней мантии в северо-западной части Индийского океана меньше средней плотности верхней мантии на 0,05 *г/см*³, то наша схематическая карта глубин поверхности Мохо будет содержать систематическую погрешность, достигающую в областях наиболь-

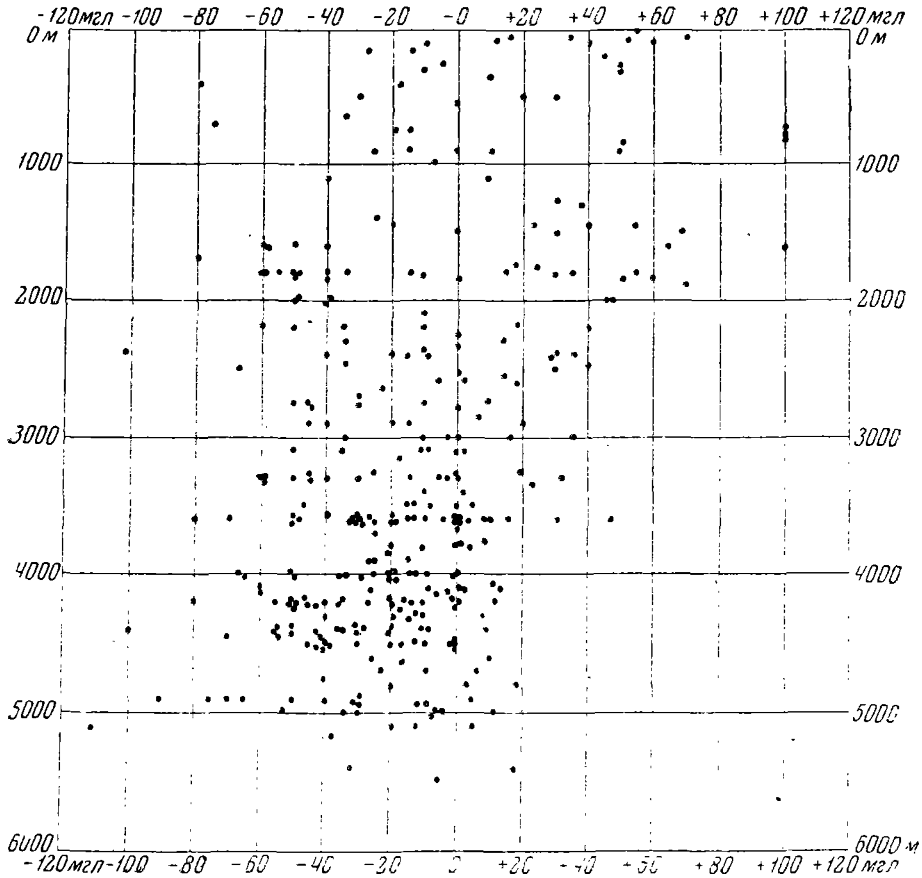

Рис. 5. График зависимости аномалии Фая от глубин дна северо-западной части Индийского океана

ших глубин до 2 *км*. В областях с глубинами поверхности Мохо 10—15 *км*, т. е. на большей части рассматриваемой акватории, систематическая погрешность, обусловленная плотностной неоднородностью верхней мантии, не превышает 1 *км*.

Кроме планетарных плотностных неоднородностей верхней мантии в последние годы в результате комплексной интерпретации детальных гравиметрических и сейсмических данных выявлены региональные, сравнительно узкие, но весьма протяженные плотностные неоднородности верхней мантии, приуроченные к срединным хребтам и переходным зонам от материков к океанам [26, 27 и др.]. Так под срединным Атлантическим и Восточно-Тихоокеанским хребтами обнаружено уменьшение мощности земной коры, однако в этом случае наблюдаемые минимумы аномалий силы тяжести в редукции Буге над хребтами объясняются разуплотнением вещества верхней мантии. Это подтверждается также уменьшением граничной скорости распространения продольных волн на границе Мохо. Не исключено, что и под Аравийско-Индийским, а возможно и под другими подводными хребтами Индийского океана будут выявлены при дальнейших исследованиях менее плотные слои верхней мантии. В этом случае изобаты поверхности Мохо под хребтами на нашей схеме будут примерно соответствовать верхнему пределу глубин разуплотнения вещества верхней мантии. Таким образом, на нашей схеме наименее уверенными являются глубины поверхности Мохо, вычисленные по гравиметрическим данным для подводных хребтов и островов.

Случайная ошибка определения глубин поверхности Мохо по гравиметрическим данным обуславливается ошибками определения аномалий Буге, локальными изменениями мощности и состава осадочных отложений и «базальтового» слоя. В среднем эти влияния редко превосходят ± 2 *км*.

В свете всего вышеизложенного изобаты поверхности Мохо проведены через 5 *км*. Уже после составления нашей схематической карты глубин поверхности Мохо были получены (устное сообщение Ю. П. Непрочнова) предварительные результаты сейсмических определений мощности земной коры в 36-м рейсе э/с «Витязь» в Маскаренской котловине. Мощность земной коры по сейсмическим данным в Маскаренской котловине 10,7 *км*, а на нашей схеме около 12 *км*. Сейсмические исследования Г. Г. Шора и Д. Д. Полларда [25] банок Сейшельской и Сайя де Мала, проведенные в 1962 г., подтвердили наличие под Сейшельской банкой «гранитного» слоя, впервые выявленного в результате сейсмических исследований Т. Гаскеллом и Дж. Своллоу [28]. На банке Сайя де Мала выявлена существенно отличная структура коры без «гранитного» слоя. Верхний слой со скоростями продольных волн от 1,72 *км/сек* до 3,0 *км/сек* предположительно отнесен к коралловым породам, подстилаемым материалом со скоростями продольных волн 4,4—4,5 *км/сек*, типичными для вулканических островов. Эти породы распространяются на глубину примерно до 8 *км* и подстилаются «базальтовым» слоем со скоростью продольных волн 6,8—7,0 *км/сек*. Таким образом, в средней части Маскаренского хребта в районе банки Сайя де Мала мощность коры до «базальтового» слоя по сейсмическим данным не менее 8 *км*, а на нашей схеме мощность земной коры до поверхности Мохо по гравиметрическим данным не менее 15 *км*.

Проведенные к настоящему времени гравиметрические исследования в северо-западной части Индийского океана позволили в общих чертах представить характер гравитационного поля, мощность земной коры, а также общие закономерности изменения толщины земной коры в различных районах этой части океана. В 1964—1965 гг. в 36-м рейсе э/с «Витязь» выполнен значительный комплекс геолого-геофизических работ в северной части Индийского океана. В их число входят сейсмические (методами МОВ и ГСЗ), гравиметрические и гидромагнитные исследования.

Результаты этих работ позволят в дальнейшем провести комплексную интерпретацию всех имеющихся геофизических и геологических данных с целью уточнения глубинного строения земной коры и верхней мантии этого региона. Так результаты предварительной интерпретации сейсмических данных, полученных в 36-м рейсе э/с «Витязь» в рифтовой зоне Аравийско-Индийского хребта, по данным Ю. П. Непрочнова, показывают, что непосредственно под осадочно-вулканогенной толщей, характеризующейся скоростями сейсмических волн порядка 5,0 *км/сек* и мощностью всего 2,0—2,5 *км*, залегают породы, характеризующиеся скоростями 7,0—7,2 *км/сек*. На основании предварительного изучения образцов основных и ультраосновных пород, собранных в 36-м рейсе э/с «Витязь» со склонов рифтовых ущелий трех ветвей Срединно-Индоокеанского хребта: Аравийско-Индийского, Западно-Индийского и Центрально-Индийского хребтов, и анализа имеющихся геофизических данных (сейсмических, магнитных и измерений теплового потока) по Срединно-Индоокеанскому хребту Г. Б. Удинцев и В. И. Чернышева высказывают предположение, что эти породы являются малоизмененными породами верхней мантии Земли[1]. Предполагается, что образование Срединно-Индоокеанского хребта обусловлено сводовым поднятием верхней мантии. Ведущими процессами формирования коры в этой зоне являются серпентинизация вещества верхней мантии, растяжение и разрывы на поверхности.

Вещество верхней мантии под Срединно-океаническими хребтами находится в условиях пониженного давления, относительно высоких температур и подвергается серпентинизации и динамометаморфизму. Все это, естественно, приводит и к соответствующим изменениям физических свойств вещества верхней мантии, в частности к уменьшению плотности и граничной скорости продольных сейсмических волн. Поэтому Срединно-океанические хребты отражаются значительным уменьшением аномалий силы тяжести в редукции Буге и, вероятно, более обосновано интерпретировать эти аномалии не увеличением мощности земной коры, а разуплотнением вещества верхней мантии под Срединно-океаническими хребтами.

ЛИТЕРАТУРА

1. Строев П. А., Гайнанов А. Г. О строении земной коры Индийского океана по данным геофизических исследований. «Океанология», **5**, вып. 4, 1965.
2. Строев П. А., Ушаков С. А., Фролов А. И. Земная кора краевой зоны Антарктиды. М., «Наука» (в печати).
3. Венинг-Мейнес Ф. А. Гравиметрические наблюдения на море. М., Геодезиздат, 1940.
4. Vening-Meines F. A. Gravity expeditions 1948—1958, with a preface Publ. «Netherl. geod. Commis.», No. 5, 1960.
5. Girdler R. W., Harrison I. C. Submarine gravity measurements in the Atlantic Ocean, Indian Ocean, Red Sea and Meditterranean Sea of 1955. «Proc. Roy. Soc.», Ser. A, No. 1217, 239, 1957.
6. Talwani M. Gravity measurements on H. M. S. «Acheron» in South Atlantic and Indian Oceans. «Bull. Geol. Soc. Amer.», **73**, No. 9, 1962.
7. Bathymetric, Magnetic and Gravity investigations H. M. S. «Owen», 1961—1962 Part I.— Text, Part 2 — Profiles. London. Hydrographic Department, Admiralty Marine science publication, No. 4, 1963.
8. Caputo M. The minimum strength of the Earth. «Journ Geophys. Res.», **70**, No. 4, 1965.
9. Morelli C. Gravity measurements on surface ships. La petrole et la mer., n°2. Paris, 1965.
10. Белоусов И. М. Батиметрическая карта северо-западной части Индийского океана. В сб.: «Океанологические исследования» № 13, М., «Наука», 1965.
11. Канаев В. Ф., Марова И. А. Батиметрическая карта северной части Индийского океана. В сб.: «Океанологические исследования», № 13, М., «Наука», 1965.
12. Шейнманн Ю. М. Об одной особенности срединных океанических хребтов. «Геотектоника», № 4, 1965.
13. Гурарий Г. З., Соловьева И. А. Строение земной коры по геофизическим данным. М., Изд-во АН СССР, 1963.
14. Кропоткин П. Н., Люстих Е. Н., Повало-Швейковская Н. Н. Аномалии силы тяжести на материках и океанах и их значение для геотектоники. Изд-во МГУ, 1958.

---

[1] Удинцев Г. Б., Чернышева В. И. Образцы пород верхней мантии земли из рифтовой зоны Индийского океана. ДАН СССР, 1965, т. 165, № 5.

15. Гайнанов А. Г., Строев П. А. Некоторые особенности гравитационного поля и строение земной коры Атлантического, Индийского и Тихого океанов. В сб.: «Геофизические исследования», вып. 2. Изд-во МГУ, 1966.
16. Корякин Е. Д. О глубинном строении земной коры в области Атлантического океана. «Изв. АН СССР», сер. геофиз., № 12, 1958.
17. Непрочнов Ю. П. Новые данные о строении земной коры под дном Индийского океана. ДАН СССР, **144**, № 2, 1962.
18. Bullard E. C. Gravity measurements in East Africa. «Phil. Trans. Roy. Soc.», **235**, Ser **A**., No. 757, 1936.
19. Муратов М. В. Проблема происхождения океанических впадин. «Бюлл. МОИП», отд. геол., **32**, вып. 5, 1957.
20. Girdler R. W. The relationship of the Red Sea to the East African rift sistem. «Quart. Journ. Geol. Soc.», London, **114**, part I, 1958.
21. Деменицкая Р. М. Основные черты строения коры земли по геофизическим данным. М., Гостоптехиздат, 1961.
22. Грушинский Н. П., Бурова Н. Г., Тарбеева М. И. Построение схематической карты толщин земной коры по рельефу и аномалиям Буге. «Вестн. Моск. ун-та», сер. физика и астрономия, № 5, 1964.
23. Гайнанов А. Г. Плотностная неоднородность верхней мантии. «Изв. АН СССР», сер. физика Земли, № 10, 1966.
24. Артемьев М. Е. Осредненные аномалии Фая — источник информации о неоднородностях в мантии. «Бюлл. МОИП», отд. геол., **10** (5), 1965.
25. Shor G. G., Pollard D. D. Seismic investigations of Seychelles and Saya de Malha Banks, northwest Indian Ocean. Science, **142**, No. 3588, 1963.
26. Гайнанов А. Г. О некоторых особенностях строения земной коры переходных зон Тихого океана по геофизическим данным. В сб.: «Геофизические исследования», вып. I. Изд-во МГУ, 1964.
27. Talwani M., Pichon X. L., Ewing M. Crustal Structure of the Mid-Ocean Ridges. «Journ. Geoph. Res», **70**, No. 2, 1965.
28. Gaskell T. F., Hill M., Swallow I. Seismic measurements made By H. M. S. «Challenger» in the Atlantic, Pacific and Indian oceans and Mediterranean sea 1950—1953. «Phil. Trans. Roy. Soc.», Ser. **A**., No. 988, 251, 1958.

Reprinted from *Bull. natn. Inst. Sci. India*, no. 38, 1968, p. 411-420

SIZE DISTRIBUTION AND CARBONATE CONTENT OF THE SEDIMENTS OF THE WESTERN SHELF OF INDIA

by R.R. NAIR *and* ABRAHAM PYLEE

Physical Oceanography Division,
National Institute of Oceanography, Ernakulam

Sediment samples collected during the 25th cruise of I.N.S. KISTNA (Indian Programme of I. I. O. E.) were analysed for grain size and carbonate content. The shelf sediments show well defined zonation, except where river-borne sediments tend to mask this zonation, as off Bombay, and the zones have been classified into two categories. (1) The innershelf, up to a depth of 20 fms is characterised by high rates of sedimentation and composed of recently deposited silts and clay with low carbonate values (<20%). (2) The outershelf (approximately 20 to 70 fms) is a zone of relict sediments, having relatively low rates of sedimentation and composed of fine to medium sands. Occasional patches of coarse iron stained sands and pebbles are also present. The carbonate content in this zone is high (30 to 80%) being contributed largely by molluscs with minor amounts due to foraminifera and other organisms. At slope depths (>70 fms), the outer shelf sands grade into foraminiferal sands.

INTRODUCTION

One of the cruises, the XXVth, carried out by I.N.S. KISTNA as part of the Indian Programme of the International Indian Ocean Expedition, covered the western shelf of India. The traverses were run normal to the coast and generally start five to ten miles offshore, and continue into slope depths. The grain size and calcium carbonate content of the bottom samples collected during this cruise forms the subject of this paper. Samples were collected by Phleger Gravity Corer with a one-metre unlined barrel as well as by a LaFond-Dietz Snapper. Core samples, after extrusion from the barrel, were logged for colour, odour, grain size, shell content etc. and later wrapped in polythene sheets and stored in wooden boxes.

Excepting for stray traverses of ships participating in the I.I.O.E., no systematic survey of the western Indian shelf has hitherto been carried out. Such published literature as are present deal with limited portions of the shelf, as off Bombay (Stewart *et al.* 1964).

LABORATORY PROCEDURE AND PRESENTATION OF DATA

Samples for analysis were taken from the top few centimetres of the core and random samples were obtained from snapper samples after thorough mixing. After separation of the samples into sand fraction ($>62.5\mu$) and silt-clay fraction, the former were sieved and the latter subjected to pipette analysis according to the methods of Krumbein and Pettijohn (1938). From the data, cumulative frequency curveswere plotted and standard statistical parameters such as median (Mdϕ), sigma phi ($\sigma\phi$) were computed according to the method of Inman (1952).

These parameters as well as sand, silt, clay percentages and the bottom notations from Admiralty Charts were incorporated in the preparation of a generalised sediment distribution map of the western shelf of India.

Calcium Carbonate in the sediments was determined by the method of Herrin *et al.* (1958). Determinations were made for the whole sample as well as for the silt-clay fraction in order to determine their relationship to the grain size of the sediments. Values for the Calcium Carbonate are plotted as histograms and presented against station locations in order to facilitate interpretation. A plot of the carbonate *vs.* depth of water also helps to bring out the trend in the offshore direction.

Physiography and Shoreline Development of the West Coast

The West Coast of India is bordered by the Western Ghats, composed largely of horizontally bedded Creto-Eocene basalts rising to heights of 6,000 ft. Precipitation in the Ghats averages hundred inches per annum and temperatures around 35°C. The combined effect of the high relief with low physiographic maturity and precipitation though seasonal but heavy, results in short seasonally flooding streams with a maximum discharge during the monsoon. Superposed on the sediments brought by these transitory rivers, is the effect of the relatively perennial rivers like the Indus debouching at the head of the Arabian Sea and the Narbada and Tapti flowing into the Gulf of Cambay.

The southward extension of the Ghats into Kerala are geologically older and lithologically different. These ranges are composed of Archean granites, charnockites and Khondalites which have attained a greater degree of physiographic maturity. The rivers draining these ranges have longer courses and debouch, with few exceptions, into inland lakes and lagoons, having flowed over a terrain of successively igneous rocks, laterites and coastal plain deposits.

The present shoreline of the west coast is one of submergence. Excepting for diastropism associated with the faulting of the west coast in the Late Tertiary (Wadia 1953; Krishnan 1960) no earth movements of a major nature have occurred in peninsular India. Therefore the submergence may be attributed to a rise in sea level against a static shoreline. Evidences of submergence are present in the form of shallow embayments along the entire length of the coast, particularly well developed along the Kerala coast, and the presence of a bordering sea floor with a gentle slope. Subsequent modification by wave action and deposition gave rise to the present configuration.

Sediments

Sedimentary and Carbonate data (Table I) for each traverse named after the major port off which they were run, are discussed below:

Bombay Section.—The traverse starts 10 miles offshore at a depth of 13 fathoms and goes up to 110 miles to a depth 250 fathoms. The continental shelf reaches its

TABLE 1

Station No.	Depth (Fms)	Location	Mdϕ	Sigmaϕ	Sand/Silt/Clay%	$CaCo_3$ % (Total Sample)	$CaCo_3$ % (Silt-Clay Fraction)
638	13	N. Lat. 18° 06.4′ E. Long. 72° 48.0′	8.0	3.0	4.0/30.0/66.0	10.0%	2.5%
639	17	N. Lat. 18° 03.0′ E. Long. 72° 43.0′	5.0	2.7	49.0/31.0/20.0	46.5	41.5
640	19	N. Lat. 18° 01.5′ E. Long. 72° 37.6′	5.0	2.7	26.6/8.6/64.8	45.0	35.0
641	19	N. Lat. 17° 57.9′ E. Long. 72° 18.1′	9.0	2.9	1.0/10-0/89.0	42.0	22.5
642	26	N. Lat. 17° 53.9′ E. Long. 72° 18.1′	8.0	2.9	1.9/34.3/63.8	31.0	20.0
643	38	N. Lat. 19° 46.4′ E. Long. 72° 00.0′	1.5	2.4	4.9/16.6/78.5	32.5	32.0
645	250	N. Lat. 17° 46.4′ E. Long. 72° 00.0′	6.9	2.5	9.0/70.0/21.0	32.0	30.00
650	108	N. Lat. 14° 22. 5′ E. Long. 73° 15.0′	4.0	2.1	48.0/30.0/21.0	56.0	50.1
651	66	N. Lat. 14° 28.0′ E. Long. 73° 24.2′	3.1	2.2	72.7/17.0/10.3	51.0	00.0
652	42	N. Lat. 14° 30.5′ E. Long. 73° 43.8′	2.9	2.4	75.6/13.3/10.1	47.0	42.0
653	32	N. Lat. 10° 33.0′ E. Long. 73° 43.8′	0.25	0.9	97.6/2.4/0.0.	33.0	0.0
654	25	N. Lat. 14° 35.2′ E. Long. 73° 53.5′	2.0	2.2	91.0/13.0/5.0	43.0	0.0
655	12	E. Lat. 14° 47.5′ E. Long. 73° 59.8′	7.0	2.8	8.3/60.6/31.1	6.0	1.5
656	10	N. Lat. 14° 40.3′ E. Long. 74° 9.2′	5.3	2.4	9.4/75.6/15.0	3.5	0.0
657	10	N. Lat. 12° 49.0′ E. Long. 74° 45.8′	5.8	2.9	3.2/63.4/33.0	7.0	4.0
658	17	N. Lat. 12° 46.7′ E. Long. 74° 41.0′	5.0	2.2	7.6/80.1/12.3	13.0	7.0
659	23	N. Lat. 12° 43.5′ E. Long. 74° 41.2′	2.9	1.9	51.0/35.0/14.0	28.0	24.0
660	43	N. Lat. 12° 35.5′ E. Long. 74° 21.0′	—	—	—	—	—
661	105	N. Lat. 12° 35.0′ E. Long. 74° 16.5′	3.1	1.6	75.0/19.0/6.0	57.0	28.5
666	46	N. Lat. 10° 13.5′ E. Long. 75° 39.0′	3.0	1.9	70.0/20.0/10.0	23.0	3.8
667	32	N. Lat. 10° 14.5′ E. Long. 75° 43.7′	3.1	1.5	69.6/22.5/7.0	21.5	19.0
668	23	N. Lat. 10° 15.4′ E. Long. 75° 49.1′	3.6	4.0	63.3/22.5/14.2	30.0	12.0
669	17	N. Lat. 10° 16.2′ E. Long. 75° 53.8′	2.8	1.5	81.0/18.0/1.0	10.0	17.0
670	13	N. Lat. 10° 17.1′ E. Long. 75° 58.3′	2.0	1.1	99.0/01.0/0.0	0.0	0.0
671	14	N. Lat. 10° 17.0′ E. Long. 76° 0.0′	3.5	2.4	1.9/97.0/1.1	2.0	0.0
672	10	N. Lat. 9° 20.7′ E. Long. 70° 16.6′	6.8	3.7	14.2/42.0/42.6	1.5	0.0
673	9	N. Lat. 9° 21.5′ E. Long. 76° 18.5′	7.4	4.0	3.6/60.4/35.6	2.0	2.0
674	20	N. Lat. 9° 18.6′ E. Long. 76° 11.5′	3.0	1.9	62.0/20.0/18.0	19.0	0.0
675	27	N. Lat. 9° 16.8′ E. Long. 76° 06.6′	2.1	1.7	89.0/10.0/1.0	16.2	16.0
676	29	N. Lat. 9° 14.9′ E. Long. 76° 02.2′	1.2	1.1	96.4/4.0/0.0	24.5	24.0
677	85	N. Lat. 9° 11.0′ E. Long. 75° 54.25′	2.4	1.3	74.0/20.0/6.0	31.5	24.0
678	250	N. Lat. 9° 07.6′ E. Long. 75° 45.0′	3.8	1.2	52.0/47.0/1.0	54.5	1.0
679	370	N. Lat. 9° 03.5′ E. Long. 75° 35.5′	2.7	0.9	90.0/6.0/4.0	59.5	31.5

maximum width in this region being about 100 miles wide. The inner shelf sediments are greenish black in colour changing to greyish green on the outer shelf. The median grain size (Mdϕ) remains uniform throughout the section, ranging between 7ϕ to 8ϕ thus falling in the coarse clay group. Stray patches of fine to medium sand are, however, also met with.

Calcium Carbonate ranges from 10% nearshore to about 45% offshore, though no systematic trend with grain size or depth of water is present.

Karwar Section.—The traverse starts at a distance of 4 miles from coast and continues to 60 miles at a depth of 110 fathoms. Relatively fine grain sediments are found nearshore, comprising largely of poorly sorted fine silt with median diameter around 6ϕ. Further offshore from a depth of 25 fathoms to 110 fathoms the grain size becomes coarser giving rise to moderately sorted sand, with median from 2ϕ to 3ϕ. An intermediate zone, at a depth of 30 fathoms with coarse (0.25ϕ) iron stained sand intermixed with shells of scaphopods, gastropods, pelecypods and foraminifera is found. In the same area, but at a shallower depth (25 fathoms) are found angular pebbles of laterite, basalt and silicified wood fragments. The true nature of these pebbles, which are masked by coatings of lime-mud, was brought out only upon treating the pebbles in sulphuric acid to remove the carbonate layer.

Calcium Carbonate increases offshore, with a nearshore value of 6% associated with the silts and clays and offshore value in excess of 50% associated with sands, the carbonate in the latter being due to mollusc shells. An exceptional feature off Karwar was the finding at two stations, 650 (110 fathoms) and 651 (66 fathoms), of cores which, excepting for about 10 centimetres of the top of the core, which was clayey, was entirely composed of fine grained carbonate with few recognisable shell fragments. Both of these cores yielded carbonate values in excess of 75%.

Mangalore Section.—The traverse starts 4 miles offshore at a depth of 10 fathoms and stops at 60 miles at a depth of 105 fathoms. Inner shelf sediments are greenish black in colour, poorly sorted and have medians between 5.3ϕ to 5.8ϕ. Proceeding outwards into the outer shelf, sediments become coarser (Mdϕ2.9-3.1) with abundant shells. Calcium carbonate ranges from 0% nearshore to 57% in the outer shelf, the latter values resulting from shells of various molluscs as well as tests of foraminifera which predominate in the slope region.

Cochin Section.—The traverse starts 8 miles from shore at a depth of 14 fathoms and continues to a depth of 45 fathoms, at a distance of 60 miles. This particular section is located off the mouth of one of the major rivers, the Periyar, in Kerala State. It is in this region that the continental shelf reaches its minimum width, being less than 30 miles. Throughout the length of the section ,the median grain size remains remarkably uniform, with medians between 2ϕ to 3.5ϕ. Sorting is good with the coarser sands being better sorted than the finer ones. It may be emphasised here that the section covers only the outer shelf, thus leaving a blank from the shore to a distance of about 8 miles offshore. However, samples collected during the course of other surveys which covered this region, testify to the presence in the inner shelf of the usual greenish black poorly sorted silty clays.

The calcium carbonate values along this section have the smallest range, from 0% nearshore to a maximum of only 23% offshore. The relatively low values of calcium carbonate in these sediments may be accounted for by the greater dilution of the shelf sediments by river-borne material particularly, Periyar and its tributaries.

Alleppey Section.—The traverse starts at a distance of 3½ miles offshore at a depth of 10 fathoms and continues to a depth of 370 fathoms. Brownish green

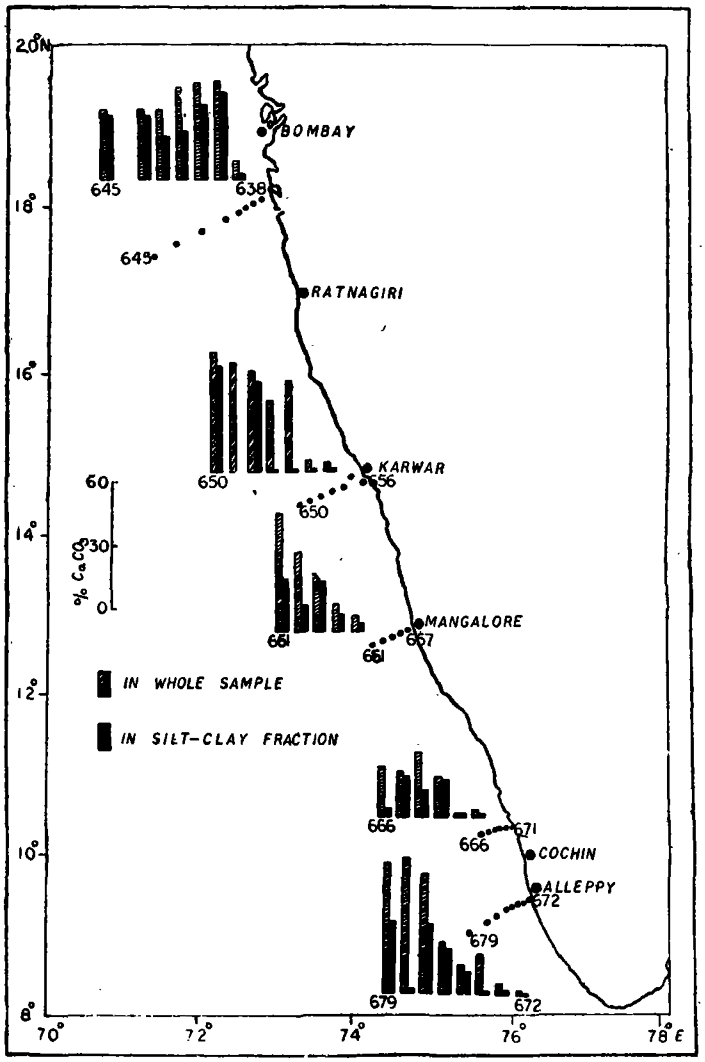

FIG. 1. Station location and distribution of calcium carbonate in whole sample and silt-clay fraction of the bottom sediments.

to greenish black, poorly sorted silts and clays are found in the inner shelf. Carbonate content is low (1-2%) both in the total sample as well as in the silt clay fraction. Seaward from 20 fathoms the silts and clays grade into moderately well sorted fine and medium sands with abundant shell fragments. Clay sized material of these sands range from 1% to 6%. This distribution changes at slope depths to greenish sands, the constituents of which are largely tests of foraminifera.

Discussion

A generalised picture of the sedimentary zonation may be obtained (Fig. 2) from the results of the five traverses shown in Fig. 1. The inner shelf, up to a depth of 20 fathoms, is floored with greenish black poorly sorted silty-clays. Northwards, the silt-clay zone is found to extend to depths of 70 fathoms. These sediments are largely terrigenous, being deposited on the shelf by the present day rivers of the West Coast of India. Seaward of this zone of silty-clays, starts the zone of fine and medium sands generally exhibiting better sorting and moderate amounts of clay size material. Succeeding those sands are the foraminiferal sands and silts at the edge of the continental shelf. In places, as off Karwar, patches of what are apparently relict iron-stained, coarse sand and shells associated with angular basalt, laterite pebbles and silicified wood are found. The sharp contrast of the inner and outer shelf sediments reflects the differences in origin of the two. The former, as mentioned earlier, are terrigenous whilst the latter seem to be relict. An obvious conclusion resulting from their exposure at the present time is the implication that little or no sedimentation takes place. Further more the close association of silicified wood, basalt and laterite pebbles, which are beyond doubt the products of subaerial weathering, lend further support to the fact that the outer shelf sediments correspond to a once lowered sea level, which probably stood at a depth of 30 fathoms below the present. The presence of bottom currents of sufficient strength to winnow the fines from these sediments is not precluded. Rao (1959) has put forth a similar depth for the Pleistocene low stands on the east coast on the basis of the presence of oolites and shallow water foraminifera.

The areal distribution of carbonate in the sediments is shown in Fig. 1 and its distribution with depth of water is shown in Fig. 3. The principal sources of carbonate in marine sediments are, (a) residual (resulting from weathering of limestone rock on the sea floor), (b) authigenic (resulting from inorganic chemical precipitation), (c) terrestrial (resulting from river and wind transport) and (d) biogeneous (accumulations of the skeletal parts of marine animals and plants). The first of these (a) is quantitatively unimportant whereas the greater part of the marine carbonates result from one or more of the latter (b), (c), (d) sources. Instances of chemically precipitated carbonates are such as those of Florida (Ginsburg 1963), precipitated as well as wind and river-borne carbonates of the Persian Gulf (Pilkey 1966). As for the biogeneous carbonates, these form the bulk of the carbonates in recent marine sediments and a vast amount of literature exists pertaining to such studies. Attempts have also been made to correlate the carbonate content of the sediments to the productivity of the overlying waters (Arrhenius 1963). The latter work, however, was carried out in the pelagic regions of the Equatorial Pacific. Correlations of this nature for shelf sediments are hampered by the very low "signal to noise" ratio of regions close to land.

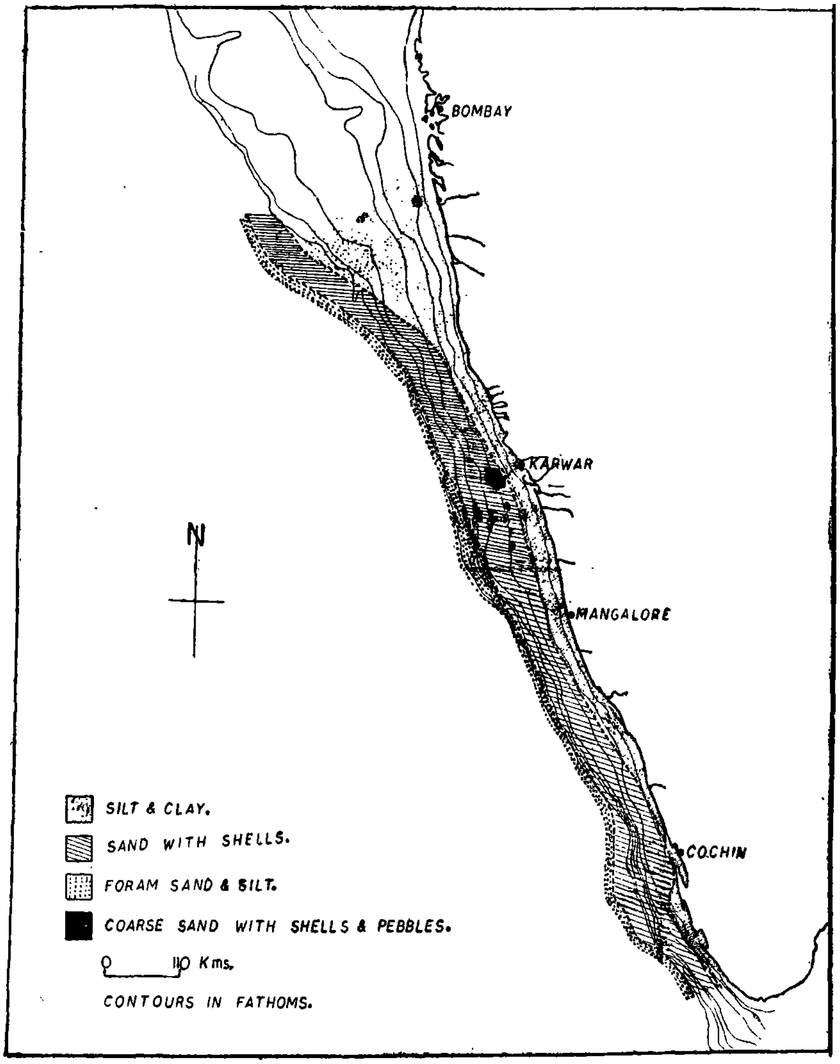

FIG. 2. Map showing distribution of surface sediments of the western shelf of India.

The carbonate content of the sediments under study seem to be mostly biogenic in origin. The carbonate content for the whole sample as well as for the silt clay fraction increases offshore. In view of the fact that in most of the samples there

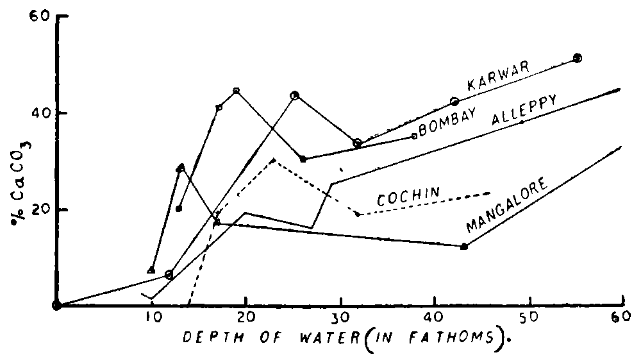

FIG. 3. Variation of carbonate content with depth of water.

is a sympathetic variation in the carbonate content of the two fractions, it is concluded that microscopic foraminiferal tests and oolites form a substantial source of carbonate. In the outer shelf, however, shells of molluscs and numerous other organisms are the predominant source. The carbonate content is thus related to grain size, being greater in the coarser grained sediments. A plot of carbonate abundance *vs.* depth (Fig. 3) brings out a well defined peak as well as a progressive increase beyond the shelf edge. The peak corresponds to the outer shelf sands with their abundant shells whereas the increase further seaward reflects the progressive preponderance of foraminiferal off tests over the other organisms. Carbonate content shows low value, as off Cochin, principally due to greater dilution of the sediments brought in by the rivers. Relating carbonate content to productivity in the overlying waters is not possible in the present study as there is little or no quantitative data regarding productivity in this region. Low rates of sedimentation in the outer shelf is also indicated by the essentially pure carbonate cores in which clastic material is conspicuous by their absence.

A preliminary examination of the constituents of the coarse fraction of cores from depths greater than 30 fathoms has brought out the presence of what are considered shallow water foraminifera. Most commonly found benthonic forms are *Amphistegina, Quiqneloculina, Robulus, Elphidium, Rotalia, Spiroloculina, Bolivina, Textularia Uvigerina.* It was also noted that samples containing abundance of shallow-water foraminifera were also associated with oolites. The latter varied from pale brown to black in color and were abundant in the finer fractions. According to Newell *et al.* (1960), the "optimum depth of formation may be around 6 feet". Thus the presence of shallow water foraminifera along with oolites on the outer shelf (depth 30 fathoms) is further proof of former low stands of sea-level on the West Coast of India.

CONCLUSIONS

(1) The continental shelf off the West Coast of India has a maximum width 100 miles, in the north (off Bombay), tapers to its narrowest point off

Cranganore (Kerala) with a width of 30 miles and again widens southward, however, not as much as in the north. Throughout the shelf is characterised by very low gradients (0.30').

(2) The inner shelf sediments are terrigenous greenish black silts and clays high in organic matter and low in carbonate, the latter being contributed by microscopic foraminifera and cocoliths.

(3) The outer shelf sediments are largely fine and medium sands with abundant molluscan shells. These sediments are at places interspersed with very coarse iron stained sands and shells, laterite and basalt pebbles with occasional fragments of silicified wood. The outer shelf sediments are relics of the past, corresponding to a once lowered sea level.

(4) Shelf edge sediments are wholly or largely composed of foraminiferal tests.

(5) Calcium carbonate increases with depth of water and is related to grain size of the sediments, being higher in the coarse grained sediments. Exceptionally high values of carbonate occur at the shelf edge, which probably are lag deposits.

(6) Absence of fine sediments on the outer shelf may also be taken as an indiaction of the presence of bottom currents.

(7) More detailed work is needed to clarify some of the doubts arising from the present work, viz., closely spaced sampling stations to bring out the extent and distribution of the relict sediments, continuous echo sounding to bring out the presence of submarine platforms and similar topographic features.

ACKNOWLEDGEMENT

We wish to thank Dr. N.K. Panikkar, Director, National Institute of Oceanography, for his interest and help during the course of this study. We are indebted to Dr. V.V.R. Varadachari, for several helpful suggestions and to Mr. P.S.N. Murty, who collected some of the samples. The co-operation of the Captain and crews of I.N.S. KISTNA is gratefully acknowledged.

REFERENCES

Arrthenius, G. (1963). Pelagic Sediments, in : *The Seas—Ideas and Observations*, (Ed. M. N. Hill Inter-science Publishers, **3**, 655-727.

Ginsburg, R. N. (1963). Shallow water carbonate sediments, in: *The Seas—Ideas and Observations*, (Ed. M. N. Hill), Inter-science Publishers, **3**, 554-571.

Herrin, E., Higka, H. S., and Robertson (1958). Rapid volumetric analysis for carbonate rocks. *Fld lab*, **26**, 139-144.

Inman, D. L. (1952). Measures for describing size distribution of sediments. *J. Sedim. Petrol.*, **22**, 125-145.

Krishnan, M. S. (1960). Geology of India and Burma, Higginbothams, Madras.

Krumbein, W. C., and Pettijohn, F. J. (1958). Manual of Sedimentary Petrology. Appleton-Centuary Crofts, New York.

Newell, N.D., Purdy, E.G., and Imbrie, J. (1960). Bahamian oolitic sands. *J. Geol.*, **68**, 481-497.
Pilkey, O.H., and Noble, D. H. (1966). Carbonate and clay mineralogy of the Persian Gulf. *Deep Sea Res.*, **13**, 1-16.
Rao, M. P., and Mahadevan, C. (1959). Studies in Marine Geology of the Bay of Bengal along the east coast of India, abstracts in the pre-prints. International Oceanographic Congress, American Association for the Advancement of Science, Washington D. C., 655-656.
Stewart, R. H., Pilkey, O. H., and Nelson, B. C. (1965). Sediments of the Northern Arabian Sea. *Mar. Geol.*, **3**, 411-427.
Wadia, D. N. (1953). Geology of India, MacMillan, London, 531.

Reprinted from *Deep Sea Res.*, vol. 16, 1969, p. 655-660

SHORTER CONTRIBUTION

Trincomalee and associated canyons, Ceylon

SAM A. BUSH* and PATRICIA A. BUSH*

(*Received* 25 *March* 1969)

Abstract—Trincomalee and associated canyons conform to Ceylon's geological structure. Trincomalee Canyon crosses the insular shelf and slope with a general northeast trend similar to the strike of charnockite–khondalite series found on the island. Deviations in the canyon's strike result from joint planes and tectonic deformation. Two secondary canyons which also trend northeast align with north and south contact zones of Wanni gneisses and charnockite–khondalites.

INTRODUCTION

AS PART of the 1964 International Indian Ocean Expedition, the USC & GSS *Pioneer* conducted a detailed bathymetric and geophysical survey over Trincomalee and two associated canyons (Fig. 1).

Trincomalee Canyon was first noted in 1908 when Somerville discussed several deep and narrow notches in the submarine plateau off the east coast of Ceylon (ADAMS, 1929a). SHEPARD (1963) published an inshore bathymetric map and described a branching, rock-walled canyon with heads in Trincomalee Harbor and Koddiyar Bay. Data collected by the *Pioneer* in 1964 were used by SHEPARD and DILL (1966) to expand Shepard's earlier compilation.

GEOLOGY

Rocks of the Koddiyar Bay area (Fig. 2) consist of biotite gneiss basement rock overlain by charnockite–khondalite series and Wanni gneisses. Khondalites are metamorphic rocks that have been intruded by charnockites. The younger Wanni gneisses outcrop both northwest and southeast of the charnockite–khondalite series. ADAMS (1929a, b) and COATES (1935) place the Wanni gneiss and charnockite–khondalite ages as Early Precambrian. AFANASSYEV, BORISOVICH and SHANIN (1964) reported K–Ar whole rock ages approximating 800 million years for charnockites on Ceylon, but ASWATHANARAYANA (1968) substantiates the Early Precambrian. Using Rb–Sr methods, he dates one group of charnockites as older than 2100 million years and mentions a younger group (1660 $\pm$ 250 million years).

In the vicinity of Koddiyar Bay, Wanni gneiss and charnockite–khondalite formations strike northeast with strong evidence of folding. According to COATES (1935) a road between the towns of Nilaveli and Trincomalee crosses the strike of two charnockite–khondalite ridges. The first ridge, 6 km wide, lies just south of Nilaveli, and the second, 1 km wide, lies immediately north of Trincomalee. At these two localities the dips are nearly vertical, but decrease southeast of Trincomalee until a northwest–southeast anticlinal arch can be seen at Dutch Point (Fig. 2). Southeast of Dutch Point the dip returns to nearly vertical (COATES, 1935).

Reversal in dip and outcropping of younger Wanni gneisses on northwest and southeast sides of the charnockite–khondalite series indicates the existence of a northeast trending synclinal fold with its axis in Koddiyar Bay.

BATHYMETRY

Within the area of this investigation the dominant feature is northeast trending Trincomalee Canyon (Figs. 2 and 3). Two of its principal heads are located in Koddiyar Bay and a third in

*Environmental Science Services Administration, Atlantic Oceanographic Laboratories, Miami, Florida 33130.

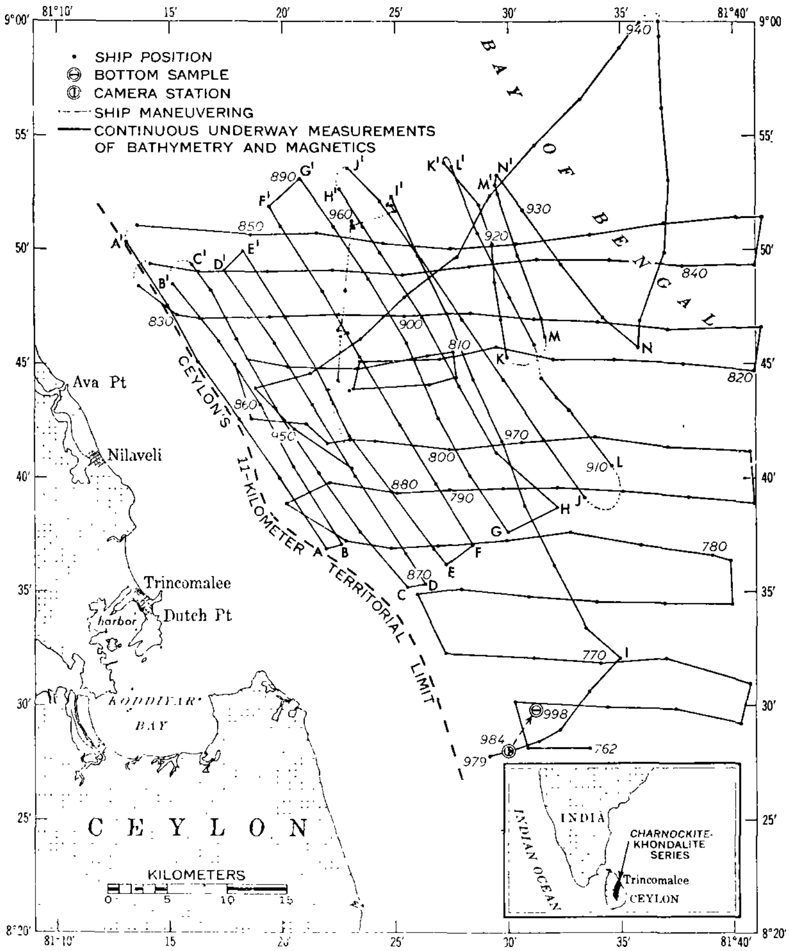

Fig.1. Index chart showing a section of track run by USC & GS Ship *Pioneer*. Positioning was established by astronomical fix, but track was adjusted on the basis of bathymetric (PDR) crossings. Broken line with arrow indicates direction and drift of underwater camera.

Trincomalee Harbor. Two tributaries enter the canyon from the south. On the broad ridge northwest of Trincomalee Canyon a northeast trending sea valley originates (Fig. 2). The valley bends east, is deflected by a rise in bottom topography (Fig. 3, profiles K–K′ to N–N′), and continues northeast parallel to Trincomalee Canyon.

Northwest of and parallel to Trincomalee Canyon is a canyon herein named North Trinco Canyon* (Figs. 2 and 3). Three northeast trending tributaries cross the insular slope and debouch into it from the west. A shoreward projection of North Trinco Canyon aligns with the northern contact zone of Wanni gneiss and charnockite–khondalite.

Southeast of and parallel to Trincomalee and North Trinco canyons is another canyon herein named South Trinco Canyon* (Figs. 2 and 3). One east and two northeast trending tributaries originate on the insular slope and debouch into it from the west. A shoreward projection of South Trinco Canyon aligns with the southern contact zone of Wanni gneiss and charnockite–khondalite.

*The authors have named the features to the north and south of Trincomalee Canyon, respectively North and South Trinco canyons. A town, harbor and submarine canyon named Trincomalee now exist within the same small geographical area, so these names are given a shortened form in keeping with the modern trend toward brevity.

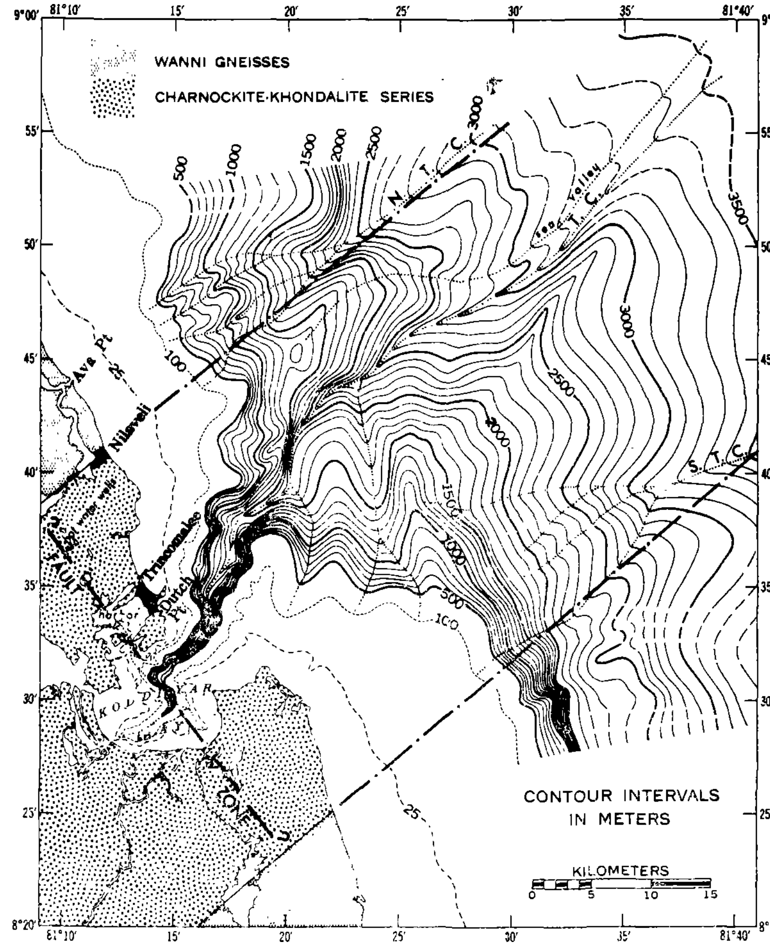

Fig. 2. Bathymetric chart contoured from PDR soundings (corrected) of the USC & GS Ship *Pioneer*. Data shoreward of Ceylon's territorial limit (Fig. 1) compiled from H. O. 3689. Dotted lines show axes of North Trinco Canyon (N.T.C.), Trincomalee Canyon (T.C.), South Trinco Canyon (S.T.C.), their tributaries, and a sea valley. Dot-dashed lines show assumed contact zones of Wanni gneisses and charnockite–khondalites. Light dashed contour lines are over areas containing fragmentary data. Heavy dashed line is the projection of Trincomalee Canyon's northwest–southeast trending segment and possible fault zone. Lengths, average gradients, and maximum wall heights of North Trinco, Trincomalee, and South Trinco canyons are respectively: 29 km, 100 m/km, 900 m; 59 km, 54 m/km, 1560 m; 28 km, 107 m/km, 350 m.

MAGNETICS

A Varian nuclear precession magnetometer recorded continuous total intensity measurements of the earth's magnetic field. The nearest magnetic observatory located near Bombay, India, furnished magnetograms which indicated such a slight diurnal variation that it has been disregarded in this study. Because of the small geographic extent encompassed by the survey, a constant of 40,450 gammas was assumed to be the value for the earth's main field (U.S. Naval Oceanographic Office, 1966). Removing this constant from total field values and contouring the resultant field (Fig. 4) leaves a gentle gradient varying from − 50 gammas in the southeast to − 300 gammas in the northwest.

Elongation of the magnetic trends along the projected contact zones of Wanni gneisses and charnockite–khondalites suggests a continuation of these rock series on to the insular slope.

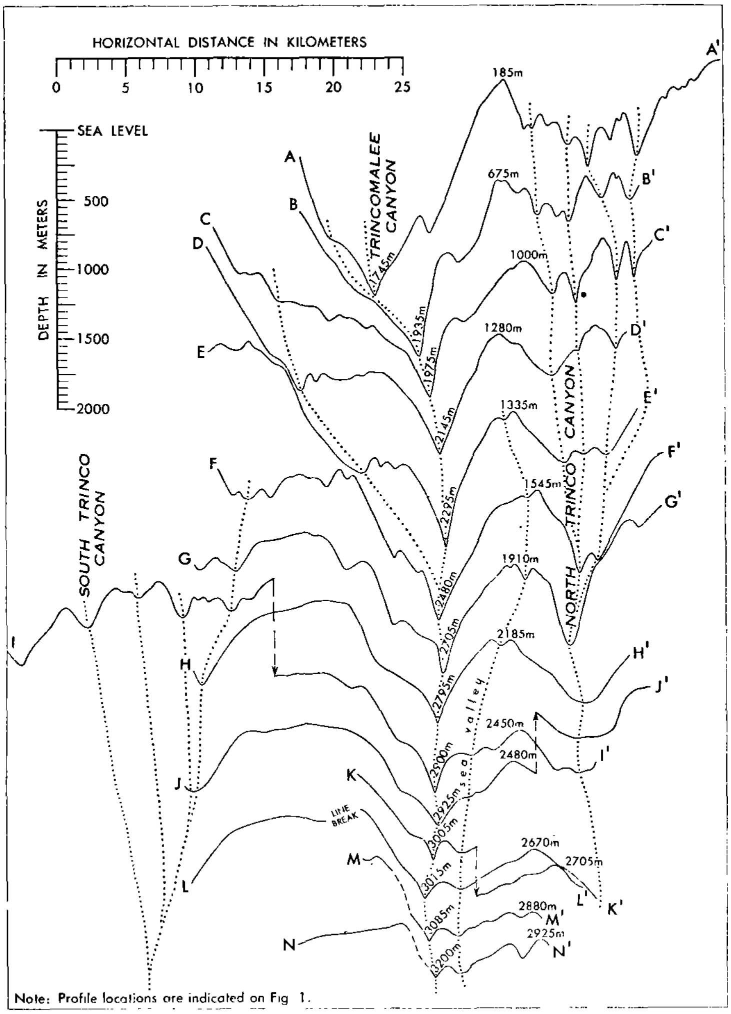

Fig. 3. Bathymetric profiles of Trincomalee and associated canyons. Vertical exaggeration is 10:1. Axes of canyons, their tributaries, and a sea valley are shown by dotted lines based on USC & GS Ship *Pioneer's* PDR data and their interpretation (Fig. 2). Broken lines with arrows indicate where profiles are broken to keep them in proper perspective (Fig. 1).

BOTTOM PHOTOGRAPHY AND DREDGING

One camera lowering was made at ship's position 984 (Fig. 1). Bottom photographs revealed a flat bottom which appeared to be composed of fine-grained sediments. As the camera drifted across the insular shelf it crossed over a rock outcrop and detritus (Fig. 5). Seaward from the talus, photographs of the bottom appear similar to the flat bottom shown landward from the outcrop. Near ship's position 998 (Fig. 1) the camera passed over an extremely steep slope (International Indian Ocean Expedition, U.S.C. and G.S. Ship *Pioneer*—1964. 1965, Vol. 1). At this location the camera was retrieved, and a chain dredge was lowered over the side. The dredge haul recovered "eight chunks of medium-grained saccharoidal dark green to black igneous rock," (International Indian Ocean Expedition, U.S.C. and G.S. Ship *Pioneer*—1964. 1965, Vol. 2).

The field description of these rocks suggests a similarity to rocks found in the Koddiyar Bay area by COATES (1935).

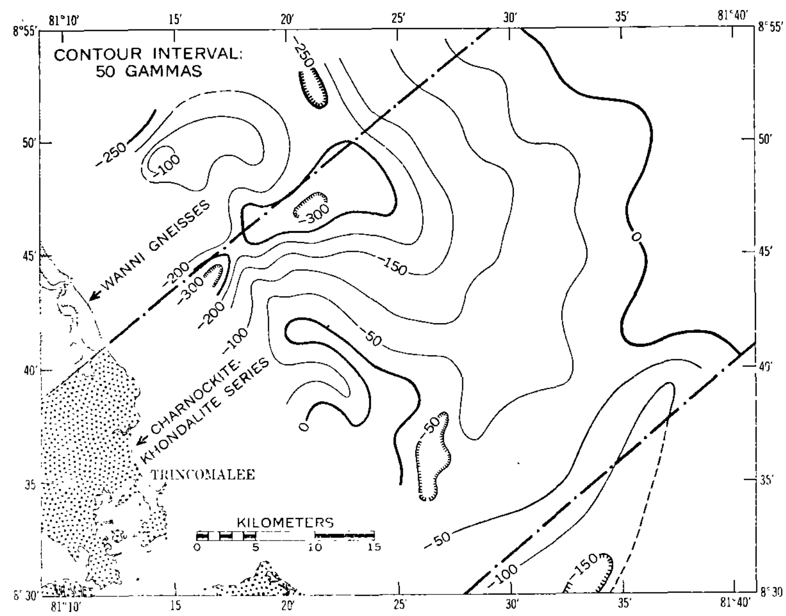

Fig. 4. Residual magnetic field off northeast Ceylon. Dot-dashed lines indicate projected contact zones of Wanni gneisses and charnockite–khondalites. Note elongation of magnetic trends along lines of projection.

DISCUSSION

The epeirogenic history of Ceylon has been positive with some minor oscillations. The last major uplift was pre-Miocene (KRISHNAN, 1953) when, according to ADAMS (1929a) the island was raised approximately 460 m above sea level. Ensuing peneplanation formed the present coastal plains which were incised before their submergence in the Miocene sea (ADAMS, 1929a). During this period of erosion, Trincomalee Canyon was probably cut along the axis of a synclinal fold and served as the major flume for denudation. Submergence was followed by a positive movement that raised the present insular shelf up to or slightly above sea level (ADAMS, 1929a). North and South Trinco were likely cut during this emergent period. Subsequent oscillations returned Ceylon to its present elevation. Feeder channels cutting across the shelf into North and South Trinco canyons were presumably buried during the depositional cycle following the last glacial stage of the Pleistocene. Trincomalee Canyon remained open because of its greater width and steeper gradient.

Like the major rock units of this area, Trincomalee Canyon has a general northeast strike. In Koddiyar Bay the axis of its main head trends northeast approximately 4 km, abruptly turns 90° northwest for a distance of 3 km, and again bends 90° northeast. The canyon's two remaining heads are in alignment with a landward projection (Fig. 2) of the northwest-southeast striking 3 km segment of Trincomalee Canyon. The northwest projection crosses a quartzite ridge (SHEPARD and DILL, 1966) and aligns with a series of hot water wells and lakes (U.S. HYDROGRAPHIC CHART 3689, 1949). The southeast projection aligns with a river mouth and series of lakes. It seems plausible that this lateral offset in Trincomalee Canyon's axis is the result of a major fault. Sharp bends which alter the northeasterly course of Trincomalee Canyon as it crosses the insular shelf are probably due to structural control. According to ADAMS (1929a) the rivers on Ceylon frequently cross quartzite ridges along joint planes so it seems reasonable to assume that joint planes may have deflected Trincomalee's path.

North and South Trinco canyons are very similar in structure. With one exception their tributaries trend northeast and enter their respective canyons from the west. Both canyons strike northeast parallel to Trincomalee Canyon, and both canyons are apparently cut along Wanni gneiss and charnockite–khondalite contact zones.

That surface geology on Ceylon continues across the insular slope is established by (1) agreement of major rock unit strikes with submarine canyon trends; (2) alignment of North and South Trinco canyons with contact zones of Wanni gneisses and charnockite-khondalites; (3) alignment of the broad ridge between North Trinco and Trincomalee canyons with the 6 km wide quartzite ridge between Nilaveli and the town of Trincomalee; (4) elongation of magnetic trends along Wanni gneiss and charnockite–khondalite contact zones; (5) rock outcrops on the insular shelf; and (6) rock type recovered from the insular slope.

Acknowledgements—We are indebted to the officers and men aboard the USC & GS Ship *Pioneer* and to members of the Atlantic Oceanographic Laboratories. We are particularly grateful to Dr. H. B. STEWART, JR. for the loan of his personal field notes and to Mr. R. K. LATTIMORE for his manuscript edits.

REFERENCES

ADAMS F. D. (1929a) The geology of Ceylon. *Can. J. Res.* **5**, 425–465.

ADAMS F. D. (1929b) The geology of Ceylon. *Can. J. Res.* **6**, 467–510.

AFANASSYEV G. D., I. V. BORISOVICH and L. L. SHANIN (1964) On the K–Ar age of certain rocks of the Indian peninsula and the Isle of Ceylon. *Dokl. sov. geologov. na 22-i sessii Mezhdunar. geol. Kongr.* Izd-vo Akad. Nauk SSSR.

ASWATHANARAYANA U. (1968) Precambrian geochronology of peninsular India and Ceylon; a reinterpretation. *Bull. geol. Soc. India* **5**, 63–64.

COATES J. S. (1935) The geology of Ceylon. Section B, Zoology and Geology. (*Spolia Zeylancia*). *Ceylon. J. Sci.* **19**, part 2, 101–191.

KRISHNAN F. N. I. (1953) The structural and tectonic history of India. *Mem. geol. Surv. India* **81**, 80–81.

INTERNATIONAL INDIAN OCEAN EXPEDITION, 1965, Vol. 1.

INTERNATIONAL INDIAN OCEAN EXPEDITION, 1965, Vol. 2.

SHEPARD F. P. (1963) Submarine canyons. In: *The Sea*, M. N. HILL, ed. Wiley, New York, **3**, pp. 480–506.

SHEPARD F. P. and R. F. DILL (1966) *Submarine canyons and other sea valleys.* Rand McNally & Co., pp. 203–204.

U.S. DEPARTMENT OF COMMERCE, ENVIRONMENTAL SCIENCE SERVICES ADMINISTRATION (1965) International Indian Ocean Expedition, USC & GS Ship *Pioneer*—1964. U.S. Govt. Printing Office, **1**, 53–58.

U.S. DEPARTMENT OF COMMERCE, ENVIRONMENTAL SCIENCE SERVICES ADMINISTRATION (1965) International Indian Ocean Expedition, USC & GS Ship *Pioneer*—1964. U.S. Govt. Printing Office **2**, 169.

U.S. NAVAL OCEANOGRAPHIC OFFICE (1966) The total intensity of the earth's magnetic force. Chart 1703, 3rd edition.

U.S. NAVY HYDROGRAPHIC OFFICE (1949) Approaches to Trincomalee. Chart 3689, 2nd edition.

Fig. 5. Bottom photograph of rock out-crop and talus. General location shown on Fig. 1.

[*facing p.* 660]

Reprinted from *Morskie gravimetričeskie issledovanija*, vol. 4, Izdatel'stvo MGU, 1969, p. 48-57

Statistical characteristics of selected marine geophysical profiles

by G. V. Aganova, A. G. Gaïnanov, E. P. Kalinina, and P. A. Stroev

IV. РЕЗУЛЬТАТЫ ГРАВИМЕТРИЧЕСКИХ ИЗМЕРЕНИЙ В МИРОВОМ ОКЕАНЕ И АНТАРКТИДЕ

Г. В. Агапова, А. Г. Гайнанов, Е. П. Калинина, П. А. Строев

СТАТИСТИЧЕСКИЕ ХАРАКТЕРИСТИКИ НЕКОТОРЫХ МОРСКИХ ГЕОФИЗИЧЕСКИХ ПРОФИЛЕЙ

В морских геолого-геофизических исследованиях при анализе и интерпретации данных обычно используется комплекс сведений об изучаемом объекте. Различные характеристики одного и того же района подвергаются сравнительному качественному анализу. Чаще всего основными данными являются результаты промеров глубин, измерения напряженности гравитационного и магнитного полей. Установлены главные закономерности распределения гравитационных и магнитных аномалий Земли и их связи (со строением земной коры), определены коэффициенты, связывающие величину аномалии силы тяжести с глубиной и высотой местности [1—5]. Однако детальные исследования последних лет, проведенные в различных океанах, показали, что зависимости между строением земной коры, рельефом дна и аномалиями гравитационного и магнитного полей Земли более сложны, что обусловлено не только особенностями регионального геологического строения, но и неоднородностью верхней мантии в различных областях [6, 7]. В связи с этим большое значение приобретают различные методы количественного, в частности статистического анализа данных гравимагнитных и эхолотных съемок [8—11]. Для оценки возможностей статистического анализа наиболее благоприятными являются данные одновременных непрерывных определений аномалий гравитационного и магнитного полей и рельефа дна. Этим требованиям удовлетворяют материалы международной индоокеанской экспедиции на и/с «Оуэн», полученные в 1961—1962 гг. [12] для северо-западной части Индийского океана и представленные непрерывными профилями дна, гравитационных и магнитных аномалий. Из всех профилей для статистического анализа нами был выбран маршрут протяженностью свыше 1500 *миль*, пересекающий основные структурные элементы западной части океана: Сомалийскую котловину, Аравийско-Индийский хребет, Аравийскую котловину и материковый склон западного побережья Индостана (рис. 1).

В работе были использованы профили дна, построенные на основании прецизионного измерения глубин. Регистрируемая величина отсчитывалась через 10-минутные интервалы. В измеренные глубины введены поправки за отклонение фактической скорости звука в морской воде от расчетной. Профили составлены в горизонтальном масштабе приблизительно 1 : 1 000 000 и дают возможность получать глубины с точностью ± 100 *м* и их положение с точностью до ± 1 *мили* вдоль галса [12].

Естественно, что в данном масштабе малые формы подводного рельефа не нашли отражения на профилях.

Измерения полного вектора напряженности магнитного поля на борту судна проводили с помощью буксируемого ядерного магнитометра.

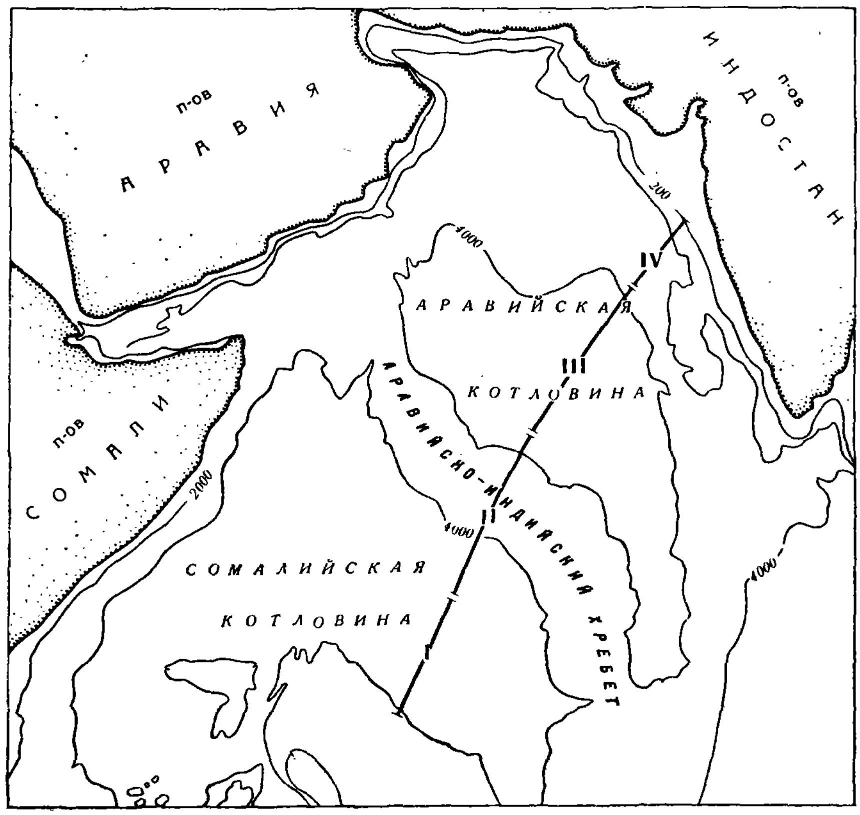

Рис. 1. Схема положения профилей

Измерения делали каждую минуту, исключая районы с резко переменным полем, где измерения осуществляли через 0,5 *мин.* Каждый отсчет регистрировали на перфокарты для электронно-счетной машины, а последние три цифры — на перовой самописец. В дальнейшем, учитывая нормальное поле, строили окончательные профили магнитных аномалий. Поправок за вековые вариации не вводили. Суточные вариации также не учитывали, так как они не превосходят 20 γ (по наблюдениям на стационарных береговых и морских якорных обсерваториях). Ошибка определения магнитных аномалий составляет около ± 20 γ.

Измерения силы тяжести на борту «Оуэна» проводили с помощью надводного морского гравиметра «Аскания — Верке», установленного на гиростабилизированной платформе фирмы Аншютц. Чувствительная система гравиметра помещена в термостат. В качестве опорных пунктов использовали наблюдения в портах заходов Ламу, Бомбей, Карачи и т. п. Эти причальные пункты привязаны гравиметром «Уордена» к мировой опорной гравиметрической сети. Все наблюдения выполнены при спокойном море, так что поправки за влияние возмущающих ускорений не вводились.

Наблюдения вели на ходу судна. Отсчеты гравиметра вместе с отметками времени автоматически регистрировались на диаграмме через каждые 5 *мин*. Значения силы тяжести отнесены к пунктам наблюдений для каждого 10-минутного интервала хода судна.

Оценка точности гравиметрических измерений проведена по контрольным и повторным пунктам. Среднеквадратическая ошибка измеренных аномалий в свободном воздухе составляет ±5—7 *мгл*.

Профиль 1 (рис. 2,I) пересекает восточную периферию Сомалийской котловины, глубины которой располагаются в диапазоне от 4000 до 5000 *м*, поверхность слегка наклонена в сторону Аравийско-Индийского хребта и, за исключением двух подводных возвышенностей с относительными высотами немногим более 1000 *м*, осложнена в основном мелкими холмами.

К северо-востоку от котловины расположен Аравийско-Индийский хребет (рис. 2,II), представляющий в структурном отношении ветвь Срединно-Индоокеанского хребта. Морфологически он выражен как типичный хребет с четкой рифтовой долиной с относительной глубиной до 1000 *м*, прослеживающейся почти на всем протяжении хребта, с характерным расчленением, в котором преобладают линейно вытянутые формы рельефа, ориентированные вдоль оси хребта. Подножье хребта расположено на глубине около 5000 *м*, а отдельные вершины поднимаются до глубины 2500 *м*.

Между материковым склоном Индостана и Аравийско-Индийским хребтом расположена Аравийская котловина (рис. 2,III). Рассматриваемый профиль пересекает ее восточную часть. Она занимает область глубин от 4000 до 5000 *м*, характерную для типичных океанических котловин. Поверхность ее слегка наклонена в сторону хребта. Небольшие подводные горы и холмы изредка нарушают в общем выровненную поверхность дна котловины. Материковый склон западного Индостана (рис. 2,IV) пересечен под некоторым углом к простиранию. Подножие склона расположено на глубине свыше 4000 *м*, верхняя часть склона крутая, нижняя выполаживается и без четких границ переходит в поверхность Аравийской котловины. Склон осложнен неглубокими депрессиями и хребтами.

Магнитное поле северо-западной части Индийского океана чрезвычайно неоднородно. Анализ магнитных профилей позволяет схематически выделить отдельные области, характеризующиеся различной степенью аномальности.

Наименее аномальные области — это:

а. Западная часть Сомалийской котловины, материковый склон и шельф Африки. Здесь средняя величина аномалий ΔT составляет $\pm 40\,\gamma$, и только в отдельных участках они достигают величины $\pm 100\ \gamma$.

б. Центральная часть Сомалийской котловины к северу от Сейшельских островов и Аравийская котловина, где аномалии ΔT в среднем колеблются в пределах ± 100—$150\ \gamma$ (рис. 2,I, 2,III). Аравийско-Индийский хребет (рис. 2,II) характеризуется типичными для срединно-океанических хребтов магнитными аномалиями. Так, на трех пересечениях в центральной и северной части хребта наблюдаются следующие изменения аномалий ΔT. Если в Сомалийской котловине наблюдаются длиннопериодные магнитные аномалии с амплитудами от —400 γ до +250 γ, то при подходе к склону Аравийско-Индийского хребта длиннопериодные магнитные аномалии затухают и выделяются короткопериодные с амплитудой от +50 до —200 γ. Над рифтовой зоной амплитуда магнитных аномалий возрастает от +200 до —400 γ.

На материковом склоне у п-ова Индостан (рис. 2, IV) наблюдаются интенсивные магнитные аномалии с амплитудой от —200 до +300 γ, которые у самого побережья затухают.

Характер гравитационных аномалий в северо-западной части Индийского океана различен для следующих основных областей: глубокие океанские котловины, океанические хребты и острова, переходные зоны от океана к материкам.

Глубоководные океанические впадины характеризуются относительно спокойным полем силы тяжести с отрицательными аномалиями Фая (—30÷—50 *мгл*) и значительными по величине аномалиями Буге (+350÷400 *мгл*).

Сильно раздробленная поверхность Аравийско-Индийского хребта (рис. 2, II) характеризуется большой изменчивостью аномалий Фая. Над самыми гребнями хребтов аномалии Фая имеют значения +30÷÷+50 *мгл*, рифтовые долины же отмечаются значительными отрицательными (до —50÷—70 *мгл*) аномалиями. Подножия океанических хребтов четко оконтуриваются изоаномалией в редукции Буге +250 *мгл*. Это относится ко всем основным хребтам: Аравийско-Индийскому, Мальдивскому и Маскаренскому. На вершинах гребней хребтов аномалии Буге уменьшаются до +150÷+100 *мгл*.

В переходных зонах от океана к материкам в северо-западной части Индийского океана аномалии Фая носят в общем спокойный характер, сохраняют свои отрицательные значения и уже у самой береговой черты резко увеличиваются, меняют знак на положительный. Аномалии Буге при подходе к берегу значительно уменьшаются, достигая нулевых значений на самом берегу и от —100 до —150 *мгл* на материке [13].

Для расчета статистических характеристик профили дна были заменены дискретными рядами значений глубин, гравитационных и магнитных аномалий, снятых с исходного материала с частотой, соответствующей на местности расстоянию 1,23 *км*.

Кривые наблюденных параметров по профилям можно рассматривать как сумму гармонических колебаний с различными периодами (частотами) и амплитудами. Гармонический анализ рельефа Земли, проведенный Преем [14] и Венинг-Мейнесом [15], показал правомочность подобных представлений для исследования мегарельефа. Гармонический анализ рельефа вдоль параллелей с частотой высот и глубин через 5-градусный интервал, проведенный в 1964 г. [16], показал, что положение и ритмичность в чередовании крупных структурных элементов Земли достаточно четко выявляется уже суммой четырех гармоник.

Можно думать, что крупные формы рельефа дна, гравитационные и магнитные аномалии формируются в основном под влиянием комплекса эндогенных процессов, различных по величине, сфере и длительности их действия относительно поверхности Земли. Разделение форм рельефа, гравитационных и магнитных аномалий на различные частотные составляющие в какой-то мере соответствует разделению формирующих их факторов на различные по характеру, величине и сфере действия составляющие. В зависимости от целей исследования проводится анализ региональных или локальных составляющих.

В данном случае под региональной составляющей подразумевается характер рельефа, гравитационных и магнитных аномалий, типичный для крупных структурно-геоморфологических регионов океана.

Под локальной составляющей подразумевают неровности рельефа, гравитационные и магнитные аномалии, осложняющие региональный характер профиля, созданные, по-видимому, комплексом факторов, действующих в пределах региона и отражающие особенности его геологи-

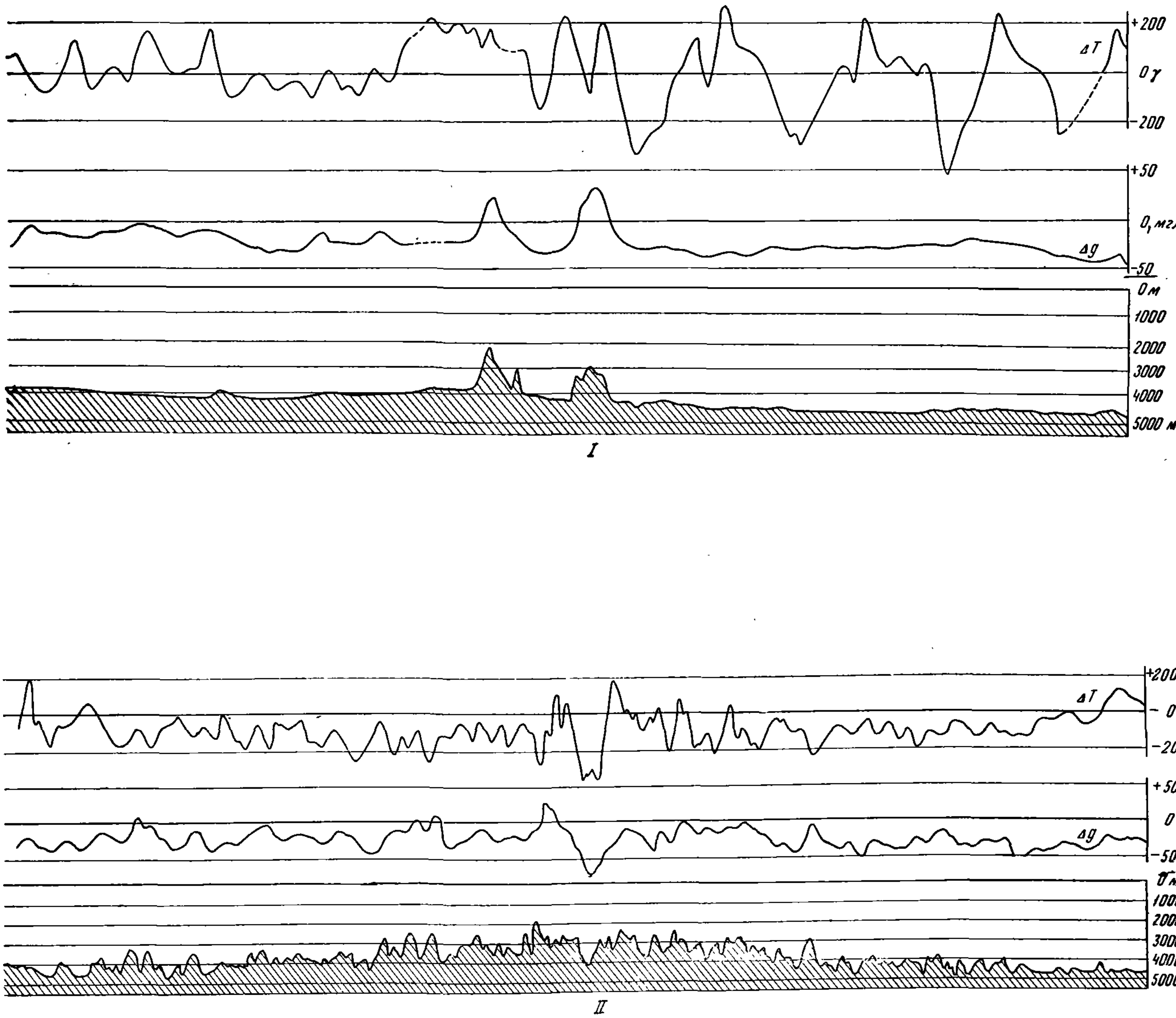

Рис. 2. Геофизические профили:
I — Сомалийская котловина; III — Аравийская котловина;
II — Аравийско-Индийский хребет; IV — Материковый склон западного Индостана

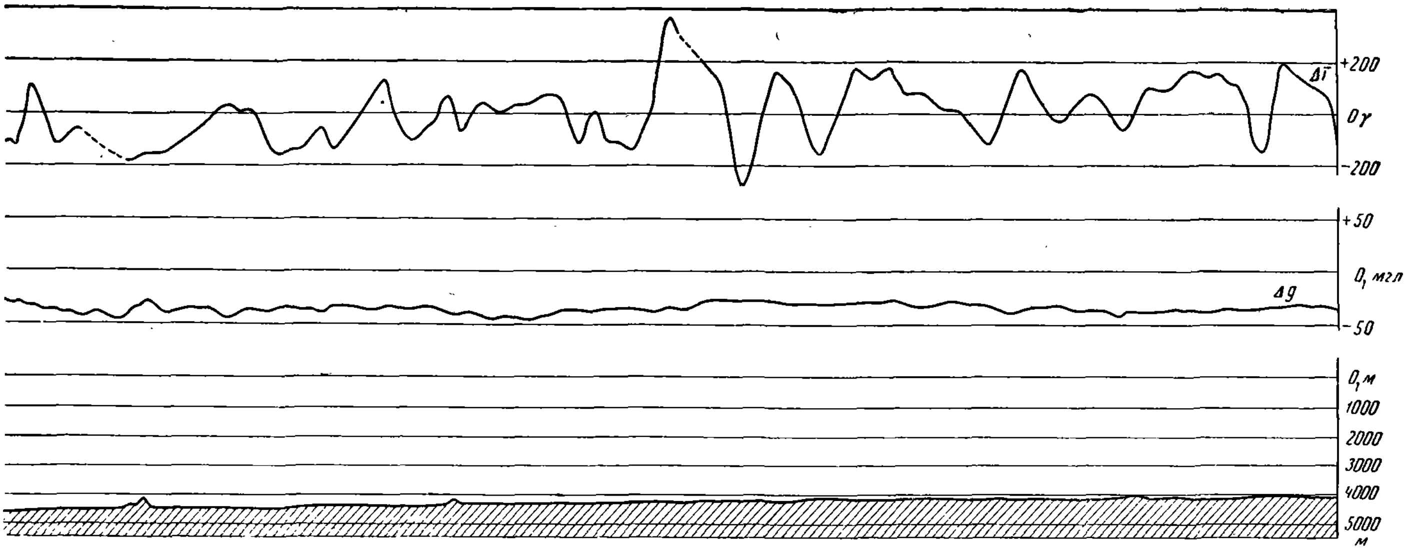

ΔT
+200
0γ
-200
+50
0, мгл
Δg
-50
0, м
1000
2000
3000
4000
5000
м

III

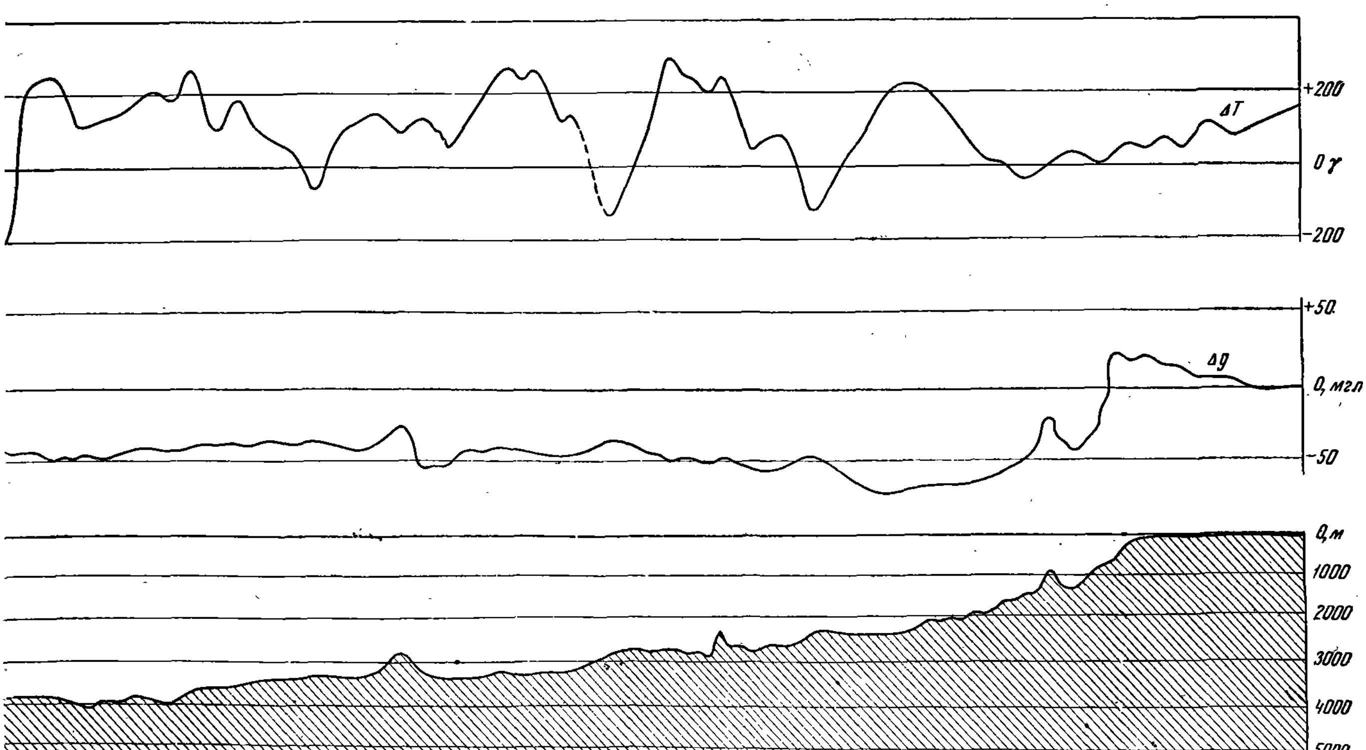

ΔT
+200
0γ
-200
+50
Δg
0, мгл
-50
0, м
1000
2000
3000
4000
5000

IV

ческого строения. Анализ последних представляет наибольший интерес.

Для выделения региональных составляющих профилей был использован метод сглаживания. Ординаты сглаженных, или региональных, профилей определены при помощи формулы

$$\tilde{x} = \sum_{j=-\frac{l}{2}}^{\frac{l}{2}} a_j x_{i+j},$$

где x_i — ординаты исходных профилей; a_j — сглаживающие коэффициенты, которые определяются ядром сглаживания, имеющим вид $1+\cos\frac{2\pi}{l} j$; l — параметр сглаживания.

При таком ядре на региональных профилях не остаются формы рельефа, аномалии ΔT и Δg, длина волны которых менее $\frac{l}{2}$ [17].

Сглаживание было произведено с параметром 123 *км*, одинаковым для всех профилей. Таким образом, на сглаженном профиле почти нет неровностей рельефа протяженностью менее 60 *км* и аномалий ΔT и Δg той же периодичности.

Наиболее общей характеристикой полей является их средняя величина, определенная для каждого профиля как

$$\bar{x} = \frac{\Sigma x_i}{n}.$$

Сглаженные профили на рис. 3 даны как отклонения от соответствующих средних.

В Сомалийской котловине (рис. 3, I) региональный профиль дна, расположенный на глубине 4000 *м*, полого наклонен к подножию Аравийско-Индийского хребта, небольшое поднятие на нем соответствует двум подводным возвышенностям. На гравитационном региональном профиле преобладают отрицательные аномалии Фая, величина которых возрастает к подножию хребта. Небольшой максимум аномалий соответствует возвышенностям. На региональном профиле магнитных аномалий среднее значение близко к нулю. Кривая регионального магнитного поля сложнее, чем кривые региональных профилей дна и аномалий силы тяжести.

В пределах Аравийско-Индийского хребта (рис. 3, II) региональные профили, вероятно, отражают основные особенности строения хребта. Сглаженный профиль рельефа выявляет массивное симметричное поднятие с несколько приподнятыми крыльями. Узкая рифтовая долина при таком большом параметре сглаживания не отражена на профиле. Судя по плавным очертаниям профиля, можно считать, что все сложное расчленение хребта создается формами, протяженность которых менее 60 *км*.

Региональные аномалии Фая над хребтом отрицательны, однако величина их незначительна. Над рифтовой зоной и у их подножия величины отрицательных аномалий возрастают до —15 — —30 *мгл* соответственно. Магнитные аномалии в районе Аравийско-Индийского хребта отрицательны, их средняя величина равна —82 γ; над рифтовой зоной величина аномалий несколько уменьшается.

Очень спокоен региональный профиль дна и гравитационных аномалий Аравийской котловины (рис. 3, III). Региональные аномалии Фая незначительно отклоняются на некоторых участках профиля от среднего значения, равного —37 *мгл*. Более сложным является профиль магнитных аномалий, у подножия аномалии отрицательны, с приближением к материковому склону появляются положительные аномалии.

У Индостана (рис. 3, IV) региональный профиль дна плавно поднимается к поверхности. Региональный профиль аномалий Фая выровнен, аномалии отрицательны, среднее значение равно —46 *мгл*. Магнитные аномалии положительны, среднее значение равно +64 γ.

Из сопоставления региональных особенностей профилей видно, что в пределах всех структурных элементов океанического дна существует довольно хорошее соответствие между рельефом дна, величинами и характером изменчивости гравитационных аномалий Фая. Характер региональных магнитных аномалий не согласуется с региональными особенностями рельефа дна и аномалий силы тяжести.

Если из ординат наблюденного параметра вычесть ординаты этого же параметра на соответствующих региональных профилях, получим локальные гравитационные и магнитные аномалии и глубины (рис. 3). Для локальных аномалий характерна значительная изменчивость величин. Количественно оценить степень изменчивости локальных аномалий можно при помощи среднего квадратического отклонения локальных составляющих от региональных. Величины средних квадратических отклонений даны в таблице.

Таблица

Характеристика профилей	Район			
	Сомалийская котловина	Аравийско-Индийский хребет	Аравийская котловина	Материковый склон Индостана
Глубины, *м*	225	334	45	141
Гравитационные аномалии, *мгл*	10	11	4	8
Магнитные аномалии, γ	118	97	81	92

В ряде случаев такая оценка не является достаточной, так как не отражает особенностей периодичности и амплитуд этих отклонений.

Для выявления структурных особенностей локальных аномалий целесообразно вычисление автокорреляционных и спектральных функций [10, 18, 19]. Автокорреляционная функция характеризует степень изменчивости аномалий. Автокорреляционные функции рассчитаны по формуле

$$C_{xr} = \frac{1}{N-r} \sum_{i=0}^{N-r} x_i x_{i+r},$$

где N — число ординат профиля; r — ряд последовательных значений от 0, 1, 2, 3, ..., m; m — величина максимального сдвига при расчете функции.

Величина максимального сдвига принята равной 96 *км*. На рис. 4 приведены нормированные автокорреляционные функции локальных гравитационных и магнитных аномалий и глубин.

Для всех профилей характерно быстрое затухание корреляционных функций, что отражает значительную изменчивость аномалий. Различаются также типы автокорреляционных функций, что отражает различный характер изменчивости рельефа, гравитационных и магнитных аномалий не только в различных районах, но и в пределах одного и

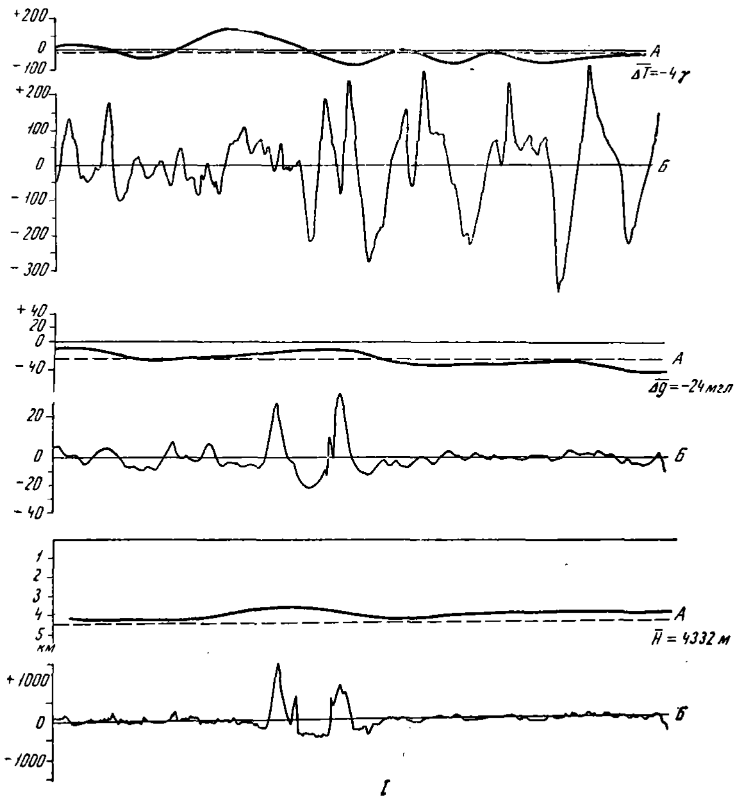

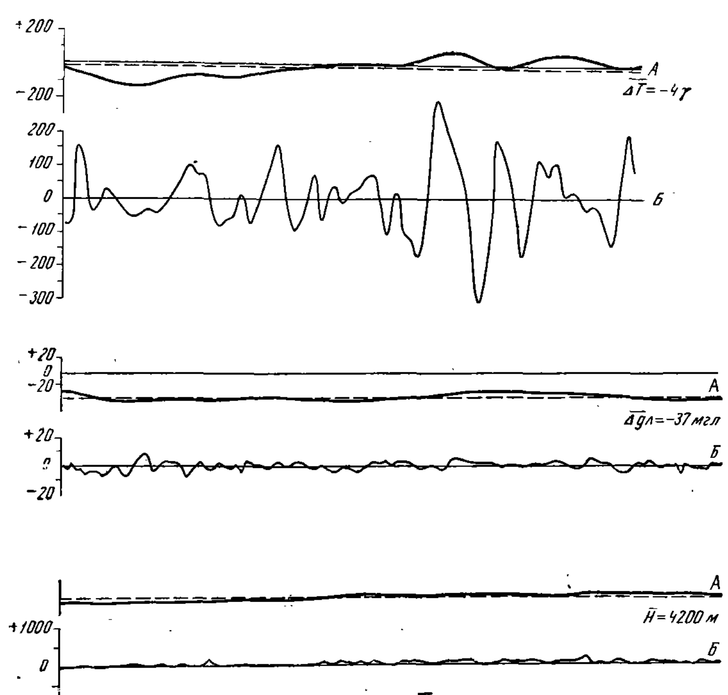

Рис. 3. Региональные (*А*) и локальные (*Б*) составляющие геофизических профилей:
I — Сомалийская котловина; II — Аравийско-Индийский хребет;
III — Аравийская котловина; IV — Материковый склон Индостана

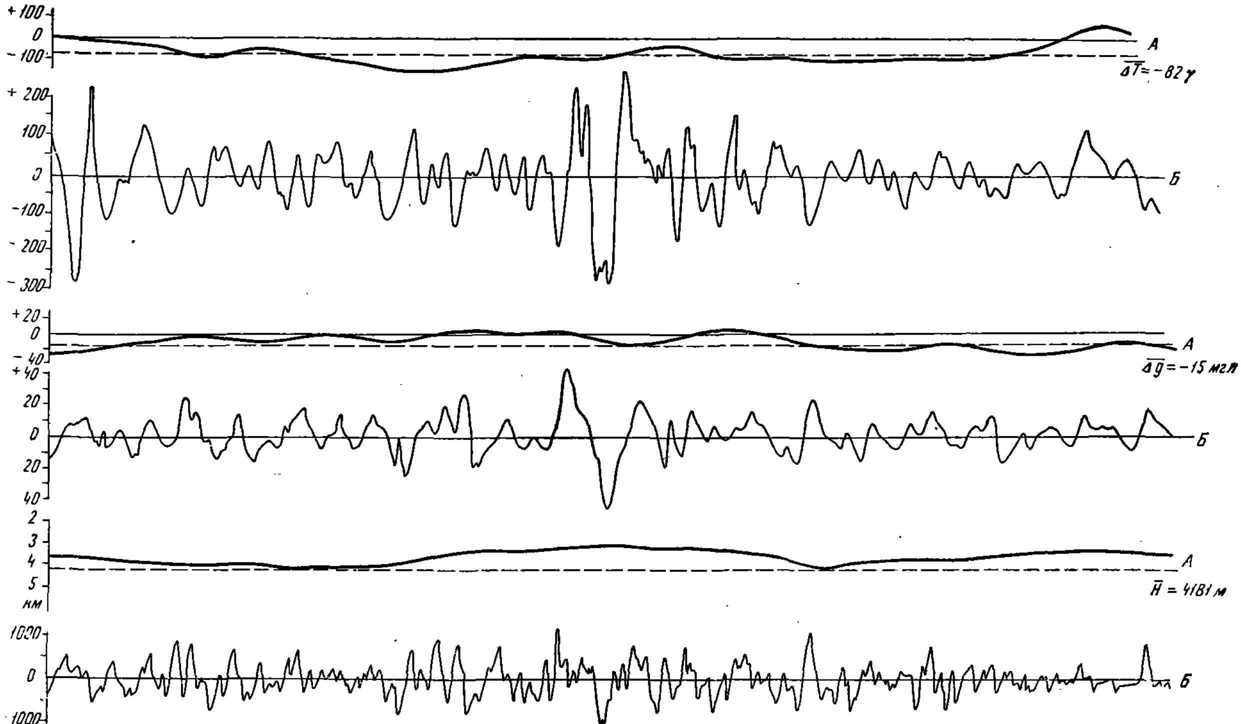

+100
0
-100
A
ΔT = -82 γ
+200
100
0
-100
-200
-300
Б
+20
0
-40
A
Δg = -15 мгл
+40
20
0
20
40
Б
2
3
4
5
км
A
H = 4181 м
1000
0
1000
Б

II

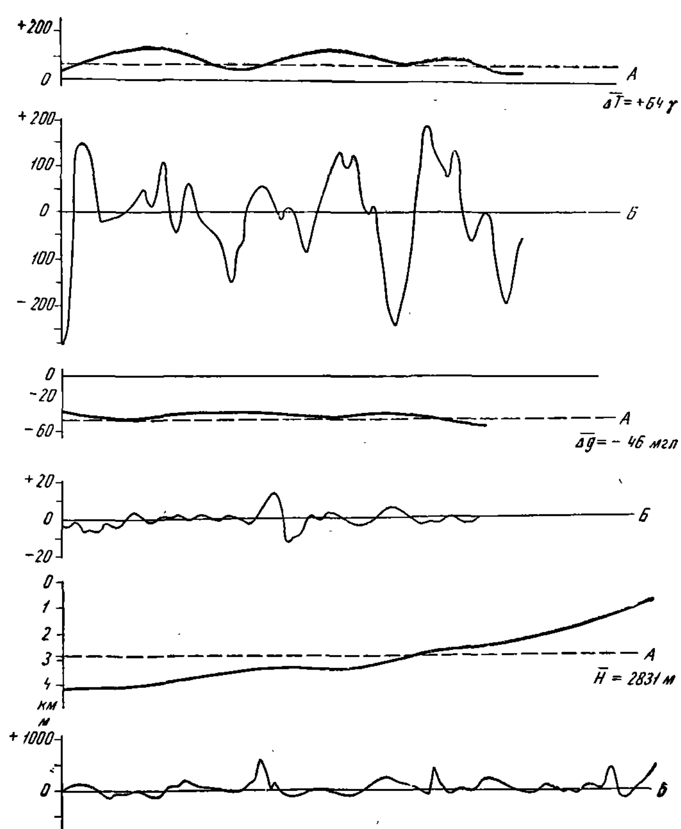

+200
0
A
ΔT = +64 γ
+200
100
0
100
-200
Б
0
-20
-60
A
Δg = -46 мгл
+20
0
-20
Б
0
1
2
3
4
км
A
H = 2831 м
м
+1000
0
-1000
Б

IV

того же района. При наличии скрытой периодичности автокорреляционная функция является знакопеременной. Расстояние между точками перехода через нуль примерно соответствует половине периода [18].

Наиболее четко выражен периодический характер автокорреляци-

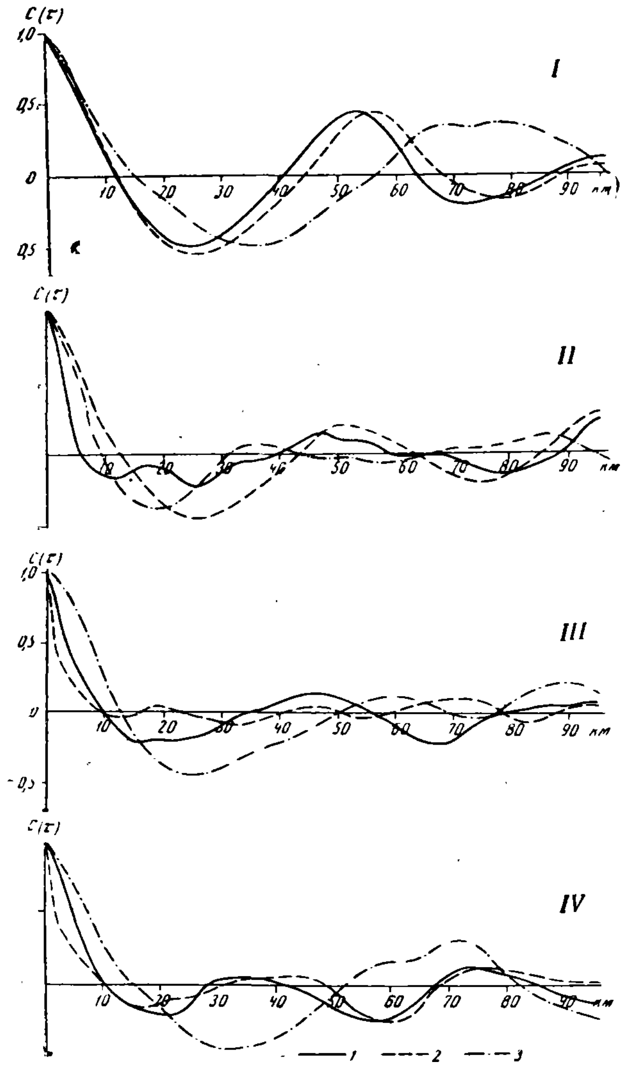

Рис. 4. Автокорреляционные функции:
I, II, III, IV — профили (см. рис. 2);
1 — глубины дна океана; 2 — аномалии силы тяжести; 3 — магнитные аномалии

онных функций Сомалийской котловины, отражающий определенную ритмичность в чередовании форм рельефа, аномалий силы тяжести и напряженности магнитного поля. Расстояние, на котором статистическая связь в значительной мере теряется — коэффициент корреляции уменьшается от 1,0 примерно до 0,3, — обычно называется радиусом автокорреляции. Автокорреляционные функции рельефа дна и аномалий силы тяжести подобны, имеют один и тот же радиус корреляции, равный 8 *км*. Несколько больше радиус корреляции магнитных аномалий, он равен 10 *км*, кроме того, вид функции свидетельствует о несколько иной периодичности в чередовании аномалий.

Автокорреляционные функцнн Аравийско-Индийского хребта характеризуются быстрым затуханием, различным обликом и низкой корреляцией на значительных расстояниях. Еще менее коррелирован рельеф дна, радиус корреляции всего 4 *км*, а значения автокорреляционной функции не превышают за первым минимумом $\pm 0{,}3$. Радиус корреляции магнитных аномалий составляет 7 *км*, а гравитационных — 9 *км*. Пожалуй, наиболее периодическим в пределах хребта остается изменение аномалий силы тяжести.

В Аравийской котловине автокорреляционная функция рельефа дна имеет радиус корреляции около 6 *км*. Радиус корреляции гравитационных аномалий еще меньше — около 4 *км*. Радиус корреляции магнитных аномалий равен 10 *км*.

На материковом склоне Индостана автокорреляционные функции рельефа и гравитационных аномалий с поправкой за угол между простиранием структур материкового склона и направлением профиля имеют радиус корреляции около 3 и 6 *км* соответственно, а радиус корреляции магнитных аномалнй около 9 *км*.

Частотная характеристика локальных аномалий может быть получена путем преобразования корреляционных функций в спектральные при помощи формулы

$$P_k = \frac{\delta_k}{m} \sum_{r=0}^{m} C_{xr} \cos \frac{kr\pi}{m},$$

где

$$\delta_k = \begin{cases} 0{,}5 \text{ при } k = 0, \quad k = m \\ 1 \text{ при } 0 < k < m. \end{cases}$$

Спектральные функции представлены на рис. 5. Доверительные пределы для рассмотренных профилей изменяются от 12,6—2,0 *км* до 11,5—2,6 *км*.

В Сомалийской котловине в спектрах преобладает один четкий максимум, который для рельефа и гравитационных аномалий связан с формами протяженностью менее 50 *км*, а для магнитных аномалий с периодичностью 50—55 *км*. Два сопряженных максимума гравитационных аномалий и глубин относятся к формам рельефа протяженностью около 26 *км*.

Наиболее сложны спектры в пределах Аравийско-Индийского хребта, особенно спектр профиля локальных неровностей рельефа, который имеет три максимума, соответствующие формам протяженностью 47, 23 и 12 *км*. Наиболее значительные по величине аномалии силы тяжести имеют периодичность 50 *км* и, по-видимому, сопряжены с максимумом отклонений рельефа. Первый максимум магнитных аномалий по сравнению с гравитационными аномалиями и рельефом смещен в область высоких частот и относится к длине волны примерно 37 *км*.

В Аравийской котловине с небольшими колебаниями глубин и гравитационных аномалий в их спектрах выделяются лишь два небольших максимума. Для рельефа первый относится к формам протяженностью 45 *км*, второй выражен очень слабо и характерен для форм протяженностью 25 *км*, а для гравитационных аномалий характерен для периодичности 58 и 22 *км* соответственно. Максимум магнитных аномалий один и характерен для периода 60 *км*.

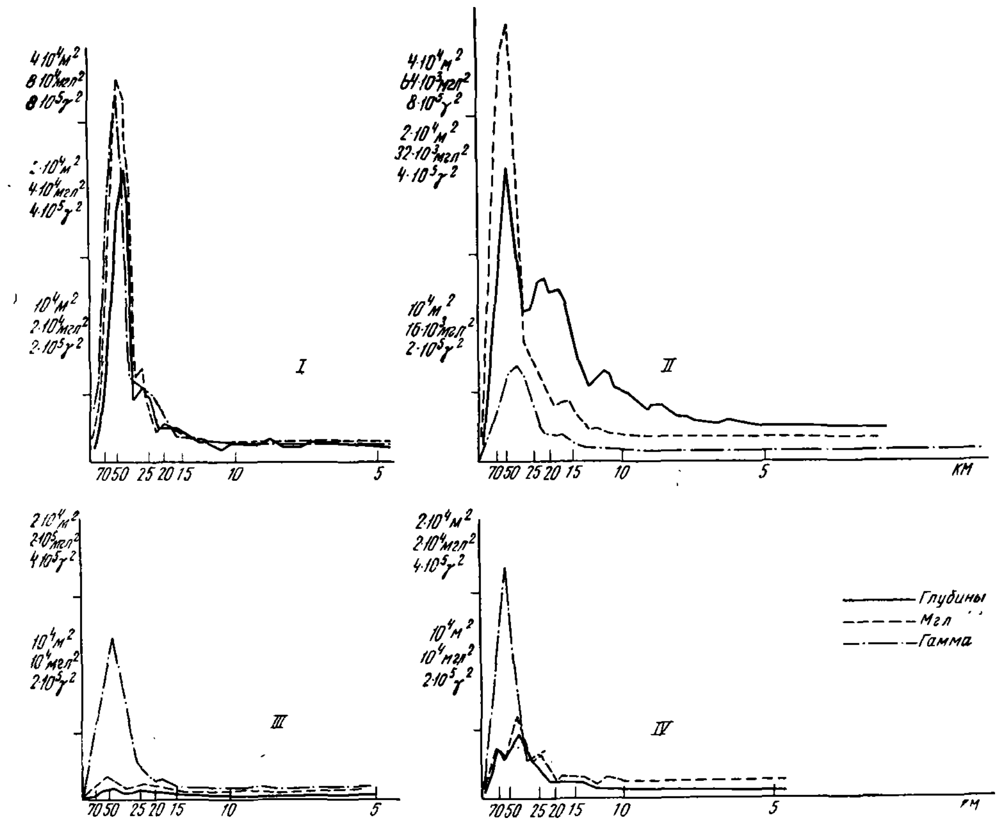

Рис. 5. Спектральные функции. Условные обозначения те же, что и на рис. 4

Спектры аномалий силы тяжести и глубин для материкового склона подобны и с учетом поправки за угол между простиранием материкового склона н направлением профиля имеют четко выраженный максимум для форм рельефа и гравитационных аномалий протяженностью около 40 *км*. В спектре магнитных аномалий преобладает один четко выраженный максимум, относящийся к локальным аномалиям протяженностью около 57 *км*.

Выявленные в результате проведенного анализа статистические характеристики позволяют более определенно судить о природе аномалий гравитационного и магнитного полей и об основных рельефообразующих факторах в океане. В частности, четко проявляющиеся в сглаженных региональных магнитных аномалиях Аравийско-Индийского хребта отрицательные аномалии с амплитудой до —150 γ (в среднем —82 γ) можно связать с подъемом изотермы точки Кюри под Срединно-Океаническими хребтами. Это хорошо подтверждается и расчетами глубин залегания нижних кромок магнитовозмущающих тел. Если нижние кромки магнитовозмущающих тел в глубоких котловинах океанов располагаются на глубинах 30 *км* и более, то под Срединно-Океаническими хребтами глубины нижних кромок уменьшаются до 10 *км* и менее [7].

Частотная корреляция магнитных и гравитационных аномалий, а также рельефа дна как над глубокими котловинами, так и над Срединно-Океаническим хребтом и материковым склоном подкрепляет точку зрения тех исследователей, которые считают причиной периодичности магнитных аномалий в океанах не чередование участков с прямой и обратной намагниченностью [20], а, скорее, структурные неоднородности земной коры и верхней мантии [7].

Сопоставление спектров гравитационных и магнитных аномалий различных моделей со спектрами наблюдаемых гравитационных и магнитных аномалий позволит более определенно судить о форме, размерах и глубине залегания аномалообразующих тел.

Все расчеты были выполнены на ЭВМ «Минск» и М-20 по программам, составленным в ГАИШ МГУ и в Институте океанологии АН СССР.

Авторы благодарят В. П. Пантелеева, М. У. Сагитова и А. Д. Ямпольского за ценные советы и обсуждение работы.

ЛИТЕРАТУРА

1. Гурарий Г. З., Соловьева И. А. Строение земной коры по геофизическим данным. М., Изд-во АН СССР, 1963.
2. Деменицкая Р. М. Основные черты строения коры земли по геофизическим данным. М., Гостоптехиздат, 1961.
3. Жонголович И. Д. Внешнее гравитационное поле Земли и фундаментальные постоянные, связанные с ним. «Тр. Ин-та теорет. астр.», вып. 3. Л., Изд-во АН СССР, 1952.
4. Кропоткин П. Н., Люстих Е. Н., Повало-Швейковская Н. Н. Аномалии силы тяжести на материках и океанах и их значение для геотектоники. Изд-во МГУ, 1958.
5. Сажина Н. Б., Грушинский Н. П. Гравитационная разведка. М., «Недра», 1966.
6. Гайнанов А. Г. Плотностная неоднородность верхией мантии. Изв. АН СССР, сер. физика Земли, № 10, 1966.
7. Гайнанов А. Г. Магнитная неоднородность верхней мантии. В сб.: «Геофизические исследования», вып. 2. Изд-во МГУ, 1966.
8. Белоусов И. М., Козлов Н. М., Ямпольский А. Д. О новой методике статистической обработки материалов промера морского дна. «Океанология», **5**, № 1, 1965.
9. Гладкий К. В. Разделение суммарных гравитационных полей как процесс частотной фильтрации. «Прикладная геофизика», вып. 25. М., Гостоптехиздат, 1960.
10. Хортон С. У., Хемпкинс У. Б., Хоффман А. А. Дж. Статистический анализ некоторых аэромагнитных карт северо-запада Канадского щита. «Аэромагнитные методы в геофизике». М., «Мир», 1966.
11. Neidell N. S. Spectral studies of marine geophysical profiles. Geophysics. **31**, No. 1, 1966.
12. Bathymetric, magnetic, gravity investigations H. M. S. OVEN, 1962—1963 London. Hydrografic Department. Admiralty. Marine Science Publication, No. 4, 1963.
13. Гайнанов А. Г., Строев П. А. Гравитационное поле и строение земной коры северо-западной части Индийского океана. В сб.: «Морские гравиметрические исследования», вып. 3. Изд-во МГУ, 1967.
14. Prey A. Darstellung der Hohen und Tiefenverhörtnisse der Erde durch eine Entwicklung hach Kugelfuktionen bis. 16 Ordnung. Abhandell Conig. Geselshaft. Goettingen Matt-Physickkl. neue Folge 11, 1, 1922.
15. Vening-Meinesz F. A., Heiskanen W. A. The Earth and its gravity field. N. Y., 1958.
16. Peixoto H., Saltman B., Feuels S. Harmonic analysis of the topografy along parallels the Earth. J. Geophys. Res., **69**, No. 8, 1964.
17. Ямпольский А. Д. О спектральных методах исследования океанологических процессов. М., Изд-во АН СССР, «Океанология», **5**, вып. 5, 1965.
18. Андреев Б. А., Клушин И. Г. Геологическое истолкование гравитационных аномалий. М., Госгеолтехиздат, 1962.
19. Сабинин К. Д., Шулепов В. А. О короткопериодных внутренних волнах Норвежского моря. «Океанология», **5**, вып. 2, 1965.
20. Vine F. S., Mattews D. H. Magnetic anomalies over oceanic ridges. Nature, **199**, No. 4897, 1963.

Reprinted from *Curr. Sci.*, vol. 39, no. 2, 1970, p. 30-32

DISTRIBUTION OF NICKEL IN THE MARINE SEDIMENTS OFF THE WEST COAST OF INDIA

P. S. N. MURTY, CH. M. RAO* AND C. V. G. REDDY*
National Institute of Oceanography, Panjim (Goa), India

THE distribution of trace elements and the possible factors influencing them in the shelf sediments off the west coast of India have been the subject of study for some time. In continuation of the results pertaining to phosphates, Murty *et al.*,[1] and Manganese, (Murty *et al.*[2]) estimations of nickel were carried out and the present paper gives an account of its distribution, and the relationship it bears to other important elements in these sediments.

The location of Stations from where the samples were collected are given in Fig. 1.

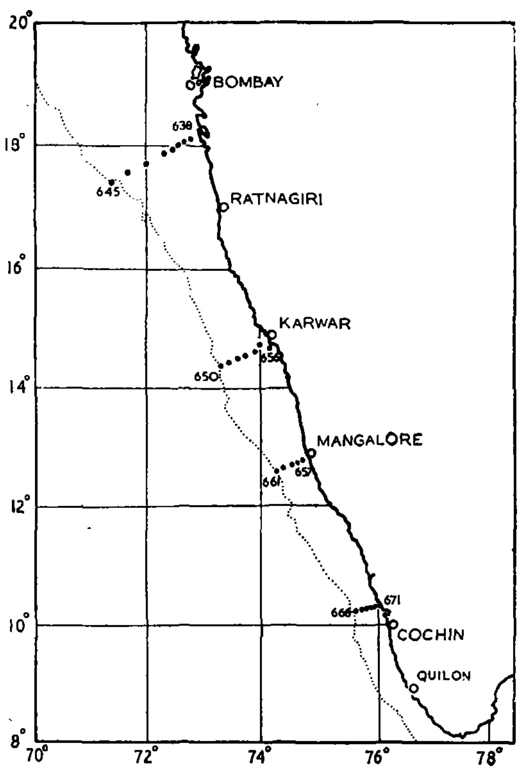

FIG. 1. Map showing the station locations.

The marine sediments fringing the west coast of India exhibit texturally, chemically and mineralogically certain well-defined distribution patterns. The inner shelf (upto 20 fms.) is covered by silty clays or clayey silts with very low carbonate content and this is followed seaward by a zone of silty or clayey sands on the rest of the shelf and slope regions characterised by a high carbonate content.[3] This is particularly so between Cochin and Karwar while off Bombay the shelf is covered for a greater part by fine-grained sediments. Studies on the organic matter (in the bulk sediments) have shown that the sediments in the inner shelf and the slope regions are characterised by a higher organic content than those in the region in between.[4] Manganese content shows a distinct trend in that it decreases in a direction seaward and away from land and also from north to south.[2] Clay minerals also exhibit regional variations. (*i*) The sediments off Bombay and Karwar are characterised by the presence of predominantly mixed layers of montmorillonite and illite with subordinate amounts of kaolinite group of minerals ; (*ii*) the sediments off Mangalore by the presence of approximately equal proportions of mixed layers of montmorillonite and illite and kaolinite group of minerals ; and (*iii*) the sediments off Kerala coast having predominantly kaolinite group of minerals with subordinate amounts of montmorillonite.

The estimations of nickel were carried out by the method described in Sandel[5] while iron and organic carbon were carried out respectively by the methods given by Snell and Snell[6] and ElWakeel and Riley.[7] All the analyses were carried out only on the silt and clay fractions and not on the bulk sample. All the colorimetric determinations were made on 'UNICAM' spectrophotometer SP 500.

Table I gives the contents of nickel, organic carbon, iron, manganese and calcium carbonate along with the depths from where the samples were collected. In order to understand the nature of relationship existing between nickel and other parameters analysed, correlation coefficients have been calculated. The values obtained between nickel and organic carbon, calcium carbonate, iron and manganese are 0·1680, − 0·2182, 0·3349 and 0·3703 respectively. The values of correlation coefficients

* From the branch establishment of National Institute of Oceanography at Cochin.

TABLE I

Stn. No.	Depth	Concentration of				
		Nickel in ppm	Organic carbon in %	Calcium carbonate in %	Manganese in %	Iron in %
638	13	40	1·59	2·5	0·077	3·65
639	17	36	1·48	41·5	0·072	2·5
640	19	24	1·14	39·0	0·064	2·3
641	19	33	1·41	22·5	0·055	4·50
642	26	45	1·86	20·0	0·037	1·55
643	38	29	2·48	32·0	0·028	1·60
645	250	34	6·24	30·0	0·009	2·15
656	10	53	2·24	0·0	0·055	3·55
654	25	30	1·21	0·0	0·058	2·20
653	32	25	1·25	0·0	0·046	1·90
652	42	19	2·00	42·0	0·029	0·20
651	55	20	2·20	0·0	0·017	0·40
650	110	27	2·57	50·1	0·027	0·30
657	10	27	2·83	4·0	0·045	3·65
658	17	21	2·73	7·0	0·037	3·65
659	23	16	2·38	24·0	0·032	1·95
660	43	28	2·17	..	0·033	1·75
661	105	22	2·93	28·5	0·039	2·75
671	13	38	3·90	0·0	0·031	5·10
670	14	34	2·98	0·0	0·028	4·25
669	17	33	2·62	17·0	0·030	4·30
668	23	38	2·76	12·0	0·020	4·85
667	32	12	2·45	18·0	0·020	3·9
666	46	33	3·73	3·8	0·014	3·60

Note: Values of manganese and calcium carbonate are borrowed from Murty *et al.*[2] and Nair *et al.*[3] respectively.

obtained in respect of nickel and iron in relation to depth along each section are given in Table II. A careful examination of the data permits the following generalizations:

TABLE II

Name of the section	r-value for nickel	r-value for iron
Off Bombay ..	−0·19	−0·65
Off Karwar ..	−0·46	−0·52
Off Mangalore ..	−0·26	−0·72
Off Cochin ..	−0·39	−0·38

r for manganese has not been calculated as it is clearly evident from the data that it decreases with depth.

(*i*) The fine-grained sediments in the inner shelf and the sediments in the slope region contain relatively a higher amount of nickel than the sediments in the outer shelf. Even among the fine-grained sediments, the sediments off Bombay, Karwar and Cochin have relatively a higher concentration of nickel than the sediments off Mangalore.

(*ii*) Nickel co-varies with both manganese and iron. Relatively, it has a stronger correlation with manganese than with iron. It does not show any relationship with organic carbon.

(*iii*) *A negative relationship exists between nickel and both calcium carbonate and depth of sampling.*

Kraus-kopf[8] made an extensive study of the factors controlling the concentration of several trace elements in sea-water including nickel. He investigated in detail four processes for the removal of these elements namely (*i*) precipitation of insoluble compounds with ions normally present in sea-water, (*ii*) precipitation by sulphide ion in local regions of low oxidation potentials, (*iii*) adsorption by materials such as ferrous sulphide, hydrated ferric oxide, hydrated manganese dioxide and clay and (*iv*) removal by metabolic action of organisms. His results have shown that adsorption is the most important process for the removal of minor and trace elements from the sea-water and their deposition in marine sediments. Nicholls and Loring[9] and Hirst[10] suggested that there is a correlation between nickel and organic carbon content of the sediments and they consider that the latter acts as an adsorbant. Hogdahl[11] has shown that nickel is enriched in marine organisms relative to sea-water to a greater extent. According to Chester[12] nickel may be probably removed permanently from sea-water under conditions of low redox potential when organic rich sulphide-bearing sediments are formed.

In the present case it is possible that precipitation of nickel as insoluble compound does not take place as the sea-water is greatly under-saturated with regard to this element. Also, precipitation of nickel by sulphide is unlikely in the areas under study, in view of the fact that considerable mixing takes place in the shelf waters. pH measurements carried out by Rao and Madhavan[13] have shown that the environment is not the reducing type. Reports of heavy mortality of bottom animals[14] during certain seasons and consequent anoxic conditions are perhaps a transient or passing feature and not long enough to maintain low redox potentials and hence reducing conditions. It may be relevant to mention here that no sulphide odour is noticed in any of the samples collected.

Organic carbon in the silt and clay fraction follows the same trend as in the bulk samples. The distribution pattern observed in the sediments of (*a*) the inner shelf, (*b*) outer shelf and (*c*) slope regions has been attributed by Murty *et al.* (*loc. cit.*) respectively to (*i*) the highly productive nature of the coastal waters as a consequence of seasonal upwelling and the presence of fine-grained sediments in the inner shelf, (*ii*) the coarse-grained nature of the sediments in the outer shelf and the presence of oxygenated waters which destroy much of the organic matter and (*iii*) the preservation of organic matter in the slope sediments under oxygen poor waters. The organic carbon does not show any relationship with nickel in the present studies which indicates that it is not bound to organic carbon. The factors that favour organic carbon to act as an effective adsorbant are (*i*) the presence of high percentage of organic carbon in the sediments, (*ii*) absence of agitated and well-ventilated waters, (*iii*) slow rate of deposition and (*iv*) the presence of a reducing environment. Considering these factors and comparing the conditions obtaining in the different parts of the shelf, it could be seen that the organic carbon in the sediments of the outer shelf cannot act as an effective adsorbant. The inshore sediments, no doubt, contain a high percentage of organic carbon but the rapid rate of sedimentation taking place in this region prevents it from acting as an adsorbant as it will not be in effective contact with the overlying waters for a considerable period.

A negative relationship exists between nickel and carbonate content. This indicates that there is no enrichment of nickel in these sediments by the organisms in their tests.

Nickel co-varies with manganese and iron. Relatively, it has a stronger correlation with manganese. A comparison of the distribution patterns of manganese and nickel shows that they are closely similar in that (*i*) both show a negative trend with depth, (*ii*) in general both are enriched in the nearshore and slope sediments relatively to the sediments in the outer shelf, and (*iii*) both show a decreasing trend from north to south except in the case of the Cochin section where though manganese content is less, the nickel content is high. This similarity in distribution might suggest that they are both closely related in these sediments. Adsorption by clay minerals on their surfaces is considered to be more effective in nearshore areas owing to the higher concentration of suspended clay particles. Information available on the manganese content in the clay fraction of a few of the samples (Table III) shows that a considerable portion of manganese is concentrated in the clay fraction and that it shows the same trend as in the silt and clay fraction. The hydrographic conditions in the shelf region being similar along the different parts of the west coast of India, this can perhaps be attributed to (*i*) the differences in the source rocks present along the different parts along the west coast and (*ii*) the differences in the adsorption capacities of the different clay minerals present in the different regions. It is quite possible that nickel may also be simultaneously getting fixed up in the sediments by this process. Thus while this process may be operating it is not unlikely that a part of nickel might have entered the basin of deposition structurally combined with the sediment and from the present studies it is not possible to determine what proportion of nickel is derived from the sea-water and what proportion is detrital in origin.

TABLE III

Name of the section	Station No.	MnO content
Off Bombay ..	638	0·05
	642	0·03
Off Karwar ..	656	0·04
	652	0·03
Off Mangalore ..	657	0·02
	659	0·01
	661	0·02
Off Cochin ..	671	0·02
	669	0·01
	666	0·01

Along the Cochin section, the nickel content is high in spite of the fact that the manganese content is low. This may perhaps be due to (*i*) the presence of the basic rocks along this coast which contain a relatively higher content of nickel and (*ii*) the high content of iron in these sediments which may be scavenging the nickel from the waters. The relatively stronger correlation observed with iron than with manganese in the sediments of this section supports this surmise.

ACKNOWLEDGEMENT

The authors wish to thank Dr. N. K. Panikkar, Director, National Institute of Oceanography, Panjim (Goa), for his keen interest and encouragement in the present investigation and Shri R. Jayaraman, National Institute of Oceanography, Panjim, for his helpful suggestions in the preparation of this paper.

1. Murty, P. S. N., Reddy, C. V. G. and Varadachari, V. V. R., *Proc. Nat. Inst. Sci. India*, 1968, **34.**
2. —, Rao, Ch. M. and Reddy, C. V. G., *Curr. Sci.*, 1968, **37.**
3. Nair, R. R, and Abraham Pylee, *Bull. Nat. Inst. Sci. India*, 1968, **38.**
4. Murty, P. S. N., Reddy, C. V. G. and Varadachari, V. V. R., *Proc. Nat. Inst. Sci. India* (in press).
5. Sandell, E. B., *Colorimetric Determination of Traces of Metals*, Interscience, New York, 1950.
6. Snell, E. D. and Snell, C. T., *Calorimetric Method of Analysis*, I, 3rd ed., D. Van Nostrand Co., New York, 1949.
7. ElWakeel, S. K. and Riley, J. P., *J. Cons. Perm. Int. Explor. Mer.*, 1957, **22.**
8. Kraus-kopf, K. B., *Geochim. et Cosmoch. Acta*, 1956, **9.**
9. Nicholls, G. D. and Loving, D. H., *Ibid.*, 1962, **26.**
10. Hirst, D. M., *Ibid.*, 1962 *b*, **26.**
11. Hogdahl, O. T., *Trace Elements in the Ocean*, The Central Institute for Industrial Research, Oslo, 1963.
12. Chester, R., *Chemical Oceanography*. eds. J. P. Riley and G. Skirro, Academic Press, London and New York, Vol. **2.**
13. Rao, D. S. and Madhavan, N., *J. Mar. biol. Ass. India*, 1964, **2.**
14. Seshappa, G., *Nature, Lond.*, 1953, **171.**

Reprinted from *Proceed. natn. Inst. Sci. India*, vol. 35, B, no. 5, 1969, p. 377-384

DISTRIBUTION OF ORGANIC MATTER IN THE MARINE SEDIMENTS OFF THE WEST COAST OF INDIA*

by P. S. N. MURTY,† C. V. G. REDDY *and* V. V. R. VARADACHARI,
National Institute of Oceanography, Ernakulam

(Communicated by N. K. Panikar, F.N.I.)

(*Received 11 July 1968*)

Organic matter has been estimated in sediment samples collected from the continental shelf and slope regions along five sections normal to the coast off Bombay, Karwar, Mangalore, Cochin and Alleppey and its distribution studied. The study has revealed that the sediments in the inner shelf and the continental slope are characterized by a higher content of organic matter while the sediments in the region in between are relatively poor in their organic matter content. The regional distribution of organic matter has been discussed in relation to the texture of the sediments and their distribution as well as upwelling and other factors.

INTRODUCTION

Except for a few values reported by Wiseman and Bennette (1940) and the recent studies by Stewart *et al.* (1965) no information is available on the organic content of the recent marine sediments forming along the eastern margin of the Arabian Sea. It is, therefore, the object of this paper to give a short account of the distribution of organic matter in the shelf and slope sediments off the west coast of India between Bombay and Quilon.

MATERIALS AND METHODS

Samples of bottom sediments from the shelf and slope regions were collected along five sections normal to the coast between Bombay and Quilon (Fig. 1) using La Fond-Dietz snapper and a gravity corer during the 25th and 26th cruises of INS *Kistna* between 22nd March, 1965 and 1st April, 1965. In the region under study, the width of the shelf is about 90 miles in the north. It gradually narrows down to about 35 miles in the south. A number of small rivers join the sea at different places but their effect on the shelf may be very local. The samples collected represent essentially the top few inches of the deposit in the case of the snapper samples and the upper 12 to 28 inches in the case of the core samples.

For the estimation of organic matter sufficient quantity of the sample was taken and washed free of salts with distilled water. In the case of the

* Paper presented at the symposium on ***Processes and products of sedimentation*** held at Waltair in December 1966.

† *Present address:* National Institute of Oceanography, Miramar, Panjim, Goa.

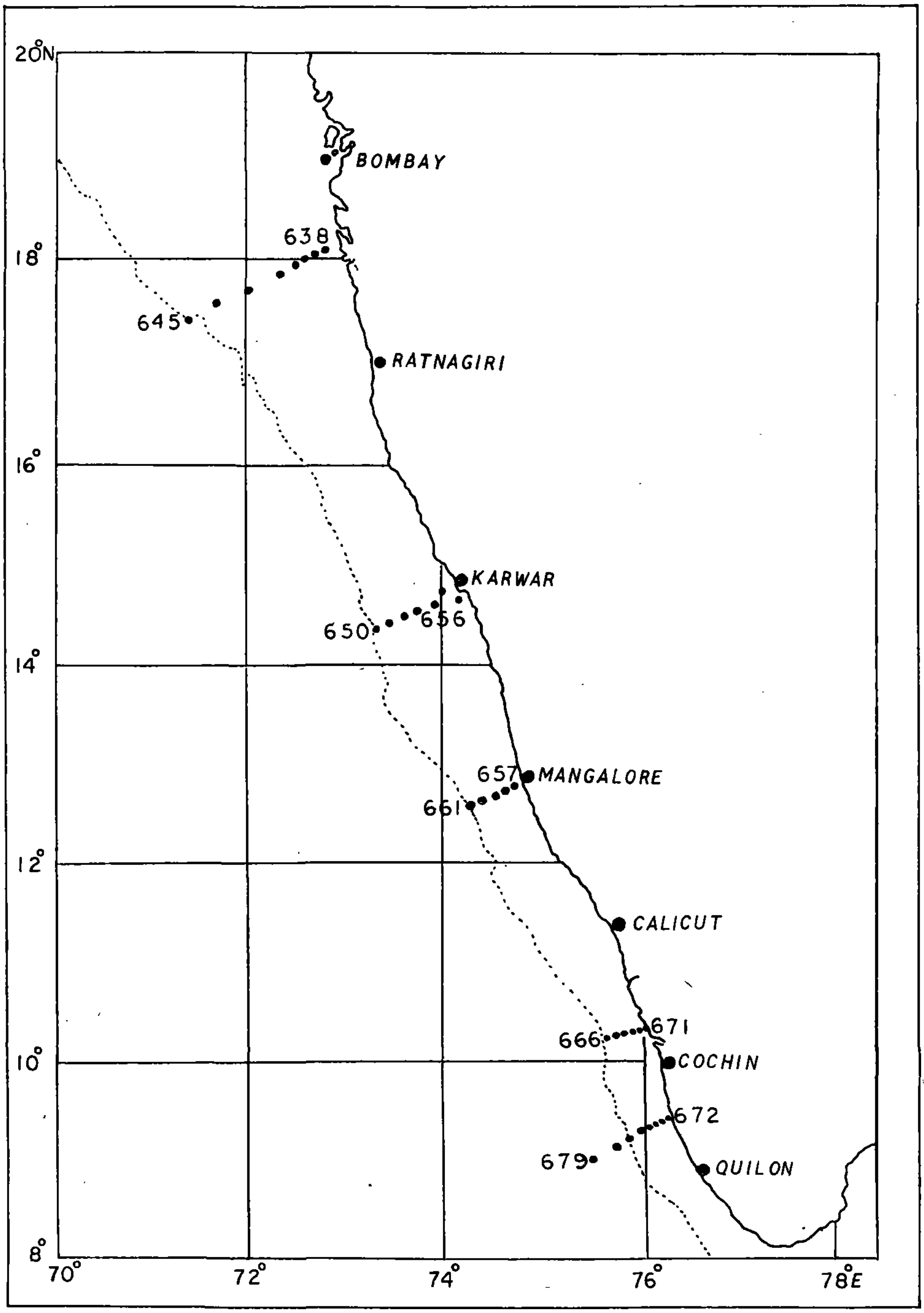

FIG. 1. Showing the locations of the sampling stations.

core samples, where the depthwise distribution of the organic content has been studied, each core was cut into 4″ long bits and washed free of salts for the determination of organic matter. The material was afterwards dried at 60 to 70 °C and then pulverized. In view of its highly complex chemical composition the organic matter in the marine sediments is determined indirectly, usually by multiplying by an appropriate factor, some property of the sediment that is related to the organic content such as the content of carbon, nitrogen, etc. In the present study organic carbon has been determined by the method of El Wakeel and Riley (1957) which consists of oxidizing the organic matter in the samples by a known quantity of chromic acid and determining the amount of acid consumed by titration against ferrous ammonium sulphate. The amount of organic matter is obtained by multiplying the organic carbon values by a factor 1·724 which is recommended by the soil chemists. This factor of 1·724 is used here as, according to Wiseman and Bennette (1940), 'the organic matter of marine muds collecting not far from land is undoubtedly partially of terrestrial origin and consequently the organic matter of these sediments is likely to have a ligno-protein with a high carbon content just as the soils'.

Results

Organic matter has been estimated in samples collected from 33 stations distributed over the five sections mentioned above. The results of the analysis are given in Table I. In view of the fact that physical characteristics such as the texture of sediment influence to some extent the accumulation of organic matter in the sediments, these characteristics have also been recorded to facilitate a better appraisal of the variations of the organic matter in the bottom sediments. Some of the salient features in the distribution of organic content of the sediments based on a study of these data are presented here.

1. On an average the organic matter constitutes about 2·55 per cent by dry weight which is just above the world average of 2·5 per cent for nearshore sediments (Trask 1939). The values, however, show a wide variation, ranging between 0·24 and 11·12 per cent.

2. The nearshore sediments and sediments on the slope have a high organic content while the sediments from the in between regions of the shelf are comparatively poor.

3. In regard to texture-organic content relationships, it is seen that invariably fine-grained sediments have a higher content of organic matter. Even within the fine-grained sediments, there is a lower percentage of organic matter in those samples collected from the shelf region off Bombay as compared to other areas.

Discussion

In a discussion of the factors responsible for the organic matter in the bottom sediments, Sverdrup *et al.* (1942) have indicated that an abundant

TABLE I

Serial No.	Station No.	Depth in fathoms	Type of sample	Sediment level in inches	Texture	% Organic matter
Off Bombay						
1	638	13	corer	0–4	Silty clay	1·92
				4–8	,,	1·94
				8–12	,,	1·73
2	639	17	snapper	0–4	Silty sand	0·24
3	640	19	corer	0–4	Sandy clay	0·89
				4–8	,,	1·43
				8–12	,,	1·07
4	641	19	,,	0–4	Silty clay	1·73
				4–8	,,	1·01
				8–12	,,	0·95
				12–16	,,	1·73
				16–20	,,	1·91
5	642	26	,,	0–4	,,	3·15
				4–8	,,	2·91
				8–12	,,	2·74
				12–16	,,	2·97
				16–20	,,	2·97
				20–24	,,	2·91
6	643	38	snapper	0–4	,,	0·89
7	645	250	corer	0–4	Clayey silt	11·12
				4–8	,,	9·52
				8–12	,,	7·79
				12–16	,,	9·12
				16–20	,,	7·61
				20–24	,,	7·67
Off Karwar						
8	656	10	,,	0–4	,,	3·81
				4–8	,,	2·50
				8–12	,,	4·45
				12–16	,,	4·39
				16–20	,,	3·86
				20–24	,,	3·76
				24–28	,,	3·31
9	655	12	,,	0–4	Silty clay	3·45
				4–8	,,	3·39
				8–12	,,	2·56
				12–16	,,	2·09
10	654	25	snapper	0–4	Silty sand	0·83
11	653	32	,,	0–4	,,	0·88
12	652	42	corer	0–4	,,	0·95
				4–8	,,	1·42
				8–12	,,	1·31
				12–16	,,	1·19
				16–20	,,	0·98
				20–24	,,	0·88
13	651	55	,,	0–4	,,	1·49
				4–8	,,	2·14
				8–12	,,	2·02
				12–16	,,	1·49
14	650	110	,,	0–4	Clayey sand	3·69
				4–8	,,	2·43
				8–12	,,	1·90
				12–16	,,	1·55
				16–20	,,	1·37
				20–24	,,	1·49
				24–28	,,	1·31

TABLE I—(*concld.*)

Serial No.	Station No.	Depth in fathoms	Type of sample	Sediment level in inches	Texture	% Organic matter
Off Mangalore						
15	657	10	corer	0–4	Clayey silt	3·93
				4–8	,,	4·70
				8–12	,,	3·75
				12–16	,,	4·04
16	658	17	,,	0–4	,,	4·40
				4–8	,,	3·33
				8–12	,,	3·83
				12–16	,,	3·33
				16–20	,,	1·96
				20–24	,,	1·96
17	659	23	,,	0–4	Silty sand	1·78
				4–8	,,	1·43
				8–12	,,	1·01
18	660	43	,,	0–4	Clayey sand	1·90
				4–8	,,	1·78
				8–12	,,	1·49
19	661	105	,,	0–4	Silty sand	3·15
				4–8	,,	2·65
				8–12	,,	2·83
Off Cochin						
20	671	13	snapper	0–4	Silty clay	3·80
21	670	14	,,	0–4	Silty sand	0·24
22	669	17	,,	0–4	,,	0·89
23	668	23	,,	0–4	,,	1·19
24	667	32	,,	0–4	,,	1·07
25	666	46	,,	0–4	Silty clay	1·71
Off Alleppey						
26	673	9	corer	0–4	Clayey silt	4·69
				4–8	,,	4·88
				8–12	,,	3·45
27	672	10	,,	0–4	Silty clay	4·52
				4–8	,,	3·35
				8–12	,,	3·45
28	674	20	,,	0–4	Silty sand	1·96
				4–8	,,	1·61
				8–12	,,	1·91
				12–16	,,	1·77
29	675	27	,,	0–4	,,	1·19
				4–8	,,	1·07
				8–12	,,	1·84
30	676	29	snapper	0–4	,,	1·31
31	677	85	,,	0–4	,,	2·44
32	678	250	corer	0–4	,,	5·34
				4–8	,,	4·94
				8–12	,,	2·91
33	679	370	,,	0–4	,,	5·04
				4–8	,,	5·17
				8–12	,,	3·86

supply of organic matter in the overlying column of water, a relatively rapid rate of accumulation of fine-grained inorganic matter and a low oxygen content of the waters immediately above the bottom sediments would favour high organic content in the bottom sediments. Deposits exceptionally rich in organic matter are encountered in areas where the upwelling waters fertilize the surface layers of the open ocean (Kuenen 1950). While sufficient data have been accumulated to show the existence of seasonal upwelling in different areas along the west coast of India (Jayaraman and Gogate 1957; Banse 1959; Carruthers *et al.* 1959; Ramamritham and Jayaraman 1960; Varadachari and Sarma 1964; Gangadhara Reddy and Sankaranarayanan 1966), not much information is available in regard to actual estimates of organic production in different shelf areas along this coast. The inference that the coastal waters along the west coast are highly productive is derived from the data on the distribution of phytoplankton as well as fishery production in different areas and during different seasons (Subrahmanyan 1959; Gogate 1960; Sudarshan 1964; Ramamurthy 1965). The high organic content of the waters could, therefore, be explained on this basis.

An examination of the texture of the sediments shows that they exhibit a distinct zonation in regard to their distribution in that the inner shelf up to a depth of about 20 fathoms is composed of silty clays or clayey silts and this is followed by zone of silty or clayey sands in the outer shelf (approximately 20 fms to the edge of the shelf) and in the slope regions. This is particularly so in the region between Alleppey in the south and Karwar in the north. Off Bombay, however, the major part of the shelf bottom consists of fine-grained sediments. The fine-grained character of the sediments as well as high organic production in the overlying waters explain the high content of organic matter in the nearshore sediments. But the slope sediments also, though coarse grained, contain a high per cent of organic matter. Coarse fraction studies on the slope sediments have revealed the presence in abundance of the tests of Globigerina and Globorotalia which indicates the existence of conditions favourable for the deposition of material in suspension. Further, the presence of glauconite in the cavities of some of the tests of Foraminifera points to the existence of a reducing environment (Jun-Ichi Takahashi 1939). Thus the existence of favourable conditions for the deposition and preservation of organic matter either present in the overlying waters or supplied to the slope from the adjacent shelf by currents may account for the high organic content in these sediments. Hydrographic studies along the west coast of India also reveal low levels of oxygen in the waters in the slope region. The sediments in the middle and outer shelf regions are relatively poor in their organic matter content when compared with the sediments in the nearshore and slope regions. Perhaps the texture of the sediments in this region is favourable for the waters to permeate through them and destroy the organic matter, deposited in them, by oxidation.

The fine-grained sediments off the Bombay coast contain a lesser amount of organic matter when compared with the sediments of similar texture in other sections. The reason for this may have to be sought in the different set of conditions obtaining off the Bombay coast. Any sediment that is supplied to the shelf is supplied during the south-west monsoon period. But the plankton bloom takes place only during the north-east monsoon period (Sudarshan 1964). Therefore the plankton debris settling to the bottom will not have enough masking cover of inorganic material and will have to remain exposed to the destructive actions of the bottom feeders and the bacteria till the next monsoon period. It is quite possible that under these conditions organic matter may not be preserved in these sediments to a higher degree.

The organic matter of the core samples does not show any systematic trend with depth. Although it is found to decrease with depth in some cases, in the majority of the cases there is a considerable degree of unsystematic variation. Correns (1937) working on 'Meteor samples' found similar trends of variations of organic carbon within the core. The organic content at any depth in a core sample is a function of several factors like the productivity of the region of sediment deposition, time of burial, rates of sedimentation and *in situ* biological and chemical activities. Present studies on the depthwise distribution of the organic matter reflects the existence of variable conditions along the shelf off the west coast of India through different periods.

Acknowledgements

The authors wish to express their deep gratitude to Dr. N. K. Panikkar, Director, National Institute of Oceanography, for his guidance and keen interest in the present investigations. They wish to express their thanks to Shri R. Jayaraman for his critical comments and helpful suggestions.

References

Banse, K. (1959). On upwelling and bottom-trawling off the south-west coast of India. *J Mar. biol. Ass. India*, **1**, 33–49.

Carruthers, J. N., Gogate, S. S., Naidu, T. R., and Leevatsu, T. (1959). Shoreward upslope of the layer of minimum oxygen off Bombay: Its influence on marine biology, especially fisheries. *Nature, Lond.*, 183, 1084–1087.

Correns, C. W. (1937). Die sedimente des aquatorialen Atlantischen Ozeans. *Wiss. Ergebn dt. atlant. Exped. 'Meteor'*, 3.

El Wakeel, S. K., and Riley, J. P. (1957). Determination of organic carbon in the marine muds. *J. Cons. perm. int. Explor. Mer.*, 22.

Gangadhara Reddy, C. V., and Sankaranarayanan, V. N. (1966). Distribution of phosphates and silicates in the shelf waters of the Arabian Sea along the west coast of India. *Abstracts, 2nd Internat. Oceanog. Congr., Moscow*, 1966.

Gogate, S. S. (1960). 'Some aspects of the hydrobiology of the Bombay waters.' Thesis submitted to Bombay University (M.Sc.).

Jayaraman, R., and Gogate, S. S. (1957). Salinity and temperature variations in the surface waters of the Arabian Sea off the Bombay and Saurashtra coasts. *Proc. Ind. Acad. Sci.*, 45, 151–164.

Jun-Ichi Takahashi (1939). 'Synopsis of Glauconitization.' *Soc. Econ. Paleon. and Mineral, Tulsa, Oklahoma*, 736 pp.

Kuenen, Ph. H. (1950). *Marine Geology.* John Wiley & Sons, New York, 551 pp.

Ramamritham, C. P., and Jayaraman, R. (1960). Hydrographical features of the continental shelf waters off Cochin. *J. Mar. biol. Ass. India,* 2, 199–207.

Ramamurthy, S. (1965). Studies on the plankton of the North Kanara coast in relation to the Pelagic fisheries. *J. Mar. biol. Ass. India,* 7, 129–149.

Stewart, Richard A., Pilkey, Orrin H., and Nelson, Bruce W. (1965). Sediments of the Northern Arabian Sea. *Marine Geol.,* 3, 411–427.

Subrahmanyan, R. (1959). Studies on the phytoplankton of the west coast of India. *Proc. Ind. Acad. Sci.,* 50.

Sudarshan, D. (1964). Observations on the plankton and trawler catches off Bombay. *J. Mar. biol. Ass. India,* 6, 222–225.

Sverdrup, H. U., Johnson, M. W., and Fleming, R. H. (1942). *The Oceans*—their physics, chemistry and general biology. Prentice Hall, New York, 1087 pp.

Trask, P. D. (1939). Organic content of recent marine sediments. *Soc. Econ. Paleon. and Mineral, Tulsa, Oklahoma,* 736 pp.

Varadachari, V. V. R., and Sarma, G. S. (1964). On the Vergence field in the north Indian Ocean. *Bull. National Geophysical Research Institute,* 2, 1–14.

Wiseman, J. D. H., and Bennette, H. (1940). Distribution of organic matter and nitrogen in the sediments from the Arabian Sea. *John Murray Expedition,* 3.

Reprinted from *Micropaleontology*, vol. 16, no. 3, 1970, p. 325-344

D. Vedantam
M. Subba Rao
Department of Geology
Andhra University
Waltair, India

Recent foraminifera from off Pentakota, east coast of India

ABSTRACT

A study of the foraminiferal content of samples of the shelf sediments off Pentakota on the east coast of India reveals that the outer shelf sediments at depths greater than 90 meters contain an abundant shallow-water warm-water benthonic fauna. A 70-cm. core taken from a depth of about 150 meters in the same area consists of oolitic sediments in the lower 45 cm. and silty clays in the upper 25 cm. The oolitic sediments of the core abound in shallow-water warm-water benthonic fossils. A comparison of the faunas in the core and in the surface sediments of the sea floor is made, and the extent of the relict fauna of the outer shelf sediments is evaluated. After the elimination of the relict elements from population counts, the living population of the sediments of the modern time surface is divided into three depth zones, ranging from 0 to 15 meters, from 15 to 40–45 meters, and greater than 40–45 meters. Sediments and fresh water discharged into the Bay of Bengal by the Godavari River to the south of Pentakota and carried northward along the coast and northeastward into deeper waters off Pentakota are found to inhibit the development of populations within the area of their influence.

INTRODUCTION

Our knowledge of the foraminifera in the bottom sediments of the Bay of Bengal is limited to a few investigations near the mainland of India and the islands scattered nearby. The earliest investigations were confined to the southern end of the Bay of Bengal, where it opens out into the Indian Ocean. Carter worked on specimens dredged up from the Gulf of Mannar, while Dakin recorded 131 species of foraminifera from the Gulf of Mannar off the coast of Ceylon, according to Ganapati and Satyavati (1958). Gnanamuthu (1943) listed 47 littoral species from near Krusadi Island in the Gulf of Mannar.

Ganapati and Satyavati (1958) were the first to report on the foraminifera of the continental shelf sediments off the east coast of India. They identified 103 species grouped into 65 genera and 23 families. Ganapati and Sarojini (1959) made a quantitative study of the foraminifera of the same samples of sediments on which Ganapati and Satyavati worked earlier, and reported the presence of another 57 species. Basing their species identifications mainly on the work of Ganapati and Satyavati (1958) and Ganapati and Sarojini (1959), Subba Rao and Vedantam (1968) reported the distributional pattern of foraminifera in the sediments across the shelf off Visakhapatnam on the east coast of India.

Bhatia and Bhalla (1964) described and illustrated 14 species of foraminifera from the shore sands at Puri, 400 km. north of Visakhapatnam. Ghose (1966) collected *Asterorotalia trispinosa* from the Digha beach about 350 km. north of Puri and made a detailed statistical study of the species. Bhalla (1968) reported 16 species from the Visakhapatnam beach sands. Raghothaman of Madras University (personal communication) has identified more than 100 species of foraminifera from the beaches of Madras State. Many species, however, are found to be common in these various reports.

The present investigation concerns the distribution of the foraminiferal populations of the continental shelf off Pentakota, a town located about 60 km. northeast of the northernmost mouth of the Godavari River on the east coast of India. The populations are compared with those from a core sample in the Holocene sediments of the same area to discover possible correlations and any reflection of change in environmental conditions since the populations in the lowest part of the core were buried.

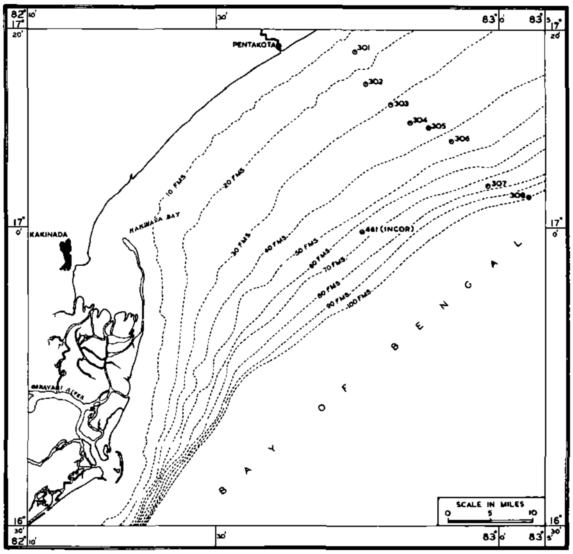

TEXT-FIGURE 1
Sample locality map, showing the western margin of the Bay of Bengal from Pentakota to Kakinada and the delta of the Godavari River.

METHODS OF STUDY

Eight samples of surface sediments were collected from the continental shelf off Pentakota on April 22, 1953, with the La Fond-Dietz snapper type of sampler by the staff of the Department of Geology, Andhra University, Waltair, India. A core of about 70 cm. in length was obtained in August, 1964, by M. Subba Rao, one of the authors, during the 18th Scientific Cruise conducted under the auspices of the Indian National Committee on Oceanographic Research (INCOR) during the International Indian Ocean Expedition Program. Station locations are shown in text-figure 1.

In his earlier studies of these sediment samples, one of the authors (M. Subba Rao) oven-dried them at 80 °C. They were subsequently treated overnight with 0.025 N sodium hexametaphosphate solution and washed on a 230-mesh sieve having openings of 0.063 mm. The sand-sized material retained on the sieve was dried and screened into different size fractions by shaking in a nest of sieves arranged on the Wentworth scale and fitted on a Ro-Tap. These well-preserved size fractions have been used in the present study for evaluating faunal differences and distributional patterns of individual species. Because of this limitation, no total population counts could be made, and so the frequency of the species in each sample is reported as very abundant, abundant, common or scarce.

TABLE 1
Characteristics of the sediments and waters of the Indian continental shelf off Pentakota. Samples collected April 22, 1953.

STATION No.	DEPTH IN METRES	% SAND	% SILT	% CLAY	SEDIMENT UNIT	% CALCIUM CARBONATE	% ORGANIC MATTER	TEMPERATURE OF WATERS °F.	SALINITY OF WATERS ‰
301	25	52.1	27.4	20.5	SAND-SILT-CLAY	19.0	1.19	SURFACE: 81 BOTTOM: 77	34.25
302	46	8.6	26.3	65.1	SILTY CLAY	10.0	1.35	SURFACE: 82 BOTTOM: 75	34.52
303	54	5.5	16.7	77.8	CLAY	9.0	1.55	SURFACE: 83 BOTTOM: 73	33.98
304	64	3.8	39.7	56.5	SILTY CLAY	10.0	1.67	SURFACE 84 BOTTOM 71	34.16
*305	72							SURFACE 84 BOTTOM: 71	33.98
306	96	58.1	22.6	19.3	SILTY SAND	48.0	1.23	SURFACE: 84 BOTTOM 67	34.77
307	156	18.5	38.6	42.9	SILTY CLAY	22.0	1.99	SURFACE 84 BOTTOM. 64	34.16
*308	205							SURFACE 83 BOTTOM 56	33.91

*SEDIMENT SAMPLES ARE NOT AVAILABLE FOR STUDY

The 70-cm. core was sampled at the top and bottom, and also at points 10, 25, 30, 40, 50 and 60 cm. from the top of the core. These samples are designated from top to bottom respectively as P_1, P_2, P_3, P_4, P_5, P_6, P_7, and P_8, the letter P standing for Pentakota. An aliquot of 5 gm. in weight was taken from each of these samples and treated in the same way as described in the foregoing paragraph. Total population counts are reduced to per gram weight of material. Percentage occurrence of each species is calculated and recorded. However, population counts in samples P_3 and P_7 are not included, as these samples do not register significant variations from the adjacent samples.

SEDIMENT SAMPLES

Sediment characteristics, such as sand, silt and clay ratios, and calcium carbonate and organic matter content, as well as the depths at which the samples were collected, are summarised in table 1. These data have been taken from the published papers of Subba Rao (1958, 1960). The outer shelf sediments are richer in calcium carbonate than the silty clays of the middle shelf. Oolitic grains and foraminiferal tests account for most of the carbonate content. Organic matter content shows a progressive increase from the inner to the outer shelf.

The coarse fraction of sample 301 contains mostly mineral grains, and these are followed in abundance by foraminifera. The rest of the fraction is composed of the shells and shell fragments of mollusks. Samples 302–304 do not contain much coarse material, and the foraminifera are not abundant. In the coarser grades of sample 306, shells and shell fragments of mollusks and oolitic grains predominate over the other constituents, while in the finer grades foraminifera constitute more than 40 per cent of the total constituents. Sample 307 contains 50 per cent shells and shell fragments of mollusks, 10 per cent globigerinids, 37 per cent benthonic foraminifera and 2 per cent ooliths in the 1–½ mm. size grade. The ½–¼ mm. size grade contains 40 per cent benthonic foraminifera, 34 per cent globigerinids, 14 per cent shells and their fragments, and 12 per cent ooliths. In the finer grades ooliths and broken fragments of globigerinids increase considerably in number.

The top 25 cm. of the core consists chiefly of a dark-grey clay, the bottom 45 cm. of a light-grey, calcareous clayey sand. Samples P_1 and P_2 of the core are 75 per cent silt and clay and 25 per cent sand-sized material, composed predominantly of foraminiferal tests. There are a few bivalves and their fragments. Ooliths are present in traces.

In sample P_3 the silt-clay content decreases considerably. Cream-coloured ooliths make their appearance in considerable numbers in all of the size grades. *Ammonia beccarii* occurs abundantly in the 1–½ mm. size grade. In the size grades greater than 1 mm., well-preserved mollusks and their fragments occur in some abundance. However, the foraminiferal population in this sample is not recorded in the present study.

In sample P_4, cream-coloured ooliths increase in number, and *Ammonia beccarii* specimens are considerably reduced in number as compared with those in sample P_3. Bryozoans are observed in the coarser grades.

In sample P_5 the cream-coloured and grey to dark-coloured ooliths occur in equal abundance.

Samples P_6–P_8 contain the largest-sized material in the entire core. It consists of corals, calcareous tubes partly worn out, unidentified calcareous fragments, and mollusks and their fragments. More bryozoans are recorded in these samples than in the upper sections of the core. Grey to dark-coloured ooliths abound.

Samples P_4–P_8 are composed of 80 per cent sand-sized material and 20 per cent silt and clay.

In no part of the core, from top to bottom, are terrigenous mineral grains observed in the coarse fractions.

SALINITY

Data on the salinity of the surface waters (Satyanarayana Rao, MS.) and on the temperature of both the surface and bottom waters (La Fond and Borreswara Rao, 1955) are also included in table 1.

Surface salinity varied from 33.1‰ to 34.77‰ on the day when the sediment samples were collected. The lowest value was recorded around the shelf edge, the highest at Station 306. Waters at Stations 303–305 are flanked by waters of higher salinity on either side. At

TABLE 2
Seasonal salinity variations at different water depths in the Bay of Bengal off Waltair.

MONTH	SALINITY (‰) AT A LEVEL OF				
	SURFACE	20 M.	75 M.	100 M.	150 M.
JANUARY	32.87	33.54			
FEBRUARY	32.71	32.96	33.95	34.30	
MARCH	33.46	34.04	34.75	34.80	
APRIL	33.30	33.60	34.10	34.60	34.60
MAY	33.70	33.90			
JUNE	33.30				
JULY	34.10				
AUGUST	33.70				
SEPTEMBER	19.35	28.00	33.91	34.50	34.50
OCTOBER	17.48				
NOVEMBER	23.05	26.01	32.15		
DECEMBER	26.46	28.23			

this time of the year the runoff from the Godavari River is at its low, and the inshore waters are affected more by upwelling (La Fond, 1957), which brings high salinity bottom waters to the surface inward of Station 303.

At Visakhapatnam, which is located about 90 km. north of Pentakota, the salinity of the surface waters increases outward from the coast. It was found to range from 18.26‰ in the 0–10 km. zone to 25.21‰ in the 30–40 km. zone in October, 1952, and from 33.78‰ to 33.31‰ in the same zones in March, 1953 (Ganapati and Murty, 1954).

Varadachari (MS.) established the vertical salinity pattern of the waters at Visakhapatnam with the use of data obtained during October, 1955–May, 1956, and in September, 1957. A portion of his data relevant to the present study is reproduced in table 2.

The surface salinity shows a very wide variation during the year, with the lowest values in October and the highest in July. The annual range of surface salinity reaches as high as 16.62‰. Such a large fluctuation is unusual for open-sea areas. However, the amplitude of the seasonal variation of salinity gradually decreases with depth, and the range becomes probably as low as 1‰ at a depth of 100 meters. The sudden and large drop in salinity taking place in September and October is associated with the flow of the southerly current bringing very dilute waters from the head of the Bay of Bengal. But these dilute low-salinity waters do not seem to influence significantly the salinity of waters at depths below 100 meters.

A similar salinity pattern may be expected to prevail at Pentakota, too.

TEMPERATURE AND CURRENTS

On the day when the sediment samples were obtained, the temperature of the surface waters was found to increase steadily from 81 °F in the inshore area to 84 °F. around the shelf edge. On the other hand, the temperature of the bottom waters decreased steadily from 77 °F. at a depth of 25 meters to 56 °F. at a depth of 200 meters.

Based on data collected from October, 1952, to April, 1953, a series of maps was constructed to show both the vertical and lateral thermal variations of the coastal waters in different seasons of the year (Rama Sastry and Balarama Murty, 1957, pp. 296–315). The following information is obtained from these maps.

1) The temperature of the bottom waters varies from 81 °F. in October and November to 71 °F. in April at Stations 304–305, and from more than 65 °F. in October and November to 64 °F. in April at Stations 306–307. Thus, the greatest temperature difference of 10 °F. is located at Stations 304–305 at depths of 70–100 meters.

2) It appears from the maps that in the Pentakota area the currents are directed northward all through the year and at all depths, except that the bottom currents at 70 meters depth (Stations 304–305) are directed southward during the October to February period.

FORAMINIFERAL FAUNA

In the surficial sediments of the continental shelf off Pentakota, a composite foraminiferal fauna totaling 85 benthonic species in 15 families and 13 planktonic species in 2 families was found, and most of the species were identified (table 3). Taxonomic notes on most of the species are omitted, but eight species of the surficial sediments and 4 species in the core sample which are identified only at the generic level are described in an appendix and illustrated in three plates. At least one of these is a new species.

Of the 15 benthonic families recognised, the Miliolidae, Buliminidae, and Rotaliidae are represented by the largest number of species in that order. Together, they account for 55 per cent of the benthonic species, while the Lituolidae, Ophthalmidiidae, Peneroplidae, Alveolinellidae, Calcarinidae and Cassidulinidae are represented by only one species each. Whereas the miliolids dominate the inner shelf populations and the buliminids the outer shelf populations, the rotaliids are well distributed over the entire shelf.

The inner shelf and the outer shelf yield the highest number of species (50–60), while the middle shelf has the smallest number (30–40). It appears that the silty clays of the middle shelf support neither a rich variety nor an abundance of fauna.

Of the 85 benthonic species, six occur in great abundance in one sample or another: *Nonion grateloupi, N. incisus, Bolivina vadescens, B. compacta, Amphistegina radiata* and *Hanzawaia concentrica*. Sixteen species occur in abundance, 26 in moderation and 37 sparingly.

Of the 13 planktonic species, *Globigerina conglomerata* and *Globigerinoides trilobus* occur in great abundance in one sample or another; *Globigerina bulloides, Globigerinoides ruber* and *Globigerinella aequilateralis* occur in abundance; *Globigerina eggeri, G. hexagona, G. rubescens, Globigerinoides sacculifer, Globigerinita glutinata* and *Pulleniatina obliquiloculata* occur in moderation; and *Sphaeroidinella dehiscens* occurs sparingly.

In the core, 89 benthonic species in 13 families and 18 planktonic species in 2 families were identified (table 3). Of the 13 benthonic families, the Miliolidae, Buliminidae and Rotaliidae are represented by the largest number in that order. Together, they account for 64 per cent of the benthonic species found in the core, while the families Ophthalmidiidae, Peneroplidae, Amphisteginidae and Cassidulinidae are represented by only one species each. The miliolids, the nonionids, and to some extent the rotaliids are represented in rich variety at the bottom of the core, while the buliminids maintain their variety all along the length of the core. There is a gradual decrease in the diversity of the fauna from the bottom to the top of the core. While the bottom section of the core contains 67 species, there are only 24 species at the top of the core. The foraminifera attain their greatest abundance in terms of the number of specimens in the middle sections of the core. The lowest number of specimens were recorded at the top of the core. Even though the middle section of the core is lithologically the same as the bottom section, the population is much smaller in the latter. It is understandable that the population at the top of the core is very much diluted by the heavy load of sediment deposition. There emerges a striking relationship in which the population with the greatest number of specimens per gram weight of sediment does not coincide with the population with the highest number of species. A similar relationship was observed off the west coast of Central America by Bandy and Arnal (1957).

Only 3 of the 89 benthonic species occur in sufficiently great abundance to constitute more than 10 per cent of the total population in any one sample (*Uvigerina peregrina, Bolivina vadescens* and *Ammonia beccarii*), 8 in sufficient abundance to constitute 5–10 per cent (*Nonion grateloupi, Buliminella elegantissima, Bolivina spathulata, B. seminuda, B. compacta, Cancris oblonga, Cassidulina laevigata* and *Hanzawaia concentrica*), 32 in moderately significant numbers (1–5 per cent), and 46 in traces (less than 1 per cent).

TABLE 3
Distribution of foraminifera in the sediments of the Bay of Bengal off Pentakota.

DISTRIBUTION IN THE CORE OF BENTHONIC FORAMINIFERA — KEY: NUMBERS REPRESENT PERCENTAGE OF EACH SPECIES IN THE TOTAL BENTHONIC POPULATIONS. S. INDICATES SCATTERED PRESENCE (LESS THAN 1 PERCENT). PLANKTONIC AND BENTHONIC POPULATIONS ARE COMPUTED SEPARATELY.

DISTRIBUTION IN SEA-FLOOR SURFACE SEDIMENTS OF BENTHONIC FORAMINIFERA — KEY: OCCURRENCE IS INDICATED BY VA: VERY ABUNDANT; A: ABUNDANT; C: COMMON; S: SCARCE. BENTHONIC AND PLANKTONIC POPULATIONS ARE REPORTED SEPARATELY.

SAMPLE No.:	P_1	P_2	P_4	P_5	P_6	P_8	SAMPLE No.:	301	302	303	304	306	307
DISTANCE OF SAMPLE FROM THE TOP OF THE CORE IN CM.	TOP	10	30	40	50	BOTTOM	DEPTH IN METRES	25	46	54	64	96	156
TOTAL BENTHONIC POPULATIONS PER GM. WEIGHT OF MATERIAL.	2400	4180	14880	12350	5200	5100	NOT ESTIMATED						
PERCENTAGE OF BENTHONIC IN THE TOTAL POPULATIONS.	64	63	85	89	86	88							
LITUOLIDAE													
1. HAPLOPHRAGMOIDES CANARIENSIS								S		S			
TEXTULARIIDAE													
2. TEXTULARIA AGGLUTINANS			1	1	1	3		S	A			S	S
3. T. CANDEIANA		S			2	S		S				S	
4. T. AFF. CANDEIANA	S			S	S								
5. T. FOLIACEA		S				S		S					
6. T. MAYORI			S	S				S				S	
7. T. AFF. XERIMBAENSIS												S	
8. BIGENERINA NODOSARIA								S	C				
VERNEUILINIDAE													
9. GAUDRYINA TRIANGULARIS ANGULATA				S									
10. CLAVULINOIDES CF. APERTURA				S	S								
MILIOLIDAE													
11. QUINQUELOCULINA AGGLUTINANS			S			S		A				C	S
12. Q. VULGARIS			1	1	2	1		A	A	C	C	C	S
13. Q. AUBERIANA				S	S	1				S		C	S
14. Q. BICOSTATA			S		S	S		A		C	S	S	C
15. Q. OBLONGA			1	1	3	S		C	S	S	S	S	S
16. Q. SCHLUMBERGERI						1							
17. Q. LAMARCKIANA								C					
18. Q. AFF. LAMARCKIANA					S			S					
19. Q. CANDEIANA						S							
20. Q. SAGRAI								S					
21. Q. CUVIERIANA								S	A	C	S	S	S
22. Q. SCHREIBERSII						S							
23. Q. RETICULATA													S
24. Q. SP.					S	S		A		S	S	S	
25. MILIOLINELLA SUBROTUNDA						1							
26. SCHLUMBERGERINA ALVEOLINIFORMIS				S					S				
27. MASSILINA SP.								S					
28. SPIROLOCULINA ARENARIA						S							
29. S. COMMUNIS				S	S	S		C	S	S	S	S	S
30. S. INDICA					S			S	S	S	S	S	S
31. S. CLARA	2	S										C	
32. S. DISPARILIS										S			S
33. S. SP.								S	S				S
34. SIGMOILINA TENUIS	S	1	1		S	S				S		S	A
35. HAUERINA INVOLUTA					S	S							
36. TRILOCULINA TRIGONULA					1	1							
37. T. TRICARINATA			2		1	1		S					
38. T. AFF. BICARINATA				S	S	1		C	A				
39. T. RUPERTIANA								S					
40. T. OBLONGA				S	1	S							
41. T. SP. A					1								
42. T. SP. B				S	S								
43. T. SP. C					S								
44. ADELOSINA LAEVIGATA								S		S	S		
45. FLINTINA BRADYANA								C	S			S	S
46. ARTICULINA SAGRAI					S								
OPHTHALMIDIIDAE													
47. OPHTHALMIDIUM SP.								S					
48. VERTEBRALINA STRIATA						S							
LAGENIDAE													
49. ROBULUS LIMBOSUS	4	2	3	2	1	S			C	S	S	C	C
50. R. CALCAR				S	S	S				S	S	C	S
51. NODOSARIA CATESBYI	S		S	S	1	S				S		C	C
52. LAGENA TENUIS									C		S	S	
53. L. STRIATA						S							
54. L. SP.					S			S		S	S	S	
55. DENTALINA VERTEBRALIS ALBATROSSI													S
56. GLOBULINA GIBBA								S	S	S			
NONIONIDAE													
57. NONION GRATELOUPI	2	2	2	2	S	2		C	C	A	VA	C	A
58. N. INCISUS		S						S	VA	VA	VA	C	
59. N. TRANSLUCENS						S							
60. ELPHIDIUM CRISPUM		S		1		S		S				S	
61. E. CRATICULATUM					S	1		S					
62. E. MACELLUM								C				C	C
63. E. DISCOIDALE						S		S	S				
64. E. STRIATOPUNCTATUM						S		C	S	C		S	C
65. E. HISPIDULUM						S							
CAMERINIDAE													
66. OPERCULINA AMMONOIDES				S		S		A				S	C
67. O. GRANULOSA				S	S	S		C				S	C
68. O. BARTSCHI						S							
69. O. BARTSCHI VAR. ORNATA						S						S	S
70. OPERCULINELLA SP.													S
PENEROPLIDAE													
71. PENEROPLIS PERTUSUS												S	
72. SORITES MARGINALIS						S							
ALVEOLINELLIDAE													
73. ALVEOLINELLA QUOYI												S	S

DISTRIBUTION IN THE CORE OF BENTHONIC FORAMINIFERA							DISTRIBUTION IN SEA-FLOOR SURFACE SEDIMENTS OF BENTHONIC FORAMINIFERA						
SAMPLE No.	P_1	P_2	P_4	P_5	P_6	P_8	SAMPLE No.	301	302	303	304	306	307
DISTANCE OF SAMPLE FROM THE TOP OF THE CORE IN CM.	TOP	10	30	40	50	BOTTOM	DEPTH IN METRES	25	46	54	64	96	156
BULIMINIDAE													
74. BULIMINA MARGINATA		S		S	1	S				S	S	S	S
75. B. AFFINIS	1	S		S	S								C
76. BULIMINELLA ELEGANTISSIMA	6	2	S	1	3	S						S	C
77. REUSSELLA ACULEATA			1	S		S							
78. ANGULOGERINA ANGULOSA		S											
79. UVIGERINA PEREGRINA	13	18	12	S	4	3						A	S
80. U. PROBOSCIDEA	S	1	S		2	S			C	C	C	S	A
81. TRIFARINA BRADYI	S	S	S	S	S	S		S		S		S	C
82. BOLIVINA VADESCENS	33	41	39	44	25	11		S	C	C	VA	A	VA
83. B. SPATHULATA	S	7	3	4	2	S						S	C
84. B. SEMINUDA	6	4	2	3	8							S	S
85. B. ROBUSTA	1	4	1	3	2	1			C		A	C	A
86. B. COMPACTA	1	1	8	S	6	13		C	A	VA	C	A	VA
87. B. SPINEA					S	S							
88. B. SP.				2	2	S				C			S
89. LOXOSTOMUM LOBATUM				S	S			S	S				S
90. L. CONVALLARIUM				S	1								
ROTALIIDAE													
91. SPIRILLINA VIVIPARA								S					
92. NEOCONORBINA PATELLIFORMIS						S							
93. DISCORBIS AUSTRALIS			S	1	1	S		S	S	S	S	S	S
94. GYROIDINA SOLDANII			S	S	S	S							
95. EPONIDES SUBORNATUS		S								S			S
96. AMMONIA BECCARII	7	4	S	1	1	10		A	A	A	C	C	C
97. A. BECCARII VAR. TEPIDA						S		C	S	C	S	S	S
98. A. PAPILLOSA	2	1	1	1	1	1		C	A	C	S	S	C
99. A. AFF. PAPILLOSA	S	S	S	S	S	2		C	A	S		S	C
100. PSEUDOROTALIA SCROETERIANA						S		A	C	C			S
101. ASTERORORTALIA TRISPINOSA			S		S	S		S	A	S	S	S	S
102. ROTALIA CALCAR		S		S									
103. CANCRIS OBLONGA	2	2	4	4	8	6		S	S	S	S	C	C
AMPHISTEGINIDAE													
104. ASTERIGERINA SP.												S	S
105. AMPHISTEGINA RADIATA		1	S	S	S	3		VA		S	S	VA	VA
CALCARINIDAE													
106. CALCARINA SPENGLERI												S	
CASSIDULINIDAE													
107. CASSIDULINA LAEVIGATA	6	3	8	S	S	S				S	S	S	A
108. CASSIDELLA BRADYI	2	1		2	2				S	S		S	S
ANOMALINIDAE													
109. CIBICIDES LOBATULUS			S	S	1	1		C	C	S	S	C	C
110. C. CICATRICOSUS					S	1							S
111. C. MARGARITIFER												A	C
112. HETEROLEPA DUTEMPLEI	S		S	1	1	1		A	S	S	S	S	S
113. HANZAWAIA CONCENTRICA	1	1	3	6	4	6		A	VA	VA	A	A	A

DISTRIBUTION IN THE CORE OF PLANKTONIC FORAMINIFERA — KEY: NUMBERS REPRESENT PERCENTAGE OF EACH SPECIES IN THE TOTAL PLANKTONIC POPULATIONS. S. INDICATES SCATTERED PRESENCE (LESS THAN 1 PERCENT). PLANKTONIC AND BENTHONIC POPULATIONS ARE COMPUTED SEPARATELY.

DISTRIBUTION IN SEA-FLOOR SURFACE SEDIMENTS OF PLANKTONIC FORAMINIFERA — KEY: OCCURRENCE IS INDICATED BY VA: VERY ABUNDANT; A: ABUNDANT; C: COMMON; S: SCARCE. BENTHONIC AND PLANKTONIC POPULATIONS ARE REPORTED SEPARATELY.

SAMPLE No.:	P_1	P_2	P_4	P_5	P_6	P_8	SAMPLE No.:	301	302	303	304	306	307
DISTANCE OF SAMPLE FROM THE TOP OF THE CORE IN CM.	TOP	10	30	40	50	BOTTOM	DEPTH IN METRES	25	46	54	64	96	156
TOTAL PLANKTONIC POPULATIONS PER GM. WEIGHT OF MATERIAL.	1350	2460	3600	1450	870	700	NOT ESTIMATED						
PERCENTAGE OF PLANKTONIC IN THE TOTAL POPULATIONS.	36	37	15	11	14	12							
GLOBIGERINIDAE													
114. GLOBIGERINA BULLOIDES	3	5	23	12	6	1		S	C	C	C	A	A
115. G. FALCONENSIS					1	3							
116. G. EGGERI	2	3	11	4	10	11		S	C	C	S	C	A
117. G. HEXAGONA	2	10	7	12	3	3			C	C	C	C	C
118. G. RUBESCENS	8	16	3	7	3	6			S	C	C	A	A
119. G. CONGLOMERATA	39	33	10	12	10	30		S	C	A	VA	A	VA
120. GLOBIGERINOIDES RUBER	11	9	13	7	3	16		S	C	C	A	A	A
121. G. SACCULIFER	S			2	1	6						C	C
122. G. TRILOBUS	5	8	8	4	13	1		S	C	C	A	A	VA
123. G. CONGLOBATUS						1							
124. G. SP.	3	2	2	2		1							
125. GLOBIGERINITA GLUTINATA	4	6	20	18	29	6			S	S	C	C	C
126. G. UVULA		1	1	9	3								
127. GLOBIGERINELLA AEQUILATERALIS	S			4	1	3		S	C	S	S	A	A
128. ORBULINA UNIVERSA			S	S	S	S							
129. PULLENIATINA OBLIQUILOCULATA	S	2	1		3			S	S	S		C	S
130. SPHAEROIDINELLA DEHISCENS						1							S
GLOBOROTALIIDAE													
131. GLOBOROTALIA MENARDII	17	5		6	13	10		S		C	S	C	A

TABLE 4
Restricted occurrence of foraminifera in the sediments of the Bay of Bengal off Pentakota.

SPECIES RESTRICTED TO THE MODERN TIME SURFACE	OCCURRENCE	SPECIES RESTRICTED TO THE CORE (HOLOCENE)	OCCURRENCE
1 HAPLOPHRAGMOIDES CANARIENSIS	S	1. TEXTULARIA AFF. CANDEIANA	S
2. TEXTULARIA AFF. KERIMBAENSIS	S	2. GAUDRYINA TRIANGULARIS ANGULATA	S
3. BIGENERINA NODOSARIA	C	3. CLAVULINOIDES CF. APERTURA	S
4. QUINQUELOCULINA LAMARCKIANA	C	4. QUINQUELOCULINA SCHLUMBERGERI	C
5. Q. SAGRAI	S	5. MILIOLINELLA SUBROTUNDA	C
6. Q. CUVIERIANA	A	6. QUINQUELOCULINA CANDEIANA	S
7. Q. RETICULATA	S	7. Q. SCHREIBERSII	S
8. MASSILINA SP.	S	8. SPIROLOCULINA ARENARIA	S
9. SPIROLOCULINA DISPARILIS	S	9. HAUERINA INVOLUTA	S
10. S. SP.	S	10. TRILOCULINA TRIGONULA	C
11. TRILOCULINA RUPERTIANA	S	11. T. OBLONGA	C
12. ADELOSINA LAEVIGATA	S	12. T. SP. A	C
13 OPHTHALMIDIUM SP.	S	13. T. SP. B	S
14. LAGENA TENUIS	C	14. T. SP. C	S
15. DENTALINA VERTEBRALIS ALBATROSSI	S	15 ARTICULINA SAGRAI	S
16. GLOBULINA GIBBA	S	16. VERTEBRALINA STRIATA	S
17. ELPHIDIUM MACELLUM	C	17. LAGENA STRIATA	S
18. OPERCULINELLA SP.	S	18. NONION TRANSLUCENS	S
19. PENEROPLIS PERTUSUS	S	19. *ELPHIDIUM* HISPIDULUM	S
20. ALVEOLINELLA QUOYI	S	20. OPERCULINA BARTSCHI	S
21. SPIRILLINA VIVIPARA	S	21. SORITES MARGINALIS	S
22. ASTERIGERINA SP.	S	22. REUSSELLA ACULEATA	C
23. CALCARINA SPENGLERI	S	23. ANGULOGERINA ANGULOSA	S
24. CIBICIDES MARGARITIFER	A	24. BOLIVINA SPINEA	S
KEY—OCCURRENCE IS INDICATED BY: A – ABUNDANT C – COMMON S – SCARCE		25. LOXOSTOMUM CONVALLARIUM	C
		26. NEOCONORBINA PATELLIFORMIS	S
		27. ROTALIA CALCAR	S
		28. GYROIDINA SOLDANII	S
		29. GLOBIGERINA FALCONENSIS	C
		30. GLOBIGERINITA UVULA	A
		31. GLOBIGERINOIDES CONGLOBATUS	C
		32. G. SP.	C
		33. ORBULINA UNIVERSA	S

Of the 18 planktonic species, 9 occur in great abundance in one sample or another, 3 species in abundance (*Globigerina uvula, Globigerinoides sacculifer* and *Pulleniatina obliquiloculata*), and 5 species in moderately significant numbers (*Globigerina falconensis, Globigerinoides conglobatus, Globigerinoides* sp., *Globigerinella aequilateralis* and *Sphaeroidinella dehiscens*). *Orbulina universa* has a scattered occurrence.

The total planktonic population reaches its zenith in the same section of the core as the benthonic population. Its numbers decline towards the bottom by 60 per cent, while toward the top the reduction in numbers is by 50 per cent. But when percentage occurrence of the planktonic specimens in the total population is considered, they range from 11 to 15 per cent in the lower section, while in the upper section they range from 36 to 37 per cent.

A comparison of populations in the core with those in modern sediments reveals that, of a total of 131 species found in the area, only 74 species are common to both the core and the modern sediments; 24 species, most of them having a scattered distribution, are restricted to the surface sediments; and 33 species, almost all of them occurring only in traces, are restricted to the core's Holocene sediments. The restricted occurrence of the species is illustrated in tables 4 and 5.

Furthermore, the uppermost clayey section of the core contains 33 species, while the deepest surface sediment sample off Pentakota contains 57 species, even though both samples come from about the same depth, the difference being that the core is located a few kilometers south of the Pentakota section. It may be noted that the deep-water sediments from corresponding

TABLE 5
Foraminiferal families in core and surface sediments.

FAMILY	TOTAL No. OF SPECIES RECORDED IN THE ENTIRE AREA	No. OF SPECIES COMMON TO SURFACE SEDIMENTS AND CORE	No. OF SPECIES RESTRICTED TO SURFACE SEDIMENTS	No. OF SPECIES RESTRICTED TO CORE
1. LITUOLIDAE	1		1	
2. TEXTULARIIDAE	7	4	2	1
3. VERNEUILINIDAE	2			2
4. MILIOLIDAE	36	15	9	12
5. OPHTHALMIDIIDAE	2		1	1
6. LAGENIDAE	8	4	3	1
7. *NONIONIDAE*	9	6	1	2
8. CAMERINIDAE	5	3	1	1
9 PENEROPLIDAE	2		1	1
10. ALVEOLINELLIDAE	1		1	
11. BULIMINIDAE	17	13		4
12. ROTALIIDAE	13	9	1	3
13. AMPHISTEGINIDAE	2	1	1	
14 CALCARINIDAE	1		1	
15. CASSIDULINIDAE	2	2		
16. ANOMALINIDAE	5	4	1	
BENTHONIC TOTAL:	113	61	24	28
17 GLOBIGERINIDAE	17	12		5
18. GLOBOROTALIIDAE	1	1		
PLANKTONIC TOTAL:	18	13		5
TOTAL *POPULATIONS:*	131	74	24	33

depths off Visakhapatnam north of Pentakota contain a much larger number of species (Subba Rao and Vedantam, 1968), and that sediments from south of Pentakota contain a much smaller number of species. It is inferred that with the increasing influence of Godavari effluents toward the south, the richness and variety of the fauna declines, probably partly due to the low salinity caused by the influx of fresh water and partly due to the rapid sedimentation of large quantities of terrigenous materials. However, 29 of the 33 species found at the top of the core, the exceptions being *Textularia* aff. *candeiana, Angulogerina angulosa* and *Rotalia calcar* which are not found in the surface sediments, and *Textularia foliacea* which is represented only in the shallowest-water sediment sample (301), are found to occur not only in sample 307 but also in other samples, with varying depth ranges and abundance.

DISCUSSION

The continental shelf between Kakinada and Visakhapatnam is on an average about 50 kilometers wide. Only ephemeral rivers debouch into the sea on this part of the coast. The shelf does not seem to be indented by submarine canyons or valleys. This part of the shelf constitutes a distinct environment, for it differs from the shelf to the north, which is cut into by numerous submarine canyons (La Fond, 1964; Subba Rao *et al.*, 1967), and also from the shelf to the south, which is covered by clays and silty clays formed by the deposition of suspended particles discharged into the Bay of Bengal by the Godavari and Krishna Rivers.

The outer part of the Visakhapatnam–Kakinada shelf is occupied by calcareous sediments, while the inner shelf at depths of less than 100 meters and the continental slope as well are occupied by clastic sediments. The calcareous sediments comprise ooliths, foraminiferal tests, and shells and shell fragments of other organisms, those of bivalves preponderating. Having considered the different aspects of these shelf sediments, Poornachandra Rao (1957) and Subba Rao (1958; 1964, p. 85) concluded that the oolitic sediments and the detrital sands to their landward side were laid down in an environment of lowered sea-level, probably in the final Pleistocene glacial stage, and that this zone of calcareous sediments, since the postglacial rise of sea-level, has not as yet been masked by Recent deposition of terrigenous sands and muds coming either from the river mouths or from coastal erosion. Numerous observations of ooliths forming in modern shallow waters, and the association between ooliths and shallow-water living foraminifera, some of which are discoloured brown and replaced by grey to greenish-black material, were advanced as evidence of their original emplacement during low stands of sea level. Naidu (1968) reports an age of 10,800±55 years B.P. for a composite sample of calcareous ooliths and littoral shells taken from the core under study at a depth of 35 cm. from the top of the core.

The calcareous sediments, which have their greatest spread off Visakhapatnam, are overlapped to the south by the Godavari sediments (Subba Rao, 1964, p. 79). Pentakota, which is located 60 km. northeast of the mouth of the northernmost distributary of the Godavari River, marks the approximate southern limit of the calcareous zone.

The calcareous sediments of the outer shelf, where net deposition of clastic sediments is insignificant in the Recent, must have been reworked, especially by waves and currents during the storms which frequently rage over the Bay of Bengal. They are also subject to large-scale contamination by the addition of planktonic debris and the remains of benthonic organisms that have entered the area from time to time with the rising sea level. Studies by Ludwick and Walton (1957) of dead and living benthonic foraminifera from the shelf edge calcareous prominences in the northeastern Gulf of Mexico, Walton's study of the living benthonic foraminifera in Todos Santos Bay, Mexico (1955), and other similar studies (Phleger, 1960, pp. 99–102) indicate that many fossil tests of shallow-water benthonic foraminifera which are observed in deeper waters are not those of living species. They concluded that these sediments were formed in an environment of a past lowered sea level.

The sediment samples of the present study were not preserved in neutralised formalin, which, if it had been used, could help in distinguishing living foraminifera from the tests of dead individuals. Nor have investigations of dead and living populations ever been reported from the area. Consequently, the occurrence of shallow-water warm-water species in anomalous association with a deep-water fauna in the middle and outer shelf sediments (table 3) renders it difficult to work out a zonal pattern for the Recent foraminifera in the area. Their comparison with the core populations is equally beset with riddles for the reasons stated below.

The lower part of the core (P_8–P_3), consisting of oolitic grains and possibly also of faecal pellets in abundance, may have been deposited in shallow warm waters about 11,000 years B.P. The upper part of the core, composed of silty clays, may have been deposited on a continuously deepening shelf immediately succeeding the oolitic sediments, or may have been deposited in the Recent, long after the cessation of oolitization processes and after the oolitic sediments had remained uncovered to be reworked over and again while the sea level was rising. However, the silty clays of the top of the core contain a shallow-water faunal element among which are *Alveolinella quoyi, Quinqueloculina* spp., *Cancris oblonga* and others which are discoloured brown, and *Amphistegina radiata* and *Elphidium* spp. which are replaced by dark-green material, probably glauconite. It is noteworthy that discolouring and replacement are symptomatic of the reworked nature of sediments (Maiklem, 1967).

That many shallow-water living species are present in the core but absent in the surface sediments and *vice versa* may be attributed to their elimination during reworking of sediments by burrowing animals, evidence for which may be considered the presence in the sediments of broken tests, sporadic frequency distribution of species, abnormally low numbers of foraminifera and large amounts of faecal pellets (Harman, 1964). However, the lowermost portion of the core is presumed to be unadulterated and to be typical of littoral sediments as they were originally laid down. The proportion of reworked material increases toward the top of the oolitic sediments. As the silty clays are deposited, ooliths, foraminiferal tests and other relict materials come from the north where the relict calcareous sediments remain exposed and get mixed into them. The reworked grains can not come from the south, for there they are buried deep under the Godavari sediments.

It is significant that, of the 89 benthonic species in the core, only 4 made their first appearance in the upper silty clays, 55 were confined to the lower oolitic part of the core, while 24 survived the drastically modified environmental conditions.

Giving due consideration to these aspects of sedimentation trends, an attempt has been made to work out the faunal assemblages of the modern time surface at Pentakota. Initially, the foraminiferal populations in the sea-floor surface sediments at Pentakota (table 3) have been divided into 17 groups on the basis of their depth ranges, and, similarly, the populations in the core have been divided into 14 groups according to their range in the core from the bottom upwards.

Of the 17 groups of foraminiferal populations of the surficial sediments (table 6), the first four groups include species restricted to the inner shelf, groups V and VI those which extend to the middle shelf as well. Groups VII through X include such species as occur both on the inner shelf inward of 60 meters as well as on the outer shelf but are conspicuous by their absence on the middle shelf at depths of 60–90 meters in the area which is covered by silty clays. Groups XI to XIII include the species which are restricted to the outer shelf, groups XIV and XV those which also extend to the middle shelf, and group XVI those which range over the entire shelf. Group XVII embraces all species of sporadic occurrence without a specific pattern.

In the core, first, species exclusive to each sample are listed (groups I–IV, table 7). Secondly, species starting at the bottom of the core and extending upward to various levels are listed (groups V–VIII). Thirdly, species that range from the bottom to the top are listed (group IX). And finally, species of sporadic occurrence (group X) are listed, followed by those with very limited vertical ranges within the core (groups XI–XIV).

Population distributions as now rearranged are correlated and certain broad patterns may be recognised.

Of the 10 species of group I (table 6) which are exclusive to sample 301 (depth: 25 meters), six are not represented in the core. They probably have entered the area in the modern environment. The remaining four are found to occur over a length of the lower part of the core. On the other hand, of the 18 species exclusive to the lowermost section of the core (group I, table 7), 12 have not been observed in the surface sediments. However, living specimens of some of these species, *Miliolinella subrotunda* and *Elphidium hispidulum*, for example, have been identified by T. Venkata Rao, a colleague of the authors, in the sediments of the lower reaches of a tidal stream at Pentakota. Obviously, the lowest portion of the core originally must have been deposited in waters shallower than 25 meters, possibly in surf and near-surf conditions, or even in a lagoonal environment.

Of the 6 species of groups II–V (table 6) having a depth range down to 30–35 meters, *Bigenerina nodosaria, Globulina gibba* and *Adelosina laevigata* are not reported in the core. *Schlumbergerina alveoliniformis* and *Elphidium discoidale* have restricted occurrences in P_8 and P_5 respectively, while *Triloculina* aff. *bicarinata* ranges from P_8 to P_5. They are all considered to be inner shelf species.

Quinqueloculina sp. and *Lagena* sp. of group VI (table 6), which are found down to 100 meters in depth, are represented only at the bottom of the core. Their specimens at depths more than 35 meters, are therefore believed to be relict. *Nonion incisus*, which occurs in abundance at 40–100 meters in depth, has a restricted appearance in the core at P_2. Thus, *Nonion incisus*, which started in deeper waters, steadily moved into shallower waters and has now established itself on the inner part of the middle shelf.

Of the 12 species of groups VI–X (table 6) that occur in shallower as well as in deeper waters, *Spiroloculina* sp. and *Elphidium macellum* are not represented in the core. *Pseudorotalia schroeteriana* and *Flintina bradyana* are restricted to the bottom of the core. *Operculina ammonoides* and *O. granulosa* range from P_8 to P_5, *Textularia agglutinans* ranges from P_8 to P_4, and *Loxostomum lobatum* has a limited range of P_6 and P_5, while the occurrence in the core of *Textularia candeiana, T.* aff. *candeiana, Quinqueloculina agglutinans* and *Elphidium crispum* is irregular and sporadic. These are all well-recognised shallow-water warm-water species, and therefore their specimens in the reworked outer shelf sediments are relict.

Of the 17 species of groups XI–XIII (table 6) that are here found only at depths greater than 100 meters, *Textularia* aff. *kerimbaensis, Quinqueloculina reticulata, Dentalina vertebralis albatrossi, Operculinella* sp., *Peneroplis pertusus, Alveolinella quoyi, Asterigerina* sp., *Calcarina spengleri* and *Cibicides margaritifer* are not found in the core. But these species are all well known for their restriction to shallow warm waters. Of the remaining 8 species, *Operculina bartschi* var. *ornata* and *Cibicides cicatricosus* are found only at the bottom of the core. These, together with the above nine species, obviously are not indigenous to the outer shelf, and their specimens, therefore, are relict in nature. *Spiroloculina clara* is a late entrant into the area and definitely is an outer shelf species. *Bulimina affinis* and *Bolivina seminuda*, which are present in the core from P_6 upwards, and *Buliminella elegantissima, Uvigerina peregrina* and *Bolivina spathulata*, which occur all along the length of the core, along with many others originally invaded the shallow water and have continued to thrive at the same place in the increasingly favourable depths for their development. The virtual absence of detrital mineral grains in the coarse fractions of the core samples and the presence of less than 20 per cent silty clay suggest that the waters were clearer and probably more saline than those of corresponding depths at present, so that the species adapted to high salinity and deep water, especially the planktonic species, could

TABLE 6
Foraminiferal depth ranges on the continental shelf off Pentakota.

KEY–OCCURRENCE IS INDICATED BY:– VA: VERY ABUNDANT; A: ABUNDANT; C: COMMON; S: SCARCE.
*SPECIES ARE NOT KNOWN TO OCCUR IN THE CORE.

STATION No.: DEPTH IN METRES:	301 25	302 46	303 54	304 64	306 96	307 156
GROUP I						
1. TEXTULARIA FOLIACEA	S					
2. *QUINQUELOCULINA LAMARCKIANA	C					
3. Q. AFF. LAMARCKIANA	S					
4. *Q. SAGRAI	S					
5. *MASSILINA SP.	S					
6. TRILOCULINA TRICARINATA	S					
7. *T. RUPERTIANA	S					
8. *OPHTHALMIDIUM SP.	S					
9. ELPHIDIUM CRATICULATUM	S					
10. *SPIRILLINA VIVIPARA	S					
GROUP II						
1. SCHLUMBERGERINA ALVEOLINIFORMIS		S				
GROUP III						
1 *BIGENERINA NODOSARIA	S	C				
2. TRILOCULINA AFF. BICARINATA	C	A				
3. ELPHIDIUM DISCOIDALE	S	S				
GROUP IV						
1. *GLOBULINA GIBBA	S	S	S			
GROUP V						
1. *ADELOSINA LAEVIGATA	S	?	S	S		
GROUP VI						
1. QUINQUELOCULINA SP.	A	?	S	S	S	
2. LAGENA SP.	S	?	S	S	S	
3. NONION INCISUS	S	VA	VA	VA	A	
GROUP VII						
1. TEXTULARIA CANDEIANA	S				S	
2. T. MAYORI	S				S	
3. ELPHIDIUM CRISPUM	S				S	
GROUP VIII						
1. *SPIROLOCULINA SP.	S	S				S
2. LOXOSTOMUM LOBATUM	S	S				S
3. PSEUDOROTALIA SCHROETERIANA	A	C	C			S
GROUP IX						
1. TEXTULARIA AGGLUTINANS	S	A			S	S
2. FLINTINA BRADYANA	C	S			S	S
GROUP X						
1 QUINQUELOCULINA AGGLUTINANS	A				C	S
2. *ELPHIDIUM MACELLUM	C				C	C
3. OPERCULINA AMMONOIDES	A				S	C
4. O. GRANULOSA	C				S	C
GROUP XI						
1. *QUINQUELOCULINA RETICULATA						S
2. *DENTALINA VERTEBRALIS ALBATROSSI						S
3. *OPERCULINELLA SP.						S
4. BULIMINA AFFINIS						C
5. CIBICIDES CICATRICOSUS						S
GROUP XII						
1. *TEXTULARIA AFF. KERIMBAENSIS					S	
2. SPIROLOCULINA CLARA					C	
3. *PENEROPLIS PERTUSUS					S	
4. *CALCARINA SPENGLERI					S	

STATION No.: DEPTH IN METRES:	301 25	302 46	303 54	304 64	306 96	307 156
GROUP XIII						
1. OPERCULINA BARTSCHI VAR. ORNATA					S	S
2. *ALVEOLINELLA QUOYI					S	S
3. BULIMINELLA ELEGANTISSIMA					S	C
4. UVIGERINA PEREGRINA					A	S
5. BOLIVINA SPATHULATA					S	C
6. B. SEMINUDA					S	S
7 *ASTERIGERINA SP.					S	S
8. *CIBICIDES MARGARITIFER					A	C
GROUP XIV						
1. ROBULUS CALCAR			S	S	C	S
2. CASSIDULINA LAEVIGATA			S	S	S	C
3. QUINQUELOCULINA AUBERIANA			S	?	C	S
4. SIGMOILINA TENUIS			S	?	S	A
5. NODOSARIA CATESBYI			S	?	C	C
GROUP XV						
1. ROBULUS LIMBOSUS		C	S	S	C	C
2. BULIMINA MARGINATA		S	S	S	S	S
3. UVIGERINA PROBOSCIDEA		C	C	C	S	A
4. CASSIDELLA BRADYI		S	S	?	S	S
5. BOLIVINA ROBUSTA		C	?	A	C	A
GROUP XVI						
1. QUINQUELOCULINA VULGARIS	A	A	C	C	C	S
2. Q. OBLONGA	C	S	S	S	S	S
3. *Q. CUVIERIANA	S	A	C	S	S	S
4. SPIROLOCULINA COMMUNIS	C	S	S	S	S	S
5. S. INDICA	S	S	S	S	S	S
6. NONION GRATELOUPI	C	C	A	VA	C	A
7. BOLIVINA VADESCENS	S	C	C	VA	A	VA
8. B. COMPACTA	C	A	VA	C	A	VA
9. DISCORBIS AUSTRALIS	S	S	S	S	S	S
10. AMMONIA BECCARII	A	A	A	C	C	C
11. AMMONIA BECCARII VAR. TEPIDA	C	S	C	S	S	S
12. A. PAPILLOSA	C	A	C	S	S	C
13. ASTEROROTALIA TRISPINOSA	S	A	S	S	S	S
14. CANCRIS OBLONGA	S	S	S	S	C	C
15. CIBICIDES LOBATULUS	C	C	S	S	C	C
16. HETEROLEPA DUTEMPLEI	A	S	S	S	S	S
17. HANZAWAIA CONCENTRICA	A	VA	VA	A	A	A
18. QUINQUELOCULINA BICOSTATA	A	?	C	S	S	C
19. ELPHIDIUM STRIATOPUNCTATUM	C	S	C	?	S	C
20. AMMONIA AFF. PAPILLOSA	C	A	S	?	S	C
21. AMPHISTEGINA RADIATA	VA	?	S	S	VA	VA
GROUP XVII						
1. *HAPLOPHRAGMOIDES CANARIENSIS	S		S			
2. *SPIROLOCULINA DISPARILIS			S			S
3. *LAGENA TENUIS		C		S	S	
4. TRIFARINA BRADYI	S		S		S	C
5. BOLIVINA SP.			C			S
6. EPONIDES SUBORNATUS			S			S

TABLE 7
Foraminiferal ranges in the core sample.

KEY: NUMBERS INDICATE PERCENTAGE OF EACH SPECIES IN THE TOTAL BENTHONIC POPULATIONS.
S. INDICATES SCATTERED OCCURRENCE.
*SPECIES ARE NOT KNOWN TO OCCUR IN THE SURFACE SEDIMENTS.

SPECIES	OCCURRENCE IN SAMPLE No.		
GROUP I	P_8		
1. *QUINQUELOCULINA SCHLUMBERGERI	I		
2. *MILIOLINELLA SUBROTUNDA	I		
3. *QUINQUELOCULINA CANDEIANA	S		
4. *Q. SCHREIBERSII	S		
5. *SPIROLOCULINA ARENARIA	S		
6. FLINTINA BRADYANA	S		
7. *VERTEBRALINA STRIATA	S		
8. *LAGENA STRIATA	S		
9. *NONION TRANSLUCENS	S		
10. ELPHIDIUM DISCOIDALE	S		
11. E. STRIATOPUNCTATUM	S		
12. *E. HISPIDULUM	S		
13. *OPERCULINA BARTSCHI	S		
14. O. BARTSCHI VAR. ORNATA	S		
15. *SORITES MARGINALIS	S		
16. *NEOCONORBINA PATELLIFORMIS	S		
17. AMMONIA BECCARII VAR. TEPIDA	S		
18. PSEUDOROTALIA SCHROETERIANA	S		
GROUP II	P_6		
1. QUINQUELOCULINA AFF. LAMARCKIANA	S		
2. SPIROLOCULINA INDICA	S		
3. *TRILOCULINA SP. A	I		
4. *T. SP. C	S		
5. *ARTICULINA SAGRAI	S		
6. LAGENA SP.	S		
GROUP III	P_5		
1. *GAUDRYINA TRIANGULARIS ANGULATA	S		
2. SCHLUMBERGERINA ALVEOLINIFORMIS	S		
NO SPECIES EXCLUSIVELY OCCURS IN SAMPLE P_4			
GROUP IV	P_2		
1. NONION INCISUS	S		
2. *ANGULOGERINA ANGULOSA	S		
3. EPONIDES SUBORNATUS	S		
NO SPECIES EXCLUSIVELY OCCURS IN SAMPLE P_1			
GROUP V	P_8	P_6	
1. QUINQUELOCULINA SP.	S	S	
2. *HAUERINA INVOLUTA	S	S	
3. *TRILOCULINA TRIGONULA	I	I	
4. ELPHIDIUM CRATICULATUM	I	S	
5. *BOLIVINA SPINEA	S	S	
6. CIBICIDES CICATRICOSUS	S	S	
GROUP VI	P_8	P_6	P_5
1. QUINQUELOCULINA AUBERIANA	I	S	S
2. SPIROLOCULINA COMMUNIS	S	S	S
3. TRILOCULINA AFF. BICARINATA	I	S	S
4. *T. OBLONGA	S	I	S
5. ROBULUS CALCAR	S	S	S
6. OPERCULINA GRANULOSA	S	S	S
7. OPERCULINA AMMONOIDES	S		S
8. BOLIVINA SP.	S	2	2

SPECIES	OCCURRENCE IN SAMPLE No.					
GROUP VII	P_8	P_6	P_5	P_4		
1. TEXTULARIA AGGLUTINANS	3	I	I	I		
2. QUINQUELOCULINA VULGARIS	I	2	I	I		
3. Q. BICOSTATA	S	S		S		
4. Q. OBLONGA	S	3	I	I		
5. TRILOCULINA TRICARINATA	I	I		2		
6. *REUSSELLA ACULEATA	S		S	I		
7. ASTEROROTALIA TRISPINOSA	S	S		S		
8. DISCORBIS AUSTRALIS	S	I	I	S		
9. *GYROIDINA SOLDANII	S	S	S	S		
10. CIBICIDES LOBATULUS	I	I	S	S		
GROUP VIII	P_8	P_6	P_5	P_4	P_2	
1. BULIMINA MARGINATA	S	I	S		S	
2. AMPHISTEGINA RADIATA	3	S	S	S	I	
GROUP IX	P_8	P_6	P_5	P_4	P_2	P_1
1. ROBULUS LIMBOSUS	S	I	2	2	2	4
2. NONION GRATELOUPI	2	S	2	2	2	2
3. BULIMINELLA ELEGANTISSIMA	S	3	I	S	2	6
4. UVIGERINA PEREGRINA	3	4	5	12	18	13
5. TRIFARINA BRADYI	S	S	S	S	S	S
6. BOLIVINA VADESCENS	11	25	44	39	41	33
7. B. SPATHULATA	5	2	4	3	7	5
8. B. ROBUSTA	I	2	3	I	4	I
9. B. COMPACTA	13	6	5	8	I	I
10. AMMONIA BECCARII	10	I	I	5	4	7
11. A. PAPILLOSA	I	I	I	I	I	2
12. A. AFF. PAPILLOSA	2	S	S	S	S	S
13. CANCRIS OBLONGA	6	8	4	4	2	2
14. CASSIDULINA LAEVIGATA	5	5	5	8	3	6
15. HANZAWAIA CONCENTRICA	6	4	6	3	I	I
16. SIGMOILINA TENUIS	S	S		I	I	S
17. NODOSARIA CATESBYI	S	I	S	S		S
18. UVIGERINA PROBOSCIDEA	S	2		S	I	S
19. HETEROLEPA DUTEMPLEI	I	I	I	S		S
GROUP X	P_8	P_6	P_5	P_4	P_2	P_1
1. TEXTULARIA CANDEIANA	S	2			S	
2. *T. AFF. CANDEIANA		S	S			S
3. T. FOLIACEA	S				S	
4. QUINQUELOCULINA AGGLUTINANS	S			S		
5. ELPHIDIUM CRISPUM	S		I		S	
6. *ROTALIA CALCAR			S		S	
GROUP XI	P_6	P_5				
1. *CLAVULINOIDES CF. APERTURA	S	S				
2. *TRILOCULINA SP. B	S	S				
3. LOXOSTOMUM LOBATUM	S	S				
4. *L. CONVALLARIUM	I	S				
GROUP XII	P_5	P_4				
1. TEXTULARIA MAYORI	S	S				
GROUP XIII	P_2	P_1				
1. SPIROLOCULINA CLARA	S	2				
GROUP XIV	P_6	P_5	P_4	P_2	P_1	
1. BULIMINA AFFINIS	S	S		S	I	
2. CASSIDELLA BRADYI	2	2		I	2	
3. BOLIVINA SEMINUDA	8	3	2	3	8	

invade waters much shallower than their normal habitat.

Of the five species of group XIV (table 6) which occur at depths of more than 50 meters, *Robulus calcar* and *Quinqueloculina auberiana* are represented only in the lower half of the core, while *Cassidulina laevigata*, *Sigmoilina tenuis* and *Nodosaria catesbyi* occur all along the length of the core. Thus, the former two are relict in the outer part of the outer shelf, the latter three being deep-water species.

The five species of group XV (table 6), *Robulus limbosus*, *Bulimina marginata*, *Uvigerina proboscidea*, *Cassidella bradyi* and *Bolivina robusta* are present virtually all along the core, although their absence in sample 301 is conspicuous. Probably they need a little higher salinity and clearer water with less turbulence. These may be reckoned as species of the middle and outer shelf.

Of the 21 species of group XVI (table 6) that are found in all of the surface sediment samples, and of the 19 species of group IX (table 7) that occur along the entire length of the core, only 9 species (*Nonion grateloupi*, ***Bolivina vadescens*, **B. compacta*, *Ammonia beccarii*, ***Ammonia papillosa*, **A.* aff. *papillosa*, **Cancris oblonga*, **Heterolepa dutemplei* and **Hanzawaia concentrica* occur in all samples of both sets. Species marked with a single asterisk increase in numbers toward the top of the core, just as they increase in numbers out to sea, while species marked with a double asterisk show a reverse relationship. Reduction in numbers of the latter group's specimens may be a result of their movement into shallower waters as the postglacial sea level rises and/or their partial destruction during the reworking of the sediments. *Nonion grateloupi* behaves the same way throughout, probably thereby showing its tolerance of large fluctuations in ecological factors. *Ammonia beccarii* is represented by a large number of specimens at the bottom of the core. Its numbers are reduced in the middle section, attain their peak in sample P_3 (not recorded in the tables), and toward the top of the core again dwindle considerably. It is most abundant in shallow-water sediments of the modern time surface. Its abundance, no matter where it is found, indicates shallow-water environment at the time of deposition.

**Quinqueloculina vulgaris* (P_8–P_4), **Q. oblonga* (P_8–P_4), **Spiroloculina communis* (P_8–P_5), *Discorbis australis*, **Ammonia beccarii* var. *tepida* (P_8), **Asterorotalia trispinosa*, ***Quinqueloculina bicostata* (P_8–P_4), *Elphidium striatopunctatum* (P_8), ***Amphistegina radiata* (P_8–P_2), *Cibicides lobatulus* (P_8–P_4) and *Spiroloculina indica* (P_6) have limited ranges of occurrence in the core. It must be emphasized that the species marked with a single asterisk occur in abundance in shallow water but are very much reduced in number in deep water. They are altogether absent in the upper half of the core. Either they must have developed tolerance for deep water or their specimens on the outer shelf are relict. Species marked with a double asterisk have a peak of abundance in shallow water and another in deep water. Like the first group of species, these are also not represented in the upper half of the core, with the exception of *Amphistegina radiata*. These species could rightly be included in group IX (table 6) but for their anomalous occurrence in the intermediate samples, too. It may safely be assumed that these are inner shelf species and that their specimens on the outer shelf must be treated as relict.

Of the 6 species of group XVII (table 6), which occur sporadically, *Haplophragmoides canariensis*, an inner shelf species, *Spiroloculina disparilis*, apparently a middle and outer shelf species, and *Lagena tenuis*, a middle shelf species, are not seen in the core, and they may have first appeared in the modern shallow waters. *Trifarina bradyi* is a species with a wide range of occurrence. *Bolivina* sp. (P_8–P_5) must be considered as relict. *Eponides subornatus* is an outer shelf species, and, like *Spiroloculina clara*, is a late entrant into the area.

Of the 18 planktonic species found in the area, *Globigerina falconensis*, *Globigerinita uvula*, *Globigerinoides conglobatus*, *G.* sp. and *Orbulina universa* are not found in the surface sediments. The other 13 species are abundant in the outer shelf sediments but occur in different ways in the core. *Globigerina falconensis*, *G. eggeri*, *Globigerinita uvulà*, *Globigerinoides sacculifer*, *G. conglobatus*, *Globigerinella aequilateralis*, *Orbulina universa* and *Sphaeroidinella dehiscens* occur in their greatest abundance at the bottom of the core. *Globigerina bulloides*, *G. hexagona*, *Globigerinoides trilobus* and *Globigerinita glutinata* occur abundantly in the middle section of the core. *Globigerina rubescens*, *Globigerinoides* sp., and *Pulleniatina obliquiloculata* occur in increasing frequencies toward the top of the core. *Globigerina conglomerata*, *Globigerinoides ruber*, and *Globorotalia menardii* have higher frequencies of occurrence both at the top and at the bottom of the core.

Globigerinita glutinata occurs in the lagoon and in the areas open to the ocean (Todd, 1961). *Globigerinoides ruber* and *G. sacculifer* are also described as lagoonal species (Phleger, 1960, p. 183). The former's abnormally high frequency of 29 per cent in P_6 and the high frequency of occurrence of the latter two in P_8 suggest lagoonal conditions at the time when samples P_8–P_6

were being deposited. However, the presence of other planktonic species in the lower part of the core in association with a shallow-water warm-water fauna indicates that the area was part of open ocean, probably with a reef complex along the coast, and that there was not much deposition of terrigenous sediments.

SALINITY, TEMPERATURE AND CURRENTS

As the salinity of the bottom waters of the shelf off Pentakota does not change appreciably from season to season, it may be presumed that it does not control the development of foraminifera. The silty clays of the shelf at depths of 40–100 meters, rich in organic content, are overlain with waters which undergo wide fluctuations in temperature through different seasons of the year. Furthermore, this is the zone where the bottom currents flow southward, instead of northward as at all other depths. These sediments contain the populations lowest both in variety and abundance. Thus, temperature appears to control the distribution of the fauna more than the other ecological factors do.

ORGANIC MATTER OF SEDIMENTS

Populations are smallest on the shelf at depths of 30–70 meters, where the sediments are silty clays and clays. These silty clays are richer in organic content than the shoaler-water sediments. In the outer shelf sediments, the planktonic foraminifera far outnumber the benthonic, particularly when the relict benthonic specimens are disregarded The sediments of the outermost shelf are the richest in organic content, and yet their benthonic populations are not as abundant as those of the coastal sands and sand-silt-clay sediments, which are the poorest in organic matter in the area. While its fine-grained nature and rapid deposition favour the preservation of organic matter in the middle and outer shelf sediments, its consumption by large communities of organisms in the coastal sediments may partly account for lower organic matter content in the latter than in the former. Furthermore, the silt-laden, relatively cold, fresh water of the Godavari River, spreading along the coast northward and out into deeper water in a northeast direction (Rama Sastry and Balarama Murty, 1957), its silt content settling out, probably at a rapid rate, along its path, seems to exert an inhibiting effect on the benthonic foraminifera.

LITHOLOGY OF SEDIMENTS

There appears to be a fair degree of correlation between benthonic populations and the nature of their substrates, sand-silt-clay sediments supporting populations greater both in variety and in abundance than the silty clays and clays. The unimpressive number of arenaceous specimens associated with any kind of substrate, except for a few species like *Textularia candeiana*, *T. foliacea*, *Bigenerina nodosaria* and *Quinqueloculina agglutinans*, is significant. It may partly be due to their elimination during the laboratory treatment of the samples with sodium hexametaphosphate. Even so, some samples which were disaggregated without the addition of chemicals do not yield arenaceous specimens in appreciable numbers. Either they were destroyed during the drying of the samples (Phleger, 1960, p. 38), or they were not abundant originally. This problem needs further investigation.

In the relict sediments, where arenaceous material is very scanty, the question of arenaceous tests being noticeably present does not arise. However, the species *Textularia agglutinans* and *Quinqueloculina agglutinans* successfully made use of the finer oolitic grains in building their tests. It is possible that certain other species of arenaceous habit could also make use of the finer oolitic grains in test-building. This possibility also needs further investigation.

It appears that, in general, the sites of active sedimentation, especially of silty clays and clays, do not favour the profuse development of foraminifera, except for a few specialised species which can adapt themselves with relative ease to such hostile environments. At any rate, this seems to be the situation on the Visakhapatnam–Kakinada shelf.

GEOGRAPHICAL PROVINCES

Cushman (1948) divided the Recent warm-water foraminiferal fauna of the world into four main geographical provinces and considered the Bay of Bengal as constituting a part of a zone which contains a mixture of the East African and Indo-Pacific faunas. Bhalla (1968, p. 389) recorded such a mixed fauna from the beach sands of Visakhapatnam. The foraminiferal assemblages off Pentakota also include elements of both the Indo-Pacific and East African geographical provinces. The relative abundances of the elements of the fauna from these two geographical realms in the foraminiferal assemblages of the continental shelf off the east coast of India will be discussed in a forthcoming publication.

CONCLUSIONS

With the elimination from consideration of the relict faunal elements of the outer shelf and, to some extent, of the middle shelf, the living foraminiferal population can be divided into three distinct depth zones, or facies, the first ranging from 0 to 15 meters in depth, the second from 15 to 40–45 meters, and the third consisting of depths greater than 40–45 meters.

Facies 1, sands
Depth: 0–15 meters. Temperature: 85°–79°F.

Quinqueloculina schlumbergeri, Q. candeiana, Q. schreibersii, Miliolinella subrotunda, Spiroloculina arenaria, Vertebralina striata, Lagena striata, Nonion translucens, Elphidium hispidulum, Operculina bartschi, Sorites marginalis and *Neoconorbina patelliformis* are restricted to this zone. The following species present in the facies continue in the next facies also (temperature: 85°–74°F.):

Triloculina tricarinata, Elphidium craticulatum, Operculina ammonoides and *O. granulosa.*

The following species which are present in this zone extend much deeper into the silty clays of facies 3-A (temperature: 85°–64°F.):

Textularia agglutinans, Quinqueloculina n. sp., *Triloculina* aff. *bicarinata, Flintina bradyana, Lagena* sp., *Elphidium discoidale* and *Pseudorotalia schroeteriana.*

Facies 2, sand-silt-clay
Depth: 15 to 40–45 meters. Temperature: 83°–74°F.

Textularia candeiana, T. foliacea, T. mayori, Quinqueloculina agglutinans, Q. lamarckiana, Q. aff. *lamarckiana, Q. sagrai, Massilina* sp., *Triloculina rupertiana, Ophthalmidium* sp., *Elphidium crispum, E. macellum* and *Spirillina vivipara* are restricted to this facies.

The following species which make their appearance in this zone extend a little seaward beyond this zone:

Bigenerina nodosaria, Spiroloculina sp. and *Loxostomum lobatum.*

The following species which also make their appearance in this zone extend much deeper into the succeeding silty clay facies, and these may be treated essentially as middle shelf species:

Adelosina laevigata and *Globulina gibba* extend down to 60 meters in depth, and *Nonion incisus* extends down to a depth of 90 meters.

Quinqueloculina vulgaris, Q. bicostata, Q. oblonga, Q. cuvieriana, Spiroloculina communis, S. indica, Elphidium striatopunctatum, Discorbis australis, Asterorotalia trispinosa, Amphistegina radiata and *Cibicides lobatulus* are abundant in facies 1 and 2 but extend deeper in much less abundance.

Facies 3-A, silty clays
Depth: greater than 40–45 meters. Temperature: 82°–64°F. or even lower.

Sigmoilina tenuis, Robulus limbosus, Nodosaria catesbyi, Bulimina marginata, Uvigerina proboscidea, Cassidella bradyi, Bolivina robusta, Eponides subornatus and *Cassidulina laevigata.*

Facies 3-B, silty clays
Depth: greater than 80 meters. Temperature: 82°–64°F. or even lower.

Spiroloculina clara, Bulimina affinis, Buliminella elegantissima, Uvigerina peregrina, Bolivina spathulata and *B. seminuda* are restricted to this zone.

Nonion grateloupi, Ammonia beccarii, A. beccarii var. *tepida, A. papillosa, A.* aff. *papillosa* and *Heterolepa dutemplei* show a wide range of distribution, but they are more abundant in the inner shelf sediments.

Bolivina vadescens, B. compacta and *Cancris oblonga* also show a wide range of distribution, but they become more abundant in the outer shelf sediments.

Hanzawaia concentrica is uniformly distributed over the entire shelf.

Other conclusions drawn from this study are:

1) Sites of active deposition of fine-grained terrigenous materials do not support large populations.

2) Organic content of the sediments does not appear to control faunal development.

3) Wide fluctuations in temperature of the bottom waters of the middle shelf inhibit population growth in the area.

4) The low salinity, the relatively cold water and the sediments of the Godavari River reach the shelf off Pentakota and tend to inhibit the populations.

5) The oolitic sediments and the associated shallow-water warm-water foraminifera forming the lower part of the core suggest that the shore line stood 11,000 years ago at not less than 100 meters below the present sea-level.

6) As the postglacial sea level rose, the water where the core sample was taken deepened steadily, resulting in the elimination of many shallow-water warm-water species. But certain species, finding themselves at more favourable depths, and finding the waters richer in nutrient salts added from the land to the postglacial rising sea, multiplied their numbers manyfold. Ecological factors should have induced certain deep-water species, including the planktonic species, to enter the shallow waters from the then offshore regions.

7) The oolitic sediments lay exposed until the Godavari sediments reached as far north as the shelf off Pentakota and covered them. Before they had been buried under the terrigenous sediment cover, they were reworked and considerably contaminated with the faunal assemblages of postglacial origin.

It is realised that, in the absence of quantitative data on populations in sediments of specific volume, and in the absence of studies on living foraminifera, the faunal assemblages presented should be considered as only approximate. It is also realised that many species which occur sparingly have been unduly overemphasized as indicators of environment. Nevertheless, this paper presents, in the opinion of the authors, a fairly dependable approximation to the true conditions. When more detailed studies are undertaken in the future, some of the species are bound to be recognised as typical zone guides. It is hoped, however, that the zonal pattern described above may help in the reconstruction of the paleogeography and in identifying the Late Tertiary shore lines, the recognition of which is very important in our quest for oil in the Bengal Basin and other Tertiary basins along the east coast of India.

ACKNOWLEDGMENTS
The writers are indebted to Miss Ruth Todd of the United States Geological Survey, who willingly gave her time in checking their identifications of the species. They are grateful to Professor D. A. Rashid of Madras University and to the authorities of the Oil and Natural Gas Commission, Dehradun, for permitting them to carry out their initial studies in their laboratories. One of them (D. Vedantam) is grateful to the Council of Scientic and Industrial Research, New Delhi, for enabling him to undertake this work by granting him a Junior Research Fellowship.

APPENDIX
Taxonomic notes on species identified to the generic level

Quinqueloculina sp.
Plate 1, figure 1

Description: The suboval test is slightly longer than broad and is subtriangular in apertural view. Five quinqueloculine chambers, four exposed on one side of the test and three on the other, are visible externally. The arcuate chambers are longer than broad and are broadest in the middle, becoming narrower towards the ends. The depressed sutures are indistinct in some specimens but in the majority are distinct. The periphery is highly rounded. The thick porcellaneous wall is polished and shining, and is ornamented with numerous evenly arranged longitudinal costae upon each of which a row of very sharp to somewhat blunt conical spines is present. A large circular aperture is situated at the end of a short neck, and has a thick lip and a thick simple tooth, broadening distally and sometimes projecting slightly above the lip.

Dimensions: Length 0.5 mm., breadth 0.48 mm., thickness 0.3 mm.

Distribution: Present sparingly in a majority of the surface sediment samples.

Remarks: The species has some resemblance to *Q. seminulum* but differs from it in having very prominent ornamentation.

Massilina sp.
Plate 1, figure 2

Description: The nearly oval test is almost three times as long as broad, quinqueloculine in the early stages, later with the chambers added in one plane, in side view subrounded, and narrow in end view. The last two chambers are half of a coil in length and equally broad throughout, the last chamber projecting at either end of the test. The distinct sutures are depressed. Periphery rounded. Wall smooth. Aperture elongate, at the end of a neck of moderate length, and usually with a simple tooth.

Dimensions: Length 1.3–1.5 mm., breadth 0.35 mm., thickness 0.28 to 0.35 mm.

Distribution: Present only in sample 301 in traces.

Spiroloculina sp.
Plate 1, figure 3

Description: The oval to subcircular test is about 1¼ to 1⅓ times as long as broad, slightly biconcave in the later stages, and laterally compressed. The two ends project slightly. The chambers are longer than broad, arcuate, and equal in breadth from one end to the other. The later chambers rapidly increase in size. The edges of the last two chambers stand out slightly above the preceding chambers. An external arenaceous layer is present on the final chamber. The chamber's thickness increases from the inner margin to near the outer. The depressed sutures are indistinct in the initial stages but distinct in the later stages. The broad periphery is concave with angular edges. The porcellaneous wall is opaque and rough due to the presence of minute pits. The circular aperture has a short cylindrical neck, a lip, and a short blunt tooth.

PLATE 1

1 *Quinqueloculina* sp.
×130. a, c, opposite side views; b, apertural view.
2 *Massilina* sp.
×35. Side view.
3 *Spiroloculina* sp.
×130. a, side view; b, apertural view.

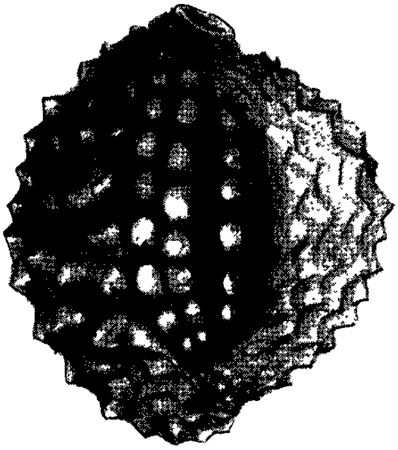

1 A

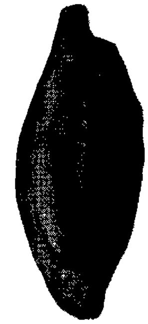

2

3 B

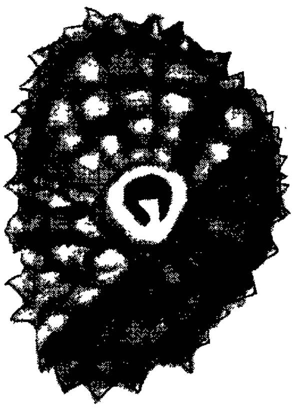

1 B

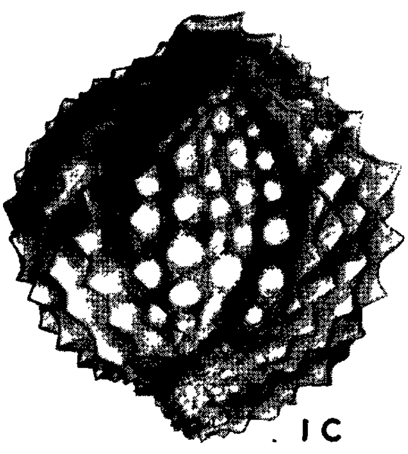

1 C

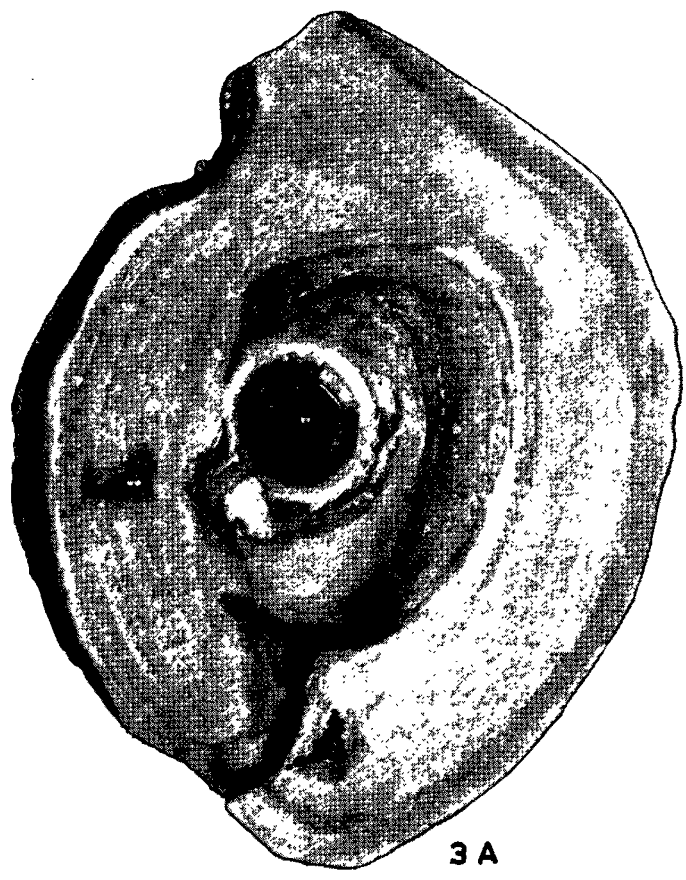

3 A

Dimensions: Length 0.85 mm., breadth 0.65 mm., thickness 0.17 mm.

Distribution: Present in surface sediments only (samples 301, 302 and 307).

Remarks: The initial chambers are completely covered with fine, pitted calcareous material, and the final chamber is covered with an arenaceous layer. But for these differences this species is quite similar to *Spiroloculina costifera* Cushman.

Triloculina sp. A
Plate 2, figure 1

Description: The elongate test is about two times longer than broad and subtriangular in apertural view. Three triloculine chambers, three exposed on one side of the test and two on the other, are visible externally. The gently curved chambers are longer than broad and are nearly equal in width from one end to the other. The middle chamber is centered well above the other two chambers. The slightly depressed sutures are somewhat indistinct. The periphery is subrounded. The thick calcareous wall is polished and shining, ornamented with numerous slightly raised longitudinal costae inclined to the longer axis of the test and curving into the inner side of the chambers. These costae are not distinct on the earliest chamber visible. The aperture is a large and wide slitlike opening cutting into the chamber on both sides. Tooth absent.

Dimensions: Length 1.1 mm., breadth 0.54 mm., thickness 0.25 mm.

Distribution: Present only in the lower section of the core.

Remarks: The species is somewhat similar to *T. oblonga* and *T. rupertiana*, but differs from the former in the absence of any tooth and in having surface ornamentation, and from the latter in the absence of pitlike surficial ornamentation.

Triloculina sp. B
Plate 2, figure 2

The suboval test is slightly longer than broad and has three externally visible triloculine chambers. Triangular in apertural view. The arcuate chambers are longer than broad, broadest at the middle, and highly inflated. Sutures distinct and depressed. Periphery subrounded or blunt. The thick calcareous wall is dull. Aperture a triangular to subcircular opening with a long broad tooth bifid at the end.

Dimensions: Length 0.62 mm., breadth 0.54 mm., thickness 0.54 mm.

Distribution: Present in traces in the core samples P_5 and P_6.

Remarks: The species differs from *Triloculina trigonula* in the position of the aperture.

Triloculina sp. C
Plate 2, figure 3

Description: Test in the adult with three visible chambers, subglobular in shape, nearly equal in length, width and thickness. All three chambers appear on one side of the test and only two on the other side. Chambers slightly longer than broad, bean-shaped and equal in width from one end to the other. The sutures are depressed and indistinct. The peripheral angles are rounded. The thick calcareous wall is dull and in some cases ornamented with faint longitudinal costae. The aperture is circular with a broad bifid tooth.

Dimensions: Length 0.45 mm., breadth 0.45 mm., thickness 0.45 mm.

Distribution: Present only in the core sample P_6.

Remarks: Very close to *T. insignis*, but the costae are not so strong as in *T. insignis*, and the aperture is very broad with the tooth occupying almost all of the area.

Ophthalmidium sp.
Plate 2, figure 4

Description: Test planispiral, evolute, circular, much compressed, consisting of a globular semitransparent proloculum, followed by a second chamber forming two coils, followed by chambers relatively shorter in length, gradually becoming a half coil in length in the final stage. Chambers nearly circular in transverse section. Depressed sutures somewhat indistinct. Peripheral margin subrounded. Numerous minute pits present on the porcellaneous wall. Aperture simple, without lip or tooth.

PLATE 2

1 *Triloculina* sp. A
×97.5. a, c, opposite side views; b, apertural view.
2 *Triloculina* sp. B
×97.5. a, c, opposite side views; b, apertural view.
3 *Triloculina* sp. C
×97.5. a, c, opposite side views; b, apertural view.
4 *Ophthalmidium* sp.
×22.5. Side view.
5 *Lagena* sp.
×97.5. a, side view; b, apertural view.

PLATE 2

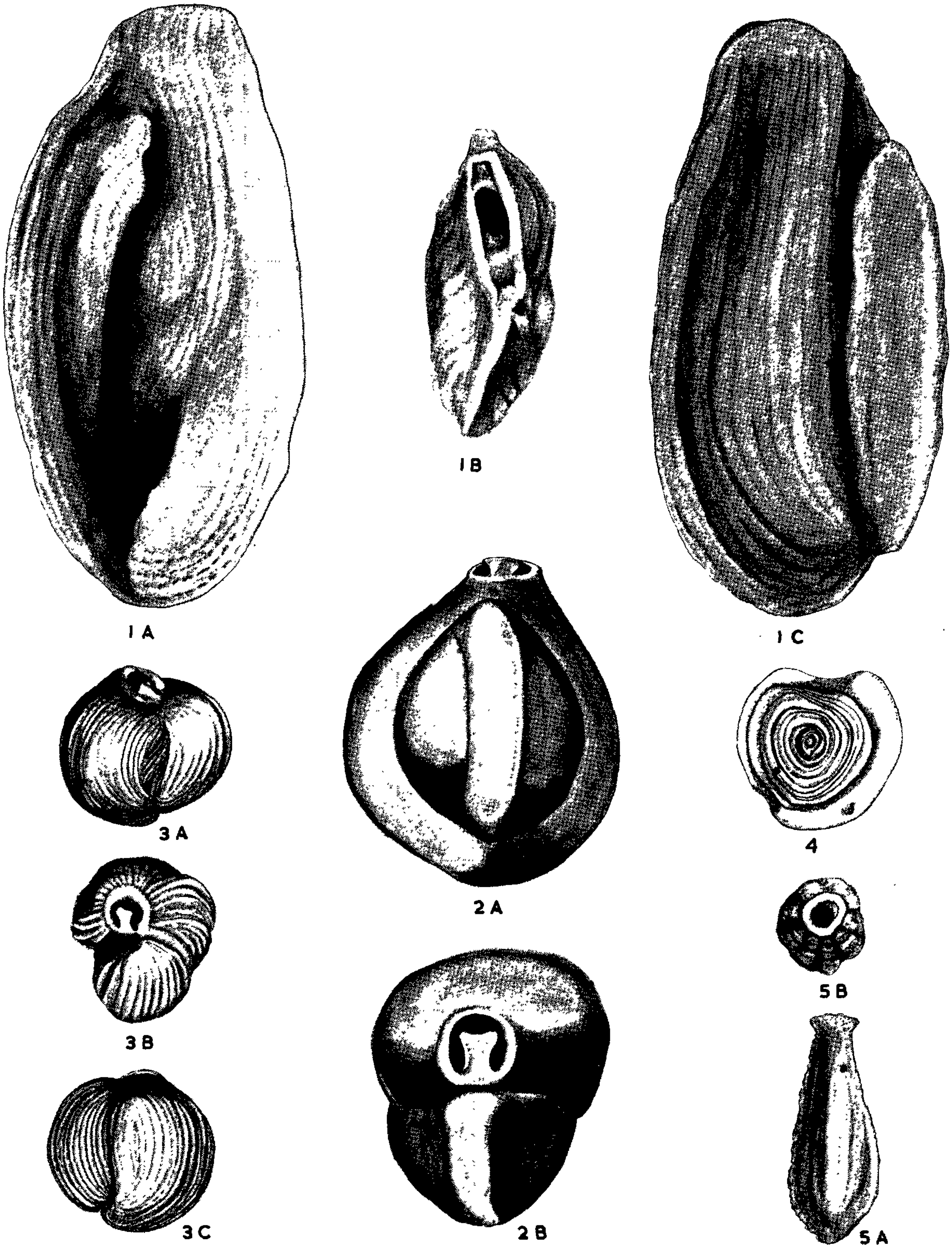

Dimensions: Diameter about 1.4 mm.

Distribution: Present in traces only in sample 301.

Lagena sp.
Plate 2, figure 5

Description: The elongate unilocular test has a slightly compressed rounded base. The apertural end is extended into a short rounded neck with a flaring lip. The thick opaque wall is smooth but in some cases ornamented with slightly raised continuous longitudinal costae, varying in number from very few to numerous. The aperture is a moderately large circular opening at the end of the rounded neck.

Dimensions: Length 0.42 mm., breadth 0.17 mm.

Distribution: Present sparingly in almost all of the surface sediment samples and in sample P_6 of the core.

Remarks: The species is somewhat similar to *L. laevis* but differs from it in having a very wide neck and longitudinal costae.

Bolivina sp.
Plate 3, figure 1

Description: The elongate test is compressed in the initial stages, tapers rapidly to the bluntly rounded initial end, and becomes broader toward the apertural end. There are about 18–20 biserially arranged chambers, broader than high, oblique to the periphery and rapidly increasing in size in the early stages, highly inflated in the later stages. The sutures are slightly inclined to the longer axis of the test and almost flush with the surface or slightly limbate in the early compressed stages, distinct and depressed in the later stages. The periphery is acute in the compressed portion, rounded and lobulate in the later portion. The thin translucent wall is finely perforate. The elongate loop-shaped aperture extends to the suture at the end of the final chamber.

Dimensions: Length 0.23 mm., breadth 0.12 mm., thickness 0.06 mm.

Distribution: Present in the lower half of the core and also in surface sediment samples 303 and 307.

Remarks: The species is somewhat close to *B. seminuda* but is bigger, less inflated, and broader at the apertural end, and has oblique sutures and more chambers.

Globigerinoides sp.
Plate 3, figure 2

Description: The low-spired trochoid test consists of 2 to 3 whorls. In the early whorls the small subglobular chambers are less distinct, while the final whorl consists of four large highly globular chambers. There exists a small, flaplike, highly inflated supplementary chamber on the ventral side, covering almost the entire umbilical region. The other chambers very rapidly increase in size. The rounded periphery is lobulate. The thin calcareous wall is perforate. The umbilicus is somewhat depressed. The aperture is a large arched opening into the umbilicus at the base of the final large chamber and is covered by the supplementary small chamber, which has a similar aperture. There are a number of supplementary apertures at the base of each chamber on the spiral side.

Dimensions: Diameter 0.25 to 0.3 mm.

Distribution: Absent in the surface sediment samples. Present throughout the entire length of the core.

Remarks: Some specimens are discoloured black. The rest are well preserved, and occur in significant numbers.

Operculinella sp.
Plate 3, figure 3

Dimensions: Length 1.25 mm., breadth 1.2 mm., thickness 0.4 mm.

Asterigerina sp.
Dimensions: Diameter 0.65 mm.

As the specimens of the last two species are heavily oolitically coated, it is practically impossible to describe their morphological features accurately. Neither of them has been recognised in the core, and they seem to be present only in the outer shelf sediments.

BIBLIOGRAPHY

BANDY, O. L., and ARNAL, R. E.
1957 *Distribution of Recent foraminifera off west coast of Central America.* Amer. Assoc. Petr. Geol., Bull., vol. 41, no. 9, pp. 2037–2053, text-figs. 1–3.

PLATE 3

1 *Bolivina* sp.
×260. a, side view; b, apertural view.
2 *Globigerinoides* sp.
×130. a, dorsal view; b, peripheral view; c, ventral view.
3 *Operculinella* sp.
×130. a, side view; b, peripheral view.

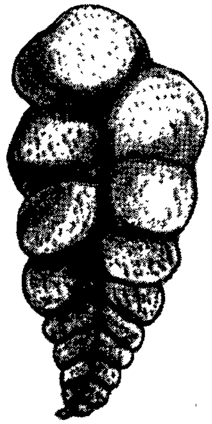

1A

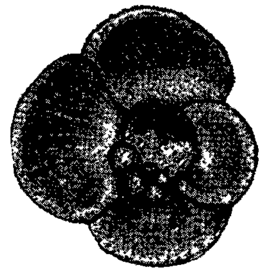

2A

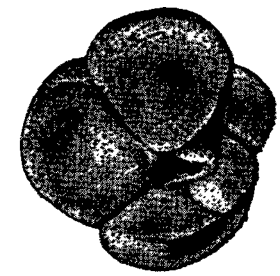

2C

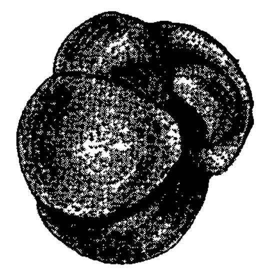

2B

1B

3A

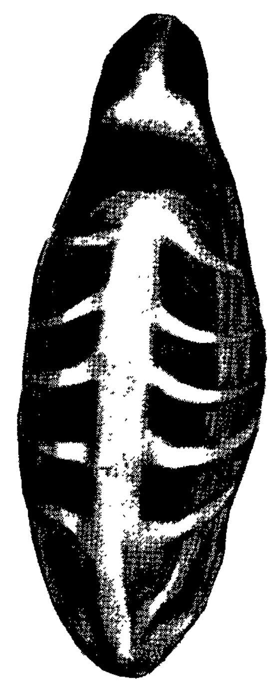

3B

BHALLA, S. N.
1968 *Recent foraminifera from Visakhapatnam beach sands and its relation to the known foramgeographical provinces in the Indian Ocean.* India, Nat Inst. Sci., Bull., no. 38, pp. 376–392.

BHATIA, S. B., and BHALLA, S. N.
1964 *Recent Foraminifera from beach sand at Puri, Orissa.* Pal. Soc. India, Jour., vol. 4 (1959), no. 1, pp. 78–81, pls. 1–2.

CUSHMAN, J. A.
1948 *Foraminifera, their classification and economic use.* Cambridge, Mass.: Harvard Univ. Press, ed 4, pp. 1–605, text-plates 1–31, key-plates, 1–55.

GANAPATI, P. N., and MURTY, V. S. R.
1954 *Salinity and temperature variations of the surface waters off the Visakhapatnam coast.* Andhra Univ., Mem. Oceanogr., vol. 1, pp. 125–141.

GANAPATI, P. N., and SAROJINI, D.
1959 *Ecology of foraminifera off Visakhapatnam coast.* All-India Congr. Zool. Inst., Proc., vol. 2, Sci. Papers, pp. 311–315.

GANAPATI, P. N., and SATYAVATI, P.
1958 *Report on the foraminifera in bottom sediments in the Bay of Bengal off east coast of India.* Andhra Univ., Mem. Oceanogr., vol. 2, pp. 100–127, pls. 1–6.

GHOSE, B. K.
1966 *Asterorotalia trispinosa (Thalmann), a spinose rotaliid from Digha beach, southern Bengal.* Cushman Found. Foram. Res., Contr., vol. 17, pt. 3, pp. 104–108, text-figs. 1–6.

GNANAMUTHU, C. P.
1943 *The foraminifera of Krusadi Island.* Madras Govt. Mus., Bull., n. ser., Nat. Hist. Sect., vol. 1, no. 2, pp. 1–28, pls. 1–4.

HARMAN, R. A.
1964 *Distribution of foraminifera in the Santa Barbara Basin, California.* Micropaleontology, vol 10, no. 1, pp. 81–96, text-figs. 1–12.

LA FOND, E. C.
1957 *Oceanographic studies in the Bay of Bengal.* Indian Acad. Sci., Proc., vol. 46, sec. B, no. 1, pp. 1–46, pls. 1–3, text-figs. 1–30.

1964 *Andhra, Mahadevan, and Krishna submarine canyons and other features of the continental slope off the east coast of India.* Indian Geophys. Union, Jour., vol. 1, no. 1, pp. 25–32.

LA FOND, E. C., and BORRESWARA RAO, C.
1955 *Vertical temperature structure of the upper layers of the sea off the east coast of India.* India, Ministry Defence, Defence Sci. Org., Publ., no. 4/55, pp. 1–21.

LUDWICK, J. C., and WALTON, W. R.
1957 *Shelf-edge, calcareous prominences in northeastern Gulf of Mexico.* Amer. Assoc. Petr. Geol., Bull., vol. 41, no. 9, pp. 2054–2101, text-figs. 1–19.

MAIKLEM, W. R.
1967 *Black and brown speckled foraminiferal sand from the southern part of the Great Barrier Reef.* Jour. Sed. Petrol., vol. 37, no. 4, pp. 1023–1030.

NAIDU, A. S.
1968 *Radiocarbon date of an oolitic sand collected from the shelf off the east coast of India.* India, Nat. Inst. Sci., Bull., no. 38, pp. 467–471.

PHLEGER, F. B
1960 *Ecology and distribution of Recent foraminifera* Baltimore: Johns Hopkins Press, pp. 1–297, pls. 1–11, text-figs. 1–83.

POORNACHANDRA RAO, M.
1957 *Some observations in the marine geology of Bay of Bengal (along the east coast of India).* Pan Indian Ocean Sci. Assoc., Congr. 3e, Tananarive, C. R., sec. C., pp. 143–148.

RAMA SASTRY, A. A., and BALARAMA MURTY, C.
1957 *Thermal field and oceanic circulation along the east coast of India.* Indian Acad. Sci., Proc., vol. 46, sec. B, no. 5, pp. 293–323, text-figs. 1–20.

SATYANARAYANA RAO, T. S.
MS. *Studies on the Chaetognatha in relation to the biology and hydrography off the Indian coast.* Unpublished doctoral thesis (1955) submitted to Andhra Univ., Waltair, India.

SHEPARD, F. P.
1954 *Nomenclature based on sand-silt-clay ratios.* Jour. Sed. Petrol., vol. 24, no. 2, pp. 151–158.

SUBBA RAO, M.
1958 *Distribution of calcium carbonate in the shelf sediments off east coast of India. Ibid.*, vol. 28, no. 3, pp. 274–285.

1960 *Organic matter in marine sediments off east coast of India.* Amer. Assoc. Petr. Geol., Bull., vol. 44, no. 10, pp. 1705–1713, text-fig. 1.

1964 *Some aspects of continental shelf sediments off the east coast of India.* Mar. Geol., vol. 1, no. 1, pp. 59–87.

SUBBA RAO, M., and VEDANTAM, D.
1968 *Distribution of foraminifera off Visakhapatnam.* India, Nat. Inst. Sci., Bull., no. 38, pp. 491–501.

SUBBA RAO, M., VENKATARATNAM, K., and CHANDRA, P. R.
1967 *Submarine canyons off the east coast of India.* Seminar Geomorph. Studies India, 1965, Univ. Saugar, India, Proc., pp. 114–120.

TODD, RUTH
1961 *Foraminifera from Onotoa Atoll, Gilbert Islands.* U. S. Geol. Survey, Prof. Paper, no. 354–H, pp. 171–191, pls. 22–25.

VARADACHARI, V. V. R.
MS. *On some meteorological and oceanographic studies of the coastal waters off Waltair in relation to upwelling and sinking.* Unpublished doctoral thesis (1958) submitted to Andhra Univ., Waltair, India.

WALTON, W. R.
1955 *Ecology of living benthonic foraminifera, Todos Santos Bay, Baja California.* Jour. Pal., vol. 29, no. 6, pp. 952–1018, pls. 99–104, text-figs. 1–24.

Reprinted from *Geologischen Rundschau*, Band 60, 1970, p. 264-275

Geologische Untersuchungen an Sedimenten des indisch-pakistanischen Kontinentalrandes (Arabisches Meer)

W. SCHOTT, U. VON STACKELBERG, F.-J. ECKHARDT, B. MATTIAT, J. PETERS & B. ZOBEL, Hannover *)

Zusammenfassung

Mit Sedimentmaterial, das von dem Forschungsschiff „Meteor" und dem pakistanischen Fischereiforschungskutter „Machhera" gesammelt wurde, sollten die Ablagerungsbedingungen auf dem Meeresboden des indisch-pakistanischen Kontinentalrandes erfaßt und unter anderem festzustellen versucht werden, wo die Schlammassen des Indus auf dem Meeresboden des Arabischen Meeres wiederzufinden sind (Abb. 1).

Enge Beziehungen zwischen den ozeanographischen Verhältnissen im Wasserraum (Chemismus und Strömungen) und der Ausbildung der Sedimente konnten erkannt werden. Rhythmisch gebänderte Sedimente auf dem oberen Kontinentalabhang spiegeln die weitreichenden Auswirkungen des Monsunwechsels wider. Indusmaterial ist bis weit in die Tiefsee zu verfolgen. Die Tonmineralien zeigen von der Küste zur Tiefsee und auch mit zunehmender Teufe in den Sediment-

*) Anschrift der Verfasser: Prof. Dr. W. SCHOTT, Dr. U. VON STACKELBERG, Dr. F.-J. ECKHARDT, J. PETERS, Dr. B. ZOBEL, Bundesanstalt für Bodenforschung, D-3 Hannover-Buchholz, Postfach 54; Dr. B. MATTIAT, Niedersächsisches Landesamt für Bodenforschung, D-3 Hannover-Buchholz, Postfach 54.

kernen die Tendenz: „Detritus" (Chlorit, Muskovit, Illit) — „Zersatz" (Montmorrillonit, mixed layer-Minerale) — „Rückbildung" (Illit).

Die biostratigraphische Bearbeitung, kombiniert mit den Ergebnissen einiger C^{14}-Datierungen ergibt u. a. Sedimentationsraten bis zu > 50 cm/1000 Jahre am oberen Kontinentalabhang abnehmend auf ca. 1 cm/1000 Jahre im offenen Ozean. Die Faunenzusammensetzung erweist das Vorhandensein eines holozänen Klimaoptimums.

Die geochemische Untersuchung der jungen Porenwässer zeigt, daß diese sehr schnell die Zusammensetzung fossiler Formationswässer erreichen können (siehe V. Marchig, i. d. Bd.).

Abstract

From the R./V. "Meteor" and the Pakistan F./V. "Machhera" sediments from the Indian-Pakistan continental margin have been investigated in order to delineate the facies distribution of the recent deposits. One of several objectives of this study was to find out how far the suspended material of the Indus River is being transported into the Arabian Sea.

A close genetic relationship was recognised between the oceanographic conditions of the water masses (chemistry and currents) and the characteristics of the sediments. The activity of the monsoons is reflected by the rhythmic lamination of the sediments of the upper continental slope. The suspended matter from the Indus River can be traced far into the Arabian Sea. The clay minerals show the following tendency from litoral to abyssal regions and from the top of the cores downward: detrital clay minerals (chlorite, muscovite, illite) — degraded clay minerals (montmorillonite, mixed-layer minerals) — "re-formational" minerals (illite).

The biostratigraphic investigation of the sediments combined with several C^{14}-dates results in sedimentation rates from > 50 cm/1000 years at the upper continental slope decreasing to about 1 cm/1000 years in the open ocean. The faunal composition proves the existence of a climatic optimum during part of the Holocene. The geochemical investigation of the recent pore fluids demonstrates that their composition very soon assumes the characteristics of fossil interstitial waters (cf. V. Marchig, in this vol.).

The results will be published in "Meteor"-Forschungsergebnisse, Reihe C.

Résumé

La tâche à remplir consista à saisir les conditions de sédimentation au fond de la mer dans la zone bordière du talus continental indo-pakistanais en se servant des échantillons de sédimentation recueillis par le navire d'exploration «Meteor» et par le cutter de pêche et de recherche scientifique pakistanais «Machhera» et, entre autres, à tenter de déterminer où les masses de boue de l'Indus se retrouvent sur le fond de la Mer d'Oman.

Il fut possible de reconnaître des relations étroites existant entre les conditions océanographiques (chimisme et courants) et la formation des sédiments. Des sédiments rubanés à stratification fine sur le talus continental supérieur reflètent les effets d'alternance des moussons. Il est possible de suivre les sédiments de l'Indus jusqu'à une grande distance dans les profondeurs de l'océan. Avec l'éloignement da la côte et, dans les carottes, avec l'augmentation de la profondeur de prélèvement les minéraux argileux montrent la tendance suivante: «matériel détritique» (chlorite, muscovite, illite) — «matériel de décomposition

chimique» (montmorillonite, minéraux de couches mixtes) — «matériel de recombinaison minéralogique» (illite).

L'étude biostratigraphique combinée aux résultats de quelques déterminations radiométriques au ^{14}C donne, entre autres, des taux de sédimentation jusqu'à $>$ 50 cm/1.000 ans au talus continental supérieur — taux qui vont décroissant jusqu'à environ 1 cm/1.000 ans en plein océan. La composition faunique prouve l'existence d'une phase climatique optimum à l'Holocène.

L'analyse géochimique des eaux interstitielles récentes montre que celles-ci peuvent atteindre, dans uns délai assez bref, la composition des eaux fossiles. (V. Marchig, en ce tome).

La publication des résultats est prévue dans les «Meteor» Forschungsergebnisse, Ser. C.

Краткое содержание

Экспедицией ,,Meteor'' и ,,Machhera'' были взяты пробы с отложений морского дна индийско-пакистанского континентального склона. — Отмечается тесная связь между гидродинамическим режимом водоема (химизм воды и направление течения) и образованием осадков. Ритмичные слои их в верхней части континентального склона отражают влияние изменения монсума. Сносний материал реки Инд удается проследить до глубин океана. — Биостратиграфические исследования и датировка по C^{14} установили скорость накопления осадков в этом районе $>$ 50 см/1000 лет на верхнем крае континентального склона, и до 1 см/1000 лет в открытом океане. Состав фауны указывает на климатический оптимум в голоцене. — Геохимические исследования поровых вод доказывают, что они очень скоро достигают зрелости таковых древних формаций.

Einführung

Von Wolfgang Schott, Hannover

Vortragskurzfassung mit 1 Abbildung

Auf der ersten Reise des Forschungsschiffes „Meteor", die 1964/65 im Rahmen der Internationalen Indischen-Ozean-Expedition durchgeführt wurde, ist auf 6 Profilen senkrecht zur indisch-pakistanischen Küste Sedimentmaterial gesammelt worden, das vor der Indusmündung mit dem pakistanischen Fischereiforschungskutter „Machhera" durch ein gemeinsames deutsch-pakistanisches Untersuchungsprogramm ergänzt wurde (Abb. 1).

Die topographischen Verhältnisse des Meeresbodens weisen in diesem östlichen Teil des Arabischen Meeres einige markante Unterschiede auf, die die Sedimentverteilung beeinflussen. Westlich von Bombay ist der Schelf über 500 km breit, westlich von Cochin dagegen nur ca. 70 km. Der Meeresboden sinkt dort erst westlich der Lakkadiven bis auf über 4000 m ab.

Die bearbeitete Meeresregion liegt innerhalb des Monsungebietes mit wechselnder Windrichtung, trotzdem ist vor der indisch-pakistanischen Küste im Oberflächenwasser vorwiegend eine nach Süden gerichtete küstenparallele Meeresströmung vorhanden. Kaltes Auftriebwasser ist vor

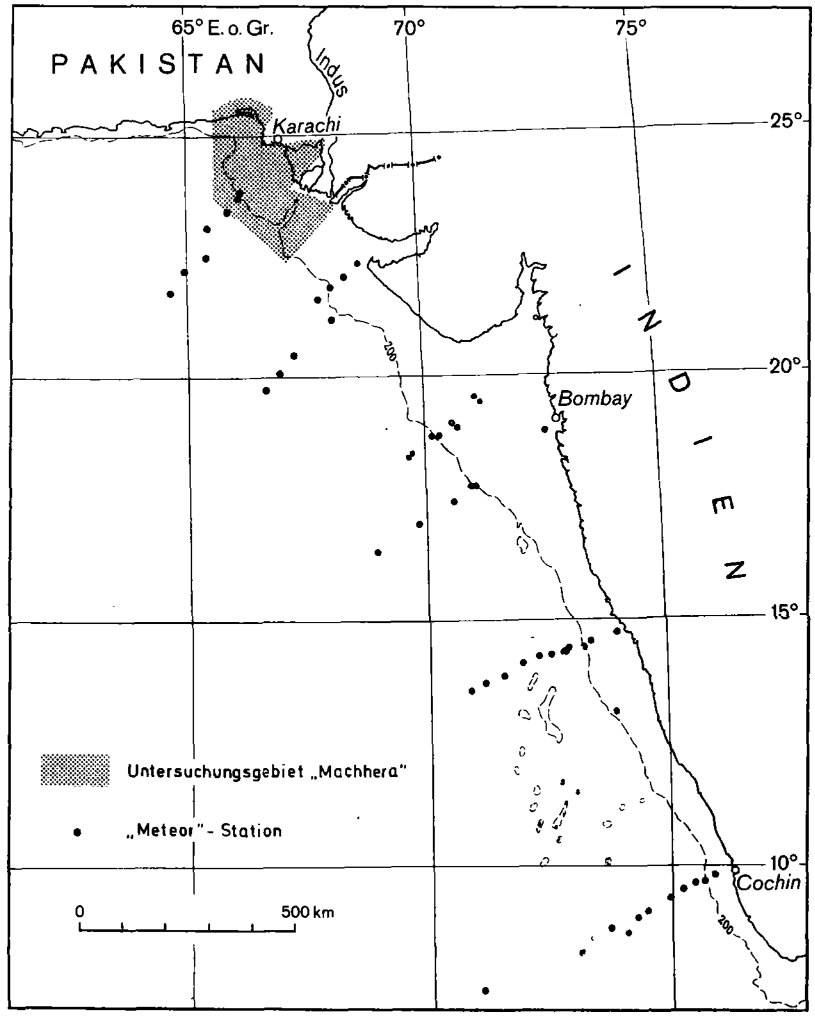

Abb. 1. Übersichtskarte des Untersuchungsgebietes. Das „Machhera"-Areal umfaßt 40 Stationspunkte. Die Untersuchungen mit der „Machhera" wurden durch Aufsammlungen von Sedimentproben im anschließenden Küstengebiet ergänzt (siehe punktiertes Gebiet auf dem Festland).

Fig. 1. Sketch map of the area of investigation. Shaded area: 40 stations from the F./V. "Machhera". The investigations from F. V. "Machhera" have been supplemented by sediment samples from the neighbouring beach (see shaded area on the main land).

Cochin und südöstlich von Karachi festgestellt worden. Diese Beobachtungen sind für die Deutung der Sedimentationsverhältnisse auf dem Meeresboden wichtig.

Durch die Bearbeitung des Sedimentmaterials sollte versucht werden, vor allem folgendes zu erfassen:

1. Überblick über den Fazieswechsel in den Oberflächensedimenten von der Küste bis in die Tiefsee.
2. Klärung der herrschenden Sedimentationsbedingungen.
3. Untersuchung der vertikalen Veränderung der organischen und anorganischen Komponenten der Ablagerungen in den Sedimentkernen.
4. Wo werden die Schlammassen des Indus auf dem Meeresboden des Arabischen Meeres sedimentiert?

Die Sedimentverteilung zeigt einen vorwiegend küstenparallelen Fazieswechsel vom Quarzfeinsand unterhalb der Küste über pleistozäne biogene Kalksande im Bereich des äußeren Schelfs zum Globigerinenschlamm der Tiefsee.

Eine größere Arbeitsgruppe, die durch die Deutsche Forschungsgemeinschaft in großzügiger Weise unterstützt wurde, hat im Rahmen einer Gemeinschaftsarbeit die Untersuchungen durchgeführt.

Die folgenden drei kurzen Berichte und der Aufsatz von V. Marchig geben einen Einblick in die Ergebnisse, die binnen kurzem in den „Meteor"-Forschungsergebnissen veröffentlicht werden.

Faziesverteilung in Sedimenten des indisch-pakistanischen Kontinentalrandes (Arabisches Meer)

Von U. von Stackelberg, Hannover

Vortragskurzfassung mit 1 Abbildung

Sedimentkerne und Oberflächenproben von 91 Stationen auf dem indisch-pakistanischen Schelf, Kontinentalabhang und Kontinentalfuß standen für die Untersuchungen zur Verfügung (Abb. 1). Die einzelnen Faziestypen der Sedimente werden vom flachen zum tiefen Wasser der Reihe nach behandelt (Abb. 2). Die hierbei geschilderten Verhältnisse gelten ± für den gesamten indisch-pakistanischen Kontinentalrand.

Auf dem Schelf beobachtet man von der Küste gegen die offene See hin folgende Sedimenttypen: Glimmerreicher, nahezu fossilleerer Quarzsand; quarz- und glimmerreicher fossilarmer Schlick; ± sandiger Pteropodenschlick; ooidreicher Kalksand (Reliktsediment). Den Kalksand unterlagert ein weißer Aragonitschlick. Der Kontinentalabhang wird bedeckt von Bänderschlick im oberen Teil, olivgrauem Schlick im mittleren und braungrauem Schlick im unteren Teil. Am Kontinentalfuß findet sich Globigerinenschlamm. Kalksand und Argonitschlick wurden im flachen Wasser während der letzten eiszeitlichen Meeresspiegelabsenkung abgelagert. Sie treten heute in Meerestiefen bis zu 160 m auf.

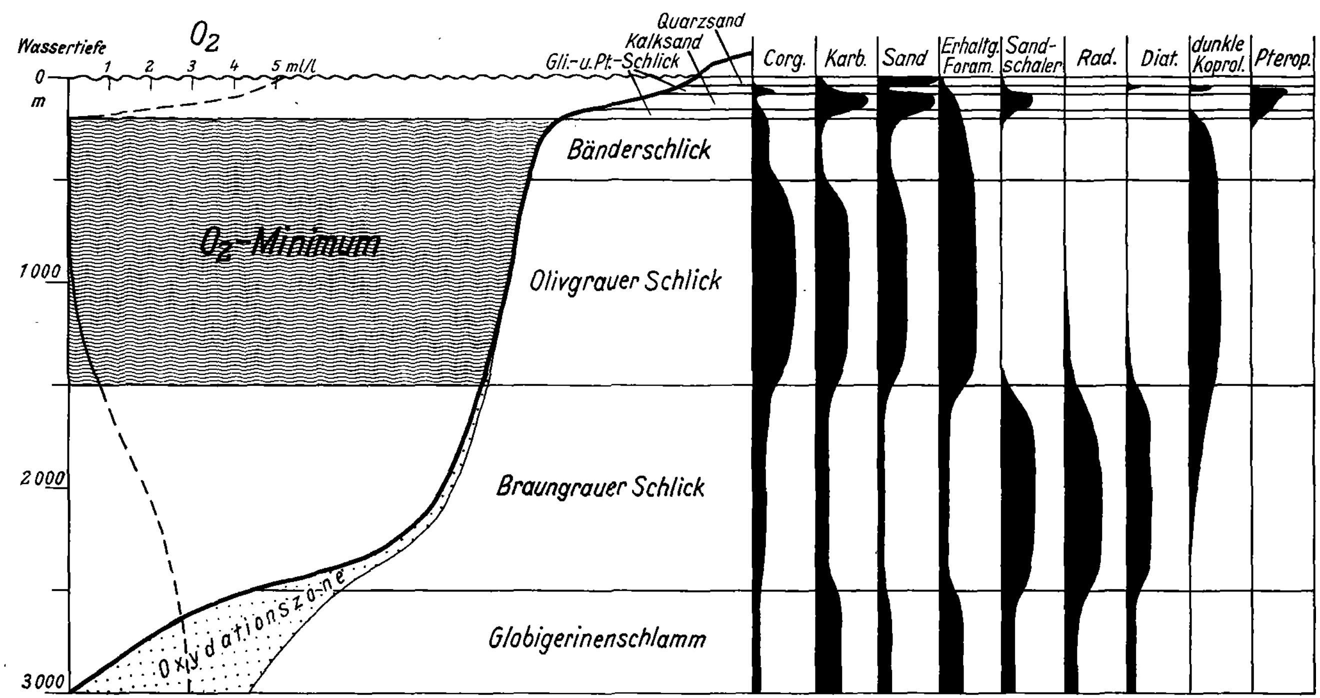

Abb. 2. Schematischer Vertikalschnitt durch den indisch-pakistanischen Kontinentalrand. Sauerstoffgehalte im Meerwasser und qualitative Gehalte ausgewählter Komponenten der Oberflächensedimente.

Fig. 2. Schematic profile of the Indian-Pakistan continental margin: Oxygen content of the seawater and qualitative content of selected components of the surface sediments.

Die Sedimente auf dem Kontinentalabhang und Kontinentalfuß werden in ihrer Zusammensetzung und in ihrem Wühlgefüge wesentlich bestimmt durch den Chemismus des Bodenwassers. Eine sauerstoffarme (min. 0,02 ml/l) Zwischenschicht, die ihre Entstehung einer extrem hohen Produktion von organischer Substanz im oberflächennahen Wasser verdankt, prallt in Wassertiefen zwischen 200 und 1500 m gegen den Kontinentalabhang. Sie liefert das sauerstoffarme Milieu für die Bildung der Bänderschlicke. Der Rhythmus der Schichtung im Bänderschlick spiegelt die Auswirkungen des Monsunwechsels auf die Sedimentation wider (Sedimentationsraten bis zu 1,5 m/1000 Jahre). Im Bereich des olivgrauen Schlicks (500—1500 m Wassertiefe) liegt das Maximum der Gehalte an organischem Kohlenstoff (max. 9%) sowie an dunklen Kotpillen. Ersteres hat seine Ursache einerseits in der starken Anlieferung von organischer Substanz, zum anderen in den günstigen Erhaltungsbedingungen aufgrund des Mangels an O_2 im Bodenwasser. Der unvollständige Zerfall der organischen Substanz hat die Entwicklung von NH_3 und H_2S zur Folge, wodurch Kieselorganismen aufgelöst werden, Kalkschaler dagegen besonders gute Erhaltung zeigen. Genau entgegengesetzt sind die Verhältnisse unterhalb des O_2-Minimums im Bereich des braungrauen Schlicks, wo unter Einwirkung von O_2 die organische Substanz weitgehend zerfällt und CO_2 frei wird. Hier bestimmen Kieselorganismen und Sandschaler das Bild der Sandfraktion. Kalkschalige Foraminiferen sind sehr schlecht erhalten. Im braungrauen Schlick beobachtet man eine besonders intensive Bioturbation. In den Sedimenten des Globigerinenschlamms tendieren die Verhältnisse wieder mehr zu denen des mittleren Kontinentalabhangs. Offenbar war wegen der größeren Entfernung vom Schelf die primäre Anlieferung von organischer Substanz nicht mehr so hoch wie im Bereich des braungrauen Schlicks, so daß sich weniger CO_2 entwickelte.

Die Mächtigkeit der Oxydationszone in den Sedimentkernen ist abhängig vom O_2-Gehalt des Bodenwassers (Abb. 2).

Die Normalfazies der Sedimente wird häufig gestört durch die Einlagerung von gutgeschichteten, gradierten Sanden, die Material vom Schelf bzw. oberen Kontinentalabhang enthalten. Diese Turbidite zeigen stets höhere Kohlenstoffwerte als ihre Umgebung, wobei das Maximum an der Basis liegt und die Gehalte nach oben parallel zur Korngröße abnehmen. Diese Tatsache stützt die Annahme einer schnellen Sedimentation. Turbidite fehlen weitgehend am oberen und mittleren Kontinentalabhang, sie erreichen ihr Maximum im Bereich des Kontinentalfußes mit $> 50\%$ der Gesamtkernlänge. Offenbar durchlaufen die Trübeströme den steileren Hang gebündelt in schmalen Rinnen. Erst unterhalb, im flachen Bereich, verbreitern sie sich fächerartig.

Petrographische Untersuchungen an Sedimenten des Indischen Ozeans im Bereich der pakistanisch-indischen Westküste

Von F.-J. Eckhardt, B. Mattiat, J. Peters, Hannover

Vortragskurzfassung mit 1 Abbildung und 1 Tabelle

Am Aufbau der Sedimente in unserem Untersuchungsgebiet sind zwei in bezug auf ihr Sedimentationsverhalten völlig verschiedenartige Komponenten beteiligt.

1. Vorwiegend silikatische Minerale, die vom Festland durch Fluß- oder Windtransport ins Meer gelangten. Ihr Sedimentationsverhalten wird beeinflußt durch Korngröße, Kornform, durch Oberflächenreaktionen mit den Ionen des Meerwassers, durch Strömungs- und Windverhältnisse und durch das Bodenrelief.
2. Die karbonatische Komponente ist in den von uns untersuchten Sedimenten bis auf sehr geringe Ausnahmen organogen und gehorcht daher ganz anderen sedimentologischen Gesetzen.

Kombiniert man für eine stoffliche Gliederung der von uns angetroffenen Oberflächensedimente die Kriterien: Korngröße und Karbonat-($CaCO_3$-) Gehalt, so ergibt sich von der Küste zur Tiefsee schematisiert folgender Aufbau:

1. Küstennaher Mineralsand, stellenweise reich an Glimmer (Biotit).
2. Karbonatarmer, küstennaher Schlick, der sich in Verlängerung der Indusmündung über den Kontinentalhang hinaus bis in die Tiefsee verfolgen läßt, und der hier im Bereich des Kontinentalfußes weit nach Süden reicht.
3. Eine Kalksandzone im Bereich des Außenschelfs.
4. Eine etwas feinerkörnige, karbonatreiche Übergangszone im Bereich des oberen Kontinentalhanges.
5. Karbonatreicher, feinkörniger Schlick im Bereich des Kontinentalanstiegs (Globigerinenschlamm, stellenweise Pteropodenschlamm).

Die Bestimmung der am Aufbau dieser Sedimente beteiligten Minerale erfolgte mit mikroskopischen und röntgenographischen Untersuchungsmethoden. Einige für das großräumige Sedimentationsgeschehen interessante Untersuchungsergebnisse sollen hier kurz mitgeteilt werden:

1. Quarzverteilung im nichtkarbonatischen Sedimentanteil: Quarzmaxima wurden angetroffen in den Küstensandbereichen und außerhalb der Schelfregion in auslaufenden „Fingern" des Indus-Schuttfächers.
   Interessant ist ferner eine deutliche Abstufung der Quarzgehalte in den Sedimenten des Kontinentalanstiegs nach Süden. Auch innerhalb des Globigerinenschlamms nehmen die Quarzgehalte in der karbonatfreien Substanz nach Süden ab und pendeln sich im westlichen Cochin-Profil auf Werte um 7% ein. Diese Quarzverteilung wird u. E. im wesentlichen durch den Indus und die von ihm transportierten Schwebstoffe verursacht. Darüber hinaus ist es möglich, daß sie im

Ergebnisse sedimentpetrographischer Untersuchungen

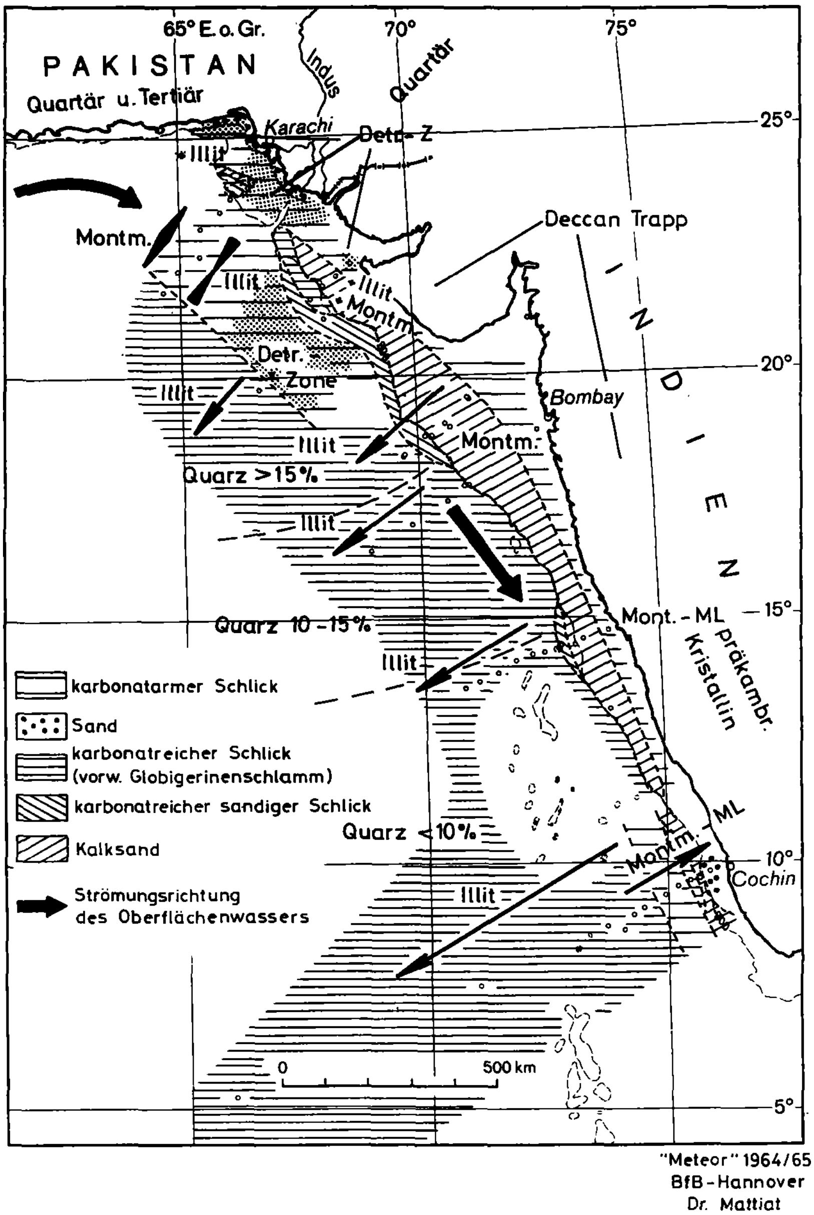

Abb. 3. Lithofaziesverteilung der Oberflächensedimente.
Fig. 3. Lithofacies distribution of the surface sediments.

Bereich der nördlichen Arabischen See auch durch äolischen Quarztransport beeinflußt wird.

2. Die Verbreitung der Tonminerale erlaubt ebenfalls einen Einblick in das rezente Sedimentationsgeschehen in diesem Raum.
   Im Indusmündungsgebiet und westlich von Karachi finden wir eine „Detritus-Zone", charakterisiert durch die Tonminerale Muskovit und Chlorit. Weiter südlich wurde diese „Detritus-Zone" auch außerhalb des Kontinentalabhanges angetroffen (Verdriftung durch südwärtsgerichtete küstenparallele Meeresströmung).
   Normalerweise finden wir, ausgehend von dieser „Detritus-Zone" mit zunehmender Entfernung von der Küste, die Abfolge: Muskovit und Chlorit → Illit → Montmorillonit → Illit. Diese Abfolge ist nach unseren bisherigen Kenntnissen im marinen Bereich zu erwarten. Illit durchläuft eine Phase der K-Abgabe und bildet sich zu Mixed-layer-Mineralen und Montmorillonit um. Im Verlauf der weiteren Diagenese kommt es dann wieder zu K-Aufnahme und Illit-Rückbildung aus Montmorillonit.
   Abweichend von diesem Schema finden wir in dem küstenparallelen Schlickstreifen entlang der Indischen Küste stark quellfähige Tonminerale, im wesentlichen Montmorillonit, stellenweise auch Mixed-layer-Minerale: Chlorit — Montmorillonit. Auch in der Kalksandzone sind dies die vorherrschenden Tonminerale. Erst im Bereich des Kontinentalanstiegs (Globigerinen-Schlamm) stellt sich dann wieder Illit als dominierendes Tonmineral ein. Diese Montmorillonit-Minerale können direkt hergeleitet werden aus den Schlammassen, die besonders zur Zeit des Sommermonsuns durch Flüsse aus dem Gebiet des Deccan-Trapp ins Meer transportiert werden.
   Aufgrund der speziellen Oberflächeneigenschaften der sie zusammensetzenden Minerale werden diese Schlammassen beim Übergang ins Meerwasser küstennah ausgeflockt. Durch küstenparallele Meeresströmungen werden sie zum Teil südwärts verdriftet.
3. Mikroskopische und elektronenmikroskopische Untersuchungen an Einzelmineralen des Aragonitschlicks (s. U. v. STACKELBERG) machen eine Flachwasserbildung dieser Aragonitkristalle wahrscheinlich.
4. In einigen Kernen westlich von Cochin wurde in bestimmten Teufenbereichen vulkanisches Glas angetroffen.
   Die optischen und chemischen Analysedaten sind in Tab. 1 wieder-

Tabelle 1. Vulkanisches Glas in Sedimenten des Indischen Ozeans im Profil westlich von Cochin

Einige chemische Daten:

SiO_2	—	70,0%	
Al_2O_3	—	11,9%	
Fe_2O_3	—	0,97%	Sonstige Daten:
CaO	—	0,80%	Brechungsquotient: n = 1,505 ± 0,01
MgO	—	0,076%	D — 2,48 g/cm³
K_2O	—	4,89%	Korngrößenmaximum: 30—70 μ ⌀
Na_2O	—	2,93%	
H_2O	—	5,33%	

gegeben. Das Auftreten dieses vulkanischen Glases eröffnete uns einige Korrelationsmöglichkeiten in dem betreffenden Gebiet.

Biostratigraphische Untersuchungen an Sedimentkernen aus dem Arabischen Meer

Von Barbara Zobel, Hannover

Vortragskurzfassung

Die biostratigraphische Gliederung der Sedimentkerne aus dem Indischen Ozean wurde mit planktonischen Foraminiferen durchgeführt. Beschrieben werden die Ergebnisse, die an den Kernen des südlichen Stationen-Profils im Bereich zwischen 5—10° N und 66—76° E von der Tiefsee auf die indische Westküste vor Cochin zu gewonnen wurden. Die Untersuchung ergab, daß die Arten-Zusammensetzung und die vertikale Abfolge der planktonischen Foraminiferen-Gemeinschaften im jüngsten Quartär in diesem Gebiet des tropischen Indischen Ozeans nicht ohne weiteres vergleichbar ist mit den bereits gut bekannten Verhältnissen im tropischen Atlantischen Ozean. So wurden in Planktonnetzfängen im Untersuchungsgebiet gewisse Arten planktonischer Foraminiferen lebend gefangen (*Globoquadrina hexagona*; *Globorotalia cultrata flexuosa*), die im Atlantischen Ozean im Holozän nicht mehr beobachtet werden konnten. Kaltes Auftriebswasser vor der indischen Westküste verursacht erhebliche Änderungen in der Arten-Zusammensetzung der Foraminiferen-Gemeinschaften mit Annäherung an den Kontinentalhang. Die Unterschiede zwischen warm- und kühlzeitlichen Faunen sind nicht so ausgeprägt wie im Atlantischen Ozean. Aus alledem ergibt sich die zwingende Notwendigkeit, die Arten-Zusammensetzung der planktonischen Foraminiferen-Gemeinschaft im heutigen Oberflächensediment jeweils an der Kernentnahmestelle als Standard für die Beurteilung klimatisch bedingter Änderungen in der vertikalen Faunenabfolge im Sedimentkern zu benutzen. Die Angabe „wärmer" oder „kälter als heute" bezieht sich auf den %-Gehalt der Foraminiferen-Gemeinschaft an Kühlwasserarten auf der heutigen Meeresbodenoberfläche am Stationsort gleichgültig, ob dieser Gehalt 3% oder 30% beträgt.

Ein sehr schnell sedimentierter Kern vom oberen Kontinentalhang vor Cochin konnte aufgrund seines hohen Gehaltes an C_{org} nach der ^{14}C-Methode datiert werden[1]; außerdem liegen einige brauchbare Einzeldatierungen sowie Vergleichswerte aus der Literatur vor. Dadurch wurde die zeitliche Einordnung der biostratigraphischen Befunde und der Vergleich mit bereits vorliegenden Ergebnissen möglich. Es ergibt sich folgendes Bild der Klimageschichte im jüngeren Quartär im Untersuchungsgebiet: Vom Hangenden zum Liegenden folgen innerhalb des Holozän den heutigen Ablagerungen sehr schnell solche, deren Fauneninhalt einem kälteren

[1]) Die ^{14}C-Datierungen führte Herr Dr. Geyh vom Niedersächsischen Landesamt für Bodenforschung, Hannover, durch.

Lebensmilieu zuzuordnen ist. Diesen schließen sich nach unten Sedimente mit einer Foraminiferen-Gemeinschaft an, die auf wärmere Bedingungen hinweist, als heute am Untersuchungsort herrschen. Diese warme Periode liegt nach Untersuchungen in Borneo zwischen 3000 und 13 000 vor heute (SABELS, 1966), im Roten Meer zwischen 6000 und 11 000 (geschätzt nach HERMAN, 1965), nach den uns vorliegenden Daten zwischen ca. 5000 und 13 000. Damit ist ein holozänes Klimaoptimum also auch für den Indischen Ozean nachgewiesen. Für den unmittelbaren Grenzbereich zwischen kalt- und warmzeitlichen Sedimenten im Untersuchungsgebiet ergibt sich danach ein etwas höheres Alter als im offenen tropischen Atlantischen Ozean.

Die Faunenabfolge im Holozän und jüngsten Pleistozän der Kerne des bearbeiteten Stationenprofiles sind miteinander parallelisierbar, wenn das eingelagerte Fremdmaterial beim Vergleich ausgeklammert wird. Dieses ist im allgemeinen unschwer an der geänderten Zusammensetzung der benthonischen Faunenelemente erkennbar. Die Sedimentationsraten in ungestörten Kernen nehmen mit Entfernung von der Küste sehr stark ab. In einem Kern, dessen Sedimentationsrate nur noch bei 2—4 cm/1000 Jahre liegt, tauchen im tieferen Teil drei charakteristische Horizonte auf, die in den Kernen mit Sedimentationsraten von 5—30 cm/1000 Jahre nicht mehr erreicht wurden. Diese Horizonte ermöglichen sowohl den Vergleich zwischen den im offenen Ozean gewonnenen Sedimentkernen (bei ca. 5° bzw. 7° N / 66° bzw. 71° E), als auch mit einem nordwestlich der Lakkadiven gelegenen Kern, mit dem dann der Anschluß gewonnen wird an die Kerne im Norden des Untersuchungsgebietes. In allen Kernen mit geringer Sedimentationsrate ist eine Lage vulkanischen Glases zu beobachten. Sie ist älter als die letzte pleistozäne Kaltzeit und jünger als ein Maximalvorkommen von *Globigerina pachyderma* var., das wahrscheinlich der vorletzten pleistozänen Kaltzeit zuzurechnen ist.

Reprinted from *Geologischen Rundschau*, Band 60, 1970, p. 275-293

Porenwässer in rezenten Sedimenten vor der indisch-pakistanischen Küste und Rückschlüsse auf frühdiagenetische Vorgänge

V. MARCHIG, Hannover

Zusammenfassung

In mehreren Sedimentkernen aus dem Indischen Ozean, vom Schelf im Bereich der Indusmündung über den Kontinentalabhang bis zum Tiefseeboden vor der süd-indischen Küste wurden die Porenwässer untersucht. Sie wurden durch Auswaschen von den Sedimenten abgetrennt und auf Na, K, Ca, Mg, Cl und SO_4 analysiert.

*) Anschrift des Verfassers: Dipl.-Ing. V. MARCHIG, Bundesanstalt für Bodenforschung, 3 Hannover-Buchholz, Postfach 54.

Die Salinität der Porenlösungen ist gegenüber der des Meereswassers schon bei geringer Sedimentteufe im allgemeinen erhöht. Das Verhältnis von Na und Cl zeigt einen schwachen Anstieg zugunsten des Na. In den Porenlösungen zeigt die Salinität gegenüber der des Meereswassers eine starke Verarmung an Mg, im allgemeinen eine deutliche Verarmung an Ca und eine sehr starke Anreicherung an K. — Die Verhältnisse der Kationen Na, Ca, Mg liegen bei den meisten Kernen bereits im Bereich der fossilen Formationswässer (nach VON ENGELHARDT, 1960).

Abstract

The author has analysed the interstitial waters of several sediment cores from the Indian Ocean, which had been sampled on the shelf within the reach of the mouth of the Indus proceeding across the continental slope as far as to the deepsea ocean floor in front of the southern coast of India. The interstitial waters were separated from the sediments by extraction and analysed for Na, K, Ca, Mg, Cl and SO_4.

The salinity of the interstitial aequous solutions generally is increased with respect to sea water little below the sediment-water interface. The proportion between Na and Cl shows a slight increase in favor of Na. Compared to sea-water there is marked impoverishment of Mg; in general there is a clear impoverishment of Ca and a very significant enrichment of K. — In mast cores, the proportions of the cations Na, Ca, and Mg are within the realm of fossil waters (according to VON ENGELHARDT, 1960).

Résumé

L'auteur a analysé les eaux interstitielles de plusieurs carottes sédimentaires de la plateforme continentale de l'Ocean Indien devant l'embouchure de l'Indus en passant par le talus continental jusqu'à la mer abyssale devant la côte indienne méridionale. Ces eaux interstitielles ont été séparées des sédiments par éluage et analysées pour la détermination de leurs teneurs en Na, K, Ca, Mg, Cl et SO_4.

C'est déjà dans le cas d'une profondeur des sédiments peu considérable que la salinité des solutions aqueuses interstitielles est en général plus élevée en comparaison de celle de l'eau de mer. La proportion existant entre le Na et le Cl accuse une faible augmentation en faveur du Na. La salinité montre, en comparaison de celle de l'eau de mer, un fort appauvrissement en Mg; elle montre, en général, un appauvrissement net en Ca et un enrichissement très fort en K. — Les proportions des cations Na, Ca, Mg se situent, dans le cas de la plupart des carottes, déjà dans le domaine des eaux fossiles d'après VON ENGELHARDT, 1960).

Краткое содержание

Исследовали поровые воды многих осадочных кернов индийского океана от шельфа у устья Инда через континентальный склон до глубин океана леред южно-индийским побережьем. Эти воды вытесняли из осадочных пород и исследовали на следующие катионы и анионы: Na, K, Ca, Mg, Cl и SO_4 Соленость поровых растворов по отношению к морской воде в общем повышена, даже если эти растворы получены из кернов, залегающих сравнительно поверхностно. В соотношении Na и Cl преобладает Na. По сравнению с морской водой эти поровые воды бедны Mg, Ca и обогащены K. — Соотношение катионов Na, Ca и Mg в большей части кернов соответствует таковому вод древних формаций.

Inhalt

1. Literaturüberblick

Die ersten Untersuchungen an Porenwässern rezenter Sedimente führten MURRAY und IRVINE 1892 durch. Das verwendete Sediment war blauer Schlick, der bei der Challenger-Expedition gesammelt wurde. Sie fanden, daß durch den Zerfall der organischen Substanz die Alkalinität gestiegen war, außerdem verminderte sich die Menge an Sauerstoff und Sulfat gegenüber dem Meerwasser.

Nach dem Aufschwung der Ölbohrungen beschäftigt man sich mit fossilen Wässern, die man in Verbindung mit Erdöl findet (KREJCI-GRAF, HECHT & PASLER, 1957; FRIEDL, 1956). Als Erklärung für die starke Salzanreicherung wird zum ersten Mal von DE SITTER (1947) und weiter von ELLIS (1954), WYLLIE (1955), DAVIS (1955), MCKELVEY, SPIEGLER & WYLLIE (1957) die Filtration durch dabei als semipermeable Membran wirkende Tone genannt.

VON ENGELHARDT (1960) hat die bisher veröffentlichten Daten über fossile Porenwässer aus verschiedenen Erdölprovinzen gesammelt und deren Abstammung vom im Sediment eingeschlossenen Meerwasser abgeleitet.

BORDOVSKIJ (1961), ŠIŠKINA (1957, 1964), ŠIŠKINA & BILJKOVA (1962), TAGAEVA & TIHOMIROVA (1962), ŠIŠKINA & ŽELEZNOVA (1964) haben in großem Ausmaße die Porenwässer aus verschiedenen Typen von Meeressedimenten untersucht. Sie kamen zu einer Abhängigkeit zwischen der Salinität und dem Redoxpotential.

DEGENS, HUNT, REUTER & REED (1964) analysierten die Sauerstoffisotopenzusammensetzung fossiler Porenwässer und kamen zu dem Ergebnis, daß diese sich nur unwesentlich von rezentem Meereswasser unterscheiden, was bedeuten würde, daß sie nicht infolge von Evaporation an Salzen angereichert sind. In der gleichen Arbeit wird auf die Ähnlichkeit der Aminosäurespektren aus fossilen Porenwässern und rezentem Meereswasser hingewiesen.

Innerhalb der letzten Jahre sind mehrere Arbeiten erschienen, die sich mit Wechselbeziehungen zwischen Mineralen und Porenwässern in rezenten Sedimenten befassen.

SIEVER, BECK & BERNER (1965) befassen sich mit den Lösungsgleichgewichten zwischen Mineralen und Porenwässern in rezenten Sedimenten.

BROOKS, PRESLEY & KAPLAN (1968) analysieren eine Reihe von Spurenelementen in Porenwässern rezenter Sedimente und diskutieren deren Herkunft.

BERRY (1969) verfolgt eine Reihe von Faktoren, die auf die selektive Filtration der Porenwässer durch Ton Einfluß haben können.

KRAMER (1969) vergleicht eine Reihe der fossilen Porenwässer mit den Gesteinen, in denen sie zu finden sind, und untersucht ihren Sättigungsgrad in bezug auf verschiedene Minerale.

2. Einleitung

Die ersten diagenetischen Prozesse in rezenten Sedimenten sind uns bisher im allgemeinen nicht zugänglich. So lassen sich z. B. in ozeanischen Sedimenten die beginnende Umwandlung der Tonminerale und das erste Auftreten authigener Minerale weder röntgenographisch — wegen geringer Gehalte — noch optisch — wegen geringer Korngröße — erfassen.

Da in solchen Sedimenten diese Reaktionen immer in Gegenwart einer flüssigen Phase ablaufen, die in ständigem Austausch mit den festen Mineralphasen steht, besteht Hoffnung, daß sich die chemischen Änderungen der festen Phasen in der Zusammensetzung der umgebenden flüssigen Phase widerspiegeln. Darüber hinaus scheint eine stufenweise Annäherung an die Zusammensetzung der Porenlösung des verfestigten Sedimentes möglich.

Um einen Beitrag zur Klärung dieser Fragen zu leisten, wurden nachfolgende Untersuchungen an Porenwässern rezenter Sedimente durchgeführt. Die Mittel hierzu stellte dankenswerterweise die Deutsche Forschungsgemeinschaft zur Verfügung.

3. Herkunft der Proben

Von den bei der „Internationalen Indischen-Ozean-Expedition 1964/65" entnommenen Kernen (SCHOTT u. VON STACKELBERG, 1965) wurden sechs zur Untersuchung ihrer Porenlösungen ausgewählt. Wie Abb. 1 zeigt, entstammen sie verschiedenen untermeerischen Regionen.

1 Kern vom Tiefseeboden nahe dem Kontinentalabhang (182),
4 Kerne vom Kontinentalabhang (183, 185, 187, 237),
1 Kern vom Schelf im Bereich des Indusdeltas (28).

Alle diese Sedimente zeigen hohe Sedimentationsraten, die größenordnungsmäßig bei 3 und mehr cm/1000 J. liegen dürften (HEYE, 1968). Am Indusdelta war die Sedimentation wahrscheinlich am stärksten. Relativ hoher Gehalt an organischer Substanz in allen 6 Sedimentkernen spricht ebenfalls für starke Sedimentation.

4. Methodik und Fehlerbetrachtung

4.1 Allgemeines

Die Abtrennung des Porenwassers von den festen Sedimentphasen ist leider immer noch mit Fehlern behaftet, denn die bisher bekannten Methoden stellen alle einen Eingriff in die empfindlichen Lösungs- und Austauschverhältnisse dar. Die zwei wichtigsten Methoden, die heute Verwendung finden, sind Wasserextraktion und Auspressen. Beide Methoden greifen entweder durch Verdünnung oder durch Druckerhöhung in das

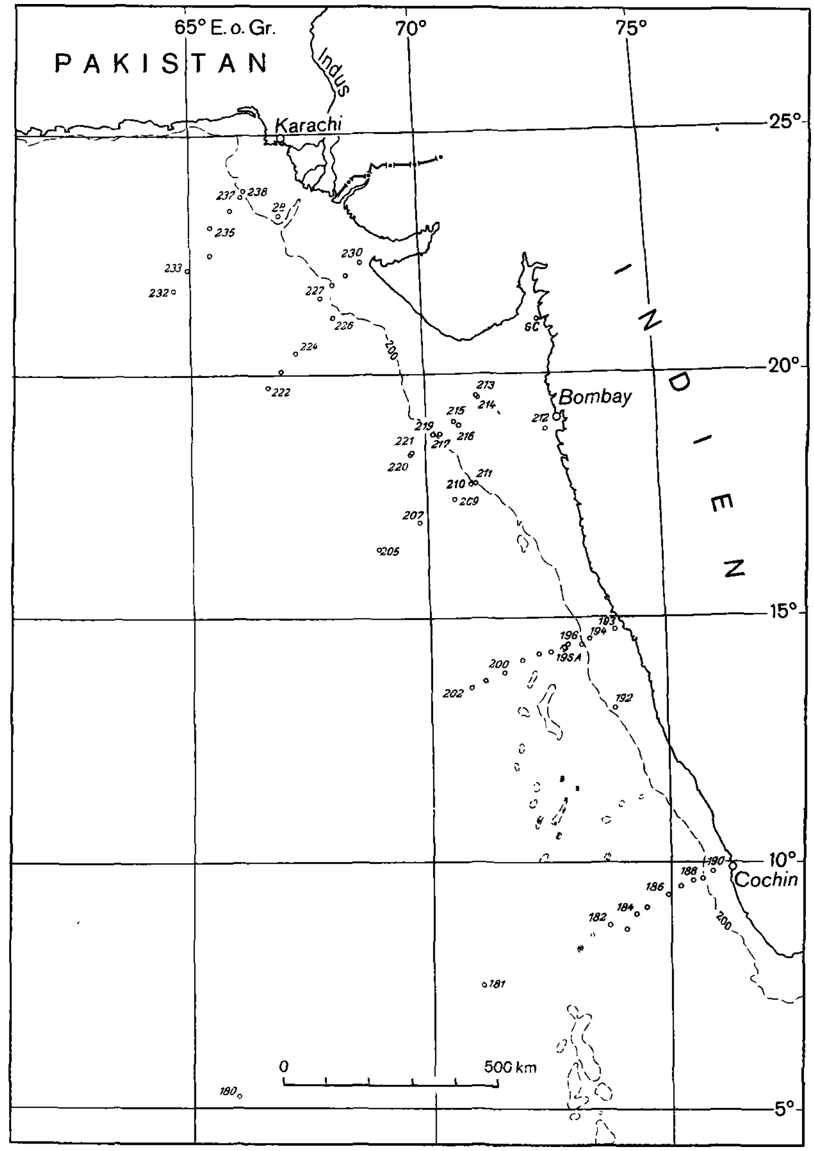

Abb. 1. Probeentnahmestellen auf dem Meeresboden vor der indisch-pakistanischen Küste.

279

Gleichgewicht Porenwasser/feste Sedimentphasen ein. Wir mußten uns aus Mangel an Probenmaterial für die Extraktion entscheiden, da das Auspressen viel mehr Substanz verlangt.

Wir bringen im folgenden die Ergebnisse der Untersuchungen am längsten der untersuchten Kerne, der als Beispiel für die anderen gelten kann.

4.2 Durchführung

4.2.1 Probenvorbereitung, Untersuchungsmethoden

Aus den untersuchten Kernen wurde alle 10—20 cm eine Probe von je etwa 2 cm Dicke entnommen. Diese Sedimentproben wurden im feuchten Originalzustand gewogen, dann in Wasser dispergiert und anschließend auf einem Membranfilter mit Porendurchmesser $\leqq 0{,}1\,\mu$ bis zum Verschwinden der AgCl-Reaktion ausgewaschen und zuletzt bei 105° C bis zur Gewichtskonstanz getrocknet. Die Differenz zwischen den Einwaagen des feuchten und des trockenen Sedimentes ist das Porenwasser oder die Porenlösung (= H_2O + gelöste Stoffe).

Das Filtrat wurde auf 250 ml eingedampft und darin folgende Ionen bestimmt:

a) Cl^- titrimetrische Bestimmung nach Mohr
b) SO_4^{2-} gravimetrische Bestimmung mit $BaCl_2$
c) Ca^{2+} komplexometrische Titration mit EDTA (photometrische Endpunktanzeige)
d) Mg^{2+} Bestimmung mit Hilfe des Atomabsorptions-Spektralphotometers
e) Na^+, K^+ flammenphotometrische Bestimmung.

Die Summe der Ionen, angegeben in Prozent der Porenlösung, bezeichnen wir als Salinität. (Sie enthält nicht sämtliche Anionen und Kationen, die im Meereswasser vorhanden sind, jedoch den überaus größten Teil davon.) Als vergleichbare Bezugsgröße gilt die mittlere Salinität des Meereswassers, die auf die gleiche Weise aus Mittelwerten dieser Ionen für das Meereswasser berechnet wird (= 3,42%).

4.2.2 Fehlerbetrachtung

Zunächst wurde geprüft, ob bei zu gründlichem Auswaschen ein Teil der von Tonen adsorbierten Ionen mit in die Lösung geht. Zu diesem Zwecke wurde die Salinität in Abhängigkeit der ausgewaschenen Sedimentmenge graphisch dargestellt (Abb. 2).

Aus der Abb. 2 geht hervor, daß bei kleineren Probenmengen die von uns bestimmte Salinität der Porenlösungen deutlich höher ist als bei größeren.

Um diese Aussage quantitativ erfassen zu können, haben wir an einem Kern für elf aufeinanderfolgende Proben je zwei Bestimmungen durchgeführt, und zwar für jede Probe einmal mit einer größeren (15—25 g) und einmal mit einer kleineren Sedimentmenge (5—10 g) als Einwaage. (Das waren ungefähr die extremen Einwaagen, mit denen vereinzelt auch bei anderen Proben gearbeitet wurde, normalerweise lagen bei den spä-

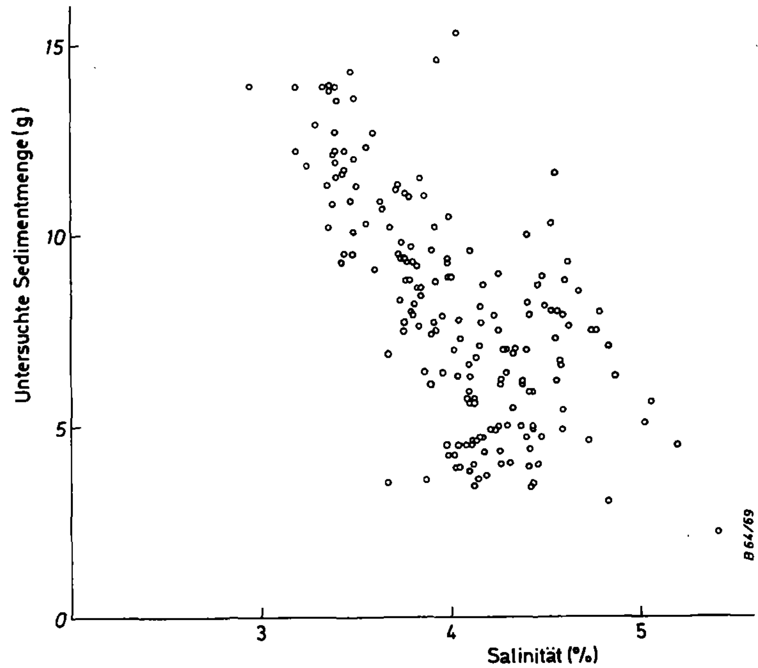

Abb. 2. Abhängigkeit der Salinität des Porenwassers von der Einwaage (der Naßsubstanz).

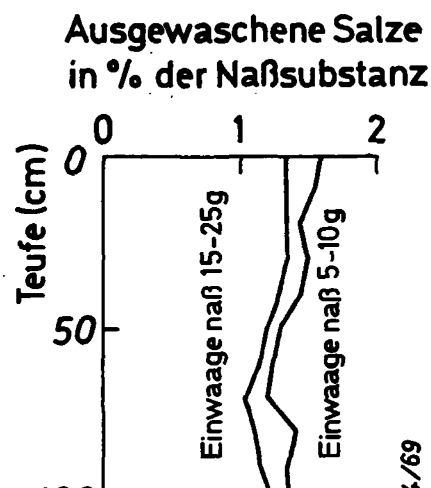

Abb. 3. Mengen der ausgewaschenen Salze in Kern 28 bei jeweils zwei verschiedenen Einwaagen vom gleichen Sediment.

281

teren Untersuchungen die Einwaagen zwischen diesen Extremen.) Wie Abb. 3 zeigt, sind bei der kleineren Einwaage im Mittel 10% mehr ausgewaschen worden. Da der Salinitätsunterschied unserer Proben (Abb. 6 und 7) teilweise bedeutend über 10% liegt, wird er also tatsächlich bestehen und nicht durch fehlerhafte Auswaschungen unterschiedlich großer Sedimentmengen vorgetäuscht sein.

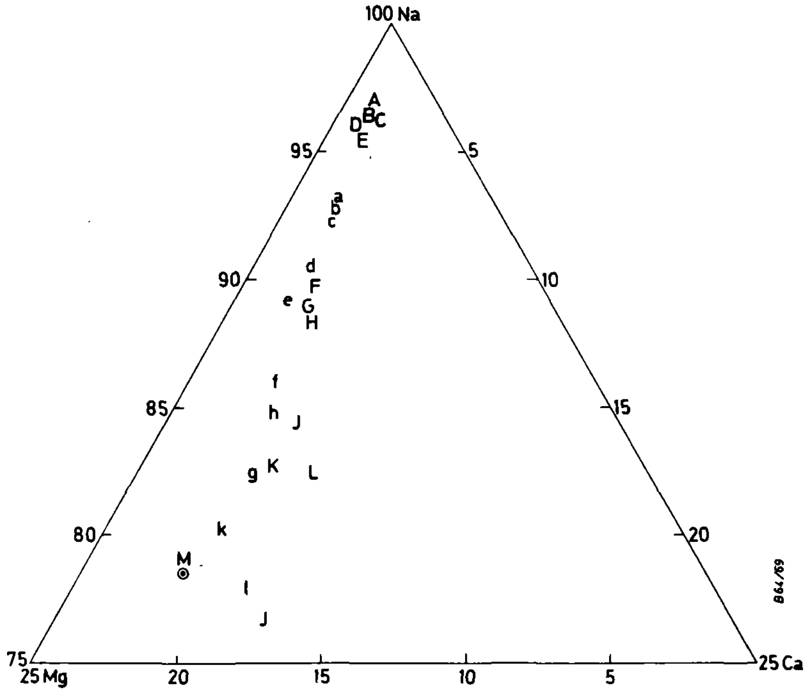

Abb. 4. Verhältnisse der Kationenäquivalente Na, Mg und Ca in den Porenwässern in Kern 28, bei jeweils zwei verschiedenen Einwaagen vom gleichen Sediment. — Kleine Buchstaben: Proben mit 15—25 g Einwaage; große Buchstaben: gleiche Proben mit 5—10 g Einwaage; M = Meerwasser.

Um zu zeigen, daß sich bei zwei verschieden großen Einwaagen einer Probe auch die Verhältnisse der Kationen verschoben haben, haben wir die Kationenäquivalente Na, Mg, Ca in das Dreieckdiagramm nach Niggli (1952) eingetragen (Abb. 4). Wie man sieht, besteht der Unterschied zwischen den zwei Bestimmungen je einer Probe hauptsächlich in der Erhöhung des Mg-Gehaltes bei der kleineren Einwaage. Die Auswaschung wurde demnach zu intensiv vorgenommen, so daß ein Teil der von Tonen adsorbierten Mg-Ionen in die Lösung gegangen ist. Da Magnesium in den ersten Stadien der Diagenese sehr labil und reversibel an Tonminerale gebunden bzw. absorbiert ist, wird man mit dieser Methode sehr schwer zu guten Ergebnissen für Mg kommen. Unsere Bemühungen sollen sich in der Richtung bewegen, den Fehler möglichst klein zu halten und die Ergebnisse durch konstante Einwaagen reproduzierbar zu machen.

Im übrigen soll bei der Darlegung der einzelnen Ergebnisse deren Verfälschung durch den Auswaschungsfehler, falls erforderlich, erneut diskutiert werden.

5. Ergebnisse

5.1 Allgemeines

Der Anteil des Porenwassers liegt in 5 der 6 untersuchten Kerne im allgemeinen zwischen 50 und 70%. Er zeigt damit gute Übereinstimmung

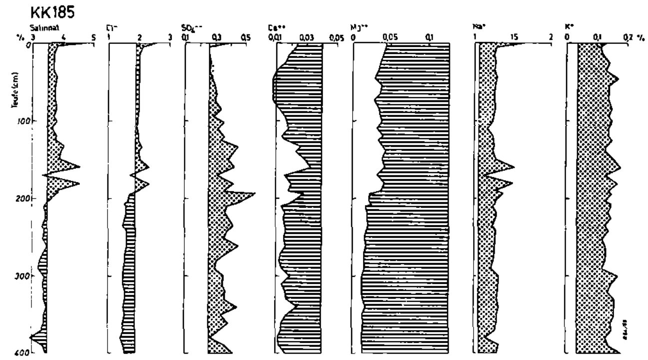

Abb. 5. Vergleich von Salinität und Gehalt an verschiedenen Ionen in den Porenwässern des Kernes 185 (in Beziehung zur Teufe) mit dem Meerwasser (die vertikale Linie zeigt jeweils den entsprechenden Gehalt des Meerwassers an). — Punktiert: Anreicherung gegenüber Meerwasser; schraffiert: Verarmung gegenüber Meerwasser.

mit entsprechenden Literaturangaben. In Schichten mit gröberem Material sinkt der Porenwasseranteil vereinzelt bis auf 17% ab, und im grobkörnigeren Kern 28 (Indusdeltanähe) liegt er generell zwischen etwa 30 und 40%. Eine eingehende Diskussion des Porenwasseranteils wird den geologisch-mineralogischen Bearbeitungen dieser Sedimente zu entnehmen sein (Schott et al. 1970).

5.2 Salinität

Stellt man die Werte für die Salinität und die für die analysierten Ionen in Abhängigkeit von der Sedimentteufe graphisch dar und zeichnet zusätzlich die entsprechenden Mittelwerte für Meerwasser ein, so ergibt sich folgendes Bild (Abb. 5).

Die Salinität liegt durchschnittlich mit Gehalten bis zu fast 5% (Abb. 7, unterer Teil des Kerns 187) deutlich über der mittleren Salinität des Meerwassers von 3,42%. Dieser große Salinitätsunterschied kann nur zum Teil mit dem bereits diskutierten „Waschfehler" erklärt werden; ein gewisser Unterschied zwischen den Salinitäten des Meerwassers und den von uns analysierten Porenwässern ist sicher vorhanden. Die niedrigere Salinität beim Kern 185 ist vielleicht auf die relativ häufigen Einschaltungen dünner, grobkörnigerer Schichten zurückzuführen. Die Porenwässer im oberen Teil des Kerns 187 könnten wegen des größten Porenvolumens aller Proben (max. 71% Porenwasser) und der damit verbundenen Austauschmöglichkeiten mit dem Meerwasser dem Meerwasser so ähnlich sein. Weitgehendere Erklärungen ergeben sich vielleicht durch die geologisch-mineralogischen Bearbeitungen (SCHOTT et al., 1970).

Die logische Deutung für die Erhöhung der Salinität des Porenwassers gegenüber der des Meerwassers in der Mehrzahl der Fälle scheint die Auspressung eines Teils des Porenwassers durch Kompaktion der Sedimente zu sein. Infolge der Wirkung des Tons als semipermeable Wand können nur Lösungen mit geringerer Ionenkonzentration den Weg ins offene Meerwasser passieren, während die Konzentration der im „Restwasser" des Sediments verbleibenden Ionen ansteigt (ELLIS, 1954). Die Erklärung der erhöhten Salinität als konservierte Paläosalinität (ŠIŠKINA-ŽELEZNOVA, 1964; GONI & PARENT, 1966) stößt dagegen bei den hier untersuchten Sedimenten auf Schwierigkeiten. In der Mehrzahl unserer Kerne tritt die Erhöhung direkt an der Sedimentoberfläche ein; das aber würde bedeuten, daß eine wesentliche Erhöhung der Meerwassersalinität in allerjüngster Zeit eingetreten sein müßte, was kaum plausibel erklärt werden könnte.

Setzen wir also die Erhöhung der Salinität im Porenwasser gegenüber der des Meerwassers durch Kompaktion der Sedimente und „Diffusionsbarriere" voraus, so ist ein Anstieg der Salinität mit zunehmender Sedimentteufe zu erwarten. Ein solcher Anstieg ist andeutungsweise nur in 2 von den 6 untersuchten Kernen (ein Beispiel zeigt Abb. 7) zu erkennen. Zur Ausbildung einer regelmäßigen, gut beobachtbaren Zunahme innerhalb eines Kerns ist jedoch sicher relativ hohe Gleichförmigkeit von Korngröße und Materialart über das ganze Sedimentprofil erforderlich, die annähernd ebenfalls nur im Kern 187 realisiert ist. Wahrscheinlich ist aber unsere Art der Salinitätsbestimmung nicht ausreichend, und weiterhin sind die Kerne vielleicht zu kurz, um bei diesen Sedimenten bereits größere Unterschiede in der Salinität zu zeigen. Aus den gleichen Gründen wurde wohl auch keine Abhängigkeit zwischen Salinität und Tongehalt in den Kernen beobachtet.

5.3 Konzentration einzelner Ionen

Wenn man die Konzentrationen der Ionen einzeln, zunächst der Anionen, in gleicher Darstellungsweise betrachtet (Abb. 5), so stellt man entsprechend dem Verhalten der Salinität im allgemeinen eine Erhöhung fest. Bei den Kationen sind die Gehalte an Na und K gegenüber dem Meerwasser erhöht; Ca und Mg dagegen gibt es in den Porenwässern weniger als im Meerwasser.

Um zu zeigen, inwieweit diese Konzentrationsunterschiede der untersuchten Ionen zu den Mittelwerten des Meerwassers durch Salinitätserhöhung der Porenwässer bedingt sind und in welchem Ausmaße noch andere Prozesse eine Rolle spielen, wurde eine andere Darstellungsweise gewählt. Zunächst wurde in den Abb. 6 und 7 der prozentuale Unterschied der Salinität zwischen Meerwasser und Porenwasser, bezogen auf 3,42% des Meerwassers als 100%, in Abhängigkeit von der Sedimentteufe graphisch dargestellt. Unter der Annahme, daß die Zusammensetzung der Salinitäten von Porenwasser und Meerwasser gleich sei, wurde sodann für jede Ionenart der prozentuale Unterschied zu den Mittelwerten für Meerwasser (= 100%) aus der Salinität der Porenwässer berechnet und auf die gleiche Weise gezeichnet. Schließlich wurden die tatsächlich gemessenen Ionenkonzentrationen auch auf diese Art in den gleichen Diagrammen den berechneten gegenübergestellt. Die Fläche zwischen den beiden Streckenzügen stellt den Unterschied in der Zusammensetzung der Salinität zwischen dem darüberstehenden Meerwasser und den untersuchten Porenwässern dar. Er soll als relative Anreicherung bzw. Verarmung der entsprechenden Ionen bezeichnet werden.

Nach dieser Darstellung zeigt sich, daß die relative Na-Anreicherung im Porenwasser im allgemeinen durchschnittlich 20% nicht übersteigt. (Es kommen jedoch auch stärkere Anreicherungen mit bis zu etwa 30% und Verarmungen von bis zu 10% vor.) Die relative Cl-Verarmung beträgt im Durchschnitt höchstens 20%. (Es kommen jedoch auch schwache Anreicherungen mit bis zu etwa 10% vor.)

Im großen und ganzen kann man feststellen, daß Na und Cl keine wesentlichen relativen Abweichungen gegenüber dem Meerwasser erfahren. Der Effekt der semipermeablen Wand wirkt sich auf beide Ionen etwa gleich aus, wofür auch die etwa gleiche Ionengröße von Na^+ und Cl^- spricht. Schließlich wird die Konzentration von Na und Cl auch nicht durch chemische Reaktionen gestört, in denen Na oder Cl verbraucht werden. Außer der sicher untergeordneten Neubildung von Zeolithen, bei der Na verbraucht werden kann, sind derartige Reaktionen zu Beginn der Diagenese nicht bekannt. Die oben beschriebene geringe Verschiebung des Na/Cl-Verhältnisses zugunsten des Na könnte höchstens mit einer Auflösung von detritischen Feldspäten erklärt werden.

Ganz anders verhält sich demgegenüber das Kalium. In allen Kernen finden wir eine starke relative Anreicherung in den Porenwässern, die zwischen 200 und 500% beträgt. Eine Erklärung für die hohen K-Gehalte ist sowohl darin zu sehen, daß die semipermeable „Tonwand" für K^+ einen überdurchschnittlich hohen Widerstand darstellt, als auch in der Mg^{2+}-Adsorbtion an die Tone, wobei K^+ verdrängt wird und in die Porenwässer gelangt. Ein Teil des K^+ in Porenwässern könnte auch aus der Verwitterung K-führender Silikate (Feldspäte und Glimmer) stammen.

Ebenfalls anders als Na und Cl, aber entgegengesetzt wie K, verhält sich das Mg. Die relative Verarmung beträgt im allgemeinen durchschnittlich mindestens 70%, meist jedoch mehr (vereinzelt sogar 95%) (in kleineren Bereichen anderer Kerne kann sie auf 20—40% absinken). Diese geringe Mg-Konzentration ist zum Teil vielleicht durch einen überdurchschnittlich kleinen Widerstand der semipermeablen Tonwand für Mg^{2+} zu erklären, wahrscheinlich aber werden dem Porenwasser durch starke Adsorbtion von Mg an Tonmineralen und Neubildung Mg-führender Schichtsilikate

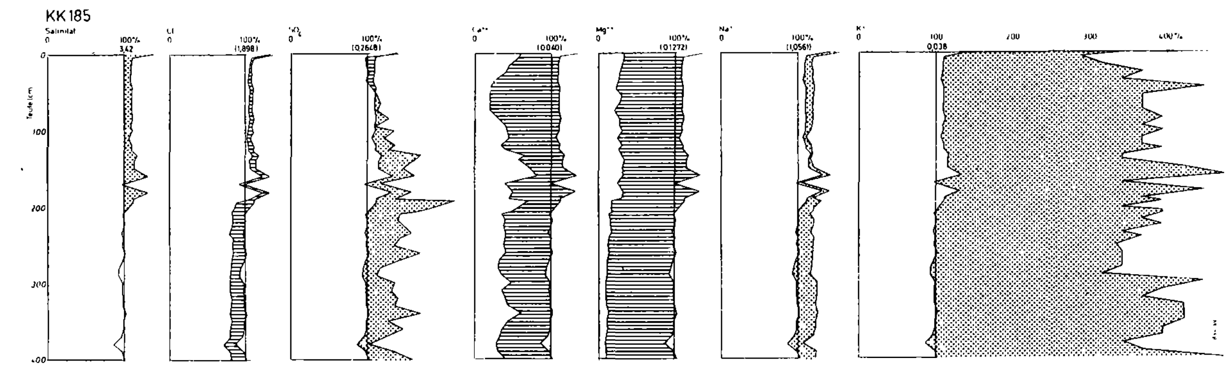

Abb. 6 (Legende S. 287, unten)

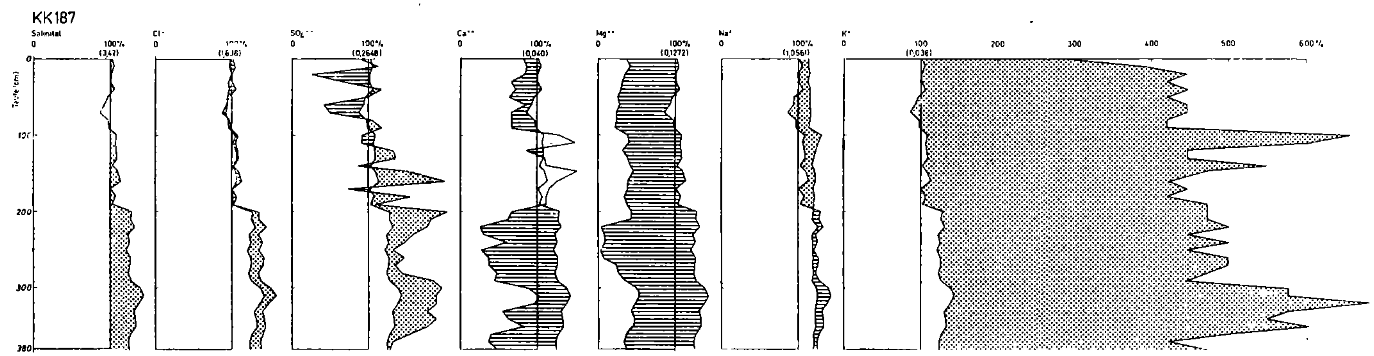

Abb. 7 (Legende S. 287, unten)

größere Mg-Mengen entzogen. Derartige Reaktionen in frühen Stadien der Diagenese sind bereits beobachtet und beschrieben worden (von Engelhardt, 1960; Siever, Beck & Berner, 1965; Brooks, Presley & Kaplan, 1968). Wahrscheinlich spielt zunächst die Adsorbtion eine größere Rolle, während sich im Laufe der Zeit das Verhältnis von adsorbiertem zu eingebautem Magnesium immer mehr zugunsten des eingebauten verschiebt.

Ca verhält sich im Prinzip wie das Mg, jedoch ist die relative Verarmung meist geringer als die des Magnesiums. (In kleinen Bereichen anderer Kerne wurden sogar teils deutliche relative Anreicherungen festgestellt.) Dennoch ist anzunehmen, daß das Verhalten des Ca durch ähnliche Faktoren wie beim Mg gesteuert wird.

Die relative Verarmung an Ca überrascht zunächst, da die vorliegenden Sedimente ziemlich reich an organischer Substanz sind. Beim Zerfall der organischen Substanz entsteht CO_2, das in diesem Milieu generell zur verstärkten Auflösung der Karbonate führen müßte (eine solche Auflösung junger Karbonatschalen wird jedoch durch deren organische Schutzschicht erheblich erschwert, wie bei Bearbeitung dieser Proben im Labor mit Säuren selbst höherer Konzentration vielfach beobachtet wurde). Mit fortschreitender Diagenese und erhöhtem Abbau dieser organischen Schutzhülle sollte aber verstärkte Auflösung von Kalkschalen und damit Anreicherung von Ca im Porenwasser möglich sein.

In allen Kernen ist mit Zunahme der Sedimentteufe eine relative Zunahme an SO_4^{2-} festzustellen. Dieser Befund konnte zunächst keine Erklärung finden. In den meisten in der Literatur beschriebenen Fällen wurde nämlich im Gegensatz zu den hier untersuchten Kernen eine Abnahme beobachtet und durch bakterielle Reduktion des Sulfates zu Sulfid und nachfolgender Ausfällung als Metallsulfid gedeutet. Volkov und Ostroumov (1960) haben dagegen auch eine Erhöhung des Sulfatgehaltes in manchen Porenlösungen von Sedimenten des Pazifiks gefunden. Sie erklären diese Erhöhung durch Zerfall von Ca-Sulfoaluminaten. Diese Erklärung scheint für die hier untersuchten Sedimente des Indischen Ozeans unbrauchbar zu sein, da hier bisher keine Ca-Sulfoaluminate festgestellt werden konnten.

Abb. 6. Vergleich von Salinität der Porenwässer mit den Gehalten an verschiedenen Ionen im Kern 185 (in Beziehung zur Teufe). Salinität und Ionenkonzentrationen sind in % ausgedrückt. Bezugsgröße ist die Salinität bzw. Konzentration an dem jeweiligen Ion des Meerwassers, die = 100% gesetzt wurde. — Punktiert: Anreicherung gegenüber dem %-Anteil des gleichen Ions im Meerwasser; schraffiert: Verarmung gegenüber dem %-Anteil des gleichen Ions im Meerwasser.

Abb. 7. Vergleich von Salinität der Porenwässer mit den Gehalten an verschiedenen Ionen im Kern 187 (in Beziehung zur Teufe). Salinität und Ionenkonzentrationen sind in % ausgedrückt. Bezugsgröße ist die Salinität bzw. Konzentration an dem jeweiligen Ion des Meerwassers, die = 100% gesetzt wurde. — Punktiert: Anreicherung gegenüber dem %-Anteil des gleichen Ions im Meerwasser; schraffiert: Verarmung gegenüber dem %-Anteil des gleichen Ions im Meerwasser.

Wir verdanken Herrn Dr. NIELSEN (frdl. mündliche Mitteilung) den Hinweis auf eine mögliche Oxydation des Sulfidanteils des Sediments zu Sulfat beim Auswaschvorgang. Unter dieser Voraussetzung würde die gefundene Sulfatanreicherung auf eine Sulfidanreicherung mit der Teufe im Sediment hinweisen.

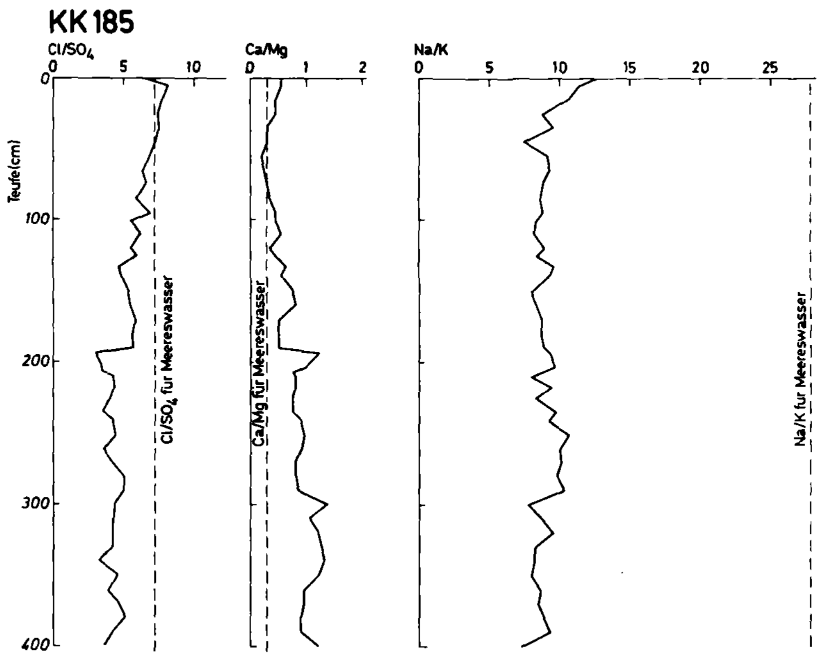

Abb. 8. Verhältnisse der Ionenkonzentrationen (in Beziehung zur Teufe) in Porenwässern des Kernes 185. Die vertikale Linie zeigt jeweils das entsprechende Verhältnis im Meerwasser an.

5.4 Verhältnis der Ionenkonzentrationen zueinander

Die Verhältnisse Cl/SO_4, Ca/Mg und Na/K (Abb. 8) bestätigen die schon angeführten Beobachtungen:

Das durchschnittliche Cl/SO_4-Verhältnis fällt deutlich mit Zunahme der Teufe, da SO_4 mit der Teufe zunimmt und Cl konstant bleibt.

Das Ca/Mg-Verhältnis ist im Mittel in den Porenwässern durchweg etwas höher als im Meerwasser, da unter den gegebenen Bedingungen offensichtlich Mg aus den Porenwässern bevorzugt vor Ca an die Tone adsorbiert wird.

Das Na/K-Verhältnis der Porenlösungen ist wegen höheren K-Gehaltes generell bedeutend niedriger als das des Meerwassers.

Wenn man die unterschiedlichen Veränderungen der Gehalte an den analysierten Ionen betrachtet, stellt sich die Frage, ob das Verhältnis der von uns bestimmten Kationen und Anionen im Gleichgewicht geblieben ist. Da das Verhältnis von Kationenäquivalenten zu Anionenäquivalenten 1 sein muß, folgt aus den Verhältnisverschiebungen der von uns

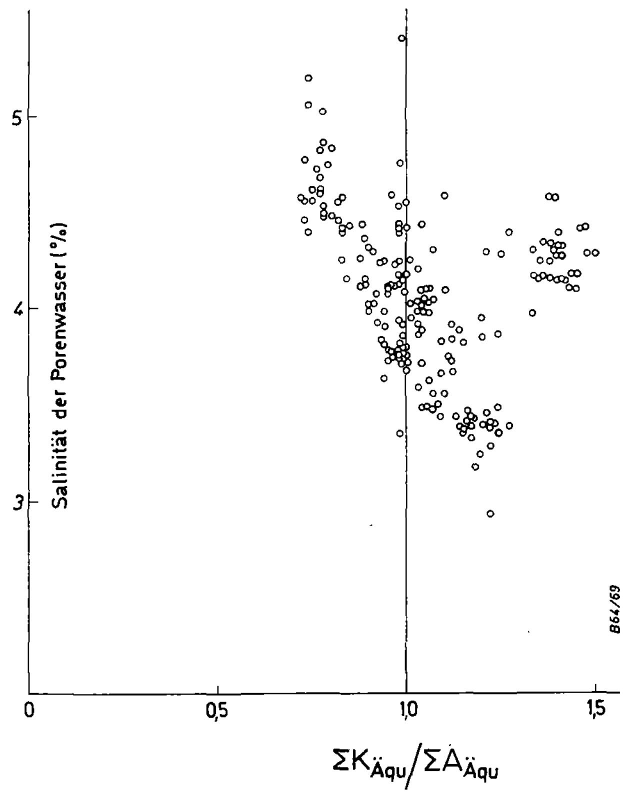

Abb. 9. Abhängigkeit des Quotienten: $\frac{\text{Summe der Kationenäquivalente}}{\text{Summe der Anionenäquivalente}}$ in den Porenwässern von der Salinität dieser Porenwässer. Die vertikale Linie zeigt den theoretischen Wert für diesen Quotienten, d. h. für den Fall, daß alle Ionen aus den Porenwässern bestimmt wurden.

bestimmten Ionen, daß andere Ionen, die in unserer Analyse nicht berücksichtigt wurden, in die Lösung gekommen sind.

Aus Abb. 9 geht deutlich hervor, daß sich das Verhältnis von Kationenäquivalenten zu Anionenäquivalenten verschoben hat, und zwar wird der Kationenmangel mit ansteigender Salinität immer stärker. Hier spiegelt sich wahrscheinlich eine Abhängigkeit zwischen der Elektrolytkonzentration und dem Kationenaustausch an den Tonen wider. Bei höherer Elektrolytkonzentration (also höherer Salinität) werden mehr Kationen ausgetauscht — also werden weniger von den primären Kationen in der Lösung bleiben. Um welche Kationen es sich bei diesem Austausch handelt, können wir zunächst nicht beweisen. Es wird unsere Aufgabe sein, bei weiteren Untersuchungen von Porenlösungen dieser Sache nachzugehen.

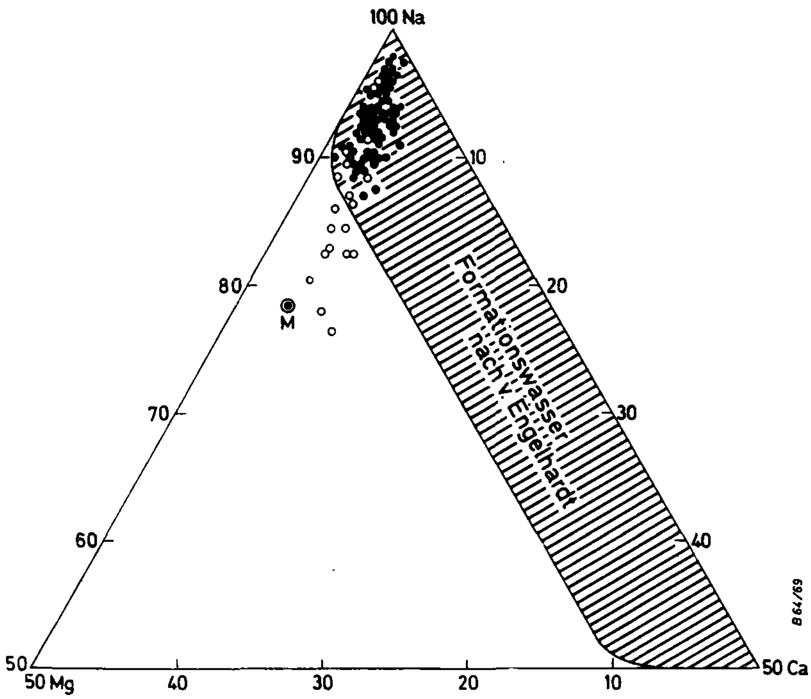

Abb. 10. Verhältnisse der Kationenäquivalente von Mg, Ca und Na in den untersuchten Porenwässern. Im Dreiecksdiagramm ist gleichzeitig der Bereich der fossilen Formationswässer nach VON ENGELHARDT (1960) eingezeichnet — Volle Kreise: Kerne 182, 183, 185, 187; leere Kreise: Kerne 28, 237; M = Meerwasser.

5.5 Vergleich der Porenlösungen rezenter und fossiler Sedimente

In unseren bisherigen Betrachtungen gingen wir von der Voraussetzung aus, daß die Veränderungen in der chemischen Zusammensetzung größtenteils auf Kompression und Wechselwirkung mit den Tonen zurückzuführen sind. Weiterhin nehmen wir an, daß die gleichen Prozesse bis zu Formationswässern, wie sie uns von den Erdölbohrungen bekannt sind, führen. Um unsere Porenlösungen mit Formationswässern vergleichen zu können, haben wir uns einer Darstellungsweise der Erdölgeologie bedient. Es handelt sich dabei um ein Dreiecksdiagramm mit den Kationenäquivalenten von Na, Ca und Mg an den Ecken. Aus der Abb.10 geht deutlich die Annäherungstendenz zu Formationswässern hervor. Den Übergang vom Meerwasser zu Formationswässern machen, wie erwartet, die Porenwässer des grobkörnigsten der hier untersuchten Kerne (Kern 28 vom Indusdelta) aus. Die wahrscheinlich sehr große Sedimentationsrate dürfte die geringste diagenetische Veränderung bewirkt haben. Die anderen Kerne konzentrieren sich im Bereich der Ca-armen Formationswässer. Die Verminderung des Mg-Gehaltes gegenüber anderen Kationen ist offensichtlich schon fast voll erreicht. Diese Darstellungsweise schließt leider das Kalium aus.

6. Zusammenfassung

Bei der Untersuchung von Porenwässern rezenter Sedimente des Indischen Ozeans wurden folgende Ergebnisse erzielt:

Die Salinität der Porenlösungen ist gegenüber der des Meerwassers schon bei geringer Sedimentteufe im allgemeinen erhöht. Das Verhältnis von Na und Cl, den Hauptträgern der Salinität, zeigt einen schwachen Anstieg zugunsten Na.

In den Porenlösungen zeigt die Salinität gegenüber der des Meerwassers:

starke Verarmung an Mg,
im allgemeinen deutliche Verarmung an Ca,
sehr starke Anreicherung von K.

Zusammenfassend kann man sagen, daß die Porenwässer gegenüber dem Meerwasser schon bei sehr geringer Sedimentteufe, sowohl bezüglich der Salinität insgesamt als auch bezüglich der Zusammensetzung der Salinität deutlich verändert sind.

Vergleicht man nun die Zusammensetzung der Salinität in unseren Porenwässern rezenter Sedimente mit der fossiler Porenwässer, so zeigt sich folgendes:

Mit Ausnahme des Kerns vor der Indusmündung ist in allen Kernen der Bereich der fossilen Formationswässer nach VON ENGELHARDT (1960) bereits nach geringer Sedimentteufe erreicht. Das Porenwasser des etwas grobkörnigeren und daher wahrscheinlich besser durchspülten Kernes stellt in seiner Zusammensetzung den direkten Übergang zwischen dem Meerwasser und den anderen Porenwässern dar. Diese Porenwässer sind sehr Na-reich, Mg- und Ca-arm. Die Abnahme ihrer Mg-Gehalte gegenüber dem Meerwasser dürfte in etwa abgeschlossen sein. Dagegen ist eine Zunahme an Ca mit zunehmender Sedimentteufe und/oder zunehmendem Sedimentalter durch Auflösung von Kalkschalen zu erwarten.

Beim Vergleich der beschriebenen Porenwässer in rezenten Sedimenten mit fossilen Porenwässern ergeben sich folgende Schlüsse über den Beginn der Diagenese:

a) Schon früh gibt es eine starke K-Zunahme, die durch eine Diffusionsbarriere oder durch Austausch mit Mg-Ionen an den Tonen bedingt sein kann. Ein Teil dieser Zunahme kann auch aus dem Zerfall K-haltiger Silikate (Glimmer und Feldspäte) stammen. Eine K-Abnahme infolge von Illit-Neubildung findet erst in viel größeren Sedimenttiefen statt (WEAVER, 1967).

b) Die Karbonatauflösung ist bei den rezenten organogenen Karbonaten wegen einer organischen Schutzhülle verzögert. Gleichzeitig wird wohl etwas Ca an Tonminerale adsorbiert. Infolgedessen sinkt der Ca-Gehalt der Porenlösung unter den Ca-Anteil der Meerwassersalinität.

c) Schon früh ist die Mg-Adsorbtion an den Tonen abgeschlossen. Das adsorbierte Mg steht später für diagenetische Mineral-Neu- und Umbildungen zur Verfügung.

Die hier vorgelegten Ergebnisse sind Teil einer größeren Arbeit von V. MARCHIG über geochemische Untersuchungen an Sedimenten vor der indisch-pakistanischen Küste, die demnächst in den „Meteor"-Forschungsberichten, Abh. Geol. u. Geoph. erscheinen wird. Dort werden dann auch sämtliche Analysendaten und weitere Einzelheiten der Porenwasseruntersuchungen mitgeteilt.

Literaturverzeichnis

BERRY, F. A. F.: Relative Factors influencing Membrane Filtration Effects in Geologic Environments. — Chem. Geol., **4**, 295—301, 1969.

BORDOVSKIJ, O. K.: On the Chemistry of the Bottom Sediments of the Indian Ocean. — Okeanol. Isled., **4**, 91—99, 1 Tab., 1961.

BREDENHOEFT, J. D., BLYTH, C. R., WHITE, W. A., & MAXEY, G. B.: Possible Mechanism for Concentration of Brines in Subsurface Formations. — Bull. Amer. Assoc. Petro. Geol., **47**, 257—269, 8 Abb., 1963.

BROOKS, R. R., PRESLEY, B. J., & KAPLAN, I. R.: Trace Elements in the Interstitial Waters of Marine Sediments. — Geochim. Cosmochim. Acta, **32**, 397—414, 7 Abb., 6 Tab., 1968.

BRUJEVICH, S. V., & KULIK, E. Z.: Causes of Decrease in Alkalinity of the Interstitial Solutions of Deep-Ocean Sediments. — Geochemistry Intern., **4**, 589—598, 7 Tab., 1967.

CHILINGARIAN, G. V., & RIEKE, H. H.: Some Chemical Alterations of Subsurface Waters During Diagenesis. — Chem. Geol., **4**, 235—252, 8 Abb., 9 Tab., 1969.

DAVIS, L. E.: Electrochemical Properties of Clays. — Proc. First Nat. Conference Clays and Clay Techn., Div. Mines Calif. Bull., **169**, 47—53, 2 Abb., 1955.

DEGENS, E. T., HUNT, J. M., REUTER, J. H., & REED, W. E.: Data on the Distribution of Amino Acids and Oxygen Isotopes in Petroleum Brine Waters of Various Geologic Ages. — Sedimentology, **3**, 199—225, 12 Abb., 6 Tab., 1964.

DE SITTER, L. V.: Diagenesis of Oil Field Brines. — Bull. Amer. Assoc. Petrol. Geol., **31**, 2030—2040, 4 Abb., 1947.

ELLIS, C. B.: Fresh Water from the Ocean. — New York Ronald Press Comp., 217 S., 41 Abb., 1954.

VON ENGELHARDT, W.: Der Porenraum der Sedimente. — Mineralogie und Petrographie in Einzeldarstellungen, 207 S., 83 Abb., 39 Tab., Springer Verlag, Berlin 1960.

FRIEDL, K.: Die Tiefenwässer der Gösting-Domung. — Erdöl und Kohle, **9**, 505—511, 3 Abb., 4 Tab., 1956.

GOLDBERG, E. D., & ARRHENIUS, G. O. S.: Chemistry of Pacific Pelagic Sediments. — Geochim. Cosmochim. Acta, **13**, 153—212, 10 Abb., 21 Tab., 1958.

GONI, J., & PARENT, C.: Étude geochimique d'une tranche des sédiments fins actuels (Baie de la Vilaine, Morbihan) Méthodologie, Paléosalinité et diagénèse. — Bull. B.R.G.M., **5,** 19—62, 23 Abb., 7 Tab., 1966.

HEYE, D.: Entwicklung von Meßmethoden zur radioaktiven und magnetischen Alterskorrelation an Sedimenten des Indischen Ozeans. — Diss. Nat. Wiss. Fak., TU Braunschweig, 67 S., 31 Abb., 9 Tab., 1968.

KRAMER, J. R.: Subsurface Brines and Mineral Equilibria. — Chem. Geol., **4,** 37—50, 8 Abb., 6 Tab., 1969.

KREJCI-GRAF, K., HECHT, F., & PASLER, W.: Über Ölfeldwässer des Wiener Beckens. — Geol. Jb., **74,** 161—210, 5 Abb., 23 Tab., 1957.

LUDWIG, G.: Die Bestimmung der Salinität des Absatzmediums oberkarbonischer Tonsteine mit Hilfe der austauschbaren Kationen und löslichen Salze. — Geol. Jb., **88,** 59—82, 9 Abb., 1969.

MCKELVEY, J. G., SPIEGLER, K. S., & WYLLIE, M. R. J.: Salt Filtering by Ion Exchange Grains and Membranes. — J. Phys. Chem., **61,** 174—178, 4 Abb., 1957.

MURRAY, J., & IRVINE, R.: On the Chemical Changes which take Place in the Composition of the Sea-Water associated with Blue Muds on the Floor of the Ocean — Transact Royal Soc. Edinburg, Vol. **XXXVII,** 481—508, 12 Tab., R. Grant & Son., Edinburgh 1892.

NIGGLI, P.: Gesteine und Minerallagerstätten. II. Exogene Gesteine und Minerallagerstätten. — 557 S., 181 Abb., 67 Tab., Verl. Birkhäuser, Basel 1952.

SCHOTT, W., VON STACKELBERG, U., ECKHARDT, F.-J., MATTIAT, B., PETERS, J., & ZOBEL, B.: Geologische Untersuchungen an Sedimenten des indisch-pakistanischen Kontinentalrandes (Arabisches Meer). — Geol. Rdsch., **60** (H. 1), 1970.

SIEVER, R., BECK, K. C., & BERNER, R. A.: Composition of interstitial Waters of modern Sediments. — J. Geol., **73,** 39—73, 10 Abb., 5 Tab., 1965.

SIEVER, R., GARRELS, R. M., KANWISHER, J., & BERNER, R. A.: Interstitial Waters of Recent Marine Muds off Cape Cod. — Science, **134,** 1071—1072, 1 Abb., 1961.

ŠIŠKINA, O. V.: Ilovlje vodi Tihogo okeana i prilegajosih morei. — Dokl. Akad. nauk SSSR, **112,** 3, 470—473, 1 Abb., 2 Tab., 1957.

—: Himiceskii sostav okeaniceskiih ilovljih vod. — Geohimija, **6,** 564—571, 2 Tab., Moskva 1964.

ŠIŠKINA, O. V., & BILJKOVA, V. S.: O himiceskom sostave ilovljih vod Atlanticeskogo okeana. — Akad. nauk SSSR, Trudi morskoi gidrof. inst., **6,** 187—194, 3 Tab., Moskva 1962.

ŠIŠKINA, O. V., & ŽELJEZNOVA, A. A.: Chlorinity of Interstitial Water of Northern Part of the Indian Ocean. — Trudi in-ta okeanologii, **64,** 144—153, 4 Abb., 3 Tab., 1964.

TAGAEVA, N. V., & TIHOMIROVA, M. M.: Géochimie des eaux interstitielles dans la diagenèse des sédiments marins (d'après l'éxemple des dépots de la mer Caspienne). — Izdat. Akad. Nauk SSSR, **1,** 246 S., 66 Abb., 84 Tab., Moskva 1962, B.R.G.M., traduction no. 4286).

VOLKOV, I. I., & OSTROUMOV, Z. A.: Raspredelenie Sulfatov v donjih otalozeniah Tihogo Okeana.— Okeanologiceskie Isledovania, No. **2,** X Razdel Programlji MGG, Izd-vo AN SSSR 1960.

WEAVER, C. E.: Potassium, Illite and the Ocean-Geochim. Cosmochim. Acta, **31,** S. 2181—2196, 3 Abb., 1 Tab., 1967.

WYLLIE, M. R. J.: Role of Clays in Well Log Interpretation. — Clays and Clay Technology, Proc. First. Nat. Conference, Div. Mines Calif. Bull., **169,** 283—305, 12 Abb., 5 Tab., 1955.

Reprinted from *Morskie gravimetričeskie issledovanija*, vol. 5, Izdatel'stvo MGU, 1970, p. 41-53

Review of over-all geophysical studies of the structure of the terrestrial crust of the Indian Ocean

by A. G. Gaïnanov, J. I. Svistounov, P. A. Stroev, and A. A. Schreider

А. Г. Гайнанов, Ю. И. Свистунов, П. А. Строев, А. А. Шрейдер

ОБЗОР КОМПЛЕКСНЫХ ГЕОФИЗИЧЕСКИХ ИССЛЕДОВАНИЙ СТРОЕНИЯ ЗЕМНОЙ КОРЫ ИНДИЙСКОГО ОКЕАНА

В результате интенсивных комплексных геофизических исследований, развернувшихся на акватории Индийского океана в период МГГ (1957—1958 гг.) и в последующие годы в связи с созданием Международной Индоокеанской экспедиции, в настоящее время Индийский океан, в особенности его северо-западная часть, является одной из наиболее геофизически изученных областей Мирового океана. По результатам гравиметрических исследований в северо-западной части Индийского океана до 1962 г. включительно были составлены схематические карты аномалий силы тяжести в свободном воздухе и редукции Буге ($\sigma = 2,8$ *г/см*^{3}) с сечением изоаномал в 50 *мгл* [1]. Комплексный анализ сейсмических данных о строении земной коры по отдельным профилям с гравиметрическими данными позволил выявить основные черты строения коры и верхней мантии в различных областях Индийского океана [2, 3]. Гравиметрические съемки в Индийском океане проводятся английскими и американскими исследователями с морскими гравиметрами Графа, «Аскания GSS-2» и Ла Коста-Ромберга. Одновременно с измерением силы тяжести проводятся непрерывные измерения по профилю полного вектора магнитного поля и глубин дна, а в некоторых рейсах и непрерывные сейсмоакустические исследования верхней осадочной толщи [4—10]. Советские исследователи на НИС «Витязь» и НИС «Курчатов» также производили непрерывные измерения силы тяжести [1] и напряженности полного вектора магнитного поля при плаваниях в Индийском океане [11].

Наиболее изученной гравиметрически областью Индийского океана к настоящему времени является северо-западная часть, для которой с учетом опубликованных до 1967 г. результатов гравиметрических измерений по профилям нами составлена схематическая карта аномалий силы тяжести в редукции Буге ($\sigma = 2,67$ *г/см*^{3}, нормальная формула международная). Средняя квадратическая ошибка определения аномалий Буге не превышает ± 10 *мгл*. Однако, учитывая редкую сеть профилей, изоаномалы проведены через 50 *мгл*. Принципиальные черты аномального гравитационного поля в сравнении с картой аномалий в редукции Буге $\sigma = 2,8$ *г/см*^{3} не изменились. Срединно-океанический

[1] См. В. А. Гладун, И. Н. Капцова. Гравиметрические работы в 40 и 41-м рейсах НИС «Витязь». Настоящий сборник.

Аравийско-Индийский, Мальдивский, Маскаренский подводные хребты характеризуются пониженными, по сравнению с глубоководными котловинами, значениями аномалий Буге. В районе поперечного разлома Оуэн юго-восточнее о. Сокотра северо-западное простирание изоаномал осложняется. Создается впечатление, что осложнение обусловлено воздействием аномальных масс северо-восточного простирания, сосредоточенных в разломной зоне Оуэн.

Гравитационное поле других частей Индийского океана освещено только на участках отдельных разрозненных профилей, пересекающих глубоководные котловины, подводные хребты, глубоководные желоба, континентальные склоны [2, 12 и др.].

По результатам наблюдений орбит искусственных спутников Земли выявлены крупная отрицательная волна геоида в северо-западной части Индийского океана, достигающая —77 *м*, а в восточной и юго-западной — положительные превышения геоида [13].

Одними из первых магнитных исследований в Индийском океане с целью изучения строения земной коры были рейсы советской немагнитной шхуны «Заря» в 1957—1958 гг. [14, 15]. Было выполнено несколько субширотных и субмеридиональных пересечений Индийского океана с непрерывной записью полного вектора земного магнитного поля T, вертикальной Z и горизонтальной H составляющих, а также магнитного склонения D. Уже в этих рейсах были выявлены характерные интенсивные короткопериодные аномалии магнитного поля над рифтовыми зонами Срединно-Индийского хребта, области слабых магнитных аномалий в районах Яванского желоба, Северо-Австралийской и Южно-Австралийской котловин. Дальнейшие магнитные съемки, проводившиеся с буксируемыми ядерными магнитометрами советскими, английскими, американскими и другими исследователями, уточнили и выявили новые области различной магнитной аномальности в Индийском океане [3—11, 16].

Наиболее полно магнитной съемкой покрыта северо-западная часть Индийского океана. Общая длина магнитных профилей к настоящему времени в этом районе превосходит 150 тыс. *км*. В результате выполненных исследований выявлены направления осей магнитных аномалий в Аравийском море и Сомалийской котловине. Намечается параллельность простираний осей магнитных аномалий основным морфоструктурам рельефа. Своеобразные мозаичные магнитные аномалии отмечены на подводном хр. Меррей, не характерные для типично океанической коры. Возможно хр. Меррей заложен на северо-восточном продолжении зоны нарушения Оуэн или является морским продолжением Оман-Пакистанской геоантиклинали [17]. Зона нарушения Оуэн по магнитным аномалиям резко отличается от примыкающих участков Аравийско-Индийского хребта. Если для последнего оси магнитных аномалий параллельны хребту с интенсивными аномалиями над рифтовой областью, то зона Оуэн характеризуется слабо аномальным полем, в среднем не превосходящим $\pm 100\ \gamma$. Наблюдается тенденция к СВ—ЮЗ простиранию осей аномалий.

Западно-Сомалийская котловина характеризуется спокойным магнитным полем, лишь изредка осложненным аномальными зонами, простирающимися, как правило, параллельно Африканскому побережью. Восточная часть Сомалийской котловины, заключенная между Маскаренским и Аравийско-Индийским хребтами, выделяется сильно расчлененным магнитным полем. Амплитуды аномалий от 150 до 300 γ с периодом 10—40 *км*. Причем характер аномалий одинаков над ровным дном и встречающимися здесь подводными горами. Над Сейшельской банкой выявлены интенсивные локальные аномалии, с амплитудой 1000—1500 γ и периодом около 1 *км*. Вероятно, эти аномалии обусловлены базальтовыми дайками, часто наблюдаемыми на Сейшельских островах. Вектора естественной остаточной намагниченности образцов базальтов, собранных на 40 дайках Сейшельских островов, оказались весьма различными по направлению [18].

Банка Сойя де Малья в отличие от Сейшельской банки выделяется слабоаномальным магнитным полем. Амплитуды магнитных аномалий, совпадающие со склонами банки, достигают 50 γ. В юго-западной части Маскаренского хребта и в южной части мелководья Каргадос-Карахос наблюдаются узкие полосовые отрицательные магнитные аномалии интенсивностью до 400 γ. Эти магнитные аномалии, протягивающиеся вдоль западного склона Маскаренского хребта до банки Сойя де Малья, возможно, отражают современную ослабленную зону в морском дне, характеризующуюся магматическими излияниями [8].

Аравийско-Индийский хребет (хр. Карлсберг по зарубежной терминологии) пересечен магнитными профилями на различных широтах. Характер аномалий на всех пересечениях остается одинаковым, меняется лишь их интенсивность [19]. Рифтовые долины Аравийско-Индийского хребта характеризуются отрицательными магнитными аномалиями. Сопоставление полигонных съемок, выполненных рядом советских и зарубежных экспедиций над различными участками Аравийско-Индийского хребта, свидетельствует о том, что оси аномалий, ассоциирующиеся с рифтовыми долинами и гребнями прилегающих гор, не являются непрерывными [11, 20]. На всех полигонах наблюдаются возмущения в магнитном поле, оси которых часто перпендикулярны основному направлению поля. Наблюдаются смещения осей магнитных аномалий, параллельных направлению хребта, в зонах возмущений порядка 10—30 *км*.

Поскольку места выбора полигонов в общем случае являются случайными, имеются основания утверждать по магнитным данным, что основные морфоструктуры в пределах хребта не являются непрерывными, а часто испытывают горизонтальные и, вероятно, вертикальные подвижки небольших амплитуд, что подтверждает представления о Срединном хребте как современной тектонически активной зоне в Мировом океане. Магнитометрическая изученность системы хребтов Лаккадивского, Мальдивского, Чагос, а также котловин и подводных хребтов южной и восточной частей Индийского океана недостаточна. Имеются только отдельные магнитные профили.

Первые сейсмические исследования методом преломленных волн в северо-западной и восточной частях Индийского океана были проведены в 1953 г. на э/с «Челенджер» [21]. В районе Сейшельской банки, расположенной на северном окончании Маскаренского хребта, под слоем коралловых рифов мощностью 30 *м*, имеющих скорость продольных волн 2,1—1,7 *км/сек*, был обнаружен слой толщиной около 2,4 *км* и скоростью продольных волн 5,5—6,0 *км/сек*. Последующие сейсмические исследования установили, что Сейшельская банка имеет материковый тип коры [22]. Гранитные породы, выходы которых на поверхность обнаружены на острове Маэ, мощностью до 13 *км* состоят из двух слоев. Первый слой со скоростью продольных волн 5,6—5,7 *км/сек*, достигает мощности до 3,5 *км*. Под этим типично «гранитным» слоем залегает слой со скоростью продольных волн 6,3 *км/сек*, который, вероятно, соответствует несколько более уплотненным гранитам. На глубине 13 *км* обнаружен слой со скоростью продольных волн 6,8 *км/сек*, типичный для «базальтового» слоя. Граница Мохоровичича (граница *М*) выявлена на глубине 32 *км* под Сейшельскими островами. Наименьшая мощность земной коры обнаружена непосредственно к западу от Сейшельской банки, где выклинивается базальтовый слой со скоростью 6,8 *км/сек*, а породы надбазальтового слоя со скоростью 4,2—6,2 *км/сек* залегают непосредственно на мантии, находящейся на глубине всего лишь 8,5 *км* ниже уровня моря. Далее в западной части Сомалийской котловины в разрезе земной коры снова появляется слой со скоростью 6,8—7,2 *км/сек*, а глубина поверхности *М* погружается до 13—15 *км* ниже уровня моря. По мере приближения к берегам Африки выклинивается надбазальтовый слой со скоростью 5,2 *км/сек* и увеличивается мощность осадочных отложений ($v_г = 2,5$ *км/сек*) до 2—3 *км*. В разрезе земной коры появляется гранитный слой со скоростями продольных волн 4,7—5,3 *км/сек*, который, вероятно, представляет собой продолжение в море отложений системы Карру. У подножья континентального склона выявлены слои со скоростями продольных волн 2,9 *км/сек* и 3,5 *км/сек*. Предполагается, что слой с $v_г = 2,9$ *км/сек* сложен осадками мелового и палеогенового возраста, а слой с $v_г = 3,5$ *км/сек* представляет собой юрские отложения [23].

В 1958 г. экспедицией на судах «Вима» и «Атлантик» было получено 5 разрезов земной коры в Аденском заливе [25, 26]. Сверху по разрезу залегают малоуплотненные осадки мощностью 0,5—1,2 *км* со скоростями 2—3 *км/сек*; ниже располагаются уплотненные осадки и вулканогенные породы со скоростями 4,0—4,5 *км/сек* мощностью 1—2 *км*. Основные и ультраосновные кристаллические породы со скоростями продольных волн 6,4—6,9 *км/сек* залегают на глубине 4—4,5 *км* и имеют мощность около 6 *км*. На двух разрезах ниже слоя со скоростью 6,4—6,9 *км/сек* обнаружен слой со скоростью 7,7 *км/сек*. Вероятно, этот слой представляет собой аномальную мантию, характерную для разреза срединно-океанических хребтов [3, 26].

Сейсмические работы на Маскаренском хребте были продолжены экспедициями на судах «Арго» и «Горизонт» в 1962 г. (экспедиция «Лузиад») и «Дискавери» и «Оуэн» в 1963 г. Совокупность результатов позволила установить неоднородность структуры хребта и прилегающей к нему с востока Маскаренской котловины.

В районе банки Сойя де Малья, расположенной южнее Сейшельских островов и являющейся частью Маскаренского хребта, гранитный слой не обнаружен. Разрез земной коры на банке Сойя де Малья типичен для океанических островов с вулканическим основанием. Под слоями небольшой мощности со скоростями продольных волн 1,72 *км/сек* и 3,25 *км/сек*, представляющими коралловый ил и коралловые породы, сходные с породами, найденными на дне Сейшельской банки, обнаружены слои со скоростями продольных волн 4,4 *км/сек* и 5,4—5,5 *км/сек* мощностью соответственно около 3 и 4 *км*, типичные для вулканических островов и подстилающиеся материалом со скоростью продольных волн 6,8—7,0 *км/сек* [22]. К западу от банки Сойя де Малья обнаружены слои со скоростями продольных волн 6,03 *км/сек* большой протяженности и мощности.

Эти слои, не типичные для вулканических структур, можно рассматривать как продолжение на юг гранитного массива Сейшельских островов. Некоторые исследователи, опираясь на эти факты, предполагают, что Маскаренский хребет образовался в результате вулканической деятельности вдоль границы массива континентального типа [24].

В экспедиции «Лузиад» были получены также сейсмические разрезы земной коры на профиле, пересекающем хребты Лаккадивский, Мальдивский и Чагос. В северной части Мальдивского хребта между

Мальдивскими и Лаккадивскими островами обнаружен типичный для вулканических островов разрез земной коры — почти 5 *км* вулканогенных пород со скоростями продольных волн 3,8 *км/сек* и 5,0 *км/сек*, подстилаемых основным океаническим («базальтовым») слоем земной коры со скоростью продольных волн 6,8 *км/сек* и мощностью 10,6 *км*. Граница *М* обнаружена на глубине 17,3 *км* под уровнем моря. Южнее в разрезе земной коры появляется слой мощностью около 5 *км* и со скоростью продольных волн 6,13 *км/сек*, который также можно отнести к вулканическим породам. Граница *М* расположена, вероятно, на глубине не менее 20 *км*, так как, несмотря на то, что сейсмический профиль был длиной более 100 *км*, волны от границы *М* не зарегистрированы. Под банкой Чагос выявлены слои со скоростями 3,01 *км/сек*, 4,76 и 6,79 *км/сек*, типичные для коралловых и вулканических пород и для основного океанического («базальтового») слоя. На основании сейсмических данных выяснилось, что Мальдивский хребет по всей длине сложен из вулканического слоя мощностью от 4 до 5 *км*, подстилаемого «базальтовым» слоем. Граница *М* на южном конце хребта вероятно расположена на большой глубине. Сейсмические данные на флангах срединного Аравийско-Индийского хребта не выявляют аномальных скоростей в мантии, характерных для срединно-океанских хребтов. На глубине около 10 *км* обнаружена граница *М*.

Экспедиция «Лузиад» провела большой объем сейсмических работ методом преломленных волн в южной и восточной частях Индийского океана. Исследованиями были охвачены Западно-Индийская и Центрально-Индийская ветви срединно-океанического хребта, Восточно-Индийский и Западно-Австралийский хребты и примыкающие к ним участки глубоководных котловин [27]. В Мадагаскарской котловине граница *М* выявлена на глубине около 10,3 *км*. Разрез земной коры представлен очень тонким ($\sim$150 *м*) слоем рыхлых осадков, надбазальтовым слоем ($v_г \approx 5,2$ *км/сек*) мощностью около 1 *км* и базальтовым слоем ($v_г \approx 6,8$ *км/сек*) мощностью около 4 *км*. На расстоянии 185 *км* от оси хребта аномальная мантия не обнаружена. На нескольких станциях в котловине Крозе к югу от развилки ветвей срединного хребта обнаружена тонкая океаническая кора. Средняя мощность коры всего 4,8 *км*, средняя глубина границы *М* около 9,0 *км*. Разрез коры состоит из слоя рыхлых осадков небольшой мощности, надбазальтового слоя мощностью 1,5 *км* ($v_г \approx 5,0$—$6,2$ *км/сек*) и базальтового слоя ($v_г = 6,8$ *км/сек*) мощностью 2,4—4,7 *км*. На расстоянии менее 50 *км* от оси Центрально-Индийского срединного хребта в разрезе земной коры на глубине 10,4 *км* выявлена аномальная мантия с граничной скоростью продольных волн 7,6 *км/сек*. Однако, в отличие от разреза земной коры в Срединно-Атлантическом хребте, надбазальтовый слой небольшой мощности, а мощность коры даже несколько больше мощности коры примыкающих глубоководных котловин. Возможно, наличие такого корня под срединным хребтом объясняется близким прохождением сейсмического профиля у островов Амстердам и Сен Поль.

Сейсмические разрезы субконтинентального типа на Западно-Австралийском хребте получены неуверенно. Граница *М* отмечена на глубине около 22 *км*. Кора многослойна, под слоем рыхлых осадков небольшой мощности выявлены уплотненные осадки ($v_г = 4,7$ *км/сек*) и слои с граничными скоростями продольных волн 5,8; 6,1; 6,4 *км/сек*, близкими к скоростям в гранитном слое [27]. На глубине около 15 *км* прослеживается граница со скоростью продольных волн 7,3 *км/сек*. У восточного подножья хребта граница *М* поднимается до 12—10 *км*, разрез коры представлен рыхлыми осадками, надбазальтовым слоем ($v_г = 5,0$ *км/сек*) и базальтовым слоем с несколько пониженной скоростью продольных волн ($v_г = 6,3$ *км/сек*). Далее к востоку в котловине между Западно-Австралийским хребтом и плато Натуралист разрез коры нормально океанический, граница *М* на глубине 10—12 *км*, кора состоит из рыхлых осадков, надбазальтового слоя ($v_г = 4,7—6,0$ *км/сек*) и базальтового слоя ($v_г = 6,7—6,9$ *км/сек*).

Единственная сейсмическая станция над гребнем Восточно-Индийского хребта выявила разрез земной коры, состоящий из рыхлых осадков мощностью около 700 *м*, небольшой мощности (2,2 *км*) слой с граничной скоростью 4,7 *км/сек*, базальтовый слой мощностью 2,9 *км* и $v_г = 6,6$ *км/сек*, подстилаемый слоем с граничной скростью 7,1 *км/сек*. Разрез не типичен для вулканических гряд. Предполагают, что структура Восточно-Индийского хребта скорее горстового происхождения, чем вулканогенного [27]. В Западно-Австралийской котловине у подножья Восточно-Индийского хребта мощность земной коры несколько меньше (~10 *км*) чем в самой котловине (~12 *км*). К юго-востоку от Кокосовых островов обнаружена необычная для глубоководных океанических котловин тонкая кора мощностью всего 2,8 *км*, подстилаемая аномальной мантией с граничной скоростью 7,7 *км/сек*. Разрез типичен для срединно-океанических хребтов. Интересно, что через эту зону проходит широкий сейсмический пояс (рис. 1)[2] северо-восточной части Индийского океана [28]. В Северо-Австралийской котловине на двух пунктах отмечена утолщенная, примерно на 3 *км*, по сравнению с Западно-Австралийской котловиной, земная кора. Утолщение коры происходит в основном за счет базальтового слоя, граница *М* расположена на глубине ~14,4 *км*. На сейсмических разрезах, пересекающих Яванский желоб в районе пролива Ломбок, отмечено увеличение мощности земной коры под главным внешним желобом. Граница *М* расположена на глубине 20—25 *км* [29, 30]. Кора утолщается в основном за счет базальтового слоя ($v_г = 6,9$ *км/сек*). В сторону островной дуги кора менее мощна, чем под внешним желобом, но более мощная, чем под примыкающей частью Индийского океана. Увеличение мощности коры по мере приближения к островам происходит за счет нарастания осадков.

Советские сейсмические исследования НИС «Витязь» Института океанологии АН СССР проводятся в Индийском океане с 1959 г. [31]. С 1964 г. начаты сейсмические исследования на полигонах в различных провинциях Индийского океана в комплексе с другими геолого-геофизическими методами [11, 32].

Глубинное сейсмическое зондирование выполнено на 12 профилях, расположенных в Андаманском море и Бенгальском заливе, в Центральной, Сомалийской и Маскаренской котловинах, в рифтовых зонах Аравийско-Индийского, Западно-Индийского и Центрального хребтов, на Мальдивском, Западно-Австралийском и Восточно-Индийском хребтах. В результате этих работ выявлено, что Центральная, Сомалийская и Маскаренская котловины имеют сходное строение земной коры. Малоуплотненные осадки имеют небольшую мощность 0,2—0,4 *км*, подстилаются надбазальтовым слоем с граничной скоростью около 5,0 *км/сек* и мощностью 1,5—2,0 *км*. Ниже залегает базальтовый, или основной, океанический слой со скоростью 6,5—6,8 *км/сек*. Общая мощность земной коры 6—7 *км*.

В рифтовых долинах Аравийско-Индийского и Западно-Индийского хребтов получены сходные колонки земной коры. Под поверхностью дна залегает слой со скоростью 4,5—5,0 *км/сек* и мощностью около 2,5 *км*. Ниже залегают породы с граничной скоростью 7,0—7,5 *км/сек*.

[2] См. Приложение 1.

Волны со скоростями 8,0 *км/сек*, характерные для границы *М*, на этих профилях не получены. Высказано два предположения: или система наблюдений была недостаточна, или же под рифтовыми долинами имеется своеобразное геологическое строение.

Для рифтовой долины Центрально-Индийского хребта строение земной коры несколько иное. Под малоуплотненными осадками мощностью 200 *м* залегают породы с граничной скоростью 4,5 *км/сек* и мощностью 1,1 *км*, подстилаемые породами со скоростью 6,5 *км/сек*.

На Западно-Австралийском и Восточно-Индийском хребтах под рыхлыми осадками, мощностью 0,3—0,5 *км*, прослежен слой со скоростью 5,4—5,5 *км/сек*, мощностью 3,5—4,5 *км*, ниже которого залегает слой со скоростью 6,5—6,7 *км/сек* и мощностью 4,5 *км*. Граница *М* выявлена на глубине 10—12 *км*. Следует отметить некоторое расхождение в результатах, полученных НИС «Витязь» и американской экспедицией на Западно-Австралийском и Восточно-Индийском хребтах [27, 32]. Однако как американские, так и советские сейсмические данные о глубине границы *М* под Западно-Австралийским хребтом получены неуверенно.

Большой интерес для изучения глубинной структуры дна Индийского океана имеет исследование сейсмичности рассматриваемой акватории.

Систематическое изучение землетрясений в Индийском океане проводится с начала XX в., но вследствие малого количества регистрирующих станций, их неравномерного расположения и несовершенных методов обработки, точность определения эпицентров землетрясений до 50-х годов была весьма низкой. В течение последних 10—12 лет точность определения эпицентров существенно повышена (до $\pm$ 10 *км*). Это удалось сделать благодаря установке более совершенных сейсмографов, организации дополнительных сейсмостанций, использования современных методов расчетов и внедрения электронной вычислительной техники [28, 33].

Распределение эпицентров землетрясений показано на рис. 1 (по К. В. Стоверу). Пояс землетрясений, совпадающих с срединно-океаническим хребтом, протягивается от южной части Атлантического океана через острова Принца Эдуарда вдоль рифтовой зоны Западно-Индийского хребта до о. Родригес, где сейсмический пояс расщепляется. Одна ветвь вдоль рифтовой зоны Аравийско-Индийского хребта простирается до Аденского залива и соединяется с сейсмическими зонами Восточно-Африканских рифтов и Красного моря, другая ветвь простирается вдоль Центрально-Индийского хребта и Австрало-Антарктического поднятия до смыкания с Тихоокеанским сейсмическим поясом. Глубины гипоцентров землетрясений Индийского океана меньше 70 *км*. Эпицентры в основном совпадают с определенными структурами и образуют зоны различного простирания. Прежде всего обращает на себя внимание тот факт, что зоны расположения эпицентров хорошо коррелируются с простиранием Аравийско-Индийского хребта. Наиболее точно сейсмическая зона совпадает с Центральной рифтовой долиной между о. Родригес и желобом Вима. Севернее желоба Вима эпицентры несколько рассеяны, но тенденция их расположения близ оси хребта сохраняется. Предполагаемое правостороннее смещение рифтовой долины по желобу Вима соответствует смещению сейсмической зоны. Сам желоб Вима не является сейсмически активным. Достигая зоны нарушения Оуэн, полоса землетрясений снова испытывает правосторонний сдвиг с амплитудой в 300 *км*. Интересно отметить, что наибольшая ширина Аденского залива также составляет около 300 *км*. Сама зона нарушения Оуэн является сейсмически активной, а ее направление как бы продолжает простирание хр. Меррей, в котором также зарегистрировано несколько эпицентров землетрясений. В Аденском заливе эпицентры расположены узкой полосой, проходящей в наиболее расчлененной по рельефу центральной части залива. Положение эпицентров здесь, возможно, соответствует срединному рифту [26], а также отдельным нарушениям типа сбросов, разломов с простиранием вкрест рифтовой зоне.

При переходе к Баб-эль-Мандебскому проливу пояс землетрясений поворачивает в Тоджирский залив и смыкается с полосой эпицентров Восточно-Африканской рифтовой системы.

В Западно-Индийском хребте эпицентры также сосредоточены вдоль рифтовой долины. Поперечная разломная зона Принца Эдуарда сейсмически активна, в отличие от асейсмичной разломной зоны Малагаси. Сейсмический пояс юго-восточной ветви Срединно-Индийского хребта по поперечной разломной зоне Амстердам смещен почти на 300 *км*. Сгущения эпицентров восточнее Амстердамской разломной зоны, возможно, также приурочены к поперечным разломам. Намечается широкий пояс сейсмичности, простирающийся примерно параллельно Яванскому желобу. Эта область повышенной сейсмичности начинается южнее острова Цейлон, пересекает Восточно-Индийский хребет южнее экватора и замыкается у Северо-Австралийской котловины. По имеющимся к настоящему времени данным еще не ясно, с какими структурами совпадают эпицентры этого сейсмического пояса.

Измерения теплового потока в Индийском океане выполнены в основном американскими экспедициями [34—38]. С 1964 г. измерения теплового потока проводятся и в советских экспедициях в Индийском океане на НИС «Витязь» и НИС «Курчатов» Института океанологии АН СССР [11]. Наибольшее число измерений теплового потока проведено в северо-западной части Индийского океана (см. рис. 1). Тепловой поток в Индийском океане изменяется в очень широких пределах: от близких к нулю до 5,0 μ *кал/см²·сек* и более. Среднее значение, вероятно, не отличается значительно от среднего значения для других океанов, равного 1,2—1,4 μ *кал/см²·сек*. Гистограмма распределения значений теплового потока в Сомалийской котловине показывает, что наиболее характерной величиной является 1,25 μ *кал/см²·сек*. Примерно такие же значения теплового потока наблюдаются в Аравийской и Маскаренской котловинах.

Для Аравийско-Индийского хребта среднее значение теплового потока составляет 1,35 μ *кал/см²·сек*. Однако в отдельных точках хребта наблюдаются высокие до 4—5 μ *кал/см²·сек* значения теплового потока.

Корреляция высоких значений теплового потока с гребнем хребта выражена слабо. Большинство повышенных значений теплового потока являются локализованными пятнами на океаническом дне. Некоторые из этих значений расположены на значительном удалении от оси хребта. В то же время часто вблизи точек с повышенным значением теплового потока регистрируются низкие значения. Гистограмма распределения величин теплового потока на Аравийско-Индийском хребте, построенная по данным 74 измерений показывает наличие нескольких мод. 43% точек имеют значение 0,5±0,2 μ *кал/см²·сек*. Это значение несколько ниже среднего для океана в целом, но оно является характерным для района хребта. Вторая мода (32% точек) соответствует значению 1,5 ± 0,2 μ *кал/см²·сек*. Это примерно соответствует среднему значению теплового потока для хребта в целом. Наконец, 9% от общего количества измерений дают величину 2,75 ± 0,25 μ *кал/см²·сек*. Такая величина потока соответствует среднему значению для рифтовых долин.

Измерения, выполненные в Аденском заливе, свидетельствуют о повышенном тепловом потоке. Среднее значение его по 5 измерениям $3{,}8 \pm 0{,}49$ μ *кал/см²·сек*, т. е. тепловой поток здесь гораздо интенсивнее, чем на срединном хребте. Кроме высоких значений в центральной зоне залива повышенные значения наблюдаются в точках, расположенных вблизи континентального склона. Таким образом, зона повышенных значений теплового потока шире зоны расположения эпицентров землетрясений.

В глубоководной котловине к северо-западу от Австралии и к югу от Яванского желоба значения теплового потока несколько меньше нормальных.

На рис. 2 и 3 приведены разрезы земной коры по профилю о. Мадагаскар — Западно-Индийский хребет — Центрально-Индийский хребет — Западно-Австралийский хребет — Австралия и по профилю пролив Ломбок — Яванский желоб.

Разрез Мадагаскар — Австралия построен, опираясь на сейсмические колонки, по аномалиям силы тяжести в редукции Буге по методу подбора. В переходной зоне от Австралии к Индийскому океану при построении разреза использованы результаты сейсмических исследований методом преломленных волн в районе Пертского бассейна [39]. Интерпретация гравитационных аномалий над Западно-Индийским хребтом выполнена для двух вариантов строения земной коры срединных хребтов:

1. При нормальной плотности верхней мантии под гребнем хребта по гравиметрическим данным должен быть корень в земной коре. Глубина границы *М* погружается до 12—14 *км*.

2. При аномально низкой плотности верхней мантии под хребтом мощность земной коры уменьшается. Мощность аномальной мантии зависит от степени разуплотнения. Если уменьшение плотности в аномальной мантии достигает 0,2 *г/см³*, то нижняя граница аномальной мантии под Западно-Индийским хребтом, вероятно, расположена на глубинах 18—20 *км*. Наименее надежные разрезы земной коры получены под Центрально-Индийским, Восточно-Индийским и Западно-Австралийским хребтами. В этих областях весьма слабо изучено гравитационное поле, а сейсмические разрезы земной коры получены неуверенно и результаты противоречивы. Если под Центрально-Индийским хребтом мантия разуплотнена примерно на 0,2 *г/см³*, то нижняя граница аномальной мантии, вероятно, располагается на глубинах 18—22 *км*. Для Западно-Австралийского хребта и области сочленения Восточно-Индийского и Западно-Австралийского хребтов интерпретация аномалий силы тяжести в редукции Буге проведена для двух вариантов строения земной коры:

1. Если подтвердится разрез коры (станция 42, рис. 2), полученный в экспедиции «Лузиад» [27], то можно предполагать, что эта область имеет субконтинентальный тип коры мощностью 18—22 *км* и с нормальной верхней мантией.

2. Если же земная кора в этой области имеет мощность порядка 10—12 *км* [32], то для согласования с гравиметрическими данными необходимо предположить наличие под этой областью разуплотненной верхней мантии. В зависимости от степени разуплотнения нижняя граница аномальной мантии, вероятно, находится на глубинах 26—34 *км*.

По профилю пролив Ломбок — Яванский желоб — Северо-Австралийская котловина разрез земной коры построен по сейсмическим данным [29, 30]. С их помощью были рассчитаны изменения аномалий силы тяжести в редукции Буге, обусловленные изменением мощности различных слоев земной коры. Вычисленные значения аномалий были

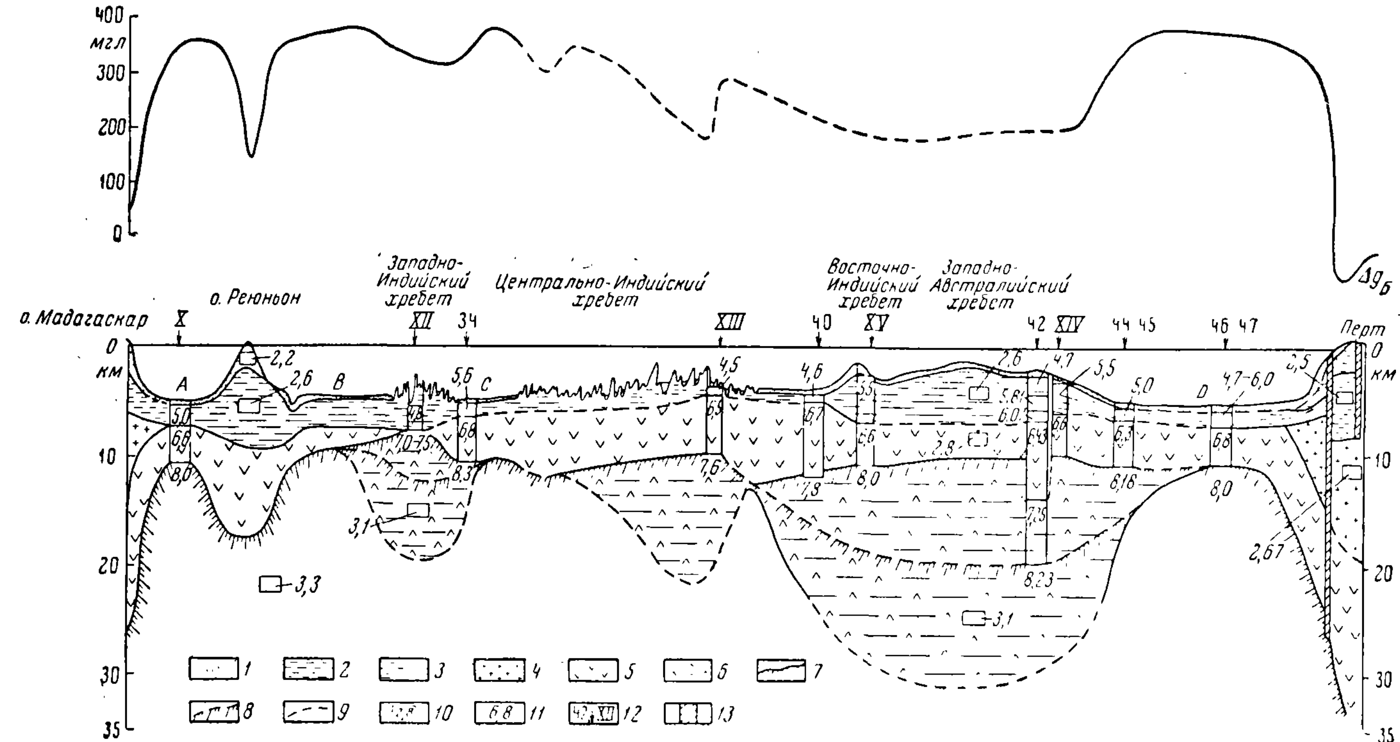

Рис. 2. Разрез земной коры Мадагаскар—Австралия:

1 — рыхлые осадки; *2* — уплотненные осадки; *3* — надбазальтовый слой; *4* — гранитный слой; *5* — базальтовый слой; *6* — породы аномальной мантии с пониженной плотностью; *7* — граница Мохоровичича; *8* — граница Мохоровичича под хребтами (верхняя мантия с нормальной плотностью); *9* — нижняя граница мантии с пониженной плотностью; *10* — плотность в *г/см*^{3}; *11* — скорость продольных волн в *км/сек*; *12* — сейсмические пункты; *13* — разломы. *А* — Маскаренская котловина; *В* — Мадагаскарская котловина; *С* — Котловина Крозе; *D* — Западно-Австралийская котловина сравнены с наблюденными аномалиями в редукции Буге, в результате чего были выявлены большие расхождения между ними, особенно в районе глубоководного желоба. Удовлетворительное согласование наблюденных и вычисленных аномалий возможно при предположении плотностной неоднородности блоков верхней мантии до глубин 60 *км*. При этом под главным внешним желобом плотность верхней мантии

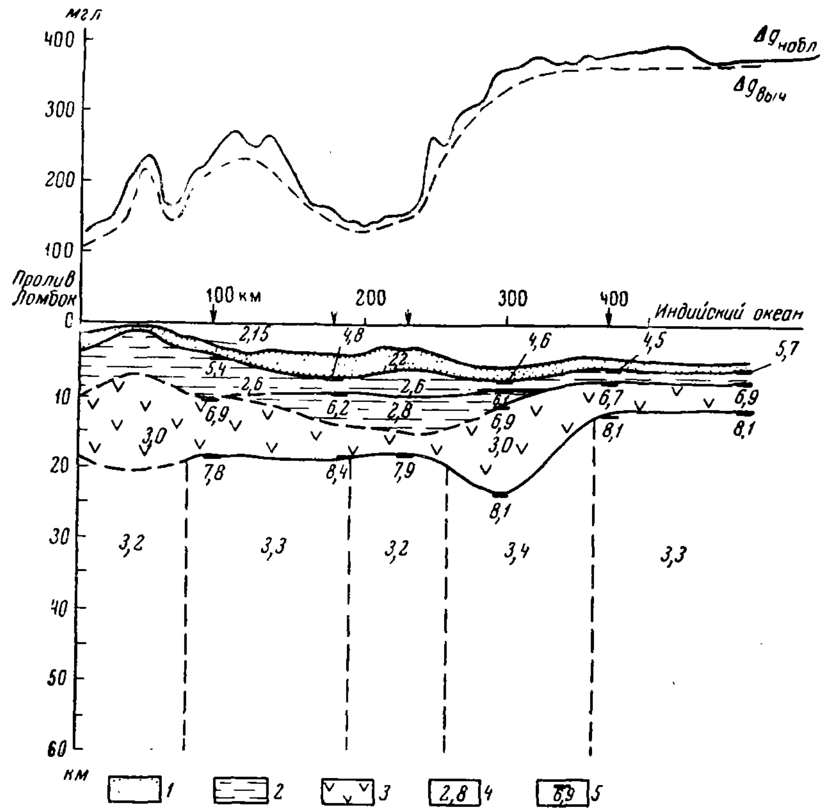

Рис. 3. Разрез земной коры пролив Ломбок—Яванский желоб—Северо-Австралийская котловина Индийского океана:
1 — рыхлые осадки; *2* — надбазальтовый слой; *3* — базальтовый слой; *4* — плотность в *г/см³*; *5* — скорость продольных волн в *км/сек*

возрастает до 3,4 *г/см³*, а под внутренней и внешней грядой плотность мантии уменьшается до 3,2 *г/см³*. Кроме того, под внешней подводной грядой, вероятно, несколько уменьшается мощность базальтового слоя за счет расслоения и увеличения мощности надбазальтового слоя. Под впадиной между внешней и внутренней грядой дуги и под примыкающей котловиной Индийского океана плотность верхней мантии близка к нормальной и равна 3,3 *г/см³*.

В результате проведенных к настоящему времени геофизических исследований в Индийском океане выявляется слоисто-блоковое строение земной коры и верхней мантии. Наиболее четко блоковая неоднородность верхней мантии проявляется под срединными хребтами и в районе развития островных дуг. Своеобразные структуры намечаются в области смыкания Восточно-Индийского и Западно-Австралийского хребтов и в глубоководной Западно-Австралийской котловине к юго-востоку от Кокосовых островов. Однако необходимы более детальные комплексные геолого-геофизические исследования для выявления особенностей глубинного строения этих областей.

ЛИТЕРАТУРА

1. Гайнанов А. Г., Строев П. А. Гравитационное поле и мощность земной коры северо-западной части Индийского океана. «Морские гравиметрические исследования», вып. 3. Изд-во МГУ, 1967.
2. Строев П. А., Гайнанов А. Г. О строении земной коры Индийского океана по данным геофизических исследований. «Океанология», **5**, № 4, 1965.
3. Гайнанов А. Г., Строев П. А. Некоторые черты строения земной коры в Красном море, Аденском заливе и северо-западной части Индийского океана. «Вестн. Моск. ун-та», сер. геология, 1967, № 6.
4. Bathymetric, magnetic and gravity investigations H. M. S. «Owen» 1962—1963. «Admiralty Marine science publication», 1966, No. 9.
5. Bathymetric and magnetic investigations H. M. S. «Dalrymple» 1961—1963. «Admiralty Marine science publication», 1966, No. 8.
6. Preliminary results of Scripps Institution of Oceanography. Investigations in the Indian Ocean during Expedition «Monsoon» and «Lusiad» 1960—1963. Univ. of California, San Diego, 1964.
7. R. R. S. «Discovery» cruises. Bathymetric and Magnetic results obtained of passage 1963. Department of Geodesy and Geophysics Cambridge University, 1964.
8. Bunce E. T., Bowin C. O., Chase R. L. Preliminary results of the 1964 cruise R. V. «Chain» to the Indian Ocean. Phil. «Trans Roy. Soc.», **259**, Ser. **A**, No. 240, 1966.
9. Bunce E. T., Langseth M. G., Chase R. L. etc. Structure of the Western Somali Basin. «J. Geoph. Res.», **72**, No. 10, 1967.
10. Peter G., Weeks L. A., Burns R. E. A reconnaissance geophysical survey in the Andaman Sea and across the Andaman Nicobar island arc. «J. Geoph. Res.», **71**, No. 2, 1966.
11. Удинцев Г. Б. 36 рейс научно-исследовательского судна «Витязь». «Океанология», **5**, № 6, 1965.
12. Vening-Meinesz F. A. Gravity expeditions 1948—1958, with a preface. «Publ. Netherl. geod. Commis», 1960, No. 5.
13. Guier W. H., Newton R. R. The Earth's gravity field as deduced from the doppler tracking of five satellites. «J. Geoph. Res.», **70**, No. 18, 1965.
14. Иванов М. М. Некоторые вопросы строения дна Атлантического и Индийского океанов по магнитным данным. «Геомагнетизм и аэрономия», **3**, № 1, 1963.
15. Иванов М. М. *Магнитная съемка океанов*. М., «Наука», 1966.
16. Taylor P. T. Geothermal and magnetic survey off the Coast of Sumatra «Bull. Earthq. Res. Inst. Tokyo», **44**, No. 2, 1966.
17. Barker P. F. A reconnaissance survey of the Murrey Ridge. «Phil. Trans. Roy Soc.», **259**, Ser. A, No. 240, 1966.
18. Matthews D. H., Davies D. Geophysical studies of the Seychelles Bank. «Phil. Trans. Roy Soc.», **259**, Ser. **A**, No. 240, 1966.
19. Vine F. J., Matthews D. H. Magnetic anomalies ower Oceanic ridges. «Nature», **199**, No. 4897, 1963.
20. Cann J. R., Vine F. J. An area on the crest of the Carlsberg Ridge: Petrology and Magnetic survey. «Phil. Trans. Roy Soc.», **259**, Ser. **A**, No. 240, 1966.
21. Gaskell T. F., Swallow S. S., Hill M. N. Seismic measurements made by H. M. S. «Challendger» in the Atlantic, Pacific and Indian oceans and the Mediterranean Sea 1950—1953. «Philos., Trans. Roy. Soc.», **251**, Ser. **A**, No. 988, 1958.
22. Shor G. G., Pollard D. D. Seismic investigations of Seychelles and Soya de Malha banks, northwest. Indian Ocean. Science, **142**, No. 3588, 1963.
23. Francis T. I. G., Davies D., Hill M. N. Crustal structure between Kenya and the Seychelles. «Phil. Trans. Roy. Soc.», **259**, Ser. **A**, No. 240, 1966.
24. Francis T. I. G., Shor G. G. Seismic refraction measurements in the northwest Indian Ocean. «J. Geoph. Res.», **71**, No. 2, 1966.
25. Nafe I. E., Hennion I. F., Peter G. Geophysical measurements in the Gulf of Aden. Preprints of Int. Ocean. Congr. N. Y., 1959.
26. Laughton A. S. The gulf of Aden. «Phil. Trans. Roy. Soc.», **259**, Ser. **A**, No. 240, 1966.
27. Francis T. I. G., Raitt R. W. Seismic refraction measurements in the southern Indian Ocean. «J. Geoph. Res.», **72**, No. 12, 1967.
28. Stover C. W. Seismicity of the Indian Ocean. «J. Geoph. Res.», **71**, No. 10, 1966.

29. Рэйтт Р. У. Сейсмические исследования методом преломленных волн в районе Индонезийской островной дуги. Второй Международный Океанографический Конгресс. Тезисы докладов. М., «Наука», 1966.
30. Деменицкая Р. М. Кора и мантия Земли. М., «Недра», 1967.
31. Непрочнов Ю. П., Ковылин В. М., Михно М. Ф. Результаты сейсмических исследований строения земной коры и осадочной толщи в Индийском океане. Геология дна океанов и морей. М., «Наука», 1964.
32. Непрочнов Ю. П., Ельников И. Н., Холопов Б. В. Строение земной коры в Индийском океане по результатам сейсмических исследований в 36-м рейсе НИС «Витязь». ДАН СССР, **174**, № 2, 1967.
33. Sykes L. R., Landisman M. The seismicity of East Africa, the Gulf of Aden, the Arabian and Red seas. «Bull. Seismol. Soc. Amer.», **54**, No. 6, 1964.
34. Von Herzen R. P., Langseth M. G. Present status of Oceanic heat flow measurements. In: «Phisics and Chemistry of the Earth.», v. 6, 1965.
35. Von Herzen R. P., Vacquier V. Heat flow and magnetic profiles on the Mid-Indian Ocean ridge. «Phil. Trans. Roy. Soc.», **259**, Ser. **A**, No. 240, 1966.
36. Sciater J. G. Heat flow in the northwest Indian Ocean and Red Sea. «Phil. Trans. Roy. Soc.», **259**, Ser. **A**, No. 240, 1966.
37. Vacquier V., Taylor P. T. Geothermal and magnetic survey off the coast of Sumatra. 1 Presentation of data. «Bull. Earthq. Res. Inst. Univ. Tokyo», **44**, No. 2, 1966.
38. Taylor P. T., Vacquier V. Geothermal and magnetic survey off the coast of Sumatra. 2. Interpretation and discussion of the resulta. «Bull. Earthq. Res. Inst. Univ. Tokyo», **44**, No. 2, 1966.
39. Hawkins L. V., Hennion J. F., Nafe J. E., Thyer R. F. Geophysical inverstigations in the area of the Perth Basin, western Australia «Geophysics», **30**, No. 6, 1965.

Part V

General reports and comments

Reprinted from *Science*, no. 3491, 1961, p. 1674-1676

The International Indian Ocean Expedition

Oceanographers will make full-scale "laboratory" studies of ocean-atmosphere relationships.

John A. Knauss

Except for the glamor and excitement of working in far-away places, why are scientists particularly interested in studying the Indian Ocean? Many of the reasons are related to the monsoon. It is well known that the circulation in the Indian Ocean north of the equator changes markedly with the seasons. This change is particularly notable in the Arabian Sea, where there appears to be a complete reversal of the surface winds between January and July. This reversal is expected to have a marked effect on the biological production of the area. The regions of divergence and upwelling change with the seasons, and a given coastal area that, in one season, exhibits all of the characteristics of high productivity may be expected to have low productivity the following season. Partly because of their obvious economic consequences, the problems connected with the natural productivity of various oceanic regions have received considerable study in recent years. The relationships between oceanic circulation and primary production are complex and not easy to separate. One of the fascinations of the Arabian Sea is that one can study a single region under widely varying conditions. The fact that the Arabian Sea apparently has large untapped fisheries and that massive fish mortalities have been reported from the area are additional stimuli to investigation.

The International Indian Ocean Expedition (IIOE) is the name given to a concerted effort by scientists to learn as much as possible about the Indian Ocean during the next few years. It will include a series of oceanographic expeditions, in which at least 20 ships from a dozen countries will participate; the probable establishment of a marine taxonomic center somewhere in India; the operation of a laboratory ship for 2 years in the Indian Ocean for the purpose of studying marine biological problems; a series of geological and geophysical reconnaissance surveys of parts of the Indian Ocean; and an increase in the network of upper-air meteorological stations for studying the monsoon circulation.

The author is assistant research oceanographer at the Scripps Institution of Oceanography, University of California, La Jolla.

Reasons for the Expedition

Although there may be some disagreement concerning our level of understanding of the steady-state relationship between the mean wind field and the major ocean currents, there is little argument concerning our understanding of the transient problem of the effect of a variable wind field on ocean currents. All are agreed that the problem is very poorly understood. Furthermore, it is a problem that is not amenable to investigation with experimental models, and our best means of attacking it would seem to be to study it in a region such as the Arabian Sea, where the winds blow steadily in one direction for several months and then reverse themselves. Unfortunately, the monsoon circulation is not that simple, but in the Arabian Sea the oceanographer probably comes closer than in any other oceanic area to achieving a "full-scale laboratory experiment" on this particular problem.

Successful laboratory experiments presuppose properly designed instrumentation, and it seems likely that a certain amount of preliminary work will have to be done in this field merely to define the scale of the phenomena we are attempting to observe. The Arabian Sea may be a fine oceanographic laboratory but it has one major drawback. The weather during the summer months can be very bad. For example, the average wind in the Arabian Sea during July is about 30 miles per hour.

Although the equator is near the southern limit of the monsoon, it too is an interesting region to study. There is a seasonal reversal of winds along part of the equator and a reversal of surface currents. The most interesting problem, however, concerns the subsurface currents. Is there a swift, subsurface, eastward-flowing undercurrent in the Indian Ocean similar to that which has been observed in the Pacific and Atlantic oceans? There is as yet no completely satisfactory explanation for the Pacific and Atlantic undercurrents. However, because the other variables along the equator in the Indian Ocean appear to be different enough, it seems possible that a good knowledge of the subsurface currents of the Indian Ocean should help in evaluating the various conflicting explanations for the Pacific and Atlantic undercurrents.

The monsoon itself poses many interesting problems. The temporal and spatial relationships of the various events which, taken together, are referred to as the monsoon circulation have yet to be adequately described or explained. For instance, although the northern summer monsoon blows predominantly from the southwest at low levels, monsoon rains originate over southern China, apparently in response to upper tropospheric changes initiated southwest of India.

These are some of the problems that make scientists want to work in the Indian Ocean. Other prospective projects are the study of a western boundary current (such as the Gulf Stream) as it crosses the equator and the study of beach development under the reversal of strong, longshore currents. As our knowledge of the oceans increases, more and more often oceanographers ask themselves where they can go to observe a certain set of conditions in order to test a hypothesis. The Indian Ocean affords many opportunities for studies of this kind.

Many have claimed that the Indian Ocean is our least known ocean. In a science in which so much is unknown there are many contenders for this rather dubious honor (the central South Pacific and the equatorial Atlantic among others), but there is little question that the Indian Ocean ranks very high on the list. Much of the effort during the next few years will be concerned with gathering biological, physical, chemical, and geological information about the land, ocean, and atmosphere, in order to provide a better description of the Indian Ocean area.

History

The International Indian Ocean Expedition was proposed at the initial meeting of the Special Committee for Oceanographic Research (SCOR) at Woods Hole, Massachusetts, 28 to 30 August 1958. At that time C. O'D. Iselin of the Woods Hole Oceanographic Institution was appointed convener of a small working group to consider exploration of the Indian Ocean. The Special Committee was established by the International Council of Scientific Unions (ICSU), and one of the reasons for its establishment was the fact that ICSU considered it important that international cooperation in field programs in oceanography be continued after the end of the IGY "on a broad basis and for a longer period."

The idea of a concerted effort in the Indian Ocean was further discussed, both informally and in formal sessions of SCOR, at the International Oceanographic Congress at United Nations Headquarters in New York, in September 1959. Shortly thereafter, SCOR asked Robert G. Snider to serve full time as Indian Ocean Coordinator. National committees were formed in many countries, including the United States.

In March 1960 the SCOR working group was reconstituted into three subcommittees under G. E. R. Deacon, director of the National Institute of Oceanography, England (*1*). Most members of the working group were able to meet in Copenhagen on 16 and 17 July 1960, at which time ideas and plans were exchanged and some matters of policy were decided. In the fall of 1960 the National Academy of Sciences Committee on Oceanography expanded its original panel for the International Indian Ocean Expedition to a series of five working groups (*2*). These groups were asked to prepare a program of work to be done in the Indian Ocean—work to be concentrated in a 2-year period beginning about July 1962.

In at least two ways the International Indian Ocean Expedition is similar to the International Geophysical Year: it requires cooperation from scientists from different disciplines and from different countries, and it is growing in size and scope well beyond the conception of the original proposal (*3*).

The original idea of SCOR can be seen in the name "International Indian Ocean Expedition." To most people, an expedition is a rather well-defined enterprise. An oceanographic expedition usually consists of a ship or a group of ships working together in an area on a given set of problems. Georg Wüst, director emeritus of the Institut für Meereskunde, Kiel, proposed such an expedition at the New York meeting in 1959. He suggested that all ships work together, making identical observations and in this way collecting the necessary data for a first-order physical, chemical, biological, and geological description of the Indian Ocean (*4*). As Wüst noted, the plan was similar in concept to that of the famed Meteor Expedition in the South Atlantic, of 1925–27. However, as the plans of the various national committees take shape it becomes apparent that the opportunity to work in the Indian Ocean means different things to different scientists. The idea of making a concerted attack on the problems of the Indian Ocean has caught the imagination of many people, and Snider, in his most recent report, was able to outline the plans of 20 different countries. As in most thriving enterprises, the report was out of date as soon as it was released.

United States Plans

Like the International Geophysical Year, the International Indian Ocean Expedition has no specific beginning or end. There will probably be a peak of activity in 1963, but there has already been a marked increase in the amount of work being done in the Indian Ocean. The Soviet vessels *Ob* and *Vitiaz* have carried out investigations in the Indian Ocean, as have the *Atlantis*, the *Vema*, and the *Argo* of the Woods Hole Oceanographic Institution, the Lamont Geological Laboratory, and the Scripps Institution of Oceanography, respectively. Oceanographic vessels from France and Japan have worked in the area recently, and there has been an increase in the oceanographic activities in several countries that border on the Indian Ocean, particularly in Australia.

The following are examples of projects planned as part of the U.S. National Program for the Expedition in the next 2 or 3 years.

1) The Woods Hole Oceanographic Institution is planning a program, in cooperation with the National Institute of Oceanography, England, to study the changing circulation pattern in the Arabian Sea during the two monsoon seasons. This work will begin in late 1962 or early 1963 and will include considerable work on the biological cycle related to these changing conditions.

2) The U.S. Coast and Geodetic Survey, in cooperation with the Committee on Mean Sea Level of the International Union of Geodesy and Geophysics, is planning to install 28 special tide gauges around the Indian Ocean, primarily to observe seasonal changes in sea level. It seems likely that seasonal changes are greater in parts of the Indian Ocean than anywhere else in the world.

3) The Scripps Institution of Oceanography of the University of California and the Narragansett Marine Laboratory of the University of Rhode Island are planning a joint expedition to the Indian Ocean, beginning in July 1962, to study the circulation in the vicinity of the equator during the two monsoon seasons. There will be two 3-month expeditions. During the first, the Scripps vessel will work in cooperation with one Australian ship. During the second, the work will be done in cooperation with several Japanese ships, with the National Institute of Oceanography, and perhaps with other groups.

4) It is expected that a "biological ship" will be stationed in the Indian Ocean for 2 years. This ship will be operated by the Woods Hole Oceanographic Institution and will be under the directorship of J. H. Ryther. It will serve as a kind of national facility for biologists from various parts of the country who would like to participate in the International Indian Ocean Expedition.

The U.S. Biological Program will consist of 2 years of operations in the western sector of the Indian Ocean, between the tips of India and Africa, during the calendar years 1963 and 1964. Approximately half the time will be spent in making a series of meridional (north-south) sections between the land and the subtropical convergence (40°S) for studies of the systematics, distribution, and abundance of marine life in relation to water masses, current systems, and the monsoonal circulation. There will be sampling of all forms of life, from microorganisms to the large pelagic fishes and from the benthos to the surface flora and fauna. The other half of the ship's operations will consist of intensive ecological or physiological investigations of the flora and fauna in regions of particular interest (the Arabian Sea, the equatorial region, the Bay of Bengal, and so on) and of such biological phenomena as plankton blooms and red water, fish mortalities, and bioluminescence. During the same period, investigations of coastal and inshore waters, of islands, and of reefs are also planned, with landing of shore parties at such island locations as the Maldives, the Laccadives, the Chagos, the Seychelles, Mauritius, and Madagascar. Biologists interested in this program should write directly to John H. Ryther, Woods Hole Oceanographic Institution, Woods Hole, Massachusetts.

5) It is planned to establish, under UNESCO sponsorship, a marine taxonomic center somewhere in India. This center will serve as a preliminary sorting center for collections made in the Indian Ocean and at the same time will provide India with a reference collection of marine organisms from the area.

6) As part of an intensive study of the monsoon circulation, it is hoped to substantially increase the number of stations in the area that are capable of measuring winds at high levels. As part of this program, the United States hopes to man two weather ships stationed on the equator for a 2-year period. Besides providing meteorological observations, the two ships will be used for making intensive physical, chemical, and biological observations.

7) The IIOE provides an excellent opportunity for making more accurate calculations of the energy flux between the ocean and the atmosphere. Such observations and calculations can be made in several more or less independent ways, and it is hoped that four different techniques may be used for intercomparison.

8) Scripps, Woods Hole, Lamont, and the U.S. Coast and Geodetic Survey all expect to conduct reconnaissance-type geological-geophysical cruises in the Indian Ocean between now and 1964. (Lamont and Scripps have each had one such cruise to the Indian Ocean in the last 2 years.) Their programs will include gravity, magnetic, and bathymetric observations while the vessels are under way and coring, heat-flow studies, bottom photography, and seismic refraction observations while they are on station. Generally speaking, Lamont will work in the southern Indian Ocean, Scripps in the west-central region, and Woods Hole in the west Indian Ocean and the Arabian Sea.

9) The newly established National Oceanographic Data Center in Washington, D.C., will process much of the data from the expedition and will assist in the dissemination of data reports to interested persons in the United States and other countries.

Foreign-Policy Implications

Presidents Eisenhower and Kennedy have both endorsed the United States' participation in the International Indian Ocean Expedition. Although presumably the President of the United States is gratified whenever this country makes progress in science, it is probable that presidential endorsement of the IIOE signifies concern not so much with verification of theories of the equatorial circulation as with matters such as cooperation between oceanographic vessels of different nations, the development of oceanography in many of the countries bordering on the Indian Ocean, and the development of new fisheries industries in these countries from local programs growing out of the International Indian Ocean Expedition.

Whether science should be an instrument of foreign policy is no longer in question, if it ever was; the question now is how and under what circumstances it can be. The one point that does seem clear is that a scientific program, to be an effective instrument of foreign policy, must first of all be good science. A scientific idea or program that is pushed primarily for political reasons will ultimately fail, not only as science but as effective politics as well. It is important, therefore, that the International Indian Ocean Expedition be justified on the basis of its scientific program. If it can be, and if the various programs are carried out successfully, then there is reason to hope that it will also be effective in furthering international cooperation in science, assisting in the growth of science in underdeveloped countries, and attaining other objectives.

Scientists who wish to learn more details about any part of the U.S. program should address their queries to Robert G. Snider, Indian Ocean Coordinator, 30 East 40 Street, New York 16, New York, or to any of the chairmen or members of the various working groups. Questions about the programs of other countries should be addressed to Mr. Snider.

References and Notes

1. Members of the SCOR working groups are as follows. *Oceanography Subcommittee (Physical and Chemical, with liaison to Marine Meteorology)*: G. E. R. Deacon (National Institute of Oceanography), chairman; Günter Dietrich (Kiel University); Fritz Fuglister and Bostwick H. Ketchum (Woods Hole Oceanographic Institution); John A. Knauss (Scripps Institution of Oceanography); John C. Swallow (National Institute of Oceanography); Paul Tchernia (Laboratoire d'Oceanographie Physique, Paris); Michitaka Uda (Tokyo University of Fisheries). *Marine Biology Subcommittee*: Ronald I. Currie (National Institute of Oceanography, United Kingdom), chairman; B. G. Bogorov (Institute of Oceanology, Moscow); David H. Davies (South African Association for Marine Biological Research, Durban); George F. Humphrey (CSIRO, Sydney, Australia); Johannes Krey (Kiel University); Shigeru Motoda (Hokkaido University); N. K. Panikkar (Fisheries Development Office, New Delhi); John Ryther (Woods Hole Oceanographic Institution); John Steele (Marine Laboratory, Aberdeen). *Geology, Geophysics, and Bathymetry Subcommittee*: Robert L. Fisher (Scripps Institution of Oceanography), chairman; Bruce C. Heezen and John Nafe (Lamont Geological Observatory); Morris N. Hill (Cambridge University); G. Nanda (Naval Headquarters, New Delhi); Hiroshi Niino (Tokyo Fisheries University); Eugen Seibold (Kiel University); A. Zhivago (Geographia Institute, Moscow).
2. Members and observers of the NAS-NRC Committee on Oceanography IIOE Panel and working groups. *Panel on Indian Ocean Expedition*: Columbus O'D. Iselin (chairman), R. D. Fusselman, H. Arnold Karo, John Lyman, Arthur E. Maxwell, Roger Revelle, Joseph L. Worzel. *Working Group on Biology*: John H. Ryther (chairman), K. Banse, Alan W. H. Be, Howard Eckles, David Keck, David McGill, John A. McGowan, Dixie Lee Ray. *Working Group on Geology, Geophysics, and Bathymetry*: Robert L. Fisher (chairman), Preston E. Cloud, Charles L. Drake, Earl E. Hays, Bruce C. Heezen, Arthur E. Maxwell, George C. Shor, Jr., Harris B. Stewart, Jr. *Working Group on Meteorology*: Robert Fleagle (chairman), Jacob Bjerknes, Alfred K. Blackadar, Andrew Bunker, Earl Droessler, Donald Portman, Colin Ramage, Morris Tepper, Jack C. Thompson.
3. In the report of the first SCOR meeting in August 1958, a tentative total budget of about $4 million was given for the total expedition [*Deep-Sea Research* **5**, 75 (1958)]. It now appears that this sum will about cover the U.S. meteorological program.
4. G. Wüst, *Deep-Sea Research* **6**, 245 (1960).

Reprinted from *Oceanogr. Mar. Biol. Ann. Rev.*, vol. 5, 1967, p. 111-118

AN INDIAN VIEWS THE INTERNATIONAL INDIAN OCEAN EXPEDITION

T. S. SATYANARAYANA RAO
National Institute of Oceanography, Bombay, India

Now that the International Indian Ocean Expedition (I.I.O.E.) is over, or at least the operational aspect of it, perhaps it is not out of place to indulge in some personal reflections—both about the various problems it has generated and those it has solved—which will supplement the review of Currie (1966) regarding what the I.I.O.E. set out to achieve and what were some of the preliminary results. It will be valuable to supplement this with a brief history of marine research in India, what I think I.I.O.E. meant to India, and in what way the nation has benefited by its own full participation in the programme.

My own association with I.I.O.E. began officially on the 1st August 1962 when I took up the post of Liaison Officer for the U.S. Programme in Biology during the I.I.O.E.; I was stationed at Bombay throughout the period of the expedition. By virtue of this position, I was not only looking after the interests of the U.S. Programme in Biology, but also maintained a close liaison with the Indian authorities who were responsible for the Indian Programme and with foreign countries participating in the expedition.

MARINE RESEARCH IN INDIA PRIOR TO I.I.O.E.

Sewell (1952) has given an account of the deep-sea oceanographical exploration in Indian waters, while Panikkar (1952, 1953) has dealt in great detail with the development of fisheries and oceanographical researches in India. I can add here very little to what they have already said, except perhaps to indicate some of the latest developments. I should, however, like briefly to recall some facts concerning marine research in India prior to I.I.O.E. Of all the different facets of marine science, marine biology is perhaps the oldest in India. Some of the more important early workers associated with marine animal studies in the Indian waters are Carter (Porifera), Canton, Day and Russel (fishes), Annandale and Kemp (Fauna of the Chilka Lake), Gardiner (Fauna of the Laccadive and Maldive Islands), Chopra (Crustacea), Fauvel (Polychaeta), Herdman (Pearl Fishery Investigation of Ceylon), Gravely (Fauna of the Madras Coast), Sewell (Copepoda), and others, all working in the early part of this century. The excellent book *The Naturalist in Indian Seas* by A. Alcock, published in 1902, gives a delightful account of the fauna and flora of the Indian Seas. Subsequently, there has been a large number of publications *mostly* dealing with the fauna of the beaches and inshore waters, and in this respect the contribution of the Madras University, Zoological Laboratories and the publications of the Madras Museum are most significant. Lt.-Col. R. B. Seymour Sewell's oceanographical researches on board H.M.I.S. INVESTIGATOR and R.V. MABAHISS in the Bay of Bengal and the Arabian Sea during the period 1925–1935 form an important chapter in the history of Marine Science in India (Sewell, 1925–38). His results were serially published by the Royal Asiatic Society of Bengal and deal with surface temperature distribution in relation to wind force, plankton studies, particularly of Copepoda, and description of various types of sediments in the Bay of Bengal and the Arabian Sea. The Reports of the John Murray Expedition include the results of R.V. MABAHISS. The Oceanographic Memoirs of the Andhra University, Waltair, Vols 1 and 2 (1954–1958), which deal with the results of the large number of cruises on board the Indian Naval Mine Sweepers conducted by the University during 1952–1955 under the leadership of Professor E. C. LaFond, Fulbright Visiting Professor of Oceanography, form another step in India's progress in marine research, particularly in the Bay of Bengal. These studies cover the physical oceanography, nutrient chemistry, plankton distribution, and sediment analysis.

Meanwhile, in 1947 the Central Government in the Ministry of Food and Agriculture set up the Central Marine Fisheries Research Institute, with headquarters at Mandapam, and this organization under the leadership of Dr N. K. Panikkar began carefully organized studies on various aspects of marine research relating to fisheries. A comprehensive scheme of sea-water analysis was initiated by the Central Marine Fisheries Research Institute in 1952 with the financial support of the Council of Scientific and Industrial Research; under this programme chemical laboratories were set up at Calcutta, Madras, and Bombay to analyse thousands of samples of sea water for salinity collected by Fishery and Merchant Navy vessels all along the Indian coastline. The Indian Naval authorities also set up a physical research centre at Cochin to study military oceanographical problems. In this connection the excellent progress made by the Forest Research Institute, Dehra Dun, in the study of marine fouling and boring organisms at different university centres all along the coast of India should be mentioned. The Universities of Kerala, Annamalai, Madras, Andhra, and Bombay have developed and expanded research and teaching facilities in marine science from 1950. Meanwhile, the Government of India constituted the Central Board of Geophysics in 1949 and an Oceanographic Committee to review problems of Oceanographic studies in India from time to time and with the ultimate object of setting up an Institute of Oceanography. Notwithstanding all this activity and expansion in the marine sciences, it should be emphasized that until 1960 there was no organization in India with sufficient funds and authority either to back up extended researches in oceanography or to co-ordinate marine studies at the national level; nor was there any organized projection of marine studies to suit India's requirements and goals. This gap was finally filled when the Central Government appointed an Indian National Committee on Ocean Research (I.N.C.O.R.) in 1960. The terms of reference of this committee were:

(*a*) to draw up a co-ordinated plan for India's participation in the I.I.O.E.,
(*b*) to advise on the allocation of a programme between Departments of Government, research organizations, universities, and other institutions,
(*c*) to consider and approve detailed plans for research in the several scientific disciplines related to India's participation and to recommend financial grants,
(*d*) to further and co-ordinate research programmes,
(*e*) to advise the Government generally on all matters connected with India's participation in the expedition.

I.I.O.E. AND INDIA

It would appear from the terms of reference of I.N.C.O.R. that besides being responsible for India's participation in the I.I.O.E., the Committee also became the focus of all developments and research projects connected with oceanographical researches. The Committee and its working groups included almost all the important scientists representing various Indian institutions concerned in different branches of oceanography. The results of the Committee's deliberations led directly to the establishment of an Indian Ocean Expedition Directorate as a department of the Council of Scientific and Industrial Research, and to the allocation of sufficient funds and staff and thus ensured full participation of India in the International Programme. The subsequent establishment of the International Meteorological Centre at Colaba (Bombay) and the Indian Ocean Biological Centre at Cochin are well known to marine scientists the world over.

The genesis of the I.I.O.E. is now well known (Currie, 1966). The expedition sought to explore in detail the oceanography of the Indian Ocean and to make the area as well known as either the Atlantic or the Pacific. It was also fashionable for all who ever spoke on the programme of I.I.O.E. to draw attention to the enormous population increase of India and neighbouring countries and the inadequacy of food and protein requirements for undernourished people and to plead fervently for the exploration and exploitation of the food resources of the sea; if the speaker were a marine meteorologist, he would say how interesting are the reversing monsoons and how unpredictable or unreliable they are for Indian agriculturists; a geophysicist would stress the possibility of unknown oil resources in the shelf areas off India. In this way all sought to justify the many cruises, ships, and nations participating in the joint enterprise of the I.I.O.E. One must consider very carefully how crucial these problems were from India's point of view.

The food problem is without any doubt serious. India's exploitation of fishery resources has been growing every year and it is reasonable to expect that given more vessels and men, it should be possible to double the gross tonnage of fish landed on our coasts. The most interesting aspect of this problem, however, is the fact that 65–75% of marine fish landed annually in India comes from the west coast (Table I). This was pointed out by Panikkar and Jayaraman (1956) at the 8th Pacific Science Congress and the picture remains the same even today. The reason for the apparent scarcity of fishery resources off the east coast of India and the rest of the Bay of Bengal should be urgently investigated and considered quite separately from the problem as

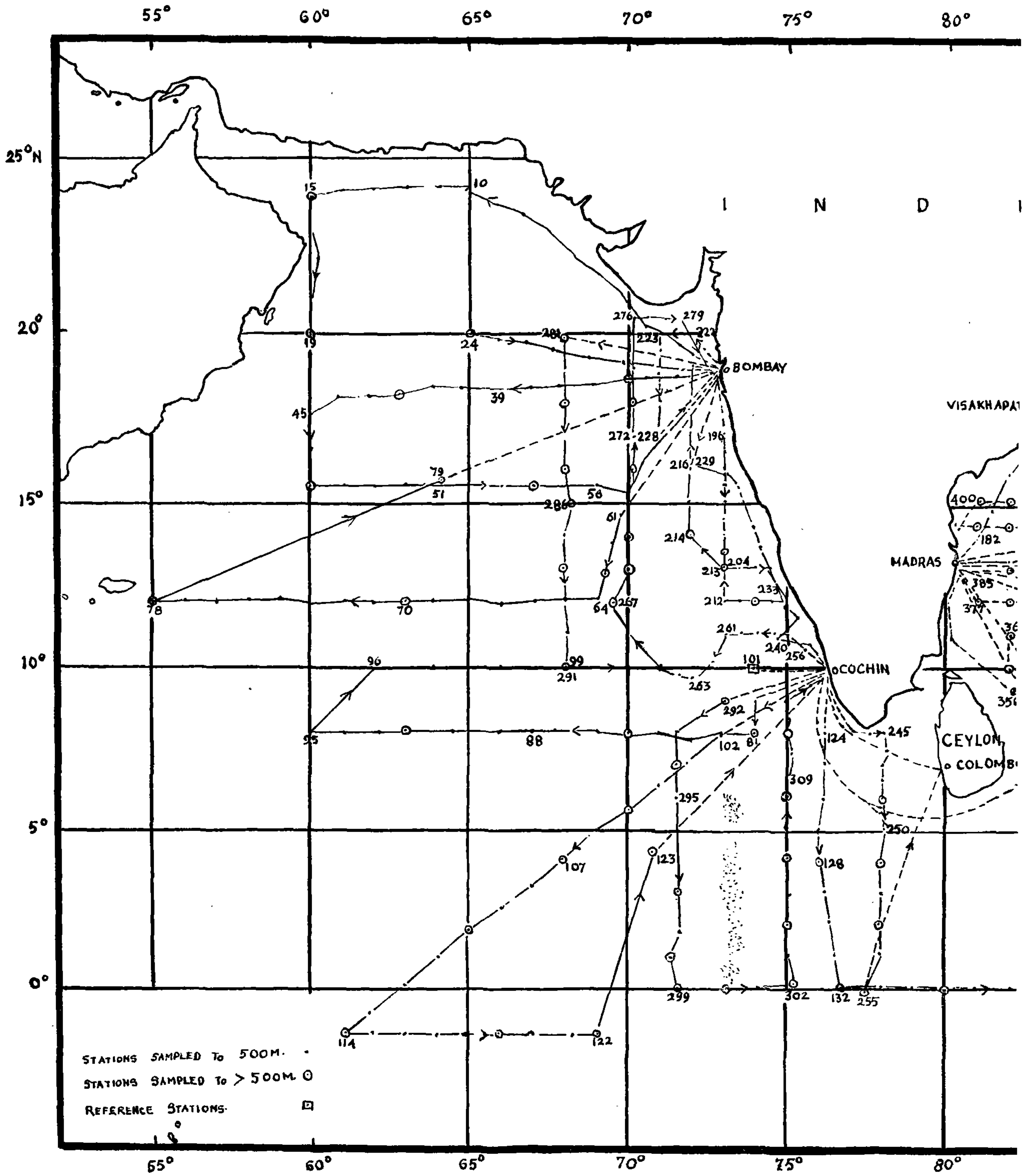

Fig. 1.—Indian programme during the I.I.O.E.;

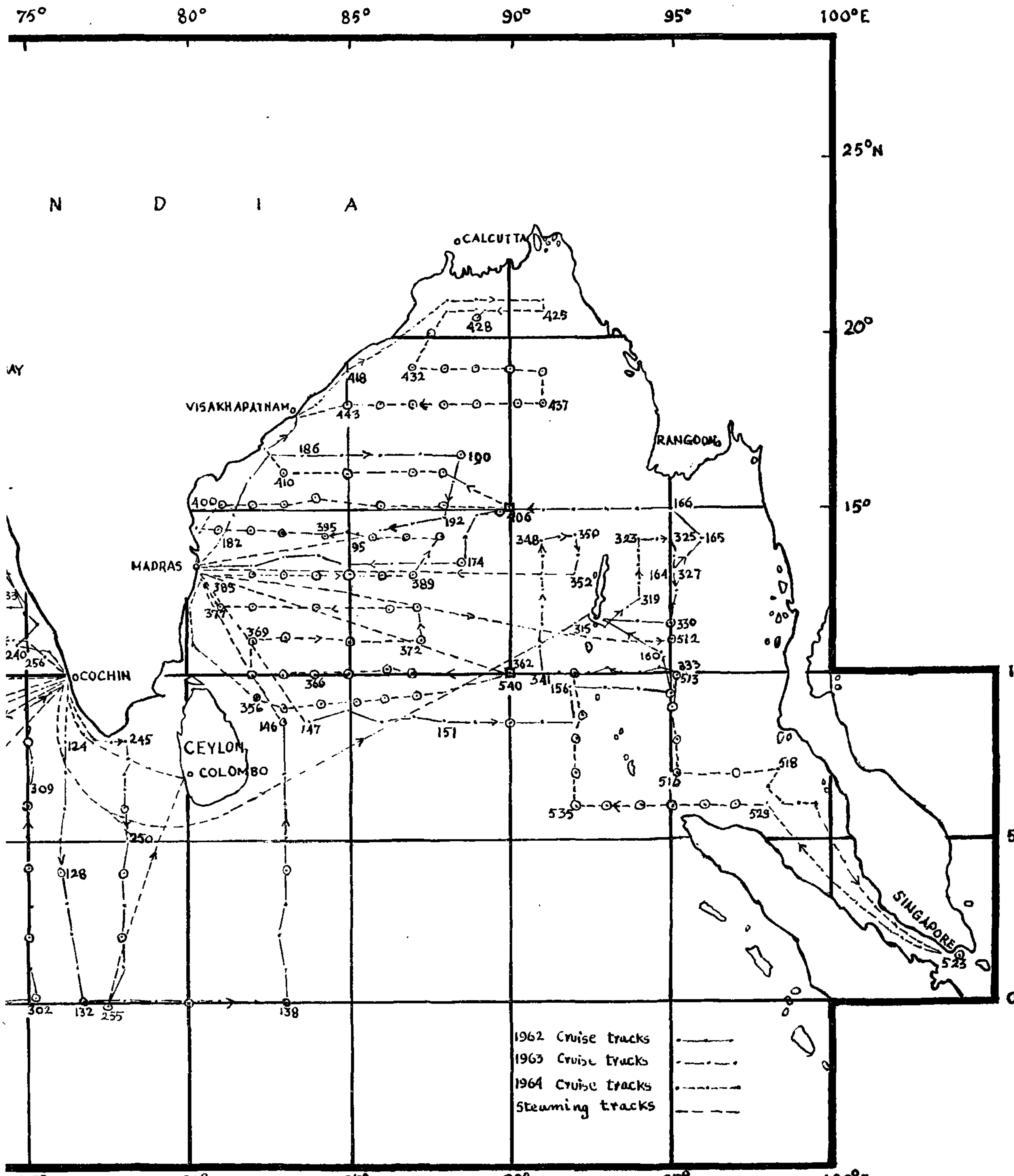

track charts of I.N.S. KISTNA, 1962–64.

to whether we are fully exploiting the available fishery off the west coast. Although in recent years mechanization of fishing vessels has increased, the fact remains that fishing is done mostly in nearshore waters while the vast shelf off the west coast remains totally unexploited. For example, off the Bombay and Gujarat coasts, the shelf extends out for nearly 200 miles and but for one or two vessels of the deep-sea section of the Food and Agriculture Ministry no large scale commercial trawlers are commissioned to fish these vast areas. Regular mapping of coastal areas rich in fishery resources was one of the immediate requirements of India.

Next we may consider the mineral resources of the sea. India lacks natural deposits of fertilizer salts and also rich deposits of fossil fuel. One of the ingenious suggestions was that the possibility of extracting nutrient salts such as phosphates and nitrates from the vast quantities of marine sediments dumped by the great river systems into the Bay of Bengal and the Arabian Sea should be considered. The possible accumulation of oil under the shelf

TABLE I

Marine fish landings of India (in metric tons)
(by the courtesy of K. V. Rao)

Year	East coast of India, including Andaman Islands	West coast of India including Laccadive and Minicoy group of islands	Total
1960	170,191	702,264	872,465*
1961	187,062	489,300	676,363*
1962	180,684	463,560	644,244
1963	185,850	469,634	655,484
1964	213,826	645,677	859,503
Annual Average	187,523	554,087	741,610

* Excludes trawler catches of 7000–8000 tons.

(offshore areas), particularly off Cambay, was also considered suitable for investigation, particularly since the nearby area of Anklesvar had yielded exploitable deposits of gas and oil.

Again, the mapping of coastal currents and the bathymetry of nearshore areas, and their importance for coastal navigation, defence, harbour construction, and so on, cannot be minimized. With the increase in industries and nuclear reactors, the question of pollution and waste disposal takes on added significance. Our knowledge of coastal bathymetry and bottom topography is totally out-of-date and the physical oceanography of the coastal currents is almost unknown; such as is known is based on visual observations of wind and water. Such observations needed to be immediately augumented by modern methods of sounding and Hi-Fix.

Finally, there is the study of the monsoons. Two problems are involved; first, how does the reversal of the monsoons affect the oceanic circulation in the North Indian Ocean, and secondly, how may the onset and intensity of the southwest monsoon be predicted. This second problem is of great agricultural importance since most of the ryots (farmers) in India depend on monsoon rains for the cultivation of summer crops (Kharif). One may illustrate this point by quoting from the 'panchangam' (Almanac, 1966), the prediction of the origin and rainfall in India for 1966–67; this shows the orthodox Hindu view of the monsoons on which our farmers pin their hopes. "This year [1966–67] a cloud by name 'Avartha' will be born at the summit of 'Meru' mountains [the present Vindhya system of Central India] and will cause 'medium' quantity of rainfall. There will be fear of war and famine in the country. The rain consists of 2 kolagas of rainfall and 4 kolagas of wind" [each kolaga measures 60 gavuda square and 100 gavuda height—each gavuda is variously described as equal to 1½ to 12 miles]. Nobody has checked statistically how accurate these predictions are, but the fact remains that the farmer has no other dependable alternative for information on monsoons.

THE INDIAN PROGRAMME

These were some of the problems in which India herself was interested at the time of launching of the I.I.O.E. Quite rightly, therefore, the planners of the Indian Programme concentrated their efforts in these directions and confined their cruises and observations to yield an intensive study of the coastal areas, both in the Arabian Sea and the Bay of Bengal. With the inauguration of the 1st Scientific Cruise of I.N.S. KISTNA on October 9, 1962, by Professor Humayun Kabir, Minister for Scientific Research and Cultural Affairs, the Indian Programme of work during the I.I.O.E. was effectively launched. Besides I.N.S. KISTNA the Indian Programme included scientific cruises by R.V. VARUNA of the Indo-Norwegian project, R.V. CONCH of the University of Kerala, and F.V. BANGADA, an exploratory fishing vessel of the Ministry of Food and Agriculture, Government of India. All the cruise tracks and programme of work were co-ordinated so that a complete coverage of important coastal areas of both in the Bay of Bengal and the Arabian Sea (see Figs 1 and 2) was effected.

I.N.S. 'KISTNA'

The participation and programme of I.N.S. KISTNA in the I.I.O.E. is unique in many respects. The Indian Navy should be congratulated for placing the frigate at the disposal of the Indian National Committee on Ocean Research solely for Oceanographical work. This was a most welcome development for the future of this work in India since by this gesture of co-operation the Indian Navy's full support for I.I.O.E. was assured.

From Figures 1 and 2 it is clear that I.N.S. KISTNA has covered fairly well both the Bay of Bengal and the Arabian Sea and in the south right up to the Equator. Commencing in October 1962, I.N.S. KISTNA has completed 28 scientific cruises, and had it not been for the unfortunate Indo-Pakistan conflict in the middle of 1965, she would have successfully accomplished the rest of the cruises planned during the fall of 1965. The vast amount of data collected by I.N.S. KISTNA is now being analysed at the data and planning division of the National Institute of Oceanography.

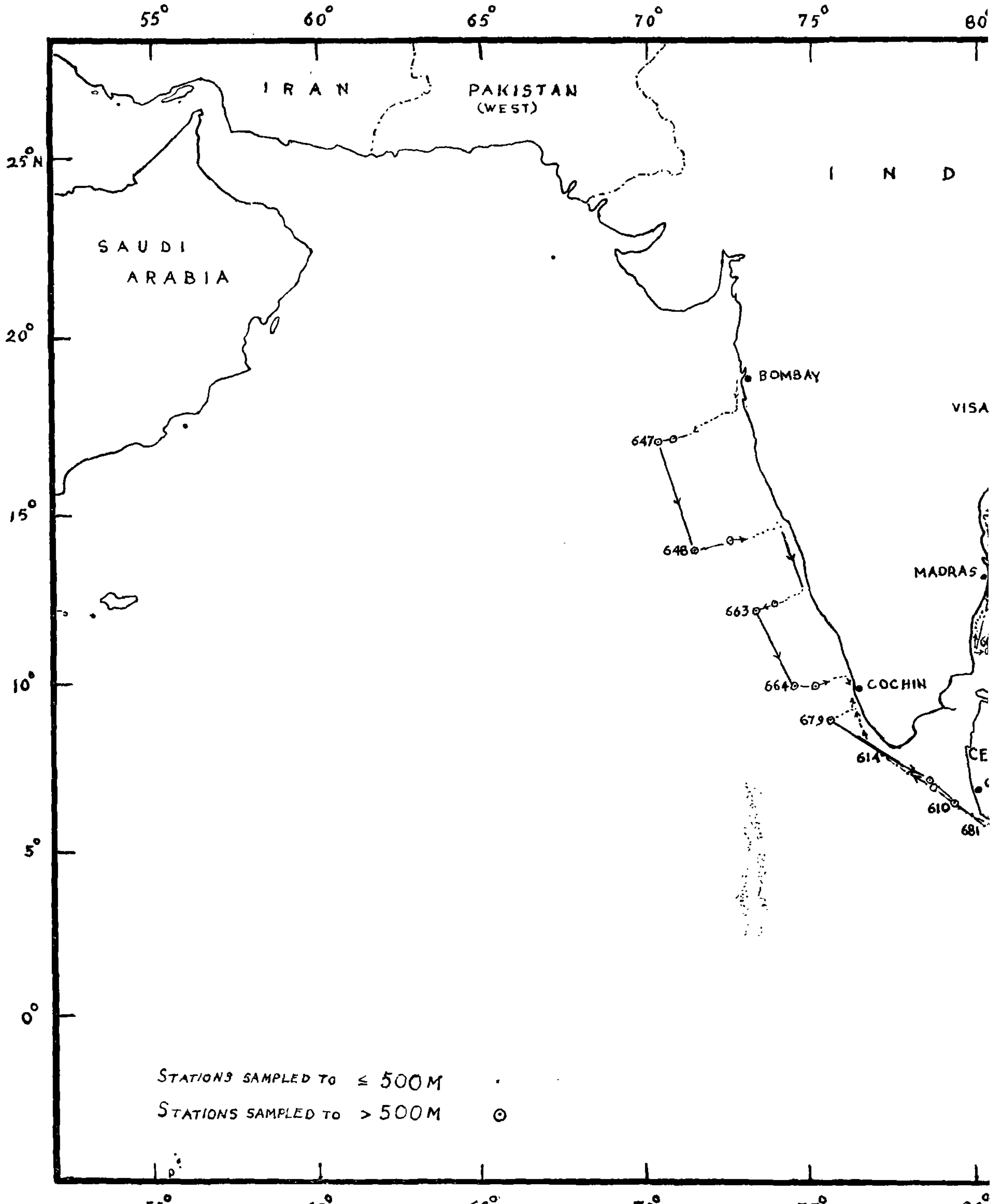

Fig. 2.—Indian programme during the I.I.O.E.;

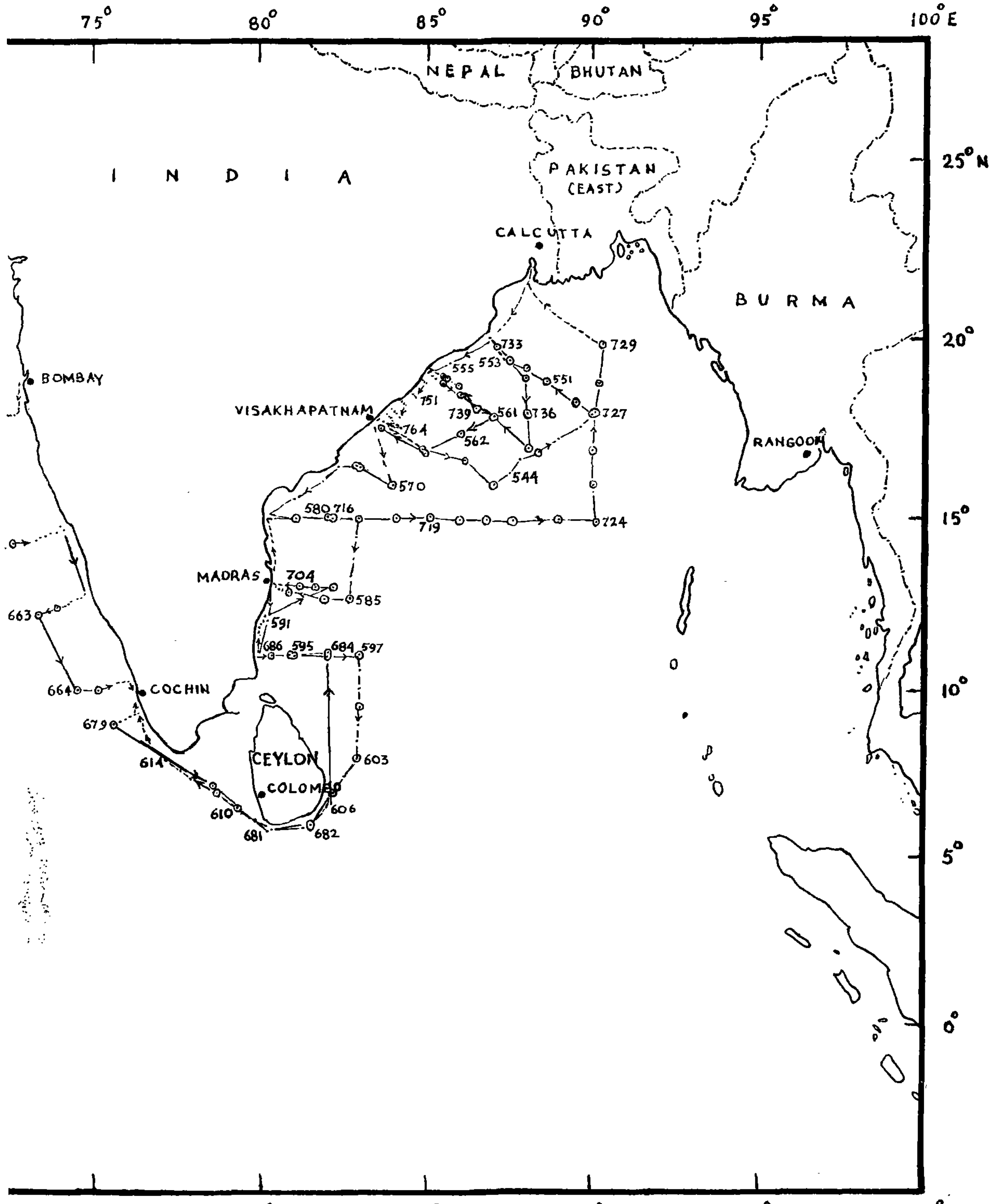

track charts of I.N.S. KISTNA, 1965.

Meanwhile, the International Meteorological Centre (I.M.C.) at Colaba, Bombay, functioned from 1st January 1962 with Professor C. S. Ramage as director. This centre was financed by the Council of Scientific and Industrial Research, and was manned by the Indian Meteorological Department. The United Nations special fund provided an I.E.M. 1620 Electronic Computer for data processing. The United States National Science Foundation had given liberal assistance through equipment and other services. The extended Indian Ocean Chart in use at I.M.C. covers the whole of the Indian Ocean plus adjacent areas. Reception of about 75 daily Radio Teletype broadcasts from Canberra, Nairobi, Singapore, and Pretoria, provided the bulk of the Southern Hemisphere coverage. Data exchanged with Tokyo and Moscow and some 40 Radio Teletype/Carrier Wave broadcasts received from Karachi, Aden, Colombo, Djakarta, and Saigon, supplemented by collections at the Meteorological communication centre, formed the coverage of the Northern Hemisphere. Ships' reports obtained over Radio Teletype circuits from Mauritius by the Indian Navy added to the coverage of the South Indian Ocean. On a typical day the total coverage amounted to:

Surface reports	1155
Ships	384
Upper air	429

Aircraft report from long distance international flights on three to four air routes.

At the I.M.C., synoptic charts are prepared for two principal times—00 and 12 hours Greenwich Mean Time—for surface and standard isobaric levels, namely 50, 100, 200, 300, 500 and 700 mb. Back plotting is also done after data reception of additional information from other centres. During the period of the I.I.O.E., perhaps the most important observations on the monsoons were carried out by specially instrumented research aircraft of the U.S. Weather Bureau Research Flight Facility and the Woods Hole Oceanographic Institution. In addition, a NOMAD automatic weather station was anchored in the Bay of Bengal half-way between Madras and the Andamans in April 1964. An Automatic Picture Transmission (A.P.T.) receiving equipment on loan from the U.S. National Science Foundation was installed at I.M.C. in December 1963, and this picked up pictures of cloud cover from TIROS VII and NIMBUS Meteorological Satellites during their orbits over the Indian subcontinent. It is too early to say that I.M.C. has solved the problem of the development of the monsoon or is able to predict the arrival of the monsoon accurately, but it has accumulated a vast quantity of information and the preliminary analysis of the data has improved our knowledge of the circulation pattern of the monsoon winds. In fact, for the first time meteorologists in India were able to get data from over the oceans for their studies and have come to realize that the weather pattern of the Indian sub-continent is greatly influenced by conditions in the sea.

The establishment of the Indian Ocean Biological Centre (I.O.B.C.) at Ernakulam marks a very important milestone in the history of marine biology in India. The Centre was organized by the Council of Scientific and Industrial Research (C.S.I.R.) in co-operation with U.N.E.S.C.O. The chief considerations which led to the selection of India for the location of the Centre were (from Indian Scientific Programme 1962–65):

1. Geographical location of India at whose ports many of the ships participating in the expedition were likely to call.
2. The very considerable interest in biological and taxonomic studies in India at scientific and university institutions.
3. The availability of a large number of trained biologists who could take up the work.
4. The advantage of a centre of this type in South Asia which would stimulate marine biological studies in the Asian region.

The principal functions of the Centre are:

1. Maintenance of a named reference collection of Indian Ocean material and duplication of it for laboratories throughout the world.
2. Sorting zooplankton samples taken by standard methods.
3. Examination of the sorted standard material or sending it to specialists throughout the world.
4. Sorting of the zooplankton samples at the request and expense of participating laboratories.
5. Training.

The development of this Centre in India has provided a unique opportunity for the training of biologists from India and other countries in the region. It is becoming almost a Mecca for visiting marine scientists and university parties from different parts of the country.

I.I.O.E. BENEFITS TO INDIA

The I.I.O.E. has achieved for itself the distinction of being one of the best examples of international co-operation between many nations both East and West. Indian scientists visited many neighbouring countries and the Indian ship I.N.S. KISTNA visited Singapore. India played host to scientists from many nations resulting in deep and abiding friendship. Many of the participating foreign research ships like R.V. ANTON BRUUN, R.V. VITYAZ, R.R.S. DISCOVERY, R.V. ARGO and R.V. HORIZON, provided facilities for ship-board training and research for many Indian scientists.

The expedition also provided opportunities for organizing seminars in which many young scientists from different parts of the country and senior scientists from abroad participated. An All-India Seminar on Marine Science was held at Waltair on 26–27th April, 1963, sponsored by the Andhra University, Waltair, the Indian National Committee on Ocean Research, the U.S. Programme in Biology and the U.S. Information Service. It was well attended and was a great success. At the time of the visit of R.V. HORIZON and R.V. ARGO at Cochin and then again at Calcutta during the visit of the U.S. Coast and Geodetic Survey Ship PIONEER seminars were arranged at which visiting scientists and their Indian counterparts participated in discussions. In July 1965 an International Symposium at Bombay on the Meteorological Results of I.I.O.E. was held and this was attended by a large number of foreign and Indian delegates.

As a finale to all this activity, a training programme was organized at the postgraduate level to train junior scientists in the subject and practice of Oceanography as a multi-disciplinary science during January–March 1966 at

Bombay. This was jointly sponsored by U.N.E.S.C.O. and C.S.I.R. A total number of 25 trainees were recruited from among the applications submitted by Indian and adjacent Asian countries to U.N.E.S.C.O. The break-up figures for the trainees were; India 20, Thailand 2, Singapore 1, Ceylon 1, and Malaysia 1.

THE FUTURE

While the Training Programme marked the end of I.I.O.E. activities, it also saw the birth of the National Institute of Oceanography (N.I.O.) of India. The Central Government approved the establishment of this institute as one of the national laboratories under the C.S.I.R. and appointed Dr N. K. Panikkar, Director of the Indian Programme under the I.I.O.E., as director of the new institute. All the activities started under the Indian Programme of the I.I.O.E., including the Indian Ocean Biological Centre, have now been merged into the National Institute of Oceanography.

The National Institute proposes to study various aspects of coastal oceanographical problems, coral reefs, oceanographical data for improved fishing and navigational charts, sedimentary history of the Indian Ocean basins, and prospecting for oil, ore, minerals, and phosphates in the sea.

Proposals are afoot for acquiring an oceanographical research ship for the institute. The institute also proposes to co-operate with other research organizations in India such as the National Geophysical Research Institute, Atomic Energy Establishment, Zoological and Botanical Surveys, and the Naval Research groups, and work on problems of mutual interest. The Institute may also have to concentrate specially on problems relating to desalination and also the pollution of coastal waters by big industries and atomic reactors.

REFERENCES

Almanac, 1966. *Prabhava Samvatsarda Mysore Panchanga*, Panchanga Mandira, V. V. Mohalla, Mysore 2, p. 27.

Andhra University Memoirs in Oceanography, 1954. **1**, Andhra University Series No. 49, 162 pp.

Andhra University Memoirs in Oceanography, 1958. **2**, Andhra University Series, No. 62, 237 pp.

Currie, R., 1966. In, *Oceanogr. Mar. Biol. Ann. Rev.*, edited by H. Barnes, George Allen and Unwin, London, **4**, 69–78.

International Indian Ocean Expedition Newsletter, India, 1965. **3**, No. 3, 23 pp.

Indian Scientific Programme, 1962–1965. Issued by the Indian National Committee on Ocean Research, C.S.I.R., New Delhi, 46 pp.

International Meteorological Centre, 1965. *Activities*, I.M.C. Brochure, issued by the Indian Meteorological Department, 20 pp.

Panikkar, N. K., 1952. *Jour. Bom. nat. Hist. Soc.*, **50**, 741–758.

Panikkar, N. K., 1953. *Proc. Eighth Pacific Sci. Congr.*, Vol. III, Oceanogr. 294–303.

Panikkar, N. K. and Jayaraman, R., 1956. *Proc. eighth Pacific Sci. Congr.*, Vol. IIIA, 111–122.

Sewell, R. B. S., 1925–3. *Mem. Asiat. Soc. Bengal*, **9**, 552 pp.

Sewell, R. B. S., 1952. *Jour. Bom. nat. Hist. Soc.*, **50**, 705–717.

Part VI

Papers presented by title or abstract only

656 Note on the formation of sand domes on the Fort Cochin beach

by V. S. Rama Raju
Physical Oceanographic Centre of Indian Ocean Expedition
(CSIR), Cochin, India.

in: Bull. natn. geophys. res. Inst. India, vol. 2, nos. 2/3, 1964, p. 74-76.

657 Red Sea fishes recently found in the Mediterranean

by Adam Ben-Tuvia
Sea Fisheries Research Station, Haifa, Israel. Present address:
Fisheries Biology Branch, FAO, Rome, Italy.

in: Copeia, no. 2, 1966, p. 254-275.

Abstract. At least 24 species of fishes have passed from the Red Sea to the Mediterranean Sea since the Suez Canal was opened in 1869. Records of another 26 species collected in the Mediterranean and alleged to be of Red Sea origin are shown to be based on misidentification or probable errors in determining the source of material. There are no reliable records of Mediterranean species penetrating into the Red Sea. Nearly all of the 24 species are confined to shallow coastal waters and have migrated mostly northward along the Asiatic coast. One is known from the Mediterranean coast of Egypt only, nine are not recorded farther north than Israel, 13 are known as far as the Anatolian coast of Turkey, and seven have reached the Aegean Sea. The extremes in westward migration so far recorded are *Parexocoetus mento* from the Gulf of Sidra and *Leiognathus klunzingeri* from the neighborhood of Lampedusa.

Several Red Sea species were observed in the Mediterranean for the first time within the last 10 years. The decrease in salinity of the Bitter Lakes, which are part of the Suez Canal, may have facilitated recent immigration.

While Red Sea species constitute only 9 % of the fish fauna of the Mediterranean coast of Israel, their ecological importance is fairly great since 18 species are among the more common in this area, and nine are commercially exploited.

658 Plankton in the Arabian Sea

by R. Raghu Prasad
Indian Ocean Biological Centre

in: Indian Seafood, vol. 6, no. 2, 1968, p. 12-15.

659 X-ray microscopy of recent planktonic Foraminifera

by Allen W. H. Bé, Willem L. Jongebloed and Andrew McIntyre
Lamont-Doherty Geological Observatory, Columbia University,

Palisades, New York, United States.

in: Jour. Paleontology, vol. 43, no. 6, 1969, p. 1384-1396.

Abstract. Twenty-three species of living planktonic foraminifers were examined with a projection X-ray microscope, revealing their internal morphology, wall thicknes and surface features without destruction of the shells. Their spatial construction and coiling pattern may be viewed from stereoscopic pairs of radiographs. Measurements of pore concentrations and pore diameters were made on shell fragments. X-ray microscopy is particularly helpful in ontogenetic studies of involute species of foraminifers.